HONI SOIT QUI MAL Y PENSE
DIEU ET MON DROIT

AGRICULTURAL RESEARCH INSTITUTE
PUSA
71472

PROCEEDINGS

OF THE

ROYAL SOCIETY OF LONDON

SERIES A

CONTAINING PAPERS OF A MATHEMATICAL AND
PHYSICAL CHARACTER.

VOL. CXVI.

LONDON:
PRINTED FOR THE ROYAL SOCIETY AND SOLD BY
HARRISON AND SONS, LTD., ST. MARTIN'S LANE,
PRINTERS IN ORDINARY TO HIS MAJESTY.
NOVEMBER, 1927.

LONDON
HARRISON AND SONS, LTD., PRINTERS IN ORDINARY TO HIS MAJESTY,
ST. MARTIN'S LANE.

CONTENTS.

SERIES A. VOL. CXVI.

No. 773—September 1, 1927.

PAGE

The Luminescence of Solid Nitrogen under Cathode Ray Bombardment. By J. C. McLennan, F.R.S., H. J. C. Ireton, and K. Thomson. (Plates 1–4) 1

The Distortion of Crystals of Aluminium under Compression. Part II.—Distortion by Double Slipping and Changes in Orientation of Crystal Axes during Compression. By G. I. Taylor, F.R.S. (Plate 5) 16

The Distortion of Crystals of Aluminium under Compression. Part III.—Measurements of Stress. By G. I. Taylor, F.R.S. 39

The Magnetic Susceptibility of some Binary Alloys. By J. F. Spencer and Miss M. E. John. Communicated by W. Wilson, F.R.S. 61

On Fresnel's Convection Coefficient in General Relativity. By N. R. Sen. Communicated by A. S. Eddington, F.R.S. 73

On the Emission of Light from Hydrogen Atoms. By R. d'E. Atkinson. Communicated by F. A. Lindemann, F.R.S. 81

On the Flexure of Thin Cylindrical Shells and other "Thin" Sections. By L. G. Brazier. Communicated by R. V. Southwell, F.R.S. 104

The Energy of the Struck String—Part II. By W. H. George and H. E. Beckett. Communicated by Sir William Bragg, F.R.S. 115

The Absorption Spectra of Aragonite and Strontianite in the near Infra-Red. By F. I. G. Rawlins and E. K. Rideal. Communicated by H. Hutchinson, F.R.S. 140

On the Measurement of Light Absorption By H. von Halban and J. Eisenbrand. Communicated by E. C. C. Baly, F.R.S. 153

The Influence of Hydrogen on Two Homogeneous Reactions. By C. N. Hinshelwood and P. J. Askey. Communicated by H. Hartley, F.R.S. 163

On the Flow of Air behind an Inclined Flat Plate of Infinite Span. By A. Fage and F. C. Johansen. (Plates 6–8). Communicated by H. Lamb, F.R.S. 170

The Photosynthesis of Naturally Occurring Compounds. I.—The Action of Ultra-Violet Light on Carbonic Acid. By E. C. C. Baly, F.R.S., J. B. Davies, M. R. Johnson and H. Shanassy 197

PAGE

The Photosynthesis of Naturally Occurring Compounds. II.—The Photosynthesis of Carbohydrates from Carbonic Acid by Means of Visible Light. By E. C. C. Baly, F.R.S., W. E. Stephen and N. R. Hood 212

The Photosynthesis of Naturally Occurring Compounds. III.—Photosynthesis *in vivo* and *in vitro*. By E. C. C. Baly, F.R.S., and J. B. Davies 219

The Electron as a Vector Wave. By C. G. Darwin, F.R.S. 227

No. 774—October 1, 1927.

The Diffraction of Light by Metallic Screens. By C. V. Raman, F.R.S., and K. S. Krishnan 254

Measurement of the Biologically Active Ultra-Violet Rays of Sunlight. By L. Hill, F.R.S. (Plate 9) 268

Intensities in the Secondary Spectrum of Hydrogen at Various Temperatures. By J. C. McLennan, F.R.S., H. Grayson-Smith and W. T. Collins 277

Bands in the Secondary Spectrum of Hydrogen—II. By H. S. Allen and I. Sandeman. (Communicated by O. W. Richardson, F.R.S.) 312

The Band Spectra of Silicon Fluoride. By R. C. Johnson and H. G. Jenkins (Plate 10) Communicated by T. R. Merton, F.R.S. 327

The Vibrations of an Infinite System of Vortex Rings. By H. Levy and A. G. Forsdyke. Communicated by S. Chapman, F.R.S. 352

The Electrical Condition of Hot Surfaces during the Adsorption of Gases. Part I.—Gold and Silver Surfaces at Temperatures up to 850° C. By G. I. Finch and J. C. Stimson. Communicated by W. A. Bone, F.R.S. 379

Contact of Flat Surfaces. By F. H. Rolt and H. Barrell. (Plates 11 and 12) Communicated by Sir Joseph Petavel, F.R.S. 401

The Theory of Metallic Corrosion in the Light of Quantitative Measurements. By G. D. Bengough, J. M. Stuart and A. R. Lee. Communicated by H. C. H. Carpenter, F.R.S. 425

The Magnetic Susceptibility of the Alkali Metals. By J. C. McLennan, F.R.S., R. Ruedy and E. Cohen 468

On the Intensity Distribution among the Lines of certain Bands in the Spectrum of the Hydrogen Molecule. By O. W. Richardson, F.R.S. 484

The Internal Conversion of Gamma Rays. By B. Swirles. Communicated by R. H. Fowler, F.R.S. 491

No. 775—November 1, 1927.

Chemical Equilibrium in a Mixture of Paraffins. By H. A. Wilson, F.R.S. 501

Further Experiments on Explosions in Gaseous Mixtures of Acetylene, of Hydrogen and of Pentane. By A. Egerton, F.R.S., and S. F. Gates 516

PAGE

Gaseous Combustion in Electric Discharges. Part II.—The Ignition of Electrolytic Gas by Direct Current Discharges. By G. I. Finch and L. G. Cowen. Communicated by Prof. W. A. Bone, F.R.S. 529

The Coagulation of Smokes and the Theory of Smoluchowski. By G. Nonhebel, J. Colvin, H. S. Patterson and R. Whytlaw-Gray. Communicated by R. Whiddington, F.R.S. 540

Investigations of the Molecular Arrangement of Uniaxial Optically Active Crystals. By W. G. Burgers. Communicated by Sir William Bragg, F.R.S. 553

Sorption of Ammonia by Glass. (Time, Pressure and Temperature Relationships.) By M. Francis and F. P. Burt. Communicated by A. Lapworth, F.R.S. 586

A Gauge-Invariant Tensor Calculus. By M. H. A. Newman. Communicated by A. S. Eddington, F.R.S. 603

The Determination of the Elastic Moduli of the Piezo-Crystal Rochelle Salt by a Statical Method. By W. Mandell. Communicated by O. W. Richardson, F.R.S. 623

Gaseous Combustion at High Pressures. Part VIII.—The Explosion of Methane with up to its own Volume of Oxygen at Initial Pressures up to 150 Atmospheres. By D. T. A. Townend. Communicated by W. A. Bone, F.R.S. 637

The Mobility of the Actinium A Recoil Atom measured by the Cloud Method. By P. I. Dee. Communicated by C. T. R. Wilson, F.R.S. 664

Further Measurements on Wireless Waves received from the Upper Atmosphere. By R. L. Smith-Rose and R. H. Barfield. Communicated by Admiral of the Fleet Sir Henry Jackson, F.R.S. 682

Tensile Tests on Alloy Crystals. Part IV.—A Copper Alloy containing Five Per Cent. Aluminium. By C. F. Elam. Communicated by H. C. H. Carpenter, F.R.S. 694

Series of Emission and Absorption Bands in the Mercury Spectrum. By Lord Rayleigh, F.R.S. 702

On Electric Phenomena in Gravitational Fields. By E. T. Whittaker, F.R.S. 720

Index 737

PROCEEDINGS OF

THE ROYAL SOCIETY.

SECTION A.—MATHEMATICAL AND PHYSICAL SCIENCES.

The Luminescence of Solid Nitrogen under Cathode Ray Bombardment.

By Prof. J. C. McLENNAN, F.R.S., H. J. C. IRETON, M.A., and K. THOMSON, M.A.

(Received June 21, 1927.)

[PLATES 1-4.]

I. *Introduction.*

An interesting development made possible by recent advances in the technique of low-temperature research has been the study of the effect produced when solid nitrogen is bombarded by cathode rays.

The present investigation is the outcome of a previous one by McLennan and Shrum* designed to test a hypothesis put forward by Vegard,† that required the auroral green line to have its origin in the luminescence of solid nitrogen suspended in a state of fine division in the upper atmosphere.

Vegard,‡ in attempting to obtain experimental confirmation of his theory, carried out some experiments in the Cryogenic Laboratory of the University of Leiden, and found that solid nitrogen exhibited a brilliant luminescence when bombarded by cathode rays or by canal rays. The radiation arising from this luminescence gave a very simple spectrum, characterized chiefly by two bands, one in the yellow-green and one in the green, which he called N_1 and N_2 respectively. Two fainter bands, designated by him as N_3 and N_4, were recorded in the red, and, in addition, a number of bands in the blue and ultra-violet region of the spectrum. The fact that the broad yellow-green band N_1

---

* 'Roy. Soc. Proc.,' A, vol. 106, p. 138 (1924).

† 'Phil. Mag.,' vol. 46, p. 193 (1923).

‡ "Commun. Phys. Lab. Univ. Leiden, No. 175," 'Ann. d. Physik,' vol. 79, p. 377 (1926).

covered a portion of the spectrum that included the position of the auroral green line led Vegard to conclude that he had succeeded in obtaining the auroral green line from solid nitrogen, and that consequently his solid nitrogen theory had been confirmed.

McLennan and Shrum,[*] who had carried out an independent investigation of the spectrum of solidified nitrogen rendered luminous by cathode rays, were forced into disagreement with Vegard by the fact that they found the yellow-green band to be broad and diffuse and to consist of three main components, with no portion of any one of the three components coinciding with the wave-length of the auroral green line. Moreover, an investigation carried out by Babcock[†] had shown the auroral green line to be an exceedingly sharp and narrow spectral line without any complex structure. In addition, McLennan and his co-workers[‡] showed that a line occupying exactly the position of the auroral line $\lambda = 5577 \cdot 35$ Å and having the characteristic sharpness of this line could be produced by an electrical discharge in pure oxygen. Lately this has been confirmed by Keys[§] and by Cario.[||]

Although the experiments carried out to test Vegard's theory did not support it, they led to the important discovery of phosphorescence exhibited by a simple element. It was found that the band N_2 with a mean wave-length $\lambda = 5230$ Å, and the band N_4 with a wave-length $\lambda = 5945$ Å were both due to nitrogen rendered phosphorescent by bombardment with high-speed electrons.

In this paper the authors describe further investigations of this phosphorescence, with special reference to the structure of the green phosphorescent band at $\lambda = 5230$ Å and to that of the red phosphorescent band at $\lambda = 5945$ Å. At the same time, the yellow-green luminescent band in the neighbourhood of $\lambda = 5577$ Å was photographed using larger dispersion than heretofore. The bands that appear in the blue and ultra-violet have been photographed with a quartz spectrograph.

II. *Apparatus.*

The apparatus in which the nitrogen was excited to luminescence was of two forms. The first was similar to that used by McLennan and Shrum.[*]

---

[*] *Loc. cit.*

[†] 'Astrophys. J.,' vol. 57, p. 209 (1923).

[‡] 'Roy. Soc. Proc.,' A, vol. 108, p. 501 (1925); *ibid.*, vol. 114, p. 766 (1927).

[§] 'Nature,' vol. 119, p. 162 (1927).

[||] 'Z. f. Physik,' vol. 42, p. 15 (1927).

In this apparatus the solid nitrogen was excited by cathode rays produced in helium at low pressure. Fig. 1 shows the details of the apparatus. The cathode rays were produced in a discharge tube of pyrex glass about 30 inches long and 1 inch in diameter. The lower part of the tube was surrounded by a glass vacuum flask G, which could be kept partly filled with liquid hydrogen. The supply of liquid hydrogen was kept in the large vacuum flask F, and when required was forced into the flask G by pressure from a cylinder of hydrogen gas. The glass vacuum flask was fitted with a German silver cap S held in place by a rubber sleeve R. The discharge tube passed through ebonite plugs placed in the German silver cap. These plugs were waxed in so as to prevent

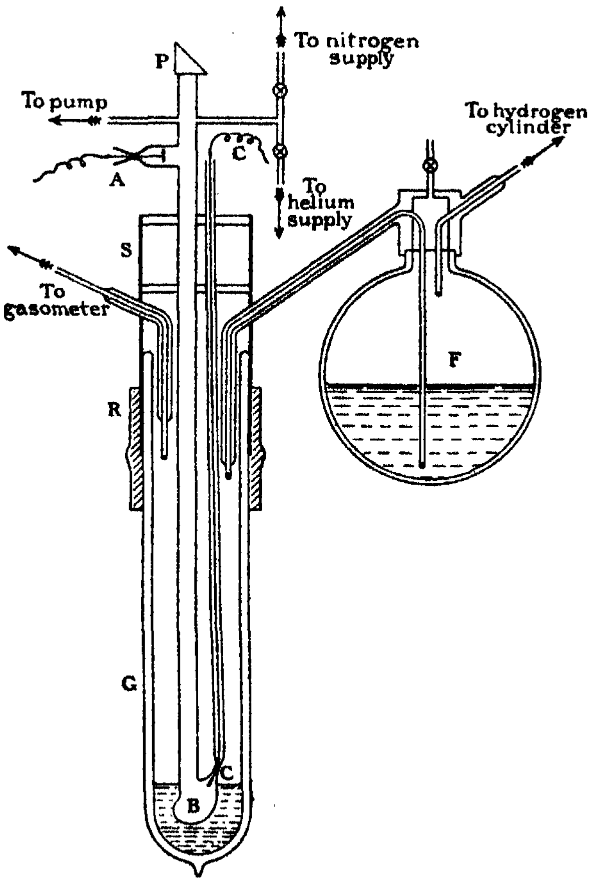

Fig. 1.

A. Anode. C. Cathode. B. Bulb containing solid nitrogen. F. Vacuum flask containing liquid hydrogen. G. Glass vacuum flask. P. Quartz prism. R. Rubber sleeve S. German silver cap over glass flask.

the escape of the evaporating hydrogen. Tubes led from the upper part of the discharge tube to a vacuum pump, the nitrogen supply and the helium supply. Pure nitrogen was prepared by heating together concentrated solutions of ammonium chloride and sodium nitrite. The nitrogen, after passing through phosphorus pentoxide and a liquid air trap, was admitted to the discharge tube. It deposited on the walls of the small bulb B at the lower end of the tube. The cathode C was placed in a side tube in such a position that when the discharge was produced a stream of cathode rays was directed against the solid nitrogen. The discharge was produced by an induction coil that gave a potential corresponding to a spark 2 inches long between points in air. The visible spectrum of the glowing nitrogen was photographed by allowing the light that issued from the bulb and that passed through the liquid hydrogen and the walls of the vacuum flask, to fall on the slit of a Hilger constant-deviation glass spectrograph. This spectrograph* was provided with an extra direct-vision prism to give greater dispersion.

The ultra-violet spectrum was obtained by directing the slit of a small Hilger quartz spectrograph towards the light issuing through a quartz prism P that was placed on the top of the discharge tube.

With the apparatus described above only the phosphorescent spectrum was photographed. The radiation from the luminescence that was produced when the solid nitrogen was being bombarded was prevented from falling on the slit of the spectrograph. This was accomplished by means of a device which brought a shutter in front of the spectrograph slit whenever the induction coil was operating. This device consisted of a wheel with a projecting sector at one side which passed in front of the slit of the spectrograph at the same time that a smaller sector on the other side of the wheel made contact and allowed the induction coil to function. The wheel was driven by a motor and worm gear.

In the second form of apparatus use was made of a special cathode ray tube recently designed by Dr. Coolidge,† of the General Electric Company. With this tube it is possible to produce high-voltage cathode rays outside the generating tube. Fig. 2 shows the details of such a tube. The source of cathode rays was a hot spiral of tungsten wire placed in a hemispherical focussing cup D similar to that used in a Coolidge X-ray tube. The anode proper N was at the same time the window of the tube, and consisted of a sheet of nickel foil 0·0005 inch thick. It was about 1 inch in diameter, and was supported against the pressure of the atmosphere by a brass honeycomb structure S soldered into a circular brass plate. The nickel window was soldered around its outer edge to this brass plate. The long copper tube F joined to the window support served as an electrostatic shield to protect the glass of the anode arm from puncturing. To prevent the fusing of the nickel window owing to the intense heat developed by bombardment a water jacket W was placed around the window support. The metallic part of the anode of the cathode ray tube was joined to the glass part by means of sealing wax.

---

* Young, 'J. Opt. Soc. Amer.,' 1923, p. 405.

† 'J. Franklin Inst.,' vol. 202, p. 693.

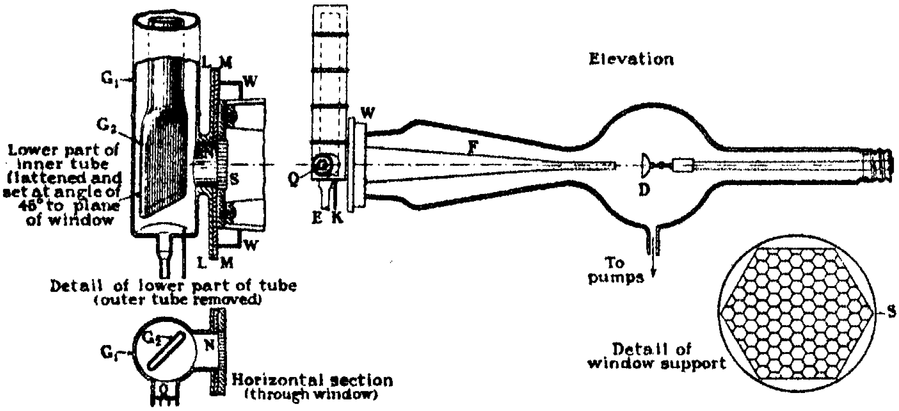
G₁
G₂
L
M
W
Lower part of inner tube flattened and set at angle of 45° to plane of window
S
W
L
M
Detail of lower part of tube (outer tube removed)
G₁
G₂
N
Horizontal section (through window)
Q
E
K
W
F
Elevation
D
To pumps
Detail of window support
S

Fig 2.

The container for the solid nitrogen took the form of a specially designed Dewar flask made of German silver the important details of which are shown in fig. 2. The outer shell G_1 had an opening in one side slightly larger in size than the nickel window of the cathode ray tube. This opening was provided with a wide flange L, which could be soldered around its outer edge to a similar flange M that extended beyond the water jacket. Thus the flask could be readily removed in case it became necessary to replace a nickel window. Another side opening in the tube G_1 carried a short tube into which a fluorite window Q was waxed. Through this window visual or spectral observations of the luminescent nitrogen could be made. The inner tube G_2 of the flask was flattened and set at an angle of 45 degrees to the plane of the nickel window. The cathode rays that passed through the window struck this flat surface. In carrying out an experiment the inner tube of the flask was kept filled above the flat surface with liquid hydrogen. The method previously described and mentioned above was used to force the liquid hydrogen into the flask. The space between the two walls of the vacuum flask was thoroughly evacuated by a mercury diffusion pump backed by a Cenco Hyvac oil pump. When pure nitrogen was admitted to this evacuated space it deposited in solid form on the flattened surface of the inner tube of the flask.

The cathode ray tube was continuously exhausted during the operation by means of a mercury condensation pump and an auxiliary oil pump. A liquid air trap was inserted between the condensation pump and the cathode ray tube. The high voltage under which the cathode ray tube was operated was supplied by a Victor Snook special transformer capable of giving voltages up to 200,000 and currents as high as 30 milliamperes.

III. *Results.*

In the experiments when the first form of apparatus was used an intense phosphorescence of the solid nitrogen was observable. Fine print could be read at a distance of 6 inches from the glowing bulb. Observations made with a small direct-vision hand spectroscope indicated that the phosphorescent spectrum consisted of a single intense green band near $\lambda = 5230$ Å. While the discharge was passing a broad yellow-green band* also appeared near $\lambda = 5577$ Å. The luminescent and phosphorescent bands appeared to come only from the form of solid nitrogen that existed below a certain temperature. When the hydrogen was allowed to evaporate the nitrogen warmed up slowly, and at a certain temperature a marked change in the appearance of the solid nitrogen occurred. Below this critical temperature it had an appearance like that of ice, but when the critical temperature was reached it suddenly changed to a powdery white form that fell off the upper parts of the bulb. This powdery form exhibited none of the luminescent effects which the ice-like form showed. The temperature at which this transformation takes place has been found by other observers† to be 35·5° K. A number of photographs of the phosphorescence spectrum was obtained with the glass spectrograph described above. Measurements of these spectrograms of the phosphorescent band showed that it was composed of five distinct components having wave-lengths as follows :—

(1)	(2)	(3)	(4)	(5)
5215 Å	5224 Å	5229 Å	5235 Å	5240 Å

These wave-lengths are given to the nearest Ångström unit and are the means of the values obtained from the measurements made on four spectrograms. No record of the red phosphorescent band N_4 was obtained upon any of the plates. Two plates taken with the quartz spectrograph exposed to the phosphorescent light showed no trace of any line or band except the green band N_2 with exposures of as long as 12 hours' duration.

---

* This band we have designated in what follows by the word "luminescent."

† W. H. Keesom and H. K. Onnes. 'Leiden Comm. No. 149A.'

In the experiments where the Coolidge cathode ray tube was used a much more intense luminescence and phosphorescence was obtained. Observations with a hand spectroscope showed that the spectrum of the radiation emitted by the solid nitrogen consisted of the intense green band N_2, the yellow green band N_1 and the fainter red band N_4. These three were observable when the cathode ray tube was in operation, but as soon as the excitation ceased the complex band N_1 disappeared and the bands N_2 and N_4 remained.

This showed that the band N_4 just as the band N_2 originated in the phosphorescence of solid nitrogen. Spectrograms obtained with the glass spectrograph with exposures of 20 hours' duration with a current of one milli-ampere through the cathode ray tube operating at 125 k.v. showed the three bands N_1, N_2 and N_4. Fig. 3 (Plate 1) is a typical spectrogram enlarged twice. It shows the three bands with the iron arc spectrum on each side for comparison. Measurements showed that the band N_2 consisted of eight definite components of a diffuse nature shading towards the red end of the spectrum. The following values were obtained for the wave-lengths of the components :—

(1)	(2)	(3)	(4)	(5)	(6)	(7)	(8)
5204·4Å	5210·4Å	5214·3Å	5220·1Å	5224·4Å	5228·8Å	5235·0Å	5240·0Å

These measurements are probably correct to within one Ångström unit since they were the mean of measurements made on a number of plates none of which varied from the mean by more than one Ångström. More accurate measurements could not be made on account of the diffuse nature of the bands.

Fig. 4 (Plate 1) is an enlargement of the phosphorescent band N_2. It shows very definitely the eight components constituting the band.

As the cathode ray tube was operated continuously the band N_1 was recorded on the plates as well as the phosphorescent bands. It was seen, however, from visual observation that the intensity of the band N_1 fell off quite rapidly as the tube was operated. In order to bring it out intensely on the photographic plates it was necessary to admit fresh nitrogen about every half hour. It was observed that after the tube had been operating for an hour or more the intensity of the light from the band N_1 was so lessened that it was scarcely visible in a direct vision spectroscope. The phosphorescent bands N_2 and N_4, however, showed no perceptible change in intensity during the operation of the tube over a period of two hours' duration. The band N_1 was recorded as a wide band with three broad diffuse components that had the following wave-lengths:

(1)	(2)	(3)
5554 Å	5617 Å	5658 Å

On account of the diffuse nature of these bands no great accuracy can be claimed for the above measurements. The agreement, however, with values obtained by other workers is quite good, as will be seen from the following table of values given by McLennan and Shrum* and by Vegard.* These values are as follows :—

	(1)	(2)	(3)
McLennan and Shrum ..	5556 Å	5617 Å	5654 Å
Vegard	5555 Å	5616·2 Å	5658·7 Å

Fig. 5 (Plate 2) is an enlargement of this band.

It was not clear from our first plates whether the red phosphorescence originated in a band with a structure or in a simple spectral line. Though its appearance, as in fig. 3 (Plate 1), was that of a faint but quite sharp line, it seemed to us reasonable, by analogy with the green phosphorescence, to suppose that it should be a band. It should be noted here that the green phosphorescence as originally observed and photographed by McLennan and Shrum* was recorded as a line at λ 5230 Å, but this was no doubt due to the fact that they had very much less intensity, and because shorter exposures were used than in our experiments. It seemed to us that if the intensity of the red phosphorescent radiation near $\lambda = 5945$ Å could be sufficiently increased, it also would be recorded as a band. In order to determine if this was the case, the cathode ray tube was operated with voltages as high as 150 k.v. With an exposure of 18 hours at this voltage the band N_4 originally observed was recorded with great intensity, and, in addition, two faint but definite components appeared near the sharp one, and on the shorter wave-length side of it. Measurements made upon these gave the following wave-lengths :—

(1)	(2)	(3)
5944·7 Å	5938·8 Å	5932·0 Å

Fig. 6 (Plate 2) shows an enlargement of the composite band with the iron arc spectrum for comparison.

In the experiments where the cathode ray tube was used several spectrograms were taken with a small quartz Hilger type E31 spectrograph. These plates showed, in addition, to the bands N_1, N_2 and N_4, a series of bands extending well down into the ultra-violet as well as a continuous spectrum extending, from about 3300 Å to 2500 Å. These bands, as will be seen from fig. 7 (Plate 3), were much fainter than the bands N_1, N_2 and N_4. Those in the visible region were never sufficiently intense to be visibly observable with a small hand spectrograph. It cannot, therefore, be stated definitely whether they were of a phosphorescent nature or otherwise. The wave-lengths of the heads of these bands obtained from carefully-made measurements were as follows :—

---

* *Loc. cit.*

$\lambda = 4573$ Å	$\lambda = 3706$ Å	$\lambda = 3381$ Å	$\lambda = 2623$ Å
4490 Å	3640 Å	3161 Å	2480 Å
4203 Å	3569 Å	2962 Å	
3954 Å	3471 Å	2783 Å	

It was at first thought that these bands might be related to the well-known second positive band system of gaseous nitrogen, but fig. 7 (Plate 3) shows that there is a marked lack of agreement. The bands obtained by the bombardment of solid nitrogen shaded off towards the red end of the spectrum, whereas the second positive bands of gaseous nitrogen shade off towards the violet.

The red band N_3 observed by Vegard* was not recorded on any of our spectrograms. According to him, this band occurs within the limits 6300 Å and 6600 Å. If it existed as the result of the excitation of solid nitrogen it should have appeared on our plates for these were extremely sensitive up to 7000 Å.

IV. *Discussion of Results.*

(*a*) *Different Forms of Solid Nitrogen.*—The phosphorescence of solid nitrogen is evidently a molecular rather than an atomic phenomenon. This is indicated by the fact that the spectrum consists of bands and not of lines. The fact that McLennan and Shrum, as well as Vegard, found that solid ammonia did not exhibit similar effects, also points in this direction. The gradual fading of the luminescent band N_1, observed while the intensities of the phosphorescent bands N_2 and N_4 remained constant, may be explained by the assumption of the existence of two slightly different forms of solid nitrogen that we might call A and B. If the radiation included in the band system N_1 be emitted by form A, it would appear that form A is transformed to form B, either by the action of the electrical bombardment, or through a natural change with time. Since the intensity of the phosphorescence does not change appreciably with long-continued bombardment, either it must be emitted from both forms or form B must be formed with extreme rapidity, and so be present in considerable amount immediately after the beginning of the bombardment. It might be noted that this fading of the N_1 radiation does not agree well with Vegard's theory of solid nitrogen in the upper atmosphere, since it shows that a necessary condition for the continued brightness of the luminescent band N_1 is a continuous supply of fresh nitrogen. At the low temperatures necessary for the luminescent effects there could be little evaporation and recrystallization, so that the freshly solidified nitrogen could not be continually produced by such a process.

---

* 'Ann. d. Physik,' vol. 79, p. 377 (1926).

(*b*) *Origin of the Band* N_3.—The reason for the non-appearance on our plates of the red band N_3, which Vegard believed to possess the same character as the luminescent band N_1, is not clear to us. Vegard in most of his work used a current of nitrogen gas streaming through his tube, so that it is possible that this band as observed by him belonged to one or other of the ordinary band systems of gaseous nitrogen. He states in one case that the path of the rays through the tube was visible, and from this it is evident that the light of some of the bands of gaseous nitrogen must have been present. This explanation might also apply to the fact that Vegard obtained a large number of the secondary bands, and with greater intensity than our plates showed. Although the path of the cathode rays was not visible in our work, it seems quite possible that the faint bands which appeared originated in nitrogen gas that must always have existed over the solid nitrogen, especially while the bombardment progressed. Although the pressure of this gas was so low that it would not carry the discharge in the discharge tube used in the first form of apparatus, its presence was shown when an attempt was made to run the cathode ray tube with an imperfect window between it and the solid nitrogen. Although the pumps were kept running on the chambers on each side of the window, a sufficiently high vacuum could not be maintained to allow the tube to be operated. With the long exposures used, the passage of the cathode rays through the gas, even with the very low pressure, might have produced a feeble radiation that was invisible but nevertheless sufficient to make an impression on the plate.

(*c*) *Violet and Ultra-Violet Bands.*—The reason for the change in form of the blue and ultra-violet bands, so that they shaded off towards the red end of the spectrum, is not as yet known to us. It seems possible, however, that the very low temperature of the gas in which they were supposedly produced, might change the distribution of energy in the molecule in some way, and thus affect the form of the bands. If, on the other hand, they originated in radiation actually emitted from nitrogen in the solid form, one would expect a radical change since the molecules would be more restricted in their motions in the solid form.

(*d*) ***The Phosphorescent Band N_2.***—In a recent note Vegard[*] pointed out that with long exposures to the light of auroræ he was able to obtain with fair intensity a band in the auroral spectrum with a wave-length very close to that of the phosphorescent band N_2 of solid nitrogen. In this note he took the view that the two bands were identical, and advanced this supposed coincidence as a proof of his theory that solid nitrogen exists in the upper atmosphere. However, it will be recalled as Lord Rayleigh[†] has already stated, there is a well-known band obtainable in the spectrum of gaseous nitrogen at ordinary temperatures which comes very close to the phosphorescent bands λλ 5240–5204 Å. This band, λ 5227 Å, as Table I shows, is the fourth member of the first negative band system of gaseous nitrogen. The first three members of this system, λ 3914 Å, λ 4278 Å, λ 4708 Å, are nearly always recorded on spectrograms of the auroral light, and it is chiefly due to this fact that the conclusion has been reached that nitrogen exists, and is present in the molecular form in the upper atmosphere in the region where the auroral light originates. Since the three bands mentioned appear on auroral spectrograms one would naturally expect some indication at least of the fourth band λ 5227 Å to appear as well. As the table shows, the emission of this band involves the vibration transition ($n' = 3$ to $n = 0$) which is quite sufficient to account for the intensity of the band being less than that of any of the other three bands since they involve transitions from the lower

Table I.—The First Negative Band System of Nitrogen.

$n \backslash n'$	0	1	2	3	4	5	6	7
0	3914	4278	4708	5227				
1	3581	3884	4237	4651	5150			
2		3563	3857	4199	4599	5075		
3		3298	3548		4167	4554	5018	
4			3296				4515	4961
5								4485

---

[*] 'Nature,' vol. 119, p. 349 (1927).

[†] 'Nature,' vol. 119, p. 525 (1927).

energy states $n'=0, 1, 2$, to that of $n=0$. Fig. 8 (Plate 3) shows a reproduction of the spectrogram taken by Vegard with an exposure to the auroral light of 70 hours. Above it is a spectrogram taken by us of the negative band system of gaseous nitrogen with a spectrograph that had approximately the same dispersion as Vegard's instrument. It will be seen that our bands λ 3914 Å, λ 4278 Å, and λ 4708 Å, register closely with the same bands on Vegard's plate, and that our negative band λ 5227 that originated in gaseous nitrogen also registers closely with the band obtained by Vegard with auroral light and assigned by him for origin to solid nitrogen.

In fig. 9 (Plate 4) there is reproduced a spectrogram of the radiation emitted by solid nitrogen under electronic bombardment and one of the light emitted by gaseous nitrogen in an ordinary Plücker tube excited with a single induction coil. Both spectrograms were taken by us with the same instrument. The one shows the phosphorescent band N_2 and the other the fourth member λ 5227 Å of the first negative band system of gaseous nitrogen. These bands, though they are close to each other, are as the photograph shows by no means identical. The problem that is before us, therefore, is to select the one with which the band obtained by Vegard in his photograph of the auroral spectrum can be identified. Had Prof. Vegard taken a photograph of the first negative band system in the spectrum of gaseous nitrogen with the instrument with which he photographed the auroral band near λ 5227, some information might possibly have been gained that could have helped towards a more or less decisive solution of the problem. It would be better, however, if the spectrum of the aurora as well as that of gaseous nitrogen and that of solid nitrogen—the latter rendered luminescent by irradiation with high-speed cathode rays—were photographed with an instrument having something like the dispersion of the one with which we obtained the spectra shown in fig. 8 (Plate 3). Spectra obtained with such an instrument would enable one to solve definitely and finally the problem presented.

It is of some importance that such spectrograms should be obtained, for the issue raised is clear and definite. If the band found by Prof. Vegard in the spectrum of the aurora is identical in wave-length with and similar in structure to the band N_2 in the spectrum of solid nitrogen, then we must conclude that nitrogen can exist in the upper atmosphere in a solid state, possibly in a finely divided state.

If, however, the auroral band in question should turn out to be identical with the fourth band λ 5227 Å, the negative band system in the spectrum of gaseous nitrogen, then it would appear impossible to reach any other conclusion regarding Prof. Vegard's solid nitrogen theory of the origin of part of the auroral spectrum than that it is invalid. It is generally agreed that the existence of the composite luminescent band with members at λ 5554 Å, λ 5617 Å, and λ 5658 Å, in the spectrum of the light from irradiated solid nitrogen cannot account for the existence of the narrow sharply defined green line λ 5577·35 Å in the spectrum of the aurora. The widths of the constituent bands referred to, together with their diffuseness as shown in fig. 5 (Plate 2), make it clear that it is quite impossible to obtain with them interference fringes of the character of those obtained by Dr. Babcock with auroral light by the use of a Fabry and Perot interferometer. The accumulated experimental evidence goes to show that in seeking for the origin of the famous green auroral line we must turn to oxygen.

V. *Moments of Inertia.*

Some information can be gained as to the nature of the modification of nitrogen that gives rise to the phosphorescent bands N_2 and N_4, by considering the structure of these bands. The band N_2, which includes, as fig. 4 (Plate 1) shows, eight components at least, is shaded off towards the violet side and also towards the red side. The strongest component is $\lambda = 5214$ Å. Two components have wave-lengths shorter than this one, namely, λ 5210 Å and λ 5204 Å, and the remaining members, λ 5220 Å, λ 5224 Å, λ 5229 Å, λ 5235Å and λ 5240 Å, are on the longer wave-length side of it. The components are almost equally spaced with a wave-length difference of about 5 Å.U., or a frequency difference of about 18·34 cm.$^{-1}$. The structure of the band can be represented approximately by a formula of the type $\nu = \nu_0 + B\,(\pm 2m + 1)$ with the zero component $\nu = \nu_0 + B$ corresponding to $\lambda = 5214$ Å, and with the line of origin of frequencies ν_0 having a wave-length close to λ 5217·5. The different components can be identified by the number m that represents the quantisation of the molecular rotational energy. If we assume integral values for m the separation of the components will be equal to 2B, and we have, therefore, $2B = 18 \cdot 34 \times C$. With 2B given by $2B = \frac{h}{4\pi^2 I_0}$, where I_0 is the moment of inertia of the radiating molecule in its final state we have

$$\frac{h}{4\pi^2 I_0} = 18 \cdot 34 \times C$$

or

$$I_0 = \frac{h}{4\pi^2 \times 18 \cdot 34 \times C}$$

$$= 3 \times 10^{-40}.$$

In the band N_4 the strongest component is λ 5944·7 Å. Like N_2 it has two components λ 5938·8 Å and λ 5932·0 Å on the short wave side of its strong component. In this case the wave separations are 6·8 Å and 5·9 Å, and the frequency separations 19·3 cm.$^{-1}$ and 16·7 cm.$^{-1}$. These lead to the values $2 \cdot 83 \times 10^{-40}$ and $3 \cdot 27 \times 10^{-40}$ for the final moment of inertia involved. From a study of both of the phosphorescent bands it would appear then that the molecule concerned in the emission of the phosphorescent light has a moment of inertia equal, approximately, to 3×10^{-40}. This it will be noted is considerably less than $16 \cdot 98 \times 10^{-40}$ and $15 \cdot 24 \times 10^{-40}$, the moments of inertia of the nitrogen molecule in its initial and final states when emitting the radiation giving rise to the second positive band system.* The approximate equality in the values of the moments of inertia deduced from the structure of the two bands may be given the interpretation that the radiation producing them originates in the transition of the molecule involved from two different energy states to one common one. On this view the difference in level of the two energy states would be represented by about 2300 cm.$^{-1}$, which is approximately the difference in the frequencies of the two bands, each considered as a single spectral entity.

At present it is not clear to us that our results can give us any more definite information regarding the molecular states of the solid nitrogen involved in the process of phosphorescence, but it is hoped that we may, by extending the investigation in other directions, make further progress shortly.

VI. *Summary.*

(1) The phosphorescent spectrum of the light from solidified nitrogen, after irradiation by high speed electrons from a Coolidge tube with a nickel window, has been shown to consist of two spectral bands designated as N_2 and N_4.

(2) The band N_2 was found to have the components 5240, 5235, 5229, 5224, 5220, 5214, 5210, and 5204 Å.U., with 5214 Å.U. having the strongest intensity.

(3) The band N_4 was shown to be composite and to have the components 5944·47, 5938·8 and 5932·0 Å.U., the strongest being 5944·47 Å.U.

(4) The spectrum of the light emitted by solid nitrogen when under electronic bombardment included in addition to the bands N_2 and N_4 three diffuse bands, N_1, that shaded into each other and had the mean wave-lengths, 5554 Å, 5617 Å and 5658 Å. This spectrum also included a number of faint diffuse bands, each shaded off towards the red in the blue and violet spectral region between λ 4573 Å and λ 2480 Å.

---

* "Molecular Spectra in Gases," 'Bulletin of the Nat. Res. Council,' vol. 11, Part 3, No. 57, Dec., 1926, p. 232.

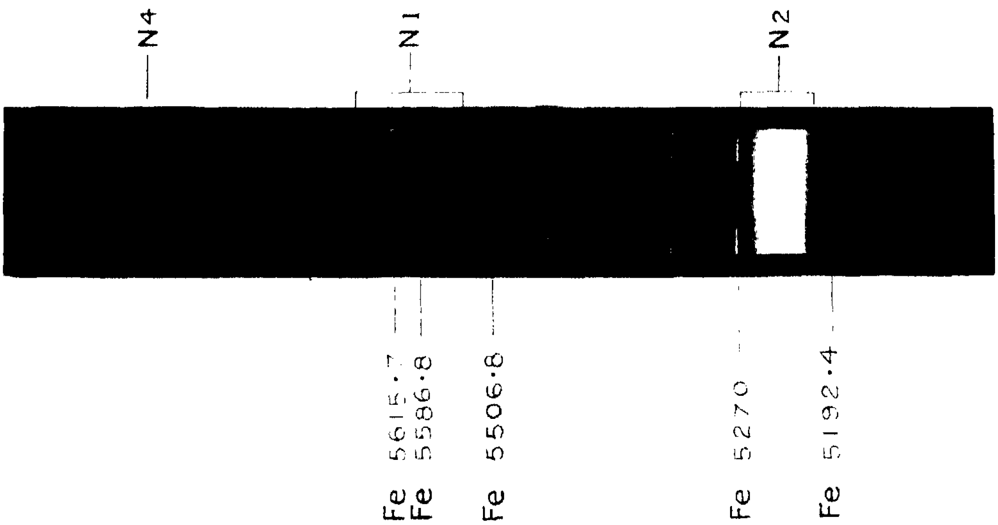
N4
N1
N2
Fe 5615·7
Fe 5586·8
Fe 5506·8
Fe 5270
Fe 5192·4

Fig. 3.

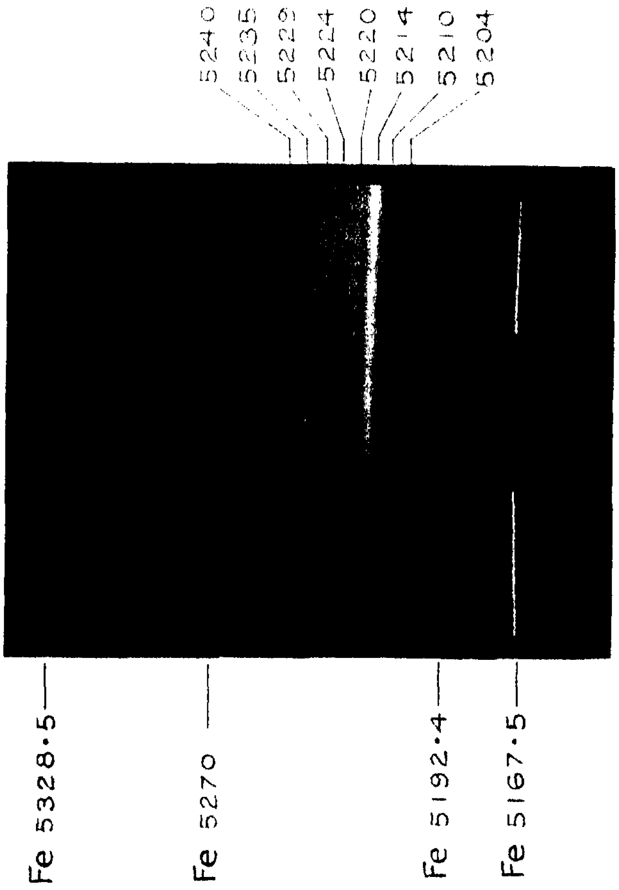
5240
5235
5229
5224
5220
5214
5210
5204
Fe 5328·5
Fe 5270
Fe 5192·4
Fe 5167·5

Fig. 4.

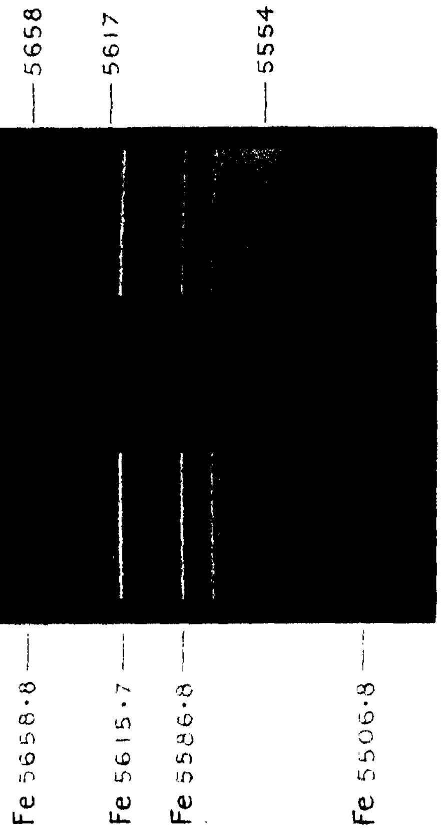
5658
5617
5554
Fe 5658·8
Fe 5615·7
Fe 5586·8
Fe 5506·8

FIG. 5.

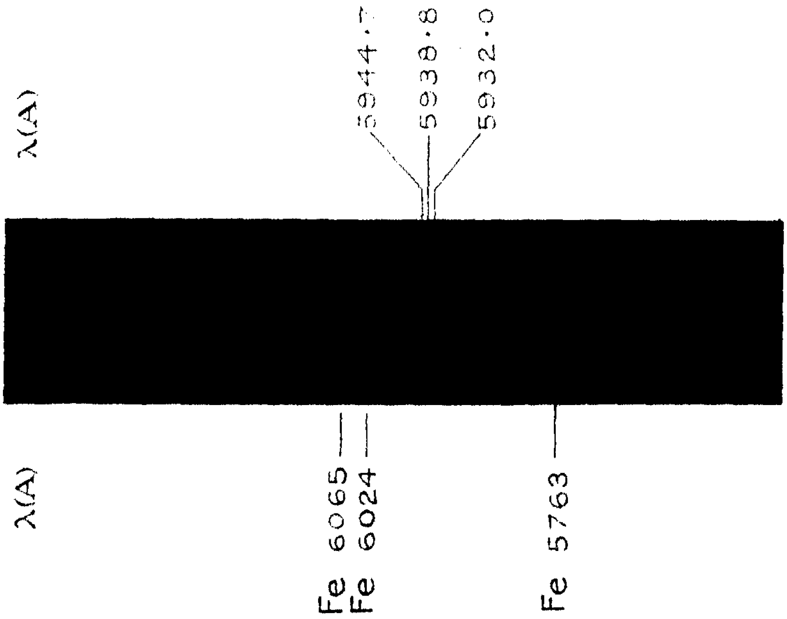
λ(A)
5944·7
5938·8
5932·0
λ(A)
Fe 6065
Fe 6024
Fe 5763

FIG. 6.

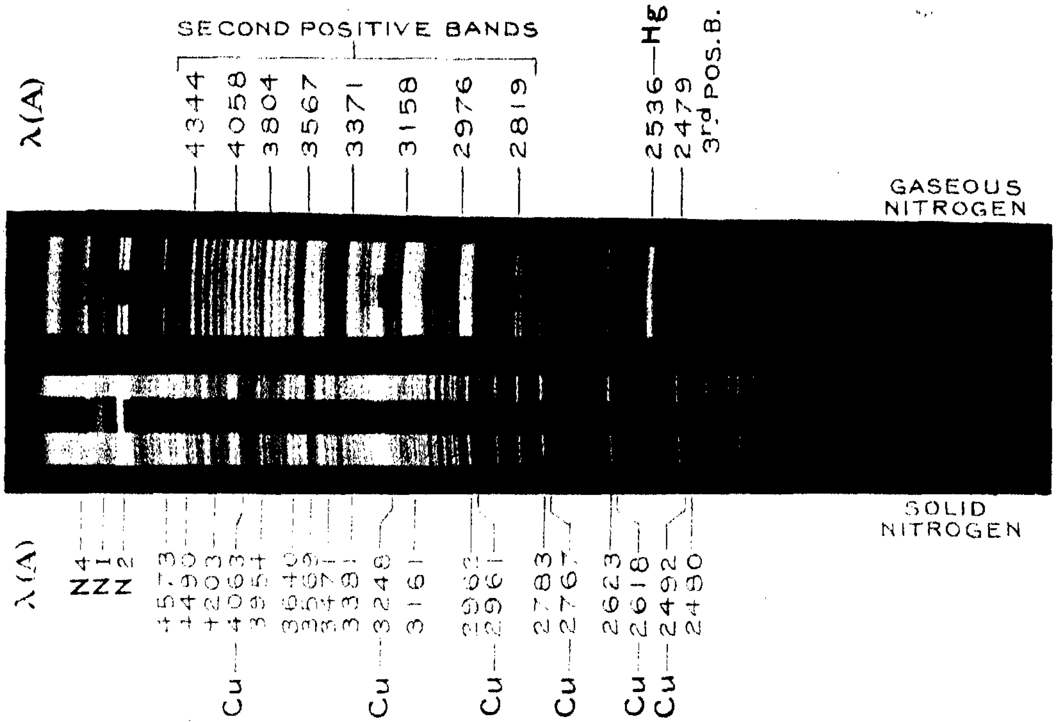
SECOND POSITIVE BANDS
λ(A)
4344
4058
3804
3567
3371
3158
2976
2819
2536—Hg
2479
3rd POS.B.
GASEOUS NITROGEN
SOLID NITROGEN
λ(A)
N4
N1
N2
4573
4490
4203
4063
3954
3646
3505
3471
3381
3248
3161
2962
2961
2783
2767
2623
2618
2492
2490
Cu
Cu
Cu
Cu
Cu
Cu

Fig. 7.

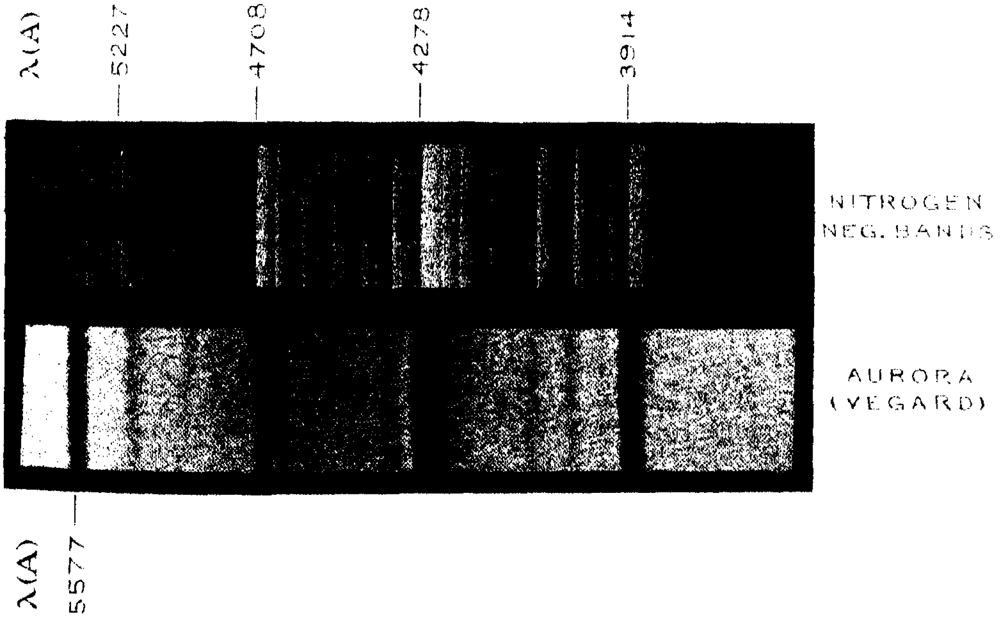
λ(A)
5227
4708
4278
3914
NITROGEN NEG. BANDS
AURORA (VEGARD)
λ(A)
5577

Fig. 8.

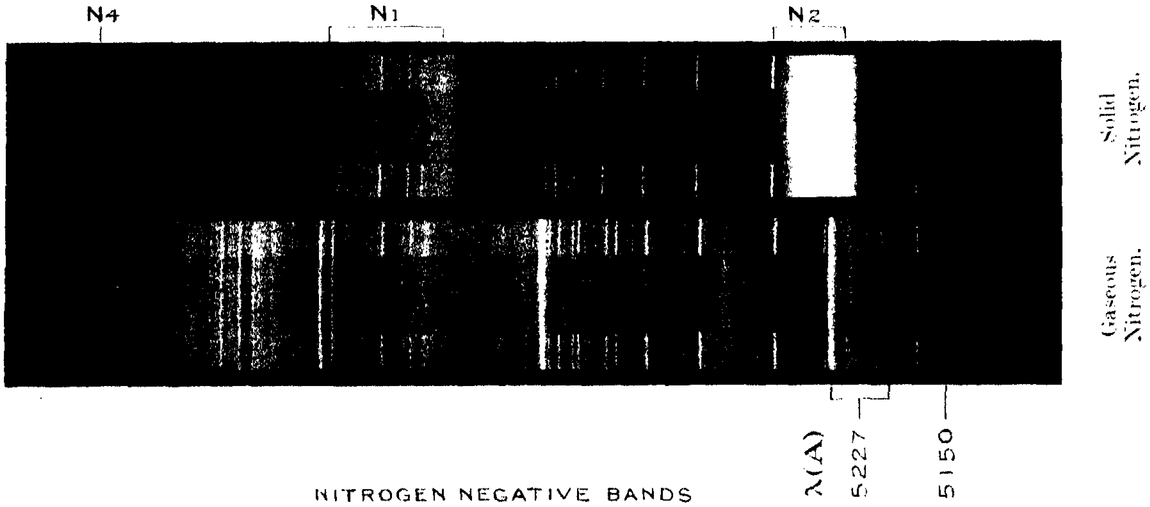
N4
N1
N2
Solid Nitrogen.
Gaseous Nitrogen.
λ(A)
5227
5150
NITROGEN NEGATIVE BANDS

Fig. 9.

(5) We failed to record on plates, that were highly sensitive to red light, even with twenty hours' exposure, any trace of a group of wave-lengths designated by Vegard as N_3, that was found by him to include one band at λ 6569 Å and one with its maximum intensity between λ 6320 Å and λ 6420 Å.

(6) The bands of group N_1 were found to be relatively strong when the solid nitrogen under irradiation was freshly deposited but with prolonged irradiation the intensities of these bands rapidly weakened. The intensities of the band groups N_2 and N_4 appeared to be unaffected by prolonged bombardment.

(7) Our experiments support the view that solid nitrogen that is initially deposited in a form A is soon transmitted under electronic irradiation or otherwise into a form B, the form B being the one that exhibited the phosphorescence investigated by us.

(8) From a study of the structures of the bands N_2 and N_4 it has been shown that the moment of inertia of the molecular system involved in the phosphorescence of solid nitrogen is approximately 3×10^{-40} m.^{1} cm.^{2}.

(9) The view has been expressed that it is not possible with the experimental evidence before us at the present time to decide whether the band recently obtained by Professor Vegard in the spectrum of the aurora near λ 5230 Å.U. is identifiable with the band N_2 in the spectrum of solid phosphorescent nitrogen, or with the band λ 5228 Å.U., the fourth member in the first negative band system of gaseous nitrogen.

One of us, Mr. K. Thomson is indebted to the National Research Council of Canada for the award to him of a Studentship that enabled him to participate in this research.

We also wish to take this opportunity of acknowledging the valuable help given to us by the physical laboratory glass-blower, Mr. R. H. Chappel, and by Mr. Plaskett and various other members of the mechanical staff in connection with the construction of the special equipment required in the investigation. Prof. McLennan desires to express his appreciation of the financial aid given by the National Research Council of Canada and by the Carnegie Corporation for the purchase of apparatus for this investigation.

The Distortion of Crystals of Aluminium under Compression. Part II.—*Distortion by Double Slipping and Changes in Orientation of Crystal Axes during Compression.*

By G. I. Taylor, F.R.S.

(Received June 10, 1927.)

[Plate 5.]

Changes in the orientation of crystal axes during compression of a disc cut from a single crystal of aluminium are discussed. They are in accordance with the prediction made on assumption that the crystal slips as determined by distortion measurements. As in case of tensile test pieces, crystal axes always take a position where two possible planes of slip are symmetrically disposed in relation to the stress, but in this case, the orientation of crystal axes relative to normal to flat surfaces of specimen is quite different from their orientation relative to axis of tensile test piece.

After the axes have taken the symmetrical position, Laue photographs show that they remain there, even when distortion is very great. Tests were continued till thickness of specimen was only 0·28 its original thickness. Distortion during period when crystal axes remain in symmetrical position is due to slipping on two symmetrically disposed planes of slip.

The bearing of the results on structure of rolled metals is discussed and distortions of cubical blocks of material, due to various types of double slipping, are compared, to find out which is most likely to occur.

It has been shown in Part I* of this paper that the distortion of an aluminium crystal during compression between parallel plates is identical in kind with the distortion of a tensile testpiece cut from a single crystal. It has been shown also that the method previously devised for predicting the slip plane and direction of slip in a tensile test from a knowledge of the orientation of the crystal axes applies also in the case of compression, provided that the normal to the two parallel steel plates in the one case is identified with the axis of the tensile test piece in the other. The direction of slip in one case is, of course, exactly opposite to that in the other. One might be inclined to suppose, therefore, that the motion of the normal to the flat surface of the specimen relative to the crystal axes during compression would be exactly opposite to that of the motion of the axis of the tensile test piece during extension, but this is not the case. The normal to the disc must move, relative to the crystal axes, in a great circle towards the pole of the slip plane, because the trace of the slip plane on the surface of the specimen remains fixed relative to the crystal axes. The normal to the specimen is necessarily perpendicular to this trace; it can, therefore, only move on a great circle relative to the crystal axes, and this great circle passes through the pole of the slip plane because that also is perpendicular to the trace.

---

* Taylor and Farren, 'Roy. Soc. Proc.,' A, vol. 111, p. 529 (1926).

To verify this, discs cut from specimen No. 59 were used. The orientations of the crystal axes were determined by reflection of X-rays at four stages of the compression, namely, at $\varepsilon = 1 \cdot 0$ (*i.e.*, material uncompressed), $\varepsilon = 0 \cdot 9134$, $\varepsilon = 0 \cdot 817$ and $\varepsilon = 0 \cdot 684$.* In each case the orientation was determined by finding reflections of homogeneous X-rays from two different planes, usually two of type {111}.† The co-ordinates of the three cubic axes (100),† (010) and (001), relative to the system described in Part I, vol. 111, p. 534, were then calculated. The results are given in columns 2 to 7 of Table I.

Table I.—Co-ordinates of cubic axes of discs cut from crystal No. 59 at various stages of compression. Co-ordinates measured in degrees.

ε.	(010).		(001).		(100).	
	θ.	ϕ.	θ.	ϕ.	θ.	ϕ.
	°	°	°	°	°	°
1·00	36	180	64	47	67	305
0·9134	36	197	57	43	77	305
0·817	35	204	57	45	80	309
0·684	35	219	55	43	87	311

To find the motion of the normal to the specimen relative to the crystal axes the co-ordinates of the three cubic axes given in Table I were used. These were set out in a stereographic diagram, the centre of which represented the normal to the surface of the specimen. The whole system was then rotated by means of a stereographic net till the axis (100), whose co-ordinates are given in columns 6 and 7 of Table I, was at the point opposite to the centre of the stereographic figure, *i.e.*, at infinity in the complete projection. The remaining two cubic axes (010) and (001) were then on the bounding circle of the stereographic diagram. Each diagram was then rotated about its centre till the crystal axes coincided in all four cases. The points representing the successive positions of the normal to the specimen were then found to lie in the spherical triangle whose vertices are represented by (010), (011), and (111). Their positions are shown by means of round dots at P_0, P_1, P_2, P_3 in fig. 1, which covers only a portion of the complete stereographic diagram.

---

* ε is the ratio of the final to the initial thickness of the disc, see Part I.

† In Parts II and III of this paper the symbol {111} is used to represent the plane {111}, while the symbol (111) is used to represent a direction, the normal to the plane {111}.

Fig. 1 may be compared with similar diagrams used in the case of tensile tests.* In the case of tensile test pieces it was shown that when slipping on one crystal plane occurs the axis of the specimen moves relative to the crystal axes in a great circle towards the direction of slip. In fig. 1 an arc of this great circle is shown by the broken line TP_0S, where S is the normal to the plane {110} which is the direction of slip, and P_0 is the point representing the initial condition of the specimen. If the motion of the normal to the specimen during compression were exactly opposite to that of the axis of a tensile test piece, points P_1, P_2, P_3 would lie on the arc P_0T. It will be seen that they do not do so.

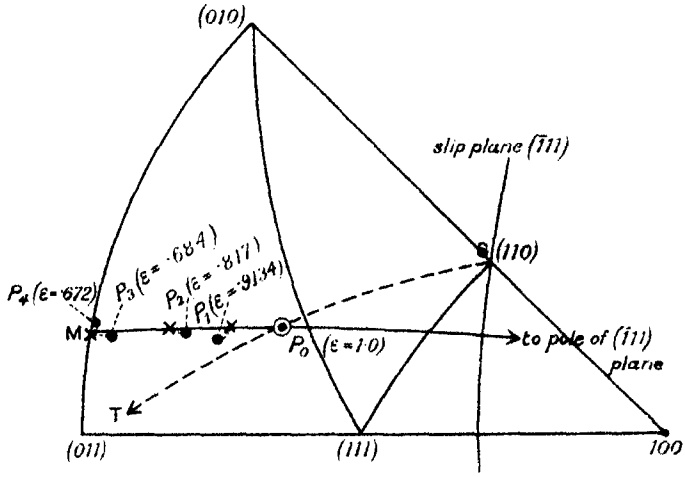
(010)
slip plane $(\bar{1}11)$
S (110)
P_4 (ϵ = ·672)
P_3 (ϵ = ·684)
P_2 (ϵ = ·817)
P_1 (ϵ = ·9134)
M
P_0 (ϵ = 1·0)
to pole of $(\bar{1}11)$ plane
T
(011)
(111)
100

FIG. I. Stereographic diagram showing motion of normal to compression disc No. 59 relative to crystal axes.

On the other hand the considerations given above lead to the prediction that P_0, P_1, P_2, P_3 should lie on the great circle which passes through P_0 and the normal to the plane {111} which is the slip plane. An arc of this circle is shown as the line P_0M. It will be seen that the observed points do lie close to this arc.

As the specimen is compressed the point P representing the normal to the flat surface of the compression disc moves from P_0 towards M, and there is a simple relationship between the amount of compression and the distance of P from P_0 along the arc. If θ is the angle between the normal to the slip plane and the normal to the disc, ϵ the ratio of the thickness of the specimen to its initial thickness, and θ_0 the initial value of θ when $\epsilon = 1$, then it can be shown that

---

* "Plastic Extension and Fracture of Aluminium Crystals," 'Roy. Soc. Proc.,' A, vol. 108, p. 38, figs. 3, 4, 5, and 9 (1925).

$$\sin \theta = \epsilon \sin \theta_0. \qquad (1)$$

In the case of specimen No. 59 the values of θ were found by laying the complete stereographic figure, of which fig. 1 is a part, over the stereographic net. Their values were 59·3°, 49·9°, 46·6°, 38·5°, corresponding with $\epsilon = 1 \cdot 0$, 0·9134, 0·817 and 0·684 respectively. Using the value $\theta_0 = 59 \cdot 3°$ the values of θ calculated from equation (1) are 59·3°, 51·7°, 44·6°, 36·0°. The predicted positions of the normal to the surface of the specimen corresponding with these values are shown in fig. 1 by means of crosses, and short lines have been drawn connecting predicted positions and the positions determined by X-ray analysis. It will be seen that the agreement is fairly good.

Further Experiments with No. 59.

As the discs are compressed the point P (fig. 1) moves along the arc towards the position M, where the arc cuts the {100} plane. At this stage the crystal axes come into a special position in relation to the plane face of the disc. The axes are symmetrical with respect to a plane through the normal to the specimen. To calculate the compression at which this should occur the angle between the point M and the direction ($\bar{1}11$) was measured and found to be 36·5°. Using formula (1) it was found that the corresponding value of ϵ is 0·69. Accordingly it is to be expected that if the orientation of the crystal axes were measured at this stage it would be found to possess this type of symmetry.

The point P_3 (fig. 1) which corresponds to $\epsilon = 0 \cdot 684$ should, in fact, be almost exactly in the cubic plane {100}. It will be seen that this symmetrical position has almost but not quite been reached.

In the course of some experiments with disc 59·9 an X-ray photograph was taken by the Laue method, using heterogeneous X-rays, at the stage when $\epsilon = 0 \cdot 672$. Since this value of ϵ differs little from the critical value $\epsilon = 0 \cdot 69$, and since the incident beam of X-rays was perpendicular to the plane of the disc, the spots of the Laue photograph should be very nearly symmetrically placed with respect to a line through the central spot. The photograph is shown in fig. 2. It will be seen that this prediction is verified with considerable accuracy.

By measuring the plate and constructing a stereographic diagram showing the position of the normal to the plane corresponding with each spot, no difficulty was found in identifying them. The two most intense ones close below the central spot correspond with the normals $(1\bar{1}1)$ and $(11\bar{1})$. The plane of symmetry through the normal to the specimen was found to be of type {100}, and it was found that the nearest (110) direction in this plane made an angle of 8° with the normal to the specimen. This enables us to place the point P_4 corresponding with $\epsilon = 0\cdot627$ on the diagram of fig. 1. It will be seen that P_4 is very close to its predicted position.

On looking at the Laue photograph, fig. 2 (Plate 5), it will be seen that the spots are not diffuse; in fact, they are very little larger than the central spot. It appears, therefore, that from the point of view of distortion measurements, at any rate, the material may still be regarded as consisting of a single crystal with axes possessing a definite orientation, when it has been compressed to a fraction 0·67 of its original thickness.

Experiments with Specimen No. 61.

In order to find out whether the results obtained with No. 59 apply to other specimens with axes in a different orientation, discs were cut from specimen No. 61, the characteristic point for which is shown in fig. 7 of Part I of this paper. It was found that in all cases, including that of No. 59, the distortion during the first 2 per cent. of compression was not due entirely to slipping on one plane, but that after this initial stage had been passed the regular régime described above set in. Accordingly disc No. 61·9 was compressed till its thickness was reduced by 3 per cent. It was then measured and compressed through another 15 per cent. and re-measured. These measurements gave the following elements* necessary for calculating the equation to the unstretched cone :—

$\alpha = 0\cdot9990$

$\beta = 1\cdot1240$

$\gamma = 0\cdot8890$

$\chi = 90° 15'$

$\chi' = 89° 15'$

$X_0 = +0\cdot152$

$Y_0 = -0\cdot176$

$X_1 = +0\cdot055$

$Y_1 = -0\cdot123$

and the equation to the first position of the unstretched cone is

$$(-0\cdot0020\cos^2\phi + 0\cdot038\cos\phi\sin\phi + 0\cdot264\sin^2\phi)\tan^2\theta + (0\cdot0723\cos\phi - 0\cdot0650\sin\phi)\tan\theta - 0\cdot2076 = 0. \qquad (2)$$

---

[*] For the meaning of these symbols see Part I, p. 537.

The stereographic projection of this cone is shown in fig. 3. As in the case of No. 59, the points lie very nearly on two planes. These planes are shown as arcs of circles.

The difference between the cone represented by equation (2) and the two planes is only appreciable in the neighbourhood of the intersection of the two planes. In this region very small changes in the measurements of the specimen make comparatively large changes in the position of the unextended cone. All directions in this region are, in fact, changed very little in length by the compression. The exact form of that part of the cone is therefore not very significant. The actual cone represented by (2) is shown by the broken curve in fig. 3. It will be seen that the unextended cone divides the whole system into two regions, one which contains all directions which are extended during compression and the other containing all those which are reduced in length. The fact that the cone cuts the bounding circle of the projection means that there is a certain range of directions on the flat surface of the disc which are decreased in length when the specimen is compressed. In No. 61·9 the ruled line ($\phi = 0$, $\theta = 90°$) happens to be in this range. The actual measured lengths between points 4 and 6[*] were 5·986 mm. before, and 5,980 mm. after compression, the contraction therefore being one part in 1000. The contraction which would be predicted on

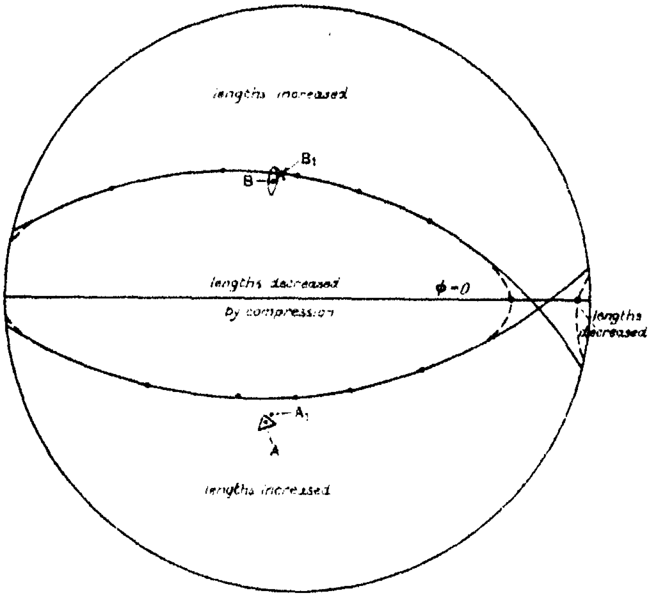

FIG. 3.—Unstretched cone for compression of disc No. 61·9 during régime of slipping on one plane.

---

[*] See Part I, p. 533.

the assumption that the distortion is entirely due to slipping on one plane is about two parts in 1000. The fact that a contraction is actually observed is remarkable. I find that if the amount of slip on any other crystallographically similar plane had been as great as 2 per cent. of that on the slip plane whose pole is at A_1, fig. 3, then the contraction along the ruled line ($\phi = 0$, $\theta = 90°$) would not have been observed. The existence of this contraction amounts therefore almost to a proof that at any rate 98 per cent. of the distortion is due to slipping on one plane.

The crystal axes were determined by Müller's method before the disc had been compressed. Two octahedral planes were determined and the co-ordinates of their poles were ($\theta = 46°$, $\phi = 255°$), ($\theta = 37°$, $\phi = 50°$). The former of these two is the slip plane and the predicted direction of slip was found for these two to be ($\theta = 46°$, $\phi = 100°$). These are marked as A and B on fig. 3, and the observed pole of the slip plane and direction of slip were found from the unextended cone. They are marked as A_1, B_1 in fig. 3, and their co-ordinates are A_1 ($\theta = 45°$, $\phi = 257\frac{1}{2}°$); B_1 ($\theta = 46\frac{1}{2}°$, $\phi = 98°$). The fact that A_1 is close to A, and B_1 close to B shows that the relationship between the distortion and the crystal axes is quite regular, but it must be remembered that the distortion figure gives the position of the slip plane when the material had already been compressed nearly three per cent., whereas the axes were measured before compression began, so that exact agreement is not to be expected.

Slipping on Two Crystal Planes.

In the case of tensile test pieces* it has been shown that the axis of the specimen moves, relatively to the crystal axes, till it gets to a position in which it is equally inclined to two octahedral planes of type {111}. Under these conditions double slipping occurs and the axis continues to be equally inclined to the two slip planes gradually moving to the position of the normal (112).

In the case of compression tests an analogous result holds. For specimen No. 59 the point M (fig. 1) represents the position of the normal to the surface of the specimen when double slipping begins. In the case of No. 61, the point A (fig. 4) represents the initial position of the normal to the slip plane. The line AB is an arc of the great circle through the pole of the slip plane and B is the point where this arc cuts the {100} plane which is represented by the edge of the stereographic diagram. The angle between A and the pole of the slip plane is 46° and the angle between B and this pole is found from fig. 4 to be 36°. Double slipping should occur therefore when

$$\epsilon = \sin 36°/\sin 46° = 0\cdot817.$$

---

* 'Roy. Soc. Proc.,' A, vol. 108, p. 38.

If it is true that slipping occurs on the plane and in the direction where the shear stress is a maximum after double slipping has begun, the rate of shear on the two slip planes should be equal. The effect of equal double slipping would be to keep the normal to the specimen in the {100} plane, but it would very gradually approach the direction (011).

The orientation of three specimens numbered 61·2, 61·7 and 61·8 were measured by X-rays, after compression to $\varepsilon = 0 \cdot 786$, $0 \cdot 769$ and $0 \cdot 781$ respectively. In each case the normal to the specimen was found to lie exactly on the {100} plane and at 7° from the direction (011).

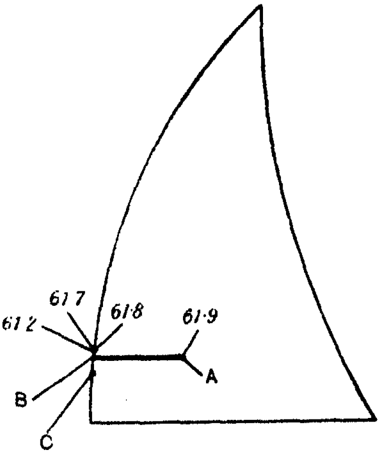

Fig. 4.—Stereographic diagram showing positions measured by X-rays of normal to specimens cut from No. 61 before and after compression.

The theory of double slipping outlined above implies that the representative point would move slowly towards the normal (011) after double slipping has begun. During the compression from $\varepsilon = 0 \cdot 817$ to $\varepsilon = 0 \cdot 769$, the point would move towards the normal (011) by an amount which is considerably less than 1°, so that to the limit of accuracy of the measurements the representative points of 61·2, 61·7 and 61·8 should coincide with B (fig. 4). It will be seen that they do so.

In order to find out whether in a large distortion the amount of slip on the two planes continues to be equal, one specimen, No. 61·19, was compressed in small stages till its thickness was only 0·298 of its initial thickness. At this stage the orientation of its axes was measured by Müller's method. Reflections were obtained from the two slip planes. Using a certain arbitrary line on the surface of the specimen as $\phi = 0$ their co-ordinates are found to be ($\theta = 35\frac{1}{2}°$, $\phi = 354\frac{1}{2}°$) and ($\theta = 37°$, $\phi = 187°$). The representative point found from these axes is very nearly on the {100} plane and is at $4\frac{1}{2}°$ from the direction (011). It is shown at C in fig. 4. It appears, therefore, that during the very large distortion which accompanies compression from $\varepsilon = 0 \cdot 817$ to $\varepsilon = 0 \cdot 289$, the amount of slip on the two slip planes is equal and the {100} plane remains, to within 1°, perpendicular to the flat faces of the specimen.

The spots on the plates due to the reflected X-rays were rather diffuse so that considerable breaking up of the crystal had evidently occurred, but the orientations of the planes of maximum intensity of reflection were still measurable to an accuracy of about 1° and the angle between the two measured normals to the octahedral planes was found to be 72°, which is within 2° of the angle between the faces of an octahedron.

Analysis of Distortion Measurements when Material Slips on two Planes.

Several sets of measurements were made in order to determine the nature of the distortion during the régime of double slipping. Measurements of specimens Nos. 59 and 61 seemed to show that the distortion can be accounted for by supposing that double slipping of the type predicted does take place, but that during the earlier stages at any rate, the amount of slip is greater on the original slip plane than it is on the second slip plane. This result is similar to that found in the case of tensile tests.* When the amounts of slip on the two planes are not equal it is difficult to calculate an equation for the unextended cone except in the case when the amounts of slip are small. On the other hand the equation to the unextended cone can be calculated for any amount of compression, provided the amount of slipping on the two planes is equal. In order to compare calculated with observed distortions specimen No. 69 was chosen. The crystal axes of this specimen were orientated in such a way that double slipping was to be anticipated even in the earlier stages of compression. The initial position of the axis of the specimen was in fact very nearly in a cubic plane, as can be seen by inspection of fig. 7 in Part I of this paper.

A disc, 69·10, cut from this crystal was compressed in small stages from $\epsilon = 1\cdot0$ to $\epsilon = 0\cdot812$. It was then cut circular and compressed in 12 stages to $\epsilon = 0\cdot667$, the surface being covered with a layer of grease before each increase in compression. It was then re-marked and again cut circular and then compressed to $\epsilon = 0\cdot5665$. The unextended cones were worked out for the compression from $\epsilon = 0\cdot812$ to $\epsilon = 0\cdot667$ and from $\epsilon = 0\cdot667$ to $\epsilon = 0\cdot5665$. These cones are shown in fig. 5. Their planes of symmetry are shown by means of broken lines. It will be seen that in each case the axis of the specimen lies very close to the plane of symmetry. This proves that if the distortion is due to double slipping the amount of slipping on the two planes concerned is nearly equal.

It remains to show that the cones are actually ones which could be due to double slipping. For this purpose it is necessary to calculate the unstretched cone for equal double slipping and to compare this with one of those shown in fig. 5. An expression for displacements of particles due to small shears δS_1 and δS_2 parallel to two planes making an angle 2α with one another is given on p. 41 of "Plastic Extension and Fracture of Aluminium Crystals."* In the case

---

* 'Roy. Soc. Proc.,' A, vol. 108, p. 39.

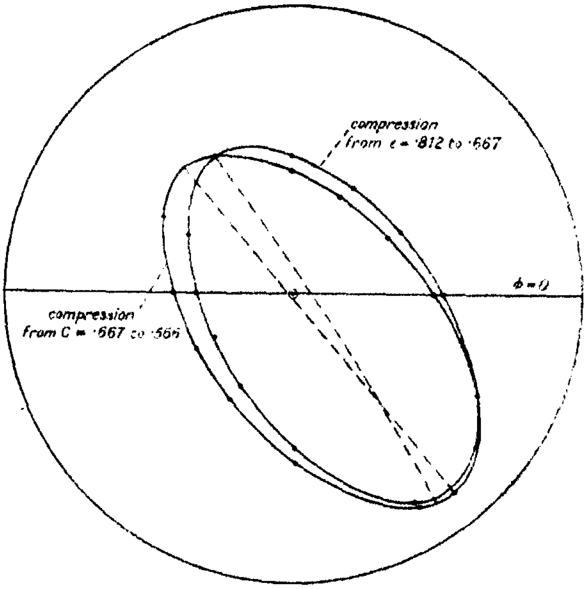

Fig. 5.—Unstretched cones for compression of No. 69·10 during régime of double slipping.

where the two shears are equal so that $\delta S_1 = \delta S_2$ the equations (2) of that paper become (after correcting an obvious misprint where cos β is written for sin β in the expression for δy) :—

$$\left.\begin{aligned}\delta x &= -z\delta s\sin\alpha\cos\beta\\ \delta y &= y\delta s\cos\alpha\sin\alpha\sin\beta\\ \delta z &= -z\delta s\sin\alpha\cos\alpha\sin\beta\end{aligned}\right\}\qquad(3)$$

where $-\tfrac{1}{2}\delta s$ has been written for δS_1 or δS_2. The negative sign is taken in order that s may have a positive value during a compression test, and the factor $\tfrac{1}{2}$ has been inserted in order to make the amount of shear for a given value of s comparable with shear by slipping on one plane. Since α and β are constant these equations can be integrated, the resultant transformation equations being

$$\left.\begin{aligned}x &= x_0 + z_0\cot\beta\sec\alpha\,(1/A - 1)\\ y &= y_0 A\\ z &= z_0/A\end{aligned}\right\}\qquad(4)$$

where $A = e^{s\cos\alpha\sin\alpha\sin\beta}$ and $s = \int ds$.

These equations give the motion of particles of the material relative to the system of co-ordinate axes shown in fig. 6, p. 40, of "Plastic Extension and Fracture of Aluminium Crystals."*

In the case when the symmetrical position of the crystal axes is arrived at by compression instead of by extension, the value of α is not the same as it was in the case previously discussed, 2α is now the internal instead of the external angle between the faces of an octahedron so that $\alpha = 54° 44'$; β is 60° as before, so that $\cos\alpha = 1/\sqrt{3}$, $\sin\alpha = \sqrt{2}/\sqrt{3}$, $\sin\beta = \frac{1}{2}\sqrt{3}$, $\cos\beta = 1/2$. Hence $\cos\alpha\ \sin\alpha\ \sin\beta = 1/\sqrt{6} = 0{\cdot}408$ and $\cot\beta\ \sec\alpha = 1$. So that formulæ (4) become

$$\left.\begin{aligned} x &= x_0 + z_0(1/\mathrm{A} - 1) \\ y &= y_0\mathrm{A} \\ z &= z_0/\mathrm{A} \end{aligned}\right\} \qquad (5)$$

And

$$\mathrm{A} = e^{0{\cdot}408\, s} \text{ or } s = \sqrt{6}\log_e \mathrm{A} = 5{\cdot}640 \log_{10}\mathrm{A}.$$

The equation to the unstretched cone may now be written down directly, it is: $x^2 + y^2 + z^2 = x_0^2 + y_0^2 + z_0^2$, and using (5) this gives for the cone in its first, or unstrained position,

$$\mathrm{A}^2(\mathrm{A}+1)\,y_0^2 - 2z_0^2 - 2\mathrm{A}x_0z_0 = 0. \qquad (6)$$

Before we can express the unextended cone in terms of γ, the ratio of the thickness of the disc after compression to that before compression, it is necessary to find the relationship between γ and A. Let i_0 be the angle between the normal to the surface of the specimen and the bisector of the two slip planes which is the axis of z in equations (5). To find γ in terms of A and i_0 consider the area of a rectangle in the flat surface of the specimen before and after compression. Let the sides of this rectangle be initially of length c and d, the side of length c being along the axis of y (which is parallel to the surface when the specimen is in the symmetrical position assumed for double slipping) and the side of length d being in the plane of symmetry $y = 0$.

If the origin of co-ordinates be taken at a corner of this rectangle, then before compression the co-ordinates of one corner are $(0, c, 0)$ while those of another are $(d\cos i_0, 0, -d\sin i_0)$.

Applying the transformation formulæ (5) it will be seen that the co-ordinates of these two points after distortion are

$$(0, \mathrm{A}c, 0) \text{ and } (d\cos i_0 - d\sin i_0(1/\mathrm{A}-1),\ 0,\ -d\sin i_0/\mathrm{A}). \qquad (7)$$

The area of the rectangle before distortion is cd, the area after distortion is

---

* *Loc. cit.*

cd A $\{[\cos i_0 - \sin i_0 (1/\mathrm{A} - 1)]^2 + \sin^2 i_0/\mathrm{A}^2\}^{\frac{1}{2}}$ and since the volume of the material is unchanged by compression this area multiplied by γ must be equal to $c\,d$. Hence

$$\mathrm{A}^2 (1 + 2 \sin i_0 \cos i_0) - 2\mathrm{A} (\sin i_0 \cos i_0 + \sin^2 i_0) + 2 \sin^2 i_0 - 1/\gamma^2 = 0. \quad (8)$$

This equation gives A and hence s when i_0 is known from X-ray measurements and γ has been measured.

To find the position of the normal to the specimen relative to the crystal axes after compression it is only necessary to note that it is in the plane $y = 0$ and at right angles to one of the sides of the rectangle cd, thus if i represents the angle which the normal to the specimen makes with the axis z after compression, we find from (7)

$$\tan i = - \left\{ \frac{- d \sin i_0/\mathrm{A}}{d \cos i_0 - d \sin i_0 (1/\mathrm{A} - 1)} \right\}$$

or

$$\cot i = \mathrm{A} (\cot i_0 + 1) - 1. \quad (9)$$

To apply these formulæ to specimen No. 69 the value of i_0 was found by X-ray reflections to be 12°. Inserting this value in (8) and (9) the equations for A and i are

$$1{\cdot}4067\,\mathrm{A}^2 - 0{\cdot}493\,\mathrm{A} + 0{\cdot}0862 - 1/\varepsilon^2 = 0, \quad (10)$$

and

$$\cot i = 5{\cdot}705\,\mathrm{A} - 1, \quad (11)$$

and inserting observed values of ε the following values for A and i are obtained:—

Table II.

ε.	A.	i.
		°
1·00	1·000	12
0·812	1·199	9·7
0·667	1·427	8·0
0·566	1·653	6·8

In the case of specimen No. 69·10 complete distortion measurements were made for the compression between $\varepsilon = 0{\cdot}667$ and $\varepsilon = 0{\cdot}566$. In order to calculate the corresponding unextended cone due to double slipping the value $\mathrm{A} = \frac{1{\cdot}653}{1{\cdot}427} = 1{\cdot}158$ must be used in (6). Inserting this value in (6) the equation to the unextended cone in the material at $\varepsilon = 0{\cdot}667$ is found to be

$$2{\cdot}900\, y_0^2 - 2{\cdot}316\, x_0 z_0 - 2 z_0^2 = 0. \quad (12)$$

In order to compare this with the unextended cone derived from external measurements it is necessary to transform the axes so that the axis of the specimen is the axis of z. The transformation formulæ necessary are

$$\left.\begin{aligned} x_0 &= x' \cos \iota + z' \sin \iota \\ y_0 &= y' \\ z_0 &= -x' \sin \iota + z' \cos \iota \end{aligned}\right\} \quad \text{where} \quad \left.\begin{aligned} x'/z' &= \tan \theta \cos \phi \\ y'/z' &= \tan \theta \sin \phi \end{aligned}\right\}. \qquad (13)$$

And θ and ϕ are the spherical polar co-ordinates with respect to axes for which $\theta = 0$ is the normal to the specimen and ($\theta = 90°$, $\phi = 0$) is the line in the surface of the specimen which is symmetrical with respect to the distortion. Taking from Table II the appropriate value $i = 8 \cdot 0°$ and inserting it in equations (13) and inserting the values of x_0, y_0 so found in (12), the equation to the unextended cone is found to be

$$(0 \cdot 281 \cos^2 \phi + 2 \cdot 900 \sin^2 \phi) \tan^2 \theta - 1 \cdot 675 \cos \phi \tan \theta - 2 \cdot 279 = 0. \qquad (14)$$

A stereographic projection of this cone is shown in fig. 6, and in order to compare it with the unextended cone calculated from the measured distortion, the cone for the compression from $\varepsilon = 0 \cdot 667$ to $\varepsilon = 0 \cdot 566$ was taken from fig. 5 and

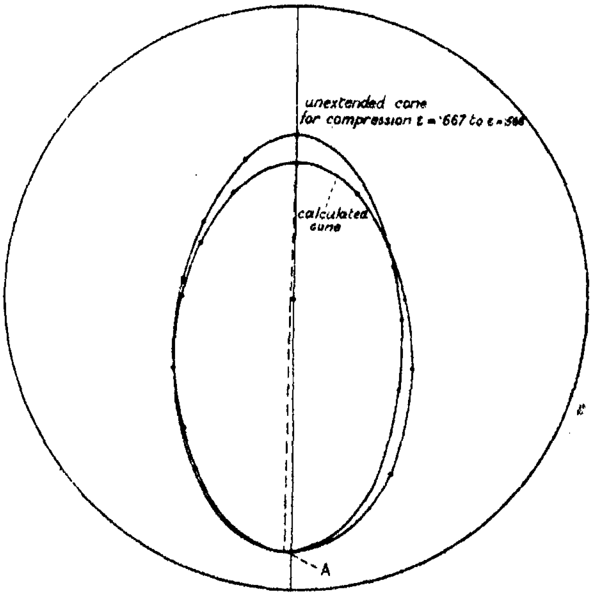

Fig. 6.—Comparison between measured form of unstretched cone for 69·10 and that deduced from assumption of equal amounts of slip on two symmetrical planes of slip.

rotated about the normal to the specimen till the cubic crystal plane which should be symmetrically disposed with respect to the distortion coincides with the co-ordinate plane $\phi = 0$ of the calculated cone. This plane is represented in fig. 6 by a vertical diameter of the bounding circle of the projection. It will be seen that the calculated cone derived from the assumption of double slipping is very close to the cone deduced fron the distortion measurements, but that the latter is rather longer and narrower than the former.

This characteristic appears in all cases that I have examined, and the fact that the cones always coincide at one end, namely the end which contains the intersection of the two slip planes marked A in fig. 6, suggests that there may be a certain amount of slipping on the same two slip planes but in one of the other possible directions of slip.

Condition of the Specimens when the Distortion is very great.

In the cases of specimens Nos. 61 and 69 the tests were continued till the distortion was very large. The details of the manner in which the tests were carried out will be described in Part III where the stress measurements are discussed, but for the present purpose it is sufficient to describe the last stage of the test in the case of one specimen, No. 69·9. This specimen had been compressed in four stages, the disc being cut circular three times. The distortion was found to be uniform all the time, and the thickness at the end of the fourth stage was 0·349 of the original thickness. It was then cut circular, the thickness being left unaltered, and marked in squares thus 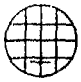

It was then compressed till its thickness was only 0·2776 of its original thickness.

A photograph of the final condition of the specimen is shown in fig. 7 (Plate 5). It will be seen that the distortion is still quite uniform, the straight lines remaining straight. The three lines which run vertically, down the page, *i.e.*, parallel to the major axis of the elliptic upper surface of the specimen, had been scratched so as to be parallel to the direction (100) in the crystal. The fact that the disc is distorted into an ellipse with its major axis parallel to the direction (100) shows that the symmetry is preserved, and the general features of the distortion are in accordance with the prediction based on equal slipping on two planes ; but we can apply a far more searching test as to how far the assumption is true. The extensions of the specimen in the flat upper surface parallel to the major and minor axes of the ellipse were measured. The distance between the intersections of two outer vertical lines and the middle horizontal line (*i.e.*, between points 4 and 6 in the notation employed in Part I, p. 533) was 3·185 mm. before compression and 3·226 mm. after compression. The extension ratio of the material parallel to the minor axis may be defined as the ratio of the two lengths 3·226/3·185 = 1·0185. *In the same way the extension ratio parallel to the major axis was found to be* 4·024/3·246 = 1·240.

The extension ratios parallel to these two directions can be calculated on the assumption of equal double slipping. The value of A corresponding with the compression from $\varepsilon = 0\cdot349$ to $\varepsilon = 0\cdot2776$ was found to be $A = 1\cdot250$. Referring to equation (7) it will be seen that the rectangle there discussed whose sides were c and d is in fact a rectangle whose sides are parallel to the scratches shown in the photograph, fig. 7. Formula (7) shows therefore that the extension ratio in the direction of the major axis should be equal to A because the initial length one side was c and the final length Ac. The predicted extension ratio in this direction was therefore $A = 1\cdot250$. Comparing this with the observed extension ratio, 1·240, it will be seen that the agreement is very good.

The extension ratio in the direction of the minor axis is, from (7)

$$\{[\cos i_0 - \sin i_0 (1/A - 1)]^2 + \sin^2 i_0/A^2\}^{\frac{1}{2}}. \tag{15}$$

At the beginning of the last stage of compression of 69·9 the value of ε was 0·349. At this stage in the compression the value of i was found by calculation to be 4·2°. Using this value for i_0 in (15), and putting $A = 1\cdot250$, the predicted extension ratio is found to be 1·014. Comparing this with the observed value 1·0185 it will be seen that again the agreement is very good.

In order to throw into as clear a light as possible the relationship between the distortion and the crystal axes the diagram fig. 8 has been prepared. This shows the specimen No. 69·9 at the end of the test. The two planes of slip {111} and $\{\bar{1}11\}$ and also the plane of symmetry {100} are shown as material sheets, and the directions of slip (110) and $(1\bar{1}0)$ are marked on them. The figure may be of some assistance in understanding the manner in which the normal to the specimen approaches the direction (011) with gradual reduction of the angle i as the compression proceeds.

Top and side views of the specimen are also shown in fig. 8. These may be compared with the photograph, fig. 7 (Plate 5).

The accuracy with which the predicted distortion is realised in practice is very surprising when the amount of breaking up which the crystal has suffered is taken into consideration. Fig. 9 (Plate 5) shows a Laue photograph of 69·9 taken

with the X-ray beam perpendicular to the plane faces of the specimen. This photograph was taken at the stage of maximum compression, *i.e.*, at $\varepsilon = 0 \cdot 2776$.

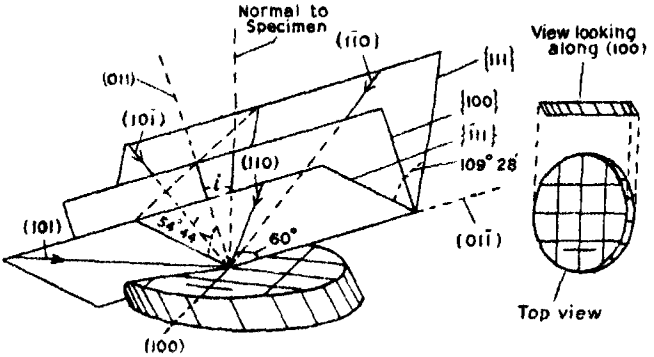

FIG. 8.—Diagram showing positions of planes and directions of slip in relation to the distortion of a compressed disc during régime of double slipping.

It may be compared with fig. 2, but in doing so it must be remembered that the distance of the photographic plate from the specimen was 1·97 cm. in the photograph, fig. 9, whereas it was only 1 cm. in the photograph of fig. 2. Allowing for this difference it will be seen that the two photographs are essentially of the same nature so far as type of symmetry is concerned. (The value of i was less in the specimen photographed in fig. 9 than in the other.) The diffuseness of the spots in fig. 9, and the smallness of their number as compared with those of fig. 2, show that the material can no longer be regarded from the point of view of X-rays, as a single crystal even approximately. On the other hand, the external measurements of the specimen show that the distortion is almost exactly what one would expect from a single crystal placed with its axes in the symmetrical position indicated by the spots in the Laue photograph, fig. 9 (Plate 5). It may be noted that the value of s appropriate to the distortion of 69·9 at $\varepsilon = 0 \cdot 2776$ is $s = 2 \cdot 8$. That is to say, the distortion is equivalent to a distortion by single slipping, in which any two planes of particles parallel to the slip plane move relatively to one another through a distance 2·8 times as great as their distance apart.

Application of Foregoing Results to the Structure of Rolled Sheets of Metal.

The nature of the distortion which occurs when metals are rolled is not well understood. Regarding the sheet as a whole, one can say that there is an extension in the direction of rolling, a contraction in thickness, and that there is little or no extension or contraction in the line perpendicular to the direction of rolling. If the distortion is uniform through the thickness of the sheet then the principal axes of strain are along and perpendicular to the direction of rolling and perpendicular to the surface of the sheet. Lines ruled on the surface of the sheet perpendicular to the direction of rolling remain perpendicular to that direction, and lines of particles originally perpendicular to the surfaces of the sheet remain so.

In rolled metals, X-ray analysis shows that the crystal axes tend to take up certain preferred orientations, and as the rolling proceeds these orientations become " stable " and remain fixed relative to the surface of the sheet. One of the fundamental problems in considering the distortion of metals during rolling is to find how these preferred orientations can remain fixed in direction as the rolling proceeds. The first successful attempt at solving a problem of this type appears to be that of Miss Elam and myself* when we showed that, if a *single crystal of aluminium could be extended indefinitely, the orientation* of the axes would come into a definite position such that the axis of the specimen was normal to a plane of type {112}.

This result was used by Polanyi and Weissenberg,† who pointed out that when the axes were in this orientation the reduction in the cross section of the bar was confined to one direction, that of a crystal direction of type (110). The dimension of the bar in the direction of type (111) which is perpendicular to (110) and (112) remaining constant. For this reason they predicted that the " stable " orientations in a rolled bar would be such that the crystal direction (112) was in the direction of rolling, (111) in the surface of the sheet but perpendicular to the direction of rolling, and (110) perpendicular to the sheet.

I had noticed this peculiarity of the distortion due to double slipping in a tensile test piece when the crystal axes were in this " stable " position, but had hesitated to apply it to the distortion of a rolled sheet because (*a*) it seems unlikely that the distortion in rolling is really uniform through the thickness of the sheet, and (*b*) the distortion of the crystal cannot be that of a rolled sheet as a whole, even if uniformity of distortion is assumed. It is true that Weissenberg's type of slipping makes the breadth of the sheet constant, the extension along the direction of rolling being equal to the contraction in thickness of the sheet. It is true also that lines of particles perpendicular to the surface remain perpendicular to it; but lines of particles initially in the surface of the sheet and

---

* " Distortion of an Aluminium Crystal during a Tensile Test," 'Roy. Soc. Proc.,' A, vol. 102, p. 643 (1923).

† See G. Masing u. M. Polanyi 'Naturwissenschaften,' Bd. II.

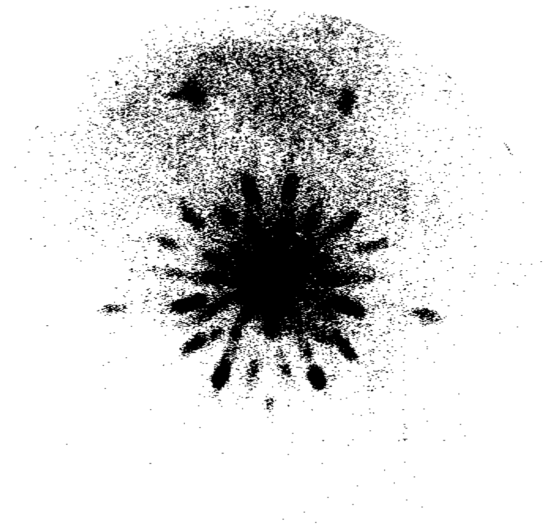

FIG. 2.—Laue photograph of specimen No. 59·9 taken when $\varepsilon = 0·672$.

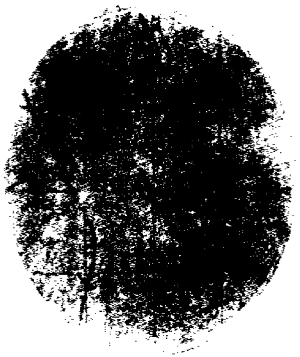

FIG. 7.—Photograph of marks on No. 69·9 after compression to $\varepsilon = 0·2776$, showing uniformity of distortion even when the distortion is very large.

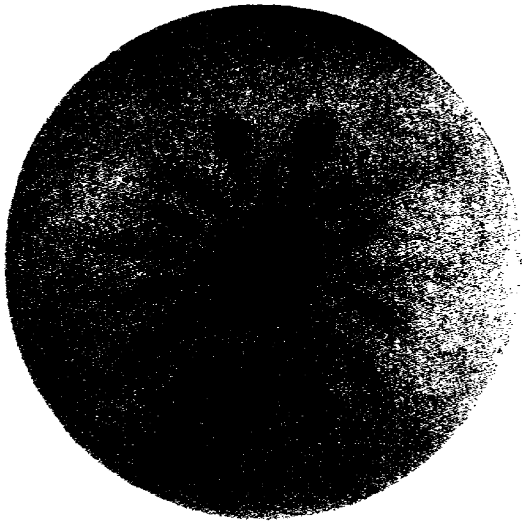

FIG. 9.—Laue photograph of 69·9 at $\varepsilon = 0·2776$, showing that symmetry about {100} plane is preserved when the distortion is very great.

perpendicular to the direction of rolling do not remain perpendicular to the direction of rolling.

To me this seems a fatal objection to Polanyi and Weissenberg's theory. It is possible that adherents of the theory might postulate an equal number of crystals with orientations in the two alternative positions consistent with the three given directions. The distortion of the material, as a whole, might be such that lines ruled across the material would, on the whole, remain perpendicular to the direction of rolling, though each element of the line became inclined to this direction; but the conditions under which the separate crystals could adjust themselves so as to fit in with the distorted positions of their neighbours are very difficult to visualise. One could for instance assume that they were very long in the direction of rolling, thus getting rid of the necessity for considering the adjustments at their ends. If the two orientations occurred alternately in grains very much elongated in the direction of rolling they could adjust themselves so far as movement relative to their nearest neighbours situated in the same plane of rolling, as themselves was concerned, but it is geometrically impossible for them to adjust themselves to the movements of neighbours in the direction perpendicular to the plane of the sheet. For this reason Weissenberg's type of slipping could only exist if the grains extended right through the sheet, their boundaries being planes parallel to the direction of rolling and perpendicular to the sheet. This distribution of grains seems highly artificial.

Application of Distortion by Compression between Parallel Plates.

Referring to fig. 8 and to equation (9) it will be seen that the "stable" position of axes to which the compressed discs tend is one for which the direction (011) is perpendicular to the disc, and the plane {100} is the plane of symmetry of the distorted specimen. In this position the distortion of the specimen is such that there is no extension in the direction $(01\bar{1})$ (which is in the face of the specimen when $i = 0$). There is a reduction in thickness in the direction (011) and a corresponding extension in the direction (100). Lines ruled on the surface in the directions (100) and $(01\bar{1})$ remain at right angles to one another after compression.

On the other hand lines of particles originally at right angles to the surface of the specimen do not remain so, as will be seen by looking at the side view of the specimen sketched in fig. 8. It appears therefore that this type of double slipping, like that of Polanyi and Weissenberg, does not give rise to a distortion which is identical with that which occurs in rolling when the assumption is made that the distortion is uniform through the thickness of the sheet.

It will be noticed that when $i = 0$ two more possible directions of slip, $(10\bar{1})$ and (101), come into positions which are symmetrical with respect to the two directions of slip $(1\bar{1}0)$ and (110) and the surface of the specimen. Their positions are shown in fig. 8. Under these circumstances it is to be expected that slipping might occur in these two new directions as well as in the old ones. As has already been pointed out the elongation of the unextended cone beyond its predicted position for the extension of 69·10 from $\epsilon = 0{\cdot}667$ to $\epsilon = 0{\cdot}566$ (see fig. 6) suggests that a certain amount of slipping in the two new directions $(10\bar{1})$ and (101) had already occurred. An examination of the unextended cone for 69·9 from $\epsilon = 0{\cdot}349$ to $\epsilon = 0{\cdot}2776$ showed that this effect was getting more pronounced as the compression increased and i decreased, the cone being more elongated than that shown in fig. 6.

If the amount of slip in both the two directions on each slip plane is equal, then the distortion of the compressed disc is identical with that assumed for rolling. If, therefore, the crystal axes are placed in accordance with the scheme shown in the right-hand bottom corner of fig. 10, the distortion due to slipping in two directions on each of the two planes of slip is identical with that assumed for rolling. Cubes in the material with their edges perpendicular to the surface of the sheet, and parallel to the direction of rolling, are distorted into rectangular blocks with one dimension unchanged.

In order to illustrate the differences in the kinds of distortion which arise from these various kinds of double slipping, the diagram shown in fig. 10 has been prepared. This shows the distortion of a cube originally whose faces and edges were originally parallel and perpendicular to the plane of rolling and the direction of rolling. W*a* and W*b* represent the distorted shape of the cube when the distortion is due to double slipping of Polanyi and Weissenberg's type. There are two possible shapes because there are two possible positions of the crystal axes, and in Weissenberg's theory both these two types of orientation occur. C_2 represents the distorted shape when the distortion is due to slipping of the type found in compression specimens, on two planes and in one direction on each plane. C_4 represents the distorted shape of the cube when the distortion is due to slipping in two directions in each of two planes. Inspection of fig. 10 shows that C_4 is the only one of these types which satisfies the assumed condition that the distortion shall be uniform through the thickness of the rolled sheet. It seems possible that if the distortion in rolling were uniform through the thickness of the sheet the slipping would, in fact, be of this type, and the " stable " position of the crystal axes would be that shown in the sketch at the right-hand bottom corner of fig. 10.

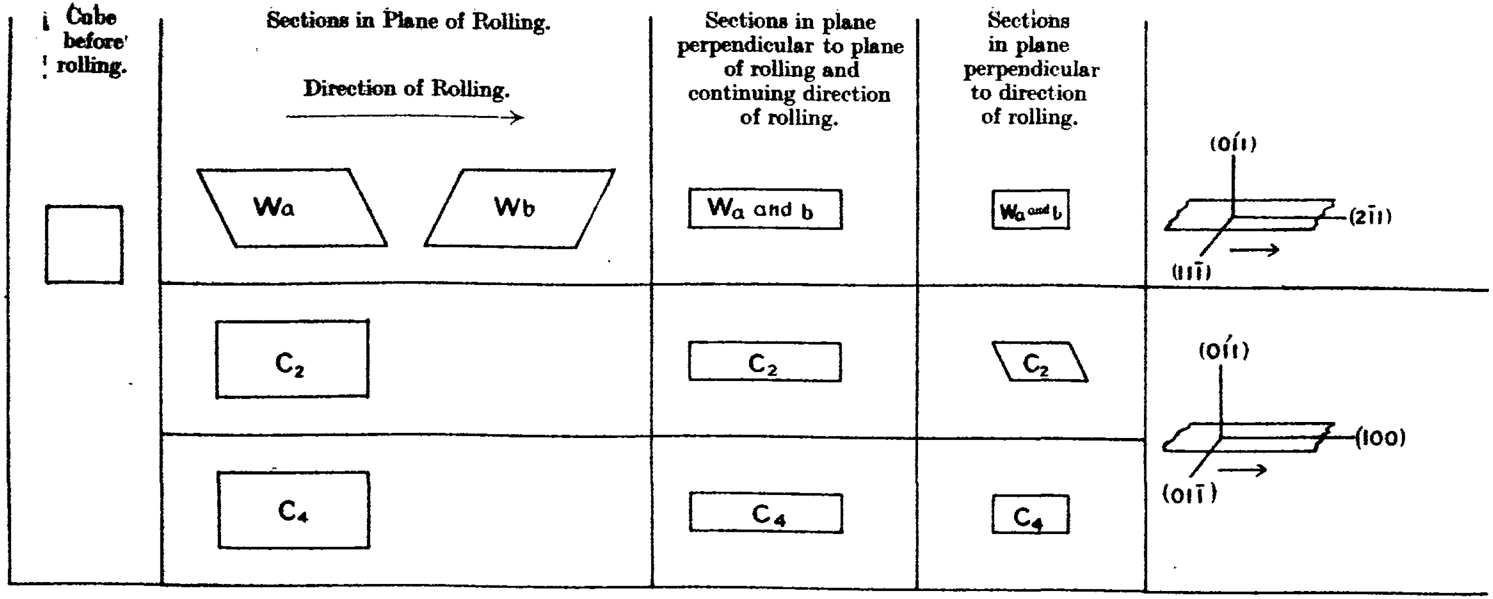
Cube before rolling.
Sections in Plane of Rolling.
Direction of Rolling.
Sections in plane perpendicular to plane of rolling and continuing direction of rolling.
Sections in plane perpendicular to direction of rolling.
Wa
Wb
Wa and b
Wa and b
C₂
C₂
C₂
C₄
C₄
C₄
(01̄1)
(21̄1)
(111̄)
(01̄1)
(100)
(011̄)

FIG. 10.—Diagram showing sections by three perpendicular planes, of shapes into which a cube is distorted, (*Wa* and *Wb*) by Polanyi and Weissenberg's type of double slipping which occurs in tensile test pieces; (C_2) by double slipping of type which occurs in compression specimens; (C_4) by double slipping on two planes in two directions on each plane. This type might be expected to occur in compression discs as the normal to the specimen gets close to its ultimate "stable" position.

Comparison with X-ray Results.

Perhaps the most complete experiments on the orientation of crystal axes in rolled foil are those of Owen and Preston.* These authors using both photographic and ionisation methods got results nearly in agreement with previous work by Wever.† They conclude that there are two sets of crystals in the material whose orientations are mirror images of one another in the plane of rolling. The individual members of each set are not all exactly in one orientation, but are rotated through a range of about 10 degrees round the transverse direction, *i.e.*, the line in the plane of rolling at right angles to the direction of rolling. This direction, which is of type (110) is common to all crystals of both sets. This feature comes out very clearly in a photograph taken with homogeneous X-rays while the specimen was rotated about the transverse direction. In this case evidently the photograph should, if the spread of crystal orientation is entirely due to rotation about this direction, be similar to a photograph of a single crystal rotated about the same axis. This photograph (Owen and Preston's, fig. 12) is, in fact, the only one of their photographs which in the least resembles a rotation photograph of a single crystal.

The crystals arrange themselves so that they all have a crystal direction of type (110) in the transverse direction. Directions of type (111) lie in the direction of rolling and in a range of about 10° on either side of it.

Comparing this result with that deduced from compression experiments combined with the assumption of uniform distortion through the thickness of the sheet, it will be seen that the crystal direction (110) sets itself in the sheet and across the direction of rolling in both cases, but in the disposition predicted from the assumption of uniform distortion the direction (100) should set itself along the direction of rolling, whereas in the observed foils (100) directions lie in ranges of 10° from 55° to 65° on either side of the plane of rolling.‡

The results of Owen and Preston could be explained by double slipping in two directions on two planes, if the distortion during rolling is not uniform through the thickness of the material. Suppose, for instance, that the distortion is such that there is no extension or shear in the transverse direction, but lines of particles originally normal to the surface of the sheet are curved in the distorted material (the curves, of course, being in planes perpendicular to the transverse direction). The sketch in fig. 11 shows the effect of distorting in this way a rectangular bar marked with lines parallel to its edges. In this case the distortion of each element could be accounted for by slipping parallel to two planes only. These two {111} type planes intersecting in the transverse direction, which would therefore be of type (110), might be in any orientation round the transverse direction. The exact orientation at any given distance from the middle of the sheet would depend on the relationship between the total extension of the material in the direction of rolling, and the amount of shear of the outer layers of material relative to the inner ones.

---

* "The Effect of Rolling on the Crystal Structure of Aluminium," 'Proc. Phys. Soc.,' vol. 38, Part 2 (1926).

† 'Z. f. Physik,' vol. 28, p. 69 (1924).

‡ See Owen and Preston, *loc. cit.*, fig. 8.

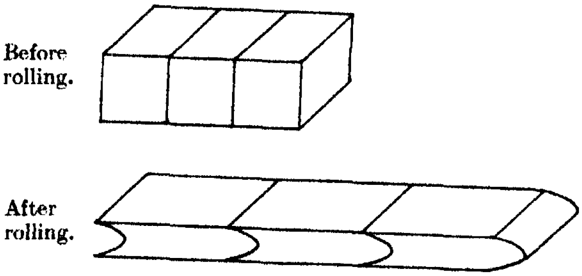

FIG. 11.—Diagram illustrating possible changes of shape in rectangular bar when rolled under conditions where distortion was not uniform through thickness of material.

In order that there may be no lateral motion of layers parallel to the plane of the sheet the amount of slip in the two directions on each plane of slip must be equal to one another, but the amount of slipping on one plane may be different from that on the other, and for any given orientation of the principal axes of strain a ratio of the amounts of slip on the two planes could be found which would bring the crystal axes into a " stable " position so that further extension would keep them in that position.

It must be remembered, however, that the distortion due to rolling is probably even more complicated than has been considered here. Though the resultant strain is necessarily of this type, the directions of the shear stresses in the material on entering the rollers are probably quite different from those in the metal when it leaves them. This question has been studied in a very interesting paper by v. Kármán,[*] who bases his work on the fact that the friction between the roller and the metal is a necessary part of the action of a rolling machine. He points out that the direction of friction may change sign as the material passes from the point where contact with the roller is first made to the point where the metal leaves the rollers. The total hydrostatic* pressure in the material also varies in a complicated manner.

---

[*] 'Z. f. Angew. Math. u. Mechanik.,' vol. 5, p. 139 (1925).

For these reasons it is impossible in the present state of knowledge to do more than give a possible reason why the crystals set themselves with a (110) direction in the plane of rolling, and at right angles to the direction of rolling. The explanation of why the orientation of the crystal axes round the transverse direction is what it is, must be left till the distortion of metals, and particularly single crystals of metals in the process of rolling, has been studied in greater detail.

In conclusion I wish to express my thanks to Sir Ernest Rutherford for allowing the work to be carried out in the Cavendish Laboratory, and to Miss C. F. Elam for giving me the single crystals used in the work, and also for carrying out some of the earlier determinations of orientation of crystal axes by X-rays. Most of the X-ray work was done with a Hadding tube presented to me by Prof. P. Debye. The Laue photographs shown in figs. 2 and 9 were very kindly made for me by Dr. A. Müller in the Davy Faraday Laboratory. I wish also to express my thanks to Mr. W. S. Farren, with whom I began this work, for his continued interest and help.

---

* Sum of the principal stresses.

The Distortion of Crystals of Aluminium under Compression. Part III.—Measurements of Stress.

By G. I. Taylor, F.R.S.

(Received June 10, 1927.)

Several experiments were devised to find out whether it is possible to measure the internal shearing stresses in a compressed disc, and the conditions under which it is possible to do so. Equations are developed for analysing shear stresses parallel to planes of slip and distortion due to double and single slipping. The relationship between shear stress and amount of shear is found for tensile and for compression specimens, when slipping is confined to one plane. The experimental results in the two cases are identical. The fact that the component of force normal to plane of slip is a pressure in one case and a tension in the other makes no measurable difference to resistance to slipping for given amount of slip.

During double slipping resistance to shear increases more rapidly for a given total amount of slipping than when all slip is confined to one plane. The experiments cover a large range and show that resistance to shear goes on increasing up to greatest amounts of distortion used.

When a bar cut from a single crystal of a soft metal is extended, the relationship which exists between the extension at any stage of the test and the force necessary to produce that extension may depend on a number of circumstances, the orientation of the crystal axes, the manner in which the load is applied, the time during which the load is on, and so forth. When a specimen of aluminium at room temperature is extended the extension does not seem to depend on the manner of loading provided the whole load is not applied very suddenly. Thus, if a given extension ϵ is obtained with a given load T and the specimen is then unloaded and afterwards gradually loaded again, then except for the small elastic extension and sometimes a very small plastic extension the specimen will not begin to extend again till the load attains the value T. It will then extend as though the load had been increasing since the beginning of the test. In the case of aluminium, therefore, at a given temperature the load necessary to produce a given extension seems to depend chiefly on the orientation of the crystal axes. In seeking to find out how the load depends on the orientation one is naturally guided by the observed type of deformation. In the case where the deformation is due entirely to slipping on a given crystal plane and in a given crystallographic direction, the force which acts across this crystal plane can conveniently be resolved into three components, a normal force perpendicular to the plane, a shearing force parallel to the direction of slip and a shearing force perpendicular to the direction of slip. Since the strengthening of the material depends on the amount of distortion it is essential in comparing specimens whose crystal axes have different orientations in relation to the direction of stress to decide on some system for measuring the distortion. Clearly the correct method in the case of slipping on one plane is to calculate the amount of shear parallel to the plane of slip. Referring to fig. 1, if A B C D is the undistorted position of a rectangular block of material, and if A D is parallel to a slip plane, the distorted position of the block is A B′ C′ D. The amount of shear will be defined as BB′/BA, that is $\tan (B\ \hat{A}\ B')$. This will be denoted by the symbol s. The shearing stress parallel to the direction of slip will be represented by the symbol S and the normal stress is N. One of the chief purposes of the work here described was to find out whether S can be regarded simply as a function of s, or whether the component of force normal to the plane of slip has any effect on the resistance to shear as it would if the phenomenon was analogous to that of solid friction. This question has already been studied by E. Schmid* who found in the case of bismuth and some other metals that the normal force does not appear to affect the resistance to shear. In his case he found S and N for a number of tension specimens, the normal force was therefore always a tension. In the present work the values of S found in extension experiments are compared with those found in compression experiments, so that the stress normal to the plane of slip is a pressure in one case and a tension in the other.

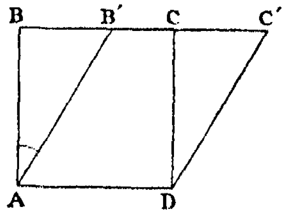

Fig. 1.—Diagram illustrating definition of amount of slip, s.

Experimental Details.

The determination of the distribution of stress in the interior of a plastic body is a matter of great difficulty unless it is possible to ensure that the stress is uniform. In the case of soft metals like aluminium in which the resistance to distortion increases steadily with the amount of distortion, it seems that a non-uniform stress would produce a non-uniform distortion. Conversely therefore, the existence of a uniform distortion implies a uniform distribution of stress. It is only when the distribution of stress is uniform that one can calculate the

---

[*] "Ueber die Festigkeit und Plasticität von Wismutkristallen," 'Z. f. Physik,' vol. 39, p. 359 (1926); and "Ueber die Schubverfestigung von Eisenkristallen bei Plastischer Deformation," 'Z. f. Physik,' vol. 40, p. 54 (1926).

stress at any point in a material from a knowledge of the total external forces applied to the specimen. For this reason, therefore, in determining the strength of materials it is essential to arrange the tests so that the distortion is uniform.

In the case of tests in which uniform bars of soft metals are extended no special precautions to ensure uniformity of distortion are necessary. The inherent stability, conferred by the rapid increase of stress with increasing extension makes the distortion uniform automatically. In the case of discs cut from single crystals of aluminium and compressed between steel plates, the conditions under which uniform distortion can be obtained were described in Part I, p. 531.* The considerations put forward above indicate that when the distortion is uniform the stress must be uniformly distributed. The existence of tangential friction at the flat surface when the specimen is squeezed into a larger and thinner disc would necessarily tend to give rise to a non-uniform distribution of stress and therefore presumably to non-uniform distortion. One is, therefore, driven to the conclusion that the precautions taken to ensure uniform distortion have so reduced the friction of the specimen on the steel plates that its effect on the stress in the material is negligible compared with the stress due to the normal load.

This conclusion is surprising, but unless it is true it is not possible to deduce the values of the shear stress S from measurements of the total compressive force on the specimen. For this reason several experiments were undertaken to verify the fact that the friction is really negligible. Some of these will now be described.

Compressive Force on Discs of Different Thicknesses.

As was pointed out in Part I the effect of friction must be greater when the disc is thin than when it is thick. Two discs of thickness 1·5 mm. were cut from specimen No. 59 and two of thickness 3 mm. The initial diameter of all of them was 14 mm. One specimen of each thickness was compressed in a few stages, the load increasing by 1000 lbs. each time. The remaining two were compressed in many stages, the load increasing each time by 100 lbs. The discs were covered with a layer of grease before each increase in load.

It was found that in the first case when the compression was carried out in a few stages the load necessary to produce a given compression was greater for the thin disc than for the thick one. On the other hand when the load was increased in 100 lb. stages the loads necessary to produce a given compression were identical, and lower than those necessary to produce the compression in a few stages.

---

* "The Distortion of Crystals of Aluminium under Compression—Part I," 'Roy. Soc. Proc.,' A, vol. 111, p. 529 (1926).

If the loads were increased in 200 lb. stages the amount of compression in the thick and thin discs was still nearly though not quite identical, but when the increase in load for each stage was 500 lbs. the load necessary to produce a given compression was appreciably increased. It appears, therefore, that for aluminium discs 14 mm. diameter one may increase the load in stages of 200 lbs. at a time, before the friction becomes appreciable compared with the normal load.

Experiment to find an Upper Limit to the effect of Friction on Measurements of Compressive Force.

As a final and apparently conclusive test as to whether the effect of the friction between the specimen and the steel plates has a measurable effect on the stresses in the specimen, an experiment was devised in which the friction on two identical discs could be applied so as to act in opposite directions in the two cases. To understand how this end can be attained it is necessary to consider the direction of relative motion of the surfaces of the specimen and the steel plates. If a uniform circular disc of non-crystalline material or of soft metal not cut from a single crystal be compressed between parallel plates without lubrication, the friction on both upper and lower surfaces of the specimen is radial and directed inwards. When a piece cut from a single crystal is compressed it becomes elliptical, and if there were no motion of the upper surface as a whole relative to the lower surface, *i.e.*, if the line joining the centres of the upper and lower elliptic faces remained perpendicular to the plane of the surfaces, the resultants of the friction forces on the upper and on the lower surfaces would each be zero. Actually, however, there is a shearing motion of the upper surface relative to the lower one.* If the upper surface of the specimen moves to the right and the lower one to the left one might expect a resultant friction acting towards the left at the upper surface and to the right at the lower surface. It appears that the effect of these friction forces would be to decrease the shearing force on the plane of slip when a given normal load is applied.

On the other hand, if the upper steel plate could be moved laterally with respect to the lower one as the load was applied the resultant friction would be made to act in any assigned direction.

In the experiment now to be described two identical discs, 69·6 and 69·10, were cut from the same crystal, No. 69. These were compressed between parallel polished steel plates which had a lateral as well as a normal movement relative to one another. In the case of 69·6 the lateral movement of the plates was in the opposite direction to the relative motion of the upper and lower surfaces of the specimen. In the case of No. 69·10 it was in the same direction. The way in which this end was attained is illustrated diagrammatically in fig. 3. In that drawing A_1 and A_2 are the polished steel plates. These were mounted on two solid steel sliders B_1 and B_2 each 1-inch square. The ends of these sliders were cut at 45° to take the steel plates which were carefully fitted to them. The sliders moved without any detectable play between two parallel steel blocks C and D and were carefully greased before every experiment. The apparatus was made so carefully that although no play could be detected in any position, the block B_1 could slide under its own weight very slowly from top to bottom of the slide.

---

* See Part I, vol. 111, p. 531 (1926).

It will be seen that when the plates A_1 and A_2 approach one another so as to decrease the distance between them by a given amount they also move an equal amount laterally because the total movement is at 45° to their polished surfaces.

The distortion of specimens cut from No. 69 has already been examined.* The direction of relative lateral motion of the upper and lower surfaces of the specimen during compression was, therefore, known. This was marked on the upper surface of each of the specimens by means of an arrow. During the tests the specimen was always placed on the lower steel plate with its marked surface up. In the case of 69·6 the specimen was always set so that the arrow pointed upwards along the line of greatest slope on the 45° plate, while in 61·10 the arrow pointed downwards. A side view of a specimen in the machine before compression is shown in fig. 2A. In figs. 2B and 2C are shown the two specimens 69·10 and 69·6 after compression. These sketches illustrate, qualitatively

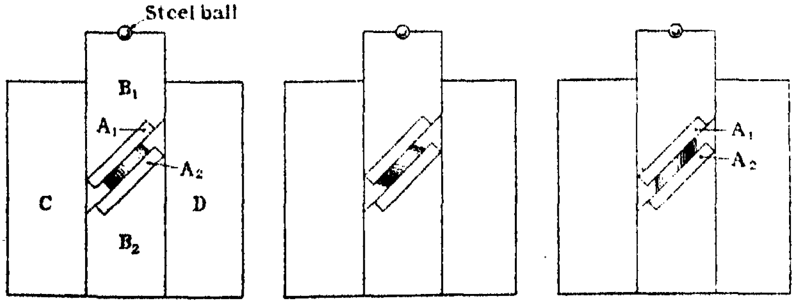

FIG. 2A.—Specimen before compression.

FIG. 2B.—No. 69·10 during compression.

FIG. 2C.—No. 69·6 during compression.

FIG. 2.—Sketch of apparatus for compression of discs between plates set at 45 degrees to their direction of motion.

---

* See Part II, pp. 24 and 29, *supra.*

at any rate, why the friction should tend to help the normal force in producing deformation in the case of 69·10 and to prevent it in the case of 69·6.

It seems unnecessary to give the results of these experiments in tabular form, but they are shown graphically in fig. 3 where the crosses refer to experiments with disc No. 69·10 and the circles to those with 69·6. The ordinates represent the load applied to the slider B, in pounds per square inch of the area of the flat surfaces of the specimens. The abscissæ are the values of ϵ, the ratio of the thickness of the disc to its initial thickness. It will be seen that in spite of the difference in the direction of the friction in the two cases the two sets of points fall almost exactly on the same curve. We may, therefore, deduce that the effect of friction on the load required to produce a given compression is negligible.

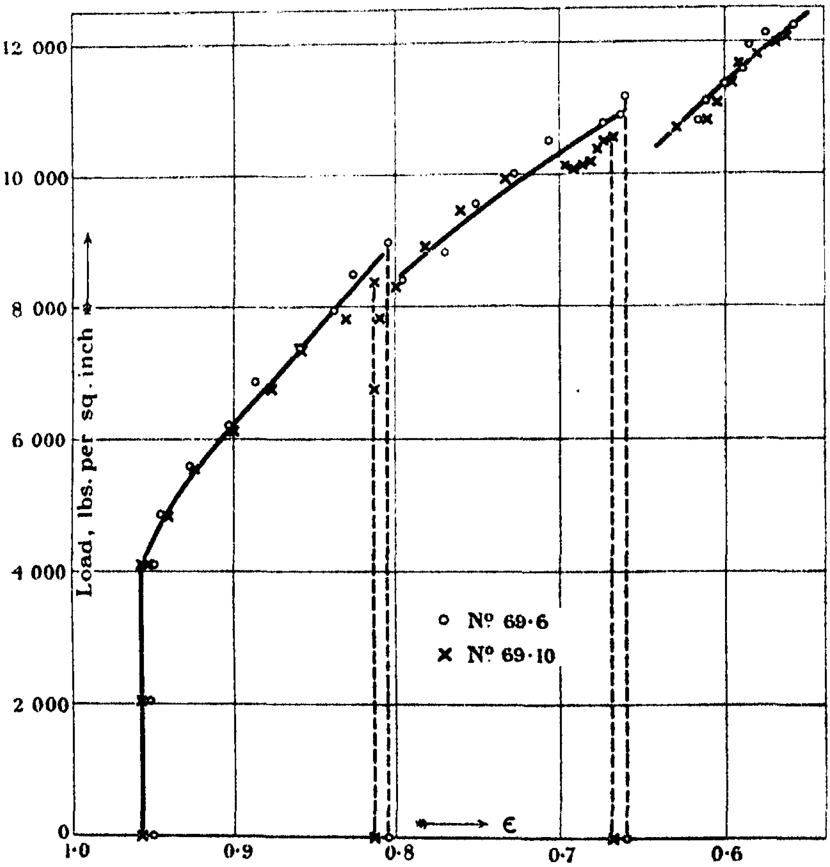

FIG. 3.—Comparison between loads when specimens are compressed with different directions of lateral motion of steel plates.

It will be noticed that the curves are divided into three parts. During the course of the experiment the shearing of the top surface relative to the bottom gave rise to excentricity of loading and to non-uniformity of distortion towards the edges of the specimens. At two stages of the test, namely, $\epsilon = 0 \cdot 804$ and $\epsilon = 0 \cdot 660$ in the case of 69·6, and at $\epsilon = 0 \cdot 813$ and $\epsilon = 0 \cdot 667$ in the case of 69·10, the specimen was reduced in area and turned circular again in order to keep the distortion from becoming non-uniform, and the breaks in the curve are due to these operations.

Another point which will be noticed is that the readings begin at $\epsilon = 0 \cdot 950$ in one case and $\epsilon = 0 \cdot 958$ in the other. This is because the specimens were first compressed about 5 per cent. between parallel plates without lateral motion in order to verify that the direction of lateral movement of the top surface of the specimen relative to the bottom was in the direction it was expected to be.

Methods of Calculation.

It has been seen that when compression experiments are carried out in the manner described above the friction is so small that no appreciable error is likely to occur if its effects are neglected. Under these circumstances one can calculate the component of shear stress parallel to a slip plane in a compression specimen by the method that was previously used in the case of tension specimens. If θ is the angle between a plane of slip and the flat surface of the specimen, η the angle between the direction of slip and the line of greatest slope in the slip plane (the specimen being placed with its flat surfaces horizontal), then the component of shear stress parallel to the direction of slip is $S = (P/a) \sin\theta \cos\theta \cos\eta$ where a is the area of cross section of the specimen and P is the total load.

To find s, the amount of shear corresponding with any degree of compression, one must know the nature of the distortion. Two sets of formulæ will be developed, the first for dealing with cases like that of No. 59 discussed in Part I where the distortion is due to slip on one plane, and the second for dealing with cases like that of 69 discussed in Part II where there is equal slipping on two slip planes situated symmetrically with respect to the axis of the specimen. In cases where the orientation of the axes changes from an unsymmetrical to a symmetrical position during the course of the test both sets of formulæ will be used, the first for the stage of single slipping and the second for the stage of double slipping.

Formulæ for Single Slipping.

Compression Tests.—Take rectangular co-ordinates x, y, z, so that the plane $z = 0$ is parallel to the plane of slip, $0x$ is the direction of slip and 0 is in the upper surface of the specimen. The spherical polar co-ordinates of the normal to the surface of the specimen are (θ, η) where θ, η have the meaning assigned them before. The relation between θ, η and x, y, z is

$$\left.\begin{aligned} x &= r \sin\theta \cos\eta \\ y &= r \sin\theta \sin\eta \\ z &= r \cos\theta \end{aligned}\right\}, \tag{1}$$

where r is the distance of the point considered from the origin.

Let (θ_0, η_0) be the values of (θ, η) before distortion. Consider two particles A and B both in a surface of the specimen. A is situated at distance a from the origin in the line of intersection of the surface of the disc and the slip plane. Its co-ordinates before distortion are evidently

$$(x = -a \sin\eta_0, \quad y = a \cos\eta_0, \quad z = 0),$$

B is situated at distance b from the origin along a line perpendicular to 0A, its co-ordinates before distortion are

$$(x = -b \cos\theta_0 \cos\eta_0, \quad y = -b \cos\theta_0 \sin\eta_0, \quad z = b \sin\theta_0).$$

The area of the rectangle contained between 0A and 0B is ab.

After distortion due to a shear of amount s defined in accordance with the scheme of fig. 1, the co-ordinates of A remain unaltered because it is in the slip plane, which is fixed with respect to the co-ordinates that we are considering. The co-ordinates of B become

$$(x = -b \cos\theta_0 \cos\eta_0 - sb \sin\theta_0, \quad y = -b \cos\theta_0 \sin\eta_0, \quad z = b \sin\theta_0).$$

The perpendicular p from the new position of B on to the line 0A is given by

$$\begin{aligned} (p^2/b^2) &= \sin^2\theta + \{\cos\eta_0(-\cos\theta_0 \cos\eta_0 - s \sin\theta_0) + \sin\theta_0 (-\cos\theta_0 \sin\eta_0)\}^2 \\ &= 1 + 2s \sin\theta_0 \cos\theta_0 \cos\eta_0 + s^2 \sin^2\theta_0 \cos^2\eta_0. \end{aligned}$$

The area of the parallelogram included between 0A and 0B is therefore

$$ab\,(1 + 2s \sin\theta_0 \cos\theta_0 \cos\eta_0 + s^2 \sin^2\theta_0 \cos^2\eta_0)^{\frac{1}{2}}.$$

Since there is no change in volume of the material the thickness multiplied by the area of this parallelogram must be constant. Hence the relationship between s and ε is

$$\varepsilon^{-2} = 1 + 2s \sin\theta_0 \cos\theta_0 \cos\eta_0 + s^2 \sin^2\theta_0 \cos^2\eta_0. \tag{2}$$

The shear stress S is

$$(\mathrm{P}/a) \sin\theta \cos\theta \cos\eta. \tag{3}$$

If a_0 is the area of the original specimen then $a = a_0/\varepsilon$. It has already been pointed out that during a compression test in which the distortion is due to slipping in one plane the axis of the specimen moves relative to the crystal axes in a great circle towards the normal to the slip plane. Hence η is constant and equal to η_0. For compression experiments the connection between θ and θ_0 is

$$\sin\theta = \varepsilon \sin\theta_0.$$

Hence

$$S = (P\varepsilon^2/a_0)\sin\theta_0\cos\eta_0(1-\varepsilon^2\sin^2\theta_0)^{\frac{1}{2}}. \qquad (4)$$

Extension Tests.—The connection between ε and s for tensile test pieces can be found in the same way as for compression tests.

Using rectangular co-ordinates x, y, z which are related to the slip plane and slip direction in the same way as before (see equation (1)) the initial co-ordinates of a point on the axis of the specimen at distance r from the origin are

$$(r\sin\theta_0\cos\eta_0,\quad r\sin\theta_0\sin\eta_0,\quad r\cos\theta_0).$$

After the material has been subjected to a shear s parallel to the plane $z = 0$, and in the direction of the axis of x, the co-ordinates are

$$(r\sin\theta_0\cos\eta_0 + sr\cos\theta_0,\quad r\sin\theta_0\sin\eta_0,\quad r\cos\theta_0),$$

ε the ratio of the final to the initial length* is given by

$$\varepsilon^2 = (\sin\theta_0\cos\eta_0 + s\cos\theta_0)^2 + \sin^2\theta_0\sin^2\eta_0 + \cos^2\theta_0$$

or

$$\varepsilon^2 = 1 + 2s\cos\theta_0\sin\theta_0\cos\eta_0 + s^2\cos^2\theta_0. \qquad (5)$$

The shearing stress S is $S = (T/a)\sin\theta\cos\theta\cos\eta$ where T is the total force applied and a is the area of cross section of the test piece. Using the formulæ† connecting θ, η with θ_0, η_0

$$\left.\begin{aligned}\varepsilon\cos\theta &= \cos\theta_0\\ \varepsilon\sin\theta\sin\eta &= \sin\theta_0\sin\eta_0\end{aligned}\right\}$$

$$S = (T/a_0)\cos\theta_0\{1-\varepsilon^{-2}(\cos^2\theta_0 + \sin^2\theta_0\sin^2\eta_0)\}^{\frac{1}{2}}. \qquad (6)$$

---

* ε has slightly different meanings in tensile and compression experiments. The same symbol is used in the two cases to make the formulæ consistent with those given in previous papers but no confusion need arise.

† "Plastic Extension and Fracture of Aluminium Crystals," 'Roy. Soc. Proc.,' A, vol. 108, p. 49 (1925).

Experimental Results for Slipping on one Plane.

Extension Experiments.—In the course of the experiments in which single crystal bars were extended, the force was measured at each stage of the test and the results are given on p. 45 of "Plastic Extension and Fracture of Aluminium Crystals."* Unfortunately when these tests were made the force was only measured at a few stages in the extension since it was not at that time realised that it would be of interest to have more points on the curves.

It was found that all the specimens had about the same strength for any given value of the extension. On the other hand all the specimens except No. 72 had been cut square so that the surface at any rate had already been slightly distorted before the test began. For this reason only the measurements on No. 72, which was not cut after being formed into a single crystal, are here analysed. The other specimens gave almost identical results, but, as will be seen in the curve (fig. 10, P.E., p. 46), they were less regular.

Referring to P.E., fig. 5, p. 38, it will be seen that No. 72† slips by single slipping up to 50 per cent. extension, but that between 50 and 60 per cent. extension the crystal axes get into the position for double slipping. Accordingly the analysis of No. 72 has only been carried out up to the stage represented by $\varepsilon = 1\cdot511$.

For No. 72 the X-ray examination gave $\theta_0 = 41\cdot9^\circ$, $\eta_0 = 23^\circ$. Using these values in (5) and (6) and the values of T given in Table IV, P.E., p. 45, the values of S and s given in the following Table (1) were found

Table I.

ε.	s.	S (lbs. per sq. in.).
1·000	0	0
1·050	0·105	1930
1·103	0·214	2760
1·202	0·392	3580
1·404	0·734	4590
1·511	0·902	4880

The relationship between S and s is shown in fig. 4 where the points are marked thus ⊙.

Compression Experiments.—Of the three single crystal bars from which compression discs were cut, only two were capable of yielding results about slipping on one crystal plane, because one of them, No. 69, happened to have its crystal axes so disposed that double slipping began almost at the beginning of the test. It has been shown in Parts I and II that slipping on one crystal plane occurred in No. 59 from $\varepsilon = 1\cdot0$ to $\varepsilon = 0\cdot67$, while in No. 61 it occurred from $\varepsilon = 1\cdot0$ to $\varepsilon = 0\cdot815$. Accordingly the measurements have been analysed in these regions by means of formulæ (2) and (4). The results are given in Table II. In the case of No. 61 the distortion was uniform from the beginning of the test whereas in the case of No. 59 the distortion at the edges of the specimen was not uniform in the early stages of the test.* The test on disc No. 59·9 was carried out in two series of stages. The initial diameter of the disc was 14·135 mm. and its thickness was 2·220 mm. It was first compressed by small steps to a thickness of 1·938 mm., *i.e.*, to $\varepsilon = 0\cdot874$. It was then cut down to a disc 8·005 mm. diameter and compressed again till its thickness was 1·496 mm., so that $\varepsilon = 0\cdot674$. During the compression from $\varepsilon = 1\cdot0$ to $\varepsilon = 0\cdot874$ the distortion at the edge of the specimen was not uniform so that the value of S calculated from (4) is not quite the true value, but the values obtained from $\varepsilon = 0\cdot874$ to $\varepsilon = 0\cdot674$, where the distortion was uniform, should be true values of the resistance to slipping. On the other hand the distortion of No. 61 was uniform over the whole disc during compression from $\varepsilon = 1\cdot0$ to $\varepsilon = 0\cdot815$, so that values obtained from formulæ (2) and (4) may be expected to be accurate.

---

* *Loc. cit.*

† There is a misprint in the text, fig. 5 refers to No. 72, not to 73 as indicated there.

The results together with the experimental data are given in Table II. They are also shown graphically in the curve fig. 4, which also shows the results of extension tests.

Table II.—Values of S and *s* for discs 59·9 and 61·17 with data from which they have been calculated.

Disc 59·9, $\theta_0 = 57°$, $\eta_0 = 13°$. Initial diameter 14·135 mm.

Thickness.	Load.	ε.	S.	*s*.
mm.	lbs.		lbs. per sq. in.	
2·220	0	1·00	0	0·000
2·220	112	1·00	199	0·000
2·220	224	1·00	388	0·000
2·218	336	0·999	596	0·002
2·215	448	0·998	796	0·004
2·210	560	0·995	994	0·011
2·208	672	0·994	1190	0·018
2·189	784	0·987	1400	0·027
2·176	896	0·980	1600	0·043
2·168	1010	0·977	1805	0·049
2·143	1200	0·966	2135	0·074
2·105	1400	0·950	2490	0·114
2·046	1600	0·922	2810	0·171
2·007	1800	0·904	3120	0·212
1·938	2000	0·874	3390	0·281

---

* See Part I, p. 543.

Table II—continued.

Disc 59·9 cut down to 8·005 mm. diameter.

Thickness.	Load.	ε.	S.	*s*.
mm.	lbs.		lbs. per sq. in.	
1·938	0	0·874	0	0·281
1·849	500	0·833	2890	0·378
1·845	550	0·831	3160	0·383
1·843	600	0·830	3450	0·385
1·808	650	0·814	3670	0·426
1·766	700	0·796	3840	0·477
1·720	750	0·774	3970	0·530
1·681	800	0·757	4110	0·577
1·643	850	0·740	4250	0·624
1·615	900	0·728	4400	0·679
1·595	950	0·718	4560	0·684
1·554	1000	0·700	4630	0·738
1·530	1050	0·689	4740	0·776
1·496	1100	0·674	4810	0·823

Disc 61·17, $\theta_0 = 46°$, $\eta_0 = 17°$. Initial diameter 14·16 mm.

Thickness.	Load.	ε.	S.	*s*.
mm.	lbs.		lbs. per sq. in.	
3·114	0	1·000	0	0
3·102	100	0·9962	194	0·007
3·090	200	0·9923	389	0·016
3·086	300	0·9910	581	0·019
3·084	400	0·9904	774	0·021
3·070	500	0·986	967	0·030
3·064	600	0·984	1157	0·033
3·048	700	0·979	1340	0·044
3·033	800	0·974	1530	0·056
3·010	900	0·967	1715	0·073
2·986	1000	0·960	1910	0·089
2·950	1100	0·950	2040	0·108
2·928	1200	0·940	2200	0·120
2·892	1300	0·929	2350	0·153
2·864	1400	0·920	2500	0·176
2·831	1500	0·909	2640	0·196
2·795	1600	0·899	2780	0·225
2·763	1700	0·887	2900	0·253
2·737	1800	0·879	3120	0·274
2·713	1900	0·871	3160	0·291
2·668	2000	0·857	3250	0·327
2·631	2100	0·845	3350	0·356
2·601	2200	0·835	3460	0·383
2·560	2300	0·822	3530	0·417
2·530	2325	0·812		
2·510	2330	0·806		

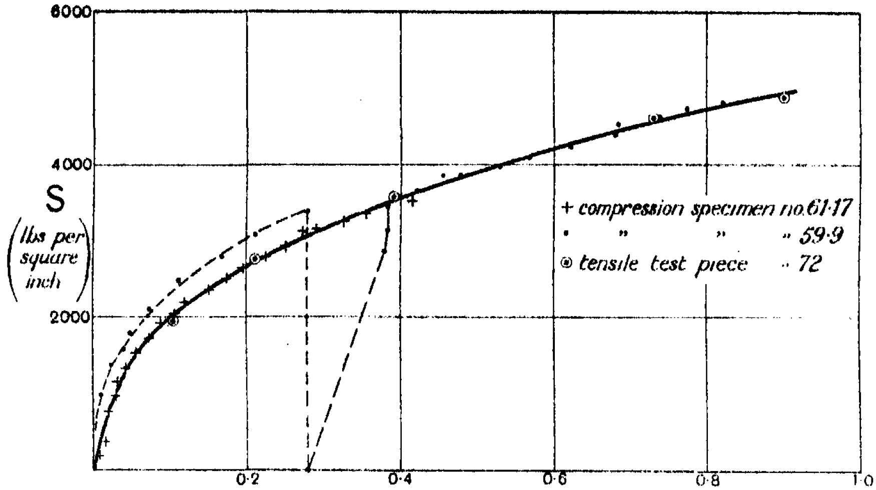

Fig. 4.—Relationship between S and ϵ for tensile and compression specimens when slipping on one plane.

Inspection of that figure reveals two facts. First the points corresponding with the compression of 59·9 from $\epsilon = 0\cdot874$ to $\epsilon = 0\cdot674$ lie in a continuous curve with the points representing the compression of 61·17 from $\epsilon = 1\cdot0$ to $\epsilon = 0\cdot815$. The points representing the compression of 59·9 from $\epsilon = 1\cdot0$ to $\epsilon = 0\cdot874$ are above the curve representing the compression for 61·17. This is evidently the effect of want of uniformity in the distortion of 59·9 in the early stages of compression, for the difference between the two specimens disappears as soon as the non-uniform part of the specimen has been removed. The points corresponding with the early stages of compression for 59·9 have been connected by a dotted curve in fig. 4. The portion between $\epsilon = 0\cdot874$ and $\epsilon = 0\cdot833$ is missing because the first load applied after cutting down the specimen was greater than it should have been.

The second point which should be noticed is that the points deduced from extension experiments lie on the same curve as the points deduced from compression experiments. This is interesting because it means that it is immaterial whether the component of force normal to the slip plane is a tension or a compression, the resistance to slipping for a given amount of distortion is identical in the two cases.

It has been shown by Dr. E. Schmid* that in the case of stretched crystals the resistance to shear parallel to the slip plane is independent of the component of tension normal to the plane of slip. The present measurements extend this result to a case where the force normal to the slip plane changes from a tensile to a compressive force.

---

* *Loc. cit.*

Double Slipping.—In the case of a material which slips equally on two planes it is necessary to define a quantity to represent the amount of slipping. Such a definition has been given in Part II where the total amount of slip s defining the state of the material at any stage is the sum of all the elements of shear on the two planes separately. Thus a small amount δs of double slipping is conceived to consist of two small shears each equal to $\frac{1}{2}\delta s$ on each of the two planes of slip concerned. These two elements of single slipping, which go to make up the element of double slipping may be conceived so far as the geometry of the distortion is concerned to occur consecutively—not simultaneously.

With slipping on one crystal plane we have seen that each increase in the amount of shear implies a corresponding increase in the resistance to shear. If each of the two elements of shear $\frac{1}{2}\delta s$ which combine to make an element δs of double slipping contribute the same increase of resistance to shear on all the crystal planes that they would if the material were undergoing distortion by slipping on one plane, then it will be seen that the values of S for any given value of s would be the same whether the distortion had proceeded by single or by double slipping. If, therefore, the values of $S = (P/a) \cos\theta \sin\theta \cos\eta$ and s, as defined, are calculated, and the results plotted on a diagram similar to that of fig. 4, any difference between the curve for double slipping, and the curve for single slipping will be due to the effect of simultaneous slipping, on two planes as distinct from the sum of the effects of slipping on each of the planes considered separately.

Formulæ for Double Slipping.—The connection between ϵ and s has been given in equation (8) of Part II.

It is

$$A^2(1 + 2\sin i_0 \cos i_0) - 2A(\sin i_0 \cos i_0 + \sin^2 i_0) + 2\sin^2 i_0 - \epsilon_2^{-2} = 0, \quad (7)$$

where

$$s_2 = 5\cdot640 \log_{10} A. \quad (7\text{A})$$

ϵ_2 is the ratio of the thickness at the stage concerned to the thickness when double slipping began. s_2 is the amount of shear which has occurred since the crystal axes got into the symmetrical position for double slipping. If s_1 is the amount of shear which occurred by single slipping before the double slipping began, then s, the total amount of shear, may be defined as $s = s_1 + s_2$. If ϵ_1 is the value of ϵ when double slipping began, then evidently ϵ, defined as the ratio of the thickness at any stage to the initial thickness at the beginning of the test, is equal to $\epsilon_1\epsilon_2$. The symbol i_0 represents the angle between the line of intersection of the two planes of slip and the flat face of the specimen at the time when double slipping began. (See fig. 8, Part II.)

The component of shear stress S is

$$(\mathrm{P}/a) \cos\theta \sin\theta \cos\eta, \tag{8A}$$

where a is the area of the disc and P the total load. In the symmetrical position both θ and η are evidently functions of i the angle between the line of intersection of the slip planes and the plane of the disc. The slip planes each make an angle of 54° 44′ with the symmetrical {100} plane which contains the normal to the plane of the disc. The direction of slip makes an angle of 60° with the intersection of the two slip planes. Using these relations it can be shown that

$$\cos\theta \sin\theta \cos\eta = \frac{1}{\sqrt{6}}\left(\frac{1 + \tan i}{1 + \tan^2 i}\right). \tag{8B}$$

The relationship between i and i_0 is given in equation (9), Part II. It is

$$\cot i = \mathrm{A}(\cot i_0 + 1) - 1. \tag{9}$$

Application to Nos. 69·9 *and* 61·17.

In the case of No. 69 where the crystal axes were in the position for double slipping at the beginning of the test $i_0 = 12°$ and $s_1 = 0$.

The equation for A is

$$1{\cdot}4067\mathrm{A}^2 - 0{\cdot}4928\mathrm{A} + 0{\cdot}0862 - \epsilon^{-2} = 0. \tag{10}$$

Using this equation a series of values of ϵ were taken and the corresponding values of A were found. These are given in columns 1 and 2 of Table III. Using the formula (7A) the values of s given in column 3 were found. The relationship between s and ϵ was then plotted in the curve shown in fig. 5.

To find the corresponding values of $\cos\theta \sin\theta \cos\eta$ the values of $\cot i$ were first calculated by means of equation (9). The corresponding values of i in degrees are given in column 4 of Table III. These were then inserted in equation (8B) and the values of $\cos\theta \sin\theta \cos\eta$ given in column 5 were calculated. These were plotted on the same diagram, fig. 5, as the values of s and the two curves were used with the measured values of P and ϵ to deduce the values of S and s given in columns 4 and 5 of Table IV.

Table III.—Showing the calculated values of A, i, and $\cos\theta\sin\theta\cos\eta$ assuming equal double slipping and $i_0 = 12°$.

ϵ.	A.	s.	i.	$\cos\theta\sin\theta\cos\eta$
1·00	1·000	0·000	12°	0·473
0·95	1·045	0·108	11·4	0·471
0·90	1·096	0·224	10·8	0·468
0·85	1·150	0·346	10·2	0·466
0·80	1·215	0·477	9·6	0·463
0·75	1·285	0·614	9·0	0·461
0·70	1·368	0·768	8·4	0·458
0·65	1·461	0·929	7·7	0·455
0·60	1·571	1·107	7·1	0·452
0·55	1·698	1·298	6·6	0·450
0·50	1·352	1·510	6·0	0·447
0·45	2·040	1·747	5·4	0·443
0·40	2·275	2·014	4·8	0·439
0·35	2·577	2·320	4·2	0·435
0·30	2·978	2·674	3·6	0·431
0·25	3·542	3·097	3·0	0·428
0·20	4·390	3·624	2·3	0·424
0·10	8·603	5·265	1·2	0·416
0	∞	∞	0	0·408

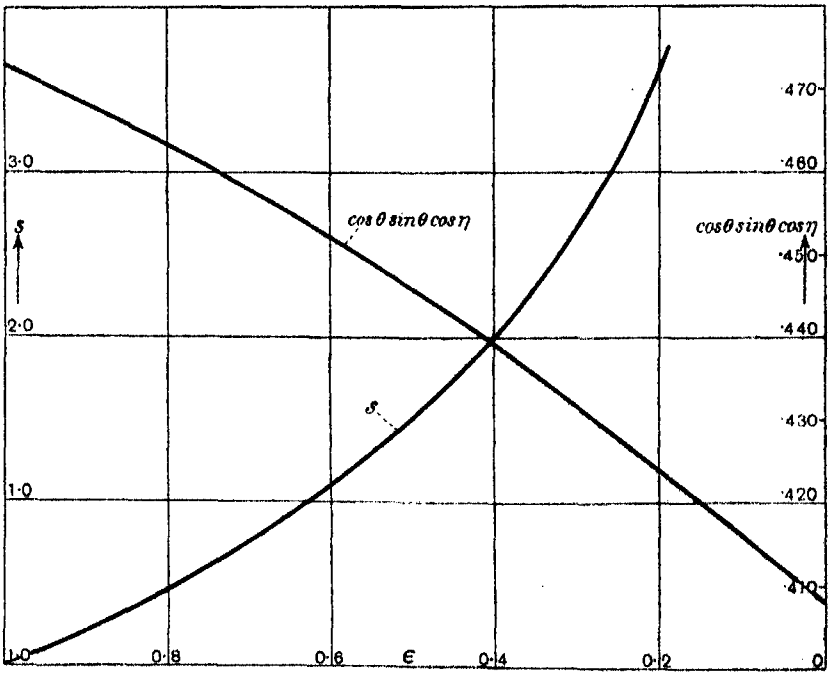

Fig. 5.—Calculated values of s and $\cos\theta\sin\theta\cos\eta$ during compression of discs cut from specimen No. 69.

Table IV.—*No. 69·9. First stage. Double slipping from beginning of test.* $i_0 = 12°$. Initial diameter 14·42 mm.

Thickness.	Load.	ε.	S.	*s*.
mm.	lbs.		lbs. per sq. in.	
2·904	0	1·00	0	0·000
2·895	100	0·997	192	0·006
2·892	200	0·996	385	0·008
2·885	400	0·994	767	0·012
2·875	600	0·990	1145	0·020
2·859	800	0·984	1520	0·032
2·833	1000	0·976	1880	0·050
2·795	1200	0·963	2220	0·080
2·753	1400	0·948	2550	0·111
2·717	1600	0·935	2860	0·142
2·674	1800	0·921	3160	0·174
2·617	2000	0·901	3430	0·220
2·562	2200	0·882	3790	0·260
2·510	2400	0·864	3930	0·304
2·490	2400	0·857	3910	0·320
2·462	2500	0·848	4020	0·342
2·424	2600	0·834	4100	0·380
2·388	2700	0·822	4190	0·415
2·366	2800	0·814	4300	0·432
2·340	2900	0·806	4400	0·453
2·305	3000	0·794	4500	0·485
2·277	3100	0·784	4570	0·510
2·246	3200	0·773	4660	0·545
2·212	3300	0·762	4720	0·570
2·189	3400	0·754	4800	0·595

No. 69·9. Second stage. Cut down to disc 10·36 mm. diameter.

Thickness.	Load.	ε.	S.	*s*.
mm.	lbs.		lbs. per sq. in.	
2·189	0	0·754	0	0·595
2·186	1000	0·753	3790	0·600
2·180	1100	0·750	4150	0·606
2·169	1200	0·746	4500	0·620
2·158	1250	0·743	4670	0·629
2·154	1300	0·742	4840	0·630
2·138	1350	0·736	4980	0·650
2·135	1400	0·735	5160	0·656
2·064	1450	0·710	5180	0·731
2·064	1500	0·710	5350	0·731
2·034	1550	0·700	5430	0·768
2·000	1600	0·689	5500	0·803
1·995	1650	0·687	5650	0·809
1·986	1700	0·684	5800	0·820
1·950	1750	0·671	5850	0·860
1·938	1800	0·667	5980	0·873
1·928	1850	0·664	6110	0·885
1·878	1900	0·646	6110	0·943
1·872	1950	0·644	6220	0·950
1·840	2000	0·634	6280	0·984
1·830	2050	0·630	6400	1·000
1·830	2050	0·630	6400	1·000
1·790	2100	0·616	6410	1·050

Table IV—continued.

No. 69·9. Third stage. Cut down to 8·560 mm. diameter.

Thickness.	Load.	ε.	S.	s.
mm.	lbs.		lbs. per sq. in.	
1·790	0	0·616	0	1·050
1·760	1150	0·606	5740	1·090
1·750	1200	0·602	5940	1·105
1·720	1250	0·592	6090	1·149
1·670	1300	0·575	6140	1·213
1·612	1350	0·554	6110	1·305
1·606	1400	0·553	6350	1·310
1·582	1450	0·544	6440	1·345
1·526	1500	0·525	6430	1·423
1·480	1550	0·509	6430	1·490
1·400	1700	0·482	6640	1·615
1·398	1750	0·481	6830	1·620
1·397	1800	0·481	7000	1·620
1·387	1850	0·477	7140	1·635
1·321	1900	0·455	6950	1·735

No. 69·9. Fourth stage. Cut down to 7·047 mm. diameter.

Thickness.	Load.	ε.	S.	s.
mm.	lbs.		lbs. per sq. in.	
1·321	0	0·4550	0	1·735
1·316	800	0·4530	5840	1·740
1·314	850	0·4525	6200	1·740
1·310	900	0·4510	6550	1·750
1·308	950	0·4505	6920	1·750
1·304	1000	0·4490	7240	1·760
1·278	1050	0·4400	7400	1·805
1·224	1100	0·4213	7460	1·900
1·178	1150	0·4055	7460	1·992
1·121	1200	0·3860	7400	2·093
1·104	1250	0·3800	7580	2·130
1·085	1300	0·3735	7710	2·173
1·032	1350	0·3553	7610	2·285
1·013	1400	0·3490	7710	2·330

No. 69·9. Fifth stage. Cut down to 6·950 mm. diameter.

Thickness.	Load.	ε.	S.	s.
mm.	lbs.		lbs. per sq. in.	
1·013	0	0·3490	0	2·330
1·010	900	0·3480	6650	2·335
0·991	950	0·3413	6990	2·385
0·982	1000	0·3382	7170	2·400
0·951	1050	0·3273	7270	2·480
0·927	1100	0·3190	7420	2·537
0·905	1150	0·3116	7560	2·595
0·875	1200	0·3013	7600	2·670
0·859	1250	0·2958	7780	2·710
0·837	1300	0·2880	7860	2·770
0·818	1350	0·2817	7980	2·820
0·806	1400	0·2776	8140	2·855

It will be noticed that in (8A) the area of the disc occurs. This was not measured in each case. The compression was carried out in a series of stages at the beginning of each of which the specimen was cut circular. Since there is no change in volume the value of $a\varepsilon$ is constant during each of these stages, and the value of a was calculated from this relationship.

In the case of 61·17 the specimen was first compressed to $\varepsilon = 0 \cdot 815$ and the formulæ applicable to single slipping were used. The value of s_1 at the end of the stage of slipping on one plane was $s_1 = 0 \cdot 435$. The value of i_0 at this stage was 7·2°. The values of S and s, *i.e.*, $s_1 + s_2$ corresponding with each value of ε during the period of double slipping are given in columns 4 and 5 of Table V.

Table V.—No. 61·17. Second stage of compression. Double slipping begins at $\varepsilon = 0 \cdot 815$ and then $i_0 = 7 \cdot 2°$ and $s_1 = 0 \cdot 435$. Disc cut down to 13·863 mm. diameter.

Thickness.	Load.	ε.	S.	$s_1 + s_2$.
mm.	lbs.		lbs. per sq. in.	
2·508	1800	0·805	3480	0·455
2·496	1900	0·802	3650	0·460
2·483	2000	0·798	3830	0·473
2·474	2100	0·795	4000	0·480
2·456	2200	0·789	4160	0·500
2·438	2250	0·783	4230	0·512
2·420	2300	0·777	4260	0·535
2·403	2350	0·772	4340	0·545
2·397	2400	0·770	4430	0·550
2·394	2450	0·769	4520	0·552
2·366	2500	0·760	4540	0·578
2·353	2550	0·756	4610	0·590
2·344	2600	0·753	4680	0·600
2·328	2650	0·748	4730	0·615
2·306	2700	0·740	4760	0·638
2·302	2750	0·739	4850	0·642
2·275	2800	0·731	4875	0·670
2·254	2850	0·724	4920	0·694
2·238	2900	0·719	4960	0·708
2·226	2950	0·715	5010	0·720
2·218	3000	0·712	5080	0·730
2·203	3050	0·708	5130	0·740
2·197	3100	0·706	5200	0·750

Table V—continued.

No. 61·17. Third stage. Cut down to disc 10·028 mm. diameter.

Thickness.	Load.	ε.	S.	$s_1 + s_2$.
mm.	lbs.		lbs. per sq. in.	
2·198	0	0·706	0	0·750
2·122	1500	0·682	5280	0·825
2·091	1550	0·671	5370	0·860
2·060	1600	0·662	5450	0·890
2·039	1650	0·654	5550	0·916
2·009	1700	0·645	5660	0·945
1·992	1750	0·640	5740	0·965
1·970	1800	0·632	5850	0·990
1·942	1850	0·623	5910	1·022
1·914	1900	0·614	5990	1·052
1·899	1950	0·610	6100	1·075
1·859	2000	0·597	6100	1·125
1·849	2050	0·593	6220	1·138

No. 61·17. Fourth stage. Cut down to disc 8·522 mm. diameter.

Thickness.	Load.	ε.	S.	$s_1 + s_2$.
mm.	lbs.		lbs. per sq. in.	
1·849	0	0·593	0	1·140
1·848	1100	0·593	5490	1·140
1·838	1150	0·590	5710	1·155
1·823	1200	0·585	5900	1·170
1·821	1250	0·584	6140	1·175
1·814	1300	0·582	6370	1·185
1·798	1350	0·577	6540	1·203
1·745	1400	0·560	6570	1·278
1·715	1450	0·559	6680	1·315
1·706	1500	0·548	6860	1·325
1·652	1550	0·530	6870	1·400
1·640	1600	0·526	6910	1·417
1·605	1650	0·515	6970	1·460
1·540	1700	0·495	6900	1·555
1·502	1750	0·482	6900	1·615

No. 61·17. Fifth stage. Cut down to disc 7·531 mm. diameter.

Thickness.	Load.	ε.	S.	$s_1 + s_2$.
mm.	lbs.		lbs. per sq. in.	
1·502	0	0·482	0	1·615
1·495	900	0·480	5670	1·625
1·493	1000	0·479	6280	1·628
1·492	1050	0·479	6600	1·630
1·488	1100	0·478	6890	1·635
1·485	1150	0·477	7160	1·640
1·446	1200	0·464	7280	1·705
1·348	1250	0·433	7050	1·863
1·342	1300	0·432	7260	1·870
1·309	1350	0·420	7360	1·940
1·275	1400	0·409	7420	1·998
1·248	1450	0·401	7530	2·040
1·208	1500	0·388	7540	2·110
1·190	1550	0·382	7650	2·140
1·175	1600	0·377	7800	2·172

In both cases the test was carried out in several stages. Specimen No. 69·9 was compressed in five stages. At the beginning of the first stage the thickness was 2·904 mm. and the diameter 14·2 mm. It was then compressed to a thickness of 2·189 mm., *i.e.*, to $\epsilon = 0\cdot754$ in 23 steps, the specimen being removed from between the steel plates and covered with a layer of grease before each of these 23 increases in load.

The successive stages were :—

Stage 2 cut down to diameter 10·36 mm. and compressed from $\epsilon = 0\cdot754$ to 0·616 in 22 steps.

Stage 3 cut down to diameter 8·56 mm. and compressed from $\epsilon = 0\cdot616$ to 0·455 in 23 steps.

Stage 4 cut down to diameter 7·047 mm. and compressed from $\epsilon = 0\cdot455$ to 0·349 in 13 steps.

Stage 5 cut down to diameter 6·950 mm. and compressed from $\epsilon = 0\cdot349$ to 0·2776 in 11 steps.

In the case of No. 61·17 the stages were :—

Stage 1 diameter 14·15 mm. compressed from $\epsilon = 1\cdot0$ to $\epsilon = 0\cdot806$ in 26 steps.

Stage 2 diameter 13·86 mm. compressed from $\epsilon = 0\cdot806$ to $\epsilon = 0\cdot706$ in 22 steps.

Stage 3 diameter 10·028 mm. compressed from $\epsilon = 0\cdot706$ to $\epsilon = 0\cdot593$ in 12 steps.

Stage 4 diameter 8·522 mm. compressed from $\epsilon = 0\cdot593$ to $\epsilon = 0\cdot482$ in 14 steps.

Stage 5 diameter 7·531 mm. compressed from $\epsilon = 0\cdot482$ to $\epsilon = 0\cdot3775$ in 15 steps.

The results given in Tables IV and V are represented in fig. 6. In that diagram the dots refer to experiments with 69·9 and the crosses to experiments with 61·17. Dotted lines have been drawn corresponding with the values of ϵ at which the specimens were cut down. For comparison the curve for single slipping has been transferred from fig. 4 and marked on fig. 6.

It will be seen that the curve for 69·9 lies above the single slipping curve, thus proving that the material hardens more rapidly when a given total amount of slipping is divided equally between two planes than when it is all on one plane. The effect is not very large, amounting roughly to about 20 per cent.

Another point which is noticeable in the curve is that the resistance to shear

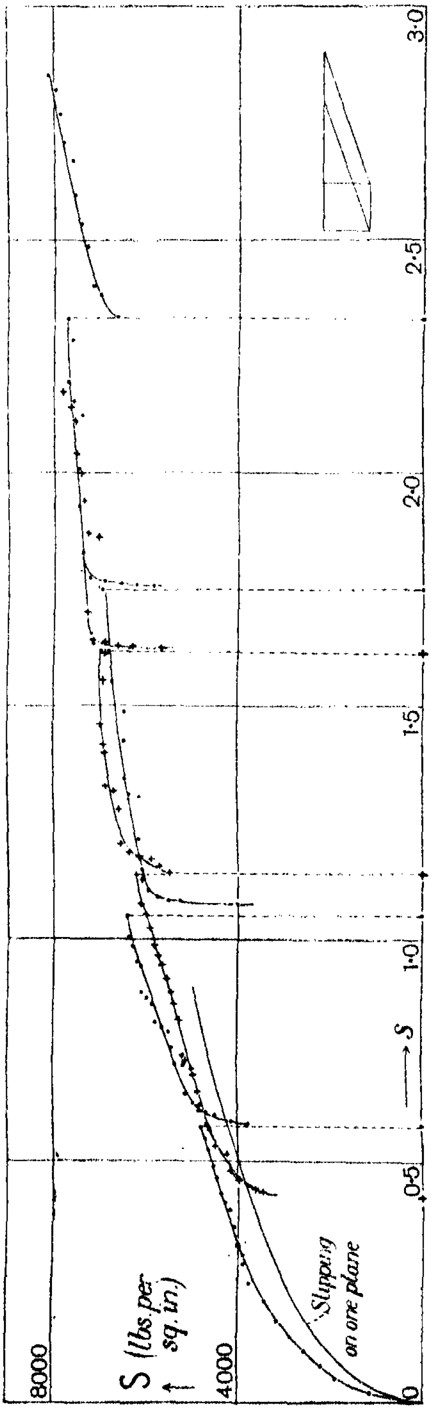

Fig. 6.—Results of compression tests on specimens Nos. 69·9 and 61·17. ● No. 69·9, + No. 61·17.

goes on increasing steadily up to the end of the test when the distortion is very great. A small diagram is inset in fig. 6 to show the amount of shear corresponding with the last point on the curve. This represents the distorted position of a cube sheared by single slipping by an amount equal to the maximum value of s.

It will be noticed that the curve corresponding with the last stage in the compression of 69·9 is not quite continuous with the curve for the first four stages of the compression. This is probably due to the fact that the material was disturbed by scratching six lines on the surface before the last compression in order to measure the distortion in the last stage.*

In conclusion I wish to express my thanks to Sir Ernest Rutherford for allowing the work to be carried out in the Cavendish Laboratory, to Miss Elam for supplying the single crystals with which the experiments were carried out, and to Mr. Farren for his help in designing some of the apparatus used, particularly that shown in fig. 2. The compression measurements were made with a Buckton compression machine in the Cambridge Engineering Laboratory, by kind permission of Prof. Inglis.

---

* This was described in Part II.

The Magnetic Susceptibility of some Binary Alloys.

By J. F. Spencer, Ph.D., D.Sc., and Miss M. E. John, M.Sc.,
Bedford College, University of London.

(Communicated by W. Wilson, F.R.S.—Received February 17, 1927.)

The object of this research has been to find a connection between the mass susceptibility and chemical composition of a number of binary alloys of several metals. The susceptibility measurements were made with the aid of a Curie and Cheneveau* magnetic balance, the permanent magnet of which produced a field with an intensity of about 640 gauss. It was found early in the work that the method of attachment of the torsion wire to the balance beam and to the torsion head was not satisfactory; consequently the hook and loop arrangement was replaced by a small clamp and screw, which was attached to the beam of the balance and the torsion head. Since the torsion wire was very thin it became necessary, in order to fasten it rigidly at both ends, to face the jaws of the clamps with thin lead foil. This arrangement ensured a perfectly satisfactory attachment of the torsion wire. The torsion wires used were of platinum 0·10 mm. diameter. To obtain concordant readings it was found necessary to anneal the wires before use. This was achieved by suspending the wire under a slight stress and passing a slowly increasing current of electricity through it, over a period of 30 minutes, until the temperature reached 150° C. When this temperature was reached, the current was maintained steady for 30 minutes and then slowly reduced to zero, a further 30 minutes being taken for the reduction. During the heating the wire was seen to untwist, so that the effect of annealing appears to be the removal of a twist imparted to the wire during drawing. Annealed torsion wires gave reproducible deflections which, on the whole, were greater than those obtained with unannealed wires.

The experiments to be described were made with materials of low susceptibility, and consequently the difference between the deflections for the two positions of the permanent magnet was rather small. To increase the accuracy of the readings, a method of oscillation was adopted. The magnet was placed in one of the positions of maximum deflection and the balance arm with its load allowed to oscillate freely. After a few minutes the oscillation had died down sufficiently for the turning points of a spot of light, reflected from a mirror on the balance arm, to be read easily on a millimetre scale situated 200 cms. from the mirror. Five successive turning points were taken, three on one side of the zero and two on the other side, from which the position of rest was calculated. This position was obtained five times for each position of the magnet, and the mean values for each position accepted as the deflection due to the specimen. Adoption of this practice enabled the deflections to be read to 0·05 mm. The readings obtained in this way were identical with those obtained by allowing the beam to come to rest, and they were obtained much more rapidly.

---

* 'J. de Physique,' vol. 2, p. 796 (1903).

Pure water, which has a mass susceptibility* at ordinary temperatures of $-0{\cdot}72 \times 10^{-6}$, was used as the comparison substance in all determinations.

Preparations of the Alloys.

The binary alloys of gold with lead, tin and cadmium, lead with silver, tin and bismuth, and tin with aluminium and cadmium, have been examined over the entire range of compositions. The metals from which these alloys were prepared were the purest obtainable. Each metal was analysed before use, particular care being taken to ascertain that iron was not present in appreciable quantity. The lead, tin, bismuth, cadmium and aluminium were obtained from Kahlbaums, and in every case a certificate of purity accompanied the metal. Gold, 0·9995 — 0·9999 fine, and pure silver were supplied by Messrs. Johnson and Matthey. Portions of the pure metals and alloys were dissolved in a suitable solvent and the neutral solution tested for the presence of iron by means of potassium thiocyanate. No specimen was measured if the neutral solution gave more than the faintest coloration by the above test.

Suitable quantities of the metals were melted together in a vitreosil crucible in an electric furnace, the molten mass was thoroughly mixed and cast into a rod, 4 mm. diameter and about 4 cm. long, in a plaster mould. When cold the rod was removed from the mould, freed from adhering plaster by scrubbing with water, and dried. A portion 8 mm. long was cut from the middle of the rod for the test specimen and a piece from either side of the test piece was analysed. The analysis of all alloys containing either gold or silver was effected by cupellation; the remaining alloys, all of which contain tin, were analysed by converting the tin into metastannic acid and weighing tin dioxide. The mean composition of the two pieces analysed was taken as the composition of the test piece provided that the composition of the contiguous pieces did not differ by more than 0·1 per cent. This difference was rarely exceeded, and when it was exceeded the alloy was remelted and recast after further mixing. The test piece was trimmed exactly to a length 0·65 cm. and a diameter 0·36 cm. It was then washed in hydrochloric acid to remove possible traces of iron which may have become attached to it during the trimming. The washing was repeated until a constant value was obtained for the susceptibility. In no case was the test piece annealed before measurement.

---

* Wills, 'Phys. Rev.,' vol. 20, p. 158 (1905); Sève, 'Ann. chim. phys.,' vol. 27, pp. 189, 425 (1912).

Method of Measurement.

For measurement the alloys were placed in a thin-walled glass tube of low susceptibility, 0·40 cm. internal diameter and 8 cm. long, which was closed by a cork to which a soft copper hook was attached. The hook was of such a length that the specimen lay in the centre of the magnetic field when the tube was attached to the balance arm. After the specimen had been suspended in the field for about 15 minutes, the deflection of the beam was measured for both positions of the magnet as described above. The deflections caused by the empty tube and by the tube containing "conductivity water" were then measured. The amount of water used was such that it filled the measuring tube to the same height as the metal specimen, thereby ensuring that the specimen and the comparison substance occupied the same position in the magnetic field. The measurements were made at room temperature. The actual temperatures are given below, with the susceptibility values.

The mass susceptibility was calculated from the measurements by Curie's formula. If Δ is the difference between the deflections of the balance arm for the two positions of the magnet, when loaded with a metal specimen of mass m, Δ' that for the same tube containing a mass of water m', and Δ'' the difference for the empty tube, then

$$\frac{k}{k'} = \frac{\Delta - \Delta''}{\Delta' - \Delta''} \frac{m'}{m} = r,$$

where k is the susceptibility per unit mass of the metal and k' that of water. The formula takes no account of the magnetisation of the air, and a correction must be applied in the form

$$\frac{k}{k'} = r\left[1 + 0{\cdot}041\left(\frac{1}{r\mathrm{D}} + 1\right)\right],$$

where D is the density of the specimen.

The density of the alloys in all cases but that of the series of gold-cadmium alloys was taken from existing measurements, those of the aluminium-tin alloys from Shepherd's[*] values, and those of the remaining series of alloys from results published by E. von Maey.[*] Values for the density of gold-cadmium alloys were obtained experimentally as described below.

---

[*] 'J. phys. Chem.,' vol. 8, p. 248 (1904).

The susceptibility values are recorded in Tables I to X, each value being the mean of five closely agreeing determinations.

Susceptibility of the Pure Metals.

The mass susceptibility of the metals from which the alloys were prepared are given in Table I, and for comparison the values determined by K. Honda[†] and M. Owen[‡] are added.

Table I.

Metal.	$k \times 10^6$.	Temperature.	Honda and Owen.
		° C.	
Silver	−0·201	19	−0·20.
Lead	−0·119	20	−0·12.
Cadmium	−0·156	19	−0·18 (Owen); −0·17 (Honda).
Tin	+0·044	20	+0·02 (Owen); +0·025 (Honda).
Gold	−0·118	20·5	−0·15.
Aluminium	+0·583	18	+0·60 (Owen); +0·65 (Honda).
Bismuth	−1·24	20	−1·40.

The susceptibility of most of the metals has been determined by others at various times, but in most cases insufficient information is given of the purity of the material used. The values of Honda and Owen take into account the iron present in the specimens measured. These two sets of measurements agree extremely well; where differences occur they are indicated in the table. The

Table II.—Silver-Lead alloys. Temperature 19° to 20° C.

Specimen.	Pb per cent.	Pb atoms per cent.	Density.	$k \times 10^6$.
Pure Pb	100·00	100·00	11·376	−0·119
Alloy A	90·38	83·04	11·220	−0·116
,, B	85·40	75·31	11·176	−0·123
,, C	79·28	66·54	11·100	−0·103
,, D	69·85	54·70	11·072	−0·116
,, E	59·86	43·63	11·000	−0·078
,, F	47·64	32·07	10·917	+0·272
,, G	38·80	24·80	10·845	+1·840
,, H	29·21	17·69	10·695	+2·032
,, I	15·11	8·39	10·626	+1·184
,, J	3·60	1·84	10·508	+0·401
Pure Ag	0·00	0·00	10·468	−0·201

---

[*] 'Z. phys. Chem.,' vol. 38, p. 295 (1901).

[†] 'Ann. d. Physik,' vol. 32, p. 1027 (1920).

[‡] 'Ann. d. Physik,' vol. 37, p. 657 (1912).

present values for silver, lead and aluminium are very close to those of Honda and Owen, whilst the remaining values are sufficiently close in view of the fact that the present measurements were made in a field of 640 gauss, whilst those of Honda and Owen were made in much larger fields.

The change of susceptibility with composition is shown in curve I, fig. 1. The alloys containing up to 30 per cent. of silver have susceptibilities which are very close to the value for pure lead, whilst the alloys containing 55 and 0·9 per cent. lead respectively are non-magnetic. The curve shows a very pronounced maximum at about 29·2 per cent. of lead. The alloys corresponding with this point contain the two metals in the atomic ratio Ag : Pb = 4·65 : 1 ; which may indicate the existence of an intermetallic compound Ag_9Pb_2, although the freezing-point curve of silver-lead alloys as determined by Friedrich* and Haycock and Neville† gives no indication of the formation of any intermetallic compounds of these elements. It is noteworthy that the maximum susceptibility of these alloys lies well inside the paramagnetic region, whilst both constituents are diamagnetic.

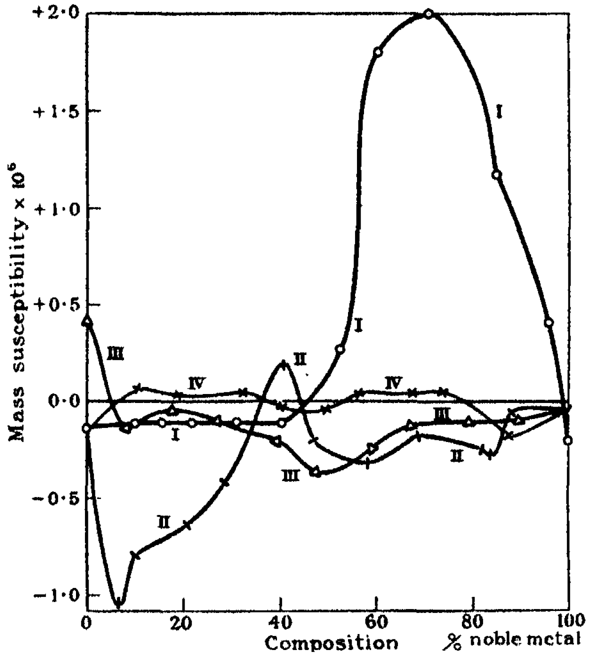

FIG. 1.—Change of Mass Susceptibility with Composition. I, Silver-lead ; II, Gold-lead ; III, Silver-tin ; IV, Gold-cadmium.

---

* 'Métallurgie,' vol. 3, p. 398 (1906).

† 'Phil. Trans.,' A, vol. 189, p. 25 (1897).

Table III.—Gold-Lead Alloys. Temperature 19° to 22° C.

Specimen.	Pb per cent.	Pb atoms per cent.	Density.	$k \times 10^6$.
Pure Pb	100·00	100·00	11·376	−0·119
Alloy A	93·995	93·79	11·68	−1·056
,, B	88·61	88·22	12·02	−0·829
,, C	79·61	78·85	12·52	−0·610
,, D	71·69	70·96	13·00	−0·438
,, E	58·54	57·31	13·92	+0·183
,, F	52·62	51·42	14·38	−0·209
,, G	41·91	40·72	15·08	−0·301
,, H	32·02	30·92	15·78	−0·191
,, I	18·58	17·76	17·22	−0·264
,, J	16·68	15·93	17·42	−0·296
,, K	11·08	10·53	17·98	−0·045
Pure Au	0·00	0·00	19·27	−0·118

The susceptibility values are plotted against composition in curve II, fig. 1, gold-lead alloys containing about 62 and 56 per cent. of lead respectively are non-magnetic, whilst the alloy containing 94 per cent. of lead and corresponding to the marked minimum in the curve is about 10 times as strongly diamagnetic as either constituent. A very sharp maximum occurs in the paramagnetic region which corresponds with an alloy containing about 58·8 per cent. of lead. Other less-pronounced points shown by the curve are minima at about 42 and 17 per cent. of lead respectively, and a maximum at about 11 per cent. of lead. With the possible exception of the maximum at 58·5 per cent. of lead, none of the maxima or minima correspond to the known intermetallic compounds deduced by Vogel* from a study of the thermal diagram of this system or by von Maey from a study of the specific volume of gold-lead alloys. The former states that Au_2Pb and $AuPb_2$ exist, whilst von Maey† finds evidence for the existence of Pb_3Au_2. The alloy represented by the maximum at 58·5 per cent. of lead contains the two constituent elements in the atomic ratio Pb : Au = 2·7 : 2, which approximates to von Maey's compound Pb_3Au_2. All the alloys of gold and lead, with the exception of those containing between 56 and 62 per cent. of lead, are diamagnetic.

The addition of a small amount of gold to tin yields a diamagnetic alloy (curve III, fig. 1); the curve crosses the zero-susceptibility line at about 6 per cent. of gold and does not re-enter the paramagnetic region at any point of its course. Minima are shown at about 52·6 and 91 per cent. of tin respectively, the former of which, being due to an alloy containing the constituent metals in

---

* 'Z. anorg. Chem.,' vol. 45, p. 17 (1905).

† 'Z. phys. Chem.,' vol. 38, p. 292 (1901).

Table IV.—Gold-Tin Alloys. Temperature 18·5° to 20·5° C.

Specimen.	Sn per cent.	Sn atoms per cent.	Density.	$k \times 10^6$.
Pure Sn	100·00	100·00	7·29	+0·044
Alloy A	91·00	94·45	7·74	−0·137
,, B	82·65	88·77	8·20	−0·042
,, C	73·70	82·36	8·68	−0·100
,, D	61·28	72·47	9·58	−0·228
,, E	52·66	64·94	10·28	−0·383
,, F	41·15	53·72	11·34	−0·246
,, G	32·40	44·32	12·50	−0·146
,, H	20·51	29·92	14·66	−0·127
,, I	10·23	15·89	16·88	−0·126
Pure Au	0·00	0·00	19·27	−0·118

the atomic ratio Sn : Au = 1·87 : 1. This minimum may therefore be regarded as indicating the presence of the compound $AuSu_2$. A maximum occurs at about 82 per cent. of tin, which is given by the alloy containing the constituents in the atomic ratio Sn : Au = 7·90 : 1, a value which is hardly likely to represent an intermetallic compound.

The freezing-point curve* of gold-tin alloys indicates the existence of three compounds, AuSn, $AuSn_2$, and $AuSn_4$. There is no indication of the compounds AuSn and $AuSn_4$ in curve III, fig. 1.

Table V.—Gold-Cadmium Alloys. Temperature 19° to 21·5° C.

Specimen.	Cd per cent.	Cd atoms per cent.	Density.	$k \times 10^6$.
Pure Cd	100·00	100·00	8·67	−0·156
Alloy A	89·04	93·50	9·58	+0·064
,, B	81·47	88·51	10·11	+0·037
,, C	67·91	78·85	11·15	+0·045
,, D	60·30	72·72	11·70	−0·046
,, E	50·12	63·84	12·57	−0·065
,, F	44·31	58·28	13·13	+0·040
,, G	33·32	46·68	14·50	+0·036
,, H	26·98	39·34	15·49	+0·038
,, I	12·78	20·36	17·69	−0·191
Pure Au	0·00	0·00	19·27	−0·118

As large quantities of these alloys were not available, the test pieces, after the magnetic deflections had been obtained, were used for the determination of the density. The alloy was powdered in an agate mortar and the volume of a known weight of the powder measured by the displacement of the level of water contained in a calibrated micro-burette, using a cathetometer for reading the levels. The values of weight, volume and density are given in Table V.

---

* Vogel, 'Z. anorg. Chem.,' vol. 46, p. 64 (1905).

Table VI.—Density of Gold-Cadmium Alloys at 18·5° to 20° C.

Specimen.	Cd per cent.	Weight.	Volume.	Density.
		g.	c.c.	
Alloy A	89·04	0·6511	0·068	9·58
,, B	81·47	0·6574	0·065	10·11
,, C	67·91	0·6134	0·055	11·15
,, E	50·12	0·6035	0·048	12·57
,, F	44·31	0·7483	0·057	13·13
,, G	33·32	1·1314	0·078	14·50
,, H	26·98	0·7746	0·050	15·49
,, I	12·70	1·0072	0·057	17·67

The susceptibility-composition curve for cadmium-gold alloys is seen in fig. 1, curve IV. It keeps close to the zero-susceptibility line over its whole length, but crosses the zero line four times, thus indicating that the alloys containing about 22, 47, 60 and 94 per cent. of cadmium respectively are non-magnetic. Very flat and ill-developed maxima evidently lie between 26 and 42 per cent. of cadmium and between 66 and 90 per cent. of cadmium. The former maximum may indicate the presence of the compound $AuCd_3$, and it is possible that this maximum might be developed were the alloy annealed and remeasured. The existence of the compounds AuCd, $AuCd_3$, and Au_4Cd_3 is shown by the freezing-point curve* of gold-cadmium alloys, but, with the exception of the possibility mentioned above, these compounds are not indicated on the susceptibility curve.

Table VII.—Aluminium-Tin Alloys. Temperature 18° to 20° C.

Specimen.	Sn per cent.	Sn atoms per cent.	Density.	$k \times 10^6$.
Pure Sn	100·00	100·00	7·29	+0·044
Alloy A	96·24	85·44	6·85	−0·017
,, B	83·17	52·99	5·54	−0·237
,, C	76·13	42·14	5·08	−0·938
,, D	65·71	30·41	4·46	−0·610
,, E	49·55	18·30	3·81	−0·364
,, F	41·86	14·09	3·54	−0·182
,, G	31·63	9·50	3·22	−0·028
,, H	19·95	5·38	3·00	−0·045
,, I	11·81	2·95	2·85	−0·039
Pure Al	0·00	0·00	2·68	+0·583

In the case of aluminium-tin alloys, fig. 2, curve I, the rather remarkable fact comes to light that, although the component elements are paramagnetic, the whole of the alloys examined are diamagnetic. On the addition of tin to aluminium, the susceptibility curve falls steeply to below the zero line; it then rises slowly for alloys containing between 11·8 and 31·6 per cent. of tin. There is an inflection at 31·6 per cent. of tin, after which the curve falls more rapidly to a very pronounced minimum at about 76 per cent. of tin. It then rises rapidly to the value for tin, but not quite regularly.

---

* Vogel, 'Z. anorg. Chem.,' vol. 48, p. 337 (1906).

The alloys containing about 10 and 97 per cent. of tin respectively are non-magnetic. The alloy corresponding to the minimum on the curve contains the constituents in the atomic ratio Al : Sn = 1·37 : 1, which may be taken to indicate the presence of the compound Al_4Sn_3, although the freezing-point curve* of aluminium-tin alloys gives no evidence of such a compound or, indeed, of any compound of aluminium and tin.

Table VIII.—Bismuth-Tin Alloys. Temperature 20° C.

Specimen.	Sn per cent.	Sn atoms per cent.	Density.	$k \times 10^6$.
Pure Bi	0·00	0·00	9·23	−1·24
Alloy A	7·84	13·01	9·57	−0·043
,, B	17·60	27·30	9·28	−0·045
,, C	30·28	43·36	8·91	−0·107
,, D	42·73	56·78	8·57	−0·165
,, E	50·04	63·78	8·40	−0·136
,, F	57·99	70·82	8·22	−0·032
,, G	68·07	79·03	7·97	−0·042
,, H	82·41	89·20	7·64	−0·032
,, I	93·62	96·33	7·42	−0·023
Pure Sn	100·00	100·00	7·29	+0·044

The influence of bismuth on the susceptibility of bismuth-tin alloys is determinative, for all the alloys examined are diamagnetic. The susceptibility-composition curve, fig. 2, curve II, rises steeply almost to the zero line on the addition of about 8 per cent of tin to bismuth, and then it falls a little up to about 17·6 per cent. of tin. At this point it falls more rapidly until it reaches 42·7 per cent. of tin, where a minimum occurs.

The atomic ratio of the constituent elements in the alloy of this composition is Sn : Bi = 4 : 3; the point may therefore indicate the presence of an intermetallic compound Sn_4Bi_3. After passing through the minimum, the curve rises fairly rapidly to 58 per cent. of tin and then more slowly, running close to the zero line, to 95 per cent. of tin, at which point it crosses the zero line. Consequently, the alloy containing 95 per cent. of tin is non-magnetic, and from the curve it is to be presumed that alloys containing more than 95 per cent. of tin

---

* Gwyer, 'Z. anorg. Chem.,' vol. 49, p. 315 (1906); Heycock and Neville, 'Trans. Chem. Soc.,' vol. 57, p. 376 (1890).

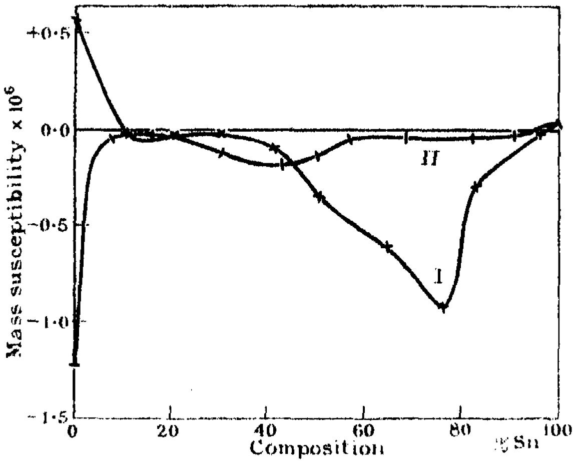

FIG. 2.—Change of Mass Susceptibility with Composition. I, Aluminium-tin; II, Bismuth-tin.

are paramagnetic. The freezing-point curve of alloys of tin and bismuth has been examined by Bucher,* who found no evidence for the existence of intermetallic compounds of these elements.

Table IX.—Cadmium-Tin Alloys. Temperature 19° to 21° C.

Specimen.	Sn per cent.	Sn atoms per cent.	Density.	$k \times 10^6$.
Pure Sn	100·00	100·00	7·29	+0·044
Alloy A	89·95	89·48	7·40	+0·027
,, B	74·76	73·73	7·58	+0·009
,, C	62·15	60·88	7·75	−0·009
,, D	51·88	50·52	7·89	−0·027
,, E	45·81	44·40	7·94	−0·045
,, F	20·94	20·02	8·33	−0·064
,, G	15·51	14·73	8·42	−0·082
,, H	9·48	8·92	8·50	−0·006
,, I	1·50	1·35	8·63	−0·027
Pure Cd	0·00	0·00	8·67	−0·156

Commencing with pure tin, the susceptibility curve falls fairly rapidly with addition of cadmium, fig. 3, up to 15·5 per cent. of tin. At this point the curve bends sharply upwards, producing a sharp minimum. The minimum corresponds with an alloy containing the constituent elements in the atomic ratio Sn : Cd = 1 : 7·14. This may indicate the presence of a compound $SnCd_7$. The curve then rises sharply, almost to the zero line, where a maximum is produced at

---

* 'Z. anorg. Chem.,' vol. 98, p. 117 (1916).

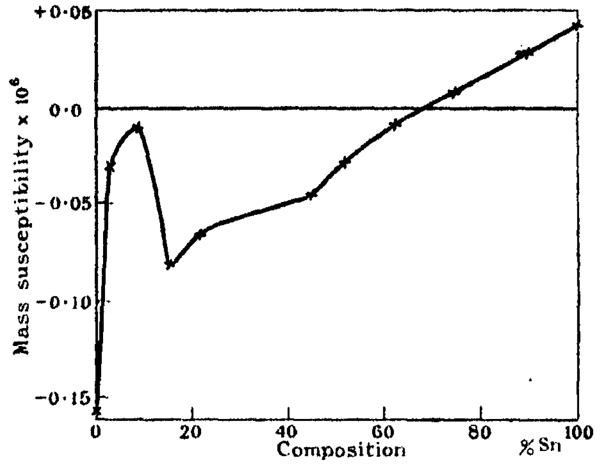

Fig. 3.—Change of Mass Susceptibility with Composition. Cadmium-tin.

9·48 per cent. of tin, after which the curve falls to the value for cadmium. The alloy containing 67 per cent. of tin is non-magnetic. Determinations of the freezing-point curve* of cadmium-tin alloys do not indicate the presence of any compounds of the two elements, although Padoa and Bovini† have stated that the compound $CdSn_4$ exists.

Table X.—Lead-Tin Alloys. Temperature 20° to 22° C.

Specimen.	Sn per cent.	Sn atoms per cent.	Density.	$k \times 10^6$.
Pure Sn	100·00	100·00	7·29	+0·044
Alloy A	96·84	98·19	7·36	+0·045
,, B	84·86	90·72	7·70	+0·016
,, C	81·84	88·51	7·78	+0·014
,, D	73·13	82·69	8·05	+0·004
,, E	52·60	66·07	8·80	−0·028
,, F	43·88	57·74	9·13	−0·046
,, G	36·08	49·64	9·45	−0·057
,, H	20·44	30·93	10·15	−0·091
,, I	13·60	21·51	10·51	−0·100
Pure Pb	0·00	0·00	11·38	−0·119

The susceptibility-composition curve for alloys of lead and tin follows practically a linear course, fig. 4. The susceptibility falls fairly regularly from the value of pure tin to that of pure lead, with increasing concentration of lead. There is no indication of the presence of compounds; the alloy containing about

---

* Bucher, *loc. cit.*; Mazotto, 'Int. Z. Metallurgie,' vol. 4, p. 13 (1913).

† 'Gazzetta,' vol. 44, p. 528 (1914).

70 per cent. of tin is non-magnetic. The susceptibility of lead-tin alloys may be calculated approximately by the mixture law from the values of the constituents and the composition of the alloy.

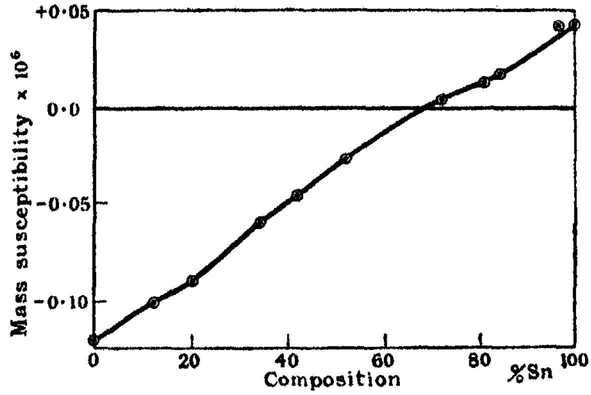

Fig. 4.—Change of Mass Susceptibility with Composition. Lead-tin.

K. Honda* has also examined the susceptibility of lead-tin alloys and finds, as we do, that the susceptibility-composition curve is practically a straight line. Freezing-point determinations of alloys of lead and tin have been made by Rosenhain and Tucker,† Degens‡ and Geurtler,§ who have failed to find any evidence of the existence of intermetallic compounds of these elements.

The expenses of this research have been met by a grant from the Government Grant Committee of the Royal Society, to whom the authors desire to express their thanks.

---

* 'Sci. Rep. Tokyo Univ.,' vol. 2, p. 11 (1913).

† 'Phil. Trans.,' vol. 209, p. 89 (1908).

‡ 'Z. anorg. Chem.,' vol. 63, p. 212 (1909).

§ 'Z. Elektrochem.,' vol. 15, p. 129 (1909).

On Fresnel's Convection Coefficient in General Relativity.

By N. R. Sen, D.Sc., Professor of Applied Mathematics, University of Calcutta.

(Communicated by A. S. Eddington, F.R.S.—Received March 28, 1927.)

It is well known that a ray of light travelling in any moving medium has only a fraction of the velocity of the medium added to its own, which is usually called Fresnel's convection coefficient. A satisfactory explanation of this phenomenon is readily furnished by Einstein's Addition Theorem for two velocities. In this explanation the velocities of light and the medium are supposed to be independent of one another, in so far as the velocity of the ray alone, in accordance with the First Postulate of Relativity, is considered to be the same as when the medium is at rest, and to this is added, according to the Relativity law, the small velocity of the medium. But, it may be argued that the light phenomenon is a distinct one governed by Maxwell's electromagnetic equations, and other auxiliary relations in case of material bodies, and the velocity of light in vacuum or in any other material medium should follow immediately from these equations alone. It appears, then, that the more direct way of obtaining the velocity of light in a moving medium would be to appeal to Maxwell's electromagnetic equations in the medium, and this would also furnish means for examining the applicability of the Addition Theorem in the present case. The two processes, however, should be mutually compatible, since Maxwell's equations, as written in accordance with restricted Relativity, are covariant with regard to Lorentz transformation in which, however, are embodied the Postulates of Relativity, and the Addition Theorem is only a consequence of this transformation. It is, therefore, more usual and also easier to deduce Fresnel's convection coefficient and Doppler effect by taking a single light-wave, say, a sine vibration, in a co-ordinate system in which the medium rests and then to subject it to Lorentz transformation, than to start from Maxwell's equations and the auxiliary relations for the moving medium and obtain the velocity from them. But in General Relativity the latter is the only course open to us; but the question now is far more complicated, since the G-field within a material body is unknown, depending on its inner dynamical conditions. Here an attempt is made to determine the velocity inside such bodies under certain hypotheses, which enable us to obtain Fresnel's coefficient in the usual form.

---

* Von Laue, 'Die Relativitätstheorie,' vol. II, pp. 146, 149.

2. We take the medium to be homogeneous, non-conducting and uncharged. In this medium the two electromagnetic tensors $F_{i\kappa}$ and $H_{i\kappa}$ are determined by the following modified Maxwell's equations* :—

$$\frac{\partial F_{j\kappa}}{\partial x_i} + \frac{\partial F_{\kappa i}}{\partial x_j} + \frac{\partial F_i{}^{j}}{\partial x_\kappa} = 0, \tag{1}$$

$$\frac{\partial}{\partial x_\kappa}(\sqrt{-g} \,.\, H^{i\kappa}) = 0. \tag{2}$$

The first set of equations can be satisfied by defining a vector potential $\kappa\,(\kappa_1,\ \kappa_2,\ \kappa_3,\ \kappa_4)$ according to the equation

$$F_{ij} = \frac{\partial \kappa_i}{\partial x_j} - \frac{\partial \kappa_j}{\partial x_i}. \tag{1'}$$

In a material medium we have the further relations*

$$u^\kappa H_{i\kappa} = \varepsilon u^\kappa F_{i\kappa}, \tag{3}$$

and

$$u_i F_{j\kappa} + u_j F_{\kappa i} + u_\kappa F_{ij} = \mu\,(u_i H_{j\kappa} + u_j H_{\kappa i} + u_\kappa H_{ij}), \tag{4}$$

ε and μ being the dielectric and the permeability constants of the body, and $(u_1,\ u_2,\ u_3,\ u_4)$ the components of velocity of the medium defined by such relations as

$$u^i = \frac{dx_i}{d\tau},$$

so that

$$\left.\begin{aligned} -d\tau^2 = ds^2 = g_{i\kappa}dx_i dx_\kappa \\ u^i u_i = -1. \end{aligned}\right\} \tag{4A}$$

In the above, as well as in all tensor equations, when an index is repeated, the equation is to be summed over that index. Multiplying equation (4) by u^i and summing over i we have

$$\mu\,(H_{j\kappa} - u_j u^i H_{\kappa i} + u_\kappa u^i H_{ji}) = F_{j\kappa} - u_j u^i F_{\kappa i} + u_\kappa u^i F_{ji}$$

and from (3)

$$\mu H_{j\kappa} = F_{j\kappa} + (\varepsilon\mu - 1)\,(u_j u^i F_{\kappa i} - u_\kappa u^i F_{ji}) \tag{5}$$

and the corresponding contravariant relation

$$\mu H^{j\kappa} = F^{j\kappa} + (\varepsilon\mu - 1)\,(u^j u_i F^{\kappa i} - u^\kappa u_i F^{ji}). \tag{5'}$$

---

* Von Laue, *loc. cit.*

For restricted Relativity, as well as for the cases we have worked out below, this equation would be sufficient, but for general treatment we shall make use of a theorem deduced by W. Gordon* from this. Equation (5′) can also be written in the form

$$\begin{aligned}\mu \mathrm{H}^{j\kappa} &= \{g^{jr}g^{\kappa s} - (\epsilon\mu - 1)(u^j u^r g^{\kappa s} + u^\kappa u^s g^{rj})\}\mathrm{F}_{rs} \\ &= \{g^{jr} - (\epsilon\mu - 1)\,u^j u^r\}\,\{g^{\kappa s} - (\epsilon\mu - 1)u^\kappa u^s\}\mathrm{F}_{rs} \\ &= \gamma^{jr}\gamma^{\kappa s}\mathrm{F}_{rs} \qquad (6')\end{aligned}$$

where

$$\gamma^{jr} = g^{jr} - (\epsilon\mu - 1)u^j u^r, \text{ etc.} \qquad (6)$$

We take γ^{jr} *to be the new metric tensor in place of* g^{jr}. The ratio of the determinants γ/g is an invariant, and consequently has the same value as in the co-ordinate system in which the medium is at rest, and it can be shown by taking $u^1 = u^2 = u^3 = 0$ that

$$\frac{\gamma}{g} = \frac{1}{\epsilon\mu}$$

and consequently

$$\sqrt{-g}\,\mathrm{H}^{j\kappa} = \sqrt{\epsilon/\mu}\,\sqrt{-\gamma}\,\gamma^{jr}\gamma^{\kappa s}\mathrm{F}_{rs}. \qquad (6'')$$

This result is due to Gordon.

Now, let us assume that the electromagnetic wave is moving in the positive direction of the axis of x with a constant velocity V, and that all the quantities are functions of $(x_1 - \mathrm{V}x_4)$. Then the integrals of (2) can be written as

$$\sqrt{-g}\,\mathrm{H}^{14} = \text{const.}, \qquad \sqrt{-g}\,(\mathrm{H}^{21} - \mathrm{VH}^{24}) = \text{const.},$$

and

$$\sqrt{-g}\,(\mathrm{H}^{31} - \mathrm{VH}^{34}) = \text{const.},$$

and since here we are concerned with phenomena changing with time we can without loss of generality take all the constants to vanish, so that we have the integrals

$$\mathrm{H}^{14} = 0, \qquad \mathrm{H}^{21} - \mathrm{VH}^{24} = 0, \qquad \text{and} \qquad \mathrm{H}^{31} - \mathrm{VH}^{34} = 0. \qquad (7)$$

Also, equation (1′) defines $\mathrm{F}_{i\kappa}$ in terms of the vector potential as follows :—

$$\begin{aligned}&\mathrm{F}_{23} = 0, \qquad \mathrm{F}_{31} = \kappa_3', \qquad \mathrm{F}_{12} = -\kappa_2', \\ &\mathrm{F}_{14} = -(\mathrm{V}\kappa_1' + \kappa_4') = -\kappa_0', \quad \mathrm{F}_{24} = -\mathrm{V}\kappa_2', \quad \mathrm{F}_{34} = -\mathrm{V}\kappa_3'. \qquad (8)\end{aligned}$$

3. *The Equation of Propagation of Waves in the Medium.*—In a recent

---

[*] 'Ann. d. Physik,' vol. 72, p. 424 (1923).

paper,* O. Baldwin and G. B. Jeffery have shown that the so-called transverse-transverse waves are the only real waves of *finite amplitude* which can be propagated in vacuum, the velocity of propagation being the signal velocity which we shall call the fundamental velocity. The authors, however, doubt if plane waves of this type are at all permitted by relativity. We shall not go into a similar discussion in the present case but limit ourselves to the determination of the velocity with which plane electromagnetic waves can be propagated in a moving material medium.

With the assumptions we have made in section 2 Maxwell's equations reduce to the three integrals (7) and the relations (8). The connecting link between these two sets is furnished by equation (6′) which determines the contravariant components of the tensor H in terms of the covariant components of F. This equation of transformation, but for the factor μ, is the same as if the metric tensor g_{ik} were replaced by γ_{ik} within the material-body and H and F were identical; or, in other words, with the new metric tensor the same equations hold as in vacuum. We first take the most general tensor g_{ik} inside, and consequently all the ten components of γ_{ik} are supposed to exist. Equations (7) are transformed with the help of (6′) and can be written in the form:

$$\left.\begin{aligned} \gamma^{1s}\gamma^{4t}\mathrm{F}_{st} &= 0 \\ (\gamma^{1t} - \mathrm{V}\gamma^{4t})\,\gamma^{2s}\mathrm{F}_{st} &= 0 \\ (\gamma^{1t} - \mathrm{V}\gamma^{4t})\,\gamma^{3s}\mathrm{F}_{st} &= 0 \end{aligned}\right\}. \tag{9}$$

If we now substitute the values of F_{st} in terms of κ_0', κ_2' and κ_3' from (8) in the above equations, we shall get three homogeneous equations in the quantities κ_0', κ_2' and κ_3', of which the coefficients are, in general, different from zero. If, now, these three quantities are themselves different from zero we can satisfy the equations by taking all the nine coefficients to vanish. If, however, any of the quantities κ_0', κ_2', κ_3' is zero then the *corresponding coefficients need not* vanish. We write these equations in the following manner:—

when $\kappa_2' \neq 0$,

$$\{\gamma^{44}\gamma^{22} - (\gamma^{24})^2\}\,\mathrm{V}^2 - 2\,\{\gamma^{22}\gamma^{14} - \gamma^{12}\gamma^{24}\}\,\mathrm{V} + \{\gamma^{11}\gamma^{22} - (\gamma^{12})^2\} = 0, \tag{10A}$$

$$\{\gamma^{44}\gamma^{23} - \gamma^{34}\gamma^{24}\}\,\mathrm{V}^2 - \{2\gamma^{23}\gamma^{14} - \gamma^{13}\gamma^{24} - \gamma^{12}\gamma^{34}\}\,\mathrm{V} + \{\gamma^{11}\gamma^{23} - \gamma^{12}\gamma^{13}\} = 0, \tag{10A′}$$

$$\{\gamma^{44}\gamma^{12} - \gamma^{24}\gamma^{14}\}\,\mathrm{V} + \{\gamma^{11}\gamma^{24} - \gamma^{12}\gamma^{14}\} = 0; \tag{10A″}$$

---

* 'Roy. Soc. Proc.,' A, vol. 111, p. 97 (1926). Eddington first showed that of the three possible types of waves of *small amplitude* only the "transverse-transverse" type has a physical significance while the other two arise out of the "sinuosities in the co-ordinate system" and can be transformed away: 'Roy. Soc. Proc.,' A, vol. 102, p. 268 (1922). The present authors have extended these results of Eddington to corresponding waves with *finite amplitude*.

when $\kappa_3' \neq 0$,

$$\{\gamma^{44}\gamma^{33} - (\gamma^{34})^2\} V^2 - 2\{\gamma^{33}\gamma^{14} - \gamma^{13}\gamma^{34}\} V + \{\gamma^{11}\gamma^{33} - (\gamma^{13})^2\} = 0, \quad (10\text{B})$$

$$\{\gamma^{44}\gamma^{23} - \gamma^{34}\gamma^{24}\} V^2 - \{2\gamma^{33}\gamma^{14} - \gamma^{13}\gamma^{24} - \gamma^{12}\gamma^{34}\} V + \{\gamma^{11}\gamma^{23} - \gamma^{12}\gamma^{13}\} = 0, \quad (10\text{B}')$$

which is the same as (10A′),

$$\{\gamma^{44}\gamma^{13} - \gamma^{34}\gamma^{14}\} V + \{\gamma^{11}\gamma^{34} - \gamma^{13}\gamma^{14}\} = 0; \qquad (10\text{B}'')$$

either $\kappa_0' = 0$, or in addition to equations (10A″) and (10B″)—

$$\gamma^{44}\gamma^{11} - (\gamma^{14})^2 = 0. \qquad (10\text{C}'')$$

There are, in fact, at most six equations. They are to be consistent and should lead to a single equation for V. We are concerned here with transverse vibrations and put $\kappa_0' = 0$, $\kappa_2' \neq 0$ and $\kappa_3' \neq 0$. The conditions for the consistency of equations (10A), (10A′) and (10B) are

$$\left.\begin{aligned} &\frac{\gamma^{44}\gamma^{22} - (\gamma^{24})^2}{\gamma^{44}\gamma^{33} - (\gamma^{34})^2} = \frac{\gamma^{22}\gamma^{14} - \gamma^{12}\gamma^{24}}{\gamma^{33}\gamma^{14} - \gamma^{13}\gamma^{34}} = \frac{\gamma^{11}\gamma^{22} - (\gamma^{12})^2}{\gamma^{11}\gamma^{33} - (\gamma^{13})^2} \\ \text{and} \quad &\frac{\gamma^{44}\gamma^{22} - (\gamma^{24})^2}{\gamma^{23}\gamma^{24} - \gamma^{24}\gamma^{34}} = \frac{2(\gamma^{11}\gamma^{22} - \gamma^{12}\gamma^{24})}{2\gamma^{14}\gamma^{23} - \gamma^{13}\gamma^{24} - \gamma^{12}\gamma^{34}} = \frac{\gamma^{11}\gamma^{22} - (\gamma^{12})^2}{\gamma^{11}\gamma^{23} - \gamma^{12}\gamma^{13}} \end{aligned}\right\} . \quad (10\text{D})$$

The resulting quadratic equation in the constant V should now be compatible with (10A″) and (10B″). There are, thus, the four relations (10D) among the ten components of γ, together with (10A″), (10B″), which must be satisfied for any wave-propagation of the type we are considering.

One obvious way in which this can be done is by putting

$$\gamma^{12} = \gamma^{13} = \gamma^{24} = \gamma^{34} = 0, \qquad (11')$$

in which case V is given by the equation

$$\gamma^{44}V^2 - 2\gamma^{14}V + \gamma^{11} = 0, \qquad (11)$$

while at least one of γ^{22}, γ^{33} and γ^{23} should be different from zero. We shall now discuss this case at some length.

Let us suppose that the medium is moving with velocity v in the direction of the axis of x. We have to connect u^1, u^2, u^3 and u^4 with v, which can be done as follows. Calling c the constant velocity of light in natural measurements, the components of the space-velocity vector are given by

$$q^i = \frac{dx_i}{dt} = c\frac{dx_i}{d\tau} = c\frac{u^i}{u^4} \qquad (i = 1, 2, 3).$$

We take the axis of time everywhere perpendicular to the ordinary space so that $g_{14} = g_{24} = g_{34} = 0$, in which case the resultant velocity

$$|q|^2 = \sum_{i=1}^{3} q^i q_i = \sum_{1}^{3} g_{i\kappa} q^i q^\kappa = -\frac{c^2}{u^{4^2}}(g_{44} u^{4^2} + 1).$$

These give

$$u^i = q^i / \sqrt{-c^2 g_{44} - q^2} \ (i = 1, 2, 3) \quad \text{and} \quad u^4 = c/\sqrt{-c^2 g_{44} - q^2}.$$

In connecting the vector q with v we should remember that the phase velocity V of the wave, according to our assumptions, being of the nature of the ratio of the two co-ordinates x_1 and x_4 is a quantity like q^1. The velocity of the medium v is, therefore, also assumed to be a quantity of the same nature and using the scale in which the constant velocity of light is unity we identify q^1 with v.* Also, since $q^2 = q^3 = 0$

$$|q|^2 = \sum_{1}^{3} g_{i\kappa} q^i q^\kappa = g_{11} q^{1^2} = g_{11} v^2.$$

Hence

$$u^1 = v/\sqrt{-g_{44} - g_{11} v^2}, \quad u^2 = u^3 = 0, \quad u^4 = 1/\sqrt{-g_{44} - g_{11} v^2}. \tag{12}$$

In order to arrive at a velocity independent of the metric tensor we have to subject the tensor components to another condition. Obviously, this should be of the form $g_{11} + \alpha g_{44} = 0$, where α is a constant. We shall, however, take $\alpha = 1$ in order to arrive at the well-known value of the velocity for restricted Relativity. This assumption gives the following equations

$$u^1 = \frac{1}{\sqrt{-g_{44}}} \cdot \frac{v}{\sqrt{1 - v^2}}, \quad u^2 = 0, \quad u^3 = 0, \quad u^4 = \frac{1}{\sqrt{-g_{44}}} \cdot \frac{1}{\sqrt{1 - v^2}},$$

and

$$\gamma^{11} = \frac{\varepsilon\mu v^2 - 1}{1 - v^2} g^{44}, \quad \gamma^{44} = \frac{\varepsilon\mu - v^2}{1 - v^2} g^{44} \quad \text{and} \quad \gamma^{14} = \frac{v(\varepsilon\mu - 1)}{1 - v^2} g^{44}. \tag{11''}$$

Substitution in (11) gives the following equation for V

$$(\varepsilon\mu - v^2)\mathrm{V}^2 - 2(\varepsilon\mu - 1)\, v \,.\, \mathrm{V} - (\varepsilon\mu v^2 - 1) = 0 \tag{13}$$

assuming

$$1 - v^2 \neq 0.$$

This quadratic equation has two real roots and can be easily solved. Putting $\sqrt{\varepsilon\mu} = n$, the refractive index of the medium, the roots of (13) can be expressed as

$$\mathrm{V} = (nv \pm 1)/(n \pm v). \tag{14}$$

---

* It should be noticed that we cannot identify v ***in natural measurement*** with $|q|$ on account of the arbitrariness in dt. But $\sqrt{-g_{44}}c$ measures the signal (light) velocity in the same scale. Hence putting $\sqrt{-g_{44}}c/|q| = c/v$, a relation from which dt cancels out, *it is evident that* $|q|$ *is to be identified with* $\sqrt{-g_{44}}v$. **This with $g_{11} + g_{44} = 0$ also leads to $g' = v$, and leaves the values of u and γ in (11″) unaltered.**

Hence the velocities of electromagnetic waves cV, in natural measurements, are

$$\frac{v \pm c/n}{1 \pm v/cn}, \tag{14'}$$

corresponding to propagation in the positive or negative direction of the axis of x. This is really the Addition Theorem for two velocities, which is thus satisfied for general Relativity under the present assumption. If we give to α a value different from unity the quadratic equation would give two entirely different velocities depending on α. But they would correspond only to a different time variable as α may be supposed to be absorbed in x_4; hence nothing is lost in generality by taking $\alpha = 1$. Fresnel's convection coefficient in the usual form can now be easily deduced from (14). The metric tensor has also to satisfy Einstein's gravitational equations, which in the present case we write in the form

$$G_{\mu\nu} - \tfrac{1}{2}g_{\mu\nu}G = -x(T_{\mu\nu} + E_{\mu\nu}), \tag{15}$$

the terms involving T and E on the right-hand side corresponding to the material and electromagnetic energy tensors respectively. But E is not here the usual tensor in empty space, which should in the present case be replaced by the following Abraham tensor.*

$$E_i^{\kappa} = H_{i\kappa}F^{\kappa\tau} - \tfrac{1}{4}F_{\tau\sigma}H^{\sigma\tau}\delta_i^{\kappa} - (\epsilon\mu - 1)u_i\Omega^{\kappa}$$

where

$$\Omega^i = u_{\kappa}F_l\{H^{i\kappa}u^l + H^{\kappa l}u^i + H^{li}u^{\kappa}\}$$

and

$$F_i = F_{i\kappa}u^{\kappa}.$$

For the wave we have been discussing there would be, according to (15), 10 equations among 10 + 4 + 2† quantities. Since $G_{12} = G_{13} = G_{24} = G_{34} = 0$ and also $E_{12} = E_{13} = E_{24} = E_{34} = 0$, as can be easily calculated four of the equations mean that the corresponding components of the material energy tensor T must vanish. The number of significant equations therefore reduces to *six* only, and the conditions of integrability would give two differential relations among the energy tensor components. The conditions, however, in their general form are extremely complicated and do not lend themselves to further discussion.

4. For the transverse waves we have just discussed κ_0' has been taken to vanish. Justification for this is also immediately obtained from equation

---

* 'Encycl. Math. Wiss.,' v. 19, p. 666.

† There are ten material energy tensor components, four independent components of the metric tensor and two components of the vector potential, viz., κ_2' and κ_3'. Four components of G, viz., G_{12}, G_{13}, G_{24}, G_{34}, vanish and the rest are different from zero.

(10c″). If, however, κ_0' is different from zero, equation (10c″) must be satisfied. For transverse waves equations (11″) and (10c″) then give

$$\varepsilon\mu = 0$$

which certainly cannot hold for a material medium. We can, however, notice that it is possible to satisfy the equations of groups (10) on a different assumption. For instance, if we take $\kappa_0' \neq 0$, (10c″) reduces (10A″) and (10B″) to

$$(\gamma^{11} - V\gamma^{14})(\gamma^{14}\gamma^{12} - \gamma^{11}\gamma^{24}) = 0$$
$$(\gamma^{11} - V\gamma^{14})(\gamma^{14}\gamma^{13} - \gamma^{11}\gamma^{34}) = 0$$

respectively. If the factors involving γ only do not vanish, the equations of group (10) can be satisfied by putting

$$\kappa_2' = 0, \quad \kappa_3' = 0, \quad \kappa_0' \neq 0. \qquad \gamma^{11} - V\gamma^{14} = 0.$$

Again, if as before we put $\gamma^{12} = \gamma^{13} = \gamma^{24} = \gamma^{34} = 0$, equations (10) can be satisfied by

$$\kappa_0' \neq 0, \qquad \kappa_2' \neq 0, \qquad \kappa_3' \neq 0, \quad \text{and} \quad \gamma^{11} - V\gamma^{14} = 0.$$

But since in each case, equation (10c″) exists the values of γ given by (11″) are not possible. The inverse problem of finding physical interpretations of these solutions appears to be difficult to solve, but the fact that no corresponding waves are known to exist in vacuum may suggest that these solutions do not actually represent any *physical waves.*

5. *Velocity for Transverse Motion of the Medium.*—If we take

$$u^1 = u^3 = 0, \qquad u^2 = \frac{1}{\sqrt{-g_{44}}} \cdot \frac{v}{\sqrt{1 - v^2}} \qquad u^4 = \frac{1}{\sqrt{-g_{44}}} \cdot \frac{1}{\sqrt{1 - v^2}},$$

and

$$\gamma^{12} = \gamma^{13} = \gamma^{14} = \gamma^{34} = 0,$$

we have the case of a material-body moving with velocity v transversely to the direction of propagation of the electromagnetic wave. With the assumptions we have made before equations (10) now reduce to

$$\gamma^{11} - \gamma^{44}V^2 = 0,$$

giving for the velocity of propagation the equation

$$V = \pm \sqrt{\frac{1 - v^2}{n^2 - v^2}}.$$

This is the same as in the restricted theory.

On the Emission of Light from Hydrogen Atoms.

By R. d'E. Atkinson, M.A., late Research Fellow, Hertford College, Oxford.

(Communicated by F. A. Lindemann, F.R.S.—Received April 4, 1927.)

When a beam of Canal-Rays passes into a high vacuum, it is well known that the light-intensity falls exponentially to a constant value which, if the pressure is sufficiently low, is very small indeed. The experiments of Wien,[*] and the theory developed by him,[†] showed that the observations could be equally well accounted for on either of two hypotheses, namely that the light from each atom falls off exponentially at the observed rate, or alternatively, that all the energy from any one atom is emitted in a very short time indeed, and that what is measured is essentially the decay-curve of those atoms that are in the initial state for the radiation in question. As to whether the maximum emission (on either theory) occurred exactly at the point of excitation, however, these experiments provided very little evidence; the excitation was in fact, so far as can be determined, distributed continuously over a region about which all that can be said is that it was bounded more or less definitely on one side by the back of the cathode, and it was possible that the curves for a point-excitation would really resemble, for instance, the activity-curve of an intermediate radioactive substance initially absent from a preparation. In fact plausible grounds for believing that this should be the true form were ready to hand, since the atom might very well be expected to spend some time in radiating infra-red lines before it reached the initial state for the radiation observed; on this point all that could be inferred from Wien's curves was that the interval must at most be appreciably smaller than the half-period of the exponential fall. This interval is not the same as the "Verweilzeit" considered by him; the Verweilzeit is the basis of a demonstration that the curves due to point-excitation should be exponential, while the present interval would have the effect that they should not.

In order to decide whether there was in fact any delay of this nature at all, it seemed desirable to try whether non-luminous canal-rays, some distance after their entry into the vacuum, could be excited anew to luminescence at approximately one known point only, so that any interval between excitation and emission could be directly measured. The experiments devoted to this object have been somewhat interrupted, and it is further necessary to discontinue them, at least for a time, once more. The present paper is thus an interim account, containing a description of the method that has been worked out and the result that has been obtained ; there are, however, a number of further questions which it was hoped to decide, and which presumably can be decided by the same method, that are still unsettled.

---

[*] 'Ann. d. Physik,' vol. 60, p. 597 (1919); vol. 66, p. 229 (1921).

[†] 'Ann. d. Physik,' vol. 70, p. 1 (1923).

When these experiments were already well advanced, a further paper by Wien[*] appeared, in which the possibility of combining the two admissible explanations of the exponential fall was considered. The result obtained was that if both Verweilzeit and Abklingungszeit existed at all, one of them must be less than one per cent. of the other. Even this result does not explicitly rule out the possibility of an interval whose effect would seem to be not so much an alteration of the shape of Wien's curves as a simple displacement of them, but it was evident from his experimental details that such a displacement, if it existed, must be small. It seemed probable, however, that the method of point-excitation would allow of greater accuracy on this question.

More recently, a paper by McPetrie[†] has been published, in which the question of this Interval (and not of the Verweilzeit) was examined ; the method employed appears, however, open to some objection, inasmuch as it consisted in visual matching of the intensities of two beams of light, and the fact on which the final inferences were based was that the difference between the beams appeared to decrease more rapidly than their absolute intensity, so that they appeared indistinguishable when they became fairly faint. The result deduced was, that between neutralisation of the canal rays and emission of the light an interval occurred which was approximately equal to the half period of the exponential decay. This conclusion appears almost impossible to reconcile with some of Wien's curves, and is certainly directly contradicted by the experiments to be described.

The relative values, and perhaps the absolute ones, of the exponential decay-constants themselves can also, in principle, be very accurately determined by the method of point-excitation, though in practice no great success has yet been obtained. Wien's measurements showed that the values for the first three Balmer lines were fairly closely equal (H_β and H_γ being apparently exactly the same) : but on the one hand the actual values obtained varied considerably in different papers, and on the other, he usually obtained only one, or less often two, of the lines on any one plate, while the use of Wellington "Spectrum" or Ilford "Rapid Process Panchromatic" plates regularly gives three and sometimes four lines at one exposure, so that it could be hoped to establish the relative values with very considerable certainty.

---

[*] 'Ann. d. Physik,' vol. 76, p. 109 (1925).

[†] 'Phil. Mag.,' vol. 1, p. 1082 (1926).

It may be added that the point-excitation method is, if experimental difficulties can be overcome, peculiarly suited to determining relative values, since it is easy to see that $I_0/(I\infty \times \mu)$ should be a constant for all lines (μ being the exponential constant per centimetre and $I\infty$ the asymptotic intensity due to excitation by the residual pressure), however much the sensitivity of the plate and the probability of excitation may vary for different lines. Further the exact value of the constant is also determinable, so that we have a very good check on the relative values of μ. The absolute decay constants (per second) involve of course a knowledge of the velocity of the rays, and since the light has hitherto always been too faint in these experiments for Doppler effect observations this has not been measured. A method of obtaining it is outlined below, but has not yet been successfully applied. Even the relative values, however, appeared at the time when these experiments were started, to be of considerable interest, since it seemed that if any variation with wave-length or with initial quantum-number could be established, its nature might be used as an argument for the wave theory or the pulse theory of the quantum. Unfortunately, the practical difficulties have so far prevented sufficient accuracy on this point; on the other hand it appears more likely now that no result will in fact be obtained which is not equally in harmony with either view.

Experimental.

It has not been possible in practice to confine the excitation region to less than about 1·5 mm. in length, but this is in effect as satisfactory as point-excitation except that the interpretation of the measurements is somewhat laborious. The distribution of excitation over the region (which is symmetrical) can be definitely determined, and the position of its maximum fixed within one or two hundredths of a millimetre, and it is thus possible, by means of a tedious approximate integration, to distinguish between an exponential curve which starts at the excitation-point and one which starts after a short interval.

The only method of point-excitation that has so far been tried with success is to pass the canal-rays either through a very small box, or across the mouth of one or more fine jets, from which air or some other gas is streaming, and to rely on rapid pumping to keep the general pressure low. The arrangement finally adopted is shown in fig. 1; it now seems likely, however, that a collimated metal-vapour stream might be more satisfactory. At the junction of the main canal-ray tube with the wide T-tube leading to the pumps, a pair of jets was placed symmetrically about the canal-ray stream, which was travelling downwards; 4 mm. above them was a small diaphragm which stopped all the rays that were not sufficiently axial, and left only a clear-cut beam that did not scatter appreciably in the distance under observation. The cathode was some centimetres above the diaphragm; the tube in it was 0·65 mm. in diameter and 2·5 cm. long, and it was held against a flat fine-ground glass seating by a spring, instead of being water-cooled. The hole in the diaphragm was also 0·65 mm. in diameter, and the air-jets were of 0·55 mm. internal diameter, and 0·75 mm. apart. Behind the jets was a shield to keep off stray light reflected from the back of the tube; the shield, jets and diaphragm were all made of iron, smoke-blackened, and built on the iron tube through which air was fed, which was held in position by sealing-wax. At the end of a run it was always found that they were still correctly in line with the tube in the cathode.

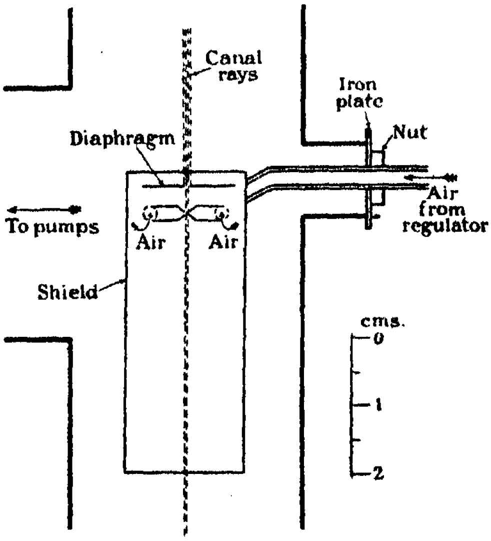

Fig. 1.

Pyrex-glass mercury-vapour pumps were used, the high-vacuum stage consisting of three pumps running in parallel; the fore-vacuum was provided by a water-pump and two mercury-vapour ones in series, and was usually about 1/40 mm. Hg; as the high-speed pumps could still run against ½ mm.

they were working under very favourable conditions. They were specially designed so that the liquid air traps employed came down inside them to within 2 cm. of the diffusion nozzles, and their combined speed at the discharge-tube was 8 to 8½ litres per second at all pressures down to $2 \cdot 10^{-4}$ mm., below which it was difficult to measure it with any certainty. The speed was determined by connecting a constant leak to the apparatus and measuring the pressure in the steady state with a McLeod gauge placed in a dead end.

After various methods had been tried, the following adjustable leak for the air supply was found to give complete satisfaction : a brass bar about 4 cm. long was bored axially with a hole about 1 mm. in diameter, which was lapped to fit as tightly as possible on a carefully-turned steel rod of the same size. An extension of this rod was threaded with 24 turns to the cm., and passed through a combined nut and packing-gland as shown (fig. 2). When air is used, the packing is obviously not directly necessary, but its purpose was to allow the supply of air to be measured, and also to allow other gases to be used if desired. The leak with this arrangement could readily be set to any desired value, being measured by the rate at which it sucked water into a 5-c.c. pipette, and once set it remained constant without attention indefinitely. The pressure behind the regulator was atmospheric, at which value it is obviously easy to keep it without attention for long periods, even if air is not the gas that is being used. The amount of air admitted was generally between ½ and 1 c.c. per minute, measured at atmospheric pressure, and the resulting general pressure in the canal-ray tube was accordingly between $8 . 10^{-4}$ and $1 \cdot 6 . 10^{-3}$ mm.

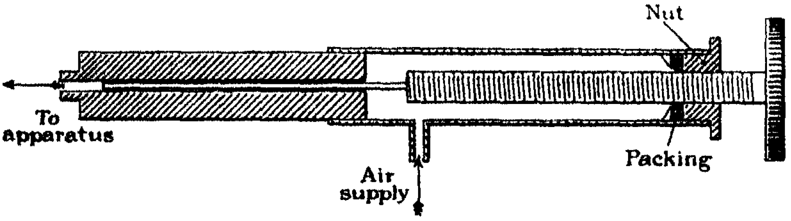

FIG. 2.

The air in the neighbourhood of the jets expands roughly as the square of the distance from the central point. If we draw a sphere of radius, say, 0·38 mm. round this point, we can calculate the density at the surface of the sphere, and can infer from it the approximate density at points inside. The speed of the air molecules is about $5 . 10^4$ cm. sec.$^{-1}$, and the area of the sphere is about $1 \cdot 5 . 10^{-2}$, (allowing for the space occupied by the jets), so that the total volume crossing it is 750 c.c. sec.$^{-1}$. The total volume leaving the observation-tube is 8 litres sec.$^{-1}$, so that the density at the surface of the sphere is 800/75 times that in the general body of the tube. Actually the density at the centre of the sphere will be considerably more than this, since the air has already expanded appreciably at the distance considered, so that roughly we may say that the maximum excitation of the canal-rays *per millimetre* at the centre of the jets is about 12 or 15 times that in the body of the tube; (see also fig. 6). This ratio is independent of the magnitude of the air leak (within the range used), and varies directly as the available pumping speed measured at the tube.

The general pressure is so low, and the high pressure region so short, that the theoretical treatment is very much simpler than that developed by Wien for his apparatus. There is no longer any question of any of the mean free paths he considers at all; they are all too long to affect the result appreciably. We simply take excitation as proportional to density for any given gas, so that the light to be observed consists of a faint uniform distribution with a stronger localised intensity superimposed on it. The question of mean free paths would only become important if we wished to determine the absolute efficiency of the arrangement; this is, in fact, very low, and most of the atoms reach the far end of the tube without suffering any effective collision at all. The intensity of light obtained is, therefore, very small, and long exposures, during which the discharge conditions had to be kept constant, were one of the difficult features of the experiment.

The apparatus was photographed through a single-prism slitless spectrograph of large size and fairly large aperture, the canal-rays themselves being at the focus of the collimator lens in place of a slit. The collimator lens was of 50 cm. focal length and $f/4{\cdot}8$, and the camera lens 70 cm. and $f/5$. The stretch (3–4 cm.) of canal-ray stream to be photographed was thus a very small fraction of the total field which either lens alone could cover; it was less, though not very much less, than could be covered *uniformly* by the two in series, with a space for the prism between. The prism was a little smaller than would have been ideal, and the beam of light was limited in all colours and for all parts of the plate solely by the size of the prism. Thus the illumination of the plate was perfectly uniform, though somewhat less than would have been possible with a larger prism. The practical advantage of having long-focus lenses was very considerable.

The spectrograph was permanently assembled with the prism approximately at minimum deviation, the lenses correctly centred on the prism, and the plateholder at the correct distance from the camera lens and correctly inclined;

there was thus only one adjustment to make, namely, to set the whole spectrograph at such a distance from the canal-ray stream that a sharp image of H_β would be formed at the centre of the plate. The stream of canal-rays, however, though plainly visible directly when the eyes had become accustomed to the darkness of the room, was completely invisible in the spectrograph; the method of focussing was therefore as follows. Between the collimator lens and the discharge tube was placed a small front-silvered mirror, in an inclined position. Reflected in this was a slit, which could be illuminated either brightly or faintly, and whose position was so arranged that its image in the mirror coincided accurately with the canal-ray beam. This adjustment was made with the illumination faint, and the slit was then strongly lighted and the spectrograph focussed on the image in the mirror.

The arrangement of the liquid-air traps, while conducing to rapid pumping at low pressures, was not economical, and the traps themselves were also small; consequently they had to be refilled about every 1½ hours. As the exposures were regularly over 24 hours in duration, it was found desirable to arrange an automatic refilling apparatus. For this purpose, a small piece of ebonite was bored with a hole near each end; two stout copper wires were passed through the holes and tightly twisted round the ebonite, and their free ends were then arranged so that at ordinary temperatures they were in firm contact. The expansion coefficient of ebonite being large, it was easy to adjust the pressure so that the contact was broken on plunging into liquid air. This switch was then placed in a glass test tube to give it a time-lag, and suspended in one of the traps. The right height had to be found by trial. The two copper wires were connected to a 2-volt relay, which thus switched on a blower whenever the ebonite warmed up. This forced air into the liquid air storage flask, driving liquid air over into the traps. The blower was sufficiently powerful to make it unnecessary also to close the evaporation outlet from the flask, and, in fact, the size of this outlet was used to control the rate of supply. It had to be adjusted to suit the time-lag of the switch. Once adjusted, the whole arrangement proved very reliable, and the copper points remained clean for a year.

It was essential to prevent mercury from collecting in the observation-space, and the high-speed pumps were never run, even in preliminary trials, without liquid air. In some of the earlier experiments this precaution was omitted, and minute drops of mercury collected on the iron-work. As this was held in place by sealing wax, the mercury could never be dislodged once it had appeared. It was not found possible in such cases to obtain a completely non-luminious beam of canal-rays, even when there was no air leak, in spite of the close proximity of the three liquid air-traps, but when proper care had been taken, it was interesting to observe the effect of suddenly turning the leak off; the parts of the beam nearest the pumps vanished at once, and the parts further down the dead end of the tube followed in order, so that after about half a second there was absolutely nothing to be seen. When the air-jets were in action the beam appeared uniform and almost perfectly parallel, with a bright stretch about a millimetre long at the jets. The light observed was for the most part due to the air, as photography revealed, and no exponential falling-off could be detected by eye.

Results.

A photograph obtained with this apparatus is shown in fig. 3. It will be observed that the air lines (mostly the nitrogen negative bands) contain the

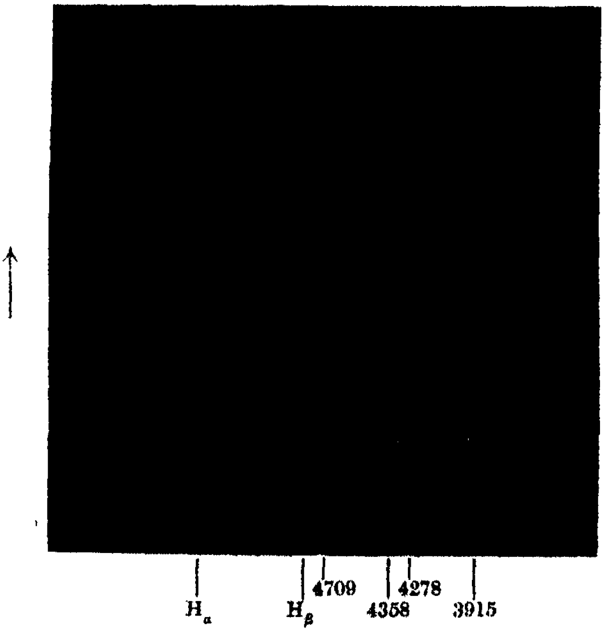

Fig. 3.

greater part of the light, and are uniform except for a bright patch at the jets; the rapid rise and gradual fall of the intensity in the Balmer lines is clearly seen, as also is the complete absence of scattering of H atoms. It appears at first sight as though the maxima in the Balmer lines are exactly on the line joining the maxima in the air lines; but measurement shows that they are displaced down the beam by about 0·54 mm. This does not, however, indicate a time-lag, after excitation, before the maximum of emission is attained; it is, as nearly as can be verified, exactly accounted for by the finite length of the high pressure region (see p. 94).

Fig. 4 is the actual photometer-curve of H_α on this plate. The curve for H_β was very similar but rose to a lower maximum. Readings were taken every fifth of a millimetre up to 24 mm. (and near the maximum every tenth), and the points cannot therefore be shown individually; about 40 points altogether fall outside the thickness of the line drawn, almost all being after 14 mm., where the glass tube seems to have had an imperfection. The slight undulations visible on the curve, and a very considerable uncertainty between 14 and 16 mm., and again at 20, were almost certainly due to irregularities in the glass tube, as they appear in the same place on the four curves (H_α, H_β, 4358 and 4709) which were accurately determined. It would certainly be preferable to use a cemented-on window. The rapid fall from 2 mm. down to 0 is due to the diaphragm. The background is neither as clear nor as uniform as is necessary for quantitative determinations in this type of work (p. 92). The line AB, which gives the abscissa of the maximum of excitation, is located from fig. 5, in which the co-ordinates on the plate of all* the most important maxima are plotted, the measurements of two different days being given. These points

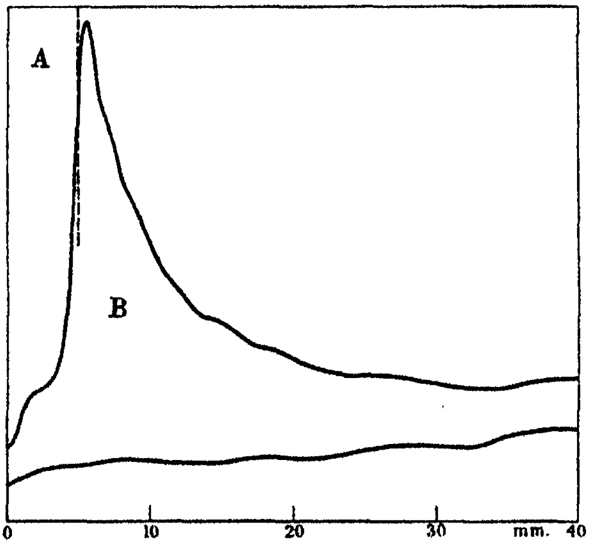

FIG. 4.

---

* 3915 and 4278 were considerably too intense for the range of the photometer, and the positions of their maxima could not be measured.

were checked every day, while the measuring (which took a week) was in progress; they did not vary more than the amount shown.

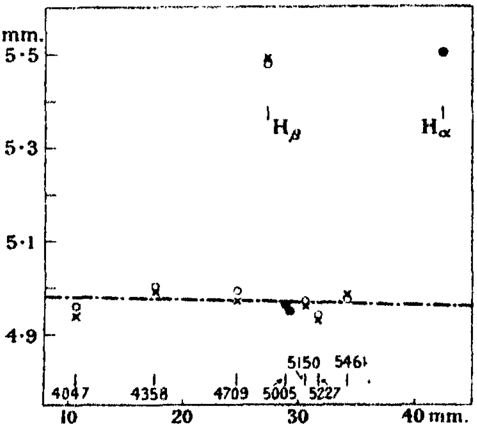

Fig. 5.

It might be suggested that this method of locating the maximum of excitation is open to the objection that possibly the air-molecules have been displaced by impact with hydrogen atoms. Since, however, the total intensity of the air-lines is much greater than the total intensity of the hydrogen, it is necessary in any case to suppose that the majority of the collisions lead to excitation of air-molecules, and only a smaller proportion excite hydrogen atoms. If now, of this majority, a large proportion do give the air-molecules an appreciable amount of momentum, it is clear that a large proportion of such hydrogen atoms as collide at all must (since they are light) be definitely stopped or turned back, and a corresponding number must be deflected through other angles. These atoms must be considerably more numerous than the ones that are excited without being deflected, and there is no evident reason why none of them should radiate: but no trace of them is to be found on the plates. Further, the symmetry of the air-maxima makes the idea unlikely.

It will be noticed that H_γ is not plotted in fig. 5. The line appearing on the plate at about the right place is evidently (from its general appearance) due for the most part to some substance coming in with the air; that it was actually mercury was proved by the presence (most of them very faint) of all the other reasonably probable mercury lines (or dots), and also by the position of its maximum on the wave-length graph, where the accuracy obtainable (in spite of the very wide "slit") was just definitely sufficient to decide against H_γ. That it was coming in with the air, and was neither a part of the canal-ray stream nor merely generally diffused through the tube, was clear from the very close resemblance of the photometer curve to that for 4709, and from the fact that the fainter mercury lines all showed a similar maximum at the jets and exactly resembled the fainter air lines.

Under the circumstances it is surprising that mercury lines should show up at all. The air used in the leak was indeed drawn from the room, and would presumably contain mercury at the usual pressure; this is, however, even neglecting the slower diffusion through the regulator, certainly not more than $2 \,.\, 10^{-6}$ of the total, and it does not seem particularly likely that the probability of excitation should be so overwhelmingly greater fór mercury, in the case of high-speed canal-ray impacts. There is a possibility that a drop of mercury was accidentally included, *on the low-pressure side* of the leak, when the apparatus was being assembled, but so far as can be judged from earlier photographs (which were obtained with a different type of apparatus and do not show the exact maximum, so that they are not quite conclusive) mercury has always come in with the air in about the same proportion. If this suggestion is really correct, it seems not unlikely that mercury would prove an extraordinarily efficient exciting agent, possibly owing to the large size of its atoms and the number of fairly loosely bound electrons round each. Since a collimated vapour-stream would offer the advantage that the general pressure in the tube would be very low indeed, the possibilities of this form of excitation appear worth exploring.

Fig. 4 shows that the method clearly allows both the exponential fall and the presence or absence of a time-lag before this begins, to be determined, provided the plate used can be properly calibrated; it was in this that the most serious difficulties were found. It was not practicable to put a comparison spectrum on the same plate at the same time as the main exposure, and it was therefore put on a separate plate subsequently, with as long an exposure as the main one (48 hours); both plates (which came, of course, from the same box) were then developed in the same tank together.* Unfortunately, the main plate was always slightly fogged with X-rays, which were not completely eliminated even in the last photograph taken, though certainly no direct or once-scattered rays could reach it. The fogging has always been enough to vitiate any accurate calibration, and such results as can be obtained in spite of it cannot be relied on for numerical accuracy. At the same time, it is evident from mere inspection of fig. 4 (though it is more fully shown below, fig. 7) that there is nothing approaching the interval inferred by McPetrie from his experiments.

---

* For details of development practice see "Photographic Photometry," Griffith, Dobson and Harrison, Clarendon Press.

The considerable difficulty with X-ray fogging is due to the long exposure, the high potential (35,000 volts peak; the H.T. source was a large coil with mercury break) and the considerable power used. In order to dissipate the energy, a very large hollow aluminium anode was used, and it ran at a red heat, emitting probably a considerable amount of white X-ray radiation of short enough wave-length to escape from the tube. Most of the spectrograph, and part of the discharge tube, were covered with lead, but apparently this protection was not adequate. A high tension D.C. supply would almost certainly have given less X-rays than a coil, for the same speed and intensity of canal-rays, and would have been preferable in other ways also. A carbon anode was tried once, to reduce the difficulty, but it made the tube unstable, by acting as a leak whenever it happened to warm up at all, and as a pump whenever its temperature fell. The apparatus was very sensitive to alterations in the hydrogen supply, since the pressure was low (9 cm. dark space) and the tube in the cathode long and narrow.

Interpretation.

Two attempts were made by the usual procedure* to convert the blackening curves into light-intensity curves. The difficulty arises in the presence on the main plate of a background which is absent on the comparison one. Clearly this background can be allowed for either in units of blackening, before the conversion, or in units of intensity after it. Neither process, of course, can be correct, but in each case a curve was obtained to which an exponential formula could be fitted exactly from 6 to 14 or 15 mm. abscissæ. The difference between calculated and observed curves was less than could be shown in a reproduction, but the equations to the curves differed considerably; the first method led to $I = I_0 e^{-2\cdot925x} + I_\infty$, where $I_0/I_\infty = 2\cdot35$, and the second led to $I = I_0 e^{-2\cdot725x} + I_\infty$, where $I_0/I_\infty = 3\cdot07$.† In each case the experimental curve fell, after about 18 mm., below the theoretical I_∞, which was, of course, additional evidence that the interpretation was faulty, but the agreement over the earlier part was sufficiently close, and for a sufficiently large range of $e^{-\mu x}$, for either curve to have appeared fairly probable if the other had not been obtained also.

It is perhaps worth mentioning, that even if the comparison spectrum had been placed on the same plate as the main one, the result could not be relied on unless the two exposures had been entirely simultaneous and concurrent, because in the early part of the main exposure the total X-ray intensity received was still small, while by the end it was larger; if the comparison spectrum had been put on after all the X-rays had been received the interpretation would still be uncertain. In Wien's work the two exposures appear to have been simultaneous, and in any case the exposures were so short, and the potentials so small, that X-ray fogging would not be expected; his values for the exponential constants are unquestionably more accurate than the present ones.

---

* Mie, 'Ann. d. Physik,' vol. 66, p. 252 (1921).

† x is in centimetres.

This question has been treated at some length because it is certainly the outstanding difficulty in this line of work, and because it happens that almost any photometer curve one is likely to obtain can be treated in a variety of ways, all of which, even if they are obviously unjustifiable, usually give a good exponential light-intensity curve over quite a considerable range.

In order to determine whether or no there is any interval before the exponential curve starts, it is necessary to know the distribution of excitation over the high-pressure region as well as the exponential decay-constant, and then to sum the effects of all points preceding a given one so as to find out the intensity of light to be expected there. The distribution of excitation might, perhaps, be calculated, but, in view of the thickness of the canal-ray stream and of the finite size of the jets, it is probably safer to infer it from measurements of the blackening in an air line, a method which appears to be completely reliable. A suitable line on grounds of intensity is 4709 Å, which can be interpreted by the calibration curve for H_β without appreciable error. The intensity curve thus obtained is given in fig. 6, and the expected curve for

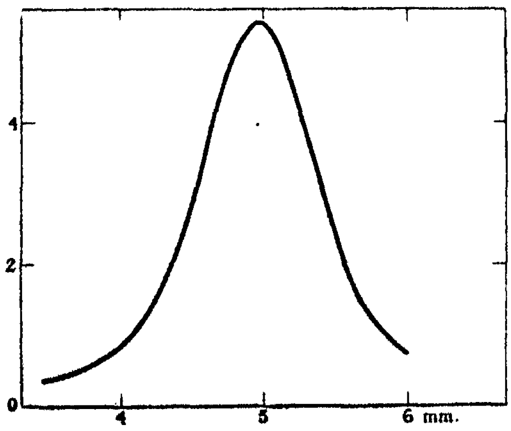

FIG. 6.

H_α is obtained by approximate integration from this (fig. 7), the assumption being made that no "interval" exists. The constant 2·925 per cm. was used for this purpose, but it is almost certainly a little too small. The experimental curve for H_α, obtained from fig. 4, is also shown in fig. 7. The vertical scale is probably slightly different for the two curves, owing to the background difficulty together with the fact that intensity-units are in any case necessarily arbitrary; it is, however, principally only the horizontal displacement of the maximum that is in question. The abscissal distance apart of the two maxima is seen to be small, and even the general shape of the curves is not very different. Part of the difference could certainly be accounted for by a distribution of velocities in the canal-rays. The fit is very much better than was obtained with the constant 2·725, which suggests that this method may even prove an accurate way of obtaining the constant, if the absence of any time-lag can be assumed. It will be noticed that the calculated maximum is actually further from the maximum of excitation (the line AB) than the observed one; since there obviously cannot really be a negative time-lag, this suggests very strongly that the discrepancy of 0·08 mm. is purely due to experimental error, so that we conclude that if the excitation could have been reduced to a point, the curve would have started from that point, and would have been exponential from the start.

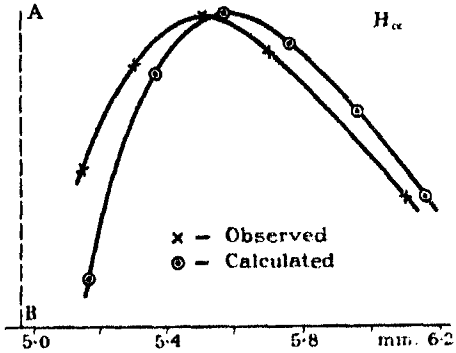

FIG. 7.

This result is, of course, only obtained for a large number of atoms, and leaves open the question whether we are observing a statistical effect analogous to a radio-active decay or whether there is a real falling-off in the light from all the atoms. Moreover, it would still be desirable to decrease the experimental uncertainty.

Further Considerations.

If it can be assumed now that "point-excitation" is a definitely feasible method of studying decay-times, and that the emission starts directly at the excitation-point, several further considerations suggest themselves, and the possibility is evident of obtaining answers to some questions of importance for which, up to the present, no experimental answer at all is available. The exact details of the whole process of excitation and emission appear, however, still to be so little known that any discussion must remain somewhat tentative; how undefined the position is may be gauged from the fact that no opinion seems as yet to have been expressed as to whether the excitation is, in fact, more usually direct or indirect—that is to say, whether the excitation, for example, of H_β in canal-rays consists, as a rule, in putting an atom directly into the four-quantum state, or whether it is more usually put into a higher state from which it jumps to that one.

It is, indeed, possible to frame hypotheses that would reconcile either view with the observed facts, but in the case of indirect excitation it must be admitted that they appear somewhat unsatisfactory. In order to account for the immediate commencement of the radiation, it would seem necessary to suppose, in effect, that an atom has two waiting times in any given stationary state—a very short one if the state was reached as the result of a fall, *i.e.*, in a radiational process, and a longer one (the one observed) if the state was reached as a result of a collision that transferred the atom from a stable state (complete ionisation or the normal state). It would be further necessary to suppose that the longer type of waiting time was practically the same for all orbits; and the explanation would fail in any case if the decay-constants of different lines were really different. In fact, exponential curves differing from one line to another do not seem to allow of the assumption of indirect excitation at all on the Verweilzeit theory, but only if we assume an Abklingungszeit; the atom could then execute all its transitions at once, and the energy be subsequently radiated in a number of independent *co-existent* trains.

If there really were these two different waiting times, absorption or fluorescence measurements could presumably demonstrate the fact. No such experiments have, of course, been attempted, and there seem to be no other data that would immediately contradict the assumption; but it is so foreign to present theory (which is more ready to credit an electron with foresight than with memory) that it is preferable to assume the excitation of canal-rays is mainly direct.

It may, perhaps, be pointed out that the difficulty of accounting for the immediate onset of maximum emission, on the assumption of indirect excitation, cannot be removed by assuming that the natural decay times of all infra-red lines are negligibly short. For we are apparently compelled to admit that the exponential constant may always be regarded as a measure of the waiting-time in the initial state, and it seems practically certain that we cannot describe any particular state as necessarily the initial state of an infra-red line at all; rather, the observed decay of any line gives us the total probability of all the possible ways by which an atom can leave the initial state in question, and this must evidently be the same whether we observe that line or any other starting from the same state.* Since the constants for, at any rate, the first three Balmer lines are approximately equal, a very considerable number of infra-red lines must also have the same rate of decay. Of course, this also is not a point which has ever been verified experimentally; the only definite experimental fact is that the strict electromagnetic view, according to which the damping is proportional to ν^2, is certainly wrong; qualitatively it is even in the wrong direction. The difficulties in the way of measurement with Paschen or Lyman lines are considerable; one could however take, say, the three lines of the mercury triplet 5461, 4358 and 4047, or the thallium doublet 5350, 3776, for which the same argument holds. In view, however, of the facts that modern theory postulates this view at every turn, and that, even though theory does not demand it, the constants appear in fact to be very similar for all visible lines, it would be desirable to be sure of being able to attain considerable accuracy before beginning the experiment. Even a rough measurement in the Lyman series would probably be more convincing.

If now we assume direct excitation there seems to be only one possibility, though the exact formulation of it depends on whether the hydrogen is supposed to be charged or neutral before excitation. We shall here assume that it is charged, but the argument can easily be adapted to the other case; the conclusion, *mutatis mutandis*, is identical. Obviously the energy necessary to ionise the exciting-molecule must come mainly from the kinetic energy of the hydrogen ion, since the neutralisation of its charge in an outer orbit provides only one or two volts. We cannot now suppose that the kinetic energy is reduced by *approximately* the right amount, and that the balance of the free energy, when the electron has definitely found a place in some hydrogen orbit, is radiated either as the limit-line of some series or as part of a continuous spectrum beyond such limit; that is once more open to all the objections that may be raised against indirect excitation, unless satisfactory grounds could be found why this particular kind of emission should have an extremely short waiting time. We must rather assume that the kinetic energy is reduced by the *exact amount necessary*, taking into account the amount required to ionise the air (or mercury) molecule, the further amount possibly required to place the resulting ion in a definite excited state,[*] and the small amount that will be gained from the hydrogen as a result of neutralising it in an outer orbit. The process in fact must be regarded as a counterpart to the ordinary Stoss zweiter Art, *i.e.*, a collision involving changes in the potential energy of both the colliding particles, but one in which the total kinetic energy, instead of being increased, is diminished. Thermodynamically it would seem inevitable that such processes must be able to occur, when the kinetic energy is high, and the effect of canal-ray observations is then to show that here they occur to the practical exclusion of all others. [It may be noted that on this view it is quite probable that in a number of cases the ion may be directly neutralised by capture into even its lowest orbit.]

---

* *Note added July* 18, 1927.—This argument is based on the apparently exponential nature of Wien's decay curves, according to which all subdivisions of a term seemed equivalent. This is probably wrong, see p. 101.

There remains, however, a difficulty, namely, that the excitation cannot in fact be entirely direct. The exact seriousness of this cannot at present be estimated, but its effect (if we reject the explanation suggested above for indirect excitation) must be that, to a greater or less extent, the decay-curves are not really exponential at all. Whether the variation from the exponential form can lie within the limits of experimental uncertainty[†] is a question for theoretical calculation, but one which is probably far from an answer as yet, since the probability of excitation of higher states by impact with air-molecules is a problem that involves several unknown quantities. Even however if the higher states could be entirely neglected, a definite fraction of the atoms excited to even the four-quantum state will ultimately emit, not H_β, but H_α; this proportion will presumably be calculable when the New Mechanics is more fully developed, and it would be interesting to see whether it is noticeable.[‡] It is in any case, at present, somewhat surprising that the Balmer lines should appear to give exponential constants at all, since they each consist primarily of two strong components having, on the old view, different values of k; on the new view the great bulk of the intensity of both components is indeed due to transitions from initial states having the same values of k, but the initial states of the two components as a whole have still different values, of j.* It would thus be desirable to extend both the range and the accuracy of the measurements, in order to ascertain how closely the curves really are exponential. Two components of equal intensity would give two exponential curves of equal area; the fact that their sum is closely an exponential itself indicates that the two constants must be either closely similar or very considerably different.

---

[*] The nitrogen radiation was that due to the ionised molecule, with a small proportion also from ionised atoms; the mercury lines, on the other hand, were the ordinary arc lines. It is not, of course, in principle necessary that the collision which excites a hydrogen atom should also be one that results in radiation of the exciting-atom at all, or at least not in visible radiation.

[†] W. Wien, *loc. cit.*, and 'Ann. d. Physik,' vol. 73, p. 483 (1924).

[‡] See Addendum, p. 101.

A further question, definitely capable of an experimental answer, but so far never apparently attacked, is whether the atoms immediately before excitation are, as has been assumed above, actually charged at all or whether they are neutral. The method of point-excitation seems particularly well-fitted to decide this question, and an apparatus was in fact constructed for the purpose; the principle was simply to deflect all charged particles through a known angle by a well-defined electrostatic field before passing them between the jets; if the radiating atoms were charged before excitation, the method obviously removes all slow-moving atoms, and also allows of a determination of the velocity of the atoms observed, so that absolute values of the decay-constants can be obtained without measuring the Doppler effect. The only result obtained, however, was that no part of the visible canal-ray stream was deflected at all; since this would have implied either that there were no charged particles in the stream (which was certainly untrue; the current was of the order of 10^{-7} amp.), or that no part of the excitation *even of the residual air molecules* was due to charged particles (which seems very unlikely), it appears most reasonable to assume that there was a faulty connection to the condenser plates. The apparatus failed after a short run, in a manner that suggested strongly that this was the case, but on dismounting it was not found possible to verify the point definitely. The state of the atom immediately before excitation thus appears still to be uncertain.

If, however, we may once again assume that the unexcited atoms are charged, the following somewhat difficult experiment appears interesting, even though only one result for it is at present predicted by theory. We consider the effect of strong incident radiation of the same frequency, on the rate of decay of a given spectral line, and the argument rests essentially on Einstein's derivation of Planck's formula. By electrostatic deflection we can obtain a beam of canal-rays consisting entirely of charged and non-radiating atoms; let it be subjected for some centimetres to intense constant radiation (from the side) of some line (preferably the lowest line of a resonance series) of the *non-ionised* atom, and early in the range of this radiation let an excitation point, *i.e.*, a neutralisation-point, be placed. The beam from this point on will consist of (1) charged atoms, which can be neglected; (2) atoms excited to other states than the initial one for the radiation in question; apparently these can also be neglected; (3) atoms excited to the initial state of the radiation; and (4) unexcited neutral atoms, whose number we shall assume (though probably this is not correct) is zero at the start. (It will be found that if this assumption is not justified the most interesting conclusion is still substantially unaffected.)

---

* Sommerfeld and Unsöld, 'Z. f. Physik,' vol. 36, p. 259 (1926); vol. 38, p. 237 (1926). In view of the question there raised about the metastability of the 2*s* term, it would be very desirable to observe the relative intensities of the components in a canal-ray stream *by the point-excitation method*; it seems, however, uncertain whether the lines are narrow enough.

In the absence of radiation the excited atoms would fall back to the normal state, giving an exponential emission curve $I = I_0 e^{-At}$. The effect of radiation, on Einstein's view, is two-fold—to lift atoms again from the normal state, and to accelerate their fall from the excited state. We should thus get an intensity-curve which starts higher than the uninfluenced one, falls with a more rapid constant, and falls not to zero but to a finite value which is in fact the ordinary resonance fluorescence value. On putting in the quantities it is found that the experiment is not quite out of the question.

Let N be the number of atoms in the excited state, and N_0 the total number of neutral atoms in either the excited or the normal state, so that in the absence of radiation $N = N_0 e^{-At}$. (We shall assume the absence throughout of unexcited atoms that were previously in other excited states, though in practice this would seldom be justified.) Let M be the number in the normal state, so that then $N + M = N_0$. Then in the presence of radiation

$$-\frac{dN}{dt} = AN + BA\rho_\nu (N - M) \quad \text{where } B = \frac{c^3}{8\pi h\nu^3}.$$

Thus it is easy to see that

$$N = N_0 [e^{-(1+2B\rho_\nu)At} (1 - Q\rho_\nu) + Q\rho_\nu],$$

where

$$Q = \frac{c}{8\pi h\nu^3 + 2c^3\rho_\nu} (= B \text{ for } \rho_\nu \rightarrow 0).$$

The radiation is not simply proportional to N or to dN/dt, but to $AN + BAN\rho_\nu$, *i.e.*, to $(1 + B\rho_\nu) N_0 A [e^{(1+2B\rho_\nu)At} (1 - Q\rho_\nu) + Q\rho_\nu]$. To get some idea of the quantities involved, we will suppose that ρ_ν has the value it would have in a black enclosure at the temperature T; if, then, α is the smallest fractional change in A that can be experimentally verified, $\frac{\nu}{T} = \frac{k}{h} . ln\left(\frac{2}{\alpha} + 1\right)$. Thus if we put $\alpha = 1$ per cent. and consider the Cs line at 8943 Å, $T = 3060°$. An adverse factor in ρ_ν of at least about 10 must presumably be introduced by necessary limitations of the solid angle from which the radiation comes, but, on the other hand, electrical excitation of lines produces much higher values of ρ_ν than temperature-excitation, so that it would appear that it should be possible to obtain enough light.

The main obstacle once this is achieved is obviously the elimination of all scattered light from the walls of the tube: perhaps the best method of avoiding this difficulty is to work with a wide doublet of which both lines have the same initial state, *e.g.*, the thallium pair. It is thus possible to use only one line for excitation, and the other alone for observation. Obviously the same theory applies as before, except that it is necessary to know the relative intensities of the two lines, and to measure the exponential constant with greater accuracy.

The equation derived above shows that an appreciable alteration in an exponential constant is to be expected only when the fluorescence-light begins to be comparable with the original canal-ray light even though the number of neutral unexcited atoms is small at the start. The density of atoms actually comprising the canal-ray stream is very small compared to that in the tube as a whole under ordinary circumstances; expressed as a pressure it may be as low as 10^{-10} mm.; even if we take a more generous figure and put the pressure at 10^{-9} mm. it is remarkable that we should apparently expect measurable fluorescence at such a pressure, and it is clear that the incident light must be intense. Special precautions would be necessary to ensure that even in the immediate neighbourhood of the canal-ray pencil the partial pressure of stationary thallium atoms was really small compared with this figure.

The experiment, if possible at all, would probably still be possible without point-excitation, but the presence of a large percentage of neutral unexcited atoms would be a disadvantage even if their number were known. If it should turn out in fact that the unexcited atoms in a canal-ray stream are not, as has been assumed in the above enquiry, charged at all, a similar line of argument shows that a focussed beam of resonance light ought to be capable of serving as a point-excitation. It is easily seen, however, that even for $\rho_\nu = \infty$ only half the atoms can be in the excited state at any one time.

Even if neither of these experiments is in practice capable of being successfully performed, the above discussion (which appears to employ the only assumptions at present available for this question) may serve to remove a possible misunderstanding. Thus Wien found that the mercury line 2537 Å decayed much more slowly than any other lines he had investigated, and it has been suggested that its character as a resonance line might be responsible for the difference, by delaying the departure of atoms from the initial state. The above argument shows that the radiation of the canal-rays themselves will be too weak to produce an observable effect (a conclusion also reached by Wien on other grounds) but it also shows that any effect there is must be in the wrong direction. Radiation does displace the equilibrium distribution of atoms in the direction of the excited state, but its effect on the time required to reach this distribution is to shorten it, not to lengthen it.

Summary.

Experiments are described in which a non-luminous beam of canal-rays was made to emit the Balmer lines by excitation at approximately one point only. The distribution of excitation round this point was determinable and the position of its maximum could be fixed within one or two hundredths of a millimetre. The distribution of intensity in the Balmer lines was measured photographically and compared, near the maximum, with that to be expected on the assumption that the intensity due to a strict point-excitation would begin at the point and would fall off exponentially from the start. The agreement obtained supports this assumption.

Several considerations arising out of this result are discussed, including some suggestions as to the nature of the excitation process ; and some further experiments made possible by the success of the method are outlined, especially a proposal for observing the " negative radiation-effect " postulated by Einstein.

This investigation was carried out in the Clarendon Laboratory, Oxford, and the author's best thanks are due to Professor Lindemann for his constant interest and advice.

[*Added, July* 18, 1927.—Since this paper was written, two important articles have appeared which, taken together, answer many of the questions raised, and correct some false assumptions. The absolute intensities and decay-constants of all the components of the Lyman, Balmer and Paschen lines have been calculated by Sugiura,* and it appears that the three portions of each Balmer line that correspond to the three possible l-transitions have appreciably different decay-constants. (The constants are necessarily always independent of j when the Burger-Dorgelo summation-rules hold.) Further, Sugiura's figures make it possible to calculate the indirectly-excited intensity of H_α that must accompany a given intensity of H_β, and so on, and it appears that this is considerable. In discussing the experimental data, however, Sugiura did not take this point into account; he also assumed that, since Wien's measurements gave a simple exponential curve, the perturbations to which the atoms were subject were large compared with the component-separations, and that this must have produced a free interchange among the various subdivisions of a term; the "average" single exponential constants thus calculated are, however, in admittedly poor agreement with Wien.

---

* 'J. Phys. et Radium,' vol. 8, p. 113 (1927).

The above assumption is open to several objections, which have been greatly strengthened by Wien's latest results; he has now, in fact, measured the decay-constants of the first two Lyman lines,* obtaining values about three times as large as in the Balmer series. This is in very fair agreement with Sugiura's calculations for the second line (the first is perhaps complicated by an incomplete metastability of the 2S term), and seems in any case conclusive evidence that the subdivisions of a term do, in fact, decay independently.

If we, then, take Sugiura's individual figures, we can plot the curves for each component and sum them. The initial ordinates are as the intensities before the cathode, *i.e.*, as *g*.A, and the resulting curves do not fit exponential formulæ well; the curves representing indirectly-excited intensity are, however, qualitatively well-suited to correct the deficiency, since they obviously start with the ordinate 0, rise fairly rapidly to a number of weak inseparable maxima, and fall fairly slowly again. It remains to consider the quantitative agreement.

The exact shape of the curve is strictly calculable, if we assume definite ratios for the intensities of the Balmer lines among themselves; on this point, however, we have experimentally so much freedom that the labour is not justified. The maximum of the curve, which is very flat, obviously cannot come so far from the right place (about 10^{-8} sec.) as to be experimentally noticeable, and the observations hardly extend as far as $3 . 10^{-8}$ sec.; it thus suffices if the area is about correct.

From Sugiura's figures, if we have initially N atoms in the 3-quantum state, correctly distributed, $0 \cdot 706$ N will emit H_α; and if we have M atoms in the 4-quantum state, $0 \cdot 292$ M will emit H_β and $0 \cdot 457$ M will ultimately emit H_α. The relative intensities of H_α and H_β are thus as $7 \cdot 06 \text{ N} \div 2 \cdot 92 \text{ M}$ if we consider

---

[*] 'Ann. d. Physik,' vol. 83, p. 1 (1927).

only direct excitation; if then we put this ratio at 9·0 for example (it is probably larger), the ratio of "4-quantum" H_α to "3-quantum" H_α is 1/5·76. Allowing a small addition for excitation from higher states again, the total indirect excitation of H_α may be say 1/4·9 of the direct, or 1/5·9 of the entire excitation. The difference between the sum of the Sugiura curves and the exponential with the same initial ordinate and a constant of 5·5 . 10^7 has also an area about 1/5·9 of that of the exponential, and any reasonable ratio for the relative intensities of H_α and H_β can be obtained by choice of an exponential constant that still remains within the range covered by Wien's results*; the agreement for H_α is thus complete.

Wien's measurements gave very much more consistent results for one apparatus, and, with each apparatus, for one velocity, than for all experiments together; if the above explanation is correct this is obviously to be expected.

The agreement for H_β is less satisfactory; the constant comes out at about 3·1 . 10^7, while Wien's lowest value was 4·35 . 10^7, and the area of the difference-curve is small. Nevertheless, there are so many possibilities which might influence the result, that it cannot be said the experiments disprove the theory.

Thus the process of excitation surmised in this paper is probably correct, namely, an instantaneous placing of the hydrogen ion (or atom) into a definite, and preferably fairly deep, quantised state; but the apparent directness of canal-ray determinations of decay-times is illusory, and particularly illusory in the case of hydrogen.]

---

* For summary see 'Ann. d. Physik,' vol. 73, p. 503 (1924).

On the Flexure of Thin Cylindrical Shells and other " Thin" Sections.

By L. G. Brazier, B.Sc.

(Communicated by R. V. Southwell, F.R.S.—Received May 28, 1927.)

It is a generally appreciated deduction from St. Venant's solution of the flexure problem that a beam in which the material is disposed at a distance from the neutral axis is superior to the solid section in economy of material. St. Venant's solution, however, suggests that this advantage increases without limit as the thickness of the material is reduced and the distance from the neutral axis is increased. It has, of course, been generally realised that this conclusion is not supported by ordinary engineering practice, and recent experience in the use of high tensile steels and problems of aircraft structure have emphasised the desirability of a further examination of the flexure problem.

St. Venant's solutions are obtained when the equations of equilibrium of an isotropic elastic solid are made linear by the neglect of terms of higher orders than the first; and by Kirchhoff's theorem of determinancy these solutions may then be considered unique and stable. To attack problems of stability it is necessary, as is shown by R. V. Southwell* in his 'General Theory of Elastic Stability,' to include some of the second order effects. It is, in fact, only when these become considerable that Kirchhoff's theorem fails and instability becomes possible. By this general treatment various classes of instability are obtained or indicated, but the only ones susceptible to analysis or of practical interest (on account of the " elastic limit " which is a feature of all practical materials) are those in which at the moment of instability the strains are still small. Bryant† has shown that this will only occur, as in the case of thin rods and shells, when one dimension of the body is small compared with others.

In a similar way we may expect that when one dimension of the *cross section* of the body is small compared with others it will be necessary to include second order terms in problems purely of flexural equilibrium. This is really evident in the case of the flexure problem from St. Venant's explicit description of the stress at any element of the cross section as a function of the *initial* position of the element. The longitudinal stress, for example, is prescribed as directly proportional to the initial distance of the element from the line of centroids or neutral axis. If, however, one dimension of the cross section is small compared with others, then even while the strains remain everywhere small, large displacements over the cross section may occur. It is then clearly inaccurate to assume that the stress in the element is a linear function of its initial position. The accurate description of the stress in the element as a function of its resultant position after including displacements due to strain, corresponds to the introduction in the problem of higher terms than the first.

---

* 'Phil. Trans. Roy. Soc.,' A, vol. 213, p. 187.

† 'Camb. Phil. Soc. Proc.,' vol. 6, p. 199 (1888).

The present paper illustrates problems of this class. It indicates the necessary corrections to St. Venant's theory of flexure for cases in which some dimensions of the cross section are small compared with others. The problem is not attacked by a direct introduction of higher terms in the equations of equilibrium, but by the variational method and the general dynamical theorem that a position of equilibrium will be a position of minimum energy. The body is supposed strained in the manner described by St. Venant. It is then allowed to undergo a system of displacements, and the system determined by the condition that the final potential energy is a minimum. The system of displacements is directed so that the applied forces do no work, and the condition then is that the strain energy of the body is a minimum.

It is interesting to find that this treatment suggests a form of instability under flexure which does not appear to have been treated before. St. Venant's solution gives a linear relation between the bending moment exerted on the beam and the resulting curvature of its central line. The effect of second or higher order terms will necessarily be to depress the bending moment progressively, below the value given by St. Venant's relation, in the manner shown in fig. 1.

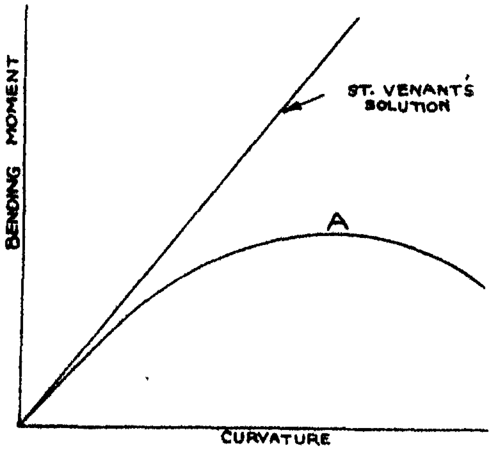

FIG. 1.

The solution obtained in this paper shows a point A at which the bending moment passes through a maximum. If the bending moment is increased above this value the beam must collapse. That is to say that the point A is a point of instability. This form of instability is characterised in comparison with the generally accepted types of instability by absence of a point of bifurcation at which an extensional and an inextensional system of displacements under the given load system become possible.* In this instability form there is no inextensional system and no bifurcation point, but a progressive reduction of the appropriate elastic rigidity through a point at which the external load system must be a maximum. In the present paper terms only of the second order have been introduced so that it will not in general give an exact expression for the maximum bending moment, but it does indicate the existence of this maximum and should give it quantitatively for sufficiently "thin" sections.

The Thin Circular Tube.

The method can conveniently be illustrated by the case of a thin circular tube subjected to flexure. To eliminate the difficulties of end effects we suppose that a long tube is bent into a circle of large radius and joined on itself. We then consider the relation between the bending moment transmitted by the tube at any section and the curvature of the tube.

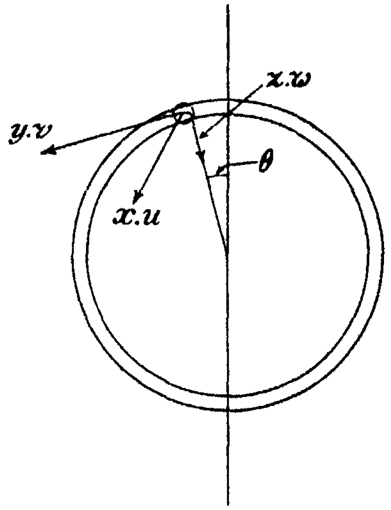

FIG. 2.

We consider, therefore, a cross section of a toroidal shell. The median radius of the cross section is r, and the thickness t. We describe a moving system of coordinates x, y, z, and of displacements u, v, w, as shown in fig. 2, the origin moving round the median circumference, and the axis of z remaining directed towards the centre and making an angle θ with the plane of symmetry of the toroid. The axis of y remains in the cross section. The plane $\theta = 0$ contains the centre of the toroid, and the curvature of the toroid is c.

---

* Curves similar to that of fig. 1 were given by Southwell in his general remarks on the collapse of struts formed of materials having finite limits of elasticity; but his curves do not pass through the origin since they contemplated initial curvature due to inaccuracies of workmanship or loading.

According to St. Venant's solution of the flexure problem the displacements in the plane of the cross section will then be:—

$$w_0 = \frac{c}{2}\sigma r^2 \cos\theta \tag{1}$$

$$v_0 = -\frac{c}{2}\sigma r^2 \sin\theta. \tag{2}$$

By expressing c in terms of Young's modulus, the maximum stress allowable and the radius we may note that for ordinary materials, including wood and metals, the maximum displacement will be of the order of $\frac{r}{1000}$.

We may conveniently imagine that when the tube was straight it was filled with a solidifying compound. When set this compound has an intelligent partiality for St. Venant's solutions, and while presenting no opposition to displacements given by his solutions, offers a complete rigidity against all other displacements. When the tube is bent to the toroid the cross section will therefore take up the form given by (1) and (2).

If the compound is now melted the cross section will be free to take up a further system of displacements v' w'. We determine v' w' by the condition that the tube will pass to a position of minimum strain energy.

As usual in problems of this type we suppose that the system v' w' is inextensional.* As w_0 v_0 have been seen to be very small the condition that w' v' are inextensional is that:—

$$w' = \frac{dv'}{d\theta}. \tag{3}$$

The total displacements are

$$w = w' + w_0 \qquad \text{and} \qquad v = v' + v_0, \tag{4}$$

and using (3) we obtain

$$w - \frac{dv}{d\theta} = w_0 - \frac{dv_0}{d\theta} = c\sigma r^2 \cos\theta \tag{5}$$

$$\frac{d^2w}{d\theta^2} - \frac{d^3v}{d\theta^3} = -c\sigma r^2 \cos\theta. \tag{6}$$

---

* *Vide* Basset, "Extension and Flexure of Cylindrical and Spherical Thin Elastic Shells," 'Phil. Trans.,' A, vol. 190, p. 433 (1890), and Rayleigh, 'Roy. Soc. Proc.,' vol. 45, p. 105 (1888). The justification for this assumption is essentially that the energy absorbed by any extensional displacement (compared with a flexural displacement) is mathematically large and therefore precluded.

The change of lateral curvature (*i.e.*, in the plane $x = 0$) at a point on the cross section is

$$c_L = \frac{1}{r^2}\left(\frac{d^2w'}{d\theta^2} + \frac{dv'}{d\theta}\right), \tag{7}$$

and using (6) we obtain

$$c_L = \frac{1}{r^2}\left(\frac{d^3v}{d\theta^2} + \frac{dv}{d\theta}\right). \tag{8}$$

The longitudinal strain at an element is proportional to the resultant distance from the neutral axis. This is

$$d = (r - w)\cos\theta - v\sin\theta. \tag{9}$$

From (9) and (8) we obtain (after neglecting products and squares of small quantities) for the total strain energy per unit length of the toroid the expression

$$\mathrm{U} = \frac{\mathrm{E}}{2}\left[\int_0^{2\pi} \frac{t^3}{(1-\sigma^2)\,12r^3}\left(\frac{d^3v}{d\theta^3} + \frac{dv}{d\theta}\right)^2 + c^2rt\left[\left\{r^2 - 2r\left(\frac{dv}{d\theta} + r^2c\sigma\cos\theta\right)\right\}\cos^2\theta - rv\sin 2\theta\right]d\theta\right]. \tag{10}$$

If this is to be a minimum then according to the calculus of variations v must satisfy the equation

$$\frac{d^6v}{d\theta^6} + 2\frac{d^4v}{d\theta^4} + \frac{d^2v}{d\theta^2} = -\frac{18c^2r^5}{t^2}(1-\sigma^2)\sin 2\theta. \tag{11}$$

The solution of this is

$$\frac{d^2v}{d\theta^2} = (\mathrm{A} + \mathrm{B}\theta)\cos\theta + (\mathrm{H} + \mathrm{E}\theta)\sin\theta - \frac{\mathrm{N}}{9}\sin 2\theta, \tag{12}$$

where

$$\mathrm{N} = \frac{18c^2r^5}{t^2}(1-\sigma^2). \tag{13}$$

Considerations of symmetry and of continuity of the circumference require that the constants, B, E and H, and the first of the two arising in the integration of (12) vanish. The second of these two and the constant A represent a rigid body displacement which can be disregarded.

We then have

$$v = \frac{\mathrm{N}}{36}\sin 2\theta,$$

$$\frac{dv}{d\theta} = \frac{\mathrm{N}}{18}\cos 2\theta, \tag{14}$$

etc.,

and

$$w = \frac{\mathrm{N}}{18}\cos 2\theta + c\,\sigma r^2\cos\theta. \tag{15}$$

It will be observed that the term containing σ is very small. It represents the St. Venant displacements (1) (2) plus a rigid body motion which is immaterial. If these expressions are substituted in (10) and the integrations effected, we obtain

$$U = \frac{E}{2}\pi r^3 t c^2 \left\{1 - \frac{3}{4}\frac{r^4 c^2 (1-\sigma^2)}{t^2}\right\}, \tag{16}$$

and the couple transmitted at a section of the toroid is given by

$$M = \frac{dU}{dc} = \frac{E}{2}\pi r^3 t \left\{2c - \frac{3r^4 c^3 (1-\sigma^2)}{t^2}\right\}. \tag{17}$$

This is a maximum when

$$c^2 = \frac{2}{9}\frac{t}{r^4 (1-\sigma^2)} \tag{18}$$

at which point the couple is

$$\bar{M} = \frac{2\sqrt{2}}{9}\frac{E\pi r t^2}{\sqrt{1-\sigma^2}}. \tag{19}$$

If (18) is substituted in (14) we obtain for the maximum radial deflection at this instant

$$\hat{w} = \frac{2}{9}r, \tag{20}$$

so that the approximations based on the smallness of w and v are justified to this extent. The form of the cross section at this point is shown at fig. 3. This figure makes it clear what is happening. The longitudinal compression on the inner side of a beam and the longitudinal tension on the outer side, both have a component directed towards the centre of the tube and tending to flatten it, in much the same way as the earth pressure tends to flatten a circular tunnel. These pressures are actually flattening the circular cross-section into the quasi-oval form shown in fig. 3. That this is the physical interpretation of the equations

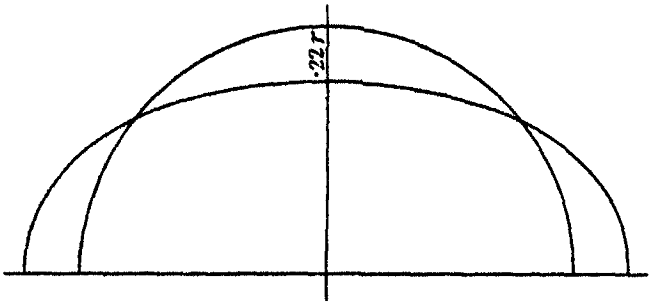

FIG. 3.—Deformation of thin tube immediately before buckling.

is clear from the following argument. The components of the longitudinal tensions and compressions directed towards the median circumference of the toroid give rise at all points of the cross-section to a pressure per unit area of amount

$$p = \mathrm{E}c^2rt \cos \theta. \tag{21}$$

And if the equilibrium of an infinitely long cylindrical shell under a vertical pressure

$$p_1 = \mathrm{E}c^2rt \cos \theta$$

is examined, it is found that the cylinder is distorted in exactly the manner defined by equations (14) and (15) without the final term of (15) which is due to St. Venant's flexure distortion.

The analysis has dealt with an endless beam strained in such a way that every section must undergo the same distortion. But we may reasonably expect the results to apply to the ordinary tubular beam provided it is sufficiently long to minimise the end effects. Then the relation between the terminal couples and the curvature of the beam will be equation (17) and not St. Venant's equation

$$\mathrm{M} = \mathrm{E}\pi r^3tc. \tag{22}$$

So long as the couple is below the value (19) there is an equilibrium position, though not a unique one. If the couple exceeds (19) the beam must necessarily collapse, even with a material of infinite elastic proportionality.

Terms of the second order only have been introduced, and it is necessary to consider if higher order terms are likely to be important. We have found that all elements of the tube are effectively subjected to a pressure tending to flatten the tube to a quasi-oval section. Elements at the top of the compression side, therefore, are in a similar condition to elements of a cylindrical shell subjected to end compression and hydraulic pressure. Southwell* deals with the problem as an example of his general theory, and finds that the tube may collapse into lobed forms of distortion which have been experimentally reproduced. In a corresponding way, therefore, a lobed deformation may occur on the compression side of the bent tube and approximate calculation suggests that this may occur before the instability point (19) is reached.

This has been experimentally confirmed. The relation between terminal couples and average curvature over the length was observed for long thin tubular beams made of celluloid and subjected to pure terminal couples. These relations are shown in fig. 4. In these experiments as the terminal couple was increased the cross section of the tube was observed to take up the quasi-oval form, and finally collapse occurred when a lobed deformation formed on the compression side. In one case the lobe occurred just as the tube was passing

---

* "On the General Theory of Elastic Stability," 'Phil. Trans.,' A, vol. 213, pp. 187–244.

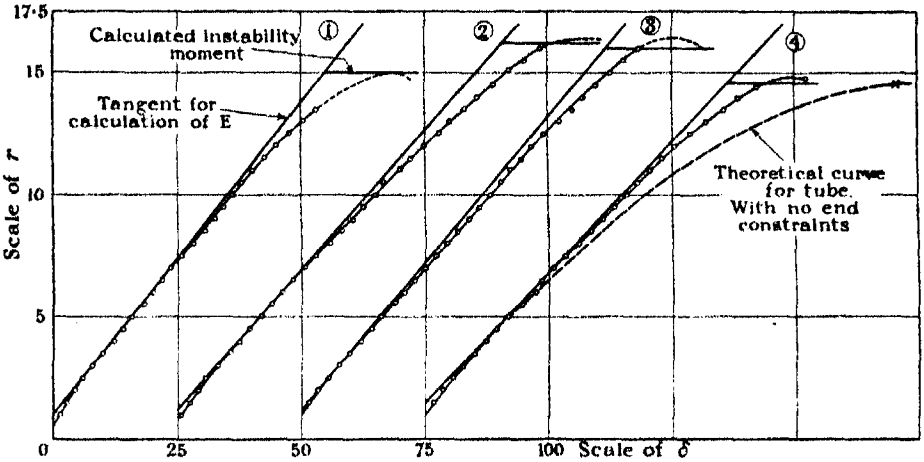

Fig. 4.—Curves showing moment-curvature characteristics of celluloid tubes.

$\Delta M = \Delta r/4{\cdot}87 - 0{\cdot}005\,\Delta\delta.$ $\Delta c = 1{\cdot}885\,.\,10^{-4}\Delta\delta.$

c = mean curvature over length of tube.

through the critical point A of fig. 1. A photograph of a lobed failure is shown at fig. 5.

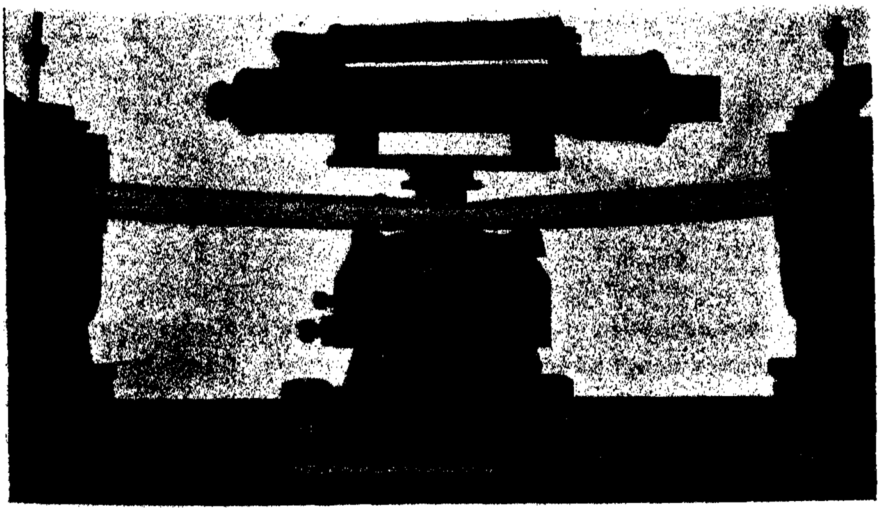

Fig. 5.

Thin Sections other than Circular.

Geometrical sections such as the ellipse can clearly be treated by the same method that has been used for the circular section. Considerable interest, however, attaches to irregular sections such as those used by aircraft engineers A typical cross-section is shown in fig. 6.

The variational method can be applied to examine the equilibrium of the flange* when the beam is bent by terminal couples. Referring to fig. 7 we describe a moving system of co-ordinates x, y, z, and of displacements u, v, w. The origin moves along the median plane of the flange. The axis of x remains parallel to the axis of the spar and the axis of z is normal to the flange at the origin. We define t as the thickness of the flange, d as the initial distance of the origin from the neutral axis, ψ the angle of the tangent at the origin to the horizontal, and ρ the initial radius of curvature of the section (in the plane $x =$

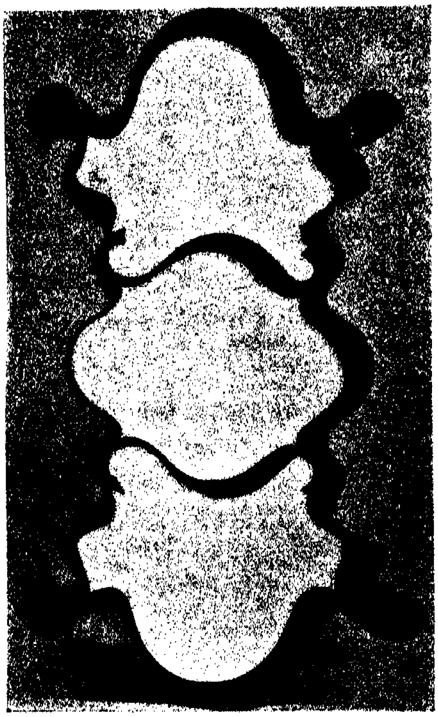

FIG. 6.

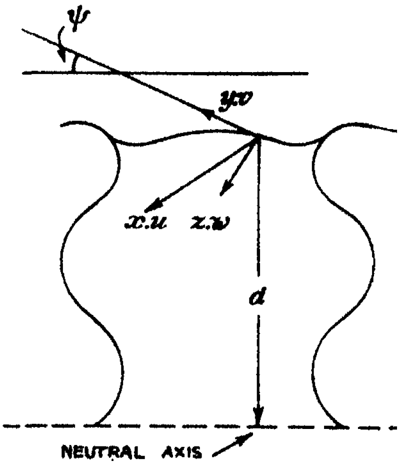

FIG. 7.

---

[*] "Flange" is used throughout in the sense that it is used by the beam engineer. That is to say, a beam has essentially two components, a "flange" and a "web."

const.) at the origin. The independent variable s is measured along the flange. (See fig. 7.)

We suppose that the spar is subjected to a constant axial curvature c and that the stress at any point is proportional to the distance from the neutral axis. As before, we then allow the flange to take up an inextensible system of deformation w, v. The condition of inextension is

$$\frac{dv}{ds} = \frac{w}{\rho}. \tag{23}$$

Using (23) we obtain for the change of curvature at a point

$$\Delta c_L = \rho v''' + 2\rho' v'' + \left(\rho'' + \frac{1}{\rho}\right) v' - \frac{\rho'}{\rho^2} v, \tag{24}$$

where the dashes denote the operation of differentiation with respect to s. For differentiations above the third order Roman numerals will be used. The resultant distance from the neutral axis is

$$d - w \cos \psi + v \sin \psi, \tag{25}$$

and we thus obtain after neglecting squares and products of the small quantities v and w with respect to d for the total strain energy between s_1 and s_2 per unit length along the spar the expression

$$\begin{aligned} U = \frac{1}{2}\Bigg[\frac{Et^3}{12(1-\sigma^2)} \int_{s_1}^{s_2} \left\{\rho v''' + 2\rho' v'' + \left(\rho'' + \frac{1}{\rho}\right) v' - \frac{\rho'}{\rho^2 v}\right\}^2 ds \\ + Etc^2 \int_{s_1}^{s_2} \{d^2 + 2dv \sin \psi - 2d\rho v' \cos \psi\}\, ds\Bigg]. \end{aligned} \tag{26}$$

As before if this is to be a minimum, v must satisfy a sixth order linear differential equation of which the coefficients are the following known functions of the independent variable :—

$$\begin{aligned} \alpha_0 &= \rho^2, \\ \alpha_1 &= 6\rho\rho', \\ \alpha_2 &= 10\rho\rho'' + 2 + 4\rho'^2, \\ \alpha_3 &= 10\rho\rho''' + 6\rho'\rho'', \\ \alpha_4 &= 5\rho\rho^{\text{iv}} - 3\frac{\rho''}{\rho} + 4\rho'\rho''' + 9\left(\frac{\rho'}{\rho}\right)^2 + \frac{1}{\rho^2}, \\ \alpha_5 &= \rho\rho^{\text{v}} + \rho'\rho^{\text{iv}} - 3\frac{\rho'''}{\rho} + 21\frac{\rho'\rho''}{\rho^2} - 18\left(\frac{\rho'}{\rho}\right)^3 - 2\frac{\rho'}{\rho^3}, \\ \alpha_6 &= -\frac{\rho^{\text{iv}}}{\rho} + 7\frac{\rho'\rho'''}{\rho^2} + 18\left(\frac{\rho'}{\rho}\right)^4 + 6\left(\frac{\rho''}{\rho}\right)^2 - 30\frac{\rho'\rho''}{\rho^3} - \frac{\rho''}{\rho^3} + 2\frac{\rho'^2}{\rho^4}, \end{aligned} \tag{27}$$

$\alpha_{(6-n)}$ being the coefficient $\dfrac{d^n v}{ds^n}$.

The second member of the equation is the known function of the independent variable

$$\frac{12c^2(1-\sigma^2)}{t^2}\{d\sin\psi + d\overline{\rho\cos\psi}'\}. \tag{28}$$

In the solution of this equation the integration constants can be determined either from the limit terms given by the calculus of variations for the free ends of the flange, or as the physical significance of the equations and terms is known by inserting the conditions that the shear and bending moments at these points are zero. The two methods give identical results.

This equation, however, will not ordinarily be conveniently integrable. We observe, however, that if we imagine all portions of the flange to be subjected to a vertical pressure directed towards the neutral plane of amount

$$p = \mathrm{E}c^2\,dt, \tag{29}$$

and investigate the equilibrium of the flange under this pressure we arrive at exactly the same equation. *Hence, although the equation cannot be solved,* the engineer may form a conception of the stresses to which the flange is subjected by supposing it subjected to the vertical pressure (29). In some cases this will lead to definite results. Thus, when there is only a single web attached to the centre of the flange, each half of the flange will have to resist the load system (29) as a cantilever. The moments arising from (29) can be obtained by graphic integration and the flange stresses accurately determined. Again, the integral of (29) taken over the flange has to be resisted by the web acting as a strut: a form of load for which it is not normally designed. The magnitude of the load is easily obtained and the suitability of the web examined. In other cases sufficient information may be obtained from tests on rubber models subjected to the load system (29) instead of a more complicated full scale test on the actual spar.

The author's acknowledgments are due to the Air Ministry for permission to publish the results contained in this paper, to the Steel Wing Company for the loan of fig. 6, to Dr. A. A. Griffith of the Royal Aircraft Establishment, in whose laboratory the experimental work was carried out, and to R. V. Southwell, F.R.S., for his detailed criticisms and advice.

The Energy of the Struck String.—Part II.

By W. H. George, M.Sc., Ph.D., F.Inst.P., Moseley Student, and H. E. Beckett, B.Sc., Research Student, University College, Nottingham.

(Communicated by Sir William Bragg, F.R.S.—Received May 30, 1927.)

The paper deals with the continuation of an investigation of the energy of the struck string studied by observation of the energy lost by the hammer during the impact. In the previous Part* an account is given of (i) the objects and theory of the work ; (ii) the experimental arrangements and results of a study of the influence of the relative position of the impact and the mass of the hammer ; and (iii) the conditions of maximum energy transference are discussed in detail. The present instalment deals with the influence of the initial velocity of the hammer, the width and nature of the hammer face, and the partition of the energy among the various partial tones of the string. The previously published results are also further discussed.

VII. *Initial Velocity* (v_0) *of the Hammer.*

An examination of the key and hammer mechanism used in pianofortes shows that just before the hammer strikes the string the hammer is quite free from the lever system of the key mechanism, and that it is in effect an inverted compound pendulum free from the influence of all external forces other than frictional and gravitational. Hence the only variable available to the pianist playing a *single* note without the use of the pedals is the initial velocity (v_0) with which the hammer strikes the string. Accordingly, the influence of this factor was studied in considerable detail.

In equations (5) and (9) of Part I, giving the energy lost by the hammer during the impact, v_0^2 occurs as a multiplying factor operating upon the whole of the right-hand sides of the equations. Under these theoretical conditions, therefore, when the impact occurs at the mid-point of the string or near one of the bridges, the fraction of its initial energy lost by the hammer is independent of the initial velocity of the hammer.

Before giving the results of the present experimental investigation, a note will be made of the accuracy attainable in the measurement of the velocity of the hammer under the conditions described in Part I. In Table I is shown the effect upon the calculated value of the hammer velocity of rebound (v) of an error of 0·1 cm. made in reading the hammer deflection (d).

---

* 'Roy. Soc. Proc.,' A, vol. 114, pp. 111–137 (1927).

Table I.

Deflection (d) of hammer (cm.).	Velocity (v) of hammer (cm./sec.).	Percentage error in v.
5	7·4	2·0
6	8·9	1·7
8	11·9	1·25
10	14·8	1·0
15	22·2	0·67
20	29·5	0·5
30	43·9	0·33
40	58·0	0·25
50	71·6	0·2
60	84·5	0·17
70	97·0	0·14
80	108·7	0·12

It will be seen that for most of the observations the error is less than 0·5 per cent.

An experimental investigation was made with three hammers of different mass (m), 4·769, 1·686 and 0·397 times that of the string (M) and at positions of impact distant 1/2, 1/4 and 1/20 the length (l) of the string from one of the bridges. For each position (a/l) of the impact, observations were made of the rebound deflection (d) of the hammer, the initial deflection (d_0) being gradually increased in successive series of observations. Some of the results are shown in Table II, in which the calculated values of the initial (v_0) and rebound (v) velocities of the hammer are shown together with the ratio v/v_0. From the constancy of this ratio it is reasonable to conclude that *at any position of the impact the energy lost by the hammer increases continuously according to a linear law with increase in the initial energy of the hammer.*

On this assumption, subsequent observations were not made in such great detail, only two or three more widely separated values of the initial velocity of the hammer being used, and the effect of change of position of impact was studied. A selection of some of the final results is shown in condensed form in Table III, which includes variations of the relative mass of hammer (m/M) from 0·5 to 4·769 and variation of the distance (a) of the impact from the nearer bridge from 6 cm. to 158·8 cm. (the midpoint of the string). The striking feature of this table is the constancy in each of the separate cases of the ratio of the rebound and initial velocities of the hammer.

The complete experimental observations are shown in figs. 1 to 5, in each of which the rebound deflections (d) of the hammer are plotted against the distance (a) of the impact from the nearer bridge. The individual points used in plotting

Table II.

Relative mass of hammer m/M.	Position of impact a/l.	Initial velocity of hammer v_0.	Rebound velocity of hammer v.	Ratio v/v_0.	Ratio v/v_0 (theoretical).
4·769	1/2	28·6	27·3	0·954	
		43·6	41·6	0·954	
		63·7	60·8	0·955	
		79·6	76·1	0·956	
	1/4	22·8	20·9	0·916	
		35·6	32·6	0·915	
		51·8	47·6	0·919	
		65·2	59·9	0·918	
		83·1	76·1	0·916	
	1/20	35·7	30·1	0·842	0·856
		48·2	40·5	0·840	0·856
		60·3	50·7	0·841	0·856
		73·4	61·9	0·843	0·856
		85·9	72·2	0·840	0·856
1·686	1/2	31·8	28·9	0·909	
		50·7	46·2	0·911	
		64·7	59·1	0·913	
		82·9	75·8	0·914	
		95·7	87·0	0·909	
	1/4	33·5	29·2	0·874	
		42·9	37·5	0·873	
		55·2	48·2	0·873	
		67·0	58·7	0·876	
		92·0	80·1	0·871	
0·397	1/2	8·4	6·0	0·713	0·733
		17·4	12·5	0·718	0·733
		27·4	19·7	0·717	0·733
		32·4	23·1	0·711	0·733
		38·9	27·6	0·709	0·733
		47·5	33·9	0·713	0·733
		56·3	40·1	0·712	0·733
		62·1	43·9	0·707	0·733
		69·7	49·4	0·710	0·733
		77·2	54·7	0·708	0·733
		99·1	64·7	0·710	0·733
		100·4	70·9	0·706	0·733
		109·0	77·0	0·706	0·733

the curves are too close together to be indicated. The striking similarity of shape of the two or three curves corresponding to the two or three different values of the initial velocities for any one hammer, and the exact coincidence of the positions of the impact for each of the main maxima and minima of the curves is at once apparent. (Hammer velocities, v_0, are given in Table III.)

It is therefore reasonable to conclude that *when a string is struck at any point by an unyielding hammer, the fraction of its initial energy lost by the hammer during the impact is independent of the initial velocity of the hammer.*

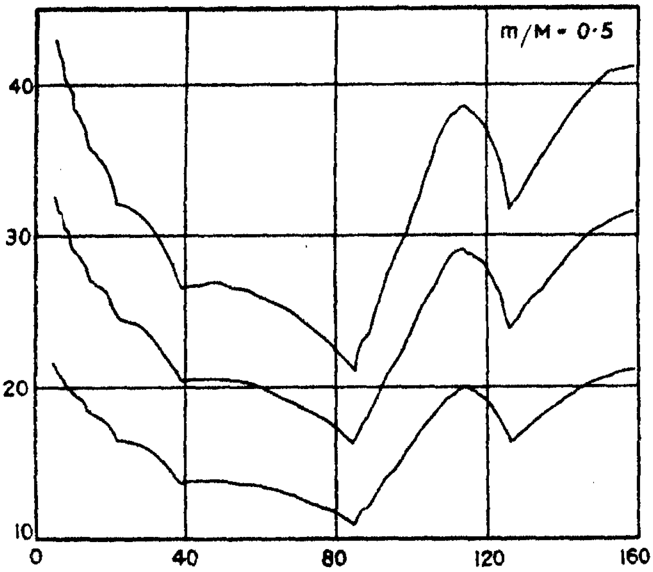

Fig. 1.

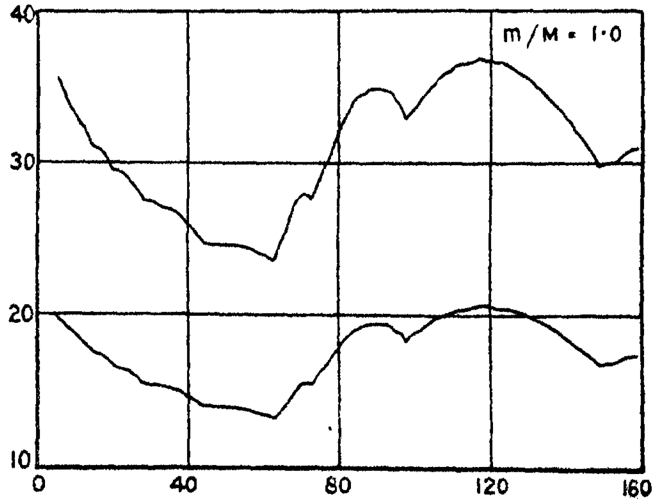

Fig. 2.

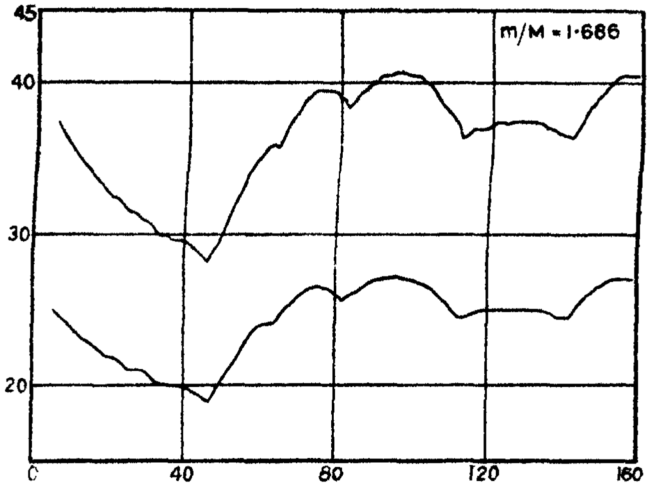

FIG. 3.

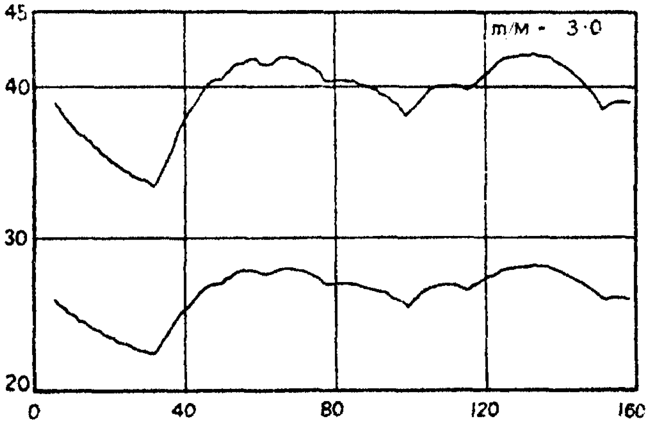

FIG. 4.

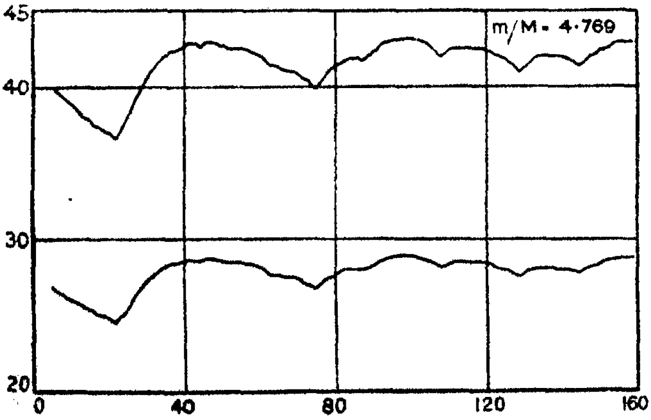

FIG. 5.

FIGS. 1–5.—Influence of initial velocity of the hammer.
Vertical axis—rebound deflection (d) of hammer in cm.
Horizontal axis—Distance (a) of impact from bridge in cm.

Table III.

m/M.	0·5			1·0		1·686		3·0		4·769	
v_0 cm./sec.	43·9	64·8	84·6	36·8	65·0	44·0	65·0	44·1	65·0	44·0	65·0
a cm.	v/v_0.										
6	0·704	0·719	0·720	0·787	0·793	—	—	0·866	0·869	—	—
10	0·658	0·659	0·658	—	—	0·800	0·800	0·836	0·840	0·870	0·873
14	0·621	0·622	0·619	0·719	0·713	0·770	0·774	0·816	0·816	0·852	0·851
20	0·585	0·579	0·582	0·668	0·666	0·735	0·735	0·787	0·789	0·834	0·830
24	0·555	0·552	—	—	—	0·715	0·719	0·773	0·773	0·840	0·841
36	0·488	0·492	0·492	—	—	0·672	0·673	0·803	0·800	0·948	0·945
42	0·466	—	0·463	0·577	0·576	0·656	0·658	0·859	0·862	0·954	0·955
50	0·469	0·467	0·465	—	—	0·682	0·680	0·902	0·905	0·954	0·950
56	0·458	0·464	0·460	—	—	0·762	0·763	0·928	0·928	0·948	0·949
60	0·455	0·455	—	0·543	0·544	0·800	0·798	0·925	0·928	0·938	0·937
70	0·427	—	0·429	0·624	0·629	—	—	0·932	0·935	0·915	0·914
76	—	0·410	0·408	0·663	0·666	0·884	0·884	0·908	0·916	0·905	0·900
82	0·387	0·386	0·382	0·743	0·744	0·856	0·859	0·902	0·905	0·932	0·928
91	0·445	—	0·443	0·783	0·785	0·902	0·905	0·887	0·892	0·948	0·947
98	0·522	0·514	0·515	0·743	0·741	0·905	0·906	0·862	0·862	0·964	0·960
106	0·612	0·601	0·610	0·799	0·797	0·871	0·873	0·895	0·894	—	—
110	0·653	0·645	0·646	0·810	0·811	0·839	0·843	0·899	0·896	0·948	0·945
116	0·665	0·650	0·654	0·828	0·823	0·828	0·830	0·891	0·894	0·951	0·949
122	0·621	0·611	0·616	0·823	0·819	—	—	0·918	0·920	0·939	0·938
128	0·565	0·556	0·559	0·814	0·808	—	—	0·935	0·937	0·921	0·916
132	0·589	0·586	0·586	0·795	0·788	—	—	0·938	0·941	0·932	0·928
138	0·631	0·624	0·628	0·763	0·754	0·821	0·823	0·936	0·933	0·938	0·937
144	0·668	0·663	0·663	0·719	0·714	—	—	0·909	0·913	0·928	0·924
152	0·697	0·697	0·698	0·680	0·678	—	—	0·865	0·864	0·951	0·949
158·8	0·708	0·710	0·705	0·701	0·700	0·902	0·905	0·869	0·873	0·961	0·956

Note on Impact at High Velocities.—In the whole of the experiments here discussed the initial velocity of the hammer does not exceed 109 cm./sec., and the apparatus in the form illustrated in Part I is not suitable for experiments involving high hammer velocities. It will be clear that the energy given to the string cannot be indefinitely increased by increasing the initial speed of the hammer, for either the string or the hammer would break. It is hoped to deal with impact at higher velocities in later work.

VIII. *Width of Contact and Yielding of Hammer.*

In the experiments so far discussed the hammer used consisted of a metal cylinder with wedge-shaped head so that the blow was given at a *point* of the string (Part I, p. 117) by an *unyielding* hammer. In a pianoforte the blow is given by a comparatively broad and felt-covered hammer. Two new conditions are therefore introduced (i) the finite width of the contact and (ii) the yielding of the hammer face. A study of the influence of these two factors was made for hammers of mass half that of the string.

Three hammers were used : (i) A *broad unyielding* hammer was made from a metal bar of square cross section (1 cm. wide) having two edges of the impinging face rounded off so as to leave a possible width of contact with the string of 0·4 cm. (ii) A *yielding* hammer was made from metal rod and bent clock spring, across which a fine wire was stretched as shown in fig. 6. By this arrangement impact at a *point* with a yielding hammer could be studied, the elastic properties of the hammer could be kept constant, and the mass of the moving spring could be made very small compared with the total mass of the hammer. (iii) The third hammer was an actual pianoforte hammer consisting of a wooden wedge covered to a thickness of 1 cm. with felt compressed by special machinery. The total mass was adjusted by the addition of a brass cylinder firmly fixed in the wooden wedge so that relative motion between these two was impossible. The added mass was fixed symmetrically so that during the impact there was no couple about a horizontal axis and therefore no tendency to set up vibrations about this axis.

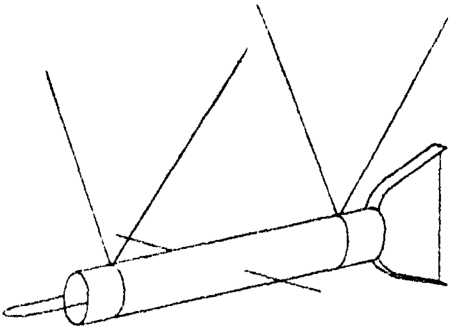

FIG. 6.

The width of the contact could be measured by smoking the string and allowing the hammer to impinge once only, when a black line, whose length could be measured, was left on the hammer face.

With each of these hammers observations were taken of the rebound of the hammer at a series of points along the string, the initial velocity being kept constant. The yielding spring hammer was then loaded so that its mass was 1·686 times that of the string, but the strength of the spring was unaltered. A set of rebound observations was again taken, but in this case the initial velocity was kept lower than before to avoid excessive yielding by the spring. The results of all these experiments are set out in Table IV, in which the first

Table IV.—Influence of Type of Hammer.

Relative mass m/M of hammer (m) and string (M).	0·5				1·686	
Type of hammer	Unyielding.		Yielding.		Un-yielding.	Yielding.
	Pointed.	Broad.	Pointed.	Broad.	Pointed.	
Initial velocity (v_0)	64·9	64·9	64·9	64·9	44·0	44·0
Position (a) of impact. (cm.)	Rebound deflections (d) of hammer. (cm.)					
6	31·9	31·8	41·9	32·9	24·8	28·9
7	31·5	31·4	41·5	32·5	24·5	—
8	30·5	30·4	41·4	32·0	24·4	28·7
9	30·4	30·2	41·0	31·7	24·0	—
10	29·3	29·4	40·5	31·1	23·9	29·4
11	29·1	28·9	40·1	30·7	23·5	—
12	28·7	28·5	39·9	30·4	23·4	27·9
13	28·3	28·2	39·3	29·9	23·1	—
14	27·4	27·4	39·0	29·5	23·0	27·6
15	27·2	27·0	38·4	29·1	22·8	—
16	27·0	27·0	38·0	28·8	22·6	27·3
17	26·9	26·8	37·9	28·5	22·5	—
18	26·7	26·5	37·4	28·1	22·3	27·0
19	26·1	26·1	37·0	27·9	22·0	—
20	25·7	25·6	36·5	27·5	21·9	26·7
21	25·1	25·1	36·2	27·1	21·9	—
22	24·5	24·5	35·8	27·0	21·8	26·5
23	24·5	24·4	35·4	26·8	21·6	—
24	24·5	24·4	35·0	26·5	21·4	26·1
25	24·5	24·4	34·8	26·4	21·1	—
26	24·4	24·3	34·4	26·1	—	25·8
27	24·3	24·3	33·9	25·9	21·1	—
28	24·1	24·1	33·6	25·7	21·0	25·6
29	24·0	23·9	33·4	25·4	—	—
30	23·8	23·7	32·9	25·1	20·9	25·4
31	23·5	23·3	32·5	25·0	20·5	—
32	23·3	23·1	32·0	24·7	20·4	25·1
33	22·9	22·8	31·9	24·4	20·1	—
34	22·6	22·5	31·4	24·0	—	24·8
35	22·2	22·1	30·9	23·6	20·1	—
36	21·7	21·8	30·8	23·4	20·0	24·6
37	21·4	21·2	30·7	23·0	20·0	—
38	21·0	20·9	30·2	23·0	—	24·4
39	20·5	20·5	29·9	22·9	20·0	—
40	20·5	20·4	29·6	22·5	—	24·1
41	20·5	20·4	29·6	22·5	19·7	—
42	20·5	20·4	29·4	22·5	19·5	24·5
43	20·5	20·5	—	22·4	19·5	—
44	20·6	20·5	28·9	22·4	—	24·9
45	20·6	20·5	—	22·4	19·2	—
46	20·6	—	28·4	22·4	19·0	25·3
47	20·6	20·5	—	22·4	19·0	—
48	20·5	—	27·9	22·3	19·5	25·6

Table IV—(continued).

Relative mass m/M of hammer (m) and string (M).	0·5				1·686	
Type of hammer	Unyielding.		Yielding.		Un-yielding.	Yielding.
	Pointed.	Broad.	Pointed.	Broad.	Pointed.	
Initial velocity (v_0)	64·9	64·9	64·9	64·9	44·0	44·0
Postive (a) of impact. (cm.)	**Rebound deflections (d) of hammer. (cm.)**					
49	20·5	20·5	—	22·3	19·9	—
50	20·5	20·5	27·0	22·1	20·3	26·0
51	20·5	—	—	22·1	20·7	—
52	20·5	20·4	26·5	22·0	21·0	26·4
53	20·4	—	—	21·9	21·4	—
54	20·4	20·4	26·1	21·9	21·9	26·7
55	20·4	—	—	21·7	22·4	—
56	20·3	20·3	25·5	21·5	22·8	27·0
57	20·1	—	—	21·5	23·1	—
58	20·1	20·1	25·0	21·4	23·5	27·2
59	20·1	—	—	21·0	23·6	—
60	20·0	20·0	24·4	21·0	23·9	27·5
61	19·9	—	—	21·0	—	—
62	19·9	19·8	23·9	20·8	24·0	27·8
63	19·8	—	—	20·5	—	—
64	19·6	19·7	23·4	20·5	24·0	27·9
65	19·5	—	—	20·4	24·5	—
66	19·4	19·5	23·1	20·2	24·9	28·0
67	19·4	—	—	19·9	—	—
68	19·3	19·3	22·7	19·6	25·4	28·1
69	19·1	—	—	19·6	25·5	—
70	19·0	19·0	22·5	19·4	—	28·3
71	18·9	—	—	19·4	26·0	—
72	18·7	18·7	22·3	19·0	26·2	28·5
73	18·6	—	—	18·9	—	—
74	18·5	18·5	22·0	18·6	26·5	28·5
75	18·4	—	—	18·4	—	—
76	18·0	18·1	22·0	18·4	26·4	28·5
77	18·0	—	—	18·0	—	—
78	17·8	17·8	22·0	17·9	26·4	28·6
79	17·5	—	—	17·9	26·2	—
80	17·4	17·5	21·9	17·5	26·0	28·7
81	17·3	—	—	17·4	25·9	—
82	17·1	17·1	21·8	17·3	25·6	28·7
83	17·0	—	—	17·0	—	—
84	16·6	16·7	21·7	17·0	26·0	28·7
85	16·4	16·5	—	17·0	26·1	—
86	17·2	17·3	21·5	17·6	—	28·6
87	18·0	17·9	—	18·0	26·5	—
88	18·0	18·0	21·5	18·6	26·6	28·5
89	18·2	18·3	—	19·1	26·7	—
90	19·0	19·0	21·5	19·5	—	28·5

Table IV—(continued).

Relative mass m/M of hammer (m) and string (M).	0·5				1·686	
Type of hammer	Unyielding.		Yielding.		Un-yielding.	Yielding.
	Pointed.	Broad.	Pointed.	Broad.	Pointed.	
Initial velocity (v_0)	64·9	64·9	64·9	64·9	44·0	44·0
Position (a) of impact. (cm.)	Rebound deflections (d) of hammer. (cm.)					
91	19·6	19·7	—	20·3	27·0	—
92	20·4	20·4	21·4	20·8	—	28·5
93	20·9	20·6	—	21·1	28·1	—
94	21·3	21·3	21·5	21·6	—	28·4
95	21·7	21·5	—	22·1	27·1	—
96	22·0	22·0	22·4	22·5	27·3	28·4
97	22·5	22·5	23·0	23·3	27·1	—
98	23·0	23·1	23·4	23·9	27·1	28·3
99	23·5	23·5	24·0	24·0	—	—
100	24·1	24·0	24·5	24·5	27·0	28·2
101	24·5	24·5	24·9	25·0	26·9	—
102	25·1	25·0	25·5	25·5	26·8	28·0
103	25·7	25·9	26·0	26·0	26·6	—
104	26·2	26·4	26·4	26·5	26·5	28·1
105	26·8	26·7	26·9	26·6	26·4	—
106	27·1	27·2	27·3	27·1	26·1	28·1
107	27·6	27·5	27·5	27·5	25·9	—
108	28·0	28·0	27·8	28·0	—	28·1
109	28·5	28·4	28·1	28·4	25·5	—
110	28·9	28·8	28·3	28·7	25·1	28·1
111	29·1	29·0	—	28·9	24·9	—
112	29·4	29·4	28·9	29·3	24·5	28·0
113	29·5	29·5	—	29·4	24·5	—
114	29·5	29·5	28·9	29·4	24·5	27·9
115	29·5	29·6	—	29·4	—	—
116	29·5	29·5	28·6	29·5	24·7	27·9
117	29·3	29·1	—	29·0	—	—
118	29·0	28·9	28·1	29·0	24·9	27·8
119	28·9	28·6	—	28·6	24·9	—
120	28·4	28·4	27·3	28·1	25·0	27·7
121	28·1	28·0	27·1	27·6	25·0	—
122	27·5	27·5	26·9	27·1	—	27·5
123	27·0	26·9	27·5	26·5	25·0	—
124	26·4	26·4	27·8	26·0	25·0	27·2
125	25·4	25·4	28·7	25·9	25·0	—
126	24·5	24·5	29·2	25·9	—	26·9
127	24·7	24·5	30·0	26·3	25·0	—
128	25·0	24·9	30·4	26·8	—	26·6
129	25·2	25·3	30·8	27·0	25·0	—
130	25·6	25·5	31·7	27·4	—	26·4
131	25·9	—	32·4	27·5	25·0	—
132	26·4	26·0	33·1	28·0	—	26·0

Table IV—(continued).

Relative mass m/M of hammer (m) and string (M).	0·5				1·686	
Type of hammer	Unyielding.		Yielding.		Unyielding.	Yielding.
	Pointed.	Broad.	Pointed.	Broad.	Pointed.	
Initial velocity (v_0)	64·9	64·9	64·9	64·9	44·0	44·0
Position (a) of impact (cm.)	Rebound deflections (d) of hammer. (cm.)					
133	26·5	—	33·4	28·5	25·0	—
134	26·9	26·5	33·9	28·9	24·8	25·8
135	27·1	—	34·5	29·0	24·8	—
136	27·3	27·2	34·9	29·5	—	25·4
137	27·8	—	35·5	29·9	24·7	—
138	28·0	27·9	36·0	30·0	24·5	25·1
139	28·2	—	36·5	30·4	24·5	—
140	28·5	28·4	36·9	30·7	—	24·9
141	28·8	—	37·0	31·0	24·5	—
142	29·1	28·9	37·5	31·4	24·5	24·5
143	29·4	—	37·9	31·6	24·9	—
144	28·7	29·4	38·3	31·9	—	24·5
145	30·0	—	38·6	32·1	25·4	—
146	30·2	30·0	38·9	32·5	—	24·8
147	30·4	—	39·4	32·8	26·0	—
148	30·5	30·3	39·5	32·9	—	25·0
149	30·9	—	—	33·2	26·4	—
150	30·9	30·7	39·8	33·3	—	25·2
151	31·0	—	—	33·4	26·6	—
152	31·1	31·0	40·4	33·6	—	25·5
153	31·3	—	—	33·6	27·0	—
154	31·4	31·2	40·5	33·6	27·0	25·5
155	31·4	—	—	33·9	27·0	—
156	31·5	31·2	40·8	34·0	—	25·5
157	31·5	—	—	34·0	27·0	—
158·8	31·5	31·3	40·9	34·0	27·0	25·7

column gives the distance (a) of the impact from the nearer bridge and the remaining columns give the mean rebound readings for (column 2) the wedge-shaped unyielding hammer used in the experiments described in Part I, (3) the broad metal hammer by which the impact was spread over 0·4 cm., (4) the yielding spring hammer, and (5) the felt-covered pianoforte hammer. In all of these experiments the mass of the hammer was one-half that of the string. The two last columns give the observations for (6) a wedge-shaped metal hammer, and (7) the corresponding spring hammer, for both of which the relative mass (m/M) was 1·686.

Discussion of Table IV.—To facilitate the discussion of the results set out in Table IV, the rebound readings for the broad metal hammer, the spring hammer, and the felt-covered hammer are shown in fig. 7 plotted against the distance (a) of the impact from the nearer bridge. Comparing the columns for the *pointed and the broad metal hammers*, the close similarity will be at once apparent. Two effects of increasing the breadth of the hammer face are the initial spreading of the impact over a greater length of the string and the complication of wave reflection from two different points of the string instead of from the single point struck by the pointed hammer. To bring out more strongly the influence of breadth of the hammer, it would be desirable to work with a much shorter string, so that large changes in the *relative* breadth could be made. It has been shown elsewhere* that there can be no tendency for the string to wrap round the hammer at the beginning of the impact. In the experiments here described the breadth of the hammer is very small compared with the length of the string. Small differences in behaviour of the pointed and broad hammers can be seen when the impact occurs near a bridge or near

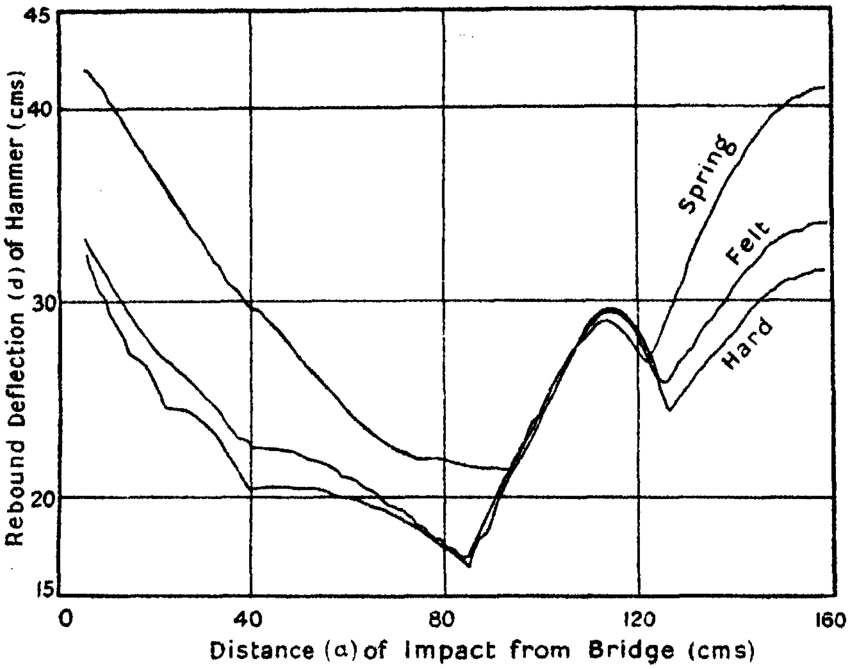

FIG. 7.—Influence of Nature of Hammer Face. $m/M = 0{\cdot}5$; $d_0 = 45$ cm.; $v_0 = 64{\cdot}9$ cm./sec.

---

* George, 'Phil. Mag.,' vol. 47, p. 593 (1924).

the mid-point, where the tendency is for the broad hammer to lose more energy than the pointed hammer. Considering now the *yielding spring hammer* (column 4 of Table IV and upper curve of fig. 7), it will be seen that almost all of the rebound readings are greater than those of the pointed or broad unyielding hammer. The most striking effects of the yielding of this hammer are (i) the decrease in the energy lost, (ii) the displacement towards the mid-point of the string of the position of impact giving maximum energy transference, and (iii) the reduction in the importance of the subsidiary maxima. A study has not yet been made of the duration of the impact with this hammer, the design of which is such that the electrical method* could readily be used. The results for the *felt-covered* pianoforte hammer (column 5 of Table IV and middle graph of fig. 7) lie between those for the pointed or broad unyielding hammers and those for the yielding metal hammer. Again we have a decrease in the energy lost and a reduction in the importance of the subsidiary maxima. The position of the impact at which the greatest amount of energy is lost is still, however, almost the same as for the unyielding hammer. It might have been expected that energy would have been lost in the inelastic yielding of the felt, for it is well known that the felt on the hammers of a pianoforte becomes, with use, more compressed. Possibly this effect would be noted in impact at higher speeds. The width of contact with the string was approximately the same as for the broad metal hammer, *i.e.*, 0·5 cm.

The results for the heavier hammer, $m/M = 1 \cdot 686$, are shown in columns 6 and 7 of Table IV and in fig. 8. Again the yielding hammer loses less energy except near the middle of the string; the subsidiary maxima are all much reduced and the position of the impact at which the energy loss is greatest is

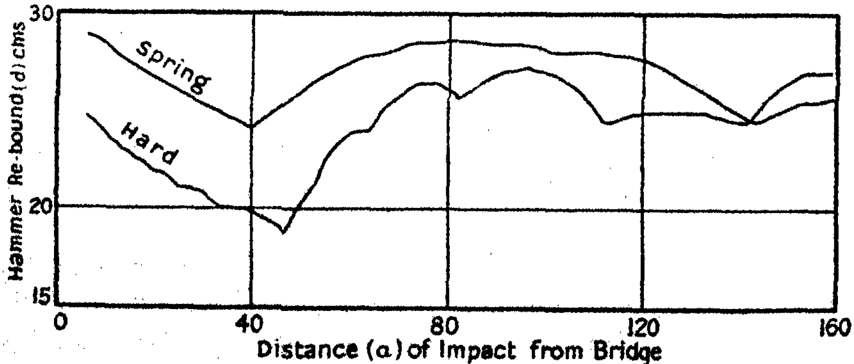

FIG. 8.—Influence of Yielding of Hammer. $m/M = 1 \cdot 686$; $d_0 = 30 \cdot 0$ cm.; $v_0 = 44 \cdot 0$ cm./sec.

---

* George, 'Roy. Soc. Proc.,' A, vol. 108, p. 284 (1925).

displaced, but in this case towards the nearer *bridge*. It was verified that the spring was not weakened by constant use, since at the end of the experiments the earliest readings were exactly repeated in four tested cases.

A noticeable feature of the results for all the lighter hammers ($m/M = 0 \cdot 5$) is the close agreement of the energy changes in the region between the two main points of greatest energy transference. This feature is not shown in the results for the heavier hammer ($m/M = 1 \cdot 686$).

IX. *Partition of the Energy among the Partial Tones of the String.*

In the discussion of the acoustics of musical instruments, much attention is given to the relative intensities of the various partial tones. It is therefore natural to examine the distribution, among the various partial tones of the resulting sound, of the total energy given to the string by the blow of the hammer. The task of making a full survey of this problem is so great that so far only 32 special cases have been examined.

Measurement of Amplitude of Partials.—There are considerable experimental difficulties in the accurate measurement of the amplitudes of the separate partials of a vibrating string, and these difficulties are still greater for the struck string on account of the transient nature of the phenomena. No sooner is the impact over but the vibrations of the string begin to diminish, due especially to the loss of energy through the ends of the string. Since the separate partials may die away at different rates, only the first few complete vibrations can be used. Where series of comparable observations are to be made, the tension and length of the string and the initial velocity of the hammer and the time which elapses between the impact and the observation must all be kept constant.

The results here discussed have been obtained by the photographic method, details of which will be found elsewhere.* Displacement time curves of the motion at various points of the string were obtained photographically, and after enlargement were analysed by use of a Mader harmonic analyser.

Some attempt was made to estimate the accuracy attained in the measurements. The greatest errors are likely to occur in the measurements of the amplitude of the higher partials, especially when the string is struck with a light hammer. The absolute values of the amplitudes to be measured are then exceedingly small, of the order $0 \cdot 01$ cm. Accordingly, the results for hammers of relative masses, $m/M = 0 \cdot 137$, $0 \cdot 397$ and $4 \cdot 769$, when the string was struck at $1/2$, $1/3$, and $(1/4)l$ and observed at $1/2$, $3/8$ and $(1/4)l$, were examined in considerable detail. Each curve (reproduced in fig. 9) was traced at least six times on the analyser,

---

* George, 'Phil. Mag.,' vol. 49, pp. 491–99 (1925).

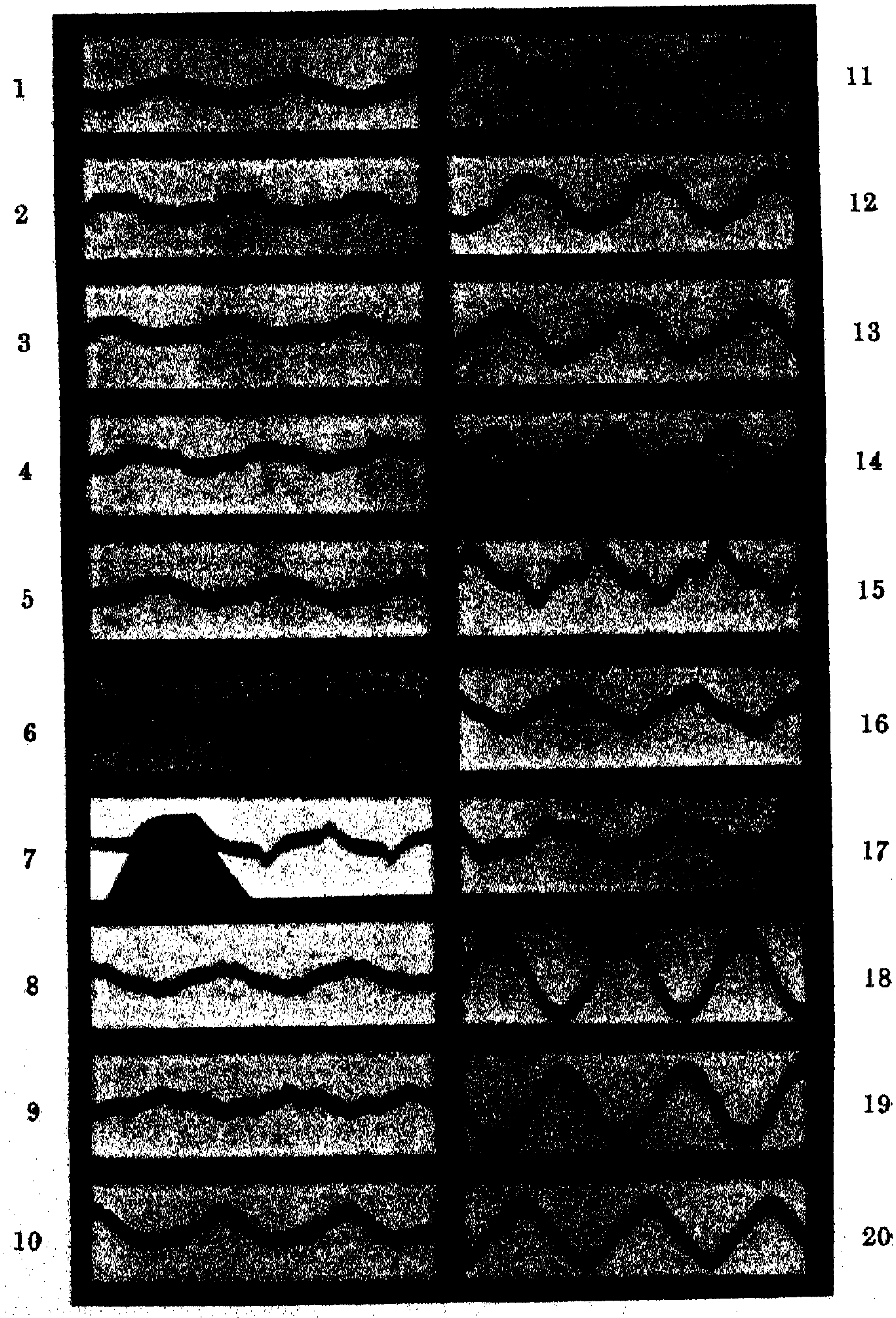

FIG. 9.—Displacement-time curves for particular points of the string (see column 4 of Table V).

Table V.—Initial Velocity of Hammer, 64·8 cm./sec.

m/M.	Impact at *a*/*l*.	Record taken at *a*/*l*.	No. in fig. 9.	Number of partial.	Sine component.			Cosine component.			Mean amplitude in cm.
0·137	1/3	1/2	1	1	0·93	0·91	0·94	0·20	0·21	0·19	†0·0421
					0·94	0·94	0·94	0·15	0·17	0·17	†0·0423
					0·14	0·14	0·14	0·30	0·29	0·30	*0·0413
		3/8	2	—	0·63	0·63	0·62	0·65	0·64	0·66	†0·0440
		1/4	3	—	0·35	0·37	0·37	0·50	0·50	0·51	†0·0397
		1/4	—	2	0·26	0·26	0·26	0·26	0·26	0·26	†0·0166
					0·27	0·26	0·27	0·24	0·24	0·23	†0·0161
					0·03	0·02	0·03	0·14	0·13	0·14	*0·0175
		3/8	—	—	0·24	0·25	0·23	0·09	0·10	0·09	†0·0164
	1/4	1/2	4	3	0·07	0·07	0·07	0·18	0·19	0·19	†0·0088
					0·02	0·03	0·02	0·07	0·07	0·08	*0·0097
		3/8	5	—	0·07	0·06	0·07	0·03	0·03	0·04	†0·0086
		1/4	6	—	0·18	0·18	0·17	0·06	0·05	0·05	†0·0117
		1/2	—	5	0·08	0·07	0·07	0·10	0·10	0·11	†0·0056
					0·07	0·08	0·08	0·11	0·11	0·12	†0·0060
		3/8	—	—	0·05	0·06	0·06	0·02	0·02	0·02	†0·0070
		1/4	—	—	0·02	0·02	0·02	0·11	0·10	0·11	†0·0069
0·397*	1/2	1/2	7	1	0·01	0·01	0·02	0·41	0·41	0·42	0·0521
					0·03	0·03	0·02	0·42	0·42	0·43	0·0534
		3/8	8	—	0·14	0·13	0·12	0·37	0·37	0·36	0·0530
		1/4	9	—	0·22	0·20	0·21	0·19	0·21	0·19	0·0516
		1/2	—	3	0·14	0·16	0·15	0·00	0·00	0·00	0·0189
					0·18	0·16	0·17	0·00	0·00	0·00	0·0214
		3/8	—	—	0·02	0·03	0·03	0·05	0·06	0·05	0·0196
		1/4	—	—	0·05	0·06	0·06	0·10	0·08	0·10	0·0194
	1/3	1/4	10	2	0·01	0·01	0·01	0·15	0·15	0·14	0·0185
					0·02	0·04	0·03	0·14	0·14	0·13	0·0176
		3/8	11	—	0·07	0·07	0·07	0·03	0·04	0·03	0·0138
	1/4·27	1/2	12	5	0·01	0·02	0·01	0·06	0·07	0·07	0·0086
					0·01	0·02	0·02	0·06	0·05	0·06	0·0074
		3/8	13	—	0·00	0·00	0·00	0·03	0·04	0·03	0·0110
		1/4	14		0·02	0·02	0·02	0·07	0·06	0·06	0·0118
4·769*	1/2	1/2	15	1	0·47	0·46	0·47	0·57	0·58	0·59	0·0938
					0·46	0·47	0·46	0·58	0·56	0·57	0·0930
		3/8	16	—	0·21	0·19	0·20	0·65	0·65	0·65	0·0927
		1/4	17	—	0·05	0·06	0·06	0·52	0·53	0·53	0·0945
	1/4	1/2	18	1	1·03	1·03	1·02	1·29	1·29	1·31	0·2083
					1·05	1·04	1·06	1·31	1·29	1·28	0·2089
		3/8	19	—	0·60	0·60	0·57	1·40	1·39	1·41	0·2070
		1/4	20	—	0·19	0·20	0·19	1·15	1·15	1·15	0·2077

* Total magnification 7·94. † Total magnification 22·5.

three times for the sine and three times for the cosine component of the particular partial under examination. A further check upon the measurement of the separate partials can be made by noting that, for example, the observations at 1/2, 3/8 and 1/4 of l can all be analysed for the amplitude (A_1) of the fundamental, the measured values of amplitude in the observations at 3/8 and 1/4 of l being multiplied by the appropriate sine factor. The results of these test measurements are summarised in Table V above, which is self explanatory.

Partition of Energy.—We deal now with the 32 special cases in which an attempt has been made to determine the partition of the total energy among the first seven partials of the string. Eight different hammers (pointed and unyielding) of relative mass (m/M), ranging from 0·137 to 4·769, were used, and the first cases studied were the specially interesting ones in which the energy lost by the hammer was a maximum. For the remaining three series the positions of impact were fixed at (1/2), (1/3) and (1/4)l from one of the bridges. Photographic records of the vibrations at distances (1/2), (3/8) and (1/4)l from the bridge were taken, and the results of their analysis are shown in Tables VI to IX. For each hammer in these tables is given (i) the amplitude in

Table VI.—Impact at Position (a/l) for which Energy lost by the Hammer is a Maximum.

a/l.	m/M.	Number (n) of partial.	1	2	3	4	5	6	7
0·0837	0·1366	Amplitude (A_n) of partial (cm.)	0·0157	0·0156	0·0117	0·0107	0·0077	0·0025	0·0026
		Energy (E_n) of partial (ergs)	117	464	588	874	707	107	158
		Ditto (in arbitrary units)	100	396	501	745	603	91·6	135
0·172	0·2896	A_n	0·0694	0·0407	0·0123	0·0071	0·0060	0·0013	0·0021
		E_n	2297	3161	649	385	429	29·1	103
			100	138	28·3	16·8	18·7	1·3	4·5
0·234	0·3973	A_n	0·1148	0·0324	0·0123	0·0054	0·0074	0·0033	0·0047
		E_n	6287	2003	649	223	653	187	52
			100	31·8	10·3	3·6	10·4	3·0	0·8
0·268	0·5	A_n	0·1297	0·0295	0·0180	0·0068	0·0081	0·0020	0·0018
		E_n	8028	1661	1391	353	782	69	76
			100	20·7	17·3	4·4	9·7	0·9	0·9
0·200	1·0	A_n	0·1956	0·0249	0·0169	0·0089	0·0026	0·0048	0·0030
		E_n	18240	1183	1226	605	81	395	210
			100	6·5	6·7	3·3	0·4	2·2	1·2
0·147	1·686	A_n	0·2545	0·0215	0·0057	0·0065	0·0033	0·0044	0·0045
		E_n	30890	882	139	322	130	332	473
			100	2·9	0·5	1·0	0·4	1·1	1·5
0·101	3·0	A_n	0·2933	0·0395	0·0098	0·0045	0·0034	0·0042	0·0016
		E_n	41030	2977	412	154	138	303	60
			100	7·3	1·0	0·4	0·3	0·7	0·1
0·0698	4·769	A_n	0·3099	0·0482	0·0149	0·0045	0·0053	0·0026	0·0039
		E_n	45820	4432	953	154	335	116	335
			100	9·7	2·1	0·3	0·7	0·3	0·8

Table VII.—Impact at $l/2$.

m/M.	Number (n) of partial.	1	2	3	4	5	6	7
0·1366	Amplitude (A_n) of partial (cm.)	0·0163	0·0002	0·0077	0·0018	0·0030	0·0005	0·0027
	Energy (E_n) of partial (ergs)	127	0·1	257	23·7	104	4·8	165
	Ditto (in arbitrary units)	100	0·0	202	18·7	82·4	3·8	130
0·2896	A_n	0·0349	0·0006	0·0138	0·0010	0·0087	0·0013	0·0042
	E_n	580	0·8	818	7·1	900	30·0	411
		100	0·1	141	1·2	155	5·1	70·8
0·3973	A_n	0·0534	0·0021	0·0214	0·0013	0·0107	0·0015	0·0057
	E_n	1360	8·7	1967	12·1	1367	39·2	751
		100	0·6	145	0·9	100	2·9	55·2
0·5	A_n	0·0722	0·0029	0·0257	0·0021	0·0126	0·0009	0·0042
	E_n	2485	16·0	2833	35·0	1891	13·3	404
		100	0·6	114	1·4	76·1	0·5	16·2
1·0	A_n	0·1505	0·0042	0·0262	0·0015	0·0072	0·0004	0·0052
	E_n	10810	33·0	2946	17·4	615	2·4	623
		100	0·3	27·2	0·2	5·7	0·0	5·8
1·686	A_n	0·0627	0·0004	0·0261	0·0013	0·0127	0·0018	0·0052
	E_n	1876	0·2	2918	12·1	1930	27·2	623
		100	0·0	155	0·6	103	1·5	33·2
3·0	A_n	0·1799	0·0015	0·0273	0·0029	0·0122	0·0030	0·0081
	E_n	15420	4·4	3207	64·0	1780	157	1519
		100	0·0	20·8	0·4	11·5	1·0	9·9
4·769	A_n	0·0930	0·0048	0·0358	0·0033	0·0078	0·0020	0·0045
	E_n	4121	43·7	5492	81·8	727	69·7	480
		100	1·1	133	2·0	17·6	1·7	11·7

centimetres of each of the first seven partials, (ii) the corresponding energy in ergs calculated by means of the equations of p. 116 of Part I, and (iii) the energies so found are recalculated in arbitrary units, the energy associated with the fundamental being fixed as 100 for each hammer.

Impact at Position of Maximum Energy Transference.—In Table VI the position of the impact is different for each hammer and is given in the column headed a/l. It was shown in Part I that this position is unique for any given hammer-mass, and if the initial velocity of the hammer is kept constant, then the energy lost by the hammer is a maximum. Considering now the partition (Table VI) of this maximum energy, it will be seen that (i) except for the very lightest hammers ($m/M < 0 \cdot 3$) by far the greater part of the energy lies in the fundamental, (ii) the energy in the fundamental, but *not* that in any other partial, increases continuously with increase in the mass of the hammer, and (iii) for

Table VIII.—Impact at $l/3$.

m/M.	Number (n) of partial.	1	2	3	4	5	6	7
0·1366	Amplitude (A_n) of partial (cm.)	0·0423	0·0161	0·0005	0·0098	0·0036	0·0005	0·0044
	Energy (E_n) of partial (ergs)	854	497	1·2	740	158	5·0	457
	Ditto (in arbitrary units)	100	58·3	0·1	86·7	18·5	0·6	53·5
0·2896	A_n	0·0883	0·0238	0·0008	0·0132	0·0030	0·0003	0·0048
	E_n	3718	1080	2·8	1332	105	2·1	532
		100	29·1	0·1	35·8	2·8	0·1	14·3
0·3973	A_n	0·1076	0·0176	0·0016	0·0150	0·0054	0·0005	0·0083
	E_n	5520	593	11·5	1714	350	4·4	1614
		100	10·7	0·2	31·1	6·3	0·1	29·2
0·5	A_n	0·0948	0·0215	0·0009	0·0059	0·0025	0·0034	0·0036
	E_n	4290	885	33·4	267	75·6	199	312
		100	20·6	0·8	6·2	1·8	4·6	7·2
1·0	A_n	0·0800	0·0521	0·0010	0·0167	0·0086	0·0004	0·0018
	E_n	3052	5188	4·4	2142	875	2·4	72·7
		100	170	0·1	70·2	28·6	0·1	2·4
1·686	A_n	0·0874	0·0563	0·0018	0·0151	0·0028	0·0023	0·0062
	E_n	3645	6047	13·3	1744	91·5	88·3	890
		100	166	0·4	47·8	2·5	2·4	24·4
3·0	A_n	0·1844	0·0140	0·0013	0·0047	0·0033	0·0009	0·0043
	E_n	16220	373	6·8	166	128	13·3	429
		100	2·3	0·0	1·0	0·8	0·1	2·6
4·769	A_n	0·0897	0·0655	0·0009	0·0127	0·0042	0·0042	0·0044
	E_n	3836	8185	3·3	1235	207	297	454
		100	213	0·1	32·2	5·4	7·7	11·8

the lightest hammer ($m/M = 0 \cdot 137$) the small amount of energy associated with the fundamental, only 1/27 of the total energy, is in strong contrast with the other results.

Impact at $l/2$, $l/3$ and $l/4$.—The results of the remaining three Tables, VII to IX, are best considered together. In these the position of the impact was arbitrarily fixed at $l/2$, $l/3$ and $l/4$ respectively, and in each table the position of the impact is the same for all hammers. It should be carefully noted that there is no justification for forming general conclusions from comparison of the results for any one hammer when the position of the impact is varied. It has already been shown elsewhere* by one of us that the amplitude of the fundamental is a fluctuating function of the position of the impact, and that the mass of the hammer has considerable influence upon the number and position of the various maxima and minima. It is not, therefore, surprising that the

* George, 'Phil. Mag.,' vol. 49, pp. 491–99 (1925).

Table IX.—Impact at $l/4$.

m/M.	Number (n) of partial.	1	2	3	4	5	6	7
0·1366	Amplitude (A_n) of partial (cm.)	0·0410	0·0106	0·0088	0·0013	0·0060	0·0040	0·0018
	Energy (E_n) of partial (ergs)	803	213	331	13·3	436	281	75·8
	Ditto (in arbitrary units)	100	26·6	41·2	1·7	54·3	35·0	9·4
0·2896	A_n	0·0874	0·0267	0·0128	0·0008	0·0094	0·0048	0·0031
	E_n	3643	1358	705	4·8	1047	389	230
		100	37·3	19·4	0·1	28·7	10·7	9·0
0·3973	A_n	0·1122	0·0325	0·0141	0·0034	0·120	0·0029	0·0044
	E_n	6008	2015	854	88·3	1707	144	454
		100	33·5	14·2	1·5	28·4	2·4	7·6
0·5	A_n	0·1332	0·0332	0·0130	0·0013	0·0067	0·0015	0·0013
	E_n	8467	2110	722	12·1	531	39·2	37·1
		100	24·9	8·5	0·1	6·3	0·5	0·4
1·0	A_n	0·1491	0·0240	0·0160	·0021	0·0014	0·0023	0·0081
	E_n	10610	1104	1098	35·0	22·9	88·3	1519
		100	10·4	10·4	0·3	0·2	0·8	14·3
1·686	A_n	0·0814	0·0496	0·0243	0·0004	0·0081	0·0026	0·0018
	E_n	3157	4699	2537	1·1	775	120	72·7
		100	149	80·3	0·0	24·5	3·8	2·3
3·0	A_n	0·1348	0·0502	0·0230	0·0009	0·0088	0·0016	0·0073
	E_n	8664	4819	2281	5·9	927	46·0	1248
		100	55·6	26·3	0·1	10·7	0·5	14·4
4·769	A_n	0·2089	0·0019	0·0113	0·0025	0·0013	0·0039	0·0050
	E_n	20820	6·8	551	48·4	18·9	262	593
		100	0·0	2·6	0·2	0·1	1·3	2·9

results of Tables VI to IX show similar fluctuation in the amplitudes of *any* partial when the position of the impact and the initial velocity of the hammer are unchanged, whilst the mass of the hammer is progressively increased from 0·137 to 4·769 times that of the string. It may be noted in passing that the results for the smallest amplitudes have probably no value as quantitative measurements. The method is not accurate to 0·001 cm., so that, for example, in Table VIII, where the impact occurred at $l/3$, the fact that a trace of the third partial is recorded when the usual theory would require its absence must not be regarded as significant.

The most striking features of the results are as follows: (i) There is no progressive change in the energy associated with the fundamental, as was shown in the results for the condition of maximum energy transference, or with any of the harmonics, as the mass of the hammer is gradually increased. (ii) In accordance with the usual theory when the impact occurs at $l/2$, $l/3$ or $l/4$, those harmonies which have nodes at the point of impact are very weak. (iii) When the amplitude of the fundamental tone is great there is a general tendency for the amplitude of the other partials to be small and vice versa. A number of remarkable cases, as, for example, when $a/l = 1/4$ and $m/M = 4{\cdot}769$, in which almost the whole of the energy lies in the fundamental and which occur under various conditions, are noteworthy. Their number would probably be increased if a systematic investigation of the influence of the position of the impact was made.

The whole of the results show the wide range of tone quality which would be available in a pianoforte if careful consideration were given to *both* the mass of the hammer and the position of the impact. It is hoped in later papers to discuss the practical application of the work to the pianoforte.

X. *Energy Changes when Impact occurs near a Bridge.*

We continue now the discussion of the results previously published in Part I. It was there shown that the energy lost by the hammer during the impact with the string is a discontinuous function of the position of the impact. We will consider now the influence of changing the mass of the hammer when the position of the impact is kept constant and near to a bridge. The calculated results are shown in fig. 10, in which the fraction of its initial energy lost by the hammer is plotted against the relative mass (m/M) of the hammer. Each curve represents the results for a different position of the impact, the distance (a) from the nearer bridge being indicated in centimetres. For comparison, the results when the impact occurs at the mid-point of the string are shown in a dotted curve. It will be seen that provided the impact lies between the bridge and the point of maximum energy transference, then the fraction of its initial energy lost by the hammer when impinging at the same point of the string *decreases continuously* with increase in the relative mass of the hammer.

Constant Fractional Energy Changes.—It was shown in Part I that as the position of the impact moves away from a bridge the energy lost by the hammer increases exponentially until a sharply defined point of maximum energy loss is revealed. Superimposed on this exponential law are small fluctuations with clearly defined subsidiary maxima (marked on figs. 9 to 14 of Part I as A, B, C, etc.). It is of interest to note that for each set of corresponding points the fraction of its initial energy lost by the hammer is approximately constant, in spite of the progressive change in the mass of the hammer. The conditions of relative mass and position of hammer are set out in fig. 11. It will be seen that (i) there is a linear relation between the relative position (a/l) of the impact and

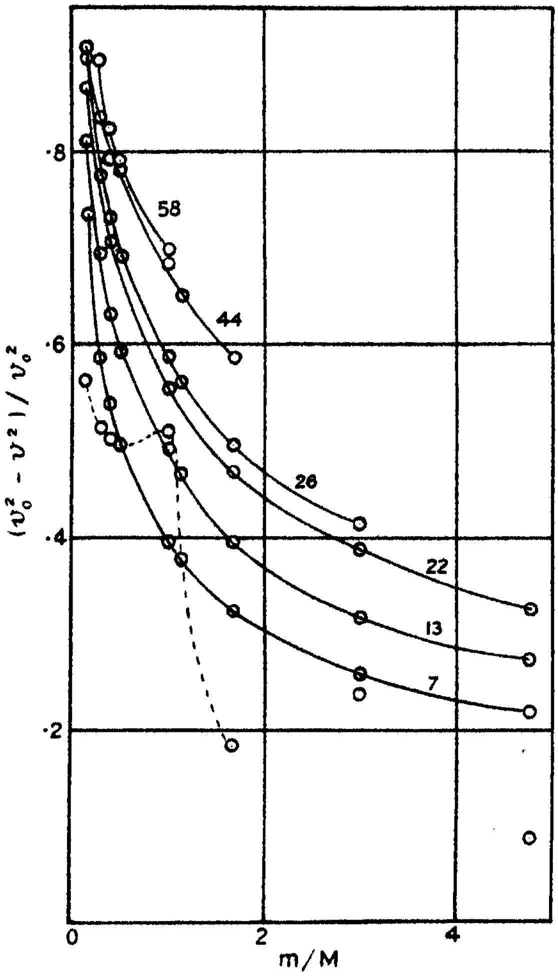

FIG. 10.—Energy Changes when Position of Impact is unaltered.

the relative mass (m/M) of hammer (m) and string (M), and (ii) the smaller the fraction of energy lost by the hammer the less is the position of the impact giving constant fractional energy loss, affected by change of mass of the hammer.

The conditions of impact just discussed are special cases chosen from the points of inflection upon the curves of figs. 9 to 14 of Part I. It is of interest to examine now arbitrarily chosen cases in which the energy changes are constant. The results for nine such cases are shown in fig. 12, in which the fraction of its initial energy lost by the hammer during the impact is indicated upon each curve. It will be seen that the same relations as were found for the special cases are valid here also, provided always that the impact is near the bridge.

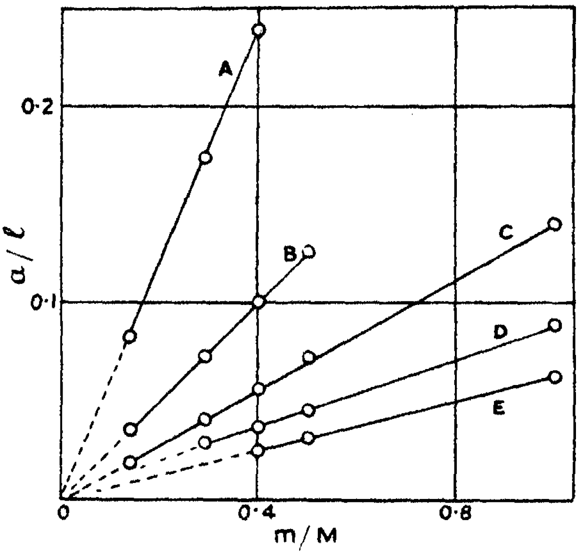

FIG. 11.

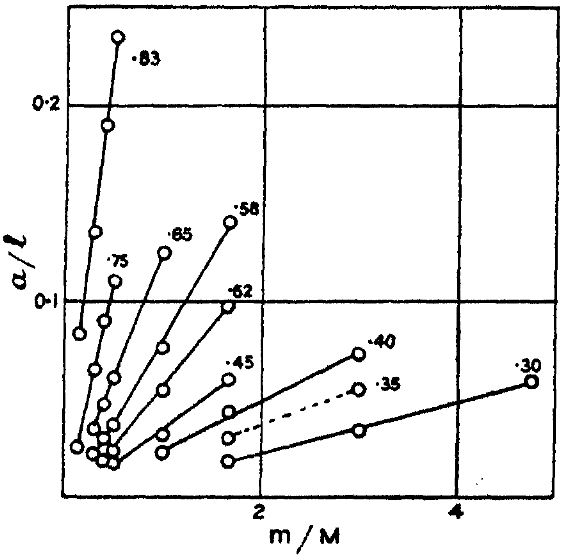

FIG. 12.—Influence of mass of hammer upon position of impact when fractional energy loss is constant at the value indicated on each line.

Constant Initial Energy.—It was shown in Part I that for each hammer mass there is a special position of the impact for which the energy lost by the hammer is a maximum. At the beginning of the present paper it was shown that this special position of the impact is independent of the initial velocity of the hammer.

It is therefore now possible to examine if there is any particular mass of hammer specially favourable to the maximum transmission of energy to the string when the initial energy of the hammer has been fixed at some particular value. A study has been made of the case when the hammer loses the greatest fraction of its initial energy. The calculations are based on the supposition that the lightest hammer ($m/M = 0{\cdot}137$) impinges with a speed of 100 cm./sec. and the heavier hammers impinge with lesser speeds, so that the initial energy of each hammer was constant. The results set out in fig. 13 show that there is no particular mass of hammer specially favourable to the transmission of energy to the string, but that (i) when the relative mass is less than 0·4, the hammer is comparatively inefficient, and (ii) the efficiency of the hammer rapidly increases between $m/M = 0{\cdot}5$ to $1{\cdot}5$.

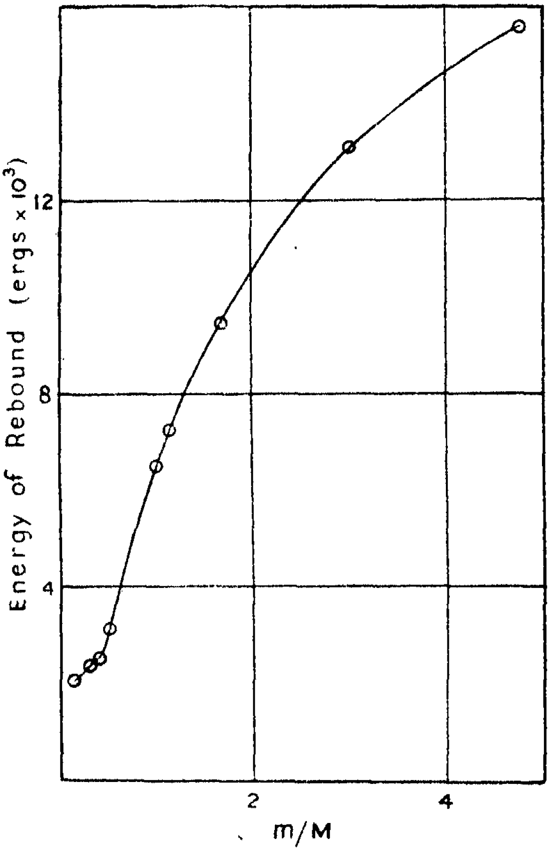

FIG. 13.—Influence of mass of hammer upon the maximum energy transmissible to the string when the hammer impinges with constant initial energy.

XI. *Summary of Results.*

(Continued from 'Roy. Soc. Proc.,' A, vol. 114, p. 136 (1927).)

(7) When a string is struck at *any* point by an unyielding hammer, the fraction of its initial energy lost by the hammer during the impact is *independent* of the initial velocity of the hammer (figs. 1 to 5).

(8) The energy changes for a *pointed* or a *broad* unyielding hammer and for an actual *felt-covered* pianoforte hammer are all remarkably similar. In any differences of behaviour the tendency is for the pointed unyielding hammer to lose more energy than do the other types of hammer (Table IV and fig. 7).

(9) The effects of a *yielding* of the hammer are (i) to reduce the importance of subsidiary maxima, (ii) to cause displacement of the position of the impact at which the greatest energy changes take place, and (iii) to reduce considerably the energy lost by the hammer at almost all positions of the impact (figs. 7 and 8).

(10) When the impact occurs at the position of maximum energy transference, then, except for the very lightest hammer, by far the greater part of the energy lies in the fundamental tone of the string. This energy in the fundamental, but *not* that in any other partial, increases continuously with increase in the mass of the hammer (Table VI).

(11) When the impact occurs at $l/2$, $l/3$ or $l/4$, there is no progressive change in the amplitude of any of the partials when the mass of the hammer is gradually increased. There is a very wide range of tone quality possible by merely varying the mass of the hammer even when the position of the impact is fixed (Tables VII to IX).

(12) When the impact occurs near a bridge, the fraction of its initial energy lost by the hammer when impinging at the same point of the string decreases continuously with increase in the relative mass of the hammer (fig. 10).

(13) When the hammer loses a constant fraction of its initial energy, there is a linear relation between the relative mass of hammer and string and the position of the impact provided that the impact occurs near a bridge (figs. 11 and 12).

(14) When the hammer impinges with constant initial energy, the mass ratio of hammer (m) to string (M), $m/\mathrm{M} = 1$, is specially efficient in the transmission of energy to the string (fig. 13).

Acknowledgments.

We wish to thank the Royal Sociey and the Department of Scientific and Industrial Research for financial aid, and Prof. P. E. Shaw for his kindness in continuing to provide for the work the facilities originally provided by the late Prof. E. H. Barton, F.R.S.

ERRATA IN PART I.

In fig. 5 (p. 126) the portion of the curve lying between $a = 98 \cdot 0$ to $158 \cdot 8$ cms. *has been displaced upwards through a distance of 0·05, e.g., the mid-point* ordinate which reads 0·56 should read 0·51.

In fig. 11 (p. 129) $m/M = 0 \cdot 397$.

The Absorption Spectra of Aragonite and Strontianite in the near Infra-Red.

By F. I. G. RAWLINS and E. K. RIDEAL.

(Communicated by A. Hutchinson, F.R.S.—Received May 31, 1926.)

Introduction.

In a series of papers dealing with some theoretical determinations of carbonate crystals, Chapman and his collaborators (1) have discussed a number of properties in calcite and magnesite, while later on they extend their work to the carbonates of zinc, iron, manganese and cadmium. They arrive at the general result that throughout the uni-axial series examined by them the CO_3 group remains almost unchanged in size. Their calculations yield a set of unique values for the rhombohedral angle, for which the limits are 101° 55′ (calcite), and 103° 28′ (calamine). In a similar way, the extremes in the size of the rhombohedral cell are shown by calcite and magnesite. Unfortunately these investigations have not yet embraced the bi-axial carbonates.

On the experimental side, Schaefer and his school (2) have recently concluded a systematic study of the absorption spectra of the uni-axial crystals calcite, magnesite, dolomite, chalybite, and of the bi-axial crystals witherite and cerussite between the wave-lengths 1 and 23μ, accessible with prisms of quartz, fluorite, rock-salt and sylvite.

Earlier work on the subject has also appeared by Coblentz (3), Nyswander (4), and Schaefer and Schubert (5), who mapped the reflection spectra of a number of carbonates between the limits indicated above. No obvious connection seems to exist between their results and the gradual transition of properties to be anticipated from Chapman's researches.

Kornfeld (6) deals with the characteristics of the CO_3^{--} ion considered as an isolated unit in free space, which is of consequence for the present work, since the absorption bands in question must be conceived as having their origin in oscillations within the CO_3 group—the so-called "internal" oscillations—in contradistinction to the "external" type which occur in the further infra-red, and are usually to be ascribed to vibrations in which the metal ion and the CO_3 group as a whole are concerned.

In virtue of Schaefer's work on the one hand, and the X-ray researches of W. L. Bragg (7) on the other, it seemed of interest to investigate aragonite and strontianite within such portions of the "internal" region as the prisms available (quartz and rock-salt) would allow. Thus, information regarding the absorption frequencies in aragonite enable a direct comparison of the two allotropic forms of $CaCO_3$ to be made, whilst with data for strontianite the series of bi-axial carbonates of the alkaline earths is naturally completed. It is, perhaps, worth noticing that the metal ions discussed in the present connection have the structure of the inert gases.

Another reason for undertaking these measurements is that in his recent paper Schaefer (2) states that the difference in wave-length between reflection and absorption maxima $\lambda_{\text{ref.}} - \lambda_{\text{abs.}}$ is positive and very considerable in amount, about $0 \cdot 2\mu$. The sign has in general been confirmed, though the magnitude would appear to be decidedly less than he finds.

A difficulty in all work of this nature arises from the fact that the absorption bands are exceedingly numerous, in addition to which, even with the limited resolution at command, the majority are doublets. Further, the asymmetric nature of the forces acting within and upon the CO_3 groups does not permit of the assemblage being treated as composed of harmonic oscillators, but are markedly anharmonic, with the consequent appearance of a number of overtones. For reasons advanced by Kratzer (7) (although intended to apply mainly to gases), it is to be anticipated that such overtones might not be exact multiples of the fundamentals, but should follow the ratio $\nu[1-x] : 2\nu[1-2x] : 3\nu[1-3x] \ldots$ where ν is the fundamental frequency and x a small term introduced by the anharmonic coupling. In addition to these overtones, Schaefer (2) has arranged some of the bands observed by him in a number of combination and difference tones. Such bands are usually of low intensity, and it seems to be necessary to invoke an "inactive" vibration at about 9μ (Kornfeld (6)) to account for the facts.

The combination of such an inactive oscillation with different real (or active) oscillations having vector properties seems somewhat artificial, and it may be well to suspend judgment for the present as to the origin of these bands.

For aragonite and strontianite, therefore, only the fundamentals (at approximately 6, 11 and 14μ (6)) will be discussed, together with their overtones lying between 2μ and 4μ.

A preliminary communication upon these overtones by the present authors, in conjunction with A. M. Taylor, has already appeared (8). Since then, further observations upon the intense band near 3·4μ have made it possible to fix its position with greater accuracy. These later figures are those embodied in the present paper.

Experimental.

In studying the absorption spectra of aragonite and strontianite two types of apparatus have been used: (*a*) an infra-red spectrometer, thermopile and moving-magnet galvanometer of the Hill-Downing pattern, and (*b*) an infra-red spectrometer (Littrow principle) together with a modified Boys' radiomicrometer. A quartz prism was employed from 1μ to 4μ, and one of rock-salt from 11μ to 14·5μ.

No further reference to method (*a*) will be made, as it has received attention before (8).

Arrangement (*b*) was adopted after considerable experience by one of the authors (F. I. G. R.) of Prof. Schaefer's apparatus at Marburg-Lahn. The chief advantage in the use of the Boys' instrument is its freedom from magnetic disturbances: its drawbacks were found to be two-fold. In the first place, the radiomicrometer is slow in action, due to the comparatively great inertia of the moving system, which made itself felt both in the time absorbed in taking readings, *i.e.* the ratio deflection through crystal : deflection in air, and in the difficulty of keeping all external conditions constant during an observation even though all work was done at night. Secondly, temperature gradients in the room were almost unavoidable, tending to set up sudden changes of zero, and a gradual drift if work is begun before all lamps, etc., have brought the room to a steady thermal state.

The instrument (R, fig. 1), as well as being itself lagged with cotton wool, was enclosed in a well-fitting box, and the space between the walls of the latter and the case of the former was lightly packed with slag wool. The whole stood upon a concrete pillar resting upon the foundations of the building.

In order to avoid disturbances arising from the observer approaching the radiomicrometer, a system of gearing was devised whereby the wave-length drum of the spectrometer could be set from an outer room. There was thus no need for anyone to come within about 15 feet, and stability of zero was successfully attained, the deflections being read at this distance by means of an appropriate telescope and scale. The relative positions of the different pieces of apparatus can be gauged from the scale diagram (fig. 1).

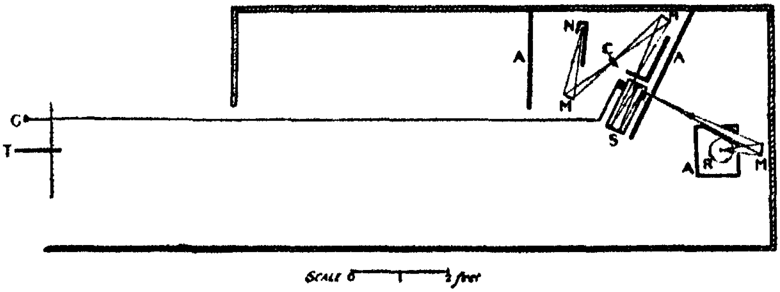

FIG. 1.—A = asbestos screens ; C = crystal holder ; G = gearing ; M = concave mirrors ; N = Nernst glower ; R = radiomicrometer ; S = spectrometer ; T = telescope.

A Nernst glower, taking about 0·7 amp. from a large constant voltage battery, served as the source of infra-red radiation.

The calibration of the spectrometer, including the absolute determination of the prism table rotation, was performed in the usual manner, using Paschen's figures for the refractive indices of quartz and rock-salt at 18° C., and checked by comparison with Schaefer's figures for the calcite absorption bands. The authors gratefully acknowledge Prof. Schaefer's kindness in putting his results for calcite at their disposal for this purpose in advance of publication.

In the neighbourhood of the trough of an absorption band readings were taken at intervals of about 0·007 μ (depending upon the dispersion of the prism at the point in question), but in other regions somewhat more widely apart.

The aim was to take about four observations within the effective slit width in the various positions of the spectrum. (By effective slit width is meant the width in μ when calculated from the calibration curves at the appropriate point.)

Average deflections by method (*a*) amounted to 100 mm. at 1·5 m. scale distance, and by method (*b*) to about 200 mm. at 5 m. In both cases readings were possible to 0·5 of a division.

The crystal sections were four in number—a thicker section of each for use between 1 μ and 4 μ, and a thinner one of each for the longer wave-lengths.

The actual thicknesses were :—

Aragonite	1·3 mm. and 0·056 mm.
Strontianite	0·33 mm. and 0·033 mm.

They were mounted upon a slider running smoothly in grooves of a rigid holder, so constructed that the specimen or air opening returned exactly to its proper position in the path of radiation after each observation. The contrivance was actuated by a system of pulleys, so that all the work of taking records could be done from one position well away from the Boys' radiomicrometer.

The results obtained are summarised in the tables and graphs which follow.

Table I.—*Calcite and Aragonite. Fundamentals and overtones arranged according to Schaefer's scheme.*

—	Calcite.	Aragonite.
$3\nu_1$	$2\cdot31\mu$ $2\cdot33$	$2\cdot25\mu$ $2\cdot30$
$2\nu_1$	$3\cdot35$ $3\cdot47$	$3\cdot35$ $3\cdot41$
ν_1	$7\cdot0$ (2) $6\cdot40$* $6\cdot7$ (2)	$6\cdot64$ (5) $6\cdot48$*
ν_3	$11\cdot35$	$11\cdot50$
ν_2	$14\cdot12$	$14\cdot39$
Minor bands	$2\cdot53$ $2\cdot79$ $3\cdot04$ $3\cdot10$	$2\cdot50$ $2\cdot79$ $3\cdot08$ $3\cdot09$

Calcite figures due to Schaefer, except ν_2 and ν_3 (authors). Aragonite figures by authors, except ν_1.

* Calculated from $(2\nu_1)_{\text{obs.}}$ using values of x in Table III.

Table II.—Calcite and Aragonite. Doublet separations at $3\nu_1$ and at $2\nu_1$.

—	$\Delta\lambda$ Calcite.	$\Delta\lambda$ Aragonite.
$3\nu_1$	$0\cdot02\mu$	$0\cdot05\mu$
$2\nu_1$	$0\cdot12\mu$	$0\cdot06\mu$

Table III.—Calcite and Aragonite. Kratzer correction at $3\nu_1$ and at $2\nu_1$.

$3\nu_1$ and $2\nu_1$, intense component of each.

	Calcite.	Aragonite.
$x =$	0·005	0·043

$3\nu_1$ and $2\nu_1$, weak component of each.

	Calcite.	Aragonite.
$x =$	0·032	0·005

Table IV.—Calcite and Aragonite. Thermodynamic and elastic properties (9).

	Calcite.	Aragonite.
Thermal expansion	$15\cdot4 \times 10^{-6}$	$61\cdot9 \times 10^{-6}$
Compressibility	$1\cdot34 \times 10^{-12}$	$1\cdot53 \times 10^{-12}$
Specific heat C_v	$80\cdot5 \times 10^{7}$	$81\cdot5 \times 10^{7}$
Grüneisen's ratio γ	0·51	1·68

Table V.—Aragonite-Strontianite-Witherite. Fundamentals and overtones arranged according to Schaefer's scheme.

	Aragonite.	Strontianite.	Witherite.
$3\nu_1$	2·25μ	—	2·35μ
	2·30	2·34	2·39
$2\nu_1$	3·35	3·39	3·45
	4·10	3·45	3·52
ν_1	6·64 (5) 6·48*	6·78 (5) 6·76*	6·85 (5) 7·10*
ν_3	11·50	11·55	11·40 ?
ν_2	14·39	14·35	14·32 ?
Minor bands—	2·50	2·55	2·59
	2·79	2·82	2·85
	3·08	3·09	3·16
	3·09	3·10	3·17
	—	3·97	3·99

Witherite figures due to Schaefer, also ν_1 for aragonite and strontianite.

* Calculated from $(2_{\nu 1})_{\text{obs.}}$ using values of x in Table VI.

Table VI.—Aragonite-Strontianite-Witherite. Kratzer correction at $3\nu_1$ and at $2\nu_1$.

$3\nu_1$ and $2\nu_1$, intense component of each.

	Aragonite.	Strontianite.	Witherite.
x =	0·043	0·019	−0·14

$3\nu_1$ and $2\nu_1$, weak component of each.

	Aragonite.	Strontianite.	Witherite.
x =	0·005	—	−0·14

Table VII.—Calcite-Aragonite-Strontianite. Values of $\lambda_{\text{ref.}} - \lambda_{\text{abs.}}$

	Calcite.	Aragonite.	Strontianite.
At ν_3	$0{\cdot}03\mu$	$0{\cdot}04\mu$	$0{\cdot}07\mu$
At ν_2	$0{\cdot}04\mu$	$0{\cdot}01\mu$	$-0{\cdot}07\mu$

Reflection figures due to Schaefer.

Discussion of Results.

Tables I to III and V to VII contain the chief results to which this study of absorption spectra has led. The graphs, figs. 2 and 3, exhibit the bands in aragonite and strontianite in the regions accessible with a quartz or rock-salt prism, as the case may be.

A general point may conveniently be made here.

As already mentioned, the metal ions involved have the inert gas structure, and thus

Mg^{++}	corresponds to	Ne
Ca^{++}	,,	A
Sr^{++}	,,	Kr
Ba^{++}	,,	X

Wasastjerna's work (10) indicates that the repulsive force between like ions varies as r^{-11} for Mg^{++}, and as r^{-9} for Ca^{++}. One might, perhaps, infer r^{-7} for Sr^{++} and r^{-5} for Ba^{++}; but the only characteristic of present interest is that these forces certainly do not have the same index throughout the series of crystals with which this paper is concerned. Even though it is the CO_3^{--}

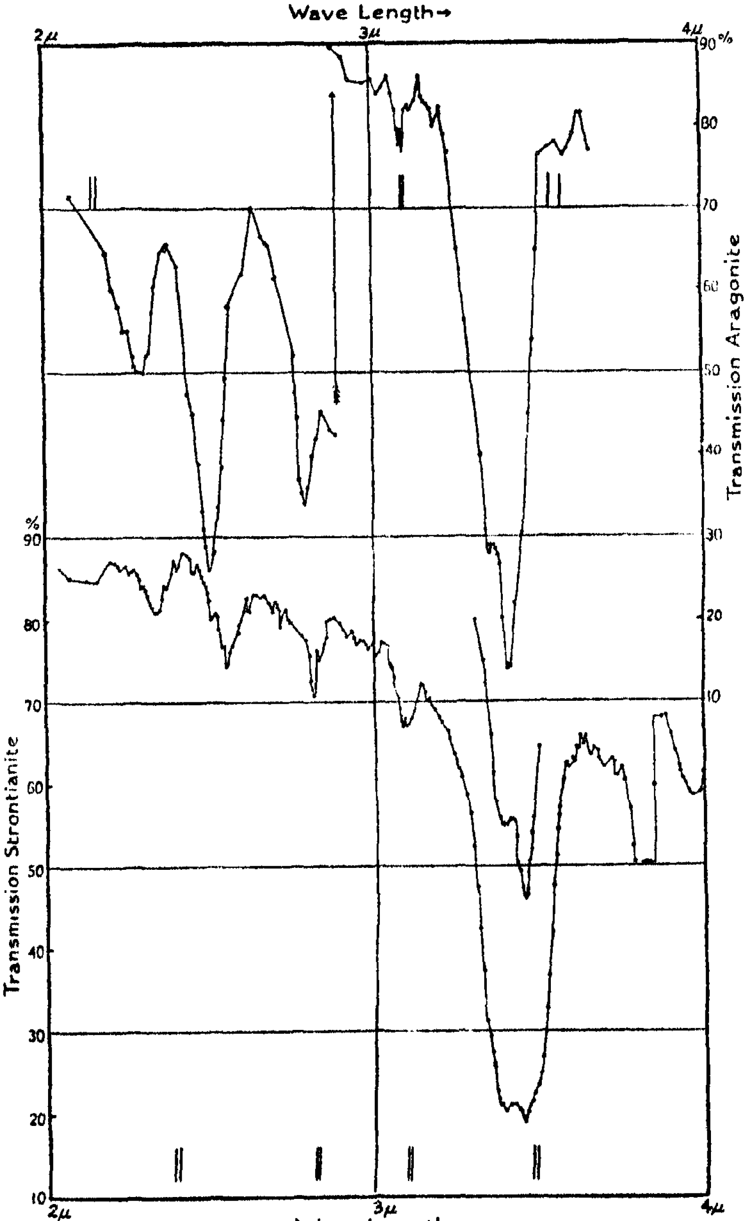

FIG. 2.—Aragonite above, strontianite below. Quartz prism.

ion that is mainly responsible for the observed bands, the indices just referred to suggest that regular transitions in absorption frequencies will probably be lacking, a feature borne out by the present results and those of Schaefer (2).

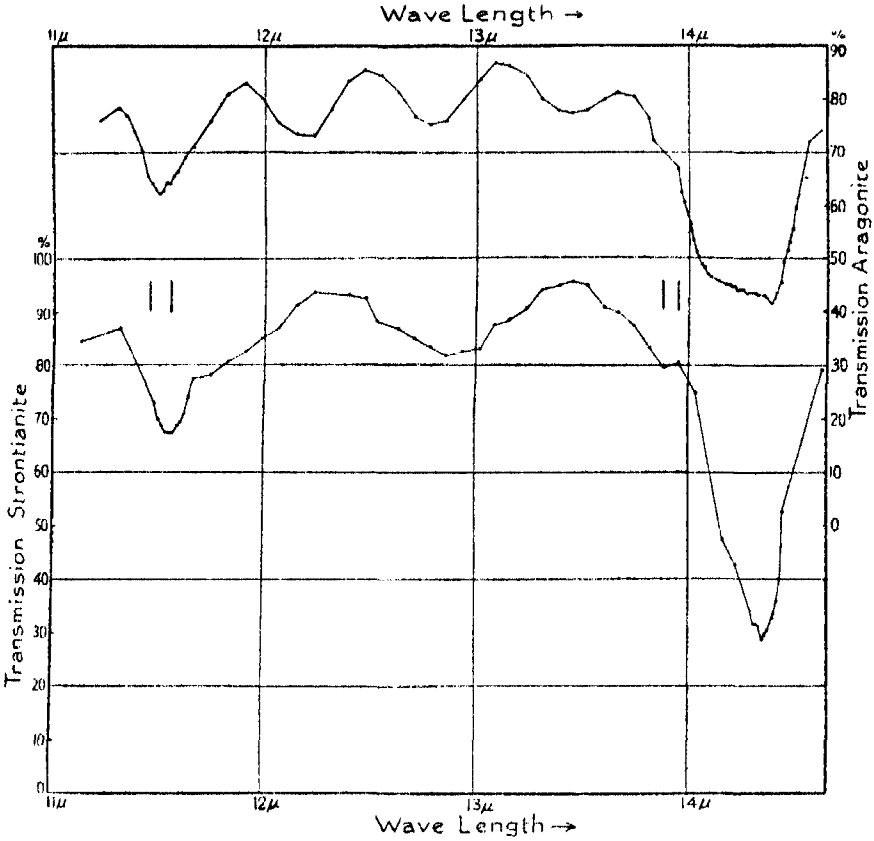

Fig. 3.—Aragonite above, strontianite below. Rock-salt prism.

It seems natural to divide the discussion into three parts :—

(*a*) Comparison of the allotropes calcite and aragonite (Tables I to IV).

(*b*) Comparison of the bi-axial carbonates of the alkaline earths—

Aragonite $CaCO_3$ Strontianite $SrCO_3$ Witherite $BaCO_3$	Tables V and VI.

(*c*) Remarks on the quantity $\lambda_{\text{ref.}} - \lambda_{\text{abs.}}$, with special reference to calcite, aragonite and strontianite (Table VII).

(*a*) All the data obtained combine to show that marked differences exist in the absorption spectra of the two forms of calcium carbonate. Coblentz (3) first hinted that the atomic weight of the metal might be a determining factor in fixing the position of the bands.

These two allotropes provide a crucial test of this view, from which it is clear that the atomic weight of the base *per se* is not of itself sufficient to account for the facts. A more likely suggestion is molecular volume [M].

Now $[M]_{\text{cal.}} = 36$, and $[M]_{\text{arag.}} = 34$, and other things being equal it might reasonably be supposed that the absorption wave-lengths should increase with [M], *i.e.* that $\lambda_{\text{cal.}} > \lambda_{\text{arag.}}$ While this seems very roughly to be true for ν_1 and its overtones, it is contradicted at ν_2 and at ν_3 (see Table I). It should be remembered, however, that ν_1 and ν_3 are oscillations in the planes of the CO_3 groups, and that ν_2 is perpendicular to them.* A knowledge of the compressibilities along the chief crystal axes might give some clue to these apparent anomalies. It is well known that the packing is different in the two forms, from which it might be inferred that the law of repulsion (perhaps r^{-9}) between like ions would influence the result by virtue of its effect upon the CO_3 complex.

The fundamental between 6μ and 7μ is unfortunately placed from an experimental point of view, and also its great intensity means that reflection measurements only are available. However, it is evident that this band (Schaefer's ν_1) and its overtones $2\nu_1$ and $3\nu_1$ are subject to very complicated relationships, *e.g.* the doublet separations are in opposite senses at the two harmonics (see Table II).

If now, from the observed data, the Kratzer term x (p. 141) is calculated for these two overtones, the values given in Table III are obtained. Naturally, it alternates in an analogous way to that of the separations. The absolute magnitude of x may be taken as a measure of the anharmonic coupling, and applying this to the intense component in each case, shows that this asymmetry is greater in aragonite than in calcite, a fact to which the relative magnitudes of the thermal expansion, compressibility and Grüneisen's ratio γ lend additional support (see Table IV).

Nevertheless the reverse is the case for the weak member in either band. With regard to this, it may be said that the experimental readings are decidedly more likely to be slightly astray in recording such small arrests, as a glance at the curves will show.

It is, perhaps, worth noticing that these doublets appear (in " ordinary " radiation) in both the uni-axial and bi-axial varieties (11).

With reference to ν_2 and ν_3 (Table I), no obvious reason can be advanced for their relative positions, except, perhaps, the difference in packing in the two directions.

It is not to be expected that agreement will be reached with Kornfeld's (6) theoretical results for these bands, for his treatment neglects the part played by the metal ion.

(*b*) The transition through the bi-axial group aragonite-strontianite-witherite allows of a little more regularity. Coblentz (3) first found that the (reflection) characteristic wave-lengths increased with the atomic weight of the base for all three fundamentals ν_1, ν_2, ν_3, which, no doubt, was the foundation of his suggestion already mentioned. Schaefer and Schubert (5) some years later found a number of irregularities in ν_2 and ν_3, confirming, however, Coblentz's order at ν_1, which is well borne out in the present results for aragonite and strontianite as regards their overtones between 1μ and 4μ (fig. 2).

The *considerations regarding ionic repulsive fields outlined in a previous paragraph* lead here also to the possibility that molecular volumes [M] as opposed to atomic weights of the particular metal might prove a more satisfactory criterion. The values of [M] with which this section is concerned are $[M]_{\text{arag.}} = 34$, $[M]_{\text{str.}} = 40$, $[M]_{\text{with.}} = 46$. Unfortunately, in absorption Schaefer's witherite specimen was imperfect, for which reason his figures are marked ? in Table V. Since ν_1 and ν_2 represent oscillations in the same plane (6) (that of the CO_3 group), and Schaefer's witherite readings involving ν_1 are fairly regular, it seems plausible to assume that his ν_2 is correct, but that the fault in his specimen mainly affected ν_3 (a perpendicular vibration), which is also reflected in his combination tone at $5 \cdot 12\mu$ (2).

If this view is permissible, it appears that whereas at ν_1 the absorption wave-lengths increase with [M], at ν_2 and ν_3 the reverse holds, and the same is true for calcite and aragonite.

Table VI gives the value of the small correction term x analogous to Kratzer's anharmonic coupling factor in gases for the bi-axial carbonates. x is calculated from the observed data for the bands near $2 \cdot 3\mu$ and $3 \cdot 4\mu$, taken by Schaefer to be the overtones $3\nu_1$ and $2\nu_1$.

Assuming x known, an estimate is obtained for the fundamental ν_1. These calculated values appear in Table V opposite Schaefer's reflection figures. Witherite excepted, the difference is much what one might expect, since it is generally accepted that $\lambda_{\text{ref.}}$ and $\lambda_{\text{abs.}}$ are not identical. As Table VII and section (*c*) indicate, experiment shows, where the fundamentals are accessible, that $\lambda_{\text{ref.}} > \lambda_{\text{abs.}}$, a fact with which $(\nu_1)_{\text{calc.}}$ is in general accord. It may be well to state that the above considerations are fully recognised to be no more than a first attempt to make any allowance for the presence of anharmonic forces on the simplest possible basis. More refined experiment might easily render them untenable, not to mention the possibility of a complete analysis of crystal dynamics.

(*c*) Table VII shows that, with the sole exception of strontianite at ν_2, the quantity $\lambda_{\text{ref.}} - \lambda_{\text{abs.}}$ is positive. Schaefer (2) finds a similar effect in all the carbonates examined by him, and his results show that the difference is very considerable, amounting to some $0 \cdot 1$ to $0 \cdot 2\,\mu$. According to the figures obtained in the course of the present work, it is much less, being some $0 \cdot 03$ to $0 \cdot 07\,\mu$. A special recalibration of the spectrometer was carried out in order to test this carefully.

Now the reflective power R is given by

$$R = \frac{(n-1)^2 + k^2}{(n+1)^2 + k^2}, \tag{1}$$

where n is the refractive index and k the coefficient of absorption. At a position of maximum reflection $(\partial R/\partial \nu = 0)$,

$$(n^2 - k^2 - 1)\, \partial n/\partial \nu + 2nk \partial k/\partial \nu = 0, \tag{2}$$

which is displaced from the positions $k_{\text{max.}}$ — *i.e.* $\partial k/\partial \nu = 0$ — by the amount $(n^2 - k^2 - 1)\, \partial n/\partial \nu$.

In such a region $(n^2 - k^2 - 1)$ is presumably negative, so that $\partial n/\partial \nu$ is also negative, or the dispersion $\partial n/\partial \lambda$ is positive. Apparently, therefore, the dispersion in these carbonates is decidedly less in actual magnitude than Schaefer's results would suggest.

Summary.

The absorption spectra of aragonite and strontianite have been examined in the near infra-red. From the results it has been found possible to compare the two allotropic modifications of $CaCO_3$ as well as the series of bi-axial crystals of the carbonates of Ca, Sr, Ba.

In the former case it is shown that definite displacements of the three fundamental frequencies of the CO_3^{--} ion occur in the two crystal forms. From the overtones of the fundamental at $7\,\mu$ it is shown that the frequencies do not follow the order ν_1, $2\nu_1$, $3\nu_1$, but that a correction must be introduced analogous to the Kratzer correction for anharmonic coupling in gases. In $CaCO_3$ this correction is greatest for the less symmetrical form.

In the bi-axial series, the absorption wave-length at ν_1 $(7\,\mu)$ and its overtones increases with the molecular volume, but the reverse is the case for the bands at ν_2 $(14\,\mu)$ and ν_3 $(11\,\mu)$. This dependence upon the molecular volumes is likewise observed in calcite and aragonite.

The values of $\lambda_{\text{ref.}} - \lambda_{\text{abs.}}$ for the various bands have been determined with the aid of Schaefer's data for $\lambda_{\text{ref.}}$ It is shown, in confirmation of Schaefer's results, that these are generally finite and positive, but less than $0 \cdot 1\,\mu$, being smaller than those obtained by this observer.

Acknowledgments.

The authors would like to take this opportunity of thanking Prof. T. M. Lowry, F.R.S., for the use of his infra-red spectrometer and thermopile. They also wish to express their gratitude to Prof. A. Hutchinson, F.R.S., for the loan of a goniometer, by the help of which the special calibration mentioned in section (*c*) of the discussion was performed. To Messrs. Brunner Mond they are indebted for a grant out of which apparatus and material was purchased. Finally, they are fully aware of the help they have received from Mr. R. Stonebridge, of the Physical-Chemistry Laboratory, in the construction of many of the special devices required.

REFERENCES.

(1) Chapman and Ludlam, 'Phil. Mag.,' vol. 50, p. 822 (1925); Chapman, Topping and Morral, 'Roy. Soc. Proc.,' A, vol. 111, p. 25 (1926); Lennard-Jones and Dent. 'Roy. Soc. Proc.,' A, vol. 113, pp. 673, 690 (1927).
(2) Schaefer, Bormuth and Matossi, 'Z. f. Physik,' vol. 39, p. 648 (1926).
(3) Coblentz, 'Carnegie Publ.' (1905–1908).
(4) Nyswander, 'Phys. Rev.,' vol. 28, p. 291 (1909).
(5) Schaefer and Schubert, 'Ann. d. Physik,' vol. 50, p. 283 (1916).
(6) Kornfeld, 'Z. f. Physik,' vol. 26, p. 205 (1924).
(7) Kratzer, 'Z. f. Physik,' vol. 3, p. 289 (1920).
(8) Rawlins, Taylor and Rideal, 'Z. f. Physik,' vol. 39, p. 660 (1926).
(9) Geiger-Scheel, 'Handbuch d. Physik,' vol. 10, p. 32 (1926).
(10) Wasastjerna, 'Soc. Sci. F.L.P.M.,' vol. 1, p. 38.
(11) Brester, 'Z. f. Physik,' vol. 24, p. 324 (1924).

On the Measurement of Light Absorption.

By H. von Halban and J. Eisenbrand.

(Communicated by Prof. E. C. C. Baly, F.R.S.—Received June 1, 1927.)

Among the physical methods which have been suggested for the elucidation of chemical problems, the measurement of light-absorption is becoming increasingly important. Opinion is, however, still very divided concerning the utility of the different methods and the measure of trust which can be reposed in the results obtained. The element of uncertainty is so great that the correctness of conclusions based on the measurements is not infrequently questioned,* and occasions have arisen in which the investigation of a problem by different methods has led to intrinsically different results. A specially clear case is found in the divergence between the photographic and photoelectric methods for the measurement of light absorption in the ultra-violet. For this reason we have thought it desirable to supplement in one or two directions the investigations of Baly, Morton and Riding† on this subject.

It must be stated at the outset that in judging the value of the methods under consideration the *aim* of the proposed investigation must first be ascertained.

The object of the work will fall into one of three main classes.

(1) The determination of extinction coefficients for a definite wave-length with the greatest possible accuracy;

(2) The mapping of absorption spectra, and finally,

(3) The kind of application which always possesses most interest for physical chemists, namely the detection of changes, which a system may undergo under definite conditions, such as, equilibrium displacements bound up with changes in light absorption, the influence of various factors on light absorption, and the investigation of the validity of Beer's Law.

It will be seen that the differences of opinion to which we have referred arise in part from the fact that the objects in view are not clearly distinguished, and in part from the lack of a strict definition of the "accuracy" of the different methods used. The next step is to draw a very clear distinction between reproducibility and absolute accuracy of the experimental data.

If we consider investigations of type (3) the absolute correctness of the results is often of little or no importance whilst the reproducibility and sensitivity of the method gain enormously in significance. Let us for instance consider an acid, the ion of which absorbs strongly in a certain region of the spectrum whilst the undissociated acid shows negligible absorption. In order to evaluate the degree of dissociation on the basis of this property it is not necessary to know the absolute value of the extinction coefficients at a definite wave-length. The problem can even be solved by colorimetric methods.* It is only necessary to make a comparison between the light absorption of a solution of the acid and that of a salt, and the trustworthiness of the result depends only on the reproducibility and the sensitivity of the method.†

---

* *Cf.* H. von Halban and J. Eisenbrand, 'Z. f. Phys. Chem.,' vol. 122, p. 337 (1926).

† 'Roy. Soc. Proc.,' A, vol. 113, pp. 709, 717 (1927).

If it is desired to test the validity of Beer's Law for a given system, the accuracy with which the wave length of light is defined may not enter into the question at all if the scope of the investigation is suitably restricted. When Beer's Law is to be tested by maintaining the product of thickness and concentration constant, the light may be quite heterogeneous, and in spite of this, suitable methods will show with great accuracy that the extinction is independent of concentration.

It is frequently stated that a method is " accurate to x per cent." This statement has no unequivocal meaning and in it several different conceptions are amalgamated.

Let the molecular extinction coefficient be ε, the concentration c, and the thickness d, and the light intensity I, then the well known equation

$$\varepsilon = \frac{1}{cd} \log \frac{I_0}{I} \text{ follows.}$$

The expression $\log (I_0/I)$ is called the extinction and we shall denote it by E.

The accuracy, *i.e.*, the relative error, of ε depends, other things being equal, on the magnitude of E, $\frac{d\varepsilon}{\varepsilon} = \frac{dE}{E}$. A critical survey of the experience and data gained by the use of the photographic method shows that an absolute error of 0·04‡ in E is normally to be expected. It follows therefore that when $E = 1$ the relative error amounts to 4 per cent., and when $E = 2$ it is 2 per cent. and so on. On the other hand the relative error increases rapidly as E decreases.§

---

* *Cf.* F. G. Donnan, 'Z. f. phys. Chem.,' vol. 19, p. 465 (1896).

† *Cf.* H. von Halban and L. Ebert, 'Z. f. Phys. Chem.,' vol. 112, p. 373 (1924).

‡ The reproducibility of the " blackening " at neighbouring points on a photographic plate as a result of equal exposures is 5 per cent. of the light intensity under favourable conditions (*cf.* F. Weigert, 'Optische Methoden in der Chemie,' Leipzig, p. 237, 1927). This would correspond to an absolute error of 0·02 in E. As a matter of fact, this degree of accuracy is only very rarely obtainable.

§ *Cf.* tables in 'Ostwald-Luther, Hand- und Hilfsbuch physikochemischer Messungen,' 4 Aufl., p. 716, and in Weigert's book referred to above.

Theoretically, the accuracy of E or ε could be much increased by making E very great. The idea however breaks down partly because of the very long times of exposure needed and partly by the very exacting demands made on the purity of the light. The principles set forth indicate that a good photographic method will give values of ε trustworthy to within a few per cent., provided only that a sufficiently large value for the extinction has been chosen. Since it is possible with the spectrographic method to work with a weak light, sufficient purity and definition in respect of wave-length can usually be obtained. In this respect no further uncertainty enters into the results.

By using the spectrographic method for investigations of type (3) it is impossible to determine the concentration of the absorbing material from the relation $\varepsilon.c.d. = \text{E}$, more accurately than E itself, *i.e.*, to within a few per cent., and that only when E is sufficiently large. For instance, two solutions of an absorbing substance, differing in concentration by 2 per cent. could only be distinguished by using the greatest care; with a difference of 5 per cent. it would at best only be possible to ascertain qualitatively the direction of the difference, but in no case could its magnitude be determined.

If we now turn to the photoelectric method we find at once a fundamental difference. The sensitivity of the photographic (and ocular) methods to differences depends on the relative difference between two light-intensities, and, therefore, on an absolute difference of E (see above), and in consequence the sensitivity cannot be increased by increasing the illumination. The electrometer, however, registers by a compensation method the absolute value of $d\,\text{I}$, and it therefore follows immediately that the sensitivity in respect of relative changes in I, may in principle be increased indefinitely by increasing the intensity of the light (stronger light source, optical train, incident intensity, wider slit).

If I_0 and the smallest value of $d\,\text{I}$ for which the apparatus is effective are defined, it can be shown that the accuracy with which E can be determined reaches a maximum when $\text{E} = 0{\cdot}4343$.*

Since, as has been mentioned, the sensitivity to differences in E depends on the light intensity, it must be higher for strong spectral lines than for weak ones.

---

* In practice, however, the assumptions underlying the deduction of this result are not fulfilled. The sensitivity is frequently conditioned not by a definite $d\,\text{I}$ but rather by a definite $d\,\text{E}$ because wedge displacements smaller than 0·01 mm. cannot be measured. As a result, the optimum sensitivity lies usually on the side of extinctions higher than 0·4343 and the sensitivity of the photoelectric arrangement cannot be used to full advantage. For further details the paper referred to above should be consulted.

In investigating two systems in which equality of absorption is to provide a criterion for equality of concentration of an absorbing substance, there is no need for the light to be specially pure. In this case an increase in light-intensity is readily obtained at the expense of purity.* The paper by H. von Halban and K. Siedentopf† contains an example of the evaluation of a small difference in concentration. Two alkaline solutions of potassium chromate, differing in concentration by 1 per cent., were compared. The photoelectric method indicated a difference of 1·04 per cent. The error expressed in terms of concentration was, therefore, 0·04 per cent. Later experiments have perhaps taken us rather further. Using the specially suitable 436 μμ line of mercury two solutions differing in concentration by 0·30 per cent. have been compared. We were not only able to recognise the direction of the difference, but also to determine approximately its magnitude. The experimental difference was 0·28 per cent. We succeeded, moreover, in carrying out similar determinations when the absolute values of the extinctions were small, as in the case of a solution of concentration $1 \cdot 121 \times 10^{-5}$. By "bracketing" between concentrations of $1 \cdot 180 \times 10^{-5}$ and $1 \cdot 062 \times 10^{-5}$ the fine-colorimetric method led to the value $1 \cdot 120 \pm 0 \cdot 002 \times 10^{-5}$.‡ In cases such as these in which the purity of light is of small consequence, the error does not reach 0·2 per cent. The *absolute* value for this small extinction was, however, determined as 0·0532 as against a value of 0·0519 calculated on the basis of the extinction coefficient for monochromatic light. The error is here greater, namely, 2·5 per cent., although it is still very small for so low an extinction.

In the case of weak lines or lines strongly absorbed by the walls of the cell, the sensitivity to differences must, in accordance with what has been said, be very much smaller. Nevertheless, except under very unfavourable conditions, *e.g.*, with the 289 μμ mercury line, an extinction difference of 0·01 (corresponding with 1 per cent. of the extinction) should be capable of detection.

As a result of the foregoing it will be seen that the photoelectric compensation method is far superior to the photographic method for the detection of differences, and, therefore, for the qualitative or quantitative determination of small changes in light absorption or small differences in the concentration of an absorbing constituent. The photoelectric method is in consequence much to be preferred as an instrument for the elucidation of problems in chemical dynamics, especially since it allows measurements with monochromatic light to be carried out relatively quickly.

---

* *Cf.* H. von Halban and L. Ebert, 'Z. f. Phys. Chem.,' vol. 112, p. 359 (1924), in which the use of this "fine-colorimetry" is described.

† 'Z. f. Phys. Chem.,' vol. 100, p. 268 (1922).

‡ The thickness in this case was 0·998 cm., and the measurements were carried out with the 366 μμ line.

We have to set against these advantages the fact that the purity of the light and the degree of definition in respect of wave-length is much poorer than in the photographic method,* because it is necessary to use an intense line in the mercury spectrum in conjunction with a relatively wide slit.† The photographic method possesses over the photoelectric method the additional advantage that the entire absorption spectrum can be obtained quickly. In this respect the photoelectric method is moreover limited to the relatively few suitable lines in the mercury spectrum, a fact which seriously reduces its utility. Since the attainable accuracy is sufficient for following the course of the absorption over the spectrum, the photographic method is unconditionally preferred for this purpose.

The views so far expressed make it easy to understand the occurrence of small incidental differences between the results of the photographic and photoelectric methods so long as they do not exceed a few per cent. The most striking example of large differences has occurred in the absorption curves of nitrates below 300 $\mu\mu$. Whilst on the long wave side of 300 $\mu\mu$, the results with the two methods were in satisfactory agreement, below 300 $\mu\mu$ the photoelectric method gave values increasingly discrepant as the wave length decreased. Instead of passing through a minimum in going from 265 $\mu\mu$ to 254 $\mu\mu$, the values continued to decrease. At the latter wave-length, the difference amounted to 75 per cent.‡ of the value obtained by the photographic method.

So great an error in the photoelectric method would seem at first sight to be impossible and inconsistent with what we have already said about the method. Baly, Morton and Riding regarded it as therefore probable that the discrepancy might be due to some hitherto unknown effect.

We have now repeated the photoelectric measurements and found the results as before, to be reproducible throughout. It therefore seemed difficult to believe that they could be absolutely false. A detailed examination has now led to the disclosure of a systematic source of error. The cells used in the measurements were made of a glass relatively opaque to short wave light. Since, however, a sufficient photo-current was generated with a moderately high applied voltage, it seemed that the glass was transparent enough for practical purposes. A closer examination, however, revealed that a very important error had in this way crept into the results. On trial it was found that a thin (0·5 *mm.*) piece of uviol glass only allowed 10 per cent. of the light of the 254 $\mu\mu$ mercury line to be transmitted. The transparency of the glass in the cells used by H. von Halban and L. Ebert was still smaller and the walls were apparently so thick that scarcely more than 0·1 per cent. of the light incident at 254 $\mu\mu$ could have reached the potassium surface.

---

* Consult G. Rössler on this point. 'Ber. d. d. Chem. Ges.,' vol. 59, p. 2609 (1926). We have in every case rounded off the wave-lengths of the line groups concerned, and for the sake of simplicity given the wave-length to the nearest $\mu\mu$.

† The use of amplification valves would apparently make for progress in this direction, *cf.* H. Rosenberg, 'Naturwiss.,' vol. 9, p. 359 (1921). For single lines the insertion of light filters would allow sufficient purity to be attained without diminishing the intensity of the light too greatly.

‡ *Cf.* G. Scheibe, 'Ber. d. d. Chem. Ges.,' vol. 59, p. 2616 (1926); E. C. C. Baly, R. A. Morton, and R. W. Riding, 'Roy. Soc. Proc.,' A, vol. 113, p. 709 (1927).

The light which emerges from the monochromator is always, however, contaminated with a " false " light. (This is due to the numerous reflecting surfaces of such an instrument and the presence of imperfections in the quartz prisms and lenses which can never be entirely eliminated.) If now the light of wave length 254 $\mu\mu$ is contaminated only to the extent of 0·001 per cent. by light of wave length 436 $\mu\mu$, it follows from the fact that this false light is absorbed neither by the glass nor the solution and causes, moreover, a very much greater effect on the potassium surface than the short wave light,* that the error must progressively increase as the extinction on the nitrate solution increases.

On these assumptions it will readily be seen that an error will arise corresponding with the discrepancy between the older photo-electric measurements and the photographic data at 254 $\mu\mu$.

It will now be shown how the correctness of this explanation has been substantiated by experiment. The first step was to check the fact that above 300 $\mu\mu$ all the cells used gave values in satisfactory agreement, whereas from 300 $\mu\mu$ downwards (always using nitrate solutions), increasing differences were recorded between the values obtained with different cells. In this way two cells of thin-walled uviol glass gave values in harmony with those of Scheibe as far as 265 $\mu\mu$. At 254 values as large as those of Scheibe could only be obtained if a chlorine filter was used to absorb blue light.†

---

* The selective photoelectric effect increases very rapidly from the ultra-violet to the blue, and indeed at 430 $\mu\mu$ it is about one hundred times that observed at 254 $\mu\mu$.

† Our new values have already been published by Scheibe in connection with his own values, 'Ber. d. d. Chem. Ges.,' vol. 59, p. 2616 (1926), and the data of Ley and Volbert, 'Z. f. Wiss. Phot.,' vol. 28, p. 141 (1924), are also in good agreement (see fig. 1).

It would now seem reasonable to expect similar errors to occur with any other absorbing material, in the same way as with the nitrates. This is, however, not the case. In the above considerations it is assumed that the "false" light is very much less absorbed than the "true" light. If, however, the absorption of the material investigated is of the same order for both the true and false lights the error will be very small, and if the false light is much more strongly absorbed than the true light, unduly high values can actually be obtained.

This explains why, with potassium chromate, in which the region of high absorption extends over the region of maximal photoelectric effect, the error is very much smaller; the values, however, obtained by H. von Halban and K. Siedentopf* were at some wave-lengths lower than those found by Scheibe. We have now obtained values for the extinction coefficients of $2 \cdot 57 \times 10^3$ at 254 μμ and $3 \cdot 16 \times 10^3$ at 265 μμ, in excellent agreement with the results of Scheibe.†

The large discrepancies between the photoelectric and photographic methods thus disappear. The curves show clearly the present position for the absorption spectra of dilute solutions of the alkali nitrates and alkaline potassium chromate. The abscissæ show wave-lengths and the ordinates the logarithms of extinction coefficients.‡

The curves now exhibit good agreement between our values and those of Scheibe, and the deviations from those of Baly, Morton and Riding are also

---

[*] See H. von Halban and K. Siedentopf, 'Z. f. Phys. Chem.,' vol. 103, p. 71 (1922); O. Oldenberg, 'Z. f. Physik,' vol. 29, p. 328 (1924); and D. St. Villars, 'J. Amer. Chem. Soc.,' vol. 48, p. 1974 (1926). Experiments with quartz-glass cells which we have recently obtained are now in progress. A systematic comparison of the different cells has already yielded interesting results which will be published in another place.

[†] See G. Rössler, 'Ber. d. d. Chem. Ges.,' vol. 59, p. 2606 (1926). It is only at 303 μμ that a difference still remains to be explained. The curve published earlier by Scheibe, 'Ber. d. d. Chem. Ges.,' vol. 57, p. 1330 (1924), contains only one point which we have used at 313 μμ near the minimum since Rössler's curve gives no point here. Scheibe's curve in the 'Chemiker-Kalender,' 1927, vol. 3, p. 324, has, however, two points which correspond with those on our curve. Thus it is only at 303 μμ that any discrepancy remains to be explained.

[‡] It is very desirable that all authors should use this mode of representation which has many advantages. See F. Weigert, 'Ber. d. d. Chem. Ges.,' vol. 49, p. 1516 (1916). The use of the extinction coefficient instead of its logarithm makes equal relative errors appear quite different according to the absolute magnitude of the extinction coefficient. Above all, the logarithmic curve is independent of any chance errors in the absolute magnitudes of concentrations and extinction coefficients.

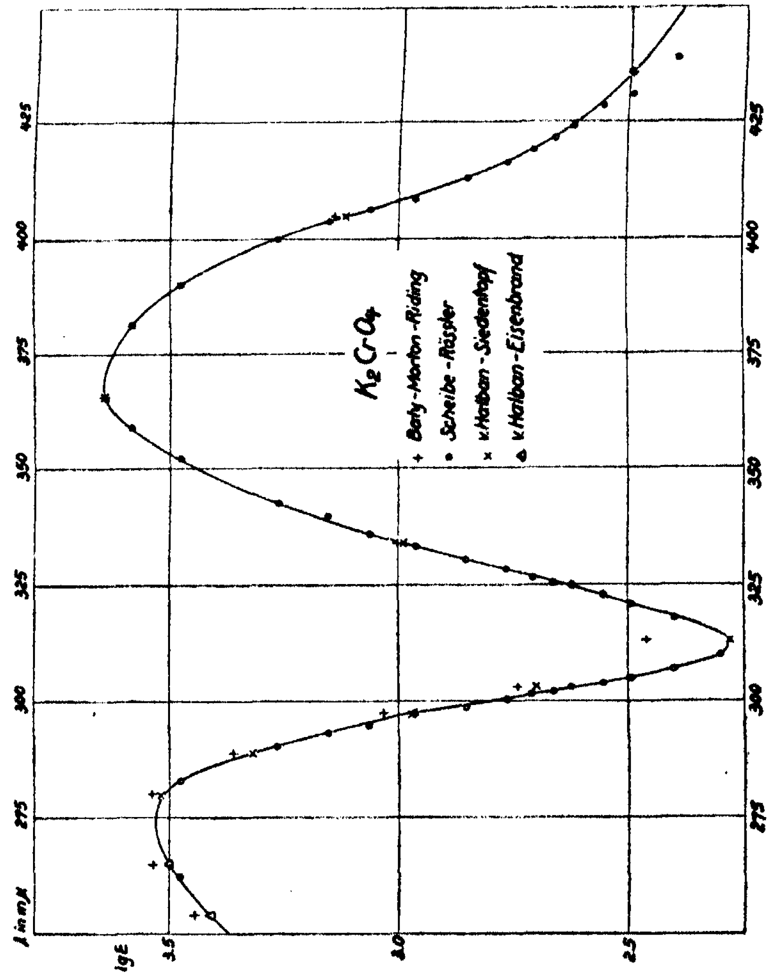
λ in mμ
275
300
325
350
375
400
425
lg E
3.5
3.0
2.5
K_2CrO_4
+ Baly-Morton-Riding
• Scheibe-Rössler
× v. Halban-Siedentopf
◇ v. Halban-Eisenbrand

FIG. 2.

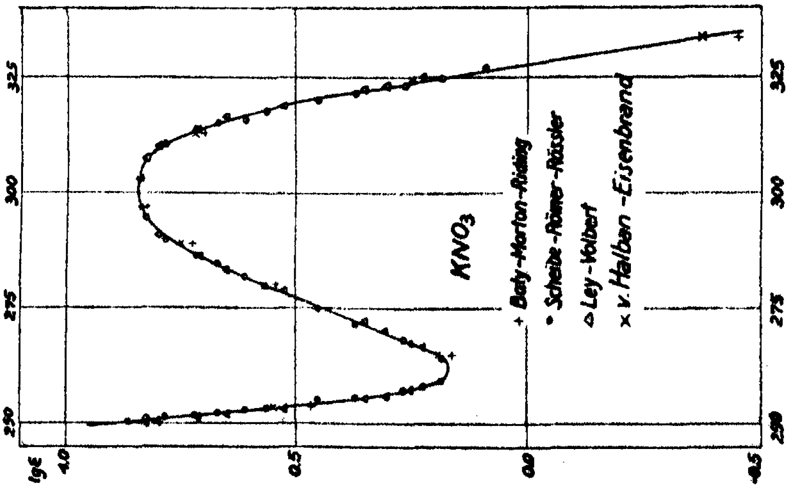
λ in mμ
250
275
300
325
lg E
1.0
0.5
0.0
-0.5
KNO_3
+ Baly-Morton-Riding
• Scheibe-Römer-Rössler
◇ Ley-Volbert
× v. Halban-Eisenbrand

FIG. 1.

on the whole similarly small, except at 313 $\mu\mu$ (K_2CrO_4).[*] The larger difference in this case is probably to be explained by the measurement of too small an extinction by these authors. The concentration of the solution used by Baly, Morton and Riding was 0·000075 N. The thickness used was 4 cm. From our value for ε we obtained $E = 0{\cdot}0586$ as against $E = 0{\cdot}087$ in the work of Baly, Morton and Riding. The difference, 0·028, is, as has been shown, well within the error of the photographic method.

We are not in a position to ascertain the reason for the differences between the photographic methods for the glass plates as duplicates are lacking.[†]

A brief discussion is necessary of a few of the data given in the work of Morton and Riding.[‡] These authors found considerable differences between the absorption spectra of dilute solutions of different nitrates. We have tested this point specifically and our results will shortly be published in full in the 'Zeitschrift für Physikalische Chemie.'

The results show that the absorption spectra of dilute solutions of the nitrates of the Alkali and Alkaline earth metals are identical. The results of H. Ley and F. Volbert[§] with silver nitrate are in agreement. The persistence, on the basis of our results, amounts to $6{\cdot}91 - 1{\cdot}56 = 5{\cdot}35$. Morton and Riding, however, find values which vary between 5·36 and 6·92. An error of this magnitude in our results appears to be quite excluded. We suggest that the maximum at 300 $\mu\mu$ is extraordinarily sensitive to the presence of impurities. We have obtained for instance with the purest commercial preparation[||] the value 7·39, and it was only after four recrystallisations from conductivity water that the value 6·91, found earlier by Ebert, was reproduced. In the case of nitric acid as yet unpublished experiments also show a lack of complete quantitative agreement with the results of Morton and Riding.

Summary.

The important factors in appraising the value of a method for the measurement of light absorption have been discussed critically. In using the photographic method it must be observed that it is characterised by a definite absolute error, or a definite absolute difference in extinction, and *not* by a definite relative error in the extinction or extinction coefficient. The accuracy with which the extinction coefficient can be determined depends rather on the absolute magnitude of the extinction used. By employing a sufficiently large extinction the photographic method permits the extinction coefficient to be determined to within a small percentage error.

---

[*] At 303 $\mu\mu$ there still remains a discrepancy which is doubtless due to the fact that in our apparatus the lines 297 $\mu\mu$ and 303 $\mu\mu$ are incompletely separated. Experiment has indeed shown that the values obtained depend to a marked extent on the slit width.

[†] 'Roy. Soc. Proc.,' A, vol. 113, p. 712 (1927).

[‡] *Ibid.*, vol. 113, p. 717 (1927).

[§] 'Z. f. Wiss. Phot.,' vol. 28, p. 41 (1924).

[||] Kahlbaum's preparation, 'Zur Analyse mit Garantieschein.'

For the evaluation of smaller differences between extinctions or of small differences in the concentration of an absorbing substance, and also for the absolute determination of small extinctions the photographic method is not suitable. On the other hand, for the quantitative exploration of absorption spectra the photographic method is entirely suitable, and on account of its greater rapidity it is for this purpose undoubtedly preferable to the photoelectric method.

In the photoelectric method we cannot at present set a lower limit to the error, *i.e.*, to the sensitivity to differences of extinction. It is, at all events, practically possible under favourable conditions (with strong lines) to raise the sensitivity to differences of extinction by about 10^2 beyond that of the photographic method.

For absolute measurements the method cannot be used to full advantage since the high intensity of light which is needed involves the use of less pure light, and poorer definition in respect of wave-length than is obtained with the photographic method.

For the exploration of complete absorption spectra the relatively small number of lines available for the method constitutes an additional disadvantage.

The large differences which occurred between the results of the two methods at wave-lengths below 300 $\mu\mu$, especially for solutions of nitrates, have been traced to a systematic error in the photoelectric measurements. The results of the two methods are in general now in satisfactory agreement.

The Influence of Hydrogen on Two Homogeneous Reactions.

By C. N. HINSHELWOOD and P. J. ASKEY.

(Communicated by H. Hartley, F.R.S.—Received June 7, 1927.)

The reactions involved in the decomposition of propionic aldehyde,* of dimethyl ether† and of diethyl ether‡ are unimolecular as long as the pressure is above a certain limit, characteristic of each reaction. At lower pressures the velocity constants fall. The presence of moderate amounts of hydrogen causes the dimethyl ether and diethyl ether reactions to remain unimolecular at low pressures, but experiments have not hitherto been made to ascertain whether the propionic aldehyde reaction is analogous in this respect. The first object of this paper is to describe experiments which fill this gap. The second object is to answer the question as to what would be the effect of hydrogen on a bimolecular reaction. The example chosen is the decomposition of acetaldehyde,§ which remains bimolecular at pressures much greater than those at which the other reactions become unimolecular, even though it may possibly follow them in this respect at some pressure sufficiently high.

The experiments were guided by some theoretical considerations which may first be briefly outlined.

Conditions under which a Reaction is Bimolecular or Unimolecular.

When a molecule in a gaseous reaction receives by collision the energy necessary for it to undergo chemical change, transformation may follow immediately, or may be delayed until the molecule next passes through a suitable internal phase. When the transformation is immediate, the rate of reaction is simply the rate at which energy can be communicated. The reaction is then kinetically bimolecular. When there is a delay, the energy gained in the first collision may be lost in a second one before the chemical change has time to occur, and if the average interval between collisions is small compared with the time-lag between receipt of energy and transformation, then, as Lindemann has pointed out,|| the reaction appears to be unimolecular.

A time-lag after activation is most probable when the structure of the molecule

---

* 'Roy. Soc. Proc.,' A, vol. 113, p. 221 (1926).

† *Ibid.*, A, vol. 115, p. 215 (1927).

‡ *Ibid.*, A, vol. 114, p. 84 (1927).

§ *Ibid.*, A, vol. 111, p. 380 (1926).

|| 'Trans. Faraday Soc.,' vol. 17, p. 598 (1922).

is complex and the energy is distributed among a number of degrees of freedom. The absence of a time-lag, on the other hand, is to be expected when the mechanism of the activation process is a very simple one.

The absolute speed of a number of simple bimolecular reactions can indeed be predicted by assuming that chemical change occurs whenever a pair of molecules collide, which are activated in a small number of degrees of freedom only. The observed speed is given by the simple exponential expression $Ze^{-E/RT}$, Z being the number of molecules entering into collision, and E being the energy of activation.

Conditions of Validity of the Simple Exponential Distribution Law for Energy of Activation.

The plain exponential form is strictly applicable when the total energy E is distributed in all possible ways in two energy terms. As pointed out in a previous paper, it may be assumed that two energy terms in *each* of the colliding molecules must be activated independently to the extents E_1 and E_2, where $E_1 + E_2 = E$. But it may equally well be assumed that one energy term in each molecule is activated, and that the total may be shared between the two without regard to any separate limits E_1 and E_2. The simplest interpretation, which is perhaps to be preferred, is that the actual translatory violence of the collision determines the activation of the molecules. Then only the components of the two velocities along the line of centres need be considered, and thus a sum total of translational kinetic energy in two energy terms will make up the energy of activation. It is obviously immaterial in what ratio this is divided between the molecules before collision, so that the separate values E_1 and E_2 disappear, and, with the limits of integration 0 to E for each molecule, the expression $e^{-E/RT}$ is found.

More Complex Molecules.

Activation by violent collision, or by any alternative mechanism simple enough to satisfy the conditions under which the expression $Ze^{-E/RT}$ is applicable, would probably be followed by immediate reaction. But in more complicated molecules the activation process may be correspondingly complex and the molecules are not transformed immediately. They are found to react, sometimes, in an apparently unimolecular fashion, in spite of the fact that collisions are ultimately responsible for activation, as is shown by the decrease in the velocity constant at lower concentrations. The apparently unimolecular behaviour necessitates the assumption of the time-lag, in order that there may be abundant activations and de-activations compared with the number of chemical transformations. Only when this condition is fulfilled can the velocity constant be independent of concentration. It is very significant, therefore, that, in reactions where this kind of behaviour is found, the absolute rate can only be accounted for if the energy of activation is assigned to a considerable number of degrees of freedom.

Two Points of View.

It should be pointed out that there are thus two separate lines of argument. First, the fact that the energy distribution law shows varying numbers of degrees of freedom to be involved in the activation of different molecules makes it probable that in some reactions the time-lag will be appreciable, while in others it may be inappreciable. Secondly, the fact that some reactions follow the bimolecular law, while some are quasi-unimolecular, shows directly that sometimes there is this time-lag and sometimes not. And this fact is quite independent of any *a priori* arguments as to whether or not it is to be expected.

Acetaldehyde and Propionic Aldehyde.

The contrast between these substances has already been referred to. The decomposition of acetaldehyde is bimolecular at least up to pressures of 500 mms. Hg, while that of propionic aldehyde becomes quasi-unimolecular at pressures above about 80 mms.

Moreover, the absolute rate of reaction of acetaldehyde can be accounted for by assuming the energy of activation to be confined to about two energy terms, while about 14 are required for propionic aldehyde.

Influence of Hydrogen on Quasi-unimolecular Reactions.

Reference has also been made to the fact that in presence of hydrogen the reactions of dimethyl and of diethyl ether remain strictly unimolecular at concentrations where the unimolecular velocity constants would otherwise fall markedly away from the normal value. The hydrogen seems to exert no effect except in some way to maintain the number of activating collisions at a suitably high value, for although it can restore the velocity constant to the normal value, it cannot increase it beyond this under any conditions.

The possibility of a further test now appears. If the interpretation which has been given to the facts is correct, hydrogen should make the decomposition of propionic aldehyde retain its unimolecular character at lower pressures. On the other hand the bimolecular decomposition of acetaldehyde, in which the Lindemann mechanism is not operative, should not be rendered unimolecular *by hydrogen; any effect that hydrogen has should be different in kind, and probably much smaller in magnitude.*

Hydrogen and Propionic Aldehyde.

Propionic aldehyde falls into line completely with dimethyl ether and diethyl ether. At low pressures, in the absence of hydrogen, the time taken for a definite fraction of the reaction to complete itself increases. In presence of sufficient hydrogen this time remains constant and independent of the concentration of the aldehyde. Moreover, in presence of increasing quantities of hydrogen the time falls to a limiting value, but no further. The following experiments were made at 523° C., the usual methods of measurement being adopted.

t_{50} is the time required for 50 per cent. of the reaction, t_{75} that for 75 per cent.

Initial pressure of propionic aldehyde.	Initial pressure of hydrogen.	t_{50}.	t_{75}.
		′ ″	′ ″
271	0	9 12	20 30
130	0	10 45	22 49
40	0	14 22	—
287	407	10 0	(20 0 calc.)
40	211	10 22	19 30
46	402	9 12	18 0
45	610	9 45	20 35

The exactness with which the reaction in presence of hydrogen conforms to the unimolecular law may be illustrated by quoting details of one experiment. The values are those observed and not those read off from a curve.

Initial pressure of propionic aldehyde = 40 mms.

Initial pressure of hydrogen = 211 mms.

Time.	Pressure increase as percentage of total increase.
′ ″	
4 36	25
10 22	50
19 30	75
29 30	87·5

Taking the time for 50 per cent. as unity, the ratio of the times for 25, 50, 75 and 87·5 per cent. in a unimolecular reaction should be 0·42 : 1·0 : 2·0 : 3·0, while the observed ratios are 0·44 : 1·0 : 1·9 : 2·9.

Hydrogen and Acetaldehyde.

The effect of hydrogen on the decomposition of acetaldehyde is by no means to make t_{50} independent of the initial pressure, and although it is not negligible it is not nearly so great quantitatively, besides being of a rather different kind.

The bimolecular reaction $2CH_3CHO = 2CH_4 + 2CO$ is unaffected, but an independent reaction $CH_3CHO + H_2 = CH_4 + CO + H_2$ is accelerated to some extent. The total rate of reaction is represented by

$$-\frac{d[CH_3CHO]}{dt} = k_1 [CH_3CHO]^2 + k_2 [H_2][CH_3CHO]$$

or

$$\frac{dx}{dt} = k_1 (a - x)^2 + k_2 (a - x)[H_2].$$

The catalytic reaction does not reach a limiting rate at 800 mms. $[H_2]$ and moreover the constant k_2 is small, being only about one-tenth as large as k_1. In the quasi-unimolecular reactions hydrogen is almost as effective as one of the reacting gases in bringing the rate to a limiting value. The counterpart of this would be that k_1 would be about equal to k_2, whence it is evident that the quantitative difference is marked.

It should be mentioned that analyses of the products of the reaction which takes place in presence of hydrogen were made, and showed that no reduction of the carbon monoxide occurred.

The above equation gives on integration

$$t_{50} = \frac{1}{k_2[H_2]} \log \frac{1 + 2(K/a)}{1 + (K/a)}$$

and

$$t_{75} = \frac{1}{k_2[H_2]} \log \frac{1 + 4(K/a)}{1 + (K/a)}$$

where t_{50} and t_{75} are the times required respectively for 50 and 75 per cent. of the reaction to take place, and

$$K = \frac{k_2[H_2]}{k_1}.$$

When $[H_2] = 0$ these expressions are indeterminate, and for small values of $[H_2]$, therefore, they are inaccurate. But a more suitable form is found by re-arranging the differential equation and integrating in the form of a series.

$$t_{50} = \frac{1}{k_1 a}\left\{1 - \frac{3}{2}\left(\frac{K}{a}\right) + \frac{7}{3}\left(\frac{K}{a}\right)^2 - \frac{15}{4}\left(\frac{K}{a}\right)^3 \ldots\right\}$$

$$t_{75} = \frac{3}{k_1 a}\left\{1 - \frac{5}{2}\left(\frac{K}{a}\right) + 7\left(\frac{K}{a}\right)^2 - \frac{85}{4}\left(\frac{K}{a}\right)^3 + \frac{341}{5}\left(\frac{K}{a}\right)^4 \ldots\right\}.$$

These reduce to the ordinary expressions for uncatalysed bimolecular reactions when $[H_2] = 0$. For moderate values of $[H_2]$ both forms of expression can be used with equal convenience, while for large values the first forms must be used.

k_1 can be found from experiments where $[H_2] = 0$. All experiments were made at 518° C., the temperature of most of the original experiments on acetaldehyde. A fresh sample of material gave results agreeing excellently with those of the original investigation.

Using mms. Hg as the units of concentration, k_1 and k_2 were found to be $0 \cdot 84 \times 10^{-5}$ and $0 \cdot 74 \times 10^{-6}$ respectively.

The following tables show that the general course of the reaction in presence of hydrogen is adequately expressed by the equations. Any deviations are mainly due to the fact that the decomposition of acetaldehyde, in the absence of hydrogen, itself deviates a little from the bimolecular law, as was shown in the earlier paper.

(*a*) *Constant pressure of acetaldehyde. Varying pressure of hydrogen.*

$[CH_3CHO]$.	$[H_2]$.	t_{50} (obs.).	t_{50} (calc.).	t_{50} as ratio.		t_{75} (obs.).	t_{75} (calc.).
				(obs.).	(calc.).		
		′ ″	′ ″			′ ″	′ ″
170	0	12 6	11 40	1·00	1·00	—	35 0
169	200	10 53	10 8	0·90	0·87	27 53	28 10
177	300	10 15	9 11	0·85	0·79	25 55	24 0
174	400	9 5	8 47	0·75	0·75	21 10	23 0
168	500	8 50	8 29	0·73	0·73	19 45	21 50
173	600	8 20	7 55	0·69	0·68	19 38	20 0
180	800	7 25	7 0	0·61	0·60	19 24	17 10

(*b*) *As* (*a*) *but with lower pressure of aldehyde.*

[CH_3CHO].	[H_2].	t_{50} (obs.).	t_{50} (calc.).	t_{50} as ratio.	
				(obs.).	(calc.).
		′ ″	′ ″		
98	0	18 8	20 15	1·00	1·00
98	200	16 25	15 55	0·91	0·79
102	500	11 50	11 50	0·65	0·58

(*c*) *Constant pressure of hydrogen. Varying pressure of aldehyde.*

[CH_3CHO].	[H_2].	t_{50} (obs.).	t_{75} (obs.).	t_{50}. In absence of hydrogen (from curve).	t_{75}. In absence of hydrogen (from curve).	$\frac{t_{50} \text{ without } H_2.}{t_{50} \text{ with } H_2.}$		t_{75}/t_{50}.	
						(obs.).	(calc.).	(obs.).	(calc.).
		′ ″	′ ″	′ ″	′ ″				
212	519	9 40	24 10	9 54	29 42	1·03	1·27	2·50	2·63
200	509	9 30	23 30	10 21	31 3	1·09	1·31	2·47	2·61
102	500	11 50	27 30	17 0	51 0	1·44	1·61	2·32	2·45
55	505	13 0	31 0	23 50	71 30	1·83	2·19	2·38	2·30

Conclusion.

The decomposition of propionic aldehyde thus falls into line completely with that of diethyl ether and dimethyl ether with regard to the influence of hydrogen; and the contrast in this respect between the decompositions of acetaldehyde and propionic aldehyde is quite what might have been expected from what was already known about the dynamics of the two reactions. The general coherence of the theoretical interpretation is thus strengthened.

Summary.

Certain reactions, namely, the decomposition of propionic aldehyde, of dimethyl ether and of diethyl ether, have recently been shown to be unimolecular at higher pressures, but to betray their dependence on molecular collisions by falling off in rate when the pressure of the reacting gas is sufficiently reduced. The second and third have been shown, further, to retain their unimolecular character at low pressures if sufficient hydrogen is present.

It is now shown that the decomposition of propionic aldehyde is analogous in this respect.

On the other hand, the bimolecular decomposition of acetaldehyde is less influenced by hydrogen, and in a different way.

Increasing pressures of hydrogen rapidly bring the propionic aldehyde reaction to a limiting rate, which is the same as the rate reached when the partial pressure of the aldehyde itself is increased. Similar pressures of hydrogen have no tendency to make the acetaldehyde decomposition appear unimolecular, and no saturation value is reached.

These phenomena are shown to be consistent with the conclusion already reached that the activation of acetaldehyde involves a few degrees of freedom only, while that of propionic aldehyde is a more complex process; and that in the acetaldehyde reaction there is no time-lag between activation and transformation, while in the propionic aldehyde reaction such a time-lag exists.

On the Flow of Air behind an Inclined Flat Plate of Infinite Span.

By A. Fage, A.R.C.Sc., and F. C. Johansen, B.Sc., of the Aerodynamics Department, the National Physical Laboratory.

(Communicated by H. Lamb, F.R.S.—Received May 23, 1927.)

[Plates 6–8.]

§ 1. *Introduction.*

The general form of the flow behind an infinitely long thin flat plate inclined at a large angle to a fluid stream of infinite extent has been known for many years past. The essential features of the motion are illustrated in the smoke photograph given in fig. 1, Plate 6. At the edges, thin bands of vorticity are generated, which separate the freely-moving fluid from the "dead-water" region at the back of the plate; and at some distance behind, these vortex bands on account of their lack of stability roll up and form what is now commonly known as a vortex street* (see fig. 2). Various theories for calculating the resistance of the plate have also been advanced from time to time. One of the earliest is the theory of "discontinuous" motion due to Kirchhoff† and Rayleigh,‡ who obtained the expression $\frac{\pi \sin \alpha}{4 + \pi \sin \alpha} \rho V_0{}^2 b$ (see symbols) for the normal force per unit length of the plate. More recently Kármán* has obtained a formula for the resistance of a plate normal to the general flow, in terms of the dimensions of the vortex system at some distance behind the plate. In spite, however, of these and other important investigations, much more remains to be discovered before it can be said that the phenomenon of the flow is completely understood.

---

* Bénard, 'Comptes Rendus,' vol. 147 (1876); also Kármán, 'Göttinger Nachr.' (1911 and 1912).

† 'Crelle,' vol. 70 (1869).

‡ "Notes on Hydrodynamics," 'Phil. Mag.' (1876).

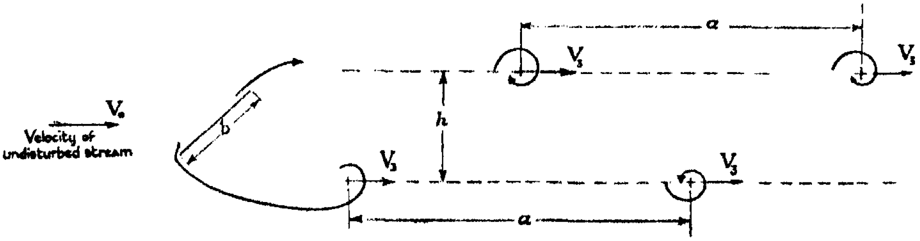

FIG. 2.

No attempt has hitherto been made, as far as the writers are aware, to determine experimentally, at incidences below 90°, the frequency and speed with which the vortices pass downstream; the dimensions of the vortex system; the average strength of the individual vortices; or the rate at which vorticity is leaving the edges of the plate. The present investigation† has been undertaken to furnish information on these features of the flow.

§ 2. *List of Symbols.*

V = average velocity at any point in the field.
V_0 = velocity of the undisturbed air relative to the plate.
V_1 & V_2 = velocity in the outer and inner boundaries of the vortex band at the edge of the plate.
V_3 = downstream velocity of the individual vortices ($V_3 = f.a$).
p_0 = pressure in the undisturbed air.
p = pressure at any point of the field.
p_m = mean pressure at the back of the plate.
α = angle of incidence of the plate (degrees).
b = breadth of plate.

---

* 'Göttinger Nachr.' (1911 and 1912); also Heisenberg, 'Phys. Z.' (1922).

† Permission to communicate the results was kindly granted by the Aeronautical Research Committee.

x, y = the longitudinal and lateral co-ordinates of a point in the field. They are measured from the centre of the plate along and at right angles to the undisturbed wind direction.

a = longitudinal spacing between two consecutive vortices in the same row.

h = lateral spacing between the vortex rows.

f = frequency per second with which the individual vortices leave each edge of the plate.

T = time interval between the shedding of successive vortices in the same row.

κ = strength of an individual vortex.

K = total strength of vorticity leaving each edge in one second.

k_N = normal force coefficient = (normal force per unit length)/$\rho b V_0^2$.

ρ = density of the air.

§ 3. *Forces on the Plate.*

(3.1.) The experiments were made on a flat, sharp-edged rectangular steel plate. The dimensions were: length 7 feet (approximately), and breadth 5·95 inches. The cross-section of the plate, normal to the span, is shown in fig. 3. To obtain the necessary rigidity, one surface (the front) was flat, and the other was slightly tapered from the centre—where the thickness is 3 per cent. of the breadth—towards the sharp edges. The plate was mounted vertically with small clearances between its ends and the floor and roof of one of the 7-foot wind-tunnels at the N.P.L. Observations, whether of pressure on the plate or of velocity in the stream were confined to the plane of symmetry, midway between the floor and roof, where for all practical purposes the flow is two-dimensional.

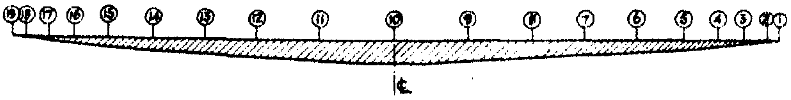

FIG. 3.

(3.2.) The forces on the plate inclined at various angles to the wind were estimated, for two-dimensional flow, from observations of pressure taken around the median section. For this purpose, a pressure tube of fine bore, into which 19 small holes were subsequently drilled—the positions are shown in fig. 3—was let in flush with the flat surface. The pressure in this tube was conveyed through a second tube, at right angles to the first and also flush with the surface, to the pressure manometer, which was a standard 26-inch Chattock tilting gauge. The holes were made airtight by thin paper discs glued to the surface of the plate. To measure the pressure, each hole was opened, in turn, to the air, by the removal of a paper disc. The pressure distribution over the front surface was measured, at a wind speed of 50 feet per second, with the plate at 18 angles of incidence, namely, 0·15°, 0·85°, 1·15°, 1·85°, 2·15°, 3·85°, 5·85°, 8·85°, 11·85°, 14·85°, 19·85°, 29·85°, 39·85°, 49·85°, 59·85°, 69·85°, 79·85°, 90°. The pressure distribution over the "back" surface was measured, at the same holes and at the same angles of incidence, by rotating the plate through 180°. In these latter experiments, the surface facing the wind is no longer flat but slightly cambered, so that the pressures at the back are probably slightly different, at small incidences, from those for an infinitely thin plate. No attempt was made to measure this difference, since a few observations taken with a total-head tube showed that, at large angles of incidence, the pressure in the dead-air region immediately behind the plate was the same, within the accuracy of measurement, whether the flat or slightly cambered surface was presented to the wind.

(3.3.) The values of the normal force coefficient, k_N, were estimated from the areas of the diagrams obtained when the pressure coefficients $(p - p_0)/\rho V^2$ were plotted on a base representing the width of the plate. To illustrate their general character, six representative diagrams are given in fig. 4.

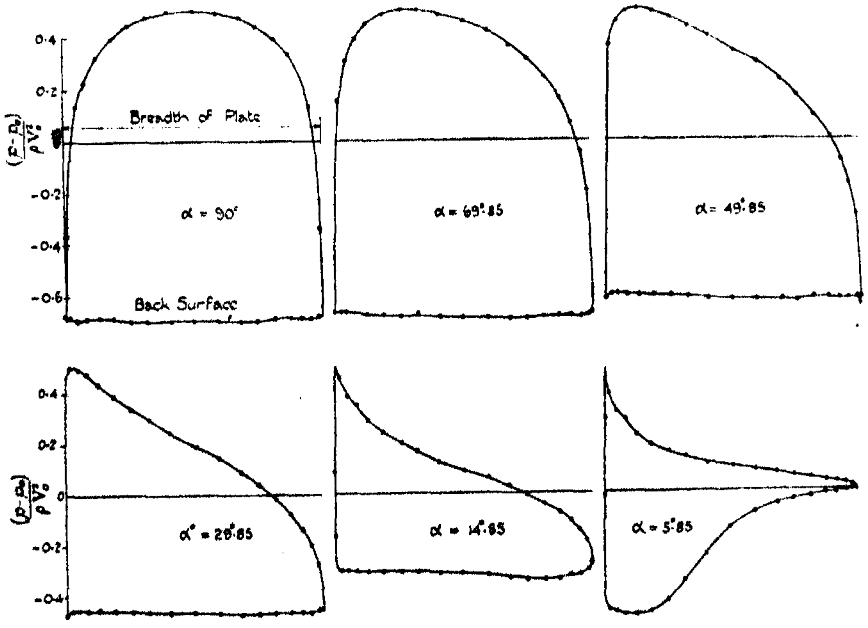

FIG. 4.

The estimated values of k_N are given in Table I (column A). These results show that k_N increases fairly rapidly with α, until a value of 0·445 is reached at $\alpha = 9°$. Beyond this incidence, k_N falls slowly to a value 0·425 at $\alpha = 15°$, and then increases continuously to a maximum value 1·065 at $\alpha = 90°$.

Table I.

$\alpha°$	k_N.			Wind-tunnel values of $(p_m - p_0/\rho V_0^2)$	$(V_1/V_0)^2$.
	Wind tunnel. (A)	Kirchhoff-Rayleigh. (B)	Ratio of wind-tunnel k_N to theoretical k_N. (C)	(D)	(E)
0	0	0	—	—	—
3	0·165	0·040	4·10	—	—
6	0·345	0·075	4·60	—	—
9	0·445	0·110	4·05	—	—
15	0·425	0·170	2·50	—	—
20	0·470	0·215	2·20	—	—
30	0·645	0·280	2·30	−0·462	1·92
40	0·785	0·335	2·35	−0·544	2·09
50	0·900	0·375	2·40	−0·615	2·23
60	0·985	0·405	2·45	−0·664	2·33
70	1·035	0·425	2·45	−0·680	2·36
80	1·060	0·435	2·45	−0·688	2·38
90	1·065	0·440	2·45	−0·690	2·38

The drag and lift coefficients, k_D and k_L, can be obtained directly from the normal force coefficient, k_N, by resolving along and normal to the undisturbed wind direction respectively. No measurements of the tangential forces acting along the surface of the plate are included. These are known to be small—the frictional coefficient of drag at $\alpha = 0°$ is of the order 0·004—and so will only slightly modify the values of k_D at very low angles of incidence. Also no corrections have been made for either the constriction or wall effects.* The correction when the plate is along the wind is, of course, zero.

(3.4.) The comparison between the experimental results and those deduced from the Kirchhoff-Rayleigh theory of the discontinuous motion of a perfect fluid past an infinitely long flat plate, is of interest. According to this theory,† the normal force coefficient k_N is equal to $\pi \sin\alpha/(4 + \pi \sin\alpha)$, and is derived on the assumptions (*a*) that the air breaks away from the plate at the sharp edges and leaves a "dead-air" region behind the plate, throughout which the pressure is uniform and equal to that in the undisturbed fluid, and (*b*) that both the pressure and velocity in the free surfaces separating the stationary from the moving fluid are equal to those in the undisturbed fluid. The theoretical values of k_N are given in Table I, together with the experimental results. It is seen that the theory considerably under-estimates the value of k_N over the entire range of incidence.

---

* See pp. 196–7.

† *Loc. cit.*

(3.5.) An explanation of the marked differences between the theoretical and experimental values of k_N may be found in the fact that the maximum velocity (V_1) in the boundary of the dead-air region behind the plate is appreciably greater than the velocity V_0 assumed in the theory, and that the mean pressure p_m behind the plate is, as a consequence, much lower than p_0. At values of α greater than 30°, the experimental pressure p_m at the back of the plate is approximately uniform, and variations from the mean value do not exceed ± 3 per cent. (see fig. 4). These mean values of $(p_m - p_0)/\rho V_0^2$ are given in column (D) of Table I. If it be assumed that the total head of the air, in the *outer boundary* of the vortex band (*i.e.*, band of discontinuity) leaving an edge of the plate is equal to that in the undisturbed stream, and that the pressure there is equal to that at the back of the plate, the velocity V_1 along this boundary is given by the relation $(V_1/V_0)^2 = 2(p_0 - p_m)/\rho V^2_0 + 1$. Values* of $(V_1/V_0)^2$ estimated from this relation are given in column (E) of Table I. It is rather remarkable that they agree very approximately—except at low values of α—with the ratios of the experimental to the theoretical values of k_N. It is for this reason that they are included in the Table.

§ 4. *Frequency of the Velocity Fluctuations behind the Plate.*

(4.1.) The plate was mounted in the manner previously described (§ 3.1). In addition, stiffening wires were fitted between the plate and the tunnel walls, to eliminate flexural vibrations. Records of the velocity fluctuations were taken behind the central part of the plate, where, for all practical purposes, the flow is two-dimensional. For this purpose, advantage was taken of the cooling effect of a current of air on a heated wire of small diameter.† The current fluctuations in the hot wire circuit due to the fluctuations of wind speed, were passed through an Einthoven galvanometer, fitted with lantern and camera, and the displacement of the string photographically recorded. Time spacings of 1/50 second, obtained from a phonic-wheel time marker controlled by a 50 ~ tuning fork, were included in the records.

---

* It will be shown in § 6.3 that these values are in close agreement with those actually measured.

† "A Hot-wire Instrument for Measuring Speed and Direction of Airflow," by L. F. G. Simmons and A. Bailey, 'Phil. Mag.' (Jan., 1927).

(4.2.) A sketch of one of the hot wires used is given in fig. 5A. The wire—of platinum 0·001-inch diameter and about 0·3 inch long—was always mounted

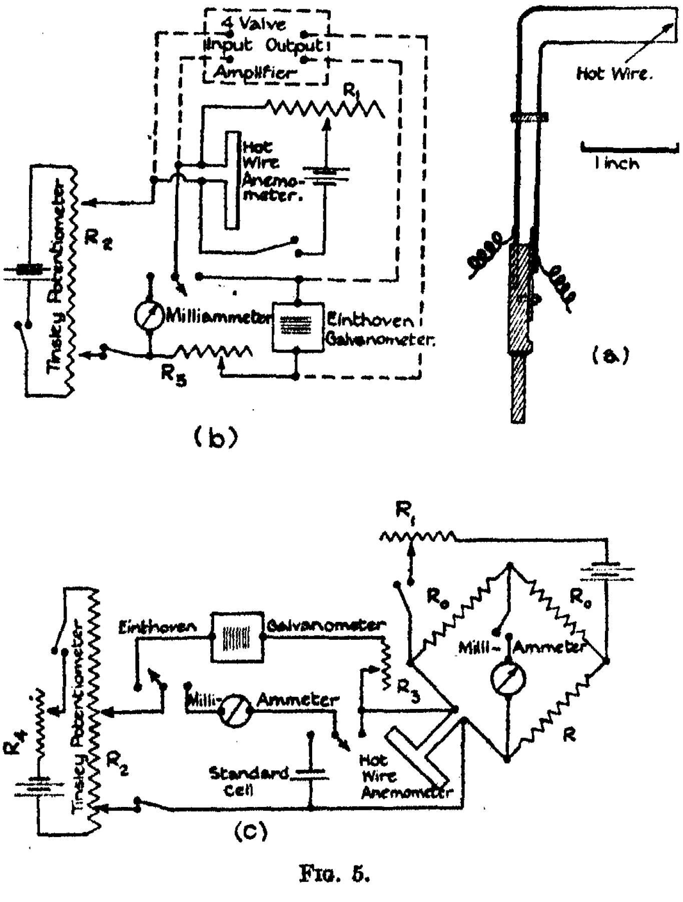

Fig. 5.

parallel to a sharp edge of the plate, that is, normal to the plane of the two-dimensional flow, and was therefore influenced only by changes of wind speed, not by fluctuations of wind direction. The general method of experiment can best be described by reference to the diagram given in fig. 5B. The wire, mounted in the wind stream at the point where the speed fluctuations were to be detected, was heated to a dull red glow by an electric current controlled by the rheostat

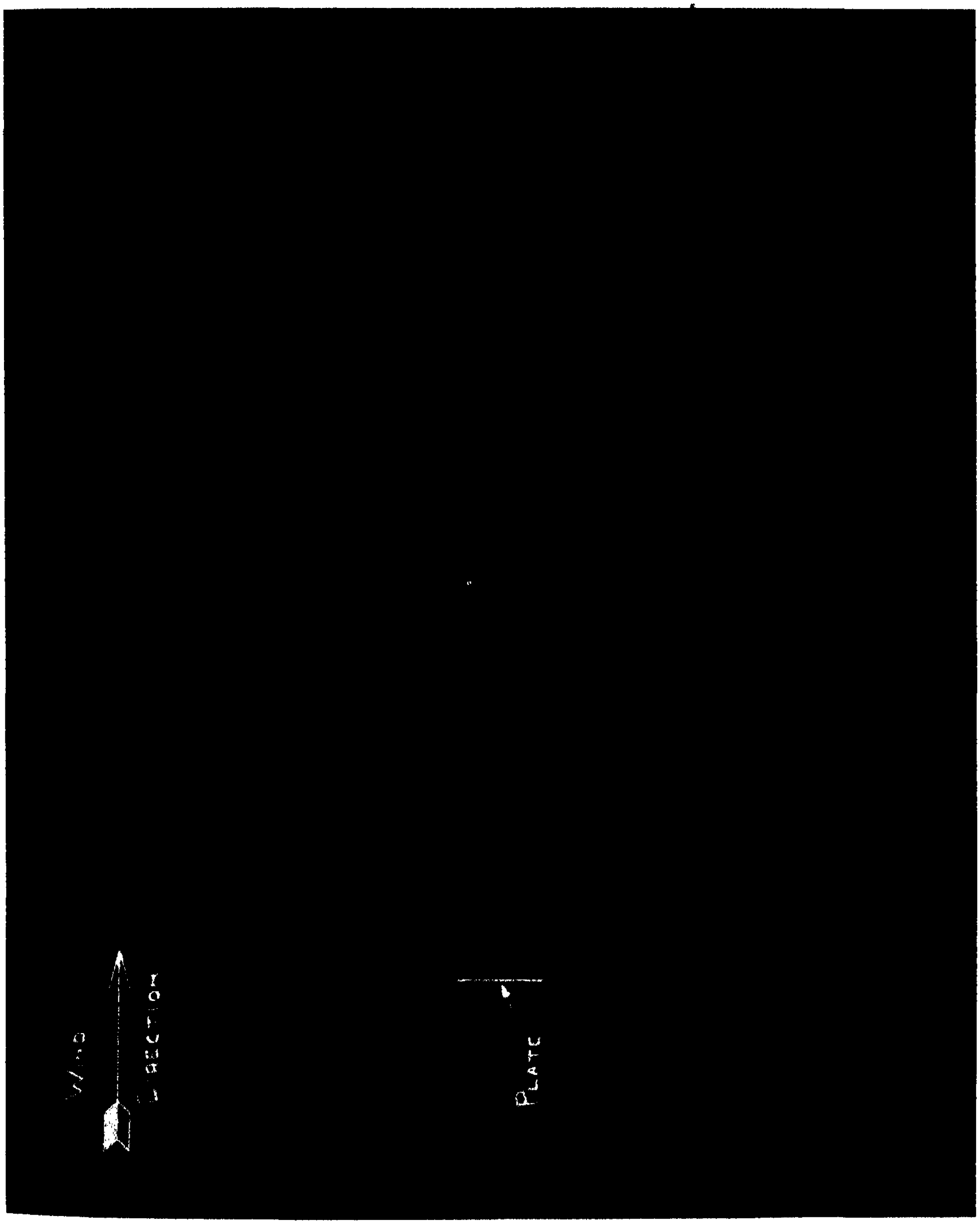

Fig. 1.

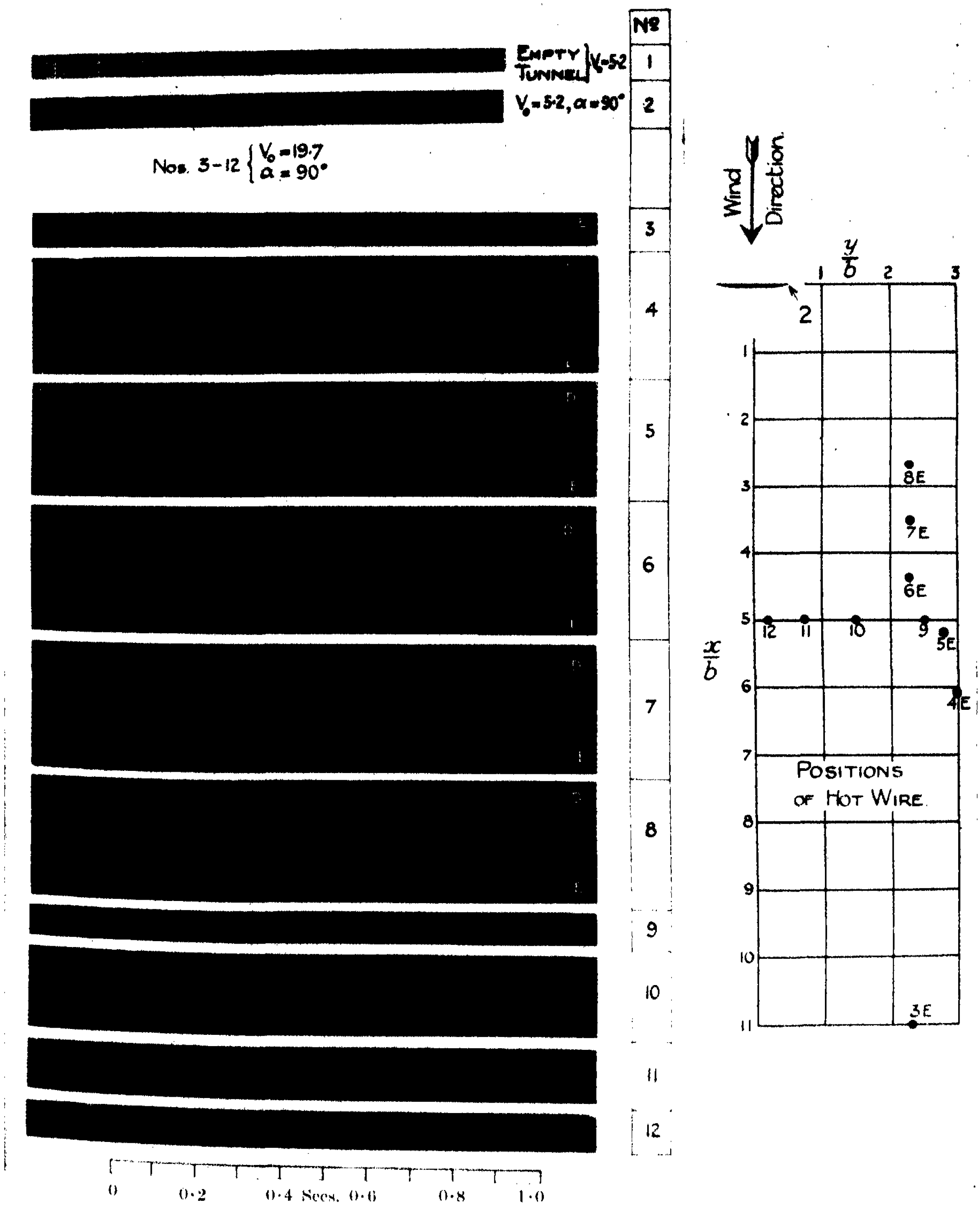
No
Empty Tunnel } V_0=5·2 1
V_0=5·2, α=90° 2
Nos. 3-12 { V_0=19·7, α = 90°
3
4
5
6
7
8
9
10
11
12
0
0·2
0·4 Secs. 0·6
0·8
1·0
Wind Direction
$\frac{y}{b}$
1
2
3
2
$\frac{x}{b}$
1
2
3
4
5
6
7
8
9
10
11
8E
7E
6E
12
11
10
9
5E
4E
3E
Positions of Hot Wire

Fig. 6.

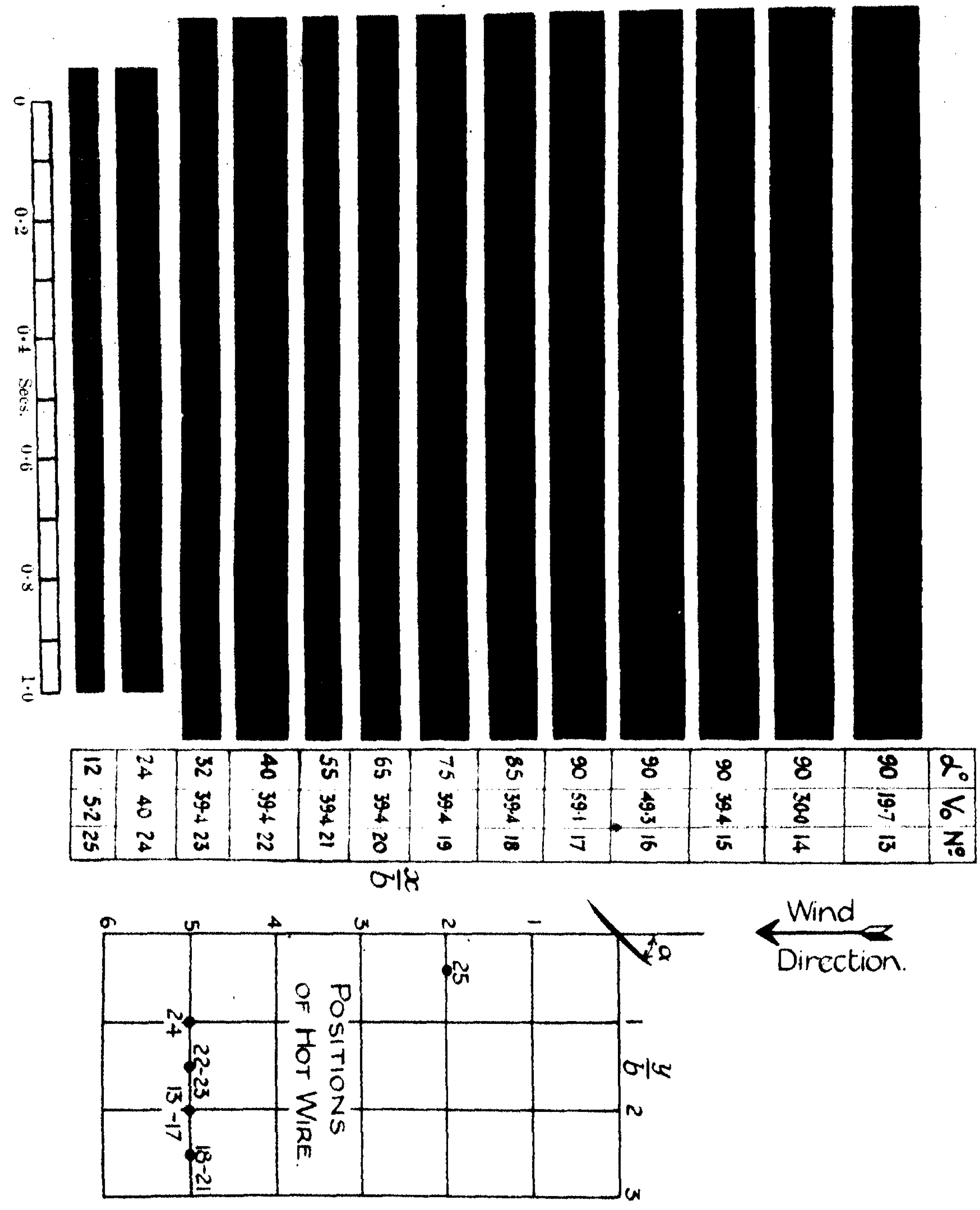

α°	V_0	No.
90	19·7	13
90	30·0	14
90	39·4	15
90	49·3	16
90	59·1	17
85	39·4	18
75	39·4	19
65	39·4	20
55	39·4	21
40	39·4	22
32	39·4	23
24	40	24
12	5·2	25

Fig. 7.

R_1. The average potential difference between the ends of the hot wire was then balanced on a potentiometer, a milli-ammeter being used as an indicator. The milli-ammeter was then switched out and the fluctuations in the potential between the ends of the hot wire put directly across the Einthoven galvanometer. A second circuit (shown dotted) containing a four-valve resistance amplifier* was used on a few occasions, when the speed fluctuations were a small proportion of the mean speed. The deflection of the Einthoven string was adjusted either by altering its tension or by a change in the resistance R_3.

(4.3.) At the outset, records of the velocity fluctuations were taken at a large number of positions in the field, with the plate at 90°. The position of a point in the field is given by the co-ordinates x and y, measured from the centre of the plate, respectively along and at right angles to the direction of the undisturbed wind. The positive direction of x is downstream, and that of y to the left when looking downstream (see Plates 7 and 8). The purpose of this exploration was to determine how the general character of the velocity fluctuations varied in different parts of the field, and also to see whether the frequency of these fluctuations was uniform. The records were taken at a low speed (19·7 feet per second) in order that any lag in the response of the hot-wire—this does not, of course, affect the recorded frequency—should not appreciably misrepresent the general character of the velocity fluctuations.

(4.4.) Records (without amplification) were taken along a longitudinal line ($y = 2.3b$) some distance outside the edge of the plate; across the wake along the line $x = 5b$; at the edge; and also in front of the plate. A representative selection of these Einthoven records is photographically reproduced in Plate 7. Records of the disturbance in the empty tunnel were also taken. In these early experiments no attempt was made to measure the actual magnitude of the velocity fluctuations. Their relative magnitudes are, however, conveyed with sufficient accuracy in the diagrams. The points of interest which arise from the records in fig. 6 (Plate 7) ($\alpha = 90°$) are summarised below. For convenience of reference the records are numbered; also a diagram is attached giving the positions of the hot wire.

(*a*) The velocity fluctuations in the empty tunnel (No. 1) are very small compared with those at the back of the plate (Nos. 3 to 12). It will be shown later that this was the case not only at 90° but at all angles of incidence greater than 12°.

---

* A comparison of diagrams taken with and without amplification, showed that the amplifier did not introduce any apparent extraneous frequencies.

(*b*) The velocity fluctuations at the edge of the plate are large but do not appear to be very regular (No. 2).

(*c*) There is a region, outside the wake and at some distance behind the plate, where the velocity fluctuations are very regular (Nos. 5 to 8), also (Nos. 13 to 17).

(*d*) The velocity fluctuations tend to become less regular as the distance behind the plate increases beyond $3b$ (Nos. 3E to 8E).

(*e*) The velocity fluctuations within the wake are more irregular than those outside (Nos. 9 to 12).

(*f*) At the same wind speed, the frequency of the fluctuations at all points behind the plate, and at some distance outside what were later decided to be the limits of the vortex street, is uniform (Nos. 4 to 8).

(*g*) The frequency of the fluctuations at the centre of the vortex street is, in general, double that outside (Nos. 9 and 12).

In addition, it was found that the velocity fluctuations at some distance forward of the plate ($4b$) were very small compared with those at the back; and also that the fluctuations in the plane of the plate and at some distance from the edge were small and irregular. It should also be noted that the amplitude of the fluctuations at $y = 1\cdot52b$ (No. 10) is greater than those on either side (Nos. 9 and 11). This is of interest because, as will be shown later, the limit of the wake is situated near the line, $y/b = 1\cdot5$.

(4.5.) The most important conclusion which may be drawn from the above summary of results is that there is a large region situated outside the wake, and at some distance behind the plate, where well-defined fluctuations of velocity of uniform frequency can be clearly determined. The photograph* of fig. 1, and also the work of previous investigators, leaves no room for doubt that these fluctuations are caused by the passage downstream of large vortices. The records demonstrate therefore that these vortices are shed from each edge of the plate with uniform frequency; and also that the frequency with which these individual vortices are generated can best be measured at some distance outside the vortex street, where the fluctuations are comparatively steady. For brevity, the frequency with which the vortices leave the edges of the plate will be referred to hereinafter as the "frequency." The variation of the magnitude of the velocity fluctuation, at any point in the field, is considered later.

(4.6.) Several records were taken to show how the frequency varied with wind speed, at a constant angle of incidence (90°). Some of these records are given in Plate 8 (Nos. 13 to 17), in order to show the regularity with which the fluctuations of velocity occur. Values of "*f*" estimated from records of this character are collected in Table II. The last column of this table shows that from $V_0 = 10$ to $V_0 = 60$ feet per second, the frequency is directly proportional to speed, within the accuracy of observation.

---

* The "smoke" was obtained by mixing ammonia and hydrochloric acid in front of the plate.

Table II.—$\alpha = 90°$.

V_0.	f.	fb/V_0.
10·6	3·13	0·146
19·7	5·75	0·144
30·05	9·00	0·148
39·40	11·60	0·146
49·25	14·55	0·146
59·10	17·35	0·146

(4.7.) A large number of records was taken to show the variation of frequency with the inclination of the plate. A representative selection of these records for values of α betwen 12° and 90° is given in Plate 8 (Nos. 17 to 25). They show that the velocity fluctuations are fairly regular, the best diagrams being obtained at high angles of incidence. The velocity fluctuations at the lowest angle of incidence (12°) are, it should be observed, much larger and easily distinguishable from the velocity disturbances in the empty tunnel (Nos. 1 and 25). The values of the frequency, estimated from these and similar records and expressed in the non-dimensional form (fb/V_0), are collected in Table III.

Table III.

$\alpha°$.	fb/V_0.	$fb \sin \alpha/V_0$.	$\alpha°$.	fb/V_0.	$fb \sin \alpha/V_0$.
90	0·146	0·146	24	0·394	0·160
85	0·147	0·146	20	0·478	0·164
80	0·152	0·150		0·503	0·172
75	0·153	0·148	16	0·548	0·151
70	0·156	0·147		0·677	0·187
65	0·163	0·148	14	0·746	0·181
60	0·173	0·150		0·900	0·218
55	0·182	0·149	12	0·874	0·182
50	0·196	0·150		0·880	0·183
45	0·205	0·145			
40	0·231	0·148	*70	0·156	0·146
36	0·253	0·149	60	0·171	0·148
32	0·280	0·148	50	0·193	0·148
30	0·307	0·153	40	0·233	0·150
28	0·330	0·155	30	0.304	0·152

---

* These observations were taken on the opposite side of the wake to that for the earlier results.

At several angles of incidence, two observations were taken, one on each side of the vortex street. In each case, the two values were in close agreement and this indicates that the vortices are shed from each edge with the same frequency. The table shows that the frequency increases, at first slowly and then more rapidly, as the angle of incidence decreases progressively from 90°. It will also be observed that $fb \sin \alpha/V_0$ is approximately constant and equal to 0·148 for values of α between 90° and 30°.

(4.8.) Records of the velocity disturbances (with and without amplification) were also taken with the plate at incidences below 12°. The results of this work are not included in the paper because the disturbances were not sufficiently regular to allow a reliable estimate of the frequency to be made. This was largely because (at low incidences) the disturbances in the region of the plate were of the same character as those in the wind of the empty tunnel. There is, however, some evidence—based on work done on the standard plate and also on another plate, 2·3 times as wide—to show that between 0° and 9° the values of (fb/V_0) probably lie somewhere between 1·0 and 1·6.

§ 5. *Longitudinal Spacing of Vortices.*

(5.1.) The method of measurement is based on the fact that the velocity fluctuations at two points situated without, and on the same side of, the vortex street are in phase, when the longitudinal distance between the points is equal to the distance between successive vortices in the same row, or a multiple of this distance. To determine the phase difference between two points, two hot wires were used and simultaneous records of the velocity disturbances taken. The average time displacement between the two series of crests (or troughs) expressed as a fraction (t/T) of the periodic time gave the phase difference.

In practice, one hot wire was fixed, and the other, usually on the opposite side of the vortex street, was moved up and down stream along a line outside the vortex street. Representative diagrams, taken with the plate at 90° incidence and the datum hot wire (D) at the position $x/b = 6 \cdot 0$, $y/b = -3 \cdot 0$, are given in Plate 7 (Nos. 4 to 8). Record No. 4 shows that when the hot wires are situated at the same distance behind the plate, but on opposite sides of the vortex street, the velocity fluctuations are 180° $(t/T = 0 \cdot 5)$ out of phase.

(5.2.) The values in Table IV give, for various angles of incidence, the variation of phase difference (t/T) with the distance downstream. At each angle of incidence, these observations plot fairly smoothly on a straight line. The longitudinal spacing (a) between consecutive vortices in the same row—that is, the change in the value of x for unit phase difference—was obtained directly from these lines.

Table IV.—Values of (t/T).

x/b.	$\alpha = 90°$.	$\alpha = 70°$.	$\alpha = 60°$.	$\alpha = 50°$.	$\alpha = 40°$.	$\alpha = 30°$.
2·02	−0·12	−0·10	−0·23	−0·21	−0·40	−0·58
3·02	+0·07	+0·10	0	−0·01	−0·16	−0·13
4·03	0·31	0·34	+0·24	+0·24	+0·13	+0·20
5·04	0·50	0·50	0·45	0·51	0·42	0·43
6·05	0·64	0·73	0·70	0·76	0·72	0·90
7·06	0·83	0·92	0·93	1·01	1·04	1·24
8·06	1·05	1·13	1·15	1·24	1·31	1·55
9·07	1·24	1·29	1·37	1·48	1·49	1·90
10·08	1·41	1·55	—	1·71	1·81	2·31
11·09	1·62	1·71	—	—	—	—
12·10	1·78	—	—	—	—	—

Table V.

$\alpha°$	(a/b)	$(a/b \sin \alpha)$	$(\mathrm{V}_3/\mathrm{V}_0 = af/\mathrm{V}_0)$
90	5·25	5·25	0·766
70	4·85	5·17	0·756
60	4·44	5·13	0·761
50	4·08	5·33	0·789
40	3·55	5·52	0·817
30	2·76	5·52	0·840

The estimated values of (a/b) are given in Table V. The longitudinal spacing is seen to decrease as the angle of incidence of the plate decreases. It will also be noted that, for values of α between 30° and 90°, the value of $(a/b \sin \alpha)$ is approximately constant, that is, the longitudinal spacing is proportional to $(b \sin \alpha)$.

(5.3.) The last column of Table V gives the ratio of the speed with which the vortices pass downstream (V_3) to the velocity of the undisturbed wind (V_0). Each value of V_3 was directly obtained from the product of "a" and "f," for, in unit time, "f" vortices spaced a distance "a" apart pass downstream. It is seen that the value of $\mathrm{V}_3/\mathrm{V}_0$ progressively increases from 0·766 at $\alpha = 90°$ to 0·840 at $\alpha = 30°$.

§ 6. *Velocity and Vorticity at the Edge of the Plate.*

(6.1.) The experiments described in this section of the paper were made to measure, at several angles of incidence, the velocity distribution near the edge of the plate. The purpose of these experiments was two-fold: to make a comparison between the velocity actually measured at the edge and that estimated from the measured pressure immediately behind the plate; and to estimate the rate at which vorticity is shed from each edge.

Two series of velocity measurements were made. In the first, Series A, the exploration was made at several angles of incidence, across the boundaries of the dead-air region, along a line normal to the edge and the undisturbed wind direction at a distance of 0·033*b* behind each edge of the plate. Explorations were also made for $\alpha = 90^\circ$ at distances 0·084*b* and 0·168*b* behind the plate. In the second series (B), the measurements were made in the plane of the plate outwards from each edge. In each series, the hot wire was mounted parallel to the edge and the time average of the velocity at a point was measured. The method of measurement is illustrated in fig. 5c (excluding Einthoven galvanometer circuit). The hot wire formed one arm of a Wheatstone Bridge, and its mean resistance (and therefore its temperature) was maintained constant at all speeds by an adjustment of the resistance R_1. The potential difference between the ends of the hot wire, measured on a potentiometer, is then a function of the *mean* wind speed at the point. The calibration curve was obtained, before and after each set of observations, by mounting the hot wire in the empty tunnel and recording changes of potential difference as the wind speed was progressively changed. The E.M.F. across the potentiometer was maintained at a constant value by adjusting the resistance R_4, so that the drop of potential along a fixed length of the potentiometer wire just balanced the constant E.M.F. of a standard cell.

(6.2.) The velocity was measured at both the leading and trailing edges, at $\alpha = 90^\circ$, 70°, 50° and 30° respectively. The observations are plotted in figs. 8 and 9. These curves show very clearly the rapid increase of velocity across the dead-air boundary at each edge of the plate. The narrow band over which the rapid change of velocity occurs will hereinafter be called the " vortex band." The more important results in figs. 8 and 9 have been collected in Table VI. From these results it is evident that:

(*a*) The velocity V_1—that is, the velocity in the outer boundary of the vortex band—measured in the plane of the plate (Series B) is in close agreement, at both the leading and trailing edges, with that measured about 0·033*b* behind the edge (Series A). Columns (*a*) to (*e*).

(*b*) The values of (V_1/V_0) at both the leading and trailing edges decrease as α decreases. Columns (*a*) to (*e*).

(*c*) At each angle of incidence, the values of (V_1/V_0) at the leading and trailing edges are in close agreement. Columns (*a*) to (*e*).

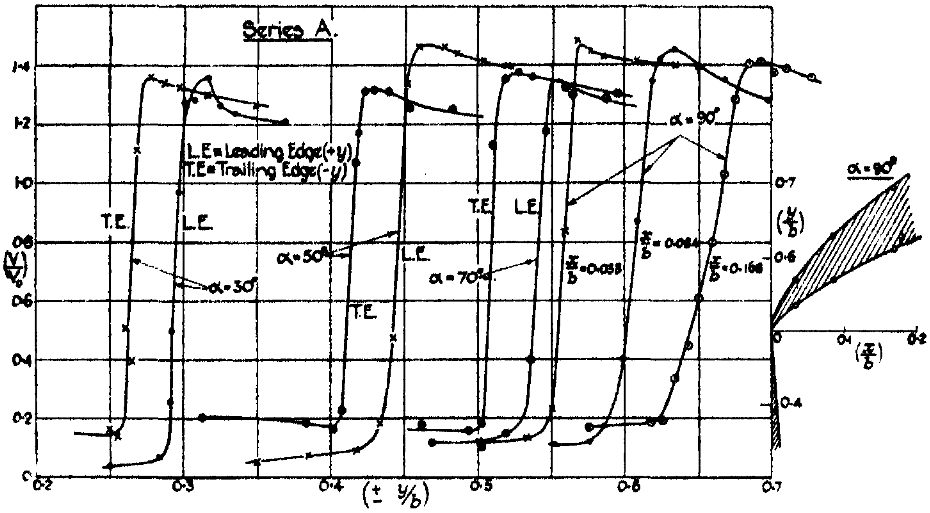
Series A.
L.E. = Leading Edge (+y)
T.E. = Trailing Edge (−y)
T.E.
L.E.
α = 30°
α = 50°
α = 70°
α = 90°
$\frac{x}{b}$ = 0·033
$\frac{x}{b}$ = 0·084
$\frac{x}{b}$ = 0·168
$\left(\frac{V}{V_0}\right)$
$\left(\pm \frac{y}{b}\right)$
$\left(\frac{y}{b}\right)$
$\left(\frac{x}{b}\right)$
0
0·2
0·4
0·6
0·8
1·0
1·2
1·4
0·2
0·3
0·4
0·5
0·6
0·7
0·7
0·6
0·4
0·1
0·2

FIG. 8.

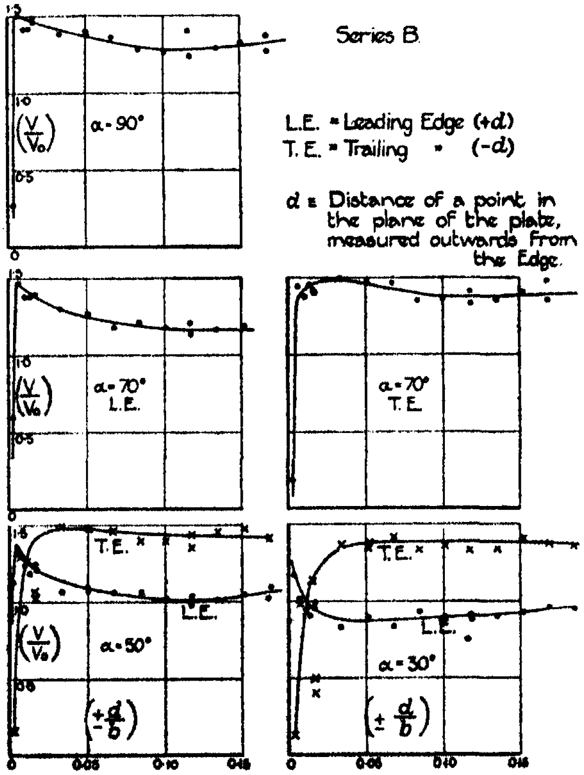
Series B
L.E. = Leading Edge (+d)
T.E. = Trailing " (−d)
d = Distance of a point in the plane of the plate, measured outwards from the Edge.
α = 90°
α = 70° L.E.
α = 70° T.E.
α = 50°
α = 30°
T.E.
L.E.
$\left(\frac{V}{V_0}\right)$
$\left(\frac{+d}{-b}\right)$
$\left(\pm \frac{d}{b}\right)$
0
0·5
1·0
1·5
0·05
0·10
0·15

FIG. 9.

Table VI.

See § 2 for symbols.

L.E. = Leading edge. T.E. = Trailing edge.

$\alpha°$	(V_1/V_0) L.E.			(V_1/V_0) T.E.			(V_1/V_0) Estimated from measured p_m.	(V_2/V_0) fig. 8.		(K/V_0^2).		
	Series A, fig. 8. (*a*)	Series B, fig. 9. (*b*)	Mean. (*c*)	Series A, fig. 8. (*d*)	Series B, fig. 9. (*e*)	Mean. (*f*)	(*g*)	L.E. (*h*)	T.E. (*i*)	L.E. (*j*)	T.E. (*k*)	Mean. (*l*)
90	1·48	1·50	1·49	1·48	1·50	1·49	1·545	0·14	0·14	1·10	1·10	1·10
70	1·35	1·47	1·41	1·37	1·48	1·43	1·540	0·14	0·16	0·99	1·01	1·00
50	1·46	1·37	1·42	1·32	1·48	1·40	1·495	0·10	0·16	1·00	0·97	0·99
30	1·35	—	1·35	1·36	1·38	1·37	1·385	0·07	0·14	0·91	0·93	0·92

* $(V_1/V_0)^2 = 1 + 2\,[(p_0 - p_m)/\rho V_0^2]$.

(*d*) If it be assumed that the total head in the outer boundary of the vortex band is equal to that in the undisturbed wind, and that the pressure throughout this band is the same as that in the dead-air region, then the value of (V_1/V_0) estimated from the average pressure (p_m) in the dead-air region is in close agreement (within 5 per cent.) with that measured in the outer boundary. Further, if the pressure across the vortex band is uniform, as assumed, then this close agreement indicates that beyond the outer boundary there is a near approach to a potential flow.

(6.3.) The strength of the vorticity shed from each edge of the plate in unit time has been estimated by a method based on that followed in the case of a perfect fluid. On the assumption that the width of the vortex band is infinitesimally small, and that the velocities on opposite sides are V_1 and V_2 respectively, the circulation around a rectangle containing a length δs of the vortex sheet, whose sides are respectively parallel and normal to the sheet, is equal to $(V_1 - V_2)\delta s$, that is $(V_1^2 - V_2^2)\delta t/2$ since $\delta s/\delta t = (V_1 + V_2)/2$. The total amount of vorticity leaving the edge in unit time is therefore $(V_1^2 - V_2^2)/2$ or $(V_1^2 - V_2^2)/2V_0^2$ expressed in non-dimensional units. In the actual flow, however, the vortex band is of finite and varying width; the radius of curvature also changes with the distance behind the plate. It is necessary, therefore, to determine the shape of the vortex band at some distance behind the edge to see whether the vortex strength can be estimated with reasonable accuracy from the relation $K = (V_1^2 - V_2^2)/2V_0^2$. The vortex band was, therefore, located for some distance behind the plate at $\alpha = 90°$, by explorations of velocity. These results are plotted in fig. 8. Data taken from this figure are tabulated in Table VII.

Table VII.—$\alpha = 90°$.

Distance behind plate (x/b):	0	0·033	0·084	0·168
(y/b) co-ordinate of point of maximum velocity, V_1	0·505	0·570	0·630	0·695
(y/b) co-ordinate of point of minimum velocity, V_2	—	0·535	0·570	0·613
Ratio of width of vortex band to the breadth of the plate	—	0·035	0·060	0·082
Value of (V_1/V_0)	1·50	1·49	1·47	1·42
Value of (V_2/V_0)	—	0·14	0·17	0·18
Value of $(V_1^2 - V_2^2)/2V_0^2$	1·11	1·10	1·07	0·99

The opening-out of the vortex band with increasing distance behind the plate is clearly shown in fig. 8. This figure together with the results in Table VII show that the width of the vortex band, although increasing with the distance downstream, is small compared with the radius of curvature of the centre line of the band, and also that the velocities along both the outer and inner boundaries are uniform, within the accuracy of measurement, for some distance behind the plate. It is concluded, therefore, that the value of $(V_1^2 - V_2^2)/2V_0^2$ measured close behind the plate gives a reasonably accurate approximation to the strength of the vorticity leaving the edge in unit time.

The estimated values of (K/V_0^2) are given in columns (*j*) and (*k*) of Table VI. These results show that only a slight diminution in the strength of the vorticity leaving each edge accompanies the considerable decrease in α from 90° to 30°; also that the vorticity is shed from the two edges of the plate at the same rate.

§ 7. *Magnitude of the Velocity Fluctuations behind the Plate.*

(7.1.) The experiments now to be described were made to measure at several angles of incidence, the mean speed and also the magnitude of the velocity fluctuations, at some distance behind the plate. The purpose in view was the determination of the average strength of the individual vortices passing downstream (see § 8). The results themselves also bring to notice some general characteristics of the flow.

The measurement of mean velocity was made by the method described in § 6.1. To measure the amplitude of the fluctuations, the mean potential difference between the ends of the hot wire was balanced on the potentiometer, and then the current fluctuations in the circuit were passed directly through the Einthoven galvanometer (fig. 5) and a record of the motion of the string taken.

To obtain a direct calibration of the string, the hot wire was mounted in the empty tunnel, and the wind speed adjusted until its value (as indicated on the potentiometer) was the same as that of the mean speed obtaining when the records of the velocity fluctuations were taken. The Einthoven galvanometer was then switched into the hot-wire circuit, and records taken of the displacement of the string as the tunnel speed was varied.

(7.2.) Observations of the mean speed and records of the velocity fluctuations were taken both within and outside the vortex street at some distance behind the plate. The distances were $5b$, $10b$ and $20b$ at $\alpha = 90°$, and $8b$ at $\alpha = 70°$ and $\alpha = 40°$. The measurements were made at a low wind speed (about 10 feet per second), to minimise errors of measurement due to any lag in the response of the hot wire to the velocity fluctuations. A comparison of results taken at speeds below and above 10 feet per second showed that if there is an error due to lag, it is smaller than the usual irregularities in the velocity fluctuations at a constant value of V_0; in fact, the records showed—except at some distance outside the limits of the vortex street—that, at any point in the field, there were large variations with time, in the values of both the maximum and minimum velocities. The average magnitude of the velocity fluctuations was estimated, therefore, from the average displacement between a large number of crests and troughs. It was also found, from an analysis of a number of records, that the difference between the average maximum velocity and the mean velocity was about 45 per cent. of the average difference between the maximum and minimum velocities. The maximum velocity has therefore been taken as the sum of the mean velocity (as measured on the potentiometer) and 45 per cent. of the average difference between the maximum and minimum velocities (obtained from the Einthoven records); and the minimum velocity as the mean velocity less 55 per cent. of this average difference. The maximum and minimum velocities could have been determined directly, with the Einthoven galvanometer, but the reason this was not done was because, as will appear later, it was the differences between these values, not their actual magnitudes, that were needed in the determination of the strength of the individual vortices.

(7.3.) The results of these experiments are given in figs. 10 and 11. At $\alpha = 90°$, and for all practical purposes at $\alpha = 70°$, the velocity curves were found to be symmetrical about the centre line of the wake ($y = 0$), so that only the curves for the positive values of y are given. This was not the case at $\alpha = 40°$, so that curves have been drawn for both positive and negative values of y. The points on each curve of maximum and minimum velocity represent mean values taken from two or more records.

It will be observed that each set of curves in figs. 10 and 11 exhibit similar characteristics. On passing through the wake from the outside, the mean velocity drops slowly at first and then more rapidly until a minimum value is reached at the centre of the wake. Each curve of maximum velocity rises to a pronounced peak which, as will be shown later, is probably the outer boundary of the vortex street, and then falls as the centre of the wake is approached. The difference between the maximum and minimum velocities is small at some distance outside the wake but rapidly increases as the vortex street is approached. At the centre of the wake the velocity fluctuations are large, especially near the plate (see $\alpha = 90°$, $x = 5b$).

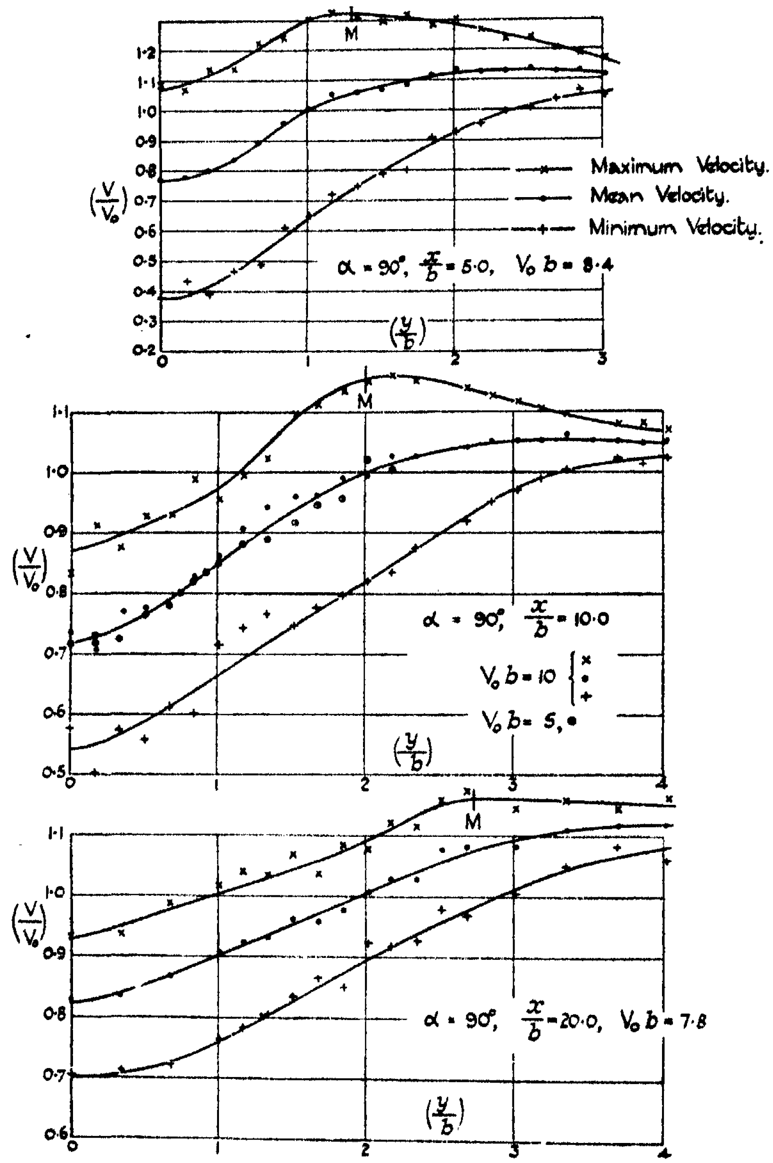

FIG. 10.

§ 8. *Vorticity in the Wake.*

(8.1.) It can easily be shown that the amplitude of the velocity fluctuations ($V_{\text{max.}} - V_{\text{min.}}$) at a point situated outside and at a distance y from the centre of a vortex street of infinite length is equal to

$$\frac{\kappa}{a}\left[\frac{1}{\sinh\frac{2\pi(y-h/2)}{a}}+\frac{1}{\sinh\frac{2\pi(y+h/2)}{a}}\right],$$

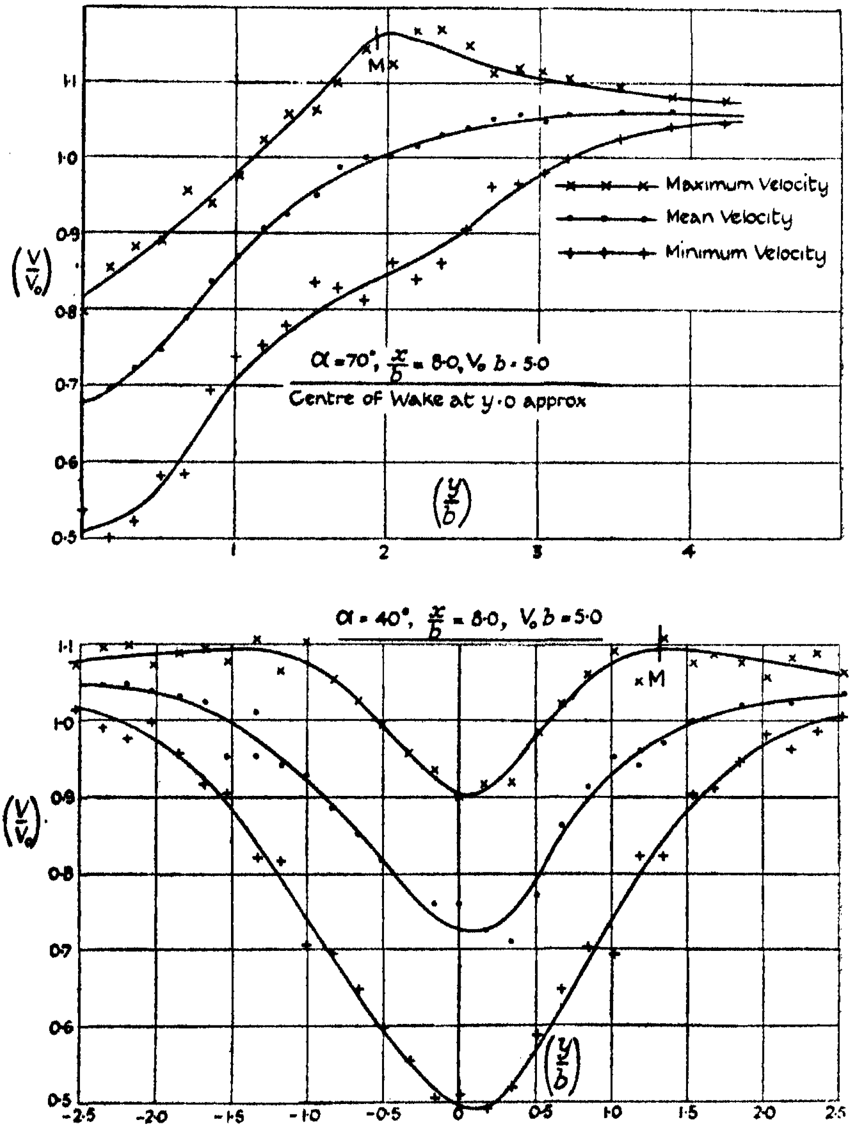

FIG. 11.

where κ is the strength of each individual vortex, and " a " and " h " are the longitudinal and lateral spacings respectively of the vortices. It follows then that when the values of " a " and " h " are known, the strength of the individual vortices can be determined from measurements of the amplitude of the velocity fluctuations outside the wake. Further, the outstanding advantage of this method of estimation is that the values of $(V_{\text{max.}} - V_{\text{min.}})$ can be measured at some distance outside the vortex street in a region where the fluctuations are comparatively steady. This method of estimating the strength of an individual vortex will now be described.

(8.2.) Further consideration is needed before the above formula can be applied to the flow in the wind tunnel. It is necessary to examine the differences which exist between the actual flow and that postulated in the theoretical régime. An outstanding difference is that the vorticity passing downstream is not concentrated in small well-defined cores, such as is assumed in the Kármán theory, but is spread over a fairly large area. This is clearly shown in the photograph of fig. 1 (Plate 6). The symbol "h" now represents the lateral spacing of the centres of the vorticity areas, and its value can be determined only when the lateral extent of the vorticity is known. If the vorticity is concentrated in circular areas of diameter d, the points of maximum velocity in the field will be where the lines $y = \pm (h + d)/2$ touch the circular peripheries; and the points of minimum velocity where the lines $y = \pm(h - d)/2$ touch the inner ends of the lateral diameters. The diameter of the vorticity area can therefore be regarded as the lateral distance between points of maximum and minimum velocity, and the value of "h" as twice the mean distance of these points from the centre line of the street.

(8.3.) An approximation to the value of "h" can thus be obtained from curves, such as those in figs. 10 and 11, which give the "y" co-ordinates of the points in the field where the velocity has maximum and minimum values. The appropriate curves in each of these figures show that, in each case, the position of maximum velocity (marked M) is quite pronounced. The position of the outer boundaries of the vortex street is therefore well-defined. The position of the inner boundaries is not so clearly defined. They are probably situated near the centre of the wake at $y = 0$, since the velocity is a minimum in this region. The diameter of a vortex core is therefore quite large and approximately equal to the lateral spacing between the vortex rows. This conclusion is supported by the photograph of the flow in fig. 1 (Plate 6). Further evidence worthy of mention was obtained from a study of a large number of records, from which it appeared that the velocity fluctuations over the region within the estimated outer boundaries of the vortex street were much more irregular in both frequency and amplitude, than those taken outside.

The values of "h" estimated from the curves of figs. 10 and 11 are given in Table VIII. Included in the table are the theoretical values obtained when the experimental values of "a" are substituted in Kármán's stability relation $h = 0{\cdot}281a$. The wind-tunnel values of (h/b) at $\alpha = 90°$ indicate an appreciable opening-out of the wake with increasing distance from the plate. A direct comparison shows that, at each angle of incidence, the wind-tunnel value of "h" is greater—except at $\alpha = 90°$, $x/b = 5$—than that estimated by the Kármán theory. This may be partly due to the impossibility of ascertaining from the curves of figs. 10 and 11, any extension of the vortices beyond the centre line ($y = 0$). At the same time there appears to be definite evidence that the vortices do not flow downstream in parallel rows.

Table VIII.

$\alpha°$	(x/b)	Wind-tunnel.			Kármán.
		(h/b)	(y/b) co-ordinate of point in outer boundary.	(a/b)	(h/b)
90	5	1·30	1·3	5·25	1·48
	10	2·0	2·0		
	20	2·75	2·75		
70	8	1·9	1·9	4·85	1·36
40	8	1·3	1·3	3·55	1·00

(8.4.) Another point which needs investigation is the extent to which the formula given in § 8.1, which has been derived on the assumption that the length of the vortex street is infinite, is applicable to the street in the wind-tunnel where the length is finite. To do this a formula was obtained which gave the magnitude of the velocity fluctuations for the actual number and spacing of the vortices in the tunnel, when the plate was at 90°. The number of individual vortices taken in each row was 5, since the distance between the plate and the after end of the tunnel was about $5 \cdot 4a$ at $\alpha = 90°$. The formula used was a simple summation series and is not included in the paper because of its cumbersome nature. The vortex strength estimated by this formula is compared with that calculated for an infinite street, having the same longitudinal and lateral spacing of vortices, in Table IX. The two methods give results which are in close agreement (within 4 per cent.). The agreement will, of course, become closer as the angle of incidence decreases and the value of "a" becomes smaller. Since only an approximate value of the vortex strength is needed it was considered that it would be sufficiently accurate to use, in all cases, the simpler formula, *i.e.*, that for the infinite street.

(8.5.) The effect of the tunnel walls on the value of $(V_{\text{max.}} - V_{\text{min.}})$ was

Table IX.

$\alpha°$	(x/b)	(y/b)	$(V_{max.} - V_{min.})/V_0$.	Series I. Kármán.			Series II. Wind-tunnel.			K/V_0^2 from Table VI.	$(\kappa f/K)$	
				(h/b)	$\kappa/V_0 b$.	$\kappa f/V_0^2$.	(h/b)	$\kappa/V_0 b$.	$\kappa f/V_0^2$.		Series I (mean).	Series II (mean).
90	10	3·0	0·151	1·475	5·1 (4·9)*	0·74 (0·72)*	2·0	3·9 (3·9)*	0·57 (0·57)*	1·10	0·65 (0·63)*	0·51 (0·49)*
		3·8	0·055	1·475	4·8 (4·5)*	0·70 (0·66)*	2·0	3·8 (3·5)*	0·55 (0·51)*			
70	8	3·0	0·128	1·365	5·3	0·83	1·9	4·1	0·64	1·00	0·82	0·63
		4·0	0·034	1·365	5·2	0·81	1·9	4·0	0·62			
40	8	1·8	0·146	1·000	2·2	0·51	1·3	1·8	0·41	0·95	0·64	0·51
		2·5	0·057	1·000	3·0	0·69	1·3	2·4	0·55			

* Finite street.

investigated and found to be negligible. This result is to be expected since the lateral spacing between the vortex rows is small compared with the width of the tunnel, so that the rows of positive and negative vorticity in each image neutralise each other in so far as their effect at a distance is concerned.

(8.6.) Estimations of the average strength of the individual vortices at some distance behind the plate (about $9b$), when $\alpha = 90°$, $70°$ and $40°$ are given in Table IX. To show the effect on $(\kappa/V_0 b)$ of a change in the value of "h," two series of results are given. In the first, the Kármán values of "h" have been taken, and in the second, the wind-tunnel values. In all cases, the calculations were made for two values of $(V_{max.} - V_{min.})$ measured in the comparatively steady region outside the vortex street. The values of the vortex strength are expressed in non-dimensional units by dividing by the product $(V_0 b)$.

The results given in Table IX show that :—

(*a*) At $\alpha = 90°$, the value of $(\kappa/V_0 b)$ calculated for the infinite and finite streets are in close agreement.

(*b*) At $\alpha = 90°$ and $\alpha = 70°$ the values of $(\kappa/V_0 b)$ calculated for the two values of $(V_{max.} - V_{min.})/V_0$ at the same value of (h/b) are in close agreement. This is, however, not the case at $\alpha = 40°$.

(*c*) At the same incidence, and for the same values of $(V_{max.} - V_{min.})/V_0$, the values of $(\kappa/V_0 b)$ are smaller in Series II (wind-tunnel) than in Series I (Kármán), (about 20 per cent.).

It may be concluded that the above method of calculation gives a reasonably good estimate of the average strength of the individual vortices, even although some uncertainty probably arises from the difficulty of estimating the exact value of "h." It is for this reason that the calculations were made both for the Kármán and experimental values of "h."

(8.7.) The most interesting results in Table IX are those which give the values of $(\kappa f/K)$, that is, the ratio of the rate at which vorticity is carried downstream in the form of well-defined vortices to the rate at which it is generated at the edge of the plate. There appears to be no systematic variation of $(\kappa f/K)$ with α, so that for the purpose of discussion it is sufficient to take the mean values in each column. These are 0·70 (Series I) and 0·55 (Series II). It follows, then, that not all the vorticity which leaves the edge travels downstream in the form of individual vortices. Of the remainder, undoubtedly a part is dissipated immediately behind the plate, by a mixture of the positive and negative vorticity from the two edges, and the rest possibly passes downstream as "unattached" vortices, which are too small to affect appreciably the measured velocity fluctuations outside the wake. It has also to be borne in mind, that even the large vortices themselves tend to break up and lose their individuality, as the distance behind the plate increases. This is clearly shown by the velocity records (Nos. 3 to 8) given in fig. 6 (Plate 7) and the photograph of fig. 1 (Plate 6). The general conclusion that can be drawn is that at a distance of $9b$ (approximately) behind the plate about 60 per cent. of the vorticity leaving the edge is passing downstream in the form of large vortices having a definite individuality; and whilst no positive evidence is available, it is highly probable that an appreciable dissipation of vorticity occurs at the back of the plate.

§ 9. *A Note on Kármán's Vortex Theory.*

(9.1.) Kármán has given a formula for the resistance of a flat plate moving normal to the stream, in terms of the dimensions of the vortex system behind the plate. This formula, given in the symbols of the paper, is

$$k_D = 0{\cdot}281\; a/b\,[2{\cdot}83\,(1 - V_3/V_0) - 1{\cdot}12\,(1 - V_3/V_0)^2].$$

If the second term be neglected the formula reduces to the approximate form $k_D = 0{\cdot}795\,.\,a/b\,(1 - V_3/V_0)$, or $k_D = 0{\cdot}281\,(\kappa/V_0 b)$ (see § 9.2). The drag is then proportional to the strength of the individual vortices. A comparison between the measured values of drag and those obtained from these two formulæ, when the wind-tunnel values of (a/b) and (V_3/V_0) are substituted, is given in Table X. Although the theory relates to a plate at 90° incidence, additional calculations have been made for values of α below 90°; this appears to be legitimate since earlier work (§§ 4.7 and 5.2) has shown that the flow pattern at some distance behind the inclined plate closely resembles that behind a plate of width ($b \sin \alpha$) mounted normal to the wind.

Table X.

$\alpha°$	Wind-tunnel.			k_D.		$\dfrac{\text{Col. B}}{\text{Col. A}}$	$\dfrac{\text{Col. C}}{\text{Col. A}}$
	(a/b)	(V_3/V_0)	k_D. (A)	Kármán's formula. (B)	Kármán's approx. formula. (C)		
90	5·25	0·765	1·065	0·895	0·980	0·84	0·92
70	4·85	0·755	0·975	0·855	0·945	0·88	0·97
60	4·44	0·760	0·850	0·770	0·850	0·91	1·00
50	4·08	0·790	0·690	0·625	0·680	0·91	0·99
40	3·55	0·815	0·505	0·485	0·520	0·96	1·03
30	2·76	0·840	0·325	0·335	0·350	1·03	1·08

The last two columns of Table X show that fair agreement exists between the wind-tunnel and the Kármán values of k_D; but a closer agreement is obtained when the approximate formula is used.

(9.2.) Another theoretical relationship given by Kármán is :—

$$(\kappa/V_0 b) = 2\sqrt{2}\,(a/b)\,(1 - V_3/V_0).$$

Table XI gives the Kármán values of $(\kappa/V_0 b)$ when the experimental values of (a/b) and (V_3/V_0) are substituted in this formula, and also the wind-tunnel values.

Table XI.

$a°$	Wind-tunnel.			Kármán.
	(a/b)	(V_3/V_0)	$(\kappa/V_0 b)$	$(\kappa/V_0 b)$
90	5·25	0·765	3·9	3·50
70	4·85	0·755	4·0	3·35
40	3·55	0·815	2·1	1·85

The agreement between the wind-tunnel ($x/b = 9·0$ approx.) and the Kármán values of $(\kappa/V_0 b)$ is reasonably close. It has already been shown in Table VIII that, in general, the wind-tunnel values of "h" are higher than those of theory.

(9.3.) It should be recorded that the Kármán values of (a/b) and (fb/V_0) measured in water, with the plate normal to the general stream, are in close agreement with those measured in the present experiments. The actual values are 5·50 and 0·145 (Kármán), and 5·25 and 0·146 (N.P.L.).

§ 10. *Summary.*

The periodic flow behind an infinitely long flat plate inclined in an air stream is examined by means of a heated hot wire used in conjunction with an Einthoven galvanometer.

The vortices generated at each edge pass downstream with a frequency which increases as the inclination of the plate decreases. The frequency is proportional to the wind speed, at a constant inclination.

The longitudinal spacing of the vortices decreases as the inclination of the plate decreases. The vortices pass downstream at a speed which increases as the inclination decreases.

Vorticity is shed from the two edges of the plate at the same rate. This rate falls slowly as the inclination is decreased from 90°.

There is a lateral opening-out of the vortex street with the passage downstream.

Only a part of the vorticity leaving the plate travels downstream in the form of vortices having a definite individuality.

Kármán's formula for the resistance of a flat plate, given in terms of the dimensions of the vortex system behind the plate, gives results in fair agreement with those measured directly. The Kirchhoff-Rayleigh theory considerably underestimates the force acting on the plate.

In conclusion, the writers desire to acknowledge their great indebtedness to Dr. H. Lamb, F.R.S., for valuable criticisms and suggestions made during the preparation of the paper, and also to Dr. S. B. Young and Mr. S. Ward, of the Admiralty Research Laboratory (Teddington), for the loan of the Einthoven galvanometer.

[*Added, August* 16, 1927.—Since the paper was communicated, Mr. H. Glauert, of the Royal Aircraft Establishment, has pointed out that the wind-tunnel values of k_D given in Table X should be corrected for the interference of the wind-tunnel, because they are compared with Kármán values of k_D for a plate in a free stream. He has also shown from theoretical considerations that the tunnel effect may be important when the plate is normal to the stream. To determine the magnitude of this effect for the 6-inch plate used in the above experiments, additional experiments have been made, in the manner described in § (3.2), to measure the drag of flat plates, of breadths 2, 4 and 8 inches respectively, set normal to the air stream in a 7-foot tunnel. From these measurements, and that previously obtained for the 6-inch plate, an approximate value of the drag coefficient (k_D) for a normal flat plate in a free stream has been obtained. The results are given below, and show that the observed drag coefficient (k_D) of 1·065 (6-inch plate) would be reduced to 0·92 approximately in the absence of the constraint of the tunnel walls. It was also estimated that the probable reduction in k_D for the plate at $\alpha = 30°$ would be 8 per cent. The wind-tunnel values of k_D in Table X should therefore be reduced by amounts varying from 13·5 per cent. at $\alpha = 90°$ to 8 per cent. at $\alpha = 30°$. These corrections bring the experimental results into much closer agreement with the Kármán values of k_D given in column B, and the general agreement with theory is satisfactory.

Breadth of Plate in inches.	$\left(\frac{\text{Breadth of Tunnel}}{\text{Breadth of Plate}}\right)$	Drag Coefficient.* k_D.
8	10·5	1·072
6	14·0	1·065
4	21·0	1·025
2	42·0	0·964
—	∞	0·920 (estimated)

* These values were obtained by dividing the measured drag per unit length of the plate by $(\rho b V_0^2)$, where V_0 is the velocity of the undisturbed wind.

[It will be apparent from the context that the comparison of

$$\frac{V_1^2 \text{ (wind-tunnel)}}{V_0^2 \text{ (Kirchhoff-Rayleigh Theory)}} \quad \text{with} \quad \frac{k_N \text{ (wind-tunnel)}}{k_N \text{ (Kirchhoff-Rayleigh Theory)}}$$

referred to at the end of § (3.5) still stands, and that the experimental values of k_N should not be corrected for the constraint of the tunnel.]

The Photosynthesis of Naturally Occurring Compounds. I.—*The Action of Ultra-Violet Light on Carbonic Acid.*

By E. C. C. Baly, F.R.S., J. B. Davies, M. R. Johnson, and H. Shanassy,
Liverpool University.

(Received July 28, 1927.)

Introduction.

In a preliminary paper one of us, in conjunction with Prof. Heilbron and Prof. Barker,* described some observations on the action of ultra-violet light on pure aqueous solutions of carbonic acid. It was found that traces of formaldehyde were present in these solutions after insolation, provided that a stream of the gas were passed through the water during the exposure to the light. These results differed from those which had previously been recorded by Moore and Webster,† who had stated that the presence of a catalyst such as colloidal ferric or uranium hydroxide was necessary.

The observation by Moore and Webster that formaldehyde in aqueous solution is converted by ultra-violet light into reducing sugars was fully confirmed, and the view was put forward that the mechanism of the photosynthesis of carbohydrates from carbonic acid consisted of two stages, first, the formation of formaldehyde, and, second, the conversion of this substance into hexoses.

---

* 'Trans. Chem. Soc.,' vol. 119, p. 1025 (1921).

† 'Roy. Soc. Proc.,' B, vol. 87, p. 163 (1914), and vol. 90, p. 168 (1918).

In two further papers the photosynthesis of nitrogen compounds was discussed, evidence being brought forward of the production of coniine* by the action of light on formaldehyde in the presence of ammonia, and of α-aminoacids by the action of light on formaldehyde in the presence of formhydroxamic acid, which was proved independently to be the first product when light acts on formaldehyde in the presence of potassium nitrite.†

This early work has been subjected to some criticisms from different angles, but out of these only one is worthy of serious consideration, namely, that published by Porter and Ramsperger.‡

Before we give an account of the present work it is necessary to point out that the view put forward in the first paper as to photosynthesis of carbohydrates from carbonic acid in two separate stages was incorrect. According to this view the carbonic-acid molecule on activation by light was converted into activated formaldehyde and oxygen, and that these two substances lost energy and appeared in their ordinary and less reactive states. In the second stage the formaldehyde was again activated by light and the activated molecules polymerised to give the reducing sugars. It is quite unnecessary to postulate the existence of these two separate stages, since the activated formaldehyde produced from the carbonic acid can itself polymerise into the reducing sugars without the necessity for the loss of energy and the subsequent re-activation. According to this view, the small amounts of formaldehyde produced when ultra-violet light acts on aqueous solutions of carbonic acid are not due to its direct formation in the first stage, but to the photo-chemical decomposition of the photosynthesised carbohydrates. This decomposition of carbohydrates into formaldehyde by means of ultra-violet light was observed by Moore and Webster, and we have also proved by many experiments that the decomposition takes place with great readiness with the hexoses and even with cellulose.

This later view was communicated to the British Association, Section B, at Saskatoon in 1924, and at the same meeting Prof. Porter communicated his criticism of the formation of formaldehyde by the action of light on aqueous solutions of carbonic acid. Briefly stated, this criticism was to the effect that, as the purity of the materials was increased, the yield of formaldehyde decreased, until in the complete absence of all impurity no trace of formaldehyde was found. The suggestion that the formation of formaldehyde observed by Moore and Webster, and also by Baly, Heilbron and Barker was due in some way to the presence of impurities at once suggested a possible explanation of the divergence in the results. In the discussion one of us (E. C. C. B.) pointed out that in all probability the action of ultra-violet light on carbonic acid was to establish a photostationary state represented by

---

* Baly, Heilbron, and Stern, 'Trans. Chem. Soc.,' vol. 123, p. 185 (1923).

† Baly, Heilbron and Hudson, 'Trans. Chem. Soc.,' vol. 121, p. 1078 (1922).

‡ 'J. Amer. Chem. Soc.,' vol. 47, p. 79 (1925).

$$6H_2CO_3 \rightleftarrows C_6H_{12}O_6 + 6O_2,$$

and that the amount of carbohydrate present in this equilibrium was very small. In the presence of oxidisable impurities the reaction would proceed from left to right with the formation of a definite amount of carbohydrate, which would be photochemically decomposed to formaldehyde. The photostationary state would be analogous to that present when potassium nitrate is exposed to ultra-violet light,[*] *i.e.*,

$$KNO_3 \rightleftarrows KNO_2 + O,$$

the stable production of the nitrite only occurring in the presence of impurities.

The reason for the introduction of the hexoses as a component of the photostationary state is to be found in the proof given by Irvine and Francis[†] that when formaldehyde is activated by ultra-violet light, glucose is produced to the extent of about one-third of the total reducing compounds formed. A systematic investigation of this photosynthesised sugar syrup is now being carried out, and it is hoped to describe the results in a subsequent communication. It may, however, be stated that, in addition to glucose, more complex carbohydrates are also present.

The Action of Ultra-Violet Light on Aqueous Carbonic Acid.

It is obvious that the first step to be taken in any further investigation of the problem is to put to the test of experiment the suggestion that ultra-violet light, when acting on aqueous solutions of carbonic acid, establishes a photostationary state, such as is represented by the equation

$$6H_2CO_3 \rightleftarrows C_6H_{12}O_6 + 6O_2.$$

A ready method of test was found in the use of Feder's[‡] solution, which consists of mercuric chloride 20 grms., sodium hydroxide 80 grms., sodium thiosulphate

---

[*] Anderson, 'J. Amer. Chem. Soc.,' vol. 46, p. 797 (1924).

[†] 'J. Ind. Eng. Chem.,' vol. 16, p. 1019 (1924).

[‡] 'Arch. Pharm.,' vol. 245, p. 25 (1907).

100 grms., dissolved in 1 litre of water. This solution is reduced by all aldehydes and is especially sensitive to formaldehyde. In order to make use of this method, two solutions were prepared, one of mercuric chloride and the other of sodium hydroxide and thiosulphate, both solutions being made with the purest conductivity water and of twice the strength indicated above. A large transparent quartz test tube, containing 80 c.c. of the mercuric chloride solution, was set up near to a quartz mercury lamp and pure carbon dioxide was passed through the solution. After about one hour's exposure half the solution was transferred by means of a pipette to a second quartz test tube, this operation being conducted in the light of the lamp. One-half of the solution was then left in the light, whilst the other half was placed in the dark. After an interval of 15 minutes, equal quantities of the sodium hydroxide-thiosulphate solution were added to the exposed solution and to the solution which had been kept in the dark. In the former case marked reduction took place, whilst in the latter case the mixed solutions remained absolutely colourless and transparent. This observation was repeated many times by independent observers with the same results.

When exactly the same procedure was followed in the complete absence of carbon dioxide, no reduction was observed with the solution either in the light or in the dark. It may be noted that the complete removal of carbon dioxide from a mercuric chloride solution is not an easy operation. The method adopted was as follows: A large quartz test tube, 9 in. × 1 in., provided with a hollow glass stopper ground in and fitted with a soda-lime tube, was used. Sufficient mercuric chloride (1·6 grm.) to form 40 c.c. of solution was weighed out into the quartz test tube, and pure conductivity water was added until the tube was nearly full. The solution was then heated and maintained in gentle ebullition until the volume was reduced to 40 c.c., this operation taking about 1½ hours The glass stopper with its soda-lime tube was then inserted and the whole allowed to cool slowly. When the tube was quite cold, it was exposed to the light from the quartz mercury lamp for an hour and then the stopper was removed and the alkaline thiosulphate solution immediately added. No trace of reduction was observed.

These results give a clear indication of the existence of a photostationary state or photochemical equilibrium, although the nature of the organic component is not established beyond the fact that it must be an aldehyde or mixture of aldehydes. It may be noted, however, that the organic component does not seem to be formaldehyde, since this substance always gives with the Feder solution a grey precipitate of metallic mercury, whereas the precipitate obtained in the above experiments was always dark brown and flocculent. An exactly similar reduction is given by solutions of glucose which have been kept for some hours, and this is suggestive in view of the equation for the photostationary state given above.

The reality of the photostationary state having been established, we next made many attempts to effect the photosynthesis of the carbohydrates by adding a harmless reducing agent to the carbonic-acid solution, hoping to shift the equilibrium to the carbohydrate side by the removal of the oxygen. Only one of these attempts met with success, and this may be described, since the results are of some interest.

Prof. Bannister drew our attention to the fact that pure iron in the presence of carbonic acid and in the absence of oxygen rusts rapidly when exposed to ultra-violet light. This suggested at once the possibility that carbohydrates are formed by the action of the ultra-violet light on the carbonic acid and that the ferrous bicarbonate takes up the oxygen with the formation of ferric hydroxide. In order to put this explanation of Prof. Bannister's results to the test of experiment, eight quartz test tubes filled with air-free conductivity water, and each containing a rod of pure Swedish iron, were arranged around a quartz mercury lamp. The water in each tube was saturated with pure carbon dioxide and kept in the dark until a saturated solution of ferrous bicarbonate was formed. This solution, when protected from the air, is quite colourless and stable, but when exposed to the light from the quartz mercury lamp ferric hydroxide is produced. After two hours' exposure, a stream of air was passed through the solution in order to oxidise the excess of ferrous bicarbonate, after which the solution was filtered and concentrated in a vacuum to a small bulk. The solution was then found to contain a substance which reduces Benedict's solution and an acid which forms an unstable silver salt. These experiments were repeated many times with the same results, but the yields were in each case very small. This small yield was attributed to the fact that a coherent layer of ferric hydroxide is formed on the walls of the quartz tubes in the light, and this layer, by absorbing the ultra-violet light, protects the solution from the further action of this light. No trace of formaldehyde could be detected in the solution after it had been exposed to light, a fact which supports the view that this substance in its ordinary form is not the first product of the action of ultra-violet light on carbonic acid.

The above photosynthesis of compounds which reduce Benedict's solution is analogous to that achieved by Stoklasa,[*] who found that substances of the nature of carbohydrates are formed by the action of light on moist carbon dioxide in the presence of alkali and nascent hydrogen.

---

[*] Stoklasa and Zdobnicky, 'Biochem. Z.,' vol. 30, p. 432 (1911); Stoklasa, Sebor and Zdobnicky, *ibid.*, vol. 41, p. 33 (1912); and vol. 54, p. 330 (1913).

The Action of Ultra-Violet Light on Carbonic Acid adsorbed on a Surface.

The very remarkable manner in which the formation of ferric hydroxide takes place on the walls of the tubes and also, it may be noted, on the surface of the iron rods when the ferrous bicarbonate solutions are exposed to ultra-violet light led us to the consideration of the possibility of the photosynthesis of carbohydrates on a suitable surface, namely, a surface capable of adsorbing carbonic acid. In this connection the results obtained by Zenghelis* are of especial interest, for he was able to demonstrate the formation of complex organic compounds when an ordinary paper fat-extraction thimble immersed in water in a uviol glass vessel, and filled with a mixture of hydrogen and carbon dioxide at a pressure equal to that of the water outside, is exposed to the light from the quartz mercury lamp. The complex compounds were recovered from the solution by evaporation, and Zenghelis concluded that they were sugars, since they were readily charred by strong sulphuric acid and gave osazones when heated with phenylhydrazine. The quantity obtained from each thimble was about 20 mgms.

We were able to confirm Zenghelis' observations in every detail, including the fact that after about ten hours' exposure the paper surface loses its efficiency. No explanation of this remarkable fact was offered by Zenghelis, but a possible explanation will be suggested in the third paper. We further observed that the presence of hydrogen is unnecessary, the same quantities of photosynthesised materials being obtained when the paper thimbles contained pure carbon dioxide.

Independent evidence of the reality of the photochemical reaction with carbonic acid on a surface was obtained in these laboratories by Dr. Morton and Dr. Riding. A Pasteur-Chamberland filter tube of the finest possible grade was immersed in conductivity water contained in a quartz vessel. Carbon dioxide was admitted into the inside of the filter tube at a pressure of several atmospheres, and the whole was exposed to the light of the quartz mercury lamp for 24 hours. The water was then found to contain formaldehyde to the extent of 0·01 per cent., the amount found in the earlier experiments described in the introduction being only about 0·00002 per cent.

We were convinced that this result gave valuable but only indirect evidence of the photosynthesis of carbohydrates, the formaldehyde being produced by their photochemical decomposition by the ultra-violet light of short wavelength. As has already been referred to, this decomposition has been conclusively established by numerous observations. In order further to test this interpretation, numerous experiments were carried out in which Pasteur-Chamberland filter tubes of different grades of fineness, containing carbon dioxide under pressure and immersed in water, were exposed to the quartz mercury lamp. Both uviol glass and quartz vessels were used, and in each case small but definite quantities of organic matter were obtained on evaporation of the solution. Formaldehyde was always found when quartz vessels were employed, but when uviol glass vessels,were used, the amount of formaldehyde was exceedingly small (1 in 5,000,000) unless the period of insolation was unduly prolonged.

---

* 'C. R.,' vol. 171, p. 167 (1920).

The position reached at this stage was one of some interest, since it had been established that photosynthesis of complex organic substances takes place when carbonic acid in the presence of a surface is exposed to ultra-violet light. The evidence, so far as it goes, favours the view that ordinary formaldehyde as such is not formed as an intermediate product, and that when found it is due to the photochemical decomposition of the complex products. The most promising method of pursuing the investigation was to make use of surfaces which have the power of adsorbing carbonic acid and to expose these when saturated to the ultra-violet light.

In view of the very suggestive results obtained on the rusting of iron by the action of light in the presence of carbonic acid, it occurred to us that aluminium powder might be a suitable substance. Apart from any other reason, it seemed very probable that this metal would rapidly become coated with a film of hydroxide and that this would form an ideal surface for adsorbing carbonic acid. Commercially pure aluminium powder was washed in turn with alcohol and ether, and kept under ether until required. Eight quartz tubes, 9 in. × 1 in., were arranged around the quartz mercury lamp, and each contained 90 c.c. of conductivity water. Into each tube a small quantity of the washed and dried aluminium powder was introduced, and through each was passed a stream of carbon dioxide. After a few minutes' interval, in order to enable the whole system to become saturated with carbonic acid, the mercury lamp was lighted and the insolation was continued for one hour. The solution was then filtered and evaporated to dryness on a water-bath in an open porcelain basin. During the evaporation small quantities of aluminium hydroxide separated and were removed by filtration. The dry residue was extracted with alcohol, and the filtered alcoholic solution gave on evaporation a gummy residue weighing about 0·020 grm. The original solution after filtration contained no measurable trace of formaldehyde, which means that, if present, the amount was less than 1 part in 10,000,000. The gummy residue was found to char very markedly on warming with concentrated sulphuric acid, but it did not appear capable of reducing Benedict's solution. This experiment was repeated several times with identical results, the times of exposure varying from one to eight hours.

Since it appeared possible that the aluminium powder might have some special effect owing to its reducing power, barium sulphate was substituted, since this substance should be able to adsorb carbonic acid on its surface. The salt was prepared by precipitation and washed until free from all soluble compounds. The experimental conditions were exactly the same as in the case of the aluminium, and the times of exposure were from one to eight hours. Once again were the complex organic substances obtained, and once again was no trace of formaldehyde to be detected in the exposed solutions.

At first sight it seemed disappointing that no evidence could be obtained of the photosynthesis of the reducing sugars in view of the statement made in the introduction as to the photostationary state. On the other hand, it is generally accepted that in the living plant the first recognisable products of photosynthesis are not hexoses, but more complex compounds, such as cane sugar or temporary starch. If, therefore, the surface mechanism enables us to realise a condition approaching that in the plant, we should not expect to find hexoses in quantity, but more complex carbohydrates. We were thus encouraged to observe the effect of acid hydrolysis on the gummy products of our experiments.

The aluminium experiments were again repeated, and the organic residue obtained on evaporation was dissolved in a little dilute hydrochloric acid and the mixture heated on a water-bath for some minutes. After neutralisation, Benedict's solution was added and the mixture was boiled, when considerable reduction took place, the precipitated cuprous oxide being contaminated with a little alumina. This experiment was repeated a number of times, in some cases with aluminium powder and in others with barium sulphate. In many cases reduction of Benedict's solution was obtained, but not in all. The gummy organic residue was invariably obtained without any evidence of formaldehyde.

Other powders were next used in place of the aluminium and barium sulphate. In the first instance freshly precipitated aluminium hydroxide was used. The compound was precipitated by the addition of ammonia solution to a solution of aluminium nitrate and was washed by centrifuging and used immediately. The time of exposure was two hours, and after evaporation 0·20 grm. of organic matter was obtained. This was dissolved in a little normal hydrochloric acid and heated at 100° for ten minutes, made alkaline with potassium carbonate, and the trace of alumina which separated was removed by filtration. On heating with Benedict's solution, marked reduction took place.

Similar results were obtained when the aluminium powder or aluminium hydroxide was suspended in solutions of potassium and sodium bicarbonates. Evidence of reduction after hydrolysis of the organic products was again obtained.

One series of results may be mentioned here in view of their special interest. It was found that if the precipitated and washed aluminium hydroxide was allowed to stand in contact with water for 24 hours before use, the yield of photosynthesised organic products was materially smaller. Indeed, after remaining under water for 60 hours, the hydroxide gave no weighable quantity of these products. It is known that aluminium hydroxide, after remaining in contact with water for many hours, changes in character and becomes acidic in its properties, and in consequence has no longer any power of adsorbing carbonic acid.

Basic aluminium carbonate was next used, this substance being prepared by the addition of a cold solution of potash alum to a cold solution of an excess of sodium carbonate. The resulting precipitate was allowed to stand for 24 hours in contact with the mother liquor, and then was filtered and washed until free from all soluble salts. After two hours' exposure a good yield of organic matter was obtained. It was noticed that in this case the suspended carbonate, originally quite white, when filtered off at the end of the exposure to light was brown in colour. This discoloured carbonate was dried on a porous tile, and a portion of it gave considerable charring when treated with concentrated sulphuric acid. Evidently, therefore, some of the organic products had been adsorbed on the surface. This is the only substance we have used which exhibits this phenomenon to any measurable extent. Lastly, we found that the basic carbonates of zinc and magnesium give equally good yields of the complex organic compounds.

In view of the results obtained in the early work and referred to in the introduction, some experiments have been carried out in which either synthetic ammonium bicarbonate or a soluble nitrite is dissolved in the water in which the fine powder is suspended. In the first experiments with the ammonium bicarbonate, the solution, after two hours' exposure with aluminium powder, was filtered, and after acidification with hydrochloric acid was evaporated to dryness on a water-bath. The residue, which was brownish-yellow in colour, was extracted with absolute alcohol, which removed much, but not all, of the brown colour. The alcoholic solution on evaporation gave some ammonium chloride which contained organic matter. This mixture in aqueous solution gave a copious yellow precipitate with potassium bismuth iodide, and the dry substance, on being rubbed in a mortar with dry borax powder, evolved a strong basic odour. In subsequent experiments the solution after two hours' exposure was filtered and evaporated to dryness under reduced pressure at 40° without previous acidification. The residue contained some aluminium salts and a considerable quantity of organic matter which, though it contained nitrogen, did not give any reactions for alkaloids. It is possible that the photosynthesised product is complex and that it undergoes hydrolysis when evaporated with hydrochloric acid at 100°. When a soluble nitrite is present, organic matter is also synthesised. These investigations are being actively pursued.

In all the foregoing experiments we used the U-shaped quartz mercury lamp made by the Hewittic Electric Company, and the lamp was operated with current at 220 volts. The quartz tubes were 9 in. × 1 in., and the uviol glass tubes were 6 in. × 2 in. These tubes were arranged round the lamp, each tube being nearly full of pure water. To each was added a small quantity of the powder, and through each was passed a fairly rapid stream of carbon dioxide. After a short time the lamp was lighted, the exposure being continued for two hours, except in those cases specially mentioned. At the end of the period the solution, which amounted in all to about 720 c.c., was filtered and evaporated to dryness on a water-bath in an open porcelain basin, any solid which separated during the evaporation being removed by filtration. In the case of the photosynthesis of nitrogen compounds, N/10 solutions of synthetic ammonia or a soluble nitrite ($Ba(NO_2)_2$ or KNO_2) were used in place of pure water.

One serious difficulty must be referred to, which very materially hindered progress until its nature was elucidated and the means of overcoming it were discovered. Transparent quartz apparatus when first made is, as is well known, transparent to ultra-violet light. On exposure to the light from the quartz mercury lamp the quartz rapidly develops an opacity to the ultra-violet rays, an opacity which extends more and more towards the longer wave-lengths with time. If the quartz be kept cool, it becomes opaque to the whole of the ultra-violet after a week's continuous exposure, this change being accompanied by the development of a marked amethyst colour. This change appears to be complex in character, since the condition characterised by the amethyst colour is completely metastable, whereas there exists an intermediate condition which is opaque to the extreme ultra-violet light and is not metastable. If the quartz tubes which have been brought into this intermediate state are kept in the dark, they slowly revert to their normal transparent state. This change is accompanied by the evolution of light which is capable of acting on a photographic plate. Prof. J. C. Drummond tells us that he has also observed this phenomenon.

The reversion to the normal state is greatly accelerated by heat or by shock, and the tubes on being heated in the blast flame exhibit a strong green phosphorescence, which disappears when the normal state has been regained. The effect of shock was discovered as the result of an accident when some quartz test tubes which had been used for some photosynthetic experiments were dropped on to the stone floor of a dark laboratory. The broken fragments phosphoresced strongly for a short time. The phosphorescence exhibited when the amethyst-coloured quartz is heated is very striking.

It may well be understood how great were the difficulties we met with before these facts were discovered. We now have found that the deterioration in transparency becomes sufficiently great to produce a marked decrease in the amount of photosynthetic material after about four hours. As a matter of routine all our quartz tubes have been subjected to the heat treatment after every exposure.

This remarkable property of fused silica has an important bearing on the efficiency of the quartz mercury lamps. As far as we are able to judge without having made quantitative measurements of the radiated energy, the 200-volt lamp suffers small deterioration, owing probably to the high temperature developed during its operation. This does not seem to be true of the 100-volt lamp, which operates at a lower temperature.

Control Experiments.

In view of the criticisms of the earlier work, it is obvious that confidence in the results now recorded can only be gained after the most rigid proof of the complete absence of all organic matter in the carbon dioxide and in the materials used. Not only was it necessary to demonstrate this, but in our opinion it was also advisable to carry out rigid control experiments which were identical with those recorded, except that powders incapable of adsorbing carbon dioxide were employed. On account of their manifest importance, these tests and control experiments may be described in some detail.

It is evident that of all the materials employed the carbon dioxide is the most probable source of impurity, especially as this gas is sometimes made by fermentation processes. We obtained the gas in cylinders from the Washington Chemical Company under written guarantee that it had been made solely by heating limestone. The usual tests proved that the gas was pure in the ordinarily accepted sense, but these, in our view, were far from being sufficiently searching, and the following special tests alone satisfied us as to the complete absence of all organic impurity:—A slow stream of the gas was passed through two litres of distilled water for many hours in the dark, and the solution on evaporation *in vacuo* gave no trace of organic residue. The same absolutely negative result was obtained when the water was irradiated with ultra-violet light during the passage of the carbon dioxide. These experiments were carried out both with and without filtration of the gas through a layer of finely powdered sodium bicarbonate between thick packing of cotton wool. It was also proved by Schryver's tests that formaldehyde was not formed in amounts greater than 1 part in 100,000,000, this being the limit of the test. There remained the possibility that the gas stream contained finely divided organic matter in the form of an aerosol, which might very possibly pass through the water without being affected. In order to prove the absence of such aerosols, the gas was passed through a quartz tube which was strongly irradiated with ultra-violet light, and then directly, without subsequent filtration, into dust-free water, both with and without irradiation. In no case was any trace of organic matter found on evaporation of the solution. These experiments, which were carried out several times, convinced us that the carbon dioxide was free from all organic impurity.

Although the absence of organic impurity in the carbon dioxide was thus established, there was still the possibility that such may have been introduced from other sources. In order to satisfy ourselves that such contamination did not take place, we carried out at frequent intervals control experiments which, in our opinion, afford the most conclusive evidence that the photosynthesis of organic matter is not due to the presence of impurity in any of the materials.

It may first be mentioned that, in confirming the results published by Zenghelis, we found that no organic compounds, including formaldehyde, were produced when the paper thimbles in water free from carbon dioxide were exposed in uviol glass tubes for eight hours. In the second place, a great number of control experiments were carried out in which powders incapable of adsorbing carbon dioxide were suspended in water by a stream of this gas and exposed to ultra-violet light in quartz vessels. A typical powder was finely powdered silica. In no case was any organic residue obtained after filtration and evaporation of the solution. Reference has already been made to the change in properties of aluminium hydroxide when kept under water for 24 hours. This afforded us an opportunity of carrying out control experiments which seem to us to be the most convincing of all. A quantity of the hydroxide was prepared, free from all soluble impurity, and after filtration this was ground up with water to form a thin paste. A portion of this paste was diluted with water and placed in the quartz tubes and a stream of carbon dioxide passed through for two hours, the vessels being irradiated with the light from the quartz mercury lamp. In every case a good yield of the organic products was obtained. The remainder of the hydroxide paste was then kept for various periods of time and the same experiment carried out, using carbon dioxide from the same cylinder. After the paste had been kept for eight hours, only a small yield of organic matter was obtained, and after 24 hours' keeping no trace of organic residue was left on evaporation of the filtered solution, nor did the recovered hydroxide contain any organic substance adsorbed on it or present in it. These particular controls, which were carried out several times, appear to us to be the most convincing of all, since the presence or absence of organic products was proved to depend solely on the physical properties of the surface used, this being the only variable factor in the experiments.

In view of the complete absence of organic impurity in the carbon dioxide used and of all organic products in the controls, we believe that the negative results recorded by Porter and Ramsperger were due to the fact that in adopting their remarkable precautions against impurities, they succeeded in materially reducing the amount of dust or other solid suspended matter, and thereby removed the small amount of surface present in the experiments of Baly, Heilbron and Barker. This suggestion is preferable to that offered by those authors, which involved the assumption that some unknown impurity was present in the earlier experiments.

Discussion of Results.

The results now brought forward give a strong indication that, whereas no measurable reaction takes place when pure carbonic acid in aqueous solution, free from all suspended matter, is exposed to light, a very definite reaction occurs when there is present in the solution a surface capable of adsorbing the carbonic acid. Furthermore, the reaction consists in the photosynthetic formation of complex organic compounds and not of formaldehyde. These complex substances char readily when heated alone or with concentrated sulphuric acid.

Their complexity is established by the fact that the power of reducing Benedict's solution is developed after hydrolysis by hydrochloric acid. It must be pointed out, however, that the presence in small quantity of reducing compounds before hydrolysis is not entirely excluded.

The results described in this communication are in accord with the view that, when carbonic acid in aqueous solution is illuminated with ultra-violet light, a photostationary state is established, involving as one of the components a complex carbohydrate. Evidence in favour of this view is given by the experiments with mercuric chloride described above. Although at this stage it is premature to advance any theory to account for the effect of the surface, it is reasonable to point out that if the carbonic acid is selectively adsorbed on the surface and the carbohydrate is not adsorbed, the photostationary state will no longer exist, with the result that the carbohydrate will be photosynthesised. The term carbohydrate is used here in a tentative sense, since the direct evidence in favour of their formation might be considered as being somewhat slender. *More definite evidence in favour of the reality of the carbohydrate photosynthesis will be adduced in the following communication.*

We would point out that in all probability these results offer the true explanation of Moore and Webster's observations with colloidal ferric and uranium hydroxides. They noted the formation of formaldehyde when these colloidal solutions saturated with carbon dioxide were exposed to light, and there is little doubt that these results were due to the colloidal surface, the formaldehyde being formed by the photochemical decomposition of the carbohydrates at first formed. In short, these authors were the first to achieve photosynthesis by the use of a surface, though this has only now been recognised.

Summary.

1. When an aqueous solution of carbonic acid in quartz tubes is exposed to ultra-violet light, a photostationary state is established. Ordinary formaldehyde is not a component of this equilibrium, but there is present an organic compound which is probably a complex aldehyde.

2. Ferrous bicarbonate in aqueous solution is converted by ultra-violet light in the absence of oxygen into ferric hydroxide, organic compounds with reducing properties being simultaneously formed. This reaction appears to take place mainly on the surface of the quartz tubes in which the solution is exposed to the light, and also on the surface of the iron rods used.

3. When an insoluble powder, capable of adsorbing carbonic acid on its surface, is suspended in water through which is maintained a stream of carbon dioxide, and when the whole is exposed to ultra-violet light, complex organic compounds are photosynthesised. These may be recovered by evaporation of the solution after removal of the insoluble powder.

4. The following materials are effective:—Aluminium powder, barium

sulphate, freshly precipitated aluminium hydroxide, and the basic carbonates of aluminium, magnesium and zinc. After remaining in contact with water for some hours, aluminium hydroxide loses its efficacy, and this is due to the well-known fact that it then has no measurable affinity for carbonic acid. Since the experimental details were identical in this case with those when the other powders were used, this result excludes the possibility that the results observed in the other cases were due to impurities.

5. Owing to the fact that quartz develops a marked opacity to rays of short wave-length when exposed to ultra-violet light, it is necessary when the photosynthetic operation is carried out in quartz tubes that these should be heated in the blast flame before use.

6. The total quantity of organic compound produced is about 0·02 grm. in two hours when eight quartz test tubes, 9 in. × 1 in., containing in all 720 c.c. of water and the suspended powder, are exposed to the light from a 220-volt U-shaped lamp at an average distance of 6 cms.

7. The organic compounds thus produced would seem to be of the nature of complex carbohydrates. They char readily when heated alone or with concentrated sulphuric acid. The quantity obtained in each experiment gives no visible reduction of Benedict's solution, but after hydrolysis with hydrochloric acid, reducing power was developed in the great majority of cases.

8. In the presence of ammonium bicarbonate complex organic compounds are produced which contain nitrogen. Photosynthesis of complex organic material containing nitrogen also takes place when nitrite of potassium or barium is present.

9. Exhaustive tests proved that the carbon dioxide and other materials used were free from all organic impurity; numerous control experiments were carried out, which consisted in the irradiation of a powder, incapable of adsorbing carbonic acid, suspended in water by means of carbon dioxide. Since entirely negative results were invariably obtained, and since the only variable factor is the nature of the surface, possibility of the results now recorded being due to organic impurities would seem to be completely excluded.

We acknowledge our indebtedness to Messrs. Brunner, Mond & Co. for their generous financial assistance which has enabled this work to be carried out.

The Photosynthesis of Naturally Occurring Compounds.—II. The Photosynthesis of Carbohydrates from Carbonic Acid by Means of Visible Light.

By E. C. C. Baly, F.R.S., W. E. Stephen, and N. R. Hood, Liverpool University.

(Received July 28, 1927.)

In the preceding communication evidence was brought forward in favour of the photosynthesis of carbohydrates when pure carbonic acid, adsorbed on a surface suspended in water, is exposed to ultra-violet light. Although possibly the results described may seem to mark a step forward towards the explanation of the phenomenon of natural photosynthesis of carbohydrates from carbonic dioxide and water, there still remains unexplained the greatest difficulty of all, namely, the utilisation by the living plant of visible light only. Furthermore, as we were the first to recognise at this stage, the evidence of the photosynthesis of carbohydrates given by the previous experiments is somewhat slender.

In all the experiments described in the preceding paper carbonic acid adsorbed on a white surface was exposed to ultra-violet light, it being assumed that in the case of aluminium powder there is formed a layer of hydroxide which is effective. The possibility occurred to one of us (W. E. S.) that if a visibly coloured powder, capable of adsorbing carbonic acid, be employed, the photosynthesis may be brought about by visible light. Two powders which satisfy the conditions are the basic carbonates of nickel and cobalt in that they are visibly coloured and undoubtedly adsorb carbonic acid on their surface when suspended in water through which carbon dioxide is passed. Preliminary experiments were carried out in which suspensions of each of these powders in water were placed in vessels of ordinary German soda glass with walls from 1·5 to 2 mm. in thickness. Carbon dioxide was passed continuously through each vessel, and the results were illuminated by the light from an ordinary tungsten filament lamp. After filtration and evaporation the exposed solutions in each yielded a gummy residue which was undoubtedly organic in nature, since it readily charred with strong sulphuric acid. This experiment was repeated several times with the same results, and these convinced us that it is possible by the use of coloured powders to photosynthesise organic compounds from carbonic acid with the help of visible light.

The photochemical reaction was then investigated in some detail, and the results which have been obtained are of considerable interest. In the early experiments the glass vessels used were the ordinary test glasses of the laboratory, each holding 250 c.c. In each 250 c.c. of water was suspended 1·25 gram of one of the two carbonates, and a fairly rapid stream of carbon dioxide was maintained through each vessel so as to keep the whole of the powder in suspension. Four of the vessels were arranged round an ordinary tungsten filament lamp and exposed for two hours.

A different method of recovering the organic substances from the exposed solutions has been adopted. After filtration, these solutions are concentrated under reduced pressure at 50°, a very slow stream of air being passed through the solution during the process. At intervals during the evaporation the precipitated carbonate is removed by filtration. The final residue consists of a gummy substance mixed with a very small quantity of the carbonate, and the former is extracted with methyl alcohol. This change in procedure has been adopted because the exposed solutions after filtration contain a considerable quantity of nickel or cobalt bicarbonate, and these salts undergo a complex decomposition when their solutions are concentrated in air at 100°.

The photosynthesised compounds are very similar in appearance to those described in the preceding paper, and it would seem that the present method of their preparation has the advantage in that the products are not so liable to undergo photochemical decomposition, since they are not exposed to ultraviolet light. No trace of formaldehyde is present in the exposed solutions, nor can it be found in the first runnings when the solutions are distilled. The test used for formaldehyde was that described by Schryver, and since this is capable of detecting one part in 10,000,000, and since on distillation of a weak solution the first runnings of the distillate are always richer in formaldehyde, the complete absence of this substance may now be accepted as conclusively proved.

This statement does not mean that carbonic acid on activation by light does not give activated formaldehyde which at once polymerises to carbohydrates. It means that this activated formaldehyde does not escape from the reaction sphere and become ordinary formaldehyde by loss of energy. That the activated form of formaldehyde is the first product seems probable from the photosynthesis of the nitrogen compounds, which it is hoped will form the subject of a further communication. It may be mentioned here in passing that, as in the case of the white powders and ultra-violet light, complex nitrogen compounds are also photosynthesised in visible light if ammonium bicarbonate is present in the solution containing a suspension of either nickel or cobalt carbonate.

In the later experiments the laboratory test glasses were substituted by rectangular glass vessels with polished sides, and in order to secure greater illumination 100-watt half-watt lamps were used in place of the ordinary tungsten filament lamp. Three of these lamps were placed close together in a row, and six of the rectangular jars containing the carbonate held in suspension by a CO_2 stream were placed close to the lamps, cooling tubes being used to prevent the temperature rising. The effective area exposed was 294 sq. cm., and 11·5 grams of the carbonate were suspended in 1,500 c.c. of water, each vessel holding 250 c.c. It was disappointing at first to find that the yield of carbohydrates was very poor after two hours' exposure. Increase of exposure was tried, and it was then found that the yield obtained in the first two hours was materially decreased by the subsequent illumination. The vessels were next removed to a distance of 6 in. from the lamps, and then a constant yield of about 0·035 gram of carbohydrate was obtained with cobalt carbonate, which compares favourably with the 0·02 gram with 400 sq. cm. exposed, such as was recorded in the previous paper, when white powders and ultra-violet light are used.

Up to the present no consideration has been paid to the question of the destination of the oxygen set free in the photosynthesis. Dr. E. K. Rideal suggested to us that the adsorption of the carbonic acid takes place by virtue of the residual affinities of the oxygen atoms, and that when photosynthesis takes place the oxygen remains adsorbed on the surface with the possible formation of a peroxide. This appears to be true for two reasons. In the first place, we have found that when nickel carbonate which is slightly damp is exposed to light in the presence of carbon dioxide it turns black on the surface owing to the formation of Ni_2O_3. The same is true of cobalt carbonate, this substance becoming brown in colour.

In the second place, we have obtained undoubted evidence of poisoning of the surface during the photosynthesis of the carbohydrates when cobalt carbonate was used. The majority of the results described in this paper have been obtained with this substance, because we were fortunate enough to obtain a quantity of commercially pure cobalt carbonate which was free from all trace of soluble impurity. The reality of the poisoning of the surface has been established by the fact already mentioned that with medium intensity of illumination the photosynthesis ceases after two hours, and also by the fact that with strong intensity the carbohydrates first formed are subsequently decomposed. We have further found that with decreasing intensity of light the quantity of carbohydrate synthesised by unit quantity of light increases. Not only do these observations prove the poisoning of the surface, but they also show that the poisoned surface tends to recover itself, the rate of this recovery being slow compared with that of the photosynthetic reaction.

Some results obtained by Mr. P. F. R. Venables in the quantities of organic matter, soluble in alcohol, obtained with aluminium powder in the presence of ammonium bicarbonate, are of interest, for he has found that the amount synthesised increases as the light intensity decreases.

As might be expected, the yield of carbohydrates with a constant intensity of illumination is increased when larger amount of the powder is used. Thus with 7·7 grams of cobalt carbonate suspended in 250 c.c. of water in each of the rectangular vessels placed at a distance of 6 in. from the half-watt lamps a yield of 0·075 gram was obtained, as against 0·035 gram with 1·9 gram of the carbonate. We have found that the carbonate, after it has become poisoned, can be re-activated by washing with hot water, and may then be used again. The material, however, develops a brown colour due to the presence of small quantities of cobaltic oxide.

It has already been noted that the photosynthesised products are similar in appearance to those obtained with white powders in ultra-violet light. They char readily on heating alone and with strong sulphuric acid. There now seems little doubt that the product is a mixture, and that one of the components of the mixture is a carbohydrate. As already described, the dry residue obtained by the evaporation of the exposed solutions under reduced pressure is extracted with pure methyl alcohol. The filtered alcoholic solution on evaporation deposits a gummy material which is not completely soluble in water, in spite of the fact that it is obtained in the first instance from an aqueous solution. Very probably this insoluble substance is colloidal in nature, and has been rendered insoluble by the subsequent treatment. It is undoubtedly organic, but the quantity obtained has as yet been too small for systematic investigation.

The aqueous solution of the residue left on evaporation of the methyl alcohol solution contains a substance which we are convinced is a carbohydrate. The reasons we have for making this statement are four in number :—

1. The solution gives a copious precipitate of cuprous oxide on warming with Benedict's solution.

2. The solution gives a well-marked Molisch reaction with α-naphthol and strong sulphuric acid. This is accepted as being specific for carbohydrates.

3. The solution, on warming for one hour with a little pure phenyl-hydrazine acetate, gives a solid osazone. This osazone is very soluble in cold alcohol, and the solution, on the addition of benzene and slow evaporation deposits the osazone again in the solid form.

4. The solution gives Rubner's test with basic lead acetate as modified by Rogerson.* This, again, is a specific test for carbohydrates.

It may further be added that the reducing power of our photosynthesised compounds is materially increased on hydrolysis by hydrochloric acid. This suggests at once the presence of complex carbohydrates of higher molecular weight than the hexoses, and, indeed, this observation strengthens our belief in the reality of the carbohydrate synthesis.

The reducing power of the products photosynthesised by means of visible light is much greater than in the case of those produced with white powders and ultra-violet light. Possibly this is due to the fact that in the latter case the photosynthesised products are photochemically decomposed by the ultra-violet light, but we have no direct evidence which proves this. It has, however, been clearly established that not only is the total quantity of material photosynthesised by means of a coloured surface in visible light greater, but the percentage reducing power is also greater than is the case with a white surface in ultra-violet light.

We find that in order to obtain the best yields of organic matter the suspended carbonate must be in the form of a fine powder. It is absolutely essential that the carbonate be free from every trace of alkali, and this is by no means easy to secure. If the solution after exposure contains even very small quantities of sodium carbonate, the carbohydrates undergo decomposition during the concentration of the solution. Furthermore, it is necessary that the carbonate be free from nitrate, chloride and sulphate.

We have found that the best method of preparation is to add a cold solution of cobalt or nickel nitrate to a cold solution of a slight excess of potassium carbonate. The nitrate is the only salt which gives a satisfactory product owing to the readiness with which the chloride and sulphate ions are adsorbed. The precipitated carbonate is collected by filtration and washed with distilled water, after which it is removed from the filter and ground up with distilled water to a thin paste. This paste is then diluted with a large volume of distilled water and steam is passed in until the temperature reaches 100°. The powder is then allowed to settle, and the supernatant liquid is poured off as far as possible. The carbonate is then again filtered and washed, the whole process being repeated until the alkali has been completely removed. We have found that the only reliable method of testing for the presence of alkali is to pass a stream of carbon dioxide through a suspension of the carbonate in water for two hours. The filtrate after evaporation to dryness must show no alkaline reaction. After the complete removal of alkali the carbonate is dried at 100°.

---

* 'Biochem. J.,' vol. 9, p. 245 (1915).

The carbonates thus prepared rarely give good yields of carbohydrates even when exposed to light in the manner described above. The photosynthesis is undoubtedly due to a type of surface catalysis, and, in consequence, such variations in the activity of the catalyst are to be expected, as are frequently found in heterogeneous catalysis. The activation of the carbonates can be achieved in two ways. In the first place, they may be heated when quite dry at 120°–140° for 20 to 30 minutes, or they may be exposed to ultra-violet light for 30 minutes, the powder being frequently stirred so as to expose new surfaces. This latter method is the better of the two, a quartz mercury lamp being held about 10 in. above the powder spread out in a large clock glass.

Although the description of the preparation and use has been restricted to the individual carbonates, excellent yields of the carbohydrates can be obtained with the mixed carbonates prepared in the manner detailed above with a solution of equivalent weights of cobalt and nickel nitrates.

Just as in the earlier work with white powders and ultra-violet light, so in the present experiments were equally rigid precautions taken against the possible presence of organic impurities in all the materials used. The carbonates were examined by passing carbon dioxide for two hours through their suspensions in water protected from all light. The filtrates on evaporation invariably gave no organic matter. These tests were identical with the photosynthetic experiments except for the fact that light was excluded. Not only was the carbon dioxide used in the successful experiments proved to be free from organic impurity by the methods described in the preceding paper, but still more conclusive experiments were also periodically carried out at frequent intervals. Preparations of nickel and cobalt carbonates known to be inactive were used, and a stream of carbon dioxide passed through their suspensions in water for two hours under illumination. No measurable quantity of organic matter, carbohydrate or otherwise, was obtained. The same powders after recovery by filtration were dried and activated, and the same process repeated under identical conditions with carbon dioxide from the same cylinder. Carbohydrates were then obtained in good yield, it having been proved that no organic matter was produced during the actual activation.

Over two hundred of these control tests were carried out at frequent intervals with entirely negative results. In view of the fact that the carbon dioxide and all the materials used were proved to be free from all organic matter, not only by direct tests, but also by very numerous control experiments periodically carried out, we feel justified in concluding that our photosynthetic products cannot be attributed to the presence of organic impurity.

Conclusions.

1. When carbonic acid, adsorbed on the surface of nickel or cobalt carbonate suspended in water, is exposed to visible light, photosynthesis of organic compounds takes place.

2. One at least of the products of this photosynthesis is a carbohydrate which reduces Benedict's solution, gives the Molisch and Rubner reactions, and forms a solid osazone.

3. The photosynthesised material contains one or more complex substances which are hydrolysed by acid to give substances which reduce Benedict's solution.

4. For equal areas of the suspension exposed to the light the yield of organic products is greater than that obtained with white powders in the light of the quartz mercury lamp.

5. The percentage of carbohydrates in the products photosynthesised with a coloured surface in white light is greater than it is when white powders are used in ultra-violet light.

6. If ammonium bicarbonate solution containing nickel or cobalt carbonate in suspension is exposed to visible light complex nitrogen compounds are photosynthesised.

7. The shift in the exciting wave-length from the ultra-violet characteristic of carbonic acid in solution to the visible region characteristic of natural photosynthesis has been achieved in the laboratory.

8. The photosynthesis by means of visible light has the advantage in that the photochemical decomposition of the products is avoided. Further, the special difficulties connected with the use of quartz apparatus with ultra-violet light are removed.

9. The oxygen set free during the photosynthesis tends to poison the surface. When moist nickel and cobalt carbonates are exposed to visible light in an atmosphere of carbon dioxide a surface film of Ni_2O_3 and Co_2O_3, respectively, is formed.

10. The surface when poisoned by oxygen slowly recovers itself under water, with the result that increased yields of the carbohydrates are obtained with unit quantity of light when the intensity of illumination is decreased.

11. When the surface has become completely poisoned the photosynthetic process ceases, and then with intense illumination the carbohydrates previously formed are photochemically decomposed.

12. Since rigid tests established the freedom of the carbon dioxide and all the materials from all organic impurity, and since over 200 control experiments, periodically carried out, invariably gave entirely negative results, it would seem impossible that the photosynthesised carbohydrates arise from organic impurity.

We acknowledge our indebtedness to Messrs. Brunner, Mond & Co. for their generous financial assistance, which has enabled this work to be carried out.

The Photosynthesis of Naturally Occurring Compounds.—III. *Photosynthesis* in vivo *and* in vitro.

By E. C. C. Baly, F.R.S., and J. B. Davies, Liverpool University.

(Received July 28, 1927.)

The evidence adduced in the two preceding communications leads to the belief that the direct photosynthesis of complex carbohydrates in a single operation from carbonic acid has now been achieved in the laboratory. There still remains, however, the question as to how far the results take us in the explanation of the natural process as it occurs in the living leaf. It must be admitted that the natural process has ever presented many difficulties, and in view of the foregoing results the problem of its explanation is one of peculiar interest.

In the first place, we may refer to the difficulty arising from the complete absence of ordinary formaldehyde in the living leaf. The elegant work of Willstätter, proving that the molecular ratio of the carbon dioxide assimilated and the oxygen transpired is unity, offers a very definite proof that the first product in the photosynthesis is formaldehyde, and, in consequence, the fact of its entire absence from the leaf during photoassimilation of carbon dioxide was very difficult to understand. This difficulty has been completely eliminated by our results. Theoretical considerations based on the formation of activated carbonic acid as the initial stage in the process lead to the view that activated formaldehyde is then produced, which at once undergoes polymerisation to give the hexoses. De-activated or ordinary formaldehyde should not, therefore, take part in the reaction and, in consequence, should not be found at any stage. These theoretical deductions have been proved to be correct, since in the photosynthetic production of carbohydrates *in vitro* the complete absence of ordinary formaldehyde has been proved. So far as this fact is concerned there is agreement between the laboratory and living processes.

The second point of interest lies in the fact that the photosynthesis *in vitro* has been achieved by the use of a surface, and the question at once arises as to whether the natural process is or is not a photochemical surface reaction. There exists a considerable amount of evidence that a limiting surface not only exists in the chloroplast but is necessary for the normal photosynthesis to take place. It is generally agreed that in the living plant the photosynthesis takes place in the chloroplasts, these being heterogeneous systems consisting of water, proteins, lipoids, and the plant pigments. Price,* as the result of ultramicroscopic observations, states that the chloroplast appears as a slightly opaque and heterogeneous body with a motionless gel structure. Stern† drew attention to the importance of the surface between the two phases of the chloroplast, namely, the lipoid and the aqueous phases. The photosynthetic process only takes place normally when this surface is intact. Then, again, Warburg‡ investigated the influence of certain surface-acting substances, such as phenylurethane and methylurethane and its homologues, and he found that they retarded natural photosynthesis, his conclusion being that their action depended on changes in a limiting surface. The relation between the rate of photosynthesis and the concentration of the narcotic is expressed by a curve which is similar to the well-known adsorption isotherm of Freundlich. These results indicate strongly that natural photosynthesis is a heterogeneous reaction, and it thus would appear that a second point of similarity has been established between the process *in vivo* and *in vitro*.

Perhaps the greatest difficulty in the way of understanding the natural photosynthetic process has been the utilisation of visible light by the leaf. This is well shown by the following values of the photosynthetic efficiency at different wave-lengths observed with Chlorella by Warburg and Negelein§ :—

	$\lambda = 660\mu\mu$	$578\mu\mu$	$546\mu\mu$	$436\mu\mu$
Efficiency	59	53·5	44·4	33·8 per cent.

---

* 'Ann. Botany,' vol. 28, p. 601 (1919).

† 'Z. f. Bot.,' vol. 13, p. 193 (1921).

‡ 'Biochem. Z.,' vol. 100, p. 230 (1919); vol. 103, p. 188 (1920); and vol. 146, p. 486 (1924).

§ 'Z. Phys. Chem.,' vol. 106, p. 191 (1923).

The difficulty can at once be realised from a consideration of the equation, derived from thermochemical data—

$$6H_2CO_3 = C_6H_{12}O_6 + 6O_2 - 673{,}800 \text{ calories.}$$

It is clear from this that the minimum quantity of energy required to activate a single molecule of carbonic acid is 112,300 calories. If the activation were achieved by photochemical means only, then we would have—

$$h\,\nu\,N = 112{,}300 \text{ calories} = 4 \cdot 6941 \times 10^{12} \text{ ergs,}$$

where h is the Planck constant, $6 \cdot 547 \times 10^{-27}$, ν is the frequency of the light, and N is the Avogadro constant $6 \cdot 1 \times 10^{23}$. The value of ν is found to be $1 \cdot 1754 \times 10^{15}$, which corresponds to a wave-length of $255 \cdot 2\mu\mu$.

This calculation is based on the minimum quantity of energy and, as can be seen, the wave-length lies far beyond the region of the spectrum which promotes photosynthesis in the leaf. As a matter of fact, carbonic acid has no power of absorbing light of the wave-length $255 \cdot 2\mu\mu$, and in the experiments described in the first communication, which proved the existence of a photo-stationary state when carbonic acid is exposed to ultra-violet light in the absence of a surface, it was found that light of a wave-length $\lambda = 210\mu\mu$ is necessary. It would follow from this that the light required to achieve photosynthesis of carbohydrates from carbonic acid by purely photochemical means must have this wave-length. This accentuates the remarkable nature of the natural process if this is considered as a purely photochemical reaction.

It has, however, been shown in these communications that in all probability the photosynthesis is a photochemical reaction on a surface, and this enables us to offer a suggestion which appears to eliminate the difficulty. We believe that the adsorbed layer of carbonic acid is partially activated—that is to say, the molecules have a higher energy content than they have in aqueous solution. In order to complete the activation to that stage required to give the activated formaldehyde, less energy will be needed than when the carbonic acid is in solution. Although we cannot at present define the increment of energy gained by the adsorbed layer of carbonic acid, it seems certain that the completion of the activation necessary for the photo-synthesis to take place is a photochemical reaction which can be achieved by means of visible light. In other words, the total quantity of energy necessary for the photosynthesis to take place is supplied in two separate amounts, one quantity being given when the adsorption on the surface takes place, and the second quantity being given by light. The first amount is sufficiently large to enable the second stage to be achieved by means of visible light. Our results justify us in offering this explanation, and if it is correct we would point out that the essential difficulty in explaining photosynthesis *in vivo* has been solved.

The question might well be asked as to the peculiar merit of a visibly coloured surface for adsorbing the carbonic acid. It is difficult to postulate that carbonic acid adsorbed on a coloured surface contains more energy than when adsorbed on a white surface, but this would seem at first sight to follow from our results. On the other hand, if it be true that the energy gained by the adsorbed carbonic acid is derived from the surface, then that surface must be re-activated by the supply of energy before it can give up energy to a fresh layer of carbonic acid, after the first layer has been converted to carbohydrates. Such re-activation of the surface would probably be secured by the absorption of light, and for this purpose a white powder would require ultra-violet light, whilst a visibly coloured powder would be re-activated by visible light. We venture to suggest this as a possible explanation of the peculiar efficacy of a coloured surface. It is also possible that the decrease in efficacy after exposure which Zenghelis observed with his paper surfaces and which was mentioned in the preceding communication is due to the want of re-activation of the surface.

In offering these suggestions, we recognise their speculative nature, which necessarily must be the case when we are dealing with a somewhat novel phenomenon, namely, a photochemical heterogeneous reaction.

In the preceding papers the poisoning of the surface by the oxygen set free in the photosynthetic reaction has been referred to, and evidence has been given which shows that the poisoned surface slowly recovers itself, the yield of carbohydrates per unit quantity of light energy absorbed being greater with smaller light intensity. In other words, the de-poisoning of the surface is a slow reaction compared with the photosynthetic reaction. It is of some interest to consider the function of the plant pigments from this standpoint.

The theory advanced by Willstätter and Stoll states that each molecule of oxygen evolved converts a molecule of chlorophyll A into chlorophyll B according to the equation

$$C_{55}H_{72}O_5N_4Mg + O_2 = C_{55}H_{70}O_6N_4Mg, H_2O,$$

and that there must be some mechanism for reversing the reaction, since the ratio of chlorophyll A to chlorophyll B remains constant during photoassimilation of CO_2. It is possible that this equilibrium is maintained by the carotin, this pigment being oxidised to xanthophyll in accordance with the equation

$$C_{40}H_{56} + O_2 = C_{40}H_{56}O_2.$$

If this be correct, it will follow that the tendency will be for the xanthophyll/

carotin ratio to increase during photoassimilation of CO_2, a change which was observed by Willstätter and Stoll. In support of this view, it may be stated that Dr. Stead, working in these laboratories, has succeeded in proving that it is possible to oxidise carotin to xanthophyll in two ways. In the first place, carotin in chloroform solution is oxidised by atmospheric oxygen, the first product being xanthophyll, and, in the second place, xanthophyll is formed when a dilute solution of ferric chloride in acetone is cautiously added to a solution of carotin in acetone. The details of this investigation will form the subject of a further communication.

It is obvious that if the molecular ratio of oxygen transpired to carbon dioxide absorbed be unity, the relative quantities of all four pigments will be constant. The fact that Willstätter and Stoll observed an increase in the xanthophyll/carotin ratio, suggests at once that one of the pigment reactions is slow compared with the photosynthetic reaction, and, indeed, that a further similarity between photosynthesis *in vivo* and *in vitro* exists. Since the chlorophyll ratio remains constant whilst the carotinoid ratio changes, it follows that the slow reaction must be the one in which the xanthophyll is reduced again to carotin, a reaction which includes the transference of the oxygen from the chloroplasts to the stomata. It also follows that for the maximum efficiency to be secured the photosynthetic reaction must proceed at a rate which is not greater than that of this slow reaction. In the laboratory we find, as already stated in the second paper, that if the photosynthesis proceeds at a greater rate than the de-poisoning of the surface, the carbohydrate yield is materially reduced, and, further, that the use of strong light for long periods causes oxidation of the carbohydrates.

These considerations offer an explanation of the fatigue effect which is well known in connection with the photosynthetic activity of the living leaf. This was demonstrated by Ursprung,* who showed that the yield of starch decreased after exposure to strong light. The phenomenon has also been studied by Ewart,† who found that prolonged exposure to intense light caused the destruction of the chlorophyll.

There is yet another phenomenon shown by the living leaf which finds a possible explanation from our results. During the day the leaves are exposed to light of varying intensities, including that of direct sunlight on a clear day. In the photosynthesis *in vitro* it is a simple matter so to adjust the light intensity that the photosynthetic rate does not greatly exceed the rate of de-poisoning of the surface. Since the plant cannot do this, it is not unreasonable to ask whether there is not present in the leaf some internal mechanism whereby the rate of photosynthesis is controlled, so that it does not at any time materially exceed the rate of the slow reaction which may be assumed to be a constant for any one leaf. We venture to suggest that the well-known variation of the orientation of the chloroplasts with respect to the light rays is one of the details of such an internal mechanism. By change in the orientation of the chloroplasts the surface exposed to the light is decreased when the light intensity is increased. The result will be that, although the quantity of carbohydrate formed on unit area of surface is increased, the total quantity formed per unit time does not exceed the limit set by the velocity of the slow reaction. In connection with this the results recorded by Puriewitsch[*] are of considerable interest. He determined the increase in the heat of combustion obtained with excised leaves of four species of plants after exposure to sunlight, the total intensity of the light being determined by means of a recording bolometer. He found that there is an inverse ratio between the amount of energy used by the leaves and the total amount of energy which fell on them, which is the result to be expected from the above considerations.

---

* 'Ber. bot. Ges.,' vol. 35, p. 57 (1917).

† 'Ann. Botany,' vol. 11, p. 439 (1897); and vol. 12, p. 379 (1898).

The quantitative data given by Puriewitsch enable us to make a comparison between the quantities of carbohydrates synthesised in our experiments and in the living leaf. Puriewitsch gives the following average values of the increase in heat of combustion in calories per sq. cm. per hour :—

Acer plantanoides	0·34, 0·27, 1·09, 0·53.
Polygonum sacchalinense ..	4·1, 1·7, 1·4, 2·0, 0·3, 0·9.
Helianthus annuus	1·3.
Saxifragia cordifolia.. ..	1·5.

As stated in our previous communication, the maximum yield of carbohydrate that we have succeeded in obtaining under the best conditions yet secured is 0·075 gram in two hours. Assuming for the present purpose that the product is glucose, this corresponds to a gain in calorific value of $674{,}000 \times 0 \cdot 075/180 = 280 \cdot 8$ calories, or 140·4 calories per hour.[†] Since the surface exposed was 294 sq. cm., the gain in calorific value was 0·48 calorie per sq. cm. per hour. It would seem, therefore, that the yield of carbohydrates obtained in the laboratory is not seriously at variance with that observed in nature.

Although the results described and discussed in this and the two preceding papers would seem to show that a definite advance has been made towards the solution of the problem of photosynthesis, it must be remembered that the actual nature of the carbohydrates synthesised in the laboratory has still to be determined. If it be true that these are the same as those which are photosynthesised by the action of ultra-violet light on ordinary formaldehyde, then valuable information will be secured by the complete study of the latter compounds. As has already been noted, Irvine and Francis have proved that glucose is one of the products. A systematic investigation of these products in these laboratories is now approaching completion, and it is hoped soon to communicate the results of this work. Sufficient evidence has already been obtained to justify the statement that the similarity between photosynthesis *in vivo* and *in vitro* is greater than is implied by the fact that glucose is formed in each case.

---

[*] 'Jahrb. wiss. Bot.,' vol. 53, p. 229 (1914).

[†] Similar results would be given if any other simple carbohydrate were assumed, since the heat of combustion is, to a first approximation, proportional to the molecular weight.

Then, again, it must be remembered that the compounds obtained in the laboratory are optically inactive, a fact which marks a sharp differentiation between the natural and the laboratory processes. Although the explanation of the asymmetric synthesis in the leaf still remains to be found, yet it may be suggested that the presence of a suitably oriented surface may be the determining factor. It is at any rate easier to envisage the possibility of asymmetric photosynthesis in a heterogeneous than in a homogeneous system.

Conclusions.

1. A marked similarity exists between photosynthesis *in vivo* and that now recorded as having been achieved *in vitro*. This is established by the following features which appear to be common to both.

2. Ordinary formaldehyde does not take part in the reaction in either case.

3. The laboratory process has been realised by the action of light on carbonic acid adsorbed on a surface. There seems little doubt that a limiting surface exists in the chloroplast and is necessary for the photosynthesis to take place.

4. A visibly coloured surface and visible light function in each of the two processes.

5. A marked fatigue effect is observed when the living leaf is exposed to too long and intense illumination, and very intense illumination destroys the chlorophyll. In the laboratory a similar fatigue effect, due to poisoning of the surface by oxygen, is observed. Intense and prolonged illumination destroys the carbohydrate, there being present nothing which is analogous to the chlorophyll.

6. In both processes there is a slow recovery reaction, and it appears that in

both the photosynthesis must not proceed at a more rapid rate than that recovery reaction.

In addition to the foregoing, the following conclusions have been reached :—

7. The total yield of organic products photosynthesised *in vitro* per hour per sq. cm. of surface is not seriously at variance with that produced in the leaves of four plant species.

8. It is possible that the constant ratio of chlorophyll A to chlorophyll B, observed by Willstätter and Stoll in the living leaf, is maintained by the carotin, which becomes oxidised to xanthophyll. Since the ratio of xanthophyll to carotin tends to increase during photosynthesis, it may be suggested that the slow recovery process present in the leaf is that in which the xanthophyll is again reduced to carotin.

9. It follows from 6 that it is to be expected that there must be present in the living leaf some internal mechanism which controls the rate of photosynthesis so that it does not exceed that of the slow-recovery reaction. It is suggested that the orientation of the chloroplasts with respect to the direction of the light rays is one of the details of this mechanism.

We again express our thanks to Messrs. Brunner, Mond & Co. for their valuable assistance. The experimental work which has led to the arguments advanced in this paper was alone rendered possible by the generous grants which this firm has from time to time made to these laboratories.

The Electron as a Vector Wave.

By Prof. C. G. Darwin, F.R.S.

(Received July 30, 1927.)

In an article in 'Nature'* last February I put forward a suggestion, of necessity in so concise a form as to be not very easily intelligible, that when the magnetic properties of the atom are regarded from the point of view of the wave mechanics, they suggest that the electron is to be taken as a wave of two components, like light, not of one like sound. The theory and its mathematical development were only outlined in 'Nature,' and the object of the present work is to give them in fuller detail. Recently Pauli† has published a paper on the same subject, and arrived at the same mathematical results, but owing to the fact that he is more disposed to regard the wave theory as a mathematical convenience and less as a physical reality, he stops short of the point which was the guiding principle to me, and refuses to interpret the two functions that we both obtain as formed from a vector. I shall therefore here develop somewhat fully the arguments and analogies which seem to me to show that the vector is the right form in which to regard it.

The chief part of the paper is concerned with developing the results given in 'Nature'; owing to other work I have not carried the matter much farther yet. The main new points are general formulæ for the intensities of spectral lines, and for the magnetic moment, and the form the theory must take for several electrons—in which my first suggestion was wrong, and which Pauli has developed from his point of view. In a future paper I hope to discuss the motion of a free electron in a magnetic field, together with other problems. Since writing the account of the theory in 'Nature' I have had the immense benefit of a visit to Prof. Bohr's Institute in Copenhagen, and have thus enjoyed the advantage of discussing the subject with him, Dr. Klein and the other members in detail. I may take the opportunity here to express my thanks to them for their interest in the matter and for many helpful criticisms.

§ 1. It may not be amiss to begin with a short review of the theory of the spinning electron and of the wave theory of matter before proceeding to the union of the two ideas, because both are still mainly to be found only in the original publications.

---

* 'Nature,' vol. 119, p. 282 (1927).

† Pauli, 'Z. f. Physik,' vol. 43, p. 601 (1927). I must thank the author for the sight of the paper in proof.

When the chief features of the Zeeman effect had been worked out,* it became apparent that the mechanical models of the atom which were in vogue were faced with a fundamental difficulty. They predicted a certain number of stationary states for the atom, whereas the Zeeman effect clearly showed that there were exactly twice as many. For example, the sodium spectrum is practically due to the action of one electron, and it would be expected that its p-levels would be singlets splitting into three in a magnetic field, whereas, in fact, they are doublets splitting into six. It is possible to imagine that some small change, such as a new law of force, might make a difference in the positions of the levels, but to obtain a different *number* of levels must certainly require a radical change of principle.

The first attempt to meet the difficulty was made by introducing a rather mystical " duality "†—in a sense the present work is something of a return to this idea—but this was soon replaced by the introduction of the spinning electron.‡ If the electron is endowed with polarity, it has more degrees of freedom than the three co-ordinates of its centre, and so it at once becomes possible to explain the doubling of the levels. Starting with this idea, the Zeeman effect determines precisely what the spinning electron must be like. It must have angular momentum $\frac{1}{2} . h/2\pi$ and it must have magnetic moment $eh/4\pi mc$. The positive and negative values of the momentum give the doubling. On account of the magnetic moment it is sometimes called the " magnetic electron," but that suggests that it is like a little bar-magnet tied to an electric charge and so tends to make us forget the mechanical angular momentum, which is just as essentially one of its qualities.

The spinning electron also explains the distance between the levels of doublets. Just as a moving electric charge experiences a mechanical force in a magnetic field, so a moving magnetic pole would experience a force in an electric field, and a moving magnet will therefore experience a couple. Corresponding to this there will be a term in the expression for the energy and so an effect on the spectrum. The first calculation of this effect indicated a doublet separation twice as great as the actual one; but the source of the error was later found to lie in a rather subtle property of the kinematics of relativity.* If a body is accelerated, but not acted on by any couples, and if it finally returns to its original position, it will nevertheless have altered its orientation. This has the effect of contributing a negative term to the energy, which happens to be just half that given by the first calculation and so halves it in the required manner.

---

* See, for instance, Andrade, 'The Structure of the Atom,' 3rd ed., ch. XV. It is not possible in this section to refer directly to much of the important work, and the references are only to a few of the more recently published papers.

† Heisenberg,' 'Z. f. Physik,' vol. 26, p. 291 (1924).

‡ Uhlenbeck and Goudsmit, 'Naturwiss.,' Nov. 20, 1925.

The "doublet effect" has a most important influence on the hydrogen spectrum. The approximation for Sommerfeld's original fine structure formula was $\frac{8\pi^4 e^8 m}{c^2 h^4 n^3} \cdot \frac{1}{k}$, with n, k integers and $n \geqslant k \geqslant 1$, and this was fully verified by experiment. Now the wave theory clearly indicates that the last factor should be not $1/k$ but $1/(k + \frac{1}{2})$. However, the doublet effect puts this right by splitting the level into two,† bringing one up to $1/(k + 1)$, and the other down to $1/k$. There are twice as many levels as before, but they are now paired so that the upper level for k coincides with the lower for $k + 1$. Thus the remarkable result emerges that the original theory was neither right nor wrong, but in a literal sense half right.

We must now turn to the wave theory. Though this has on the whole been chiefly used as a calculus of stationary states,‡ yet its inception by de Broglie and some of its developments§ show that for many purposes we must regard the electron as a wave. The motion of an electron in free space, or in the presence of weak electric and magnetic fields can be treated by the ordinary theory of waves, and is only more complicated than, say, the theory of sound, by the fact that the phenomenon of group-velocity plays a very important part. Such a problem is, however, unduly simple, because it is possible to regard the wave of the electron as in ordinary space, whereas in any general mechanical system the wave is in a peculiar space, the "co-ordinate space" of the system. For example, the wave equation for the spin of a rigid body is in a space of the three Eulerian angles, and as these have cyclic ranges of admissible values it is very hard to visualise.

If we attack the problem of the spinning electron by regarding it as a rotating body, we have the wave in a space of six dimensions, and since three of them are the Eulerian angles, we lose all simplicity of visualisation. We also encounter more fundamental difficulties. For the wave calculus shows that the stationary states correspond to angular momenta which must be *integral* multiples of $h/2\pi$, whereas the value $\frac{1}{2} . h/2\pi$, which is required to the exclusion of all others, is inadmissible. Instead of doubling the number of states, we have multiplied them by infinity, and even then have not got those we wanted. So we have to make two special hypotheses, which apply to no other problem. First we have to suppose that for the spin only the lowest quantum state is allowable ; this is perhaps not unnatural, but still it is an extra assumption. Then, and this is more serious, it can be shown that the wave function associated with each state is not single-valued, as it is in all other problems, but is double-valued* ; for only so can we get the value $\frac{1}{2} . h/2\pi$. If it is hard to visualise even a single-valued function in the space of the Eulerian angles, a double-valued function forces us to give up the attempt altogether.

---

* Thomas, 'Nature,' vol. 117, p. 514 (1926), and 'Phil. Mag.,' vol. 3, p. 1 (1927); Frenkel, 'Z. f. Physik,' vol. 37, p. 243 (1926).

† Several writers simultaneously worked this out. The formulæ may be found in a rather later paper by Heisenberg and Jordan, 'Z. f. Physik,' vol. 37, p. 263 (1926).

‡ Schrödinger, 'Ann. d. Physik,' vol. 79, pp. 361 and 489, etc. (1926).

§ Davisson and Germer, 'Nature,' vol. 119, p. 558 (1927).

The main objections to making a direct application of the accepted wave theory to the spinning electron thus are—(1) that the simplicity of visualisation is entirely lost by the spin, (2) that we only require to double the number of states and have multiplied them by infinity, (3) that the wave problem is entirely exceptional in that we have to introduce double-valued functions. All these objections are met at the outset if we take the analogy of light and assume that, just as there are two independent polarised components in a wave of light, so there are two independent components in the wave of an electron. We cannot expect any exact similarity in the wave equations, because when a light *wave* is analysed into its components, as when considering the *rays* traversing a doubly refracting medium, the polarisations are mutually perpendicular ; but when the electron *wave* is analysed by a Stern-Gerlach experiment, the associated *rays* (or particles) are polarised anti-parallel.

Under these circumstances (and after a good many unsuccessful direct attacks on the problem) it seemed best to proceed by empirically constructing a pair of equations to represent the fine structure of the hydrogen spectrum. All the features of the spinning electron are embodied in this spectrum, so that, if we can fit it, we can be sure that all other known cases will also work. When we

---

* If we admit double-valued functions, doublet spectra can be worked out by the methods applied to all multiplets in a recent paper of the present writer (' Roy. Soc. Proc.,' A, vol. 115, p. 1). If χ, λ, μ are the Eulerian angles, the proper functions for the rotation are

$$\cos\frac{\chi}{2}\, e^{i(\lambda+\mu)/2}, \quad \sin\frac{\chi}{2}\, e^{i(-\lambda+\mu)/2}.$$

The functions f, g, which we shall meet later, are from this point of view the coefficients of these two expressions.

have got the two equations for hydrogen, we shall readily see how they can be put into vector form, so as to correspond to the guiding physical idea from which the investigation started.

The hypothesis does not and is not intended to abolish the spinning electron, but only the representation of its wave by means of a rotating body. To understand this we may turn for a moment to the problem of two electrons, since the case of one has the special simplification that the co-ordinate space in which its wave equations occur is so like the ordinary space of geometry that it is quite possible to confuse the spaces together. In forming the wave equation for two " point-electrons " (electrons without spin), we cannot avoid proceeding as follows :—We first suppose them as points in geometrical space and set down the Hamiltonian. Then we reinterpret this as a differential equation in an essentially different space—the co-ordinate space of the two electrons. In fact, the passage from the wave equation of one electron to that of two must lead through the Hamiltonian, and the process cannot be short-circuited. If this is true for the electric charges, it would be most unnatural to expect a short-circuiting for the magnets. To go from the vector waves of one electron to those of two, we must pass through a Hamiltonian stage, and in this stage the expression of the vector character is embodied in the spinning electron.

We may conclude with a general argument, which theory is still too incomplete to develop further. The Schrödinger calculus works absolutely correctly only when there are no magnetic forces, and this implies that the field is determined by the electrostatic potential, the vector potentials vanishing. We thus have a correspondence between the one potential and the one Schrödinger wave function. There are really four potentials, and so, if the correspondence is to be maintained, there should be four wave functions, and this is exactly what we shall obtain.

§ 2. We require to invent two functions f and g of x, y, z, which shall obey equations with the following properties :—To account for the gross properties of the hydrogen spectrum, f, g must both approximately satisfy Schrödinger's equation for hydrogen. They must not, however, exactly satisfy it because they have to explain the fine structure. Each level given by the Schrödinger equation must become two, and when there is a magnetic field these levels must " perturb " one another, so as to explain the Paschen-Back effect.

The most natural, and perhaps the only, way of getting these qualities is to take equations of the form

$$\begin{aligned} \mathrm{D}f + \alpha f + \beta g &= \mathrm{W}f \\ \mathrm{D}g + \gamma f + \delta g &= \mathrm{W}g, \end{aligned} \tag{2.1}$$

where $D\psi = W\psi$ is the Schrödinger equation for the stationary states of the gross structure, while α, β, γ, δ are small perturbing operators in x, y, z. Consider how such equations are solved by successive approximation. To simplify the matter we will first suppose that the solution of $D\psi = W\psi$ is not degenerate. Then there will be a sequence of proper values W_n and proper functions ψ_n which are orthogonal and which we suppose normalised. We have to find what solutions will give proper values of W near W_n. Extending Schrödinger's method of approximation we take

$$\begin{aligned} f &= a\psi_n + \Sigma_m a_m \psi_m \\ g &= b\psi_n + \Sigma_m b_m \psi_m, \end{aligned} \tag{2.2}$$

and substitute in our equations. As the solution is to be near W_n, the coefficients a_m, b_m will all be much smaller than a, b. We can expand the function $\alpha\psi_n$ in a sequence of proper functions, say, $\Sigma_m\, \alpha_n{}^m \psi_m$, and so for the others.

Substitute in (2.1) and carry out the usual method of approximation. We start with the null approximation, which may be seen to depend only on the coefficients a, b. We thus obtain

$$\begin{aligned} a(W - W_n) &= a\alpha_n{}^n + b\beta_n{}^n \\ b(W - W_n) &= a\gamma_n{}^n + b\delta_n{}^n, \end{aligned} \tag{2.3}$$

whence

$$(W - W_n - \alpha_n{}^n)(W - W_n - \delta_n{}^n) = \beta_n{}^n\gamma_n{}^n, \tag{2.4}$$

a quadratic for $(W - W_n)$, and so two roots as required. The roots will be near W_n, but will depart from it by amounts depending on $\alpha_n{}^n \ldots \delta_n{}^n$ in a non-linear manner, so that we can expect to be able to represent the interaction of solutions typified by the Paschen-Back effect. For each root we get a ratio $a : b$. By substituting back we obtain as next approximation $a_m = (a\alpha_n{}^m + b\beta_n{}^m)/(W_n - W_m)$, etc., and then proceed in the usual way for the further approximations. In the present work we shall only require the null approximations for a, b which are given by (2.3), for these will suffice to give the next approximation (2.4) for W.

In the case where $D\psi = W\psi$ is degenerate and has k mutually orthogonal solutions $\psi_1 \ldots \psi_k$ all with the proper value $W = W_n$, we must make the substitution

$$\begin{aligned} f &= a_1\psi_1 + \ldots + a_k\psi_k + \Sigma_m a_m \psi_m, \\ g &= b_1\psi_1 + \ldots + b_k\psi_k + \Sigma_m b_m \psi_m, \end{aligned}$$

where ψ_m refers to values of W other than W_n and a_m, b_m are small. By a process similar to the above we at once see that there will be $2k$ solutions near W_n, that is, double the number given by Schrödinger's single equation. Associated with them there will be $2k$ pairs of functions for f and g. These will not be in general the same sets of combinations of $\psi_1, \ldots \psi_k$, but there is no need for us to examine them further. In the particular case that we require, it happens that the natural choices for $\psi_1, \ldots \psi_k$, the spherical harmonic functions, are themselves the proper functions f, g when suitably paired and multiplied by suitable factors a, b.

The form of α, β, γ, δ for our problem was found by setting down a simple system of equations which give all doublet levels—it is given below in (3.6) as derived from our solution. By examining the p-levels, terms in $\alpha, \ldots \delta$ can be found which easily suggest general forms, and these forms are then readily verified in the general case. It will suffice here to pursue the opposite course, and, taking the equations as given, to show how they lead to the hydrogen spectrum.

§ 3. We write the equations in the general form suitable for the relativity transformation—this involves the introduction of t as one of the independent variables. Let e be the numerical value of the charge of the electron,[*] m its mass, N the atomic number of the nucleus and H the external magnetic field acting along z. Then if

$$\mathrm{D} = \Delta - \frac{1}{c^2}\frac{\partial^2}{\partial t^2} - \left(\frac{2\pi mc}{h}\right)^2 + 2\,.\,\frac{2\pi i}{c^2 h}\,.\,\frac{\mathrm{N}e^2}{r}\frac{\partial}{\partial t} + \frac{2\pi i e\mathrm{H}}{ch}\left(x\frac{\partial}{\partial y} - y\frac{\partial}{\partial x}\right) + \left(\frac{2\pi \mathrm{N}e^2}{ch}\right)^2\frac{1}{r^2}, \tag{3.1}$$

the equation $\mathrm{D}\psi = 0$ is the Schrödinger equation for the hydrogen spectrum, written as by Dirac[†] and Klein.[‡]

Let

$$y\frac{\partial}{\partial z} - z\frac{\partial}{\partial y} = \mathrm{R}_1, \quad z\frac{\partial}{\partial x} - x\frac{\partial}{\partial z} = \mathrm{R}_2, \quad x\frac{\partial}{\partial y} - y\frac{\partial}{\partial x} = \mathrm{R}_3.$$

Then our equations are given as

$$\left.\begin{aligned}\left(\mathrm{D} - \frac{2\pi e\mathrm{H}}{ch}\right)f + \tfrac{1}{2}\frac{\mathrm{N}e^2}{mc^2}\frac{1}{r^3}\left(-i\mathrm{R}_1 g - \mathrm{R}_2 g + i\mathrm{R}_3 f\right) = 0 \\ \left(\mathrm{D} + \frac{2\pi e\mathrm{H}}{ch}\right)g + \tfrac{1}{2}\frac{\mathrm{N}e^2}{mc^2}\frac{1}{r^3}\left(-i\mathrm{R}_1 f + \mathrm{R}_2 f - i\mathrm{R}_3 g\right) = 0\end{aligned}\right\}. \tag{3.2}$$

We solve these by approximations. The null approximation will be given by omitting the last two terms in D and neglecting terms in $1/c^2$. This we call D_0. The solution of $D_0\psi = 0$ is, in polar co-ordinates, of the form

---

[*] We mean that $e = +4\cdot77 \times 10^{-10}$ ESU.

[†] 'Roy. Soc. Proc.,' A, vol. 112, p. 661 (1926).

[‡] 'Z. f. Physik,' vol. 41, p. 407 (1927).

$$\begin{aligned}\psi &= \psi_{n,k,u}\\ &= f_n^k\left(\frac{4\pi^2 Ne^2 m}{h^2(n+1)}\,r\right)P_k^u(\cos\theta)\,e^{iu\phi}e^{-i\frac{2\pi}{h}(mc^2+W_n)t},\end{aligned} \tag{3.3}$$

where

$$f_n^k(z) = e^z z^k\left(\frac{d}{dz}\right)^{n+k+1} e^{-2z}z^{n-k} \qquad (k \leqslant n),$$

$$P_k^u(x) = (k-u)!\,(1-x^2)^{u/2}\left(\frac{d}{dx}\right)^{k+u}\frac{(x^2-1)^k}{2^k\,.\,k!} \qquad (-k \leqslant u \leqslant k),$$

$$W_n = -\frac{2\pi^2 N^2 e^4 m}{h^2(n+1)^2} \qquad (n \geqslant 0).$$

This is precisely the original Schrödinger solution and calls for no further comment.

The system is degenerate in both k and u. To solve we therefore change the time factor in $\psi_{n,k,u}$ into exp. $-\frac{i2\pi}{h}(mc^2 + W_n + \overline{W})$ and take

$$\left.\begin{aligned} f &= \Sigma_{k,u}a_{k,u}\psi_{n,k,u}\\ g &= \Sigma_{k,u}b_{k,u}\psi_{n,k,u}\end{aligned}\right\}, \tag{3.4}$$

omitting at once all the smaller terms corresponding to other values of n, as these are only required for the higher approximations. We have

$$D\psi_{n,k,u} = \left\{\frac{8\pi^2 m}{h^2}\Big[W + C(r)\Big] - \frac{2\pi eH}{ch}u\right\}\phi_{n,k,u},$$

where

$$C(r) = \frac{8\pi^4 N^4 e^8 m}{c^2 h^4 (n+1)^4}\left\{\frac{1}{4} - \frac{(n+1)^2 h^2}{4\pi^3 Ne^2 m}\frac{1}{r} + \left[\frac{(n+1)^2 h^2}{4\pi^2 Ne^2 m}\right]^2\frac{1}{r^2}\right\}.$$

We next work out the perturbation terms. It is easy to show that

$$\begin{aligned}(R_2 + iR_1)\,\psi_{n,k,u} &= e^{-i\phi}\left(\frac{\partial}{\partial\theta} - i\cot\theta\,\frac{\partial}{\partial\phi}\right)\psi_{n,k,u}\\ &= (k+u)\,\psi_{n,k,u-1}\end{aligned}$$

$$\begin{aligned}(R_2 - iR_1)\,\psi_{n,k,u} &= e^{i\phi}\left(\frac{\partial}{\partial\theta} + i\cot\theta\,\frac{\partial}{\partial\phi}\right)\psi_{n,k,u}\\ &= -(k-u)\,\psi_{n,k,u+1}.\end{aligned}$$

(The reason for the slightly unusual definition of the spherical harmonic P_k^u is that it is available for both positive and negative u, makes $P_k^{-u} = (-)^u P_k^u$, and enables us to run scales of relation through the zero value without trouble.)

We also have $R_3 \psi_{n,k,u} = iu\psi_{n,k,u}$.

Substitute these results in (3.2) and we have

$$\Sigma a_{k,u} \left\{ \frac{8\pi^2 m}{h^2} [\overline{W} + C(r)] - \frac{2\pi e H}{ch}(u+1) \right\} \psi_{n,k,u} + \tfrac{1}{2} \frac{Ne^2}{mc^2} \frac{1}{r^3} \left\{ -\Sigma b_{k,u}(k+u)\psi_{n,k,u-1} - \Sigma a_{k,u} u \psi_{u,k,u} \right\} = 0$$

$$\Sigma b_{k,u} \left\{ \frac{8\pi^2 m}{h^2} [\overline{W} + C(r)] - \frac{2\pi e H}{ch}(u-1) \right\} \psi_{n,k,u} + \tfrac{1}{2} \frac{Ne^2}{mc^2} \frac{1}{r^3} \left\{ -\Sigma a_{k,u}(k-u)\psi_{n,k,u+1} + \Sigma b_{k,u} u \psi_{n,k,u} \right\} = 0. \tag{3.5}$$

We next multiply these equations by one of the conjugate quantities $\psi^*_{n,k,u}$ with some particular values of k, u and integrate over all space. By virtue of the orthogonal properties of spherical harmonics only one term out of each sum will survive. As to the radial integrations we have terms involving

$$\int (f_n^k)^2 r^2 dr \,.\, r^{-s},$$

with $s = 0, 1, 2, 3$. These have been worked out,[†] so that we may quote the results. We thus find that for every pair of admissible[‡] values of k and u:[§]

$$\begin{gathered} a_{k,u}\{\overline{W} - W_1 - \beta u - \omega(u+1)\} - b_{k,u+1}\,\beta(k+u+1) = 0 \\ -a_{k,u}\,\beta(k-u) + b_{k,u+1}\{\overline{W} - W_1 + \beta(u+1) - \omega u\} = 0, \end{gathered} \tag{3.6}$$

where

$$W_1 = \frac{8\pi^4 N^4 e^8 m}{c^2 h^4 (n+1)^3} \left(\frac{3}{4} \cdot \frac{1}{n+1} - \frac{1}{k+\frac{1}{2}} \right)$$

$$\beta = \frac{4\pi^4 N^4 e^8 m}{c^2 h^4 (n+1)^3} \, \frac{1}{k(k+\frac{1}{2})(k+1)}$$

$$\omega = \frac{eHh}{4\pi mc}.$$

[†] See, for example, Waller, 'Z. f. Physik,' vol. 38, p. 635 (1926).

[‡] The value $u = -k-1$ is admissible, because the coefficient $b_{k,-k}$ is so, though $a_{k,-k-1}$ is not.

[§] Equations equivalent to these were given by Heisenberg and Jordan, *loc. cit.*

These give all the levels of a doublet spectrum. Since k has the same value in all the suffixes of (3.6) we see that the degeneracy in k plays no part in the positions of the levels. Taking a given value of k we only have to fill in all permissible values of u in (3.6).

There are first two exceptional cases obtained by putting $u = k$ and $-k-1$, because there are no coefficients $b_{k,\,k+1}$ and $a_{k,\,-k-1}$. For these

$$\overline{\mathrm{W}} = \mathrm{W}_1 + \beta k + \omega (k+1)$$

$$\overline{\mathrm{W}} = \mathrm{W}_1 + \beta k - \omega (k+1)$$

at all strengths of field. These give the two extra components of one member of the doublet.

For other values of u we have

$$[\overline{\mathrm{W}} - \mathrm{W}_1 - \beta u - \omega (u+1)]\,[\overline{\mathrm{W}} - \mathrm{W}_1 + \beta (u+1) - \omega u] = \beta^2 (k-u)(k+u+1), \qquad (3.7)$$

so that in weak fields ($\omega \ll \beta$)

$$\overline{\mathrm{W}} = \mathrm{W}_1 + \beta k + \omega \frac{(u+\frac{1}{2})(k+1)}{k+\frac{1}{2}} \text{ and } \mathrm{W}_1 - \beta (k+1) + \omega \frac{(u+\frac{1}{2})\,k}{k+\frac{1}{2}}$$

and in strong fields ($\omega \gg \beta$)

$$\overline{\mathrm{W}} = \mathrm{W}_1 + \beta u + \omega (u+1) \text{ and } \mathrm{W}_1 - \beta (u+1) + \omega u.$$

The quantum number m is thus equal to $u + \frac{1}{2}$.

In the absence of a magnetic field we have

$$\overline{\mathrm{W}} = \mathrm{W}_1 + \beta k = \frac{8\pi^4 \mathrm{N}^4 e^8 m}{c^2 h^4 (n+1)^3} \left[\frac{3}{4} \cdot \frac{1}{n+1} - \frac{1}{k+1}\right]$$

and

$$\overline{\mathrm{W}} = \mathrm{W}_1 - \beta (k+1) = \frac{8\pi^4 \mathrm{N}^4 e^8 m}{c^2 h^4 (n+1)^3} \left[\frac{3}{4} \cdot \frac{1}{n+1} - \frac{1}{k}\right] \qquad (3.8)$$

which shows how the doublet separation leads to Sommerfeld's original expression for the fine structure of hydrogen.

From the evidence of X-ray spectra it is believed that Sommerfeld's expression should be exactly verified, whereas (3.8) is only its first approximation and is only verified to that degree.* Pauli has attempted a second approximation, but does not get the exact result. So we can only claim that our equations (3.2) are valid to the first approximation, and must be prepared for a future addition of still smaller terms.

---

* It should be observed that our work, like that of Heisenberg and Jordan, gives a wrong result for $k = 0$. This is hardly surprising as we are expanding in inverse powers of k. The Zeeman effect is, however, still correct.

§ 4. The equations (3.2) have the property that by a suitable recombination they can be restored to the same form when axes are changed in direction—apart from the special choice we have made for the external magnetic field. For example, if we wish to use x as prime axis instead of z, we can restore the equations to their original form by taking the equations in $f+g$ and $f-g$. The general rule of recombination is not hard to work out, and depends on the use of the "Cayley-Klein parameters" of a rigid body.* This is the method used by Pauli, but we need not enter into it here. It is the very essence of the present work that this invariance connotes the existence of a vector, and when we have obtained one there is no need for such a complicated procedure.

Consider the following analogy:—Suppose that we were doing experiments with ordinary light, and trying to work out the wave equations of light from them. We should find that the light depended on two quantities, really the two polarised components. We should set up two wave equations involving two independent unknowns—we might, for example, have equations for E_x, E_y but without E_z. These equations would be quite unsymmetrical in appearance—or at any rate the associated formulæ for intensity would be so†—but would have the property that by changes in the dependent variables E_x, E_y they could be made to assume the same form for a change of axes. We should, therefore, try to modify them by the introduction of a new variable until they become invariant in *form* as well as in *fact*. As soon as we have succeeded in doing so, we have obtained a vector. In the example we, of course, should introduce the quantity E_z and the relation div. $E = 0$, and should then find that if E_x, E_y, E_z obey the same law of transformation as x, y, z, the equations can be put in the invariant form $\Delta E = \frac{1}{c^2}\frac{\partial^2 E}{\partial t^2}$; div. $E = 0$, and that perfectly symmetrical and invariant formulæ will then give the intensity. This is the condition for the existence of E as a vector. The *necessary and sufficient condition* for the existence of a vector is that equations can be set down which are invariant in form for a change of axes, when the dependent variables obey the same law of transformation as x, y, z. In more general cases of invariance it may be necessary to use a tensor instead of a simple vector. Thus the existence of a set of equations with solution independent of changes of axes implies that, provided we can obtain an invariant *form*, we shall have a tensor associated with the variables. This is purely a matter of definition. Anyone

[*] See, for instance, Whittaker's 'Analytical Dynamics,' ch. I.

[†] This alternative must be given because the equations will actually be $\Delta E = \frac{1}{c^2}\frac{\partial^2 E}{\partial t^2}$ for both E_x and E_y.

who rejects this argument for the electron must be prepared for consistency to reject the whole ordinary interpretation of the electromagnetic theory.

We may consider our example somewhat further. There are many different ways in which the equations for light can be put into invariant form. For example, we might by chance have been led to equations in the magnetic forces, or to the electromagnetic equations in both electric and magnetic forces; the process of modification will throw no light on which the vector we get will be. A historical example of this point arises in the discussions of the nineteenth century as to whether in a doubly refracting medium the electric force, magnetic force, or electric current was the light vector. In particular we might have arrived at the four electromagnetic potentials; these involve an undetermined vector relation between them, and the process would not help to decide what this relation should be. It is only by a comparison with phenomena derived from other sources (electrostatics and current electricity) that we can decide—or even define—more precisely the physical meaning of our vector. We therefore conclude that when we have the equations of the electron in vector form, we may quite possibly not have them in the best vector form. Improvement can only come from importing some new principle, and even so as far as concerns the theory of spectra all forms must prove mathematically equivalent.

§ 5. The process of deriving a system of equations in invariant form from (3.2) is simple. Take any two arbitrary constants α, β, and form the equations for the following quantities:—

$$\begin{aligned} X_1 &= \alpha f + \beta g \\ X_2 &= i\alpha f - i\beta g \\ X_3 &= -\beta f + \alpha g \\ X_4 &= i\beta f + i\alpha g \end{aligned} \qquad (5.1)$$

They are

$$\begin{aligned} DX_1 - U_1X_4 - U_2X_3 + U_3X_2 &= 0, \\ DX_2 - U_2X_4 - U_3X_1 + U_1X_3 &= 0, \\ DX_3 - U_3X_4 - U_1X_2 + U_2X_1 &= 0, \\ DX_4 + U_1X_1 + U_2X_2 + U_3X_3 &= 0, \end{aligned} \qquad (5.2)$$

where

$$U_1 = \tfrac{1}{2}\frac{Ne^2}{mc^2}\frac{1}{r^3}\left(y\frac{\partial}{\partial z} - z\frac{\partial}{\partial y}\right),$$

$$U_2 = \tfrac{1}{2}\frac{Ne^2}{mc^2}\frac{1}{r^3}\left(z\frac{\partial}{\partial x} - x\frac{\partial}{\partial z}\right),$$

$$U_3 = \tfrac{1}{2}\frac{Ne^2}{mc^2}\frac{1}{r^3}\left(x\frac{\partial}{\partial y} - y\frac{\partial}{\partial x}\right) + i\frac{2\pi eH}{ch}.$$

The operators U are of vector form when we allow for the specialisation that H has been taken along the z axis. We can generalise them by putting in the three components of H, but must, of course, at the same time put in the other two in D in (3.1). We also observe that $\mathrm{N}e\frac{x}{r^3}$ is the x component of the electric force acting on the electron, so that we take as general form of U the vector of which the x component is

$$\mathrm{U}_1 = \tfrac{1}{2}\frac{e}{mc^2}\left(\mathrm{E}_y\frac{\partial}{\partial z} - \mathrm{E}_z\frac{\partial}{\partial y}\right) + i\,\frac{2\pi e}{eh}\,\mathrm{H}_x. \tag{5.3}$$

Then if we regard X_1, X_2, X_3 as the components of a vector and X_4 as a scalar we can write (5.2) in the vector notation

$$\begin{aligned} \mathrm{DX} - \mathrm{U}\,.\,\mathrm{X}_4 - [\mathrm{U}, \mathrm{X}] &= 0, \\ \mathrm{DX}_4 + (\mathrm{U}, \mathrm{X}) &= 0, \end{aligned}$$

and it is now evident that our system is independent of the choice of axes, and by definition we have a vector wave.

In a footnote in Pauli's paper, he mentions that Jordan drew his attention to the use of quaternions in connection with the magnetic properties of the electron. He does not follow up the suggestion, but it is admirably suited to develop the whole matter, and enables us to express the system of equations (5.2) in a single form. Quaternions obey the rule

$$\begin{aligned} j_1^2 = j_2^2 = j_3^2 &= -1, \\ j_1 j_2 = -j_2 j_1 &= j_3, \text{ etc.} \end{aligned} \tag{5.4}$$

Take

$$\left.\begin{aligned} \mathrm{U} &= j_1\mathrm{U}_1 + j_2\mathrm{U}_2 + j_3\mathrm{U}_3 \\ \mathrm{X} &= \mathrm{X}_4 + j_1\mathrm{X}_1 + j_2\mathrm{X}_2 + j_3\mathrm{X}_3 \end{aligned}\right\},$$

and we have as expressing all four equations

$$\mathrm{DX} = \mathrm{UX}.$$

The four equations (5.2) are really only two, for whatever axes are chosen they can be combined into a pair in $\mathrm{X}_1 + i\mathrm{X}_2$ and $\mathrm{X}_3 + i\mathrm{X}_4$ (or any other grouping), and as all results, levels, intensities, etc., depend only on products of conjugate quantities, no different results would arise from the equations in $\mathrm{X}_1 - i\mathrm{X}_2$, $\mathrm{X}_3 - i\mathrm{X}_4$, so that the first pair completely express the problem. It is this fact that makes our vector indeterminate, and from the argument of the last section there is nothing in the theory of spectra which can give the smallest help in making it more precise. Any pair of quantities α, β in (5.1) will fulfil all the necessary conditions, but they must be chosen *once for all*, and not different for each proper value. To see this we may recall that the wave equation is by itself only a calculus of stationary states, and so is a very incomplete account of the quantum theory. It requires supplementing by something which describes the interconnections of the various levels, and at present these interconnections are only expressible by means of intensity formulæ. We shall see that those formulæ would go wrong unless we take the same values for α, β for both the levels of each line. For many purposes the most convenient choice is to take $\alpha = 1$, $\beta = 0$, and so have $X_1 = f$, $X_2 = if$, $X_3 = g$, $X_4 = ig$, but any subsequent change of axes will make this simplicity disappear, since the first three are transformed as a vector, and the fourth is unchanged.

It would be very satisfactory to have some definite physical way of removing the arbitrariness of the vector, and there is some hint of one given by considering an electron in free space. I hope to discuss this in a future paper, but it involves somewhat lengthy consideration of Schrödinger's "wave-packets," which cannot be entered into here ; and as long as we do not go outside the present field of knowledge we cannot expect to find any cogent argument for a definite selection.

An analogy from optics suggests a good reason for expecting the ambiguity. Consider a beam of right-handed circularly polarised light going along z. Provided that we allow of imaginary vectors, this is fully specified by a vector E, which may be taken quite indifferently in any direction in the xy plane. The admission of complex values has imported an extra element of arbitrariness into the vector. Now the whole wave theory of matter is expressed always in terms of complex quantities, though from its strong resemblance to the theory of light it is hard to believe that this is essential. So we may conjecture that the exclusion of complex quantities may be expected to give a much more precise meaning to the vector. Up to the present I have had no success in making this step. It does not appear possible with a single vector, and if we try with two—very loosely analogous to the electric and magnetic forces—a further degree of arbitrariness is imported. All this illustrates the fact that we cannot improve the form of the vector without importing some foreign principle to help, for any of the vectors admitted by (5.1) are equally good to give all the results about which we know.

§ 6. We shall now derive the formulæ for the intensity of spectral lines and for the magnetic moment of the atom. The complete theory is complicated by the fact that a moving magnet emits radiation, and so it is not sufficient simply to take the electric density in the manner of Klein[†] and calculate the emission on that basis. A preliminary investigation shows that in consequence of this extra radiation there are minute changes in the intensities of the lines of the doublet spectra, but no new lines or polarisations. In triplet spectra, of course, the new terms are of capital importance in determining the triplet-singlet intercombinations. We shall here omit these considerations and derive the ordinary formulæ for intensity empirically, limiting ourselves to the relative intensities of the components of each multiplet.

In Schrödinger's theory intensities are calculated by finding the normalised proper functions ψ_p, ψ_q of the levels concerned, and then taking $\psi_p\psi_q^*$ as electric density. The obvious generalisation is to take $\sum_{\lambda=1}^{4} X_\lambda^p X_\lambda^{q*}$ as electric density, normalising the X's so that $\int \sum_{\lambda=1}^{4} |X_\lambda|^2\, dx\, dy\, dz = 1$. We shall show that this gives the correct relative values.

If we substitute from (5.1), assuming that α and β can be chosen differently for the two levels, we obtain as the density $2(\alpha_p\alpha_q^* + \beta_p\beta_q^*)(f_pf_q^* + g_pg_q^*)$, while in the two normalisations there will occur respectively factors $2(\alpha_p\alpha_p^* + \beta_p\beta_p^*)$ and $2(\alpha_q\alpha_q^* + \beta_q\beta_q^*)$. Thus the factors in α, β will affect the value of the intensity if they are chosen to be different for the two levels.[‡] Since we obtain the observed results by taking them the same, we conclude that α, β must be the same constants for all levels of the atom. This principle goes beyond those which depend on the wave equation, but is just as essential a part of the complete theory.

We can now set down the formulæ for *intensity*. For the three types of polarisation we have (omitting a factor for the absolute value)

$$[p \rightarrow q] = \frac{\left|\int \left\{\begin{matrix} x+iy \\ 2z \\ x-iy \end{matrix}\right\} \sum_{\lambda=1}^{4} X_\lambda^p X_\lambda^{q*}\, dx\, dy\, dz\right|^2}{\int \sum_{\lambda=1}^{4} |X_\lambda^p|^2\, dx\, dy\, dz \,.\, \int \sum_{\lambda=1}^{4} |X_\lambda^p|^2\, dx\, dy\, dz}$$

$$= \frac{\left|\int \left\{\begin{matrix} x+iy \\ 2z \\ x-iy \end{matrix}\right\} (f_pf_q^* + g_pg_q^*)\, dx\, dy\, dz\right|^2}{\int (|f_p|^2 + |g_p|^2)\, dx\, dy\, dz \,.\, \int (|f_q|^2 + |g_q|^2)\, dx\, dy\, dz}. \qquad (6.1)$$

[†] *Loc. cit.*

[‡] Apart from an arbitrary phase factor which does not seem of much interest.

We substitute in these the known values of f and g in terms of spherical harmonics, and integrate over space. The harmonic formulæ are well known and the radial integration is the same for all components, and so does not matter. We obtain the following results :—

In any solution of (3.6) the quantum number m corresponds to $u + \frac{1}{2}$. Normalise so that

$$a^2_{k,u}(k+u)!\,(k-u)! + b^2_{k,u+1}(k+u+1)!\,(k-u-1)! = 1. \qquad (6.2)$$

Then the intensities of the lines observed from a direction perpendicular to the magnetic field are

$$\begin{bmatrix} k & \rightarrow & k-1 \\ m & & m-1 \end{bmatrix} = \{a_{k,u}a'_{k-1,u-1}(k+u)!\,(k-u)!$$
$$+ b_{k,u+1}b'_{k-1,u}(k+u+1)!\,(k-u-1)!\}^2$$

$$\begin{bmatrix} k & \rightarrow & k-1 \\ m & & m \end{bmatrix} = 4\,\{a_{k,u}a'_{k-1,u}(k+u)!\,(k-u)!$$
$$+ b_{k,u+1}b'_{k-1,u+1}(k+u+1)!\,(k-u-1)!\}^2$$

$$\begin{bmatrix} k & \rightarrow & k-1 \\ m & & m+1 \end{bmatrix} = \{a_{k,u}a'_{k-1,u+1}(k+u)!\,(k-u)!$$
$$+ b_{k,n+1}b'_{k-1,u+2}(k+u+1)!\,(k-u-1)!\}^2 \qquad (6.3)$$

These formulæ readily yield all the well-known results.†

We now turn to the magnetic moment of the atom in any stationary state, and shall proceed in the same empirical manner. The magnetic moment is determined by the energy in a magnetic field; in fact, if W is the energy and H the field strength, $\partial W/\partial H$ is by definition the magnetic moment. Now from (3.7)

$$\left[\frac{\partial \overline{W}}{\partial \omega} - (u+1)\right]\left[\overline{W} - W_1 + \beta(u+1) - \omega u\right]$$
$$+ \left[\frac{\partial \overline{W}}{\partial \omega} - u\right]\left[\overline{W} - W_1 - \beta u - \omega(u+1)\right] = 0,$$

and so multiplying by $a_{k,u}\,b_{k,u+1}$, and using (3.6) we get

$$\left[\frac{\partial \overline{W}}{\partial \omega} - (u+1)\right]a^2_{k,u}(k-u) + \left[\frac{\partial \overline{W}}{\partial \omega} - u\right]b^2_{k,u+1}(k+u+1) = 0,$$

---

† They are immediately comparable with (4.4) (4.5) (4.6) of my paper (' Roy. Soc. Proc.,' vol. 115, p. 1) if we take for the symbols $a_{k,u}$, $b_{k,u+1}$ here, those that are there $a^{kj}_{m-\frac{1}{2},\frac{1}{2}}$, $a^{kj}_{m+\frac{1}{2},-\frac{1}{2}}$.

and hence for the z-component

$$\mu_3 = \frac{eh}{4\pi mc} \frac{(u+1)\, a^2_{k,u}\,(k+u)!\,(k-u)! + u\, b^2_{k,u+1}(k+u+1)!\,(k-u-1)!}{a^2_{k,u}\,(k+u)!\,(k-u)! + b^2_{k,u+1}\,(k+u+1)!\,(k-u-1)!}. \tag{6.4}$$

We have to make an integral formula corresponding to this. Now obviously a chief part of the moment will be given by the convection of electricity. In Schrödinger's theory this gives rise to a density of moment proportional to $\frac{1}{2i}[\psi^* R_3\psi - \psi R_3\psi^*]$, where $R_3 = x\frac{\partial}{\partial y} - y\frac{\partial}{\partial x}$, and this has to be integrated over space. We therefore expect that we shall have a term in

$$\frac{1}{2i}\sum_{\lambda=1}^{4}(X_\lambda^* R_3 X_\lambda - X_\lambda R_3 X_\lambda^*). \tag{6.5}$$

In addition we shall have a term corresponding to the intrinsic magnetism. As a matter of pure vector calculus we should conjecture that this must be proportional to

$$X_1^*X_2 - X_1X_2^* - X_3^*X_4 + X_3X_4^*, \tag{6.6}$$

and, in fact, we easily show that if the X's are normalised by (6.2) we may take

$$\mu_3 = \frac{eh}{4\pi mc}\int\Big\{-\tfrac{1}{2}i\sum_{\lambda=1}^{4}(X_\lambda^* R_3 X_\lambda - X_\lambda R_3 X_\lambda^*) - i\Big(X_1^*X_2 - X_1X_2^* - X_3^*X_4 + X_3X_4^*\Big)\Big\}\,dx\,dy\,dz. \tag{6.7}$$

It we substitute the values of the X's for any level and carry out the integrations, we get the moment as given by (6.4). Since (6.7) is in vector form, we can set down the components of moment in other directions.

The quaternion notation suggests an interesting unity between the electric charge and the magnetic moment. If we make the convention that the quantity conjugate to j_1 is $-j_1$, etc., and form the quaternion XX*, the coefficients are respectively proportional to the electric density and to the expressions of the type (6.6) which are the intrinsic parts of the density of magnetic moment.

§7. It will be useful to compare our work shortly with Pauli's. It must first be emphasised that there is absolutely no difference in mathematical result between them, but only a question of interpretation. Pauli has two functions ψ_α, ψ_β identical with f, g above, and his fundamental assumption that it requires two functions to represent the electron is the essential point of his proceedings. He then works from the general principles of quantum mechanics and arrives at equations for the proper functions identical with (3.2). As these general principles were originally derived from a study of the hydrogen spectrum, etc., it is clearly indifferent whether we use them to describe the hydrogen spectrum, as he does, or use the spectrum to derive them, as has been done here.

He makes use of the principle of angular momentum and derives certain operators s_x, s_y, s_z corresponding to the angular momentum of spin. These operators obey the equations

$$s_x^2 = 1, \text{ etc.},$$

$$s_x s_y = -s_y s_x = -i s_z, \text{ etc.}, \qquad (7.1)$$

and he derives

$$\begin{array}{ll} s_x f = g & s_x g = f \\ s_y f = -ig & s_y g = if \\ s_z f = f & s_z g = -g. \end{array} \qquad (7.2)$$

He then has a rather laborious task, for it is necessary to show that the resulting processes are invariant for changes of axes, which is by no means self-evident with such unsymmetrical formulæ. This he does by means of the Cayley-Klein parameters, and the whole process is rather long. By introducing vectors, even if they are only regarded as a mathematical artifice, his work would be shortened, and if quaternions are used the process reduces to only a few lines, for s_x can be identified with $-ij_1$——in (7.1) (7.2), s_x, etc., have been expressed in units $h/4\pi$, so that we should really take $s_x = \frac{h}{4\pi i} j_1$, etc. All considerations of the Cayley parameters can then be dispensed with.†

There is one problem treated by Pauli which we will next consider. He supposes an assembly of electrons in a magnetic field which suddenly changes its direction. The electrons are first all pointing along, and none away from, the field, and he shows that if the field changes suddenly through an angle θ, a fraction $\cos^2 \theta/2$ will point along and $\sin^2 \theta/2$ away from the new direction. This he urges gives a direct measure of $|f^2|$ and $|g^2|$, and so invests them with a physical reality not possessed by the vector. I hope to discuss the whole matter in a future communication, but as it introduces certain considerations lying rather deep in the whole quantum theory, it would take too long to do so here. But his result does not seem in any way to oppose the vector idea. For what he is really doing is to measure the component of magnetic moment of the electrons in the new direction of the field. As they start with moment $\cos\theta$ and end with ± 1, it is natural that the numbers should be in the ratio $(1 + \cos\theta) : (1 - \cos\theta)$. Moreover, by another experiment, he could determine the component in another direction, and this would give him a definite measure of another combination of f and g, for example $fg^* + gf^*$. Thus he has by no means exhausted the possibilities of experiment, and could find out more than he has claimed.

---

† His formulæ (6″), which also look very unsymmetrical, go immediately into the quaternion form as components of XX^*.

It is perhaps arguable that though we can take it as a matter of definition that the wave is a vector, it is not usefully so regarded. For example, the displacement of a rigid body is often treated by consideration of Eulerian angles, though really independent of any axial system. This is because the problems to be dealt with are concerned with such things as the position of a marked point on the body. As soon as this is not required, as in dealing with angular momentum or velocity, we at once make use of vector methods. As there are certainly no marked points on the electron, it seems natural to do the same here.

The main trouble with the vector method is the arbitrariness of the vector, which we so far lack any principle to fix. In fact, we set down four equations and then at once reduce them to two, which are the same equations as those of Pauli. There is an exact analogue to this in optics, for there we set down no less than eight electromagnetic equations and then express the unknowns in terms of only two, the magnitudes of the amplitudes of the two component waves, and these are not vectors.

Apart from the greater elegance of the formulæ, the real advantage of the vector conception is that it should more readily suggest extensions of application. This it undoubtedly will do, but in the most important such extension, the relativity transformation, the simplest form of the generalisation gives a wrong result, as we shall see. From this point of view all that we can at present claim is that the vector principle helps to make explicit the widespread difficulties in the way of uniting the quantum theory with relativity. If, with Pauli, we do not go beyond the two functions f and g, there is no point of attack on the relativity problem at all.

In conclusion, it may be well to reiterate that there is no difference between the mathematics of Pauli and of the present work. There is thus no question of devising any *experimentum crucis* to discriminate between them. The choice depends only on what is the most convenient set of physical conceptions for us to adopt.

§ 8. The question of several electrons can be treated by similar processes. In my 'Nature' article I only described a very cursory investigation of it which was as a matter of fact wrong, through a partial confusion of ordinary space with the space of the electrons. Pauli has described how the problem must be treated, and his method is readily adapted. It will suffice to treat of two electrons, and we shall only consider the general character of the equations.

The vector (including in the term the scalar fourth component) must be replaced by a quantity that is vectorial for each electron separately, but the equations only have the invariant form for a *simultaneous* change of axes for both electrons. Thus the vector is replaced by a tensor of the second rank. It is not quite like an ordinary tensor, for the ordinary tensor is a function of xyz, whereas this is a function of $x_1y_1z_1$, $x_2y_2z_2$, and invariant only for simultaneous transformation of both sets of co-ordinates. As was pointed out in §1, we cannot expect to proceed directly from the wave equation for one electron to that of two, but must go through the Hamiltonian and the spinning electron, which is the dynamical expression of the vector character of the electron.

The complete system of equations involves 16 unknowns which may be classified as (1) an invariant X_{44}, (2) two vectors X_{14}, X_{24} ... and X_{41} ... , (3) a second-rank tensor X_{11}, X_{12} ... . If, then, we wish to use a tensor notation, we shall have to write down four equations, and this is rather cumbersome. A much quicker method is to use quaternions, or, rather, "double quaternions." We take two incoherent sets $j^{(1)}$, $j^{(2)}$. Among themselves the components of $j^{(1)}$ obey the rules for quaternions (5.4), as do $j^{(2)}$, while such quantities as $j_1^{(1)}j_3^{(2)} = j_3^{(2)}j_1^{(1)}$ are irreducible. Heisenberg* gives the dynamical form for the extra energy of a pair of electrons. It consists of terms

$$Q = V + M^{(1)}s^{(1)} + M^{(2)}s^{(2)} + \sigma\,(s^{(1)}s^{(2)}) + (\rho s^{(1)})\,(\rho s^{(2)})$$

where V is the mutual potential energy, $M^{(1)}$ is a vector function of co-ordinates and momenta of both electrons linear in the momenta, $M^{(2)}$ is the same with interchanged electrons and σ and ρ are symmetric functions of their positions, the latter a vector. To obtain the wave equations we substitute $\frac{h}{4\pi i}\,j^{(1)}$ for $s^{(1)}$, etc., and replace the momenta by $\frac{h}{2\pi i}\,\frac{\partial}{\partial x_1}$, etc., in the usual way. This makes Q into a quaternion operator. We put

$$X = X_{44} + j_1^{(1)}X_{14} + \ldots + j_1^{(2)}X_{41} + \ldots + j_1^{(1)}j_1^{(2)}X_{11} + j_1^{(1)}j_2^{(2)}\,X_{12} + \ldots,$$

and have as the wave equation $DX + QX = 0$, where D is the Schrödinger operator for the gross structure. It is then only necessary to multiply out, and select coefficients of the j's to obtain the 16 wave equations.

---

* 'Z. f. Physik,' vol. 39, p. 499 (1926); see p. 514.

It would take too long to develop here the whole of the formulæ which give the helium spectrum, so I shall only describe the results. Just as with one electron we can reduce the four equations to two, so here we can reduce the sixteen to four, the choice being largely arbitrary. If we have a magnetic field along z, we may conveniently take

$$\begin{aligned}
F_1 &= X_{11} + i\, X_{12} + i\, X_{21} - X_{22} \\
F_2 &= X_{13} + i\, X_{14} + i\, X_{23} - X_{24} + X_{31} + i\, X_{41} + i\, X_{32} - X_{42} \\
F_3 &= X_{33} + i\, X_{34} + i\, X_{43} - X_{44} \\
G &= X_{13} + i\, X_{14} + i\, X_{23} - X_{24} - X_{31} - i\, X_{41} - i\, X_{32} + X_{42}.
\end{aligned}$$

We find that a set of equations, now, of course, not symmetrical, can be constructed between these four quantities. From the forms of the operators it can be seen that if $F_1\, F_2\, F_3$ are antisymmetrical in the co-ordinates of the two electrons, then G is symmetrical, and vice versa. In the case that the coefficients σ and ρ in Q are negligible compared to M, the equations separate into precisely those for a singlet and a standard triplet spectrum.

The exclusion principle of Pauli* (which forbids the two electrons from ever having the same four quantum numbers) takes a very simple form in the present theory. It is simply that for all the sixteen components,

$$X_{\alpha\beta}(x_1\, x_2) = -\, X_{\beta\alpha}(x_2\, x_1).$$

There is no need to discuss the question of more than two electrons, as it obviously goes in the same way, but involves very heavy work. Since this work will occur whatever the fundamental principles, it gives no help in those principles. This sketch will suffice to show how the many-electron problem must be treated from the present point of view.

§ 9. One of the strongest recommendations of the spinning electron is that the anomalous Zeeman effect and the formula for doublet separation can be imputed to the same cause. As was mentioned in the introduction, the first attempt gave a separation twice too great for the doublets. This was by means of the direct relativity transformation, and it required the rather subtle correction of Thomas to halve it. The ordinary form of direct relativity transformation as applied to a system of particles treats of a uniform translatory velocity, and shows that this is equivalent to a rotation of the four-dimensional space-time axes. In the present problem no idea of translatory velocity is comprehensible, but the rotation of the axes retains its meaning and so allows us to carry out the process. Our transformation thus does not really get to the bottom of the problem, and it is hardly surprising that, as will appear, it suggests a doublet separation twice as great as the actual value.

---

* 'Z. f. Physik,' vol. 31, p. 765 (1925).

We must first review a few of the properties of four-dimensional tensors, as these are not very familiar. We only deal with rectangular transformations made according to the annexed scheme. On account of the orthogonal relations it is easy to prove that the determinant formed out of any three rows and columns is (with appropriate sign) equal to the complementary member of the scheme. For example

	x_1	x_2	x_3	x_4
x_1'	l_{11}	l_{21}	l_{31}	l_{41}
x_2'	l_{12}	l_{22}	l_{32}	l_{42}
x_3'	l_{13}	l_{23}	l_{33}	l_{43}
x_4'	l_{14}	l_{24}	l_{34}	l_{44}

$$l_{21} = -\begin{vmatrix} l_{12} & l_{32} & l_{42} \\ l_{13} & l_{33} & l_{43} \\ l_{14} & l_{34} & l_{44} \end{vmatrix}. \qquad (9.1)$$

Also the determinant made of any two rows and columns is equal to the complementary determinant made of the other two rows and columns. For example,

$$\begin{vmatrix} l_{11} & l_{31} \\ l_{12} & l_{32} \end{vmatrix} = -\begin{vmatrix} l_{23} & l_{43} \\ l_{24} & l_{44} \end{vmatrix}. \qquad (9.2)$$

In consequence of (9.1) it is possible to work out the analogy to what is in three dimensions a vector product or curl. If $T_{\alpha\beta\gamma}$ is a tensor of the third rank, it is transformed according to the rule

$$T'_{\delta\epsilon\zeta} = \Sigma_{\alpha\beta\gamma} T_{\alpha\beta\gamma} l_{\alpha\delta} l_{\beta\epsilon} l_{\gamma\zeta}.$$

If $T_{\alpha\beta\gamma} = -T_{\alpha\gamma\beta} = -T_{\beta\alpha\gamma}$ we call it skew-symmetric, and there will be six terms in the sum with the same numerical value, three positive and three negative. The l's of these then form a determinant which reduces to the complementary l, and so T can be regarded as a vector. In any example the quickest way of showing the skew-symmetry is to write T symbolically as a determinant. Thus if $A_\alpha B_\beta C_\gamma$ means symbolically $T_{\alpha\beta\gamma}$, we have

$$\begin{vmatrix} A_1 & A_2 & A_3 \\ B_1 & B_2 & B_3 \\ C_1 & C_2 & C_3 \end{vmatrix}$$

as the 4-component of a vector.

Next consider a skew-symmetrical tensor of the second rank—a so-called six vector. We have

$$T_{\alpha\beta} = -T_{\beta\alpha} \quad \text{and} \quad T'_{\gamma\delta} = \Sigma_{\alpha\beta} T_{\alpha\beta} l_{\alpha\beta} l_{\beta\delta}.$$

We shall show that the system of equations

$$T_{12} = T_{34}, \quad T_{23} = T_{14}, \quad T_{31} = T_{24} \tag{9.3}$$

is invariant for a change of axes when T is skew-symmetrical. This we prove by a direct transformation

$$T'_{12} - T'_{34} = \Sigma_{\alpha\beta} T_{\alpha\beta} (l_{\alpha 1} l_{\beta 2} - l_{\alpha 3} l_{\beta 4}).$$

To save writing a rather long expression we will select the coefficients of T_{12} and T_{34} only. Remembering that $T_{21} = -T_{12}$ we get

$$\begin{aligned} &T_{12} (l_{11} l_{22} - l_{13} l_{24} - l_{21} l_{12} + l_{23} l_{14}) \\ &+ T_{34} (l_{31} l_{42} - l_{33} l_{44} - l_{41} l_{32} + l_{34} l_{43}) \\ &= (T_{12} - T_{34}) (l_{11} l_{22} - l_{12} l_{21} - l_{13} l_{24} + l_{23} l_{14}) \end{aligned}$$

by virtue of the relations (9.2). Similarly for the other coefficients. It follows that if for one system of axes we can throw a set of equations into the form (9.3), that form will hold for any other.

From the general argument of § 4 we know that it may be that we have not got our equations (5.2) into the best possible form, but that that does not matter, as all forms must be mathematically equivalent. Now we have equations involving a vector X_1 X_2 X_3 and a scalar X_4, and nothing could be more natural than to regard X_4 as the time component of the vector—it might need some constant multiplier, but we shall see that none is required.

In generalising we encounter a difficulty at the outset because the equations (5.2) are not right in tensor dimensions. We shall write x_1, x_2, x_3, x_4 for x, y, z, ict and ϕ_1, ϕ_2, ϕ_3, $-i\phi_4$ for vector and scalar potentials. Then in

$$\mathrm{U}_1 = \tfrac{1}{2}\frac{e}{mc^2}\left(\mathrm{E}_y\frac{\partial}{\partial z} - \mathrm{E}_z\frac{\partial}{\partial y}\right) + i\frac{2\pi e}{ch}\mathrm{H}_x$$

we have $\mathrm{E}_y = i\left(\frac{\partial\phi_4}{\partial x_2} - \frac{\partial\phi_2}{\partial x_4}\right)$, so that $\mathrm{E}_y\frac{\partial}{\partial z}$ is the 243 component of a tensor. So, too, $\mathrm{E}_z\frac{\partial}{\partial y}$ is the 342 component, but H_x is a 23 component and of the second, not the third, rank, and so requires an extra x_4 or t component. Now all four components of X involve the time in the form exp. $-i\frac{2\pi}{h}(mc^2 + \mathrm{W})t$, and so to a first approximation $\frac{\partial}{\partial t}\mathrm{X} = -i\frac{2\pi}{h}mc^2 . \mathrm{X}$. Then we may take

$$mc^2\mathrm{U}_1 = \tfrac{1}{2}e\left(\mathrm{E}_y\frac{\partial}{\partial z} - \mathrm{E}_z\frac{\partial}{\partial y}\right) - \frac{e}{c}\mathrm{H}_x\frac{\partial}{\partial t},$$

and this is now the 234 component of a tensor. Taking X as a vector, the first equation of (5.2) may now be written, as far as concerns tensor dimensions, as

$$mc^2\,\mathrm{D} . 1 - (234) . 4 - (134)\,3 + (124)\,2 = 0.$$

It is evident that to make this a possible equation we must first replace the mc^2 by $\partial/\partial t$, for otherwise the first term would be of odd rank and the rest of even, which is impossible. Then, since D is invariant, the first term becomes a 14 component, and the rest must reduce to that too, which it can only do if the bracketed quantities (234), etc., reduce to a vector. They do not so reduce, and therefore the simple relativity generalisation cannot be carried out.

As mentioned above, this is because we are trying to do without the Thomas correction, and that is not permissible. In default of seeing how it is to be brought in, we will imagine the doublet separation to be twice as great as it really is, and shall find that then the whole process can be easily carried through. The terms $\mathrm{E}_y\frac{\partial}{\partial z} - \mathrm{E}_z\frac{\partial}{\partial y}$ are those which fix the doublet separation, and we double their coefficient. Then

$$mc^2\mathrm{U}_1' = e\left(\mathrm{E}_y\frac{\partial}{\partial z} - \mathrm{E}_z\frac{\partial}{\partial y} - \frac{\mathrm{H}_x}{c}\frac{\partial}{\partial t}\right),$$

and this we may write symbolically as

$$-ie\begin{vmatrix} \dfrac{\partial}{\partial x_2} & \dfrac{\partial}{\partial x_3} & \dfrac{\partial}{\partial x_4} \\ \phi_2 & \phi_3 & \phi_4 \\ \dfrac{\partial}{\partial x_2} & \dfrac{\partial}{\partial x_3} & \dfrac{\partial}{\partial x_4} \end{vmatrix}$$

where the first row only operates on the second. It is therefore the 1-component of a vector.

To reduce our equations to invariant form, it now only remains to introduce a number of insignificant terms which are required for symmetry. The equations (5.2) were developed on the basis that the magnetic force is very small compared to the electric, and that the operator $\partial/\partial t$ is much more important as to magnitude than the other differentials. Thus we have only had terms in H which are multiplied by $\partial/\partial t$, but may introduce others in H $\partial/\partial x$, etc., without affecting the approximation. By taking account of these facts we can set down the general form and verify that the added terms are insignificant. First we have to add on to D terms corresponding to the squares of the magnetic field. These bring it to the form

$$\mathrm{D} = \Sigma^4_{\lambda=1}\left(\frac{\partial}{\partial x_\lambda} + i\frac{2\pi e}{ch}\phi_\lambda\right)^2 - \left(\frac{2\pi mc}{h}\right)^2, \tag{9.4}$$

which was used by Dirac and by Klein. This calls for no comment. Next set down the vector

$$\left.\begin{aligned} \mathrm{T}_1 &= \frac{\partial}{\partial x_1}\mathrm{D} + i\frac{2\pi e}{ch}\left\{\left(\frac{\partial\phi_4}{\partial x_3} - \frac{\partial\phi_3}{\partial x_4}\right)\frac{\partial}{\partial x_2} + \left(\frac{\partial\phi_2}{\partial x_4} - \frac{\partial\phi_4}{\partial x_2}\right)\frac{\partial}{\partial x_3} + \left(\frac{\partial\phi_3}{\partial x_2} - \frac{\partial\phi_2}{\partial x_3}\right)\frac{\partial}{\partial x_4}\right\} \\ &\cdot\ \cdot\ \cdot\ \cdot\ \cdot\ \cdot\ \cdot\ \cdot\ \cdot\ \cdot\ \cdot\ \cdot\ \cdot\ \cdot\ \cdot\ \cdot\ \cdot\ \cdot\ \cdot\ \cdot\ \cdot\ \cdot\ \cdot\ \cdot\ \cdot\ \cdot\ \cdot \\ \mathrm{T}_4 &= \frac{\partial}{\partial x_4}\mathrm{D} + i\frac{2\pi e}{ch}\left\{\left(\frac{\partial\phi_3}{\partial x_2} - \frac{\partial\phi_2}{\partial x_3}\right)\frac{\partial}{\partial x_1} + \left(\frac{\partial\phi_1}{\partial x_3} - \frac{\partial\phi_3}{\partial x_1}\right)\frac{\partial}{\partial x_2} + \left(\frac{\partial\phi_1}{\partial x_2} - \frac{\partial\phi_2}{\partial x_1}\right)\frac{\partial}{\partial x_3}\right\} \end{aligned}\right\} \tag{9.5}$$

Then our equations become

$$\begin{aligned} \mathrm{T}_4\,\mathrm{X}_1 - \mathrm{T}_1\,\mathrm{X}_4 - \mathrm{T}_2\,\mathrm{X}_3 + \mathrm{T}_3\,\mathrm{X}_2 &= 0 \\ \mathrm{T}_4\,\mathrm{X}_2 - \mathrm{T}_2\,\mathrm{X}_4 - \mathrm{T}_3\,\mathrm{X}_1 + \mathrm{T}_1\,\mathrm{X}_3 &= 0 \\ \mathrm{T}_4\,\mathrm{X}_3 - \mathrm{T}_3\,\mathrm{X}_4 - \mathrm{T}_1\,\mathrm{X}_2 + \mathrm{T}_2\,\mathrm{X}_1 &= 0 \\ \mathrm{T}_4\,\mathrm{X}_4 + \mathrm{T}_1\,\mathrm{X}_1 + \mathrm{T}_2\,\mathrm{X}_2 + \mathrm{T}_3\,\mathrm{X}_3 &= 0. \end{aligned} \tag{9.6}$$

Here $T_4 X_1 - T_1 X_4$ is a component of a skew-symmetrical tensor of second rank, so that the first three equations are of type (9.3) and therefore covariant for changes of axes. The fourth equation is also invariant. They represent the best that we can do at present for showing the identity of the doublet effect with the Zeeman effect.

It remains to show that the added terms are insignificant. We take the X's as of order unity and consider how they are affected by the various operators. The "radius of the first hydrogen orbit" is $h^2/4\pi^2 e^2 m$, so that we may say that $\partial/\partial x_1$ introduces a factor of order $e^2 m/h^2$, so, too, for $\partial/\partial x_2$, $\partial/\partial x_3$. On the other hand, $\partial/\partial x_4$ introduces a factor $\frac{1}{c} . \frac{2\pi}{h} mc^2$ of order mc/h. The relevant part of space is that at distances comparable with $h^2/4\pi^2 e^2 m$, and so the electric force E is of order $e \Big/ \left(\frac{h^2}{4\pi^2 e^2 m}\right)^2 = \frac{e^5 m^2}{h^4}$, and this is much greater than H, the magnetic force. Finally, the operator D has magnitude determined by the fact that DX differs from zero by an amount determined from the separation of the fine structure, so that we may say that it is of the order $\frac{8\pi^2 m}{h^2} . \frac{8\pi^4 e^8 m}{c^2 h^4}$ or $\frac{e^8 m^2}{c^2 h^6}$. Thus the first term of T_4 is of order $\frac{mc}{h} . \frac{e^8 m^2}{c^2 h^6} = \frac{e^8 m^3}{ch^7}$, and the other three are of order $\frac{e}{ch} . H . \frac{e^2 m}{h}$, which bears to the first the ratio H/E, which is negligible. The first term of T_1 is $\frac{e^2 m}{h^2} . \frac{e^8 m^2}{c^2 h^6} = \frac{e^{10} m^3}{c^2 h^8}$. The second and third are of order $\frac{e}{ch} . \frac{e^5 m^2}{h^4} . \frac{e^2 m}{h} = \frac{e^8 m^3}{ch^3}$. The first bears to this a ratio e^2/ch, which is the "fine structure constant," and so negligible. The fourth is of order $\frac{e}{ch} . H . \frac{mc}{h}$, which bears to the second a ratio $H \Big/ \left(E \frac{e^2}{ch}\right)$, which is not negligible because of the second factor in the denominator. We have thus shown that the first term in T_4 and the second, third and fourth terms in T_1 T_2 T_3 are of the same order of magnitude and greater than the other terms in these expressions. This justifies the equations (9.6).

In view of the fact that we have carried out the same process as Uhlenbeck and Goudsmit, it is quite natural that we have obtained the same result. It is not clear how Thomas's effect is to be brought in, but the above work shows that, as in the dynamical model, we must regard the separation of the doublets as composed of two parts, a doubled separation which we have explained and a negative amount equal to the actual separation, for which a formulation is still to be found. This will doubtless be connected with the fact that the deduction of the Sommerfeld formula for separation ought to be exact and not merely a first approximation. In view of these considerations we cannot regard the theory as at all complete—as, indeed, is true of the whole interconnection of the quantum theory with relativity—but in spite of these blemishes we may hold that to regard the electron wave as a vector wave does provide a promising point of attack on this fundamental problem.

Summary.

In spite of the great success of the spinning electron in the theory of spectra, there are grave difficulties in its interpretation in terms of the wave theory. These are met by making the hypothesis that the wave of an electron, like a wave of light, has two components. Once this hypothesis is made, the consequences here developed follow almost inevitably.

The wave equations are worked out so as to fit the hydrogen spectrum, and this ensures that they will conform to all known conditions of quantum mechanics. They are found to be unsymmetrical, so that they take a different form according to what direction of space is chosen as prime axis.

A general argument from analogy shows that they should therefore be interpreted in terms of a vector, so as to be invariant in form as well as fact. The vector is found to be in some degree arbitrary, and nothing in the theory of spectra can hope to remove this arbitrariness.

Formulæ are developed in vector form for the intensities of spectral lines and for the magnetic moment of the atom.

A short comparison is made with a recent paper of Pauli, who makes the same fundamental hypothesis and therefore gets the same mathematical development, but is unwilling to interpret it in terms of vectors.

The theory is sketched for the case of two or more electrons.

A relativity transformation is applied, so as to identify the "doublet effect" with the Zeeman effect. This encounters the difficulty that it is not at present possible to see what form the Thomas correction should take in the wave theory, and so gives a value for the doublet separation twice as great as it should be. The trouble is no doubt connected with the fact that the hydrogen spectrum has only been verified to a first approximation and goes wrong in the second—a difficulty at present shared by all theories.

The Diffraction of Light by Metallic Screens.

By Prof. C. V. Raman, F.R.S., and K. S. Krishnan.

(Received June 13, 1927.)

1. *Introduction.*

Gouy[*] discovered that when a metallic screen with a sharp and highly-polished edge is held in the path of a pencil of light, its boundary appears as a luminous line diffracting light through large angles, both into the region of shadow (interior diffraction) and into the region of light (exterior diffraction). He noticed further that this diffracted light is strongly polarised, but in perpendicular planes in the two regions mentioned; the colour of the diffracted light and its state of polarisation depend in a remarkable manner on the material of the screen and on the extent to which its edge is rounded off in the process of polishing. When the edge is viewed through a double-image-prism from within the shadow, only that image appears coloured which is more intense and is polarised with the magnetic vector parallel to the edge. The second image which is fainter and is polarised with the electric vector parallel to the edge, appears perfectly white. When the incident light is polarised in any arbitrary azimuth, the diffracted light is found to exhibit elliptic polarisation. These and other results have been confirmed by later observers.[†]

Gouy's experimental results were discussed by Poincaré on the basis of the electromagnetic theory of light in two memoirs published in the "Acta Mathematica."[‡] The special case of an ideal screen (plane or wedge-shaped), supposed perfectly-reflecting and having a sharp edge, is amenable to complete theoretical treatment, and was dealt with by Poincaré himself, and later in a rigorous manner by Sommerfeld,[§] and following him by numerous other mathematicians. The behaviour of actual metallic screens, however, differs considerably from that found theoretically for this ideal case. Though attempts have been made by Poincaré himself in the memoirs quoted, and later also by Epstein,[||] to take the nature of the screen and the rounding of its edge into account, it cannot be said that Gouy's observations have so far received a complete or satisfactory explanation. We propose in this paper to discuss more particularly the

[*] 'Ann. Chim. et Physique,' vol. 8, p. 145 (1886).

[†] W. Wien, 'Wied. Ann.,' vol. 28, p. 117 (1886).

[‡] 'Acta Mathematica,' vol. 16, p. 297 (1892), and vol. 20, p. 313 (1896).

[§] 'Math. Annalen,' vol. 47, p. 317 (1896).

[||] 'Diss. Munich'; also 'Encyklop. d. math. Wissensch.,' vol. V (3), p. 491.

influence of the material of the screen on the diffraction by a sharp edge, and to show how it may be explained in a very simple manner. The case of rounded edges is reserved for discussion in a separate paper.

In the fifth section of his first memoir, Poincaré discussed the electromagnetic boundary conditions at the surface of an imperfectly conducting screen, and made the important remark that the extreme smallness of the depth to which an optical disturbance penetrates into any actual metal, should considerably simplify the theory. In his actual attempt, however, to discuss the problem of diffraction by an imperfectly conducting screen, he made no use of the elegant mathematical methods and results contained in the earlier parts of his memoir, and contented himself with a qualitative discussion on the basis of the Kirchhoff formulation of Huygens' Principle. The treatment given does not, as was indeed remarked by Poincaré himself, appear capable of leading to quantitative results. In the course of our paper, we shall show how it is possible to apply the Fresnel-Huygens' Principle with success to the problem of diffraction by imperfectly-conducting screens. It is more convenient, however, to base our treatment in the first instance on a modification of the known exact solutions for the case of perfectly-reflecting screens or wedges.

2. *Theory.*

Sommerfeld's solution of the wave-equation in cylindrical co-ordinates for the case of a semi-infinite screen which is a perfect reflector and lies in the xz-plane, with its edge along the z-axis, is

$$u = \mathrm{F}(\rho, \phi, \phi_0) \mp \mathrm{F}(\rho, \phi, -\phi_0). \tag{1}$$

The upper (minus) sign refers to the case in which the plane of polarisation and the plane of incidence are parallel to each other; (we shall refer to this as the $\|^{l}$ case), and u then denotes the electric force parallel to the edge. The lower (plus) sign refers to the case in which the plane of polarisation of the incident light is perpendicular to the plane of incidence (we shall refer to this as the $\perp^{r}$ case), u then denoting the magnetic force parallel to the edge.

$$\mathrm{F}(\rho, \phi, \phi_0) = \left(\frac{i}{\pi}\right)^{\frac{1}{2}} e^{i\frac{2\pi t}{\mathrm{T}}} e^{ik\rho\cos(\phi-\phi_0)} \int_{-\infty}^{\tau} e^{-i\lambda^2}\, d\lambda, \tag{2}$$

where

$$\tau = \sqrt{2k\rho} \,.\, \cos\tfrac{1}{2}(\phi - \phi_0).$$

The expression (2) has the property that when τ is positive and sufficiently large, which is the case when $\pi + \phi_0 > \phi > 0$, the function tends to the limiting value $e^{i\frac{2\pi t}{\mathrm{T}}} e^{ik\rho\cos(\phi-\phi_0)}$, which represents a train of plane waves incident on the screen in a direction making an angle ϕ_0 with its plane; when τ is negative and sufficiently large, which is the case when $\pi + \phi_0 < \phi < 2\pi$, the function tends to the limit zero. $F(\rho, \phi, -\phi_0)$ is obtained by writing $-\phi_0$ for ϕ_0. When $\pi - \phi_0 > \phi > 0$ it tends to the limit $e^{i\frac{2\pi t}{T}} e^{ik\rho\cos(\phi+\phi_0)}$, which represents a plane train of waves reflected from the screen. When $\pi - \phi_0 < \phi < 2\pi$, $F(\rho, \phi, -\phi_0)$ tends to the limit zero.

Now the solutions (1) satisfy the conditions $u = 0$ and $\frac{\partial u}{\partial \phi} = 0$ respectively, on both faces of the screen, supposed to be infinitely thin and perfectly reflecting, that is, when $\phi = 0$ and also when $\phi = 2\pi$. Now any actual screen to be opaque must be of finite thickness, hence a solution of the form (1) or any simple modification of it cannot be expected to represent the behaviour of such screens *completely*. Nevertheless, as already mentioned above, a metallic screen of a thickness which is only a small fraction of a wave-length, is practically opaque, and this makes it possible to represent its behaviour with a high degree of accuracy by a comparatively simple modification of (1). Consider expressions of the form

$$u = F(\rho, \phi, \phi_0) - (C_s + iD_s) \,.\, F(\rho, \phi, -\phi_0) \tag{3}$$

and

$$u = F(\rho, \phi, \phi_0) + (C_p + iD_p) \,.\, F(\rho, \phi, -\phi_0) \tag{4}$$

in which the (numerical) factors $C_s + iD_s$ and $C_p + iD_p$ are so chosen that they represent the amplitude of the wave reflected at the illuminated face of the particular screen used, for the particular angle of incidence under consideration. Equation (3) refers to the $\|^l$ case, and (4) to the $\perp^r$ case. Since $C_s + iD_s$ and $C_p + iD_p$ are functions only of the angle of incidence ϕ_0, (3) and (4) continue to satisfy the wave-equation and represent distributions of light and shadow of the same general character as those indicated by (1), with this difference, however, that the disturbance on the illuminated face of the screen expressed by (3) and (4) will have the actual values corresponding to the screen used, while (1) corresponds to a screen with properties which cannot be physically realised. We are therefore justified in expecting that (3) and (4) would represent the disturbance throughout the whole field in the actual problem much more accurately than the Sommerfeld formulæ.

To understand the physical significance of the formulæ, it is best to use the asymptotic expressions for the functions for large values of ρ. We have, when $\cos\frac{1}{2}(\phi - \phi_0)$ is positive,

$$F(\rho, \phi, \phi_0) \backsim e^{i\frac{2\pi t}{T}} e^{ik\rho\cos(\phi-\phi_0)} + \frac{i^{3/2} e^{i\frac{2\pi t}{T}} e^{-ik\rho}}{2\sqrt{2\pi k\rho}\,.\cos\frac{1}{2}(\phi - \phi_0)}, \tag{5}$$

while when $\cos \frac{1}{2} (\phi - \phi_0)$ is negative, there is a similar expression in which the first term is missing. Similarly when $\cos \frac{1}{2} (\phi + \phi_0)$ is positive, we have

$$F(\rho, \phi, -\phi_0) \backsim e^{i\frac{2\pi t}{T}} e^{ik\rho\cos(\phi+\phi_0)} + \frac{i^{3/2} e^{i\frac{2\pi t}{T}} e^{-ik\rho}}{2\sqrt{2\pi k\rho}\,.\cos\frac{1}{2}(\phi+\phi_0)}, \tag{6}$$

and a similar expression in which the first term is missing, if $\cos \frac{1}{2} (\phi + \phi_0)$ is negative. The general expression for the light diffracted by the edge is either

$$E_z = \frac{i^{3/2} e^{i\frac{2\pi t}{T}} e^{-ik\rho}}{2\sqrt{2\pi k\rho}} \left[\frac{1}{\cos\frac{1}{2}(\phi-\phi_0)} - \frac{C_s + iD_s}{\cos\frac{1}{2}(\phi+\phi_0)}\right] \tag{7}$$

or

$$H_z = \frac{i^{3/2} e^{i\frac{2\pi t}{T}} e^{-ik\rho}}{2\sqrt{2\pi k\rho}} \left[\frac{1}{\cos\frac{1}{2}(\phi-\phi_0)} + \frac{C_p + iD_p}{\cos\frac{1}{2}(\phi+\phi_0)}\right]. \tag{8}$$

3. *An Alternative Treatment.*

The formulæ (7) and (8) may also be derived in the following manner based on the Fresnel-Huygens' Principle. It is readily shown that the wave-equation in cylindrical co-ordinates,

$$\frac{\partial^2 u}{\partial\rho^2} + \frac{1}{\rho}\frac{\partial u}{\partial\rho} + \frac{1}{\rho^2}\frac{\partial^2 u}{\partial\phi^2} + \frac{\partial^2 u}{\partial z^2} - \frac{1}{c^2}\frac{\partial^2 u}{\partial t^2} = 0, \tag{9}$$

is exactly satisfied by putting

$$u = e^{i\frac{2\pi t}{T}} \frac{e^{-ik\rho}}{2\sqrt{2\pi k\rho}} \cos\tfrac{1}{2}(\phi + \epsilon), \tag{10}$$

which represents a cylindrical wave of Poisson's type diverging from the z-axis. A plane wave incident on the xz-plane in the direction ϕ_0 is transmitted through the part of the plane to the left of the edge and is reflected from the part on the right. To find the disturbance diverging from the edge of the screen, at any point very distant from it, we divide the area of the xz-plane adjacent to the edge into half-period strips parallel to it on either side, and show in the usual way that the effect of the transmitted wave reduces to one-half of the first half-period strip on one side of the edge, and that the effect of the reflected wave reduces to that of a similar strip on the other side. Assuming that each of these strips is the origin of a cylindrical wave of the type appearing in (10), we may write the total disturbance at (ρ, ϕ) diverging from the origin, in the form

$$u = e^{i\frac{2\pi t}{T}} \frac{e^{-ik\rho}}{2\sqrt{2\pi k\rho}} \left[A_0\cos\tfrac{1}{2}(\phi+\alpha) + B_0\cos\tfrac{1}{2}(\phi+\beta)\right], \tag{11}$$

where A_0, B_0, α and β have to be so chosen as to give the amplitudes and phases of the divergent waves correctly. Now the width of either half-period strip is easily shown to be

$$\frac{\lambda}{4 \cos \frac{1}{2} (\phi - \phi_0) \cos \frac{1}{2} (\phi + \phi_0)},$$

and we may assume, as is usual in the elementary diffraction theory, that the amplitudes A_0 and B_0 are proportional to this width. It is necessary that the term in (11) proportional to A_0, contributed by the transmitted wave, remains finite when $\phi = \pi - \phi_0$, and that proportional to B_0, contributed by the reflected wave, remains finite when $\phi = \pi + \phi_0$, as these directions do not coincide with the respective directions of travel of these waves. We are thus obliged to assume that $\alpha = \phi_0$ and that $\beta = -\phi_0$. The equation (11) then reduces to

$$u = e^{i \frac{2\pi t}{T}} \frac{e^{-ik\rho}}{2\sqrt{2\pi k\rho}} \left[\frac{A}{\cos \frac{1}{2} (\phi - \phi_0)} + \frac{B}{\cos \frac{1}{2} (\phi + \phi_0)} \right], \tag{12}$$

where A and B are suitably chosen constants. As in the elementary diffraction theory we write

$$A = e^{-i\frac{\pi}{4}} = i^{3/2},$$

which expresses the difference of path of $\lambda/8$ between a parent plane wave and the divergent cylindrical wave from a laminar strip cut out of it. The value of B relatively to A evidently depends on the change of amplitude and phase occurring in reflection at the surface of the screen. We write therefore

$$B/A = -(C_s + i D_s) \quad \text{or} \quad +(C_p + iD_p),$$

according to the state of polarisation of the incident beam. The formulæ (7) and (8) are then reproduced.

4. *Explanation of Ellipticity of the Diffracted Light.*

From expressions (7) and (8) the ellipticity of the light diffracted through large angles, when the incident light is polarised in any arbitrary azimuth, follows as an immediate consequence. We shall consider first the case of normal incidence on a plane screen. We have then

$$C_s + iD_s = C_p + iD_p = \frac{n(1 - i\kappa) - 1}{n(1 - i\kappa) + 1}.$$

Taking for the case of a steel edge and for $\lambda = 5 \cdot 80 \times 10^{-5}$ cm., $n\kappa = 3 \cdot 24$ and $n = 2 \cdot 46$, we have $C_s + iD_s = C_p + iD_p = 0 \cdot 69 - i \times 0 \cdot 29$. With these numerical values and writing the expressions in the square brackets on the right-hand side of (7) and (8) in the form $F_s + iG_s$ and $F_p + iG_p$ respectively, the values of $F_s^2 + G_s^2$ and of $F_p^2 + G_p^2$ for various angles of observation, and the phase differences between these two components are shown in Table I.

Gouy noticed that with a sharp steel edge, the light diffracted into the region of shadow shows no sensible ellipticity when the deviation is less than 45°. For larger deviations, it becomes sensible, the $\|^l$ component being in advance of the $\perp^r$ component, the difference of path being, however, always numerically less than $\lambda/4$. It will be seen that this is in general agreement with the figures for the difference of path shown in the fifth column of Table I. The table also indicates the interesting result that in the region of exterior diffraction, the path difference changes sign and increases in a continuous manner up to the boundary of reflection, when it becomes half a wave-length, while according to the Sommerfeld formulæ there is a sudden reversal of phase when the diffracted ray lies in the continuation of the plane of the screen.

Table I.—Diffraction by Steel Edge : Normal Incidence.

$\|^l$ and $\perp^r$ *indicate plane of polarisation parallel and perpendicular respectively to the plane of incidence.*

$\lambda = 5{\cdot}80 \times 10^{-5}$ cm.

Region of observation.	Direction of diffracted ray ϕ.	Intensity of $\|^l$ component $F_s^2+G_s^2$.	Intensity of $\perp^r$ component $F_p^2+G_p^2$.	Difference of path between the components $\frac{\delta_p-\delta_s}{\lambda}$.	Difference of path according to Sommerfeld formulæ.
Boundary of reflection....	90°	—	—	0·50	0·50
Exterior diffraction (region of illumination)	120	15·0	3·9	0·45	0·50
	150	6·7	0·38	0·35	0·50
	180	5·9	0·36	0·15	—
	210	8·0	1·55	0·06	0
	240	21·1	10·0	0·03	0
Boundary of shadow........	270	—	—	0	0
Interior diffraction (region of shadow)	285	49	70	−0·01	0
	300	10·0	21·1	−0·03	0
	315	3·6	11·4	−0·04	0
	330	1·55	8·0	−0·06	0
	345	0·72	6·4	−0·09	0
	360	0·36	5·9	−0·15	—

5. *Effect of Oblique Incidence.*

When the light is incident on the screen obliquely at an angle θ (measured as usual from the normal) we have

$$C_s + iD_s = -\frac{\cos\theta - \sqrt{n^2(1-i\kappa)^2 - \sin^2\theta}}{\cos\theta + \sqrt{n^2(1-i\kappa)^2 - \sin^2\theta}}, \tag{13}$$

and

$$C_p + iD_p = \frac{n^2(1-i\kappa)^2\cos\theta - \sqrt{n^2(1-i\kappa)^2 - \sin^2\theta}}{n^2(1-i\kappa)^2\cos\theta + \sqrt{n^2(1-i\kappa)^2 - \sin^2\theta}}. \tag{14}$$

At normal incidence (13) and (14) are equal, and at grazing incidence they are again equal but opposite in sign. At the principal incidence (which lies between 70° and 80° for most metals) the difference of path between the || and ⊥ʳ components of the reflected wave amounts to $\lambda/4$ and then rapidly diminishes to 0 as grazing incidence is approached. With the help of the formulæ (7), (8), (13) and (14) the intensity of the two components of the diffracted light and their phase-difference can be calculated for any angle of incidence and of observation. Let us first consider moderately oblique incidence. Two cases have naturally to be distinguished, viz., when the incidence is from the screen-side of the normal, and when it is from the farther side. Tables II and III give the values for a steel screen when $\phi_0 = 135°$ and 45°, respectively, for yellow light. It can be seen that the effects observed in interior and exterior diffraction are no longer similar to each other.

Table II.—Diffraction by a Steel Edge. $\phi_0 = 135°$.

Region of observation.	Direction of diffracted ray ϕ.	Intensity of ||ʳ component $F_s^2+G_s^2$.	Intensity of ⊥ʳ component $F_p^2+G_p^2$.	Difference of path between the components $\frac{\delta_p-\delta_s}{\lambda}$.
Exterior diffraction	135°	4·6	0·30	0·23
	180	3·8	0·35	0·14
	225	4·9	0·8	0·09
	270	12	4·0	0·04
	285	24	11	0·03
	300	75	48	0·02
Boundary of shadow............	315	—	—	0
Region of shadow	330	41	75	−0·02
	345	6·0	27	−0·05
	360	0·7	18	−0·17

In the case considered in Table II, the region of shadow is of much smaller angular width, and the degree of polarisation and also the ellipticity increase rapidly as we approach the plane of the screen ($\phi = 360°$). On the other hand, in Table III the region of shadow is much wider, and the polarisation and ellipticity of the diffracted light increase less rapidly with increasing deviation of the diffracted ray. In exterior diffraction these effects are reversed.

Table III.—Diffraction by a Steel Edge. $\phi_0 = 45°$.

Region of observation.	Direction of diffracted ray ϕ.	Intensity of $\|\|^l$ component $F_s^2+G_s^2$.	Intensity of $\perp^r$ component $F_p^2+G_p^2$.	Difference of path between the components $\frac{\delta_p - \delta_s}{\lambda}$.
Exterior diffraction	135°	—	—	0·45
	165	28	2·3	0·32
	195	31	8·4	0·06
Boundary of shadow	225	—	—	0
Region of shadow	255	9·6	22	−0·03
	285	1·5	7·0	−0·06
	315	0·5	4·2	−0·09
	345	0·2	3·3	−0·14
	360	0·1	3·1	−0·17

6. *Diminished Intensity of Diffracted Light.*

If we compare the figures shown in Tables II and III with those calculated from Sommerfeld's formulæ for a perfectly reflecting screen, we find that the effect of imperfect conductivity of the screen is not only to introduce elliptic polarisation, but also to diminish the total intensity of the diffracted light and the ratio of the components of vibration for specified angles of incidence and diffraction. In fact, these effects are all closely related to one another, and become the more striking when the incidence is very oblique.

In Table IV the case of oblique incidence on a steel edge has been worked out and shown. It is assumed that $\phi_0 = 170°$, that is, only 10° short of grazing incidence. The figures for the steel edge and for a perfectly reflecting screen are shown side by side for comparison, and it will be seen that the intensity of the $\perp^r$ component is diminished to one-fifth of its value, on the surface of the screen, by reason of the imperfect conductivity, while that of the $\|^l$ component is very slightly increased. Nevertheless, the ratio of the $\perp^r$ and $\|^l$ components remains large, showing that even at such incidences the polarisation remains large. We have to approach grazing incidence still more closely before the

Table IV.—Diffraction by a Steel Edge. $\phi_0 = 170°$.

Region of Shadow.

Direction of diffracted ray ϕ.	Intensity of $\|'$ component for a *perfect conductor.*	Intensity of $\|'$ component for *steel* $F_s^2 + G_s^2$.	Intensity of $\perp^r$ component for *steel* $F_p^2 + G_p^2$.	Intensity of $\perp^r$ component for a *perfect conductor.*	Difference of path between the components for *steel* $\frac{\delta_p - \delta_s}{\lambda}$.
350°	—	—	—	—	0
352	2590	2600	3100	4060	−0·01
354	460	480	750	1280	−0·02
356	119	128	313	746	−0·04
358	23	28	170	571	−0·07
360	0	0·9	109	527	−0·23

diminution of the $\perp^r$ component is such as to produce a striking diminution of the completeness of polarisation. From formulæ (7), (8), (13) and (14) it follows that, at grazing incidence, the diffracted light should be unpolarised at all angles.

The foregoing considerations help to explain, at least in part, the interesting observation of Gouy that for given directions of the incident and diffracted rays, the intensity of the diffracted light is a *maximum* when the plane of the screen bisects the angle between these two directions. According to Sommerfeld's formulæ the intensity should be a *minimum* for this position of the screen. Owing, however, to the imperfect conductivity of actual screens, as we have seen, the intensity falls off in approaching the extreme cases in which the light is incident grazingly on the screen from either direction. As we shall see later, other circumstances, as, for instance, the finite angle formed by the faces of the screen at the edge, or the actual rounding off of the latter, would also operate in the direction of diminishing the intensity of the diffracted light in the two extreme positions of the screen. Hence the intermediate position for the screen actually gives the maximum instead of the minimum intensity for the diffracted rays in the particular direction.

7. *Explanation of Diffraction Colours.*

The wave-length enters in the expression for the intensity of the diffracted light in two distinct ways. Referring to (7) and (8) it will be seen that the intensity is inversely proportional to k, that is, proportional to the wave-length. The longer wave-lengths would thus tend to be more prominent in the light diffracted by the edge than in the incident light. This effect would operate both on the parallel and perpendicular components of vibration in the diffracted light. The colour of the diffracted light is also influenced, and in an entirely different way, by the factors $C_s + iD_s$ and $C_p + iD_p$ appearing in (7) and (8), which are, in general, functions of the wave-length of the incident light. If we confine ourselves to the case of normal incidence, $C_s + iD_s$ and $C_p + iD_p$ are identical in magnitude. But the former appears with a negative sign in (7) and the latter with a positive sign in (8). Hence, if a particular wave-length appears with a strengthened amplitude in (8) it will appear with a weakened amplitude in (7), and *vice versa*. This, taken together with the proportionality to λ already mentioned, furnishes an explanation of the difference in the colour of the parallel and perpendicular components of the light diffracted into the region of shadow, which was discovered by Gouy for metals such as copper and gold. It can easily be seen that in the region of shadow, the longer wave-lengths which are strongly reflected by the metal would be much enhanced in the perpendicular component, while the corresponding weakening in the parallel component would be almost insensible. In the region of exterior diffraction, these features are interchanged.

Table V.—Gold Screen. $\phi_0 = 90°$ (Normal Incidence).

Direction of diffracted ray ϕ.	$(F_s^2+G_s^2)\,\lambda \times 10^8$, for $\lambda \times 10^5 =$			$(F_p^2+G_p^3)\,\lambda \times 10^8$, for $\lambda \times 10^5 =$		
	4·20.	5·80.	7·00.	4·20.	5·80.	7·00.
°						
270	—	—	—	—	—	—
285	217	282	326	279	408	508
300	48·3	59·0	64·4	80·4	125	159
315	19·1	22·1	22·1	41·8	68·3	88·7
330	9·56	10·7	9·50	28·1	48·5	63·9
345	5·44	6·36	4·87	22·1	40·2	53·6
360	3·41	4·86	3·48	19·5	37·6	50·7

In Table V the intensity of the diffracted light has been calculated for the case of a gold screen using the following data :—

$\lambda = 7{\cdot}00 \times 10^{-5}$ cm. ; $n = 0{\cdot}280$, $n\kappa = 3{\cdot}800$;
$\lambda = 5{\cdot}80 \times 10^{-5}$ cm. ; $n = 0{\cdot}415$, $n\kappa = 2{\cdot}750$;
$\lambda = 4{\cdot}20 \times 10^{-5}$ cm. ; $n = 1{\cdot}570$, $n\kappa = 1{\cdot}800$.

From the table it will be seen that in the region of shadow $(F_s^2 + G_s^2)\lambda$ has practically the same value for different wave-lengths, while $(F_p^2 + G_p^2)\,\lambda$

increases in value as we proceed towards the red end of the spectrum. The increase with wave-length is much more marked for large angles of diffraction than for small angles. Further, $F_p^2 + G_p^2$ is always greater than $F_s^2 + G_s^2$, the ratio between the two increasing with the angle of diffraction. From these facts, it follows that when the region of shadow is examined, the $\|^l$ component of the diffracted light will be perfectly white, while the $\perp^r$ component, which is in fact much stronger than the other, will exhibit an orange-yellow tint, the colouration being the more marked, the further we go into the region of shadow. The same colour effects will be noticeable also in the region of exterior diffraction, the $\|^l$ and $\perp^r$ components now, however, exchanging places.

8. *Intensified Colours at Oblique Incidences.*

While the variation with wave-length of the intensity of the $\perp^r$ component shown in Table V is marked enough, it is not exceptionally large, being in fact of the same order of magnitude as the variation of the reflecting power of the metal with wave-length. This is in agreement with observation, for Gouy found that the sharpest metallic edges do not show particularly vivid colours by diffraction. When, however, the incidence on the screen is made oblique, the colours of the $\perp^r$ component should become more lively. To understand why this should be the case, we have only to refer to section 6 above, in which it was shown that the imperfect reflectivity of the metal results in a diminution of the intensity of the diffracted light in comparison with the theoretical value for a perfectly reflecting screen, and that this diminution becomes the more marked as the incidence of the light on the screen becomes more oblique. Those wave-lengths, however, for which the reflecting power of the metal approaches unity, persist in nearly full strength in the $\perp^r$ component of the diffracted light, and hence determine its colour in increasing measure as the obliquity of the screen is increased. It is to be noted also that the colour should appear at smaller deviations of the ray in interior diffraction, and at larger deviations in exterior diffraction, or *vice versa*, according to the position of the screen.

In Table VI the case of a gold screen, for a position of the screen 10° short of grazing incidence, has been worked out and the intensities of the $\|^l$ and $\perp^r$ components are shown for six different wave-lengths, the direction of observation considered being along the surface of the screen in the region of shadow. The normal reflecting power of the metal for the same wave-lengths is also shown for comparison.

Table VI.—Gold Edge. $\phi_0 = 170°$, $\phi = 360°$.

$\lambda \times 10^5$ (cm.).	Intensity of $\|^l$ component $(F_s^2+G_s^2)\,\lambda \times 10^5$.	Intensity of $\perp^r$ component $(F_p^2+G_p^2)\,\lambda \times 10^5$.	The reflection coefficient.
4·00	9·9	200	0·360
4·60	12·5	210	0·358
5·20	17·5	240	0·608
5·80	10·5	470	0·827
6·20	8·8	650	0·889
7·00	7·1	1000	0·930

It will be noticed that the intensity of the $\|^l$ component varies but little with wave-length, while the $\perp^r$ component shows large intensities in the orange and red regions in the spectrum. The effect in the latter case is of a highly selective character, becoming pronounced only for the wave-lengths for which the reflecting power of the metal approaches unity.

When the figures shown in Table VI are computed after the manner employed by the late Lord Rayleigh* for discussion of the colours of thin plates, and plotted in Maxwell's colour-triangle, it is found that the $\|^l$ component is perfectly white, while the $\perp^r$ component is of a rich orange-yellow colour.

The case of other metals may be worked out in a similar manner. In Table VII are given the reflection-coefficients and the colour of the diffracted light as observed by Gouy and Wien, for a number of metals. The general relationship between them is fairly clear from the figures. In the case of the whiter metals, of course, the colour is largely determined by the factor λ appearing in the expression for the intensity of the diffracted light.

Table VII.—Reflection Coefficients and Diffraction Colours.

For $\lambda \times 10^5 =$	4·20	4·50	5·00	5·50	6·00	6·50	7·00	*Colour of* $\perp^r$ component of diffracted light.
Silver	0·866	0·905	0·913	0·927	0·926	0·935	0·946	Pale yellow.
Copper	0·33	0·37	0·44	0·48	0·72	0·80	0·83	Red.
Steel	0·52	0·54	0·55	0·55	0·55	0·56	0·58	Reddish white.
Platinum	0·518	0·547	0·584	0·611	0·642	0·663	0·69	Yellow.
Zinc	0·803	0·806	0·805	0·789	0·774	0·771	0·770	Colour insensible.
Tin	—	0·605	0·670	0·686	0·706	0·713	0·716	Greenish yellow.

---

* Lord Rayleigh, 'Scientific Papers,' vol. 2, p. 498.

9. *Diffraction by Metallic Wedges.*

Poincaré considered the case of a perfectly reflecting wedge in his first memoir, and showed that if the surfaces of the wedge are given by the angles $\phi = 0$ and $\phi = \chi$, the rays diffracted from its edge have an amplitude proportional to

$$\left[\frac{1}{\cos\frac{\pi^2}{\chi} - \cos\frac{\pi}{\chi}(\phi - \phi_0)} \mp \frac{1}{\cos\frac{\pi^2}{\chi} - \cos\frac{\pi}{\chi}(\phi + \phi_0)}\right]. \tag{15}$$

As the result of a more elaborate analysis, Wiegrefe[*] found for the cylindrical wave diverging from a wedge-shaped edge the identical expression given by (15) with the multiplying factor

$$-i^{3/2} e^{i\frac{2\pi t}{T}} e^{-ik\rho} \sqrt{\frac{\lambda}{\rho}} \cdot \frac{\sin\frac{\pi^2}{\chi}}{2\chi}. \tag{16}$$

On putting $\chi = 2\pi$, the formulæ (15) and (16) reduce to those for the case of a perfectly reflecting plane screen. In the case of an imperfectly conducting wedge, we modify expression (15) and write it in the form.

$$\left[\frac{1}{\cos\frac{\pi^2}{\chi} - \cos\frac{\pi}{\chi}(\phi - \phi_0)} - \frac{C_s + iD_s}{\cos\frac{\pi^2}{\chi} - \cos\frac{\pi}{\chi}(\phi + \phi_0)}\right], \tag{17}$$

or

$$\left[\frac{1}{\cos\frac{\pi^2}{\chi} - \cos\frac{\pi}{\chi}(\phi - \phi_0)} + \frac{C_p + iD_p}{\cos\frac{\pi^2}{\chi} - \cos\frac{\pi}{\chi}(\phi + \phi_0)}\right], \tag{18}$$

where C_s, D_s, C_p, D_p have the same significance as previously, and are functions of the angle of incidence of the light on the illuminated side of the wedge.

From formula (15) it appears that along the two surfaces of the wedge $\phi = 0$ and $\phi = \chi$, the diffracted light should be completely polarised with the intensity of the $\|^l$ component zero, and that of the $\perp^r$ component finite. As the rear surface of the wedge limits the region of shadow, it follows as a consequence that the polarisation-effects should usually appear at smaller deviations of the diffracted ray in the case of a wedge than for a plane screen. When the imperfect reflecting power of the metal is taken into account, as in formulæ (17) and

---

[*] A. Wiegrefe, 'Ann. d. Physik,' vol. 39, p. 449 (1912).

(18), it would also follow, for the reasons stated, that the colours of the diffracted light should also be observable at smaller deviations and be generally more striking than for a plane screen.

10. *Summary.*

1. The paper contains a discussion of the observations of Gouy on the intensity, colour and polarisation of the light diffracted through large angles by metallic screens and wedges with polished edges. The well-known expressions due to Poincaré and Sommerfeld referring to diffraction by perfectly-reflecting screens and wedges, are modified so as to take into account the changes of phase and amplitude which occur when light is reflected at the surface of a metal. The modified formulæ are then discussed.

2. The formulæ show that when the incident light is plane-polarised in any arbitrary azimuth, the light diffracted through large angles is elliptically polarised, the sign of the ellipticity being different in interior and exterior diffraction.

3. In interior diffraction, the component polarised in the plane of incidence is white, while the perpendicular component is coloured, the colour depending on the nature of the metal. In exterior diffraction, these effects are reversed.

4. The effect of imperfect conductivity is to make the intensity of the diffracted light less and less as the incidence becomes more and more oblique. This diminution is least for the wave-length for which the reflection-coefficient is largest. The colour-effects arise in this way and therefore become more prominent at oblique incidences.

Measurement of the Biologically Active Ultra-Violet Rays of Sunlight.

By LEONARD HILL, F.R.S., National Institute for Medical Research.

(Received February 2, 1927,—Revised June 8, 1927.)

[PLATE 9.]

Methods of Measurement.

The ultra-violet radiation was measured by the acetone methylene-blue method described by Webster, Hill and Eidinow.* Readings were taken at the Meteorological Office, Kingsway, The Royal Observatory, Greenwich, the States Meteorological Station, Guernsey, the National Institute for Medical Research, Hampstead, and by voluntary observers elsewhere, viz., by Dr. Adams, Liverpool Sanatorium, Frodsham, Cheshire; Dr. Paul Tozer, Peppard Common Sanatorium, Oxon; Dr. Segaller, St. Ives, Cornwall; A. R. Tankard, Esq., Hull; Dr. Wyatt, Wingrave, Lyme Regis; H. J. Sargent, Esq., Bexhill; C. L. Rivers, Esq., Harrogate; Dr. Dorno, Davos, Switzerland; J. Fyfe, Esq., Stirling; S. M. Bower, Esq., Huddersfield; R. Robertson, Esq., Lowestoft; F. R. Gray, Esq., Ventnor; R. L. Massey, Esq., Khartoum; Dr. P. W. Moore, Assouan; Dr. Rosenheim (some records in Egypt).

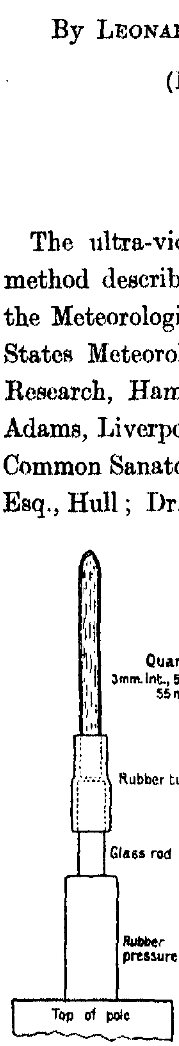

FIG. 1.—Standard Silica Tube and Mounting.

The standard acetone methylene-blue is made up from a 0·1 per cent. solution of Paulene Frères methylene-blue; 5·8 c.cm. of this is added to 30 c.cm. of pure distilled acetone, and made up to 100 c.cm. with water; this gives a standard labelled 10. The standard solution is kept in brown glass bottles. A standard silica tube, as shown in fig. 1, 3 mm. in diameter, is filled with this solution and exposed to the sunlight. At the end of the exposure the colour is compared with the colour of eight standard tubes (fixed and unbleachable). These standard tubes are marked 3, 4, 5, 6, 7, 8, 9 and 10, and are placed in a suitable frame for comparison.† The standard solution used for bleaching in the silica tube is matched against these standard tubes not only after the period of exposure, but also before exposure, since the standard solution (10) may very gradually fade, while also the refractive power of the silica tubes may vary.

---

* *Lancet*, vol. 206, p. 745 (April, 1924).

† The apparatus is made by Siebe, Gorman, Ltd., 187, Westminster Bridge Road, S.E.1.

The difference between the readings, before and after exposure, gives a measurement of the shorter wave-lengths of the ultra-violet sunlight for the time and place of exposure.

A solution of acetone in water is decomposed by ultra-violet light with the formation of acetic and formic acids, and other substances. The extent of this decomposition can be measured by means of the reduction of methylene-blue, which acts as a hydrogen acceptor in this reaction. Exposed to a constant source of ultra-violet rays, the bleaching of the methylene-blue is proportional to the time of exposure. The acetone-blue solution in a 3 mm. layer transmits λ 3342, partly absorbs λ 3132 of the spectrum of the mercury vapour lamp, and wholly absorbs rays shorter than λ 3132 (fig. 2, Plate 9).

The degrees of the colour scale are equal and were biologically standardised, using a mercury vapour lamp, against both the killing of infusoria in a quartz cell, and the erythema dosage of the white skin. In the case of the mercury vapour lamp one unit of fading on the scale is equal to twice the infusoria killing dose, and to 2–4 times the erythema dose, the sensitivity of skin varying in individuals. The skin of the inner surface of the upper arm was used for the erythema dose. How far this quantitative scale can be applied to sunlight is considered later.

Dr. A. B. Hill has tested for us among 53 people the accuracy in matching the acetone-blue of different tints against the fixed scale, and found it of quite high order, 80 per cent. of the readings lying within a quarter of a unit of the mean.

The temperature coefficient was determined between 1·5 and 35° C., and found to be 1·15 to 1·2 for 10° C. A difference of 10° C. above or below 20° will make a difference of about half a degree of the scale. Such a correction may be required in the tropics or cold climates.

Fig. 1 shows the correct method of mounting the tube. At Hampstead the tube is thus mounted on the end of a long bamboo, hinged at its bottom, and supported by movable guys. This allows the tube to be brought down for changing the solution, and supports it clear of all roofs and obstructions.

Ultra-violet rays reach us diffusely from the blue sky and bright clouds as well as direct from the sun. Dorno has shown that the ultra-violet radiation from the clear sky at Davos is greater than that from the low sun. Taking the diffuse ultra-violet from the sky as 100, that from the direct sun was found by Dorno to be:—

Height of Sun.	
10°	1·7
20°	12·3
40°	47·6
60°	85·1

The silica tube containing the standard acetone-blue solution must then be exposed to the sky right down to the horizon line. Fig. 3 shows the difference between the readings taken on the roof and in the grounds at Hampstead.

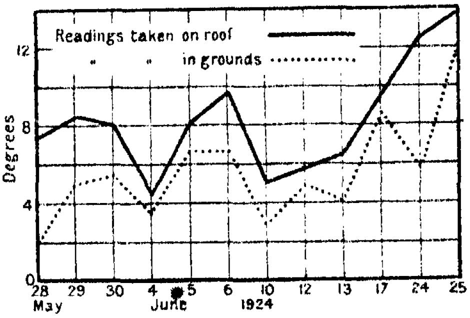

Fig. 3.—Effect of Skyshine.

At one station the reading appeared to be 30–40 per cent. too low. The full exposure of the tube to the sky was found to be obstructed by trees. It was agreed that the tube should be exposed in future on the top of a tall mast. The

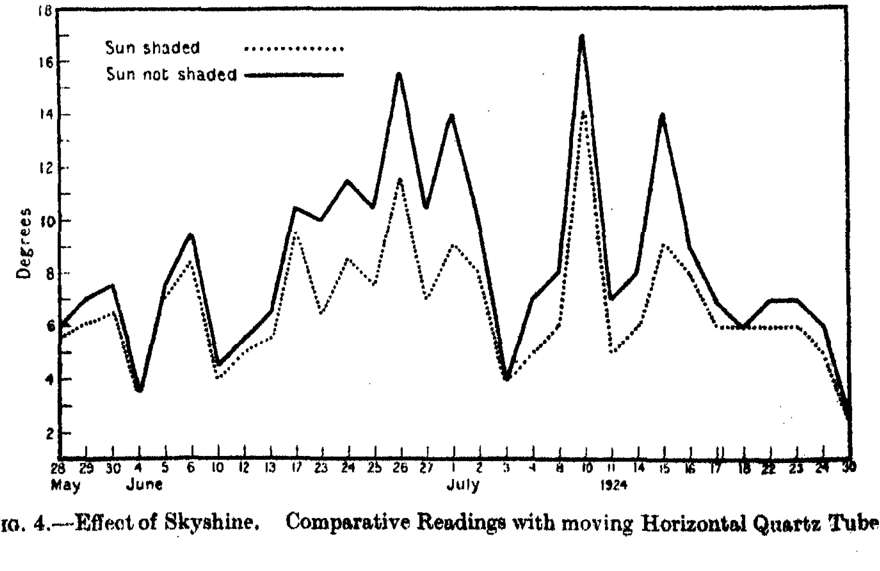

Fig. 4.—Effect of Skyshine. Comparative Readings with moving Horizontal Quartz Tube.

readings continued to be too low. The tube was then found to be screened from the northern half of the sky by an obstruction on the top of the mast. On raising the tube above the obstruction the true readings were obtained.

Fig. 4 shows records taken by the acetone-blue method with two silica tubes at Hampstead. The tubes were suitably affixed for me by Mr. T. C. Angus to a clock so as to be carried round in the horizontal position and kept normal to the sun. A small strip of brass attached sufficed just to shade one tube from the direct sun. Thus, one tube was exposed to the skyshine and sun, while the other was shaded from the direct sun, and exposed to the skyshine only. The graph shows that the ultra-violet rays come mostly from the skyshine.

Ultra-Violet Rays of Sunlight which fade Acetone-Blue.

While the spectrum of the sun may extend to λ 2900, λ 3000 is the practical limit. Using a Hilger quartz spectroscope and a bromine screen, we have found the spectrum of the sun scarcely reached λ 3000 at Hampstead. A saturated solution of uric acid (1 in 40,000) in a stratum 6 cm. thick absorbs all rays of shorter wave-length than λ 3200,* cutting out from the spectrum of the mercury vapour lamp the intense band λ 3132 (fig. 2). Exposing under such a stratum a sealed silica tube full of the standard solution of acetone-blue to a mercury vapour lamp, a similar tube being under distilled water, the fading of the latter was 6, while that of the former was insignificant. On another occasion the fading was 9 under water, 1 under uric acid solution. On the other hand, exposing similarly the tubes to sunlight, the fading on several days in May at Hampstead on the top of the hill was :—

Under uric-acid solution.	Under distilled water.
3·0	3·5
3·5	4·5
4·5	6·5
4·0	5·0
5·0	6·0
Average.... 4·0	Average.... 5·1

While the active rays for fading acetone-blue of the mercury vapour lamp are then λ 3142 and of shorter wave-length than this, those of the sun in England are chiefly of longer wave-length than λ 3142. (In one observation carried out for us at Assouan by Dr. P. W. Moore, the fading was twice as great under water as under uric acid, an indication of the greater intensity of the shorter wave-lengths of the ultra-violet rays of the sun there.)

---

* According to Dhéré this solution absorbs all rays shorter than λ 3060.

Under 3 per cent. quinine sulphate solution, which absorbs rays of the mercury vapour lamp shorter than λ 4200 (fig. 2), the fading of the acetone-blue in sunlight during a certain period was found to be insignificant, while under distilled water it was 4½. The rays of the sun in England active in fading acetone-blue are certainly then of shorter wave-length than λ 4200. As the acetone-blue solution partly absorbs λ 3132 and some of the other rays of shorter wave-length than λ 3342 (fig. 2), it must be rays between λ 3342 and λ 3000 which produce the fading in sunlight.

The Erythema-Producing Rays of Sunlight.

Sunlight focussed on the skin through the solution of quinine sulphate does not produce erythema if the skin is kept cool by running water. The erythema-producing rays are then in the ultra-violet region. Further, to determine these rays the effect of Chance's Vitaglass as a screen was compared with that of silica and of green window glass (fig. 5, Plate 9). Vita and green window glass were found by Bourdillon to have the following percentage transparency :—

	Thickness in mm.	Wave-length in Angstrom units.								
		λ 4046	3655	3342	3131	3022	2967	2893	2804	2655
Green window glass.	2·8	87·0	76·6	26·0	0·12	—	·01	—	—	—
Vitaglass† (1926 sample).	1·3	91·0	89·1	86·5	66·5	48·1	34·5	18·6	5·3	0·4

† *The transmission of recent samples has been improved.*

Exposed for two hours to the mid-day summer sun, the skin of the abdomen reacted with a slight erythema under green window glass, distinct under Vita glass, well marked under silica or no screen (fig. 6, Plate 9).

As silica lets through about 90 per cent. all along the U.V. spectrum, while Vitaglass let through about 75 per cent. of the rays between λ 3300 to λ 3000, and green window glass let through 25 per cent. of those rays at λ 3342 and little below λ 3200,* and as in the sun a slight production of erythema occurs

---

* Coblentz and Fulton, 'Bur. Stand. Sci. Paper No. 495,' fig. 4 (1924).

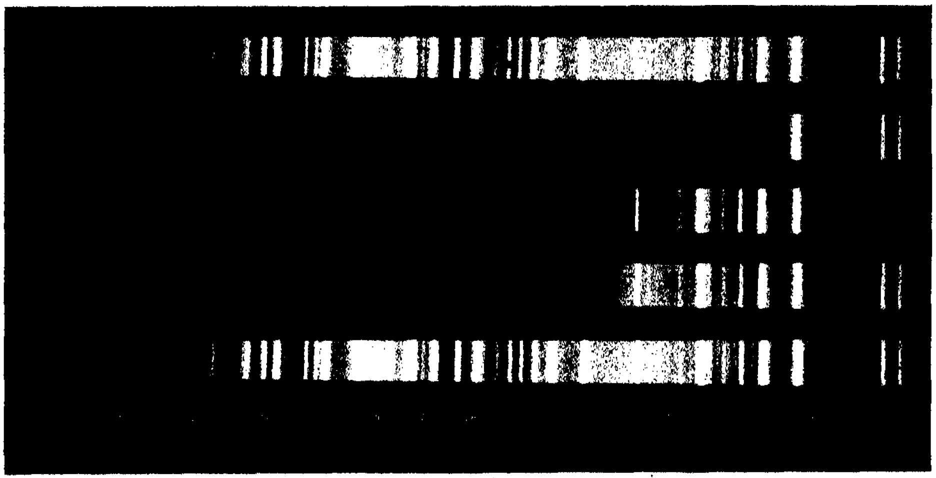

2

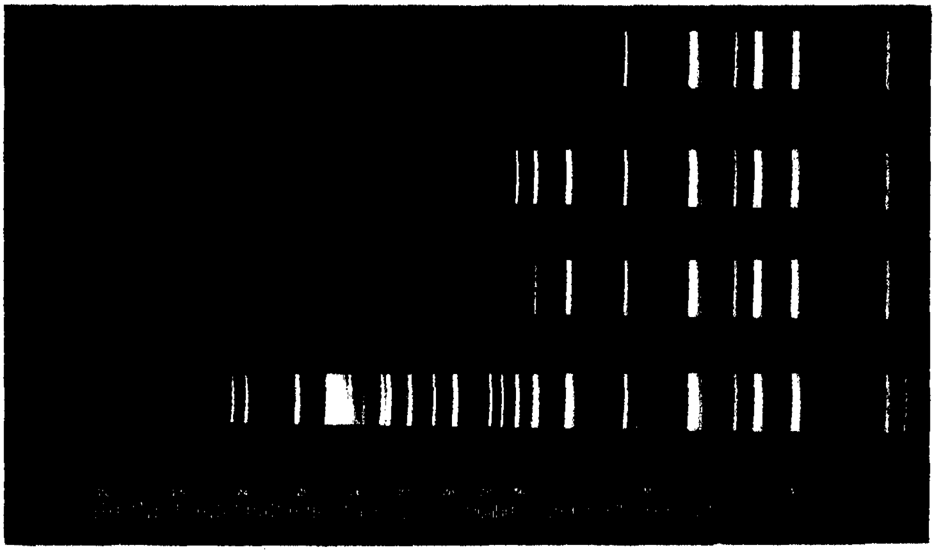

5

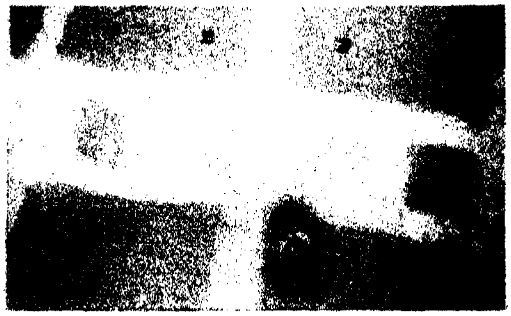

6

1. Vita glass.
2. Chance's ultra-violet glass.
3. Green window glass.
4. Silica.

under green window glass, a greater one under Vitaglass, and still greater under silica, we may conclude that the erythema-producing rays of the sun mainly lie between λ 3300–3000. Chance's ultra-violet glass transmits rays particularly about λ 3600, and no erythema results under this.

Exposed to the summer sun the average fading of acetone-blue on a number of days was 8½ under silica, 7½ under Vitaglass, 4 under green window glass. There is then a correspondence between the acetone-blue fading and the erythema-producing power of the sun's rays, and exposure to the summer sun about noon, sufficient to fade the acetone-blue one on the scale, produces well-marked erythema.

While as a quantitative method the fading of acetone-blue in sunlight can be claimed to give only approximate values, it enables one to compare in a qualitative way the value of the sunlight in various places.

In the case of pure acetone, Henri* has shown that the maximal absorption is at λ 2706 (fig. 7). Hausser and Vahle,† using the bands of the spectrum of the mercury-vapour lamp and equal intensities as determined by the thermopyle,

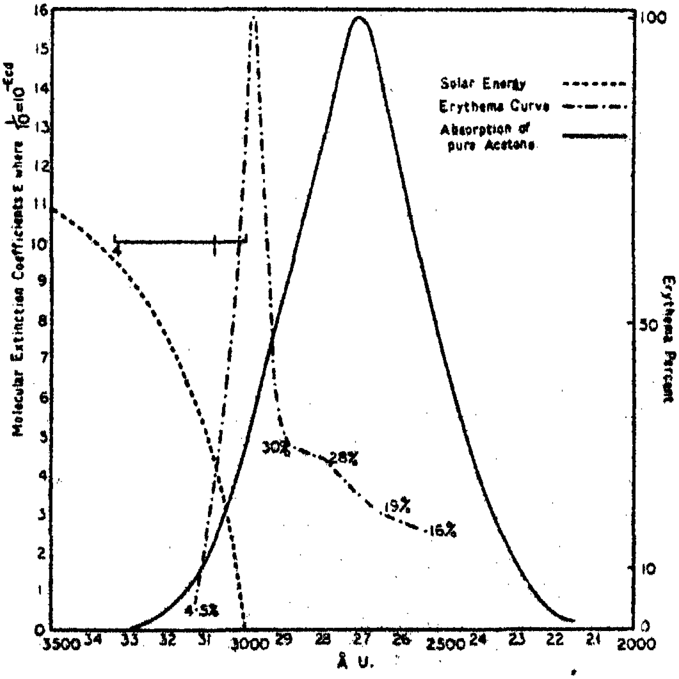

FIG. 7.

---

* 'C.R.,' vol. 156, p. 230 (1915).

† 'Strahlentherapie,' vol. 13, p. 59 (1922).

have found the maximal erythema production to be at λ 2967. At λ 3131 the erythema production was only 4·5 per cent. of that at λ 2967. While the erythema-producing action of rays about λ 3131 are then relatively weak, the intensity of the sun in this region is sufficient to be effective. So, too, in the case of the fading of acetone-blue. The rays of the sun which activate ergasterol and so, by forming vitamin D, prevent rickets, lie between λ 3200 and λ 2900.

In the case of biological reactions produced by ultra-violet rays there is a minimal value below which no biological reaction results, (*a*) for time, (*b*) for intensity of the source. While interrupted excitations, each below the threshold value, may be summated and provoke a reaction, with sufficient intervals such interrupted excitations become ineffectual. Weak ultra-violet radiation which produces a fading effect on acetone-blue in the course of 24 hours may therefore have no erythema-producing effect. It is known, however, that a curative effect can be produced in the absence of erythema.

Records of the biologically active Ultra-Violet Rays.

Tables I, II and III show the average monthly readings taken with the acetone-blue gauge for 1925 and 1926 and first five months of 1927 in the places of observation. The highest British ultra-violet reading obtained so far has been 23 at Peppard on July 10, 1924. At Hampstead the reading on this day was 18. Fig. 8 shows the monthly daily averages for Hampstead, Peppard

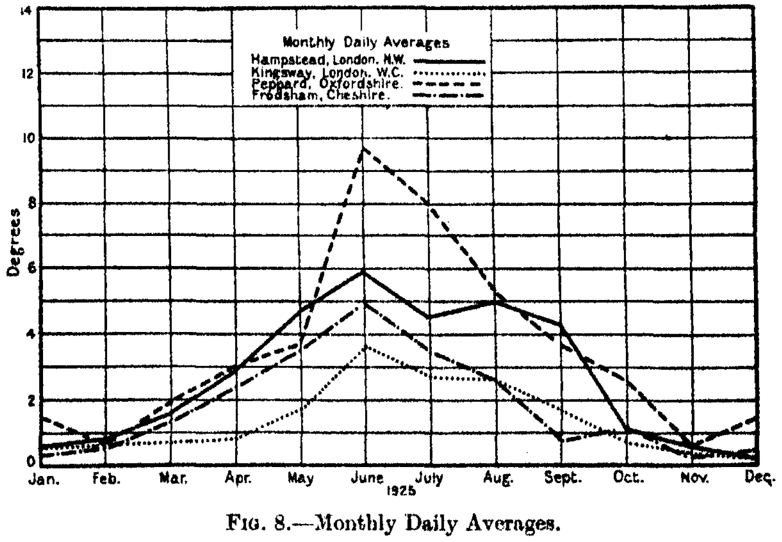

FIG. 8.—Monthly Daily Averages.

(Oxon), Kingsway and Frodsham (Cheshire). The readings are highest in the summer and lowest in the winter months.

Places remote from towns, such as Peppard Common and the top of Hampstead, which is singularly free from smoke during the greater part of the year owing to its height and position to the North-west of London, receive considerably more ultra-violet light than those more exposed to the smoke clouds of industrial areas, *e.g.*, Kingsway and Hull. Ultra-violet intensity is clearly more dependent upon artificial air pollution than upon natural causes due to geographical position in England. The readings in Davos and still more in Assouan gain greatly from geographical position. At Assouan the readings in the winter months are very high. The readings at Davos or Assouan on clear days may not be higher than those in summer in clean country or seaside places in South England, but the monthly average is much higher in the first two places, and particularly so in Assouan. On two humid, overcast days at Assouan the readings were 3 and 2, against 12 to 18 for clear sunny days. At Ventnor a reading of 5 was obtained on the sea front bathed in sun, and 1 on the cliffs shrouded in mist on the same day.

A series of readings was taken on the East Coast in August with one tube at the edge of the cliff exposed to the seashine, and the other inland. As no difference in reading was found, it was concluded that the ultra-violet rays reflected from the sea, at least on the East Coast, are insignificant. Periodic variations of ultra-violet radiation have been recorded by hourly readings at Khartoum during continuous sunshine on some days with no obvious cause.

Table I.—Ultra-Violet Light. Daily Average for the Month.

Place.	1925.											
	Jan.	Feb.	Mar.	Apl.	May.	June.	July.	Aug.	Sept.	Oct.	Nov.	Dec.
Hampstead....	0·6	0·8	1·6	3·0	4·8	5·9	4·5	5·0	4·3	1·1	0·6	0·2
Peppard (Oxon)	1·5	0·6	2·0	3·0	3·7	9·7	8·0	5·3	3·7	2·6	0·6	1·6
Kingsway	0·6	0·6	0·7	0·8	1·7	3·6	2·7	2·6	1·8	0·7	0·4	0·2
Frodsham (Cheshire)	0·4	0·5	1·3	2·4	3·5	5·0	3·5	2·6	0·8	1·1	0·4	0·5
Harrogate	0·6	0·8	1·2	2·1	4·1	5·2	6·1	4·5	—	—	—	—
Hull	0·2	0·3	0·9	1·1	2·8	3·4	3·3	2·5	1·5	0·7	0·4	0·2
St. Ives (Cornwall)	—	1·3	2·1	3·0	3·4	10·5	—	—	—	—	—	—
Greenwich	0·7	1·0	1·5	2·7	3·5	4·0	4·3	4·2	3·3	2·5	1·6	1·1
Lyme Regis	—	—	1·6	3·1	5·8	7·7	—	5·9	5·3	2·9	—	0·8
Guernsey	—	—	—	—	3·7	—	—	—	—	4·2	1·9	1·5
Huddersfield	—	—	—	—	—	—	4·5	3·3	1·9	0·7	0·5	0·2
Stirling	—	—	—	—	—	—	—	—	—	1·9	0·8	0·5
Bexhill	—	1·2	2·0	3·3	5·2	4·6	2·9	3·7	2·7	1·7	1·2	0·7
Davos (Switzerland)	—	—	—	—	—	—	—	—	6·3	—	3·0	1·9

Table II.—Ultra-Violet Light. Daily Average for the Month.

Place.	1926.											
	Jan.	Feb.	Mar.	Apl.	May.	June.	July.	Aug.	Sept.	Oct.	Nov.	Dec.
Hampstead....	0·4	0·6	1·8	2·9	4·4	5·3	6·2 (11)	5·8 (3)	3·6	1·3	0·3	0·4
Peppard	0·6	1·0	2·8	3·3	3·2	6·5	6·8	5·0	3·1	2·1	0·8	0·9
Kingsway	0·3	0·3	1·2	2·0	1·7 (25)	3·2	3·4	3·6 (26)	2·5	0·8	0·6	0·2
Frodsham (Cheshire)	0·3	0·4	0·7	3·0	3·3	3·8	3·3	3·2	—	—	—	—
Hull	0·3	0·4	0·4	1·2	2·0	2·5	3·7	3·6	2·2	1·7	0·4	0·3
Greenwich	1·0	—	—	—	—	—	—	—	—	—	—	—
Lyme Regis	0·7	1·1	2·4	3·8	5·0	6·9	7·2	6·9	5·2	2·3	1·5	1·5
Guernsey	1·8	2·2	2·0	2·4	4·1	6·9	6·4	4·8	3·7	2·3	1·4	0·7
Huddersfield	0·2	0·5	0·9	1·2	2·1	3·2	3·8	3·1	2·2	1·3	0·6	0·4
Bexhill	0·7	1·2	2·2	2·7	3·1	4·8	6·9	6·3	4·8	2·0	1·6	2·0
Ventnor	—	—	—	—	(12)	—	—	6·7	5·9	3·4	2·5	2·5
Lowestoft	0·6	0·4	1·5	1·8	5·0	4·8	6·7	6·6	5·9	4·8	1·2	1·3
Stirling	0·2	0·5	0·9	1·3	3·0	4·2	6·0	5·4	4·1	2·1	0·8	0·3
Davos (Switzerland)	1·7	2·0	2·8	5·1	5·9	6·0	9·0	10·4	8·4	4·4	3·5	2·3
Agra	—	1·0	2·0	2·5	3·8	6·0	9·5	7·7	6·8	2·5	1·5	1·3
Lugano (Switzerland)	—	—	—	—	—	—	—	—	—	—	—	—
Egypt (Khartoum)	—	—	—	—	—	—	—	(8) 13·0	(16) 10·6	—	—	—
Assouan	—	—	—	—	—	—	—	—	—	—	—	11·4

The figures in brackets indicate number of observations in the month. At Lowestoft up to August the readings were too low owing to screening of skyshine by trees.

Table III.—Ultra-Violet Light. Daily Averages for the Month.

Place.	1927.					
	Jan.	Feb.	March.	April.	May.	June.
Hampstead	0·39	0·55	1·34	2·55	3·9	3·22
Peppard	0·97	0·97	2·10	3·56	5·87	—
Kingsway	0·21	0·21	0·74	1·50	3·45	2·57
Hull	0·18	0·23	0·55	0·86	1·43	2·13
Huddersfield	0·48	0·89	1·97	2·83	2·69	—
Bexhill	1·55	1·39	2·74	4·13	5·27	3·88
Lyme Regis	1·18	1·71	3·52	4·50	4·71	4·72
Lowestoft	1·50	1·39	3·16	2·96	3·48	3·66
Guernsey	0·97	1·82	2·61	3·36	4·96	6·33
Ventnor (I.O.W.)	2·77	2·48	3·29	3·86	5·19	5·42
Torquay	—	—	—	3·45	4·05	4·50
Dagenham (Essex)	—	—	—	2·36	5·43	4·75
Davos (Switzerland)	3·00	4·25	4·55	7·60	7·72	5·92
Assouan (Egypt)	12·90	12·75	—	—	—	—

Summary.

Daily values of biologically active ultra-violet radiation taken during 1925, 1926 and part of 1927 at many places show that there is a great loss of this radiation in smoky cities. The winter readings are much lower than the summer.

While Davos in Switzerland receives a greater amount of ultra-violet radiation than the most favoured British place, Assouan in Egypt receives a greater amount than Davos.

I am indebted to Mr. C. Pergande for his care in keeping the records.

Intensities in the Secondary Spectrum of Hydrogen at Various Temperatures.

By Prof. J. C. McLennan, F.R.S., H. Grayson-Smith, Ph.D., and W. T. Collins, M.A.

(Received June 22, 1927.)

Introduction.

In recent years a great deal of progress has been made in the classification of the lines of the secondary spectrum of hydrogen. In particular, O. W. Richardson* has included a large number of lines in a system involving electronic, vibrational and rotational terms, of which the Fulcher bands form an important part. This includes a number of band systems due to electronic transitions from a series of *m*P levels to a 2S level, and one system due to the electronic transition from the 3S to the 2P level. Fig. 1 shows the electronic energy levels as compared with the corresponding levels in the helium atom. Fig. 2 shows the vibrational levels included in the *m*P → 2S series, and fig. 3 some of the rotational levels included in the 3P → 2S system. In most of these bands, Q-branches only have been identified. Following Richardson's notation,

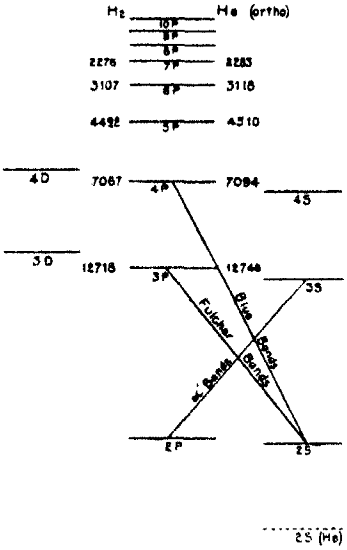

Fig. 1.—Electronic Levels of Hydrogen and Orthohelium.

---

* 'Roy. Soc. Proc.,' A, vol. 111, p. 714 (1926); vol. 113, p. 368 (1926); vol. 114, p. 643 (1927).

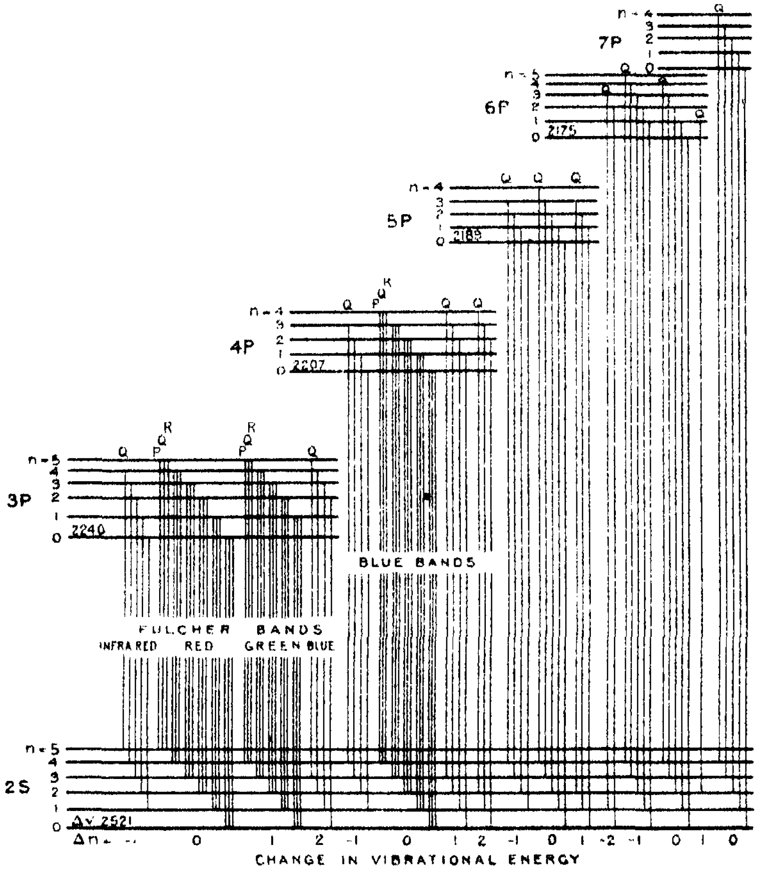

FIG. 2.—Vibrational Levels in H_2.

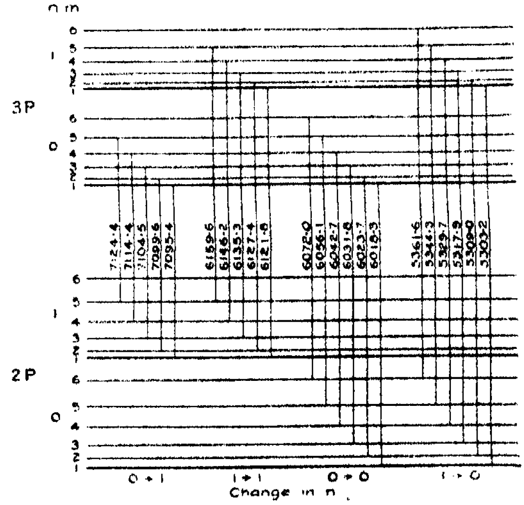

FIG. 3.—Rotational Levels in H_2.

the different systems of the $mP \rightarrow 2S$ series have been denoted by α, β, γ, etc., and for further convenience the $3S \rightarrow 2P$ system has been denoted by α'. The different bands are denoted by $n'' \rightarrow n'$, etc., where n'' and n' are the initial and final values of the vibrational quantum numbers. Thus $0 \alpha 0Q1$ indicates the first line of the Q-branch of the $0 \rightarrow 0$ band of the $3P \rightarrow 2S$ system.

Many other regularities have been pointed out from time to time in the secondary spectrum. Allen and Sandeman* have arranged a number of lines which are enhanced at high pressure in a band system which they believe to be due to H_3. Isolated series, some of which perhaps have no real significance, have been picked out by Richardson and Tanaka† and by Richardson‡ on the basis of the characteristics of the lines at different voltages. Some similar regularities are due to Curtis§ and Kiuti.‖

Since it is well known that band lines due to transitions between energy levels involving large rotational quantum numbers should be reduced in intensity at low temperatures, measurements of the intensities of the lines of these band series at different temperatures should form a valuable criterion as to the accuracy of the classifications so far made, and should be of assistance in the further analysis of the spectrum. A certain amount of work has already been done in this direction. McLennan and Shrum¶ have published a list of lines which are either enhanced or reduced at the temperature of liquid hydrogen. Goos** has measured the relative intensities at different temperatures of the lines of the Fulcher bands. McLennan, Grayson-Smith and Lea†† have given preliminary measurements of the intensities at two temperatures of a number of the stronger lines. In the present paper relative measurements are given of the intensities at the temperatures obtained by cooling the discharge tube with water and with liquid air. These measurements include most of the lines from λ 6532 A to λ 3777 A in Merton and Barratt's table‡‡ of the lines of the secondary spectrum.

---

* 'Roy. Soc. Proc.,' A, vol. 114, p. 293 (1927).

† 'Roy. Soc. Proc.,' A, vol. 106, p. 640 (1924); vol. 107, p. 602 (1925).

‡ 'Roy. Soc. Proc.,' A, vol. 108, p. 553 (1925); vol. 109, pp. 35, 239 (1925).

§ 'Phil. Mag.,' vol. 1, p. 695 (1926).

‖ 'Proc. Phys. Math. Soc.,' Japan, vol. 5, p. 9 (1923).

¶ 'Trans. Roy. Soc. Can.,' III, vol. 18, p. 177 (1924).

** 'Z. f. Physik,' vol. 31, p. 229 (1925).

†† 'Roy. Soc. Proc.,' A, vol. 113, p. 183 (1926).

‡‡ 'Phil. Trans.,' A, vol. 222, p. 369 (1922).

Experimental.

A specially constructed discharge tube was used, with a capillary portion about 12 cm. long and 0·4 cm. in diameter, made of thin-walled Pyrex glass. This was bent into the form shown in fig. 4, so that it could be fitted into a liquid air flask with the capillary vertical. The light from the end of the capillary was reflected on to the slit of the spectrograph by means of a right-angled prism. By this means it was possible to avoid passing the light through the liquid air, which absorbs strongly, and at the same time to take advantage of the added intensity obtained by viewing the discharge longitudinally. The discharge was excited by means of a 20,000 volt ½-k.w. transformer, without capacity, using a gas pressure of about ½-mm.

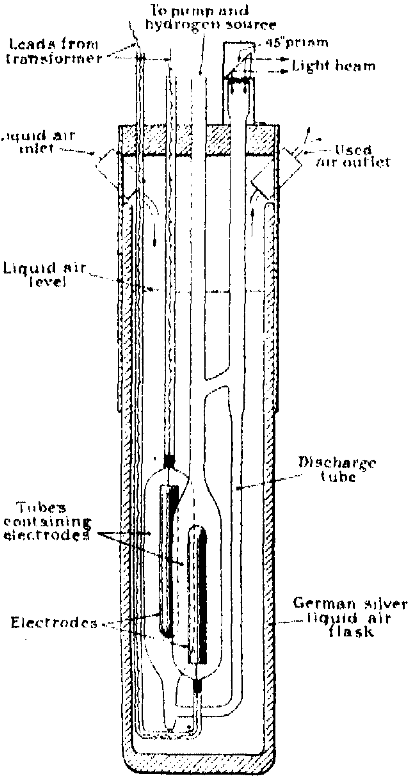

FIG. 4.

In order to develop the secondary spectrum to the best advantage, it is necessary to use very pure hydrogen. The tube was operated for several hours in order to drive occluded gas out of the terminals, and then highly exhausted, using liquid air traps to condense mercury vapour, etc. Finally hydrogen was admitted by heating a palladium tube. No lines due to any impurities were identified on the plates finally used for measurement.

The spectra were photographed on a Hilger E1 quartz spectrograph, using Ilford panchromatic plates for the greater part of the spectrum. For the region from λ 5728 A to λ 4867 A, where these plates have a minimum of sensitivity, they were supplemented by Eastman "Astronomical Green" plates. The two exposures at room temperature and at the temperature of liquid air were made successively on the same day without re-exhausting the discharge tube, and special care was taken that nothing except the temperature should be changed.

The intensities were obtained from the plates by means of a Moll self-registering microphotometer, using the formula $I = \log \frac{h_0}{h_0 - h}$ where h_0 is the total galvanometer deflection in the absence of a line, and h is the height of the trace of the line (*see* fig. 5). This is equivalent to $I = \log \frac{\text{(Incident light)}}{\text{(Transmitted light)}}$ and is sufficiently accurate for relative measurements of lines of moderate intensity. This, of course, takes no account of the change of the sensitivity of the plates with the wave-length, and therefore little importance can be attached to the relative intensities of lines which are widely separated on the plates. Fig. 5 shows a portion of the microphotometer curves obtained,

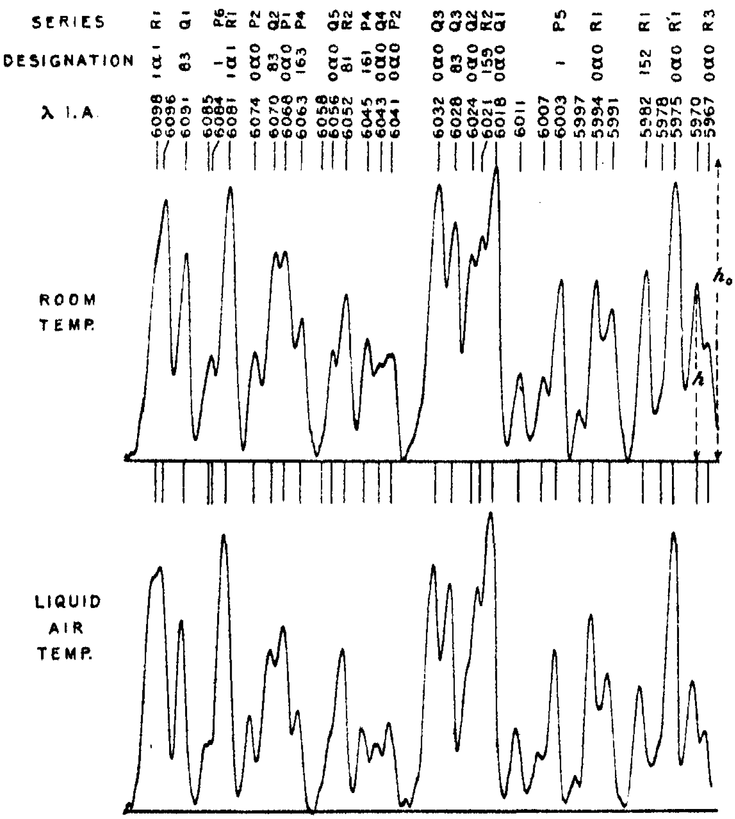

FIG. 5.

including the 0α0 band and neighbouring lines. The variations in the intensities at the two temperatures are quite obvious in the reproduction.

Richardson's Series System.

The results of the measurements of the intensities of the lines included in Richardson's series system are given in Table I. The first two columns of the table give the series designations, the third the wave-length (from Merton and Barratt), and the fourth and fifth the measured intensities on the plates taken at room temperature and at the temperature of liquid air respectively. "*a*" indicates lines whose intensities may be affected by their proximity to a stronger line; "*b*" indicates lines, which on our plates, are masked by a neighbouring strong line. In the column headed "Remarks," alternative assignments for some of the lines are given; "*d*" in this column indicates lines whose assignments are given as doubtful in Richardson's papers. The table is far from complete, bands and portions of bands which were too faint to make intensity measurements having been omitted. The confirmation of the system as a whole is excellent. A few lines appear to be out of place, or possibly in certain cases the line which is given as a component and whose intensity has been measured is in reality a multiple line. An example of this is the line 0α0P2, which is reduced at liquid air temperature, while other P2 lines are slightly enhanced. Similar examples will be found on inspection of the table.

Table I.—Intensities of Richardson's Series Bands.

System 3P → 2S (α).

Series.	Member.	Wave-length.	Intensities.		Remarks.
			R.T.	L.A.	
0*a*0	Q 1	6018·29	130	110	
	Q 2	6023·74	47	27	
	Q 3	6031·80	96	60	
	Q 4	6042·70	16*a*	10*a*	or 28Q8
	Q 5	6056·10	17*a*	12*a*	or 1*a*′1R2
	R 1	5994·05	38	40	
	P 2	6067·70	47	36	or 3P2
	P 3	6100·18	*b*	*b*	
	P 4	6137·91	13	10½*a*	
1*a*1	Q 1	6121·76	110	105	
	Q 2	6127·40	53	29	
	Q 3	6135·34	82	63	
	Q 4	6146·17	13	5	

Table I—continued.

Series.	Member.	Wave-length.	Intensities.		Remarks.
			R.T.	L.A.	
1a1	R 1	6098·23	48	65	
	R 2	6074·39	18	15	or 0a′0P3
	R 3	6053·27	*b*	*b*	
	R 4	6035·02	8*a*	5*a*	or 1a′1R3
	P 2	6169·63	24	29	
2a2	Q 1	6224·81	90	95	
	Q 2	6230·23	30	18	
	Q 3	6238·39	41	25	
	Q 4	6249·15	7	4½*a*	or 3a3R3
	Q 5	6262·49	8	4	
	R 1	6201·15	*b*	*b*	
	R 2	6174·88	*b*	*b*	
	R 3	6151·47	12½	12	
	P 2	6271·31	19	24	
3a3	Q 1	6327·07	61	68	
	Q 2	6332·46	19*a*	10½	
	Q 3	6340·57	17½	12	
	R 1	6303·46	17	20	
	R 2	6274·86	21	20	
	R 3	6249·15	7	4½*a*	or 2a2Q4
	R 4	—	—	—	
	R 5	6207·31	3½	2	
	P 2	6372·19	9½	12	
	P 3	6411·77	*b*	2½	or 4a′4Q3
4a4	Q 1	6428·10	29	30	
	Q 2	6433·47	9*a*	4½*a*	
	Q 3	6441·50	11	8½	
	Q 4	6452·13	3	—	
	R 1	6404·01	—	—	
	R 2	6376·11	3½*a*	1½	or 3a′3P2
5a5	Q 1	6527·35	9	10½	
	Q 2	6532·62	1½	1	
1a0	Q 1	5303·15	45	38	
	Q 2	5309·03	14	8	
	Q 3	5317·90	20	12½	
	Q 4	5329·74	6½	4	
	R 1	5283·30	*b*	*b*	
	R 2	5270·41	20	6	
	R 3	5259·69	—	—	
	R 4	5250·15	2½	2	
	P 2	5340·84	8	10	or 1a′0Q1
2a1	Q 1	5419·90	58	55	
	Q 2	5425·96	41	24	

Table I—*continued.*

Series.	Member.	Wave-length.	Intensities.		Remarks.
			R.T.	L.A.	
2*a*1	Q 3	5434·83	31	19	
	Q 4	5446·70	6½	2½	
	Q 5	5461·50	14	8½	
	Q 6	5479·2	*b*	*b*	
	Q 7	5499·56	35	22	*d* probably 3*a*2R2
	Q 8	5521·87	13	8½	*d*
	R 1	5401·06	25	29	
	P 2	5456·97	16	18	
	P 3	5488·48	—	—	
	P 4	5524·01	8½	8	
3*a*2	Q 1	5537·45	63	60	
	Q 2	5543·41	31	19	
	Q 3	5552·52	24	14	
	Q 4	5564·53	17	11	
	Q 5	5579·47	14	11	
	R 1	5518·48	21	24	
	R 2	5499·56	35	22	
	R 3	5483·90	7	3½	
	P 2	5573·86	13½	16½	or 186R4
	P 3	5606·8	2*a*	2*a*	
	P 4	5646·12	6	5	
4*a*3	Q 1	5655·75	40	40	
	Q 2	5661·72	32	23	
	Q 3	5670·89	19½	14	
	R 1	5634·31	*b*	*b*	
	R 2	5616·24	7½	5½	
	P 2	5689·19	61	51	or K5
	P 3	5725·87	—	—	
	P 4	5766·98	35	26	or 0β2Q5
	P 5	5812·56	77	55	probably 28Q3
5*a*4	Q 1	5774·98	42	43	doublet ? or G4
6*a*5	Q 1	5889·96	—	*b*	
	Q 2	5893·95	13	9½	
	Q 3	5900·48	8½	7	
	Q 4	5909·37	*b*	*b*	
	Q 5	5920·65	35	30	*d* probably 157Q3
2*a*0	Q 1	4768·10	—	—	
	Q 2	4774·29	2½	2	
	Q 3	4783·47	—	—	
	Q 4	4795·14	*b*	*b*	
	Q 5	4811·67	3	3	*d*
3*a*1	Q 1	4891·22	10½	10½	
	Q 2	4897·49	—	—	
	Q 3	4906·27	13	11½	*d*
	Q 4	4919·11	14½	7½	
	Q 5	4934·29	68	46	*d*

Table I—continued.

Series.	Member.	Wave-length.	Intensities.		Remarks.
			R.T.	L.A.	
4α2	Q 1	5016·43	28	18	or 202P4
	Q 2	5022·63	2	1	
	Q 3	5032·19	5	—	
	Q 4	?	—	—	
	Q 5	5061·73	12	8½	
5α3	Q 1	5143·53	13½	10	or 83Q11
	Q 2	5150·09	2	1½	
	Q 3	5159·80	7	4½	*d*
3α0	Q 2	4360·34	6	—	
5α2	Q 3	4625·39	20	12	*d*

System 4P → 2S (β).

0β2	Q 1	5759·51	*b*	*b*	
	Q 2	5760·37	29	21	or 152R3
	Q 3	5762·70	6½	6	or 201R7 or 158R5
	Q 4	5766·08	*b*	4½*a*	*d*
	Q 5	5766·98	19	12	or 4 3P4
0β1	Q 1	5063·84	22	14	
	Q 2	5067·47	—	—	*d*
	Q 3	5069·73	*b*	*b*	
	Q 4	5075·44	17½	12	*d* or 53P4
	Q 5	5080·47	28	21	
1β2	Q 1	5109·32	11½	9½	
	Q 2	5111·78	—	—	
	Q 3	5115·37	8½	5	
	Q 4	5120·97	5½	4	*d*
	Q 5	5127·94	5	5	*d*
2β3	Q 1	5153·87	11	11	
	Q 2	5156·30	8½	6	
	Q 3	5160·55	—	—	*d*
	Q 4	5164·67	5	3	
	Q 5	5170·96	10	6	
3β4	Q 1	5197·30	*b*	*b*	
	Q 2	5199·61	17½	12½	
4β5	Q 1	5239·04	6	7	
0β0	Q 1	4490·45	35	34	
	Q 2	4493·67	13½	9	
	R 1	4474·24	15½	10½	or 26P4
	R 2	4464·12	8	5½	or 61Q3
	R 3	4455·67	15½	12½*a*	
	R 4	4449·42	—	—	
	R 5	4445·24	23	22	

Table I—continued.

Series.	Member.	Wave-length.	Intensities.		Remarks.
			R.T.	L.A.	
System 4P → 2S (β)—continued.					
$0\beta0$	P 2	4515·47	8½	6	or IIA*b*Q6
	P 3	4534·17	31	29	or IIA*c*Q3
	P 4	4555·87	—	—	
	P 5	4580·04	57	50	and others
	P 6	4607·38	20	8	or 101R2
$1\beta1$	Q 1	4554·13	25	28	
	Q 2	4557·32	18½	14	
	Q 3	4562·24	13½	8	
	R 1	4537·83	15	11½	
	R 2	4524·95	*b*	*b*	
	R 3	4514·27	9½	6	or IIA*a*Q7
$1\beta1$	P 2	4577·23	—	—	or $1\beta1$Q5
	P 3	4597·22	6	5½	
	P 4	4620·72	7	3	or $2\beta2$Q2
$2\beta2$	Q 1	4617·49	42	29	
	Q 2	4620·72	7	3	or $1\beta1$P4
	Q 3	4625·39	20	12	
	R 1	4605·35	—	—	or 111P5
	R 2	4591·84	3½	3	or $3\gamma4$Q2
	R 3	4580·04	57	50	and others
	P 2	4643·83	—	—	
	P 3	4667·05	10	7½	
	P 4	4692·04	10½	8½	or $0\delta2$Q3
	P 5	4721·56	10	6½*a*	or $4\beta4$R3
$3\beta3$	Q 1	4680·43	12½	11½	
	Q 2	4683·79	36	36	
	R 2	4657·83	5*a*	2½	
	P 2	4705·24	2	4	
	P 3	4732·81	3½	4	probably $4\beta4$R1
	P 4	4763·82	11	13	probably $1\delta5$R1 or IIB*b*Q2
$4\beta4$	Q 1	4742·75	17	17	or IIB*a*Q2
	R 1	4732·81	3½	4	
	R 2	4726·13	—	—	or $3\delta5$Q1
	R 3	4721·56	10	6½	or $2\beta2$P5
	R 4	4719·02	29	31	
	P 5	4869·42	19	9½	
$1\beta0$	Q 1	4085·18	19	24	or $1\gamma1$Q3
$2\beta1$	Q 1	4159·31	7½	9	
$3\beta2$	Q 1	4233·60	13	14½	or $4\gamma4$Q1
	Q 2	4237·57	2	2	
	Q 3	4243·27	7	6	
$4\beta3$	Q 1	4308·60	5	6	

Table I—continued.

Series.	Member.	Wave-length.	Intensities.		Remarks.
			R.T.	L.A.	
		System 5P → 2S (γ).			
0γ1	Q 1	4478·97	6½	7	
2γ3	Q 2	4557·32	18	14	probably 1β1Q2
3γ4	Q 2	4591·84	3½	3	or 2β2R2
	Q 3	4594·72	—	—	
	Q 4	4598·48	6½	4	
0γ0	Q 1	4024·79	6	5	
	Q 2	4027·42	8½	—	or IIDcQ2
	Q 3	4031·60	6½	6	or IID*b*Q2
1γ1	Q 1	4078·88	21	25	
	Q 2	4081·46	—	—	
	Q 3	4085·18	11½	13	or 1β0Q1
	Q 4	4090·74	—	—	
	Q 5	4097·47	4	8½	
	Q 6	4106·22	4½	4½	
2γ2	Q 1	4131·50	8	7½	
	Q 2	4133·99	6½	6	
	Q 3	4138·18	—	—	
	Q 4	4143·86	—	—	
	Q 5	4151·55	3	2½	or IIC*a*Q4
3γ3	Q 1	4182·14	22	24	
	Q 2	4184·67	—	—	
	Q 3	4188·24	3	1½	*d*
4γ4	Q 1	4233·60	13½	15	or 3β2Q1
3γ2	Q 2	3825·01	2½	—	
	Q 3	3829·07	—	—	*d*
	Q 4	3836·48	7	3	*d*
4γ3	Q 1	3884·21	4½	9½	or 1δ0Q1
		System 6P → 2S (δ).			
0δ2	Q 2	4690·16	15½	15½	
	Q 3	4692·04	10½	8½	or 2β2P4
1δ3	Q 3	4709·52	17	17	
0δ1	Q 1	4217·7	—	—	
	Q 2	4219·49	2½	4	
	Q 3	4222·30	24	25	doublet ?
2δ3	Q 1	4290·15	6	5	
4δ5	Q 2	4350·78	2	1½	

Table I—continued.

Series.	Member.	Wave-length.	Intensities.		Remarks.
			R.T.	L.A.	
		System 6P→2S (δ)—continued.			
1δ1	Q 1	3863·22	14	16	
	Q 6	3887·90	4½	3	*d* or 4ε4Q5
3δ3	Q 3	3960·07	4½	2	
4δ4	Q 1	4000·85	7½	7	
		System 7P→2S (ε).			
2ε2	Q 1	3792·98	—	—	
	Q 2	3794·47	3½	2	
	Q 3	3797·62	*b*	*b*	
	Q 4	3803·05	12	16	
4ε4	Q 1	3872·38	19	20	
	Q 5	3887·90	4½	3	*or* 1δ1Q6
		System 3S←2P (α′).			
0α′0	Q 1	5989·22	*b*	*b*	
	Q 2	5991·92	*b*	*b*	
	Q 3	5998·02	—	—	
	Q 4	6006·91	14	9	
	R 1	5975·43	105	84	
	R 2	5957·26	*b*	*b*	
	R 3	5941·95	18½*a*	18*a*	
	P 2	6041·01	18*a*	14	
	P 3	6074·39	18	15	or 1α1R2
	P 4	6112·80	4*a*	2*a*	
	P 5	6155·61	14	9	probably 2α2R2
1α′1	Q 1	6093·83	*b*	*b*	
	Q 2	6095·96	76	69*a*	
	R 1	6080·78	89	83	
	R 2	6056·10	17	11½	or 0α0Q5
	R 3	6035·02	8	5	or 1α1R4
	P 4	6232·99	17½	10½	probably 3α′3R3
2α′2	Q 1	6197·05	*b*	*b*	
	Q 2	6199·38	73	68	
	R 1	6182·98	45	45	
	R 2	6155·61	14	9	
	P 2	6264·89	3	3	

Table I—*continued.*

Series.	Member.	Wave-length.	Intensities.		Remarks.
			R.T.	L.A.	
System 3S←2P (α′)—continued.					
3α′3	Q 1	6299·42	42	41	
	Q 2	6302·27	*b*	*b*	
	Q 3	6309·01	—	—	
	Q 4	6318·65	5½*a*	4	
	R 1	6285·37	26	28	
	R 2	6257·63	2½*a*	3*a*	
	R 3	6232·99	17½	10½	
	P 2	6376·11	3½*a*	1½	or 4α4R2
4α′4	Q 1	6399·45	28	30	
	Q 2	6404·01	—	—	
	Q 3	6411·77	*b*	2½	or 3α3P3
	R 1	6391·04	4½	3½	
	R 2	6362·48	18	12	or 159Q′2
	P 2	6487·76	1½	1½	or 163P6
	P 3	6524·63	2	4	*d*
5α′5	Q 1	6499·87	2½	2	
1α′0	Q 1	5340·84	8	10	or 1α0P2
	Q 2	5344·82	11½	8	
	Q 3	5351·75	5	3½	
3α′2	Q 3	5597·63	33	31	probably K7

An attempt has been made to compare the observed intensities of the lines of the Q-branches which have been definitely measured with the intensities calculated by means of Kemble's formula,* which reduces to $I \propto (2m+1)\,\epsilon^{-e_m}/kT$ for the Q-branches, where m is the quantum number expressing the total angular momentum, e_m is the corresponding rotational energy, and T is the absolute temperature. In agreement with the theoretical requirements of Mullikan† m has been taken to be 1, 2, 3, . . . for the Q-branches. In order to find the effective temperature of the discharge, it is necessary to assume that the intensities of at least two lines follow the formula. The two taken were the lines Q1 and Q3 of the 0α0 band, which appear to be regular, giving temperatures of 315° A and 240° A when the tube was cooled with water and with liquid air respectively. These temperatures were then used to calculate the relative intensities of the lines of the Q-branches with respect to Q1 = 100. In Table II, the observed intensities of the Q-branches for which definite measurements have been possible are compared with these calculated intensities. Strictly, the calculated intensities should vary with each band, owing to the variation in e_m. This variation, however, is only of the order of magnitude of the error of measurement, and has not been considered. While this calculation is of little real value, owing to the small number of members in each band, certain features of the intensity arrangement in the bands are more clearly brought out by it.

---

* 'Phys. Rev.,' vol. 25, p. 1 (1925).

† 'Phys. Rev.,' vol. 28, pp. 481, 1202 (1926).

One of the most noticeable features of the hydrogen bands is the alternation of intensity between the odd and even numbers of the series. This has been shown to be a necessary characteristic of band spectra due to homopolar molecules, such as H_2, and the occurrence of the phenomenon in these bands may be considered as a further support of their assignment to the H_2 molecule. Generally, the intensities of the Q2 and Q4 lines are about one-third of the calculated values at room temperature, and are still less at the temperature of liquid air. This reduction of the relative prominence of the even members with change of temperature is quite marked, and probably has some bearing on the anomalous behaviour of the specific heat of hydrogen at low temperatures. Some exceptions appear in which the Q2 line is stronger than the above, for example, in the bands 1α1, 3α2, 2α1, 4α3, 1β1. The line 2β2Q2 is much too faint.

The Q3 line appears to be weak in many of the bands included in Table II, and in some other bands. In a few bands, Q5 is too strong, for example, in 2α1, and 3α2, and also in 4α2, 0β1, 2β3. In the bands 6α5 and 3α1, the correct Q5 line is probably masked by the line at present assigned to that position.

For the bands of systems other than α and β the information afforded by the intensity measurements is too incomplete to justify their inclusion in Table II. As will be seen from Table I, the general characteristics are the same for the other bands of the $m\text{P}\rightarrow 2\text{S}$ series. In the P-branches which have been classified by Richardson for part of the α system, the even members are very much stronger than the odd, the latter being so weak that no comparison can be made. This must be taken to indicate that the anomalous behaviour of the even members belongs principally to the initial levels. The P-branches of the system, and the R-branches generally, are rather irregular, and little can be said about them. In the Q-branches of the α′ system, there is some evidence that the even members are strong and the odd weak.

Table II.—Calculated and Observed Intensities.

Member.	Calc.	0α0	1α1	2α2	3α3	4α4	1α0	2α1	3α2	4α3	0β0	1β1	2β2
							At room temperature.						
1	100	100	100	100	100	100	100	100	100	100	100	100	100
2	105	36	48	33	31	30	31	71	49	80	39	74	17
3	74	74	75	46	29	38	44	54	38	49	—	54	48
4	38	12½	12	8	—	10	14	11	27	—	—	—	—
5	14½	13	—	9	—	—	—	24	22	—	—	—	—
							At liquid air temperature.						
1	100	100	100	100	100	100	100	100	100	100	100	100	100
2	93	25	28	19	15½	15	21	44	31	58	27	50	10
3	55	55	60	26	18	28	33	35	23	35	—	29	41
4	22	9	5	4½	—	—	10½	4½	17	—	—	—	—
5	6	11	—	4	—	—	—	15	17	—	—	—	—

The Bands of Allen and Sandeman.

The lines included in the band system picked out by Allen and Sandeman are all lines which are enhanced at high pressure, and most of them are faint on our plates. Those that have been observed with measurable intensity are given in Table III. The intensities of these lines are very irregular, and not much can be said from the information given by the intensity measurements about the justification of this system. It is possible that some of the lines observed by us with considerable strength at low pressure in reality mask faint lines which are the true band members.

Table III.—Bands due to Allen and Sandeman.

Series.	Member.	Wave-length.	Intensities.		Remarks.
			R.T.	L.A.	
IIAa	Q 1	4579·43	—	—	
	Q 2	4578·00	24	12	
	Q 3	4572·73	38	29	
	Q 4	4563·68	10	4½	
	Q 5	4550·96	23	17	
	Q 6	4534·56	—	—	
	Q 7	4514·27	9½	6	or 1β1R3
	Q 8	4490·45	35	34	belongs to 0β0Q1

Table III—continued.

Series.	Member.	Wave-length.	Intensities.		Remarks.
			R.T.	L.A.	
IIA*a*	R 2	4575·86	22	25	
	R 3	4568·10	41	40	
	R 4	4555·85	—	—	
	R 5	4541·12	3	3½	
	P 4	4582·58	35	28	
	P 5	4580·04	57	50	and others
IIA*b*	Q 2	4558·50	22	15½	
	Q 5	4515·47	8½	6	or 0β0P2
IIA*c*	Q 2	4539·15	15	14½	
	Q 3	4534·17	31	29	or 0β0P3
IIA*d*	Q 5	4493·67	13½	9	probably 0β0Q2
IIB*a*	Q 2	4742·75	17	17	or 4β4Q1
	Q 3	4737·39	—	—	
	Q 4	4727·75	—	—	
	Q 5	4713·93	11	15	
	Q 6	—	—	—	
	Q 7	4674·53	16*a*	17*a*	
IIB*b*	Q 2	4763·82	11	13	or 185R1
IIB*c*	Q 1	4786·04	8*a*	7*a*	*d* probably 53P1
	Q 2	4784·85	7½*a*	6½*a*	
IIB*d*	Q 1	4807·33	6	4½	*d* probably 110Q5
IIB*e*	Q 4	4811·67	3	3	
	Q 5	4797·76	19½	20	*d*
IIC*a*	Q 2	4163·52	13	7½	
	Q 3	4159·31	7½	9	probably 2β1Q1
	Q 4	4151·55	3	2½	or 2γ2Q5
	Q 5	4140·80	—	—	
	Q 6	—	—	—	
	Q 7	4110·17	5½	4	
IIC*b*	Q 2	4179·54	28	32	
	Q 3	4175·13	17½	12	or 20Q2
	Q 4	4167·60	2½	3	
	Q 5	4156·70	17½	13	or 20Q5
IIC*c*	Q 2	4195·65	30	26	
IIC*d*	Q 4	4199·77	21	27	
IIC*e*	Q 3	4223·89	15	13	
	Q 4	4214·27	—	—	
	Q 5	4205·10	43	51	
IID*a*	Q 2	4057·50	4	1½	

Table III—continued.

Series.	Member.	Wave-length.	Intensities.		Remarks.
			R.T.	L.A.	
IID*b*	Q 1	4043·57	13	12	
	Q 2	—	—	—	
	Q 3	4038·56	3½	2	
	Q 4	4031·60	6½	6	or 0γ0Q3
IID*c*	Q 1	4028·35	14½	16½	
	Q 2	4027·42	8½	—	or 0γ0Q2
IID*d*	Q 6	3978·33	5½	4	
IID*e*	Q 3	3991·96	22	23	

Miscellaneous Regularities.

The intensities of the lines included in the various disconnected regularities picked out by Richardson and others are given in Table IV. In some of these series it was necessary to use measurements made on the "Green plates" in the same series as measurements from the ordinary plates. In such cases the intensities given in brackets are those taken from the "Green plates." A large number of series given by Richardson have been omitted from the table, for which intensity measurements could be made for only one or two lines. Only the following series can be said to be justified by the intensity measurements at the two temperatures: 59Q, 20Q, 185R, 61Q. 181Q appears to be a reversed R-series. In a large number of series all the lines are affected in the same way by the change of temperature, and it is therefore suggested that the following series may be in reality sequences of corresponding members of associated bands: 1P, 28Q, 201R, 202P, 3P, 11R, 27P, 53P, 81R, 83Q, 83R, 152R, 185Q, 85Q, 157Q, 154Q, K, H, Ki. Of these, 201R, 202P, 11R, 83R, 154Q, K, H, appear to be composed of lines with low rotational quantum numbers; 83Q appears to be composite with members alternately of low and higher quantum number; the remainder appear to be composed of lines with higher quantum numbers. Other series included in Table IV are indefinite, or have irregular intensities.

Table IV.—Miscellaneous Series due to Richardson.

Series.	Member.	Wave-length.	Intensities.		Remarks.
			R.T.	L.A.	
1P	P 2	5816·39	—	—	
	P 3	5869·18	35	27	
	P 4	5931·33	77	60	
	P 5	6002·81	39	30	
	P 6	6084·22	16½	10½*a*	
28Q	Q 1	5778·96	19	12	
	Q 2	5791·74	26	18	or 201R8
	Q 3	5812·56	77	50	or Ki1
	Q 4	5841·41	7	3½	
	Q 5	5878·43	34	34	
	Q 6	—	—	—	
	Q 7	5978·02	9	10½	
	Q 8	6042·70	15½*a*	10	or 0*a*0Q4
201R	R 1	5754·61	—	—	
	R 2	5736·88	67	61	or K4
	R 3	5725·87	*b*	*b*	
	R 4	5723·44	24	20	
	R 5	5728·54	61	49	or G5
	R 6	5741·80	27	24	
	R 7	5762·70	13	11½	*or 0β2Q3 or 158R5*
	R 8	5791·74	40	29	or 28Q2
202P	P 2	4849·34	40	30	
	P 3	4928·62	64	45	
	P 4	5016·43	28	18	or 4*a*2Q1
110Q	Q 1	4751·59	3½	2½	
	Q 2	4756·92	4½	5½	
	Q 3	4768·10	—	—	or 2*a*0Q1
	Q 4	4784·85	7½*a*	6½*a*	probably IIB*c*Q2
	Q 5	4807·33	6	4½	
59Q	Q 1	4867·05	22	19	or 41Q2 or 185Q3
	Q 2	4875·92	27	17	
	Q 3	4891·22	10½	10½	probably 3*a*1Q1
	Q 4	4912·32	4½	3	
3P	P 1	5959·70	46	27	
	P 2	6067·70	47	36	or 0*a*0P2
	P 3	6174·03	32	25	or 158R1
	P 4	6278·32	—	—	
	P 5	6380·11	13½	13	
11R	R 1	5103·56	(15½)	(11½)	
	R 2	5003·40	(21)	(17)	
	R 3	4896·46	(11½)	(7)	or 104Q3
	R 4	4784·85	(12)	(9)	probably IIBcQ2
	R 5	4669·25	—	—	
	R 6	4550·96	23	17½	probably IIA*a*Q5 or 111P4
27P	P 1	5180·59	16	9	
	P 2	5256·61	23	12	
	P 3	5329·74	6½	4	probably 1*a*0Q4

Table IV—continued.

Series.	Member.	Wave-length.	Intensities.		Remarks.
			R.T.	L.A.	
20Q	Q 1	4177·40	48	51	
	Q 2	4175·13	17½	12	or IIC*b*Q3
	Q 3	4171·29	23	16½	
	Q 4	4165·17	7	4	
	Q 5	4156·70	17½	13	or IIC*b*Q5
	Q 6	4146·22	6	6	
	Q 7	4133·99	6½	6	probably 2γ2Q2
53P	P 1	4786·04	13	7	or IIB*c*Q1
	P 2	4883·82	9½	5½	
	P 3	4980·47	19	14	
	P 4	5075·44	17½	12	or 0β1Q4
	P 5	5168·25	10	7	
81R	R 1	6134·27	*b*	*b*	
	R 2	6052·34	34	30	
	R 3	5970·24	38	23	
	R 4	5888·14	57	43	
	R 5	5806·09	26	21	
	R 6	5724·55	—	—	
	R 7	5642·78	(23)	(7½)	or K6
	R 8	5561·65	(15)	(12)	
83Q	Q 1	6090·92	47	38	
	Q 2	6070·00	47	30	
	Q 3	6027·98	63	52	
	Q 4	5967·31	20	13	
	Q 5	5889·04	*b*	*b*	
	Q 6	5794·65	19½	13	
	Q 7	5686·10	—	—	
	Q 8	5564·53	(17)	(11)	probably 3α2Q4
83Q or 83R	Q 10	5291·59	(22)	(18)	
	Q 11	5143·53	(13½)	(10)	or 5α3Q1
	Q 12	4990·16	(6½)	(5½)	
	Q 13	4832·79	9	8	or 41Q3
	Q 14	4673·12	11	9½	
162R or 52P	R3 P4	5340·84	8	10	probably 1α'0Q1
	R4 P3	5272·29	33	29	
	R5 P2	5214·64	11½	9½	
171P	P 2	5743·05	*b*	*b*	
	P 3	5884·66	48	35	
	P 4	6045·44	21	12½	or 161P4
159R	R 1	6161·59	38	24	
	R 2	6021·28	56	50	
	R 3	5916·24	42	31	
	R 4	5843·45	4	2	
	R 5	5801·14	12½	9	or 156Q5
	R 6	5788·25	18	14	
152R	R 1	5982·54	43	21	
	R 2	5864·47	15	12½	
	R 3	5760·37	29	21	or 0β2Q2

Table IV—continued.

Series.	Member.	Wave-length.	Intensities.		Remarks.
			R.T.	L.A.	
185Q	Q 1	4878·10	9	7½	
	Q 2	4874·28	*b*	*b*	
	Q 3	4867·05	22	19	or 59Q1 or 41Q2
	Q 4	4856·54	34	25	
	Q 5	4842·45	15*a*	7*a*	
	Q 6	4824·58	9	6	*d*
185R	R 1	4763·82	11	13	or IIB*b*Q2
	R 2	4686·79	20	18½	
	R 3	4609·14	—	—	
	R 4	4531·14	6	6½	
	R 5	4453·02	16	10½	
61Q	Q 1	4434·31	8½	5	or 112Q1 (double ?)
	Q 2	4447·56	38	39	
	Q 3	4464·12	8	5½	or 0β0R2
	Q 4	4487·80	24	15	
112Q	Q 1	4434·31	8½	5	or 61Q1 (double ?)
	Q 2	4429·29	—	—	
	Q 3	4417·32	22	14	
	Q 4	4398·19	5½	2½	
84R	R 1	4813·61	7	7	
	R 2	4723·01	26	16½	
	R 3	4631·44	—	—	
	R 4	4539·15	15	14½	probably IIA*c*Q2
85Q	Q 0	4379·38	11	7½	
	Q 1	4390·89	14½	9	or 26P3
	Q 2	4414·22	26	16	
	Q 3	4449·92	14½	10	
157 Q	Q 1	5956·42	14½	10½	
	Q 2	5947·27	37	23	
	Q 3	5920·65	35	30	
	Q 4	5871·81	34	31	or G2
	Q 5	5801·14	12½	9	
	Q 6	5709·74	(20)	(27)	or 157R2
	Q 7	5601·66	*b*	*b*	or 4*a*3R3
	Q 8	5481·08	(36)	(30)	
157 R	R 0	5891·31	*b*	*b*	
	R 1	5803·93	*b*	16*a*	
	R 2	5709·74	(20)	(27)	or 157Q6
	R 3	5600·38	(26)	(15)	
	R 4	5474·89	(19½)	(12½)	
153 P	P 1	5893·95	13	9½	or 6*a*5Q2
	P 2	5982·54	43	21	
	P 3	6090·92	47	38	
156 Q	Q 1	5712·19	—	*b*	
	Q 2	5716·00	(20)	(12)	
	Q 3	5731·92	(52)	(40)	
	Q 4	5759·51	—	—	or 0β2Q1
	Q 5	5798·95	(13)	(10)	or 159R5
	Q 6	5850·89	—	—	or 159R8
	Q 7	5916·24	42	31	probably 159R3

Table IV—continued.

Series.	Member.	Wave-length.	Intensities.		Remarks.
			R.T.	L.A.	
158 R	R 1	6174·03	32	25	or 3P3
	R 2	6067·70	47	36	probably 0*a*0P2 or 3P2
	R 3	5963·46	19	16	
	R 4	5861·56	—	—	
	R 5	5762·70	6½	6	or 0β2Q3 or 201R7
	R 6	5667·40	(9)	(7½)	
154 Q	Q 1	5949·90	60	55	or 186R1
	Q 2	5924·82	38	38	
	Q 3	5859·79	16	13	
	Q 4	5757·33	(37)	(30)	
	Q 5	5620·90	(14)	(7½)	
	Q 6	5455·33	(10½)	(10)	
	Q 7	5266·04	(34)	(24)	
186 R	R 1	5949·90	60	55	or 154Q1
	R 2	5822·80	27	40	or G3
	R 3	5697·46	(27)	(22)	
	R 4	5573·86	(13½)	(16½)	or 3*a*2P2
	R 5	5452·54	(10½)	(10)	
181 Q	Q 1	3869·29	*b*	*b*	
	Q 2	3869·99	16½	10	
	Q 3	3871·62	19	24	

Table IVA.—Series due to Curtis and Kiuti.

Series.	Member.	Wave-length.	Intensities.		Remarks.
			R.T.	L.A.	
K	1	5887·35	—	—	
	2	5835·98	58	51	
	3	5785·81	68	63	
	4	5736·88	67	61	or 201R2
	5	5689·19	61	51	or 4*a*3P2
	6	5642·78	23	7½	or 81R7
	7	5597·63	33	31	
G	1	5922·01	*b*	*b*	
	2	5871·81	31	27	or 157Q4
	3	5822·80	48	45	or 186R2
	4	5774·98	62	58	or 5*a*4Q1
	5	5728·54	61	49	or 201R5
H	1	5989·22	—	—	
	2	5936·02	20*a*	19½*a*	
	3	5883·88	*b*	*b*	
	4	5832·89	24*a*	21	
Ki	1	5812·56	77	50	or 28Q3
	2	5819·39	19	12	
	3	5831·00	22*a*	13½*a*	
	4	5847·29	*b*	*b*	
	5	5868·23	*b*	*b*	
	6	5893·95	13	9½	probably 6*a*5Q2

Intensities of the Lines of Merton and Barratt's Table.

Table V gives a complete list of the lines whose intensities have been measured. The first column gives the wave-lengths, taken for the most part from Merton and Barratt's table. A few additional lines from Tanaka's table* have also been included. The second and third columns give the intensities at room temperature and at the temperature of liquid air respectively. Where two values of the intensities are given for the same line, those in brackets were taken from the "Green plates." The last three columns of the table give the classifications in Richardson's series system, in the system of Allen and Sandeman, and in the miscellaneous regularities respectively.

Table V.—Intensities of Lines in Secondary Spectrum.

Wave-length.	Intensities.		Identifications.		
	R.T.	L.A.	Rich.	A. & S.	Misc.
6522·62	1½	1	5*a*5Q2	—	(159Q'4)
27·35	9	10½	5*a*'5Q1	—	—
24·63	2	4*a*	4*a*'4P3	—	—
20·0 ?	4*a*	2½	—	—	—
17·69	8½	6½	5*a*5Q1	—	—
6499·87	2½	2	5*a*'5Q1	—	—
87·76	1½	1½	4*a*'4P2	—	163P6
78·9 ?	1½	3	—	—	—
75·32	5½*a*	8 *a*	—	—	—
73·63	8	10½	—	—	—
70·7 ?	4½*a*	5½*a*	—	—	—
66·56	4½*a*	4 *a*	—	—	—
64·1 ?	5	4½	—	—	—
57·3 ?	2½	4	—	—	—
55·02	4½	4½	—	—	—
52·13	3	—	4*a*4Q4	—	—
45·31	3½	5	—	—	—
41·50	11	8½	4*a*4Q3	—	—
37·81	9½	9	—	—	—
34·80	8 *a*	6½	—	—	161P6
33·47	9 *a*	4½*a*	4*a*4Q2	—	—
28·10	29	30	4*a*4Q1	—	—
17·0	1	1	3*a*'3P3	—	—
18·33	4½	3	—	—	—
11·77	*b*	2½	{ 4*a*'4Q3 3*a* 3P2	— —	— —
6399·45	28	30	4*a*'4Q1	—	—
91·04	4½	3½	4*a*'4R1	—	—
87·87	2½	2	—	—	159Q5

---

* 'Roy. Soc. Proc.,' A, vol. 108, p. 592 (1925).

Table V—continued.

Wave-length.	Intensities.		Identifications.		
	R.T.	L.A.	Rich.	A. & S.	Misc.
6382·88	6	3½	—	—	—
80·11	13½	13	—	—	3P5
76·11	3½*a*	1½	3*a*'3P2 4*a* 4R2	— —	— —
72·19	9½	12	3*a* 3P2	—	—
70·09	3	3 *a*	—	—	—
62·48	18	12	4*a*'4R2	—	159Q'2
46·93	3½	3½	—	—	—
40·57	17½	11½	3*a* 3Q3	—	—
32·46	19 *a*	10½	3*a* 3Q2	—	—
27·07	61	68	3*a* 3Q1	—	—
20·37	6 *a*	6	—	—	—
18·65	5½*a*	4½	3*a*'3Q4	—	—
16·38	2½*a*	2½	—	—	—
03·46	17	20	3*a* 3R1	—	—
6299·42	42	41	3*a*'3Q1	—	—
89·70	6	3½	—	—	—
85·37	26	28	3*a*'3R1	—	—
74·86	21	20	3*a* 3R2	—	—
71·31	19	24	2*a* 2P2	—	—
67·96	9	8½	—	—	—
64·89	3	3	2*a*'2P2	—	—
57·63	2½*a*	3½*a*	3*a*'3R2	—	(159Q3)
49·15	7 *a*	4½*a*	3*a* 3R3 2*a* 2Q4	— —	(157P5) —
38·39	41	25	3*a* 3R3 2*a* 2Q3	— —	— —
32·99	17½	10½	3*a*'3R3 (1*a*'1P4)	— —	— —
30·23	30	18	2*a* 2Q2	—	—
24·81	90	94	2*a* 2Q1	—	(157P4)
18·53	3 *a*	2	—	—	(157P7)
14·3 ?	1½*a*	2½	—	—	—
09·75	2	1	—	—	—
07·31	3½	2	3*a* 3R5	—	—
03·6 ?	3	3	—	—	—
6199·38	73	68	2*a*'2Q2	—	—
86·52	5	3	—	—	—
82·98	45	45	2*a*'2R1	—	—
74·03	32	25	—	—	3P3 158R1
69·63	24	29	1*a* 1P2	—	—
61·59	38	24	—	—	159R1
55·61	14½	9½	2*a* 2R2 (0*a*'0P5)	— —	— —
51·47	12½	12	2*a* 2R3	—	—
48·47	—	4	—	—	—
46·17	12½	5	1*a* 1Q4	—	—
44·06	—	5	—	—	—
39·36	10½	10½*a*	—	—	—
37·91	13	10½*a*	0*a* 0P4	—	—
35·34	81	63	1*a* 1Q3	—	—
27·40	53	29	1*a* 1Q2	—	—
21·76	110	105	1*a* 1Q1	—	—

Table V—continued.

Wave-length.	Intensities.		Identifications.		
	R.T.	L.A.	Rich.	A. & S.	Misc.
6117·86	7 a	5 a	—	—	—
12·80	4 a	2	0α′0P4	—	—
12·10	4 a	3	—	—	—
07·86	4½	2	—	—	157P2
6098·23	48 a	65 a	1α 1R1	—	—
95·96	76	69 a	1α′1Q2	—	—
90·92	47	38	—	—	83Q1 (153P3)
85·20	15½a	10½a	—	—	—
84·22	16½a	10½a	—	—	1P6
80·78	89	[illegible]	1α′1R1	—	—
74·39	18	15	1α 1R2 0α′0P3	— —	— —
70·00	47	30	—	—	83Q2
67·70	47	36	0α 0P2	—	3P2 (158R2)
63·28	26	16	—	—	163P4
58·28	4 a	3½a	—	—	—
56·10	17	11½	0α 0Q5 1α′1R3	— —	— —
52·34	34	30	—	—	81R2
45·44	21	12½	—	—	171P4 (161P4)
42·70	15½a	10	0α 0Q4	—	—
41·01	17½a	14	0α′0P2	—	—
35·02	8 a	5 a	1α 1R4 1α′1R3	— —	(157P1) —
31·80	96	60	0α 0Q3	—	—
27·98	63	52	—	—	83Q3
23·74	47	27	0α 0Q2	—	—
21·28	56	50	—	—	159R2
18·29	130	110	0α 0Q1	—	—
11·38	14	13	—	—	—
06·91	13½	9	0α′0Q4	—	—
02·81	39	30	—	—	1P5
5997·0 ?	7½	5	—	—	—
94·05	38	40	0α 0R1	—	—
90·51	30	24	—	—	—
82·54	43	21	—	—	152R1 (153P2)
78·02	9 a	10½a	—	—	28Q7
75·43	105	84	0α′0R1	—	—
70·24	38	23	—	—	81R3
67·31	20	13	—	—	83Q4
63·46	19	16	—	—	158R3
59·70	46	27	—	—	3P1
56·42	14½	10½	—	—	157Q1
49·90	60	55	—	—	154Q1
47·27	37	23 a	—	—	157Q2 186R1
42·95	19½a	18½a	—	—	—
41·95	18½a	18 a	0α′0R3	—	—
38·60	81	60	—	—	—
36·02	20 a	19½a	—	—	H2

Table V—continued.

Wave-length.	Intensities.		Classifications.		
	R.T.	L.A.	Rich.	A. & S.	Misc.
5931·33	77	60	—	—	1P4
24·82	38	38	—	—	154Q2
20·65	35	30	(6*a* 5Q5)	—	157Q3
16·24*	42	31	—	—	159R3 (156Q7)
10·15	19	14½	—	—	—
04·97	9 *a*	6½*a*	—	—	—
03·47	9 *a*	6 *a*	—	—	—
00·48	8½	7	6*a* 5Q3	—	—
5897·72	2	3½	—	—	—
93·95*	13 (7½)	9½ (7)	6*a* 5Q2	—	Ki6 (153P1)
88·14	57 (41)	43 (32)	—	—	81R4
84·66	48 (38)	35 (26)	—	—	171P3
78·43	34 (30)	34 (26)	—	—	28Q5
76·05	6½	5½*a*	—	—	—
71·81*	34 (31)	31 (27)	—	—	157Q4 G2
69·18*	35 (31)	27 (24)	—	—	1P3
66·65	6½	4½*a*	—	—	—
64·47	15 (14)	12½ (10½)	—	—	152R2
59·79	16 (16)	13 (12)	—	—	154Q3
57·09	6½ (5½)	5 (4½)	—	—	—
51·67	16½ (20)	11½ (14)	—	—	—
49·31	25 (27)	18 (19)	—	—	—
43·45	4*a*	2	—	—	159R4
41·41	7*a* (6½)	3½ (4)	—	—	28Q4
39·83	11½	5½*a*	—	—	—
35·98	58 (58)	54 (51)	—	—	K2
32·89	24*a* (29)	21 (26)	—	—	H4
31·00	22*a*	13½*a*	—	—	Ki3
22·80	27 (48)	40 (45)	—	—	186R2 G3
19·31	19 (27)	12 (20)	—	—	Ki2
15·00	38 (47)	27 (36)	—	—	(169Q6)
12·56	77 (77)	50 (55)	(4*a* 3P5)	—	28Q3 Ki1
08·26	6½*a*	13*a*	—	—	—
06·09	26 (44)	21 (30)	—	—	81R5
03·93	*b*	16*a*	—	—	157R1
01·14	12½ (21)	9 (16)	—	—	157Q5
5798·95	8*a* (13)	6 (10)	—	—	156Q5 159R5
94·65	19½ (30)	13 (22)	—	—	83Q6
91·74	26 (40)	17½ (30)	—	—	28Q2 201R8
88·25	18 (32)	14 (27)	—	—	159R6
85·81	56 (68)	50 (63)	—	—	K3
78·96	19 (34)	12 (24)	—	—	28Q1
74·98*	42 (62)	43 (58)	5*a* 4Q1	—	G4
66·98	19 (35)	12½ (26)	0β2Q5 4*a* 3P4	— —	— —
66·08*	*b*	4½*a*	0β2Q4	—	—
62·70	6½	6*a*	0β2Q3	—	158R5 201R7

* Given by Merton and Barratt as probably double.

Table V—continued.

Wave-length.	Intensities.		Classifications.		
	R.T.	L.A.	Rich.	A. & S.	Misc.
5760·37	29 (48)	21 (41)	(0β2Q2)	—	152R3
57·33	19*a* (37)	12*a* (30)	—	—	154Q4
56·54	19*a*	13*a*	—	—	—
53·54	3½	2½	—	—	—
48·99	3½ (6)	2½ (5½)	—	—	169Q5
45·35	4	3	—	—	161P2
41·80	11½*a* (27)	10½ (24)	—	—	201R6
40·08	9½	7	—	—	—
36·88	39 (67)	38 (61)	—	—	201R2 K4
31·92	25 (52)	18½ (40)	—	—	156Q3
	“ Green	Plates ”			
28·54	61	49	—	—	201R5 G5
23·44	24	20	—	—	201R4
16·00	20	12	—	—	156Q2
13·30	39	27	—	—	—
09·74	20	27	—	—	{ 157R2 157Q6
03·75	46	37	—	—	—
00·63	40	18	—	—	—
5097·46	27	22	—	—	186R3
94·11	22	18½	—	—	—
89·19	61	51	4*a* 3P2	—	K4
84·09	47	29	—	—	—
72·73	13	11½	—	—	—
70·89	19½	14	4*a* 3Q3	—	—
67·40	9	7½	—	—	158R6
61·72	32	23	4*a* 3Q2	—	—
57·78	21	40	—	—	—
55·75	41	40	4*a* 3Q1	—	—
53·32	9	7½	—	—	—
46·12	6	5	3*a* 2P4	—	—
42·78	23	7½	—	—	{ 81R7 K6
34·78	38	28	—	—	—
30·74*	35	12	—	—	—
27·45	14½	11½	—	—	—
23·04	13½	11½	—	—	—
20·90	14	7½	—	—	{ 154Q5 (170Q1)
16·24	7½	5½	4*a* 3R2	—	(169Q1)
12·53	39	28	—	—	—
06·8	2*a*	2*a*	3*a* 2P3	—	—
04·61*	15	7½	—	—	—
00·38	26	15	—	—	157R3
5597·63	33	31	3*a*′2Q3	—	K7
91·38	9	9	—	—	—
83·10	5	—	—	—	—
79·47	14	11	3*a* 2Q5	—	—
73·86	13½	16½	3*a* 2P2	—	186R4
69·51	6½	4	—	—	—
64·53	17	11	3*a* 2Q4	—	(83Q8)
61·65	15	12	—	—	81R8
55·14	15	9	—	—	—

* Given by Merton and Barratt as probably double.

Table V—continued.

Wave-length.	Intensities.		Classifications.		
	R.T.	L.A.	Rich.	A. & S.	Misc.
5552·52	24	14	3*a* 2Q3	—	—
49·67	12	9	—	—	—
47·63	14½	9½	—	—	—
43·41*	31	19	3*a* 2Q2	—	—
37·45	63	60	3*a* 2Q1	—	—
34·08	10	9	—	—	—
29·81	7	5	—	—	—
27·36	13	10	—	—	—
24·01	8½	8	2*a* 1P3	—	—
21·87	13	8½	2*a* 1Q8 ?	—	—
20·91	5	—	—	—	—
18·48	21	24	3*a* 2R1	—	—
07·89	16	12½	—	—	164R1
05·51	40	16½	—	—	—
5499·56	35	22	3*a* 2R2 (2*a* 1Q7)	— —	— —
95·98	22	14	—	—	—
93·05	6½	5½	—	—	—
83·90	7	3½	3*a* 2R3	—	—
81·08	36	30	—	—	157Q8
74·89	19½	12½	—	—	157R5
71·61	9½	8½	—	—	—
65·21	20	8½	—	—	—
61·50	14½	8½	2*a* 1Q5	—	—
59·63	19	14½	—	—	—
56·97	16	18	2*a* 1P2	—	—
55·33	10½	10	—	—	154Q6
52·44	10½	10	—	—	186R5
46·70	6½	2½	2*a* 1Q4	—	—
38·82	10½	8½	—	—	—
34·83	31	19	2*a* 1Q3	—	—
29·97	14	8	—	—	—
29·00	14½	7	—	—	—
25·96	41	24	2*a* 1Q2	—	—
19·90	58	55	2*a* 1Q1	—	—
17·80	28	20	—	—	—
09·68	17½	14½	—	—	—
05·38	14½	12	—	—	—
01·06	25	29	2*a* 1R1	—	—
5399·00	20	20	—	—	—
94·70*	11½	7½	—	—	—
92·32	18½	15½	—	—	—
88·21	41	35	—	—	—
86·74	23	16	—	—	—
78·41	9	6½	—	—	—
73·32	23	13½	—	—	—
65·91	23	21	—	—	—
62·86	9	4½	—	—	—
58·72	9½	7	—	—	—
55·92	21	15	—	—	—
51·75	5	3½	1*a*′0Q3	—	—
44·82	11½	8	1*a*′0Q2	—	—
43·18	11½	9½	—	—	—
40·84	8	10	1*a*′0Q1 1*a* 0P2	— —	(162R3) —

* Given by Merton and Barratt as probably double.

Table V—continued.

Wave-length.	Intensities.		Classifications.		
	R.T.	L.A.	Rich.	A. & S.	Misc.
5336·42	24	18½	—	—	—
34·28	14½	11½	—	—	—
31·51	9½	9	—	—	—
29·74	6½	4	1α 0Q4	—	27P3
26·80	7	5½	—	—	—
20·44	11	9½	—	—	—
17·90	20	12½	1α 0Q3	—	—
14·34	8½	7½	—	—	—
09·03*	14½	8½	1α 0Q2	—	—
03·15	45	38	1α 0Q1	—	—
5299·71	8½	7	—	—	—
96·10	5	3½	—	—	164R4
91·59	22	18½	—	—	83Q10
84·50	20	20	—	—	(185P6)
78·36	9½	9	—	—	—
72·29	33	29	—	—	162R4
70·41	20	6½	1α 0R2	—	—
66·04	34	24	—	—	154Q7
64·67	26	17	—	—	—
61·18	17½	11½	—	—	—
56·61	23	12	—	—	27P2
50·15	2½	2	1α 0R4	—	—
43·75	7	4½	—	—	—
39·04	6	7	4β5Q1	—	(84P4)
31·75*	7	4½	—	—	—
29·52*	16	11	—	—	—
26·77	13	11½	—	—	—
23·56	11½	—	—	—	—
22·76	14½	13½	—	—	—
21·32	9½	7	—	—	—
14·64	11½	9½	—	—	162R5
05·09	7	5½	—	—	—
5199·61	17½	12½	3β4Q2	—	—
96·38	29	20	—	—	—
93·02	4	3	—	—	—
91·05	9½	4	—	—	—
88·31	7½	7	—	—	—
80·59	16	9½	—	—	27P1
74·71	17½	12½	—	—	—
73·83	10	6	—	—	—
70·96	10	6	2β3Q5	—	—
68·25	10	7	—	—	53P5
64·67	5	3	2β3Q4	—	—
59·80	7	4½	5α3Q3	—	—
58·28	7½	5½	—	—	—
56·30	8½	5½	2β3Q2	—	—
53·87	11	11	2β3Q1	—	—
50·09	2	1½	5α3Q2	—	—
46·35	13	11½	—	—	—
43·53	13½	10	5α 3Q1	—	{ 83Q11 (185P4)
37·10	5	5	—	—	—
34·14	5½	3½	—	—	—
32·04	5	3½	—	—	—
27·94	5	5	1β2Q5	—	—

* Given by Merton and Barratt as probably double.

Table V—continued.

Wave-length.	Intensities.		Classifications.		
	R.T.	L.A.	Rich.	A. & S.	Misc.
5122·59	8	8	—	—	—
20·97	5½	4	1β2Q4	—	—
16·90	5½	4	—	—	—
15·37	8½	5	1β2Q3	—	—
13·17	24	18	—	—	—
09·32	11½	9½	1β2Q1	—	—
07·66	11½	10½	—	—	—
03·56	15½	11½	—	—	11R1
5099·76	5½	3½	—	—	—
96·26	6½	4½	—	—	—
94·71	5	3	—	—	—
92·32	4½	2½	—	—	—
90·22	5	3½	—	—	—
84·83	28	23	—	—	—
80·47	28	21	0β1Q5	—	—
75·44	17½	12	0β1Q4	—	53P4 (84P2)
72·42	10	6½	—	—	—
70·22	11½	7½	—	—	—
68·16	28	21	—	—	—
63·84	21	14	0β1Q1	—	—
61·73	12	8½	4a 2Q5	—	—
55·08	33	28	—	—	—
49·38	8½	2½	—	—	—
47·98	12	12	—	—	—
41·63	17	13	—	—	—
39·83	21	14	—	—	—
32·19	5½	—	4a 2Q3	—	—
30·37	18½	16½	—	—	—
24·98	3	1½	—	—	—
22·63	2	1	4a 2Q2	—	(10P5)
20·76	7	5½	—	—	—
16·43	28	18	4a 2Q1	—	202P3
15·12	34	19	—	—	—
13·05	42	33	—	—	—
11·19	17½	12½	—	—	—
08·58	22	17	—	—	—
03·40	21	17	—	—	11R2
00·19	3½	1½	—	—	—
4997·94	13½	9	—	—	—
96·73	15½	10½	—	—	—
94·11	6	3	—	—	185P2
90·16	6½	5½	—	—	83Q12
83·38	4	2½	—	—	—
80·47	19	14	—	—	53P3
78·25	15	12	—	—	—
76·64	15	10	—	—	—
73·27	37	28	—	—	—
69·24	17½	13	—	—	—
66·85	25	15½	—	—	—
65·11	6	—	—	—	—
60·93	5½	4	—	—	—
55·74	25	16½	—	—	38R1
52·57	7	3½	—	—	—
49·53	4½	5	—	—	—
44·81	7	4½	—	—	84Q1

Table V—continued.

Wave-length.	Intensities.		Classifications.		
	R.T.	L.A.	Rich.	A. & S.	Misc.
4942·53	9	5	—	—	—
39·17	25	19½	—	—	—
34·29	68	46	3*a* 1Q5	—	—
32·22	34	23	—	—	—
28·62	64	45	—	—	202P3 (203P2)
25·20	10	4½	—	—	84Q3
24·00	8½	4	—	—	—
21·15	6½	4	—	—	60R1
19·11	14½	7½	3*a* 1Q4	—	(58R0)
12·32	4½	3	—	—	59Q4
08·80	17	8½	—	—	104Q2
06·27	13	11½	3*a* 1Q3	—	—
03·55	3	2	—	—	—
01·81	10	6	—	—	—
4896·46	11½	7	—	—	11R3 104Q3 (58R1) (41Q0)
91·22	10½	10½	3*a* 1Q1	—	(59Q3)
88·44	5	3½	—	—	41Q1
86·40	10½	10	—	—	10P4 84Q5
83·82	9½	5½	—	—	53P2
81·55	8½	5½	—	—	—
78·10	8½	7	—	—	185Q1
75·92	27	17	—	—	59Q2
73·05	46	29	—	—	—
69·42	19	9½	4β4P5	—	38R2 (58R2)
67·05	22	19	—	—	41Q2 185Q3 59Q1
	“ Blue	Plates ”			
56·54	17 (36)	16 (25)	—	—	185Q4
49·34	22 (40)	22 (30)	—	—	202P2
43·35	11*a* (19½)	7*a* (10)	—	—	60R2
42·45	11*a* (15)	7*a* (7)	—	—	185Q5
38·25	10½ (22)	8 (13)	—	—	58R3
32·79	8½ (17)	8 (9½)	—	—	41Q3 83Q13
31·60	5*a* (8½)	5½ (5)	—	—	—
24·58	6 (9)	8 (6)	—	—	185Q6 ?
22·96	8½ (16)	10 (12)	—	—	—
19·38	3½ (5)	3½ (4)	—	—	—
17·51	4½ (8)	5½ (7½)	—	—	—
13·61	7 (12)	7 (9½)	—	—	84R1
11·67	3 (5½)	3 (3)	(2*a* 0Q5)	IIB*e*Q4	—
07·33	6 (11)	4½ (7)	—	(IIB*d*Q1)	110Q5
02·03	3½ (8)	3½ (5½)	—	—	—
4797·76	19½ (30)	20 (24)	—	(IIB*e*Q5)	—
93·95	9 (17)	9½ (14)	—	—	102–3
90·82	7*a* (8)	*b* (5½)	—	—	—
89·40	7*a* (11½)	6½ (8½)	—	—	—
86·04	8*a* (18)	6½ (7)	—	(IIB*c*Q1)	53P1 41Q4
84·85	7½*a* (12½)	6½*a* (9½)	—	IIB*c*Q2	110Q4 11R4

Table V—continued.

Wave-length.	Intensities.		Classifications.		
	R.T.	L.A.	Rich.	A. & S.	Misc.
4780·94	10½ (19)	8½ (11½)	—	—	—
77·42	7½ (13)	7 (10)	—	—	38R3
74·29	2½ (5½)	2 (3½)	2α 0Q2	—	—
70·71	5 (11)	4 (6½)	—	—	60R3
67·24	4½ (8)	4 (6½)	—	—	—
63·82	11 (19)	13 (16)	(3β3P4)	IIB*b*Q2	185R1
60·06	3	1½	—	—	56R2
56·92	4½ (8½)	5½ (6½)	—	—	110Q2
51·59	3½ (4½)	2½ (2½)	—	—	110Q1
42·75	17 (23)	17 (17)	4β4Q1	IIB*a*Q2	—
40·98	9½ (12)	9 (8½)	—	—	—
32·81	3½ (6)	4 (3)	4β4R1 (3β3P3)	— —	— —
30·77	5 (6½)	3½ (3½)	—	—	—
28·78	4 (5½)	2 (2½)	—	—	—
23·01	26 (34)	16½ (17½)	—	—	84R2 (56R3)
21·56	10	6½*a*	2β2P5 4β4R3	— —	— —
19·02	29	31	(4β4R4)	—	—
13·93	11	15½	—	IIB*a*Q5	—
10·05	9	8½*a*	—	—	—
09·52	17	17	1δ3Q3	—	—
05·24	2	4	3β3P2	—	—
02·55	6½	6	—	—	60R4
4692·04	10½	8½	0δ2Q3 (2β2P4)	— —	(56R4) —
90·16	15½	15½	0δ2Q2	—	—
86·79	19½	18½	—	—	185R2
83·79	36	36	3β3Q2	—	—
82·35	22	18½	—	—	—
80·43	12½	11½	3β3Q1	—	38R4
79·11	12½	7½*a*	—	—	—
74·53	16*a*	17*a*	—	IIB*a*Q7	—
73·12	11	9½	—	—	83Q14
71·33	23	17	—	—	—
67·05	10½	8	2β2P3	—	(56R5)
65·58	13½	11½	—	—	10P2
62·79	27	22	—	—	102–1 101R1
61·39	29	26	—	—	—
57·83	5½	2½	3β3R2	—	—
53·04	28	23	—	—	—
49·47	7*a*	4*a*	—	—	—
45·33	8	5	—	—	—
33·95	81	72	—	—	—
31·89	64	54	—	—	—
27·96	44	41	—	—	—
25·39	20	12	2β2Q3 (5α 2Q3)	— —	— —
20·72	7	3	2β2Q2 1β1P4	— —	— —
17·49	42	29	2β2Q1	—	—
13·10	3½	3½	—	—	—
07·38	20	8	0β0P6	—	101R2
4598·48	6½	4	3γ4Q4	—	—

Table V—continued.

Wave-length.	Intensities.		Classifications.		
	R.T.	L.A.	Rich.	A. & S.	Misc.
4597·22	6	5½	1β1P3	—	—
95·13 T	3½	2	—	—	—
91·84	3½	3	3γ4Q2 2β2R2	— —	— —
88·67	6	5	—	—	—
84·48	12½	12½	—	—	—
82·58	35	28	—	II*a*AP4	—
80·04	57	50	(0β0P5) (2β2R3)	(IIA*a*P5) —	(41Q7) —
78·00	24	12	—	IIA*a*Q2	—
75·86	22	25	—	IIA*a*R2	—
72·73	38	29	—	IIA*a*Q3	—
68·10	41	40	—	IIA*a*R3	—
65·56	4	5	—	—	—
63·68	10	4½	—	IIA*a*Q4	—
62·24	13½	8	1β1Q3	—	—
58·50*	22	15	—	IIA*b*Q2	(101R3) (26P5)
57·32	18½	14	1β1Q2 (2γ3Q2)	— —	— —
54·13	25	28	1β1Q1	—	—
50·96	23	17	—	IIA*a*Q5	(111P4) (11R6)
47·93	7	6½	—	—	—
43·68	10½	9½	—	—	—
41·12	3	3½	—	IIA*a*R5	—
39·15	15	14½	—	IIA*c*Q2	(84R4)
37·83	15	11½*a*	1β1R1	—	—
34·17	31	29	0β0P3	IIA*c*Q3	—
33·08	24*a*	19*a*	—	—	—
31·14	6	6½	—	—	185R4
29·09	12	12½	—	—	—
27·74	6	8	—	—	—
24·13	21	16	—	—	—
21·44	10½	8	—	—	—
19·95	6½*a*	*b*	—	IIA*d*Q2	—
17·47	7½	8½	—	—	—
15·47	8½	6	0β0P2	IIA*b*Q6	(101R4)
14·27	9½	6	1β1R3	IIA*a*Q7	—
11·70	15	12½	—	—	—
09·13	4½	6	—	—	—
05·63	15	8½	—	—	111P3
01·91	16	13½	—	—	(20P5)
4498·10	51	47	—	—	—
93·67	13½	9	0β0Q2	(IIA*d*Q5)	—
90·45	35	34	0β0Q1	(IIA*a*Q8)	—
87·80	24	15	—	—	61Q4
86·05	26	29	—	—	—
82·03	10	6½	—	—	—
78·97	6½	7	0γ1Q1	—	—
77·05	12	13½	—	—	—
74·24	15½	10½	0β0R1	—	26P4
71·94	10½	10½	—	—	—
67·12	24	21	—	—	—
64·12*	8	5½	0βOR2	—	61Q3

* Given by Merton and Barratt as probably double.

Table V—continued.

Wave-length.	Intensities.		Classifications.		
	R.T.	L.A.	Rich.	A. & S.	Misc.
4460·96	39	38	—	—	—
58·86	15½	10	—	—	—
56·77	24	21	—	—	—
55·67	15½	12½	0β0R3	—	—
53·02	16	10½	—	—	185R5
49·92	14½	10	—	—	85Q3
47·56	38	39	—	—	61Q2
45·24	23	22	0β0R5	—	—
41·45	4½	4	—	—	—
38·26	6½	5	—	—	—
34·31	8½	5	—	—	{ 61Q1 112Q1
25·92	12	8½	—	—	—
23·18	15	14	—	—	—
19·48	19	15½	—	—	—
17·32	22	14	—	—	{ 112Q3 (204R1)
14·22	26	16	—	—	85Q2
12·26	35	30	—	—	—
10·57	10	4½	—	—	—
04·57	7½	6½	—	—	—
00·81	13½	9½	—	—	—
4398·19	5½	2½	—	—	112Q4
90·89	14½	9	—	—	{ 26P3 85Q1
89·08	9	7	—	—	—
84·40	5½	5	—	—	—
79·38	11	7½	—	—	85Q0
70·70	4	2½	—	—	—
67·73	4	3	—	—	—
60·34 T	6	—	3α 0Q2	—	—
54·51	3½	4	—	—	—
50·78 T	2	1½	4δ5Q2	—	—
35·50	4	4	—	—	—
32·57	4½	5	—	—	—
30·34	3	3	—	—	—
27·95	6½	7	—	—	—
19·4 ?	2	3½	—	—	—
12·89	3½	3	—	—	—
08·60	5	6	4β3Q1	—	(26P2)
06·26	9½	1½	—	—	—
03·40	15	11½	—	—	—
4295·49	5	4½	—	—	—
92·84 T	3	2½	—	—	—
90·15 T	6	5	2δ3Q1	—	—
53·30	7½	6	—	—	—
43·27	7	6	3β2Q3	—	—
37·57	2	2	3β2Q2	—	—
33·60*	13½	15	{ 3β2Q1 4γ4Q1	—	—
27·36	3½	3½	—	—	26P1
23·89	15	13	—	IICeQ3	—
22·30*	24	25	(0δ1Q3)	—	—
19·49 T	2	4	0δ1Q2	—	—
12·50	31	24	—	—	—

* Given by Merton and Barratt as probably double.

Table V—*continued.*

Wave-length.	Intensities.		Classifications.		
	R.T.	L.A.	Rich.	A. & S.	Misc.
4210·10	27	15	—	—	—
09·16	15½	11½	—	—	—
05·10	43	51	—	IIC*e*Q5	—
02·30	3	4	—	—	—
00·91	9½*a*	10½*a*	—	—	—
4199·77	21	27	—	(IIC*d*Q4)	—
98·20	7½	7	—	—	—
95·65	30	26	—	IIC*c*Q2	—
89·40	5½	4	—	—	—
88·24 T	3½	2	3γ3Q3	—	—
82·14	22	24	3γ3Q1	—	—
79·54	28	32	—	IIC*v*Q2	—
77·04	48	51	—	—	20Q1
75·13	17½	12	—	IIC*b*Q3	20Q2
71·29	23	16½	—	—	20Q3
67·60	2½	3	—	IIC*b*Q4	—
65·17	7	4	—	—	20Q4
63·52	13	7½	—	IIC*a*Q2	—
61·90	14	14	—	—	—
59·31	7½	9	2β1Q1	(IIC*a*Q3)	—
56·70	17½	13	—	IIC*b*Q5	20Q5
52·61	4	2	—	—	—
51·55	3	2½	2γ2Q5	IIC*a*Q4	—
46·22	6	6	—	—	20Q6
33·99	6½	6	2γ2Q2	—	(20Q7)
31·50	8	7½	2γ2Q1	—	—
30·07 T	5	3½	—	—	—
16·33 T	3	3½	—	—	—
13·53	4½	5½	—	—	—
10·17	5½	5 *a*	—	IIC*a*Q7	—
09·35	5	5½*a*	—	—	—
07·79	3	3	—	—	—
06·22	4½	4½	1γ1Q6	—	—
4097·47	4	8½	1γ1Q5	—	—
87·75	19	24	—	—	—
85·18	11½	13	1β0Q1 1γ1Q3	— —	— —
83·90	5	3½	—	—	—
82·38	10½	15½	—	—	—
78·88	21	24	1γ1Q1	—	—
74·07	10½	8	—	—	183P3
72·98	10	8	—	—	—
71·28	13½	12	—	—	—
69·65	33	41	—	—	—
66·90	41	38	—	—	20R1
65·57	15½*a*	12½	—	—	—
63·62	19½	16*a*	—	—	—
62·49	31	32	—	—	—
59·23	3½	4	—	—	—
57·50	4	1½	—	IID*a*Q2	—
56·41	4½	4	—	—	—
55·29	5½	2½	—	—	—
54·00 T	4	4	—	—	—
48·45	11	9½	—	—	—
43·57	13	12	—	IID*b*Q1	—
38·56	3½	2	—	IID*b*Q3	—
35·56	5	5	—	—	—

Table V—continued.

Wave-length.	Intensities.		Classifications.		
	R.T.	L.A.	Rich.	A. & S.	Misc.
4031·60	6½	6	0γ0Q3	IID*b*Q4	—
28·35	14½	16½	—	IID*c*Q1	—
27·42	8½	*b*	0γ0Q2	IID*c*Q2	—
26·58	6½	4½	—	—	—
24·79	6	5	0γ0Q1	—	—
21·62 T	7	8½	—	—	—
19·00	4½	4	—	—	—
16·53 T	4	3	—	—	—
09·57 T	4½	4½	—	—	—
05·96	17½	14½	—	—	—
02·59	10	10	—	—	—
00·85	7½	7	4δ4Q1	—	—
3997·18	16	19½	—	—	—
93·92	8½	8½	—	—	—
93·27	8½	11½	—	—	(181P4)
91·96	22	23	—	IID*e*Q3	—
90·04	19	22	—	—	—
86·96	4½	2½	—	—	—
83·98	6	6	—	—	—
82·61	7	2½	—	—	182P4
78·33	5½	4	—	IID*d*Q6	—
77·02	3	2½	—	—	—
75·70	10	5	—	—	—
74·32	10	5	—	—	—
63·17	8	12	—	—	—
62·36	7½	7	—	—	—
60·07	4½	2	3δ3Q3	—	—
50·59	5	3	—	—	—
47·09	3½	3	—	—	—
44·30	7	7	—	—	—
24·44	8	9½	—	—	—
3887·90	4½	3	1δ1Q6 4ε4Q5	— —	— —
84·21	4½	9½	4γ3Q1	—	180Q1
79·60	8	9½	—	—	—
72·38	19	20	4ε4Q1	—	—
71·62	18½	24	—	—	181Q3
70·82	26	13	—	—	—
69·99	16½	10	—	—	181Q2
67·09	10	5	—	—	—
64·22	10	4	—	—	—
63·22	14	16	1δ1Q1	—	—
61·53	14	12	—	—	—
60·73	14	13½	—	—	—
59·93	14	10	—	—	—
58·74	9½	8	—	—	182Q3
57·81	9½	4½	—	—	—
51·29	3½	3½	—	—	—
36·48	7	3	3γ2Q4	—	—
25·01	2½	—	3γ2Q2	—	—
12·85	4½	4½	—	—	—
09·07	3	—	—	—	—
08·05	12	16	(2ε2Q4)	—	(20R5)
3799·02	7	10	—	—	—
96·63	17½	19	—	—	183R1
94·47	3½	2	2ε2Q2	—	—
91·43	5	3½	—	—	—
77·03	3½	3½	—	—	—

Summary.

The intensities of most of the lines measured by Merton and Barratt in the secondary spectrum of hydrogen have been measured by means of a microphotometer at two temperatures. These lines include the greater part of Richardson's series system, for which the change of intensity with temperature has been found to be generally in good agreement with theory. The alternation of intensity between the odd and even members of the series is also clearly shown, and shown to be further affected by change of temperature. Other regularities which have been found in the spectrum have also been examined, and from the change in intensity, many of these appear to be sequences of corresponding members of different bands, rather than actual band series.

In conclusion, the authors wish to express their gratitude to Dr. R. Ruedy for the continued interest he has shown in this work and for the valuable assistance he has given, and also to the Laboratory Glassblower, Mr. R. H. Choppell, for much kind help on numerous occasions.

Bands in the Secondary Spectrum of Hydrogen—II.

By H. Stanley Allen, M.A., D.Sc., Professor of Natural Philosophy in the University of St. Andrews, and Ian Sandeman, Ph.D., late Carnegie Research Scholar in the University of St. Andrews.

(Communicated by O. W. Richardson, F.R.S.—Received June 10, 1927.)

In a previous communication,* evidence has been given for the existence of an extensive system of bands of a distinctive type, extending over a wide range of the visible and infra-red spectrum of hydrogen. These are called in the writers' notation the "Type-II Bands," and are characterised by parallel groups of Q series, each group comprising from three to five bands. The individual bands of a group are spaced out at intervals of very nearly 92 wave-numbers, the spacing being in some cases approximately constant and in some cases varying in such a way as to indicate that the null lines of the group are given by a quadratic law. For certain bands P and R series have also been identified obeying the Simple Combination Principle. All such series are closely parallel to the corresponding branches of a band (II_A, *a*) described by one of us,* which comes out strongly in an arc struck between tungsten electrodes in an atmosphere of hydrogen at higher pressures. The Type-II Bands have for various reasons been ascribed to triatomic hydrogen, H_3.

---

* Allen and Sandeman, 'Roy. Soc. Proc.,' A, vol. 114, p. 293 (1927).

In the present paper, our purpose is to extend the study of these regularities. We begin by giving a group occurring in the green, which bears a strong resemblance to the infra-red groups described in detail previously.

A Band Group in the Green resembling the Infra-red Groups, II_F and II_G.—The Q series of this group (II_H) are given in Table I, in which we have used the same notation as before. The wave-numbers of the lines are those given

Table I.—Band Group II_H, Q Series.

	a.		*b.*		*c.*
Q(1)					19405·75 (Drd^2, *p*, *p*) *5·99*
Q(2)	19226·88* (M3, –, –) *24·40*	*92·49*	19319·37 (M3H, 4, 1) *24·16*	*92·37*	19411·74* (M0, –, –) *24·75*
Q(3)	19251·28 (M0, –, –) *43·36*	*92·25*	19343·53 (M2, 0, 0) *42·93*	*92·96*	19436·49* (M3H, 5, 5) *43·55*
Q(4)	19294·64 (Missing) *62·32*	*91·82*	19386·46 (M0, ‖, ‖)	*93·58*	19480·04 (M1, 1, 0) *63·47*
Q(5)	19356·96† (M1, 3, 3) *80·69*				19543·51* (M2, –, –) *79·23*
Q(6)	19437·65‡ (Missing ?) *100·01*	*92·19*	19529·84 (T*p*, 1, –)	*92·90*	19622·74 (M0, 0, *p*)
Q(7)	19537·66§ (M, 1, 1) *116·77*				
Q(8)	19654·43 (Missing) *136·11*				
Q(9)	19790·54 (D*r*, *p*, –)	*93·57*	19884·11 (M0, 2, 1)	*92·04*	19976·15 (D*rd*, –, –)

* Members of Richardson's Fulcher System. There is, however, some evidence, drawn from the intensity and character of the lines, that we have in each case a real coincidence.

† Claimed by Richardson as his ${}_2\beta_3$ Q(4). Richardson admits, however, that the line may be a little too strong for this. Moreover, the strength of the line in the arc indicates a real coincidence, since ${}_2\beta_3$ Q(1) and Q(3) have not been observed in the arc, while Q(2) appears faintly.

‡ Comes very near the strong line 19436·49 (M3H, 5, 5), *c*, Q(3).

§ Appears on Merton and Barratt's helium plates. The wave-number seems rather high.

‖ Not resolved on our arc plates from 19388·38 (M0). Arc intensities of the combined line: At. Press. 1, 45 cm. 1.

---

* Sandeman, 'Roy. Soc. Proc.,' A, vol. 108, p. 607 (1925).

by Merton and Barratt,* by Tanaka,† or by Deodhar,‡ and the observed intensities are placed in brackets underneath, an "M," a "T," or a "D" being prefixed to indicate which observations are referred to. The other two figures given refer to observations made in St. Andrews, and indicate the intensities of the line in the arc at atmospheric pressure and at 45 cm. of mercury. "H" or "L" signifies that the line is recorded by Merton and Barratt as enhanced at high or low pressure respectively.

Table I is very like the previous tables of Q series. The *a* column shows distinct twofold intensity sequence, since the even members Q (4), Q (6), and Q (8) are missing, and the odd members, Q (5), Q (7), and Q (9) come out both in the arc and Geissler-tube. The table also shows evidence of threefold intensity sequence, since the lines Q (3), Q (6), and Q (9) are present in all the series.§ There are, moreover, three lines that come in the positions which Q (12) should occupy in each series. These have been omitted from the table, since two of them are somewhat intense.

In addition to the lines given, there is a line, 19135·39 (M1, —, —), that may be Q (2) of the column immediately to the left of the *a* column, which we may call the "*z*" column. There are also traces of a *d* column.

The value 19294·64 for *a*, Q (4) was originally obtained by quadratic interpolation from the lines *a*, Q (2), Q (3), and Q (5), and, since this value has been found to be in good agreement with the Combination Principle, it has been retained. The values of the remaining missing lines of the *a* series have been obtained by a graphical method. It is worthy of mention that the lines 20118·22 (M3, 4, 4) and 20309·56 (M0, —, —) come closely into the positions which *a*, Q (11) and Q (12) should occupy, and, in fact, taking the formula representing this series as

$$\mathrm{II_H},\ a,\ \mathrm{Q}\,(m) = 19232\cdot182 - 21\cdot1977\,m + 9\cdot24732\,m^2,$$

we obtain the following residuals for the lines :—

Q(2) + 0·10, Q(3) —0·53, Q(4) (—0·71), Q(5) —0·42,
Q(6) (—0·25), Q(7) +0·74, Q(8) (0·00), Q(9) +0·10,
Q(10) ———, Q(11) +0·29, Q(12) +0·14.

It may also be mentioned that many of the Type-II series have been found to extend to higher members, and to deviate from a quadratic law for the lower members in a manner very similar to the above.

---

* Merton and Barratt, "Bakerian Lecture," 'Phil. Trans,' vol. 222 (1922).

† Tanaka, 'Roy. Soc. Proc.,' A, vol. 108, p. 592 (1925).

‡ Deodhar, 'Roy. Soc. Proc.,' A, vol. 113, p. 420 (1926).

§ *a*, Q(6) is missing, but it is probable that part of the arc intensity of the line 19436·49 is attributable to it. The dispersion of our plates was insufficient to test this point.

Such members of the R and P branches as are present are given in Tables II and III. A few higher members may be present, but these cannot be identified with certainty. The R and P series of the *b* band are almost entirely missing, while those of the *c* band are supplied by Deodhar's measurements of some of the very faint lines. We shall see later that the same peculiarity, viz., that of the *a* and *c* bands being more intense than the *b* band in the P and R branches appears in the R branches of another group (II_D).

The Combination Principle applied to Bands II_H, *a* and II_H, *c* gives :—

Band II_H, *a*.

Differences.

$$Q(2) + Q(3) = 38478{\cdot}16, \quad R(2) + P(3) = 38478{\cdot}13, \quad {}_2\Delta_3 = -0{\cdot}03,$$
$$Q(3) + Q(4) = 38545{\cdot}92, \quad R(3) + P(4) = 38546{\cdot}39, \quad {}_3\Delta_4 = +0{\cdot}47,$$
$$Q(4) + Q(5) = 38651{\cdot}60, \quad R(4) + P(5) = 38651{\cdot}46, \quad {}_4\Delta_5 = -0{\cdot}14.$$

Band II_H, *c*.

$$Q(2) + Q(3) = 38848{\cdot}23, \quad R(2) + P(3) = 38848{\cdot}25, \quad {}_2\Delta_3 = +0{\cdot}02,$$
$$Q(3) + Q(4) = 38916{\cdot}53, \quad R(3) + P(4) = 38916{\cdot}99, \quad {}_3\Delta_4 = +0{\cdot}46.$$

In spite of the fact that in the former band the missing line in each series has been calculated by quadratic interpolation from its neighbours, the Combination Principle appears to fit very well.

Table II.—Band Group II_H, R Series.

	a.		*b*.		*c*.
R(1)	19230·73 (M,[*] 4, 1) *38·02*				
R(2)	19268·75 (M1, 0, 0) *55·59*				19455·59 (*Drd*^{a}, –, –) *55·65*
R(3)	19324·34 (Missing) *73·17*				19511·24 (*Drd*, –, –) *73·65*
R(4)	19397·51[†] (M3L, –, –)	*94·44*	19491·95 (*Drd*, –, –)	*92·94*	19584·89[‡] (M3, 5, 4)

[*] Appears on Merton and Barratt's helium plates. R(2) also shows helium effect.

[†] The same line as $_2\beta_3$ Q(1). There are, however, grounds for believing that the line is a doublet.

[‡] The same line as 11 R(1).

Table III.—Band Group II_H, P Series.

	a.	*b.*	*c.*
P(2)			
P(3)	19209·38 (MO, –, –) *12·67*		19392·66 (D*r*, –, –) *13·09*
P(4)	19222·05 (D*r*, –, –) *31·90*		19405·75* (D*rd*^{2}; *p*, *p*)
P(5)	19253·95 (Missing) *51·14*		
P(6)	19305·09 (T*p*, –, –)		

* An overlap with II_H, *c*, Q(1). The "*d*^{2}" feature of Deodhar's observation suggests that there are two lines close together.

The term differences deducible for the two bands are shown in Table IV. Here we have adopted the same numeration for the series as before, viz. :—

$$
\begin{aligned}
P(m) &= \nu_0 + F(m-1) - f(m), \\
Q(m) &= \nu_0 + F(m) - f(m), \\
R(m) &= \nu_0 + F(m+1) - f(m).
\end{aligned}
$$

It is interesting to note that with this numeration the missing lines of the *a* band are P(5), Q(4), and R(3), suggesting that the initial term F(4) is responsible for the failure of these lines. Moreover, the strength of Q(5) in the arc and the appearance of R(4) and P(6) seem attributable to the initial term F(5), a term which has already been found to be associated with intensity in the case of Bands II_F, *a*, II_G, *a*, and II_A, *a*.

A comparison between Table IV and Table IX of our previous paper shows that both initial and final term differences for Band II_H, *a* are closely similar

Table IV.—Bands II_H, *a* and II_H, *c*, Term Differences.

Initial Term Differences.

Band.	*m*.	F (*m* + 1) – F (*m*).	Δ{F (*m* + 1) – F(*m*)}.	Δ^2{F(*m* + 1) – F(*m*)}.
II_H, *a*	1			
	2	41·885	30·94	–0·825
	3	72·825	30·115	–0·495
	4	102·94	29·62	
	5	132·56		
II_H, *c*	1			
	2	43·84	30·89	–0·79
	3	74·75	30·10	
	4	104·85		

Final Term Differences.

Band.	m.	$f(m+1)-f(m)$.	$\Delta\{f(m+1)-f(m)\}$.	$\Delta^2\{f(m+1)-f(m)\}$.
II_H, *a*	1			
	2	17·485	11·745	−0·425
	3	29·23	11·32	0·00
	4	40·55	11·32	
	5	51·87		
II_H, *c*	1			
	2	19·09	12·11	−0·66
	3	31·20	11·45	
	4	42·65*		

* Obtained by taking II_H, *c*, Q(5) as 19542·24, a value arrived at by a graphical method. The wave-number given in Table I (an overlap with ${}_1\beta_2$ Q(3)) is too high.

to those of the two infra-red bands II_F, *a* and II_G, *a*, showing that this system is not confined to the infra-red region, but extends into the visible. The similarity is indeed so great, that it seems permissible to associate the three groups together as the "F—G—H System." It is also noteworthy that the difference between the null lines (*see* Table V) of the Bands II_H, *a* and II_G, *a* comes out as

$$19220{\cdot}2 - 15069{\cdot}5 = 4150{\cdot}7$$
$$= 45 \times 92{\cdot}24,$$

and so appears to be an integral multiple of the fundamental 92 difference which separates the bands of a group.

In Table V we give the band constants deducible from the term differences of Table IV, although, owing to missing lines, no great numerical accuracy can be attributed to these figures. As before we have assumed a general quadratic form for the term :—

$$F(m) = B(m + E)^2,$$

where B is taken to represent the factor $h/8\pi^2 I_1$, I_1 being the initial moment

Table V.—Band Constants.

Band.	B cm.$^{-1}$.	I_1 gm. (cm.)^2.	E.	b cm.$^{-1}$.	I_2 gm. (cm.)^2.	e.	ν_0 cm.$^{-1}$.
II_H, *a*	15·06	$18{\cdot}4 \times 10^{-41}$	−1·08	5·66	$48{\cdot}8 \times 10^{-41}$	−0·92	19220·2
II_H, *c*	15·25	$18{\cdot}1 \times 10^{-41}$	−1·06	5·89	$46{\cdot}9 \times 10^{-41}$	−0·87	19405·9
II_F, *a*	15·059	$18{\cdot}35 \times 10^{-41}$	−1·095	5·736	$48{\cdot}18 \times 10^{-41}$	−0·961	13464·75
II_G, *a*	15·189	$18{\cdot}19 \times 10^{-41}$	−1·105	5·846	$47{\cdot}28 \times 10^{-41}$	−0·963	15069·53
II_A, *a*	15·178	$18{\cdot}21 \times 10^{-41}$	−0·919	6·145	$44{\cdot}98 \times 10^{-41}$	−0·648	21830·95

of inertia of the molecule. Table V also shows similar values for Bands II_F, *a*, II_Q, *a*, and II_A, *a* for comparison. We may note the close similarity between certain pairs of the moments of inertia in the table.

A very curious circumstance is that both initial and final term differences for the *c* band have come out greater than the corresponding differences for the *a* band, although the *c* band lies higher in the spectrum. This casts doubt on the supposition that the 92 difference is traceable to the vibration quantum number. It seems also unlikely that the P and R branches of the *c* band have been wrongly identified, since the Combination Principle holds with considerable accuracy. A similar increase in the values of the term differences in passing up the group will be shown to hold in the case of Band Group II_D, which we shall now proceed to describe.

The R Series of Group II_D.—The Q series of this group which occurs on the short-wave side of the primary line H_δ have been given in our previous paper. In Table VI we give the R series. The line 24911·07 (*a*, R(5)) comes very near

Table VI.—Band Group II_D, R Series.

	a.		*b.*		*c.*
R(1)	24652·22 (M0) *36·82*	*91·99*	24744·21* (T*rd*) *37·40*	*93·68*	24837·89‡ (Missing) *36·92*
R(2)	24689·04 (T*p*) *55·17*	*92·57*	24781·61 (T*p*)	*93·20*	24874·81 (M0) *55·07*
R(3)	24744·21* (T*rd*) *74·45*				24929·88 (T*r*) *74·06*
R(4)	24818·66† (Missing) *92·41*				25003·94 (T*q*) *92·21*
R(5)	24911·07 (T0) *110·45*				25096·15 (Missing) *110·79*
R(6)	25021·52 (Missing) *129·64*				25206·94 (T*q*)
R(7)	25151·16 (T*p*) *146·74*				
R(8)	25297·90 (Missing) *165·79*				
R(9)	25463·69 (T*rd*)				

* An overlap.

† Comes near the comparatively strong line 24817·09 (M2), II_D, *c*, Q(1).

‡ Comes near the line 24839·05 (M0L), $_2\gamma_0$ Q(1).

where *b*, R(4) should be, so that a weak member of the *b* column may be present here overshadowed by this line.

Just as in II_H, the R series of the *b* band is weaker than those of the *a* and *c* bands. Here, however, we have to deal with a region much less crowded with lines, and can draw more certain evidence from intensities, since there are fewer overlaps. It seems not unreasonable to suppose that in the *b* and *d* bands of Group II_D the intensity has gone mainly into the Q series, whereas the *a* and *c* bands which possess fainter Q series have their R series better developed.

The missing lines of the *a* column have been inserted by calculating a quadratic formula to represent the series. Taking this formula as:

$$II_D,\ a,\ R(m) = 24633{\cdot}46 + 9{\cdot}542m + 9{\cdot}1892m^2,$$

we obtain the following residuals: R(1) + 0·03, R(2) −0·26, R(3) −0·58, R(4) (0·00), R(5) +0·17, R(6) (0·00), R(7) +0·64, R(8) (0·00), R(9) + 0·03. The two missing lines of the *c* column have been similarly calculated. It is noteworthy that the series II_D, *a*, R is of the same alternating-intensity type as the corresponding Q series and resembles it in length.

P series obeying the Simple Combination Principle have not been observed in this group, although it is possible that P series, or fragments of P series which do not obey this principle, may be present. This weakness of the P and R branches in comparison with the Q is no new thing in band spectra: Richardson* remarks that, in the Red, Green, and Blue Fulcher Systems which he has discovered, the P branches are weaker than the R branches and the R than the Q; Dieke† has deduced a similar conclusion from theoretical considerations for general band spectra; and in the recently discovered Lyman Bands‡ in the ultra-violet spectrum of hydrogen Q series *only* seem to be present.

As stated in our previous paper, another group has been found closely parallel to II_D but occurring a little higher in the spectrum. Since, however, the second group shows a number of coincidences with the lines of Richardson's Fulcher System, we shall for the present omit it.

The term differences for the bands of Group II_D are shown in Table VII. These figures must be regarded as approximate owing to the number of missing lines. The missing lines of the Q series have been calculated, where possible, by a process of averaging horizontal differences, while those of the R series have been arrived at from the quadratic formula representing the series—a questionable procedure, since the series appear to show systematic divergence from a parabolic law, particularly for low quantum numbers. Nevertheless, the general resemblance of the term differences for the various bands is sufficiently striking. Both initial and final term differences show a small but appreciable increase in passing up the group—a peculiarity which has already been noted in the case of Group II_H.

---

* Richardson, 'Roy. Soc. Proc.,' A, vol. 111, p. 739 (1926).

† Dieke, 'Z. f. Physik,' vol. 33, p. 161 (1925); *see* also Mulliken, 'Phys. Rev.,' vol. 29, p. 391 (1927).

‡ Lyman, 'The Spectroscopy of the Extreme Ultra-Violet,' p. 79 (1914); *see also* Witmer, 'Proc. Nat. Acad. Sci.,' vol. 12, p. 238 (1926) and 'Phys. Rev.,' vol. 28, p. 1223 1926).

Table VII.—Band Group II_D, Term Differences.

Initial Term Differences.

Band.	m.	$F(m+1)-F(m)$.	$\Delta\{F(m+1)-F(m)\}$.	$\Delta^2\{F(m+1)-F(m)\}$.
II_D, *a*	1	19·37	30·87	+0·48
	2	50·24	31·35	−0·22
	3	81·59	31·13	−0·09
	4	112·72	31·04	−0·96
	5	143·76	30·08	−0·06
	6	173·84	30·02	−1·84
	7	203·86	28·18	
	8	232·04		
II_D, *b*	1	20·56	31·34	
	2	51·90		
II_D, *c*	1	20·80	31·18	−0·96
	2	51·98	30·22	+1·41
	3	82·20	31·63	
	4	113·83		

Final Term Differences.

Band.	m.	$f(m+1)-f(m)$.	$\Delta\{f(m+1)-f(m)\}$.	$\Delta^2\{f(m+1)-f(m)\}$.
II_D, *a*	1	13·42	13·00	−1·15
	2	26·42	11·85	+1·23
	3	38·27	13·08	−1·04
	4	51·35	12·04	−1·21
	5	63·39	10·83	+0·25
	6	74·22	11·08	
	7	85·30		
II_D, *b*	1	14·50	12·80	
	2	27·30		
II_D, *c*	1	15·06	12·07	+0·57
	2	27·13	12·64	
	3	39·77		

For the sake of comparison we have calculated the constants for Band II_D, *a* from the same data as were employed previously in the case of Bands II_F, *a*, II_G, *a*, and II_H, *a*. These are given in Table VIII. On comparing Table VIII with Table V, it will be seen that Band II_D, *a* shows appreciably lower values of the moments of inertia, as well as numerically smaller E and *e* constants, than the other bands.

Table VIII.—Band Constants.

Band.	B cm.$^{-1}$.	I_1 gm. (cm.)^2.	E.	*b* cm.$^{-1}$.	I_2 gm. (cm.)^2.	*e*.	ν_0 cm.$^{-1}$.
II_D, *a* …	15·54	$17 \cdot 8 \times 10^{-41}$	−0·88	6·28	$44 \cdot 0 \times 10^{-41}$	−0·44	24633·6

The accuracy of the data provided by Table VII is insufficient to enable us to say definitely whether the values of the moments of inertia, which depend on the quantities $\Delta\{F(m+1) - F(m)\}$ and $\Delta\{f(m+1) - f(m)\}$, increase or decrease in passing up the group. We can, however, deduce that the E and *e* constants are not the same for the different members of the group, and are, in fact, numerically smaller for the *c* band than for the *a* band. This result can be shown for example by taking successive values of the quantities $\dfrac{F(m+2) - F(m+1)}{F(m+1) - F(m)}$ which are independent of B.

It may be noted that the analysis of the various Type-II bands, embodied in Tables V and VIII, has been carried out from the same or closely similar data for each band, and so affords an effective method of comparing these bands with one another. It cannot, however, claim to be fundamental, since it is based on an approximate series representation for the bands. Many of the Type-II series have been found to deviate from a parabolic law in a characteristic manner, and it seems probable that, were it possible to discover the correct series representation, many of the difficulties presented by the bands would vanish.

Other Groups of Q Series.—In Table IX we give a group of Q series (II_I) occurring in the green. This group resembles II_B of our first paper in possessing five columns spaced out at intervals of very nearly 92 wave-numbers, the interval being slightly greater at the right-hand edge of the table than at the left-hand edge. Here Tanaka's and Deodhar's observations, except in two cases, one involving an overlap, have not served to fill up the gaps. In spite of these gaps the regularity of the horizontal and vertical differences indicates a considerable degree of probability for the group. It may also be noted that

Table IX.—Band Group II_I, Q Series.

	e.		d.		c.**		b.		a.
Q(1)	—								18673·69 (D*rd*, 0, 0)
									6·62
Q(2)	18311·19 (M1L, –, –)	*91·76*	18402·95§ (T*q*, –, –)	*92·01*	18494·96 (M0, 3, 2)	*92·75*	18587·71 (M3, –, –)	*92·60*	18680·31 (M0, 0, 0)
	24·14		*24·22*		*24·83*		*24·69*		*24·21*
Q(3)	18335·33 (M0, 0, –)	*91·84*	18427·17 (M0, 0, –)	*92·62*	18519·79 (M1, –, –)	*92·61*	18612·40 (Missing)	*92·12*	18704·52* (M1L, –, –)
	43·20		*42·87*		*43·45*		*43·58*		*43·83*
Q(4)	18378·53 (Missing)	*91·51*	18470·04 (Missing)	*93·20*	18563·24‡ (M3L, 0, –)	*92·74*	18655·98 (M1, 1, 1)	*92·37*	18748·35 (Missing)
	62·27		*61·52*				*62·48*		*63·45*
Q(5)	18440·80 (M0, –, 1)	*90·76*	18531·56 (M1, –, –)				18718·46† (M1, 0, 0)	*93·34*	18811·80 (M0, –, –)

* The same line as $_1a_0$ Q(5).

† The same line as $_1a_0$ P(2).

‡ The same line as $_2a_1$ R(2).

§ The same line as IV_A, 7, Q(9).

** Of the three lines forming the *c* column, *c*, Q(2) shows enhancement in the condensed discharge, *c*, Q(3) diminution, and *c*, Q(4) (an overlap) great diminution according to the observations of Merton and Barratt. *b*, Q(5) (an overlap) and *d*, Q(5) also show diminution. On the other hand, *e*, Q(3) and *e*, Q(5) show enhancement. It is doubtful how much of this is to be ascribed to overlaps. In Richardson's Fulcher System the effect of the condensed discharge is always to weaken the lines of low rotation quantum number and to enhance the lines of high rotation quantum number.

three of the gaps occur at the line Q(4) which, by analogy with Band Group II_B, we should expect to find fainter than Q(5).

Bearing in mind the supposition that there is a structural relationship between Band Groups II_I and II_B, we may note the curious fact that the interval separating the two groups comes out approximately as

$$2398 = 26 \times 92 \cdot 2 \text{ cm.}^{-1},$$

i.e., an integral multiple of the fundamental 92 difference like the interval separating Groups II_H and II_G.

Traces of the same configuration have been found in other portions of the spectrum. Many of these are too fragmentary to be given with confidence. One, which contains a Q series complete from Q(1) to Q(5) as well as traces of a horizontal spacing of the order found previously, is given in Table X.

Table X.—Band Group II_J, Q Series.

	a.		*b.*
Q(1)	23273·73 (MO)		
	6·72		
Q(2)	23280·45 (MO)	*90·97*	23371·42 (T*p*)
	24·96		*24·81*
Q(3)	23305·41 (TO)	*90·82*	23396·23 (Missing)
	42·76		*42·95*
Q(4)	23348·17 (T*p*)	*91·01*	23439·18 (T*p*)
	61·1		*61·09*
Q(5)	23409·3 (T)	*91·0*	23500·27 (MO)

This group (II_J) occurs just on the short-wave side of the primary line H_γ. The vertical differences are so like those of previous groups that it seems likely that this group will turn out to be a weaker member of the same extensive system to which the others belong. Curiously enough, the intensity sequence of the *a* series of Group II_J is perfectly smooth, while the *b* series shows abnormal strength in the line Q(5), a peculiarity characteristic of some of the other groups.

In Table XI we give a group appearing in the ultra-violet just on the short-wave side of the primary line H_ζ. This group (II_K), occurring not far from the limit of Merton and Barratt's observations in a region where lines are becoming exceedingly scarce, affords strong confirmation of the validity of the arrangement.

Table XI.—Band Group II_K, Q Series.

	z.		*a.*		*b.*		*c.*
Q(1)	25724·47 (M0)	*92·17*	25816·64* (M1L)	*91·24*	25907·88 (M1)		
			5·07		*6·24*		
Q(2)			25821·71 (M2L)	*92·41*	25914·12 (M0)	*92·19*	26006·31 (D*r*)
			24·29		*24·33*		*24·31*
Q(3)			25846·00 (T*p*)	*92·45*	25938·45 (Missing)	*92·17*	26030·62† (T*pd*)
			43·17		*43·20*		*42·14*
Q(4)			25889·17 (M1)	*92·48*	25981·65 (D*rw*)	*91·11*	26072·76‡ (D*r*)
			61·46		*62·12*		*63·59*
Q(5)			25950·63 (D*r*)	*93·14*	26043·77 (T*r*)	*92·58*	26136·35§ (M0)
			79·99				*78·51*
Q(6)			26030·62† (T*pd*)				26214·86 (T*r*)

* The same line as ${}_4\epsilon_4$ Q(1).
† An overlap. The "*d*" feature of Tanaka's observation suggests two lines.
‡ The same line as ${}_3\epsilon_3$ Q(3). Since ${}_3\epsilon_3$ Q(2) is missing, this may well be a real coincidence.
§ The same line as ${}_3\gamma_3$ Q(2). The line seems too intense to be claimed solely by either series.

It may be noted, that it is in some cases possible to find a head-formula that will link three of the groups together. Taking the line Q(2) as representative of the band in the head-formula—

$$Q(2) = 20486 \cdot 39 + n\,(1351 \cdot 866 - 0 \cdot 2533n) - n'\,(1259 \cdot 703 - 0 \cdot 1933n'),$$

we should have the three bands of Group II_H corresponding to vibration transitions 0 → 1, 1 → 2, and 2 → 3, Band II_A, *a* corresponding to the transition 1→0, and the two bands of Group II_J to transitions 3 → 1 and 4 → 2. There would also be traces of bands corresponding to some of the null transitions.

This representation, however, cannot be accepted as convincing, since it would mean that the *b*, *c*, and *d* bands of Group II_A are somewhat displaced from their proper positions. Also, the evidence deducible from the R series is rather against allotting Groups II_H and II_A to the same Deslandres system. Again, if the groups are to be ascribed to the vibration quantum number in this way, we should expect the E and *e* constants not to alter and the moments of inertia to increase in passing from the long-wave to the short-wave side of a group, so that we should have successively diminishing term differences. Instead of this, at least in the case of Group II_H, there is a progressive increase of the term differences in passing up the group.

When we review the regularities that have just been described, it seems somewhat surprising that so many well marked groups occur which are unrelated either by the head-formula of Deslandres or by that of Rydberg, and the conviction has forced itself on the writers, that the groups given are merely the strongest members of a very extensive system of which the structure will not be fully unravelled until experimental means have been found of favouring the emitter.

The Distribution of the Type-II Regularities in the Spectrum.—This is shown in diagrammatic form in Table XII. Vertical differences between the successive figures in each column have been shown, although, where successive groups differ markedly in structure, such differences can have little physical significance. And, indeed, there is little apparent relationship between these differences, except that some of them appear to be integral multiples of the fundamental 92 interval, *e.g.* :—

$$\begin{array}{c} \mathrm{II}_K\ 25821\cdot71 \\ \mathit{3984\cdot21} = \mathit{43} \times \mathit{92\cdot7} \\ \mathrm{II}_A\ 21837\cdot50 \\ \mathit{6764\cdot25} = \mathit{73} \times \mathit{92\cdot7} \\ \mathrm{II}_G\ 15073\cdot25, \end{array}$$

and

$$\begin{array}{ccc} \mathrm{II}_H\ 19226\cdot88 & \mathit{1852\cdot07} = \mathit{20} \times \mathit{92\cdot6} & \mathrm{II}_B\ 21078\cdot95 \\ \mathit{4153\cdot63} = \mathit{45} \times \mathit{92\cdot3} & & \mathit{2398\cdot64} = \mathit{26} \times \mathit{92\cdot3} \\ \mathrm{II}_G\ 15073\cdot25 & & \mathrm{II}_I\ 18680\cdot31. \end{array}$$

Table XII provides strong evidence for the view put forward, that the groups which have been given are only the strongest out of a very extensive system. If this be so, further progress will depend on whether experimental conditions can be found that will favour the emitter. It seems likely that the arc spectrum at higher pressures will serve to bring out some of the weaker lines due to triatomic hydrogen, and it is hoped to pursue investigations in this direction.

One fact that calls for theoretical interpretation is the horizontal spacing of 92 wave-numbers which forms a prominent feature of these regularities. We have been at first inclined to attribute this spacing to the vibration quantum number. The evidence provided by the present paper, however, points to some other cause.

In the theory of molecular spectra at present accepted only three quantum numbers are employed, associated respectively with rotational, nuclear vibrational, and electronic energy. Several workers in this field have emphasised the connection between molecular spectra and atomic spectra. Now, in the latter at least three quantum numbers are necessary to specify a spectroscopic term. It must follow that in dealing with a molecule more than three quantum

Table XII.—Band System II.

Table showing the positions of the groups in the Spectrum.

(The Q(2)'s of the *a* bands are taken as representing the groups.)

	Groups having their *a* series on the long-wave side.		Groups having their *a* series on the short-wave side.	
Infra-red	II$_F$	13470·42		
		1602·83		
	II$_G$	15073·25		
Green		*4153·63*	II$_I$	18680·31
	II$_H$	19226·88		*2398·64*
Blue		*2610·62*	II$_B$	21078·95
	II$_A$	21837·50		
		1442·95		*2932·44*
Violet	II$_J$	23280·45		
		1358·35	II$_C$	24011·39
	II$_D$	24638·80		
		1182·91		
Ultra-violet	II$_K$	25821·71		

numbers will be required.* It is at least possible that the 92 difference which is found in the spacing of the groups is dependent on a new quantum number which has not as yet been given a specified place in band theory.

It is probable that a satisfactory analysis of these bands, once it has been accomplished, will not only serve to disentangle a considerable portion of the secondary spectrum of hydrogen, but will prove a starting point for the experimental study of triatomic spectra, and so open up a field of spectroscopic investigation as yet but little understood.

Summary.

In a recent communication (' Roy. Soc. Proc.,' A, vol. 114, p. 293 (1927)), evidence has been given for the existence of a system of bands of a distinctive type, occurring in groups throughout a wide range of the visible and infra-red spectrum of hydrogen. The bands in a group are spaced out at intervals of very nearly 92 wave-numbers. Various reasons have been given for attributing the system to triatomic hydrogen, H_3. To the bands already given a considerable number of new bands has now been added, and there is evidence to show that these are only the strongest in a very extensive system.

---

* See in particular Mecke, ' Phys. Z.,' vol. 26, p. 217 (1925); and Birge, ' Bulletin of Nat. Research Council,' No. 57 (1926).

The structure of some of the better defined bands has been investigated from a theoretical standpoint, and reasons are given for the view that the spacing in groups with a difference of 92 wave-numbers is not to be attributed to the vibration quantum number. Based on the analogy with line spectra, a tentative suggestion is made that this difference is dependent on a new quantum number.

We have to thank Prof. O. W. Richardson for supplying information about the lines of his system.

The Band Spectra of Silicon Fluoride.

By R. C. JOHNSON, M.A., D.Sc., Lecturer in Physics in the University of London, King's College, and H. G. JENKINS, M.Sc., Musgrave Research Student in the Queen's University of Belfast.

(Communicated by T. R. Merton, F.R.S.—Received May 5, 1927—Revised July 13, 1927).

[PLATE 10.]

Introduction.

This investigation of the band spectra of silicon fluoride originated in an attempt to produce the band spectra of boron fluoride. The latter would be of considerable interest in view of the close similarity which should exist between the BF and the CO molecule, and of the fact that our knowledge of the band spectra of CO is very extensive. We have made several attempts to obtain the boron fluoride spectra free from silicon fluoride, but without success. The boron fluoride is broken up by the discharge and the free fluorine attacks the silica in the glass. In order to interpret properly the plates obtained, it was necessary to know the systems due to silicon fluoride, and an examination of the literature revealed the fact that very little is known of the band spectra of this compound. Porlezza* has examined the spectrum produced by admitting SiF_4 into a discharge tube, using a three-metre grating having 10,000 lines to the inch. He studied the violet end of the spectrum chiefly and records wave-lengths of about 60 heads in the region λλ 5475–3870. Some of these have been related in empirical formulæ: these are obviously some of the sequences of Table I. Dufour has examined the Zeeman effect on some of these bands, but apart from this work very little appears to be known about the band spectra of silicon fluoride.

---

* 'Rend. Accad. Linc.,' vol. 20, p. 488 (1911); and vol. 33, p. 283 (1924).

Experimental.

The method we used for preparation of the silicon fluoride was as follows: A mixture of finely powdered silicon (or pure silica) and calcium fluoride was treated with concentrated sulphuric acid, and the resulting gas was passed over caustic potash and phosphorus pentoxide into a flask attached to the discharge tube. The tube was usually kept on the pump system during the exposure, and from the reservoir attached fresh supplies of gas could be admitted to the tube at intervals without interrupting the exposure. The discharge tubes used were both wide bore and capillary, fitted with small side bulbs of KOH and P_2O_5 and quartz windows. The exciting currents were varied over a wide range, the maximum current from the secondary of the transformer being about 80 milli-amps. The pressure of silicon tetra-fluoride in the discharge tubes was usually about 1 mm. of mercury. Photographs have been taken on a glass prism spectrograph giving a dispersion of 3·2 inches from λλ 7000–3900, and a quartz prism spectrograph of dispersion 4 A.U. per mm. at λ 2100 and 16·5 A.U. per mm. at λ 3000. For high dispersion work the first and second orders of a 21-foot concave grating were used.

The Band Systems Obtained.

The discharge through silicon fluoride is of a strong blue colour. This is due to a system of intense bands in the blue region, degraded to the red, and as seen under low dispersion, apparently doublets. These are the bands obtained and measured by Porlezza. Under various conditions a large number of band systems have been obtained, and it will be convenient to describe them at this stage. For the sake of reference each system is denoted by a Greek letter.

(1) *The α group.*—This is the system of bands referred to above in the blue region. Its wave-lengths are given in Table I. The system appears strongly under all conditions except those of low current density. Good second order grating plates have been obtained of this group, by use of a capillary tube through which a constant stream of silicon tetra-fluoride was passed at about

1 mm. pressure. Owing to the breaking up of the silicon fluoride by the heavy discharge used, a deposit gradually collected in the capillary, and this had to be cleaned at intervals. It was found that a blast of air easily carried the deposit into the wider part of the tube, and in this manner the exposure was continued without having to remove the tube itself—a very important point in obtaining high dispersion photographs. Plate 10, Spectrum 1, shows this system under low dispersion, and Nos. 5 and 6 show a portion of the system in the second order of the 21-foot grating.

Table I.—Wave-Lengths of the α-System.

Int. (Porlezza).	λ (Porlezza).	Int.	λ (I.A.).	ν (Vacuo).	Series.
—	—	0*da*	5015	19936	
—	—	1*a*	4970·8	20112	
—	—	0*a*	4964·6	20137	C (3, 6)
—	—	2*a*	4928·6	20284	A (6, 8)
—	—	1*a*	4920·9	20316	D (3, 6)
—	—	2*a*	4895·6	20421	
—	—	4	4889·0	20448	B (6, 8), A (5, 7)
—	—	2	4879·8	20487	C (6, 8).
—	—	2	4861·3	20565	
—	—	6	4850·5	20611	B (5, 7), A (4, 6)
—	—	2	4838·7	20661	C (5, 7).
—	—	2	4819·6	20743	
—	—	4	4815·3	20761	B (4, 6), A (3, 5)
—	—	3	4812·5	20773	
—	—	3	4794·7	20850	B (8, 9) ?
—	—	2	4780·9	20911	B (3, 5)
—	—	3	4776·4	20930	
—	—	1*d*	4758·4	21010	
—	—	2*d*	4752·6	21037	B (7, 8)
—	—	2	4738·1	21099	C (7, 8)
—	—	3 ?	4722·1	21171	
—	—	1	4704·0	21252	B (10, 10), A (5, 6)
—	—	2	4668·7	21413	B (5, 6), A (4, 5)
—	—	2*d*	4659·5	21456	D (6, 7), C (5, 6), B (9, 9)
—	—	3*d*	4650·5	21497	A (8, 8)
—	—	2	4648·0	21508	C (9, 9)
—	—	3 ?	4633·2	21577	A (3, 4), B (4, 5)
—	—	3	4624	21622	D (5, 6), C (4, 5)
0	4616·57	4	4616·5	21655	B (8, 8)
1	4609·61	5	4609·6	21689	A (7, 7)
0	4605·25	3	4605·2	21709	C (8, 8)
—	—	2*c*	4586·7	21796	D (4, 5)
1	4575·18	6	4575·076	21851·45	B (7, 7)
2	4569·45	8*d*	4569·492	21878·16	A (6, 6)
1	4564·98	6	4564·94	21900·0	C (7, 7)
2	4535·91	7*c*	4535·911	22040·13	B (6, 6), A (0, 1
3	4531·62	9*d*	4531·628	22060·96	A (5, 5)
2	4526·45	7*d*	4526·407	22086·40	C (6, 6)
4	4498·64	7	4498·595	22222·95	B (5, 5)
5	4495·82	9	4495·772	22236·91	A (4, 4)
1	4492·71	2*c*	4492·56	22252·8	D (6, 6), C (0, 1)
4	4489·75	7	4489·618	22267·38	C (5, 5)

a = approximate measure only. *c* = confused with other bands. *d* = diffuse.

Table I—*continued.*

Int. (Porlezza).	λ (Porlezza).	Int.	λ (I.A.).	ν (Vacuo).	Series.
4	4463·41	7	4463·217	22399·10	B (4, 4)
6	4462·06	8	4461·964	22405·39	A (3, 3)
3	4456·24	—	—	22434·2	D (5, 5)
5	4454·55	7	4454·524	22442·81	C (4, 4)
9	4429·98	10	4430·231	22565·87	A (2, 2)
—	—	9	4429·788	22568·13	B (3, 3)
—	—	3	4421·96	22608·1	
—	—	4	4421·44	22610·7	D (4, 4), C (3, 3)
6	4421·00	6	4420·92	22613·4	
10	4400·58	10	4400·498	22718·34	A (1, 1)
10	4398·38	9	4398·257	22729·91	B (2, 2)
4	4388·64	4	4388·563	22780·12	D (3, 3)
3	4387·11	0*c*	4386·77	22789·4	
15	4368·50	20	4368·221	22886·20	A (0, 0)
3	4365·58	5 ?	4365·35	22901·3	C (6, 5)
—	—	0	4355·10	22955·2	
—	—	1	4354·49	22958·4	
3	4353·92	3*a*	4353·80	22962·0	
3	4338·71	6	4338·735	23041·74	B (5, 4)
4	4334·39	8	4334·351	23065·04	A (4, 3)
—	—	2	4334·11	23066·3	D (6, 5)
2	4329·73	7	4329·650	23090·08	C (0, 0), C (5, 4)
3	4304·21	7	4304·186	23226·69	B (4, 3)
3	4301·31	7	4301·274	23242·41	A (3, 2)
3	4298·79	1	4298·746	23256·08	D (5, 4)
—	—	3	4299·04	23254·5	
—	—	1	4297·14	23264·8	D (0, 0)
2	4295·84	5	4295·732	23272·39	C (4, 3)
1	4283·35	—	—	23339·7	
3	4271·59	8	4271·523	23404·29	B (3, 2)
3	4270·45	8	4270·192	23411·59	A (2, 1)
—	—	—	4265·52	23437·2	
2	4265·06	5	4264·99	23440·14	D (4, 3)
—	—	0	4264·62	23442·2	
—	—	0	4263·99	23445·6	
—	—	2	4263·64	23447·6	
2	4263·47	6	4263·495	23448·36	C (3, 2)
—	—	2	4262·936	23451·43	
1	4256·91	8	4256·84	23485·0	
1	4254·65	7	4254·52	23497·8	
—	—	4*da*	4243·2	23560	A (1, 0)
4	4240·92	10 ?	4240·795	23573·87	B (2, 1)
1	4234·28	6*d*	4233·7	23613	
1	4233·02	—	—	23617·2	D (3, 2)
1	4215·39	—	—	23715·9	B (1, 0)
2	3905·25	—	—	25599·3	
3	3882·99	—	—	25746·1	
1	3870·75	—	—	25827·5	

a = approximate measure only. *c* = confused with other bands. *d* = diffuse.

(2) *The* β *group.*—This is a well defined system of close doublets in the region λλ 3200–2680, with heads degraded towards the further ultra-violet. The system appeared best when the α group was radiating strongly and was

weak under low current density conditions. Good low dispersion plates of the system have been obtained and a few less satisfactory plates in the first order of the grating. On Plate 10 Nos. 1 and 2 are photographs of the system. Wave-length data are given in Table II. A vibrational isotope effect can be readily detected in the most refrangible group of bands on the original plate.

Table II.—Wave-lengths of the β System.

Int.	λ (I.A.).	Nature of head.	n'	n''	ν (Vacuo).
0	3205·9	P 28	0	4	31184
0	3203·1	Q 28			31211
0	3185·8	P 28	1	5	31381
0	3182·8	Q 28			31410
0	3165·8	Q 28	2	6	31578
0	3162·9				31607
0	3149·9	P 28	3	7	31738
0	3147·3	Q 28			31764
2	3121·1	Q 28	0	3	32031
2	3119·9	—	—	—	32043
0	3105·3	P 28	1	4	32194
2	3103·5	Q 28			32212
2*a*	3102·3				32225
1	3087·8	P 28	2	5	32376
2*c*	3086·3	Q 28			32392
2*c*	3085·0				32405
1	3070·7	P 28	3	6	32556
2*c*	3069·5	Q 28			32569
2*vc*	3053	Q 28	4	7	32745
4	3042·4	P 28	0	2	32859
5	3041·4	Q 28			32870
3	3027·5	P 28	1	3	33021
6	3026·5	Q 28			33031
6*c*	3025·4				33044
3	3011·8	P 28	2	4	33193
5	3010·8	Q 28			33204
3*c*	3009·6				33217
2	2996·2	P 28	3	5	33366
4	2995·3	Q 28			33375
0	2980·9	P 28	4	6	33537
1	2979·9	Q 28			33548
10	2967·06	P 28	0	1	33693·6
10	2965·76	Q 28			33708·4
10	2952·82	P 28	1	2	33856·0
10	2951·67	Q 28			33869·3
7	2938·61	P 28	2	3	34019·7
8	2937·53	Q 28			34032·3
3	2924·4	P 28	3	4	34185
4	2923·4	Q 28			34197
1	2910·5	P 28	4	5	34348
1	2909·5	Q 28			34360
10	2894·41	P 28	0	0	34539·3
10	2893·03	Q 28			34555·7
4	2880·85	P 28	1	1	34701·8
9	2879·62	Q 28			34716·6

Note.—Column 3 has not been completed, in view of the discussion in the text as to the precise molecule or molecules which are responsible for the subsidiary heads.

a = approximate measure only. *c* = confused with other bands. *vd* = very diffused.

Table II—*continued*.

Int.	λ (I.A.).	Nature of head.	n'	n''	ν (Vacuo).
2*c*	2867·9	P 28	2	2	34858
2*c*	2866·8	Q 28			34871
1*vd*	2843·2	P 28	4	4	35161
2*vd*	2830·3	P 28	5	5	35322
1*vd*	2817·6	P 28	6	6	35481
8	2812·98	P 28	1	0	35539·0
8	2811·52	Q 28			35557·5
4	2801·4		2	1	35686
8	2800·0	P 28			35703·5
7	2798·8	Q 28			35719·5
1	2790·1		3	2	35830
6	2788·7	P 28			35848
5	2787·5	Q 28			35864
0	2778·8		4	3	35976
2	2777·5	P 28			35993
2	2776·4	Q 28			36007
0	2766·3	P 28	5	4	36138
0*a*	2765·2	Q 28			36153
2*c*	2736·5	P 28	2	0	36532
3*c*	2735·3	Q 28			36549
2	2726·5		3	1	36666
3	2725·09				36685·2
3	2724·5	P 28			36693
2	2723·15	Q 28			36711·3
2	2716·49		4	2	36801·3
3	2715·06				36820·7
3	2714·47	P 28			36828·7
2	2713·17	Q 28			36846·4
1	2706·49		5	3	36937·3
2	2705·13				36955·9
2	2704·53	P 28			36964·1
1	2703·21	Q 28			36982·0
1	2696·5		6	4	37075
2*d*	2694·6	P 28			37100
1	2693·4	Q 28			37117
0*a*	2686·8	P 28	7	5	37208
0*d*	2684·8	Q 28			37236

a = approximate measure only. *c* = confused with other bands. *d* = diffuse.
vd = very diffused.

(3) *The* γ *group*.—This is a curious system of three groups of bands in the region λλ 2654–2525. Table III gives wave-length data. Under the microscope each of the three groups is seen to be a double double-headed band associated with a number of other weaker bands and degraded to the more refrangible side.

Table III.—Wave-lengths of the γ System.

Int.	λ (I.A.).	ν (Vacuo).	Int.	λ (I.A.).	ν (Vacuo).
1	2654·24	37664·4	2*c*	2587·3	38638·8
3	2652·77	37685·25	3	2585·90	38659·7
1*vd*	2649·21	37735·9	5	2584·29	38683·8
1	2647·47	37760·7	2	2584·17	38685·6
1*d*	2645·99	37781·8	2	2583·02	38702·8
1	2644·80	37798·8	2	2581·4	38727·1
2	2642·81	37827·3	2	2580·5	38740·6
3	2641·42	37847·2	2	2578·91	38764·5
2	2639·39	37876·3	2	2578·15	38775·9
2	2637·94	37897·1	2	2576·50	38800·7
1	2637·19	37907·9	2	2575·91	38809·8
1	2635·93	37926·0	1*d*	2574·26	38834·5
1	2634·61	37945·0	4	2541·50	39335·0
1	2633·00	37968·2	7	2539·22	39370·3
2	2596·87	38496·55	3	2537·20	39401·7
5	2595·09	38522·8	3	2535·38	39430·0
3	2594·94	38525·0	2	2532·36	39477·0
	2594·17	38536·5	5	2530·68	39503·2
2	2592·25	38565·0	6	2528·87	39531·5
	2591·59	38574·8	3	2526·90	39562·3
2	2589·74	38602·4	1	2525·04	39591·4
	2589·25	38609·7			

c = confused. *d* = diffuse. *d* = very diffuse.

(4) *The* δ *group*.—This is a system of bands of the headless type, measured in the region λλ 2600–2250 and possibly extending further into the ultra-violet. Some of the strong bands at first sight appear to group themselves in threes, but analysis shows that the quartet appears to be the unit. They occur more or less faintly, but persistently, under all conditions, but a low current density appears to favour them particularly. This is possibly due to the comparative absence, in the latter case, of the continuous spectrum which masks the system under high current density conditions. Plate 10, Spectrum 4 (left-hand side), shows this system, of which Table IV gives details.

Table IV.—Wave-lengths of the δ System.

Wave-length.	Int.	ν (Vacuo).	Δν
2610·3	1*a*	38298	
2600·6	1*a*	38441	
2595·3	3*a*	38520	
2588·6	0*a*	38619·5	
2585·7	1	38662	
2584·5	3	38681	
2578·7	1*a*	38768	

a = approximate.

Table IV—continued.

Wave-length.	Int.	ν (Vacuo).	Δν.	
2573·1	1	38852		
2567·9	1	38931	79	
2562·6	1	39012	81	324
2557·3	2	39091	79	329
2551·8	1	39176	85	329
2546·3	1	39260	84	
2541·2	3	39341	81	
2539·3	5	39369	157	322
2530·4	3	39498		329
2528·8	5	39532	91	333
2525·2	1	39589		
2519·8	2	39674	85	338
2516·1	2	39733	59	334
2514·8	4	39753	20	331
2509·5	3	39836	83	336
2504·1	2	39923	87	
2498·9	2	40005	82	336
2493·7	4	40089	84	337·5
2488·5	3	40172	83	332
2483·1	2	40260·5	88·5	335
2478·3	1	40337	76·5	338
2473·0	4	40424	87	336·5
2467·8	4	40510	86	346
2462·6	2	40596	86	339
2457·3	1*a*	40683·5	87	341
2452·5	4	40763	80	343
2447·2	5	40851	88	347
2441·9	3	40939	88	339
2432·3	3	41100	161	337
2427·1	5	41190	90	354
2422·0	5	41276	86	
2416·5	1*a*	41370	94	340
2411·6	1*a*	41454	84	340
2407·2	4	41530	76	333
2402·2	4	41616	86	
2397·2	1*a*	41703	87	348
2387·1	0	41878	175	343
2382·5	4	41959	81	344
2377·5	3	42047	88	344
2373·4	1	42121	74	343
2363·2	2	42303	182	343
2358·3	2	42390	87	342
2354·2	1	42464	74	344
2349·3	1	42550	86	
2339·4	1	42732	182	344
2335·3	0	42808	76	345
2330·6	1	42894	86	
2320·7	0	43077	183	344
2312·1	0	43238	161	
2307·2	0	43328	90	337
2298·7	0	43489	161	339
2289·4	0	43665	176	
2280·9	0	43828	163	
2276·3	0	43918	90	348
2271·3	0	44013	95	

a = approximate.

(5) ***The* ε *System.***—These are two sets of bands, well defined and single-headed and degraded towards the more refrangible end. The intensity of the system is, however, rather low. The former set resembles the Ångström bands somewhat in position and appearance, the latter set in the same way resembles the second positive nitrogen bands. The appearance and occurrence together of the two sets suggests that they are members of the same system, but there is not enough data to demonstrate their relationship. The sets occur well under high current density. Plate 10, Spectrum 1 (middle), shows several members of the more refrangible set; the less refrangible set does not appear on the reproduction. Wave-length data are found in Table V.

Table V.—Wave-lengths of the ε System.

λ Int.	λ (I.A.).	ν (Vacuo).	Notes.
00	5710	17508	*b*
00	5693	17560	*b*
1	5671·7	17626	*bm*
00	5644	17713	*m*
2	5592	17878	
0	5549	18016	*mc*
0	5480	18243	
5	5388	18555	
1	5290	18898	
5	5193·6	19249	
0	5015	19935	*m*
0	4975	20095	*m*
2	4818·6	20747	
6	4229·7	23636	
8	4183·3	23898	
5	4143·1	24130	*bm*
2	4071	24557	
8	4011·8	24919	
2	3962	25233	
4	3811	26232	
1	3765·5	26549	
0	3711	26939	*bm*
1	3710	26946	*md*
0	3641	27457	
0	3632	27525	
0	3592	27832	
0	3570	28003	
0	3544·7	28203	
00	3515	28441	
0	3509	28490	
00	3479	28736	
00	3436	29095	
00	3395	29447	
00	3330	30021	

b = band or line ?
c = confused.
d = close doublet.
m = micrometer setting on middle.

(6) ***The ζ Group.***—This group consists of four or five double-headed bands in the region λλ 6200–6500 which appear to degrade towards the violet side. These bands are not the same as the fluorine bands described by Gale and Monk.* The fluorine bands are degraded towards the red, and there is no agreement of wave-lengths. In diffuse and extended bands of this type precise wave-length measurements under low dispersion are not possible. Approximate wave-lengths for identification purposes are: $\lambda\lambda \frac{6270}{6285}$; 6397; 6416; $\frac{6492}{6512}$; 6594. Low current density seems to favour this group, which is seen on the Plate No. 3*b* (extreme right).

(7) *The η Band.*—This is a remarkable isolated band in the region λλ 3368–3340. It has a maximum of intensity very near to that of the curious isolated ammonia† band, and it was at first suspected of being identical with it. A plate showing the ammonia band was obtained, and superposition clearly demonstrated that the two bands were not the same. The band appears well on Plate 10, No. 1. On our negatives it appears well only when the blue system is strong, *i.e.*, with high current density. The chief features under low dispersion are two close doublets superposed on a strong continuous background—a formation which strongly suggests the structure of the γ system, to which we believe it to be related.

(8) *The θ bands of the Cathode glow.*—In every case in which silicon fluoride was present in the discharge tube a yellow glow appeared at the cathode. With the aid of a direct vision spectroscope this was seen to be due to a system of narrow bands in the yellow region. Attempts to photograph this system from specially constructed tubes failed, owing to the comparative faintness of the radiation, but it should be possible to photograph it with an instrument of very large light gathering power. Their occurrence at the cathode indicates that the bands arise in an ionised molecule.

The Origin of the Band Systems.

Owing to the great chemical activity of the free fluorine liberated in the discharge tube we have tested carefully the possibility that some of the above systems may arise in impurities such as fluorine, hydrogen fluoride, carbon fluoride, mercury fluoride, aluminium fluoride and sulphur fluoride. The band systems are not due to F_2. The band spectrum of fluorine has been carefully investigated by Gale and Monk (*loc. cit.*). The bands attributed to fluorine by these writers have not appeared on any of our plates. It is further very unlikely that any of the systems originate in HF which is a polar molecule, but special precautions were taken to eliminate it from the discharge tube. If present, however, it would probably react immediately, whereas all the band systems have been obtained from silicon fluoride which has been in the tube for a considerable time.

---

* 'Astrophys. J.,' vol. 59 (1924).

† Fowler and Gregory, 'Phil. Trans.,' A, vol. 218, p. 351 (1919).

In order to find out if any of the band systems were due to carbon fluoride we endeavoured to eliminate carbon impurity from our apparatus. We were not able to do this absolutely, but with special precautions we reduced carbon contamination to a *very* small amount and found that the above band systems appeared with undiminished intensity. Furthermore, Gale and Monk refer to some attempts of Porter and Blackburn to secure the band spectrum of carbon fluoride, using for this purpose carbon tetra-fluoride. These were unsuccessful. We feel confident therefore that none of our systems originate in carbon fluoride.

The band systems were, moreover, independent of the presence of mercury impurity, or of the use of aluminium for tube electrodes. All the band systems occurred as before when nickel and copper were substituted for aluminium.

The method of preparation of silicon tetra-fluoride, involving the use of sulphuric acid, led to the production of two band systems which were ultimately attributed to sulphur fluoride. These exhibited a high degree of variability and could not be obtained when the silicon fluoride was prepared in other ways. The one system occurs in the green between λ 4900 and λ 5200, the other between λ 3300 and λ 2700. We propose to reserve details of these for another communication. From the experimental evidence outlined above we feel justified in concluding that the eight systems already described arise from a silicon fluoride molecule.

The Structure of the α System.

This complex system of bands has been analysed, and presents some notable features. The data recorded in Table I consist of one very intense band sequence with a moderately strong sequence on its more refrangible side, and at least two much fainter ones on its less refrangible side. The intensely strong clear head at λ 4368·22 suggests itself as the (0, 0) band, and its structure is of the simplest type of PR band. The band is clearly single-headed and there is little, if any, confusing structure work superposed. The other bands on the red side among which we expect to find succeeding members of the (0, 0)

Table VI.—Assignment of Vibrational

n'' \ n'	→ 0	1	Diff.	2	Diff.	3	Diff.	4	Diff.
↓ 0	22886·2§ — — 23264·8?	22040·1† — 22252·8† —							
1	23560? 23716·6? — —	22718·3* — — —							
2		23411·6 23573·8 — —	843·7 843·9	22568·9 22729·9 — (Present)					
3				23242·4 23404·3 23448·4 23617·2	837·0 838·4 837·7 837·1	22405·4 22565·87 22610·7 22780·1	828·2	21577·2?†	
4						23065·0 23226·7 23272·4 23440·1	828·1 827·6 829·6 829·4	22236·9 22399·1 22442·8 22610·7	823·9 822·1 820·8 815
5								— 23041·7 23090·1 23256·1	818·8 822·7 821·7
6									
7									
8									
9									
10									

§ = Perturbed about 6 units to violet side.
* = Perturbed about 9 units to red side.

Quantum Numbers to the α System.

5	Diff.	6	Diff.	7	Diff.	8	9	10
20761† 20911 — —		— — 20137*a* 20315*a*						
21413† 21577† 21622† 21796*c*	802 816	20611?† 20761† — —						
22060·9 22222·9 22267·4 22434·4	809 809·9 812·4 812·4	21252† 21413† 21455*d*† 21622†	804 802 794	20448† 20611† 20661? —				
— — 22901·3 23066·3	814·9 813·5	21878·1 22040·1† 22086·4*d* 22252·8*c*	798	— — — 21455*c*†		20284 20448† 20487 —		
				21689·5 21851·4 21900·0 —	801	— 21037*d* 21099 —		
						21497·2 21655 21708·7 —	— 20850·5 — —	
							— 21455·7† 21508·5 —	
								— 21252·4† — —

† = Coincident with another radiation. (See Table I.)
c = Confused. *d* = Diffuse.

sequence are doublets in every case (see Plate 10, No. 5), or apparently so. The doublet widths show considerable variation, being 11·57, 2·26, 6·29, 13·96 and 20·83, and it is found impossible to account for these in terms of the vibrational isotope effect, Q branches, or other such cause. Proceeding on the assumption that we are dealing with two distinct band systems superposed so as to give a spurious doublet effect, it is possible to separate two band systems presenting very similar features. When these were arranged in the usual (n', n'') diagrams, it was apparent that within the limits of error the first differences of the one were the same as those of the other. The two sub-systems, which for the sake of brevity we will call A and B, are disposed in Table VI in the same diagram. (They are given by the first and second of the four wave-numbers in each square.) Subsequently, most of the remaining data of Table I were sifted into two other systems C and D similar to the above, and these fit reasonably well into the (n', n'') scheme of Table VI, and constitute the third and fourth members of each square. Critical examination of the identity of the first differences of these four sub-systems is not possible, as they are not extensive in either the n' or n'' dimension. Examination of the intervals AB, BC, and CD along a sequence is interesting. While the interval AB is constant at about 162 units, both BC and CD show an appreciable drift. It is possible that this is accounted for, wholly or in part, by the existence of an n' n'' product term in the vibrational energy function, owing to measurements having been made on the band heads not on the null lines. One feature of very considerable significance is the sudden beginning of the B system at ν 22729·9, recorded as the (2, 2) band in Table VI. The intensity fall down the sequence is 9, 10, 7, 7 (<7), 6, 4, etc., which suggests that if ν 22729·9 is really the (2, 2) band of the B system we might expect to find the (1, 1) band of quite appreciable intensity. There is no trace of it however, and it seems probable that the band at ν 22729·9 is really the (0, 0) band of the B system, so that the n' and n'' values of Table VI require to be reduced by 2. The band at ν 23573·8 raises no serious difficulty being of a doubtful linelike character. Furthermore, if it belonged to the B system, it would on this new view be the (0, 0) band, and as a consequence the B system would, unlike the A system, have $\Delta n = +1$ and not $\Delta n = 0$ as the dominating sequence. The level of the B system is therefore 156·3 units below that of the A system (and not as at first supposed 162 units above it). The true assignment of quantum numbers to the C and D systems is less certain, as there is a tendency for the intensities to fall off towards the origin. We consider, however, that the vibrational quantum numbers of these systems are those of Table VI also diminished by 2 units. These are considered more probable than ($n' - 3$) and ($n'' - 2$), which would involve the disappearance of the $\Delta n = -1$ sequence altogether.

Anticipating later results, it is found that the β system has its final electronic state in common with the α system. Now the two electronic levels associated with the β system are certainly single, so that it is reasonable to interpret the four levels of the α system as a singlet level (A), and a triplet level (BCD). The scheme of electronic levels of the emitting molecule is now as shown in fig. 1.

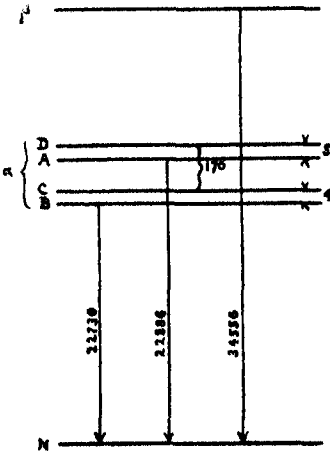

FIG. 1.

It has not been thought necessary at present to obtain accurate expressions for the band heads of the α system. These probably contain considerable terms in n'^3, n''^3 and $n'n''$. We have, however, found by graphical methods that the following formula holds reasonably well for the smaller values of n' and n'' (say less than 5):

$$\text{(A bands) } \nu = 22880 \cdot 5 + (709 \cdot 5n' - 7 \cdot 05n'^2) - (860 \cdot 5n'' - 4 \cdot 55n''^2) \quad (1)$$

Perturbations.—Examination of the $\Delta n = 0$ sequence shows that ν 22718·3 is perturbed from its expected position (viz., ν 22727) by about 8·7 units towards the low frequency side (provided, of course, that we identify this band with the (1, 1) band of the A system). Further, the (0, 0) band appears at ν 22886·2, and is therefore perturbed by some 5·7 units towards the high frequency side. The determination of which vibrational levels of the molecule are actually displaced is difficult, owing to the scarcity of data in the neighbourhood of the origin. Anticipating the data obtained by analysis of the β system it is possible to arrive at definite conclusions, and these are presented in fig. 2.

The Intensity Distribution and the Stability of the Molecule.—It will be observed from Table VI that bands in the neighbourhood of the origin are curiously few in number, but they multiply as we proceed outwards for values of $n > 4$. This attenuated character of the intensity distribution in which radiation is chiefly confined to one, or perhaps two sequences, is an indication of very little interaction between the excited electron and the vibrational energy of the molecule. It implies that the expression for the potential energy of the nuclei as a function of r (the inter-nuclear distance) is almost identical in the initial and final states of the molecule. This is strikingly confirmed by fine structure analysis of the (0, 0) band, the inter-nuclear distances before and

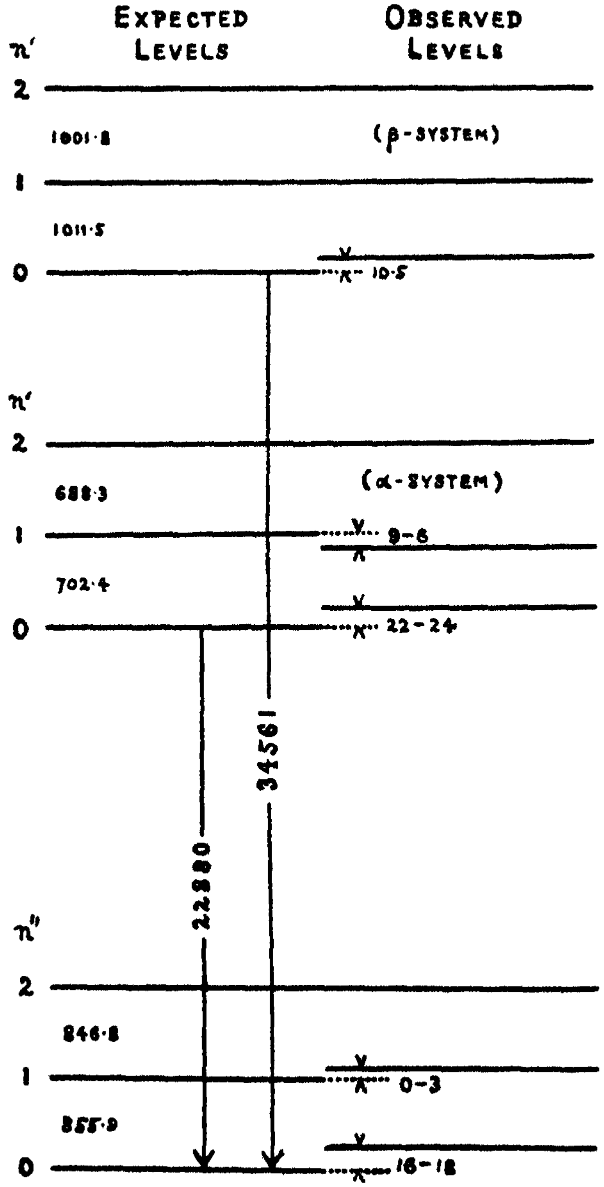

Fig. 2.

after the electron transition being respectively: 1·566 A.U. and 1·564 A.U. To this same cause the α system probably owes its great stability under energetic conditions of excitation, as in the condensed discharge and condensed spark. In general, the destruction of a band system by energetic conditions of excitation is due to dissociation of the molecule, and this will result when its vibrational energy is equal to its heat of dissociation. Franck* has shown that the communication of energy to a molecule is largely indirect, being due to electronic excitation in the first instance : the secondary effect of collisions only becoming important at high temperatures. The vibrational energy of a molecule is therefore a measure of the excess of potential energy which remains with the nuclei when they acquire a new equilibrium position as a consequence of the electronic transition. We have already observed that the inter-nuclear distance scarcely changes during the above transition, so that the stability of the molecule is a consequence.

The Structure of the β System.

This well defined system, for which the data are given in Table II, is degraded towards the more refrangible side. All the heads are close doublets due to the presence of Q branches. In Table VII is made an assignment of vibrational quantum numbers. Only the wave numbers of the more refrangible Q heads are recorded there, the separations from the associated P heads are recorded in parenthesis above each wave-number. As already mentioned, this system and the α system have a common final electronic state, and as in the latter case, the vibrational constants have been found approximately by graphical methods. The Q heads are given by :

$$\nu = 34561 \cdot 4 + (1015 \cdot 8n' - 4 \cdot 75n'^2) - (860 \cdot 5n'' - 4 \cdot 55n''^2). \qquad (2)$$

Perturbations.—The perturbation of the final level $n'' = 0$ by some 16–18 units towards the low frequency side is common to both the α and β systems. The initial level $n' = 0$ associated with this system is also perturbed by some 10½ units to the high frequency side (*vide* fig. 1). A most remarkable feature, however, is the perturbation relative to its neighbours of the (0, 1) band at $\nu \begin{cases} 33693 \cdot 6 \\ 33708 \cdot 4 \end{cases}$ by some 8–9 units to the low frequency side. The whole $n' = 0$ level is as we have seen perturbed by some 10½ units to the high frequency side, so that the net effect is a perturbation of some 2 or 3 units to the high frequency side. The recorded wave-lengths and wave-numbers have been checked carefully and were obtained from three different plates taken in the second order of the 21-foot grating. We have here, therefore, a remarkable case in which the perturbation is not associated with either of the vibrational levels, but

---

* 'Trans. Faraday Soc.' (December, 1926).

Table VII.—Quantum Analysis of the β System.

n'' → n' ↓	0	Diff.	1	Diff.	2	Diff.	3	Diff.	4	Diff.	5	Diff.	6	Diff.	7
0	(16·4) 34555·7 (1001·8)	847·3	* (14·8) 33708·4 (1008·2)	837·9	(11·5) 32870·5 (998·8)	839·5	32031 (1000·4)	820	31211*a* (1001)						
1	(18·5) 35557·5 (991·5)	840·9	(14·8) 34716·6 (1002·9)	847·3	(13·3) 33869·3 (1001·7)	837·9	(10·4) 33031·4 (1000·9)	819·4	(18) 32212*a* (992)	802	31410*a* (982)				
2	(17) 36549*c*	829·5	(16·0) 35719·5 (991·8)	848·5	(13) 34871 (993)	839	(12·6) 34032·3	828·3	(11) 33204 (993)	812	(16) 32392*c* (983)	814	31578*a* (991)		
3			(18) 36711·3	847·2	(16) 35864·1 (982·3)		—		(12) 34197	822	(9) 33375 (985)	806	(13) 32569*c* (979)	805	31764*a* (981)
4					(17·7) 36846·4	839·4	(14) 36007				(12) 34360	812	(11) 33548*a*	803	32745*c*
5							(18) 36982·0	829	(15) 36153*a* (964)						
6									(17) 37117						
7											(28) 37236*d*				

* Perturbed towards the low frequency side by some 9 or 10 units.

with the emission or absorption of a certain critical amount of vibrational energy (in this case 856 hc. ergs).

The vibrational isotope effect.—In view of the existence of three isotopes of silicon, of masses 28, 29 and 30, examination of both the α and β systems was made in order to detect any vibrational isotope effect. The theory of the isotope effect in electronic bands has been worked out by Mulliken[*] and we have adopted his notation below. The isotopic separation is proportional to $\nu_1{}^n$, and will therefore become appreciable in those sequences well removed from the origin. In the α system the strong sequences are $\Delta n = 0$ and ± 1, and the representatives of the sequence $\Delta n = +2$ are quite weak. The effect would therefore not be expected in the α system to any great extent. Probably some of the unassigned data in the first part of Table I is isotopic in origin. In the β system the effect is very distinct in the sequence $\Delta n = -2$ and is also measurable though not very precisely, in the sequences $\Delta n = +2$ and $+3$. In fig. 3 is exhibited the isotopic separation for the more reliable data of Table II.

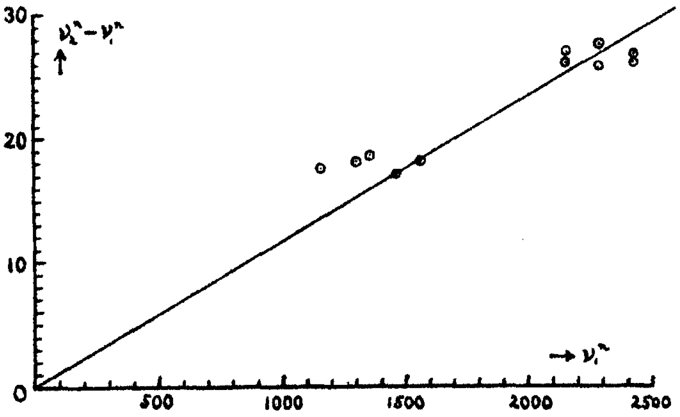

Fig. 3.

The line has been drawn after due consideration of the weight to be attached to the various points, and gives for the isotopic co-efficient $(\rho - 1) = -0 \cdot 0117 \pm 0 \cdot 0009$. Now if the emitting molecule be assumed SiF, then the calculated values of $(\rho - 1)$ are

$$\text{for} \left.\begin{matrix} \text{Si}^{28}\text{F} \\ \text{Si}^{30}\text{F} \end{matrix}\right\} -0 \cdot 01357 \text{ and for } \left.\begin{matrix} \text{Si}^{28}\text{F} \\ \text{Si}^{29}\text{F} \end{matrix}\right\} -0 \cdot 00700.$$

Unfortunately for those elements which have more than two isotopes, there is no precise quantitative data as to the proportions in which these occur. From the above figures it is easy to show that if Si^{30} atoms are twice as abundant as Si^{29} atoms, then the *mean* calculated value of $(\rho-1)$ would be $-0\cdot0114$. From the fine structure analysis of the band λ 4368 (*vide* later section) and for other reasons, it seems probable that the emitting molecule is FSi—SiF. On this assumption the isotopic co-efficient $(\rho-1)$ is for the following molecules:

---

[*] 'Phys. Rev.,' vol. 25, p. 119 (1925).

$$\left.\begin{array}{l} FSi^{28}-Si^{28}F \\ FSi^{30}-Si^{28}F \end{array}\right\}-0\cdot01026 \text{ and } \left.\begin{array}{l} FSi^{28}-Si^{28}F \\ FSi^{29}-Si^{28}F \end{array}\right\}-0\cdot00722.$$

Such molecules as $FSi^{30}-Si^{30}F$ and $FSi^{29}-Si^{29}F$ give for $(\rho-1)$ relative to the main head $-0\cdot02062$ and $-0\cdot01047$ respectively; these molecules will, however, probably be few in number compared to the previous type. Under the dispersion used, none of these isotopic components were separated from each other, and it is difficult therefore to deduce anything definite about the molecule from the experimental value.

Heat of Dissociation of the Molecule.

From a knowledge of the vibrational states of a non-polar molecule, Birge and Sponer* have shown that it is possible, within certain limits, to evaluate the energy required to dissociate it. For this purpose the data of equations (1) and (2) are available, but they are only approximate, and therefore no great accuracy is to be attributed to the figures deduced (especially as the relation between ω_n and n is probably not linear). From the data of the final state of the molecule (presumably the normal state) we have $n_0 = 94\cdot56$, giving $D = 40685$ wave-number units or $5\cdot022$ volts. From the initial level of the α system we have $n_0 = 50\cdot32$ giving $D = 40730$ units or $5\cdot028$ volts. The exceptional closeness of these values is fortuitous, but we feel justified in concluding that the heat of dissociation will be of the order of 5 volts, which is equivalent to 116000 calories. From the initial state of the β system we find $D = 11$ volts. While this value may be considerably in error it is sufficient to show that in this case the dissociation into two SiF groups leaves one or both of them with several volts of electronic energy.

The Structure of the γ System.

These groups are always to some extent obscured by the δ system and the continuous spectrum which seems to accompany the latter. Wave-number data and certain regularities are exhibited in Table VIII. The minor doublet

---

* 'Phys. Rev.,' vol. 28, p. 259 (1926).

Table VIII.—Structure of the γ System.

	37827·3	(162·9)	37664·4	
	37847·2	(161·9)	37685·3	
49·0 49·9				50·65
	37876·3		—	
	37897·1	(161·2)	37735·9	
31·6 28·9				24·8
	37907·9		—	
	37926·0	(165·3)	37760·7	
37·1 42·2				38·1
	37945·0	(163·2)	37781·8	
	37968·2	(169·4)	37798·8	
	38659·7	(163·1)	38496·6	
	38683·8	(161·0)	38522·8	
25·9 19·0				28·45 13·7
	38685·6	(160·6)	38525·0	
	38702·8	(166·3)	38536·5	
41·5 37·8				40·0 38·3
	38727·1	(162·1)	38565·0	
	38740·6	(165·8)	38574·8*c*	
37·4 35·3				37·4 34·9
	38764·5	(162·1)	38602·4	
	38775·9	(166·2)	38609·7	
36·2 33·9				36·4
	38800·7	(161·2)	38638·8	
	38809·8		—	
33·8				
	38834·5*d*		—	
	—		—	
	39503·2	(168·2)	39335·0	
	39531·5	(161·2)	39370·3	
59·1 59·9				66·7 57·7
	39562·3	(160·6)	39401·7	
	39591·4	(161·4)	39430·0	
				75·3
	—		39477·0	
	—		—	

interval is probably a Q branch. The major interval of about 162 units has already been encountered in connection with the α system. It seemed at first sight possible that the three groups of the γ system might be the (0, 0), (0, 1) and (0, 2) bands associated with an electron transition from an initial triple level down to the A, B, C and D levels, especially as this would account for a maximum of 12 bands in each group (which is suggested by Group 2 of Table VIII). The intervals between corresponding bands of the three groups are from 830 to 850 units, while the above arrangement would give 702, 688, etc., and must therefore be abandoned. The interval of 830 to 850 units suggests the final (normal) electronic level with its intervals of 856, 847 and 838, and it seems possible that the γ system represents another transition from a triple electronic level down to the normal one. There is no doubt from the available data that the molecule which is responsible for the α and β systems radiates the γ system also.

With regard to the δ system, no relationship of this to the other systems has yet been found. Its character suggests that it arises from a more complex molecule.

The Fine Structure of the Band at λ 4368·22.

Plate 10, No. 6, shows the structure of this band which is of the simple PR type and has only one missing line. Table IX gives detail of the band obtained from an excellent second order plate. Absolute values of the wave-lengths are reliable to within 0·01 A.U. and relative values to within much less than this. The band has been rigorously analysed using the method of least squares to evaluate coefficients. If the rotational energy function is $B\ (j-\varepsilon)^2 + D\ (j-\varepsilon)^4$, the constants for the initial and final electronic states of the molecule have been found to be : $B' = 0\cdot2897595$; $D' = +0\cdot00011226$; $\varepsilon' = +0\cdot5497296$; $B'' = 0\cdot2903813$; $D'' = +0\cdot00008990$; $\varepsilon'' = +0\cdot5070601$. From these we find for the moments of inertia $I' = 95\cdot622\ 10^{-40}$ grm.-cm.^{2}, and $I'' = 95\cdot418\ 10^{-40}$ grm.-cms.^{2}. Now if we assume that the emitting molecule is $Si^{28}\ F$ we find for the inter-nuclear distances $r'_0 = 2\cdot263\ 10^{-8}$ cms. and $r_0'' = 2\cdot260\ 10^{-8}$ cm., values which are too large for a molecule of this kind with but 23 electrons. AlO and SiN, each with 21 electrons, have values in the normal state of 1·62 A.U. and 1·55 A.U. respectively. For I_2 with its 106 electrons we have an inter-nuclear distance of but 2·66 A.U. Assuming that the emitting molecule is $FSi^{28} - Si^{28}\ F$, and that it is capable of rotating like a symmetrical dipole of nuclear masses 47, we then find for the inter-nuclear distances : $r'_0 = 1\cdot571$ A.U. and $r_0'' = 1\cdot569$ A.U. This is of the anticipated order of size. Although of a different type, the AgH molecule with its 48 electrons has a value for r_0'' of 1·63 A.U. in the normal state. The derived values of r_0' and r_0'' here represent the distances between the centres of gravity of the two SiF nuclei constituting the molecule. No other assumption as to the nature of the molecule gives so reasonable a value for the size. Furthermore, the absence of Q branches lends support to the highly symmetrical character of the emitter, and, in addition, an "even" type molecule such as FSi—SiF is in harmony with the odd multiplicity of the electronic levels. One feature calls for special notice, viz., that the coefficients D′ and D″ are definitely positive, while according to the theoretical relation, $\omega_n = \sqrt{-4B^3/D}$ the coefficient D should be essentially negative if the molecule is capable of vibration. We know from equation (1)

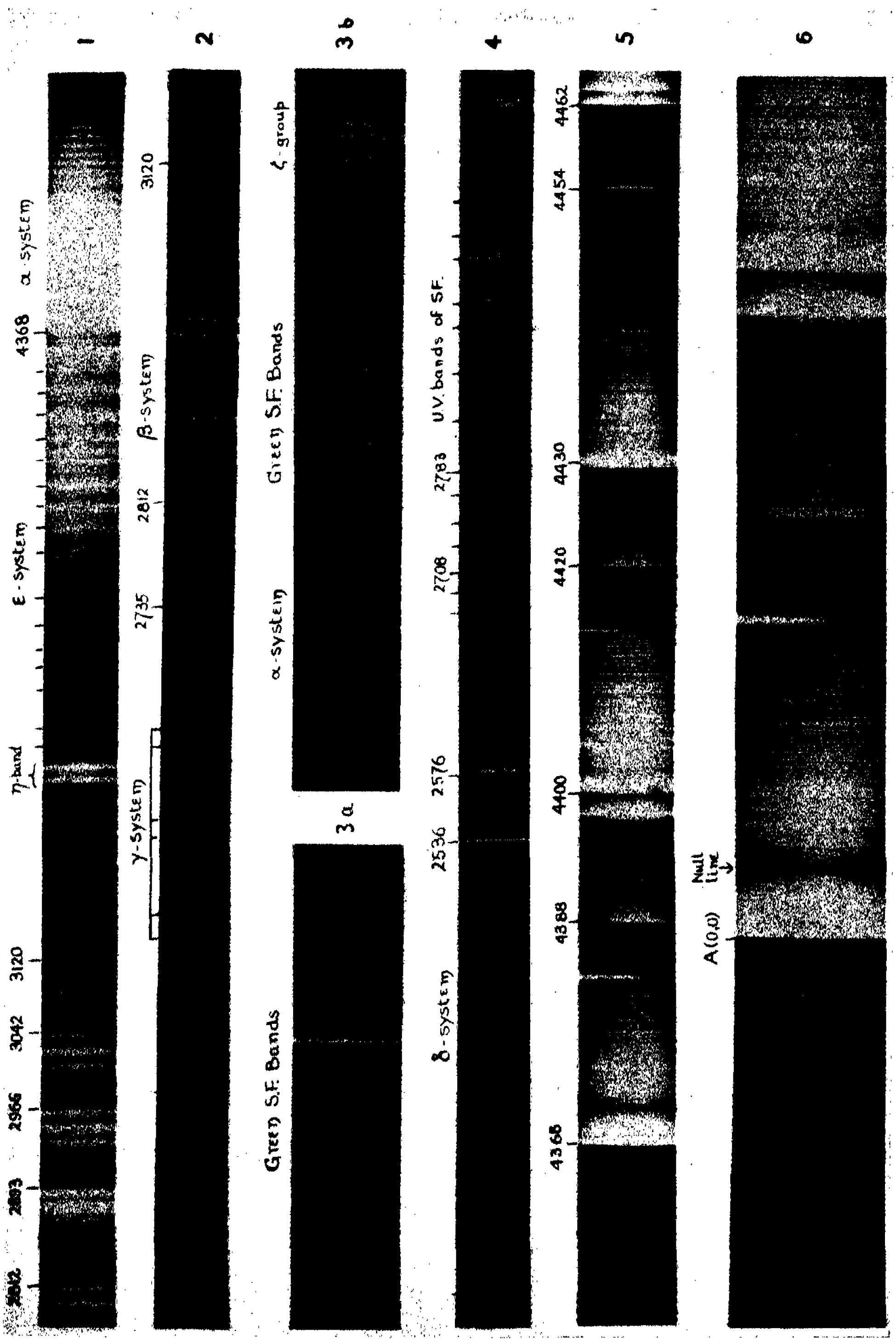
1
2
3 b
3 a
4
5
6
α-system
4368
ε-System
η-band
3120
3042
2966
2883
2802
3120
β-System
2812
2735
γ-System
ζ-group
Green S.F. Bands
α-system
Green S.F. Bands
U.V. bands of S.F.
2783
2708
2576
2536
δ-system
4462
4454
4430
4420
4400
4388
4368
Null line
A(0,0)

(*Facing p.* 348.)

Table IX.—Fine Structure of the Band at λ 4368.

Int.	λ (I.A.).	ν (Vacuo).	Series.
head	4368·213	22886·25	
5	69·186	81·15	R (26)
5	69·263	80·75	R (25)
5	69·330	80·40	R (24)
8	69·410	79·98	R (23)
5	69·491	79·55	R (22)
6	69·567	79·15	R (21)
7	69·650	78·72	R (20)
7	69·735	78·28	R (19)
7	69·822	77·82	R (18)
7	69·909	77·36	R (17)
7	69·995	76·91	R (16)
7	70·080	76·47	R (15)
7	70·175	75·97	R (14)
7	70·264	75·505	R (13)
7	70·358	75·02	R (12)
7	70·454	74·51	R (11)
7	70·549	74·01	R (10)
6	70·651	73·48	R (9)
6	70·747	72·98	R (8)
6	70·851	72·43	R (7)
5	70·951	71·91	R (6)
4	71·051	71·39	R (5)
3	71·162	70·805	R (4)
2	71·261	70·29	R (3)
1	71·372	69·71	R (2)
0	71·475	69·17	R (1)
—	—	—	N
0	71·691	68·04	P (2)
1	71·812	67·41	P (3)
2	71·916	66·86	P (4)
3	72·032	66·255	P (5)
4	72·150	65·64	P (6)
5	72·268	65·02	P (7)
6	72·384	64·41	P (8)
6	72·505	63·78	P (9)
6	72·625	63·15	P (10)
6	72·743	62·54	P (11)
7	72·861	61·92	P (12)
7	72·989	61·25	P (13)
7	73·112	60·61	P (14)
7	73·238	59·95	P (15)
7	73·365	59·285	P (16)
7	73·494	58·61	P (17)
7	73·626	57·92	P (18)
7	73·759	57·225	P (19)
8	73·892	56·53	P (20)
8	74·027	55·825	P (21)
8	74·161	55·125	P (22)
8	74·285	54·48	P (23)
8	74·439	53·67	P (24)
9	74·581	52·93	P (25)
10	74·723	52·19	P (26)
9	74·869	51·43	P (27)
9*d*	75·022	50·60	P (28)
9	75·167	49·87	P (29)

d = diffuse.

Table IX—continued.

Int.	λ (I.A.).	ν (Vacuo).	Series.
9	4375·317	22849·09	P (30)
9	75·470	48·29	P (31)
9	75·623	47·49	P (32)
9	75·781	46·62	P (33)
9	75·942	45·83	P (34)
10	76·103	44·985	P (35)
8	76·269	44·12	P (36)
10	76·442	43·22	P (37)
8	76·609	42·34	P (38)
10	76·781	41·45	P (39)
8	76·955	40·44	P (40)
1	77·090	39·835	P (41)
10	77·138	39·58	
1	77·268	38·905	P (42)
8	77·310	38·685	
1	77·460	37·90	P (43)
10	77·497	37·71	
1	77·631	37·01	P (44)
7	77·682	36·75	
2	77·825	36·00	P (45)
9	77·864	35·795	
1	78·013	35·02	P (46)
6	78·066	34·74	
7*s*	78·198	34·05	P (47)
7	78·263	33·72	
0	78·415	32·92	P (48)
6	78·466	32·66	
6	78·666	31·61	P (49)
1*c*	78·830	30·76	P (50)
9*d*	78·896	30·41	
0	79·017	29·78	P (51)
5	79·085	29·43	
9	79·281	28·41	P (52)
1	79·451	27·52	P (53)
5	79·517	27·18	
5	79·739	26·02	P (54)
0*d*	79·911	25·12	P (55)
8	79·988	24·72	
0	80·136	23·95	P (56)
4	80·176	23·74	
6	80·437	22·38	P (57)
4*c*	80·683	21·10	P (58)
0	80·866	20·15	P (59)
4	80·927	19·83	
3	81·177	18·53	P (60)
c	—	—	P (61)
0	81·621	16·215	P (62)
3	81·702	15·79	
4	81·965	14·425	P (63)
c	—	—	P (64)
2	82·525	11·51	P (65)
0	82·725	10·47	P (66)
2	82·807	10·04	
1	83·097	08·53	P (67)

c = confused. *d* = diffuse. *s* = superposed.

that the values of ω_0' and ω_0'' are 790·5 and 860·5. We believe that this unusual feature is related to the perturbations of the $n' = 0$ and $n'' = 0$ vibrational levels already referred to.

Using the extensive data of the P branch up to P (60) we have found a least squares formula for the lines of this branch :

$$\nu = 22869 \cdot 153 - 0 \cdot 56650 j - 0 \cdot 0030917 j^2 + 0 \cdot 0_5 3643 j^3 - 0 \cdot 0_6 48441 j^4.$$

Substituting $j = 1$ we find the origin is at ν22868·58. The value of m_{H} is 91.

The Rotational Isotope Effect.—From Table IX it will be seen that beyond about P (41) a faint component appears on the more refrangible side of, and resolved from the main line. The satellite is of small intensity and its separation increases as we travel out from the origin. These features suggest an isotope effect. We have examined this quantitatively but found that agreement with the expected value is poor, a feature which we attribute to the faintness of the component and its proximity to the very strong main line.

We should like, in conclusion, to express our thanks to Mr. Barratt of University College, London, for the opportunity of checking some of our data on his calculating machine. We also tender sincere thanks to Prof. J. J. Nolan, of Dublin, for the loan to one of us of the concave grating which has been invaluable in this work.

The Vibrations of an Infinite System of Vortex Rings.

By Prof. H. Levy, M.A., D.Sc., and A. G. Forsdyke, A.R.C.Sc., B.Sc.

(Communicated by S. Chapman, F.R.S.—Received March 17, 1927.)

§ 1. The vibrations that may be set up and maintained in the central filament of a single vortex ring of small but finite section have been investigated by Thomson[*] and others, but no corresponding investigation appears to have been undertaken for a system of parallel rings, although the matter is of some importance in connection with the state of motion behind a moving body. In a previous paper[†] the authors have examined the stability of an infinite system of equal vortex rings situated in parallel planes with their centres evenly spaced along an infinite line and with their planes at right angles to that line. Instability was there found to occur for disturbances confined to displacements of the centre of each ring along the central axis, the filament of each ring still remaining circular. In the present paper the investigation is extended to deformation of the vortex filaments, and some interesting conclusions are drawn regarding natural modes of vibration of the infinite system of vortex rings, such as may occur without the longitudinal instability referred to in the previous paper becoming apparent.

It is found, for example, that for any given ratio of radius of ring section to radius of ring there exists a critical ratio of ring spacing to radius, separating the region of stable oscillation from that of instability, a result in some respects closely analogous to that found by Kármán for the stability of two infinite parallel rows of rectilinear vortices.[‡]

§ 2. The deformations of the filaments will be taken to be of the first order of small quantities compared to the radius of the rings, and the latter will be assumed to perform such oscillations as will give rise to no change in the position of the centre of mass, to the same order. The analysis then resolves itself into an investigation of the conditions in which the presumed oscillations will persist unchanged.

---

[*] J. J. Thomson, 'Motion of Vortex Rings'; Pocklington, 'Phil. Trans.,' A, vol. 186, p. 603 (1895); Carslaw, 'Proc. Lond. Math. Soc.,' vol. 28, p. 97 (1897).

[†] 'Roy. Soc. Proc.,' A, vol. 768, p. 594 (1927).

[‡] 'Phys. Z.,' vol. 13, p. 49 (1912); 'Gött. Nachr.,' p. 547 (1912).

The notation employed throughout this paper is as follows :—

κ = strength of each vortex.

b = radius of each vortex ring.

a = spacing interval of the centres of the vortex rings along the axis.

(x, y, z) rectangular co-ordinates of any point A on the central vortex ring, the origin being at the centre of this ring and the y-axis coincident with the axis of the system.

(x', y', z') co-ordinates of any point B on the nth ring of the system where by "the nth ring" is meant the vortex ring whose centre lies at a distance na from the origin, along the y-axis.

ϵ = radius of cross section of each vortex filament.

δ_n, β_n = axial and radial displacements respectively at the point (x', y', z') on the nth ring, δ_0 β_0 denoting the corresponding displacements on the central ring.

θ, ϕ denote the measure of azimuth round the circumference of the central and nth rings respectively.

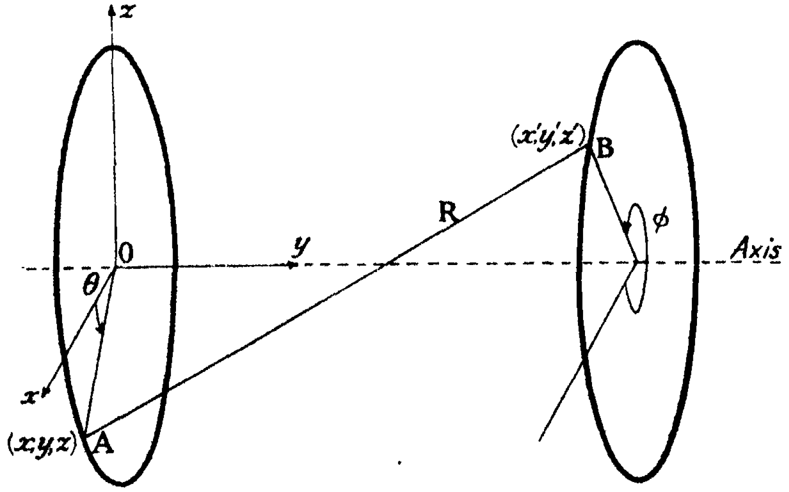

FIG. 1.

We consider displacements which do not involve changes in the position of the centre of gravity of any vortex ring, and, for this purpose, assume

$$\delta_n = \gamma_n \cos r\phi, \tag{1}$$

$$\beta_n = \alpha_n \cos r\phi, \tag{2}$$

where α_n, γ_n are small functions of the time. The number r, which characterises the displacement may take certain positive integral values. The limitations imposed upon r will be discussed later in the paper. At present, however, we notice that the case $r = 0$ has been discussed in a previous paper. Further, the case $r = 1$ is excluded from the present investigation for the radial displacement given by (2) when $r = 1$ results in a displacement of the centre of the ring, of amount α_n along the radius vector $\phi = 0$, the circular form of the ring remaining unchanged to the first order of small quantities. For positive integral values of r other than unity it can be easily proved that the displacements assumed are such that the centre of gravity of each vortex ring remains stationary, so that displacements characterised by these values of r are of the type to be considered. Such displacements take the form of stationary waves on the circumference of each vortex ring.

§ 3. The equations of motion of the system are found to involve functions whose properties cannot be determined without considerable numerical calculation. For this purpose it is necessary to use Zonal Toroidal Harmonic functions, and as no tables of these are available they and their first and second derivatives, which are also required, were calculated for certain sets of values of the variables. The method of calculation is described and the functions tabulated separately at the end of this paper.

The investigation may be conveniently divided into two parts, since the velocity at any point of a vortex ring of the system is due in part to the self-influence of that ring, the other part of the velocity arising from the effect of the remaining rings of the system. The former has been investigated by J. J. Thomson in the paper to which reference has been made in § 1. The equations of motion there determined involve the radius of cross section of the vortex filament, assumed circular in form, this quantity being involved in the form $\log b/\epsilon$. Provided the ratio ϵ/b is small the shape of the cross section of the vortex filament will remain approximately circular, except when two vortex rings approach one another so closely that the shortest distance between them is of the same order as the radius of cross section of either.[*] This possibility will be excluded in virtue of the fact that the ratio a/b, as will be proved, must exceed a certain value, great in comparison with ϵ/b, in order that vibrations of the system may be possible. It will be convenient to fix an upper limit to the ratio ϵ/b; we shall here assume the value 0·1. For larger values the error involved in the approximations would be too great to be neglected. This definite maximum value allows exact calculations of the quantities arising in the equations of motion to be made, for it will be seen that if vibrations are possible with a certain spacing ratio and the maximum value of ϵ/b, then they are certainly possible for all smaller values of ϵ/b and the same ratio of spacing.

---

[*] Lamb's 'Hydrodynamics,' 5th edition, p. 213.

In investigating the effect, upon any vortex ring, of the remaining vortices of the system we may consider the filament to be concentrated in its central line and, without appreciable error, neglect the fact that it has a definite cross section. The equations of motion will be derived to a degree of approximation involving the displacements α_n, β_n, to the first order. They are then linear, so that the effects of the separate rings may be superposed.

It is found that for a particular kind of displacement characterised by r, the functions arising in the equations of motion are multiplied by terms linear in r. It is therefore questionable whether the accuracy of our approximation will suffice for large values of r. This can only be decided by an examination of the second order terms in the velocity components—an investigation which would involve considerable labour and must be left for future treatment. Large values of r will therefore here be excluded; for a reason which will appear the discussion is restricted to values of r equal to 2, 3, 4, 5, 6, for which our degree of approximation suffices.

§ 4. At the point A on the central vortex ring the effect of the nth ring is to produce velocity components u, v, w. We neglect for the present the self-influence of the central ring. Then

$$u = \frac{\kappa}{4\pi}\int_0^{2\pi}\left\{\frac{dz'}{d\phi}(y-y') - \frac{dy'}{d\phi}(z-z')\right\}\frac{d\phi}{\mathrm{R}^3}, \tag{3}$$

where R denotes the length of AB.

Now

$$\left.\begin{aligned}(x-x') &= (b+\beta_0)\cos\theta - (b+\beta_n)\cos\phi\\ (y-y') &= \delta_0 - na - \delta_n\\ (z-z') &= (b+\beta_0)\sin\theta - (b+\beta_n)\sin\phi\end{aligned}\right\}, \tag{4}$$

and

$$\left.\begin{aligned}\frac{dx'}{d\phi} &= \frac{d\beta_n}{d\phi}\cos\phi - (b+\beta_n)\sin\phi\\ \frac{dy'}{d\phi} &= \frac{d\delta_n}{d\phi}\\ \frac{dz'}{d\phi} &= \frac{d\beta_n}{d\phi}\sin\phi + (b+\beta_n)\cos\phi\end{aligned}\right\}. \tag{5}$$

The expression

$$\frac{dz'}{d\phi}(y-y') - \frac{dy'}{d\phi}(z-z')$$

therefore becomes

$$\begin{aligned}
&\left\{\frac{d\beta_n}{d\phi}\sin\phi + (b+\beta_n)\cos\phi\right\}\{\delta_0 - na - \delta_n\} \\
&\qquad\qquad - \frac{d\delta_n}{d\phi}\{(b+\beta_0)\sin\theta - (b+\beta_n)\sin\phi\} \\
&= -nab\cos\phi + b\frac{d\delta_n}{d\phi}(\sin\phi - \sin\theta) - na\frac{d\beta_n}{d\phi}\sin\phi \\
&\quad - na\beta_n\cos\phi + b\cos\phi\,(\delta_0 - \delta_n) \quad \text{correct to the first order} \\
&= -nab\cos\phi + \tfrac{1}{2}b\gamma_n\{(r-1)\cos(r+1)\phi - (r+1)\cos(r-1)\phi\} \\
&\quad + rb\gamma_n\sin r\phi\sin\theta + \tfrac{1}{2}na\alpha_n\{(r-1)\cos(r-1)\phi \\
&\qquad\qquad - (r+1)\cos(r+1)\phi\} + b\gamma_0\cos\phi\cos r\theta. \qquad (6)
\end{aligned}$$

Similarly

$$v = \frac{\kappa}{4\pi}\int_0^{2\pi}\left\{\frac{dx'}{d\phi}(z-z') - \frac{dz'}{d\phi}(x-x')\right\}\frac{d\phi}{\mathrm{R}^3}$$

$$\begin{aligned}
&\left\{\frac{dx'}{d\phi}(z-z') - \frac{dz'}{d\phi}(x-x')\right\} \\
&= \left\{\frac{d\beta_n}{d\phi}\cos\phi - (b+\beta_n)\sin\phi\right\}\{(b+\beta_0)\sin\theta - (b+\beta_n)\sin\phi\} \\
&\quad - \left\{\frac{d\beta_n}{d\phi}\sin\phi + (b+\beta_n)\cos\phi\right\}\{(b+\beta_0)\cos\theta - (b+\beta_n)\cos\phi\} \\
&= b^2 - b^2\cos\phi\cos\theta - b^2\sin\phi\sin\theta \\
&\qquad\qquad - b\alpha_0(\cos\phi\cos\theta\cos r\theta + \sin\phi\sin\theta\cos r\theta) \\
&\quad - \tfrac{1}{2}b\alpha_n\sin\theta\{(r+1)\sin(r+1)\phi + (r-1)\sin(r-1)\phi\} + 2b\alpha_n\cos r\phi \\
&\quad + \tfrac{1}{2}b\alpha_n\cos\theta\{(r-1)\cos(r-1)\phi - (r+1)\cos(r+1)\phi\}. \qquad (7)
\end{aligned}$$

Finally

$$w = \frac{\kappa}{4\pi}\int_0^{2\pi}\left\{\frac{dy'}{d\phi}(x-x') - \frac{dx'}{d\phi}(y-y')\right\}\frac{d\phi}{\mathrm{R}^3}$$

$$\begin{aligned}
&\left\{\frac{dy'}{d\phi}(x-x') - \frac{dx'}{d\phi}(y-y')\right\} \\
&= \frac{d\delta_n}{d\phi}\{(b+\beta_0)\cos\theta - (b+\beta_n)\cos\phi\} \\
&\qquad\qquad - \left\{\frac{d\beta_n}{d\phi}\cos\phi - (b+\beta_n)\sin\phi\right\}\{\delta_0 - na - \delta_n\} \\
&= -nab\sin\phi - \tfrac{1}{2}na\alpha_n\{(r+1)\sin(r+1)\phi + (r-1)\sin(r-1)\phi\} \\
&\quad - rb\gamma_n\cos\theta\sin r\phi + \tfrac{1}{2}b\gamma_n\{(r+1)\sin(r-1)\phi + (r-1)\sin(r+1)\phi\} \\
&\qquad\qquad + b\gamma_0\cos r\theta\sin\phi. \qquad (8)
\end{aligned}$$

To simplify the integrations involved in the expressions for u, v, w the function R^{-3} will be expanded in a series of the form $\sum_{m=0}^{\infty} C_m \cos m(\phi - \theta)$, where the coefficients C_m have now to be determined. Let A_m be the value of C_m when the displacements δ_0, β_0, δ_n and β_n are all zero. When this is the case let $(b \cos \theta, \zeta, b \sin \theta)$ denote the co-ordinates of the point A and $(c \cos \phi, \eta, c \sin \phi)$ the co-ordinates of B, where $b = c$ and $(\zeta - \eta) = na$. During a small displacement the quantities b, c, ζ, η undergo small independent changes db, etc. Therefore,

$$C_m = A_m + \frac{\partial A_m}{\partial b} \,.\, db + \frac{\partial A_m}{\partial c} dc + \frac{\partial A_m}{\partial \zeta} d\zeta + \frac{\partial A_m}{\partial \eta} \,.\, d\eta.$$

But
$$db = \alpha_0 \cos r\theta, \qquad dc = \alpha_n \cos r\phi,$$
$$d\zeta = \gamma_0 \cos r\theta, \qquad d\eta = \gamma_n \cos r\phi.$$

Therefore

$$C_m = A_m + \alpha_0 \cos r\theta \frac{\partial A_m}{\partial b} + \alpha_n \cos r\phi \frac{\partial A_m}{\partial c} + \gamma_0 \cos r\theta \frac{\partial A_m}{\partial \zeta} + \gamma_n \cos r\phi \frac{\partial A_m}{\partial \eta}, \tag{9}$$

where after differentiation c is put equal to b and $(\eta - \zeta) = na$. To find A_m we have, in the undisplaced position,

$$\begin{aligned} R^2 &= (c \cos \phi - b \cos \theta)^2 + (\eta - \zeta)^2 + (c \sin \phi - b \sin \theta)^2 \\ &= \{(\eta - \zeta)^2 + b^2 + c^2 - 2bc \cos(\phi - \theta)\}. \end{aligned}$$

Therefore
$$R^{-3} = (2bc)^{-3/2}\{q - \cos(\phi - \theta)\}^{-3/2},$$

where
$$q = \frac{(\eta - \zeta)^2 + b^2 + c^2}{2bc}. \tag{10}$$

Now
$$R^{-3} = \sum_{m=0}^{\infty} A_m \,.\, \cos m(\phi - \theta).$$

Therefore
$$\pi A_m = \frac{1}{(2bc)^{3/2}} \int_0^{2\pi} \frac{\cos m\psi \,.\, d\psi}{(q - \cos\psi)^{3/2}}, \tag{11}$$

$$2\pi A_0 = \frac{1}{(2bc)^{3/2}} \int_0^{2\pi} \frac{d\psi}{(q - \cos\psi)^{3/2}}. \tag{12}$$

Write
$$\pi A_m = \frac{1}{(2bc)^{3/2}} \chi_m.$$

Then
$$\begin{aligned} \pi \frac{\partial A_m}{\partial b} &= \frac{\chi_m}{2\sqrt{2}} \frac{\partial}{\partial b} \frac{1}{(bc)^{3/2}} + \frac{1}{(2bc)^{3/2}} \frac{\partial \chi_m}{\partial b} \\ &= -\frac{3}{2\sqrt{2}} \frac{\chi_m}{b^4} + \frac{1}{2\sqrt{2}} \frac{\partial \chi_m}{\partial q} \,.\, \frac{\partial q}{\partial b}, \end{aligned}$$

and
$$\pi \frac{\partial A_m}{\partial \eta} = \frac{1}{2\sqrt{2}b^3} \frac{\partial \chi_m}{\partial q} \,.\, \frac{\partial q}{\partial \eta}.$$

Now
$$\frac{\partial q}{\partial b} = \frac{2bc \,.\, 2b - n^2a^2(2b) - 2b(b^2 + c^2)}{4b^4}$$

$$= -\frac{n^2a^2}{2b^3} = \frac{\partial q}{\partial c}. \tag{13}$$

$$\frac{\partial q}{\partial \eta} = \frac{na}{b^2} = \frac{\partial q}{\partial \zeta}. \tag{14}$$

Now if Q_m denotes the Zonal Toroidal Harmonic* of the second kind and of order m,

$$Q_m = \frac{1}{\sqrt{2}} \int_0^\pi \frac{\cos m\psi \,.\, d\psi}{(q - \cos\psi)^{\frac{1}{2}}}.$$

Therefore

$$\frac{dQ_m}{dq} = -\frac{1}{2\sqrt{2}} \int_0^\pi \frac{\cos m\psi \,.\, d\psi}{(q - \cos\psi)^{3/2}}.$$

It follows that $\chi_m = -4\sqrt{2}\,\dfrac{dQm}{dq}$, and, therefore, that

$$A_m = -\frac{2}{\pi b^3}\frac{dQ_m}{dq}, \tag{15}$$

$$\frac{dA_m}{dc} = \frac{\partial A_m}{\partial b} = \frac{3}{\pi b^4}\frac{dQ_m}{dq} + \frac{n^2a^2}{\pi b^6}\frac{d^2Q_m}{dq^2}, \tag{16}$$

$$\frac{\partial A_m}{\partial \eta} = -\frac{\partial A_m}{\partial \zeta} = -\frac{2na}{\pi b^5}\frac{d^2Q_m}{dq^2}. \tag{17}$$

Moreover, since

$$2Q_0 = \frac{1}{\sqrt{2}} \int_0^\pi \frac{d\psi}{(q - \cos\psi)^{\frac{1}{2}}}$$

it follows from (12) that (15) (16) and (17) are true when $m = 0$.

§ 5. To obtain u, v, w the expressions (6) (7) (8), respectively, must be multiplied by $\sum_m C_m \cos m(\phi - \theta)$, and the products integrated from 0 to 2π. It is convenient to divide this process into three parts (a) involving finite terms from both C_m and (6) (7) (8); (b) involving first order terms from C_m and (c) involving first order terms from (6) (7) (8). The formula

$$\begin{aligned} \int_0^{2\pi} \cos m\psi \cos n\psi \, d\psi &= 0 \qquad n \neq m \\ &= \pi \qquad n = m, \text{ is used.} \end{aligned}$$

In the expression for u the finite terms are given by

$$\frac{\kappa}{4\pi}\sum_m \int_0^{2\pi} \{-nab\cos\phi \,.\, A_m(\cos m\phi\cos m\theta + \sin m\phi \sin m\theta)\} \,.\, d\phi$$
$$= -\tfrac{1}{4}\kappa \,.\, nabA_1 \cos\theta.$$

---

* Bassett, 'Hydrodynamics,' § 277.

First order terms from (6)

$$\frac{\kappa}{4\pi}\sum_m\int_0^{2\pi}[\tfrac{1}{2}b\gamma_n\{(r-1)\cos(r+1)\phi-(r+1)\cos(r-1)\phi\}$$
$$+\,rb\gamma_n\sin r\phi\sin\theta+b\gamma_0\cos\phi\cos r\theta$$
$$+\,\tfrac{1}{2}na\alpha_n\{(r-1)\cos(r-1)\phi-(r+1)\cos(r+1)\phi\}]\,\mathrm{A}_m$$
$$\times\,(\cos m\phi\cos m\theta+\sin m\phi\sin m\theta)\,.\,d\phi$$
$$=\frac{\kappa}{4}[\tfrac{1}{2}b\gamma_n\{\mathrm{A}_{r+1}(r-1)\cos(r+1)\theta-\mathrm{A}_{r-1}(r+1)\cos(r-1)\theta\}$$
$$+\,rb\gamma_n\mathrm{A}_r\sin r\theta\sin\theta+b\gamma_0\mathrm{A}_1\cos r\theta\cos\theta$$
$$+\,\tfrac{1}{2}na\,\alpha_n\{(r-1)\,\mathrm{A}_{r-1}\cos(r-1)\,\theta-(r+1)\,\mathrm{A}_{r+1}\cos(r+1)\,\theta\}].$$

First order terms from C_m

$$\frac{\kappa}{4\pi}\sum_m\int_0^{2\pi}\Big[-nab\cos\phi\,.\,(\cos m\phi\cos m\theta+\sin m\phi\sin m\theta)$$
$$\times\left(\alpha_0\cos r\theta\,\frac{\partial\mathrm{A}_m}{\partial b}+\alpha_n\cos r\phi\,\frac{\partial\mathrm{A}_m}{\partial c}+\gamma_0\cos r\theta\,\frac{\partial\mathrm{A}_m}{\partial\xi}+\gamma_n\cos r\phi\,\frac{\partial\mathrm{A}_m}{\partial\eta}\right)\Big]\,d\phi$$
$$=-\frac{\kappa}{4}\Big[nab\cos\theta\left(\alpha_0\cos r\theta\,\frac{\partial\mathrm{A}_1}{\partial b}+\gamma_0\cos r\theta\,\frac{\partial\mathrm{A}_1}{\partial\zeta}\right)$$
$$+\,\tfrac{1}{2}nab\left\{\alpha_n\cos(r+1)\,\theta\,\frac{\partial\mathrm{A}_{r+1}}{\partial c}+\gamma_n\cos(r+1)\,\theta\,\frac{\partial\mathrm{A}_{r+1}}{\partial\eta}\right\}$$
$$+\,\tfrac{1}{2}nab\left\{\alpha_n\cos(r-1)\,\theta\,\frac{\partial\mathrm{A}_{r-1}}{\partial c}+\gamma_n\cos(r-1)\,\theta\,\frac{\partial\mathrm{A}_{r-1}}{\partial\eta}\right\}\Big].$$

Collecting terms we obtain

$$u=\frac{\kappa}{4}\Big[-nab\,\mathrm{A}_1\cos\theta+\tfrac{1}{2}na\alpha_n\{(r-1)\,\mathrm{A}_{r-1}\cos(r-1)\,\theta$$
$$-(r+1)\,\mathrm{A}_{r+1}\cos(r+1)\,\theta\}$$
$$+\,b\gamma_0\mathrm{A}_1\cos r\theta\cos\theta+\tfrac{1}{2}b\gamma_n\{(r-1)\,\mathrm{A}_{r+1}\cos(r+1)\,\theta$$
$$-(r+1)\,\mathrm{A}_{r-1}\cos(r-1)\,\theta\}$$
$$+\,rb\gamma_n\mathrm{A}_r\sin r\theta\sin\theta-nab\cos\theta\left(\alpha_0\,\frac{\partial\mathrm{A}_1}{\partial b}+\gamma_0\,\frac{\partial\mathrm{A}_1}{\partial\zeta}\right)\cos r\theta$$
$$-\,\tfrac{1}{2}nab\left\{\alpha_n\,\frac{\partial\mathrm{A}_{r+1}}{\partial c}+\gamma_n\,\frac{\partial\mathrm{A}_{r+1}}{\partial\eta}\right\}\cos(r+1)\,\theta$$
$$-\,\tfrac{1}{2}nab\left\{\alpha_n\,\frac{\partial\mathrm{A}_{r-1}}{\partial c}+\gamma_n\,\frac{\partial\mathrm{A}_{r-1}}{\partial\eta}\right\}\cos(r-1)\,\theta\Big].\qquad(18)$$

Similarly in the expression for v we have

$$\frac{\kappa}{4\pi}\sum_m \int^{2\pi} [(b^2 - b^2 \cos\phi \cos\theta - b^2 \sin\phi \sin\theta) \\ \times \mathrm{A}_m (\cos m\phi \cos m\theta + \sin m\phi \sin m\theta)]\, d\phi$$

$$= \frac{\kappa}{4}[2b^2\mathrm{A}_0 - b^2\mathrm{A}_1 (\cos^2\theta + \sin^2\theta)],$$

$$\frac{\kappa}{4\pi}\sum_m \int_0^{\pi} [-\tfrac{1}{2}b\alpha_n \sin\theta \{(r+1)\sin(r+1)\phi + (r-1)\sin(r-1)\phi\} + 2b\alpha_n \cos r\phi \\ + \tfrac{1}{2}b\alpha_n \cos\theta \{(r-1)\cos(r-1)\phi - (r+1)\cos(r+1)\phi\} \\ - b\alpha_0 \{\cos\phi\cos\theta\cos r\theta + \sin\phi\sin\theta\cos r\theta\}] \\ \times \mathrm{A}_m (\cos m\phi \cos m\theta + \sin m\phi \sin m\theta)\, d\phi.$$

$$= \frac{\kappa}{4}[-\tfrac{1}{2}b\alpha_n \sin\theta \{(r+1)\mathrm{A}_{r+1}\sin(r+1)\theta + (r-1)\mathrm{A}_{r-1}\sin(r-1)\theta\} \\ + \tfrac{1}{2}b\alpha_n \cos\theta\{(r-1)\mathrm{A}_{r-1}\cos(r-1)\theta - (r+1)\mathrm{A}_{r+1}\cos(r+1)\theta\} \\ + 2b\mathrm{A}_r\alpha_0 \cos r\theta - b\alpha_0 (\cos^2\theta + \sin^2\theta)\cos r\theta \,.\, \mathrm{A}_1],$$

$$\frac{\kappa}{4\pi}\sum_m \int_0^{2\pi} \Big[(b^2 - b^2\cos\phi\cos\theta - b^2\sin\phi\sin\theta)\ (\cos m\phi\cos m\theta + \sin m\phi \sin m\theta) \\ \times\left(\alpha_0 \cos r\theta \frac{\partial \mathrm{A}_m}{\partial b} + \alpha_n \cos r\phi \frac{\partial \mathrm{A}_m}{\partial c} + \gamma_0 \cos r\theta \frac{\partial \mathrm{A}_m}{\partial \zeta} + \gamma_n \cos r\phi \frac{\partial \mathrm{A}_m}{\partial \eta}\right)\Big] d\phi$$

$$= b^2 \cos r\theta \left(\alpha_n \frac{\partial \mathrm{A}_r}{\partial c} + \gamma_n \frac{\partial \mathrm{A}_r}{\partial \eta}\right) \\ - b^2\cos^2\theta\left(\alpha_0 \cos r\theta \frac{\partial \mathrm{A}_1}{\partial b} + \gamma_0 \cos r\theta \frac{\partial \mathrm{A}_1}{\partial \zeta}\right) \\ - b^2\sin^2\theta\left(\alpha_0 \cos r\theta \frac{\partial \mathrm{A}_1}{\partial b} + \gamma_0 \cos r\theta \frac{\partial \mathrm{A}_1}{\partial \zeta}\right) \\ - \tfrac{1}{2}b^2\cos\theta\cos(r+1)\theta\left\{\alpha_n \frac{\partial \mathrm{A}_{r+1}}{\partial c} + \gamma_n \frac{\partial \mathrm{A}_{r+1}}{\partial \eta}\right\} \\ - \tfrac{1}{2}b^2\cos^2\theta\cos(r-1)\theta\left\{\alpha_n \frac{\partial \mathrm{A}_{r-1}}{\partial c} + \gamma_n \frac{\partial \mathrm{A}_{r-1}}{\partial \eta}\right\} \\ - \tfrac{1}{2}b^2\sin\theta\sin(r+1)\theta\left\{\alpha_n \frac{\partial \mathrm{A}_{r+1}}{\partial c} + \gamma_n \frac{\partial \mathrm{A}_{r+1}}{\partial \eta}\right\} \\ + \tfrac{1}{2}b^2\sin\theta\sin(r-1)\theta\left\{\alpha_n \frac{\partial \mathrm{A}_{r-1}}{\partial c} + \gamma_n \frac{\partial \mathrm{A}_{r-1}}{\partial \eta}\right\}.$$

Therefore

$$
\begin{aligned}
v = \frac{\kappa}{4}\Big[& 2b^2\mathrm{A}_0 - b^2\mathrm{A}_1 - \tfrac{1}{2}b\alpha_n(r+1)\,\mathrm{A}_{r+1}\cos r\theta + \tfrac{1}{2}b\alpha_n(r-1)\,\mathrm{A}_{r-1}\cos r\theta \\
& - \mathrm{A}_1 b\alpha_0\cos r\theta + 2b\mathrm{A}_r\alpha_n\cos r\theta + b^2\cos r\theta\left(\alpha_n\frac{\partial\mathrm{A}_r}{\partial c} + \gamma_n\frac{\partial\mathrm{A}_r}{\partial\eta}\right) \\
& - b^2\cos r\theta\left(\alpha_0\frac{\partial\mathrm{A}_1}{\partial b} + \gamma_0\frac{\partial\mathrm{A}_1}{\partial\zeta}\right) - \tfrac{1}{2}b^2\cos r\theta\left(\alpha_n\frac{\partial\mathrm{A}_{r+1}}{\partial c} + \gamma_n\frac{\partial\mathrm{A}_{r+1}}{\partial\eta}\right) \\
& - \tfrac{1}{2}b^2\cos r\theta\left(\alpha_n\frac{\partial\mathrm{A}_{r-1}}{\partial c} + \gamma_n\frac{\partial\mathrm{A}_{r-1}}{\partial\eta}\right)\Big]. \qquad (19)
\end{aligned}
$$

Finally, considering the expressions for w,

$$
\begin{aligned}
& \frac{\kappa}{4\pi}\sum_m\int_0^{2\pi} - nab\sin\phi\,.\,\mathrm{A}_m(\cos m\phi\cos m\theta + \sin m\phi\sin m\theta)\,d\phi \\
& \qquad = -\frac{\kappa}{4}\,.\,nab\mathrm{A}_1\sin\theta,
\end{aligned}
$$

$$
\begin{aligned}
& \frac{\kappa}{4\pi}\sum_m\int_0^{2\pi}[-\tfrac{1}{2}na\alpha_n\{(r+1)\sin(r+1)\phi + (r-1)\sin(r-1)\phi\} - rb\gamma_n\cos\theta\sin r\phi \\
& \qquad + \tfrac{1}{2}b\gamma_n\{(r+1)\sin(r-1)\phi + (r-1)\sin(r+1)\phi\} \\
& \qquad + b\gamma_0\cos r\theta\sin\phi]\,\mathrm{A}_m\,.\,(\cos m\phi\cos m\theta + \sin m\phi\sin m\theta)\,d\phi \\
& \quad = \frac{\kappa}{4}[-\tfrac{1}{2}na\alpha_n\{(r+1)\,\mathrm{A}_{r+1}\sin(r+1)\theta + (r-1)\,\mathrm{A}_{r-1}\sin(r-1)\theta\} \\
& \qquad + b\gamma_0\cos r\theta\sin\theta\,\mathrm{A}_1 - rb\gamma_n\mathrm{A}_r\cos\theta\sin r\theta \\
& \qquad + \tfrac{1}{2}b\gamma_n\{(r+1)\,\mathrm{A}_{r-1}\sin(r-1)\theta + (r-1)\,\mathrm{A}_{r+1}\sin(r+1)\theta\}],
\end{aligned}
$$

$$
\begin{aligned}
& \frac{\kappa}{4\pi}\sum_m\int_0^{2\pi}\Big[-nab\sin\phi(\cos m\phi\cos m\theta + \sin m\phi\sin m\theta) \\
& \quad \left(\alpha_0\cos r\theta\frac{\partial\mathrm{A}_m}{\partial b} + \gamma_0\cos r\theta\frac{\partial\mathrm{A}_m}{\partial\zeta} + \alpha_n\cos r\phi\frac{\partial\mathrm{A}_m}{\partial c} + \gamma_n\cos r\phi\frac{\partial\mathrm{A}_m}{\partial\eta}\right)\Big]d\phi \\
& \quad = -\frac{\kappa}{4}\Big[nab\sin\theta\cos r\theta\left(\alpha_0\frac{\partial\mathrm{A}_1}{\partial b} + \gamma_0\frac{\partial\mathrm{A}_1}{\partial\zeta}\right) \\
& \qquad + \tfrac{1}{2}nab\sin(r+1)\theta\left(\alpha_n\frac{\partial\mathrm{A}_{r+1}}{\partial c} + \gamma_n\frac{\partial\mathrm{A}_{r+1}}{\partial\eta}\right) \\
& \qquad - \tfrac{1}{2}nab\sin(r-1)\theta\left(\alpha_n\frac{\partial\mathrm{A}_{r-1}}{\partial c} + \gamma_n\frac{\partial\mathrm{A}_{r-1}}{\partial\eta}\right)\Big],
\end{aligned}
$$

giving

$$\begin{aligned} w = \frac{\kappa}{4}\Big[& - nab\,A_1 \sin\theta - \tfrac{1}{2} na\alpha_n \{(r+1)\,A_{r+1} \sin(r+1)\,\theta \\ & \qquad\qquad + (r-1)\,A_{r-1} \sin(r-1)\,\theta\} \\ & + b\gamma_0 \cos r\theta \sin\theta A_1 - rb\gamma_n \cos\theta \sin r\theta\, A_r \\ & - \tfrac{1}{2} nab \sin(r-1)\,\theta \left(\alpha_n \frac{\partial A_{r-1}}{\partial c} + \gamma_n \frac{\partial A_{r-1}}{\partial \eta}\right) \\ & - nab \sin\theta \cos r\theta \left(\alpha_0 \frac{\partial A_1}{\partial b} + \gamma_0 \frac{\partial A_1}{\partial \zeta}\right) \\ & - \tfrac{1}{2} nab \sin(r+1)\,\theta \left(\alpha_n \frac{\partial A_{r+1}}{\partial c} + \gamma_n \frac{\partial A_{r+1}}{\partial \eta}\right) \\ & + \tfrac{1}{2} b\gamma_n \{(r+1)\,A_{r-1} \sin(r-1)\,\theta + (r-1)\,A_{r+1} \sin(r+1)\,\theta\}\Big]. \quad (20) \end{aligned}$$

The velocity v is that produced in the direction of the axis at the point " θ " on the central vortex ring, due to the action of the nth ring of the system. If the corresponding radial velocity be denoted by μ then

$$\begin{aligned} \mu &= u \cos\theta + w \sin\theta \\ &= \frac{\kappa}{4}\Big[- nab\,A_1 + \tfrac{1}{2} na\alpha_n \{(r-1)\,A_{r-1} \cos r\theta - (r+1)\,A_{r+1} \cos r\theta\} \\ & \qquad\qquad\qquad\qquad + b\gamma_0 A_1 \cos r\theta \\ & \quad - \tfrac{1}{2} b\gamma_n \{(r+1)\,A_{r-1} \cos r\theta - (r-1)\,A_{r+1} \cos r\theta\} \\ & \quad - \tfrac{1}{2} nab \cos r\theta \left(\alpha_n \frac{\partial A_{r-1}}{\partial c} + \gamma_n \frac{\partial A_{r-1}}{\partial \eta}\right) \\ & \quad - nab \cos r\theta \left(\alpha_0 \frac{\partial A_1}{\partial b} + \gamma_0 \frac{\partial A_1}{\partial \zeta}\right) \\ & \quad - \tfrac{1}{2} nab \cos r\theta \left(\alpha_n \frac{\partial A_{r+1}}{\partial c} + \gamma_n \frac{\partial A_{r+1}}{\partial \eta}\right)\Big]. \quad (21) \end{aligned}$$

If U_1', V_1' denote the radial and axial velocities produced on the central ring by the remaining rings of the system they will be obtained by the summation of expressions (19) (21) for all values of n excluding zero. To indicate the way in which n is involved in the expressions to be summed let μ_n, v_n denote the radial and axial velocities produced by the nth vortex ring at a point on the central ring, and let $A_m^{(n)}$ denote the corresponding value of A_m, while

$$q_n \equiv \frac{n^2 a^2}{2b^2} + 1.$$

Thus

$$A_m^{(n)} = \frac{1}{2\sqrt{2}\pi b^3}\int_0^{2\pi} \frac{\cos m\psi \,.\, d\psi}{(q_n - \cos\psi)^{3/2}}. \tag{22}$$

Then,

$$U_1' = \sum_{n=-\infty}^{\infty}{}' \mu_n \quad\text{and}\quad V_1' = \sum_{n=-\infty}^{\infty}{}' v_n, \tag{23}$$

where the symbol Σ' indicates that the value $n = 0$ is to be excluded from the summation.

The terms in U_1', V_1', which are independent of the small displacements of the system, must be omitted from a consideration of the motion which arises as a result of these displacements. They are, in fact, the corresponding velocities which are produced on the central vortex ring when the system is in the neutral position. The term in question in U_1' is

$$\frac{\kappa}{4}\sum_{n=-\infty}^{\infty}{}' \{-nab\,A_1^{(n)}\},$$

which vanishes, for $A_1^{(n)}$ contains only even powers of n. The term in V_1' is

$$\begin{aligned}&\frac{\kappa}{4}\sum_{n=-\infty}^{\infty}{}' \{2b^2A_0^{(n)} - b^2A_1^{(n)}\}\\ &= \frac{\kappa}{4}\sum_{n=-\infty}^{\infty}{}' \left\{\frac{1}{2\sqrt{2}b^3}\int_0^{2\pi}\frac{(1-\cos\psi)\,d\psi}{(q_n - \cos\psi)^{3/2}}\right\}\\ &= \frac{\kappa b^2}{4}\sum_{n=-\infty}^{\infty}{}' \left\{\int_0^{2\pi}\frac{(1-\cos\psi)\,d\psi}{\{2b^2(1-\cos\psi)+n^2a^2\}^{3/2}}\right\},\end{aligned}$$

which, in a previous paper has been shown to be that part of the velocity of advance of the central ring along the axis, due to the other vortex rings. Then, if U′, V′ denote the parts of U_1', V_1' which arise solely owing to the small displacements to which the system is subjected,

$$\begin{aligned}U' = \frac{\kappa}{4}\sum_{n=-\infty}^{\infty}{}' \Big[&\tfrac{1}{2}na\,\alpha_n\{(r-1)\,A_{r-1}^{(n)} - (r+1)\,A_{r+1}^{(n)}\} + b\gamma_0 A_1^{(n)}\\ &- \tfrac{1}{2}b\gamma_n\{(r+1)\,A_{r-1}^{(n)} - (r-1)\,A_{r+1}^{(n)}\} - nab\left\{\alpha_0\frac{\partial A_1^{(n)}}{\partial b} + \gamma_0\frac{\partial A_1^{(n)}}{\partial \zeta}\right\}\\ &- \tfrac{1}{2}nab\left\{\alpha_n\frac{\partial A_{r+1}^{(n)}}{\partial c} + \gamma_n\frac{\partial A_{r+1}^{(n)}}{\partial \eta}\right\}\\ &- \tfrac{1}{2}nab\left\{\alpha_n\frac{\partial A_{r-1}^{(n)}}{\partial c} + \gamma_n\frac{\partial A_{r-1}^{(n)}}{\partial \eta}\right\}\Big]\cos r\theta.\end{aligned} \tag{24}$$

$$\mathrm{V}' = \frac{\kappa}{4} \sum_{n=-\infty}^{\infty}{}' \Big[-\mathrm{A}_1 b\alpha_0 + \tfrac{1}{2} b\alpha_n \{(r-1)\,\mathrm{A}^{(n)}_{r-1} - (r+1)\,\mathrm{A}^{(n)}_{r+1}\} + 2b\mathrm{A}_r^{(n)}\alpha_n$$
$$- \tfrac{1}{2} b^2 \left\{ \alpha_n \frac{\partial \mathrm{A}^{(n)}_{r+1}}{\partial c} + \gamma_n \frac{\partial \mathrm{A}^{(n)}_{r+1}}{\partial \eta} \right\} - \tfrac{1}{2} b^2 \left\{ \alpha_n \frac{\partial \mathrm{A}^{(n)}_{r-1}}{\partial c} + \gamma_n \frac{\partial \mathrm{A}^{(n)}_{r-1}}{\partial \eta} \right\}$$
$$+ b^2 \left\{ \alpha_n \frac{\partial \mathrm{A}_r^{(n)}}{\partial c} + \gamma_n \frac{\partial \mathrm{A}_r^{(n)}}{\partial \eta} \right\} - b^2 \left\{ \alpha_0 \frac{\partial \mathrm{A}_1{}^{(n)}}{\partial b} + \gamma_0 \frac{\partial \mathrm{A}_1{}^{(n)}}{\partial \zeta} \right\} \Big] \cos r\theta. \tag{25}$$

§ 6. Two equations of this type will hold for each vortex ring of the system, ultimately leading to a set of equations of motion infinite in number. A normal mode of displacement is clearly given by

$$\alpha_n = (-1)^n \alpha_0, \quad \gamma_n = (-1)^n \gamma_0, \tag{26}$$

for then the displacements of every ring are related in the same way to the displacements of the remaining vortices of the system. The infinite set of equations of the form (24), (25) reduces to two equations only which are applicable to any particular vortex of the system.

The relations (15), (16), (17) show that $\frac{\partial \mathrm{A}_m^{(n)}}{\partial \eta}$ and $\frac{\partial \mathrm{A}_m^{(n)}}{\partial \zeta}$ are odd functions of n, while $\mathrm{A}_m^{(n)}$, $\frac{\partial \mathrm{A}_m^{(n)}}{\partial b}$, $\frac{\partial \mathrm{A}_m^{(n)}}{\partial c}$ are even functions. These, in conjunction with (26) enable us to reduce (24) and (25) to

$$\mathrm{U}' = \frac{\kappa b}{2} \gamma_0 \sum_{n=1}^{\infty} \Big[\mathrm{A}_1{}^{(n)} - \tfrac{1}{2}(-1)^n \{(r+1)\,\mathrm{A}^{(n)}_{r-1} - (r-1)\,\mathrm{A}^{(n)}_{r+1}\} - na \frac{\partial \mathrm{A}_1{}^{(n)}}{\partial \zeta}$$
$$- \tfrac{1}{2} na\,(-1)^n \frac{\partial \mathrm{A}^{(n)}_{r+1}}{\partial \eta} - \tfrac{1}{2} na\,(-1)^n \frac{\partial \mathrm{A}^{(n)}_{r-1}}{\partial \eta} \Big] \cos r\theta, \tag{27}$$

$$\mathrm{V}' = \frac{\kappa b}{2} \alpha_0 \sum_{n=1}^{\infty} \Big[-\mathrm{A}_1{}^{(n)} - \tfrac{1}{2}(-1)^n \{(r+1)\,\mathrm{A}^{(n)}_{r+1} - (r-1)\,\mathrm{A}^{(n)}_{r-1}\}$$
$$+ 2(-1)^n \mathrm{A}_r^{(n)} + b(-1)^n \frac{\partial \mathrm{A}^{(n)}}{\partial c} - b \frac{\partial \mathrm{A}_1{}^{(n)}}{\partial b}$$
$$- \tfrac{1}{2} b\,(-1)^n \frac{\partial \mathrm{A}^{(n)}_{r+1}}{\partial c} - \tfrac{1}{2} b\,(-1)^n \frac{\partial \mathrm{A}^{(n)}_{r-1}}{\partial c} \Big] \cos r\theta. \tag{28}$$

Let

$$\mathrm{H}^{(n)} = \mathrm{A}_1{}^{(n)} - na \frac{\partial \mathrm{A}_1{}^{(n)}}{\partial \zeta},$$

$$\mathrm{H}_r{}^{(n)} = -\tfrac{1}{2} \{(r+1)\,\mathrm{A}^{(n)}_{r-1} - (r-1)\,\mathrm{A}^{(n)}_{r+1}\} - \tfrac{1}{2} na \frac{\partial \mathrm{A}^{(n)}_{r+1}}{\partial \eta} - \tfrac{1}{2} na \frac{\partial \mathrm{A}^{(n)}_{r-1}}{\partial \eta},$$

$$\mathrm{G}^{(n)} = -\mathrm{A}_1{}^{(n)} - b \frac{\partial \mathrm{A}_1{}^{(n)}}{\partial b},$$

$$\mathrm{G}_r{}^{(n)} = -\tfrac{1}{2} \{(r+1)\,\mathrm{A}^{(n)}_{r+1} - (r-1)\,\mathrm{A}^{(n)}_{r-1}\} + 2\mathrm{A}_r^{(n)}$$
$$+ b \frac{\partial \mathrm{A}_r^{(n)}}{\partial c} - \tfrac{1}{2} b \frac{\partial \mathrm{A}^{(n)}_{r+1}}{\partial c} - \tfrac{1}{2} b \frac{\partial \mathrm{A}^{(n)}_{r-1}}{\partial c}.$$

Then,

$$U' = \frac{\kappa b}{2}\gamma_0 \cos r\theta \sum_{n=1}^{\infty} \{H^{(n)} + (-1)^n H_r^{(n)}\}, \tag{29}$$

$$V' = \frac{\kappa b}{2}\alpha_0 \cos r\theta \sum_{n=1}^{\infty} \{G^{(n)} + (-1)^n G_r^{(n)}\}. \tag{30}$$

So far we have neglected the effect of each ring upon itself. If U'', V'' are the velocities produced by this cause for a displacement of the type here contemplated, J. J. Thomson finds

$$U'' = -r^2 L_r \gamma_0 \cos r\theta, \tag{31}$$

$$V'' = (r^2 - 1) L_r \alpha_0 \cos r\theta, \tag{32}$$

where

$$L_r = \frac{\kappa}{2}\left\{\log\frac{8b}{\varepsilon} - 2f(r) - \tfrac{1}{2}\right\}\Big/ 2\pi b^2,$$

and $f(r)$ is equal to $1 + \frac{1}{3} + \frac{1}{5} + \ldots + \frac{1}{2r-1}$. Write $L_r = \frac{\kappa b}{2} M_r$, so that

$$M_r = \frac{1}{2\pi b^3}\left\{\log\frac{8b}{\varepsilon} - 2f(r) - \tfrac{1}{2}\right\}.$$

If now we put $U = U' + U''$ and $V = V' - V''$ we shall have

$$U = \dot{\alpha}_0 \cos r\theta,$$

$$V = \dot{\gamma}_0 \cos r\theta,$$

and the equations of motion of the system of vortex rings are therefore,

$$\dot{\alpha}_0 \cos r\theta = \frac{\kappa b}{2}\gamma_0 \left[-r^2 M_r + \sum_{n=1}^{\infty} \{H^{(n)} + (-1)^n H_r^{(n)}\}\right] \cos r\theta,$$

$$\dot{\gamma}_0 \cos r\theta = \frac{\kappa b}{2}\alpha_0 \left[(r^2 - 1) M_r + \sum_{n=1}^{\infty} \{G^{(n)} + (-1)^n G_r^{(n)}\}\right] \cos r\theta.$$

The appearance of the factor $\cos r\theta$ in each term of these equations shows that the type of displacement contemplated is a permanent one provided the amplitude remains small. This is true even if no relation of the form (26) exists between the amplitudes of the wave displacements of a given period, since the factor $\cos r\theta$ appears throughout in equations (24), (25), where the amplitudes are all arbitrary.

At this stage, owing to the complicated and widely differing natures of the functions M, G, H, it becomes necessary to resort to numerical calculation. Accordingly we proceed to express $H^{(n)}$, $G^{(n)}$, $H_r^{(n)}$ $G_r^{(n)}$ in terms of Toroidal Functions and their derivatives by means of equations (15), (16), (17)

$$\begin{aligned} \mathrm{H}^{(n)} &= \frac{1}{\pi b^3} h^{(n)} \text{ (say)} \\ &= \mathrm{A}_1^{(n)} - na \frac{\partial \mathrm{A}_1^{(n)}}{\partial \zeta} \\ &= \frac{1}{\pi b^3} \left\{ -2 \frac{d\mathrm{Q}_1}{dq_n} - 4 (q_n - 1) \frac{d^2\mathrm{Q}_1}{dq_n^2} \right\}, \end{aligned} \tag{33}$$

$$\begin{aligned} \mathrm{G}^{(n)} &= \frac{1}{\pi b^3} g^{(n)} \\ &= \frac{2}{\pi b^3} \frac{d\mathrm{Q}_1}{dq_n} - \frac{3}{\pi b^3} \frac{d\mathrm{Q}_1}{dq_n} - \frac{n^2 a^2}{\pi b^5} \frac{d^2\mathrm{Q}_1}{dq_n^2} \\ &= \frac{1}{2} \cdot \frac{1}{\pi b^3} h^{(n)}, \end{aligned} \tag{34}$$

$$\begin{aligned} \mathrm{H}_r^{(n)} &= \frac{1}{\pi b^3} h_r^{(n)} \\ &= \frac{1}{\pi b^3} \left\{ (r+1) \frac{d\mathrm{Q}_{r-1}}{dq_n} - (r-1) \frac{d\mathrm{Q}_{r+1}}{dq_n} \right\} + \frac{n^2 a^2}{\pi b^5} \frac{d^2\mathrm{Q}_{r+1}}{dq_n^2} + \frac{n^2 a^2}{\pi b^5} \frac{d^2\mathrm{Q}_{r-1}}{dq_n^2} \\ &= \frac{1}{\pi b^3} \left\{ (r+1) \frac{d\mathrm{Q}_{r-1}}{dq_n} - (r-1) \frac{d\mathrm{Q}_{r+1}}{dq_n} \right\} + 2 (q_n - 1) \left\{ \frac{d^2\mathrm{Q}_{r+1}}{dq_n^2} + \frac{d^2\mathrm{Q}_{r-1}}{dq_n^2} \right\}, \end{aligned} \tag{35}$$

$$\begin{aligned} \mathrm{G}_r^{(n)} &= \frac{1}{\pi b^3} g_r^{(n)} \\ &= \frac{1}{\pi b^3} \left\{ (r+1) \frac{d\mathrm{Q}_{r+1}}{dq_n} - (r-1) \frac{d\mathrm{Q}_{r+1}}{dq_n} \right\} - \frac{4}{\pi b^3} \frac{d\mathrm{Q}_r}{dq_n} + \frac{3}{\pi b^3} \frac{d\mathrm{Q}_r}{dq_n} \\ &\quad + \frac{n^2 a^2}{\pi b^5} \frac{d^2\mathrm{Q}_r}{dq_n^2} - \frac{3}{2} \cdot \frac{1}{\pi b^3} \left\{ \frac{d\mathrm{Q}_{r+1}}{dq_n} + \frac{d\mathrm{Q}_{r-1}}{dq_n} \right\} - \tfrac{1}{2} \frac{n^2 a^2}{\pi b^5} \left\{ \frac{d^2\mathrm{Q}_{r-1}}{dq_n^2} + \frac{d^2\mathrm{Q}_{r+1}}{dq_n^2} \right\} \\ &= \frac{1}{\pi b^3} \left\{ (r - \tfrac{1}{2}) \frac{d\mathrm{Q}_{r+1}}{dq_n} - (r + \tfrac{1}{2}) \frac{d\mathrm{Q}_{r-1}}{dq_n} - \frac{d\mathrm{Q}_r}{dq_n} \right. \\ &\qquad \left. + 2 (q_n - 1) \left(\frac{d^2\mathrm{Q}_r}{dq_n^2} - \tfrac{1}{2} \frac{d^2\mathrm{Q}_{r+1}}{dq_n^2} - \tfrac{1}{2} \frac{d^2\mathrm{Q}_{r-1}}{dq_n^2} \right) \right\}. \end{aligned} \tag{36}$$

Further, let $\mathrm{M}_r = \frac{1}{\pi b^3} m_r$. The equations of motion now take the form

$$\frac{2}{\kappa} \pi b^2 \dot{\alpha}_0 = \left[-r^2 m_r + 2 \sum_{n=1}^{\infty} \{ h^{(n)} + (-1)^n h_r^{(n)} \} \right] \gamma_0, \tag{37}$$

$$\frac{2}{\kappa} \pi b^2 \dot{\gamma}_0 = \left[(r^2 - 1) m_r + 2 \sum_{n=1}^{\infty} \{ g^{(n)} + (-1)^n g_r^{(n)} \} \right] \alpha_0. \tag{38}$$

We consider in detail the first case $r = 2$. The radial increment experienced by the nth vortex ring is $\alpha_n \cos 2\phi$. This alone would cause the vortex ring to assume an approximately elliptical shape, with its major axis in the direction of the radius vector $\phi = 0$. Owing, however, to the axial displacement $\gamma_n \cos 2\phi$ the ellipse becomes twisted out of its plane, the form assumed being saddle-shaped. Since $\alpha_n = (-1)^n \alpha_0$ and $\gamma_n = (-1)^n \gamma_0$, the major axes of the figures formed by successive vortices will lie in mutually perpendicular directions. The appearance of the system will be of the form indicated in fig. 2, where, however, the displacements are much exaggerated in magnitude.

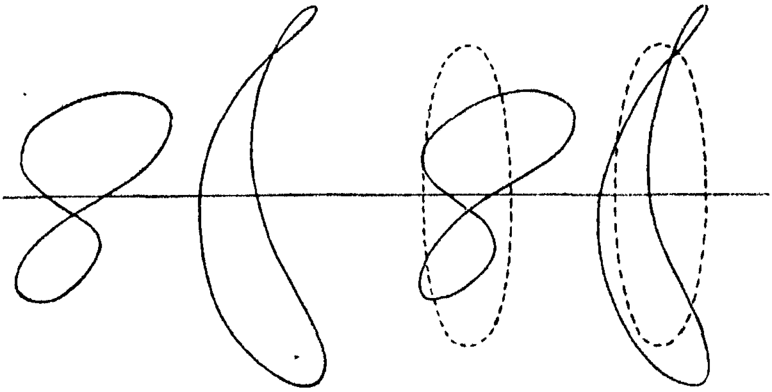

Fig. 2.

From the tables of Toroidal Functions we can calculate the values of $h^{(n)}$, $g^{(n)}$, $h_2^{(n)}$, $g_2^{(n)}$ for various values of q_n. Let λ denote the quantity

$$\sqrt{2}\sqrt{q_n - 1} = \frac{na}{b}.$$

The following table shows the results of these calculations :—

Table I.

q_n	1·030	1·062	1·144	1·265	1·435	1·981	3·000	5·079
λ	0·246	0·353	0·536	0·728	0·933	1·408	2·000	2·856
$h^{(n)}$	−34·4	−17·04	−7·534	−4·068	−2·428	−0·918	−0·328	−0·095
$h_2^{(n)}$	27·5	11·85	3·98	0·989	0·688	0·193	0·061	0·018
$g^{(n)}$	−17·2	−8·52	−3·77	−2·034	−1·214	−0·459	−0·164	−0·048
$g_2^{(n)}$	35·2	17·05	7·05	3·69	1·75	0·462	0·106	0·018
$\log_{10} g$	1·237	0·931	0·577	0·304	0·085	$\bar{1}$·664	$\bar{1}$·215	$\bar{2}$·678
$\log_{10} g_2^{(n)}$	1·546	1·231	0·848	0·567	0·243	$\bar{1}$·664	$\bar{1}$·027	$\bar{2}$·255

Consider first the quantities $h_r^{(n)}$ and $h^{(n)}$, and in particular the sums of these quantities as they occur in the equations of motion. They depend upon the spacing ratio a/b which we will denote by λ_1, the particular value assumed by λ when $n = 1$. Then $\sum_{n=1}^{\infty} h^{(n)}$ will be formed by the addition of the values of $h^{(n)}$ corresponding to $\lambda = \lambda_1, 2\lambda_1, 3\lambda_1, \ldots$. The series thus obtained will converge rapidly since $h^{(n)}$ ultimately behaves like $1/n^3$. Therefore, for purposes of calculation it will only be necessary to take a few terms of the series. Moreover, the sign of the sum of the series will be determined by the sign of the first few terms.

When λ_1 is greater than the maximum value of λ given in the table (2·85) it is clear that those terms in the equations of motion which involve $g^{(n)}$ and similar quantities are negligible compared with the terms in m_r. The equations of motion are then approximately the same as those for a single isolated vortex ring, so that the system will perform oscillations about its mean configuration, each ring vibrating as it would do in the normal mode characterised by $r = 2$, were it remote from other vortices.

It is therefore necessary to consider only those values of $\lambda < 2\cdot85$. $\sum_{n=1}^{\infty} h^{(n)}$ is then clearly negative.

Again, $\sum_{n=1}^{\infty} (-1)^n h_2^{(n)}$ is an alternating series whose terms steadily diminish in absolute value. The sum of this series will be of the same sign as the first term of the series, *i.e.*, negative. Finally we see that m_2 is positive for all admissible values of b/ε. For if b/ε takes its minimum value 10 (which we may denote by b/ε'), $\log 8b/\varepsilon' = 4\cdot35$, so that $m_r = 4\cdot35 - f(2) - \frac{1}{2} = 1\cdot18$. Since $b/\varepsilon \geqslant 10$, $m_r \geqslant 1\cdot18$ and therefore necessarily positive. It follows that the coefficient of γ_0 in (37) is negative. Vibrations will, therefore, be maintained in the normal mode characterised by $r = 2$ if the coefficient of α_0 in (38) is positive. For the differential equations

$$\dot{x} = \mathrm{A}y,$$

$$\dot{y} = \mathrm{B}x,$$

lead to

$$\frac{d^2\chi}{dt^2} = \mathrm{AB}\chi, \qquad (39)$$

and the solution of (39) is periodic if AB is negative.

On reference to Table I we see that $\sum_{n=1}^{\infty} g^{(n)}$ and $\sum_{n=1} (-1)^n g_2^{(n)}$ are both negative. The system will therefore be capable of executing vibrations if $3m_2 > 2\left|\sum\limits_{n=1}^{\infty} g^{(n)} + \sum\limits_{n=1}^{\infty}(-1)^n g_2^{(n)}\right|$. For the minimum value of b/ε, $3/2\ m_2 = 1{\cdot}79$ so that the condition for small oscillations of the system is $\left|\sum\limits_{n=1}^{\infty} g^{(n)} + \sum\limits_{n=1}^{\infty}(-1)^n g_2^{(n)}\right| < 1{\cdot}79$. To evaluate this quantity the curves of $\log_{10} g^{(n)}$ and $\log_{10} g_2^{(n)}$ were plotted to the base λ. Series of ordinate readings were taken at $\lambda = \lambda_1,\ 2\lambda_1,\ 3\lambda_1 \ldots$ for various values of the spacing ratio λ_1, and the sums $\sum\limits_{n=1}^{\infty} g^{(n)}$ and $\sum\limits_{n=1}^{\infty}(-1)^n g_2^{(n)}$ formed by addition. Table II gives the results of these calculations where κ_2 denotes $\sum\limits_{n=1}^{\infty} g^{(n)} + \sum\limits_{n=1}^{\infty}(-1)^n g_2^{(n)}$.

Table II.

λ.	0·5	0·75	1·0	1·25	1·5	2·0	2·5	3·0
$\sum\limits_{n=1}^{\infty} g^{(n)}$	− 6·904	− 2·529	− 1·994	− 0·732	− 0·434	− 0·176	− 0·079	− 0·040
$\sum\limits_{n=1}^{\infty}(-1)^n g_2^{(n)}$	− 7·127	− 2·966	− 1·365	− 0·678	− 0·345	− 0·101	− 0·036	− 0·014
κ_2.	−14·031	− 5·495	− 3·39	− 1·410	− 0·779	− 0·277	− 0·115	− 0·054

κ_2 assumes the critical value 1·79 for a value of λ lying between 1·0 and 1·25. Let us denote this spacing ratio by ξ'. Then for the minimum ratio of radius of vortex ring to cross section of filament, b/ε', the system can maintain vibrations provided the ratio of spacing distance to radius is greater than ξ'. Now clearly, there will be a critical ratio of spacing ξ (say) for all values of b/ε. Since $b/\varepsilon \geqslant b/\varepsilon'$, it follows that $\xi \geqslant \xi'$. Thus oscillations about the mean position are possible in the normal mode characterised by $r = 2$, provided that $a/b \geqslant \xi'$, which we know to be less than 5/4.

The relation between the critical ratio of spacing, ξ, and the value of b/ε is exhibited in fig. 3 by two curves drawn to the same ordinate axis. The function $\frac{3}{2}m_2 = \frac{3}{2}\left\{\log\frac{8b}{\varepsilon} - 3\frac{1}{6}\right\}$ is plotted to the base b/ε over a range extending indefinitely upwards from the critical value 10. This is shown to the left of the figure. On the right κ_2 is plotted to the base a/b, the curve C being obtained. Then, the respective abscissæ corresponding to equal ordinates on the two curves give corresponding values of ϵ/b and ξ. Thus, to determine the value of ξ corresponding to the value of b/ϵ given by the point A, we draw the ordinate AB to the curve B, and project horizontally to cut the second curve in C. Dropping the perpendicular CD, D will give the required value of a/b by direct reading. The critical value, ξ' corresponding to the minimum value of b/ϵ, is found by this means to be 1·20.

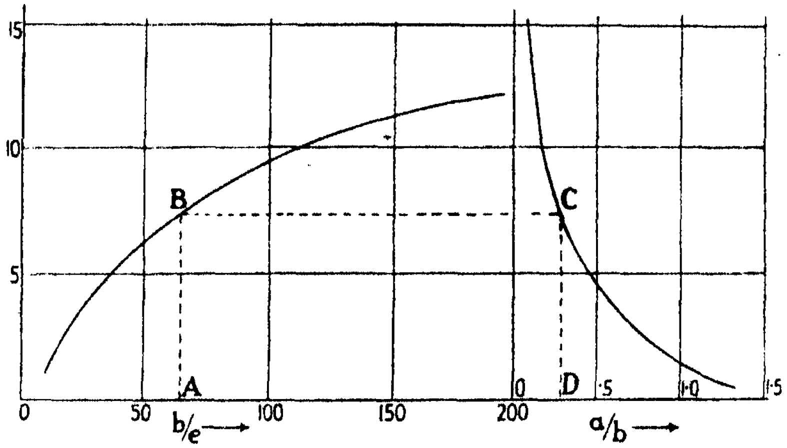

Fig. 3.

The curve C divides the plane into two parts. For values of a/b, b/ϵ corresponding to points lying in the region to the right of this curve, the system is capable of executing vibrations in the normal mode for which $r = 2$.

§ 7. By the use of certain properties of toroidal functions it is possible to determine whether the system is capable of maintaining vibrations for which $r = 3, 4, 5$ and 6. An alternative expression for the toroidal harmonic is

$$Q_m = \int_0^\infty \frac{d\theta}{(q + \sqrt{q^2 - 1}\cosh\theta)^{\frac{1}{2}(2m+1)}}.$$

Writing the continuous variable x in place of m let us regard

$$Q_x = \int_0^\infty \frac{d\theta}{(q + \sqrt{q^2 - 1}\cosh\theta)^{\frac{1}{2}(2x+1)}} \tag{40}$$

as a continuous function of x, which becomes identical with the toroidal function Q_m when x assumes the positive integral value m. We deduce the following properties of Q_x:

(*a*) Q_x is positive for all admissible values of q and x, *i.e.*, $x \geqslant 0$, $q \geqslant 1$.

(*b*) Q_x diminishes steadily to zero as q and x become great.

It follows that $\partial Q_x/\partial q$ and $\partial Q_x/\partial x$ are always negative. The equation

$$(q^2-1)\frac{d^2Q_x}{dq^2} = -2q\frac{dQ_x}{dq} + (x^2-\tfrac{1}{4})\,Q_x, \tag{41}$$

then shows that d^2Q_x/dq^2 is always positive. Therefore, dQ_x/dq increases steadily as q increases, and, being negative, it must tend to a limit $\leqslant 0$. The relation

$$\frac{dQ_x}{dq} = \frac{(2x-1)}{2\,(q^2-1)}\{qQ_x - Q_{x-1}\} \tag{42}$$

shows that this limit has the value zero.

Write the equations of motion in the form :—

$$\frac{2}{\kappa}\pi b^2\dot{\alpha}_0 = \{-r^2 m_r + 2\mathrm{J}_r\}\gamma_0, \tag{43}$$

$$\frac{2}{\kappa}\pi b^2\dot{\gamma}_0 = \{(r^2-1)\,m_r + 2\kappa_r\}\alpha_0, \tag{44}$$

where

$$\mathrm{J}_r = \sum_{n=1}^{\infty} h^{(n)} + \sum_{n=1}^{\infty}(-1)^n h_r^{(n)} \quad\text{and}\quad \kappa_r = \sum_{n=1}^{\infty} g^{(n)} + \sum_{n=1}^{\infty}(-1)^n g_r^{n}.$$

Consider only those values of r for which m_r is > 0. It is readily seen that this is true for $r = 3, 4, 5, 6$. The only term in (43) other than m_r, which depends upon r is $2\sum_{n=1}^{\infty}(-1)^n h_r^{(n)}$.

Now

$$h_r^{(n)} = (r+1)\frac{dQ_{r-1}}{dq_n} - (r-1)\frac{dQ_{r+1}}{dq_n} + 2\,(q_n-1)\left\{\frac{d^2Q_{r+1}}{dq_n^2} + \frac{d^2Q_{r-1}}{dq_n^2}\right\}.$$

We investigate the behaviour of this quantity as r increases, r being $\geqslant 2$. Consider

$$\begin{aligned}\mathrm{P}(x) &= x^2Q_x\\ &= \int_0^{\infty}\frac{x^2\,d\theta}{\mathrm{A}^{x+\frac{1}{2}}},\end{aligned}$$

where

$$\mathrm{A} = (q + \sqrt{q^2-1}\cosh\theta).$$

$$\frac{d\,.\,\mathrm{P}(x)}{dx} = \int_0^{\infty}\frac{\{2x - x^2\log\mathrm{A}\}\,d\theta}{\mathrm{A}^{x+\frac{1}{2}}}.$$

Now

$$\begin{aligned}2 - x\log\mathrm{A} &< 2 - x\log(q+\sqrt{q^2-1})\\ &< 2 - 2\log(q+\sqrt{q^2-1}) \quad\text{since}\quad x \geqslant 2\\ &< 0 \quad\text{if}\quad (q+\sqrt{q^2-1}) > e\\ &\textit{i.e.}\ \text{if}\quad q > \tfrac{1}{2}\left(e+\frac{1}{e}\right) = 1{\cdot}55.\end{aligned}$$

For $q = 1 \cdot 55$, $\sqrt{2(q-1)} = 1 \cdot 05$, which is less than the critical value which we have found to be $1 \cdot 20$. Hence for values of $x \geqslant 2$ and $a/b > 5/4$, $x^2 Q_x$ is a function which diminishes in value as x increases. (45)

Again, consider

$$\begin{aligned} \mathrm{R}(x) &= \frac{dQ_x}{dq} \\ &= \frac{d}{dq}\int_0^\infty \frac{d\theta}{\mathrm{A}^{x+\frac{1}{2}}} \\ &= -\int_0^\infty \frac{(x+\frac{1}{2})\dfrac{d\mathrm{A}}{dq} \, . \, d\theta}{\mathrm{A}^{x+3/2}} \, . \end{aligned}$$

Therefore,

$$\begin{aligned} \frac{d \, . \, \mathrm{R}(x)}{dx} &= -\int_0^\infty \frac{\left[\mathrm{A}^{x+3/2}\left\{\dfrac{d\mathrm{A}}{dq} - (x+\frac{1}{2})\dfrac{d\mathrm{A}}{dq}\log \mathrm{A}\right\}\right] d\theta}{\mathrm{A}^{2x+3}} \\ &= \int_0^\infty \frac{\dfrac{d\mathrm{A}}{dq}\{(x+\frac{1}{2})\log \mathrm{A} - 1\}\, d\theta}{\mathrm{A}^{x+3/2}} \, . \end{aligned} \qquad (46)$$

Now

$$\frac{d\mathrm{A}}{dq} = 1 + \frac{q}{\sqrt{q^2-1}} \cosh \theta > 0.$$

Therefore, $\dfrac{d\mathrm{R}(x)}{dx}$ is certainly positive if $x \geqslant 2$, $\log \mathrm{A} \geqslant 1$, from which it follows that $\dfrac{dQ_x}{dq}$ is an increasing function of x in the range considered; being negative, this function, therefore, diminishes in absolute value as x increases.

Again,

$$x\frac{dQ_x}{dq} = -\int_0^\infty \frac{(x^2+\frac{1}{2}x) \, . \, \dfrac{d\mathrm{A}}{dq} \, d\theta}{\mathrm{A}^{x+3/2}} \, ,$$

Therefore,

$$\begin{aligned} \frac{d}{dx}\left\{x \, . \, \frac{dQ_x}{dx}\right\} &= -\int_0^\infty \frac{\mathrm{A}^{x+3/2}\left\{(2x+\frac{1}{2})\dfrac{d\mathrm{A}}{dq} - (x^2+\frac{1}{2}x)\log \mathrm{A}\dfrac{d\mathrm{A}}{dq}\right\} d\theta}{\mathrm{A}^{2x+3}} \\ &= \int_0^\infty \frac{\dfrac{d\mathrm{A}}{dq}\{(x^2+\frac{1}{2}x)\log \mathrm{A} - 2x - \frac{1}{2}\}\, d\theta}{\mathrm{A}^{x+3/2}} \, , \end{aligned} \qquad (47)$$

and this is positive if $x \geqslant 2$, $\log \mathrm{A} \geqslant 1$.

Therefore, $x\dfrac{dQ_x}{dq}$ is negative and diminishes in absolute value as x increases. It follows from (41), (45), (46), that $(q^2-1)\dfrac{d^2Q_x}{dq^2}$, and, therefore, $\dfrac{d^2Q_x}{dq^2}$ is a positive decreasing function of x in the range we are considering.

Moreover, since

$$Q_m = \int_0^\pi \frac{\cos m\theta\,.\,d\theta}{(q-\cos\theta)^{1/2}},$$

$$(q-1)\frac{d^2Q_m}{dq^2} = \tfrac{3}{4}\int_0^\pi \frac{(q-1)\cos m\theta\,.\,d\theta}{(q-\cos\theta)^{5/2}}.$$

This function diminishes as q increases, behaving ultimately like $q^{-3/2}$.

Returning now to $h_r^{(n)}$ we see that all its terms diminish in absolute value as q_n increases, and also as r increases. $\sum\limits_{n=1}^{\infty}(-1)^n h_r^{(n)}$ may be written in the form

$$\sum_{n=1}^{\infty}(-1)^n(r+1)\frac{dQ_{r-1}}{dq_n}$$
$$+\sum_{n=1}(-1)^n\left[2(q_n-1)\left\{\frac{d^2Q_{r+1}}{dq_n^{\,2}}+\frac{d^2Q_{r-1}}{dq_n^{\,2}}\right\}-(r-1)\frac{dQ_{r+1}}{dq_n}\right].$$

The first of these series is one whose terms steadily diminish and whose first term is positive. Hence

$$\sum_{n=1}^{\infty}(-1)^n(r+1)\frac{dQ_{r-1}}{dq_n} \text{ is positive and } < -(r+1)\frac{dQ_{r-1}}{dq_1}$$

where the suffix 1 is used to indicate the first term of the series.

Similarly

$$\sum_{n=1}^{\infty}(-1)^n\left[2(q_n-1)\left\{\frac{d^2Q_{r+1}}{dq_n^{\,2}}+\frac{d^2Q_{r-1}}{dq_n^{\,2}}\right\}-(r-1)\frac{dQ_{r+1}}{dq_n}\right]$$

is negative.

Hence $\sum\limits_{n=1}^{\infty}h_r^{(n)}$ is $< -(r+1)\dfrac{dQ_{r-1}}{dq_1}$, and this by (47) is $\leqslant$ the corresponding term of the series obtained when $r=2$. This term is $-\dfrac{3dQ_1}{dq_1}$, which from the table of toroidal functions is seen to be $3\cdot996$ for $q=1\cdot265$, while the corresponding value of $h^{(n)}$ is $-4\cdot068$. Therefore, for this particular value of q, and for $r=2$, $\sum\limits_{n=1}^{\infty}h^{(n)}+\sum\limits_{n=1}^{\infty}(-1)^n h_r^{(n)}$ is negative. It follows that this quantity is always negative in the range of values of q_n and r considered.

Turning to the second equation of motion (44) we have to investigate the behaviour of

$$g_r^{(n)} = r\left\{\frac{dQ_{r+1}}{dq_n} - \frac{dQ_{r-1}}{dq_n}\right\} - \left\{\frac{dQ_r}{dq_n} + \tfrac{1}{2}\frac{dQ_{r-1}}{dq_n} + \tfrac{1}{2}\frac{dQ_{r+1}}{dq_n}\right\}$$
$$+ 2(q_n - 1)\left\{\frac{d^2Q_r}{dq_n^2} - \tfrac{1}{2}\frac{d^2Q_{r+1}}{dq_n^2} - \tfrac{1}{2}\frac{d^2Q_{r-1}}{dq_n^2}\right\}$$

as r increases.

Now

$$\frac{dQ_{r+1}}{dq_n} = \frac{2r+1}{2(q_n^2-1)}\{q_nQ_{r+1} - Q_r\}$$
$$\frac{dQ_{r-1}}{dq_n} = -\frac{(2r-1)}{2(q_n^2-1)}\{q_nQ_{r-1} - Q_r\}.$$

Therefore,

$$\left\{\frac{d^2Q_{r+1}}{dq_n} - \frac{d^2Q_{r-1}}{dq_n}\right\} = \frac{1}{2(q_n^2-1)}\{-4rQ_r + q_n\,.\,(2r+1)\,Q_{r+1} + q_n\,(2r-1)\,Q_{r-1}\}$$
$$= \frac{1}{2(q_n^2-1)}\{4r\,.\,(q_n^2-1)\,Q_r\},$$

since $4rq^2\,Q_r + q\,(2r+1)\,Q_{r+1} + 2\,(2r-1)\,Q_{r-1} = 0.$

Therefore $r\left\{\frac{dQ_{r+1}}{dq_n} - \frac{dQ_{r-1}}{dq_n}\right\} = 2r^2Q_r$, which by (45) is a positive decreasing function of r.

Also $-\left\{\frac{dQ_r}{dq_n} + \tfrac{1}{2}\frac{dQ_{r+1}}{dq_n} + \tfrac{1}{2}\frac{dQ_{r-1}}{dq_n}\right\}$ is a positive decreasing function of r.

Then, as regards these parts of $\sum\limits_{n=1}^{\infty}(-1)^n g_r^{(n)}$, *i.e.*

$$\sum_{n=1}^{\infty}(-1)^n\left[r\left\{\frac{dQ_{r+1}}{dq_n} - \frac{dQ_{r-1}}{dq_n}\right\} - \left(\frac{dQ_r}{dq_n} + \tfrac{1}{2}\frac{dQ_{r+1}}{dq_n} + \tfrac{1}{2}\frac{dQ_{r+1}}{dq_n}\right)\right]$$

we shall have a negative quantity whose absolute value diminishes as r increases.

There remains the quantity

$$\sum_{n=1}^{\infty}(-1)^n\left[2(q_n-1)\left\{\frac{d^2Q_x}{dq_n^2} - \tfrac{1}{2}\frac{d^2Q_{x-1}}{dq_n^2} - \tfrac{1}{2}\frac{d^2Q_{x+1}}{dq_n^2}\right\}\right] = \sum_{n=1}^{\infty}(-1)^n\,S_n(x)$$

say.

Now $\frac{d^2Q_x}{dq_n^2}$ is positive. If we can show that $\frac{d}{dx}\left\{\frac{d^2Q_x}{dq^2}\right\}$ is negative, and that the curve $y = \frac{d^2Q_x}{dq_n^2}$ (plotted to the base x) is convex to the x axis, which requires that $\frac{d^2}{dx^2}\left\{\frac{d^2Q_x}{dq_n^2}\right\}$ is negative, it will follow that

$$2(q_n-1)\left\{\frac{d^2Q_x}{dq_n^2} - \tfrac{1}{2}\frac{d^2Q_{x+1}}{dq_n^2} - \tfrac{1}{2}\frac{d^2Q_{x-1}}{dq_n^2}\right\} = S_n(x)$$

is negative and diminishing in absolute value as x increases. $\sum_{n=1}^{\infty} S_n(x)$ will then be a positive decreasing function of x.

Now from (48) it follows that $\frac{d}{dx}\left\{\frac{d^2 Q_x}{dq^2}\right\}$ is negative.

From (46)

$$\frac{d^2}{dx^2}\left\{\frac{dQ_x}{dq}\right\} = \int_0^\infty \frac{\left[A^{x+3/2}\frac{dA}{dq}\log A - \frac{dA}{dq}\{(x+\frac{1}{2})\log A - 1\}A^{x+3/2}\log A\right]d\theta}{A^{2x+3}}$$

$$= \int_0^\infty \frac{\frac{dA}{dq}\log A\{2 - (x+\frac{1}{2})\log A\}\,d\theta}{A^{x+3/2}}.$$

Therefore,

$$\frac{d^2}{dx^2}\left\{-2q\frac{dQ_x}{dq}\right\} = \int_0^\infty \frac{2q\frac{dA}{dq}\log A\{(x+\frac{1}{2})\log A - 2\}\,d\theta}{A^{x+3/2}}.$$

Now

$$\frac{dA}{dq} = 1 + \frac{q}{\sqrt{q^2-1}}\cosh\theta.$$

Therefore,

$$q\frac{dA}{dq} = q + \frac{q^2}{\sqrt{q^2-1}}\cosh\theta > A.$$

Therefore,

$$\frac{d^2}{dx^2}\left\{-2q\frac{dQ_x}{dq}\right\} > \int_0^\infty \frac{2A\,.\log A\{(x+\frac{1}{2})\log A - 2\}\,d\theta}{A^{x+3/2}} > 0$$

for values of q and x in the range considered.

Again, from (45)

$$\frac{d^2}{dx^2}\{x^2 Q_x\} = \int_0^\infty \frac{[A^{x+1/2}\{2 - 2x\log A\} - A^{x+1/2}\log A\{2x - x^2\log A\}]\,d\theta}{A^{2x+1}}$$

$$= \int_0^\infty \frac{[2 - 4x\log A + (x\log A)^2]\,d\theta}{A^{x+1/2}}.$$

Therefore,

$$\frac{d^2}{dx^2}\left\{-2q\,.\frac{dQ_x}{dq} + x^2 Q_x\right\}$$

$$> \int_0^\infty \frac{A[2\log A\{(x+\frac{1}{2})\log A - 2\} + 2 - 4x\log A + (x\log A)^2]\,d\theta}{A^{x+3/2}}. \quad (50)$$

This is certainly > 0 if $(x^2+2x+1)(\log A)^2 - 4\log A - 4x\log A + 2 > 0$.

Taking $x = 2$ the condition becomes

$$9\,(\log A)^2 - 12 \log A + 2 > 0.$$

This requires $\log A > 1{\cdot}14$

or
$$q + \sqrt{q^2 - 1}\,\cosh\theta > e^{1\cdot 14}.$$

Since the minimum value of $\cosh\theta$ is unity the expression (50) will certainly be positive if

$$q + \sqrt{q^2 - 1} > e^{1\cdot 14},$$

or if

$$q > 1{\cdot}73.$$

This requires $a/b = \sqrt{2\,(q - 1)} > 1{\cdot}205$, which is within our limits of accuracy equal to the critical value of ξ' obtained by measurements from the curves of fig. 3.

From (41) and (50) it follows that $\dfrac{d^2}{dx^2}\left\{\dfrac{d^2 Q_x}{dx^2}\right\}$ is positive for $x \geqslant 2$, $a/b \geqslant 1{\cdot}2$, and, therefore, $S_n\,(x)$ is a positive decreasing function of x. Now $\sum\limits_{n=1}^{\infty} (-1)^n S_n\,(x) < -S_n\,(x)$, where the suffix unity denotes the first term of the series. We find from the tabulated values of toroidal functions that for $a/b = 5/4$, $-S_n\,(x) = 0{\cdot}1$, which, compared with the corresponding value of $\sum\limits_{n=1}^{\infty} \{g^{(n)} + (-1)^n g_2^{(n)}\}$, is negligible in its influence on the possibility of vibrations. The whole effect of this term can be annulled by a slight alteration in the value of m_r. The maximum change required to be made in m_r is, from equation (38), of amount $\dfrac{2 \times 0{\cdot}1}{r^2 - 1}$. Having already considered $r = 2$ we take $r = 3$ to obtain the maximum alteration in m_r, of amount $0{\cdot}025$. This is easily seen to involve a change of $< \frac{1}{2}$ per cent. in the ratio b/ε, and is, therefore, negligible and outside the limits of accuracy of our equations of motion.

In connection with equations (43), (44) we have proved that for $2 \leqslant r \leqslant 6$ and $a/b > 1{\cdot}20$, J_r is negative. κ_r, negative for $r = 2$, but increasing with r, is always negative, but since $(r^2 - 1)\,m_r + 2\kappa_r$ is positive for $r = 2$, it is positive for all values of r considered. We conclude, therefore, that the system is capable of maintaining the vibrations considered for all values of spacing ratio in excess of the value $1{\cdot}20$.

APPENDIX.—Tables of Toroidal Functions by A. G. Forsdyke.

The accompanying tables give the values of the Zonal Toroidal Harmonics of the second kind (Q_m) of order m, for $m = 0, 1, 2, 3$, together with the first and second derivatives of these functions. The method of calculation is here outlined :—

$$Q_m = \frac{1}{\sqrt{2}}\int_0^\pi \frac{\cos m\phi \,.\, d\phi}{(q - \cos\phi)^{1/2}},$$

q, the argument of Q_m being always greater than unity. The harmonics of order zero and unity are immediately expressible in terms of Complete Elliptic Functions of the first and second kinds. The reduction is here given :—

$$Q_0 = \frac{1}{\sqrt{2}}\int_0^\pi \frac{d\phi}{(q - \cos\phi)^{1/2}}.$$

Put

$$k = \frac{\sqrt{2}}{\sqrt{q+1}}, \quad \theta = \phi/2,$$

and we have

$$\begin{aligned} Q_0 &= \frac{\sqrt{2}}{\sqrt{q+1}}\int_0^{\pi/2} \frac{d\theta}{(1 - k^2\cos^2\theta)^{1/2}} \\ &= \frac{\sqrt{2}}{\sqrt{q+1}} F_1(k). \end{aligned}$$

Also

$$\begin{aligned} Q_1 &= \frac{1}{\sqrt{2}}\int_0^\pi \frac{\cos\phi \,.\, d\phi}{(q - \cos\phi)^{1/2}} \\ &= \frac{\sqrt{2}}{\sqrt{q+1}}\int_0^{\pi/2} \frac{(2\cos^2\theta - 1)\,d\theta}{(1 - k^2\cos^2\theta)^{1/2}} \\ &= \frac{\sqrt{2}}{\sqrt{q+1}}\left\{-(q+1)\int_0^{\pi/2}(1 - k^2\cos^2\theta)^{1/2}\,d\theta + q\int_0^{\pi/2}\frac{d\theta}{(1 - k^2\cos^2\theta)^{1/2}}\right\} \\ &= \frac{\sqrt{2}}{\sqrt{q+1}}\{qF_1(k) - (q+1)E_1(k)\}. \end{aligned}$$

The elliptic functions are usually tabulated to the argument $\chi = \sin^{-1} k$. In the tables that were available the complete elliptic functions $F_1(\sin\chi)$ and $E_1(\sin\chi)$ were given to the required degree of accuracy only for every fifth degree in χ. Consequently the functions Q_m could only be calculated for values of q corresponding to these values of χ, which accounts for what appears to be a very arbitrary choice of value of q in the table. The calculations were carried out to eight figures, so that the tabulated values may be taken as being correct to six figures.

Table I.

q	1·030152	1·062182	1·143594	1·264949	1·434886	1·980581	3·000000	5·079213	10·197821
k	0·992546	0·984808	0·965926	0·939693	0·906308	0·819152	0·707107	0·573576	0·422618
$F_1(k)$	3·500433	3·153385	2·768063	2·504550	2·308787	2·034715	1·854075	1·731245	1·648995
$E_1(k)$	1·022313	1·040114	1·076405	1·118378	1·163828	1·258680	1·350644	1·432291	1·498115
Q_0	3·474331	3·105478	2·673744	2·353507	2·092472	1·666741	1·311029	0·993001	0·696895
Q_1	1·519109	1·186265	0·828923	0·596760	0·434173	0·227988	0·112889	0·049420	0·017131
Q_2	0·928441	0·644880	0·372686	0·221993	0·133161	0·046452	0·014545	0·003688	0·000632
Q_3	0·618841	0·384209	0·184569	0·091239	0·045210	0·010409	0·002082	0·000318	0·000034

Table II.

q	1·030152	1·062182	1·143594	1·264949	1·434886	1·980581	3·000000	5·079213	10·197821
Q_0'	− 16·82623	− 8·236356	− 3·620385	− 1·983273	− 1·212717	− 0·525734	− 0·238762	− 0·100697	− 0·034417
Q_1'	− 15·59641	− 7·195772	− 2·803377	− 1·331985	− 0·693874	− 0·207889	− 0·060773	− 0·014960	− 0·002535
Q_2'	− 13·78801	− 5·863825	− 1·962540	− 0·789752	− 0·344370	− 0·069792	− 0·012985	− 0·001856	− 0·000156
Q_3'	− 11·88225	− 4·616252	− 1·312551	− 0·444014	− 0·161229	− 0·022100	− 0·002594	− 0·000209	− 0·000007
Q_0''	552·1443	130·3929	24·73006	7·380599	2·792626	0·569963	0·138102	0·031239	0·005124
Q_1''	543·5530	126·1468	22·85055	6·361206	2·188023	0·340257	0·056163	0·007624	0·000627
Q_2''	520·9512	116·00015	19·12331	4·716665	1·404877	0·154189	0·016557	0·001318	0·000261
Q_3''	488·3890	102·6919	14·999795	3·202225	0·810541	0·061114	0·004222	0·000198	0·000030

Having obtained Q_0 and Q_1 it was only necessary to perform two successive applications of the recurrence relation

$$(2m+1)\,Q_{m+1} - 4mqQ_m + (2m-1)\,Q_{m-1} = 0$$

in order to obtain Q_2 and Q_3.

The first derivatives of the Q-functions were calculated from the formulæ

$$\frac{dQ_0}{dq} = Q' = -\frac{1}{2\,(q^2-1)}\,(qQ_0 - Q_1),$$

$$Q_m' = \frac{(2m-1)}{2\,(q^2-1)}\,(qQ_m - Q_{m-1}),$$

and the second derivatives are given by

$$(q^2-1)\,Q_m'' = -2qQ_m' + (m^2 - \tfrac{1}{4})\,Q_m.$$

These formulæ are taken from Bassett, 'Hydrodynamics,' § 277 *et seq.*, where toroidal functions are discussed in some detail. Table I gives the function Q_m together with the Complete Elliptic Functions corresponding to the selected values of q. The second Table gives the first and second derivatives of Q_m.

The Electrical Condition of Hot Surfaces during the Adsorption of Gases. Part I.—*Gold and Silver Surfaces at Temperatures up to* 850° C.

By G. I. Finch and J. C. Stimson.

(Communicated by W. A. Bone, F.R.S.—Received June 11, 1927.)

Introduction.

In 1914, Dr. H. Hartley[*] published an account of an investigation upon the electrical condition of a gold surface heated in contact with various gases, in the course of which he found, *inter alia*, that gold acquired a negative charge when in contact with hydrogen or carbonic oxide, or a mixture of either of these gases with oxygen, and a positive charge when in contact with oxygen alone. In view of the fact that these interesting and significant results indicate a possible clue to the mechanism and nature of the heterogeneous catalysis of gaseous reactions by hot surfaces, the present investigation was undertaken with the object of confirming and extending Dr. Hartley's work.

---

[*] 'Roy. Soc. Proc.,' A, vol. 90, p. 61 (1914).

Experimental.

The main difficulty encountered in the course of this investigation lay in the avoiding of spurious electrical effects. We believe, however, that the design and arrangement of apparatus finally adopted by us were such as to preclude the occurrence of such effects. It was also found necessary to employ a pumping system which would permit of the rapid attainment of a high degree of vacuum, and to prevent ingress of any traces of mercury vapour into the vessel containing the metal surface, which would otherwise have been contaminated with mercury.

The Apparatus.

The apparatus consisted essentially of an electrically heated transparent quartz vessel containing the gold or silver surface under examination. The vessel could be evacuated or filled with gas to any required pressure. The electrical charge on the surface was measured by means of a quadrant electrometer connected to the metal under examination. One silver and two gold surfaces were used. Experiments with one of the latter surfaces, a gold gauze, were carried out in a horizontal quartz vessel, the charge being measured by means of a Dolezalek quadrant electrometer, whilst the other surfaces (gold and silver sheets) were suspended in a vertical quartz vessel and connected to a Lindemann quadrant electrometer. The apparatus is shown in fig. 1.

The Horizontal Vessel.—The surface, S_1, was that previously employed by Dr. Hartley; it consisted of a piece of gold gauze, 9 by 20 cm., with 22 strands (each 0·15 mm. in diameter) per cm. and weighed 49 grams. The gauze was wrapped round a quartz rod supported in the axis of the horizontal quartz vessel. A gold wire, fused to the gauze, passed through a quartz capillary, into the far end of which it was sealed with sealing wax, to the insulated pair of quadrants of a Dolezalek quadrant electrometer. A steady circulation and drying of the gas surrounding the gauze was ensured by the difference in temperature between the main horizontal vessel situated in the furnace, F_1, and the side tube, H, containing purified phosphoric oxide.

The electric furnace, F_1, consisted of nichrome strip, wound non-inductively over a layer of mica and asbestos paper round an earthed iron tube, the windings being suitably spaced in order to ensure as nearly as possible a uniform temperature throughout that section of the furnace occupied by the gold gauze. The furnace tube was lagged externally with a thick, loosely packed layer of asbestos wool, maintained in position by a wider tube of refractory material concentric with the core of the furnace. A platinum, platinum-rhodium thermocouple,

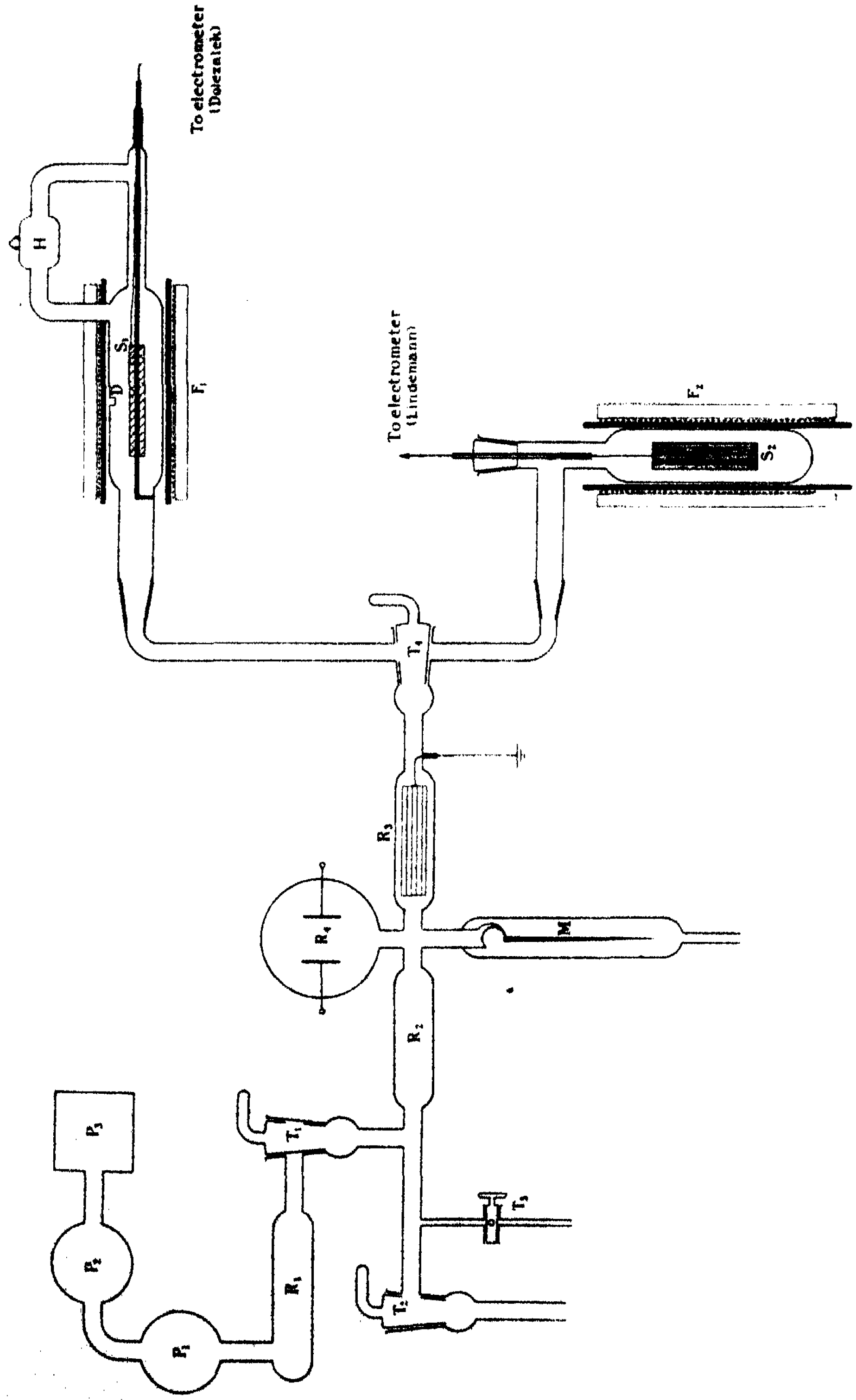
To electrometer (Dolezalek)
H
D
S_1
F_1
To electrometer (Lindemann)
F_2
S_2
T_4
R_3
R_4
M
R_2
T_1
P_3
P_2
R_1
P_1
T_2
T_3

FIG. 1.

the junction of which was situated in the recess, D, in the main quartz vessel, served to measure the temperature of the gold gauze.

The Vertical Vessel.—The surface, S_2, consisted of a 22 S.W.G. sheet, 6 by 10 cm., of either pure gold or silver supplied by Messrs. Johnson and Matthey of Hatton Garden. The sheet, rolled into a loose spiral, was suspended centrally in the vertical quartz vessel by means of a fused-on wire of the same metal, which passed through a capillary in a ground-in quartz stopper and hence to the Lindemann electrometer.

The furnace, F_2, was similar in construction to F_1, nichrome strip being wound non-inductively on, and insulated from, an earthed iron tube. The latter was fixed vertically inside an asbestos-lined metal casing packed with asbestos wool. The temperature of the surface was measured by means of a thermocouple placed in the furnace tube in contact with the quartz vessel and level with the metal sheet.

The Pumping System.—A high degree of vacuum could be maintained in the quartz vessels by means of two all-steel mercury vapour pumps, P_1 and P_2, in series with each other and backed by the "Hyvac" oil pump, P_3. Ingress of mercury vapour into the apparatus was prevented by means of the mercury vapour trap, R_1, in which the vapour was absorbed by means of a liquid alloy of sodium and potassium.* The wide-bore tap, T_1, enabled the apparatus to be shut off from the pumping system, and the taps, T_2 and T_3, served for the preliminary evacuation of the apparatus before bringing the mercury vapour pumps into action, and for the admission of gas respectively. The tube, R_2, contained purified phosphoric oxide, and R_3 a roll of earthed aluminium foil, for the drying of, and removal of charges from, the gases admitted to the apparatus. Into the tube, R_4, two platinum wires were fused, to which aluminium discs were attached, the latter being 5 cm. apart. By previous calibration with a McLeod gauge, it was found that when the discharge from an induction coil passed an external and parallel 7 cm. spark-gap in air without any visible sign of discharge from the tube, the vacuum was of the order of 10^{-6} mm. of mercury. M was a null manometer consisting of a pointer fused to a drawn-in glass bulb, the interior of which was in communication with the apparatus and the exterior with an ordinary mercury U-tube manometer, one limb of which was closed. When the internal and external pressures were equal, the position of the pointer was at zero. By suitably adjusting the latter pressure, the pointer could be brought to the zero position, the pressure in the apparatus then being equal to that registered by the mercury manometer.

---

* 'Nature,' vol. 119, p. 856 (1927).

Another wide-bore tap, T_4, served to connect the pumping system to either of the quartz vessels containing the metal surfaces.

The glass portion of the apparatus was attached to the mercury vapour pumps and the quartz vessels by means of dry ground joints, rendered vacuum-tight with sealing wax. All taps were lubricated with Ramsay grease. At first this gave off considerable quantities of gases, but after prolonged evacuation this evolution of gas practically ceased.

Shielding of the Apparatus from External Electrical Effects.—The whole of the apparatus from the tap, T_4, up to and including the electrometers was protected from external electrical effects by being completely encased in an electrically continuous and earthed coating of metal, *i.e.*, the iron furnace tubes in the case of the heated sections, and tin-foil elsewhere.

The Quadrant Electrometers.—The connections of the electrometers are not shown in fig. 1. In the case of the Dolezalek quadrant electrometer, one pair of quadrants was permanently connected to earth, the other pair being insulated from earth and connected to the gold gauze, S_1, by means of a gold wire fused to the gauze. The surface and the insulated quadrant pair could be earthed by means of an earthing key (not shown in fig. 1). The needle was brought as nearly as possible into a position symmetrical with respect to the quadrants and was then accurately adjusted until there was no appreciable difference in the scale reading of the beam of light reflected from the needle mirror, when the needle was either connected to earth, or charged to +72 or —72 volts, both quadrant pairs being earthed. With the needle charged to +72 volts the sensitiveness of the instrument was 140 scale divisions per volt.

The Lindemann quadrant electrometer has been described by F. A. and A. F. Lindemann and T. C. Keeley.* The surface, S_2, was connected to the needle of this electrometer and could be earthed by means of a switch, and the two pairs of quadrants were charged oppositely. Readings were made by observing the position of the needle through a microscope. The electrometer was adjusted as follows :—With the needle and quadrants earthed, the position of the former was made to coincide with the zero position of the Leitz micrometer eyepiece of the microscope. Then, with the needle still earthed, but the quadrants charged (top terminal +12, bottom terminal —16 volts), the needle was brought back to the zero position again by the fine adjustment of the potentials of the quadrants by means of a potentiometer across the high-tension accumulator battery. Under these conditions, the sensitivity of the Lindemann electrometer was 350 eyepiece divisions per volt.

---

* 'Phil. Mag.,' vol. 47, p. 578 (1924).

The insulation of the electrical circuits was tested frequently throughout the course of this investigation by charging up the surfaces to 2 volts and determining the subsequent rate of leak of this charge.

Preparation of the Gases.

Oxygen, hydrogen and electrolytic gas were prepared by the electrolysis of a saturated solution of thrice recrystallised barium hydroxide. Carbonic oxide was obtained by the interaction of pure formic acid and concentrated sulphuric acid. All the above gases were purified by passage through spiral washers containing a concentrated potassium hydroxide solution followed by concentrated sulphuric acid. Carbon dioxide was generated from a saturated solution of sodium bicarbonate and dilute sulphuric acid, both solutions being freed from air by flushing with carbon dioxide. Carbonic oxide " Knall " gas was prepared by mixing carbonic oxide and oxygen in their combining proportions in an eudiometer over mercury, and subsequently checking the mixture by analysis in a " Bone and Wheeler " gas-analysis apparatus. Argon was prepared by passing the commercial gas over a heated magnesium-lime mixture. Nitrogen was obtained by the passage of a mixture of ammonia and air over red-hot copper turnings, and then through a potassium hydroxide solution and concentrated sulphuric acid in spiral washers.

Before admission into the apparatus, all gases were finally sharply dried by slow passage through a 1 metre long tube containing purified phosphoric oxide.

EXPERIMENTAL PROCEDURE AND RESULTS.

Series A. Experiments with the Gold Gauze up to 510° C.

(i) *In Vacuo.*—The vessel containing the gold gauze was evacuated at room temperature to below 10^{-5} mm., and the temperature then raised to 510°. At first the charge on the gauze was positive ($+0 \cdot 3$ volt) at this temperature, but it fell gradually, and after seven days had settled down to $-0 \cdot 55$ volt, the " in vacuo " charge for the gold gauze at 510°, at which value it remained unchanged during a further seven days' (168 hours') continuation of this treatment. In this, and in all further experiments to be described below, the electrometer needle and the gold gauze were frequently earthed. After each such earthing the charge was rapidly re-established at a rate depending on the gas (if any), the temperature of the surface and the electrical capacity of the system.

The temperature was now lowered by steps to room temperature and once more raised in a similar manner to 510°, during which operations the variation of the charge on the gauze with temperature was observed. At each step in the temperature a pause was made sufficiently long to ensure constancy in the value of the charge having been attained. The results are recorded in fig. 2, curve Vacuo.

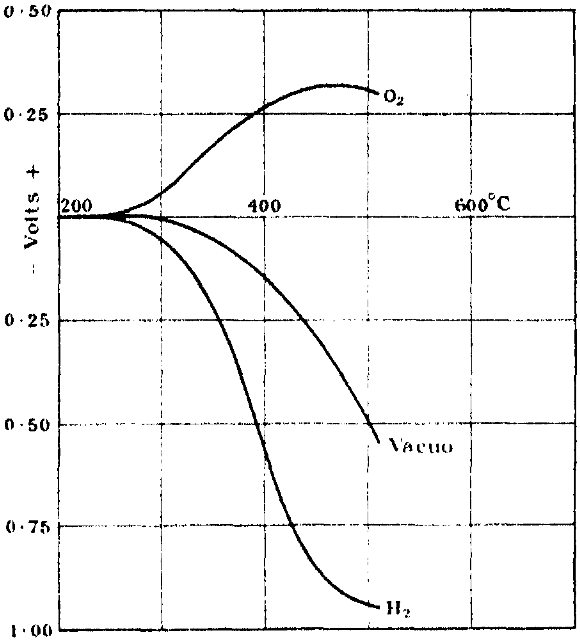

FIG. 2.

(ii) *In Gases. Oxygen.*—With the gauze heated to 510° and showing the constant in vacuo charge of − 0·55 volt corresponding to this temperature, oxygen was rapidly admitted to a pressure of 10 mm. The negative in vacuo charge now gave way to a positive one, a constant "oxygen" charge of +0·30 volt being attained within 50 minutes after admission of the gas. The rate of change of the charge on the surface from the in vacuo to the oxygen charge is shown in fig. 3, curve O_2 510°.

The temperature was now lowered by steps to room temperature and raised in like manner to 510°. The observed variation of the oxygen charge with temperature is recorded in fig. 2, curve O_2. On rapidly evacuating to below 10^{-5} mm., the oxygen charge went back steadily to the in vacuo value. The corresponding rate of change of charge curve obtained on evacuation after the gauze had been heated during three hours in oxygen is shown in fig. 4, curve Vacuo 510°. In the course of further experiments it was found that the time of evacuation necessary to re-establish the in vacuo charge depended upon the duration of previous heating of the gauze in contact with oxygen. Thus, when the gauze had been heated at 510° in contact with oxygen during 3, 20 or 48 hours, the duration of heating to the same temperature in vacuo required for

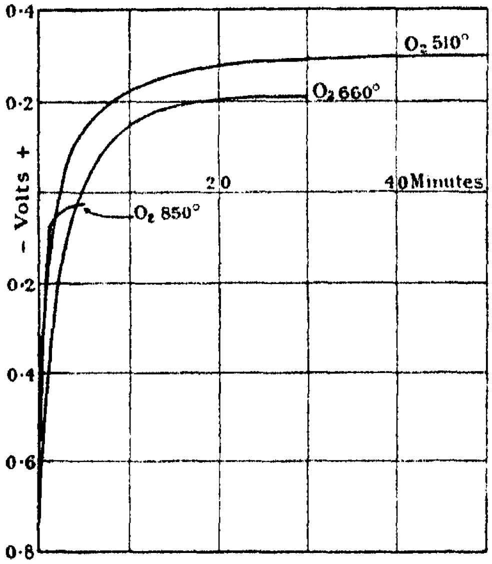

Fig. 3.

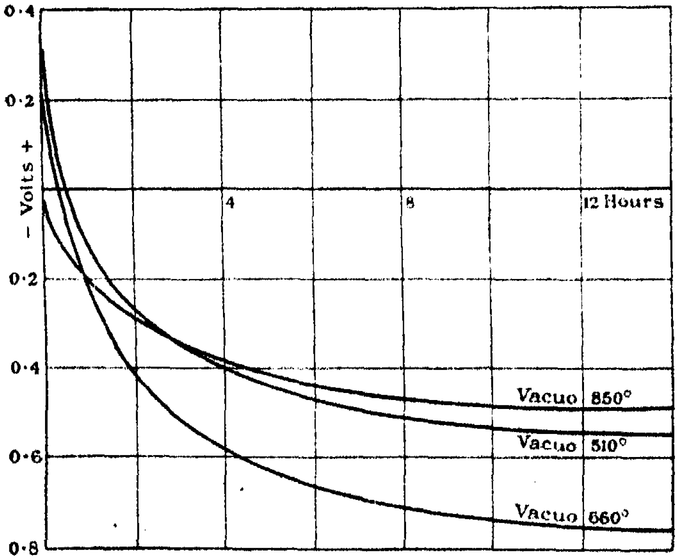

Fig. 4.

the complete re-establishment of the in vacuo charge was 12, 48 or 84 hours respectively.

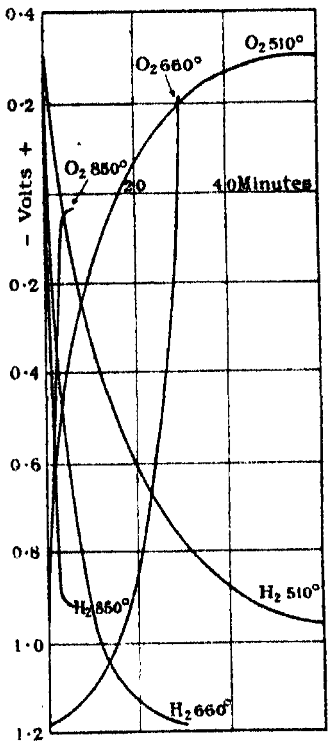

FIG. 5.

All the above experiments were repeated with oxygen pressures between 1 and 600 mm., with the result that the value of the oxygen charge at all temperatures up to 510°, the rate of attainment of the same, and the rate of re-establishment of the in vacuo charge were found to be independent of the pressure of the oxygen within the limits stated.

In contrast to the length of time necessary to remove the oxygen charge from the surface at 510° by evacuation alone, it was found that it could be rapidly removed by introducing hydrogen, after previous rough evacuation of the oxygen, whereupon the charge reached the in vacuo value in 15 minutes, and the hydrogen value within an hour, no matter how long the oxygen had previously been in contact with the gold gauze. The corresponding rate of change of oxygen to hydrogen charge curve is shown in fig. 5, curve H_2 510°.

Hydrogen.—Hydrogen was rapidly admitted into the apparatus to a pressure of 10 mm. with the gold gauze showing the in vacuo charge of — 0·55 volt at 510°. The charge immediately commenced to change and finally reached the constant "hydrogen" charge of — 0·95 volt in one hour (fig. 6, curve H_2 510°). The variation of the hydrogen charge with temperature is recorded in fig. 2, curve H_2. On evacuation, the hydrogen charge changed within 15 minutes to — 0·65 volt, the in vacuo charge being finally attained within 2 hours. The duration of the time of contact of the gold with hydrogen (up to 60 hours) had no influence on the time of evacuation necessary to restore the in vacuo charge. The rate of re-establishment of the in vacuo charge from the hydrogen charge is shown in fig. 6, curve Vacuo 510°.

The above experiments were repeated with fresh quantities of hydrogen between 1 and 600 mm., and the results were similar to those detailed above, the value of the hydrogen charge being independent of the gas pressure. The hydrogen charge could be removed rapidly by admitting oxygen to the surface, the charge then passing the in vacuo value within 5 minutes, and giving the full oxygen charge within one hour. The corresponding rate of change of charge curve is shown in fig. 5, curve O_2 510°.

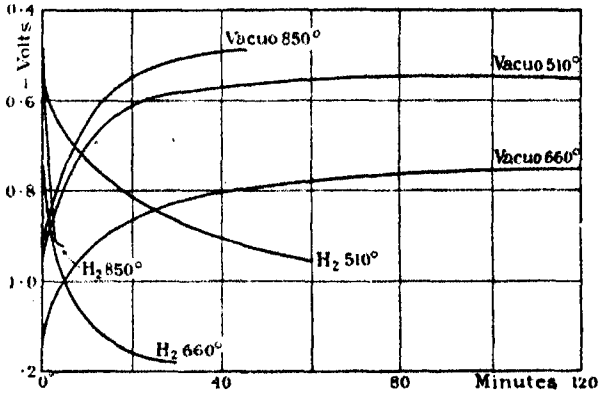

Fig. 6.

Series B. Experiments with the Gold Gauze up to 660° C.

(i) *In Vacuo.*—On conclusion of the above series of experiments the temperature of the gauze was raised to a new maximum of 660° in a vacuum below 10^{-5} mm., and maintained under these conditions for several days until the charge on the surface, which changed steadily but exceedingly slowly, became constant at $-0\cdot75$ volt. The variation of this in vacuo charge with temperature was determined as before, the results being recorded in fig. 7, curve Vacuo. This new in vacuo charge-temperature curve still resembled in character that obtained when the gauze had not been heated above 510°, but the surface did not commence to give a charge until 420° instead of at 290° as in the previous case.

The gauze was brought into contact with, and heated in, various gases, after which the 660° in vacuo charge-temperature curve could be repeated an indefinite number of times after sufficiently prolonged evacuation.

(ii) *In Gases. Oxygen.*—On admission of oxygen, the in vacuo charge changed steadily until the gold gauze showed a constant oxygen charge of $+0\cdot21$ volt at 660° within 30 minutes after the first rapid admission of oxygen (fig. 3, curve O_2 660°). The charge-temperature curve is shown in fig. 7, curve O_2. The time of evacuation necessary in order to restore the in vacuo charge was long and depended, as before, on the previous time of contact of the gauze with oxygen, the actual times being almost as long as those previously quoted for the removal of the oxygen charge in Series A. The oxygen charge could be removed rapidly, after preliminary rough evacuation of the oxygen to about 0·1 mm., by either hydrogen or carbonic oxide (fig. 5, curve H_2 660°).

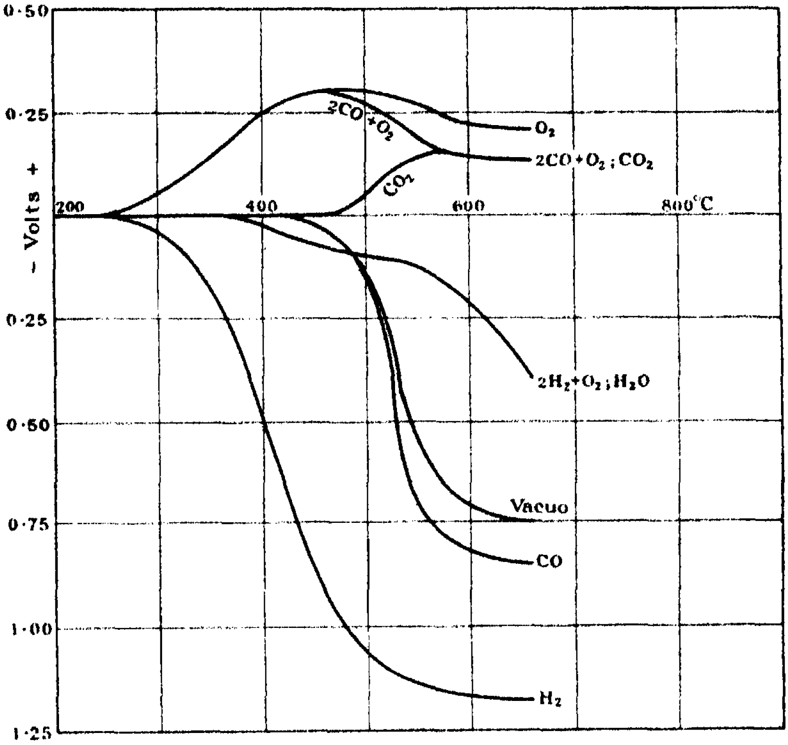

FIG. 7.

Hydrogen, Carbonic Oxide and Carbon Dioxide.—Immediately after the introduction of any one of these gases, the gold gauze acquired a constant charge, the value of which was characteristic of the gas, within 30 minutes (fig. 6, curve H_2 660°). These charges were found to be independent of the gas pressure. Evacuation to below 10^{-5} mm. sufficed to restore the in vacuo charge within two hours (fig. 6, curve Vacuo 660°). The corresponding charge-temperature curves are recorded in fig. 7, curves H_2, CO and CO_2.

Electrolytic and Carbonic Oxide "Knall" Gases.—The charge-temperature curves for these gases are recorded in fig. 7, curves $2H_2 + O_2$ and $2CO + O_2$. During the determination of these curves, a steady stream of the gaseous mixture under examination was admitted at a rate sufficient to maintain the pressure constant within the apparatus. The charge-temperature curves for these explosive mixtures were intermediate between those of their respective component gases. The "Knall" gas and carbon dioxide curves coincide between

580° and 660°. Below 580° the former approaches, and finally merges into, the oxygen charge-temperature curve. This result was found to be independent of whether the "Knall" gas contained a slight excess of either oxygen or carbonic oxide.

Water Vapour.—The phosphoric oxide was removed from the tube, H, and a tap funnel sealed in place of the plug by which the tube was normally closed. The apparatus was then evacuated, closed off at T_4 from the pumping system, and a few drops of air-free distilled water admitted through the tap funnel. The resulting charge-temperature curve was then determined as before and is recorded in fig. 7, curve H_2O. It coincided throughout with the curve for electrolytic gas.

Series C. Experiments with the Gold Sheet up to 850° C.

(i) *In Vacuo.*—In the foregoing experiments it was shown that the in vacuo charge-temperature curve was permanently altered on raising the maximum temperature to which the surface was heated. In order to see if the same effect occurred with the gold sheet, three experiments were carried out as follows :—

(*a*) The sheet was heated at 510° in vacuo until the charge on the surface was constant. The charge-temperature curve was then determined and is shown in fig. 8, curve Vacuo 510°.

(*b*) The temperature was now raised to 660° and evacuation continued until a constant in vacuo charge for this temperature was obtained. The corresponding charge-temperature curve was thereupon determined and is shown in fig. 8, curve Vacuo 660°.

(*c*) Finally, the sheet was evacuated at 850° and the corresponding charge-temperature curve, recorded in fig. 8, curve Vacuo 850°, determined.

(ii) *In Gases.*—The gases used in this series of experiments fell, as before, into one of two groups, according to whether a comparatively brief or prolonged evacuation was necessary in order to reduce the respective gas charge to the in vacuo charge. Oxygen and air alone called for prolonged evacuation. As previously, in no case did the pressure of the gas within wide limits (between 1 and 760 mm.) have any influence on the magnitude of the charge.

Oxygen and Air.—The oxgyen charge at 850° was attained within five minutes after the admission of the gas (fig. 3, curve O_2 850°). The time of evacuation required to restore the in vacuo charge varied with the previous duration of heating of the sheet in oxygen. Thus, when the surface had previously been heated at 850° in contact with oxygen during 1 minute, 15 minutes, 1 hour, 3 hours or 20 hours, the times of evacuation required to re-establish the in vacuo charge were 8, 10, 12, 14 (fig. 4, curve Vacuo 850°) or 16 hours respectively. The oxygen charge could be "burnt off" the surface by either hydrogen or carbonic oxide in five minutes (fig. 5, curve H_2 850°).

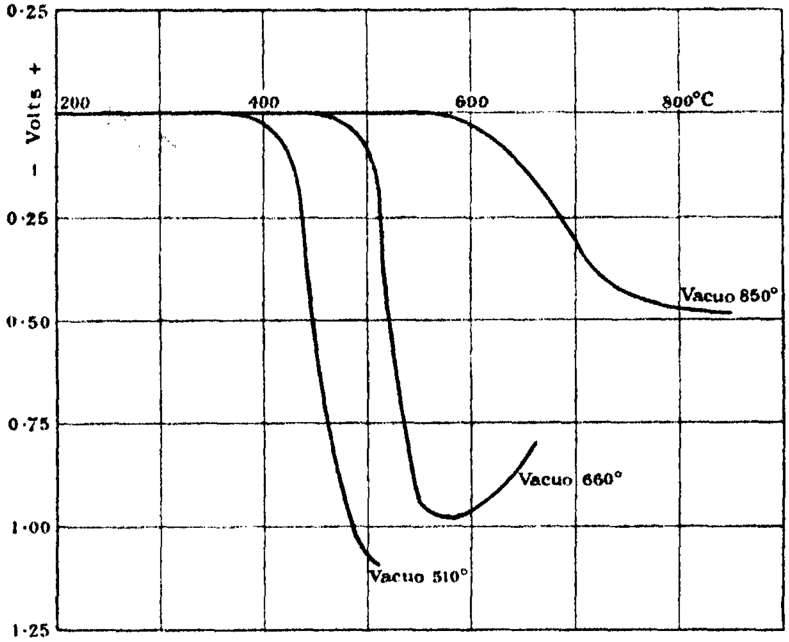

FIG. 8.

The air charge was removable in exactly the same way and at the same rate as that of oxygen by evacuation or by "burning off." The charge-temperature curves for oxygen and air are shown in fig. 9, curves O_2 and Air.

Hydrogen, Carbonic Oxide, Argon and Nitrogen.—On admission of any of these gases, the in vacuo charge at 850° gave place to a charge characteristic of the gas in question, the charge being completely attained within five minutes after the admission of the gas (fig. 6, curve H_2 850°). The in vacuo charge could be restored by evacuation at 850° within 45 minutes in the case of hydrogen (fig. 6, curve Vacuo 850°), and within one hour in the case of the other gases. The charge-temperature curves are recorded in fig. 9, curves H_2, CO, Ar and N_2.

Electrolytic and Carbonic Oxide "Knall" Gases; Water Vapour and Carbon Dioxide.—The charge-temperature curves for these gases and gaseous mixtures are shown in fig. 9, curves $2H_2 + O_2$, $2CO + O_2$, H_2O and CO_2. At 850° the corresponding charge was exhibited within five minutes of admission of the gas (as in fig. 6, curve H_2 850°). In all cases the charge was readily removed and the in vacuo charge restored by evacuation at 850° (as in fig. 6, curve Vacuo 850°).

On completion of the above series of experiments, the vertical quartz vessel containing the gold sheet was disconnected from the apparatus and withdrawn from the furnace. It was then observed that a minute quantity of gold had sublimated and been deposited on the cooler portions of the vessel in the form of an exceedingly thin film. In reflected light this film was yellowish-brown in colour and reddish-purple in transmitted light. The time of heating of the gold sheet at 850° in vacuo had been about eight months in all.

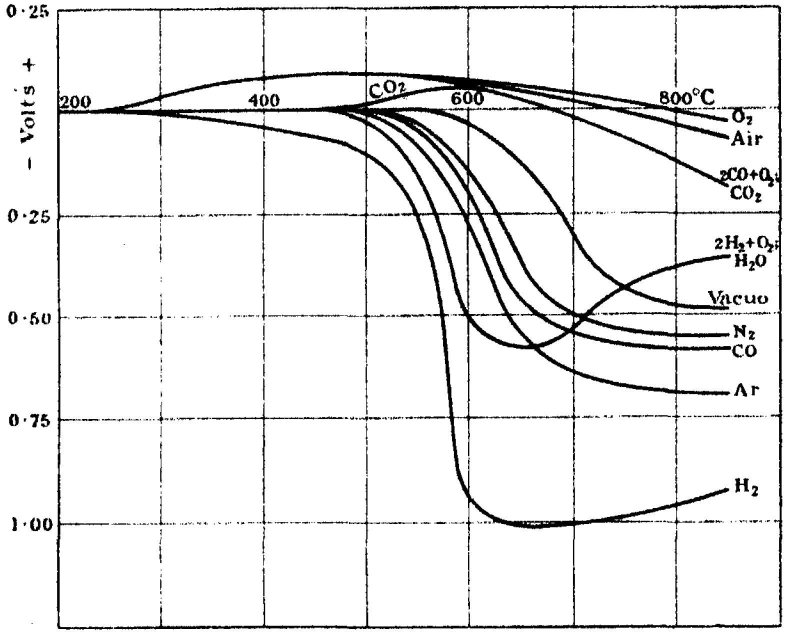

FIG. 9.

Series D. Experiments with the Silver Sheet up to 850° C.

The experiments in this series were carried out in the same manner as those described under Series C.

(i) *In Vacuo.*—The charge-temperature curves for silver in vacuo up to 510°, 660° and 850° are recorded in fig. 10.

(ii) *In Gases. Oxygen, Air and Hydrogen.*—The charge-temperature curves for these gases are recorded in fig. 11, curves O_2, Air and H_2. It was found that, unlike the hydrogen charge on gold, the time required for the removal not only of the oxygen and air, but also of the hydrogen charge on silver, and the re-establishment of the in vacuo charge by evacuation was long and depended on the previous time of heating of the silver in contact with the gas. The

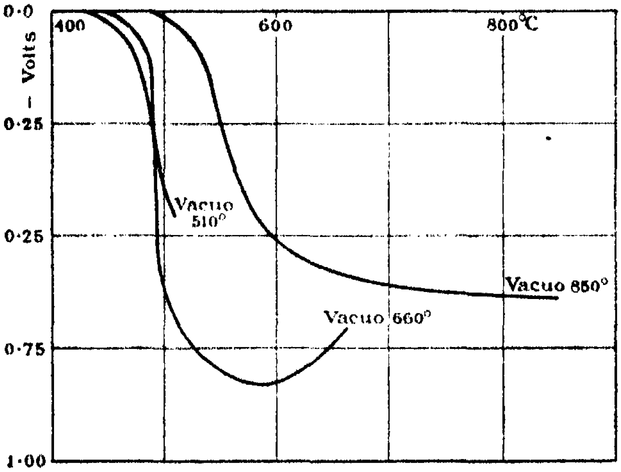

FIG. 10.

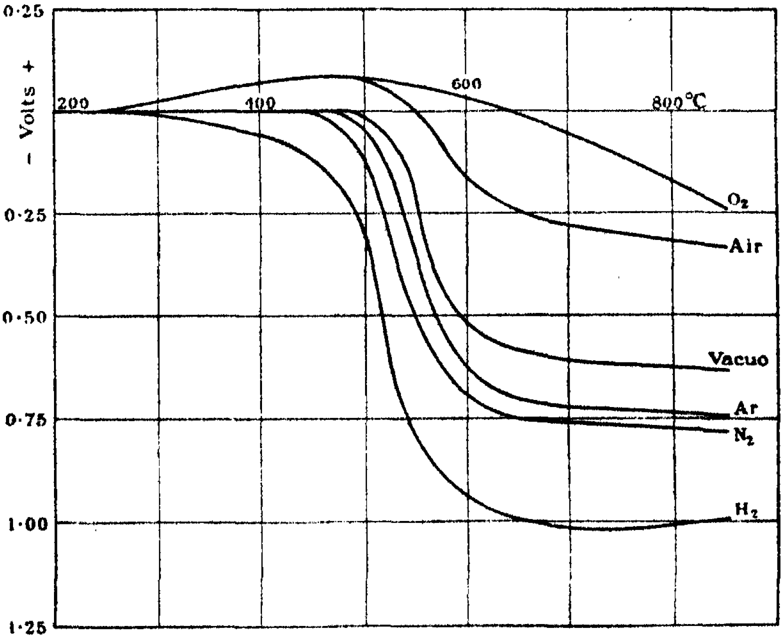

FIG. 11.

necessary time of evacuation in the case of the oxygen, air or hydrogen charge on silver was practically the same as that required in the case of the oxygen or air charge on gold (fig. 4, curve Vacuo 850°).

Nitrogen and Argon.—The charge-temperature curves for these gases are recorded in fig. 11, curves N_2 and Ar. The charge due to either gas was removed, and the in vacuo charge as readily restored as, for example, in the case of the hydrogen charge on gold (fig. 6, curve Vacuo 850°).

On completion of these experiments and prior to a contemplated determination of the charge-temperature curve for carbonic oxide, the silver was maintained at a temperature of 850° in a vacuum below 10^{-5} mm. for a continuous period of nearly three months, with the object of severely testing the constancy or otherwise of the in vacuo charge. Towards the end of this period, a change was indeed observed, the charge gradually approaching towards zero, which fact was at first attributed to a state of almost complete de-gassing of the silver having been brought about by this prolonged treatment. Soon afterwards, however, a breakdown in the furnace winding necessitated the disconnection of the vertical vessel, and it was then found that the gradual fall of the in vacuo charge was due to the fact that the whole of the silver in the high-temperature zone had sublimated on to the cold portions of the quartz vessel protruding from the furnace. During the carrying out of the experiments described under Series D, the silver had been heated in a high vacuum for about, in all, seven months at 850°.

DISCUSSION OF THE RESULTS.

Whilst several alternative hypotheses might be advanced to account for the fact that a gold or silver surface acquires a charge when heated in contact with a gas, the following interpretation appears to us to be most in accordance with the facts established in the course of this investigation :—

When a gas is brought into contact with a hot gold or silver surface, it is at first adsorbed and condensed into a layer of electrically neutral molecules on the surface of the metal. In the case of oxygen, a small fraction of the molecules thus condensed are " activated " (dissociated or ionised, or otherwise electrically charged) and continue in this state to remain adsorbed on the surface, the corresponding negative charges (in the event of ionisation) escaping into space. The surface thus becomes positively charged. This charge is a measure of an equilibrium in a system existing at the surface of the metal, of which active oxygen, *i.e.*, charged oxygen particles, form one component. Further, on becoming activated, a small proportion of the condensed oxygen molecules either quit the surface positively charged, the corresponding negative charges remaining on the surface, or are negatively charged and retained in such condition by the surface. Thus, the value of the oxygen charge is also a measure of the ratio of the number of positively charged oxygen particles remaining on the surface to the number, either of similar particles emitted from the surface, or of negatively charged oxygen particles retained by the surface. Above 790°, in the case of gold, and 640°, in the case of silver, the latter preponderate and the oxygen charge is negative.

In the case of all other gases examined, with the exception of such gaseous compounds or mixtures as contained oxygen, no evidence was obtained of such gases ever giving rise to a positive charging of the surface; which would indicate that a small fraction of the molecules in the condensed layer of such negatively charging gases are, on activation, either emitted from the surface in a positively charged condition, the corresponding negative charges remaining behind on the surface which thus acquires a negative charge, or are negatively charged by, and remain in this condition on, the surface. In this case also the magnitude of the charge on the surface is a measure of the state of an equilibrium of which either the charged molecules emitted from the surface (or, rather, the corresponding negative charges retained by the surface), or the negatively charged molecules remaining on the surface form one component. Thompson* has shown that thermionic emission commences from a platinum wire when raised to the temperature at which the union of hydrogen and oxygen on the surface begins. Further, Langmuir† observed that, when poison had been admitted to a reacting system containing a catalytically acting tungsten wire sufficient to stop the catalysis, the thermionic emission was simultaneously suppressed.

The magnitude of the charge alone thus affords by itself no measure of the activity of the surface, *i.e.*, its effect upon the rate of attainment of the equilibrium of which charged gaseous particles form a part. Such a measure would, however, be obtained by observing the rate of charging up of the electrical system (surface-connecting lead-electrometer) of known capacity after reduction of the charge to zero by earthing. We have carried out, and are continuing experiments on these lines, the results of which will be embodied in a further communication. It will suffice at this stage to state that the current which can be drawn from the surface, and hence the activity of the latter, increases rapidly with temperature.

No evidence has been obtained of deep-seated occlusion of any of the gases with which the surfaces have been brought into contact in the course of our experiments. It is true we have found that oxygen, in the case of gold, and

* 'Phys. Z.,' vol. 14, p. 11 (1913).

† 'Trans. Farad. Soc.,' vol. 17, p. 641 (1921).

either oxygen or hydrogen, in the case of silver, is only slowly removed from the heated metal by prolonged evacuation, and that the difficulty of such removal increases with the length of previous time of contact of the heated surface with the gas; whereas in the case of all other gases removal is effected far more easily, the necessary time of evacuation being also independent of the previous duration of heating of the surface. At first sight, this might be construed as evidence of occlusion of oxygen by gold and of both oxygen and hydrogen by silver, but against this view, it will be sufficient to cite the fact that the oxygen charge can be " burnt off " the surface with ease and rapidity by either hydrogen or carbonic oxide. Dr. Hartley found that a sudden increase or decrease in pressure respectively reduced or increased the charge, which observations he considered as pointing to occlusion effects. We have, however, not been able to confirm this result, but have found that sudden evacuation, admission of gas or lowering or raising of the temperature is followed only by a smooth and gradual change in the charge towards the value corresponding to the new set of conditions. We believe that the charge fluctuations observed by Dr. Hartley were essentially spurious and due to electrostatic effects resulting from rapid flow of gas, either past the surface on evacuation or reduction of pressure, or through a plug of cotton wool on increasing the pressure within his apparatus. A possible explanation of the difficulty of removing the oxygen on gold, or either oxygen or hydrogen on silver, charges by evacuation alone is that it may be due to the formation of compounds. But, while Bone and Wheeler* in their experiments on the catalytic combustion of hydrogen and oxygen in contact with silver found distinct evidence of the formation of silver hydride at high temperatures, according to Carnelly and Walker,† silver oxide is unstable at such temperatures, the decomposition of silver oxide being quite complete between 300° and 430°. Nor is there, as far as we are aware, any evidence of the direct formation of gold oxide, other than that afforded by the work of D. L. Chapman and his co-workers,‡ and by the results of the present investigation. Nevertheless, viewed in the light of the hypothesis previously advanced in order to account for the charging of a surface in contact with gases, the fact is significant that the oxygen charge is positive only below 790° in the case of gold, and below 640° in the case of silver, and negative at all higher temperatures.

We believe that if compound formation is the true explanation of the tenacity with which oxygen is held by gold, and oxygen and hydrogen by silver, then the mechanism of the charging up of these surfaces by these gases proceeds as follows :—

---

* 'Phil. Trans.,' A, vol. 206, p. 1 (1906).

† 'Trans. Chem. Soc.,' vol. 53, p. 79 (1888).

‡ 'Roy. Soc. Proc.,' A, vol. 107, p. 92 (1925).

(i) On admission, the gas is first adsorbed and condensed on the surface into a layer of electrically neutral molecules.

(ii) A compound is formed between the metal and a proportion of the condensed gas molecules, which process tends towards a state of equilibrium existing between electrically neutral molecules, the metal and the resulting compound.

(iii) The compound dissociates, the liberated gas molecules being activated by the surface which thus becomes charged.

(iv) Simultaneously with step (ii) another fraction of the condensed molecules are activated by the surface without the intermediate formation of a compound.

Whilst our experimental results afford no positive evidence of deep occlusion of the gases by the surfaces examined, their evidence on this point should be regarded as neutral rather than negative.

The results obtained with gaseous mixtures are of particular interest. The charge-temperature curve for air on gold at the higher temperature ranges lies between those for oxygen and nitrogen, but nearer the former. As the temperature is lowered, the air charge-temperature curve steadily approaches that of oxygen, until at 550° they merge together. At 510° the nitrogen charge falls to zero. Hence the conclusion may be drawn that the surface at all temperatures examined by us activates oxygen more readily than nitrogen. For example, at 850°, if this interpretation of the above facts is the true one, and if the effect of the in vacuo charge be neglected, then the proportion of oxygen activated by the surface to the similarly activated nitrogen is as 0·48 to 0·04, *i.e.*, 12 molecules of oxygen are activated to 1 of nitrogen. Similarly, the conclusion may be drawn that silver at 850° is five times more active towards oxygen than towards nitrogen. It should be pointed out that neither the value of the air charge, nor that of any of the other gaseous mixtures examined, can be accounted for on the supposition that the leakage of the nitrogen or other gas charges exceeded that of the oxygen charge.

The above interpretation may also be applied to a mixture of two combining gases. The charge-temperature curve for carbonic oxide "Knall" gas lies between those for oxygen and carbonic oxide separately, but nearer the former. Thus at all temperatures the activity of the surface towards oxygen is greater than towards carbonic oxide; at 850° in the proportion of 0·39 to 0·16.

With falling temperature the " Knall " gas curve approaches and finally, at 540°, merges into that of oxygen, *i.e.*, about 30 degrees above that temperature at which the gold surface ceases to activate carbonic oxide. The charge-temperature curve for carbon dioxide coincides with that of the " Knall " gas between 620° and 850°. In view of these facts, it is difficult to avoid the conclusion that the " activation " of carbon dioxide consists in, at the least, the dissociation of this gas into its constituents; and further that, for every two active oxygen molecules thus formed at 850° and retained at the surface, only about one carbonic oxide molecule contributes to the charging of the surface, the remaining three escaping from, or remaining adsorbed upon, it in an electrically neutral condition. Below 620°, the carbon dioxide charge-temperature curve leaves that of the " Knall " gas to approach and finally fall to zero at 475°. This effect is readily explained on the basis of the free carbonic oxide originating from the dissociation of carbon dioxide " burning off " the oxygen from the surface, whilst below 475° the surface is no longer able to bring about the dissociation of carbon dioxide.

A similar line of reasoning may be followed in the cases of electrolytic gas and water vapour. Both hydrogen and oxygen are activated by the surfaces at all temperatures above 250°. Thus the fact that the charge-temperature curves for electrolytic gas and water vapour coincide throughout the whole temperature range examined by us, constitutes further evidence in support of the explanation put forward to account for the nature of the carbonic oxide " Knall " gas and carbon dioxide curves. Although the water-vapour charge-temperature curve falls to zero at 470°, it is quite possible that the surface is still capable of bringing about the dissociation of water vapour at all temperatures down to 250°, the lowest temperature at which activation of either oxygen or hydrogen takes place.

In view of the profound effect which the previous history of heating has been found to have upon the gold and silver surfaces, it will be of interest to record briefly their history. The gold and silver sheets were supplied by Messrs. Johnson and Matthey and were first employed by us for the purposes of this investigation. Prior to Dr. Hartley's experiments, the gold gauze had been used by Professor Bone in the course of his studies on catalytic combustion, the maximum temperature to which it was then subjected being 600°. When used by Dr. Hartley, 500° were never exceeded. In 1922, Mr. Derringer, in the course of an investigation carried out in these laboratories, heated the gauze during several months to about 480° in oxygen, after which treatment the gauze was stored away until the present investigation was undertaken. On our first heating the gauze to 510° in vacuo, it exhibited a charge of +0·3 volt at that temperature, which positive charge gradually became negative, and after seven days' continuous heating finally reached a constant value of −0·55 volt. We conclude, therefore, that the positive charge exhibited by the gauze in the early stages of our first experiment was due to oxygen which was completely removed from the surface after seven days' evacuation. The remaining constant negative charge on the oxygen-free surface must be ascribed to some gas leaving the metal and being activated in the process. In view of the constancy of this in vacuo charge, which in the case of all three surfaces remained completely unaffected by several months' heating in vacuo, it is unlikely that the in vacuo charge is due to any deeply occluded gas making its way to the surface and leaving the metal. In all probability, the in vacuo charge is due to activation by the surface and emission therefrom in the charged state of its own vapour.

The reasons for the profound and permanent effect which the maximum temperature to which the metal has been previously subjected has upon the activating powers of the surface, especially at the lower temperature ranges, is still obscure. It is possibly due to some radical alteration in the structure of the surface.

From the considerations put forward in the above, it seems possible to evolve an explanation of the principal facts observed by Prof. Bone and his co-workers in their studies on the catalytic combustion of hydrogen and carbonic oxide with oxygen mixtures over gold and silver surfaces on the basic supposition, which has been made by them, that both of the reacting gases require to be activated at the surface before combustion can take place. We are conferring with Prof. Bone and Dr. Hartley about this subject and hope in the near future, on completion of the experiments upon the rate of charging up of such surfaces in contact with gases, which are now under way, to put forward in conjunction with them a common explanation of catalysis in regard to gold and silver surfaces.

Summary.

The main facts established in the course of this investigation are as follows:—

(i) A gold or silver surface becomes charged when heated either in contact with a gas or in a high vacuum.

(ii) The magnitude of the charge is characteristic of the gas and dependent on the temperature and previous history of heating of the metal, but independent of the gas pressure.

(iii) Evacuation of a gas removes the corresponding charge slowly in the case of oxygen or air on gold, and oxygen, air or hydrogen on silver, but rapidly in the case of all other gases examined.

(iv) The rapidity of removal of all gas charges, other than those due to oxygen or air on gold, or oxygen, air or hydrogen on silver, by evacuation increases with temperature.

(v) The oxygen charge on gold or silver, and the hydrogen charge on silver can be removed rapidly by "burning off" with either hydrogen or carbonic oxide in the former case, and by oxygen in the latter.

(vi) Sudden evacuation, admission of gas, or lowering or raising of the temperature, is followed by a smooth and gradual change in the charge towards the value corresponding to the new set of conditions.

(vii) The value of the charge due to a mixture of two gases, whether reacting with each other or not, is intermediate between the charges of the component gases.

(viii) The value of the charge due to the reaction product of a mixture of combining gases is the same as that due to the gaseous mixture, provided the surface commences to activate both gases at the same temperature. Otherwise, whilst at the higher temperature ranges the charge-temperature curves of the gaseous mixture and the reaction product still coincide, in the neighbourhood of that temperature at which one of the constituents is no longer activated, the charge-temperature curve of the mixture approaches and finally merges into that of the more readily activated gaseous component.

(ix) The previous heat treatment of the surface has a profound effect upon its powers of activation.

From the above facts we conclude (i) that the charge on a hot gold or silver surface in contact with a gas is due to an "activation" of the gas, whereby its molecules become electrically charged; and that (ii) the activation of a compound molecule such as water vapour or carbon dioxide involves at least its dissociation.

One of us (J. C. S.) wishes to thank the Court of the Skinners' Company, the Kent Education Committee, the Board of Education and the Department of Scientific and Industrial Research for personal grants which have enabled him to devote his full time to this research.

Contact of Flat Surfaces.

By F. H. Rolt and H. Barrell.

(Communicated by Sir Joseph Petavel, F.R.S.—Received June 11, 1927.)

[Plates 11 and 12.]

(1) Introduction.

It is well known that two clean glass plates with optically worked flat surfaces adhere to one another when brought into intimate contact. Considerable force is required to separate the plates; in fact, it often happens that their surfaces become damaged during the process. Such adherence is clearly due to molecular cohesion.

Similar evidence of cohesion is observed when contact is made between accurately flat, polished surfaces of steel and of steel and glass.

A somewhat different kind of contact occurs between the faces of the block gauges which are extensively used in modern workshop practice. These gauges usually consist of blocks of hardened steel having two faces, optically flat and parallel, whose distance apart defines the length of the gauge. If the faces of a pair of block gauges are quite clean their adherence is not so strong as in the case of glass plates. This is due to the fact that block gauges, as ordinarily produced, do not possess scratchless polished surfaces. The method of finishing them by a lapping process—rubbing over a flat, cast-iron surface impregnated with abrasive material—gives rise to surfaces which are covered with innumerable fine scratches, lying generally in one direction. Fig. A (Plate 11) is a microphotograph ($M = 19$ diameters) showing these scratches on a lapped surface of a typical block gauge. It should be mentioned that when examined for optical flatness by interference fringes there is little to distinguish such a surface from one having an optical polish.

It will be readily understood that when two clean lapped surfaces are brought together, mutual contact can only take place over a fraction of the total area owing to the presence of scratches, and the adherence is less marked than with polished surfaces.

If, however, a very minute trace of liquid, such as paraffin oil, is interposed between two such surfaces, experience shows that they will adhere with greatly increased tenacity. Indeed, Budgett[*] has found that the direct pull required to separate a pair of lapped steel surfaces, the liquid being condensed water vapour, was sometimes as high as 90 lbs. per square inch. The separation is more easily effected by sliding one surface over the other.

---

[*] 'Roy. Soc. Proc.,' A, vol. 86, p. 25 (1912).

This operation of bringing two surfaces into intimate contact with the aid of a minute trace of liquid is commonly known as "wringing."

Another degree of contact can be realised between clean surfaces of glass and lapped steel. As would be expected the adherence is better than that between two clean lapped surfaces, and can be further improved by interposing a trace of liquid between the surfaces.

It should be mentioned that polished surfaces, whether of glass or steel, can also be brought together with the aid of a very thin liquid film. The adherence appears to be as good as that obtained between clean surfaces, but there is less risk of damaging the surfaces when they are separated, for, according to Budgett (*loc. cit.*), the separation of wrung surfaces takes place within the liquid film.

Since the wringing process is used so extensively to build up combinations of different lengths from separate gauges it is of importance to know whether the liquid film between two wrung surfaces has any appreciable thickness. The experiments described in this paper are chiefly concerned with measurement of this thickness, but with the results obtained it is possible to give a qualitative explanation of the general phenomenon of wringing.

(2) PREVIOUS WORK.

Pérard and Maudet* obtained an apparent negative value of 0·06 μ for the thickness of an oil wringing film between two lapped surfaces. They attributed this result to the superposition of two quantities of opposite sign: the real thickness of the oil film, which they considered to be of extreme order of smallness and not measurable, and the mutual crushing of the two surfaces caused by the large cohesive forces between them. The latter effect, they suggested, gave rise to a certain amount of interpenetration of the two scratched surfaces in contact.

They also found that the size of a combination of block gauges was unchanged when vaseline, vaseline oil and petrol were used as the wringing media, provided care was taken to ensure that a minimum quantity was used to form each film.

Peters and Boyd† have stated that when the wringing film is of alcohol its thickness between lapped surfaces is not greater than 0·025 μ, but with films of grease or moisture from the hands the thickness is uncertain and may amount to 0·07 μ.

---

* 'Trav. et Mém. Bureau Internat.,' vol. 17, p. 74 (1921).

† 'Sci. Papers Bureau Standards,' vol. 17, p. 691 (1922).

Previous work in the Metrology Department of the National Physical Laboratory[*] has indicated that the thickness of films of paraffin oil and condensed water vapour, formed between wrung lapped surfaces, is of the order of 0·025 μ, but that for the more viscous liquids like vaseline oil and olive oil, the thickness may be two or three times greater.

In the present experiments the measurement of film thickness has been made by two methods. The first, called the Area Method, depends upon measurement of the area attained by a known volume of liquid placed between two flat surfaces which are wrung together, and therefore gives the average thickness of a wringing film. The second, called the Interferometer Method, is based upon the comparison of the length of a wrung combination of block gauges with the sum of their individual lengths. The measurements are made optically, using light waves and their property of interference. This method gives the value of a quantity which is a function of the separation of the metallic surfaces due to the wringing film interposed between them.

(3) THE AREA METHOD.

(3)—(a) *General Description.*

A cylindrical block of hardened steel, 1 inch in length and 2 inches in diameter, had one of its end faces lapped so that it was flat to within 0·05μ over its whole surface. The opposite face was polished so as to be free from scratches, whilst the same accuracy of flatness was retained. To the centre of one of these flat surfaces a small drop of paraffin oil of known weight was transferred by means of a fine wire, and an accurately flat glass proof plane 3 inches in diameter and ⅝ inch thick was gradually wrung to the steel surface. As this was being done the oil drop flattened out to a disc which had, in general, a circular outline on both lapped and polished surfaces in its early stages. When the wringing process was complete the block and proof plane were left undisturbed, and it was found that the area of the disc continued to increase for about one hour on the lapped surface, and for three to six hours on the polished surface. Fig. 1 shows the rate of growth in diameter of the disc in one experiment with the lapped surface.

When the maximum area of disc had been attained its value was obtained by measurements through the glass plate. Knowing the weight, area and density of the oil film its average thickness could be calculated.

---

[*] 'Annual Report, N.P.L. (1922),' p. 113.

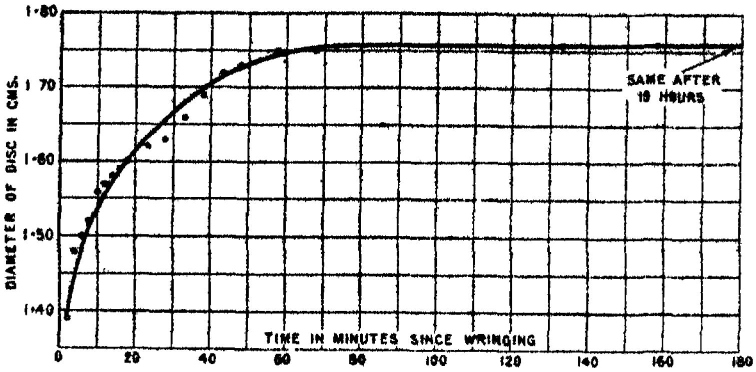

FIG. 1.—Growth in diameter of Wringing Film of Paraffin Oil on Lapped Surface.

(3)—(*b*) *Standardisation of Oil Drops.*

To determine the weight of oil used to form the film a pool of paraffin oil was formed on a glass plate, and into this the end of a fine copper wire of diameter 0·022 inch was dipped. The oil adhering to the end of the wire was then transferred to the centre of one of the steel surfaces by bringing the tip of the wire into contact with the steel. Observations showed that although no special precautions were taken to regulate the depth of the supply pool, the amount of oil transferred by successive dips was fairly constant.

The average weight of an oil drop was determined by transferring 30 drops to one surface of a block-gauge of known weight. The gauge was weighed after the addition of the 30 drops of oil, and the average weight of one drop was calculated. A correction for evaporation losses was applied.

Two sets of observations were taken. The first gave a value of $5 \cdot 0 \times 10^{-6}$ gm. as the average weight of one drop, and the second gave a value of $4 \cdot 8 \times 10^{-6}$ gm., the mean value being $4 \cdot 9 \times 10^{-6}$ gm.

(3)—(*c*) *Experimental Notes.*

A marked difference was observed in the manner in which the oil film expanded on the lapped and polished surfaces of the block after the initial wringing. On the lapped surface it was noticed that the oil film when viewed through a microscope, spread at a greater rate along the scratches than across them, the scratches obviously acting as channels for the oil.

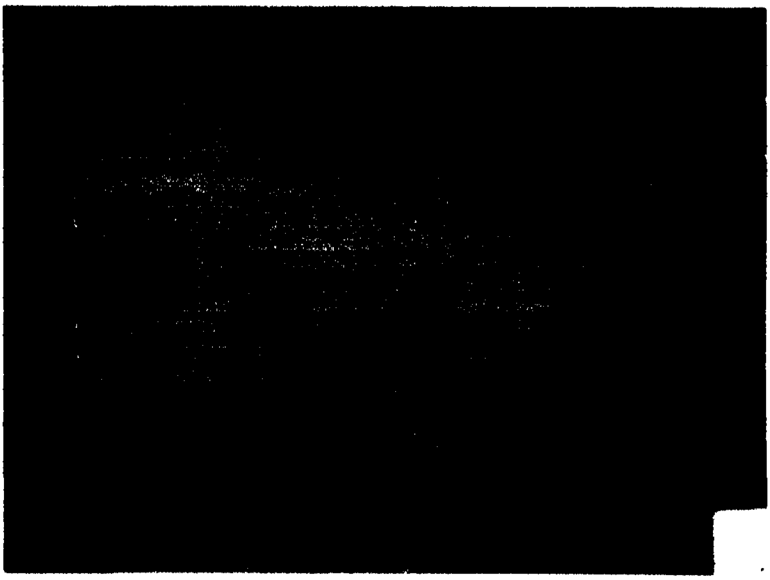

FIG. A.

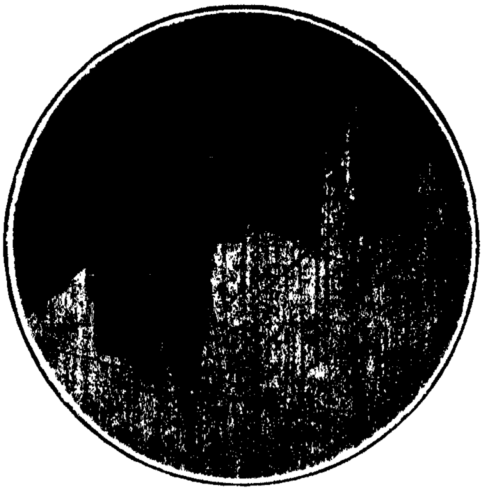

Fig. B.

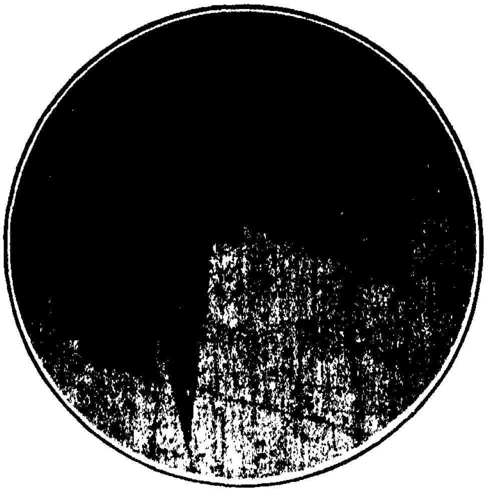

Fig. C.

Fig. D.

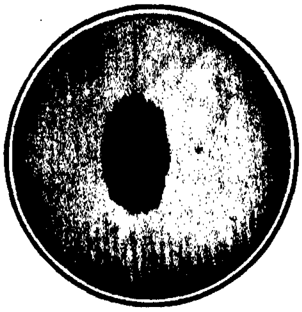

Fig. E.

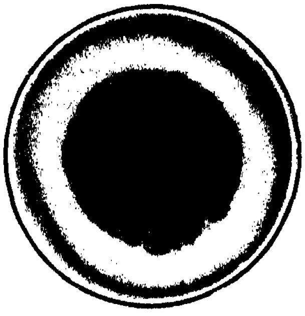

Fig. F.

This plate is Crown Copyright, and is contained in the Report of the National Physical Laboratory for 1926.

Figs. B and C (Plate 12)* are microphotographs (M = 19 diameters) showing two stages in the expansion of the edge of an oil film on the lapped surface of the steel cylinder, the time interval being five minutes. It will be seen that the film is bounded by scratches on the surface, and expansion of the film at a point is temporarily arrested until the trough formed by a scratch has been filled. For comparison the edge of a film formed between glass and the polished surface of the steel cylinder is shown in fig. D (Plate 12), and the disturbance due to a single scratch is plainly visible.

Fig. E (Plate 12) is a photograph of the final shape of a film on the lapped steel surface where the lapping marks are mostly in one direction. The outline of the film is roughly elliptical, due to the oil travelling faster along the scratches than across them. Fig. F (Plate 12) shows the corresponding shape attained by the same amount of oil on the polished surface of the steel. The outline here is practically circular, since, in the absence of scratches, there is no tendency for the film to spread more in one direction than another. It is also quite evident that the absence of scratches also allows the oil to spread over a larger area.

Measurement of the maximum area attained by an oil film between the steel and glass was made through the glass plate either with a travelling microscope, using normal illumination, or with a planimeter. The latter instrument could be used quite successfully, and values of a given area obtained by the two methods of measurement agreed within 2 per cent.

The adherence of the glass plate to the steel block was much greater when the polished surface of the latter was used. When applied to the lapped surface the glass plate could be readily removed after wringing by a sliding motion, an indication that the average thickness of the wringing film was large enough to allow shearing between the liquid molecules. This method of separation could not be applied, however, to the glass and polished steel surfaces. The contact had to be broken by a kind of peeling operation—the surfaces being gradually pulled apart in a direction normal to themselves. This peeling operation was greatly assisted by cooling with ether the glass surface not in contact with steel, so that the other surface assumed a convex shape; in this condition the glass readily parted company with the steel surface.

It need hardly be stated that the surfaces used in these wringing experiments were maintained as clean as possible. Cleaning was effected with cotton wool saturated with a cleaning mixture containing alcohol, ether and ammonium hydrate. The surfaces were then dried off with a special cotton wool that left no debris on them.

---

* Figs. B, C, D, E, F of Plate 12 are Crown Copyright and are contained in the Report of the National Physical Laboratory for 1926.

(3)—(*d*) *Results.*

(i) *Glass and Lapped Surface of Steel.*—Measurements were made of the minimum thicknesses attained by a series of films of paraffin oil formed between the glass plate and the lapped surface of the steel block. The values are plotted against corresponding order numbers in fig. 2. It will be seen that the values of the thickness lie evenly about a curve, showing that the average thickness of the oil film becomes less as the number of wringing increases, until an approximately constant value of 0·017 μ is reached between the fifteenth and twentieth wringings. It appears, therefore, that the process of wringing tends to wear down the high points of a freshly lapped surface, so that the scratches become less deep and the oil is forced to spread over a larger area.

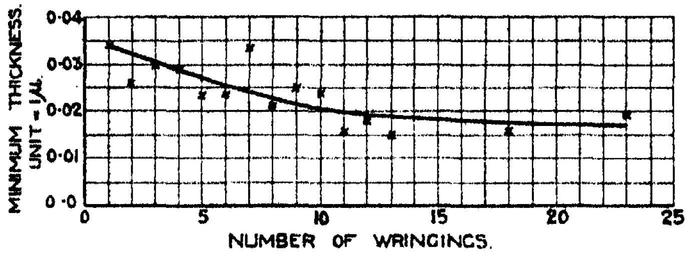

Fig. 2.—Films of Paraffin Oil between Glass and Lapped Steel.

(ii) *Glass and Polished Surface of Steel.*—It was found that a wringing film of paraffin oil formed between glass and the polished surface of the steel block required an average period of six hours to attain its maximum area. Using, as before, a standardised oil drop, the maximum area was always considerably greater than that between glass and lapped steel, *i.e.*, the film was much thinner. The following values of maximum area and minimum thickness were obtained in five experiments.

Table I.—Paraffin Oil Film between Optically Polished Steel and Glass Surfaces.

Area (sq. cm.)	12·6	9·5	9·6	14·7	13·1
Thickness ($\mu \times 10^{-3}$)	4·9	6·4	6·4	4·2	4·7

Mean Thickness = 0·0053 μ.

The average thickness of a wringing film of paraffin oil between optically polished steel and glass surfaces is therefore closely 0·005 μ. Referring back to fig. 2, the mean of the last five values of the thickness of the film between glass and lapped steel surfaces is 0·017 μ. The difference is undoubtedly due to the fact that the oil has to fill the scratches on the lapped surface.

(3)—(*e*) *Experiments with other Oils.*

Wringing experiments were also made with the optically polished steel and glass surfaces using vaseline oil and a heavy lubricating oil as the wringing media. After the initial wringing with these oils it was found that, owing to their viscous nature, the films spread with extreme slowness, and did not attain a constant area within three weeks. The thickness of the films was even then two or three times greater than the minimum thickness which had been obtained when using paraffin oil. The adherence was not strong and the glass plate could be made to slide off the steel block with comparative ease.

Artificial means were employed to spread these viscous oils to a state of minimum thickness. The adherence then became as great as that for paraffin oil.

It has been mentioned earlier that the glass surface in contact with the steel block could be made to assume a convex shape by cooling its other surface with ether. This was done immediately after placing the glass on the polished surface of the steel block, which had on it a drop of known weight of one of the viscous oils. Under these conditions the oil drop became enlarged to a disc about 5 mm. in diameter. The action of wringing the glass plate to the steel block caused the disc of oil to roll between the two surfaces, leaving in its track a faint smear which gradually increased in area at the expense of the liquid disc until it eventually covered a large portion of the steel surface. Then, as the glass recovered a uniform temperature and assumed its normal flatness, a black film of roughly circular outline appeared over the steel surface covered by the smear, and the glass plate became firmly attached to the block. The area of this dark film was measured and it was assumed that it represented the maximum area to which the oil could spread between the polished surfaces.

In contrast to the viscous oils paraffin always expanded continuously from the original drop and the film could be seen at all stages of its growth.

A series of experiments with paraffin oil drops showed that the method of accelerated spreading produced wringing films of the same average minimum thickness as those obtained when the drops expanded naturally. It is permissible, therefore, to use the method of accelerated spreading to derive the average minimum thickness of films of the viscous oils.

Drops of vaseline oil and the heavy lubricating oil were standardised by the method already described for paraffin oil, and the means of five measurements of minimum thickness for each of the oils were as follows :—

Vaseline oil	$0 \cdot 007\ \mu$
Lubricating oil	$0 \cdot 008\ \mu$

The mean value for paraffin was $0 \cdot 005\ \mu$, and it is evident that the more viscous oils can be forced to attain approximately the same minimum thickness. With this condition the adherence of the glass plate and polished steel surface appears to have the same quality whatever oil is used to form the wringing film.

(3)—(*f*) *Discussion of Results.*

It is of interest to note that the thickness of a wringing film of paraffin oil between polished surfaces, viz., $0 \cdot 005\ \mu$, is nearly equal to the limiting thickness ($0 \cdot 006\ \mu$) of black films of a solution of sodium oleate in water as obtained experimentally by several observers, notably Johonott and Chamberlain.* In addition, from theoretical considerations, Bakker† has stated that the minimum thickness of a liquid film in the free state is approximately three times the radius of molecular attraction. Lord Rayleigh‡ has also shown that the radius of molecular attraction is of the order of $0 \cdot 002\ \mu$ by determinations of the thickness of an oil film just necessary to arrest the motion of camphor particles on water. It would therefore seem that the minimum thickness of a wringing film between polished surfaces is about twice the radius of molecular attraction.

(4) THE INTERFEROMETER METHOD.

(4)—(*a*) *General Description and Theory.*

Two sets of nominally equal block gauges, of size 0·125 inch, and numbered respectively from 1 to 8 and 9 to 16, were specially made for this work by The Pitter Gauge and Precision Tool Co., Ltd., of Woolwich. All the gauges had lapped surfaces which were flat and parallel within $0 \cdot 05\ \mu$, many of them within $0 \cdot 02\ \mu$. They were arranged into eight pairs so that the difference in size of the members of any pair was not greater than $0 \cdot 03\ \mu$.

Their sizes at 62° F. (16°·67 C.) were determined by mechanical comparison with a standard block gauge, and are expressed in terms of the errors from nominal size (0·125 inch) in microns.

---

* 'Phys. Rev.,' vol. 31, pp. 170–182 (1910).

† 'Phil. Mag.,' vol. 17, p. 337 (1909).

‡ 'Roy. Soc. Proc.,' A, vol. 47, p. 364 (1890).

Table II.—Unit of error = 1 μ.

Pair.	(*a*)		(*b*)	
	Gauge No.	Error at 62° F.	Gauge No.	Error at 62° F.
g_1	1	− 0·30	2	− 0·30
g_2	3	− 0·30	4	− 0·30
g_3	5	− 0·33	7	− 0·36
g_4	8	− 0·31	6	− 0·31
g_5	9	− 0·26	10	− 0·26
g_6	12	− 0·26	15	− 0·25
g_7	14	− 0·25	11	− 0·22
g_8	16	− 0·28	13	− 0·29
$\Sigma(g)$	(A)	− 2·29	(B)	− 2·29

Each of these pairs of gauges was used in turn as the separator, approximately 0·125 inch in length, between two optically flat glass plates, the gauges being arranged one on each side of partially reflecting silver films $\frac{1}{4}$ inch wide, centrally deposited upon the faces of the glass plates (fig. 3). The glass plates were in wringing contact with the faces of the pair of gauges. In this manner a Fabry-Perot étalon was constructed whose optical length could be determined by observing the diameters of the circular interference fringes formed by the action of the parallel, semi-reflecting, silver films upon a convergent beam of monochromatic light.

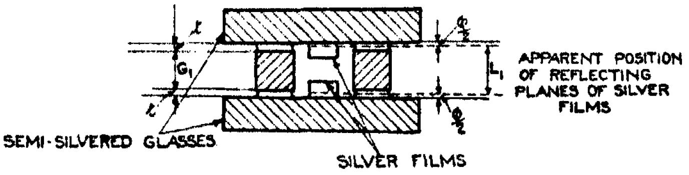

Fig. 3.

If L_1 represents the optical length of the étalon which has the gauge pair g_1 as separator, then :—

$$L_1 = G_1 + 2t - \phi, \tag{1}$$

where :—

G_1 = mean value of lengths of the gauge pair g_1, as defined by the separation of their ends,

t = separation of wrung surfaces of glass and lapped steel,

ϕ = correction due to the displacement of the reflecting planes of the silver films from the mechanical surfaces of the glass plates (see fig. 3).

It may be assumed that the correction is $\phi/2$ at each surface. The displacement is due partly to a phase loss suffered by light waves in normal reflection at a silver surface and partly to the thickness of the silver films.

Similar equations are derived for the gauge pairs $g_2, g_3 \ldots g_8$:—

$$\left.\begin{aligned} L_2 &= G_2 + 2t - \phi \\ L_3 &= G_3 + 2t - \phi \\ &\cdots\cdots \\ L_8 &= G_8 + 2t - \phi \end{aligned}\right\} \tag{2}$$

if the same pair of semi-silvered glasses is used throughout and t is constant.

From equations (1) and (2) :—

$$\Sigma\,(L) = \Sigma\,(G) + 16t - 8\phi, \tag{3}$$

where :—

$$\Sigma\,(L) = L_1 + L_2 + \ldots + L_8$$
$$\Sigma\,(G) = G_1 + G_2 + \ldots + G_8.$$

Now suppose that all the gauges of column (*a*), Table II, are wrung together into one combination (A), and those of column (*b*) into another combination (B). The two groups $\Sigma\,(g)$ may then be used as the separator, approximately 1 inch long (fig. 4) of the same semi-silvered glasses, forming a Fabry-Perot étalon

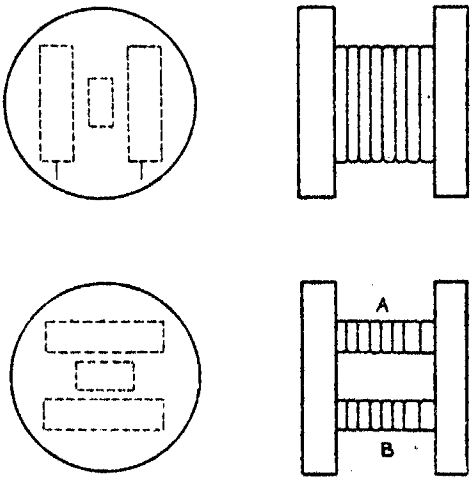

Fig. 4.

whose optical length L′ is given by the expression :—

$$L' = \Sigma\,(G) + 7t' + 2t - \phi, \tag{4}$$

where t' = separation of two wrung surfaces of lapped steel, t and ϕ remaining unchanged.

From equations (3) and (4) :—

$$\Sigma (L) - L' = 7 (2t - t' - \phi). \qquad (5)$$

The value of ϕ may be determined from another experiment, so that :—

$$(2t - t') = \frac{1}{7} [\Sigma (L) - L'] + \phi. \qquad (6)$$

The interferometer method is unable to determine separately the values of t and t'. In this respect it is not so useful as the area method, but it can be shown that the value of $(2t-t')$ obtained by the interferometer method is in good agreement with the value that may be derived from a consideration of the results of the area method. Furthermore, it will be seen later that the interferometer method provides a very accurate means of comparing wringing films of different liquids.

(4)—(*b*) *Experimental Notes.*

For measurement each étalon was placed with its optical axis vertical in the apparatus shown diagrammatically in fig. 5. One of the glass plates rested upon three $\frac{1}{4}$-inch steel balls, whose position with respect to the gauges is given in inset to fig. 5. This manner of support was found necessary to prevent any distortion of the glass plates by the action of the weight of the gauges upon them.

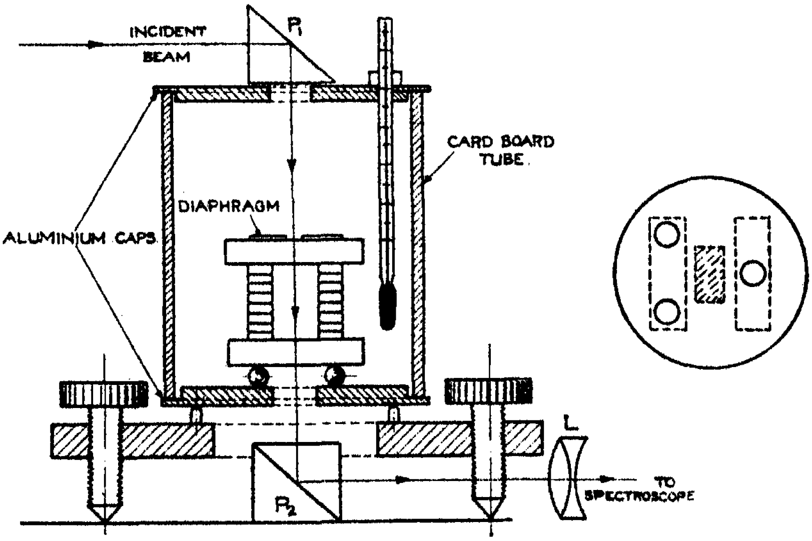

Fig. 5.

The étalon was shielded from draughts by a short length of cardboard tube which was closed at each end by aluminium caps having apertures at their centres about ½ inch in diameter. This simple means of protection enabled a sufficiently steady temperature of the étalon to be maintained. The tube and its caps stood upon a levelling table so that the direction of the axis of the étalon could be controlled.

The source of monochromatic radiations was a tube containing neon at low pressure excited to luminescence by a discharge from an induction coil. A convergent beam of light from the neon tube was directed vertically downwards through the étalon by the totally reflecting prism P_1. After passing the étalon the beam fell upon P_2 and was reflected towards the slit of a constant deviation spectroscope. A 12-inch lens L, between P_2 and the slit, focussed the system of interference fringes in the plane of the slit.

Photographs of the fringes in radiations from the region λ 5852 to λ 7032 of the neon spectrum were taken on Ilford Special Rapid Panchromatic Plates, with exposures of about 10 minutes. A travelling microscope instrument was used to measure linear diameters of the first three or five fringes in about five radiations on the photographic negatives. In visual work, measurements were made with an eyepiece micrometer fitted to the spectroscope.

If ε is the excess fraction of a light wave contained in the path difference set up by an étalon, then it can be shown that the following relation exists between ε and the squares of the linear diameters of interference fringes:—

$$\varepsilon = \frac{nd_n^2 - (n-1)\,d_{n+1}^2}{d_{n+1}^2 - d_n^2}$$

where d_n = linear diameter of the nth-fringe, counting outwards from the centre of the system. When $(n+1)$ fringes are measured, n values of ε are obtained, but the best value is derived by a least squares solution.

The excess fraction was calculated from measurements in three or five different radiations of known wave-length, and then the orders of interference for these radiations were derived by the usual method of coincidences, assuming an approximate value for the path difference (or twice the separation of the reflecting planes of the étalon). Since the orders of interference and the corresponding wave-lengths were then known the optical length of the étalon could be calculated in terms of each radiation used. Corrections were applied for the effect of varying refractive index of air upon the wave-lengths.

The phase loss of light reflected at metallic surfaces varies with the wave-length, so that ϕ (see equation 6) also varies with wave-length. For this reason the optical lengths of étalons were calculated only in terms of the bright yellow neon line at λ 5852 in the present measurements, because it was possible to measure most accurately the value of ϕ for that region of the spectrum.

The wringing process was standardised in the following way: Two surfaces to be wrung together were cleaned thoroughly with the cleaning mixture and cotton wool. One of the standard paraffin oil drops was transferred by the fine wire to the centre of one of the surfaces; the two surfaces were then brought together and wrung until they adhered firmly.

Each pair of gauges was wrung to the glass surfaces in four different arrangements with the object of compensating for the small errors of parallelism of the gauge surfaces. Four measurements of the combination $\Sigma\ (g)$ were made in the same way, treating (A) and (B) as single gauges. The whole 16 gauges were wrung anew for each measurement, but care was taken to ensure that the same gauge surfaces were in contact throughout.

An étalon made up with a single gauge pair was left in the apparatus for at least one hour after wringing before it was measured. Observations showed that this period was sufficient to allow the étalon to reach a steady temperature. Étalons made up with the combinations (A) and (B) were left at least two hours in the apparatus before measurement. Fig. 6, curve (1), shows the change in length of $\Sigma\ (g)$ with time after the gauges had been wrung with paraffin oil. The change in length was due partly to loss of heat absorbed by the gauges during wringing and partly to spreading of the oil films (see fig. 1).

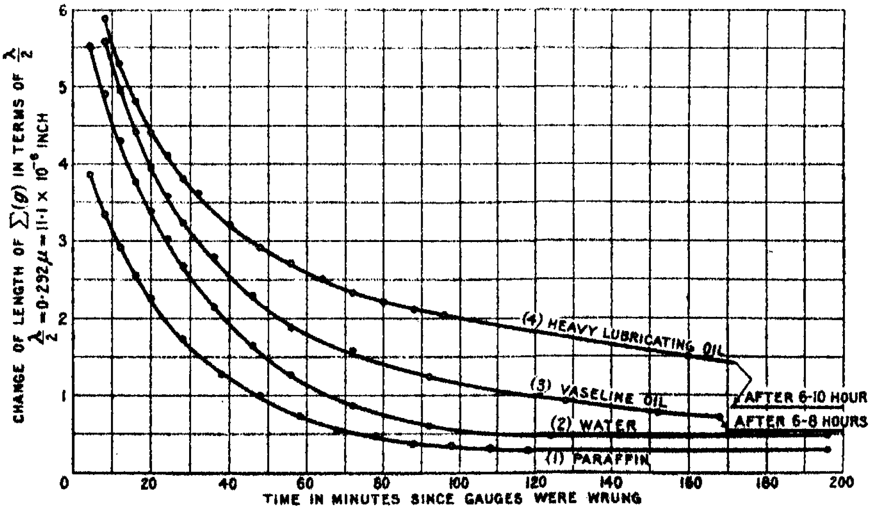

FIG. 6.

Room temperatures during the whole series of measurements varied from 15° C. to 20° C., but the optical lengths of étalons were reduced to values at a mean temperature of 18°·25 C. The coefficient of expansion of the gauges was obtained by measuring the optical length of the Σ (g) étalon at a series of temperatures near 16° C., 17°·5 C. and 19° C.

(4)—(*c*) *Measurement of* ϕ.

For the measurement of ϕ the surfaces of the two semi-silvered glasses were placed face to face, but separated by strips of thin paper, so that they enclosed a wedge-shaped air film of small thickness. This wedge interferometer was examined in a parallel beam of yellow monochromatic light (λ 5875) from a helium tube, observing the silvered portions by transmitted light and the unsilvered portions by reflected light.

Suppose that in fig. 7 the dotted lines represent the apparent positions of the reflecting planes in silver for yellow light. If these planes are coincident with the adjacent glass surfaces bright fringes in the transmitted system coincide with dark fringes in the reflected system. There was, actually, a small displacement between the two systems, and its value ϕ (equation 1, p. 409) was measured. From fig. 7 it is obvious that $\phi = \text{KL} - \text{MN}$.

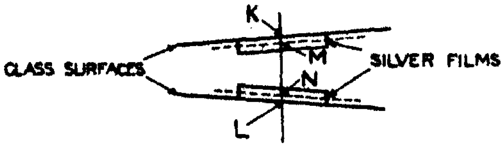

Fig. 7.

The displacement was measured by both visual and photographic means.

(4)—(*d*) *Results.*

(i) *Value of* ϕ.—

By visual method, $\phi = 0{\cdot}003_2\ \mu$
By photographic method, $\phi = 0{\cdot}008_5\ \mu$
Mean value of $\phi = 0{\cdot}006\ \mu$

Equal weights were assigned to the values in calculating the mean. For the visual method the result was obtained from measurements of 18 fringes, and for the photographic method the result was obtained from measurements of three negatives, each of which showed five fringes. The mean value of ϕ refers to light of wave-length λ 5875.

Since the value of ϕ is very small the experimental error appears very large by comparison, and in deriving the final result of the interferometer method it is necessary to associate with ϕ a possible range of $\pm\ 0{\cdot}003\ \mu$. It will be found that the interferometer method is affected throughout by the fact that the experimental errors are of the same order of magnitude as the quantity which it finally derives. For this reason alone, the method, so far as it relates to the determination of the absolute magnitude of ϕ, can be regarded only as a check upon the results obtained by the more direct method described in section (3). As such, the result found is satisfactory.

(ii) *Optical Lengths of Étalons.*—In the following table the quantities $L_1 \ldots L_8$ are those defined by equations (1) and (2); L' and L'' are, respectively, the optical lengths of the étalon Σ (g) before and after the optical lengths $L_1 \ldots L_8$ were determined. The only difference in conditions was that the same surfaces were not in contact for L' as for L''. The values are expressed in microns, and at a temperature of 18°·25 C. Temperature corrections were made using a coefficient of $11 \cdot 52 \times 10^{-6}$ per 1° C., which was determined in the way already described.

Table III.

		Optical length (μ) at 18°·25 C.	Means.			Optical length (μ) at 18°·25 C.	Means.
L'	*a*	25,398·086	25,398·075	L_5	*a*	3,174·789	3,174·767
	b	·051			*b*	·758	
	c	·125			*c*	·754	
	d	·038			*d*	·768	
L_1	*a*	3,174·713	3,174·714	L_6	*a*	3,174·814	3,174·822
	b	·726			*b*	·831	
	c	·703			*c*	·844	
	d	·716			*d*	·798	
L_2	*a*	3,174·736	3,174·712	L_7	*a*	3,174·802	3,174·817
	b	·711			*b*	·802	
	c	·692			*c*	·819	
	d	·710			*d*	·846	
L_3	*a*	3,174·720	3,174·738	L_8	*a*	3,174·717	3,174·734
	b	·767			*b*	·745	
	c	·705			*c*	·734	
	d	·761			*d*	·738	
L_4	*a*	3,174·767	3,174·756	L''	*a*	25,397·980	25,398·028
	b	·745			*b*	8·041	
	c	·766			*c*	·014	
	d	·747			*d*	·079	

The eight values for L' and L'' are plotted on the left of fig. 8 against the number of wringings the gauges had experienced, making due allowance for the four complete wringings which were made in the determinations of $L_1, L_2, \ldots, L_8$. The points enclosed by dotted circles were obtained by calculation from the values of $L_1, L_2, \ldots, L_8$ given in the table. For instance the value for the 59th wringing was obtained by calculation from the sum of all the values marked "*a*" for L_1 to L_8, and so on. The curve of fig. 8 starts at the 55th wringing because the gauges had experienced 54 wringings during preliminary work.

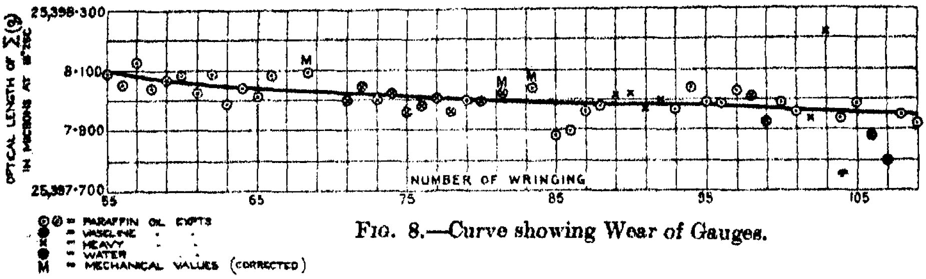

FIG. 8.—Curve showing Wear of Gauges.

The gradual shortening of the combination Σ (*g*) is quite obvious on the figure, and amounts to about 0·06 μ for twelve wringings. It is undoubtedly due to wear of the gauge surfaces.

For the calculation of $(2t-t')$ the mean of L′ and L″ was taken in order to eliminate the effect of wear.

(iii) *Calculation of* $(2t - t')$

$$\left.\begin{aligned}\Sigma\,(\mathrm{L}) &= 25{,}398\cdot060\ \mu\\ \text{Mean L}' &= 25{,}398\cdot052\ \mu\end{aligned}\right\}\text{from Table III.}$$

By equation (6),

$$(2t-t') = \tfrac{1}{8}\,[\Sigma\,(\mathrm{L}) - \mathrm{L}'] + \phi$$

$$(2t-t') = 0\cdot001\ \mu + 0\cdot006\ \mu$$

$$= 0\cdot007\ \mu.$$

It is possible to calculate the probable effect of the small variations shown in Table III, and the difference between the two values of ϕ upon the value of $(2t-t')$. Such calculations show that the probable range of values of $(2t-t')$ is $\pm\,0\cdot005\ \mu$. The value of $(2t-t')$ is therefore $0\cdot007\ \mu \pm 0\cdot005\ \mu$.

Suppose that the thicknesses of wringing films of paraffin oil formed under certain conditions are represented by the following expressions:—

t'', between two polished surfaces,
t, between a polished surface and a lapped surface,
t', between two lapped surfaces.

Then it may reasonably be assumed that the value of t is a mean between the values of t' and t'', or that,

$$2t = t' + t''.$$

The area method has shown that the thickness t'' of a wringing film of paraffin oil between polished surfaces of glass and steel is $0 \cdot 005\ \mu$. On the above assumption, therefore, by the area method,

$$(2t - t') = 0 \cdot 005\ \mu.$$

The difference between $2t$ and t', actually derived by the interferometer method, is $0 \cdot 007\ \mu$, and is in good agreement with the value derived by the area method.

In both methods the magnitude of the quantity to be measured is so small that observational errors appear relatively large. But since the area method measures the film thickness by practically direct means, it is of greater value than the interferometer method, which does not produce a simple result and can only be regarded as a useful check upon the former method. For the purposes of comparing films of different liquids and of observing the wear of gauge surfaces during successive wringings the interferometer method is, however, of great importance.

(5) COMPARISON OF FILMS OF DIFFERENT LIQUIDS BY THE INTERFEROMETER METHOD.

Having confirmed the results of the area method, using paraffin oil as the wringing medium, the interference method was used with the heavier oils, viz., vaseline oil and heavy lubricating oil. Two experiments were also made with water as the medium.

The combination $\Sigma\ (g)$ was wrung together, using an approximately constant amount of liquid to each film, in the manner described for paraffin oil. The glass plates, however, were wrung to the combination with paraffin oil in every measurement, so that any difference in optical length would be due solely to seven steel-steel wringing films. Owing to wear of the gauges by repeated wringings, measurements of the combination wrung with paraffin oil were made frequently to give reference points.

The results are shown in fig. 8, where the optical lengths are plotted against the number of wringings the gauges had experienced. Here again the results of the area method are well confirmed. Since the observations for the viscous oils are fairly evenly distributed about the curve of wear of the gauges, as determined by paraffin oil observations, wringing films of the three oils must have approximately the same thickness.

Observations marked M in fig. 8 were calculated from mechanical measurements made by comparison of the combination of the 16 gauges with a standard 2-inch end-gauge. It will be noted that there is fair agreement between the optical and mechanical lengths, the latter being on the average about 0·04 μ greater than the former.

It will be observed that the paraffin oil observations corresponding with wringing numbers 85 and 86 are low, the heavy oil observation at 103 is high and the water observations at 106 and 107 are low. The paraffin oil observations at 85 and 86 were not reliable owing to abnormal temperature changes that took place during these two measurements. The high value for the heavy oil at 103 was probably due to faulty wringing. No explanation can be advanced for the low water observations.

The vaseline and heavy lubricating oils, having greater viscosities than paraffin, took longer to settle down to the minimum film thickness. The effect is shown in curves (3) and (4) of fig. 6. Unless excess oil was used little change occurred after three hours, but in all experiments with the heavier oils a period of at least six hours was allowed to elapse after wringing the gauges together.

(6) COMPARISON OF FILMS OF DIFFERENT LIQUIDS BY A MECHANICAL METHOD.

As a check on the equality of film thickness with different oils a series of comparisons of the length of the combination of 16 ⅛-inch gauges with a standard 2-inch gauge was made when the gauges were wrung together in turn with paraffin oil, vaseline oil and the heavy lubricating oil as the wringing medium. Additional comparisons were made with the combination brought together in as clean a state as possible. The comparisons of the combination with the 2-inch standard were carried out on a level comparator.*

The wringing of the gauges together was performed in the manner already described, using the minimum quantity of oil for each film consistent with good adherence. After each comparison the oil was cleaned off with the special cleaning mixture.

In the following table the sizes of the combination are given in terms of the error from nominal size (2 inches), the unit being one hundred-thousandth of an inch.

Table IV.—Unit of Error = 1 × 10^{-5} inch.

Medium.	Readings.					Means.
Paraffin oil	−19·1	−19·1	−19·1	−19·3	−19·3	−19·18
Vaseline oil	−18·9	−19·3	−19·1	−19·2	−19·2	−19·14
Lubricating oil	−19·1	−19·1	−19·1	−18·9	−19·1	−19·06
No film	—	−18·9	−18·8	−18·9	−18·9	−18·87

---

* 'Annual Report N.P.L. (1919),' pp. 85–87.

The table shows that the size of the combination is constant, within about one-millionth of an inch (0·025 μ), irrespective of the wringing medium. When the combination is wrung together without any film it is, if anything, slightly larger than when wrung together with oil. This difference is probably due to the fact that the adherence between gauges was appreciably diminished when no films were interposed and the contact was somewhat uncertain.

A description of similar comparisons by mechanical means of the size of a combination of gauges wrung together with different liquids appeared in the Annual Report of the National Physical Laboratory for 1922, p. 113. These comparisons showed that a film of vaseline oil was on the average about 0·025 μ thicker than a film of paraffin or petrol, a result which does not conform with the present work.

In order to find an explanation of this disagreement some further experiments were performed, and it was found that by wringing with an excess of one of the viscous oils the size of the combination was appreciably enlarged, but could still be approximately reproduced in successive wringings by repeating the quality or "feel" of the contact. These enlarged films showed no tendency to diminish when left undisturbed, but in all cases the minimum size could be attained by cleaning off the excess of oil and rewringing.

(7) WEAR OF GAUGE SURFACES DURING WRINGING.

Reference to fig. 8 will show that wear of the gauge surfaces was still in progress, even after 100 wringings, but it was less rapid than at the fiftieth wringing. The total loss in length of the combination from the fifty-fifth to the one hundredth-and-ninth wringing was approximately 0·15 μ. In all there were 18 surfaces in contact for this étalon, including the two glass surfaces. Therefore, the average amount of wear at one surface per wringing was about 0·00015 μ or $1 \cdot 5 \times 10^{-8}$ cm.—a quantity which is of the same order of magnitude as the molecular diameter.

In fig. 9 is given a set of curves which show the effect of different grades ot lapped finish upon the rate of wear of gauge surfaces. Three sets of eight ¼-inch block gauges were made. Those of Set I had surfaces of fine finish, Set III had surfaces of coarse finish, and Set II had surfaces of finish intermediate between those of Set I and Set III. Each set was wrung together repeatedly with paraffin oil and its overall length measured by means of a millionth comparator* (surface contact type). The curves show diminution of this length during 200 wringings in units of 1×10^{-5} inch.

---

* 'Annual Report N.P.L. (1919),' pp. 86, 87.

The rate of wear of each set was most rapid during the first 50 wringings, being greatest for the set of coarsely finished surfaces. After this the sets of fine and intermediate finish tended to reach a constant state, the latter being apparently better than the former. On the other hand, with the gauges of coarse finish the wear quite evidently persisted after 200 wringings. From the

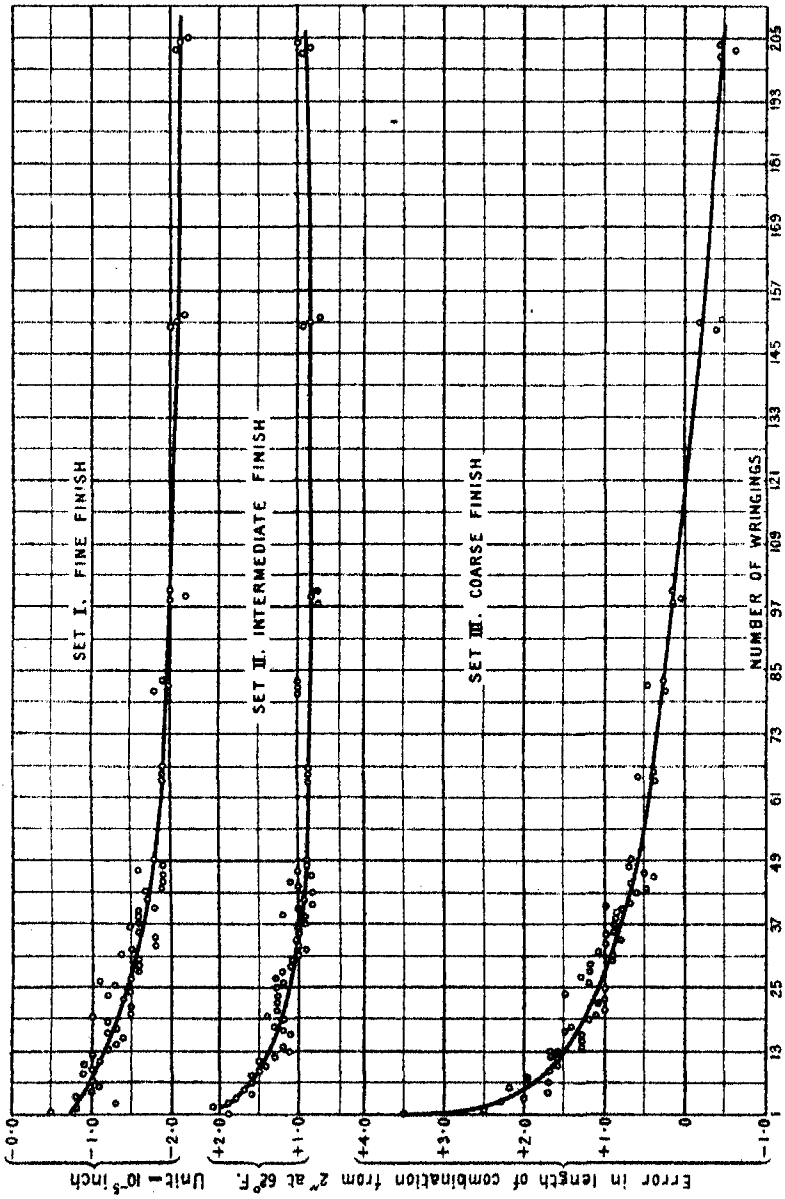

FIG. 9.—Wear of Block Gauges due to Wringing.

curves, the total wear of eight gauges during 200 wringings was $1\cdot4 \times 10^{-5}$ inch or $0\cdot36\ \mu$ for Set I, $1\cdot2 \times 10^{-5}$ inch or $0\cdot30\ \mu$ for Set II, and $3\cdot2 \times 10^{-5}$ inch or $0\cdot81\ \mu$ for Set III. The average wear per surface per wringing was therefore $1\cdot1 \times 10^{-8}$ cm. for Set I, $1\cdot0 \times 10^{-8}$ cm. for Set II, and $2\cdot5 \times 10^{-8}$ cm. for Set III; all these quantities are of the same order of magnitude as the molecular diameter.

(8) DISCUSSION.

The results of experiments described in this paper may be summarised as follows:—

(i) The thickness of wringing films of paraffin oil between flat, polished surfaces of steel and glass is $0\cdot005\ \mu$. It is somewhat less than the limiting thickness of free films of a solution of sodium oleate in water, as determined by Johonott and Chamberlain, and is roughly twice the accepted value of the radius of molecular attraction. Lubricants, such as vaseline oil and ordinary lubricating oil, form wringing films between polished surfaces of steel and glass of thicknesses $0\cdot007\ \mu$ and $0\cdot008\ \mu$ respectively, when artificial means of spreading them between the surfaces is applied.

(ii) Owing to the presence of scratches upon lapped surfaces the average thickness of a wringing film between such surfaces, as determined by the area method, does not represent the thickness of that part of the film which separates the planes containing the high regions on the surfaces. The interferometer method only gives the value of a quantity which is a function of this separation; the magnitude of this quantity does, however, confirm the results of the area method for polished surfaces.

(iii) Wringing films of lubricants between lapped surfaces have the same thickness as films of paraffin oil.

(iv) The contact between flat surfaces which are wrung together with the liquids mentioned above can be repeated to an accuracy of about $0\cdot01\ \mu$ to $0\cdot02\ \mu$.

(v) The lapped surfaces of end-gauges show evidence of wear during repeated wringings. Wear is most rapid when the surfaces are new, and its rate declines as the number of wringings increases. Averaged over a large number of wringings the wear per surface is of molecular dimensions each time a contact is realised.

With this data it is possible to put forward qualitative explanations of certain properties of wrung surfaces.

Consider first the circumstances of contact between a liquid and a flat solid surface. In fig. 10 (*a*) the influence of solid molecules extends to a distance R into the liquid, where R is their radius of attraction. The layer of liquid molecules in immediate contact with the solid is in the most intense region of the molecular field extending from the solid. Proceeding upwards from the solid surface the field diminishes in intensity until, at the dotted line, it has a vanishingly small value. Above the dotted line liquid molecules exist in a field of force due to other liquid molecules alone. For these reasons it is probable that the stratum of liquid within a distance R of the solid surface has a structure corresponding to a gradual transition from the solid to the liquid phase.

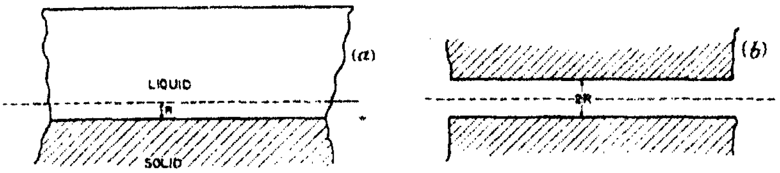

Fig. 10.

Furthermore, Hardy* states that the molecules at the surface of a solid or liquid are highly oriented by the normal component of the forces of attraction. At a solid-liquid interface this orientation of liquid molecules persists until a critical distance from the solid is reached, where the attraction of the liquid for itself is greater than its attraction for the solid. Beyond this the random arrangement of molecules which permits fluidity in a liquid is in existence, and the orientation is destroyed. Hardy therefore assigns a peculiar significance to the plane defined by the dotted line in fig. 10 (*a*). He describes it as a natural plane of cleavage or slip in the liquid when tangential stress is applied, and shows that it is of fundamental importance in the problems of boundary lubrication.

Let us further consider a film of thickness 2R between two flat solid surfaces of the same material. It is clear that in fig. 10 (*b*) every liquid molecule is under the influence of solid molecules. The film has lost its property of fluidity and is in a condition which may be described as quasi-solid.

Since Hardy† has obtained results in experiments on boundary lubrication which indicate that the value of R for different solids may vary, a film of thickness ($R_1 + R_2$) between solid surfaces of different materials whose molecules possessed radii of attraction R_1 and R_2 would have similar properties to the one described above.

---

* 'Phil. Mag.,' vol. 38, p. 37 (1919); 'Roy. Soc. Proc.,' A, vol. 100, p. 565 (1922).

† 'Roy. Soc. Proc.,' A, vol. 108, p. 27 (1925).

It was noted in section (3) that a wringing film between two flat polished surfaces of glass and steel offered great resistance to shearing, and that the only means of breaking it was by a "peeling" operation of the surfaces. These properties are capable of explanation if its thickness is $(R_1 + R_2)$, where R_1 and R_2 are the radii of attraction of molecules in steel and glass surfaces. In normal displacement of the two surfaces, the motion is resisted solely by the attractive forces between molecules. A shearing displacement is resisted partly by the same forces and also by a disinclination of the film molecules to disturbance of their orientation in the molecular fields due to the two solids. The latter factor may be as great or even greater than the resistance to displacement of the liquid molecules along the normal to the interface.

From these considerations it would seem that the maximum thickness of a wringing film between solid surfaces must be of the same order of magnitude as twice the radius of attraction of the solid molecules.

If the film has a thickness greater than 2R or $(R_1 + R_2)$ there is a stratum outside the range of the molecular fields of the solid surfaces. This stratum exists as a normal liquid possessing fluidity and does not offer great resistance to shearing stresses. Lapped surfaces have scratches upon them which may be assumed to be relatively deep compared with the quantities 2R or $(R_1 + R_2)$. Thus, between lapped surfaces the film has a thickness greater than 2R or $(R_1 + R_2)$ in the neighbourhood of scratches so that, on the whole, the film must be appreciably weaker than that formed between polished surfaces. A film between glass and lapped steel should have properties, by this reasoning, which are intermediate between those already considered.

In practice it has been found that the adherence between glass and lapped steel surfaces is better than that between two lapped steel surfaces, and in both cases the adherence is inferior to that between two polished surfaces. It is also well known that a pair of freshly lapped surfaces adhere better when their high points have been reduced by wear, that is, when a film of less average thickness can be produced.

In order to account for surface wear in the wringing of lapped surfaces it appears necessary to assume that relatively high points may come into absolute contact. Absolute contact of two surfaces implies that molecules in each surface come within the range of both the repulsive and attractive fields of forces, and that at separation the surface layers are greatly disturbed or even torn away from the parent bodies. Hardy has shown that the thickness of a lubricating film is a function of the pressure upon it. Thus between a spherical surface and a plane the film may be only two molecules thick, owing to the enormous pressure that may be set up over a small area. Tomlinson* in some experiments on friction between a sphere and plane has obtained results which he considers can only be explained by assuming that absolute contact between the two bodies takes place locally when the pressure is sufficiently great, even though a lubricating film is present. It is therefore conceivable that points of elevation on lapped surfaces may be forced through the wringing film and set up absolute contact, while the rest of the surfaces are still separated by film. Damage occurs to these elevated points upon separation, and therein lies the probable explanation of the wear of lapped surfaces. It has been already mentioned that, on the average, the amount of wear per surface per wringing is of molecular dimensions. The curves of rate of wear show that the rate declines as the number of wringings increases. This can be taken as a proof that, as the elevated points break down there is less likelihood of the surfaces meeting in absolute contact.

It is not necessary to suppose that this reduction in thickness of a gauge of approximately one molecular diameter per wringing connotes the removal of a complete layer of molecules from the surface. Only a comparatively small proportion of the total surface, on the highest points, would be forced into the intimate contact which results in detachment of the molecules.

The fact that liquid films entirely within the influence of solid molecules may have a quasi-solid structure leads to another possible explanation of the mechanism of wear not dependent upon absolute contact of the solids. On this view it must be supposed that the quasi-solid film may affect the surface molecules of the solid surfaces upon separation in the same way that the molecules of solid surfaces affect each other when they are separated after absolute contact. This implies that the thickness of a wringing film between lapped surfaces cannot be of greater magnitude than twice the radius of attraction of solid molecules.

Whatever view is taken of the cause of wearing the upper limit of the separation of lapped steel surfaces cannot be greater than twice the radius of attraction of steel molecules.

If it be assumed that the separation of wrung surfaces is exactly twice the mean radius of attraction of the solid molecules, then the mean radius of attraction of glass and steel molecules is between $0 \cdot 002\ \mu$ and $0 \cdot 003\ \mu$.

The adherence of flat surfaces in wringing contact has its origin in the cohesion of molecules of the film. As Guillaume* has pointed out, the experiments of Berthelot and Worthington demonstrate that liquids possess strong cohesive forces. For instance, Worthington† was able to exert on ethyl alcohol a tension corresponding to 17 atmospheres when the liquid was contained in a glass bulb which it entirely filled. Guillaume (*loc. cit.*) gives a figure of 15 kg. per square centimetre for the direct pull necessary to separate two block gauges wrung together with a lubricant. This corresponds to a tension of about 15 atmospheres, and is, therefore, of the same order of magnitude as Worthington's values for the tensile strengths of liquids.

---

* 'Roy. Soc. Proc.,' A, vol. 115, p. 472 (1927).

The writers wish to thank Sir Joseph Petavel and Mr. J. E. Sears for their encouragement and for facilities for carrying out the experiments at the National Physical Laboratory.

The Theory of Metallic Corrosion in the Light of Quantitative Measurements.

By G. D. BENGOUGH, J. M. STUART and A. R. LEE.

(Communicated by H. C. H. Carpenter, F.R.S.—Received June 11, 1927.)

The principal object of the present research is the discovery of a satisfactory way of measuring the corrosion of metals in water and dilute salt solutions, and the use of it to test the adequacy of the newer electrochemical theory of corrosion as applied to such media. The theory suggests that a large number of factors can influence the rate of corrosion, but does not indicate quantitatively their relative importance in given conditions, in fact, the theory is based at present upon qualitative or only roughly quantitative measurements. It is desirable, therefore, that a determined attempt should be made to place it upon a sounder basis, on account, both of the inherent interest of the theory and of its importance in technical problems of steadily increasing insistence.

The present communication is the first portion of an extensive research; it is divided into three sections, the first gives an outline of the theory as understood by the authors; the second, a brief review of the kind of measurement upon which it rests; the third an improved method of measuring corrosion as applied to the metal zinc, together with an interpretation of the results so far obtained.

---

* 'Récents Progrès du Système Métrique,' p. 11 (1921).

† 'Phil. Trans.,' A, vol. 183, p. 355 (1893).

SECTION I.

The Electrochemical Theory of Corrosion.

By the term corrosion of a metal the present authors mean the chemical or electrochemical oxidation of that metal. In the present communication chemical oxidation of a metal means oxidation without passage into solution; electrochemical oxidation connotes passage into solution at the moment of oxidation. At elevated temperatures, in the absence of liquid electrolytes, the oxidation may be regarded as typically chemical; at atmospheric temperatures, in the presence of electrolytes, as typically electrochemical.

The work of W. H. J. Vernon* and of U. R. Evans† suggests that chemical oxidation may take place to a small extent even at laboratory temperatures and in the presence of liquids, but there is now a general agreement that the oxidation of metals immersed in water or salt solutions at atmospheric temperatures is *mainly* an electrochemical process.

The work upon which this general agreement is based is extensive and only a very brief review can be given. Whitney,‡ in 1903, was the first to formulate a general theory of corrosion on electrochemical lines. His paper contained very little experimental work and no quantitative corrosion measurements, and related to a single metal, iron. His theory was really based on general chemical knowledge, and he left it to future workers to test it experimentally.

He considered that iron when suffering from corrosion always passes into or through a state of solution, " and . . . we have really to consider the effect of conditions upon the potential difference between iron and its surroundings. The whole subject of corrosion of iron is, therefore, an electrochemical one, and the rate of corrosion merely a function of electromotive force and resistance of circuit. If now we apply Nernst's conception of the source of electromotive force between a metal and a solution we must conclude from the measured potential difference that iron in contact with an aqueous solution tends to dissolve, ionise or oxidise with a force expressed as equivalent to about 10,000 atmospheres pressure at ordinary temperature." Whitney further stated that " iron should tend to dissolve in any aqueous solution until the concentration of the electrically charged iron ions reaches such a concentration that the osmotic pressure is equal to the above value." In order that the tendency to dissolve should be translated into practice Whitney argued (by analogy with a Daniell cell) that the presence of a second electrode having a lower electrolytic solution pressure than iron, and in electrical connection with it, was necessary; he thus brought into prominence the idea that the presence of a second phase with a relatively low solution pressure was necessary to the corrosion of an ordinary metal. This idea certainly suggests that a pure homogeneous metal would not corrode and that increased purification would reduce corrosion. Bancroft[*] points out that Whitney did not make a definite statement to that effect, nevertheless, a majority of the exponents of the theory adopted the idea, particularly Cushman,[†] Walker[‡] and Lambert,[§] and his associates, who regarded it as a central feature of the theory. Whitman,[||] on the other hand, considers that two contiguous molecules of a pure metal may serve as anode and cathode and set up corrosion, and N. K. Chaney[¶] considers that the same point on a metal surface may serve as both anode and cathode.

---

* Reports to the Atmospheric Corrosion Research Committee. 'Trans. Faraday Soc.,' vol. 19, p. 839 (1924), vol. 23, p. 113 (1927).

† 'J. Chem. Soc., vol. 127, p. 2484 (1925), vol. 131, p. 1020 (1927).

‡ 'J. Amer. Chem. Soc.' vol. 25, p. 394 (1903).

Whitney further stated that "iron, when placed in a solution containing hydrogen ions will dissolve as the hydrogen precipitates, just exactly as when placed in the copper salt solution. That iron does oxidise or dissolve in all solutions containing appreciable quantities of hydrogen ions is well known. This electrochemical relationship between iron and hydrogen is the primal cause of rusting."

Whitney's original theory has been examined experimentally, emended and expanded from time to time by so many workers that only a small minority can be mentioned here. Walker,[**] Cederholm and Bent were the first to indicate the true function of oxygen in corrosion, namely, cathodic depolarisation. Bancroft[††] and others emphasised the importance of the formation of electrolytic double layers and of over-voltage. Lambert[‡‡] and his associates showed that visible corrosion of a highly purified iron did not take place in highly purified water in presence of oxygen, but could take place in certain solutions in the absence of acid or any substance likely to produce acid—a matter upon

[*] 'J. Phys. Chem.,' vol. 28, p. 785 (1924).

[†] 'Trans. Amer. Electrochem. Soc.,' vol. 12, p. 403 (1907).

[‡] 'Trans. Amer. Electrochem. Soc.,' vol. 39, p. 53 (1921).

[§] 'J. Chem. Soc.,' vol. 97, p. 2426 (1910), vol. 101, p. 2056 (1912), vol. 107, p. 218 (1915).

[||] 'Publ. Massachusetts Inst. Techn.,' Nos. 154 and 419 (1926).

[¶] 'Trans. Amer. Electrochem. Soc.,' vol. 29, p. 447 (1916).

[**] 'J. Amer. Chem. Soc.,' vol. 29, p. 1251 (1907).

[††] *Loc. cit.*

[‡‡] 'J. Chem. Soc.,' vol. 101, p. 2068 (1912), and vol. 107, p. 218 (1915).

which acute disagreement had occurred. J. Aston[*] drew attention to the peculiar effect of differences of oxygen distribution in causing corrosion; Bancroft, Bengough and Stuart[†] and others have stressed the effects of films of corrosion products.

Newton Friend[‡] studied the effect of alkalies and drew attention to the importance of the presence of colloids. Speller[§] and R. E. Wilson[||] suggested that the factors which control the corrosion process vary with the conditions, particularly the hydrion concentration. The work of U. R. Evans,[¶] from the year 1923 onwards, has been especially important in explaining a number of facts which did not previously seem to be covered satisfactorily by the theory; more detailed reference is made to his work later.

As a result of the labours of these and other workers a corrosion theory has now been built up which appears to give a satisfactory account of the process on a qualitative or roughly quantitative basis. The theory may be briefly summarised as follows:—

(1) $M + 2H^{\cdot\cdot} \rightarrow M^{\cdot\cdot} + 2H$ (nascent);

(2) $2H + \frac{1}{2}O_2 \rightarrow H_2O$ (a little H_2O_2 is also sometimes formed)

$\downarrow$

or (2*a*) $2H \rightarrow H_2$ (molecular)

according to the nature of the metal M and the concentration of hydrogen ions and oxygen; with relatively inert metals, low hydrion and high oxygen concentration (2) will take place; with reactive metals high hydrion and low oxygen concentration (2*a*) will occur; in intermediate conditions both reactions may occur side by side; when hydrogen is evolved as gas over-voltage may become an important factor in corrosion.

Equation (1) may be divided into an anodic reaction:—

$$M + 2 \bigcirc\!\!\!\!\!+ \rightarrow M^{\cdot\cdot}$$

and a cathodic reaction:—

$$2H^{\cdot} \rightarrow 2H + 2\oplus.$$

From these reactions it is clear that corrosion will usually cause a general increase in alkalinity, since hydrogen ions are being replaced by metal ions. In solutions of salts of alkali metals alkalinity will be specially noticeable at cathodes, but *local* acidity may occur at anodes, owing to hydrolysis of anodic products such as metallic chlorides.

---

[*] 'Trans. Amer. Electrochem. Soc.,' vol. 29, p. 449 (1916).

[†] 'J. Inst. Metals,' vol. 28, p. 31 (1922).

[‡] 'Proc. Chem. Soc.,' vol. 26, p. 179 (1910); 'Trans. Chem. Soc.,' vol. 119, p. 932 (1921), vol. 121, p. 41 (1922); also several papers in J. Iron and Steel Inst. and J. Inst. of Metals.

[§] 'Ind. and Eng. Chem.,' vol. 17, p. 339 (1925).

[||] 'Ind. & Eng. Chem.,' vol. 15, p. 127 (1923).

[¶] 'J. Inst. Metals,' vol. 30, p. 239 (1923); 'Chem. Ind.,' vol. 43, p. 222 (1924); 'Trans. Faraday Soc.,' vol. 19, p. 789 (1924); 'Ind. & Eng. Chem.,' vol. 17, p. 363 (1925), and other papers.

This statement of the type-actions of corrosion suggests that they are simple and should not be difficult to study experimentally. Unfortunately the reactions are not ordinarily spaced uniformly over the whole of a metallic surface placed in water or salt solution, and both distribution and speed are affected by a large number of factors, some of which are difficult to control.

The irregular distribution of corrosion was formerly believed to be caused by heterogeneity, chemical or physical, of the metal, but this explanation, though true in many cases, has been found to be inadequate in others. Aston* however, showed that wet rust could assist the further corrosion of iron by screening the underlying metal from the direct access of oxygen—such screened metal becoming anodic to metal freely exposed to oxygen, and, therefore, selectively attacked. This line of work was developed by U. R. Evans,† whose work brought out some important points; for instance, he provided a satisfactory explanation of the well-known fact that corrosion often takes place in an especially marked degree at just those places to which oxygen has least direct access, by showing that such places become relatively anodic and are actively attacked in consequence. The screening of oxygen may be due either to the presence of quite extraneous substances (even non-conductors such as glass), or to the products of the corrosive action (particularly hydroxides formed from a soluble anodic product), or to cracks or pores in the metal. This explanation of the irregular distribution of corrosion has provided, in many cases, a solution of the difficulty that pitting, *i.e.*, locally intensified corrosion, could not be correlated either with the distribution of second phases or with local variations in physical properties which were the explanations formerly offered.

One of the omissions from earlier versions of the electrochemical theory was adequate consideration of the nature, distribution and state of aggregation of the products of corrosion. These products may be soluble bodies, colloids, gels or crystalline aggregates, and may be distributed by diffusion, convection, cataphoresis and gravity. That a film or scale of corrosion products might interpose a resistance in the circuit was recognised by Whitney in his original paper, and Bancroft* also called attention to the interfering effect of "films." In recent years much work has been done on the matter, and it is now believed that corrosion products can affect the amount and distribution of corrosion in several ways. Products of low solubility can operate :—

---

* 'Trans. Amer. Electrochem. Soc.,' vol. 29, p. 449 (1916).

† 'J. Inst. Metals,' vol. 30, p. 257 (1923); 'Chem. Ind.,' vol. 43, p. 315T (1924); 'Trans. Faraday Soc.,' vol. 19, p. 789 (1924).

(1) By forming a compact resistant film in contact with the metal either locally or generally, and so slowing down corrosion of the underlying metal. A thin film may thus "ennoble" the underlying metal but yet allow current to pass cathodically and corrosion to take place elsewhere. Films may be formed either anodically or cathodically; the passivifying films formed in chromate solutions† are often considered to be due to films formed at anodes, though it is equally possible that these are due to chemical oxidation. The cathodic production of films in the presence of dissolved oxygen has been specially studied by U. R. Evans.‡ These usually consist of oxidised metal and may protect and "ennoble" the underlying metal and so render the neighbouring metal relatively anodic. Such films are often thick enough to show interference colours of several orders.

It has been shown by several authors that a film of corrosion product may be so thin as to be invisible and yet affect the behaviour of a metal towards solutions.

(2) By forming porous "oxygen screens," not in actual contact with the metal. Certain corrosion products, even when insoluble, have a remarkable power of movement from their seat of production§; thus they do not always blanket down corrosion as rapidly as might be expected. It seems probable that they are first formed as colloids and are slightly moved cataphoretically under the action of the electrochemical cell by which they are formed. Sometimes "screens" are formed late in a corrosion process owing to a previously adherent film losing its adhesive power through some physical or chemical change.

---

* 'Trans. Amer. Electrochem. Soc.,' vol. 9, p. 17 (1906).

† For the nature of these films see U. R. Evans, 'J. Chem. Soc.,' vol. 131, p. 1020 (1927).

‡ 'Ind. and Eng. Chem.,' vol. 17, p. 363 (1925); 'J. Chem. Soc.,' vol. 127, p. 2484 (1925).

§ Bengough and Hudson, 'J. Inst. Metals,' vol. 21, p. 64 (1919); see figs. 12 and 13, Plate III.

Soluble products can operate :—

(3) By maintaining a higher concentration of metal ions at some areas on the metal surface than on others, and so causing concentration cells which give rise to local attack at areas of low concentration.*

(4) By dissolving, peptising or otherwise loosening a protective film or porous scale.

(5) By diffusing away from the anode and forming precipitates elsewhere.

Conditions Governing Corrosion and the Arrangement of Corrosion Experiments.

From the foregoing brief summary of the modern theory of corrosion the following factors, all independent of the corroded metal, would be expected to influence the process :—

(1) The temperature.
(2) The pressure of the oxygen gas.
(3) The hydrion concentration.
(4) The amount and distribution of the oxygen supply.
(5) The nature and distribution of corrosion products.
(6) The conductivity of the liquid.
(7) The metal ion concentration.

The action of light, particularly of ultra-violet rays, is also a possible factor.†

Factors (1) and (2) can be accurately controlled ; the others can only be fixed initially, and must be allowed to take their own course during the experiment : they depend on the specific nature of the corroding liquid.

If corrosion products accumulate at the surface of the metal the concentrations of ions there may differ from those in the bulk of the solution, and may be dictated largely by the corrosion products.

In most published researches on aqueous solutions the oxygen supply to the reactive surface has been allowed to depend largely upon convection currents. This has been clear from the work of Adeney, Leonard and Richardson,‡ who showed that the quantity of oxygen supplied by diffusion to the interior of a solution was small relatively to that supplied by convection ; they suggested that convection is set up in a salt solution by evaporation at the surface, which produces a relatively concentrated and heavy layer of liquid; this layer then sinks carrying oxygen in solution. This movement of oxygen constitutes an undetermined factor in the great majority of published research on corrosion; it can be made very small by accurate control of temperature and gas pressure or by very shallow immersion; both methods of control have been used in the present research.

---

* See Bengough and Stuart, 'World Power,' 1 (1924), and Bengough and May, 'J. Inst. Metals,' vol. 32, p. 129 (1924), for discussion of conditions favouring such action.

† Cribb and Arnaud, 'Analyst,' vol. 30, p. 225 (1905) ; Newton Friend, 'J. Iron and Steel Inst.,' Carnegie Mem., vol. 11, p. 116 (1922).

‡ 'Phil. Mag.,' vol. 45, p. 835 (1923).

The foregoing list of factors which influence corrosion includes only those external to the metal. Factors relating to a highly purified metal include :—

(1) The electrical properties of the metal, particularly the electrode potential.
(2) The state of aggregation, including crystal size and character, presence of pores and cracks, nature of the surface film or "skin."
(3) The presence of internal stresses.
(4) The over-voltage (in cases where hydrogen gas may be evolved).

For a solid solution or two-phase material there must be added :—

(5) The nature and concentration of impurities in solid solution.
(6) The nature, amount and distribution of the second phase.

For a given highly purified metal, carefully prepared and annealed, some of these factors can be eliminated or made small; probably the most difficult to control are the occurrence of minute invisible pores and the nature of the surface film or skin.

This skin differs from the metal beneath it in important properties and is produced by all the ordinary mechanical processes by which a flat metallic surface is produced such as cutting, grinding or working in contact with some other substance. In this skin may be found traces of the substance used for the cutting or grinding process; nevertheless, some such process appears to be necessary if metal is to be tested in compact form and definite shape.

Most experimenters in the past have prepared their metal surface by grinding on emery paper. Turned surfaces have been less used, and these are probably less liable to contain "inclusions" derived from the preparatory process. The comparative behaviour of several kinds of surface has been studied in the present research.

Consideration of the above list of factors, which are believed to affect the rate of corrosion, suggests that experiments must be very carefully devised and carried out if they are to be interpreted quantitatively for the purpose in view. It is important, therefore, to consider whether the methods at present in use for measuring corrosion in water and dilute salt solutions are adequate, and, if not, whether they can be improved.

SECTION II.

Existing Quantitative Data.

Quantitative methods which have been used in the investigation of corrosion in water and nearly neutral salt solutions are :—

(1) The loss of weight method.
(2) The increase of weight method.
(3) The oxygen consumption method.
(4) Method based on the solution of the corrosion product and determination of metal in it.

Sometimes measurements of the depth of pits have been added as a subsidiary method.

(1) This is most generally used. The specimen is weighed before the experiment, placed in the corroding medium and removed from it at the end of a specified time ; the corrosion product is then stripped from it by mechanical or chemical means, *e.g.*, by rubbing or weak acid ; the specimen is then reweighed after some process of drying. Mechanical methods of removing corrosion products are open to the objections that part is liable to remain in the deeper corrosion pits, and that loosened metal may be entirely removed ; they are quite useless for the present research on zinc. The chemical method is better in some cases, but the nature and strength of the solution must be carefully chosen so that the metal is not appreciably dissolved. This method, with a correction, has been used in the present research for comparison with the oxygen absorption method.

It should be noted that loss of weight methods reckon both oxidised and "chemically exfoliated" metal as corroded, but the latter is metal merely mechanically loosened or excised by the progress of corrosion along preferential paths.

(2) The increase of weight method consists in weighing the specimen at the end of the experiment with the corrosion products *in situ.* It has been successfully used in atmospheric corrosion tests in which the product adheres tightly to the specimen, and the weighing process does not generally interfere with the further progress of the test.* It has also been used by Basch and Sayre† with certain aluminium alloys in order to ascertain their relative resistance to industrial waters. With "wet" tests it is not easy to decide

---

* W. H. J. Vernon, 'Trans. Faraday Soc.,' vol. 19, p. 839 (1924).

† 'Mech. Engineering,' vol. 46, p. 199 (1924).

upon the best method for the desiccation of the specimen at the end of the experiments.

Except in atmospheric corrosion tests, methods based on weight variation, as usually carried out, only give a result at the *end* of each corrosion test; they do not allow determinations to be made at intervals during the course of a single experiment.

(3) The determination of oxygen consumption has been comparatively seldom used as a means of measuring corrosion. Kröhnke* and Arndt† used it for measurements of corrosion of iron and steel by moist air, but the apparatus was designed for technical rather than critical measurements; moreover, the experimental data obtained cannot be interpreted, as the distribution of oxygen between ferrous and ferric iron was not determined. Shipley and McHaffie‡ carried out a couple of experiments with iron, using an oxygen-absorption method in which the specimens were joined to graphite rods to stimulate corrosion. They also determined the iron in the corrosion products by solution and titration. The results showed a fairly good agreement between the two methods, titration giving slightly higher results.

Speller and Kendall§ developed a method based on measurements of the volume of oxygen in a stream of water before entering and after leaving iron pipes usually about 200 feet long—a method particularly adapted to the solution of practical problems which has given good results in their hands, but not suitable to the purposes of the present authors.

The oxygen consumption method is complicated if hydrogen is evolved. This hydrogen must be measured and a correction applied to determine the real volume of oxygen absorbed; the corrosion corresponding to the hydrogen evolved must be calculated.

When the method is used for a metal which exhibits two valencies, oxygen may be absorbed in raising it to a higher valency, and the amount so used must be determined by analysis of the corrosion products. At the present stage of the work only zinc, a single valency metal, has been used.

(4) This method has been used by Shipley and McHaffie‖ and by U. R. Evans.¶ It suffers from similar drawbacks to No. 1.

Results of corrosion experiments are usually stated as weight lost per unit

---

[*] 'Metallrohren-Ind.' (April 10, 1910).

[†] 'Chem.-Z.,' vol. 34, p. 425 (1910).

[‡] 'Canadian Chem. and Metall.,' vol. 8, p. 121 (1924).

[§] 'Ind. and Eng. Chem.,' vol. 15, p. 134 (1923).

[‖] 'Canadian Chem. and Metall.,' *loc. cit.*

[¶] 'J. Soc. Chem. Ind.,' vol. 43, p. 315T (1924).

area per day, and Wilson* has proposed to add per unit of concentration of oxygen. These methods of statement are not satisfactory unless all the conditions of the experiments to be compared are precisely defined, since the rate of corrosion varies greatly with time as well as other factors ; in no research known to the authors have the necessary data been given.

Comparatively few papers give sufficient details of experiments carried out at least in duplicate, to enable judgment to be formed on the accuracy achieved; some typical results are given below.

Heyn and Bauer's† extensive researches on iron and aluminium, mainly of a technical nature, contain experiments in duplicate and even quadruplicate, and an examination of some of their results show variations from the means of 2·5 to 8 per cent. Some measurements by Bengough and Hudson‡ on zinc, also of technical nature, showed variations from the mean of 3 to 10 per cent. ; with very slight corrosion the variations were still greater. Newton Friend,§ referring to the corrosion of iron, stated in 1923, " rates of corrosion exhibit marked variation, which may amount to 100 per cent. even when the experimental conditions appear to be identical " ; but this author has published || experiments carried out in triplicate in which variations from the mean in four experiments were about 4, 4·2 and 9 per cent. ; in another paper duplicates differed by 2 and 17 per cent.

Whitman and Russell,¶ working on the relatively simpler problems of corrosion in acid, stated : " The reported results are probably not reproducible to within better than 25 per cent."

Speller and Kendall** in a paper entitled 'A New Method of Measuring Corrosion in Water' (an oxygen absorption method), only give single figures for their results, though the statement is made, in some instances, that these are means from two experiments. The only reference to accuracy of results occurs in some remarks about the relative amounts of ferrous and ferric iron in the corrosion product. A knowledge of these amounts is vital to an oxygen absorption method of measuring corrosion, and they state that : " The variation is

---

* 'Ind. and Eng. Chem.,' vol. 15, p. 127 (1923).

† 'Mitt. aus d. k. Material-prüfungsamt,' vol. 26, p. 1 (1908); vol. 28, p. 62 (1910); vol. 29, p. 2 (1911).

‡ 'J. Inst. Metals,' vol. 21, p. 63 (1919).

§ 'J. Chem. Soc.,' vol. 123, p. 2996 (1923).

|| 'J. Iron and Steel Inst.' (Carnegie Mem.), No. 11, p. 142 (1922) ; 'J. Inst. Met.,' vol. 33, p. 19 (1925).

¶ 'Ind. and Eng. Chem.,' vol. 17, p. 348 (1925).

** 'Ind. and Eng. Chem.,' vol. 15, p. 134 (1923).

sufficiently small to come within an experimental error of 10 per cent." It seems, therefore, that these authors would not claim a high "overall" accuracy.

U. R. Evans* carried out a series of experiments in duplicate by the usual loss of weight method, the specimens of sheet-steel being partially immersed in the liquid. The loss of weight was measured at the end of 21 days; some results were as follows:—Variations from mean: in distilled water, 10 per cent.; in N/20 sodium chloride, 1·5 per cent.

The points brought out in the foregoing discussion of quite typical methods and results appear to the authors to be:—

(1) The accuracy attained by existing methods of measurement varies between wide limits, and is usually low.

(2) It is not clear whether the discrepancies between supposedly duplicate experiments are due to some inherent characteristic of the corrosion process or to the fact that in the experiments control has not been kept over all the controllable factors.

(3) The shapes of curves connecting time and corrosion should be accurately determined. Till this is done the usual method of recording results in terms of metal corroded per unit of time is unsatisfactory.

Section III of this paper describes the attempts made to throw light on some of these points.

SECTION III.

New Quantitative Data and Attempted Interpretation.

An oxygen absorption method of measuring corrosion has been devised in which the following factors are known and controllable:—

(*a*) Temperature.

(*b*) Pressure.

(*c*) The initial hydrion concentration.

(*d*) The initial amount and distribution of oxygen supply.

(*e*) The initial composition and conductivity of the liquid.

"Adeney streaming" has been almost or quite eliminated, and similar metal specimens can be always tested in similar positions in similar vessels.

Principle of the Apparatus.

The principle of the apparatus used is shown in diagram, fig. 1

The metal specimen M is supported on three fine glass points (*n*) in a corrosion vessel J. Water is introduced into the vessel through capillary (*h*), which is then sealed off. Oxygen or other gas can be introduced through the side tube (*p*). The pressure at which the experiment is to be carried out is determined by

---

* 'J. Soc. Chem. Ind.,' vol. 44, p. 163T (1925).

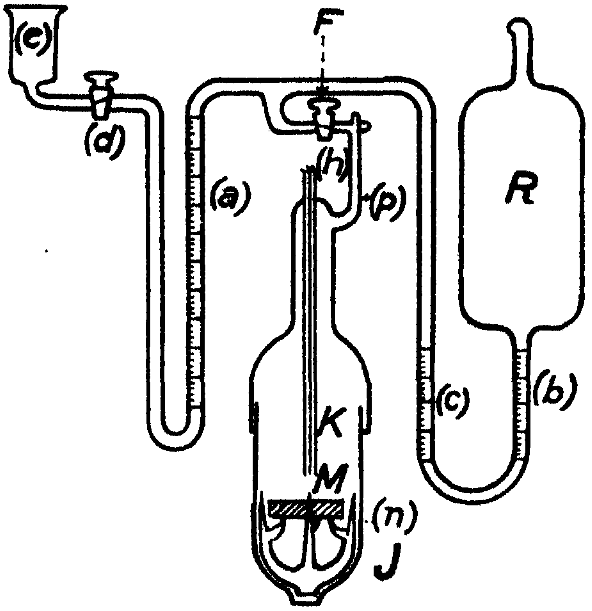

FIG. 1.—Diagram of Oxygen Absorption Apparatus.

the pressure in the manometer bulb R, which is filled with oxygen and connected to manometer limbs (*c*) and (*b*) containing water; the corrosion vessel can be put into communication with the manometer by opening tap F, and its pressure adjusted to that of R; the manometer levels will then be equal. When corrosion takes place oxygen will be absorbed and the level will rise in the manometer limb (*c*). This oxygen can be replaced from a graduated gas burette (*a*) by introducing water from (*e*) by opening tap (*d*). Oxygen is forced in until the heights in the two manometer limbs (*c*) and (*b*) are again equal. The volume of oxygen in (*a*) will then be found to have diminished by an amount corresponding to that absorbed by corrosion. The whole apparatus, including gas burette, corrosion-vessel and manometer bulb is placed in a thermostat, consequently an experiment can be carried through at constant temperature and pressure; in the present experiments 25° C. and 760 mm., except in so far as the pressure in the corrosion-vessel changes by absorption of oxygen between replacements of gas; usually such replacements were relatively small and were carried out every 24 hours, or in special experiments every two hours.

The actual apparatus fulfils the following conditions:—

(1) The tests are carried out in vessels made of "redline" Jena glass,* Durosil or transparent silica.

(2) The corroding liquid never passes through a greased tap.

(3) The liquid can be saturated with oxygen at the temperature and pressure used in the test before being brought into contact with the metal; in the absence of true saturation false readings would be obtained.

(4) A known quality of water, as indicated by its conductivity and *p*H number, can be used for each test. The transfer of this water from the still to the corrosion-vessel can be conducted out of contact with the laboratory air in the way described later, and the conductivity of the water can be measured actually in the thermostat in the presence of oxygen.

(5) The metal specimens can be kept of uniform size and shape, usually circular discs, 2·5 mm. in diameter and 0·6 mm. thick were used. They are arranged horizontally, and both the flat surfaces and the sides of the discs are exposed to the liquid.

Attempts were made to coat all except one horizontal surface so that an expression could be obtained for the rate of corrosion at a definite depth. Many coating materials were tried and applied with or without the use of heat and pressure. The conditions to be met by a suitable material are the formation of a watertight joint between metal and material, and the absence of effect on the water-conductivity. Vulcanite and Bakelite applied with heat and pressure, gave watertight joints, but both affected the conductivity of the water to an important extent; paraffin wax does not give a permanently watertight joint. Much time was spent in making and testing coatings, none of which was successful.

Detailed Description of the Corrosion Apparatus.

The actual apparatus was designed so that the conductivity water or other liquid under test could be forced into the corrosion-vessel through the capillary (*h*), fig. 1, by the oxygen or other gas used as an atmosphere. This capillary was connected to a separate vessel (shown in fig. 2) through tube G by a short rubber connection.†

---

* See paper by H. V. Renn, 'The Industrial Chemist,' vol. 2, p. 271 (1926), for amounts of alkali extractable by distilled water at 100° C., from Jena glass.

† Except for this and connection D, fig. 2, the conductivity water from the still never came into contact with any solid except glass and platinum electrodes.

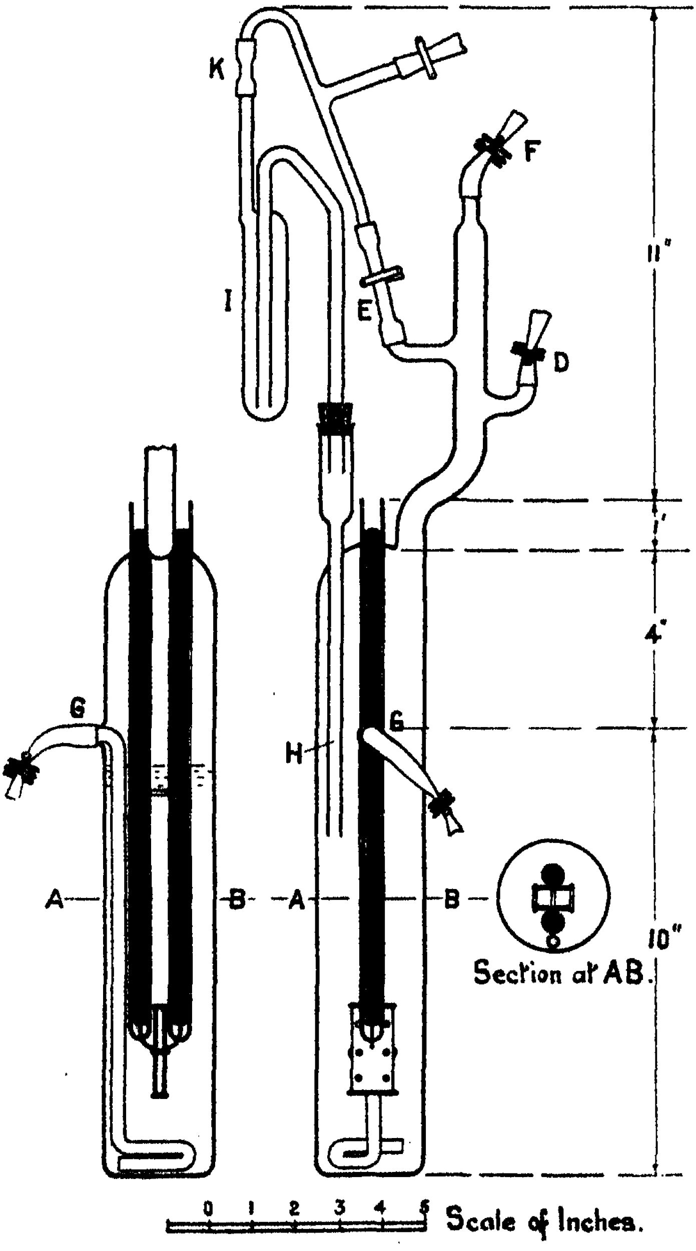

FIG. 2.—Electrode Vessel.

The component parts of the actual apparatus are shown in figs. 3A, 3B and 3C. Fig. 3A shows the oxygen burette (*a*) and manometer (*b*). The reservoir R is filled at the beginning of the experiment with oxygen at the pressure, namely,

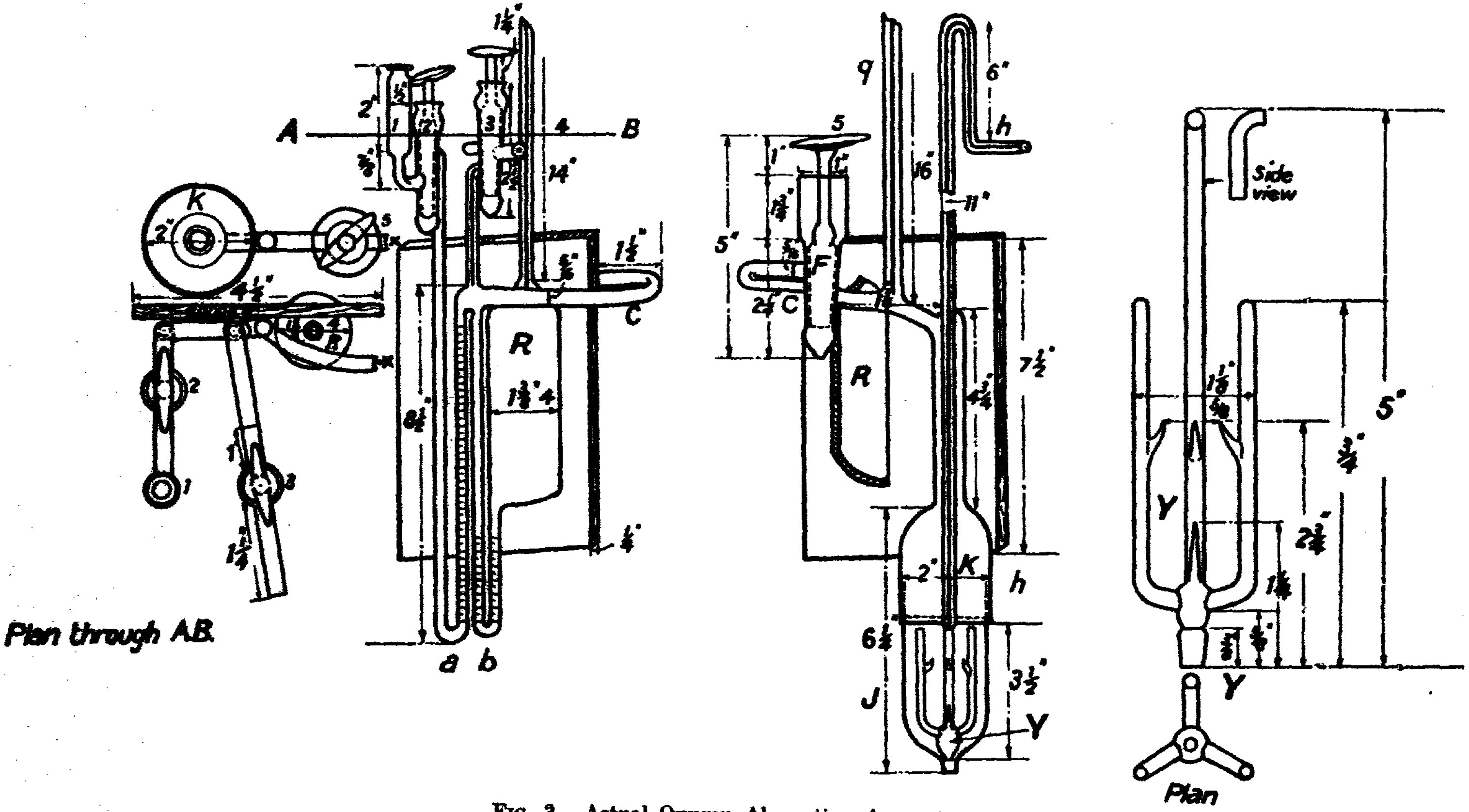

Fig. 3a.

Fig. 3b.

Fig. 3c.

Fig. 3.—Actual Oxygen Absorption Apparatus.

760 mm., at which the experiment is to be conducted; hence, when the levels in (*b*) are identical the oxygen in (*a*) is at a pressure of 760 mm. The tube (C) joins that marked (C) in fig. 3B, which leads to the corrosion-vessel when tap F is open. The oxygen absorbed is replaced by running in water through the tap (2) until the water-levels in the manometer become identical. By attaching a length of rubber tubing to the wide tube (1) water can be sucked back into (1) if necessary for adjusting the level.

The oxygen burette (*a*) for the most sensitive work has a capacity of 1 or 2 c.c. and is graduated to 0·01 or 0·02 c.c. Since several c.c. might be used in a single experiment it is necessary to arrange that it can be refilled with oxygen during the experiment.

To do this the oxygen supply is connected to the outer open tube on the three-way tap (3), which can be put into communication either with the other open tube or with the oxygen burette. It is first put in communication with the former and the tubing is swept out with oxygen. Then the pressure of the oxygen supply is brought to 760 mm., and the tap (3) is turned to communicate with the oxygen burette and water is withdrawn from the latter until the graduated tube is practically full of oxygen. Tap (3) is then closed.

The oxygen burette could be read to 0·01 c.c. with an error of ± 0·005 in the most sensitive form of apparatus, but most work was done with a 2-c.c. burette graduated to 0·02 c.c. with an error of ± 0·01 c.c.; 1 c.c. of oxygen corresponds to nearly 5·35 mgrm. of zinc, so that the corrosion of about 0·05 mgrm. can be detected in the most sensitive apparatus.

The corrosion-vessel J fits into a ground-joint at K and has a ground recess into which fits the base of the stand Y. This should be notched (if solid) or have an opening (if hollow) to release any air trapped underneath.

The ground joint X must be very effectively sealed, since it is under a slight hydrostatic pressure when placed in the thermostat.

An actual corrosion experiment consisted in bringing together the purified oxygen, the metal specimen and the water or salt solution in the corrosion-vessel. It will be convenient to consider the preparation of each of these materials separately and then to describe the method by which they were brought together in the vessel.

Preparation of the Oxygen.

Electrolytic oxygen was supplied in cylinders by the British Oxygen Company, and contained about 0·5 per cent. of hydrogen. To remove this and other possible impurities the gas was passed through a thick-walled copper tube partly filled with copper gauze and heated to a red-heat. The oxygen was then cooled, filtered through cotton wool and passed through concentrated KOH solution and distilled water. It was then dried over P_2O_5. Finally it was passed through a dust-filter of special type. It was found that the passage of a stream of the purified oxygen through conductivity water contained in the "electrode-vessel," shown in fig. 2, did not appreciably alter its conductivity.

Preparation of Metallic Specimens.

The selection of the metal zinc for preliminary investigation was due to its two properties of fairly rapid oxidation and single valency. An additional advantage is that it can be obtained in large quantities in a well-purified condition.

It was realised that so much metal would be required during the course of the research (several kilos at least) that it would be impossible to rely solely upon laboratory methods of preparation.

Accordingly three samples of zinc were obtained for the research. The main supply consisted of about 25 kilos of Australian electrolytic zinc. This was part of a specially picked ingot exceptionally free from impurities. Several analyses carried out on large quantities of the metal gave the following results:—

Iron	0·005 per cent.
Lead	0·005 ,,
Cadmium	Trace.

These percentages are below the probable limits of solubility in zinc, consequently none of these metals would be present as a separate phase. No other metals could be detected by the ordinary methods of chemical analysis.

The other two samples of about 500 grms., each consisted of re-distilled zinc kindly furnished by the New Jersey Zinc Company. These were called "Spectroscopic Zinc," grade A and grade C. Ordinary chemical methods failed to show the presence of any foreign metals in these samples. The Company claimed that even spectroscopic analysis did not show any impurities in A and only traces in C. An examination of these samples, kindly carried out by Mr. L. J. Freeman, of the Astro-Physics Department of the Royal College of Science, confirmed the claim.

The method of preparing the electrolytic zinc for test was as follows: The original ingot was wrapped in cloth and broken down by hammer into a few large lumps. These were melted in a gas-fired furnace in a salamander crucible and cast in iron moulds into ingots about 40 cm. long and 3 cm. in diameter.

The ingots were sawn into short lengths and remelted in a small salamander crucible over a gas-ring; they were then cast in an iron mould giving rods about 10 cm. long and 3 cm. in diameter, which were apparently quite sound.

It was necessary to prepare specimens of definite shape and size, as shown in fig. 1. The rods were turned down by the authors in a small precision lathe to a diameter slightly greater than 2·5 cm. They were then cut with a hacksaw into sections about 1 cm. thick. Each section was turned down approximately to 0·7 cm. thickness and boiled for half an hour in conductivity water; after this treatment the specimen was always handled through two thicknesses of filter paper and wash-leather gloves. For accurate turning to size it was held in a carefully cleaned collet lined with filter paper. The two plane surfaces were then turned parallel to one another within a limit of about 0·01 mm. and the total thickness of the finished specimen was brought to 0·6 mm., the "final cut" was kept very fine and as uniform as possible for all specimens. After turning the specimens were kept in a desiccator till required. A number were used for corrosion tests without any further treatment; some were ground on emery papers finishing on Hubert 0000, and others were annealed in glass tubes at various temperatures in an atmosphere of argon.

Commercial argon contains oxygen and nitrogen. The oxygen was removed by passing the gas over copper gauze heated to 700° C. in an electric furnace. Copper oxide was also used in the purifying train to remove any trace of hydrogen. The gas was then passed over "sofnolite" to remove traces of CO_2, dried in a P_2O_5 tower, and finally filtered through a plug of carefully dried cotton wool.

Some of the specimens that had been annealed in argon showed coloured interference films. This was found to be due to the presence of moisture, probably from the walls of the tube in which the metal was annealed or from the filter originally used in the argon purification train. This filter was replaced by a Jena glass filter and the walls of the tube were carefully dried as follows: A tube about 30 inches long, open at one end, with a narrow tube sealed on at the other, was cleaned, dried and baked at about 400° C. for ten minutes. The zinc specimens were then placed in the cooled tube and the open end sealed off, the specimens were then moved down to the sealed end. The other half of the tube was then heated to about 450° C., and the tube was exhausted and filled with dried nitrogen. It was then allowed to cool, the specimens were shifted to the portion of the tube that had been heated and the tube was sealed off in the middle. Immediately after sealing off a rubber connection on the narrow end of the tube was clipped off and left closed till it was joined to the argon purifying and drying train. The tube was then evacuated and filled with argon several times. Finally it was sealed off and placed in the annealing furnace. The specimens were annealed either at 300° C., or later 250° C., for a week. After annealing the specimens were kept in a vacuum desiccator till used.

The "spectroscopic zinc," grade C, was used in the cast condition only. It was treated similarly to the electrolytic zinc except that it was melted and cast in clear silica vessels.

One experiment was made with grade A zinc. This arrived from America in glass tubes in the form of rods about 0·8 cm. in diameter. A portion of a rod was broken off (by continued bending) of such length that its total surface was approximately the same as that of a standard specimen; it was then placed in the corrosion-vessel in a nearly vertical position. The metal was handled only through wash-leather gloves and two thicknesses of filter paper, and so never came into contact with any metal during preparation for the test. The result of this experiment is given on p. 449.

The process of placing the metal specimen in the corrosion measurement apparatus necessitated its exposure for a short time after removal from the desiccator to atmospheric oxidation and to the presence of aerial dust particles. The metal surface must, therefore, be presumed to be coated with a thin, though invisible, film of oxide formed by the action of the atmosphere. The work of Vernon shows, however, that such a film is of an open or granular nature, and it does not seem likely to exert any great protective action against the action of electrolytes.

Preparation of Water and Salt Solutions.

The water was prepared in a specially designed still which is being described elsewhere. The conductivity of water actually used in different corrosion experiments varied from $0 \cdot 047 \times 10^{-6}$ mhos to $0 \cdot 10 \times 10^{-6}$ mhos; within these limits the speed and amount of corrosion appeared to be independent of the conductivity of the water for reasons to be mentioned later. For making up salt solutions water of similar quality was used.

The conductivity water used in the corrosion tests was collected in a special vessel similar to fig. 2, through which purified air could be passed. The vessel was provided with a tube, sealed through the side (*cf.* G, fig. 2), so that several batches could be run through before finally collecting the water for the corrosion test. The outlet of this tube was finally connected to the corrosion apparatus as previously described. This arrangement was designed to avoid risk of contamination by CO_2, etc., in collecting and transferring the water.

For salt solutions the vessel shown in fig. 2 was employed. The tube D was connected by rubber tubing to the outlet of the still and the tubes F and E formed the inlet and outlet respectively for the purified air. G represents the tube sealed through the side of the vessel.

The additional fittings necessary for the introduction of the salt consisted essentially of (1) a tube H, sealed into the vessel and ending below a mark indicating a fixed volume (650 c.c.), and (2) a vessel connected, as shown, to the air outlet E.

By detaching the connection K strong salt solution could be introduced into I in the amount required for converting the above volume of water into salt solution of the required concentration. By closing the clip on the rubber connection at E purified air could be driven through I, and the salt solution evaporated to dryness (I being generally heated with hot water); the connection to the still should be closed during this evaporation.

After evaporating to dryness K was reconnected and the clip at E opened. Water was then collected (after preliminary washing), the volume was adjusted to 650 c.c., and the clip on the still-connection D closed. By closing and opening E water could be driven up into I and allowed to run back and the salt thereby brought into solution.

The conductivity of solutions was measured in the thermostat at 25° C., and the values are given in the General Table; these differ slightly in some cases from what would be expected from their descriptions on the scale of normality; the conductivity values should be preferred in such cases.

Starting an Experiment.

The essential operations to be carried out in bringing together the metal, oxygen and liquid for the experiment are :—

(1) Thorough cleaning of the apparatus and especially of the bottom vessel—the latter with nitric acid, distilled water and final steaming and drying.

(2) Sealing the ground-joint of the corrosion-vessel with red wax.

(3) Connecting together in the thermostat the corrosion-vessel and the electrode-vessel containing the corroding liquid.

(4) Connecting up the source of purified oxygen in such a manner that the gas can be passed either into the corrosion-vessel or into the electrode-vessel, and arranging that the gas exit can be connected up to an apparatus for adjusting the pressure in the whole system to 760 mm.

(5) Connecting the corrosion-vessel to a vacuum pump.

After making these connections the manipulations are as follows: (*a*) The corrosion-vessel is alternately pumped out and filled with oxygen several times. (*b*) Oxygen is then bubbled through the liquid in the electrode-vessel for about half an hour to saturate the latter after it has reached the temperature of the thermostat. (*c*) The liquid under test is driven into the corrosion-vessel by oxygen pressure. (*d*) The pressure in the apparatus is adjusted to 760 mm. (*e*) The capillary connections are then sealed off. A detailed account of the procedure followed in making the experiments has been deposited with the corrosion of Metals Research Committee of the Department of Scientific and Industrial Research, and may be inspected on request.

Comparison between Loss of Weight and Oxygen Consumption Measurements.

Since loss of weight measurements of corrosion have been so largely used by previous workers it was thought to be desirable to compare them with those obtained by the method just described.

The loss of weight method was carried out as follows: Before the beginning of a corrosion experiment the metal specimen was dried in a desiccator and weighed; this weight was called A; at the end of the corrosion experiment it was placed in 10 per cent. acetic acid in a glass dish and observed under a binocular microscope, giving a visual magnification of 50 diameters. The time taken to dissolve all the corrosion products was noted. When solution was complete the specimen was removed, washed in distilled water, dried in a desiccator and weighed; this weight was called B. Then A–B was the apparent loss of weight due to corrosion. But this loss of weight was obviously too great, as bubbles of hydrogen, due to acid attack, were always seen coming off from metal points, etc. In order to find a correction for this the specimen* was again placed in acid for a similar time to that taken to remove the corrosion products, washed, dried and weighed again; this weight was called C, and B–C is the correction required. Then (A–B)–(B–C) is called the "corrected loss of weight." The correction (B–C) is very slightly too large, since no corrosion products were present during the second acid treatment to hinder the attack on the metal, nevertheless hydrogen can be seen coming out of the pits at an early stage of the treatment even when undissolved corrosion product is still present. The corrosion products on specimens corroded in conductivity water were rapidly attacked by the acid, but in the experiments with chloride solutions

* A blank specimen cannot be used because the rate of evolution of hydrogen is largely dependent upon the details of the metal surface such as sharp points, etc., hence the specimen itself must be used to give the closest possible approximation. A newly turned specimen would give a nearly negligible correction.

the time necessary to dissolve all the products out of the deep pits varied from half an hour to more than an hour.

Results are given in Table I, which show that in all cases but two the oxygen consumption measurement indicates similar or, generally, less corrosion than the loss of weight method. This difference is no doubt partly due to loss of exfoliated metal in the loss of weight method—that losses due to this cause actually took place could usually be seen with the microscope.

In the two experiments in which loss of weight gave the smaller figure one result (A45) is due to over-correction; the other (A22) is probably due to the fact that the total corrosion is extremely small, and the consequent experimental errors relatively large, especially in the loss of weight method.

Table I.—Comparison between oxygen-absorption and loss of weight methods of measuring corrosion.

Specimen No.	Corroding liquid.	Zinc by calculation from oxygen absorbed. mgrs.	Zinc by loss of weight.		Time taken to remove corrosion product by acid. minutes.
			(*a*) Uncorrected. mgrs.	(*b*) Corrected. mgrs.	
A 22	Con. water	2·04	1·4	1·2	8
A 29	,,	1·58	2·2	1·6	1
A 33	,,	10·40	12·0	—	—
A 36	,,	4·47	6·60	6·40	1¾
A 48	,,	0·96	2·2	1·2	7
A 40	KCl N/10,000	20·7	27·3	—	—
A 41	KCl N/5,000	41·17	59·0	52·8	34
A 42	KCl N/20,000	22·36	26·4	24·4	44
A 44	KCl N/10,000	71·69	85·0	77·6	45
A 45	KCl N/100,000	5·19	8·2	4·6	45
A 53	KCl N/20,000	26·64	29·5	28·4	13
A 49	KCl N/10,000	58·58	69·8	65·4	63
A 52	KCl N/5,000	100·95	117·7	114·7	75
A 50	KCl N/10,000	67·25	83·6	78·6	73
A 54	KCl N/ 20,000	40·18	47·0	39·2	98
A 59	KCl N/1,000	242·00	262·20	252·2	71

Viewing the results as a whole it is clear that the loss of weight method is not suitable for critical work for zinc when a difficultly soluble corrosion product is formed and deep pits occur in the metal. In such conditions considerable corrections must be applied and the errors that are liable to occur seem to be far greater than any likely to happen in a carefully arranged oxygen consumption experiment.

A detailed discussion of the time-corrosion curves obtained in various experiments will now be given.

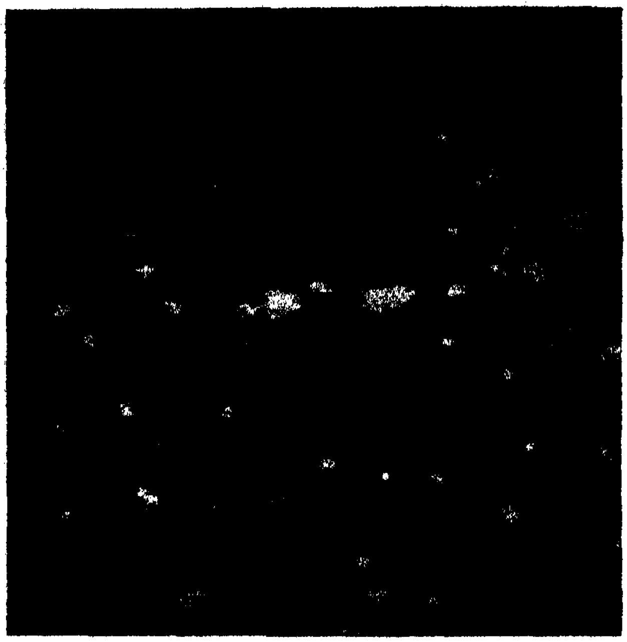

Fig. 4.—Typical micro. showing "pits."

General Features of the Curves.

(All the figures given for corrosion refer to discs of zinc 2·5 cm. in diameter and 0·6 cm. thick, tested at 25° C., and 760 mm. pressure, at a depth of 1·6 cm. usually in 100 c.c. of water or solution.)

A measurable amount of corrosion took place even when the most highly purified zinc and water (conductivity $0\cdot047 \times 10^{-6}$ reciprocal ohms) were used, and signs of corrosion would usually be seen within 24 hours. Grade A (spectroscopically pure) zinc corroded quite as rapidly as the Australian electrolytic zinc in N/10,000 potassium chloride solution, as shown in Table II.*

Nearly one hundred curves have been taken showing the relation between corrosion and time, and data relating to many of them are incorporated in the General Table of Results (pp. 464–5), which summarises the experimental conditions. A selection of typical curves showing the actual experimental data is given in figs. 5 to 11.†

---

* Compare H. M. Cyr, 'Trans. Amer. Electrochem. Soc.,' vol. 51, p. 169 (1927).

† Tables giving the full experimental data for all the curves have been deposited with the Corrosion of Metals Research Committee of the Department of Scientific and Industrial Research and may be inspected on request.

Table II.—Oxygen Absorbed in N/10,000 Potassium Chloride Solution.

	"Grade A" Zinc. (S 1.)	Australian Electrolytic Zinc. (A 50.)
Days 0·75	0·04	0·17
1·75	1·40	1·11
2·75	2·50	2·18
3·75	3·46	3·17
4·75	4·51	4·07
5·75	5·42	4·84
6·75	5·96	5·61
7·75	6·60	6·27
8·75	7·17	6·88
9·75	7·73	7·33

The following experimental facts seem worth remark :—

(1) For a period of about two days the curves are typically concave upwards, *e.g.*, fig. 6 : corrosion appears to be slow for the first few hours. The rate then appears to increase rapidly, and a maximum is usually reached in three or four days.

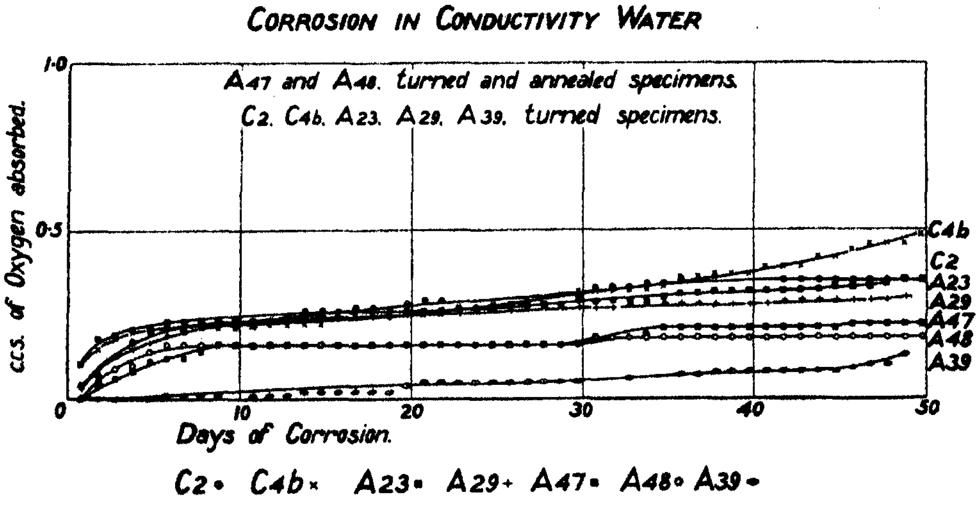

FIG. 5.—Curves for Conductivity Water.

(2) After the third or fourth day the rate of corrosion usually begins to fall off and the curves become convex upwards, and, finally, nearly parallel to the time-axis.

(3) Certain small step-like changes in the direction of the curves may occur at irregular intervals with conductivity water and very dilute salt solutions, especially with emeried or turned surfaces (see fig. 6). They usually last only

a day or two, and correspond to slight and temporary increases in corrosion rate.

(4) A few curves were obtained with conductivity water and turned specimens which showed little or no corrosion for many days. Thereafter the rate increased, corrosion finally reaching more or less the usual values. Examples of this type of curve are Nos. A 21, fig. 6, A 39 and A 43. When corrosion once starts it may continue for long periods; thus No. A 43 showed the highest corrosion at the end of a hundred days of any specimen tested in conductivity water for that length of time. Such curves have never been obtained with specimens that have been annealed after turning.

(5) The method of preparing the surface of the specimens had an important effect on the rate and amount of corrosion. Five methods were used, namely :—

(*a*) Turning followed by emery treatment finishing on 0000 Hubert paper.
(*b*) Turning only.
(*c*) Annealing in argon, followed by turning.
(*d*) Turning followed by annealing in argon.
(*e*) Burnishing with an agate tool.

After completion of these preparatory processes the specimens were kept in vacuum desiccators till required for use. Of the various treatments much the best was (*d*), especially as regards reproducibility.

(6) Many additions to conductivity water gave greatly increased corrosion even when the addition favoured the formation of a low-solubility corrosion product, *e.g.*, potassium hydrogen phosphate and potassium carbonate (see fig. 6). But in N/10,000 barium hydroxide solutions no visible or measurable

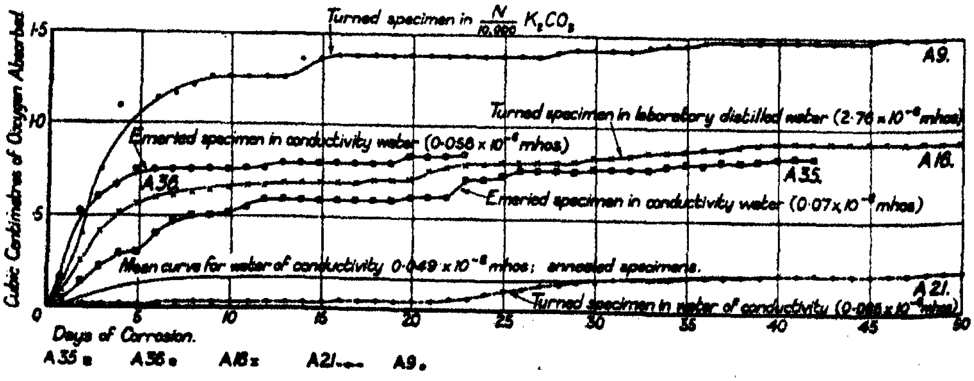

FIG. 6.—Curves for Conductivity Water with "Impurities."

corrosion took place in 30 days on an annealed specimen, *i.e.*, the total corrosion was certainly less than two or three-hundredths of a milligram.

(7) Estimations of the amount of chlorine in the filtered liquid at the end of experiments with dilute potassium chloride solutions lasting 50 days or more were made for several specimens. The results are shown in Table III. In the weaker solutions all the chlorine was removed; in the stronger part only.

(8) Comparison of the results for the turned specimen of the more highly purified "spectroscopic C zinc" with those for electrolytic zinc shows that the influence of purification within the limits of these experiments is quite small relatively to the influence of surface treatment.

Table III.

Specimen and concentration of solution.	Volume of liquid in corrosion-vessel.	Total oxygen absorbed.	Cl. in solution.
	c.c.	c.c.	mgm.
A,48 N/10,000 KCl	100	10·95	Trace.
A 50 N/10,000 KCl	100	13·12	—
A 51 N/10,000 KCl	100	10·10	—
A 52 N/5,000 KCl	100	18·87	0·13
A 54 N/20,000 KCl	100	7·51	Nil.

Nil means less than 0·03 mgm.

Discussion of Accuracy and Reproducibility.

In spite of the care taken to ensure uniform conditions it was obvious that corrosion was not uniformly distributed over the surfaces of the zinc specimens in any of the liquids used, but was largely concentrated at certain areas or "pits" (shown white in fig. 4). Hence the total amount of corrosion depended mainly upon the number and depth of such areas or pits. The position of the deepest pits could not be predicted and did not seem to be related in any definite way to the shape of the specimen. On many specimens, but not on all, the glass points of the stands which supported the specimens caused deep pits. Many pits seemed to be definitely related to the crystal boundaries or twinning planes and to penetrate along certain most favoured paths determined by the arrangement of the crystals. On emeried specimens rows of pits were sometimes observed to be situated along scratches, but many scratches did not show this.

The number and depth of pits varied greatly. In conductivity water the number might be less than 100 on an upper horizontal surface though often over that figure, and most of the pits were less than 0·02 mm. in depth. In

N/10,000 KCl the number on a similar surface might rise to about 1,000, and was nearly always over 500. The depth occasionally might reach 0·59 mm., but for the great majority was less than 0·04 mm., and sometimes hundreds of pits never reached a depth of 0·01 mm. Many of these were invisible to the unaided eye, but were detected at a magnification of 10 diameters. A large proportion of the total corrosion was due to a relatively small number of deep pits, and anything which affected the number and activity of these would notably affect the total corrosion.

Table IV.

Six lowest results for 50 days in conductivity water.

Specimen No.	Total oxygen absorbed. c.c.	Conductivity. mhos.	Treatment.
A 39	0·13	$0 \cdot 065 \times 10^{-6}$	Annealed and turned.
A 48	0·18	$0 \cdot 050 \times 10^{-6}$	Turned and annealed.
A 21	0·21	$0 \cdot 065 \times 10^{-6}$	Turned.
A 47	0·21	$0 \cdot 047 \times 10^{-6}$	Turned and annealed.
A 18 (1)	0·21	$0 \cdot 064 \times 10^{-6}$	Turned.
A 29 (2)	0·29	$0 \cdot 075 \times 10^{-6}$	Turned and emery polished.

Mean 0·205 = c.c. = 1·0 mgrm. zinc.

(1) Shallow immersion ; 2 mm. instead of standard depth of 1·5 cm.

(2) The only low result for an emery polished specimen ; usual result about three times this amount.

A general survey of the curves shows clearly that the nearest approach to agreement between duplicate results is obtained with specimens whose surfaces have been turned and subsequently annealed. In distilled water the total amounts of oxygen absorbed at the end of 50 days in duplicate experiments, A 47 and A 48, were 0·21 c.c. and 0·18 c.c., *i.e.*, the divergence from the mean figure corresponded to ± 7·5 per cent. ; this is a reasonable agreement considering the smallness of the total quantities of gas involved. Table IV shows six results obtained in conductivity water in various conditions, and fig. 5 the curves for A 47 and A 48, and two curves for spectroscopic zinc grade C, namely C 2 and C 4*b*.

In N/20,000 potassium chloride solutions very close agreement was obtained between the two annealed specimens, the curves for the most part lying over or close to one another for a period of approximately 10 days, which was the full period of one of the experiments. At the end of this time the total amount of oxygen absorbed was 5 c.c. in both experiments (see fig. 7).

In N/10,000 the following results were obtained in two experiments, Nos. A 49 and A 50, which were regarded as typical :—

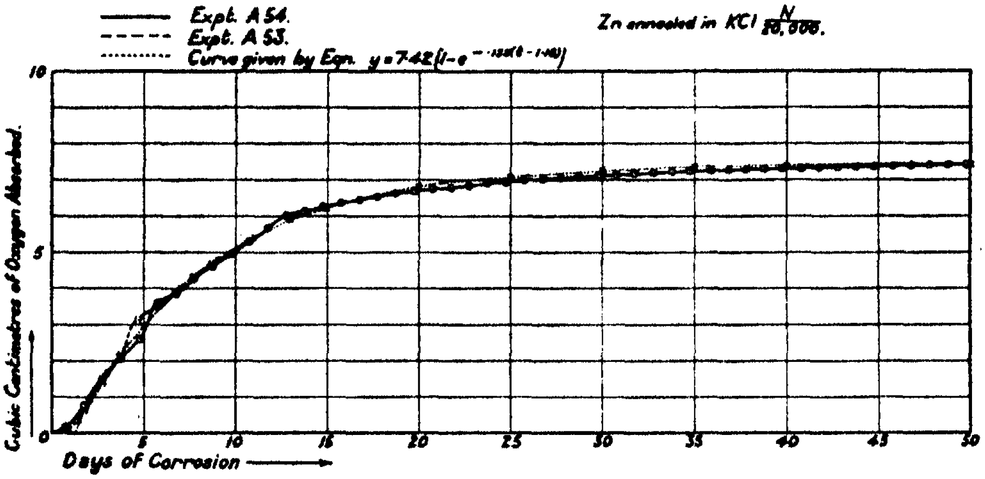

Fig. 7.—A 53, A 54, and their Theoretical Curve.

Table V.

—	Cubic centimetres of oxygen.		Difference.	Per cent. variation from mean (corrected for area).*
	A 49	A 50		
5 days	4·6	4·25	0·35	± 6·7
10 days	8·0	7·5	0·5	± 5·9
20 days	10·0	10·9	0·9	± 1·7
30 days	10·5	12·0	1·5	± 3·9
40 days	10·8	12·4	1·6	± 4·2
50 days	11·0	12·6	1·6	± 4·2

* A 49 was slightly smaller than the usual standard specimen.

The curves obtained for A 50 (fig. 8) and A 40, which were tested in N/10,000 potassium chloride, were sufficiently smooth to be investigated mathematically, and were found to be of the exponential type for a certain part of their course. The equations are given and the interpretation discussed on pp. 458–9.

In solutions of N/5,000 potassium chloride the curves also corresponded with the exponential form of equation for considerable periods (see A 52, fig. 9). The cause of the smoothness of such curves seems to be the presence of a sufficiently large number of deep pits to give an average result; the total corrosion may then be expected to resemble, fairly closely, the curve characteristics of one large pit.

Fig. 8.—Experiment A 50—Zn (annealed in N/10,000 KCl).

General Equation :—$y = A\{1 - e^{-k(t-b)}\}$.

Constants used : $A = 13 \cdot 3$, $k = 0 \cdot 0906$; $b = 0 \cdot 76$.

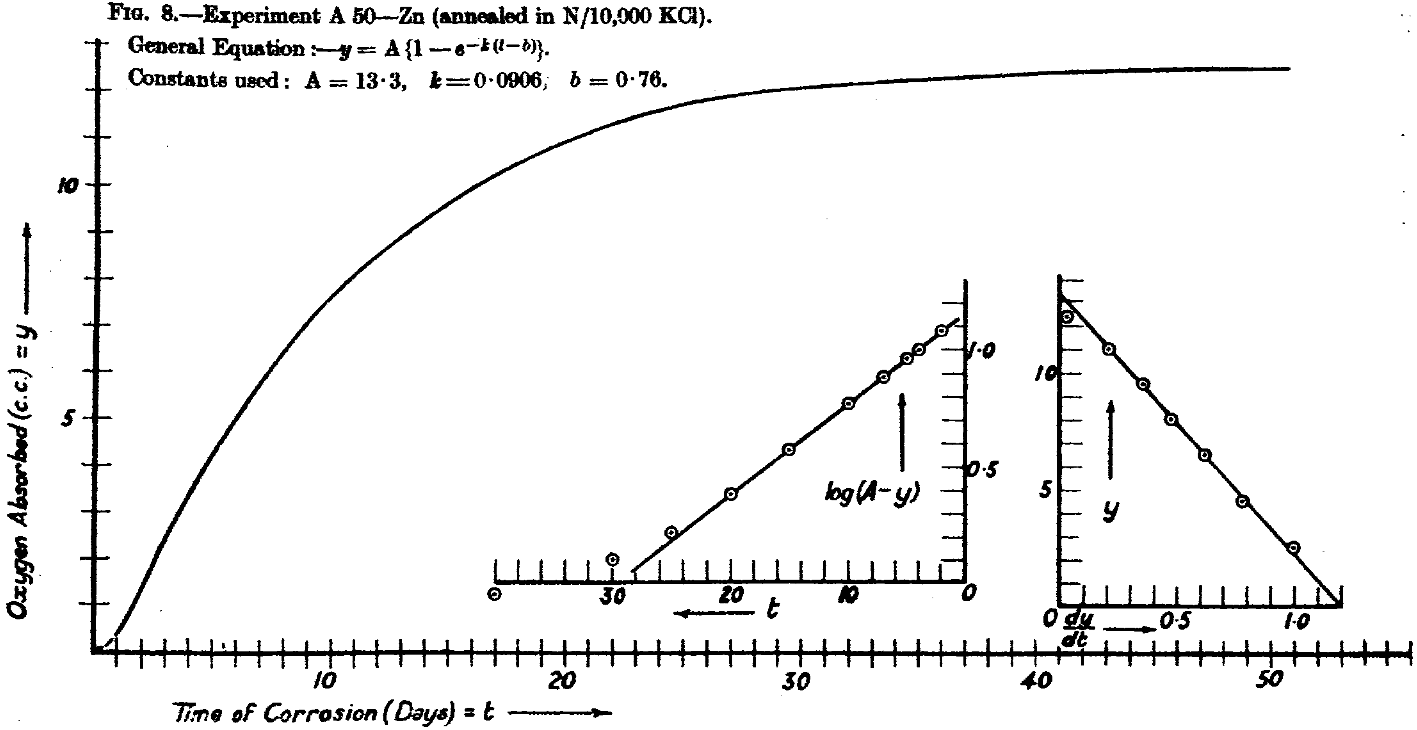

t (days).	y (expt.).	y (calc.).	t (days).	y (expt.).	y (calc.).
2	1·40	1·40	20	10·94	10·97
4	3·42	3·38	25	11·70	11·82
5	4·27	4·24	30	12·05	12·36
7	5·77	5·74	40	12·41	12·92
10	7·53	7·54	55	12·63	13·20
15	9·65	9·64	103	13·00	13·30

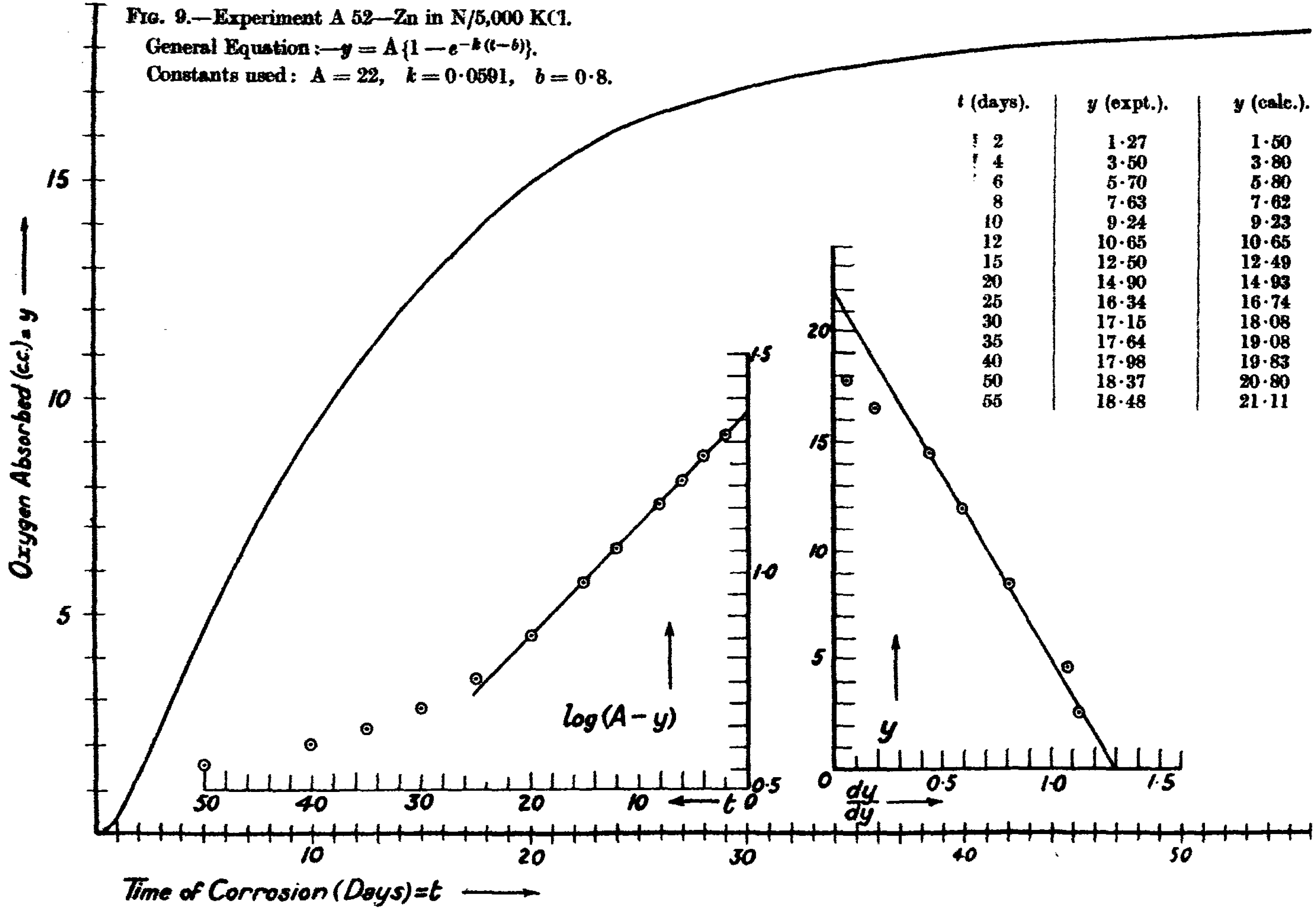

FIG. 9.—Experiment A 52—Zn in N/5,000 KCl.
General Equation :—$y = A\{1 - e^{-k(t-b)}\}$.
Constants used : $A = 22$, $k = 0\cdot0591$, $b = 0\cdot8$.

t (days).	y (expt.).	y (calc.).
2	1·27	1·50
4	3·50	3·80
6	5·70	5·80
8	7·63	7·62
10	9·24	9·23
12	10·65	10·65
15	12·50	12·49
20	14·90	14·93
25	16·34	16·74
30	17·15	18·08
35	17·64	19·08
40	17·98	19·83
50	18·37	20·80
55	18·48	21·11

The failure to get reasonable agreement between specimens that had been either turned or turned and subsequently ground on emery paper is remarkable. Differences between two turned specimens tested in N/10,000 KCl might amount to more than 100 per cent. in 50 days, *e.g.*, A 34 and A 40, fig. 10; usually the corrosion was less than that characteristic of annealed specimens (*cf.* figs. 10 and 11). The behaviour of turned specimens may be briefly summed

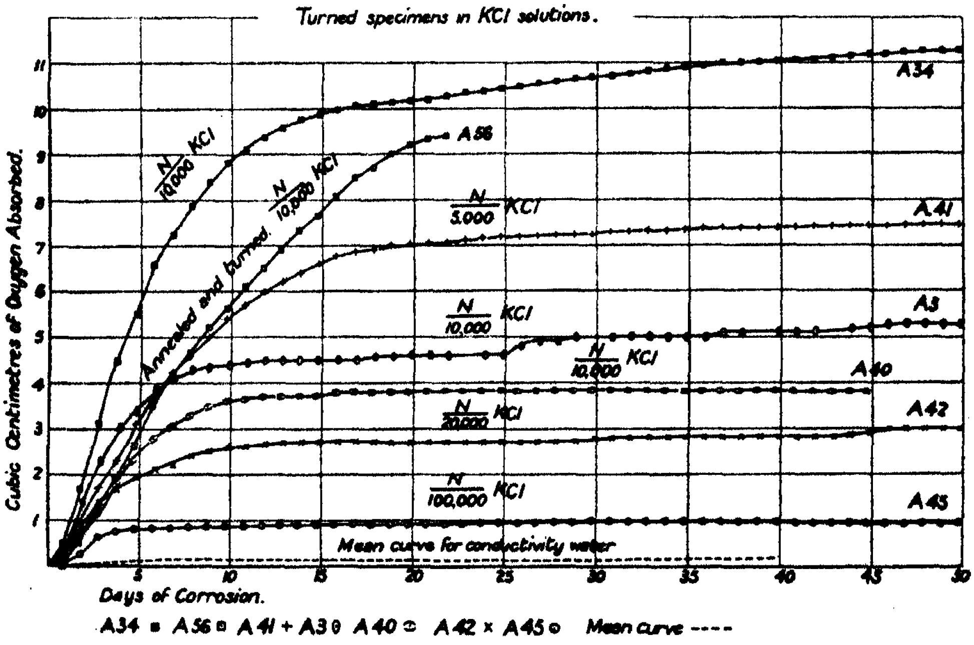

Fig. 10.—Turned Specimens in KCl.

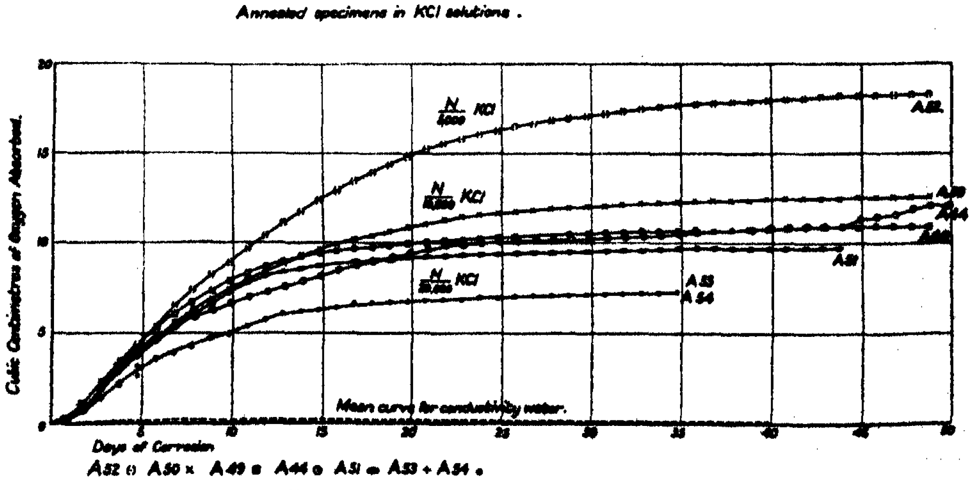

Fig. 11.—Annealed Specimens in KCl.

up by saying that it is unpredictable but sometimes very resistant to corrosion. The surface of the turned metal was covered by a metallic layer that was apparently structureless even when viewed at high magnification and after treatment with acid, and this layer seemed to be the cause of considerable resistance to corrosion wherever it was intact, but especially when a smoothing effect rather than a definite cut was obtained in the lathe when preparing the specimen. Unfortunately this property was not closely reproducible at will. A specimen, A 64, lightly burnished with agate, also gave much less corrosion than annealed specimens.

The behaviour of specimens ground on emery paper was quite different from that of turned specimens. The former usually showed increased corrosion during the first few days, both in conductivity water and N/10,000 potassium chloride, *e.g.*, A 36 and A 58. It was thought at first that the increased rate of corrosion in conductivity water as compared with turned or annealed specimens, was due to traces of impurities acquired from the emery paper, which would slightly enhance the conductivity of the water. This view was negatived by the fact that a similar enhancement of corrosion took place in a chloride solution of such high conductivity ($15 \cdot 5 \times 10^{-6}$ mhos) that the effect of traces of impurity would be negligibly small. No explanation based upon the amount of " work " put upon the metal by the rubbing process could be framed, since turning, on the whole, tended to cut down the rate of corrosion. As a tentative hypothesis it may be suggested that the surface and pores of the emeried metal contain a certain amount of very finely laminated or finely divided metal as a result of the rubbing process, and that such metal is specially reactive, perhaps owing to surface considerations. The amount and distribution would differ in different specimens and closely agreeing results could not be expected. It was noted, however, that the distribution of pits over the surface of a turned and emeried specimen was more regular than over a turned surface, and that after the first few days fairly smooth corrosion-time curves were obtained in N/10,000 potassium chloride ; this suggested that the initial effect of the emery treatment gradually dies away ; it was, in fact, found that the total corrosion of A 58, an emeried specimen, for 20 days was rather less than that of A 49, a turned and annealed specimen, for a similar time.

Preliminary Interpretation of the Curves.

From the foregoing description of the general form of the curves and the statement of the factors which influence accuracy and reproducibility, a preliminary attempt will now be made to deduce the factors which control the process of corrosion in the particular experimental conditions used.

(1) Using standard-sized specimens in potassium chloride solutions of concentration N/10,000 and N/5,000, it is clear that there is always sufficient oxygen present at the metallic surface to carry on corrosion continuously at the maximum rate that has been observed with turned and annealed specimens, for the curves are smooth, and specimens that have been emery-treated as well as those tested in stronger solutions, show a still faster rate in the earlier stages of corrosion.

(2) Consequently the different rates of corrosion that have been observed with different specimens, and with the same specimen at different periods of the test, must be due to factors independent of the oxygen supply.

(3) Typical curves of annealed specimens in N/10,000 and N/5,000 potassium chloride such as A 50 and A 52, have three branches. The first extends from zero time to two or three days, and is concave upward, the next extends to about 30 days, and is convex upwards; the last branch extends to the end of the experiment, and is approximately a straight line, nearly parallel to the time-axis.

(4) The first branches correspond to increases in the rates of corrosion gradual at first but more rapid afterwards. The explanation seems to be that corrosion starts at a slow rate dependent probably upon slight differences of oxygen distribution. These differences are increased by such factors as the formation of screens of corrosion products round, and partially above, the initial centres of corrosion until a maximum is reached, when oxygen is nearly or completely excluded from the corroded areas. The maximum difference of potential that can be set up by an oxygen-concentration cell in the conditions of the experiment will then have been reached and will remain nearly constant for the rest of the experiment.

This explanation of the shape of the first branch of the curve offers no suggestion about the feeble initial cause which starts the whole process, but merely suggests that it may be supplemented and finally brought to a maximum. The nature of the initial cause is the subject of a separate microscopic investigation.

(5) The second branches of the curves have been found to correspond to the equation—

$$y = A(1 - e^{-kt}),$$

in which y is the oxygen absorbed in time t and A and k are constants. Figs. 8 and 9 show the curves for A 50 and A 52, also the derived curves, the values of the constants and tables showing the calculated and experimental values. If extrapolated the curve for A 50 would cut the t axis at 0·76, and the equation may be stated as—

$$y = A\,(1 - e^{-k\,(t-0{\cdot}76)}),$$

for A 52 a similar extrapolation gives a value of 0·81 and a corresponding change may be made in the equation.

The values of the constants of these and other curves are given in Table VI. It will be observed that for similar specimens the value of A rises with increase in initial concentration of the solution, and that of k decreases. It is also clear from the form of the equation that the limiting value of A is that of y, the total oxygen absorbed, but it will only reach this value if t is infinitely great. The value of A depends mainly upon the initial concentration of chlorine ions, but also upon the rate of diminution of their concentration, since if these are withdrawn more rapidly from solution it is obvious that the value of y will be proportionally reduced. The constant k also depends upon the rate of diminution of the chlorine ions, and it has been found experimentally that A and k vary inversely for a given concentration, *i.e.*, the product Ak has an approximately constant value as shown in Table VI.

(6) If the whole process of corrosion is electrolytic the total corrosion will depend on Q the quantity of electricity that has passed. This will depend on :—

(*a*) *The effective conductivity of the liquid for corrosion-generated currents* which, in the conditions of the experiment, is proportional to the amount of chlorine ions present.* The concentration of chlorine ions diminishes as the experiment proceeds, for it has been found that the chlorine is gradually removed from the liquid and locked up in insoluble zinc oxychloride or some equivalent body.

(*b*) *The electrical potential E which actuates the process.*—If E be assumed constant for the greater part of the experiment, as suggested in (4) above, it can be shown that at time t,

$$\frac{dQ}{dt} = K^1\,(A^1 - Q),$$

where Q is the total quantity of electricity that has passed at time t and K^1

---

* (OH) ions present are considered to be mainly film-formers and only corrosion-current-carriers to a relatively slight extent ; this seems justified by the relatively very slight corrosion characteristic of conductivity water, and N/10,000 Ba $(OH)_2$ solution.

and A^1 are constants depending upon the amount of chlorine ions left at time t and their initial concentration.*

But by hypothesis Q varies as y, the amount of oxygen absorbed as found by experiment, and the equation can be written as follows—

$$\frac{dy}{dt} = \mathrm{K}\,(\mathrm{A} - y),\ i.e.,\ y = \mathrm{A}\,(1 - e^{-kt}),$$

an equation which is identical with that found for the second branches of the experimental curves.

Table VI.

Specimen No.	Solution.	Total oxygen absorbed c.c. at 50 days.	Values of constants in equation $y = \mathrm{A}\,(1 - e^{-k\,(t-b)})$.			
			A.	k.	b.	Ak.
(Annealed) A 52	N/5,000	18·36	22·00	0·059	0·81	1·3
(Turned) A 41	N/5,000	7·50	7·70	0·143	1·15	1·1
(Annealed) A 50	N/10,000	12·57	13·30	0·091	0·76	1·2
(Turned) A 40	N/10,000	3·87	4·10	0·29	1·73	1·2
(Annealed) A 54	N/20,000	7·42	7·42	0·13	1·18	0·96

The above relations suggest that the whole process of corrosion in the conditions of experiment is electrolytic in character and determined mainly by the conductivity of the liquid for corrosion currents, *i.e.*, on the amount of the available chlorine ions present.

(7) The reactions characteristic of the second branches of the curves may, therefore, be regarded as :—

(1) At anodes $\mathrm{Zn} + 2\mathrm{Cl} \rightarrow 2\mathrm{Zn\ Cl_2}$.

(2) At cathodes $\begin{cases} 2\mathrm{H}\cdot + \mathrm{O} \rightarrow \mathrm{H_2O}\ ;\ \mathrm{K}\cdot + (\mathrm{OH}) \rightarrow \mathrm{KOH}, \\ \mathrm{Zn\ Cl_2} + 2\mathrm{KOH} \rightarrow \mathrm{Zn\ (OH)_2} + 2\mathrm{KCl}. \end{cases}$

(3) In the liquid away from pits and cathodes :—

$$6\mathrm{Zn\ Cl_2} + (\mathrm{X} + 5)\mathrm{H_2O} \rightarrow \mathrm{Zn\ Cl_2},\ \ 5\mathrm{Zn\ O}\cdot\mathrm{XH_2O} + 10\mathrm{CHl}$$

or some similar insoluble oxychloride or "adsorption compound," by dilution of this solution.

Owing to the last reaction the chlorine is gradually locked up ; the formula has been suggested by the work of G. Andre and F. L. Perrot,† but probably merely represents an average composition of the insoluble product. Obviously equation (3) will provide only a small proportion of the total insoluble corrosion product in the very dilute solutions used; the product will be mainly zinc hydroxide.

---

* The complete argument is given in the Appendix.

† See Mellor, "Treatise on Inorganic and Theoretical Chemistry,' vol. 4, 1923, for discussion of the formulæ of zinc oxychlorides and full references to literature.

8. Third branches of the curves. For N/5,000 potassium chloride solution (A 52, fig. 11) analysis showed at the end of 88 days that 0·13 mgm. of chlorine was left in the solution, *i.e.*, only 83 per cent. of that originally in solution had been used; comparison between the final experimental value of the oxygen absorbed and the maximum value calculated from the equation showed the proportion $\left(\frac{18\cdot 87}{22}\right) = 86$ per cent. This suggests that the decided falling away of the third branch of the experimental curve from the calculated curve, as shown in the tables in fig. 9, is mainly due to the barring out of some of the chlorine ions from the anodic areas by means of accumulation of corrosion products. If this be so, the discrepancies between the calculated and experimental curves should increase in stronger solutions which give greater corrosion, and decrease in more dilute solutions. So far experimental confirmation of this prediction has been obtained in dilute solutions only.

There is, possibly, another factor which tends to decrease the total corrosion when this is concentrated upon a relatively small number of deep pits. Experiment has shown that the deep pits become narrower as they penetrate into the metal and terminate as very fine passages; it is clear that diffusion of zinc chloride out of such pits will become increasingly difficult as the pits deepen, with the result that there is probably a continually increasing concentration of zinc ions in the deep pits. The anode potential will be affected, and this will result in the gradual slowing down of corrosion and set a limit to the depth to which a pit can penetrate.

For N/10,000 solution (A 50, fig. 8) the experimental curve had approached to within about 2 per cent. of the maximum value for the calculated curve at the end of 103 days, but the third branch falls very slightly below the calculated value from 25 days onward.

In the N/20,000 solution (A 54) the third branch of the curve had not been reached in 50 days, since at the end of this time the calculated exponential and experimental curves were still in close agreement, as shown in Table VI and fig. 7.

9. The suggestion that chlorine ions may be barred out from pits raises the question of the effect of the films of corrosion products on the earlier part of the curve. Since the course of the curve for A 50 between 2 and 12 c.c. of oxygen absorbed is dictated mainly by the concentration of chlorine ions, it is

reasonable to assume that the electrical resistance offered by films of corrosion products is relatively unimportant during that part of the curve. This assumption receives experimental support from: (*a*) The fact that in experiment A 52 with a stronger solution N/5,000, and much more corrosion product than occurred with A 50, the exponential form of the curve is maintained to 14 c.c. of oxygen corresponding to 18 days. (*b*) Micrographic observations which have shown that some at least of the more important pits remain open and free from visible films of corrosion products for several days at least; these products are probably in colloidal or gel form in and near the pits. (*c*) The fact that corrosion in K_2CO_3 N/10,000 solution is several times greater than in conductivity water, yet $ZnCO_3$, which is a low solubility product, will be formed at the anode, otherwise the addition of the salt would have no effect on the corrosion. Consequently the current which is conveyed by (CO_3) ions must be able to pass fairly freely through the film of $ZnCO_3$ (or basic carbonate). It seems possible that a *thin* film of precipitated zinc hydroxide gel, even when formed across the entrance of a pit, may not offer a very large electrical resistance to the passage of a current nor to diffusion of Cl ions; the opaque appearance of the dried corrosion product on a specimen is deceptive, since the film has parted with the water, of which it largely consisted when wet.

The foregoing considerations were based upon curves for annealed specimens A 50 and A 52, and the question arises whether they apply to such specimens as A 40, which was turned and tested in N/10,000 KCl similarly to A 50, but which gave only about one-third of the total corrosion of that specimen. This small amount of corrosion was correlated with a relatively very small number of pits; there were only about 50 in all on the upper surface instead of 500–1000 or more, and none shallower than 0·04 mm. An examination of the curve for this specimen showed that the second branch, namely, that corresponding to the exponential equation, occurred between three and nine days, corresponding to 1·3 and 3·5 c.c. of oxygen; as the total corrosion corresponded only to 3·87 c.c. of oxygen it is evident that the equation satisfactorily represents the course of corrosion except for a short initial period roughly similar to that observed for A 50 and A 52. The difference between the curves for A 40 and A 50 lies in the values of the constants A and *k* (see Table VI), and it seems that they have been affected indirectly by the nature of the metal surface which, for A 40, has enormously reduced the number of the pits.

It is clear that the effect must be indirect since the constant A is dependent mainly upon the initial concentration of chlorine ions and the constant *k* upon the rate of diminution of these ions in the solution. Since the initial concentration of chlorine ions was the same for both A 40 and A 50, it is reasonable to seek the cause of the change in value of the constants in the change in the rate of removal of ions from solution, and it is known, from inspection of equations for A 50 and A 52, that if k be changed A will also be changed, but in the opposite sense.

Since the amount of corrosion was much less for A 40 than for A 50, it may be tentatively assumed that the chlorine ions were more rapidly removed from solution, because if these be rapidly locked up the total amount of corrosion will be cut down. Since the outstanding differences between the two specimens were the much smaller number the deeper penetration and the less regular spacing of the pits on A 40, it is reasonable to seek a relation between these differences and the rapid precipitation of the chlorine ions. It is clear that zinc will only be precipitated by dilution, according to equation (3) above, if it escape contact with KOH solution (which would precipitate it as $Zn(OH)_2$, and reform KCl, which would carry on corrosion). The question, therefore, arises whether the chances of precipitation of the chlorine ions as an " oxysalt " are greater when the number of pits is reduced and their spacing made less regular.

With a small number of active pits irregularly distributed over the surface of the specimen, the cathodic areas at which KOH is produced will probably be somewhat restricted. In the initial stages of corrosion zinc chloride will meet the KOH and rapidly build up walls of corrosion product round each pit, which will soon form considerable tubular barriers between the chloride-producing anode and the potash-producing cathode. After this formation the chances of the escape of the chloride out into the liquid without being precipitated would seem to be increased as compared with conditions consisting of a much larger number of much smaller barriers distributed over the surface of the metal.

For potassium chloride solutions of concentration N/20,000, two curves were obtained for annealed specimens A 53 and A 54 (fig. 11). For the first five or six days these curves wavered slightly about a mean position and then settled down to identical readings for a further five days, at the end of which time A 53 had to be removed from the thermostat. A smoothed curve was drawn through the mean positions of the two curves where they differed, then through their identical paths, and, finally, following the data for A 54 only. It was found that this curve could be closely represented by the general equation already given with the following values for the constants :—

$$A = 7 \cdot 42,\ k = 0 \cdot 133,\ \text{and}\ b = 1 \cdot 18\ \text{(see fig. 7).}$$

General Table of Results.

Specimen number.	Metal sample.	Treatment.	Corroding liquid.	Conductivity of liquid.	Time of experiment. Days.	Depth of deepest pit on upper surface.	Total oxygen consumption.	Material of corrosion vessel.	Effect of glass supports.
				mhos.		mm.	c.c.		
A 3	Australian electrolytic zinc, No. 3	Turned	KCl N/10,000 approx.	—	165	0·27	6·41	Durosil	Not definite.
A 4	"	"	c. water aerated	$0{\cdot}28 \times 10^{-4}$	115	0·13	2·32	"	None.
A 6	"	"	K_2SO_4 N/10,000	—	88	0·235	4·91	"	"
A 8	"	"	KH_2PO_4 N/10,000	—	117	—	1·80	"	"
A 9	"	"	K_2CO_3 N/10,000	—	78	0·05	1·66	"	"
A 10b	" cracked	"	c. water	$0{\cdot}065 \times 10^{-4}$	20	—	0·247	—	"
A 13	Australian electrolytic zinc	"	c. water	$0{\cdot}10 \times 10^{-4}$	7	—	0·68	Silica	Not definite.
A 14	"	"	c. water	$0{\cdot}087 \times 10^{-4}$	10	—	0·437	Jena glass	None.
A 16	"	"	Laboratory distilled water	$2{\cdot}76 \times 10^{-4}$	50	—	0·91	"	Not definite.
A 18	"	"	c. water, shallow immersion.	$0{\cdot}064 \times 10^{-4}$	78	0·03	0·285	Durosil	Noticeable.
A 21	" No. 2 casting	"	c. water	$0{\cdot}065 \times 10^{-4}$	68	0·117	0·245	—	"
A 23	" "	"	"	$0{\cdot}067 \times 10^{-4}$	57	0·09	0·35	Jena glass	None.
A 29	Australian electrolytic zinc, No. 3 casting	Emery polished	"	$0{\cdot}075 \times 10^{-4}$	49	0·04	0·295	—	"
A 33	"	Annealed and emery polished	"	$0{\cdot}079 \times 10^{-4}$	40	0·155	1·954	Jena glass	Noticeable.
A 34	"	Turned	KCl N/10,000	—	61	—	11·42	Durosil	—
A 35	"	Annealed and emery polished	c. water	$0{\cdot}070 \times 10^{-4}$	42	0·165	0·835	—	None.
A 36	"	"	"	$0{\cdot}058 \times 10^{-4}$	23	0·07	0·836	—	"
A 37	"	Turned	"	$0{\cdot}061 \times 10^{-4}$	164	0·18	1·15 for 163 ds.	Durosil	Noticeable.
A 38	"	Annealed and emery polished	"	$0{\cdot}094 \times 10^{-4}$	12	—	0·445	—	Not definite.

A 39	,,	Annealed and turned	,,	$0 \cdot 065 \times 10^{-6}$	71	0·07	0·131 for 50 ds.	Jena glass	Noticeable.
A 40	,,	Turned	KCl N/10,000	$15 \cdot 5 \times 10^{-6}$	66	0·28	3·872 for 46 ds.	Durosil	,,
A 41	Australian electrolytic zinc No. 4 casting.	,,	KCl N/5,000	$30 \cdot 8 \times 10^{-6}$	83	0·13	7·695	Jena glass	,,
A 42	,,	,,	KCl N/20,000	$8 \cdot 4 \times 10^{-6}$	151	0·21	4·18	Silica	,,
A 43	,,	,,	c. water deep immersion.	$0 \cdot 067 \times 10^{-6}$	140	—	1·755	Jena glass	,,
A 45	,,	,,	KCl N/10,000	$1 \cdot 92 \times 10^{-6}$	51	0·20	0·97	Durosil	Not definite.
A 46	,,	Turned and annealed in argon	,, ,,	$15 \cdot 7 \times 10^{-6}$	24	—	12·87 for 20 ds.	,,	Noticeable.
A 47	,,	,,	c. water	$0 \cdot 047 \times 10^{-6}$	53	—	0·215	—	,,
A 48	,,	,,	,,	$0 \cdot 05 \times 10^{-6}$	52	0·055	0·18	—	,,
A 49	,,	,,	KCl N/10,000	$15 \cdot 5 \times 10^{-6}$	50	0·446	10·95	Durosil	,,
A 50	,,	,,	KCl N/10,000	$15 \cdot 7 \times 10^{-6}$	117	0·505	13·12	Jena glass.	—
A 51	,,	,,	KCl N/10,000	$15 \cdot 5 \times 10^{-6}$	50	—	9·77	Silica	—
A 52	,,	,,	KCl N/5,000	$30 \cdot 6 \times 10^{-6}$	50	—	18·36	Durosil	—
A 53	,,	,,	KCl N/20,000	$7 \cdot 7 \times 10^{-6}$	10	0·27	4·98	,,	Noticeable.
A 54	,,	,,	KCl N/20,000	$7 \cdot 7 \times 10^{-6}$	62	—	7.51	,,	—
A 56	,,	Annealed and turned	KCl N/10,000	$15 \cdot 5 \times 10^{-6}$	81	0·59	10·26	Jena glass	Noticeable.
A 57	,,	Turned and emery polished	c. water	$0 \cdot 082 \times 10^{-6}$	26	—	0·97	,,	Not definite.
A 58	,,	,,	KCl N/10,000	$15 \cdot 6 \times 10^{-6}$	21	—	8·37	Durosil	Noticeable.
A 64	,,	Agate-burnished	KCl N/10,000	$15 \cdot 5 \times 10^{-6}$	64	—	5·83	,,	,,
C 1	Grade C*	Turned	c. water	$0 \cdot 088 \times 10^{-6}$	9	0·035	0·37	Jena glass	Not definite.
C 2	,,	,,	,,	$0 \cdot 14 \times 10^{-6}$	102	0·08	0·44	,,	None.
C 3	,,	,,	,,	$0 \cdot 09 \times 10^{-6}$	55	—	0·91	,,	Noticeable.
C 4b	,,	,,	,,	$0 \cdot 065 \times 10^{-6}$	100	—	0·815	Silica	Not definite.
S 1	Grade A*	As cast	N/10,000 KCl	$15 \cdot 2 \times 10^{-6}$	55	—	12·68	Durosil	Noticeable.

---

* Redistilled zinc supplied by N. Jersey Zinc Co.

The experimental curve and the theoretical curve deduced from these values are in remarkably good agreement for the period 2 to 50 days.

In conductivity water and N/100,000 KCl no parts of the curves correspond to the typical equation. After the initial concave-upwards branch the paths could usually be represented by straight lines connected by small steps. The most probable interpretation of the step phenomena seems to be the temporary and partial breakdown of membranes of corrosion products blocking the pits, which allow a short period of renewed activity.

It will be observed that the curves for chloride solutions rarely show an acceleration of the rate of corrosion after the first few days, except in the case of emeried specimens; after the initial rise in the rate there is a continuous drop. It may be tentatively suggested that few, if any, new pits are developed after the first day or two; their positions seem to be fixed early in the corrosion process, probably by the details of the metal surface, but their rate and period of operation may be determined mainly by conditions external to the metal, such as the nature of the corroding liquid, temperature, pressure and diffusion currents. These factors probably also determine, to some extent, the number of the pits. These suggestions are mainly based upon observations made during microscopic work and are now being developed more fully.

It is important to notice that the factors which are believed to control the corrosion of zinc over the main portions of the curves in the solutions described in this paper do not include the rate of oxygen supply. This may be taken to mean that there was always sufficient oxygen available for the fastest rate of corrosion which could occur in the particular conditions studied. The rate of corrosion can be increased by the use of solutions of greater concentration and conductivity, and it is to be expected that conditions would soon be reached in which the rate of oxygen supply would become the controlling factor. A new branch should then appear in the time-corrosion curves and take the form of a straight line, the slope of which would depend largely upon the rate of oxygen supply. It has already been found that a straight-line branch occurs in the curve for N/1,000 potassium chloride solution, and investigation of this and stronger solutions is now being pursued.

This research has been carried out under the direction of the Corrosion of Metals Research Committee of the Advisory Council of the Department of Scientific and Industrial Research in the Metallurgical Laboratories of the Royal School of Mines. The authors wish to thank the Chairman, Prof. H. C. H. Carpenter, for much advice and many facilities afforded to them.

They also wish to thank Miss Ruth Pirret, who has made numerous measurements with great care during the course of the work.

APPENDIX.—DEVELOPMENT OF AN EQUATION CONNECTING TIME AND CORROSION.

At time t suppose :—

total quantity of electricity which has passed $= Q$
and momentary current at time t .... $= i$
and electrolytic resistance.................. $= R$.

Let E.M.F. $= E$.

Let C = amount of chlorine present at beginning and
C' = amount of chlorine used up at time t.
Then amount of chlorine left $= C - C'$.

Now

$$i = \frac{dQ}{dt}, \tag{1}$$

and also

$$i = \frac{E}{R}. \tag{2}$$

At time t:—

the electrolytic conductivity for corrosive current varies as the chlorine left, *i.e.*,

$$\frac{1}{R} = K\,(C - C'). \tag{3}$$

And C' is proportional to total quantity of electricity that has passed during time t, therefore,

$$C' = A\,Q.$$

Therefore conductivity

$$\frac{1}{R} = K\,(C - A\,Q.).$$

Therefore

$$i = \frac{E}{R} = E\,K\,(C - A\,Q.) = A\,E\,K\left(\frac{C}{A} - Q\right).$$

$$= K^1\,(A^1 - Q).$$

Hence

$$\frac{dQ}{dt} = K\,(A^1 - Q).$$

But if Q varies as y (*i.e.*, the oxygen absorbed),

then $$\frac{dy}{dt} = K\,(A - y),$$

therefore $$y = A\,(1 - e^{-Kt}).$$

The Magnetic Susceptibility of the Alkali Metals.

By Prof. J. C. McLennan, F.R.S., Dr. Richard Ruedy and
Elizabeth Cohen, M.A.

(Received August 5, 1927.)

1. *Introduction.*

In a recent paper, Miss L. Crow found the alkali metals to be diamagnetic: they seemed in this respect to resemble copper, silver and gold, which have in the vapour state one Bohr magneton per atom, but are diamagnetic when solidified. In view of the statement made by Miss Crow that the susceptibility of the glass containers used was negligibly small, it seemed to us necessary to repeat her work. The following paper gives the results of our investigation.

In a series of experiments, Gerlach and Stern,[*] and also Taylor,[†] showed that for elements of the first column the vapour molecules possess one Bohr magneton $m_0 = 5550/\mathrm{N}$ gauss cm., N being Avogadro's number. When placed in a magnetic field H the velocity of the valence electron increases, and the energy of the molecule changes by the amount $(m_0\mathrm{H}) + (e^2\mathrm{H}^2/8mc^2)\Sigma r^2$,[‡] m being the mass of the electrons, e its charge, c the velocity of light, and r the distance from the nucleus. The second member, the diamagnetic effect, is usually negligible. The first term, the paramagnetic effect, leads to an orientation of the molecule parallel to the magnetic field, an orientation which remains, however, incomplete on account of the energy of thermal agitation and the collisions of the atoms. In the case of the alkali vapours for which the molecules are free to orientate themselves in any direction, the molecular susceptibility may be shown to be $\chi_m = \frac{1}{3}\mathrm{N}m_0^2/k\mathrm{T}$. In solid bodies the number of positions which the molecule is free to assume is limited by the action of the neighbouring atoms with which it composes the crystal lattice, and the magnetic field may not be able to overcome the forces in the solid body and not succeed in orientating the magnetons. The paramagnetic properties are then hidden, and the diamagnetic factor may become predominant. Furthermore, lower electron shells become important, as is known in the case of the rare earths.

The band spectrum of the sodium molecules, which exist in a small amount in sodium vapour even up to temperatures of 400° C., corresponds to transitions between single electronic states, the normal state of the molecule being a $^1S_0$ state. This shows that, as in the case of the formation of the hydrogen molecule, the two sodium atoms orientate themselves when combining in such a way that their magnetic moments are compensated, the two electrons, for instance, spinning in opposite directions. That a similar co-ordination takes place in the solid is clear from mere geometric conditions; for in the sodium atom the distance in the aphelion position of the electron from the nucleus is 2·55 Å,* whilst the distance between the nuclei in the crystal lattice (at 90° K.) is only 4·24 Å; in potassium the valence electron reaches a point 3·1 Å from the centre, whilst the distance between the two neighbouring atoms in the solid is only 5·25 Å. There is then not enough space for both electrons to move independently. Furthermore, as copper, silver and gold crystallise as face centred cubes, and the alkalies as body centred cubes, where the atoms are farther separated from each other, the two groups of substances may clearly differ in their magnetic properties in the solid state, although as vapours they all possess one Bohr magneton per atom gramme. Similar variations occur in all the columns of the periodic system as occur in the first column. In a large number of elements† the susceptibility of the solid differs thus in sign and magnitude from that of the vapour, even in elements belonging to the same group and having the same crystal structure.

---

[*] 'Ann. d. Physik,' vol. 74, p. 673 (1924), and vol. 76, p. 163 (1925).

[†] 'Phys. Rev.,' vol. 28, p. 576 (1926).

[‡] Herzfeld, 'Phys. Z.,' vol. 26, p. 824 (1925).

The most extended measurements of the magnetic properties of the elements have, however, been made at a time when the metallurgy of many of the elements was insufficiently developed, and their crystal structure unknown, so that new measurements over large ranges of temperatures are desirable and necessary before a theory can be formulated. This is particularly true for the magnesium group, the members of which crystallise in the dihexagonal system. Their magnetic properties ought to be different in different directions, but no definite observations have been made as yet.

The following work contains the results obtained in our re-investigation of the alkali metals.

2. *Preparation of the Alkali Metals.*

The metals to be investigated were introduced into the experimental tube by a vacuum distillation of the metal from a side arm. The side arm consisted of a series of pyrex bulbs sealed to a piece of pyrex glass tubing, into which the metal was first introduced. The bulbs were about one and a half inches in diameter, with a short constriction of one-eighth inch diameter between them. The repeated distillations of the metal through the series of bulbs was to increase the purity of the material that finally reached the experimental tube. The system was first heated to drive off all moisture. The end of the distillation arm was then opened and the metal inserted. The bulbs were again heated and the tubes then raised to a temperature of about 250° C. This temperature was maintained until all oil and gas had been completely removed. The metal was then gently distilled through the side arm. For this purpose a bunsen burner with a soft flame was used.

---

* Simon, 'Naturwiss.,' vol. 15, p. 398 (1927).

† Stoner, 'Magnetism and Atomic Structure.'

The sodium and potassium were prepared from the pure commercial metal, cæsium and rubidium by the action of calcium on halides of these alkalies, according to the method due to Hackspill.* The cæsium was prepared from cæsium chloride mixed with four times the theoretical combining weight of calcium filings. The chloride used was first well dried by heating it in the presence of dry hydrogen chloride gas. The mixture was placed in the tubes TTTT of the distillation apparatus shown in fig. 1, a glass wool plug in each tube serving to prevent any of the contents of the tube from sputtering out when the reaction took place. These four tubes were then joined to the series of bulbs BBBB as shown. While the system was being evacuated the tubes were gently heated to drive off any occluded gases. When no more gas came off the tubes were heated to a temperature of about 500° C., the reaction took place, and the cæsium collected from each tube was distilled slowly through the series of five bulbs and thence into the experimental tube L. The vacuum pump was kept running throughout the process. To determine whether any calcium distilled over with the cæsium, calcium filings were heated in the manner just explained. There was no metal condensed even in the first bulb.

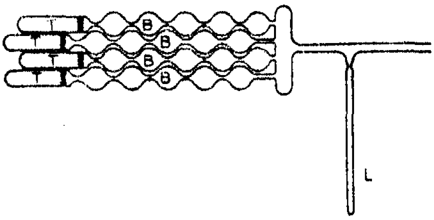

Fig. 1.

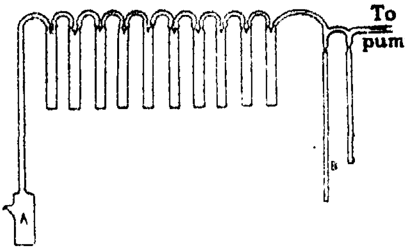

Fig. 2.

After readings in the magnetic field were taken this cæsium was re-distilled several times, and the susceptibility re-determined. For a second set of readings fresh cæsium was made and then distilled through a series of ten tubes (fig. 2). The tubes were heated for an hour at a temperature of about 300° C. while on the vacuum pump, the whole of the distilling apparatus except the end tube A, which contained the cæsium, being placed in an electric oven. The cæsium was slowly distilled through the tubes in succession, and thence into the experimental tube B. The distillation process took in all about seven hours. The melting point of the cæsium prepared in this manner was determined and found to be 28° C. Melting points for cæsium tabulated in Landolt-Börnstein vary from 25·30 to 28·2° C., the latter being according to Bidwell the latest and presumably the most accurate value. The International Critical Tables have adopted 26° C. as the melting point of cæsium. As a result of extended work on cæsium, Bridgman gives 29·7° C. as the melting point of very pure cæsium.

---

* 'Ann. Chim. Phys.,' vol. 28, p. 613 (1913).

The rubidium was prepared in a similar manner to that described for cæsium, rubidium bromide being used in place of cæsium chloride.

Sodium was also prepared by electrolysis through glass,* so as to obtain the metal free from iron. A piece of the glass tube used for weighing the metal was sealed to the neck of a 200-watt lamp. The system was evacuated, and the lamp bulb dipped into a bath of molten sodium nitrate that was connected to the positive pole of the electric mains supplying current to the lamp. Sodium was liberated and deposited on the cooler parts of the inner surface of the lamp bulb. By prolonging the process of electrolysis it was found that several grammes of sodium could be finally obtained inside the lamp. The metal was then driven into the attached tube. It was found possible to accomplish this operation successfully if the narrow tube was connected to the lamp by means of a short wide tube of 2 or 3 cm. length, into which most of the diffusing sodium settled during the electrolysis. By following this procedure it was not necessary to heat the upper part of the bulb, where two different kinds of glass, that of the stem and that of the bulb, were sealed together. The results obtained with a sample of this material are contained in Table II.

3. *Method of Measurements.*

The method used, due to Plücker and Gouy,† was that of weighing the metals in the presence and absence of a strong uniform magnetic field H. This field was obtained by the use of an electromagnet of the rectangular frame type.

---

* Pirani, 'Z. techn. Physik,' vol. 2, p. 232 (1922); Burt, 'J. Opt. Soc.,' vol. 11, p. 6 (1925).

† Stoner, 'Magnetism and Atomic Theory.'

The field was measured by the induction method, the change in magnetic flux through a small coil of many turns, due to the application of the field, being measured by means of a ballistic galvanometer that had previously been calibrated by means of a Duddell standard inductance. The field was determined for different currents through the electromagnet from 12 to 25 amps. The square of the field was plotted against the current in the electromagnet. The value of H^2 could then be read directly from the chart for any current in the electromagnet coils.

If the material to be tested, in the form of a slab of uniform cross section, were hung from one arm of a balance so that the lower end came between the pole pieces of the electromagnet, the susceptibility of the substance should be given by

$$k = 2gP/A\,(H^2 - H'^2),$$

where

A = the area of horizontal cross section of the metal;
H = the strength of the field at the lower end of the slab;
H′ = the strength of the field at the upper end of the slab; and
P = the pull in grammes due to the application of the field.

In our experiments the metals were contained in slender evacuated glass tubes, which were suspended from the balance arm so that the upper end of the metal came in the strongest part of the magnetic field, midway between the pole pieces of the electromagnet (fig. 3). The great advantage of this method was that the effect of the glass tubing was eliminated, provided the tubes were uniform. This was tested experimentally with an exhausted tube, and found to be so.

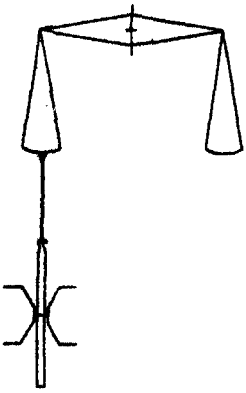

Fig. 3.

Experiments showed that at a distance of three and a half centimetres from the centre of the pole pieces the field strength was only about one-fifteenth of its value midway between the pole pieces: that is, H'^2 is here less than 0·5 per cent. of H^2. As the metals in the tubes were all six centimetres or more in length, H'^2 could be neglected, and the formula would become

$$k = (2g/A)\,(P/H^2).$$

To calculate the susceptibility the pull P on the metal was plotted against the square of the magnetic field H, producing that pull (fig. 4), and the value of P/H² taken as the slope of the straight line thus obtained.

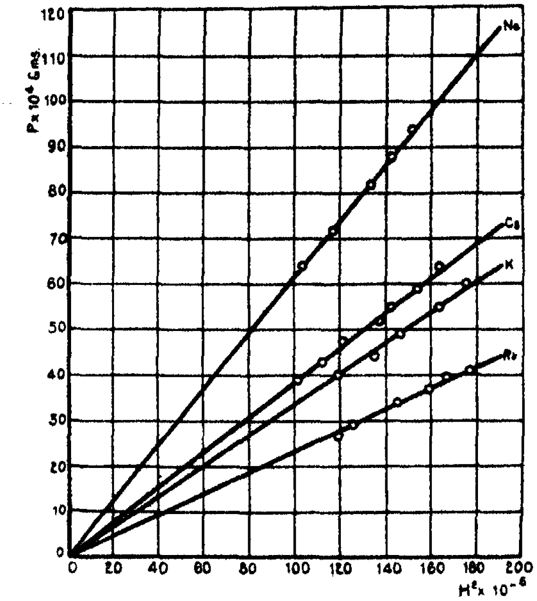

Fig. 4.

4. *Results.*

The results are given in Tables I–V.

Table I.—Sodium.

Current in electro-magnet.	Weight in scale pan.	Pull of field on metal.	Mean current c.	Mean pull for current c. P.	Square of field corresponding to c. $H^2 \times 10^{-4}$.
amps.	gms.	gms.	amps.	gms.	H in gauss.
0	32·4900				
13·3	32·4834	0·0066			
0	99	65			
13·1	36	63	13·1	0·0064	103
0	99	63			
13·0	36	63			
0	99	63			
15·4	28	71			
0	98	70			
15·0	26	72	15·2	0·0072	116
0	98	72			
15·3	26	72			
0	98	72			
18·0	16	82			
0	97	81			
17·9	15	82	17·9	0·0082	133
0	97	82			
17·8	15	82			
0	97	82			
19·7	08	89			
0	96	88			
19·7	08	88	19·6	0·0088	142
0	96	88			
19·5	08	88			
0	96	88			
21·5	00	96			
0	94	94			
21·7	00	94	21·6	0·0094	151
0	94	94			
21·6	00	94			
0	94	94			

The mean value P/H^2 is obtained by plotting column 5 against column 6 (fig. 4).

An average of ten readings gave the inner diameter of the tube as 0·504 ± 0·0005 cm. It followed then that

$$A = 0·199 \text{ cm}^2.$$

$$P/H^2 = 0·615 \times 10^{-10} \text{ (from graph) fig. 4}$$

and

$$k = 2 \times 981 \div 0·199 \times 0·615 \times 10^{-10}$$

$$= 0·61 \times 10^{-6}.$$

Table II.—Sodium Prepared by Electrolysis through Glass.

Current in electro-magnet.	Weight in scale pan.	Pull of field on metal.	Mean current. c.	Mean pull for current c. P.	Square of field corresponding to c. $H^2 \times 10^{-6}$.
amps.	gms.	gms.	amps.	gms.	H in gauss.
0	24·2738				
13·4	12	0·0026			
0	36	24			
13·3	10	26			
0	36	26	13·5	0·0026	217
13·7	09	27			
0	36	27			
13·5	09	27			
0	36	27			
15·6	07	29			
0	36	29			
15·8	07	29			
0	37	30	15·6	0·0030	235
15·7	07	30			
0	38	31			
15·5	08	30			
0	38	30			
18·0	05	33			
0	38	33			
18·0	05	33	18·0	0·0033	252
0	38	33			
17·9	03	35			
0	37	34			
20·2	01	36			
0	37	36			
20·4	99	38	20·4	0·0036	266
0	35	36			
20·6	99	36			
0	35	36			

From graph, $P/H^2 = 0 \cdot 129 \times 10^{-10}$.
Mean of ten readings gave $d = 0 \cdot 228 \pm 0 \cdot 001$ cm., therefore $k = 0 \cdot 62 \times 10^{-6}$.

Table III.—Potassium.

Current in electro-magnet.	Weight in scale pan.	Pull of field on metal.	Mean current c.	Mean pull for current c. P.	Square of field corresponding to c. $H^2 \times 10^{-6}$.
amps.	gms.	gms.	amps.	gms.	H in gauss.
0	31·9979				
13·4	39	0·0040			
0	79	40			
13·4	39	40	13·5	0·0040	110
0	79	40			
13·6	40	39			
0	79	39			
15·5	36	43			
0	79	43			
15·7	35	44	15·6	0·0044	135
0	80	45			
15·7	35	45			
0	81	46			
17·5	32	49			
0	81	49			
17·4	32	49	17·4	0·0049	146
0	80	48			
17·3	30	50			
0	80	50			
20·2	27	53			
0	80	53			
20·0	23	57	20·2	0·0055	163
0	78	55			
20·4	23	55			
0	78	55			
22·4	18	60			
0	78	60			
22·4	18	60	22·4	0·0060	175
0	77	59			
22·4	17	60			
0	77	60			

From graph $P/H^2 = 0·337 \times 10^{-10}$.
Mean of eight readings gave $d = 0·336 \pm 0·0005$ cm., therefore $k = 0·42 \times 10^{-6}$.

Table IV.—Rubidium.

Current in electro-magnet.	Weight in scale pan.	Pull of field on metal.	Mean current c.	Mean pull for current c. P.	Square of field corresponding to c. — $H^2 \times 10^{-6}$.
amps.	gms.	gms.	amps.	gms.	H in gauss.
0	30·7344				
13·6	16	0·0028			
0	44	28			
13·4	16	28	13·4	0·0028	119
0	44	28			
13·3	17	27			
0	43	26			
14·5	14	29			
0	43	29			
14·4	13	30	14·5	0·0029	126
0	42	29			
14·4	13	29			
0	42	29			
17·3	08	34			
0	42	34			
17·4	07	35	17·4	0·0034	145
0	41	34			
17·4	07	34			
0	41	34			
19·8	04	37			
0	41	37			
19·9	04	37	19·8	0·0037	159
0	40	36			
19·7	03	37			
0	39	36			
21·3	00	39			
0	39	39			
21·2	30·7299	40	21·3	0·0040	166
0	·7338	39			
21·5	·7298	40			
0	·7338	40			
23·2	·7297	41			
0	·7338	41			
23·3	·7296	42	23·3	0·0041	177
0	·7337	41			
23·3	·7296	41			
0	·7337	41			

From graph $P/H^2 = 0·232$.
Mean of twelve readings gave $d = 0·422 \pm 0·001$ cm., therefore $k = 0·31 \times 10^{-6}$.

Table V.—Cæsium.

Current in electro-magnet.	Weight in scale pan.	Pull of field on metal.	Mean current c.	Mean pull for current c. P.	Square of field corresponding to c. $H^2 \times 10^{-6}$.
amps.	gms.	gms.	amps.	gms.	H in gauss.
0	29·1972				
12·2	33	0·0039			
0	72	39			
12·3	34	38	12·3	0·0039	101
0	73	39			
12·3	33	40			
0	70	37			
13·9	26	44			
0	69	43			
14·0	26	43			
0	71	45			
13·8	28	43	13·9	0·0043	112
0	71	43			
15·2	26	45			
0	71	45			
15·1	25	46	15·1	0·0045	121
0	70	45			
15·1	25	45			
0	70	45			
17·8	18	52			
0	71	53			
17·7	18	53	17·8	0·0052	137
0	70	52			
17·8	18	52			
0	71	53			
18·8	17	54			
0	71	54			
18·6	15	56	18·7	0·0055	142
0	70	55			
18·8	14	56			
0	69	55			
21·2	09	60			
0	69	60			
21·2	10	59	21·1	0·0059	154
0	69	59			
21·0	10	59			
0	69	59			
23·2	04	65			
0	69	65			
23·1	06	63	23·1	0·0064	163
0	69	63			
23·1	06	63			
0	69	63			

From graph $P/H^2 = 0{\cdot}383 \times 10^{-10}$.
Mean value of sixteen readings gave $d = 0{\cdot}476 \pm 0{\cdot}0004$, therefore $k = 0{\cdot}42 \times 10^{-6}$.

Similar experiments, carried out with the different samples of cæsium obtained as explained, make $k = 0{\cdot}41$, $0{\cdot}37$, $0{\cdot}38$, $0{\cdot}40$, and $0{\cdot}41 \times 10^{-6}$, giving a mean value of $0{\cdot}40 \times 10^{-6}$.

The metals used were tested in turn for the presence of iron as an impurity by a colorimetric analysis. In each case the metal was dissolved in hydrochloric acid, and this solution compared with solutions made up of the same amount of acid and different known amounts of iron trichloride. The solutions used as standards contained 1, 3 and 5 times 10^{-6} grammes of iron. Equal quantities of a solution of ammonium thiocyanate were added to each test tube, together with about five cubic centimetres of ether. The tubes were shaken thoroughly and then allowed to stand. The red colour of the ether layer was then observed, and the amount of iron in the solution determined by comparison with the standard solutions. In all cases it was found that the iron content was only about two parts in a million by weight. The magnetic susceptibility of 2×10^{-6} grammes of iron in the free state and at 12,000 gauss is $0 \cdot 04 \times 10^{-6}$, assuming 217 as the specific intensity of maximum magnetisation (Weiss). We see, therefore, that this quantity of iron could in no way account for the paramagnetic results obtained.

Moreover, Honda* has shown that although we may accurately determine the iron content of a substance by chemical analysis, we cannot, from data so obtained, determine the effect of the iron on the magnetic susceptibility of the element. The total amount of iron present may not be free, but partly or entirely combined in a non-magnetic form. The correction due to the iron content can best be determined by a method due to and used by Owen. If the specific susceptibility be determined for different fields the results can be represented by the formula $\chi = \chi_a + \sigma/H^2$. Where χ is the specific susceptibility at field H, χ_a and σ are constants, σ being the constant saturation intensity of the free iron. Estimated in this way, Owen found the amount of free iron to be considerably less than the total iron content as determined by chemical analysis; it was about 50 per cent. for sodium. In the present experiment the range of fields used was too limited to show this difference due to the small amount of iron known to be present in the metal.

The results obtained are summarised in the following table. Column (ii) gives the experimentally determined volume susceptibility and column (iii) the specific susceptibility. In the data given in column (iv), the maximum correction for iron has been made. Columns (v) and (vi) give the values as obtained by Sucksmith, Honda and Owen. The seventh column contains the atomic susceptibility calculated from the values in (iii). Fig. 5 shows the relation between the atomic susceptibility of the alkali elements and their atomic number.

---

* 'Ann. d. Physik,' vol. 32, p. 1048 (1910).

Table VI.

(i) Element.	(ii) Volume susceptibility. k.	(iii) Specific susceptibility.	(iv)	(v) Sucksmith 0° C.	(vi) Honda and Owen 18° C.	(vii) Atomic susceptibility χ_{Pt}.	(viii) Density.
		χ.	$\chi - \chi_{Fe}$.				
Lithium	—	—	—	—	$0{\cdot}50 \times 10^{-6}$	—	—
Sodium	$0{\cdot}61 \times 10^{-6}$	$0{\cdot}63 \times 10^{-6}$	$0{\cdot}59 \times 10^{-6}$	$0{\cdot}59 \times 10^{-6}$	0·51	14×10^{-6}	0·971
Potassium	0·42	0·49	0·45	0·51	0·40	19	0·862
Rubidium	0 31	0·21	0·17	0·07	0·07	17	1·532
Cæsium	0·42	0·22	0·18	−0·05	−0·10	28	1·97

The alkali metals have been investigated by K. Honda* (sodium and potassium) and by M. Owen† (lithium, sodium, potassium, rubidium and cæsium) from the temperature of liquid air to above the melting point. The metals, supported inside a copper vessel or gelatine box, were placed in a non-uniform field with a stream of carbon dioxide or nitrogen protecting the samples from oxidation. The material contained an appreciable amount of iron, for which a correction was made by measuring the susceptibility in weak and strong fields. Owen observed no change in the susceptibility of the alkali metals near the melting point. Quite generally the paramagnetic elements show no appreciable change in susceptibility at the melting point.

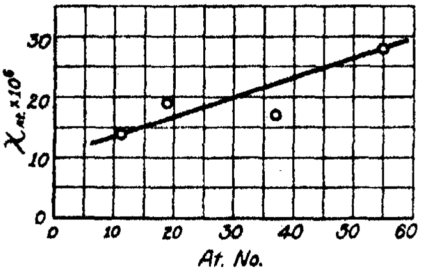

Fig. 5.

More recently Sucksmith‡ undertook the interesting problem of investigating the susceptibility of the alkali metals as they changed from the liquid to the vapour state, but "unfortunately the difficulty of finding a suitable container above 500° C. proved prohibitive." However, he studied the susceptibility of these elements in the liquid state to a temperature of about 500° C. The method he used was essentially that of Faraday, in which the force exerted on a small quantity of the substance in a non-uniform field is measured. The sodium and potassium used contained no detectable trace of iron. The slight quantity of iron found to be present in rubidium and cæsium was corrected for by taking measurements at different fields and eliminating the effect of the ferromagnetic impurity by the method due to Owen. His results are given in curves between the temperatures 0° C. and 500° C. for sodium, potassium, and rubidium, and between 0° C. and 300° C. for cæsium. Sucksmith found that for all four metals the paramagnetism increased slightly at the melting point,* decreasing again when the metal has become molten, and then slightly increasing with increasing temperature. But, as Sucksmith pointed out, if in the vapour state the atoms possess one Bohr magneton, very great increases of susceptibility in the range between 500° C. and the boiling points must still take place.

---

* 'Ann. d. Physik,' vol. 32, p. 1027 (1910).

† 'Ann. d. Physik,' vol. 37, p. 657 (1912).

‡ 'Phil. Mag.,' vol. 2, p. 21 (1926).

Experiments at Liquid Air Temperature.

Honda and Owen found that the magnetic susceptibility of sodium and potassium was constant down to a temperature of — 190° C. As the metals used in Honda's and in Owen's experiments contained considerably more iron than those prepared in the present investigation, it was thought advisable to re-determine the susceptibility of the alkalis at low temperatures. The tubes containing the alkali metals were hung inside a double walled glass vessel, and liquid air was kept bubbling between the walls. The following results were obtained with cæsium and sodium.

Table VII.—Sodium.

Room temperature.		Liquid air temperature.	
Current in E.M.	Pull due to *c*.	Current in E.M.	Pull due to *c*.
	gms.		gms.
0		0	
20·7	0·0007	21·0	·0009
0	0·0007	0	0·0003
21·0	0·0007	21·1	0·0007
0	0·0006	0	0·0007
20·6	0·0005	20·4	0·0006
0	0·0005	0	0·0006
20·4	0·0007	20·2	0·0006
0	0·0006	0	0·0006
Mean 20·7	0·0006	20·7	0·0006

Here $H^2 = 49 \times 10^6$; $P/H^2 = 0\cdot12 \times 10^{-10}$; $k = 0\cdot57 \times 10^{-6}$.

---

* Attempts to reproduce this increase in the present work with cæsium were not successful.

Table VIII.—Cæsium.

Room temperature.		Liquid air temperature.	
Current in E.M.	Pull due to *c*.	Current in E.M.	Pull due to *c*.
	gms.		gms.
0		0	
0·6	0·0010	20·6	0·0010
0	0·0011	0	0·0011
20·8	0·0010	20·4	0·0011
0	0·0010	0	0·0011
20·9	0·0010	20·4	0·0011
0	0·0009	0	0·0012
20·2	0·0010	20·6	0·0012
0	0·0012	0	0·0011
Mean 20·8	0·0010	20·5	0·0011

$H^2 = 49 \times 10^6$. At room temperature $P/H^2 = 0{\cdot}20 \times 10^{-10}$, $d = 0{\cdot}185$ cm., therefore $k = 0{\cdot}40 \times 10^{-6}$. At liquid air temperature $P/H^2 = 0{\cdot}22 \times 10^{-10}$, therefore $k = 0{\cdot}44 \times 10^{-6}$.

The results given in Table VII show that the susceptibilities of these elements were constant down to − 190° C.

To ascertain whether the temperature of the metal was that of the liquid air, some cobalt sulphate heptahydrate, contained in a glass tube similar to the ones used with the alkali metals, was examined, and its susceptibility was found to increase from 39×10^{-6} to 112×10^{-6}, when the temperature was lowered. A comparison of our results with those recorded by Jackson[*] for this salt showed that the temperature must have been about 85° A. The constancy in susceptibility found by us could not be taken as applying at temperatures lower than 85° A.

In a recent paper Pauli has[†] deduced the formula

$$\chi_0 = 2{\cdot}209 \times 10^{-14} n^{1/3}$$

for the susceptibility of the alkali metals near 0° K. by considering the valence electrons as gas molecules possessing angular momentum and subject to quantum conditions, n being the number of metal atoms per unit volume. The values thus obtained are in good agreement with the experimental values found at room temperature. However, the theory predicts a change of paramagnetism with temperature, whereas the paramagnetism of the alkali metals is constant up to near the melting point. Moreover, the formula, when applied to copper, silver and gold, predicts that these should be more strongly paramagnetic than the alkali metals, whereas they are all diamagnetic.

---

[*] 'Comm. of Phys. Lab.,' Leiden, § 163; 'Phil. Trans.,' A, vol. 224, p. 1 (1923).

[†] 'Z. f. Physik,' vol. 41, p. 81 (1927).

There is, then, at present no quantitative theory to account for the paramagnetism of the alkali metals. The paramagnetism of potassium, for example, is smaller than that of the V‴ ion in a solid salt, despite the fact that V‴ has the same number of outer electrons.

A still more puzzling problem is the fact that the paramagnetism of so many elements is quite independent of the temperature. This is the more remarkable as the alkali metals, with the exception of lithium, are amorphous at ordinary temperatures; sodium shows crystal structure* only below 0° C., potassium below − 120° C., rubidium below − 35° C., and cæsium below − 80° C. The electrical resistance shows a change near these transition points, the thermoelectric power† changes, and recently, in a study of the heat conductivity‡ of sodium from the temperature of liquid hydrogen to above room temperature, it was shown that the heat conductivity too gave indications of a variation.

Weiss has proposed the hypothesis that intense atomic fields exist in the solid elements which show no change in the paramagnetism with temperature, but the values to be assumed would be of the order of 10^8 to 10^9 gauss, whereas the fields arising from atoms at distances of the order of those between atoms and molecules are not greater than those which can be applied artificially.

Further experimental work is then necessary upon the anomalous paramagnetics, which, as Stoner hopes, might shed much light on many obscure problems.

We desire to record our indebtedness to Mr. R. H. Chappell for his valuable help in connection with the glass work and the distillation of the metals. We are also greatly obliged to the Sunbeam Lamp Works of the Canadian General Electric, Toronto, for a generous supply of lamps. Elizabeth Cohen, one of the authors, was enabled to participate in this investigation through the award to her of a Bursary by the National Research Council of Canada.

---

* Bidwell, 'Phys. Rev.,' vol. 27, p. 381 (1926).

† Bidwell, 'Phys. Rev.,' vol. 23, p. 357 (1924).

‡ Bidwell, 'Phys. Rev.,' vol. 28, p. 384 (1926).

On the Intensity Distribution among the Lines of Certain Bands in the Spectrum of the Hydrogen Molecule.

By O. W. Richardson, F.R.S., Yarrow Research Professor of the Royal Society.

(Received July 29, 1927.)

There is a definite alternation of intensity in the successive lines of a given branch of this spectrum. This is particularly evident in the Q branches, which are the strongest, the lines usually denoted by Q (1), Q (3) and Q (5) being much more intense than the intervening lines Q (2) and Q (4). For some time I have had evidence which, though in some respects incomplete, pointed to the conclusion that in any band the mean value of the intensities of any two consecutive odd-numbered lines such as Q (1) and Q (3) was nearly equal to three times the intensity of the intervening line such as Q (2). An examination of the much more comprehensive measurements which have recently been obtained by McLennan, Grayson-Smith and Collins[*] seems to remove all doubt from this matter.

In the second row of Table I, I tabulate a the sums of their measured intensities of the lines Q (1) and Q (3) for the successive bands denoted by ${}_0\alpha_0$, ${}_1\alpha_1$, ${}_2\alpha_2$, ${}_3\alpha_3$ and ${}_4\alpha_4$ in Structure, Part V.[†] These are followed in the third row by b, twice the intensity as measured of the corresponding Q (2) line. The fourth row contains the resulting values of $b \div a$. All the foregoing are the

Table I.

			${}_0\alpha_0$	${}_1\alpha_1$	${}_2\alpha_2$	${}_3\alpha_3$	${}_4\alpha_4$
R.T.	a	Q(1) + Q(3)	226	191	131	78½	40
,, ...	b	2Q(2)	94	106	60	38	18
,, ...	$b + a$		0·416	0·555	0·458	0·484	0·451
L.A.	a	Q(1) + Q(3)	170	168	119	79½	38½
,, ...	b	2Q(2)	54	58	36	21	9
,, ...	$b + a$		0·318	0·345	0·303	0·264	0·234
R.T.	and L.A.	Mean $b + a$	0·367	0·450	0·380	0·372	0·342

---

[*] *V. supra*, p. 277.

[†] O. W. Richardson, 'Roy. Soc. Proc.,' A, vol. 113, p. 368 (1926).

data got at Room Temperature (R.T.). These are followed in the same order by similar data got with the thin-walled discharge tube immersed in liquid air (L.A.). Finally, the eighth row contains the average of the two values of $b \div a$ got at the two temperatures.

The data in a table like this must, of course, be regarded critically. The lines have been identified by means of Merton and Barratt's Tables,* and the resolution employed by McLennan, Grayson-Smith and Collins is certainly not superior to that used by Merton and Barratt. On a plate taken for me by Mr. Wilfred Hall on his 21-foot Rowland grating, the following are resolved into close doublets : ${}_0\alpha_0$ Q (3), ${}_1\alpha_1$ Q (1), ${}_1\alpha_1$ Q (2), ${}_3\alpha_3$ Q (3) and ${}_3\alpha_3$ Q (5). It is obvious that the measured intensities of these lines will all be too high. This interference will be most serious when the weak Q (2) line is concerned. It is satisfactory that there is only one case of visible interference with the Q (2) line, namely, in the ${}_1\alpha_1$ band, and also that the values of $b \div a$ got from this band are distinctly higher than the corresponding values got from every other band.

The only bands in which all three lines are free from visible interference and from claims by lines from other systems which are not of negligible intensity are the bands ${}_2\alpha_2$ and ${}_4\alpha_4$. In the case of ${}_4\alpha_4$ the intensity of the weak Q (2) line 15539·43 = λ 6433·47 (2) is hardly measurable with accuracy on account of its proximity to 15536·22 = λ 6434·80 (3), which is of similar intensity. It is probable that the ${}_2\alpha_2$ data are most reliable, and these give a mean value of 0·380. The others do not differ from this by an amount which exceeds the elements of uncertainty in the data, and it is evident that none of them are very far from one-third.

The value of $b \div a$ should be greater at room temperature than at the lower temperature, as is found to be the case. This is due to the fact that at the room temperature the intensity distribution curve among the lines as a function of the rotational quantum number m ($m = 1, 3, 5$, etc., or $m = 2, 4, 6$, etc., but not $m = 1, 2, 3$, etc.) is convex to the m axis in the region from about $m = 1$ to $m = 3$. This is because the value of m for maximum intensity is $>$ about 1. At the lower temperature the maximum shifts to $m < 1$ and the curve between $m = 1$ and $m = 3$ becomes concave to the m axis.

It may be urged that the intensity data are almost as complete for the green bands ${}_1\alpha_0$, ${}_2\alpha_1$, ${}_3\alpha_2$ and ${}_4\alpha_3$, and if they were used instead of the data in Table I the following very unconvincing set of values of $b \div a$ would be obtained, viz. : 0·390, 0·780, 0·614 and 0·929. The testimony of the first three bands is valueless as the second line (Q (2)) is a known blend in each case (see Part V,

---

* Merton and Barratt, 'Phil. Trans.,' A, vol. 222, p. 369 (1922).

p. 375) and the Q (2) line of the fourth band may well be, as there are a lot of lines of uncertain classification in this part of the spectrum.

[*Note added August* 19, 1927.—Since this was written I have had the opportunity of examining two additional plates of this region taken by Mr. Hall. On both plates ${}_4\alpha_3$Q (2) is clearly double, and on one plate the constituents are definitely resolved. On these plates the bands ${}_1\alpha_0$, ${}_2\alpha_1$ and ${}_3\alpha_2$ show a distinct alternation of intensity similar to that in the red bands. The Q (3) line is stronger than the Q (2) line in each case, even when the intensities of the two lines which occupy the position of Q (2) are lumped together. This is in agreement with Merton and Barratt's estimates of the intensities, although it does not accord with the numbers given by McLennan, Grayson-Smith and Collins for ${}_2\alpha_1$ and ${}_3\alpha_2$. This additional information shows that the intensities in the green bands in reality support the conclusions which have been drawn from the other bands.]

The fact that the data in Table I involve each of the initial vibration states 0, 1, 2, 3 and 4 shows that the ratio is about one-third for transitions starting from each of these states in the three-electron state. The only bands for which there are enough data with the four-electron initial state are ${}_1\beta_1$ and ${}_2\beta_2$. These give mean values 0·870 and 0·186 respectively. However, ${}_1\beta_1$ Q (2) is also claimed as ${}_2\gamma_3$ Q (2) and ${}_2\beta_2$ Q (1) is claimed as ${}_0$A${}_0$ Q′ (4), which may be a strong line in that system and ${}_2\beta_2$ Q (3) is known to be too intense and otherwise irregular (see Part V, p. 383); so that such deviations as there are from the values given by the ${}_x\alpha_x$ bands are of the character to be expected from the nature of the lines. The only other band from which sufficiently complete data are available is ${}_1$A${}_0$ Q (*m*).* These give a mean value 0·424 for $b \div a$. The initial state here is probably a three-electron state. These examples suggest that the ratio about 3 : 1 for these alternating intensities is a general, or at least fairly widespread, feature of this spectrum.

The matter can be made more interesting if we consider the theory of the phenomena a little. The intensity of a spectral line is proportional jointly to the number of emitters in the initial state, and to the probability of a "jump" from that state to the relevant final state. The number of emitters is equal to $cpe^{-E/kT}$, where E is the energy and p the *a priori* probability of the emitters in the initial state, c is a constant, k Boltzmann's constant, and T the temperature. I shall assume that the probability of a jump is the same for all lines of a Q branch of a given band. This can be justified by an appeal to the Correspondence Principle, according to an application of which the probability of a jump from a given initial state is, to a first approximation, independent of the rotational energy of that state. This makes the relative intensities of the lines simply proportional to the respective numbers of emitters in the initial states, and therefore proportional to $cpe^{-\mathrm{E}/k\mathrm{T}}$. The different initial states of a given band will only differ as to their rotational energy, so that for E it is sufficient to put the rotational part of the energy. Except for second order refinements, which it is unnecessary to consider, this, according to the formulæ of the wave mechanics, for the m state is $(m + \frac{1}{2})^2h^2/8\pi^2\mathrm{I}$, h being Planck's constant and I the moment of inertia of the molecule about the axis of rotation (perpendicular to the line joining the nuclei). The *a priori* probability p will be proportional to $m + \frac{1}{2}$, but to account for the alternation of intensity of the lines I take the factor c to be different for the odd and even values of m. According to these hypotheses the intensities of the Q (1), (3), (5) lines are given by

---

* This is the same as 20 Q (*m*) of Richardson and Tanaka, 'Roy. Soc. Proc.,' A, vol. 107, p. 164 (1925).

$$\mathrm{I} = c\,(m + \tfrac{1}{2})\,e^{-(m+\frac{1}{2})^2h^2/8\pi^2\mathrm{I}k\mathrm{T}}, \tag{1}$$

and the intensities of the Q (2), (4), (6) lines by

$$\mathrm{I} = c'\,(m + \tfrac{1}{2})\,e^{-(m+\frac{1}{2})^2h^2/8\pi^2\mathrm{I}k\mathrm{T}}. \tag{2}$$

For testing this equation it is desirable to have the intensities of at least four successive lines. On examination of the data it appears that there is only one band whose first four lines are free from visible blends or from interferences with other systems which are so indefinite that the intensities of the suspected lines cannot be estimated. The favourable band is ${}_2\alpha_2$. Even with this band interferences with the following lines have been claimed :—With Q (1) by AP (6), 157P (4), and IV*a*7P (2) with Q (4) by 157P (5) and DR (3) with Q(5) by IV*a*7P (3). By an examination of the intensities found by McLennan, Grayson-Smith and Collins for the other lines of these systems I estimate the intensities of the following lines expressed in their scale of numbers to be negligible on their plates, viz., AP (6), IV*a*7P (2), P (3), 157P (4), P (5), whilst DR (3) is about 4 at room temperature and about 2½ at L.A. As regards AP (6), IV*a*7P (2) and 157P (4), which are claimed to be covered up by ${}_2\alpha_2$ Q (1), this conclusion is confirmed by the work of Merton and Barratt,* who examined the fine structure of this line 6224·81 (9) and found it to have the normal width for the molecule H_2. This result implies that if there are three lines mixed with it their frequencies must be coincident to a degree which is highly improbable or their intensities must be relatively negligible. It thus appears that the only line whose intensity requires correction is Q (4), which is reduced from R.T. 7 L.A. 4½ to about R.T. 3 L.A. 2. The corrected values of the measured intensities of the ${}_2\alpha_2$ Q (m) lines at room temperature (R.T.) and in the tube cooled by liquid air (L.A.) are given in Table II.

---

* *Loc cit.*, p. 383.

Table II.

${}_2\alpha_2$ Q (m) $m \rightarrow$	1	2	3	4	5	(?) 6
Intensity at R.T.	90	30	41	3	*	*
,, L.A.	94	18	25	2	*	*

* Not present in McLennan, Grayson-Smith and Collins' Tables. Presumably too faint to measure.

Considering the lines Q (1), (2), (3), (4) and (5), these data yield for ½ the sum of the intensities of the lines for m even divided by ⅓ the sum of the intensities for m odd 0·378 at R.T. and 0·252 at L.A., the average being 0·315.

If we apply equation (1) to Q (1) and Q (3), we find the values of $\log_{10} c$ and $b = h^2 \div 8\pi^2 IkT \log 10$. From this value of b we obtain the value of $\log_{10} c'$ by applying equation (2) to Q (2). This can be done both for the R.T. and the L.A. data. From these values of b and c or c', according as odd or even lines are concerned, the intensities I_m of the remaining lines can be calculated. In this way I have compiled the data in the second and third rows of Table III. The fourth and fifth rows contain similar data computed with the formula

$$I_m = (c \text{ or } c')\,(m+1)\,10^{-(m+\frac{1}{2})^2 b}, \tag{3}$$

and the sixth and seventh rows the like data, but using

$$I_m = (c \text{ or } c')\,10^{-(m+\frac{1}{2})^2 b}. \tag{4}$$

Table III.

	$\log_{10} c$.	b.	$\log_{10} c'$.	c/c'.	mean c/c'.	I_4 calc.	I_5 calc.	I_6 calc.	T.
R.T.	1·9378	0·071	1·523	2·60	3·13	3·62	3·38	0·216	227° K
L.A.	2·0093	0·0944	1·4464	3·66		1·55	0·79	0·0186	170° K
R.T.	1·7958	0·0639	1·3994	2·49	2·99	6·36	4·38	0·35	259° K
L.A.	1·8693	0·0877	1·3261	3·49		1·77	0·988	0·0292	183·5° K
R.T.	2·031	0·0342	1·6908	2·19	2·42	9·97	9·92	1·76	471° K
L.A.	2·1024	0·0575	1·6144	2·64		2·82	2·31	0·153	280° K

The observed intensities of Q (4), Q (5) and Q (6) seem definitely too low to be compatible with equation (4) and are more favourable to equations (1) and (2) than to (3). At first sight it seems strange that Q (5) 6262·49 (4) should not be recorded, at any rate in the R.T. list. There is, however, a line very close to it, 6264·89 (0), which is given as 3 R.T. → 3 L.A. As 6262·49 is given as of intensity (4) by Merton and Barratt, it is a fairly strong line for that part of the spectrum, and it seems almost certain that it must be present on McLennan, Grayson-Smith and Collins' plates. It is most probable that their intensity represents the composite intensity of the two lines unresolved.

The values of T in the last column are got by substituting the value of $J_0 = 10{\cdot}72 \times 10^{-41}$, the moment of inertia for the vibrationless 3 state (Part V, p. 410), for I in

$$b = h^2 \div 8\pi^2 IkT \log_e 10. \tag{5}$$

Actually this value of J_0 should be increased about 10 per cent. on account of the fact that we are dealing with the 2 quantum vibration state (2 → 2). I have not troubled to make this correction, as a comparison with the data got from the green bands 1 → 0, 2 → 1, etc., which look rather reliable in this matter as the blended Q (2) lines are not involved, suggests that the experimental data for b from ${}_2\alpha_2$ Q (1) and Q (3) are affected by an error which will just about cancel this correction and leave T unaltered. The estimated temperatures from (3) and from (1) and (2), particularly from the latter, are undoubtedly too low for R.T. However, the absolute values of J_0 in the table on p. 410 of Part V may all be somewhat too high. Furthermore, under the spectroscopic experimental conditions the state of these emitters must be far removed from any condition of temperature equilibrium; so that it is probably straining the applicability of the formula too much to expect a better agreement.

One thing at any rate emerges with definiteness from this discussion. Every method of treating the data agrees in making the weights of the alternate sets of states differ by a factor which is very closely 3 to 1. It will be seen that the stronger states are those which have the same weights and rotational quantum numbers as the antisymmetric states of Hund* (except for the difference between $m\,(m+1)$ and $(m+\frac{1}{2})^2$, which is mainly a question of notation) and the alternate weaker states have the same weights and quantum numbers as the symmetric states.

In a recent note† I concluded from a combined analysis of the Q branches of

---

* 'Z. f. Physik,' vol. 42, p. 119 (1927).

† O. W. Richardson, 'Roy. Soc. Proc.,' A, vol. 114, p. 649 (1927).

Werner's ultra-violet bands as arranged by Dieke and Hopfield, and of some related lines in the visible, that the moment of inertia of the unexcited hydrogen molecule was $4 \cdot 52 \times 10^{-41}$. It was pointed out that this value was high compared with any value which seemed probable from the values of the specific heat of hydrogen at various temperatures. More recently Hori,* by a more complete analysis of Werner's ultra-violet bands, without using data from the visible spectrum, has arrived at practically the same value, viz., $4 \cdot 67 \times 10^{-41}$. Dennison† has shown that these values are in agreement with the value calculated from the specific heats of hydrogen if it is assumed that in the rotational states of unexcited H_2 both symmetric and antisymmetric states are present, but there are no transitions between one class of state and the other, so that the gas behaves like a mixture of two separate gases, and, finally, the antisymmetric molecules are three times as numerous as the symmetric molecules.

In the present paper we have found that the antisymmetric molecules are three times as numerous as the symmetric for the initial three-electron states of the H_α bands of Part V, and probably also for the initial four states of the H_β bands, and also probably for the initial state of the ${}_1A_0$ band. Dennison's interpretation of the specific heat of hydrogen means that it holds also for the one-electron state. Furthermore, he quotes Hori to the effect that in the ultra-violet (Werner's) bands the transitions between antisymmetrical terms are three times as strong as between symmetrical. If this is true, it means that the same statement can be made of the two-electron state also.

The only other case I know of in which the intensities of the alternate lines of homopolar band spectra have been measured is that of N_2^+,‡ and here also the ratio is not very different from 3 to 1. It does not seem, however, that this ratio can be completely general, since it is believed, on what appear to be pretty adequate grounds, that in the helium band spectrum one of the alternate sets of lines has zero intensity.

In the visible hydrogen band spectrum there are no lines which are known to involve combinations between symmetric and antisymmetric terms, and it is improbable that there are any strong lines which involve undiscovered combinations of this character. This circumstance will establish the persistence of the 3 to 1 ratio which is attributed, perhaps more fundamentally, to the fact that the antisymmetric states have a paramagnetic combination of the nuclei with three possibilities of orientation, and the symmetric states have not.

---

* Quoted by †Dennison, 'Roy. Soc. Proc.,' vol. 115, p. 483 (1927).

‡ Fassbender, 'Z. f. Physik,' vol. 30, p. 90 (1924).

In conclusion, I wish to thank Prof. McLennan for permission to use the data which he and his collaborators have obtained, in advance of publication, and Mr. Wilfred Hall for taking a number of plates for me on his 21-foot Rowland grating.

The Internal Conversion of γ-Rays.

By Bertha Swirles, B.A., Yarrow Research Student, Girton College, Cambridge.

(Communicated by R. H. Fowler, F.R.S.—Received July 12, 1927.)

§ 1. *Introduction.*

Ellis and Wooster have discussed in two recent papers* the experimental evidence for the absorption of γ-rays in the X-ray levels of the atom in which they are emitted. In the present paper this absorption will be investigated on the lines of quantum mechanics. The problem is that of the perturbation of a heavy atom by a Hertzian doublet placed at its centre. It will be assumed that the characteristic functions corresponding to the orbits considered are those of a hydrogen-like atom. The normalised expressions for all these functions are given by Oppenheimer.† If A be the perturbing term in the potential energy it may be shown by an extension of an argument given by Dirac,‡ that the increase in the number of systems in a given state r (or in the case of positive energies in an interval of length $2\pi h$) from time $-\mathrm{T}$ to T, where T is large compared with the periods of the atom, is

$$\Delta \mathrm{N}(r) = \frac{1}{h^2}\Big(\sum_s + \int\Big)(\mathrm{N}(s) - \mathrm{N}(r))\left|\int_{-\mathrm{T}}^{\mathrm{T}} \mathrm{A}(rs)\, dt\right|^2, \qquad (1)$$

where $\mathrm{N}(s)$ and $\mathrm{N}(r)$ are the numbers of systems initially in the states r and s, and h is here (Planck's constant)/2π. Of these the number of transitions from the state s to an interval of positive energy $(E_r, E_r + dE_r)$ is, supposing $N(r) = 0$,

---

* 'Roy. Soc. Proc.,' A, vol. 114, p. 276 (1927); 'Proc. Camb. Phil. Soc.,' vol. 23, p. 717 (1927).

† 'Z. f. Physik,' vol. 41, p. 268 (1927).

‡ 'Roy. Soc. Proc.,' A, vol. 112, p. 661 (1926). See also J. A. Gaunt, 'Proc. Camb. Phil. Soc.,' vol. 23, p. 732 (1927).

$$\frac{1}{h^2} N(s) \left| \int_{-T}^{T} A(rs)\, dt \right|^2 \frac{dE_r}{2\pi h}. \tag{2}$$

$A(rs)$ is the (rs) matrix component of A, and can be calculated from the known characteristic functions of Schrödinger's wave equation.

The vector potential of a Hertzian doublet with its axis along the axis of z and its moment equal to $f(t)$ is

$$0, \quad 0, \quad \frac{1}{cr} f'(t - r/c), \tag{3}$$

and its scalar potential is

$$-\frac{\partial}{\partial z}\left(\frac{1}{r} f(t - r/c)\right). \tag{4}$$

The generalised wave equation is, neglecting squares and higher powers of $f(t)$,*

$$h^2 \nabla^2 \psi + 2m\left(ih\frac{\partial}{\partial t} - mc^2 + \frac{Z\varepsilon^2}{r}\right)\psi + \frac{1}{c^2}\left(ih\frac{\partial}{\partial t} - mc^2 + \frac{Z\varepsilon^2}{r}\right)^2 \psi$$
$$= -2ih\frac{\varepsilon}{c^2 r} f'(t - r/c)\frac{\partial \psi}{\partial z} + 2m\varepsilon\frac{\partial}{\partial z}\left(\frac{1}{r} f(t - r/c)\right)\psi. \tag{5}$$

The left-hand side is the wave equation for the hydrogen atom, including the relativity terms which may here be neglected. The reason for introducing this generalised equation is that in the non-relativity form the order of the operators in the perturbing terms is ambiguous.

Expanding the characteristic functions of the perturbed equation as a series and integral of those of the unperturbed equation

$$\psi = \left(\sum_s + \int\right) a_s \psi_s e^{-iE_s t/h} \tag{6}$$

we obtain

$$ih\dot{a}_r = \left(\sum_s + \int\right) a_s \left[-\frac{ih\varepsilon}{c^2 m}\int \frac{1}{r} f'(t - r/c)\frac{\partial \psi_s}{\partial z}\psi_r e^{i(E_r - E_s)t/h}\, dv \right.$$
$$\left. + \varepsilon \int \frac{\partial}{\partial z}\left(\frac{1}{r} f(t - r/c)\right)\psi_s \psi_r e^{i(E_r - E_s)t/h}\, dv \right]. \tag{7}$$

By comparison with equation (25) of Dirac's paper† we see that

$$A(rs) = -\frac{ih\varepsilon}{c^2 m}\int \frac{1}{r} f'(t - r/c)\frac{\partial \psi_s}{\partial z}\psi_r e^{i(E_r - E_s)t/h}\, dv$$
$$+ \varepsilon \int \frac{\partial}{\partial z}\left(\frac{1}{r} f(t - r/c)\right)\psi_s \psi_r e^{i(E_r - E_s)t/h}\, dv, \tag{8}$$

---

* See O. Klein, 'Z. f. Physik,' vol. 41, p. 407 (1927).

† *Loc. cit.*, p. 674.

and putting

$$(E_r - E_s)/h = \nu, \tag{9}$$

the expression (2) becomes

$$\frac{1}{h^2}N(s)\left|\int_{-T}^{T}\int\left(-\frac{ih\epsilon}{c^2 m}\frac{1}{r}f'(t - r/c)\frac{\partial\psi_s}{\partial z}\psi_r + \epsilon\frac{\partial}{\partial z}\left(\frac{1}{r}f(t - r/c)\right)\psi_s\psi_r\right)e^{i\nu t}\,dt\,dv\right|^2\frac{d\nu}{2\pi}. \tag{10}$$

Here ν is the angular frequency and is equal to 2π times the frequency.

Let $f(t)$ from time $t = -T$ to $t = T$, where T is very large, be resolved into its harmonic components, and suppose all these to vanish except for a small range of frequencies from ν to ν + $d\nu$. Let M be the number of γ-rays of frequency ν, per unit frequency range, emitted from time $t = -T$ to $t = T$. Then,

$$Mh\nu\,d\nu = \frac{4\nu^4}{3c^3}\left|\int_{-T}^{T}f(t)\,e^{i\nu t}dt\right|^2\frac{d\nu}{2\pi}, \tag{11}$$

and

$$f'(t) = -i\nu f(t). \tag{12}$$

Then putting

$$N(s) = 1$$

the expression (10) becomes

$$\frac{3c^3}{4h\nu^3}\left|\int\left\{\epsilon\frac{\partial}{\partial z}\left(\frac{1}{r}\right)e^{i\nu r/c}\psi_s\psi_r - i\nu e^{i\nu r/c}\left(-\frac{\epsilon}{c}\frac{1}{r}\frac{\partial r}{\partial z}\psi_s\psi_r - \frac{ih\epsilon}{mc^2}\frac{1}{r}\frac{\partial\psi_s}{\partial z}\psi_r\right)\right\}dv\right|^2 M\,d\nu$$

$$= \frac{3c^3\epsilon^2}{4h\nu^3}\alpha_{\nu z}M\,d\nu, \text{ say.} \tag{13}$$

Then, averaging over all directions of the axis of the doublet, we have that the probability of the emission of an electron from the state s to the state r is

$$\alpha_\nu = \frac{c^3\epsilon^2}{4h\nu^3}(\alpha_{\nu x} + \alpha_{\nu y} + \alpha_{\nu z}). \tag{14}$$

§ 2. *The Absorption in the K-levels.*

The expressions for the ψ's in polar co-ordinates (r, θ, ϕ) are given by Oppenheimer* in the form

$$u(r)\,v(\theta)\,w(\phi),$$

where

$$w(\phi) = \cos m\phi + i\sin m\phi,$$

$$v(\theta) = P_k^m(\cos\theta)$$

and $u(r)$ satisfies the equation

$$\frac{1}{r^2}\frac{d}{dr}\left(r^2\frac{du}{dr}\right) + \left(\gamma^2 + \frac{2\alpha}{r} - \frac{k(k+1)}{r}\right)u = 0, \tag{15}$$

---

* *Loc. cit.*, p. 276.

where

$$\gamma = +\sqrt{\frac{-2m\mathrm{E}}{h^2}}, \quad \alpha = \frac{\mathrm{Z}\varepsilon^2 m}{h^2}.$$

m and k are integers. If E is positive and equal to E′, the equation (15) is satisfied by

$$u = r^{k'} \int_{\mathrm{C}} e^{zr} (z - \gamma')^{k' - in'} (z + \gamma')^{k' + in'} \, dz, \tag{16}$$

where C is a certain double circuit and

$$n' = i\alpha/\gamma'.$$

If E is negative $u(r)$ may be put in the form

$$2\pi i \, (-2\gamma)^{2k+1} r^k e^{-\gamma r} \sum_{j=0}^{n-k-1} \frac{(-2\gamma r)^j}{j\,!} \binom{n+k}{n-k-1-j}, \tag{17}$$

where $n = \alpha/\gamma$, and is an integer.

For k-terms $n = 1$, $k = 0$, $m = 0$, Then

$$\psi(s) \equiv \psi(1, 0, 0) = -4\pi i \gamma e^{-\gamma r}.$$

Therefore,

$$\frac{\partial \psi(1, 0, 0)}{\partial x} = -\gamma \psi(1, 0, 0) \frac{\partial r}{\partial x}, \quad (x = x, y, z)$$

Then it is readily found that the θ, ϕ integrals in $\alpha_{\nu x}$, $\alpha_{\nu y}$, $\alpha_{\nu z}$ vanish unless $k' = 1$, and that the sum of the squares of these integrals is 1.*

Therefore,

$$\alpha_\nu = \frac{c^3 \varepsilon^2}{4h\nu^3} \left| \int \left(\frac{1}{r^2} e^{i\nu r/c} - \frac{1}{r} e^{i\nu r/c} \cdot \frac{\nu}{c} \left(i + \frac{h\gamma}{mc} \right) \right) \times u_{1,0,0}(r) \, u_{n'k'm'}(r) \, r^2 \, dr \right|^2 \tag{18}$$

$$= \left| \frac{4\pi^2 c^3 \varepsilon^2 \xi^2 \xi'^2 \gamma^2}{h\nu^3} \right| \left| \int_0^\infty e^{i\nu r/c - \gamma r} \cdot r \int_{\mathrm{C}} e^{zr} (z - \gamma')^{1-in'} (z + \gamma')^{1+in'} \, dz \, dr - \frac{\nu}{c} \left(i + \frac{h\gamma}{mc} \right) \int_0^\infty e^{i\nu r/c - \gamma r} \cdot r^2 \int e^{zr} (z - \gamma')^{1-in'} (z + \gamma')^{1+in'} \, dz \, dr \right|^2 \tag{19}$$

where ξ, ξ' are normalising factors given by

$$\xi^2 = -\alpha/2\pi^2 \tag{20}$$

[*Note added August* 8, 1927.—**This factor ξ^2, which has twice the value of the square of the normalising factor, is used as there are two K-electrons in an atom. α_ν is then the K-internal conversion coefficient of an atom and is directly comparable with the experimental results.**]

---

* See J. R. Oppenheimer, *loc. cit.*, pp. 279, 284.

$$\xi'^2 = \frac{\frac{2m}{h}\,|\,2\gamma'\,|^{-3}\,e^{3\pi n'}}{(1-e^{2\pi n'})\,(1-e^{-2\pi n'})\,\Gamma(2+in')\,\Gamma(2-in')} \tag{21}$$

$$= \tfrac{1}{4}\frac{m}{2\pi h\alpha^3}\,\frac{n'^2}{n'^2+1}\,(1-e^{-2\pi n'})^{-3}.$$

We have to consider the two integrals

$$\text{(A)} \int_0^\infty \int_C e^{i\nu r/c-\gamma r+zr}\,.\,r\,(z-\gamma')^{1-in'}\,(z+\gamma')^{1+in'}\,dz\,dr.$$

$$\text{(B)} \int_0^\infty \int_C e^{i\nu r/c-\gamma r+zr}\,.\,r^2\,(z-\gamma')^{1-in'}\,(z+\gamma')^{1+in'}\,dz\,dr.$$

Let

$$\nu/c = \beta = b\alpha$$

$$\frac{h\gamma}{mc} = \kappa = 0{\cdot}603 \quad (\mathrm{Z} = 83).$$

Integral A becomes, integrating, first with respect to r

$$\int_C \frac{(z-\gamma')^{1-in'}\,(z+\gamma')^{1+in'}}{(-z-i\beta+\gamma)^2}\,dz. \tag{22}$$

and, similarly, integral B becomes

$$2\int_C^B \frac{(z-\gamma')^{1-in'}\,(z+\gamma')^{1+in'}}{(-z-i\beta+\gamma)^3}\,dz. \tag{23}$$

Integrals of this type have been considered by Fues.* The double circuit integral is equal to $(1-e^{-2\pi n'})$ times a simple positive integral round the branch line, and this can be reduced to negative curves round the poles at $\gamma - i\beta$ and at ∞. Therefore, each integral is equal to

$$-\,2\pi i\,(1-e^{-2\pi n'})\ (\text{residue at } (\gamma - i\beta) + \text{residue at } \infty\,).$$

Integral A. The residue at $\gamma - i\beta$ is

$$\alpha\left(\frac{in'-1+bn'}{in'+1+bn'}\right)^{in'}(4-2ib). \tag{24}$$

The residue at ∞ is

$$2ib\alpha. \tag{25}$$

---

* 'Ann. d. Physik,' vol. 81, p. 288 (1926).

Integral B. The residue at $\gamma - i\beta$ is

$$-2\left(\frac{in'-1+bn'}{in'+1+bn'}\right)^{in'}(1+n'^2)+(n'^2+2n')\left(\frac{in'-1+bn'}{in'+1+bn'}\right)^{in'+1}$$
$$+(n'^2-in')\left(\frac{in'-1+bn'}{in'+1+bn'}\right)^{in'-1}. \tag{26}$$

The residue at ∞ is

$$2. \tag{27}$$

Therefore (19) becomes

$$\left|\frac{4\pi^2c^3\epsilon^2\xi^2\xi'^2\alpha^2}{h\nu^3}(1-e^{-2\pi n'})^2\,.\,4\pi^2\alpha^2\right|\times$$
$$\times\left|\begin{aligned}&\left(\frac{in'-1+bn'}{in'+1+bn'}\right)^{in'}(4+2b\,(\kappa+n'^2\,(i+\kappa)))\\&+\left(\frac{in'-1+bn'}{in'+1+bn'}\right)^{in'+1}n'b\,(i+\kappa)\,(-i-n')\\&+\left(\frac{in'-1+bn'}{in'+1+bn'}\right)^{in'-1}n'b\,(i+\kappa)\,(i-n')\\&-2\kappa b\end{aligned}\right|^2. \tag{28}$$

Now

$$\nu = 2\pi RZ^2\,(1+n'^{-2}). \tag{29}$$

Then putting the limiting wave-length for κ absorption, c/RZ^2, equal to λ_0, we have

$$\frac{\lambda}{\lambda_0}=(1+n'^{-2})^{-1}, \tag{30}$$

and

$$b=\frac{2\pi RZh^2}{c\epsilon^2m}\left(\frac{\lambda}{\lambda_0}\right)^{-1} \tag{31}$$

$$=0{\cdot}304\left(\frac{\lambda}{\lambda_0}\right)^{-1},\quad (Z=83). \tag{32}$$

We have also

$$\left|\frac{4\pi^2c^3\epsilon^2\xi^2\xi'^2\alpha^2}{h\nu^3}(1-e^{-2\pi n'})^2\,.\,4\pi^2\alpha^2\right| \tag{33}$$

$$=\frac{m\epsilon^2\alpha^2c^3}{8\pi^2h^2R^3Z^6}\left(\frac{\lambda}{\lambda_0}\right)^3\cdot\frac{n'^2}{n'^2+1}(1-e^{-2\pi n'})^{-1} \tag{34}$$

$$=1{\cdot}345\left(\frac{\lambda}{\lambda_0}\right)^4(1-e^{-2\pi n'})^{-1},\quad (Z=83.) \tag{35}$$

Now

$$\frac{m\epsilon^2\alpha^2c^3}{8\pi^2h^2R^3Z^6\lambda_0{}^4}\propto Z^4.$$

The expression (35) is, therefore, about 5 per cent. larger for $Z = 84$. .

It remains to evaluate the square of the modulus of the other factor in (28). This can be obtained simply for wave-lengths very near the limit and for very small wave-lengths.

I. *Approximation for Wave-lengths near the Limit.*

$$\frac{\lambda}{\lambda_0} \simeq 1 - n'^{-2}.$$

$$b = 0 \cdot 304\, (1 + n'^{-2}).$$

n' is large and n'^{-3} and higher powers of n'^{-1} will be neglected.

$$\left(\frac{in' - 1 + bn'}{in + 1 + bn'}\right)^{in'} = \exp\left(\frac{in'}{2} \log\left(\frac{(bn'-1)^2 + n'^2}{(bn'+1)^2 + n'^2}\right) - n' \tan^{-1} \frac{2n'}{b^2 n'^2 - 1 + n'^2}\right) \quad (36)$$

$$\simeq \exp\Bigg(\frac{in'}{2} \log\left(\frac{1 + 0\cdot 092\,(1 + 2n'^{-2}) - 0\cdot 608 n'^{-1}\,(1 + n'^{-2}) + n'^{-2}}{1 + 0\cdot 092\,(1 + 2n'^{-2}) + 0\cdot 608 n'^{-1}\,(1 + n'^{-2}) + n'^{-2}}\right)$$

$$- n' \tan^{-1} \frac{2n'^{-1}}{1 - n'^{-2} + 0\cdot 092\,(1 + 2n'^{-2}}\Bigg)$$

$$\simeq \exp\Bigg(\frac{in'}{2} \log\left(\frac{1\cdot 092 - 0\cdot 608 n'^{-1} + 1\cdot 184 n'^{-2} - 0\cdot 608 n'^{-3}}{1\cdot 092 + 0\cdot 608 n'^{-1} + 1\cdot 184 n'^{-2} + 0\cdot 608 n'^{-3}}\right)$$

$$- n' \tan^{-1} \frac{2n'^{-1}}{1\cdot 092 - 0\cdot 816 n'^{-2}}\Bigg)$$

$$\simeq \exp\,(in'\,(-0\cdot 557 n'^{-1} - 0\cdot 011 n'^{-3}) - 1\cdot 831 + 0\cdot 678 n'^{-2}), \quad (37)$$

$$\simeq 0\cdot 160\,(0\cdot 849 - 0\cdot 529 i)\,(1 + (0\cdot 678 - 0\cdot 011 i)\, n'^{-2})$$

$$\simeq 0\cdot 136 + 0\cdot 092 n'^{-2} - i\,(0\cdot 085 + 0\cdot 058 n'^{-2}). \quad (38)$$

The required expression therefore becomes

$$(0\cdot 136 + 0\cdot 092 n'^{-2} - i\,(0\cdot 085 + 0\cdot 058 n'^{-2})\,) \times \Bigg\{4 + 1\cdot 206 b$$

$$+ \frac{4n'^2 b[(1\cdot 206 + 1\cdot 206 n'^2 + b - b^3 n'^2 - 3bn'^2) + i\,(2 + 2n'^2 - 0\cdot 603\,(b - b^3 n'^2 - 3bn'^2))]}{(\,(bn'+1)^2 + n'^2)\,(\,(bn'-1)^2 + n'^2)}\Bigg\}$$

$$-1\cdot 206 b, \quad (39)$$

$$\simeq (0\cdot 136 + 0\cdot 092 n'^{-2} - i\,(0\cdot 085 + 0\cdot 058 n'^{-2})) \times$$

$$\times\,(4\cdot 638 + 0\cdot 659 n'^{-2} + i\,(2\cdot 567 + 0\cdot 213 n'^{-2})) - 0\cdot 367\,(1 + n'^{-2}), \quad (40)$$

$$\simeq 0\cdot 482 + 0\cdot 306 n'^{-2} + i\,(-0\cdot 045 - 0\cdot 060 n'^{-2}). \quad (41)$$

Therefore, the square of the modulus of (41) is

$$0\cdot234 + 0\cdot300\, n'^{-2}$$

and, from (28), (35) and (42)

$$\alpha_\nu \simeq 0\cdot31\left(\frac{\lambda}{\lambda_0}\right)^{2\cdot72}.$$

II. *Approximation for very Short Wave-lengths.*

Here

$$\frac{\lambda}{\lambda_0} \simeq n'^2, \tag{42}$$

and

$$b = \sigma\,(n'^2 + 1)/n'^2. \quad \sigma = 0\cdot304. \tag{43}$$

Then,

$$\left(\frac{in' - 1 + bn'}{in' + 1 + bn'}\right)^{in}$$

$$\simeq \exp\left\{\frac{in'}{2}\log\left(\frac{\sigma^2 - 2\sigma n' + n'^2\,(1 + 2\sigma^2) - 2\sigma n'^3}{\sigma^2 + 2\sigma n' + n'^2\,(1 + 2\sigma^2) + 2\sigma n'^3}\right)\right.$$

$$\left. - n' \tan^{-1}\frac{2n'}{n'^2 - 1 + \sigma^2\,(n'^2 + 1)^2/n'^2}\right\}$$

$$\simeq \exp\left(in'\left(-\frac{2n'}{\sigma} - \frac{2n'^3}{\sigma} + \frac{2n'^3\,(1 + 2\sigma^2)}{\sigma^3} - \frac{8}{3}\frac{n'^3}{\sigma^3}\right) - \frac{2n'^4}{\sigma^2}\right). \tag{44}$$

Similarly

$$\left(\frac{in' - 1 + bn'}{in' + 1 + bn'}\right)^{in'+1}$$

$$\simeq \exp\left((in' + 1)\left(-\frac{2n'}{\sigma} - \frac{2n'^3}{\sigma} + \frac{2n'^3\,(1 + 2\sigma^2)}{\sigma^3} - \frac{8}{3}\frac{n'^3}{\sigma^3}\right) + \frac{2in'^3}{\sigma^2} + O\,(n'^4)\right) \tag{45}$$

and

$$\left(\frac{in' - 1 + bn'}{in' + 1 + bn'}\right)^{in'-1}$$

$$\simeq \exp\left((in' - 1)\left(-\frac{2n'}{\sigma} - \frac{2n'^3}{\sigma} + \frac{2n'^3\,(1 + 2\sigma^2)}{\sigma^3} - \frac{8}{3}\frac{n'^3}{\sigma^3}\right) - \frac{2in'^3}{\sigma^2} + O\,(n'^4)\right). \tag{46}$$

Therefore the expression whose modulus is required becomes approximately

$$\begin{aligned}&\left(1-\frac{2in'^2}{\sigma}+\frac{n'^4}{\sigma^3}\left(-4\sigma+2i\left(\sigma^2-\tfrac{1}{3}\right)\right)\right)\left(4+2\sigma\kappa\left(1+n'^{-2}\right)+2\sigma\left(1+n'^2\right)(i+\kappa)\right)\\ &\quad+\left(1-\frac{2n'}{\sigma}-\frac{2in'^2}{\sigma}+\frac{2n'^2}{\sigma^2}+\frac{n'^3}{\sigma^3}\left(2\left(\sigma^2-1\right)+6i\sigma\right)\right)\\ &\qquad\qquad\qquad\qquad\qquad\qquad(\sigma\,(i+\kappa)\left(-1-n'^2-i\left(n'+n'^{-1}\right)\right)\\ &\quad+\left(1+\frac{2n'}{\sigma}-\frac{2in'^2}{\sigma}+\frac{2n'^2}{\sigma^2}-\frac{n'^3}{\sigma^3}\left(2\left(\sigma^2-1\right)+6i\sigma\right)\right)\\ &\qquad\qquad\qquad\qquad\qquad\qquad(\sigma\,(i+\kappa)\left(-1-n'^2+i\left(n'+n'^{-1}\right)\right)\\ &\quad-2\sigma\kappa\left(1+n'^{-2}\right).\end{aligned}\tag{47}$$

The first term which does not vanish is that in n'^2.

Therefore for very short wave-lengths

$$\alpha_\nu \propto \lambda^{5 \cdot 5}. \tag{48}$$

The general case of an atom for which the field differs slightly from a Coulomb field, and for which k and k' are not integers, has not been considered here. For external absorption Oppenheimer* found that for very short wave-lengths the required integrals, considered as functions of k and k', are discontinuous if $k + k'$ is an odd integer. For the present case this point has not yet been fully investigated.

§ 3. *Discussion of Results.*

The calculations have been carried out for $Z = 83$, but for values of Z of this order the variation of α_ν with Z is small (*i.e.*, α_ν is about 4 per cent. greater for $Z = 84$). The variation with Z is, therefore, similar to that for external absorption.

The approximation I is valid only for values of n'^{-1} less than 0·54, *i.e.*,

$$0 \cdot 78 < \frac{\lambda}{\lambda_0} < 1,$$

and the approximation II holds only for values of n' less than 0·12, *i.e.*, we must have

$$\frac{\lambda}{\lambda_0} \leqslant 0 \cdot 02.$$

The range of wave-lengths investigated experimentally lies between these two ranges, *i.e.*,

$$0 \cdot 03 < \frac{\lambda}{\lambda_0} < 0 \cdot 5.$$

---

* *Loc. cit.*

For this range it has not been found possible to obtain a convenient approximation. The values of α_ν have been calculated directly from (28) for some values of λ. These are given in Table I for comparison with the values given by the empirical formula obtained by Ellis and Wooster. The values given by the present theory are about one-eighth too small, but this discrepancy probably arises from the screening effect of the other electrons. There is some reason to suppose, from the way that Z occurs in the formulæ, that if we could include the change of Z with r the values of α_ν would be substantially increased. This calculation would, however, involve at present insuperable difficulties.

Table I.

λ/λ_0.	Ellis and Wooster. $a_\nu = 4\cdot104\,(\lambda/\lambda_0)^{2\cdot65}$.	a_ν from (28).
0·038	0·0007	0·00003*
0·10	0·0092	0·0024
0·20	0·0576	0·0063
0·30	0·1688	0·0145

* Last figure unreliable.

The theory in its present form may be applied to the L-absorption. These calculations are now in progress, and it is hoped to obtain an estimate of the relative absorption in the K and L levels and in the different L-levels.

In conclusion I wish to express my thanks to Mr. R. H. Fowler, F.R.S., for his help and encouragement during the course of this work.

Summary.

The internal conversion of γ-rays has been investigated experimentally by Ellis and Wooster. It is here discussed on the lines of the quantum mechanics. The problem is that of the perturbation of a hydrogen atom of nuclear charge Z by a Hertzian doublet at its centre. An expression is obtained for the coefficient of absorption in the K-levels. This expression gives values about one-eighth smaller than the experimental ones, but the discrepancy is probably due to a neglect of the screening by the other electrons.

Chemical Equilibrium in a Mixture of Paraffins.

By H. A. Wilson, F.R.S., Rice Institute, Houston, Texas.

(Received March 7, 1927.)

In this paper the theory of chemical equilibrium is applied to a mixture of paraffins C_nH_{2n+2}, and it is shown that the equilibrium composition of the vapour and liquid phases can be approximately calculated at any given temperature and pressure.

Such a mixture has two independent constituents so that according to the phase rule the composition of the phases, whenever there are two, will be determined by two independent variables such as the temperature and pressure.

Consider the reaction

$$C_{n-1}H_{2(n-1)+2} + C_{n+1}H_{2(n+1)+2} = 2C_nH_{2n+2}.$$

The equilibrium constant $p_n^2/p_{n-1}p_{n+1}$ is given by the equation

$$\log \frac{p_n^2}{p_{n-1}\,p_{n+1}} = \frac{H}{RT} + \frac{2C_n - C_{n-1} - C_{n+1}}{R} \log T + \frac{2k_n - k_{n-1} - k_{n+1}}{R},$$

where p_n denotes the partial pressure of C_nH_{2n+2} in the vapour phase, C_n the heat capacity of one molecule of C_nH_{2n+2} at constant pressure, k_n the entropy constant for one mol of C_nH_{2n+2}, R the gas constant for one mol, T the absolute temperature, and H the heat of the reaction.

It was found by Julius Thomsen that the heats of formation of paraffins can be expressed as

$$(2n + 2)\,14 \cdot 9 + (n - 1)\,14 \cdot 71 \text{ calories.}$$

Here $n - 1$ is the number of linkages between carbon atoms and $2n + 2$ the number between H and C atoms.

The following table gives the heats of formation found experimentally and calculated by Thomsen :—

	Found.	Calculated.
CH_4	59·55	59·59
C_2H_6	104·16	104·11
C_3H_8	148·51	148·62
C_4H_{10}	193·65	193·13
C_5H_{12}	238·88	237·64

The agreement is good so we may conclude that Thomsen's formula is correct for any paraffin.

The heat of the reaction we are considering will be the heat of formation of $2C_nH_{2n+2}$ minus the heats of formation of $C_{n-1}H_{2(n-1)+2}$ and $C_{n+1}H_{2(n+1)+2}$, and Thomsen's formula makes this zero. Hence $H = 0$. For example, in the case

$$C_2H_6 + C_4H_{10} = 2C_3H_8,$$
$$H = 2 \times 148 \cdot 51 - 104 \cdot 16 - 193 \cdot 65 = -0 \cdot 79$$

according to the experimental values and $H = 0$ according to the formula.

The quantity $2C_n - C_{n-1} - C_{n+1}$ is also nearly zero. This is so because the heat capacity of $C_n H_{2n+2}$ must be nearly the mean of those of $C_{n-1}H_{2(n-1)+2}$ and $C_{n+1}H_{2(n+1)+2}$. The experimental values of C_n available, which are very few, agree with this within the limits of error. The fact that all hydrocarbon oils have nearly equal specific heats shows that $2C_n - C_{n-1} - C_{n+1}$ cannot differ much from zero.

The quantity $2k_n - k_{n-1} - k_{n+1}$ also cannot differ much from zero, for k_n must be nearly the mean of k_{n-1} and k_{n+1}.

The equation for the equilibrium constant is therefore approximately

$$\log p_n^2/p_{n-1}\,p_{n+1} = 0,$$

so that $p_n^2 = p_{n-1}\,p_{n+1}$. From this it follows that $p_n = p_1 f^{n-1}$, where f is a constant, so that the total pressure P is given by

$$\begin{aligned} P &= p_1 + p_2 + p_3 + p_4 + \ldots \\ &= p_1 (1 + f + f^2 + f^3 + \ldots) \\ &= p_1/(1 - f). \end{aligned}$$

This shows that f must be a fraction less than 1 and greater than 0.

This result is in general agreement with experience, for it is found that the amounts of the different paraffins present in natural gases decrease with increasing molecular weight.

Let m_n denote the number of mols of $C_n H_{2n+2}$ present in a volume V of the vapour. Let $k = V/RT$ so that $m_n = kp_n$. The mols of H in V is equal to

$$\begin{aligned} &4m_1 + 6m_2 + 8m_3 + \ldots \\ &= 2kp_1 (2 + 3f + 4f^2 + \ldots) \\ &= 2kp_1 \frac{2 - f}{(1 - f)^2}. \end{aligned}$$

The mols of C in V is equal to

$$\begin{aligned} & m_1 + 2m_2 + 3m_3 + \ldots \\ & = kp_1 (1 + 2f + 3f^2 + \ldots) \\ & = kp_1 \frac{1}{(1-f)^2}. \end{aligned}$$

If the composition of the vapour is CH_x, that is, x atoms of hydrogen to one atom of carbon, then

$$x = \frac{2kp_1 \dfrac{2-f}{(1-f)^2}}{kp_1 \dfrac{1}{(1-f)^2}} = 4 - 2f,$$

so that $f = 2 - x/2$. The weight in grams of $C_n H_{2n+2}$ in the volume V of the vapour is

$$m_n (14n + 2) = kp_1 f^{n-1} (14n + 2),$$

so that the fraction by weight of $C_n H_{2n+2}$ in the vapour is

$$\frac{kp_1 f^{n-1} (14n + 2)}{\dfrac{12kp_1}{(1-f)^2} + 2kp_1 \dfrac{2-f}{(1-f)^2}} = \frac{(7n+1) f^{n-1} (1-f)^2}{8-f}.$$

By means of this expression the percentages by weight of the different paraffins in the vapour for different values of $x = 4 - 2f$ can be calculated. The following table gives the percentages for $x = 2{\cdot}2$, $2{\cdot}3$, $2{\cdot}4$, $2{\cdot}5$, $2{\cdot}6$, $2{\cdot}7$, $2{\cdot}8$, for values of n from 1 to 15.

n.	$x = 2{\cdot}2$	2·3	2·4	2·5	2·6	2·7	2·8
1	1·13	2·53	4·44	6·90	9·90	13·3	17·3
2	1·90	4·00	6·67	9·70	13·0	16·3	19·5
3	2·51	4·98	7·82	10·70	13·3	15·5	17·1
4	2·98	5·59	8·24	10·50	12·3	13·3	13·5
5	3·33	5·88	8·14	9·80	10·7	10·7	10·1
6	3·57	5·97	7·78	8·80	8·9	8·3	7·3
7	3·83	5·92	7·30	7·66	7·25	6·26	5·05
8	3·86	5·72	6·64	6·55	5·80	4·65	3·50
9	3·90	5·48	5·97	5·51	4·55	3·39	2·35
10	3·90	5·17	5·30	4·59	3·64	2·45	1·55
11	3·85	4·83	4·65	3·78	2·72	1·75	1·02
12	3·76	4·46	4·06	3·09	2·07	1·24	0·67
13	3·66	4·10	3·51	2·51	1·58	0·87	0·43
14	3·54	3·76	3·05	2·02	1·19	0·61	0·28
15	3·42	3·44	2·59	1·63	0·89	0·43	0·18

We see that as x increases the percentage of any particular paraffin in the vapour increases to a maximum value and then diminishes. It can easily be shown that the molecular fraction of any paraffin in the vapour is a maximum when the composition of the vapour is the same as the composition of the paraffin in question.

The composition of the liquid in equilibrium with the vapour will now be considered. Let p_n denote the partial pressure of $C_n H_{2n+2}$ in the vapour and p_n' the vapour pressure of the pure liquid C_nH_{2n+2}. Then we have approximately

$$\log \frac{p_n}{C_n p_n'} = \frac{v}{V}\left(1 - \frac{p_n'}{P}\right),$$

where C_n is the molecular concentration of C_nH_{2n+2} in the liquid or the ratio of the number of molecules of C_nH_{2n+2} in the liquid to the total number of molecules in the liquid, v is the volume of one mol of pure liquid C_nH_{2n+2}, and V the volume of one mol of the vapour of pure C_nH_{2n+2} at the total pressure P. In most cases the expression $v/V\,(1 - p_n'/P)$ is a rather small fraction, so that we shall assume

$$\log \frac{p_n}{C_n p_n'} = 0,$$

or

$$p_n = C_n p_n'.$$

The errors due to using this rather rough approximation are not serious as regards the composition of the liquid calculated, in such cases as are of practical importance. The composition of the liquid will be denoted by $CH_{x'}$, so that x' is the number of atoms of hydrogen in the liquid to one atom of carbon.

Since

$$C_n = p_n/p_n' \quad \text{and} \quad p_n = p_1 f^{\,n-1},$$

we have

$$C_1 + C_2 + C_3 + \ldots = 1 = p_1\left\{\frac{1}{p_1'} + \frac{f}{p_2'} + \frac{f^2}{p_3'} + \ldots\right\},$$

so that

$$p_1 = \frac{1}{\left\{\frac{1}{p_1'} + \frac{f}{p_2'} + \frac{f^2}{p_3'} + \ldots\right\}},$$

and the total pressure P is given by

$$P = \frac{1}{(1-f)\left\{\frac{1}{p_1'} + \frac{f}{p_2'} + \frac{f^2}{p_3'} + \ldots\right\}}.$$

The number of mols of carbon (C) in the liquid is given by

$$C = m_1' + 2m_2' + 3m_3' + \ldots,$$

where m_n' denotes the mols of C_nH_{2n+2} in the liquid, and the mols of hydrogen is given by

$$Cx' = 4m_1' + 6m_2' + 8m_3' + \ldots,$$

so that

$$x' = 2\left\{\frac{2m_1' + 3m_2' + 4m_3' + \ldots}{m_1' + 2m_2' + 3m_3' + \ldots}\right\}.$$

The fraction by weight of C_nH_{2n+2} in the liquid is equal to

$$\frac{m_n'(14n+2)}{\Sigma\, m_n'(14n+2)}.$$

Also

$$\Sigma\, m_n'(14n+2) = C(12 + x'),$$

$$\Sigma n m_n' = C,$$

so that

$$\Sigma m' = C(x'/2 - 1).$$

Hence the fraction by weight of C_nH_{2n+2} in the liquid is equal to

$$\frac{(7n+1)(x'-2)\,p_n}{(12+x')\,p_n'}.$$

To make further progress it is necessary to calculate the values of the series

$$\sum_{n=1}^{n=\infty} \frac{f^{n-1}}{p_n'} = \frac{1}{p_1'} + \frac{f}{p_2'} + \frac{f^2}{p_3'} + \ldots$$

and

$$\sum_{n=1}^{n=\infty} \frac{nf^{n-1}}{p_n'} = \frac{1}{p_1'} + \frac{2f}{p_2'} + \frac{3f^2}{p_3'} + \ldots.$$

For this purpose it will be sufficient to use an approximate expression for the vapour pressures p_n'. We have

$$L_n = \frac{RT^2}{p_n'}\frac{dp_n'}{dT},$$

where L_n is the latent heat of evaporation of one mol of C_nH_{2n+2}. Integrating, this gives

$$\log p_n' = -\frac{L_n}{RT} + \text{constant}.$$

If B_n denotes the boiling point of C_nH_{2n+2} and if p_n' is expressed in atmospheres, then, when $T = B_n$, we have that $p_n' = 1$, so that

$$\log p_n' = \frac{L_n}{R}\left(\frac{1}{B_n} - \frac{1}{T}\right).$$

This expression will give p_n' approximately when the temperature does not differ greatly from the boiling point.

The present theory is only valid at temperatures at which the paraffins react chemically with each other, which are probably above 600° K. At such temperatures the early terms in the series $1/p_1' + f/p_2'$, etc., are small. The above expression then gives very large values for p_1', p_2', etc., and so is sufficiently accurate for these small terms. Also for large values of n when B_n is much greater than T, the factor f^{n-1} becomes so small that the terms in the series are small. Thus the above expression for p_n' may be used to calculate the values of the series in question.

According to Trouton's Law we have $L_n = 20B_n$ approximately for the paraffins and B_n is nearly equal to $140\sqrt{n}$, except when n is very small, which does not matter since when n is very small the terms in the series are small.

Hence we have, since $R = 2$

$$\log p_n' = 10\left(1 - \frac{140\sqrt{n}}{T}\right),$$

or

$$p_n' = e^{10\,(1-140\sqrt{n}/T)}.$$

Hence

$$\Sigma\frac{f^{n-1}}{p_n'} = e^{-10}\Sigma f^{n-1}e^{1400\sqrt{n}/T}.$$

Put $1400/T = \alpha$ and let $f^{-1} = g$ and $\log g = \beta^2$, so that

$$\Sigma\frac{f^{n-1}}{p_n'} = ge^{-10}\Sigma e^{-\beta^2 n+\alpha\sqrt{n}}.$$

Since the terms in the series are small when n is very small and also when n is very large, and a large number of the terms are appreciable for intermediate values of n, we may replace the series by an integral and so get

$$\Sigma\frac{f^{n-1}}{p_n'} = ge^{-10}\int_0^\infty e^{-\beta^2 n+\alpha\sqrt{n}}\,dn.$$

Let $n = x^2$, so that

$$\Sigma\frac{f^{n-1}}{p_n'} = 2ge^{-10}\int_0^\infty e^{-\beta^2 x^2+\alpha x}\,x\,dx,$$

or

$$\Sigma\frac{f^{n-1}}{p_n'} = 2ge^{-10+\alpha^2/4\beta^2}\int_{-\alpha/2\beta}^\infty e^{-y^2}\left(\frac{y}{\beta} + \frac{\alpha}{2\beta^2}\right)dy,$$

where

$$y = \beta x - \alpha/2\beta.$$

If $\alpha/2\beta$ is greater than about 2 this gives approximately

$$\frac{g\alpha e^{-10+\alpha^2/4\beta^2}}{\beta^3}\int_{-\infty}^{+\infty} e^{-y^2}\,dy = \frac{g\alpha}{\beta^3}\sqrt{\pi}e^{-10+\alpha^2/4\beta^2}.$$

Hence

$$\Sigma\frac{f^{n-1}}{p_n'} = \sqrt{\pi}g\frac{1400}{\mathrm{T}\,(\log g)^{3/2}}\,e^{-10+1960000/4\mathrm{T}^2\log g}.$$

But P, the total pressure, is given by

$$\mathrm{P} = \frac{1}{(1-f)\,\Sigma f^{n-1}/p_n'}.$$

Hence

$$\mathrm{P} = \frac{\mathrm{T}\,(\log g)^{3/2}}{1400\sqrt{\pi}\,(g-1)}\,e^{10-490000/\mathrm{T}^2\log g}.$$

Since $x = 4 - 2/g$ we have $g = 2/(4-x)$. By means of this equation for P the following values of P have been calculated:—

Pressure in Atmospheres.

Temperature	$CH_{2\cdot 2}$.	$CH_{2\cdot 3}$.	$CH_{2\cdot 4}$.	$CH_{2\cdot 5}$.	$CH_{2\cdot 6}$.	$CH_{2\cdot 7}$.	$CH_{2\cdot 8}$.
300° K						0·0045	0·03418
350° K						0·1509	0·6751
400° K			0·00164	0·05023	0·3286	1·523	4·84
450° K			0·03274	0·4122	2·238	7·598	19·14
500° K	0·0000113	0·00947	0·2864	2·230	9·046	24·58	52·32
550° K	0·0003225	0·08465	1·446	8·153	25·81	59·55	111·9
600° K	0·003994	0·4532	5·021	21·83	61·62	118·5	202·7
650° K	0·02918	1·694	13·42	47·51	110·5	204·8	
700° K	0·1433	4·878	29·58	89·13	186·5		
750° K	0·524	11·57	56·62	150·0			
800° K	1·518	23·68	96·83				
850° K	3·695						

To determine the composition of the liquid in equilibrium with the vapour we require also the value of the series

$$\Sigma\frac{nf^{n-1}}{p_n'} = \frac{1}{p_1'} + \frac{2f}{p_2'} + \frac{3f^2}{p_3'} + \dots.$$

This may be shown to be approximately equal to

$$2ge^{-10}\int_0^\infty e^{-\beta^2x^4+\alpha x}\,x^3\,dx,$$

where $\alpha = 1400/\mathrm{T}$, $g = f^{-1}$, $\log g = \beta^2$, and $x^2 = n$ as before.

Let $y = \beta x - \alpha/2\beta$, so that

$$\Sigma \frac{nf^{n-1}}{p_n'} = \frac{2ge^{-10+\alpha^2/4\beta^2}}{\beta^4} \int_{-\alpha/2\beta}^{\infty} e^{-y^2}\left(y^3 + \frac{3\alpha y^2}{2\beta} + \frac{3}{4}\frac{\alpha^2 y}{\beta^2} + \frac{\alpha^3}{8\beta^3}\right) dy.$$

When $\alpha/2\beta$ is greater than about 2 this gives approximately

$$\Sigma \frac{nf^{n-1}}{p_{n'}} = 2\alpha g e^{-10+\alpha^2/4\beta^2} \int_{-\infty}^{+\infty} e^{-y^2}\left(\frac{3y^2}{2} + \frac{\alpha^2}{8\beta^2}\right) dy$$

$$= e^{-10+\alpha^2/4\beta^2} \frac{\alpha g\sqrt{\pi}}{\beta^5}\left\{\frac{3}{2} + \frac{\alpha^2}{4\beta^2}\right\}.$$

Hence

$$x' = 2\left\{1 + \frac{\Sigma f^{n-1}/p'_n}{\Sigma nf^{n-1}/p'_n}\right\}$$

$$= 2\left\{1 + \frac{\beta^2}{\frac{3}{2} + \frac{\alpha^2}{4\beta^2}}\right\}.$$

or

$$x' = 2\left\{1 + \frac{\log g}{\frac{3}{2} + \frac{490000}{T^2 \log g}}\right\}.$$

The following table gives values of x' calculated by means of this expression :—

Values of x' in $CH_{x'}$ the Composition of the Liquid.

Vapour →	$CH_{2\cdot 2}$.	$CH_{2\cdot 3}$.	$CH_{2\cdot 4}$.	$CH_{2\cdot 5}$.	$CH_{2\cdot 6}$.	$CH_{2\cdot 7}$.	$CH_{2\cdot 8}$.
800° K	2·0241	2·0524	2·0904	2·1382	2·1948	2·2630	2·3410
750° K	2·02164	2·04728	2·0824	2·1268	2·1800	2·2444	2·3188
700° K	2·0192	2·0424	2·0746	2·1154	2·1650	2·2250	2·2954
650° K	2·01686	2·0376	2·0666	2·1038	2·1494	2·2060	2·2712
600° K	2·0147	2·03292	2·0587	2·0922	2·1334	2·1846	2·2460
550° K	2·01254	2·0285	2·0509	2·0806	2·1176	2·1634	2·2186
500° K	2·0105	2·0240	2·0434	2·0690	2·1014	2·1424	2·1918
450° K	2·00864	2·01982	2·0362	2·0580	2·0856	2·1210	2·1640
400° K	2·0069	2·01574	2·0293	2·0473	2·0704	2·0998	2·1366

By means of the table of values of the equilibrium pressure P at different temperatures and for different values of x, and the table of values of x' for different values of x and the temperature, a chart can be drawn showing the values of x and x' corresponding to any temperature and pressure. By means of this chart x and x' can be immediately obtained when T and P are given.

Strictly speaking, such a chart should only be used for temperatures above about 600° F., but when vapour has been heated above 800° F. and then cooled down it is possible that its composition will not differ much from that indicated by the chart. This is due to the fact that the condition of equilibrium $p_n = p_1 f^{n-1}$ is independent of the temperature. The chart may therefore be used for approximate calculations on vapour at temperatures down to perhaps 500° F., provided the vapour was originally produced above 700 or 800° F. and kept hot long enough for equilibrium to be approximately established between the hydrocarbons present.

The amount of vapour stopped by a reflux condenser, heat exchanger or other similar apparatus may be calculated as follows: Let M_1 be the weight of vapour entering the condenser and let its composition be CH_{x_1}. Let M_2 be the weight of vapour coming out of the condenser and let its composition be CH_{x_2}, and let M be the weight of liquid condensed and its composition $CH_{x'}$. Then the hydrogen in M_1 must be equal to the hydrogen in $M_2 + M$, so that

$$M_1 \frac{x_1}{12 + x_1} = M_2 \frac{x_2}{12 + x_2} + M \frac{x'}{12 + x'}.$$

Also the carbon in M_1 must be equal to the carbon in $M_2 + M$, so that

$$M_1 \frac{12}{12 + x_1} = M_2 \frac{12}{12 + x_2} + M \frac{12}{12 + x'}.$$

These equations give

$$\frac{M_2}{M_1} = \frac{x_1 - x'}{x_2 - x'} \times \frac{12 + x_2}{12 + x_1}.$$

The theory has been compared with the results obtained in large scale operations on paraffin oils and appears to give results which agree approximately with the results obtained at temperatures above 600° F.

It seems probable therefore that when a mixture of paraffins is kept at temperatures above about 800° F. for a sufficient time, chemical equilibrium is approximately established in the mixture. Provided therefore that the mixture forms two phases, the composition of each phase will be determined by the temperature and pressure.

If the liquid phase (usually called the tar) is $CH_{x'}$ the vapour phase CH_x and the oil from which the tar and vapour are formed is CH_{x_1}, then

$$CH_{x_1} = f\,CH_x + (1 - f)\,CH_{x'}$$

where f is the fraction of the carbon which goes into the vapour phase.

Hence

$$x_1 = f x + x' - f x'$$

or

$$f = \frac{x_1 - x'}{x - x'}.$$

If the oil used has the same composition as the vapour formed, so that $x_1 = x$, then $f = 1$, so that no tar will be formed. The amount of tar formed can therefore be diminished by adding hydrocarbons which contain more hydrogen than the oil so as to increase x_1 and make it more nearly equal to x. For example,

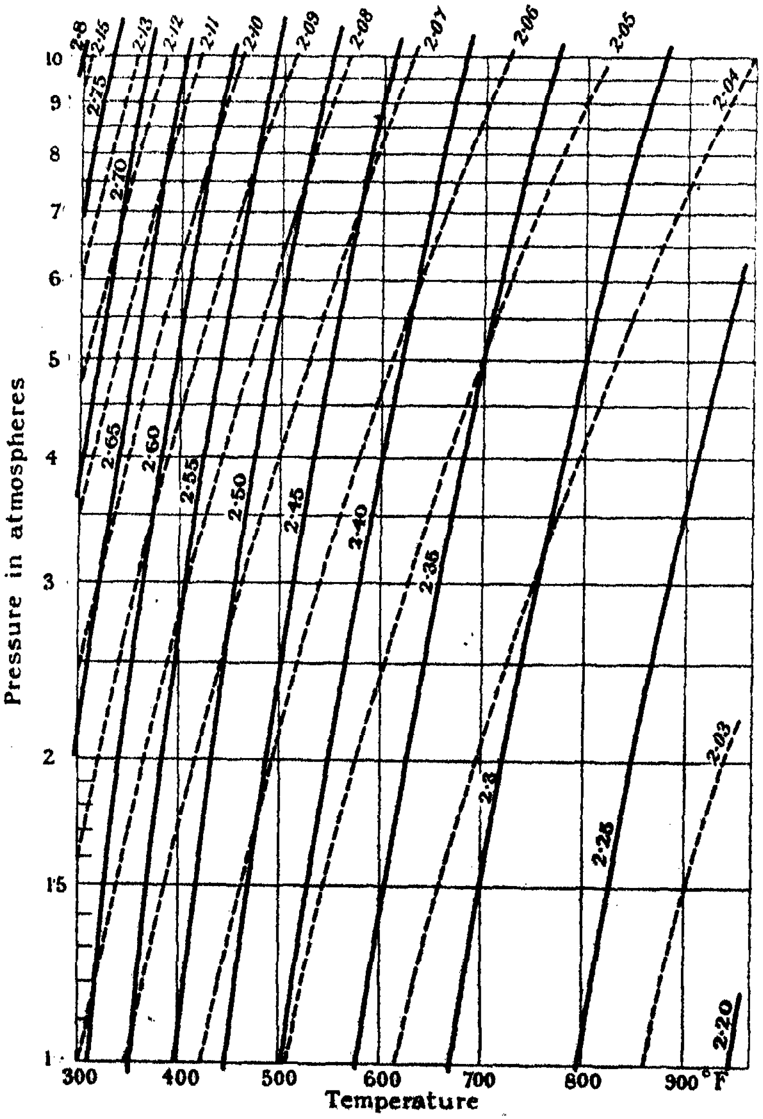

Fig. 1.—Composition of Liquid and Vapour when in Equilibrium with each other.

Solid lines (———) represent Composition of Vapour.
Broken lines (– – –) represent Composition of Liquid.

methane or hydrogen or any volatile hydrocarbon might be pumped in with the oil so as to increase x_1.

The composition of the vapour formed is determined by the temperature

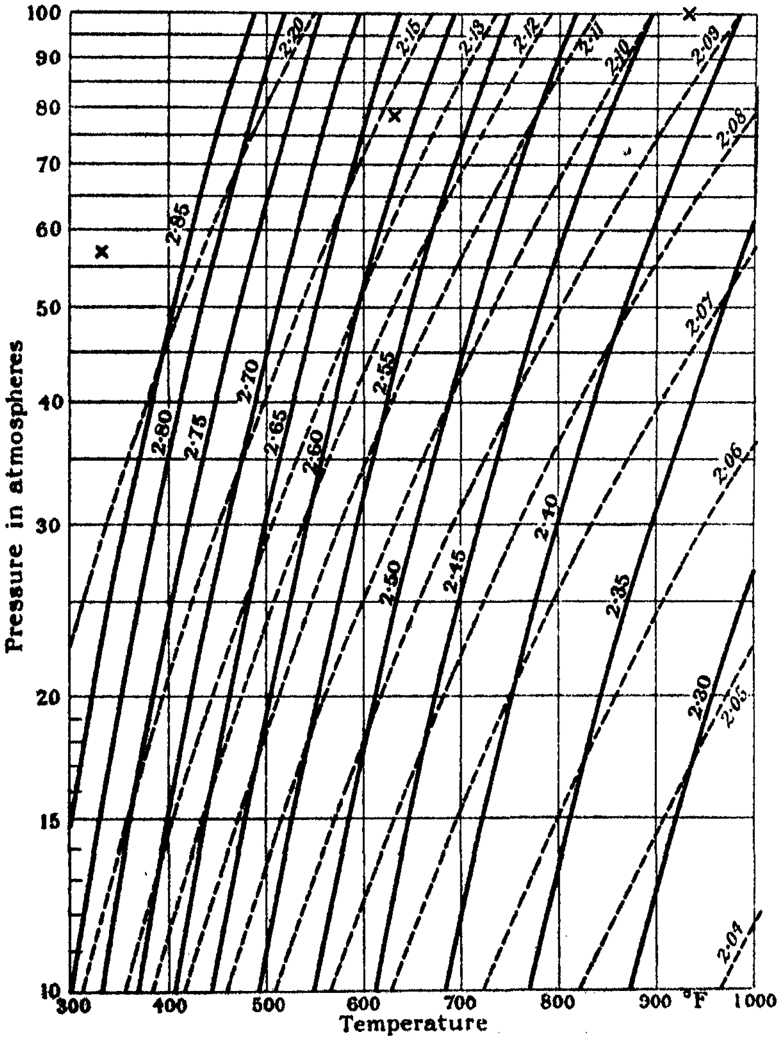

FIG. 2.—Composition of Liquid and Vapour when in Equilibrium with each other.
Solid lines (———) represent Composition of Vapour.
Broken lines (— — —) represent Composition of Liquid.

and pressure, so that, provided some tar is formed, the effect of adding volatile hydrocarbons or hydrogen to the mixture will therefore be merely to increase the amount of the vapour without altering its composition.

The composition of the vapour can be altered by changing the pressure or the temperature. Raising the pressure increases the proportion of volatile hydrocarbons in the vapour and raising temperature diminishes it.

The chart shows that, roughly speaking, raising 100° F. has about the same effect as halving the pressure. Of course, raising the temperature greatly accelerates the reactions, so that it diminishes the time required for equilibrium to be reached.

To obtain vapour containing the greatest possible molecular percentage of any particular hydrocarbon, the temperature and pressure should be so chosen that the composition of the vapour as given by the chart is the same as the composition of the hydrocarbon. For example, the molecular percentage of C_5H_{12} will be the maximum possible when $x = 2 \cdot 4$, which is the case at the following temperatures and pressures :—

Temperature.	Pressure (atmospheres).
600° F.	4·0
700° F.	12·0
800° F.	30·0
900° F.	61·0

The percentage by weight of C_5H_{12} in the vapour is then 8·14, according to the table of percentages. The maximum percentage by weight of C_5H_{12} in the vapour is about 10·7 when $x = 2 \cdot 65$.

APPENDIX.

(*Added May* 30, 1927.)

The following appendix was written in response to criticisms of the above paper. The use of the hypothetical reaction

$$C_{(n-1)}H_{2(n-1)+2} + C_{(n+1)}H_{2(n+1)+2} = 2C_nH_{2n+2}$$

for the purpose of obtaining the equilibrium condition in the vapour of a mixture of paraffins does not involve the assumption that such reactions actually occur. The equilibrium condition is the condition of maximum entropy, so that if m_n denotes the number of mols of C_nH_{2n+2} in the mixture in equilibrium, then if we suppose any possible small changes made in the m's the resulting total change of entropy must be zero. We may therefore suppose only three of the m's to be changed, viz., m_n, m_{n-1}, and m_{n+1}, and that

$$2\delta m_n + \delta m_{n-1} + \delta m_{n+1} = 0,$$

since this is a possible change in the m's corresponding to the above reaction. The equation for the equilibrium constant is then obtained by equating the change of entropy to zero.

The same result, of course, is obtained by considering any other possible reaction. For example, consider the reaction

$$C_nH_{(2n+2)} = C_{(n-m)}H_{2(n-m)+2} + C_mH_{2m},$$

which involves the production of a possibly unsaturated hydrocarbon C_mH_{2m}.

Replacing n by $n - 1$ and then by $n + 1$ we get

$$C_{(n-1)}H_{2(n-1)+2} = C_{(n-1-m)}H_{2(n-1-m)+2} + C_mH_{2m}$$

and

$$C_{(n+1)}H_{2(n+1)+2} = C_{(n+1-m)}H_{2(n+1-m)+2} + C_mH_{2m}.$$

Subtracting the two last equations from twice the previous one we get

$$2C_nH_{2n+2} - C_{(n-1)}H_{2(n-1)+2} - C_{(n+1)}H_{2(n+1)+2}$$
$$= 2C_{(n-m)}H_{2(n-m)+2} - C_{(n-1-m)}H_{2(n-1-m)+2} - C_{(n+1-m)}H_{2(n+1-m)+2} = 0,$$

which is the same as the equation

$$C_{(n-1)}H_{2(n-1)+2} + C_{(n+1)}H_{2(n+1)+2} = 2C_nH_{2n+2}.$$

The condition of equilibrium among the paraffins in the vapour is therefore approximately $p_n = p_1f^{n-1}$, whatever reactions occur and whatever other compounds besides paraffins may be present.

The condition of equilibrium for any other homologous series of compounds present in the vapour is similar to that for the paraffins. Thus if A_n denotes a member of any homologous series, then a possible hypothetical reaction is

$$2A_n = A_{n-1} + A_{n+1},$$

so that provided the relevant physical properties of A_n are nearly the means of those of A_{n-1} and A_{n+1} it follows, as for the paraffins, that the condition of equilibrium between the A's in the vapour is $p_{A_n} = p_{A_1}f_A{}^{n-1}$, where p_{A_n} denotes the partial pressure of A_n in the mixture and f_A is a quantity less than unity and nearly independent of n.

The value of the fractions f_A is determined by the physical properties of the compounds in question when a liquid and gaseous phase are present, as in the case of the paraffins. Now the physical properties of the ethylenes, cyclo-paraffins and paraffins are very similar. For example, the boiling point of the paraffin C_9H_{20} is 151° C., that of nonylene C_9H_{18} is 153° C., and those of the various cyclo-paraffins C_9H_{18} range from 140 to 170° C. It follows that in the case of a mixture of paraffins and other hydrocarbons having similar physical properties provided the paraffins compose the greater part of the mixture, the fraction of the mixture in equilibrium boiling between any given limits of temperature will be nearly the same as for a mixture of paraffins only. That is to say, any other compound A_n of nearly equal physical properties may replace a fraction of each paraffin in C_nH_{2n+2} without altering the proportion of the equilibrium mixture boiling between given limits.

This is probably the reason that the results of the theory of the mixture of paraffins, in the absence of other compounds, appear to be applicable in many cases to the mixtures of hydrocarbons obtained in commercial work on oil, for these mixtures frequently contain a large proportion of paraffins.

The results of the theory will presumably not be found to agree with experimental results on mixtures not containing a large proportion of paraffins, or containing appreciable amounts of compounds having properties greatly different from those of the paraffins.

The approximate solution of the problem of the equilibrium composition of a mixture of paraffins, in the assumed absence of other compounds, is of scientific interest even if the mixtures obtained in practice always contain other compounds besides paraffins. The equilibrium of, for example, a mixture of paraffins and ethylenes can of course be worked out in a similar way to that of a mixture of paraffins only. This is a somewhat more complicated problem than the one considered, and the writer does not desire to discuss the solution of it in the present paper.

The solution of the problem considered depends on the laws of thermodynamics and so must be correct unless errors have been made in the calculations. The approximations made of course limit the validity of the solution to the range of temperature and pressure within which the approximations are near enough to the truth.

It is found that when oil, not initially containing any easily volatile but non-gaseous constituents, is kept at a constant and sufficiently high temperature, then the amount of such constituents present increases with the time at first rapidly and then more slowly, and finally only increases very slowly. This appears to indicate an approach to an equilibrium composition.

It is found that the rate of reaction in oil increases rapidly with the temperature, as with most chemical reactions. The theory indicates that the percentage of the easily volatile but non-gaseous compounds $C_4H_{10} + C_5H_{12} + \dots + C_{12}H_{26}$ in the vapour is nearly constant at 60 per cent. for all compositions between $CH_{2 \cdot 4}$ and $CH_{2 \cdot 6}$. At 25 atmospheres the equilibrium composition of the vapour is $CH_{2 \cdot 4}$ at 800° F. and $CH_{2 \cdot 6}$ at 530° F., according to the theory.

It is found that the percentage of easily volatile but non-gaseous constituents in the vapour obtained by heating oil to temperatures in the neighbourhood of 800° F. at 25 atmospheres pressure, for a long enough time for approximate equilibrium to be reached, is nearly independent of the temperature and of the time and is equal to about 60 per cent. of the vapour obtained. For example, an oil giving 30 per cent. of tar usually gives about 40 per cent. by weight (47 per cent. by volume) of easily volatile products and $(100 - 30) \times 6/10 = 42$, which is nearly equal to 40. If an equilibrium was not reached, then we should expect the amount of the products formed in a given time to increase rapidly with the temperature and at a constant temperature to go on increasing with the time. When oil is heated to temperatures around 800° F., then compounds of both higher and lower molecular weight than those originally present are produced in it. This result, which agrees with the present theory, has been known for a long time.

The results mentioned seem to show that an equilibrium state is approached, and, since the mixtures obtained consist largely of paraffins, the equilibrium state must be one of equilibrium between the paraffins present. The proportion of easily volatile constituents agrees approximately with that calculated, which suggests that the actual state is similar to the calculated equilibrium state.

Further Experiments on Explosions in Gaseous Mixtures of Acetylene, of Hydrogen and of Pentane.

By A. Egerton, F.R.S., and S. F. Gates, B.Sc., M.A. (Oxon).

(Received August 5, 1927.)

[Plate 13.]

An account of experiments on detonation in gaseous mixtures of acetylene and pentane has already been published.* Certain further observations are here recorded as an addendum to the former papers.

(*a*) *Influence of Pressure on Velocity of Detonation.*

It was mentioned on p. 157 of the second paper referred to, that further measurements of the velocities of the detonation waves set up in the explosive mixtures investigated were necessary to determine the precise extent of the increase in velocity occasioned by rise of initial pressure.

In order to arrive at reliable results from the photographic records obtained in the manner described in the previous paper, certain precautions were necessary. Spot lights arranged at the ends of the explosion tube provided reference lines along the two edges of the photographic paper at right angles to the line of travel of the explosion (*vide* fig. 2, Plate 13). By setting a plate accurately ruled in squares† against these reference lines, one of the cross lines on the plate could be used as a base line. The distances to the start of the lines, which form the record of the light from the windows of the tube during the explosion, were then measured by a Hilger micrometer as detailed below. The rate of rotation of the wheel was obtained by means of a tuning fork, standardised at the National Physical Laboratory. The light from an arc lamp was reflected from a mirror on the fork and focussed by means of quartz lenses on to the photographic paper; a shutter was arranged to admit the light for one revolution of the wheel. If L_D length of film after development and drying, L_V length of film on which N_V vibrations are counted, f the frequency of fork, n the actual distance of travel of wave in centimetres during which the distance of travel of the film measured by the micrometer is h, and p is the

---

* 'Roy. Soc. Proc.,' A, vol. 114, pp. 137 and 152 (1927).

† Specially constructed to our instructions by Messrs. Rheinberg.

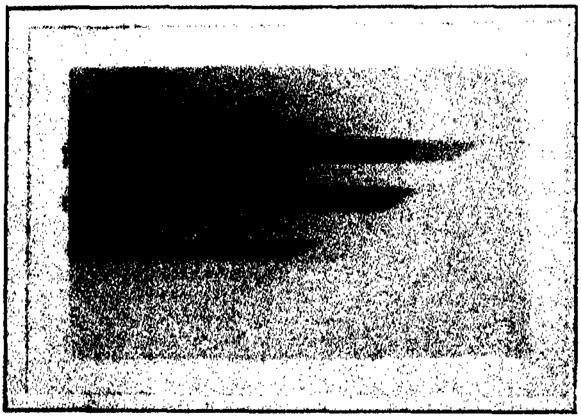

Fig. 1.—Mixture $C_2H_2 : 2 \cdot 5O_2 : 10N_2$. 15° C. 96 lbs.

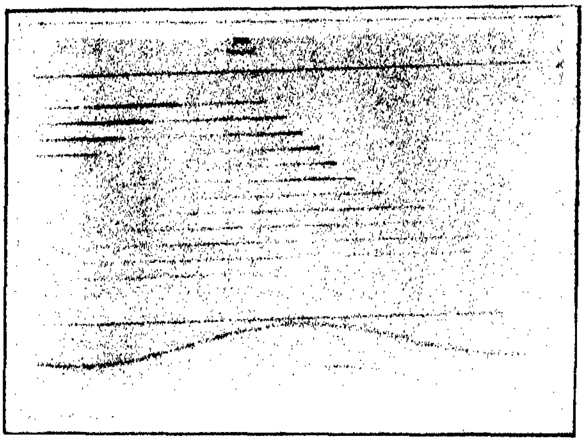

Fig. 2.—Mixture $2H_2 : 1O_2 : 2N_2$. 140° C. 21·2 lbs.

(*Facing p.* 516.)

periphery of the wheel with paper attached, then V the velocity of the wave is given by

$$V = \frac{p f L_V n}{h N_V L_D}.$$

L_D the length of the film and p both vary with the tightness with which the film is placed on the wheel. The shrinkage on drying was found to be about 3 mm. on the total length of film 95·9 cms. The variations of ± 1 mm. in 956 mm. were attributed to these two causes combined. The mean value for L_D, 95·6 cms., was therefore sufficiently accurate to be used in all cases. The frequency of the fork carrying the mirror being 1021 (at the temperature of the room),

$$V = \frac{10{,}242\ L_V n}{h N_V} \text{ metres per second.}$$

The following is an example of the measurement of a film :—

Sheet 141 (2). Mixture : 1 $C_2H_2 : 2{\cdot}5 O_2 : 3$ Argon.
Pressure 50 lbs.

Distance between guide lines : 2·721 cms.

Film length (L_D) : 95·65 cms. Vibrations (N_V) : 17 = 87·44 cms. (L_V).

Window.	2	3	4	5	6	7	8	9	10	12	13
Base line	12·643	12·642	12·641	12·640	12·639	12·638	12·636	12·635	12·634	12·631	12·630
Start of line	12·540	12·321	12·057	11·804	11·553	11·299	11·047	10·797	10·544	10·039	9·788
Difference	0·103	0·321	0·584	0·836	1·086	1·339	1·589	1·838	2·090	2·592	2·842
Step difference		0·218	0·263	0·252	0·250	0·253	0·250	0·250	0·252	0·502	0·250

h = 2·006 cms.

The wave in all cases is found to be considerably more rapid for the first 10 to 20 cms. after the point of detonation; h is measured after the wave has settled down to its uniform velocity, *i.e.*, when the step differences as determined above become constant.

With the precautions described it has been possible to measure the velocity of the detonation waves to an accuracy of at least ½ per cent.

The results obtained for various mixtures of acetylene, of hydrogen, and of pentane with oxygen, nitrogen or argon are given in the tables (I to III). The mixtures were made in the manner described in the previous paper ; the pressure gauge was calibrated at the National Physical Laboratory.

Table I.—Acetylene.

Mixture.	Temperature.	Press. lbs. (abs.).	Position of detonation. cms. from spark.	Velocity of detonation. metres/sec.	Other figures (Dixon).
$1C_2H_2 : 2{\cdot}5O_2 : 5N_2$	15° C.	15	73	1998	
		50	50	2049	
		85	40	2061	
		115	40	2064	
$1C_2H_2 : 2{\cdot}5O_2 : 3N_2$	,,	15	41	2108	
		50	15	2165	
		85	12	2193	
		115	12	2202	
$1C_2H_2 : 2{\cdot}5O_2$	,,	15	5	2399	2391 (2482 Berthelot)
		50	at spark	2469	
		85	,,	2508	
$1C_2H_2 : 1{\cdot}5O_2$	,,	15	at spark	2688	2716
		50	,,	2806	
		73	,,	2814	
$1C_2H_2 : 1{\cdot}5O_2 : 1N_2$	,,	15	20	2669	
		50	8	2740	
		60	at spark	2739	
$1C_2H_2 : 1{\cdot}5O_2 : 3N_2$	,,	15	55	2140	
		50	24	2243	
		85	6	2266	
		115	almost at spark	2308	
$1C_2H_2 : 1{\cdot}5O_2 : 5N_2$	,,	15	100	2167	
		50	70	2085	
		85	56	2068	
		115	56	2095	
$1C_2H_2 : 2{\cdot}5O_2 : 5A$	,,	15	35	1847	
		50	13	1916	
		85	2	1999	
		115	2	2014	
$1C_2H_2 : 2{\cdot}5O_2 : 3A$	,,	15	30	2016	
		15	30	2021	
		50	10	2101	
		85	4	2134	
		115	at spark	2166	

Table II.—Pentane.

Mixture.	Temperature.	Press. lbs. (abs.).	Position of detonation. cms. from spark.	Velocity of detonation. metres/sec.
$1C_5H_{12} : 8O_2 : 15N_2$	15° C.	15	95	1212
		50	80	2021
		85	70	2017
		102	70	2024
$1C_5H_{12} : 8O_2 : 6N_2$	,,	15	78	2113
		50	49	2134
		73	38	2139
$1C_5H_{12} : 8O_2$	,,	15	17	2261
		37	8	2334
$1C_5H_{12} : 5{\cdot}5O_2$	,,	15	7	2458
		36	7	2501
$1C_5H_{12} : 8O_2 : 15A$	,,	15	76	1857
		50	50	1870
		85	45	1891
		115	43	1948
$1C_5H_{12} : 8O_2 : 6A$	,,	15	35	2034
		50	10	2097
		80	14	2081

Table III.—Hydrogen.

Mixture.	Temperature.	Press. lbs. (abs.).	Position of detonation. cms. from spark.	Velocity of detonation. metres/sec.	Other figures (Dixon).
$2H_2 : 1O_2 : 2N_2$	15° C.	15	58	2148	2121
		50	38	2180	
		85	38	2226	
		115	38	2226	
$2H_2 : 1O_2 : 1N_2$	,,	15	48	2302	
		50	24	2432	
		85	20	2468	
		115	20	2470	
$2H_2 : 1O_2$	,,	15	30	2769	2820 (2810 Berthelot) 2872 at 30 lbs.
		50	14	2877	
		85	8	2898	
		115	8	2913	
$2H_2 : 1O_2 : 1H_2$	,,	15	40	2993	
		50	14	3166	
		85	7	3184	
		115	7	3195	

Table III—(continued).

Mixture.	Temperature.	Press. lbs. (abs.).	Position of detonation. cms. from spark.	Velocity of detonation. metres/sec.	Other figures (Dixon).
$2H_2$ $1O_2$: $2H_2$	15° C.	15	57	3053	
		50	28	3332	
		85	16	3354	
		115	16	3413	
$2H_2 : 1O_2 : 2A$	,,	15	42	1960	
		50	30	2088	
		85	14	2132	
		115	13	2144	
$2H_2 : 1O_2 : 1A$	,,	15	30	2251	
		50	18	2320	
		85	15	2352	
		115	15	2366	
$2H_2 : 1O_2 : 1N_2$	140° C.	21·2	46	2331	
		71	22	2391	
		120	12	2402	
		163	11	2423	
$2H_2 : 1O_2 : 2N_2$	,,	21·2	69	2178	
		71	48	2120	
		120	40	2244	
		163	40	2276	

The positions of detonation are in fair agreement with the figures given for corresponding mixtures in the previous communications. The fact that as the pressure increases detonation takes place earlier, but only up to a certain limiting pressure, is confirmed. The same applies in the case of hydrogen, figures for which we have not previously given.*

The velocities behave similarly with rise of pressure; at high pressures the same increase of pressure makes less difference to the velocity than at lower pressures.

Certain figures obtained by Prof. Dixon (1893) are given in column 6; agreement is best in the case of acetylene.† It would be possible from a knowledge of the specific heat of the gases to calculate the velocity of the detonation wave according to the method of Jouguet.‡ Such a calculation would be unconvincing owing to dissociation and the uncertainty of the specific heat data.

---

* *Cf.* Dumanois and Lafitte, 'C. R.,' vol. 183, p. 284 (1926).

† The hydrogen contained 0·7 per cent. N_2, which may account for the slight difference for these mixtures.

‡ 'J. de Math.,' vol. 2, p. 5 (1906).

It would be more to the point to do the reverse and determine the specific heat from the velocity and the maximum temperature. It is hoped to extend this work and to determine the temperature by optical methods.

(*b*) *On "Autoignition."*

On p. 159 of our paper it was stated that compression waves set up by the ignited charge may cause "autoignition" of another part of the charge, but that the work did not provide any evidence for such a view. The following record of experiments continues investigation of this point:—

Table IV.

Mixture.	Pressure.	Length of tube.	Position of detonation.
$1C_2H_2 : 2{\cdot}5O_2 : 6N_2$	50 lbs.	136 cms.	53 cms.
		121 ,,	58 ,,
		91 ,,	68 ,,
		61 ,,	(no detonation)
		31 ,,	n. d.
$1C_2H_2 : 2{\cdot}5O_2 : 3N_2$	50 ,,	61 ,,	16 cms.
		31 ,,	17 ,,
		21 ,,	14 ,,
		11 ,,	10 ,,
$1C_2H_2 : 2{\cdot}5O_2 : 3N_2$	15 ,,	136 ,,	28 ,,
		121 ,,	28 ,,
		91 ,,	28 ,,
		61 ,,	30 ,,
		31 ,,	30 ,,
		21 ,,	20 ,,
		11 ,,	n. d.
$1C_2H_2 : 1{\cdot}5O_2 : 4N_2$	15 ,,	61 ,,	60 cms.
		31 ,,	n. d.
		21 ,,	n. d.
		11 ,,	n. d.
$1C_2H_2 : 2{\cdot}7O_2 : 2{\cdot}9N_2$*	15 ,,	61 ,,	32 cms.
		31 ,,	30 ,,
		21 ,,	n. d.
		11 ,,	n. d.
$1C_2H_2 : 2{\cdot}7O_2 : 2{\cdot}9N_2$	50 ,,	61 ,,	12 cms.
		31 ,,	12 ,,
		21 ,,	12 ,,
		11 ,,	11 ,,

---

* See Woodbury, Canby and Lewis, 'J. S. Aut. Eng.,' vol. 8, p. 209 (1921).

(1) *Experiments with the Long Tube.*

Into the same steel explosion tube as[*] had previously been employed, lengths of steel rod were closely fitted so that the tube could be shortened to any required length. Table IV gives the points of detonation measured from the spark, when the tube length was varied in the manner described.

The last mixture was similar to that used by Woodbury, Canby and Lewis[*] in their 12-inch by 4-inch bomb. They recorded evidence of autoignition considerably in front of the main combustion zone for this mixture.

In our experiments there is no evidence of autoignition in any case, and the virtual shortening of the bomb by insertion of the steel rods makes little difference to the points of detonation.

The experiments show that the length of tube does not affect the position of detonation to an appreciable extent except when detonation is about to occur in the neighbourhood of the end of the tube, presumably owing to local increase of pressure. The weak mixture ($1C_2H_2 : 2{\cdot}5O_2 : 6N_2$), however, appeared to behave differently; the shorter the tube the later the detonation, an effect which possibly may be connected with the oxidation of the nitrogen. With nitrogen as diluent it appears not to be as easy to repeat results as with other mixtures.

Table V.

Mixture.	Initial pressure.	Temperature.	Notes.
$1C_2H_2 : 2{\cdot}5O_2 : 10N_2$	96 lbs.	15° C.	Loud crack, glow lasts half second.
,, ...	,,	,,	,,
,, ...	,,	,,	,,
,, ...	,,	,,	,,
,, ...	100 lbs.	,,	Loud crack, yellow light.
,, ...	,,	,,	,,
,, ...	,,	,,	,,
$1{\cdot}1C_5H_{12} : 8O_2 : 32N_2$	,,	,,	No knock.
,, ...	,,	,,	Burnt gently.
$1{\cdot}1C_6H_{14} : 9{\cdot}5O_2 : 38N_2$	95 lbs.	,,	Did not burn.
$1C_6H_{14} : 6{\cdot}4O_2 : 25{\cdot}6N_2$	,,	91° C.	Burnt slowly, no knock.
,, ...	110 lbs.	89° C.	Burnt slowly, high-pitched whistle.

(2) *Experiments with Short Bomb of Large Diameter.*

A bomb was constructed measuring 19 cms. by 10·7 cms. internal diameter, so that experiments could be carried out under circumstances similar to those conducted by R. W. Fenning at the National Physical Laboratory,[†] a photographic record of flame travel being obtained instead of a record of pressure rise. The aperture of the three windows in the side of the bomb measured 2·8 cms. by 2 mm., and there was a space of 2·9 cms. between each window. Particular care was expended in order to render the windows gas tight. The bomb could be placed in an oil bath heated by a coil through which steam was passed; the bomb was then placed horizontally, windows uppermost, and a mirror arranged to reflect the light from the windows toward the lens of the camera. Combustion was initiated at the centre of one of the end plates of the bomb by means of a spark plug. The experiments summarised in Table V have been carried out with the above arrangement, but further work is contemplated when an indicator has also been fitted to give a simultaneous record of pressure rise.

---

[*] *Loc. cit.*

[†] 'Rep. Aero. Research Comm. No. 979,' p. 20 (1925).

The sound of the explosion of the mixture $C_2H_2 : 2 \cdot 5O_2 : 10N_2$ was definitely of the nature of a knock, but for the other mixtures the combustion was quiet. The visible combustion continued for about half a second after commencement. The records were taken on the wheel (1 metre circumference) at 2 revolutions per second.

The records for the acetylene mixture are quite different from the others (see fig. 1, Plate 13). The rate of combustion at the first window is about 12 metres per second, at the second window about 16 metres per second; somewhere between the second and third windows a change in rate occurs and the main combustion front travels with a decreasing instead of an increasing velocity at about 13 metres per second. There is faint luminosity shown at the third window, which seems to start, sometimes abruptly, almost before the combustion has travelled half-way along the bomb. There is no such appearance prior to combustion at the second window, neither does the intensity of the faint image at the third window follow the apparent intensity of the light from the second window; that it should be due to light reflected from the inside of the bomb seems therefore unlikely. Apart from such a possibility, other explanations of the effects observed can be offered. "Autoignition" may occur well in front of the combustion zone. The combustion spreading from the spontaneously ignited portion of the gas would meet the advancing main combustion zone and check its progress, though enhancing the luminosity. That no autoignition occurs with such mixtures in the long steel tube of small diameter, while it is a possible explanation of the effects observed in the bomb, is not surprising, as heat would be dissipated more rapidly in the former case, so preventing autoignition. Some of the photographs show distinct closely spaced bands, indicating that the combustion has a vibratory character. The number of vibrations per second in the after-flame is about 2500, and the spacing is consistent with the view that successive sound waves are reflected from the end plates. In fact, the general character of the combustion (apart from the faint initial luminosity at the third window already described) is vibratory, and the effects observed are similar to those which would be shown by a horizontal section through a record such as given by Prof. Bone.* The initial vibration appears to exhibit a frequency of about 250 to 300 vibrations per second and of the order to be expected from the dimensions of the bomb. This vibratory condition is not set up by any "give" at the windows; the records show clearly the moment at which a "blow out" occurs. If it occurred, a "blow out" generally took place long after the explosion had reached the end of the bomb. The pentane mixtures burnt slowly with a speed of flame at the first window of about 1·7 metres per second, at the second of about 3 metres per second, and at the third of 0·6 metre per second. The rich hexane mixture behaved similarly to the pentane mixture. There was no "knock" or "crack" in these cases.

The inference from the above results that "knock" is associated not necessarily with detonation, but with a vibratory type of combustion, seems to be similar to that which Dr. Morgan† has come to as a result of experiments in closed bombs of different lengths. He attributes the initiation of the vibratory condition to a correlation of the rate of generation of heat with the normal vibration frequency of the gaseous charge. Indeed, if there is any irregularity in the rate of burn, some vibrations will be set up (and are faintly visible in the initial stages of combustion in some of the records) and the gaseous charge in the bomb will pick out from this noise its suitable wave. A stationary wave will be formed which gives rise to the necessary conditions for vibratory combustion and the enhancement of the sonorous effects accompanying the pressure fluctuations.‡

These rapid changes of pressure are also the conditions favouring "auto-ignition" which, if it occurs, would still further increase the rate of rise of pressure. There is, perhaps, no very great difference in the nature of the combustion process, whether it be uniform, vibratory, spontaneously generated or detonating. The flame will move with increased velocity as the pressure increases in its offing, and if the pressure is great enough, ignition may occur adiabatically ahead of the combustion zone, but will not be propagated particularly rapidly, because the rate of reaction will only be sufficient to generate heat adequate to keep the flame going as in the ordinary combustion zone. If, on the other hand, the rate of rise of pressure in front of the combustion zone is great enough and conditions are such that a very large number of molecules are activated, the rate of reaction may be great enough to supply sufficient excess energy to maintain the initial rate of reaction and the detonation wave may be set up. Detonation cannot be set up unless sufficient molecules are activated by the immediate proximity of the high-temperature combustion zone. It seems clear from the extreme sensitiveness to composition of the explosive mixture to transmission of a detonation wave* that it is necessary to achieve a certain reaction rate before a detonation can be initiated. Adiabatic ignition by mechanical compression in front of the combustion zone is alone insufficient; a certain rate of reaction is also essential.

---

* See 'Roy. Soc. Proc.,' A, vol. 114, Pl. 30, p. 429 (1927).

† 'Phil. Mag.,' vol. 3, p. 161 (1927).

‡ In an engine the movement of the piston and turbulence of the charge might influence, but not prevent, such a condition of affairs.

Although the rapid rise of pressure accompanied by temporary increase in rate of combustion which is associated with vibratory combustion is akin to the phenomenon of "pseudo-detonation"—(a tendency for the gas to detonate locally, but no detonation wave propagated)—it is very improbable that true detonation occurs in an internal combustion engine. Rate of rise of pressure is much greater for detonation than is experienced with "knocking" and would lead to greater damage than knocking causes; and, further, explosions in bombs for the mixtures of the strength used in an engine do not give evidence of true detonation.

Brown and Watkins† provide evidence that rate of rise of pressure is the dominant factor that determines the tendency of a fuel to initiate the detonation wave, but that the relative tendency of different fuels to detonate is different from their tendency to "knock" in an engine. These authors state that the self-igniting temperature is an important factor besides the rate of rise of pressure; we have discussed the significance of this factor‡ and shown its influence on the knocking characteristics of a fuel. The processes of slow combustion prior to ignition affect the formation of ignition centres and the propagation of ignition —factors which control autoignition. Both autoignition and the rapid rise of pressure which occurs in vibratory combustion are manifestations of the same influence. High local temperature occasions the necessary activation to produce rapid combustion, which is delayed again in regions of less density.

---

* See Wendlandt, 'Z. f. Phys. Chem.,' vol. 116, p. 227 (1925).

† 'J. Ind. Eng. Chem.,' vol. 19, p. 363 (1927).

‡ 'J. Inst. Pet. Technologists,' vol. 13, p. 244 (1927).

That autoignition occurs and leads to vibratory combustion is probable, that hot regions (*e.g.*, valves) assist "knocking" and would favour autoignition is also significant; but it is not essential that autoignition precedes the establishment of a vibratory condition, and it remains to be proved that autoignition is essential to the production of "knocking."

The slow processes of combustion which precede inflammation have been discussed in our papers (*loc. cit.*). Taking a simple case, in the combustion of hydrogen and oxygen the encounters of the hydrogen and oxygen molecules result first in a temporary formation of a peroxide of hydrogen, and the oxygen produced by its subsequent decomposition is in an active state. The subsequent processes of energy exchange we do not yet know sufficient about to discuss, but there seems little doubt that the process of combustion is controlled by the rate of such activation and deactivation, and that, unless there is a very large amount of excess heat available, the rate of combustion can be considerably modified by the preliminary processes. We had found that "anti-knocks" act in these preliminary stages of combustion, and that was the reason for their failure to influence the rate of combustion when plenty of heat was available, as in the rapid combustions which give rise to true detonation. It is clear from our discussion that autoignition and vibratory combustion are influenced by the igniting characteristics of the fuel, and these in turn by the nature of the preliminary processes of combustion, so that "anti-knocks" can here influence the combustion processes. Our contention is further borne out by the work of Lovell, Coleman and Boyd,* who find from an analysis of the burning charge at various stages in the cylinder of an internal combustion engine (using gasoline as fuel) that the rate of combustion of the fuel is delayed by the presence of the "anti-knock," and accelerated by a "pro-knock." Their work shows that combustion spreads outwards from the spark, but continues just as in a bomb for a very considerable time after the flame has travelled throughout the charge. If the contention was right that "anti-knocks" influence processes of slow combustion, then they should influence to some extent the rate of combustion of slow-burning mixtures. This we have now shown to be the case.

(3) *Effect of Anti-Knocks on Slow-Burning Mixtures.*

The mixture $1C_5H_{12} : 8O_2 : 32N_2$ at 100 lbs., at 80 lbs. and at 73 lbs. in the long steel tube burnt quietly with no knock and a yellow flash. A mean velocity of about 20 metres per second was obtained for the rate of flame travel in the latter case, the record showing an irregular rate of burn. With 0·96 per cent. lead ethyl present in this mixture, the flame was bluish in colour and travelled irregularly and much slower (about 1 metre per second).

---

* 'J. Ind. Eng. Chem.,' vol. 19, p. 373 (1927).

Experiments have also been made with slow-burning acetylene and pentane mixtures at ordinary pressures. A long glass tube fitted with flanged ends was furnished with brass electrodes at certain fixed positions. The method of recording the velocity of flame travel electrically by taking advantage of the conductivity of the flame was similar to that described by Bone, Fraser and Winter* and by Crowe and Newey.† In order to simplify the arrangement, the sparks were caused to puncture a strip of thin squared paper wrapped round the metal flange of a 6-inch wheel driven at constant speed by a gramophone motor (the speed of which was checked by a tuning-fork kindly lent by Prof. J. Gunn of the Department of Pharmacology). The acetylene results (see Table VI) were obtained using a tube 175 cms. long by 1·3 cms. diameter and ignition by a spark 10 cms. from the open end of the tube; the pentane results (see Table VII) with a tube 371 cms. long by 1·2 cms. diameter and ignition by spirit flame at the mouth of the tube. The far end was closed by a brass plate in both cases.

The lead ethyl vapour was introduced by passing the gas mixture on its way to the explosion tube through a small U tube containing glass wool soaked with

Table VI.—Acetylene.

Mixture.	Speed cms./sec.		Notes.
	(*a*.)	(*b*.)	
5 per cent. C_2H_2 95 per cent. air	93	100	Narrow combustion zone.
,, ...	96·5		,,
,, ...	99		,,
,, ...	93	92	,,
Do. + lead tetraethyl	98·5	91·5	Flame 3 inches long and cone-shaped.
,, ...	106	95·5	,, ,,
Do. without lead tetraethyl	—	92	Narrow combustion zone.
,, ...	101	92	,,
,, ...	104	99	,,
,, ...	104	104	
Do. + 0·4 per cent. lead tetraethyl	105	142	Flame 6 inches long.
Do. + 0·4 per cent. lead tetraethyl	110	111	Flame 5 inches long.

(*a*) Flame velocity over a distance of 40 cms. commencing at 55 cms. from the spark.
(*b*) Flame velocity over a distance of 40 cms. commencing at 95 cms. from the spark.

---

* 'Roy. Soc. Proc.,' A, vol. 114, p. 407 (1927).

† 'Phil. Mag.,' vol 49, p. 1112 (1925).

Table VII.—Pentane.

Mixture.	Speed. cms./sec.		Notes.
	(*a.*)	(*b.*)	
3 per cent. C_5H_{12} 97 per cent. air	55	—	Flame goes out after 220 cms. travel.
,,	56	—	,, ,,
Do. + 0·4 per cent. lead tetraethyl	51	51·5	
Do. + 0·8 per cent. lead tetraethyl	49·5	53·5	Went out 15 cms. from end.
Do. without lead tetraethyl	56	—	Similar to first two.

(*a*) Flame velocity over a distance of 50 cms. commencing at 71 cms. from the mouth of the tube.

(*b*) Flame velocity over a distance of 50 cms. commencing at 279 cms. from the mouth of the tube.

the liquid. The tube containing the lead ethyl was accurately weighed, before and after, so as to give the quantity of lead ethyl which was vaporised.

The only effect of the lead ethyl on the rate of travel in the case of the acetylene mixture was an accelerating one and then only in certain experiments. The effect on the character of the flame was considerable, a long cone-shaped blue tail being formed. The effect of the lead ethyl on the rate of travel of the pentane mixture is definitely a delaying one. The flame of this mixture is not steady but is inclined to vibrate and extinguish; the lead ethyl tends to maintain, but at the same time to delay, the propagation of the flame. As expected, there is a definite retardation of the process of combustion in pentane mixtures in the presence of an "anti-knock," provided the combustion is not too rapid. The effect on other mixtures is being investigated.

The above results lend support to the inference on p. 524. Together, the results provide evidence that "knock" is associated with a vibratory type of combustion, not necessarily involving "autoignition," and is not due to the establishment of a detonation wave.

We have to thank the Asiatic Petroleum Company for permission to continue to utilise the apparatus which was erected mainly at their expense, and the Aeronautical Research Committee of the Air Ministry for a grant to enable one of us (S. F. G.) to continue the work.

Summary.

(1) Measurements are given of velocities and positions of detonation of acetylene, of pentane and of hydrogen mixtures with oxygen, nitrogen and argon, at initial pressures up to 6 atmospheres in a steel tube 1·5 cms. diameter.

(2) The influence of length of tube on the position of detonation is investigated.

(3) Experiments in a bomb of comparatively large diameter are described, giving some evidence of autoignition during the progress of combustion of a vibratory character in certain acetylene mixtures.

(4) The influence of lead tetraethyl on the rate of uniform movement of flame is recorded for certain mixtures of acetylene and of pentane. The lead tetraethyl delays the rate of combustion of the pentane under such circumstances.

Gaseous Combustion in Electric Discharges. Part II.—*The Ignition of Electrolytic Gas by Direct Current Discharges.*

By G. I. Finch and L. G. Cowen.

(Communicated by Prof. W. A. Bone, F.R.S.—Received July 7, 1927.)

[Plate 14.]

Introduction.

In Part I* of the present series of researches an account was given of an investigation of the slow, non-self-propellant combustion of electrolytic gas in direct-current discharges. Owing to the limited output of the generator then available, it was not possible, except in a few isolated cases, to extend the investigation to the study of the ignition of electrolytic gas. Some time after the completion of the above-mentioned work, however, a larger high-tension direct-current generator, together with suitable smoothing chokes and condensers, became available, thus enabling us to carry out a systematic investigation of the conditions of ignition of electrolytic gas.

Experimental.

In the experiments to be described below, precautions were taken to eliminate as far as possible any conditions favourable to ignition, particularly heat and catalytic combustion at the electrodes, other than those due to ionisation of the gas; and then to study the effect of variations of the gas pressure upon the least-igniting current. We have been able to establish a gas pressure-least

* 'Roy. Soc. Proc.,' A, vol. 111, p. 257 (1926).

igniting current relationship of such a nature that the conclusion may be drawn that ignition of electrolytic gas is determined, under the conditions of our experiments, by the attainment of a definite concentration of ions due to the passage of the electric current; and, further, it has been found that flame is propagated more rapidly in the gas when ionised by the electric discharge than otherwise.

Description of the Electrical Circuit.

The electrical circuit was similar to that previously employed and described and illustrated in Part I, fig. 1. The new generator was capable of a maximum output of 100 milliamperes at 5,000 volts. The normal full speed of the rotor was 2,700 r.p.m., and the output commutator was built up of 192 segments. The secondaries of four one-kilowatt high-tension transformers served as smoothing chokes, the inductance of each being over 300 henrys. The storage condenser of the smoothing circuit was capable of withstanding without breakdown a steady sustained pressure of up to 6,000 volts and had a capacity of three microfarads. Owing to the experimental procedure which it was found necessary to adopt, in the majority of the experiments the potential drop across the electrodes could not be determined with sufficient accuracy with the apparatus at our disposal. The electrostatic voltmeter and the tapped non-inductive resistance shunting the electrodes were, therefore, dispensed with. The output of the generator was controlled partly by means of a variable water resistance, and partly by varying the speed of the generator by means of a sliding resistance connected in the primary 220-volt circuit.

The Explosion Vessel and Electrodes (fig. 1).

It was found necessary to employ an explosion vessel of considerably greater volume than that previously used in our slow-combustion experiments, in order to reduce, as far as practicable, the fall in gas pressure due to slow combustion preceding ignition. The explosion vessel finally adopted after numerous trial experiments consisted of a horizontally disposed glass tube of 7·5 cm. diameter, the total volume of the vessel and manometer being approximately 480 c.c. It was provided with a two-way tap, one branch of which served for the admission of the electrolytic gas, the other for evacuation by means of a "Hyvac" oil pump. The electrodes were fitted by means of ground-in greased joints into ports situated near the centre of the vessel and were so disposed that the arc burning between them was horizontal. A mercury U-tube manometer, one limb of which was closed, communicated with the vessel through a

T-piece let in between the latter and the two-way tap. The explosion vessel was surrounded by a water-jacket, maintained at a temperature of 20° C. and consisting of a wooden box fitted with a glass cover through which the discharge could be viewed or photographed. The vessel contained 50 c.c. of concentrated sulphuric acid, which was renewed at suitable intervals, the specific gravity of the discarded acid being determined as a check.

In studying the slow combustion of electrolytic gas it had been found that the soft-soldering of short sections of pointed 1-cm. lengths of 20 S.W.G. wire to stout copper wire or rod was sufficient to ensure that the electrodes remained so cool with the relatively small currents then passed that no appreciable catalytic combustion of the gas in contact with the electrodes could be detected. With the much heavier currents which could be furnished by the new generator, however, and which were required to bring about ignition, it was frequently observed, particularly in the case of platinum electrodes at the higher pressure ranges and smaller gap widths, that vigorous catalytic combustion would occasionally set in, and rapidly, or even sometimes abruptly, raise the temperature of the cathode to a bright red heat, thus bringing about ignition of the gas or causing the electrode point to become unsoldered. It was therefore decided to employ, as electrodes for the purpose of the experiments to be described below, small thimbles pressed or spun out of thin sheet metal of 30 S.W.G., and to water-cool these. The base of such a thimble was struck with a radius of approximately 12 mm. The diameter of the cylindrical portion of the thimble was 8 mm. The construction of the holders into which these electrodes were secured is shown in fig. 1, in which one electrode complete with holder and

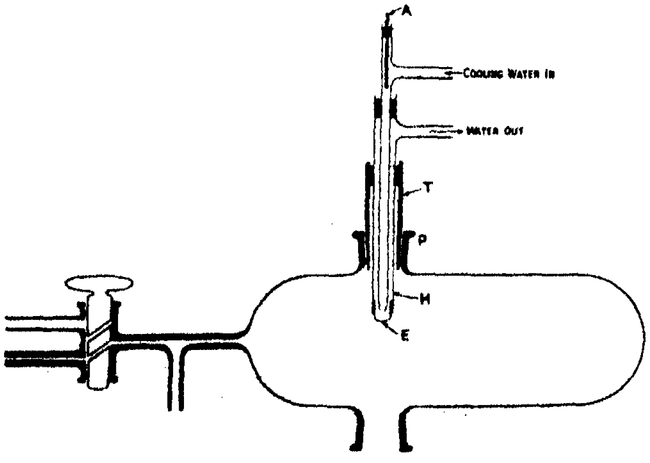

FIG. 1.

water-cooling arrangements is shown fitted into the explosion vessel. The electrode thimble, E, was sealed with sealing wax into the holder, H, with the rim of the thimble-base proud of the end of the former by 1½ mm. The holder was likewise secured with sealing-wax into a glass tube, T, the ground-in end of which was fitted into the port, P, provided for its reception in the explosion vessel. The gap width could be adjusted by softening the sealing-wax joint between H and T. Connection was made to the stout copper wire, A, sealed into the cooling-water tube, a column of cooling water thus acting as the final steadying resistance and reducing the capacity effects of the electrodes to a minimum. The cooling-water systems of both electrodes were independent of each other and insulated throughout. Insulation tests were frequently carried out under a pressure of 5,000 volts.

The Electric Discharge between Water-Cooled Electrodes.

Three photographs of the direct-current discharge in electrolytic gas between 30 and 90 mm. between pointed wire electrodes were shown in Part I.* When the current is below about 0·8 milliampere the appearance of the discharge was as in fig. 5, Plate 5.* On increasing the current above this value, the positive column shrank abruptly, fig. 4,* showing a sharply defined stage in the transition from the long to the short positive column, and became only feebly luminous except in the vicinity of the anode spot. Further increase in the current up to the independence value, *i.e.*, that current at which combustion in the positive column sets in was attended only by an increase in this faintly glowing positive column and in the area of the cathode covered by the cathode glow. On exceeding the independence current, however, a strongly luminous core commenced to grow out from the anode spot into the faint portion of the positive column. In the case of the discharge shown in fig. 3,* the independence current was exceeded by about 1 milliampere. Owing to its feeble luminosity, the fainter portion of the positive column does not, however, appear on the photograph. With further rise in current, the brightly luminous section of the positive column continued to increase until it almost bridged the gap.

The manner in which the discharge in electrolytic gas between water-cooled platinum or copper electrodes varied with current differed in several important particulars from the above. In the first place, the faint, usually striated discharge shown in fig. 5, Plate 5,* appeared only below about 0·25 milliampere.

---

* *Loc. cit.*, Plate 5, p. 265.

FIG. 3.—$i = 2\cdot25$ m-amp.; $p = 13\cdot7$ cm.; $d = 15$ mm. Positive column glow adjacent anode is brighter than positive glow near the cathode. Faraday dark space is about $1\cdot5$ mm. wide and well defined. Crookes dark space just visible.

FIG. 4.—$i = 5\cdot25$ m-amp.; $p = 7\cdot65$ cm.; $d = 15$ mm. Both positive column glows are approximately equally bright. Faraday dark space very narrow.

FIG. 5.—$i = 9\cdot4$ m-amp.; $p = 5\cdot6$ cm.; $d = 15$ mm. Positive glow adjacent the cathode is brighter than the positive glow near the anode.

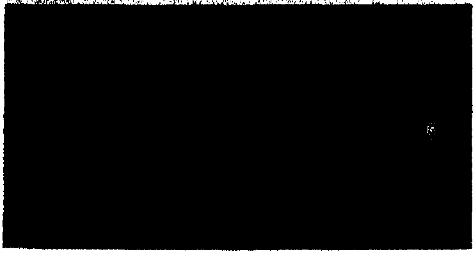

FIG. 6.—$i = 5\cdot0$ m-amp.; $p = 5\cdot4$ cm.; $d = 30$ mm. Showing the extension of positive column glow nearest the anode with increase in gap width.

In all cases both positive column glows are joined by a faint blue-violet track which is not visible on the photographs owing to its feeble luminosity.

On slightly exceeding this value, the positive column practically disappeared and became limited to two widely separated bright glows of minute volume; one, the brighter of the two, was rooted on the anode spot or glow, while the other and less luminous was close to, but separated from, the cathode glow by a sharply defined dark space. Both these bright positive column glows faded gradually away towards each other in such a manner that the intervening space between the glows was completely bridged by a narrow, feebly luminous track of violet-blue light. As the current was increased the areas of the electrodes covered by the anode and cathode glows likewise increased, though their luminosity remained constant; at the same time the Faraday dark space was narrowed down until with higher currents it could be no longer distinguished. The two bright portions of the positive column also increased in volume and brightness; an increase in luminosity which was, however, more pronounced in the case of that positive glow which was nearest the cathode, with the result that, whilst at the lower current ranges the latter was not so intense as the glow near the anode, with higher currents it altogether eclipsed the latter in brilliancy.

Under similar conditions of current and gas pressure, the main effect of decreasing the gap width was to widen, *i.e.*, broaden out, the two positive column glows in a direction at right angles to the path of the discharge. Otherwise, except for the shortening of the positive column, the appearance of the discharge remained unchanged.

Experimental Procedure.

The fact was recorded in Part I (p. 278) that, in the few ignition experiments then carried out, a definite interval elapsed after attaining the ignition current before ignition took place. In the course of a series of preliminary experiments carried out with the purpose of determining the most suitable type of electrode for use in the ignition experiments to be described below, it was found, however, with wire electrodes that the true cause of this lag effect was due to the more or less abrupt setting in of catalytic combustion on the cathode. With the new type of water-cooled electrode, no such lag could ever be observed. Thus, for instance, if the current passed by the discharge in electrolytic gas, maintained at constant pressure, were increased to a definite value and ignition failed to occur immediately on attaining that value, it would not take place at all, no matter how long these conditions of current and gas pressure were kept constant. When, however, ignition did occur it was found that, particularly at the lower ranges of gas pressure, the values of the corresponding igniting currents depended to some extent upon the rate of increase of the current. Thus, a rapid increase in the current from a low value resulted in ignition occurring at a current below that needed to ignite the gas when the rate of current increase was slow. The effect, however, was not to be confused with lag, with which it had nothing in common. As will be seen later, it was due solely to the water-vapour concentration in the gaseous mixture in the ignition zone of the discharge. The results of these preliminary experiments, however, clearly indicated the need of a uniform experimental procedure in regard to the rate of current increase when determining least igniting currents. A rapid increase of the current was found to be impracticable, owing to the difficulty thereby introduced of reading the milliammeter with sufficient accuracy. Eventually, the following procedure was decided upon and adhered to throughout all the experiments to be described below :—

The combustion vessel was first evacuated and a discharge carrying a current of approximately 1 milliampere passed between the electrodes. Electrolytic gas was slowly admitted to a few millimetres above that pressure, the least igniting current of which it was sought to determine. As the pressure rose in the explosion vessel, and hence also the resistance of the discharge, the generator was gradually speeded up in order to maintain the current approximately constant. When the pressure in the explosion vessel had attained the desired value the generator was rapidly, within between 1 and 2 seconds, further speeded up to such an extent, previously determined by pilot experiments, that the discharge current now amounted to as nearly as possible 85 per cent. of the least igniting current. By means of an automatic control consisting of a weighted plunger, released by a trigger and moving under the influence of gravity, a variable water resistance was now cut out at such a rate that the remaining 15 per cent. of the least igniting current was thrown into the circuit in the space of three seconds. Pressure and igniting current readings were taken simultaneously at the moment of explosion, which was indicated on the manometer and milliammeter by sudden deflections.

The Experimental Results.

Experiments were carried out with platinum, aluminium and copper electrodes and combinations thereof. The results obtained with aluminium and copper are, however, being reserved for a further communication, those with platinum electrodes alone being recorded in what follows. Pressures of electrolytic gas above 180 mm. were not employed, as it was thought that the force of the ensuing explosion might shatter the explosion vessel.

In fig. 2 are recorded the results obtained with water-cooled platinum electrodes in four series of experiments, three (Curves I, II and III) over

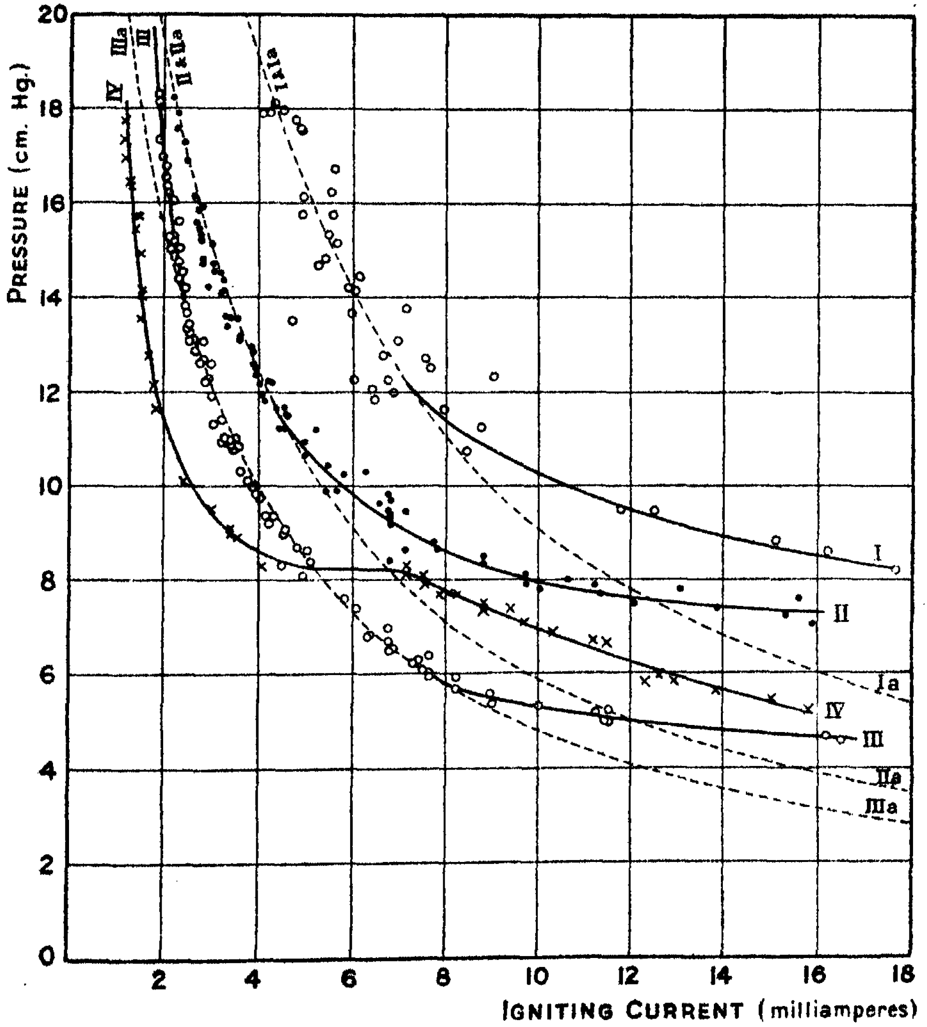

FIG. 2.

Hyperbola Ia: $p\,(i + 1 \cdot 5) = 105$

Hyperbola IIa: $p\,(i + 1 \cdot 5) = 68$

Hyperbola IIIa: $p\,(i + 1 \cdot 5) = 55$

concentrated sulphuric acid with gap widths of 3·8, 7·5, and 15 mm. respectively, and one (Curve IV) with a gap width of 15 mm., but without sulphuric acid, the igniting current being in all cases plotted against gas pressure. All points observed are recorded.

It will be seen that the experimental errors increase with decrease in gap width. This was due to various distortion effects, such as bowing or curvature of the discharge as a result of the seating of the cathode and anode glows on diametrically opposed points on the electrode surfaces, all of which effects virtually amounted to an increase in the effective gap width. With the 15-mm. gap, the discharge origins, particularly with platinum electrodes, showed less tendency to settle down elsewhere than on the centre of the electrode face, and even when this was not the case the ensuing virtual increase in the effective gap width was proportionately much smaller than in the case of the narrower gaps.

Discussion of the Results.

Since the experiments obtained with a 15-mm. gap show the greatest freedom from experimental error, the following discussion is based primarily upon the results recorded in fig. 2, Curve III: The most striking feature of this curve is that it shows that the igniting current varies with the pressure over a considerable range in a hyperbolic manner. For purposes of comparison, a dotted curve has been drawn, which is a rectangular hyperbola satisfying the equation $p \times (i + 1\cdot5) = 55$, where $p =$ pressure of electrolytic gas in centimetres and $i =$ the current in milliamperes (fig. 2, Curve IIIa). It will be seen that over the igniting current range between 2·3 and 7·6 milliamperes, the experimental results obtained actually lie, within the limits of experimental error, upon this hyperbola. This proves that, under the conditions of our experiments and over the range of pressure and current in question, *ignition is determined solely by the attainment in some portion of the gas traversed by the discharge of a certain definite concentration of suitable ions or electrically charged particles*, because on kinetic grounds the concentration of ions varies in a hyperbolic manner with the gas pressure. The curve cannot be accounted for on any purely thermal grounds, because of the complete absence of lag, ignition invariably taking place immediately on attainment of the igniting current. Hence we are left with the only supposition that will explain the facts disclosed by our experiments, namely, that ignition is essentially determined by concentration of ions; and inasmuch as flame propagation consists essentially in the communication of ignition from one layer to the next, the conclusion may be drawn that flame propagation is also essentially an electrical phenomenon.

Reduction in gap width results in an increase in igniting current; an effect which may be reasonably ascribed to the widening of, and hence also lowering of, the concentration of ions in the two bright positive column glows, in one of which, probably in the brighter, where the luminosity of the discharge as a whole is at its maximum, ignition without doubt originates; since from a consideration of the experimental results recorded in Part I of this series it is evident that ignition cannot occur in either the cathode or anode glows unless indeed the character of the discharge should undergo a radical change in the neighbourhood of the igniting current; and no such change was ever observed in the course of these experiments.

Below 2·3 and above 7·6 milliamperes the pressure-igniting current curves for the 15-mm. gap gradually diverges from the dotted hyperbola in such a manner that the igniting currents exceed those which would have been obtained had the experimental results actually conformed throughout to the hyperbola. Similar divergencies were observed over the lower pressure and higher current ranges with 7·5 and 3·8 mm. gaps, and are recorded in fig. 2, Curves I and II.

In order to throw light upon the reasons for the above-mentioned deviations of the pressure-igniting current curves from rectangular hyperbola, it will be necessary to consider more closely what goes on in that section of the discharge in which ignition will eventually originate, as the ignition current is approached. The concentration of ions on a plane at right angles to the path of, and intersecting the discharge through, the brightest positive glow, *i.e.*, the zone of most intense ionisation, will be at a maximum at the centre, and will fall away thence to practically zero at the limit of the discharge on this plane. Since the discharge is burnt between horizontal electrodes, electrolytic gas enters from below, and is drawn through, the discharge by convection. At high pressures and consequently with small igniting currents, both of which conditions result in constriction of the positive glow in the directions of the intersecting plane, the distance which the gas must travel in order to pass from the outer edge to the centre, *i.e.*, the most active zone of the discharge, approaches a minimum; whereas at low pressures where the igniting current is much larger, and, in consequence of both these conditions, the thickness of the positive glow considerably greater, the gas will require more time in order to travel from the outer zone to the centre of the discharge where ignition will be set up. In passing through the less active outer portions or sheaths enclosing the zone of maximum ionisation in the discharge, some of the electrolytic gas which was dry prior to entering the discharge is slowly burnt, with the result that the gas arriving in the ignition zone is charged to a lesser or greater extent with water vapour, the relative concentration of which will depend mainly upon the pressure and current conditions. Thus, at the higher pressure ranges and consequently with low igniting currents the moisture contents of the gas will be at a minimum, whereas under conditions of low pressure and heavy current the state of the gas will tend to approach saturation with water vapour.

In the light of these considerations it is difficult to resist the conclusions that (i) the observed deviations of the pressure-igniting current curves from a rectangular hyperbola at the two extremes of the curve (*i.e.*, outside the pressure range over which there is no such divergence) are due to the extent to which the electrolytic gas in the ignition zone of the discharge is charged with water vapour, (ii) under given experimental conditions there exists a certain definite concentration or range of concentration of water vapour which is most favourable to ignition, and above and below which ignition becomes more difficult to effect, (iii) deviation from the hyperbola in the range of higher pressures and lower currents in Curve III is due to deficiency of water vapour in the ignition zone, (iv) on the other hand, deviations in the region of low pressures and higher currents are due to an excess of moisture vapour, and, finally, (v) a suitable concentration of water vapour materially assists in the building up of that concentration of ions which must be attained in order to determine ignition in electrolytic gas, and the rôle played by water vapour in ignition is, therefore, essentially of an electrical nature.

Confirmation of these interpretations is afforded by the experimental results obtained without sulphuric acid in the explosion vessel, which are recorded in fig. 2, Curve IV. Although dry when passed into the vessel, the gas became charged to a certain extent with water vapour as a result of slow combustion preceding the attainment of the igniting current. Over the range of higher pressures Curve IV lies to the left of both the hyperbola IIIa and the pressure-igniting current Curve III, *i.e.*, in the region of easier conditions of ignition. At 5·2 milliamperes Curves IV and III intersect each other and the former continues thence into the region of more difficult conditions of ignition. The comparatively abrupt sweep of Curve IV from the zone of easier to that of more difficult ignition is possibly due to a more or less abrupt change of the igniting zone from one bright positive glow to the other.

Reasons have been given above for concluding that ignition occurred nowhere else in the discharge other than in one or other of the brightly luminous sections of the positive columns. Attempts were made to obtain direct experimental confirmation of the correctness of this conclusion by photographing the discharge at the moment of ignition on a photographic plate moving at a rate of 1,200 cm. per second at right angles to the path of the discharge taking place between horizontal electrodes set at a distance of 30 mm. apart. Whilst failing in their main object these experiments disclosed a fact of considerable significance, namely, that the velocity of propagation of flame was far more rapid along the path of the electric discharge than elsewhere in the explosion vessel. It was owing to this high rate of travel of the flame in the path of the discharge that the exact location of the ignition point could not be accurately determined with the apparatus at our disposal, though in many of the photographs distinct evidence was obtained of ignition being first set up in the vicinity of the anode. We estimate that the rate of flame propagation in the path of the discharge was very roughly at least 300 metres per second, and possibly much higher, and at least 10 times greater than elsewhere in the explosion vessel where the flame speed was of the order of 30 metres per second. This circumstance proves that the speed of flame propagation is greatly accelerated in regions where the medium is highly ionised.

Summary.

In the foregoing experiments it has been shown that :—

(i) Ignition of electrolytic gas by means of a direct-current discharge occurs without lag immediately on attainment of the igniting current.

(ii) A hyperbolic relationship exists between the gas pressure and the igniting current over a considerable range of conditions.

(iii) The value of the igniting current is raised by either a deficiency or an excess of water vapour in the gas in the ignition zone.

(iv) A decrease in the gap width, which results in a broadening out of the bright positive glows, increases the value of the igniting current.

(v) The rate of flame propagation in electrolytic gas along the path of the discharge is at least ten times greater than elsewhere.

From these facts, the conclusions are drawn that ignition is conditioned by the attainment in some portion of the gas traversed by the discharge of a certain definite concentration of suitable ions or electrically charged particles in the building of which water vapour materially assists, and that flame propagation is also essentially an electrical phenomenon.

One of us (G.I.F.) wishes to thank the Government Grants Committee of the Royal Society for a grant with part of which the cost of some of the apparatus employed in this investigation was defrayed.

The Coagulation of Smokes and the Theory of Smoluchowski.

By G. Nonhebel, J. Colvin, H. S. Patterson and R. Whytlaw-Gray.

(Communicated by R. Whiddington, F.R.S.—Received July 14, 1927.)

In a previous communication[*] it has been shown that smokes are unstable disperse systems which spontaneously coagulate from the moment of formation. In this respect they differ from hydrosols, which are stable normally and coagulate only on the addition of an electrolyte. For these latter systems there is evidence to show that the so-called "rapid coagulation" begins when the complete discharge of the double layer has been effected, and that the particles are brought together mainly by Brownian motion. With smokes, too, chance collision brought about by molecular bombardment is probably the chief factor in aggregation, so that a close analogy between the rapid coagulation of hydrosols and the spontaneous coagulation of smokes would appear to exist. Further, if it is admitted that every chance collision between the particles in the two types of system results in a union, then the equations developed by Smoluchowski[†] for the rate of coagulation of colloids might be expected to be equally valid for smokes after making allowance for the difference in properties of the two dispersion media. Reliable experimental data on sol coagulation are not easily obtained, for the process is completed in a relatively short period, but the measurements of Zsigmondy,[‡] Westgren,[§] and others[||] show a satisfactory agreement with theory. In a smoke, conditions are more favourable, for coagulation can be followed at much greater dilutions, so that the whole process is slowed down, and observations may be extended over several hours.

On account of the interest presented by the above analogy, and the possibility of testing it quantitatively, we have measured the velocity of coagulation of various smokes by a method which we believe to be free from any serious experimental errors.

Experimental.

In the previous work the particles were counted with the ultramiscroscope, using a modification of the slit instrument of Zsigmondy. Most of the number time curves contained in the previous paper are not in conformity with the equation of Smoluchowski, the rate of coagulation observed being smaller than that predicted by the equation, and the deviation increasing progressively with time. To explain this it was suggested that a diminution of the proportion of effective collisions might be brought about by the progressive adsorption of gas around the particles. Alternatively, the breaking up of the large aggregates formed as the cloud aged would yield an apparent rate of coagulation slower than that demanded by the equation. Support for both these hypotheses could be found in the literature.* Finally, the divergence between experimental and theoretical results might be attributed to errors which are inherent in the method of counting, and the first step evidently was to examine this possibility. Some attention must now be given to a discussion of the experimental arrangements used in the earlier work.

---

[*] Whytlaw-Gray and Speakman, 'Roy. Soc. Proc.,' A, vol. 102, p. 600 (1923).

[†] 'Z. f. Phys. Chem.,' vol. 92, p. 129 (1918).

[‡] 'Z. f. Phys. Chem.,' vol. 92, p. 600 (1918).

[§] 'Z. f. Phys. Chem.,' vol. 92, p. 750 (1918).

[||] Kruyt and Arkel, 'Rev. Trav. Chim. Pays-Bas,' vol. 39, p. 656 (1920); Tuorila, 'Kolloid Z.,' vol. 38, p. 3 (1926).

Originally the depth of the volume in which particles were counted was taken as that of the depth of the illuminating ribbon of light. This depth was determined by the Zsigmondy method of rotating the slit through an angle of 90°. It was assumed that only particles lying within the ribbon of light were counted, all others outside this region being invisible, and it is upon this assumption that the validity of the method is entirely dependent. For the observation of coarse clouds a weak source of illumination was used in conjunction with a microscope of low numerical aperture. Under these conditions the results were in satisfactory agreement with the equation of Smoluchowski. The investigation of fine clouds, however, necessitated powerful illumination and a lens system of high aperture, in which case the results showed a progressive discrepancy from theory as the cloud aged. In view of this divergence when using lenses of high numerical aperture, it seemed probable that scattered or reflected light either from the illuminated particles themselves, or from the cell, was rendering visible particles outside the defined volume. The correctness of this view was finally proved by a direct measurement of the depth of the zone in which particles could be counted at different periods during the coagulation of the smoke. This depth should, of course, be constant and agree with the thickness of the beam of light measured by the usual Zsigmondy procedure. To test this the viewing microscope was replaced by an instrument with a fine, graduated focussing adjustment, and a number of measurements were made of the limiting distance between particles which were just visible on the near and far sides of the illuminating ribbon of light. The same lenses were used as in the counts of fine clouds, namely, a 16-mm. Watson's Holos on the microscope and a 25-mm. Holos on the projection lens, but a pointolite lamp was substituted for the arc in order to avoid fluctuations of the light intensity during the observations. Although no special accuracy was claimed for the measurements, it was clear that with fine particles in the early stages of aggregation, such as tobacco smoke, the depth of the beam did not differ markedly from that estimated in the usual way; but that as coagulation proceeded and the particles grew larger and larger, the apparent depth of the beam increased progressively and particles well outside the true zone of illumination became visible. It appeared that this effect increased rapidly when the particles had grown on the average beyond some definite size. When the microscope was focussed on the centre of the illuminated zone, the same effect was shown by the appearance at a certain stage of coagulation of a large number of minute points and ill-defined discs of low luminosity. These corresponded to particles outside the beam on its near and far sides. It is evident that the counts were vitiated by this error, for a practice was made of counting every particle, including those on the limit of visibility, and it was not possible to discriminate between faintly illuminated particles outside the beam and minute particles within it. The explanation of the first results, which agreed with Smoluchowski's equation, is that the illuminating beam was of such low intensity that particles outside the beam did not become visible at any stage during coagulation. It must therefore be concluded that a progressive error is inherent in the Zsigmondy ultramicroscope when it is used for particles as large as those found in smokes, and that this error may be very considerable when high-intensity illumination and lenses of high numerical aperture are used. Similar criticism has been made by Westgren* when counting the particles in gold sols, and he claimed that the errors could be reduced by using a broad slit and cutting down the intensity of illumination.

---

* Bancroft, 'Applied Colloid Chemistry,' p. 147 (1921); Gibbs, 'Clouds and Smokes,' p. 93 (1924).

To eliminate this error, experiments were undertaken by Mr. W. Sever to test the possibility of using a cell in which the depth of the observed volume was limited by the walls of the cell itself, as in the cardioid ultramicroscope used for sols. On account of the lively Brownian movement of the particles, the concentration of a smoke contained in a shallow cell rapidly diminishes, so that provision had to be made for sucking a stream of smoke from a reservoir through the cell. In a series of experiments with a cell of this type, Mr. Sever established the possibility of counting by this means. The wedge-shaped form of the cell was entirely his design; but in the first cell made it was difficult to ensure that the depth of the observed volume remained constant. The arrangement of the apparatus and the form of the cell we have finally adopted is shown in the diagram.

---

* 'Arkiv. Matem. Astron. Fys.,' vol. 11, No. 8 (1918).

The cell consists essentially of two glass blocks AA fitting together on optically ground surfaces to form an airtight join, and hollowed out in the manner shown in fig. 1, which shows a horizontal section through the cell. Glass plates BB fitting on to the ground surfaces serve to close the cell at each end of the hollowed-out portion. The smoke enters by a 2-mm. bore tube C through the end plate opposite to the illuminating objective D, and passes into a wedge-shaped chamber 1 cm. long, the apex of which merges into a narrow slit 0·1 mm. wide between two optically plane surfaces E, 2 mm. broad. With this arrangement it is possible to take the cell to pieces for cleaning, and to reassemble it without altering the depth of the illuminated volume. The smoke is viewed in this part of the cell by an optical system, the depth of focus of which is greater than the distance between the two plane surfaces E. It then passes into a similar wedge-shaped chamber, 0·5 cm. long, and out by a tube F at right angles to the illuminating band of light. The angle at the apex of the wedge is approximately 20°. Fig. 1 (side elevation) shows a vertical section through the cell at the essential surfaces E, and indicates the line of junction of the two glass blocks. The cell is held tightly together by spring bands in a brass case, as shown in fig. 1 (end elevation), which gives a view of the cell from the position of the observation microscope F. The cell and case were constructed to our design by Messrs. Hilger.

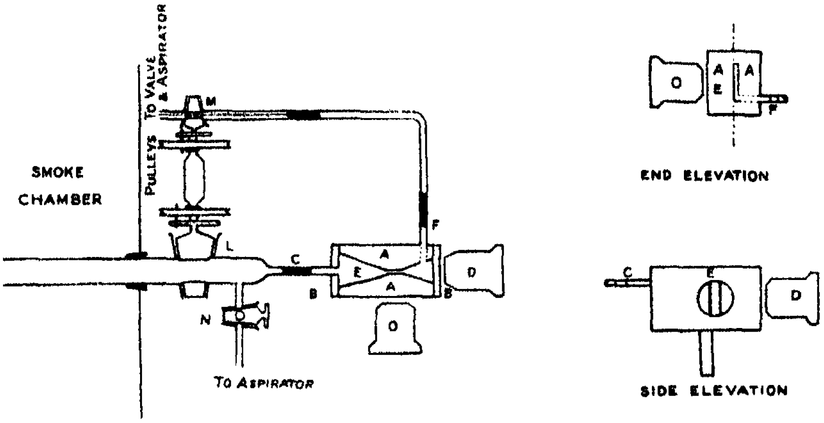

FIG. 1.

The illumination system consisted of a 5-ampere Zeiss automatic arc, with a water-cooled slit placed within 1 cm. of the carbons. A small condensing lens was placed immediately behind the slit, and the image of the anode was focussed on to the back of the illumination objective D, a 25-mm. Holos of N.A. 0·3. The light from this objective fell on to a slit in the brass case and so into the cell, being focussed into the space between the essential surfaces E, and completely filling it from side to side. Any light which struck the sides of the wedge was reflected internally in the cell, and was unable to pass into the viewing objective.

The observation microscope consisted of a 25-mm. Holos objective, stopped down to approximately N.A. 0·07, in combination with a series of × 10 eyepieces carrying square diaphragms of various sizes. The depth of focus of this combination was somewhat greater than the depth of the cell, and consequently both walls of the cell were held in focus, and there was no parallax. This is important; earlier counts with an objective of N.A. 0·3 gave irregular results with the larger diaphragms, which were traced to the fact that both walls of the cell were not completely in focus at once. That the system finally used suffered from no parallax was proved by substituting a micrometer scale for the cell, and moving it relatively to the microscope over a range of 0·1 mm., when the size of the diaphragm remained unchanged.

In the old method of counting the particles, a continuous slow stream of smoke was sucked through the cell, and the number of particles in each field was counted as it passed across the field of view. It will readily be understood that the correct estimation of the number of fields which contained no particles was difficult. By placing taps L and M (see fig. 1) on each side of the cell and rotating them in phase, however, it was possible to suck fresh quantities of smoke into the cell and count the number of particles in the fields obtained when the taps were closed. As it was essential that no particles should be lost in their passage from the smoke chamber to the cell, the tap L and tubing were made of 1 cm. internal bore. The tube projected 15 cm. into the tank, but the tap was almost flush with its side, and was then drawn off sharply to a jet of 2-mm. diameter, which was connected with the cell by a short length of rubber tubing. A T-piece carrying a small tap N served to flush out tap L and the leading tube with smoke before a fresh charge was admitted to the cell. The cell exit F was connected to the second rotating tap M, which was of fine-bore capillary, so that it opened and shut sharply. From this, connection was made to the aspirator through a fine needle valve, by means of which the flow of smoke through the cell when the taps were open could be delicately adjusted. It was found essential that all the connections between the taps L and M and the cell should be airtight and rigid, otherwise the particles in the field of view were not steady during the time the taps remained closed. The taps were rotated mechanically at the rate of 30 revolutions per minute by means of a geared-down electric motor, and were carefully synchronised.

In our first experiments it was found that particles which struck and adhered to the surfaces E appeared as bright spots of light which obscured the field. But by coating the cell walls with a thin film of quinoline these particles were rendered invisible. The quinoline was applied by sweeping down the surfaces with a swab of cotton-wool wrapped round the end of a thin glass rod and moistened with a mixture of dust-free redistilled quinoline and acetone. A fresh coating of quinoline had to be applied only after every six counts. Several other substances, such as immersion oil, were tried in place of quinoline, but none of them gave such a thin and stable film upon the glass.

The method of making a count was as follows: Taps L and N were opened and the tubes flushed out with smoke. N was then closed, M opened, and a slow stream of smoke sucked through the cell until all the air had been displaced. The needle valve was then closed down so that the particles appeared as streaks as they passed across the field of view. The motor was switched on, and the number of particles in each field obtained when the taps were closed was counted. Except during the early stages of a run, when the Brownian motion was considerable, the particles appeared as steady points of light and were easy to count. The average of 70 fields was taken for each point, and the time taken over each such count was approximately 1½ minutes. Within limits the speed of the motor was immaterial. The number of particles per c.c. of smoke at the mean time of counting could then be calculated from the depth of the cell, and the area viewed by the eyepiece. During the course of a run about 10 litres of smoke were sucked out of the chamber and replaced by dust-free air, which entered at a point remote from the intake tube for the cell.

The smokes were generated in an air-tight metal cistern of 0·87 cubic metre capacity, with two detachable glass windows. The internal arrangements were similar to those previously described,* and the air inside was kept dry and free from carbon dioxide by trays containing fused calcium chloride and soda lime.

Numerous clouds of various concentrations of ammonium chloride were investigated. The clouds were dispersed by heating a weighed amount of resublimed ammonium chloride in a porcelain boat; but in an effort to discover some method of quantitatively reproducing a cloud, various types of heater were tried. These were:—

---

* Whytlaw-Gray and Speakman, *loc. cit.*

1. A silica plate heated electrically by bare nichrome wire raised to red heat. 15 mgms. of ammonium chloride could be dispersed in one minute.

2. Two mica plates, placed horizontally one above the other at a distance of 2 cms., the boat being inserted between the two plates, which were wound with nichrome wire. In this case evaporation was extremely rapid, and 15 mgms. were dispersed in less than 30 seconds.

3. A small silica U-tube containing the heating coil inside and sealed so that no electrons could escape from the heated metal into the atmosphere around the boat. The smoke should therefore be formed in an atmosphere comparatively free from ions. The boat was of thin aluminium, resting across the arms of the U-tube. Sublimation of the chloride was slow, and two minutes were required for complete dispersal of 15 mgms.

The fan in the chamber was kept running for three minutes after the first appearance of smoke, in order to ensure complete homogeneity.

Results.

If the particulate volume, σ (*i.e.*, the reciprocal of the number of particles per cubic centimetre), or the volume containing a single particle, was plotted against the age of the cloud in minutes, t, a straight line was in all cases obtained. This is one of the predictions of Smoluchowski's theory of coagulation and will be discussed later. The coagulation was usually followed for about 120 mins. Straight lines have been obtained up to 250 mins., but counting became less accurate after two hours because of irregularities in the uniformity of the cloud, due to dilution and to settling out of the particles. In order to eliminate a personal error in counting, the counts were made by two observers taking alternate readings. The following table gives the results obtained during a typical run :—

Table I.—Run, LXVI.

Weight of ammonium chloride = 30 mgms. Heater, type II.
Cloud dispersed in 25 secs. Fanned for 3 minutes.

Time in minutes.	Average number per diaphragm.	Volume of smoke viewed, cu. cm.	No. per cubic centimetre $\times 10^{-6}$.	Particulate vol., cu. cm. $\sigma \times 10^{7}$.
				σ
6·0	2·67	$1 \cdot 576 \times 10^{-6}$	1·70	5·90
11·0	1·87	—	1·19	8·40
16·0	1·79	—	1·14	8·8
19·5	1·37	—	0·87	11·5
24·0	1·31	—	0·83	12·0
32·0	2·81	$4 \cdot 034 \times 10^{-6}$	0·694	14·4
36·5	2·40	—	0·595	16·8
42·5	2·49	—	0·617	16·2
48·0	1·97	—	0·488	20·5
60·5	1·56	—	0·388	25·8
67·0	1·49	—	0·369	27·1
72·0	1·44	—	0·357	28·0
79·0	1·43	—	0·355	28·2
83·0	2·20	$7 \cdot 373 \times 10^{-6}$	0·299	33·5
89·5	2·20	—	0·299	33·5
103·5	1·91	—	0·259	38·6
98·0	1·76	—	0·239	41·9

A graph of σ against time is shown in fig. 2.

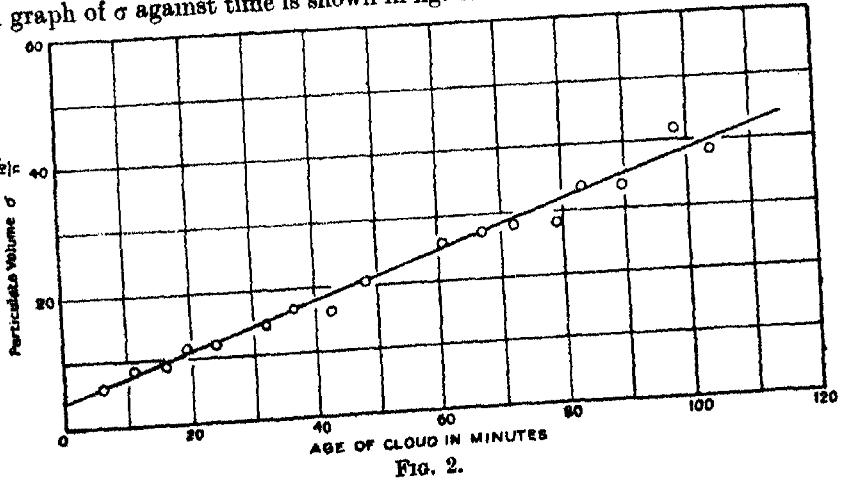

Fig. 2.

Owing to the intense Brownian motion of the particles in a freshly dispersed cloud, the accuracy of the counting was always less during the early stages of a run. The constants of the equation

$$\sigma = \sigma_0 + Kt \tag{1}$$

were, therefore, always calculated—by the method of least squares—from the points obtained with the larger diaphragms.

σ is the reciprocal of the number of particles at time t, σ_0 at the time of dispersal, and K is the coagulation constant of the cloud.

A few runs were also made with smokes of antipyrin and arsenious oxide, both prepared by sublimation, and with smokes of cadmium oxide prepared by striking an arc between two electrodes of the metal. In all cases straight-line graphs of σ against time were obtained. The experimental results are summarised in Table II, which gives the constants σ_0, n_0, and K of equation (1). The quantity δ is the initial number of particles per c.c. per mgm. of smoke dispersed. It will be seen that it is not constant, but that the values are more nearly constant if we compare the figures for each weight concentration. In general also the numbers obtained with the closed heater were smaller than those obtained when the smoke was formed in a highly ionised atmosphere such as that which would exist in the immediate vicinity of the red-hot elements of heaters 1 and 2.

Table II.

Run.	Wt. dispersed. mg.	Type heater.	$n_0 \times 10^{-6}$.	$\sigma \times 10^7$ cu. cm.	K c.c./min. $\times 10^8$.	$10^{-5}\,\delta$.	s.
			Ammonium Chloride.				
63	4·2	2	1·47	6·79	4·73	3·50	2·54
64	4·2	2	1·08	9·23	4·89	2·57	2·77
69	4·2	2	0·89	11·27	4·71	2·11	2·76
71	4·2	2	0·96	10·37	5·20	2·29	3·00
44	8·4	3	0·61	16·46	6·00	0·724	4·12
56	8·0	2	1·30	7·71	4·66	1·63	2·84
57	8·2	2	0·96	10·44	4·50	1·17	2·53
58	8·0	2	0·91	10·95	4·57	1·14	2·94
43	14·6	3	0·89	11·22	5·60	0·610	3·93
45	15·0	3	1·27	7·88	4·93	0·846	3·31
46	15·6	3	1·24	8·09	4·03	0·794	2·73
47	15·2	2	1·49	6·71	4·74	0·950	3·12
51	15·0	2	1·24	8·04	4·34	0·826	2·92
52	15·0	2	1·19	8·40	4·03	0·840	2·71
53	14·8	2	1·05	9·54	3·15	0·708	2·17
32	28·6	1	2·48	4·04	3·88	0·863	3·34
33	30·6	1	3·04	3·29	4·68	0·990	3·07
35	32·2	1	2·56	3·91	4·50	0·792	3·05
38	31·6	3	1·33	7·53	3·24	0·420	2·38
39	28·4	3	3·22	3·11	4·77	1·13	3·08
65	30·0	2	2·40	4·17	3·29	0·799	2·22
66	30·0	2	3·80	2·63	3·61	1·27	2·29
67	30·0	2	1·14	8·77	3·01	0·380	2·24
68	60·0	2	17·2	0·58	3·60	2·87	1·95
70	60·0	2	4·1	2·44	3·67	0·690	2·54
			Arsenious Oxide.				
19	78·6	1	1·92	5·20	4·40	0·244	3·10
			Antipyrin.				
54	40·0	2	4·60	2·17	3·86	1·15	2·57
55	40·0	2	2·02	4·91	3·01	5·20	2·23

Table II—(continued).

Cadmium Oxide.

The weight concentrations were unknown, but were of the order of 50 mg. Consequently only values of σ_0 and K can be calculated from the experimental results.

Run.	59	60	61	62	28	29	....
$n_0 \times 10^{-6}$ ...	1·36	3·44	6·54	1·44	1·15	1·04	...
$\sigma_0 \times 10^7$ ...	7·35	2·90	1·53	6·94	8·69	9·60	—
$K \times 10^8$ ...	5·10	5·30	5·50	3·96	5·20	4·60	—

Accuracy of Results.

One of the largest sources of error is due to averaging over so few particles; in general the numbers counted in 70 fields were between 100 and 200. If a larger number of fields were viewed, inaccuracies might arise due to settling of particles in the narrow leading tube of the cell, and if a larger diaphragm were used errors of observation would be magnified because of the difficulty of counting the particles in the large groups which occasionally appear. Errors in the calculation of the volume of smoke viewed may amount to 5 per cent., and actual errors in counting may be of the same magnitude. We do not think that our individual points have a greater accuracy than 10 per cent., but the value of the coagulation constant K has probably a higher accuracy. The error in the constant σ_0, the reciprocal of the initial number of particles, may be as great as 20 per cent., partly because of the error in determining the zero time itself, and partly because of the smaller accuracy of the counts during the first few minutes when a very small diaphragm was used, and the particles were in rapid Brownian motion. As already mentioned, these counts were neglected in calculating the equation to the lines, and consequently the errors due to extrapolation over a longer time-interval become magnified.

These errors concern only the particles which actually reached the field of view. There was certainly a slight loss of particles during the passage of the smoke from the chamber to this point, but, as the leading tube was wide, no serious error was introduced in this way. The numbers showed no tendency to fall off during a count of 70 fields, except when the taps were rotated very slowly, and the amount of smoke passed through the cell was very small. Usually about 10 c.c. were sucked through the cell during a count of 70 fields. A certain proportion of particles were lost by striking the walls of the cell at the narrow portion, but this was estimated to be only about 2 per cent. There was also the possibility of a slight leakage of air into the cell at the junction of the end plate B with the prisms AA, but this again would not lead to serious error. Taking the whole of the possible errors into account, it is believed that the actual numbers counted are not likely to be more than 10 per cent. too low, and this is offset slightly by the error of observation which lies on the side of counting too many particles. Nevertheless, this latter error was small because analyses of the numbers counted in 100 fields shows them to lie well on distribution curves.

It is to be noted that the initial numbers we have obtained are distinctly smaller than those given in the paper by Whytlaw-Gray and Speakman* for clouds of similar weight concentration, and it is obvious that the particulate number-time curves are of a different shape. We have been privileged to see some figures of Mr. H. L. Green (which will be published shortly), obtained by another method of counting, involving the use of the Aitken effect, which are in satisfactory agreement with our own. The concordance between these two independent methods indicates that there can be no serious error in our numbers.

The Theory of Smoluchowski.

On the assumption that the particles in a colloidal solution unite when they approach within a definite distance of each other not much greater than twice their radius, Smoluchowski has shown that coagulation can be formulated in terms of diffusion. If all the particles are initially of the same size, the total number present at any time can be expressed by a simple equation similar to the bimolecular equation of chemical kinetics. If n is the total number of particles present at time t and n_0 the initial number, then

$$n = \frac{n_0}{1 + n_0 \mathrm{K} t}, \tag{2}$$

where K should be a constant if certain simplifying assumptions are made. This equation has been experimentally verified for colloidal solutions by many workers.†

If we assume that the mechanism of coagulation in smokes is similar, the same equation should be valid and a linear relationship should be obtained when the particulate volumes are plotted against the time, for equation (2), when rearranged, becomes the same as equation (1). The theory of Smoluchowski predicts, therefore, the correct form of the coagulation curve for smokes.

---

* *Loc. cit.*

† Zsigmondy, Westgren, Kruyt, Tuorila, *loc. cit.*

The constant K is given by the formula

$$\mathrm{K} = 4\pi \mathrm{DS}, \tag{3}$$

where D is the diffusion constant of Einstein and S is the radius of the sphere of action of the particles initially. Einstein's equation for D is

$$\mathrm{D} = \mathrm{RT} \,.\, \mathrm{B}/\mathrm{N}, \tag{4}$$

where N is the Avogadro number and B is the mobility. For colloidal solutions we may assume that the mobility is given, to a first approximation, by Stokes's equation, so that

$$\mathrm{D} = \frac{\mathrm{RT}}{\mathrm{N}} \cdot \frac{1}{6\pi\eta r}, \tag{5}$$

where r is the radius of the particles and η the viscosity of the medium. If we write $\mathrm{S} = sr$, equation (3) becomes

$$\mathrm{K} = \frac{2}{3} \cdot \frac{\mathrm{RT}}{\mathrm{N}} \cdot \frac{s}{\eta}. \tag{6}$$

If now the sphere of influence is always the same for a given smoke, *i.e.*, if s is a constant, K should always have the same value. Actually, as inspection of Table II will show, K is not a constant, but varies from cloud to cloud. The same is true also of hydrosols.

At first sight it would seem possible that this may be due to the fact that in smokes the size of the particles is comparable with the mean free path of the molecules of the medium, so that the mobility cannot be deduced from Stokes's law. If we substitute the Stokes-Cunningham expression for the mobility, namely,

$$\mathrm{B} = (1 + \mathrm{A}\lambda/r)/6n\eta r,$$

where λ is the mean free path and A is a constant, we obtain

$$\mathrm{K} = \frac{2}{3} \cdot \frac{\mathrm{RT}}{\mathrm{N}\eta}(1 + \mathrm{A}\lambda/r)s. \tag{7}$$

In this case it is evident that K is no longer a constant, but becomes smaller as the average size of the particles increases. Using Millikan's value for A, $\mathrm{A}\lambda = 9 \times 10^{-6}$, and putting $\mathrm{R} = 8{\cdot}3 \times 10^{7}$, $\mathrm{N} = 6{\cdot}1 \times 10^{23}$, $\mathrm{T} = 293$, $\eta = 1{\cdot}82 \times 10^{-4}$, and reckoning time in minutes, we find that

$$\mathrm{K} = 8{\cdot}76 \times 10^{-9}(1 + 9 \times 10^{-6} \,.\, r^{-1})\, s \text{ cms.}^3/\text{min.} \tag{8}$$

Values of s, the ratio of the radius of the sphere of action to the initial radius of the particles calculated from this equation, are given in Table II, the values of r being calculated from the weight of the particles and the density* of the dispersed substance in the solid state. It will be seen that the values of s are far from constant, but, nevertheless, lie in groups for each weight concentration. The most consistent results were obtained when the cloud was dispersed from the open heater, type II, probably because dispersal was accomplished more rapidly. That the Stokes-Cunningham expression gives a slightly better representation of the curves is shown by the fact that the rate of coagulation is generally greater the smaller the initial size of particles. On the other hand, the curves for σ do not show the curvature predicted by the equation, but this may be due to the error introduced by the settling out of the particles, which tends to make the experimentally found values of σ too large. The curvature to be expected is small in all cases.

---

* The density of antipyrin was found to be 1·18 at 18° C.

A possible explanation of the lack of constancy of the values of s and of their high value, approximately 3 instead of 2, is that the particles are charged electrically, both positively and negatively; but until more reliable data on this branch of the subject are available, it is not possible to test this hypothesis. It is also possible that the weight concentrations themselves might be in error, due to incomplete dispersal of the heated substance into a fine particulate state; but calculation shows that the values are not greatly altered even if only half of the material weighed out was present as smoke. Thus, for run 47, where the weight concentration was 15 mgm., and the value of s 3·12, the latter is only lowered to 2·83 on the assumption that the actual weight of solid in the smoke was 7·5 mgm. Again, in calculating the radius of the particles, the densities of the substances have been taken as those of the material in bulk; but if we were to use a lower density, such as has been found by us* for cadmium oxide particles, the values of s obtained would be even greater. Assuming a normal density of cadmium oxide, and a weight concentration of 50 mgm, the average value for s for the clouds given in Table II is approximately 2·8.

Finally, it must be remembered that Smoluchowski derived his equation on the assumption that the particles are spherical and coagulate to spherical aggregates. Actually, it has been shown* that such is not the case for particles of cadmium oxide, which form chains of smaller particles. The particles of ammonium chloride appear in the ultramicroscope to be loose but apparently spherical aggregates, whilst those of antipyrin, by their brightness, appear to be liquid. If this is so, spherical particles would be formed on coagulation. We hope at some later date to make a further study of this substance and of substances which are known to yield liquid particles, such as heavy paraffin.

---

* Patterson and Whytlaw-Gray, 'Roy. Soc. Proc.,' A, vol. 113, p. 302 (1926).

In conclusion, we must express our thanks to Professor Conrady for valuable advice on the optical and illuminating system we have employed.

Summary.

1. The slit ultramicroscope has been criticised as an instrument for determining the number of particles in a smoke.

2. A special cell has been designed for counting smoke particles and has been shown to give reliable results.

3. The coagulation of clouds of ammonium chloride, antipyrin and cadmium oxide has been studied and has been shown to obey the same general law, which is probably valid for all smokes composed of non-volatile particles.

4. The experimental data agree as closely as those obtained for sols with the theory of Smoluchowski.

Investigations of the Molecular Arrangement of Uniaxial Optically Active Crystals.

By W. G. Burgers (Ramsay Memorial Fellow).

(Communicated by Sir William Bragg, F.R.S.—Received July 15, 1927.)

The present paper deals with the X-ray investigation of certain optically active uniaxial crystals. The investigation was undertaken for several reasons. In the first place it was hoped to obtain evidence on the disputed question as to whether their optical activity must be ascribed to pseudo-symmetrical intergrowths of biaxial lamellæ (their rotatory power thus being produced in a similar way as that exhibited by definite spiral piles of thin mica plates) or whether special arrangements of the atoms within the unit cells proved to be present in the structures of such crystals. It was therefore necessary to discuss in how far X-rays are able to reveal the presence and the true nature of a lamellar structure. The cases of both relatively large lamellæ and of lamellæ which are too small to give individual X-ray reflections must be discussed. The latter case has been dealt with especially in connection with recent statements of G. Friedel* with regard to the value of X-ray analysis of structures of this type. The crystals discussed in this paper have been investigated with particular reference to this difficulty. The conclusions arrived at are given in the Summary at the end of the paper. They suggest that the rotatory power of the crystals is really due to some special arrangement of atoms within a unit of structure. For the crystals investigated these arrangements have been considered more in detail. The principal points discussed are put together in the Summary.

---

* 'Leçons de Cristallographie,' Paris (1926); 'C. R.,' vol. 182, p. 741 (1926).

THEORETICAL.

I.—Since von Reusch[*] showed that definite spiral piles of thin mica plates exhibit the property of rotating the plane of polarisation of light waves, optically active crystals have in many cases been considered as mimetic forms, being in fact pseudo-symmetrical intergrowths of biaxial lamellæ. The theory of the optical behaviour of piles of such lamellæ was worked out by Mallard[†] and Sohncke[‡] for different types of piles. In their view the theory could be extended to lamellæ of "molecular"-thickness, thus offering an explanation of the phenomena in both pseudo-symmetrical and true uniaxial crystals. Sohncke especially deduced which of his 65 point-groups could represent optically active crystals, each point-group being considered as a pile of lamellæ, arranged in such a way that the symmetry of the whole corresponded to that of the point-group under consideration.

The determination of the presence or absence of a lamellar structure in the case of an active crystal is therefore essential to the explanation of its rotatory power.

Several crystallographers, especially Wyrouboff,[§] were convinced supporters of the lamellar theory. Wyrouboff even considered a pseudo-symmetrical structure far more probable than a structure in which all molecules were arranged in such a beautifully regular way as is necessary for a true uniaxial crystal.[||]

There seems to be little doubt that in several cases optical activity is caused by lamellar growth. A well-known example of this kind is ammonium lithium sulphate. Crystals of this substance were observed by Wyrouboff,[¶] which consisted of pseudo-hexagonal orthorhombic sections, the principal directions of which made angles of 60° with each other. Those parts of the crystals where different lamellæ overlapped were more or less uniaxial and exhibited rotatory power. Another example of this kind is trans-camphortricarboxylic acid, $C_{10}H_{14}O_6$, investigated by Pope.*

---

[*] 'Pogg. Ann. d. Physik,' vol. 138, p. 628 (1869).

[†] 'Traité de Cristallographie," vol. II (1884).

[‡] 'Pogg. Ann.,' vol. 8, p. 16 (1878); 'Z. f. Krist.,' vol. 19, p. 530 (1891); vol. 25, p. 530 (1896). The problem was also treated by Prof. H. A. Lorentz in 1905. See F. M. Jaeger, 'Principe de Symmétrie,' p. 216 (1925).

[§] 'Ann. Chim. Phys.,' vol. 8, p. 340 (1886).

[||] *Loc. cit*, p. 349.

[¶] 'Bull. Soc. fr. Min.,' vol. 13, p. 215 (1890).

With regard to other substances, however, the views of different authors do not agree. This is, for example, the case with the optically active crystals of sodium periodate, ethylenediamine sulphate and guanidine carbonate. Wyrouboff† considered these crystals as pseudo-symmetric. He founded this opinion on a study of the anomalous character of their optical properties. Brauns‡ and Martin,§ on the contrary, considered the observed anomalies as consequences of internal strains, which may be due to several causes, such as skeletal growth (Martin), loss of water of crystallisation, and so on.

Similarly differences of opinion are found with regard to quartz,‖ benzil,¶ potassium lithium sulphate,** and other substances.

On account of the fact that optical investigations have led to different conceptions about the constitution of optically active uniaxial crystals, it is worth while to see how far X-rays are able to reveal the true nature of such crystals. In order to do this we must distinguish between two possibilities with regard to the size of the lamellæ.

(*a*) They are so large ($> 10^{-6}$ cm.)†† that the X-ray diffraction effect of the whole structure may be considered as a superposition of the effects due to the individual lamellæ.

(*b*) They are exceedingly small and involve only a relatively small number of unit-cells each.

These two possibilities must be considered in connection with the experimental results which show that all the uniaxial crystals investigated so far give X-ray diffraction effects such as would be expected from true single crystals.‡‡

On account of this fact the presence of case (*a*) requires that the geometrical pseudo-symmetry of the *lattice*, which underlies the twin-structure, is so pronounced that, on oscillation photographs about various crystallographic directions, spots due to different lamellæ either coincide or lie on the same (or intermediate) hyperbolæ. We may expect this, for example, for a twin-structure such as is represented in fig. 1. In this case pseudo-hexagonal orthorhombic lamellæ built upon the base-centered orthorhombic lattice Γ'_0 twin on {110} (the *c*-axis is vertical for all the lamellæ). The original lattice cell underlies the whole structure (disregarding its contents and possible irregularities introduced at the twin boundaries).

---

* 'Z. f. Krist.,' vol. 27, p. 408 (1896).

† 'Ann. Chim. Phys.,' vol. 8, pp. 367, 394 (1886); 'Bull. Soc. fr. Min.,' vol. 29, p. 351 (1906).

‡ 'Die optischen Anomalien,' pp. 200 and 156 (1891).

§ 'N. Jahrb. f. Min., Beil.,' vol. 7, p. 26 (1891).

‖ See, *e.g.*, Tutton, 'Crystallography,' vol. 2, p. 1266 (1922), and G. Friedel, 'C. R.,' vol. 182, p. 741 (1926).

¶ Wyrouboff, 'Ann. Chim. Phys.,' *loc. cit.*, p. 369.

** Wyrouboff, 'Bull. Soc. fr. Min.,' vol. 13, p. 215 (1890); H. Traube, 'Neues Jhrb. f. Min.,' vol. 1, p. 171 (1894).

†† G. L. Clark, 'Applied X-Rays,' p. 181.

‡‡ With the exception of irregularities observed in the symmetry of Laue photographs in some cases (F. M. Jaeger, *loc. cit.*, p. 225).

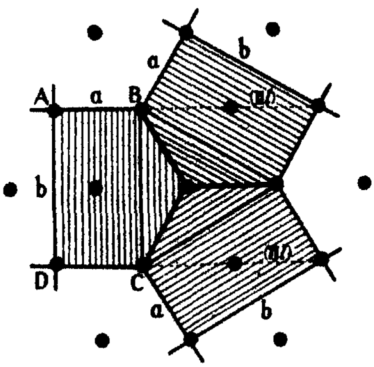

Fig. 1.

Another example would be realised if an orthorhombic or monoclinic crystal, built upon a pseudo-tetragonal lattice, twinned in such a way that the different lamellæ occupied perpendicular orientations with regard to each other.*

In such cases, if doubt exists with regard to the true crystal symmetry (ethylenediamine sulphate, etc.), the values calculated for periodicities and spacings have to be critically considered, and in particular attention must be paid to the determination of abnormal spacings. Indeed, a halving of a definite plane may remain unobserved on account of the fact that planes with different indices (belonging to different lamellæ) may occupy parallel positions and therefore reflect in the same direction. Thus, for example, in the twin structure represented in fig. 1, the (0*kl*) planes of one set of lamellæ coincide with the ($\frac{1}{2}k$ $\frac{1}{2}k$ l) planes of the other sets (for example, 01*l* with $\frac{1}{2}$ $\frac{1}{2}$ *l*; 02*l* with 11*l*).

Let us assume that the space-group underlying the orthorhombic lamellæ is C_{2v}^{12}. The abnormal spacings are† :—

{*hkl*} halved if $(h + k)$ is odd.

All (0*kl*) halved.

The first set of (general) halvings, due to the base-centering of the orthorhombic lattice, is not affected by the twinning because the distribution of *lattice-points*

---

[*] Compare, *e.g.*, pseudo-tetragonal crystals of monoclinic potassium ferrocyanide, K_4FeCy_6, for which $\beta = 90° 1'$, and $a : b : c = 0\cdot3947 : 1 : 0\cdot3983$, they twin frequently in a similar way (Brauns, *loc. cit.*, p. 58; Jaeger, *loc. cit.*, p. 220).

[†] Astbury and Yardley, 'Phil. Trans.,' A, vol. 224, p. 233 (1924).

remains the same if we pass from one lamella to another. Of the halvings of the second set we shall observe only that of {001} and those which are already included in the first set. The remaining halvings, namely, those for which k is even, will not be observed on account of the first order reflections of $(\frac{1}{2}k\ \frac{1}{2}k\ l)$ planes (compare for example the {021} and {111} planes in two different lamellæ).

It is, however, possible for the presence of one or more special halvings to be decisive in certain cases, for instance in the crystals of ethylenediamine sulphate and guanidine carbonate, which have been investigated in this paper. It is shown (see experimental part) that these crystals are not built up of lamellæ of the size we are now considering, but that they are either truly tetragonal or belong to class (*b*), which we shall discuss later on.

As will be clear from the experimental part, the decision with regard to the first point rests finally on the *quartering* of the *c*-plane. If, instead of being quartered, this plane had been halved, then the argument, based on the *directions* of the diffraction effects only, would have been inconclusive.

Similar criteria are possible in the hexagonal and trigonal systems. The fact that the spacing of the basal plane in the crystals of sodium periodate $NaIO_4 . 3H_2O$ and potassium rhodium oxalate $K_3[Rh(C_2O_2O_2)_3] + 1H_2O$ is equal to *one-third* of the observed translation parallel to the *c*-axis is a strong argument against a structure of lamellæ of type (*a*). The reasoning followed in the case of the tetragonal crystals (see experimental part) seems even superfluous here. Indeed, optically active piles of thin mica plates are constructed in such a way that the plates all lie with the basal plane horizontal, successive plates occupying different orientations only with regard to horizontal axes of reference. Therefore it is highly probable on account of the optical activity of the crystals that their basal plane corresponds to the same plane in all the lamellæ, unless the twinning is of a more complicated character. The thirding of a plane in orthorhombic, monoclinic and triclinic crystals is, however, improbable. It can only be accidental, because the abnormal spacings required by space-group properties for crystals of these systems are either halvings or quarterings.

On the other hand, on considering crystals of potassium lithium sulphate, $KLiSO_4$, we notice that with regard to X-rays they behave as true hexagonal crystals built upon the hexagonal lattice Γ_h, with the *halving* (not thirding) of the basal plane as only abnormal spacing.* From the point of view of X-ray analysis alone and without detailed intensity investigations it is difficult to decide as to the absence or presence of, for example, orthorhombic lamellæ

---

* A. J. Bradley, 'Phil. Mag.,' vol. 49, p. 1225 (1925).

(compare fig. 1 and also p. 556). Of course such an ambiguity includes marked pseudo-hexagonal shape in the cells of the latter. This condition is fulfilled in the two crystals mentioned in the beginning of this paper, one of which, NH_4LiSO_4, is closely related to the substance under discussion. For a crystal of this kind the final decision must be made from intensity considerations.

The question of the absence or presence of lamellæ is of particular interest in this substance on account of the fact that its structure, as revealed by X-rays on the assumption that the crystals are really hexagonal, takes a rather exceptional place among optically active crystals (see p. 568). The point of view that the crystals are lamellar was defended by Wyrouboff.* The fact that the rotatory power was different for different crystals, and that for a definite crystal the rotation was not always proportional to its thickness, and not even constant in different places of the same crystal plate, was explained by Traube† as a consequence of different kinds and various degrees of twinning of left- and right-handed crystals. This was deduced from a study of etch figures and pyroelectric properties. Wulf,‡ who discovered their rotatory power and who observed Airy-spirals in them, states that all the crystals investigated by him (which are described as really magnificent) showed considerable differences ($\pm\frac{1}{2}°$) in the angles in the vertical zone and in the parallelism of the planes.

We must now consider the possibility of case (*b*), *i.e.*, crystals in which the successive lamellæ are individually too small to give separate X-ray reflections. It is especially on account of such structures ("pseudo-paramorphic") that G. Friedel§ is dissatisfied with the results of X-ray analysis.

Friedel's arguments are based on the experimental fact that the faces of the different components of a twin crystal can be deduced, within a certain degree of accuracy, from one and the same primitive form. It is therefore assumed by this author ('Leçons de Cristallographie,' p. 426) that in a twin crystal we can pick out a lattice-cell which, disregarding its contents, propagates itself in a more or less rigorous way throughout the whole structure. This cell may be either simple or a *multiple* of the original lattice-unit. Fig. 1 (cell ABCD) represents the simpler case; fig. 2 a more complicated case. This latter figure shows an imaginary twinning of monoclinic cells (for example PQRS) on {100} (= PQ or AB). If, for a moment, we assume that fig. 2 could represent a twin structure of the black circles only, then this structure would be only periodic (or quasi-periodic) with regard to a certain number of special points, namely, the corners

---

* 'Bull. Soc. fr. Min.,' vol. 13, p. 224 (1890).

† 'Neues Jhrb. f. Min.,' 1892, vol. II, p. 58; 1894, vol. I, p. 171.

‡ 'Z. f. Krist.,' vol. 17, p. 595 (1890).

§ 'Leçons de Cristallographie' (Paris, 1926), pp. 392 to 398; see also 'C. R.,' vol. 182, p. 741 (1926).

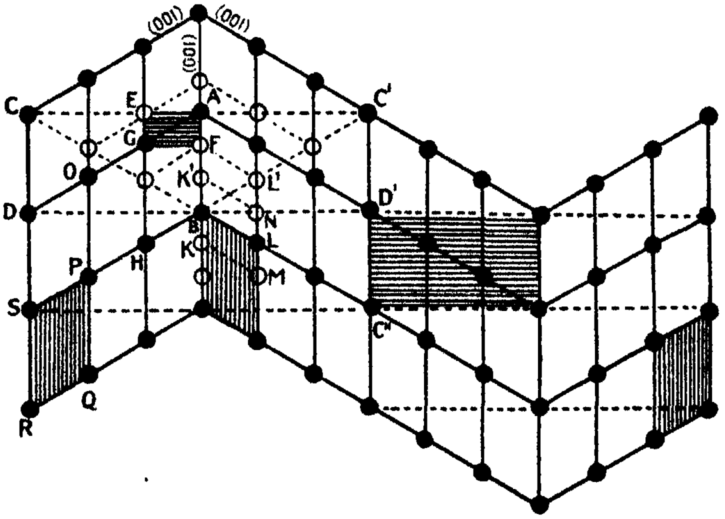

FIG. 2.

of the lattice cell ABCD. The contents of these cells, however, occupy different orientations in the individual lamellæ (*cf.* the diagonals AD and AD′). Similar conditions hold for the contents of the cells ABCD in fig. 1.

The sharp photographs of the pseudo-paramorphic crystals are due, according to Friedel, to the presence of these pseudo-lattice-units ABCD (*cf.*, *loc. cit.*, p. 397), and they may be expected only if the individual size of the lamellæ is smaller than a certain minimum ; in which case the periodicities peculiar to each lamella individually will not be revealed separately,* but the values observed for them will lie between those of the separate lamellæ, just as is shown by photographs of mixed crystals.† Friedel fears, therefore, that the structure arrived at will have an "illusory" value, both because it relates to a unit which may be a multiple of the real unit and because the value of the individual periodicities cannot be found.

With regard to this conclusion it cannot be denied that certainly such micro-twin-structures would offer considerable difficulties in the determination of the true symmetry of the underlying lamellæ. But it seems probable that the danger of the X-ray analyst coming to a totally wrong conclusion is less than Friedel supposes.

---

* In general the periodicity of points corresponding to ABCD in figs. 1 and 2 will not be mathematically exact as in the ideal cases of the figures.

† Friedel's conception of mixed crystals (' C. R.,' *loc. cit.*) differs in several points from that advanced by Vegard and Schjelderup (see, *e.g.*, ' Z. f. Physik,' vol. 42, p. 1 (1927)). However, whatever the true facts of the case, the observed periodicities cannot be far from the individual ones (see especially Vegard, ' Z. f. Physik,' vol. 5, p. 17 (1921)).

It is natural to attribute the fact that sharp single-crystal X-ray diffraction effects are observed to the presence of a unit of structure which underlies, in a more or less rigorous way, the whole pseudo-paramorphic crystal. It seems, however, probable that the smallest unit deduced from the photographs will correspond, if not to the true unit of the lamellæ, then to some *sub-multiple* of it, *not to a multiple.*

Indeed, the twinning of a crystal is based on the fact that, at a certain stage of its growth, the constituent atomic groups may take up two or more positions of equilibrium which are quasi-equivalent (see especially Friedel, *loc. cit.*, p. 422). One of these positions corresponds to the continuation of the homogeneous crystal, the others to the formation of twins. The possibility of the twinning must, therefore, be connected with a definite pseudo-symmetrical character of the structure of the untwinned crystal. This feature is only partly expressed in the already-mentioned fact that the faces of a twin crystal can be deduced from one and the same primitive form (*cf.*, fig. 2, cell ABCD). It seems, however, reasonable to assume that *in cases where twinning occurs in every few unit-cells* (" pseudo-paramorphic crystals ") the cause of the twinning must be due to very pronounced pseudo-symmetrical relations in the immediate neighbourhood of such a point as B. If, again, fig. 2 (black circles only) is supposed to represent a case of very frequent twinning, then the directions B→ C′ and B→ C″ represent directions of growth of nearly equal probability. We may expect that a group similar to that at L is present somewhere near at L′ (open circle), both groups occupying symmetrical or pseudo-symmetrical positions with regard to DD′. If this is true, then, on account of the periodicities of the monoclinic lattice, such groups are present near at, for example, F, K, M, etc., and possibly again, because of the nearly equal probability of BC′ and BC″ as directions of growth, a similar group near at K′, N, and so on.

It can be easily seen that in the resulting structure all points of a lattice built upon the pseudo-unit AEGF are occupied by more or less identical groups (only a few of them are indicated in the figure). If sharp photographs are obtained, then they will arise from the presence of this pseudo-unit AEGF,* and the analysis of the photographs will give its structure. Although it is possible that the periodicities calculated for this sub-unit are intermediate ones (as in an ordinary mixed crystal), this is not a serious objection, for the X-ray analysis leads to a structure for the contents of the small cell, which is, with only slight distortions, repeated throughout the whole twin. For many of the conclusions to be drawn from this structure, the *exact* size of the true cell and the *exact* orientation of the atomic groups is immaterial.

---

* Moreover, if the smallest unit deduced from the photographs corresponded to some *multiple* of the real cell of the untwinned crystal (*cf.* ABCD in fig. 2), it seems not unlikely that the presence of *lattice-points* inside this unit (*cf.* G, O) would betray itself by the occurrence of a number of abnormal spacings (better : abnormal *mean*-spacings, on account of what is said on page 559) of general planes.

This general argument applies to the whole phenomenon of repeated twinning. It can, for example, be applied to the pseudo-paramorphic structure shown in fig. 1, if the distribution of scattering centres in the original lattice-cells is similar in directions which make angles of 60° with each other.* This means that the structure is very nearly trigonal or hexagonal. And, of course, this is what one would expect if such a twinning occurs so frequently as it is here assumed.

Finally, we come to the following conclusion: We may safely assume that the uniaxial optically active crystals investigated by X-rays up to the present, with the possible exception of potassium lithium sulphate, are not built up of relatively large lamellæ (case (*a*)) of very pronounced pseudo-symmetrical character with regard to the geometrical properties of their underlying lattices. The structure deduced from their "single crystal" diffraction effects is then either that of a true uniaxial crystal, or it refers to a "pseudo-unit" of the nature ascribed above. Conclusions drawn from this structure with regard to a possible spiral arrangement of successive molecules will in all probability be valid even if the true unit-cell is a (more or less approximate) multiple of this sub-unit. Therefore, with regard to this point we may as well consider the crystals as uniaxial and their optical activity due to the arrangement and properties of the crystal molecules themselves. This point of view is adopted in the following discussion.

II.—The connection between optical activity and a spiral arrangement of the atoms (molecules, ions) in crystals has often, after Sohncke, been discussed by several authors.† Oseen,‡ in his mathematical treatment of the rotation of the plane of polarisation, showed that in general optical activity is to be expected for such arrangements.§ It seems therefore natural to conclude* that optically active uniaxial crystals are built upon space-groups which possess screw-axes. This is really the case with the crystals investigated by X-rays up to the present. They are collected in Table I, together with those which are dealt with in this paper. The fifth column shows the presence of screw-axes in all of them. With regard to these results there are several points which are worth mentioning.

---

* Compare the twinning of aragonite, Bragg, 'Roy. Soc. Proc.,' A, vol. 105, p. 16 (1924).

† See, *e.g.*, Barlow, 'Z. f. Krist.,' vol. 27, p. 473 (1896); Larmor, 'Roy. Soc. Proc.,' A, vol. 99, p. 1 (1921); Tutton, 'Crystallography,' vol. 2, p. 1272.

‡ 'Ann. d. Physik,' vol. 48, p. 1 (1915).

§ A phenomenon closely analogous to the rotation of the plane of polarised light was demonstrated by K. F. Lindman ('Ann. d. Physik,' vol. 74, p. 541 (1924)), who showed that the plane of polarisation of electro-magnetic waves was rotated by a spiral arrangement of isolated spherical metal-resonators.

Table I.

Substance.	Crystal class.	Space group.	Bravais lattice.	Screw axis parallel to opt. axis.	Investigated by
Sodium periodate .... $NaIO_4 \cdot 3H_2O$.	Trigonal pyramidal	C_3^4	Γ_{rh}	▲ ▲	—
Quartz .... SiO_2	Trigonal trapezohedral	D_3^4 (D_3^6)	Γ_h	▲	Bragg and Gibbs.*
Cinnabar .... HgS	Trigonal trapezohedral	D_3^4 (D_3^6)	Γ_h	▲	Mauguin Buckley and Vernon.†
Benzil	Trigonal trapezohedral	D_3^4 (D_3^6)	Γ_h	▲	Allen.‡
Potassium rhodium oxalate .... $K_3[Rh(C_2O_2O_2)_3] \cdot 1H_2O$	Trigonal trapezohedral	D_3^4 (D_3^6)	Γ_h	▲	—
Lithium potassium sulphate .... $KLiSO_4$	Hexagonal pyramidal	C_6^6	Γ_h	⬢ ⬬	Bradley.§
Iodosuccinimide	Tetragonal pyramidal	C_4^3 (C_4^4)	Γ_t	◆ ⬬	Yardley.¶
Guanidine carbonate	Tetragonal trapezohedral	D_4^4 (D_4^8)	Γ_t	◆ ⬬	—
Ethylene-diamine sulphate	Tetragonal trapezohedral	D_4^4 (D_4^8)	Γ_t	◆ ⬬	—

* 'Roy. Soc. Proc.,' A, vol. 109, p. 405 (1925).
† 'C. R.', vol. 176, p. 1483 (1923); 'Min. Mag.', vol. 20, p. 382 (1925).
‡ 'Phil. Mag.', vol. 3, p. 1037 (1927).
§ 'Phil. Mag.', vol. 49, p. 1225 (1925).
¶ 'Roy. Soc. Proc.,' A, vol. 108, p. 542 (1925).

---

* H. Hilton, 'Mathematical Crystallography,' p. 257 (1903).

Quartz, cinnabar and benzil are built upon space-groups for which Sohncke already deduced optical rotatory power (alternating three point screw-system), comparing them to a pile of mica lamellæ rotated through 120° with regard to each other.

The same is true for potassium rhodium oxalate. This salt, which was described and investigated by F. M. Jaeger,* is the only one of the substances mentioned which gives optically active solutions. The crystals of such a substance would be expected to exhibit rotatory power even though the underlying space-group did not possess screw-axes.

The question arises if the absence or presence of screw-axes in the crystals can be detected by an investigation of their rotatory power. For this purpose it is not trustworthy to compare the absolute values of [α] and [ρ]† for a definite wave-length. Indeed, even if the solvent had no influence on the rotatory power of the substance in question, there remains the fact that in a solution the molecules have all possible orientations with regard to the incident light vibrations, whereas in the crystal the molecules occupy a limited number of orientations and a certain definite distribution. Therefore a dependence of the rotatory power of a molecule on its orientation may already be the cause of a difference between [ρ] and [α], as has been pointed out especially by Longchambon.‡ This author showed at the same time§ that for a number of substances the rotatory *dispersion* is the same in the crystalline and in the dissolved state ($\alpha_{\lambda_1} : \alpha_{\lambda_2} : \ldots = \rho_{\lambda_1} : \rho_{\lambda_2} : \ldots$), so that at least for the substances investigated, the rotatory *dispersion* of the molecules seems to be independent of their orientation.

The equality of the two dispersions might be accounted for by the absence of structure rotation.|| This is, of course, not a necessary condition.¶

On the other hand, it seems not unlikely that (in special cases) a "spiral arrangement" in the crystal may influence the rotatory dispersion. For example, the difference in dispersion between crystalline tartaric acid and its dilute solution is accounted for in a comparable way if we accept Astbury's**

---

[*] 'Rec. Trav. Chim. Pays-Bas,' vol. 38, p. 262 (1920).

[†] [α] = rotation per d.M. of a solution containing .1 gram of the active substance per centimetre; [ρ] = rotation of a crystal plate of 10/*d* cm. thickness (*d* is the density of the crystal).

[‡] 'Thèses,' Paris, p. 87 (1923); 'C. R.,' vol. 173, p. 89 (1921).

[§] Longchambon, *loc. cit.*, pp. 88 to 90; 'C. R.,' vol. 175, p. 174 (1922).

[||] This expression is generally used to denote the rotation due to some special dissymmetric arrangement in the crystalline state.

[¶] Longchambon, *loc. cit.*, p. 90.

[**] Astbury, 'Roy. Soc. Proc.,' A, vol. 102, p. 506 (1923).

structure of the crystals of this substance. In this case, however, a special spiral is introduced in the crystal as a consequence of the difference between the crystal molecule and the chemical molecule, and not by the arrangement itself of the crystal molecules.

The rotatory dispersion curve of potassium rhodium oxalate has been measured for aqueous solutions containing from 0·5 to 11 per cent. anhydrous salt by Jaeger,[*] and is shown in fig. 3, curve I. For wave-lengths shorter than $\lambda =$ 5970 the solution is dextrorotatory, whereas it is lævorotatory for greater values of λ. Longchambon[†] has remeasured the same dispersion for a very dilute solution (0·065 per cent.), curve II,[‡] and also the rotatory power and dispersion of the crystals. Curve III gives the values for $[\rho]$ deduced from his

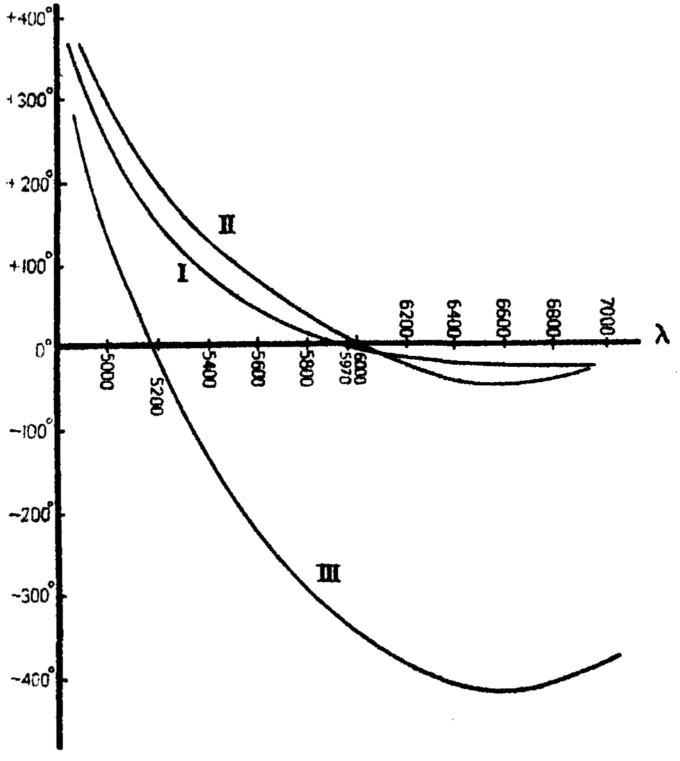

FIG. 3.—Rotatory Dispersion of $d-K_3[Rh(C_2O_2O_2)_3] + 1H_2O$.
I. Aqueous Solution $[\alpha]$ (Jaeger). II. Aqueous Solution $[\alpha]$ (Longchambon). III. Crystal $[\rho]$ (Longchambon).

---

[*] *Loc. cit.*, p. 262.

[†] 'C. R.,' vol. 178, p. 1828 (1924).

[‡] One value (for $\lambda = 5000$) does not fit on the curve.

figures. The curves for [α] and [ρ] have a similar appearance; only $\lambda_{[\rho=0]}$ is shorter than $\lambda_{[\alpha=0]}$. As Longchambon states, the shift of the rotatory dispersion curve by transition from solution to crystal can be explained by assuming that in the crystal a left-handed rotation is superimposed on the rotation of the molecules. He rejects this explanation on the following grounds: The crystals of $K_3[Rh(C_2O_2O_2)_3]$ belong to the trigonal trapezohedral class like quartz. They have indeed a great resemblance to quartz crystals. The symmetry of this class, one trigonal axis perpendicular to three dyad axes, is also ascribed to the complex ion $[Rh(C_2O_2O_2)_3]$, according to Jaeger.* Therefore Longchambon concluded from the similar appearance of the two dispersion curves and the resemblance between ion- and crystal-symmetry that the crystal molecules were probably all parallel. In that case a structure rotation is not expected, and this would explain the similarity of the two curves. The shift of the zero point was accounted for by the molecular anisotropy which shows its influence as a consequence of the definite orientations of the ions in the crystalline state.

Now the parallel orientation of all ions would be possible only if there was one ion per unit-cell. This ion would then possess the full D_3 symmetry. This would be possible if the space-group of the crystal was D_3^1, D_3^2 or D_3^7. The present X-ray investigation shows, however, that the space-group is D_3^4 (or D_3^6) and that the hexagonal unit-cell contains six molecules. This space-group possesses a three-fold screw-axis. A group of two ions $[Rh(C_2O_2O_2)_3]^{---}$, possessing a dyad axis, can be compared with the group SiO_2 in quartz. These groups are arranged in spirals round the vertical axes. A definite spiral arrangement is present in the structure of the crystals (see fig. 4, which shows the general positions of the equivalent points) which certainly would produce optical activity even if the ions were inactive. The suggestion that the shift in the rotatory dispersion curve on transition from solution to crystal is wholely or partly due to the screw-axes in the latter can therefore not be rejected on the grounds advanced by Longchambon.

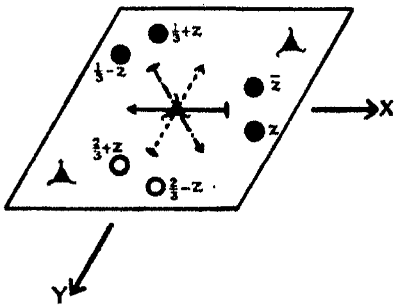

Fig. 4.

Common camphor is another uniaxial crystal which gives active solutions.

---

* 'Rec. Trav. Chim.,' *loc. cit.*, pp. 17, 18.

For this substance the rotatory dispersion in the crystalline and liquid and dissolved states is the same.* An attempt to show the absence or presence of screw-axes in the space-groups of camphor crystals was not successful because good crystals could not be grown.†

The remaining five crystals in Table I are of interest with regard to the special type of screw-axes in their space-groups. Three of them, viz., $NaIO_4 . 3H_2O$, $KLiSO_4$ and iodo-succinimide have space-groups which do not belong to those for which Sohncke from lamellar considerations deduced the possibility of optical activity. We shall discuss them separately.

$NaIO_4 . 3H_2O$.—Sohncke supposed that the crystals of this salt belonged to his three-point screw system‡ which may be compared to a pile of triclinic lamellæ rotated through 120° with regard to each other. This would "explain" their optical activity. The corresponding Schönfliess space-group is $C_3^2(C_3^3)$ which is based on Γ_h and has a three-fold screw-axis of definite rotatory sense.

It is, however, shown in this paper that the space-group is C_3^4, which is based on the rhombohedral lattice Γ_{rh}. The unit-cell, built upon this lattice, contains left- and right-handed three-fold screw-axes. But, as a matter of fact, because of the absence of vertical symmetry planes in the structure, they belong to screws which are not mirror-images. A more detailed consideration of the structure will make this clear.

Although the actual structure of the crystal has not been worked out, we can say a good deal about it from symmetry considerations. There is only one group of $NaIO_4 . 3H_2O$ in the rhombohedral unit-cell. As a consequence of the symmetry elements of the space-group, such a group has three-fold symmetry of its own. This means that the sodium, the iodine and one of the oxygen atoms lie on a vertical axis, and that the three remaining oxygen atoms of the salt molecule form an equilateral triangle perpendicular to this axis. The same holds for the three oxygen atoms of the three water molecules. Therefore, if we omit the hydrogen atoms, we can project the group $NaIO_4 . 3H_2O$ on a horizontal plane as one of the groups in fig. 5. The circles in the centre of the two triangles of oxygen atoms are the projection of the three atoms Na, I, O. The triangles lie at different heights with regard to the vertical axis; their relative orientations in the horizontal planes are not fixed by the symmetry elements of the space-group. We have to place such a group at all the rhombohedral lattice-points in parallel positions. This is represented in fig. 5, which is

---

* L. Longchambon, *loc. cit.*, p. 89.

† W. G. Burgers, 'Nature,' vol. 118, p. 116 (1926).

‡ 'Z. f. Krist.,' vol. 19, p. 531 (1891), and vol. 25, p. 529 (1896).

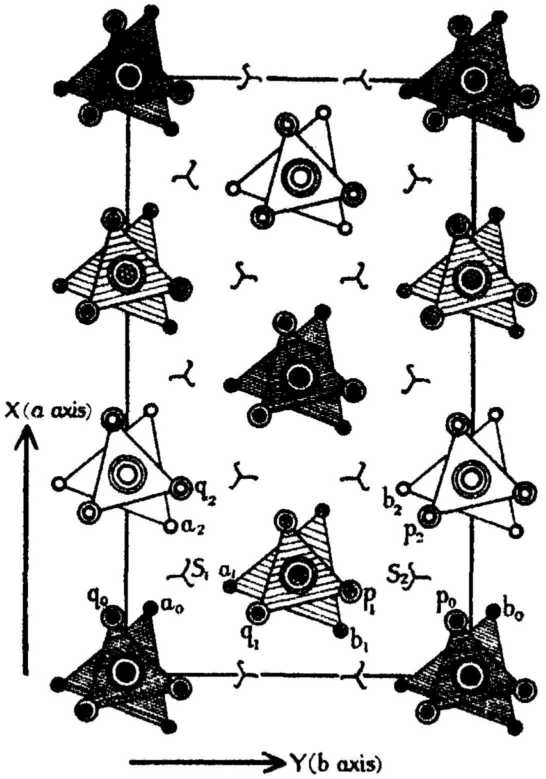

Fig. 5.

a horizontal projection of the orthohexagonal unit corresponding to the rhombohedral cell under discussion.* The orthohexagonal cell contains six groups $NaIO_4 . 3H_2O$ at points with co-ordinates :—

$$x = 0, y = 0, z = 0 \qquad x = \tfrac{1}{6}, y = \tfrac{1}{2}, z = \tfrac{1}{3} \qquad x = \tfrac{5}{6}, y = \tfrac{1}{2}, z = \tfrac{2}{3}.$$
$$x = \tfrac{1}{2}, y = \tfrac{1}{2}, z = 0 \qquad x = \tfrac{2}{3}, y = 0, z = \tfrac{1}{3} \qquad x = \tfrac{1}{3}, y = 0, z = \tfrac{2}{3}.$$

In the drawing the groups are shaded according to their distance from the plane of the paper. The difference in height between two oxygen triangles of the same molecule is indicated only by a difference in direction of the shading lines.

This schematic structure shows clearly the presence of right- and left-handed screw-axes (S_1 and S_2). Equivalent oxygen atoms can therefore be considered as forming both right- and left-handed spirals, for example, $a_0\, a_1\, a_2$ (S_1) and $b_0\, b_1\, b_2$ (S_2); in the same way $p_0\, p_1\, p_2$ (S_2) and $q_0\, q_1\, q_2$ (S_1). If now vertical planes of symmetry were present in the structure, then the oxygen triangles would occupy symmetrical positions with regard to the boundaries of the orthohexagonal cell, and there would be no difference between two opposite spirals of equivalent oxygen atoms, except in rotatory sense. On the other hand, the absence of such planes requires for the triangles an arbitrary orientation such as is shown in the figure, and now the two spirals are not mirror-images. There is, so to say, a definite surplus of left-handedness or right-handedness, according to the two kinds of crystals which are possible. The absence of vertical planes of symmetry is clear from the habit of the crystals (see Groth). It was also shown by a Laue photograph perpendicular to the basal plane.

---

* See P. Niggli, 'Geom. Krist. d. Disk.,' p. 220.

$KLiSO_4$.—It has already been mentioned in the first part of this paper that this salt occupies in some way an exceptional place as an optically active crystal. The structures discussed so far show clearly a spiral arrangement of definite rotatory sense on account of the presence of three-fold screw-axes. The space-group of $KLiSO_4$ (C^6, Sohncke's triple-threaded six-point screw system), however, possesses only screw-axes of translation $c/2$, either six-fold or two-fold (see fig. 6, which shows the general positions of the equivalent points). We can bring the structure into coincidence with itself by rotating it through 60° about a vertical axis either way, yet using a translation $c/2$ in the same direction. Of course the structure as a whole is enantiomorphous on account of the absence of a centre and planes of symmetry, but a definite screw direction is not present. There are, moreover, no asymmetric atomic groups present in the structure which could act as optically active units of some importance, because the oxygen-tetrahedra are found to be regular as nearly as could be estimated from the experimental data. This suggests once more the possibility of a structure which is in reality lamellar and pseudo-hexagonal (*cf.* pp. 557, 558).* Optical activity would then be produced as in the case of NH_4LiSO_4.

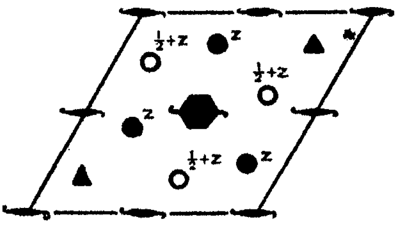

Fig. 6.

Tetragonal Optically Active Crystals.—They belong either to the pyramidal class (iodo-succinimide) or to the trapezohedral class (ethylenediamine sulphate, guanidine carbonate).

---

* The writer would like to state here that he does not maintain that the structure assigned to $KLiSO_4$ is wrong. The substance is only discussed to show the difficulty of making sure about the absence of lamellæ in a similar case and in connection with the rotatory power of its crystals.

There is a remarkable difference between the crystals of these two classes with regard to their rotatory power. In the trapezohedral class several crystals are known which are strongly optically active (of the order of 15° per mm. for sodium light), although their solutions are inactive. It is otherwise in the pyramidal class. Iodo-succinimide is (so far as it is known to me) the only crystal belonging to this class for which, while inactive in solution, the presence of optical activity is suggested by experiment.* The value of ρ could, however, not be measured. The other crystal of this class, which is known to be optically active, will be mentioned farther on.

It looks indeed from the experimental results that the symmetry difference between these two classes is of vital importance with regard to the production of rotatory power. The pyramidal class has a four-fold axis as the only element of symmetry, whereas in the trapezohedral class there are, in addition, four dyad axes perpendicular to it. In some of the space-groups of these two classes the four-fold axis is a screw axis. The X-ray investigation showed this to be the case for all three crystals mentioned. They contain each four molecules per unit-cell, which are arranged in a spiral round the vertical axis (compare fig. 7).

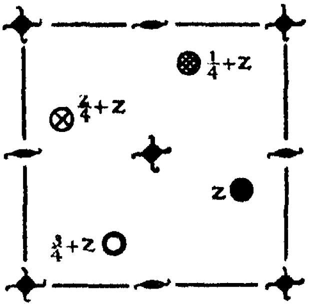

FIG. 7A.

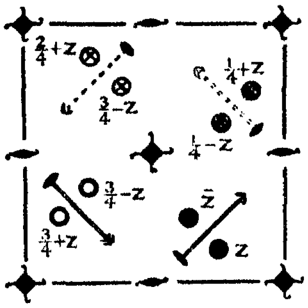

FIG. 7B.

In iodo-succinimide [space-group $C_4^2(C_4^4)$, Sohncke's four-point screw system (fig. 7A)] these molecules are asymmetric (they have at least no symmetry which is "effective" in the crystal structure), but the molecules of both guanidine carbonate and ethylenediamine sulphate [space-group D_4^4 (D_4^8), Sohncke's alternating four-point screw system (fig. 7B)] have a dyad axis.

The question arises now whether four-fold screw-axes alone can produce optical activity, or whether the presence of two-fold axes also is a necessary condition.

To obtain experimental evidence with regard to this point it is necessary to investigate a crystal, the molecules of which do not possess rotatory power

---

* Tutton, 'Roy. Soc. Proc.,' A, vol. 108, p. 548 (1925).

For example, the fact that the tetragonal pyramidal crystals of barium antimonyl tartrate $Ba(SbO)_2(C_4H_4O_6)_2 + H_2O$* are optically active can be ascribed to the presence of optically active molecules, and the rotatory power would be expected even if all the molecules were in parallel positions. This same argument may be applied to iodo-succinimide, for, although this crystal gives an inactive solution, the crystal-molecules are possibly asymmetrical, as already stated. The observed rotatory power might therefore be due to this asymmetry of the crystal molecules.

For the trapezohedral crystals, however, there seem to be good reasons for the conception that their rotatory power is, at least for the greater part, due to the spiral arrangement of the molecules. The fact that in the trapezohedral case this property is far more pronounced than in the pyramidal case makes it improbable that it is due to mere distortion of molecules which are inactive in solution. Furthermore, the order of magnitude of ρ is nearly the same for the two substances investigated (15½° and 14½° per millimetre) and comparable to that of strychnine sulphate crystals [13¼° (Traube), 9° to 10° (Descloizeaux)], although the last substance mentioned gives an optically active solution.†

Sohncke and Mallard discussed the difference between the pyramidal and trapezohedral crystals from the point of view of their lamellar theory. Sohncke‡ dismissed the possibility of optical activity for the former on account of the fact that a pile of perpendicularly crossed mica plates, although behaving as a whole like a uniaxial crystal, does not produce rotation of the plane of polarisation. Tetragonal trapezohedral crystals, however, if built upon certain point-groups which possess four-fold screw-axes, were compared with piles of mica, successive plates of which made angles of 45° with each other (the mica plates have alternately equal thickness).§ A pile of this type does rotate the plane of polarisation, and optical activity was expected for those crystals of this class which possess four-fold screw-axes of definite rotatory sense. Although this view is interesting as a possible way of representing the facts, it does not solve the question, because it is not at all clear whether we can argue from mica plates, how ever thin they may be, to lamellæ of the thickness of a few atoms only.

---

* W. Mamontow, 'Z. f. Krist.,' vol. 32, p. 503 (1900). The magnitude of the rotation is not given.

† $[\rho]_D$ is for this substance more than twenty times $[\alpha]_D$ (see Groth). Although this fact seems to indicate the presence of structural rotation in the crystals, it cannot be used as a strong argument. Longchambon ('Thèses,' p. 88) has measured the rotation of monoclinic crystals (*e.g.*, ammonium tartrate) for which $[\rho]$ is more than ten times $[\alpha]$. For these latter crystals this is probably for the greater part due to differences between the crystal molecule and the chemical molecule (see p. 563) on account of the fact that only two-fold screw axes are possible in the monoclinic system.

‡ *Loc. cit.*

§ See also Mallard, 'Traité de Cristallographie,' vol. 2, p. 320, for a similar explanation.

A sound point of view is to be found in Oseen's* and Born's† theories of optical activity. Especially, the results of Oseen's calculations are given in a form which make it probable that they can be applied to the point under consideration.‡

EXPERIMENTAL.

Method of Investigation.

The dimensions of the unit-cells and the corresponding space-groups were determined chiefly by means of 20°-oscillation photographs about various crystallographic directions. A Shearer gas-tube was used, with copper or molybdenum anticathode. Except in the case of guanidine carbonate, a few important spacings were measured with a Bragg ionisation spectrometer of molybdenum anticathode. For one substance (potassium rhodium oxalate) most of the spacings were determined in that way. Laue photographs were taken to confirm the crystal symmetry, and, for the substance last mentioned, to test the unit-cell deduced from the spectrometer measurements. The oscillation photographs were analysed by Bernal's method.§ Astbury and Yardley's tables and diagrams,‖ together with Wyckoff's tables,¶ were used for the determination of the space-groups and the minimum symmetry and position of the molecules (ions).

d-Potassium Rhodium Oxalate, $K_3[Rh(C_2O_2O_2)_3] + 1H_2O$.

Crystallographic data** :

Trigonal trapezohedral (D_3).

$$a : c = 1 : 0{\cdot}8938.$$

$$\alpha = 100^\circ\ 38'.$$

Specific gravity : $d_{4^\circ}^{20^\circ} = 2{\cdot}255$.

The crystals investigated were grown by Prof. Jaeger, and are fully described in the paper just quoted.

---

* 'Ann. d. Physik,' vol. 48, p. 1 (1915).

† 'Z. f. Physik,' vol. 8, p. 390 (1922).

‡ No more time was available to continue this research for the present, so that this question had to be left as it stands.

§ 'Roy. Soc. Proc.,' A, vol. 113, p. 117 (1926).

‖ 'Phil. Trans.,' A, vol. 224, p. 221 (1924).

¶ 'Carn. Inst. Wash.,' Publ. 318.

** F. M. Jaeger, 'Rec. Trav. Chim. Pays-Bas,' vol. 38, p. 262 (1920).

Results of X-Ray Measurements.

Space-groups : D_3^4 (D_3^6).

Bravais lattice : Γ_h.

Dimensions of unit-cell : $\left.\begin{array}{l} a = 11{\cdot}28 \text{ Å} \\ c = 20{\cdot}2^5 \text{ Å} \end{array}\right\} a : c = 1 : 1{\cdot}80.$

Number of groups $K_2[Rh(C_2O_2O_2)_3] + 1H_2O$ per cell : *six.**

Minimum symmetry of this group : *none.*

Discussion.—The space-group was found in the following way : fig. 8 shows the position of the digonal axes (which coincide in this class with the Bravais-Miller hexagonal axes *h*, *k*, *i*) with regard to the boundaries of the unit-cells in the different space-groups.† A relates to D_3^1, D_3^3, D_3^5 ; B to D_3^2, D_3^4, D_3^6 (lattice Γ_h) ; C represents D_3^7 (lattice Γ_{rh} ; A_1 A_2 A_3 are the Miller rhombohedral axes). Now for the spacing of {10$\bar{1}$0} is found the value 9·74 Å, and for that of {11$\bar{2}$0} 5·64 Å, so that $d_{10\bar{1}0} = \sqrt{3} \, . \, d_{11\bar{2}0}$. This is only possible for fig. 8B. D_3^2 is further excluded by the thirding of the *c*-plane. Therefore the underlying space-group is D_3^4 (or D_3^6).

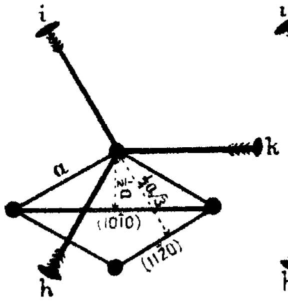

FIG. 8A.

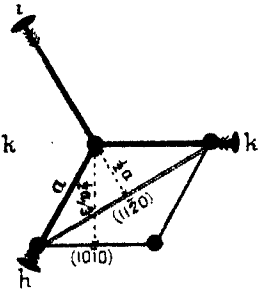

FIG. 8B.

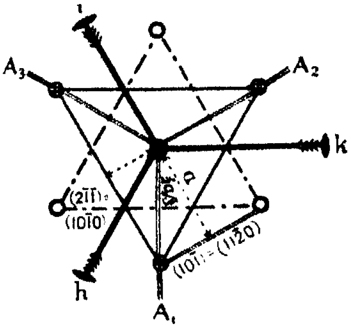

FIG. 8C.

The spacings in Table II are calculated for a hexagonal cell with $a = 11{\cdot}28$ and an axial ratio which is twice that given by Jaeger. A Laue photograph‡ perpendicular to {0001} confirms this unit-cell (Table III). The applied voltage was 56 k.v., which corresponds to a low wave-length limit for the white radiation $\lambda = 0{\cdot}22$ Å. No spots are present for which $n\lambda$ is below this value.§ The gnomonic projection (fig. 9) shows a three-fold axis and three planes of symmetry, as is expected for the D_3-class.

---

* The figures quoted give 6·07.

† See Astbury and Yardley's diagrams.

‡ This photograph was kindly taken for me in Prof. Jaeger's laboratory.

§ See R. W. G. Wyckoff, 'The Structure of Crystals' (1924).

Table II.

Indices of planes.		Spacings.		Relative intensities from successive orders.
True cell.	Original cell.	Obs.	Calc.	
0001	0001	6·76	20·17	III>VI>IX.
$10\bar{1}0$	$10\bar{1}0$	9·74	9·77	II>I>IV and VI ; III, V abs.
$11\bar{2}0$	$11\bar{2}0$	5·64	5·64	
$12\bar{3}0$	$12\bar{3}0$	3·70	3·69	
$13\bar{4}0$	$13\bar{4}0$	2·68	2·71	
$14\bar{5}0$	$14\bar{5}0$	2·16	2·14	
$10\bar{1}1$	$20\bar{2}1$	8·8	8·79	I>II.
$10\bar{1}2$	$10\bar{1}1$	7·00	7·02	I>II.
$10\bar{1}3$	$20\bar{2}3$	5·50	5·53	I v. w. ; II str.>III>I.
$10\bar{1}4$	$10\bar{1}2$	4·50	4·48	II>I ; III v.w.
$10\bar{1}5$	$20\bar{2}5$	3·69	3·73	
$20\bar{2}3$*	$40\bar{4}3$	3·99	3·95	
$30\bar{3}2$*	$30\bar{3}1$	3·13	3·10	
$30\bar{3}4$*	$30\bar{3}2$	2·80	2·74	
$40\bar{4}1$*	$80\bar{8}1$	2·46	2·42	
$11\bar{2}1$	$22\bar{4}1$	5·43	5·41	II>I.
$11\bar{2}2$	$11\bar{2}1$	4·92	4·90	I str.>II ; III v. w.
$11\bar{2}3$	$22\bar{4}3$	4·32	4·28	II>I.
$11\bar{2}4$	$11\bar{2}2$	3·76	3·71	I>II.
$11\bar{2}7$*	$22\bar{4}7$	2·62	2·57	
$12\bar{3}6$*	$12\bar{3}3$	2·52	2·49	
$13\bar{4}5$*	$26\bar{8}5$	2·30	2·25	
$14\bar{5}2$*	$14\bar{5}1$	2·12	2·09	
$14\bar{5}4$*	$14\bar{5}2$	1·99	1·96	

* Calculated from oscillation photographs.

Table III.

Indices.	Spacing = d.	$2d$.	Sin θ.	$2d \sin \theta = n\lambda$.
$20\bar{2}1$	4·74	9·48	0·236	2·237
$3\bar{1}\bar{2}1$	3·63	7·26	0·179	1·300
$22\bar{4}1$	2·80	5·60	0·139	0·778
$4\bar{1}\bar{3}1$	2·69	5·38	0·136	0·732
$40\bar{4}1$	2·42	4·84	0·119	0·576
$5\bar{1}\bar{4}2$	2·09	4·18	0·204	0·853
$50\bar{5}2$	1·92	3·84	0·186	0·714
$33\bar{6}2$	1·85	3·70	0·180	0·666
$6\bar{1}\bar{5}2$	1·73	3·46	0·168	0·581
$7\bar{1}\bar{6}4$	1·43	2·86	0·280	0·801

The space-group D_3^4 contains six equivalent positions (see fig. 4), which have the following co-ordinates :—

x	y	z	$y-x$	$\bar{x}$	$z+\frac{1}{3}$	$\bar{y}$	$x-y$	$z+\frac{2}{3}$
$x-y$	$\bar{y}$	$\bar{z}$	$\bar{x}$	$y-x$	$\frac{1}{3}-z$	y	x	$\frac{2}{3}-z$

They form a double trigonal spiral about the trigonal axis, and represent Sohncke's *alternating three-point screw system.*

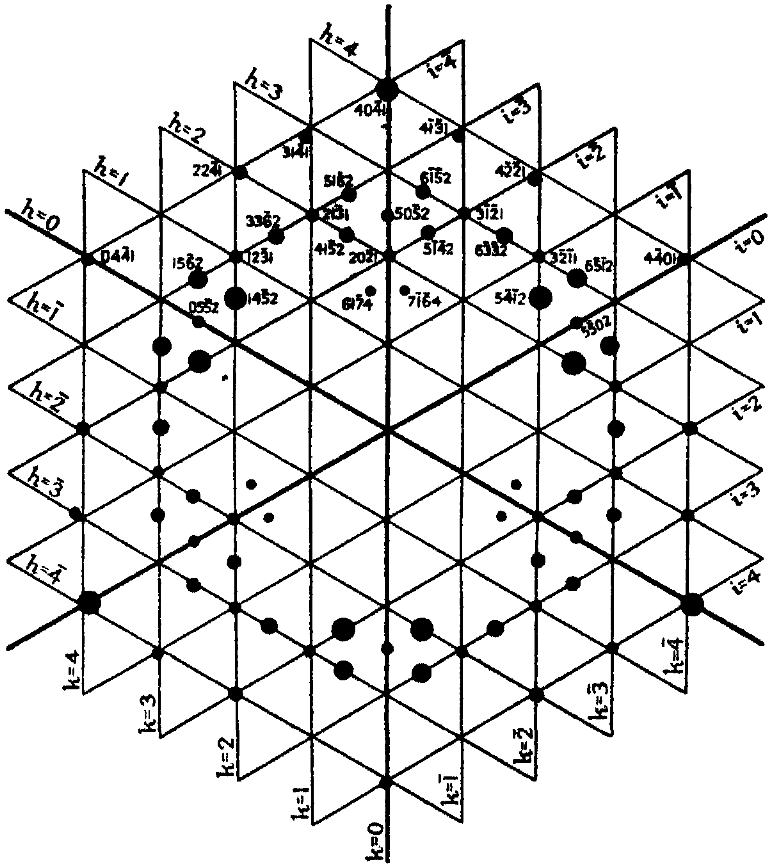

Fig. 9.—d-$K_3[Rh(C_2O_2O_2)_3] + 1H_2O$. Gnomonic projection of Laue photograph perpendicular to {0001}.

Each of these positions is associated with a group $K_3[Rh(C_2O_2O_2)_3] + 1H_2O$. It is reasonable to assume that the complex ion $[Rh(C_2O_2O_2)_3]^{---}$ exists as a definite entity in the crystalline structure. These ions are therefore also arranged in a spiral way. If we place a rhodium atom in a certain position, then the positions of the other atoms of the same ion are not related to that of the rhodium atom by any symmetry-element of the space-group.

This means that, crystallographically speaking, the ion is asymmetric, although it may possess symmetry properties which are not directly " effective " in the construction of the cell. It is probable that the symmetrical arrangement ascribed to them by Jaeger (see theoretical part) is more or less preserved in the crystal. Recently W. T. Astbury[*] has shown that in the case of the tervalent metallic acetylacetones, which have a molecular structure similar to that of the present ions, there is much evidence that the crystal molecules of these compounds have the octahedral habit.

Sodium Metaperiodate, $NaIO_4 . 3H_2O$.

Crystallographic data[†]:

Trigonal pyramidal (C_3).

$\bar{a} : c = 1 : 1 \cdot 0942 \qquad \alpha = 94° 8'$.

Specific gravity: $d = 3 \cdot 219$.

Rotation of the plane of polarised light per millimetre: $\rho_D = 23 \cdot 3°$.

Beautiful crystals were grown from a solution of 10 grams of secondary sodium paraperiodate $Na_2H_3IO_6$[‡] and 40 grams of sodium nitrate[§] in 100 c.c. water, to which 5 c.c. concentrated nitric acid had been added. The crystals obtained in this way showed two trigonal pyramids, $r\{100\}$ and $e\{11\bar{1}\}$, and the basal plane $c\{\bar{1}\bar{1}\bar{1}\}$ (see Groth).

Results of X-Ray Measurements.

Space-group: C_3^4.

Bravais-lattice: Γ_{rh}.

Dimensions of the orthohexagonal unit-cell:

$a = 10 \cdot 38$ Å $\quad b = 6 \cdot 00$ Å $= \frac{1}{3}a\sqrt{3} \quad c = 13 \cdot 13$ Å[‖]

$a : c = 1 : 2 \cdot 188$.

Length of the edge of the rhombohedral unit-cell: $a' = 5 \cdot 58$ Å.

Rhombohedral angle: $\alpha = 65° 1'$.

Number of groups $NaIO_4 . 3H_2O$—

In the orthohexagonal cell: *six*.

In the rhombohedral cell: *one*.[¶]

Minimum symmetry of this group: three-fold rotation axis.

Discussion.—The relation between the orthohexagonal axes a, b, c (indices $h\ k\ l$), which correspond to the cell mentioned in the first part of this paper, and the Bravais-Miller hexagonal axes a_1, a_2, a_3, c (indices $h\ k\ i\ l$) is shown in fig. 10.

---

[*] 'Roy. Soc. Proc.,' A, vol. 112, p. 448 (1926).

[†] Groth, 'Chem. Krist.,' vol. 2, p. 178.

[‡] See J. W. Mellor, 'Inorganic Chemistry,' vol. 2, pp. 387, 407.

[§] For the influence of $NaNO_3$ on the crystallisation of $NaIO_4 . 3H_2O$ see Eakle, 'Z. f. Krist.,' vol. 26, p. 558 (1896).

[‖] Calculated from a by means of the axial ratio. The mean experimental value was 13·07 Å.

[¶] The figures quoted give 0·99.

The c-axis is for both sets perpendicular to the plane of the drawing. $A_1\,A_2\,A_3$ are the Miller rhombohedral axes. The orientation of the boundaries of the crystal with regard to these axes is indicated in the centre of the figure.

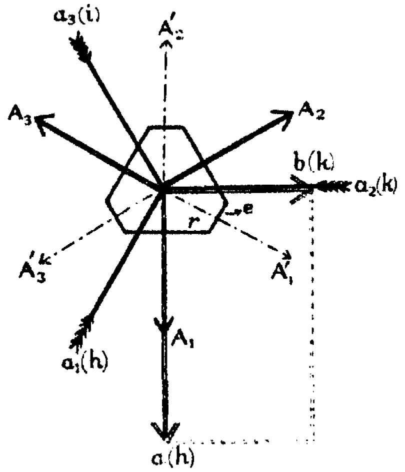

FIG. 10.

The presence of a rhombohedral lattice was evident from the following facts:—

(*a*) Oscillation photographs were taken with the orthohexagonal axes a, b, c as axes of oscillation. Only those about the b-axis were symmetrical under and above the equator so far as the *presence* of the spots was concerned (the intensities were often different). Fig. 5 shows that, while a plane perpendicular to this axis is a plane of symmetry of the rhombohedral *point lattice*, this is not the case for planes perpendicular to the a and c axes.

(*b*) Table IV gives the observed planes. Both the orthohexagonal and the corresponding Bravais-Miller hexagonal indices are given. These latter indices belong to planes which either correspond directly to those in the first column, or which are equivalent to them with regard to the reflection of the X-rays.

If the lattice is rhombohedral, then the orthohexagonal cell contains six lattice points, the co-ordinates of which are given on page 567. A set of planes of this latter cell can give a first order reflection if, and only if, successive planes of the set contain all these six points (or points which are equivalent to them). This means that the substitution of their co-ordinates in the equation of the planes ($hx + ky + lz = p$) must give a set of values for p which differ only by whole numbers. This necessary condition is fulfilled for all the planes in the first column of the table.

By means of well-known transformation formulæ* we can transfer the hexagonal indices of these planes into rhombohedral indices. These latter do not correspond to the indices given by Groth and Eakle, because, as can be seen from the figures quoted, the axial ratio adopted by them must be doubled, and the true fundamental rhombohedron differs from the rhombohedron deduced from crystallographic measurements. The original rhombohedral

---

* See, *e.g.*, Tutton, 'Crystallography,' I, p. 338.

Table IV.—$NaIO_4 . 3H_2O$. Planes observed on Oscillation Photographs.

$00\bar{3}$	0003	m. str.	$0\bar{2}0$ $\bar{3}\bar{1}0$	$11\bar{2}0$	str.	$\bar{4}2\bar{1}$	$21\bar{3}\bar{1}$	w.
$00\bar{6}$	0006	m. w.				512	$21\bar{3}2$	m.
$00\bar{9}$	0009	m.	$31\bar{3}$	$11\bar{2}3$	str.	$51\bar{4}$	$21\bar{3}\bar{4}$	m. w.
			$3\bar{1}3$	$11\bar{2}\bar{3}$	w.	515	$21\bar{3}5$	m.
$20\bar{1}$	$10\bar{1}1$	str.	$\bar{3}16$	$11\bar{2}6$	m. str.	$51\bar{7}$	$21\bar{3}\bar{7}$	m. str.
202	$10\bar{1}2$	str.	$\bar{3}1\bar{6}$	$11\bar{2}\bar{6}$	m.	518	$21\bar{3}8$	m. w.
$20\bar{4}$	$10\bar{1}\bar{4}$	m. str.	319	$11\bar{2}9$	w.	$\bar{4}2\overline{10}$	$21\bar{3}\overline{10}$	m.
205	$10\bar{1}5$	m.	$31\bar{9}$	$11\bar{2}\bar{9}$	m.			
$20\bar{7}$	$10\bar{1}\bar{7}$	m. str.				242	$31\bar{4}\bar{2}$	m. str.
$\bar{1}18$	$10\bar{1}8$	str.	$6\bar{2}0$	$22\bar{4}0$	m. w.	$2\bar{4}2$	$13\bar{4}2$	m. str.
			$\bar{6}2\bar{3}$ $62\bar{3}$	$22\bar{4}\bar{3}$	m.	$24\bar{4}$	$31\bar{4}4$	m. w.
401	$20\bar{2}1$	w.				$2\bar{4}\bar{4}$	$13\bar{4}\bar{4}$	m. w.
$40\bar{2}$	$20\bar{2}\bar{2}$	m.						
404	$20\bar{2}4$	m. str.	$\bar{5}11$	$12\bar{3}1$	m. w.	$35\bar{3}$	$41\bar{5}3$	m.
$40\bar{5}$	$20\bar{2}\bar{5}$	m.	$\bar{5}1\bar{2}$	$12\bar{3}\bar{2}$	w.	$3\bar{5}\bar{3}$	$14\bar{5}\bar{3}$	m.
$\bar{2}27$	$20\bar{2}7$	m. w.	$\bar{5}14$	$12\bar{3}4$	m.	$\bar{3}5\bar{3}$	$14\bar{5}3$	m.
$\bar{2}2\bar{8}$	$20\bar{2}\bar{8}$	m.	$\bar{5}1\bar{5}$	$12\bar{3}\bar{5}$	m.w.	$\bar{3}\bar{5}\bar{3}$	$41\bar{5}\bar{3}$	m. str.
2211	$20\bar{2}\overline{11}$	m.	$\bar{5}17$	$12\bar{3}7$	m. w.			
			$\bar{5}1\bar{8}$	$12\bar{3}\bar{8}$	m.	$82\bar{4}$	$32\bar{5}\bar{4}$	m. w.
600	$30\bar{3}0$	m. str.	$42\overline{11}$	$12\bar{3}\overline{11}$	m.	$\bar{8}2\bar{5}$	$23\bar{5}\bar{5}$	m.
603	$30\bar{3}3$	m.						
$60\bar{3}$	$30\bar{3}\bar{3}$	m.						
$\bar{3}36$	$30\bar{3}6$	w.						
$\bar{3}3\bar{6}$	$30\bar{3}\bar{6}$	w.						

indices can easily be transfered into the true ones via the hexagonal indices. This is done for three planes in the following Table V :—

Table V.

Trigonal indices. (Groth).	Corresponding hexagonal indices.	True hexagonal indices.	True trigonal indices.	As preceding column. Trigonal axes rotated over 60°.
$r\{100\}$ $e\{11\bar{1}\}$ $a\{10\bar{1}\}$	$\{10\bar{1}1\}$ $\{02\bar{2}1\}$ $\{11\bar{2}0\}$	$\{10\bar{1}2\}$ $\{01\bar{1}1\}$ $\{11\bar{2}0\}$	$\{411\}$ $\{22\bar{1}\}$ $\{10\bar{1}\}$	$\{101\}$ $\{100\}$ $\{1\bar{1}0\}$

This transformation shows that *e* is the principal trigonal pyramid and not *r*. If we rotate the trigonal axes A_1 A_2 A_3 (fig. 10) through 60° into the positions A_1' A_2' A_3', the indices of the last column are obtained. The form *a*, which is a right trigonal prism of the second order in the original description, is the corresponding left prism in the true description. This fact is mentioned because Eakle (*loc. cit.*) observed this form only on crystals which had a left-handed rotatory power, and he mentions it as an exception to the rule, observed for quartz crystals, that the position of the tetrahedral forms corresponds to the character of the rotation of the crystals. Although there seems to be no reason that this relation should be a general one,* the supposed exception is only apparent in this case.

A general description of the structure of the crystals has been discussed already with regard to its rotatory power (see fig. 5). A Laue photograph perpendicular to $\{\bar{1}\bar{1}\bar{1}\}$ shows a trigonal axis as only symmetry-element. However, the absence of planes of symmetry is not very pronounced, being evident only in small intensity differences of certain spots. The symmetry of the structure is therefore closely related to that of one of the three classes C_{3v} (tourmaline), D_3 (quartz) or D_{3d} (calcite). Only the first class comes into consideration on account of the hemimorphic character of the crystals, which is clearly shown by their habit, etch figures and pyro-electric properties (see Groth). The space-group to which the structure corresponds most is probably C_{3v}^5, which is also based on the rhombohedral lattice. This means that the group $NaIO_4 . 3H_2O$ itself has nearly three planes of symmetry.

In order to determine the positions of the atoms, eight parameters have to be fixed, even if we leave the hydrogen atoms out of consideration, viz., four along the *c*-axis (O, I, O_3, O_3) and four to fix the oxygen triangles with regard to the horizontal axes. The fact that three atoms lie in one line, and the approach of the structure to higher symmetry (as shown by the Laue photograph) will be of use in this determination, for which especially intensities of the basal and prism planes require to be measured.† The intensities given in the table represent the appearance of the spots on the plates and they give only an approximate idea of the true relative values on account of the absorption of the crystals. The presence of one group $NaIO_4 . 3H_2O$ in the rhombohedral unit-cell excludes for this salt the formula $Na_2I_2O_8 . 6H_2O$ which is, *e.g.*, given in Groth. The single formula was also found for the tetragonal modification.‡

Ethylenediamine Sulphate, $C_2H_4(NH_2)_2 . H_2SO_4$.

Crystallographic data§:

Tetragonal trapezohedral (D_4).

$$a : c = 1 : 1{\cdot}4943.$$

Rotation of the plane of polarised light per millimetre: $\rho_D = 15° 30'$.

---

* It follows from a study of the morphology of quartz crystals by Niggli ('Z. f. Krist.,' vol. 63, p. 311 (1926)), that for this substance it must be considered as a special consequence of their structure.

† The intensity investigation and analysis of the structure have unavoidably had to be left incompleted.

‡ Merle Kirkpatrick and Dickenson, 'Trans. Am. Chem. Soc.,' vol. 48, p. 2327 (1926).

§ Groth, 'Chem. Krist.,' vol. 3, p. 54.

The crystals investigated showed the {001} and {221} faces, as described by von Lang.* Their density was determined by the suspension method in a mixture of tetrabromoethane and chloroform; for its value was found: $d_{4^\circ}^{16^\circ} = 1\cdot62^5$.

Results of X-Ray Measurements.

Space-group: D_4^4 (D_4^8).
Bravais-lattice: Γ_t (simple tetragonal lattice).
Dimensions of the unit-cell:

$$\left.\begin{array}{l} a = 5\cdot96 \text{ Å} \\ c = 17\cdot99 \text{ Å} \end{array}\right\} a : c = 1 : 3\cdot016.$$

Number of molecules $C_2H_4(NH_2)_2 \cdot H_2SO_4$ in this cell: *four*.†
Minimum symmetry of the crystal-molecule: two-fold rotation axis.

Discussion.—In this substance the absence of a twin-structure built up of lamellæ, large enough to give individual X-ray reflections (type *a*, see theoretical part), can be demonstrated as follows: The crystals behave with regard to X-rays as true tetragonal crystals. The values of the maximum periodicities in the direction of the axes (calculated from the first hyperbola on oscillation photographs) are found to be $a = b = 5\cdot96$, $c = 17\cdot99$. If we assume that the periodicity in the direction of the *c*-axis is common to all the lamellæ (see p. 557), then from the fact that the periodicities in the directions of the *a* and *b* axes possess the same maximum value, we may infer that, if the structure is lamellar, the lamellæ are perpendicularly crossed.‡ It is further evident that for a definite lamella the periodicity in the direction of either the *a* or *b* axis is equal to 5·96, whereas for the same lamella the periodicity perpendicular to this direction can have all values $\frac{5\cdot96}{n}$, where *n* is a whole number. Figs. 11A, B, C, represent the cases for which $n = 1$, 2 and 3.

A consideration of the spacings of the planes belonging to the prism zone shows that fig. 11A is the only possibility. The two largest spacings calculated from the photographs for planes of this zone are $2\cdot97 = \frac{1}{2}a$, and $4\cdot22 = \frac{1}{2}a\sqrt{2}$ (they correspond in reality to the (200) and (110) planes respectively). They exclude figs. 11B and 11C, because no prism spacing equal to $\frac{1}{2}a\sqrt{2}$ is possible in these cases. We have still to consider the possibility of lattice points within the rectangular cell built upon the square base of fig. 11A. The two prism spacings $\frac{1}{2}a$ and $\frac{1}{2}a\sqrt{2}$ leave as only possibility a point in the centre of the base, or in the centre of the cell. The first alternative can be dismissed on account of the fact that for the maximum periodicity in a direction of 45° to the sides of the square the length $8 \cdot 44 = a\sqrt{2}$ is found. A point in the centre of the cell is excluded because first order reflections of planes are present such as (111) and (115) (see Table VI; the indices refer to the crystallographic axes, which correspond to the sides of the square in fig. 11A). Possible halvings of planes $(11l)$ cannot be affected by the simultaneous presence of perpendicular lamellæ based on quadratic cells, because planes of the same form $\{11l\}$ have parallel positions in all the lamellæ. A centreing of the cell under consideration would halve them all, if l is odd. Therefore the lattice built upon the square basis of fig. 11A is a simple lattice. It is, of course, possible that not the sides, but the diagonals of this square coincide with two of the (for example, orthorhombic) crystallographic axes. In that case the unit-cell is twice as large and is base-centered.

---

* Groth, 'Chem. Krist.,' vol. 3, p. 54.

† The figures quoted give 3·99.

‡ F. M. Jaeger, 'Proc. Roy. Acad. Amst.,' vol. 22, p. 815 (1920) came to a similar conclusion from a study of Laue photographs of piles of mica plates.

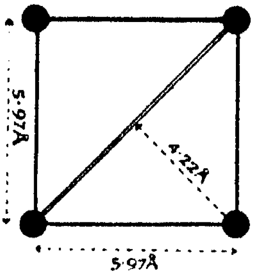

Fig. 11A.

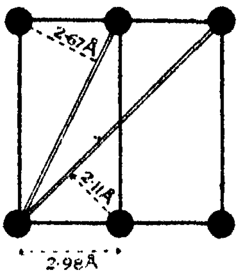

Fig. 11B.

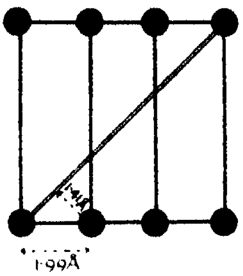

Fig. 11C.

We consider now the fact that only the fourth and eighth order reflections are observed for the (001) plane. This means that the (001) plane of the separate lamellæ is quartered, for the c-planes are parallel for all of them. A consideration of the space-groups of the triclinic, monoclinic and orthorhombic systems built upon a simple lattice or a lattice with one pair of opposite faces centered, shows that none of them requires a quartering for a lattice plane. The quartering of the c-plane excludes* therefore those systems and with that the possibility of lamellæ of the corresponding symmetry.

As a consequence of these results and of arguments adduced in the first part

---

* This is only true if the quartering is considered as real. If the possibility of an accidental quartering is accepted, then the foregoing considerations, based on geometrical facts, are not conclusive with regard to this question, and, for example, orthorhombic space-groups can be found which are in agreement with the observed reflections of all the planes.

Table VI.—Planes observed on Oscillation Photographs.

Ethylenediamine sulphate.			Guanidine carbonate.			
Cell according to Groth.	True cell, based on Γ_t (=) Γ_0.	Relative intensity.	Cell according to Groth.	True cell, based on		Relative intensity.
				Γ_t (=) Γ_0'.	Γ_t (=) Γ_0.	
The indices for this column can be obtained from those in the next column by dividing the *l*-index by two.	004	str.	The indices for this column can be obtained from those in the next column by dividing the *l*-index by two.	004	004	w.
	008	mod.		008	008	mod.
	200, 020	str.		220	020	w.
	202, 022	str.		221	021	mod. w.
	203, 023	v. w.		222	022	mod.
	204, 024	mod. str.		223	023	w.
	206, 026	mod. str.		224	024	str.
				227	027	w.
	040	mod. str.				
	043	mod. w.				
	101, 011	str.		111	011	v. w.
	102	v. w.		*112*	*012*	*v. str.*
	103, 013	str.		113	013	str.
	104, 014	mod. w.		114	014	str.
	105, 015	mod. str.		115	015	str.
	106, 016	mod. str.		116	016	mod.
	017	mod. str.		117	017	mod.
	110	w.		200	110	v. w.
	111	mod. str.		201	111	str.
	112	*v. str.*		202	112	w.
	114	mod.		203	113	mod.
	115	mod. str.		205	115	w.
	116	w.		207	117	mod. w.
	224	mod. w.		400	220	mod.
	225	mod. w.		401	221	mod.
	210, 120	v. w.		310	120	v. w.
	211, 121	w.		311	121	w.
	212, 122	w.		312	122	mod.
	214, 124	mod. w.		313	123	w.
	215, 125	mod. w.		314	124	mod.
	216, 126	mod.		315	125	w.
	311, 131	mod. w.		420	130	v. w.
	312, 132	mod.		421	131	w.
	134	w.				
	136	w.				
	137	v. w.				
	144	v. w.				
	244	w.				
	155	mod. w.		510	230	v. w.
				513	233	w.

of this paper we conclude that the crystals are really tetragonal and built upon the simple lattice Γ_t. The crystal-class is not evident from the habit of the crystals, which is, in fact, holohedral. The trapezohedral class D_4 has been ascribed to them on account of their rotatory power. This class is confirmed by the X-ray investigation. A Laue photograph possesses full tetragonal symmetry, thus showing that the crystal belongs to one of the four following classes: D_{4h}, D_4, D_{2d} or C_{4v}. The observed abnormal spacings (*cf.* Table VI) are {100} halved and {001} quartered. They exclude the classes D_{4h}, D_{2d} and C_{4v} and give as space-group at once D_4^4 (D_4^8).

The fact that only four molecules are present in the unit-cell requires a dyad axis as minimum symmetry condition for the molecules. Their arrangement in the unit-cell is shown in fig. 7B (corresponding to Astbury and Yardley's diagram No. 116), each molecule being represented by its dyad axis and two crystallographically equivalent atoms. The co-ordinates of the latter with regard to the c-axis are given in the figure. The dyad axes are parallel to {110}; equivalent points on them possess the co-ordinates:—

$$x, y, 0;\ y, \bar{x}, \tfrac{1}{4};\ \bar{x}, \bar{y}, \tfrac{1}{2};\ \bar{y}, x, \tfrac{3}{4}.$$

The molecules form a four-fold spiral about a tetragonal screw-axis.

The formula of the compound, on the assumption that it is ionised, may be written 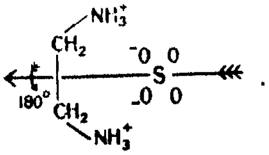

. The presence of the dyad axis in the molecule requires this same minimum symmetry for the $C_4H_4(NH_3)_2{}^{++}$ group, and therefore probably also for the ethylenediamine molecule

$$\begin{array}{l} CH_2\,.\,NH_2 \\ | \\ CH_2\,.\,NH_2 \end{array}$$

This seems of interest in connection with the above-mentioned symmetry of complex ions of the type $[C_0(\text{acine})_3]^{---}$ (see preceding crystal). In these ions a dyad axis is attributed to each ethylenediamine molecule.

Guanidine Carbonate $(CN_3H_5)_2 \,.\, H_2CO_3$.

Crystallographic data*:

Tetragonal trapezohedral (D_4):

$a : c = 1 : 0\cdot9910.$

Specific gravity: $d = 1\cdot25$.

Rotation of the plane of polarised light per millimetre: $\rho_D = 14^\circ\ 35'$.

---

[*] Groth, 'Chem. Krist.,' vol. 3, p. 569.

The crystals investigated showed the planes {111}, {001} and {100}. They had an octahedral habit. A definite direction in a crystal was identified with the aid of its optical character.

Results of X-Ray Measurements.

Space-groups: D_4^4 (D_4^8).

Bravais-lattice: Γ_t (simple tetragonal lattice).

Dimensions of the unit-cell:

$$\left.\begin{array}{l} a = 6{\cdot}95\ \text{Å} \\ c = 19{\cdot}4^5\ \text{Å} \end{array}\right\} a : c = 1 : (0{\cdot}989 \times 2\sqrt{2}).$$

Number of molecules $(CN_3H_5)_2 \,.\, H_2CO_3$ per cell: *four.*[*]

Minimum symmetry of this crystal-molecule: two-fold rotation axis.

Discussion.—The absence of lamellar twinning of type *a* was demonstrated for this crystal in exactly the same way as is described for the preceding substance. A Laue photograph showed the full tetragonal symmetry also in this case.

Again the cell deduced from X-ray measurements does not correspond to the original cell adopted by the crystallographers. The relation between the two cells is shown in fig. 12. The dimensions given for *a* and *c* correspond to AK and AE, and the cell AKDMELHN. This cell, which is built upon the

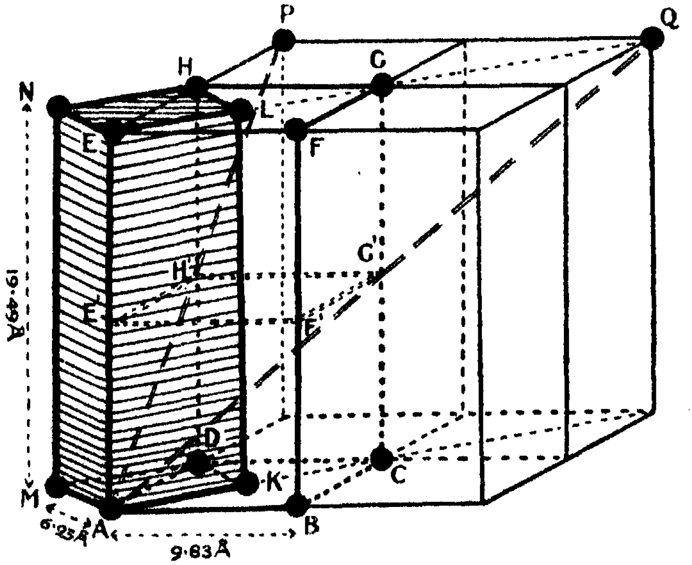

Fig. 12.

---

[*] The figures quoted give 3·95.

simple tetragonal lattice $\Gamma_t (=) \Gamma_0$, is equivalent to the cell ABCDEFGH, which has the square faces centred $[(\Gamma_t (=) \Gamma_0']$, and which contains eight molecules.

The cell adopted in Groth's description is ABCDE'F'G'H'. The *c*-axis of this cell must, therefore, be doubled. Table VII gives the lengths of the periodicities in different crystallographic directions as deduced from rotation photographs. The figures in the sixth column are calculated from a = AK = 6·95, and a value for the axial ratio which is $2\sqrt{2}$ times that given by Groth.

The observed planes are collected in Table VI; the indices are given for both $\Gamma_t (=) \Gamma_0$ and $\Gamma_t (=) \Gamma_0'$. Those according to Groth's cell can be easily deduced in the way indicated in the table. With regard to the simple tetragonal lattice the abnormal spacings are the same as in the preceding case, viz., {100} halved and {001} quartered, the resulting space-group being D_4^4 (D_4^8).

Table VII.—Guanidine Carbonate.

Periodicities in different crystallographic directions.

Original cell.	True cell, based on		Periodicities in fig. 12.	Observed value.	Calculated value.
	$\Gamma_t (=) \Gamma_0'$.	$\Gamma_t (=) \Gamma_0$.			
[100]	[100]	[110]	AB = AD	9·89 A	9·83 Å
[001]	[001]	[001]	AE = MN	19·38	19·49
[110]	[110]	[100]	AK = AM	6·95	6·95
[011]	[021]	[221]	AP	27·55	27·68
[111]	[221]	[401]	AQ	33·5	33·9

The minimum symmetry and the positions of the molecules in the unit-cell are the same as for ethylenediamine sulphate (see fig. 7 on p. 569). The fact that the crystal-molecule $(CN_3H_5)_2 \cdot H_2CO_3$ possesses a dyad axis does not give us any direct evidence with regard to a possible symmetry of the guanidine molecule itself. If we write the formula according to current conceptions thus:— 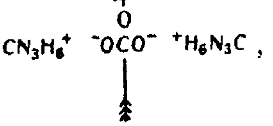 $CN_3H_6^+\ {}^-O\overset{\overset{180°}{\updownarrow}}{\overset{O}{C}}O^-\ {}^+H_6N_3C$, we can only say that the CO_3^{--} group has a dyad axis, but each of the guanidinium ions may be asymmetric. They are related to each other only by a rotation through 180°.

Summary.

1. The following uniaxial optically active crystals have been investigated by X-rays:

d-Potassium rhodium oxalate, $K_3[Rh(C_2O_2O_2)_3] + 1H_2O$.

Sodium metaperiodate, $NaIO_4 + 3H_2O$.

Ethylenediamine sulphate, $C_2H_4(NH_2)_2 . H_2SO_4$.

Guanidine carbonate, $(CN_3H_5)_2 . H_2CO_3$.

2. The fact that sharp single-crystal X-ray diffraction effects are observed from these crystals has been discussed with special reference to the question as to how far such effects are able to give information about the presence or absence of a lamellar twin-structure (Theoretical part I). The conclusions arrived at suggest that their rotatory power is not due to a spiral arrangement of biaxial lamellæ (*cf.* piles of mica plates), but to some special arrangement of atoms within a unit of structure (see, however, under 5).

This unit is a real unit if the crystal is truly uniaxial; but it is a pseudo-unit if the crystal is built up out of very many twinned lamellæ which individually are too small to give X-ray reflections ("pseudo-paramorphic" crystal). In *this later case this pseudo-unit corresponds either to a real elementary cell of* the lamellæ, or to some sub-multiple of one.

3. The space-groups or "pseudo" space-groups of these units (see 2) have been determined (Experimental part), and the spiral arrangements within them have been discussed in connection with the rotatory power of the crystals (Theoretical part II).

4. It is shown that the similarity between the rotatory dispersion curves of crystals and solutions of $K_3[Rh(C_2O_2O_2)_3] + 1H_2O$ is not due to the presence of parallel molecules in the crystalline state. The molecules occupy a spiral arrangement in the crystal which may account at least partly for the movement of the inversion point of the dispersion curve on transition from the dissolved to the crystalline state.

5. The rather exceptional place of potassium lithium sulphate as an optically active crystal, and the difficulty of making sure about the absence of lamellæ in the case of this salt, is discussed.

6. The marked difference in rotatory power between tetragonal pyramidal and tetragonal trapezohedral crystals has been considered in connection with the spiral arrangements within their units of structure.

In conclusion, I wish to thank most sincerely Sir William Bragg for his interest in the work and for his unfailing kindness. I am very much indebted to the Managers of the Royal Institution for allowing me to carry out this research in the Davy-Faraday Research Laboratory. My sincere thanks are also due to Mr. W. T. Astbury for his valuable criticism of the work and his interest throughout. For most of the crystals investigated I am much indebted to Profs. H. J. Backer and F. M. Jaeger of Groningen. The research was carried out by means of a grant from the Ramsay Memorial Fellowship Trust.

Sorption of Ammonia by Glass. (Time, Pressure and Temperature Relationships.)

By M. Francis and F. P. Burt.

(Communicated by A. Lapworth, F.R.S.—Received May 3, 1927.)

The sorption of ammonia by glass wool at 0° C. and at different pressures was investigated by Bangham and Burt.* The glass wool, after being cleaned *in situ* with chromic acid and washed with water, was out-gassed at 200° C. After each experiment the ammonia was expelled from the sorbent by heating to this temperature while part of the system was cooled with liquid air. Under these conditions reproducible results were obtained, and it was found possible to express the sorption at any time during an experiment as a function of the pressure and the time from the start. A small correction was needed to take account of the diminution of pressure as sorption progressed. An outstanding feature of the phenomenon investigated was the extraordinary slowness of the later stages of the process, as a result of which the experimental attainment of equilibrium proved quite impracticable. When the logarithms of the quantities of gas taken up were plotted against the logarithms of the time from the start, the resulting graphs were nearly linear over their whole course, and of very small gradient (about $\frac{1}{12}$), a large fraction of the sorption being completed before any observations could be taken. It therefore proved impossible to assess limiting values, and the present work was undertaken with the hope of throwing more light on this question. Regarded as a sorbent, glass is a highly unsatisfactory material, mainly because of the impossibility of freeing it from water. Since, however, the primary object of these investigations has been to find the order of correction that should be applied for sorption effects in glass apparatus used for accurate gas measurement, we have submitted our sorbent to such heat treatment as would be feasible, say, in the case of a calibrated density bulb, instead of aiming at the highest possible degree of desiccation. The tenacity with which water and traces of gas are held, even at far higher temperatures, is illustrated in a recent paper by Durau.* That the water content of glass can be kept very nearly constant by careful regulation of the temperature of out-gassing has been established both by the work of Sherwood† and by the earlier experiments carried out in this laboratory, and finds further confirmation in the present research.

---

* 'J. Phys. Chem.,' vol. 29, p. 113 (1925).

The Sorption Apparatus.

Into the exhausted bulb A, containing glass wool, ammonia was displaced by means of mercury, the weight of mercury required defining the volume of gas admitted to the sorption vessel. To facilitate rapid observations, a microburette B, graduated in hundredths of a cubic centimetre, was included in the system. Except during an initial period which rarely exceeded a minute, the pressure in the system could be kept constant by introducing mercury as sorption proceeded, reference being made through a differential gauge C to the pressure obtaining in a large volume D of the experimental gas, kept at the temperature of melting ice. The working pressure was determined at the beginning of an experiment from the readings of a wall-bracket barometer of the Fortin type and a double point-tube manometer, the open limb of which was provided with an external point moving over a millimetre scale.

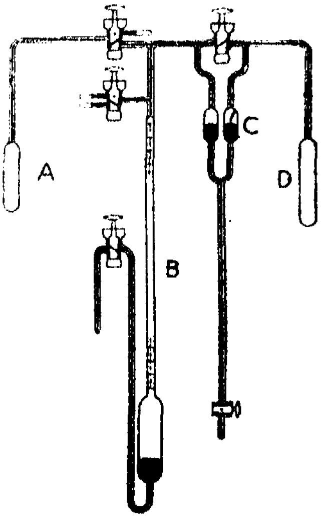

FIG. 1.

For experiments at 0° C., the sorption-bulb was surrounded by powdered ice; for higher temperatures an electrically heated and controlled oil-bath was used.

In reducing volumes of gas to normal temperature and pressure, allowance was made for deviations from the gas laws. Corrections were also applied to compensate for errors in the micro-burette and thermometers, for variations in the temperatures of the exposed capillaries, and for slight departures from the pressure taken as standard for a series of experiments covering a range of temperatures.

---

* 'Z. f. Physik,' vol. 37, p. 419 (1926).

† 'J. Amer. Chem. Soc.,' vol. 40, p. 1645 (1918).

The dead-space volume of the sorption-bulb was determined by a water calibration and checked at the beginning and end of the experiments by calibration *in situ* with hydrogen.

An estimate of the surface of the glass wool was made by measuring the mean diameter of a large number of fibres, assuming them to be cylindrical. Microscopic examination failed to disclose the presence to any appreciable extent of capillary pores or air-bubbles.

Before incorporation with the apparatus the wool-bulb was cleaned by treatment with alkali followed by chromic and sulphuric acid mixture, and thoroughly washed with distilled water. The major portion of the water having been removed by drainage, further desiccation was effected by passing through the bulb a stream of dry, dust-free air, while the temperature was slowly raised to 180° C. The last stages of drying were carried out *in vacuo*, after the bulb had been sealed to the apparatus.

Preparation of Ammonia.

The gas was liberated by aqueous caustic potash from a meal of ammonium chloride crystals which contained no organic bases. After liquefaction and removal of air, the gas received a preliminary drying by passage over asbestos-potash and phosphorus pentoxide, and was then absorbed by copper sulphate, previously dehydrated by evacuation at 350° C. *in situ*. The cupric hexammino-sulphate thus formed was slowly heated, the liberated ammonia being removed at intervals, until the residue corresponded to a mixture of the di- and tetrammino-compounds. At this stage a quantity of ammonia was condensed and fractionated, and a middle fraction was stored for subsequent use. The "tailings" were tested qualitatively for moisture by exposure to a few crystals of phosphorus pentoxide previously distilled in oxygen. To ensure against accumulation of traces of water slowly given up by the glass, the ammonia was allowed to evaporate into the sorption apparatus at the beginning of each experiment from the surface of distilled phosphorus pentoxide.

Preliminary Experiments.

Before a systematic series of experiments was undertaken, the glass wool was heated to temperatures as high as 250° C. for long periods of time in presence of ammonia. The effect of this treatment on the course of the sorption process was examined at intervals by conducting sorption experiments at 0° C. under a uniform pressure of 550 mm.; the sorbent being rendered "gas-free" before each experiment by heating to 200° C., condensing out the bulk of the ammonia, and finally exposing the system to charcoal cooled in liquid air for at least three hours.

The results of these preliminary experiments are shown in fig. 2. Log sorption (cubic centimetres at N.T.P.) is plotted against log time (minutes). The early isothermals were flat and nearly linear, like those of Bangham and Burt. As the treatment was continued the graphs became steeper and more curved, so that a much larger fraction of the whole process came within the range of experimental observation. It may be noted that, though the early parts of the isothermals follow such different courses, they are all tending towards limits not so very far apart.

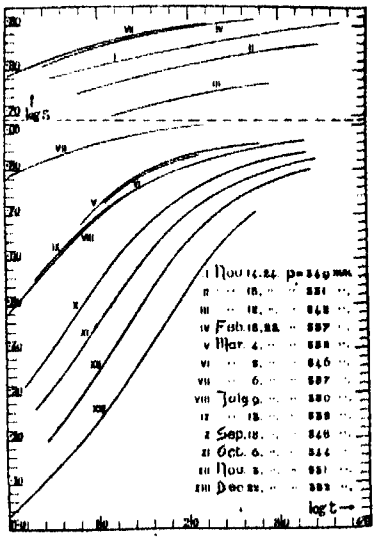

FIG. 2.

The progressive change is ascribed to the gradual removal of water, since the flat type of graph could always be recovered by treating the sorbent with water, drying in a current of air and out-gassing in the usual way. (Curve VII in fig. 2 is an example of this.) Heating in presence of ammonia would appear to be more effective in reducing the water content of the glass than heating *in vacuo*. Ultimately a state was reached when further treatment produced no more change, and the subsequent experiments indicate clearly that this condition of the sorbent was closely reproduced after out-gassing. That the temperature normally employed for this purpose (200° C.) was adequate was confirmed at a later date, when it was found that increasing this temperature by 100° C. left the activity of the sorbent unaltered.

Systematic Experiments.

The numerical data for a single experiment are tabulated at the end of the paper. Fig. 3 shows a series of isothermals at 0° C. under constant pressures ranging from 774 to 115 mm.

The isothermals form a series of S-shaped curves, running roughly parallel to each other. The central part of each curve is nearly linear, and the sorption values can be seen to increase regularly with the pressure.

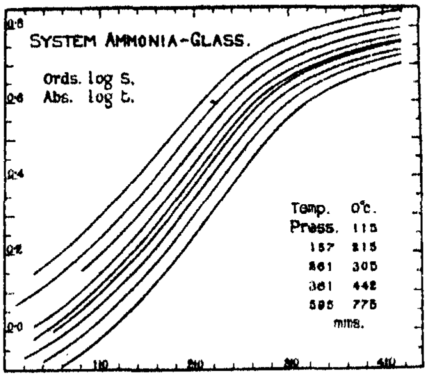

FIG. 3.

Figs. 4 and 5 represent two series of experiments at pressures of 115 and 305 mm. respectively, and covering a temperature range of 0° to 200° C. Here the isothermals form a complicated network. On examination it can be seen that the high-temperature experiments have the advantage at the start, but are ultimately overtaken by the low-temperature ones. In the case of the higher temperatures only the latter part of the S is seen.

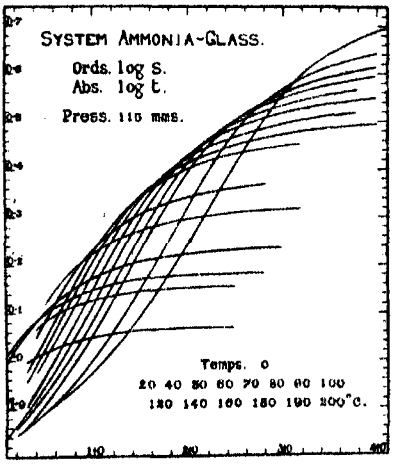

FIG. 4.

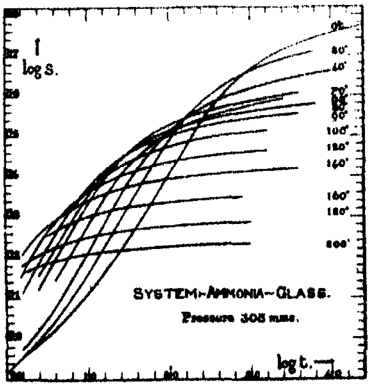

FIG. 5.

Rate of Sorption.

No satisfactory equation has been found to fit the whole course of the sorption process, but some interesting regularities appear when different co-ordinates are chosen. If log (sorption rate), instead of log sorption, is plotted against log time, graphs of the type shown in fig. 6 are obtained. These refer to experiments at 0° C., and, in order to avoid confusion, only three pressures have been depicted. The values of $d \log s/d \log t$ were obtained from the curves drawn through the experimental log s, log t points, by assuming these curves linear over short consecutive log time intervals (0·1). From these values the rates were calculated from the relationship $\frac{ds}{dt} = \frac{d \log s}{d \log t} \cdot \frac{s}{t}$. Each graph consists of two linear portions linked by a short curve. The two linear portions have been produced to intersection. The highest pressure graph starts off above the others, but, after bending over, the second limb falls at the bottom of the series. The first limbs run closely parallel to each other, and so do the second. The common slope of the first part is $-0·54$; that of the second $-1·36$. The " elbow " of each graph—the point of intersection of the two straight lines —is displaced to the left progressively as the pressure increases, and it may be noticed that the locus of these intersecting points is a straight line.

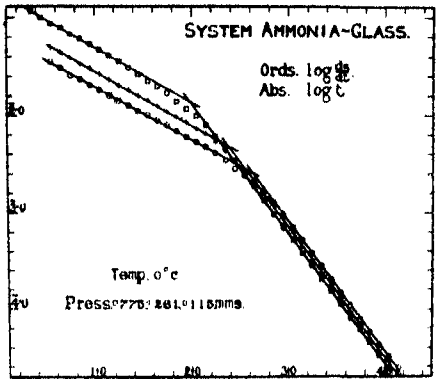

FIG. 6.

Evaluation of the Sorption Limits.

Assuming that the second limb of these rate graphs continues linear indefinitely, we may write an equation

$$\log ds/dt = a + b \log t,$$

where s is the sorption, t the time, and b the slope, $-1·36$. On integration we have :—

$$s = - \text{const.}/t^{0·36} + \sigma,$$

where σ represents the limiting value of sorption for $t = \infty$.

The experimental sorption values were plotted against $1/t^{0 \cdot 36}$ and the linear graphs so obtained were extrapolated to find the sorption limits. Table I gives the logarithms of these limits and the logarithms of the corresponding pressures, for the experiments at 0° C.:—

Table I.

Pressure (millimetres of Hg).	Log p.	Log σ (cubic centimetres at N.T.P.).	Chronological order of experiment.
774·4	2·8889	0·8808	9
594·5	2·7742	0·8586	8
442·4	2·6458	0·8405	7
360·6	2·5570	0·8218	6
305·9	2·4856	0·8124	1
305·0 (mean of 3)	2·4843	0·8224	10, 11, 12
260·6	2·4160	0·8119	5
215·1	2·3326	0·7941	4
157·6	2·1976	0·7870	3
114·8	2·0600	0·7709	2

These values are plotted in fig. 7 (at the top of the diagram), and it will be noted that from $p = 774$ to $p = 305$ mm. the points lie fairly well about a straight line, so that over this pressure range the Freundlich equation, $s = kp^{1/n}$, is applicable, n having the value 6. In the neighbourhood of 300 mm. pressure there appear to be alternative values for the sorption. One experiment falls into line with the higher pressures, while three other concordant experiments (of which the mean has been taken) yield a much higher result which seems to be associated with the curve running through the low-pressure points. An examination of the chronological order of the experiments makes it highly improbable that the discrepancies in this region are due to any progressive change in the nature of the sorbent. There would appear to be a real discontinuity, associated with a labile condition in the neighbourhood of 300 mm., a view which is supported by the fact that a similar break is observable when the logarithms of the sorption values at long equal times from the start are plotted against

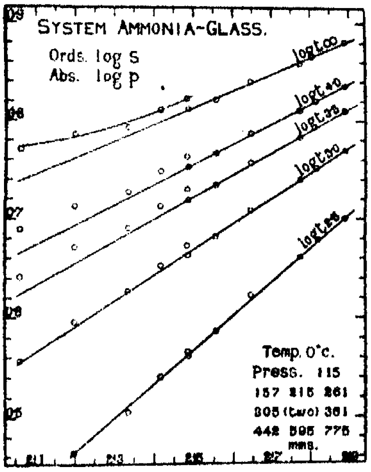

FIG. 7.

the logarithms of the pressures (fig. 7). On the other hand, the total change in the sorption limit over the experimental pressure range is small, and the points have been plotted with a very open ordinate scale. The apparent discrepancies are certainly greater than the probable experimental error, but not overwhelmingly greater.

In Table II the values of $d \log p/d \log s$ between 0·5 and 1 atmosphere pressure are given for a series of times.

Table II.

Log (time from start) (minutes)	$n = \dfrac{d \log p}{d \log s}$.	Log (time from start) (minutes).	$n = \dfrac{d \log p}{d \log s}$.
∞	6·0	2·5	2·88
4·0	4·86	2·0	2·39
3·5	4·47	1·5	2·30
3·0	3·90	1·0	2·42

At log time = 3, $d \log p/d \log s$ is constant over the whole pressure range: at 3·5, the discontinuity which is so conspicuous in the limit is just beginning to make its appearance.

The above table indicates that too small values may be assigned to the exponent n in the Freundlich equation if equilibrium is assumed to be attained in a few hours. According to our data, the sorption of ammonia by glass at 0° C. is, in the limit, proportional to $p^{1/6}$, over a pressure range of 300 to 770 mm.

Time, Pressure, and the Sorption Fraction.

In the log rate, log time graphs, the points of intersection of the two linear portions of each graph were found to lie on a straight line. When the sorption values corresponding to the times defined by these "elbow" points were read from the experimental log s, log t isothermals, they were found to represent very closely half the "equilibrium" values, and this striking regularity lends considerable support to the validity of these limits. The fact that the "elbow" time in the rate graph corresponds in every case to 50 per cent. sorption, suggests that the first half of the sorption process is of a different nature to the second half, where the rate of change of log ds/dt with log t is more than doubled. In Table III, log times at 50 per cent. sorption are compared with the "elbow" times as read from the rate graphs.

Table III.

Pressure (millimetres of Hg).	Log time at 50 per cent. sorption.	Log time at "elbow."
774·4	2·00	2·00
594·5	2·09	2·10
442·4	2·19	2·18
360·6	2·27	2·26
305·9	2·325	2·32
305·0 (mean of 3)	2·35	2·34
260·6	2·40	2·40
215·1	2·46	2·44
157·6	2·57	2·54
114·8	2·68	2·63

Composite Rate Graph.

When log time corresponding to 50 per cent. sorption is plotted against log pressure, the points fall closely about a straight line of negative slope 0·8. That is, d log t/d log p = constant = $-$ 0·8, so that $(p^{4/5}\,t)$ is a constant for

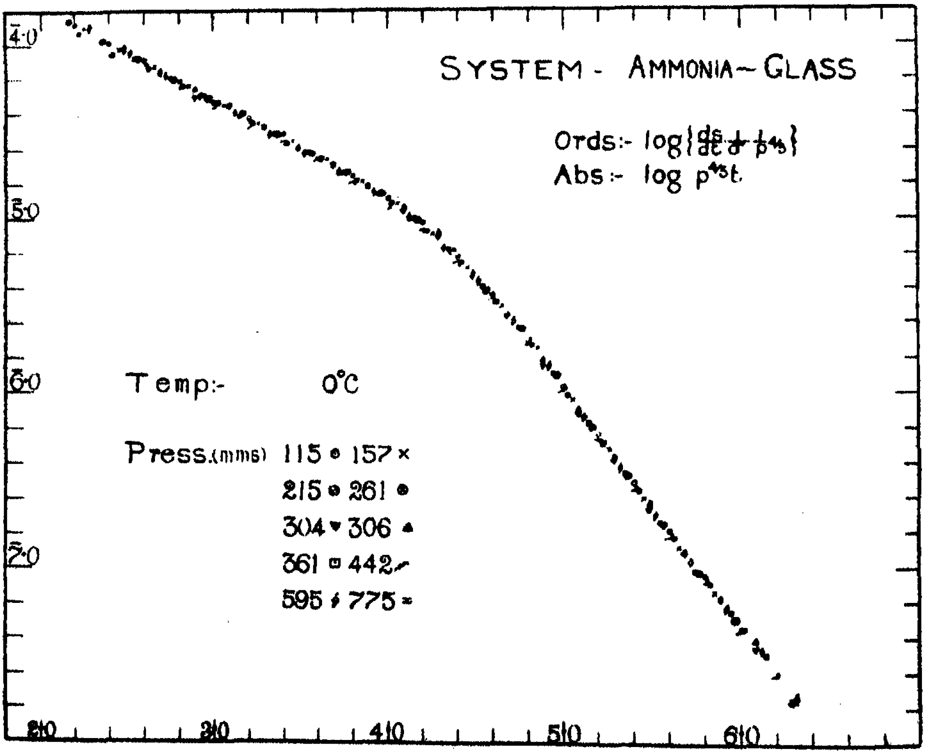

Fig. 8.

50 per cent. sorption. Now the slope of the straight line joining the "elbow" points in the rate graphs is $-1 \cdot 15$. If, instead of log ds/dt, we plot log (fractional rate)—log $(ds/dt \,.\, \sigma^{-1})$—against log time, each graph suffers a vertical displacement, and the locus of the elbow points, though still linear, now has a slope of unity $(-0 \cdot 99)$. The substitution of log $(p^{4/5}\,t)$ for log t brings all the elbow points on the same vertical line, and, finally, the introduction of the same pressure term into the ordinate denominator superimposes not only the elbow points, but the whole graphs, since the limbs are parallel.

Accordingly, when log $(ds/dt \,.\, \sigma^{-1}\, p^{-4/5})$ is plotted against log $(p^{4/5}\,t)$, there results a single composite graph which includes every experiment in the series at 0° C. This is shown in fig. 8.

Sorption Fraction Graphs.

A composite graph in terms of the sorption fraction can also be prepared. When s/σ is plotted against log time, the isothermals at 0° C. form a series of curves whose tangents at the same ordinate values are all parallel, the horizontal intercepts between any pair of curves being equal and independent of the ordinate value.

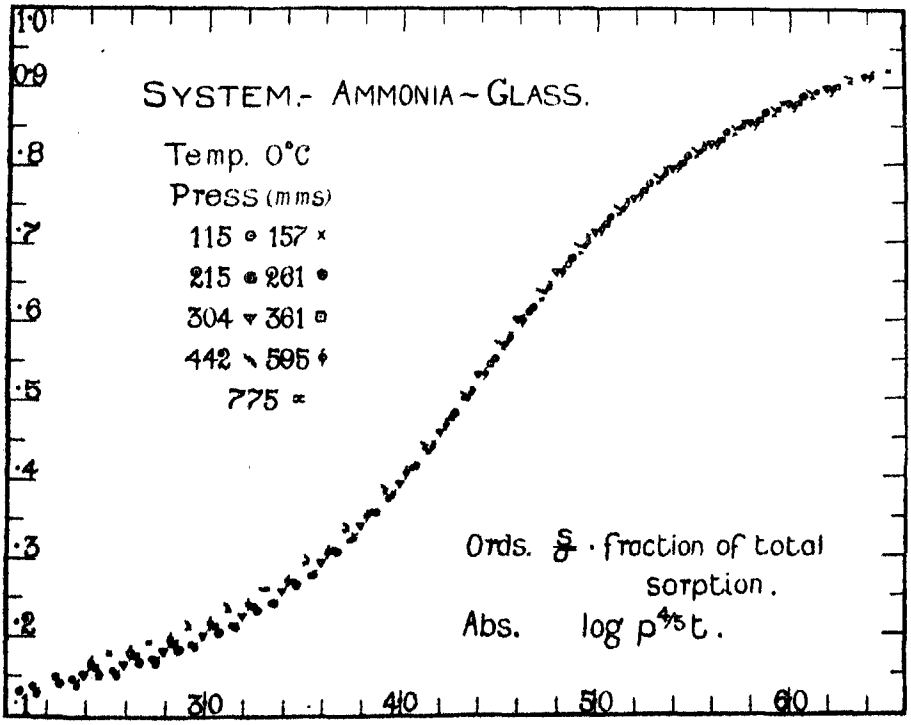

FIG. 9.

Such a system of curves can be superimposed by a suitable lateral shift, and this is achieved by adding log $p^{4/5}$ to all abscissa values. That is to say, the sorption fraction at constant temperature is a single-valued function of the product $(p^{4/5}\,t)$. This is shown in fig. 9. The divergence of the early points may be due in part to experimental error connected with the assessment of the time origin, since the introduction of the gas to the glass wool is by no means an instantaneous process. A more rigorous examination of the data, however, indicates that the pressure exponent is not quite constant, but tends towards unity for small values of the sorption fraction.

Temperature Relationships.

Extending the foregoing considerations to a series of isothermals for a number of temperatures under the same pressure, precisely analogous conclusions were reached. The log rate, log time graphs for the 115 mm. and the 305 mm. series are shown in figs. 10 and 11. Here the highest temperature isotherm starts off at the top and finishes at the bottom of the series. The slopes of the two limbs are essentially the same as in the pressure experiments. The "elbow" points, which again define the time for 50 per cent. sorption, lie on a straight line of slope − 0·87, and this slope again becomes unity (− 1·02) if the fractional rates are substituted for the absolute values. Log time for 50 per cent. sorption plotted against log absolute temperature yields a straight line of negative slope 13·7, so that $T^{13\cdot 7}\,t$ is a constant for 50 per cent. sorption, and a composite graph can be constructed as before.

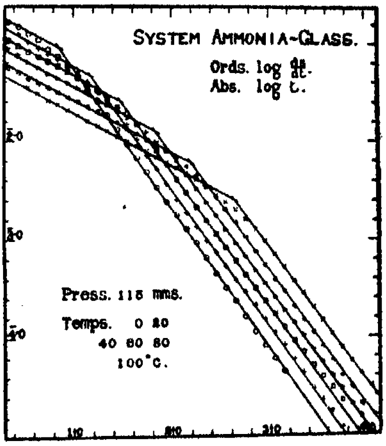

FIG. 10.

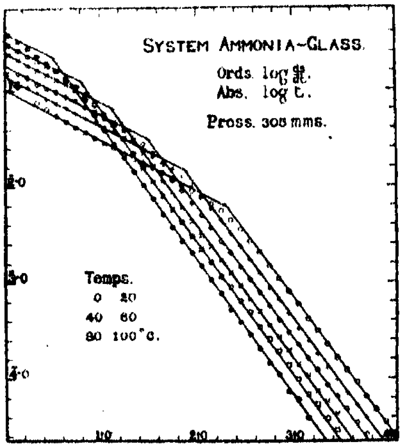

FIG. 11.

In the case of the temperature series, however, there is a significant alteration in the slope of the second limb of the rate graph with the temperature, so that perfect superposition cannot be achieved. Under 115 mm. pressure the extreme variation in this slope is from 1·36 at 0° C. to 1·68 at 200°, and, under 305 mm. pressure, from 1·36 to 1·52, over the same temperature range. Combining both temperature and pressure data, the sorption fraction can be expressed as a single-valued function of the product ($tp^{4/5}$ $T^{13 \cdot 7}$), accurately in the neighbourhood of 50 per cent. sorption, and approximately over a wide range of sorption. The close concordance for 50 per cent. sorption is indicated in Table IV, which also contains the sorption limits.

Table IV.

	115 mm.				305 mm.		
° C.	Log ($T^{13 \cdot 7}$)	Log time at 50 per cent. sorption.	Log ($T^{13 \cdot 7} t$)	σ (cubic centimetres at N.T.P.)	Log time at 50 per cent. sorption.	Log ($T^{13 \cdot 7} t$)	σ (cubic centimetres at N.T.P.)
0	33·38	2·68	36·06	5·900	2·33	35·71	6·493
20	33·80	2·19	35·99	4·885	1·88	35·68	5·685
40	34·19	1·84	36·03	4·438	1·50	35·69	4·872
50	34·38	1·68	36·06	4·220	—	—	—
60	34·56	1·49	36·05	3·945	1·12	35·68	4·232
70	34·73	1·32	36·05	3·680	0·97	35·70	4·240
80	34·90	1·14	36·04	3·433	0·79	35·69	3·920
90	35·07	0·98	36·05	3·193	0·63	35·70	3·705
100	35·23	0·83	36·06	2·973	0·52	35·75	3·405
120	35·54	0·49	36·03	2·425	0·19	35·73	3·005
140		Mean	36·042	2·108	Mean	35·704	2·655
160		Log $p^{4/5}$	1·649	1·738	Log $p^{4/5}$	1·987	2·285
180		Log ($tT^{13 \cdot 7}$ $p^{4/5}$)	37·691	1·548	Log ($tT^{13 \cdot 7}p^{4/5}$)	37·691	1·970
190				1·447			—
200				1·190			1·723

This value for the composite product may be compared with that deduced from all the experiments at 0° C.

For temperatures higher than 120° C. it is impossible to assess the position of the elbow in the rate graph, since the first limb is becoming vanishingly short. For the same reason no accurate time can be assigned to the half-sorption point on the log s, log t isothermal.

Table V.

Pressure.	Log $p^{4/5}$.	Log time for 50 per cent. sorption.	Log $(p^{4/5}\,t)$.
774·4	2·311	2·00	4·311
594·5	2·219	2·09	4·309
442·4	2·117	2·19	4·307
360·6	2·046	2·27	4·316
305·9	1·989	2·325	4·314
260·6	1·933	2·40	4·333
215·1	1·866	2·46	4·326
157·6	1·758	2·57	4·328
114·8	1·648	2·68	4·328
		Mean	4·319
		$t^\circ = 0$, log $T^{13.7}$ =	33·376
		Log $(t T^{13.7}\, p^{4/5})$	37·695

Temperature Relationships in the Limit.

When the limiting sorption values are plotted against the reciprocals of the absolute temperatures, a linear relationship is indicated (fig. 12), whereas the logarithms of sorption plotted against any function of the temperature yield a curve. There is, however, a disappointing want of regularity about the distribution of the points, which show definite re-entrant angles. Thus the limiting value for sorption at 70° C. and 305 mm. pressure is greater than that for 60° C. at the same pressure; yet the times corresponding to 50 per cent. sorption fall in their correct positions on the log time, log T graph. The fact that the discrepancies observable when absolute values of sorption are under consideration disappear when the sorption fraction is substituted, suggests that, from experiment to experiment, the capacity of the sorbent was subject to

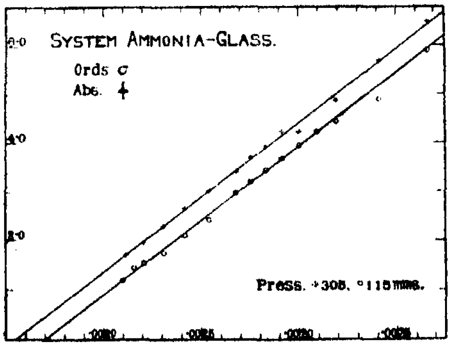

FIG. 12.

small variations. Such variation, implying a vertical shift of the isothermal as a whole, does not alter the course of the sorption process (as considered in terms of the sorption fraction), and is therefore to be distinguished from the progressive change in behaviour observed during the preliminary experiments. Some accidental variation of procedure affecting the rate of heating during out-gassing, or the subsequent rate of cooling, may have modified the capacity of the sorbent in an indeterminate manner. Further, it seems not unreasonable to suppose that the "available capacity" of the sorbent might increase with temperature in a manner not necessarily uniform.

If the straight lines in fig. 12 are extrapolated to zero sorption, they cut the temperature axis at points corresponding to 370° C. and 315° C. for the 305 mm. and the 115 mm. series, respectively.

No particular significance is to be attached to the numerical values of the exponents of pressure and temperature employed to construct the composite graphs. The figure selected is in each case a compromise, peculiarly appropriate to 50 per cent. sorption. Thus, if log time is plotted against log T for 25 per cent. and for 75 per cent. sorption, a linear graph is obtained in each case, but the values of $d \log t/d \log T$ are now $-13\cdot0$ and $-14\cdot4$ respectively, as compared with $-13\cdot7$ for 50 per cent. sorption. The temperature and pressure exponents found may also be characteristic of the high degree of desiccation of the glass, but in this connection it is noteworthy that the Freundlich exponent for the pressure range $0\cdot5-1$ atmosphere has the same value, namely, 6, as that previously found by Bangham and Burt with glass that certainly contained more water. This suggests that, while the condition of the sorbent may have a marked effect on the early course of the sorption process, the pressure coefficient in the limit, or after a very long time, may be largely independent of this condition.

Desorption.

The apparatus used in these experiments was not adapted for desorption measurements. It had been found by Bangham and Burt that if, at the end of a long period of sorption, the pressure in their apparatus was reduced in a series of steps, a linear relationship existed between the logarithms of the quantities of gas remaining on the glass and the logarithms of the corresponding pressures. Moreover, these quasi-equilibrium values were very much greater than the limits being approached from the other direction; the reciprocal slopes of the sorption and desorption lines being 6 and 12 respectively. The striking change in the slope of the rate graphs in the neighbourhood of 50 per cent. sorption suggests that the glass presents to the ammonia molecules alternative types of accommodation; one-half of the total accommodation being more readily available than the other half. If the further assumption is made that half the gas taken up cannot be removed by isothermal reduction of pressure, a plausible explanation of desorption hysteresis is afforded, and it becomes possible to construct a hypothetical desorption line from the sorption data.

If s_1 represents the limiting value of sorption at a particular pressure p_1, then on reducing the pressure to p_2, where the sorption limit is s_2, the corresponding point in the desorption line will be $(s_1 + s_2)/2$. This method of calculation leads to a nearly linear desorption line of reciprocal slope 12·3, which is almost identical with the earlier experimental value (12·6). The experimental value, however, refers to a lower pressure range.

The Rate of Sorption.

The limiting quantity of ammonia taken up by the glass wool at 0° C. and one atmosphere pressure is about 7·5 c.c. measured at N.T.P. This is some twelve times the quantity required to form a monomolecular layer on the glass surface as measured (1·6 sq. metres). The extraordinary feature of the low-temperature experiments is the enormous length of time apparently needed to attain, say, 99 per cent. sorption.

It was estimated that nearly seven years would be necessary in the case of the 774 mm. experiment at 0° C., and more than half a century at 115 mm. at the same temperature; 50 per cent. sorption was reached in one hundred minutes and in eight hours, respectively.

At a temperature of 200° and a pressure of half an atmosphere, 50 per cent. sorption is achieved in a few seconds, and 99 per cent. inside an hour, but, even at this temperature, the later stages of the process are slow.

For the purpose of examining the variation in the rate of sorption with pressure and temperature, we may select for comparison the half-sorption values as distinctive points. For a constant temperature series we have at 50 per cent. sorption

$$\frac{d \log t}{d \log p} = -0\cdot 8 \text{ and } \frac{d \log \frac{ds}{dt}}{d \log t} = -1\cdot 15.$$

Therefore

$$\frac{d \log \frac{ds}{dt}}{d \log p} = 0\cdot 9, \text{ whence } \frac{ds}{dt} = Cp^{0\cdot 9}.$$

That is, at constant temperature the rate of sorption is very nearly directly proportional to the pressure.

For a constant pressure series, at 50 per cent. sorption,

$$\frac{d \log t}{d \log \mathrm{T}} = -13\cdot 7 \text{ and } \frac{d \log \frac{ds}{dt}}{d \log t} = -0\cdot 87.$$

Therefore

$$\frac{d \log \frac{ds}{dt}}{d \log \mathrm{T}} = 12, \text{ whence } \frac{ds}{dt} = \mathrm{C}'\mathrm{T}^{12}.$$

At constant pressure the rate of sorption is approximately doubled for every 20° C. rise in temperature.

Typical Experiment.

The numerical results of a typical experiment are given below :—

Temperature, 0° C. Pressure, 775 mm. of Hg.

Log time (minutes).	Log sorption (cubic centimetres at N.T.P.).	Log time (minutes).	Log sorption (cubic centimetres at N.T.P.).	Log time (minutes).	Log sorption (cubic centimetres at N.T.P.).	Log time (minutes).	Log sorption (cubic centimetres at N.T.P.).
0·28	0·1446	1·449	0·4174	2·114	0·6113	3·033	0·7727
0·43	0·1729	1·512	0·4355	2·230	0·6400	3·100	0·7793
0·57	0·1985	1·585	0·4579	2·322	0·6616	3·185	0·7868
0·70	0·2246	1·651	0·4776	2·378	0·6744	3·462	0·8060
0·80	0·2483	1·712	0·4958	2·518	0·7028	3·657	0·8195
0·91	0·2741	1·765	0·5119	2·591	0·7157	3·763	0·8255
1·029	0·3034	1·826	0·5280	2·607	0·7191	3·946	0·8341
1·130	0·3303	1·898	0·5509	2·774	0·7458	4·066	0·8384
1·209	0·3520	1·978	0·5743	2·819	0·7503	4·202	0·8449
1·316	0·3802	2·045	0·5935	2·926	0·7623	4·416	0·8531

Summary.

1. Though complete desiccation of glass is impracticable, it is possible, by suitable treatment, to maintain it indefinitely in such a condition that its behaviour towards ammonia can be closely recovered.

2. The shape of the sorption curve depends on the dryness of the sorbent. For a state of maximum desiccation it is S-shaped, only the top section of the S being available for observation in the case of the higher temperature experiments.

3. The sorption process can be divided into two parts, represented by straight lines when log sorption rate is plotted against log time. The slope of both lines is independent of pressure and varies only slightly with temperature. Their point of intersection corresponds, in all cases, to 50 per cent. sorption.

4. By a suitable choice of co-ordinates the complete sorption process can be represented as a single-valued continuous function of temperature, pressure and time. As regards temperature variation, this is only approximately true.

5. At 50 per cent. sorption the rate of sorption is nearly proportional to the pressure at constant temperature, and is doubled for every 20° C. rise in temperature at constant pressure.

6. At constant temperature, log sorption, in the limit, was found to be a linear function of log pressure between 0·5 and 1 atmosphere. At lower pressures a departure from linearity was observed.

7. At constant pressure, sorption, in the limit, was found to be a linear function of the reciprocal of the absolute temperature.

The "constant-pressure" apparatus was based on a design suggested by Prof. D. H. Bangham.

A grant from the Brunner-Mond Research Fund partly defrayed the expenses of this investigation, and we are also indebted to the Department of Scientific and Industrial Research for a maintenance grant to one of us (M. F.).

A Gauge-Invariant Tensor Calculus.

By M. H. A. NEWMAN, M.A., Fellow of St. John's College, Cambridge.

(Communicated by A. S. Eddington, F.R.S.—Received June 14, 1927.)

It has been pointed out by Weyl, Eisenhart, Veblen and others,* that the differential equations of geodesics in a manifold with a general affine structure do not remain unchanged in form when a new parameter is adopted. If in the equation

$$\frac{d^2x^i}{d\tau^2}+\Gamma^i_{rs}\frac{dx^r}{d\tau}\frac{dx^s}{d\tau}=0 \qquad (0.1)$$

τ is replaced by $\bar\tau(\tau)$, the resulting equation is

$$\frac{d^2x^i}{d\bar\tau^2}+\Gamma^i_{rs}\frac{dx^r}{d\bar\tau}\frac{dx^s}{d\bar\tau}-\frac{d\bar\tau}{d\tau}\frac{d^2\tau}{d\bar\tau^2}\frac{dx^i}{d\bar\tau}=0. \qquad (0.2)$$

This means that the equations (0.1) not only give the *form* of the geodesic with an assigned direction at a given point, but also select a parameter, which, when two arbitrary constants (" origin " and " unit ") have been fixed, may be taken as a *measure* of any arc of the curve. (For example, when $\Gamma^i_{rs}=0$, the geodesics may be represented parametrically by

$$x^i=a^if(\tau)+b^i,$$

where $f(\tau)$ is any steadily increasing function; but the equations $d^2x^i/d\tau^2=0$ are satisfied only by $x^i=a^i\tau+b^i$.)

It is natural to enquire whether the definition cannot be modified so that the equations of geodesics shall have invariant form under changes of parameter as well as under changes of co-ordinates. The equations themselves will then no longer provide a natural measure of length, so that it is a species of *gauge-invariance* that is required. The question has some physical interest, for it is the *form* of the path of a particle that is the primary subject of investigation in field theories; the interpretation that can be given to the *measure* of an arc in the space-time manifold is at any rate much less obvious. It is possible that the equations of physics should have "gauge-invariant," as well as tensor form.

---

* Weyl, 'Gött. Nachr.,' p. 99 (1921); L. P. Eisenhart, 'Proc. Nat. Acad. Sci.,' vol. 8, p. 233 (1922); O. Veblen, *ibid.*, p. 347. Numerous papers on cognate subjects by Eisenhart, Veblen and T. Y. Thomas have appeared since 1922 in the 'Proc. Nat. Acad. Sci.'

A set of equations having this new invariance property was given by Weyl, namely,

$$\frac{d^2x^i}{d\tau^2} + \Gamma^i_{rs}\frac{dx^r}{d\tau}\frac{dx^s}{d\tau} - \phi_r\frac{dx^r}{d\tau}\frac{dx^i}{d\tau} = 0, \tag{0.3}$$

where ϕ_r is a vector field which is replaced by

$$\phi_r - \frac{1}{\lambda}\frac{\partial\lambda}{\partial x_r},$$

when $d\tau$ is replaced by $\lambda d\tau$; but the themes pursued in Weyl's paper were purely geometrical, and he was not led to construct a general invariant calculus, capable of dealing with quantities of any "weight." Indeed, such a calculus seems to be lacking at present: even in Weyl's original metrical gauge theory* the covariant derivative of a tensor of weight m ($\neq 0$) has not itself "gauge character," *i.e.*, is not simply multiplied by a scalar when the gauge changes.

The calculus developed in the present paper is a purely analytical one, in the sense that the choice of definitions is governed by numerical considerations. The antitheses

	Change of component-system	Change of gauge-system
	tensor character	gauge character
(for displacements)	direction(†)	measure
	Γ^i_{rs}	ϕ_r,

are strictly observed (the last replacing Weyl's antithesis:

$$g_{ik} \qquad\qquad \phi_r$$

with Γ^i_{rs} "above" both). The analysis is simplified by the fact that if a fundamental tensor is subsequently introduced and

$$\sqrt{g_{ik}dx^i dx^k}$$

identified with measure of dx^i, the new "covariant" derivative of g_{ik} is zero: raising and lowering of indices is commutative with invariant derivation, just as it is in an ordinary Riemann manifold.

It is hardly necessary to say that the ideas elaborated in § 1 of this paper lie very near the surface in the works mentioned in the footnote on p. 603.‡

---

* *Cf. e.g.*, 'Raum, Zeit, Materie,' 5th Edn., pp. 121, *seq.* (All references "RZM" are to the 5th edition of this book.)

† The *direction* of the vector a^i is the set of ratios $a^1 : a^2 : a^3 : \ldots : a^n$.

‡ [*Note added in proof.*—I find that M. P. Apfell has considered "weighted derivatives" in his 'Mécanique rationelle,' vol. 5, p. 143 (1926), obtaining the equations 4.6 and 8.2 of this paper; but the calculus does not seem to have been applied to obtain the identities of § 2.]

§ 1. *Weighted Affine Structure.*

1. Let M_n be an n-dimensional manifold provided not only with a co-ordinate system—a rule for assigning n co-ordinates to every point—but also a *measure-system*, that is, a rule for assigning a positive scalar *measure* $|PP'|$, to every small displacement $\overrightarrow{PP'}$. The connection between the components and measure of $\overrightarrow{PP'}$ must be such that, if k is any scalar, then

$$|kPP'| = k\,|PP'|,$$

but it is otherwise unrestricted, save for the usual continuity assumption: if P and P′ are near Q and Q′, $|PP'|$ is nearly equal to $|QQ'|$.

This being premised, a *measure* can be assigned to any finite arc γ of simple character* by taking points $P_1, P_2, \ldots, P_q$, in order along the curve and defining $|\gamma|$ to be the limit of

$$|P_1P_2| + |P_2P_3| + \ldots + |P_{q-1}P_q|$$

when the density of the points P_i on γ is indefinitely increased. If P_0 is a fixed point on γ the measure, τ, of the arc P_0P can be taken as the parameter, and the equations of γ given as

$$x^i = x^i(\tau).$$

Suppose that a second measure-system, $\bar{\tau}$, is set up, *i.e.*, that a fresh measure, $d\bar{\tau}$, is assigned to every small displacement. We shall consider only *gauge* changes, *i.e.*, changes of the measure-system such that *for all displacements at the same point the ratio $d\bar{\tau}/d\tau$ is the same.* This ratio

$$\lambda = \frac{d\bar{\tau}}{d\tau}$$

is, then, a *function of position* in M_n. By this restriction we are, in fact, supposing a *metric* set up at every point, for the ratios of the measures of two displacements at the same point is independent of a mere "gauge" change. In particular, displacements at the same point are *equally long* if they have equal measures in any one gauge-system; it then follows that their measures are equal in all systems. Between displacements at different points equality of measure is *not* a gauge-true relation, and a more elaborate definition will be necessary.

2. If the measure τ is taken as the parameter of a curve, the vector

$$u^i = \frac{dx^i}{d\tau}$$

---

* A rigorous discussion of necessary conditions for "rectifiable" character cannot suitably be undertaken here. For an axiomatic treatment of such matters. *cf.*, K. Menger, 'Proc. Amsterdam,' vol. 29, p. 1 (1926).

is called the *gradient*. Its components not only vary with the co-ordinate system; they are multiplied by λ^{-1} when $\lambda d\tau$ replaces $d\tau$. We are led then to consider tensors whose components are multiplied by a function of position when the gauge changes. Such quantities have a double character, *tensor character*, which determines how they behave under a change of co-ordinates, and *gauge character*, which settles what power of λ they are multipled by when $d\tau$ is replaced by $\lambda d\tau$. If the multiplying factor is λ^m the tensor is said to have *weight m*. Thus, u^i is of weight -1, while dx^i is of weight 0, or *gauge-invariant*.

A *gauge-true* relation is one which remains true if the quantities on both sides are replaced by their components in another gauge-system. Evidently both sides of a gauge-true relation must have the same weight, and the quantity $a^i + b^i$ has not gauge-character at all unless the weights of a^i and b^i are the same. On the other hand, any product of tensors has both tensor- and gauge-character: its weight is the sum of the weights of the factors.

3. For each separate gauge system an affine-structure can now be introduced in the way that has been made familiar by Levi-Cività and Weyl; that is, n^3 functions of position, K^i_{rs}, are chosen, and then if a^i is a contra variant vector at the point (x) the vector

$$a^i + \mathbf{d}a^i = a^i - K^i_{rs}\, a^r\, dx^s \tag{3.1}$$

at $(x + dx)$ is defined to be *affine-equal** to a^i at (x).

There is, however, one modification. *Since tensors of different weights may not be added, there is no need to assume that the affine components, K^i_{rs}, are the same for the different weight-categories, i.e.*, we may assume that if a^i is a vector of weight m at (x), the affine-equal vector at $(x + dx)$ is

$$a^i - K^i_{rs}\,(m)\, a^r\, dx^s, \tag{3.2}$$

where $K^i_{rs}\,(m)$ may be a function of m as well as the co-ordinates.

This modification has important consequences. Let us return for a moment to the gaugeless affine theory. There is, of course, an expression similar to 3.1, say

$$b_i + \mathbf{d}b_i = b_i + \Lambda^r_{is}\, br\, dx_s,$$

for the projection of a covariant vector b_i. It is usually assumed that

$$\Lambda^i_{rs} = K^i_{rs},\dagger$$

the reason being as follows (if geometrical arguments are set aside) :—

---

* There seems to be no name already current for this relation shorter than "obtained from a^i by parallel projection."

† But see Schouten, 'Der Ricci-Kalkül,' Chap. II.

If it is assumed that the "affine-increment" of a function of vectors follows the usual rule for calculating total differentials,

$$\mathbf{d}\Phi(\mathrm{A}, \mathrm{B}, \ldots) = \frac{\partial\Phi}{\partial\mathrm{A}}\,\mathbf{d}\mathrm{A} + \frac{\partial\Phi}{\partial\mathrm{B}}\,\mathbf{d}\mathrm{B} + \ldots \tag{3.3}$$

(where A, B, . . . denote tensors or tensor-densities of any character), it follows that, in particular,

$$\mathbf{d}\mathrm{AB} = \mathrm{A}\mathbf{d}\mathrm{B} + \mathrm{B}\mathbf{d}\mathrm{A}$$

and therefore

$$\begin{aligned} \mathbf{d}\,(a^i b_i) &= (a^i \Lambda^r_{is} b_r - \mathrm{K}^i_{rs} a^r b_i)\, dx^s \qquad (3.4) \\ &= a^r b_i\,(\Lambda^i_{rs} - \mathrm{K}^i_{rs})\, dx^s. \end{aligned}$$

Now it is imperative for the unity of the (gaugeless) affine calculus that the affine-increment of all tensors of the same character shall be given by the same rule, and in particular that if c is a *scalar* the affine increment of c shall be

$$\mathbf{d}c = \mathrm{F}(c, dx)$$

where the form of F does not vary from scalar to scalar. This can only be made compatible with (3.3) by taking F to be zero:

$$\mathbf{d}c = 0.$$

For we must have, in particular, for all values of a and b,

$$\mathrm{F}(ab, dx) = a\mathrm{F}(b, dx) + b\mathrm{F}(a, dx)$$

and the only solution of this functional equation is

$$\mathrm{F}(a, dx) \equiv 0,$$

as may at once be seen by differentiating it for b and then letting $b = 0$. Thus in the gaugeless theory purely analytical considerations compel us to identify affine and numerical equality between scalars. Applied to (3.4), in which $a^r b_i$ can have any values, this gives

$$\Lambda^i_{rs} = \mathrm{K}^i_{rs}.$$

With our new assumptions, however, the grounds for supposing $\mathbf{d}c$ zero, and therefore for taking Λ and K to be equal, disappear. Scalars of different weights may very well have affine-increments formed by different rules, *i.e.*, if c is of weight m the proper assumption is

$$\mathbf{d}c = \mathrm{F}_m(c, dx)$$

and if the weights of a and b are m and m' equation (3.5) is replaced by

$$\mathrm{F}_{m+m'}(ab, dx) = a\mathrm{F}_{m'}(b, dx) + b\mathrm{F}_m(a, dx).$$

We assume then that the new increments, $\underset{\bullet}{\mathbf{d}}a^i$ and $\underset{\bullet}{\mathbf{d}}b^i$, are given by

$$\underset{\bullet}{\mathbf{d}}a^i = -\,\mathrm{K}^i_{rs}(m)\,a^r\,dx^s$$
$$\underset{\bullet}{\mathbf{d}}b_i = \quad \Lambda^r_{is}(m)\,b_r\,dx^s.$$

4. The argument for making $\mathbf{d}c$ zero has still its full force when applied to scalars of weight 0; for the product of two such scalars is of weight zero. Hence, if a^i and b_i are of weights m and $-\,m$ respectively, we must have

$$a^ib_i = (a^i - \mathrm{K}^i_r\,(m)\,a^r dx^s)\,(b_i + \Lambda^r_{is}(-m)\,b_r dx^s),$$

and therefore

$$\mathrm{K}^i_{rs}(m) = \Lambda^i_{rs}(-\,m). \tag{4.1}$$

In particular

$$\mathrm{K}^i_{rs}(0) = \Lambda^i_{rs}(0)$$
$$= \Gamma^i_{rs},$$

say.

The affine-increment of a *zero* scalar must clearly be zero, whatever its weight. If then a^i is of weight m and b_i is of weight 0, and

$$a^ib_i = 0, \tag{4.2}$$

it must follow that

$$(a^i - \mathrm{K}^i_{rs}(m)\,a^r dx^s)\,(b_i + \Gamma^r\;b_r dx^s) = 0,$$

i.e.,

$$a^rb_i(\mathrm{K}^i_{rs}(m) - \Gamma^i_{rs}) = 0.$$

That this should be true when a^i and b_i are any vectors satisfying (4.2) requires that there should exist a vector $\phi_s(m)$ with the property that

$$\mathrm{K}^i_{rs}(m) - \Gamma^i_{rs} = \delta^i_r\,\phi_s(m). \tag{4.3}$$

Hence (using 4.1) if a^i and b_i are *any* vectors of weights m and m' respectively,

$$\underset{\bullet}{\mathbf{d}}(a^ib_i) = -\,a^ib_i dx^s[\phi_s(m) - \phi_s(-\,m')].$$

But a^ib_i is of weight $m + m'$, and therefore, if unity is to be preserved within each "weight-category",

$$\phi_s(m) - \phi_s(-\,m')$$

must be a function of $m + m'$. This entails

$$\phi_s(m) = m\phi_s(1)$$
$$= m\phi_s,$$

say, *i.e.*,

$$\mathrm{K}^i_{rs}(m) = \Gamma^i_{rs} + m\delta^i_r\phi_s, \quad \Lambda^i_{rs}(m) = \Gamma^i_{rs} - m\delta^i_r\phi_s.\;*$$

---

* The writers mentioned on p. 603 find

$$\mathrm{K}^i_{rs}(-1) = \Gamma^i_{rs} - \tfrac{1}{2}\,(\delta^i_r\phi_s + \delta^i_s\phi_r),$$

but since K is only used by them in the equations of geodesics

$$\frac{du^i}{ds} + \mathrm{K}^i_{rs}u^ru^s = 0,$$

the presence of an unsymmetrical part in K^i_{rs} would be without significance in their work.

If then $\mathbf{d}$ denotes the ordinary affine-increment formed with the components Γ^i_{rs}, viz.,

$$\mathbf{d}a^i = -\Gamma^i_{rs}a^r dx^s, \qquad \mathbf{d}b_i = \Gamma^r_{is}b_r dx^s,$$

then

$$\underset{\bullet}{\mathbf{d}}a^i = -\mathrm{K}^i_{rs}(m)\,a^r dx^s = \mathbf{d}a^i - ma^i\phi_s dx^s,$$

$$\underset{\bullet}{\mathbf{d}}b_i = \Lambda^r_{is}(m)\,b_r dx^s = \mathbf{d}b_i - mb_i\phi_s dx^s;$$

i.e., in both cases $\underset{\bullet}{\mathbf{d}}$ and $\mathbf{d}$ are connected by the symbolical relation

$$\underset{\bullet}{\mathbf{d}} = \mathbf{d} - m\phi_s\,dx^s. \tag{4.4}$$

If the analogue of (3.3) is assumed to hold for the operator $\underset{\bullet}{\mathbf{d}}$:

$$\underset{\bullet}{\mathbf{d}}\Phi(\mathrm{A}, \mathrm{B}, \dots) = \frac{\partial\Phi}{\partial\mathrm{A}}\underset{\bullet}{\mathbf{d}}\mathrm{A} + \frac{\partial\Phi}{\partial\mathrm{A}}\underset{\bullet}{\mathbf{d}}\mathrm{B} + \dots, \tag{4.5}$$

the rule (4.4) holds for all tensors and tensor-densities: *if A is any tensor quantity*

$$\underset{\bullet}{\mathbf{d}}\mathrm{A} = \mathbf{d}\mathrm{A} - m\mathrm{A}\phi_s dx^s. \tag{4.6}$$

An example will suffice. Let c^{ik} be a $(2:0)$ tensor of weight m, let $a^i_{(r)}$ $(r = 1, 2, \dots n)$ be n independent vectors of weight m, $b^i_{(r)}$ n independent vectors of weight 0. Then there exist scalars κ_{rs} of weight 0, such that

$$c^{ik} = \sum_{rs}\kappa_{rs}\,a^i_{(r)}\,b^k_{(s)},$$

Hence, by (4.5),

$$\begin{aligned}\underset{\bullet}{\mathbf{d}}c^{ik} &= \sum_{rs}\kappa_{rs}(a^i_{(r)}\,\underset{\bullet}{\mathbf{d}}b^k_{(s)} + b^k_{(s)}\,\underset{\bullet}{\mathbf{d}}a^i_{(r)})\\ &= \mathbf{d}c^{ik} - m\sum_{rs}\kappa_{rs}\phi_t a^i_{(r)}\,dx^t\,b^k_{(s)}\\ &= \mathbf{d}c^{ik} - mc^{ik}\phi_s\,dx^s.\end{aligned}$$

In particular, if c is a scalar of weight, m,

$$\underset{\bullet}{\mathbf{d}}c = -mc\phi_s dx^s.$$

5. Having thus set up an affine-structure in each gauge system we must now consider how these structures are related to each other. Our object will be to make the projection,

$$\mathrm{A} + \underset{\bullet}{\mathbf{d}}\mathrm{A},$$

independent of the gauge system, *i.e.*, to arrange that the quantities

$$\mathrm{A} + \mathbf{d}\mathrm{A} - m\mathrm{A}\phi_s\,dx^s$$

in the various gauge systems shall be the components in those systems of a tensor at $(x + dx)$, of the same weight as A.

This requires in the first place that if a^i is of weight 0, $a^i + \underset{\bullet}{\mathbf{d}}a^i$ (in this case identical with $a^i + \mathbf{d}a^i$) shall be unaltered by a change of gauge. *The quantities* Γ^i_{rs} *are gauge-invariants.*

If A is a tensor or tensor-density of weight m its components in a new gauge-system, ($d\bar{\tau} = \lambda(x)\, d\tau$), are

$$\bar{A} = \lambda^m A,$$

and its projection at $(x + dx)$ is

$$\bar{A} + \mathbf{d}\bar{A} - m\bar{A}\bar{\phi}_s\, dx^s = \lambda^m (A + \mathbf{d}A - mA\bar{\phi}_s dx^s). \tag{5.1}$$

These are to be the $\bar{\tau}$-components of the tensor at $(x + dx)$ whose τ-components are $A + \underset{\bullet}{\mathbf{d}}A$; *i.e.*, the right-hand side of (5.1) must be equal to

$$\{\lambda(x + dx)\}^m (A + \mathbf{d}A - mA\phi_s dx^s) = \lambda^m \left[A + \mathbf{d}A - mA\left(\phi_s - \frac{1}{\lambda}\frac{\partial\lambda}{\partial x_s}\right)dx^s\right],$$

where λ means $\lambda(x)$. Hence *the necessary and sufficient condition that all the quantities* $A + \underset{\bullet}{\mathbf{d}}A$ *should be the components of the same tensor, of weight* m, *at* $(x + dx)$ *is that*

$$\bar{\phi}_s = \phi_s - \frac{1}{\lambda}\frac{\partial\lambda}{\partial x_s}.$$

This unique tensor will be called the *projection* of A at $(x + dx)$, and said to be *affine-equal* to A. $\underset{\bullet}{\mathbf{d}}A$ will be called the *weighted affine-increment.*

(It will be noticed that while Γ^i_{rs} has gauge- but not tensor-character the reverse is true of ϕ_i, in agreement with the antitheses set out on p. 604.)

Let P_0 have co-ordinates x^i_0, let ϕ^0_s stand for $\phi_s(x_0)$, and let

$$\lambda(x) = 1 + \sum_s x^s \phi^0_s.$$

If a new gauge system

$$d\bar{\tau} = \lambda\, d\tau$$

is introduced,

$$\bar{\phi}_s = \phi_s - \frac{1}{\lambda}\phi^0_s,$$

$$= 0 \text{ at } P_0.$$

Thus *a gauge-system can always be introduced in which the field* ϕ_s *vanishes at an assigned point* P_0. Such a system will be said to be *normal* at P_0.

6. The relation that has been called "affine-equality" is usually interpreted geometrically as "equal and parallel." The fields Γ^i_{rs} and ϕ_s, which together determine the "weighted" relation, lead naturally to separate definitions of "parallel" vectors of any weight, and of "equally long" displacements.

A vector b^i at $(x + dx)$ is *parallel* to a^i at (x) if it has the *same direction* as $a^i + \underset{\bullet}{\mathbf{d}}a^i$, *i.e.*, if

$$b^i = \kappa\,(a^i + \underset{\bullet}{\mathbf{d}}a^i),$$

where κ is a scalar. Now

$$\begin{aligned} a^i + \underset{\bullet}{\mathbf{d}}a^i &= a^i - \Gamma^i_{rs}\,a^r\,dx^s - m a^i \phi_s\,dx^s \\ &= (a^i - \Gamma^i_{rs}a^r\,dx^s)\,(1 - m\phi_s\,dx^s), \end{aligned}$$

if second order quantities are neglected. Hence *the direction of vectors at $(x + dx)$ parallel to a^i at (x) is determined by the field Γ^i_{rs} alone, being the direction of*

$$a^j - \Gamma^i_{rs}a^r\,dx^s.$$

A displacement δy^i at $(x + dx)$ is *as long as* δx^i at (x)* if it is as long as $\delta x^i + \underset{\bullet}{\mathbf{d}}\,(\delta x^i)$; *i.e.*, if

$$|\,\delta y^i\,| = |\,\delta x^i + \underset{\bullet}{\mathbf{d}}\,(\delta x^i)\,|\,.$$

The form of the relation thus set up between the measures of equally long displacements depends on the variation of the function

$$|\,dx^i\,|$$

from point to point, but it is interesting to follow the consequences of an additional assumption.

Let $\delta\tau$ be the measure of δx^i, let u^i be $\delta x^i/\delta\tau$, and let

$$u^i + \underset{\bullet}{\mathbf{d}}u^i = \delta z^i/\delta\tau.$$

If it is assumed that the *projection of a gradient is itself the gradient of a displacement* (an assumption which restricts Γ^i_{rs} and ϕ_s), $\delta\tau$ is also the measure of δz^i, *i.e.*, of

$$\begin{aligned} \delta\tau\,(u^i + \underset{\bullet}{\mathbf{d}}u^i) &= \delta\tau\,(u^i - \Gamma^i_{rs}u^r\,dx^s + u^i\phi_s\,dx^s) \\ &= (\delta x^i - \Gamma^i_{rs}\,\delta x^r\,dx^s)\,(1 + \phi_s\,dx^s). \end{aligned}$$

Hence the measure of $\delta x^i - \Gamma^i_{rs}\,\delta x^r\,dx^s$, which is $\delta x^i + \underset{\bullet}{\mathbf{d}}\,(\delta x^i)$, is

$$\delta\tau\,(1 - \phi_s\,dx^s).$$

The ratio of the measures of equally long displacements at $(x + dx)$ and (x) is determined by the field ϕ_s alone, being equal to

$$1 - \phi_s\,dx^s.$$

---

* Phrases involving the noun *length* are purposely avoided. There is no number which is the common length of δx^i and δy^i.

If the vector a^i of weight m is projected round the parallelogram

$$x^i, \quad x^i + dx^i, \quad x^i + dx^i + \delta x^i, \quad x + \delta x^i,$$

the increment of its i-component is

$$\Delta a^i = -a^r \mathrm{T}^i_{rst}(m)\, dx^s\, \delta x^t,$$

where $\mathrm{T}^i_{rst}(m)$ is the Riemann-Christoffel tensor formed with the quantities $\mathrm{K}^i_{rs}(m)$:

$$\mathrm{T}^i_{rst}(m) = \frac{\partial \mathrm{K}^i_{rt}}{\partial x_s} - \frac{\partial \mathrm{K}^i_{rs}}{\partial x_t} + \mathrm{K}^p_{rt}\,\mathrm{K}^i_{ps} - \mathrm{K}^p_{rs}\,\mathrm{K}^i_{pt}.$$

Direct substitution of the values of $\mathrm{K}^i_{rt}(m)$ gives

$$\mathrm{T}^i_{rst}(m) = \mathrm{R}^i_{rst} - 2m\, \delta^i_r \phi_{[s,\, t]},$$

$$\mathrm{T}_{ik}(m) = \mathrm{R}_{ik} + 2m\phi_{[i,\, k]},$$

where R^i_{rst} is the curvature tensor formed with the Γ's:

$$\mathrm{R}^i_{rst} = \frac{\partial \Gamma^i_{rt}}{\partial x_s} - \ldots,$$

and the comma denotes plain differentiation:

$$\phi_{s,\, t} = \frac{\partial \phi_s}{\partial x_t}.$$

The brackets are Bach and Schouten's notation*: if a_{ik} is any covariant tensor

$$a_{[ik]} = \tfrac{1}{2}(a_{ik} - a_{ki}), \qquad a_{(ik)} = \tfrac{1}{2}(a_{ik} + a_{ki}).$$

(Notice that both R^i_{rst} and $\phi_{[s,\, t]}$ are tensors of weight 0.)

Thus

$$\Delta a^i = -a^r \mathrm{R}^i_{rst}\, dx^s\, dx^t + 2ma^i \phi_{[s,\, t]}\, dx^s\, \delta x^t,$$

and,

$$a^i + \Delta a^i = (a^i - a^r\, \mathrm{R}^i_{rst}\, dx^s\, \delta x^t)\,(1 + 2m\phi_{[s,\, t]}\, dx^s\, \delta x^t).$$

Hence the necessary and sufficient condition for the integrability of direction is

$$\mathrm{R}^i_{rst} = 0 \tag{6.1}$$

at all points, and for integrability of length

$$\phi_{[s,\, t]} = 0 \tag{6.2}$$

A proof is given by Weyl (*op. cit.*, p. 1) that (6.1) and (6.2) are sufficient conditions for the existence of everywhere-normal co-ordinate and gauge systems.

7. From the definitions that have now been given a calculus very similar to the ordinary tensor calculus can be built up. If V is a tensor field the "true"

---

* Bach, 'Math. Z.,' 9, p. 113 (1921); extended by Schouten to tensors of all ranks.

excess of the field at $(x + dx)$ over its value at (x) is the excess of $\mathrm{V} + d\mathrm{V}$, the actual value at $(x + dx)$, over $\mathrm{V} + \underset{\bullet}{\mathbf{d}}\mathrm{V}$, the tensor affine-equal to V. Hence $\mathrm{V}_{|s}$, the "true" rate of change of the field with respect to x_s, is the coefficient of dx_s in $d\mathrm{V} - \underset{\bullet}{\mathbf{d}}\mathrm{V}$, *i.e.*,

$$\mathrm{V}_{|s} = \mathrm{V}_{;s} + m\phi_s \mathrm{V}, \tag{7.1}$$

where $\mathrm{V}_{;s}$ denotes the ordinary covariant derivative, formed as if V were of weight 0. Evidently $\mathrm{V}_{|s}$ has the same weight as V. The equation of geodesics is

$$\frac{du^i}{d\tau} + \Gamma^i_{rs} u^r u^s - u^i u^s \phi_s = 0, \tag{7.2}$$

that is,

$$u^r u^i_{|r} = 0.$$

*The difference between the two repeated derivatives, $v^i_{|rs}$ and $v^i_{|sr}$ of a vector field v^i of weight m is given by

$$\begin{aligned} v^i_{|[rs]} &= -\tfrac{1}{2}\mathrm{R}^i_{jrs} v^j + m v^i \phi_{[r,s]} \\ &= v^i_{;[rs]} + m v^i \phi_{[r,s]}. \end{aligned}$$

More generally, if V is any tensor or tensor-density

$$\begin{aligned} \mathrm{A}_{|rs} &= (\mathrm{A}_{;r} + m\mathrm{A}\phi_r)_{;s} + m\phi_s(\mathrm{A}_{;r} + m\mathrm{A}\phi_r) \\ &= \mathrm{A}_{;rs} + 2m\mathrm{A}_{;(r}\phi_{s)} + m\mathrm{A}\phi_{r,s} + m^2\mathrm{A}\phi_r\phi_s. \end{aligned}$$

And therefore

$$\mathrm{A}_{|[rs]} = \mathrm{A}_{;[rs]} + m\mathrm{A}\phi_{[r,s]}.$$

8. *Introduction of a Fundamental Tensor.*—We now consider the effects of choosing a special form for the function $|\underset{\bullet}{\delta x^i}|$, viz.,

$$\sqrt{g_{ik}\,\delta x^i \delta x^k}.$$

The tensor g_{ik} must evidently be of weight 2.

The projection of δx^i at $(x + dx)$, namely

$$\delta x^i - \Gamma^i_{rs}\,\delta x^r dx^s,$$

has measure $\delta\tau$, where

$$\begin{aligned} \delta\tau^2 &= g_{ik}(x + dx)(\delta x^i - \Gamma^i_{rs}\delta x^r dx^s)(\delta x^k - \Gamma^k_{rs}\delta x^r dx^s) \\ &= g_{ik}\delta x^i \delta x^k + dx^s \delta x^i \delta x^k \left(\frac{\partial g_{ik}}{\partial x^s} - \Gamma^r_{is} g_{rk} - \Gamma^r_{sk} g_{ir}\right). \end{aligned}$$

But it also follows from the assumption on p. 611 that the measure of $\delta x^i - \Gamma^i_{rs}\,\delta x^r dx^s$ is $(1 - \phi_s dx^s)$ times that of δx^i:

$$\delta\tau^2 = (1 - 2\phi_s dx^s)\, g_{ik}\,\delta x^i \delta x^k.$$

---

* From this point it is assumed that

$$\Gamma^i_{\ r} = \Gamma^i_{sr}.$$

Since (dx) and (δx) are arbitrary this gives

$$\frac{\partial g_{ik}}{\partial x^s} - \Gamma^r_{is} g_{rk} - \Gamma^r_{sk} g_{ir} + 2\phi_s g_{ik} = 0. \tag{8.1}$$

i.e., since g_{ik} is of weight 2

$$g_{ik|s} = 0, \tag{8.2}$$

the relation between Γ^i_{rs} and ϕ_s. More generally, if the measure of δx^i is

$$(g_{ij\ldots k}\, \delta x^i\, \delta x^j \ldots \delta x^k)^{1/q},$$

then

$$g_{ij\ldots k|s} = 0.\text{[*]}$$

It follows at once from (8.2) that

$$g^{ik}_{|s} = 0,$$

$$(\sqrt{g})_{|s} = 0,$$

and so if A is any tensor

$$(\mathrm{A}g^{rs})_{|s} = \mathrm{A}_{|s} g^{rs},$$

$$(\mathrm{A}\sqrt{g})_{|s} = \mathrm{A}_{|s}\sqrt{g} \quad :$$

the raising and lowering of indices, and the passage from tensors to tensor densities, are commutative with weighted covariant differentiations just as they are in an ordinary Riemann manifold.

From (8.1) it follows that

$$\Gamma^i_{rs} = \begin{Bmatrix} i \\ rs \end{Bmatrix} + 2\delta^i_{(r}\phi_{s)} - g_{rs}\phi^i ;$$

if the gauge structure is fixed, the metrical structure determines the affine structure. If this expression for Γ^i_{rs} is substituted in the equation of geodesics (7.2) the result is

$$\frac{du^i}{d\tau} + \begin{Bmatrix} i \\ rs \end{Bmatrix} u^r u^s + \phi_s u^s u^i = \phi^i$$

(for $u_r u^r = 1$).

Note.—It is rather easy to slip into the supposition that when $g_{ik|s} = 0$ the derivative of vector a^i of weight m is

$$\frac{\partial a^i}{\partial x_r} + \begin{Bmatrix} i \\ qr \end{Bmatrix} a^q + m a^i \phi_r.$$

This is, of course, not the case. The derivative is

$$\frac{\partial a^i}{\partial x_r} + \Gamma^i_{qr} a^q + m a^i \phi_r = \frac{\partial a^i}{\partial x_r} + \begin{Bmatrix} i \\ qr \end{Bmatrix} a^q + (m+1)\, a^i \phi_r + \delta^i_r a_q \phi^q - a_r \phi^i.$$

---

[*] Veblen, Eisenhart, and Thomas have given conditions that an integral of (7.2) of type (8.3) should exist for given Γ^i_{rs} and ϕ_s. See Veblen and Thomas, 'Trans. Amer. Math. Soc.,' vol. 26, p. 551 (1923).

§ 2. *Fundamental Identities and Field Laws.*

The methods of infinitesimal changes of gauge and co-ordinate systems[*] will now be used to find, in two typical cases, the condition that a function of tensors of known character should itself have assigned gauge and tensor character. The identities found in this way include those that appear as "momentum and energy equations" in field theories, *i.e.*, they are the identities that ensure the compatibility of the equations of motion with the absence of matter:

$$u^i = 0.$$

Case 2 has already been investigated by Weyl[†] but the results are not given by him as tensor, and, of course, not as gauge-true relations.

9. *Case* 1.—Let a general weighted affine structure (Γ^i_{rs} and ϕ_i) be adopted, Γ^i_{rs} being symmetrical, and let $\mathfrak{A}$ be a scalar density of weight 0 which is a function of Γ^i_{rs}, ϕ_i, and their first derivatives.

This case hardly differs from the corresponding problem in the purely affine-theory, which I have considered in an earlier paper.[‡] If the increment of $\mathfrak{A}$ when Γ^i_{rs} and ϕ^i receive general small increments is

$$\delta\mathfrak{A} = \mathfrak{A}_i^{rs}\,\delta\Gamma^i_{rs} + \mathfrak{a}^i\,\delta\phi_i + \frac{\partial}{\partial x^t}(\delta\mathfrak{x}^t), \qquad (\mathfrak{A}_i^{rs} = \mathfrak{A}_i^{sr}),$$

then $\mathfrak{A}_i^{rs}$ and $\mathfrak{a}^i$ are tensor-densities of weight 0, and satisfy

$$\frac{\partial\mathfrak{a}^i}{\partial x^i} = 0, \tag{9.1}$$

$$\mathfrak{A}_{i\,|\,rs} - \mathrm{R}^t_{rsi}\,\mathfrak{A}_t^{rs} = 2\mathfrak{A}^r\phi_{[i,r]}. \tag{9.2}$$

These are the "equations of motion" and "conservation of charge" in a field theory with the law

$$\delta\int\mathfrak{A}\,dx = 0. \tag{9.3}$$

For example, if

$$\mathfrak{A} = \sqrt{\|\mathrm{R}_{ik} + a\phi_{[i,k]}\|},$$

and

$$\delta\mathfrak{A} = \mathfrak{H}^{ik}\,(\delta\mathrm{R}_{ik} + a\,\delta\phi_{[i,k]}),$$

then[§]

$$\mathfrak{A}_i^{rs} = \mathfrak{H}^{(rs)}_{;\,i} - \delta_i^{(r}\mathfrak{H}^{s)t}_{;\,t}, \quad \mathfrak{a}^r = -a\,\frac{\partial\mathfrak{H}^{[rs]}}{\partial x_s}.$$

---

[*] *Cf.* RZM, p. 111, &c. Also Pauli, 'Relativitätstheorie,' p. 616; Weitzenböck, 'Invariantentheorie,' p. 372.

[†] RZM, pp. 300, *seq.*

[‡] 'Proc. Camb. Phil. Soc.,' 23, p. 262 (1926).

[§] *Cf.* Einstein, 'Sitzungsber. der Preuss. Acad.,' p. 35 (1923).

There are further identities, obtainable either by the closer consideration of $\delta\mathfrak{x}^i$ (this is carried out in detail in any paper cited above) or by the introduction of an arbitrary scalar factor, in the manner described below. But these identities are less important, since they are not among the equations obtained from (9.3).

10. *Case* 2.—More interesting is the case where a fundamental tensor g_{ik} has been introduced, connected with Γ_{rs}^{i} and ϕ_i by

$$g_{ik|r} = 0.$$

It is natural, in view of (8.3) (although hardly in the spirit of the antitheses on p. 603) to consider Γ_{rs}^{i} as a function of g_{rs} and ϕ_i, and, therefore, to investigate functions $\mathfrak{W}$ of ϕ_i, g_{rs} and their derivatives. We proceed to find conditions that $\mathfrak{W}$ shall be a scalar density of weight m.

Let

$$\delta\mathfrak{W} = \mathfrak{W}^{ik}\,\delta g_{ik} + \mathfrak{w}^i\,\delta\phi_i + \frac{\partial}{\partial x^r}(\delta\mathfrak{y}^r), \quad (\mathfrak{W}^{ik} = \mathfrak{W}^{ki}).$$

In general $\mathfrak{W}^{ik}$ and $\mathfrak{w}^i$ have neither tensor nor gauge character.

(*a*) Suppose that the *gauge-system* is slightly changed:

$$d\bar{\tau} = d\tau\,(1 + \varepsilon).$$

Then

$$\delta g_{ik} = 2\varepsilon g_{ik}, \qquad \delta\phi_i = -\frac{\partial\varepsilon}{\partial x^i},$$

and therefore

$$\int\delta\mathfrak{W}\,dx = \int\varepsilon\left(2\mathfrak{W}^{ik}g_{ik} + \frac{\partial\mathfrak{w}^i}{\partial x^i}\right)dx + \int\frac{\partial}{\partial x^r}(\varepsilon\mathrm{X}^r)\,dx + \int\frac{\partial^2}{\partial x^r\,\partial x^s}(\varepsilon\mathrm{Y}^{rs})\,dx.$$

If $\mathfrak{W}$ is of weight m we must also have

$$\delta\mathfrak{W} = m\varepsilon\mathfrak{W}.$$

Hence

$$0 = \int\varepsilon\left(2\mathfrak{W}_i^i + \frac{\partial\mathfrak{w}^i}{\partial x^i} - m\mathfrak{W}\right) + \int\frac{\partial}{\partial x^r}(\varepsilon\mathrm{X}^r)\,dx + \int\frac{\partial^2}{\partial x\,\partial x}(\varepsilon\mathrm{Y}^{rs})\,dx.$$

If ε vanishes on the boundary of the domain of integration, the last two integrals vanish separately. It follows that

$$2\mathfrak{W}_i^i + \frac{\partial\mathfrak{w}^i}{\partial x^i} = m\mathfrak{W} \tag{I}$$

at all points. It also follows that

$$\mathrm{X}^r = 0, \qquad \mathrm{Y}^{(rs)} = 0,$$

but the explicit forms of these relations will be found by another method.

(*b*) Next consider a small change in the co-ordinate system,

$$\bar{x}^i = x^i + \xi^i \quad (\xi^i \text{ is a small displacement}).$$

It can be shown without difficulty† that the effect of this change on the integral

$$\int \mathfrak{W}\, dx$$

is to increase it by

$$\int \delta^* \mathfrak{W}\, dx + \int \frac{\partial}{\partial x^i} (\xi^i \mathfrak{W})\, dx, \tag{10.1}$$

where, if f is any quantity with a transformation rule,

$$\delta^* f = \bar{f}(x) - f(x).$$

Hence, for $\mathfrak{W}$ to be a scalar density (10.1) must be zero whatever the small vector field ξ^i. Using

$$\delta^* f = \bar{f}(\bar{x}) - f(x) - \xi^i \frac{\partial f}{\partial x^i},$$

we find

$$\delta^* g_{ik} = -\xi^r g_{ik,r} - \xi^r_{,i} g_{rk} - \xi^r_{,k} g_{ir},$$
$$\delta^* \phi_i = -\xi^r \phi_{i,r} - \xi^r_{,i} \phi_r.$$

The condition imposed on $\mathfrak{W}$ by its tensor character is therefore

$$\int \xi^r [\mathfrak{W}^{ik} g_{ik,r} - 2\mathfrak{W}^i_{r,i} + \mathfrak{w}^i \phi_{i,r} - (\mathfrak{w}^i \phi_r)_{,i}]\, dx + \int \frac{\partial}{\partial x^r} (\delta_\delta^r)\, dx = 0,$$

which gives

$$\mathfrak{W}^{ik} g_{ik,r} - 2\mathfrak{W}^i_{r,i} + \mathfrak{w}^i \phi_{i,r} - (\mathfrak{w}^i \phi_r)_{,i} = 0. \tag{10.2}$$

Now

$$g_{ik,r} = \Gamma^p_{ir} g_{pk} + \Gamma^p_{kr} g_{ip} - 2\phi_r g_{ik}.$$

Hence (10.2) is

$$2\mathfrak{W}^i_{r;i} + 2\mathfrak{W}^i_i \phi_r - 2\mathfrak{w}^i \phi_{[i,r]} + \phi_r \mathfrak{w}^i_{,i} = 0, \tag{10.3}$$

the covariant derivative $\mathfrak{W}^i_{;i}$ being calculated as if $\mathfrak{W}^i_r$ were a (1 : 1) tensor-density of weight 0.‡ In view of I, this is equivalent to

(II) $$\mathfrak{W}^i_{r;i} = \mathfrak{w}^i \phi_{[i,r]} - \tfrac{1}{2} m \mathfrak{W} \phi_r.$$

---

† RZM., p. 233; Pauli and Weitzenböck, *op. cit.*, p. 615.

‡ There is no objection to the covariant derivation of quantities that are not tensor or have not gauge-character, provided it is made clear how they are to be treated; *e.g.*, we may set

$$\Gamma^i_{rs;t} = \Gamma^i_{rs,t} + \Gamma^i_{pt}\Gamma^p_{rs} - \Gamma^p_{rt}\Gamma^i_{ps} - \Gamma^p_{st}\Gamma^i_{pr},$$

which leads to the compact formula

$$R^i_{jrs} = -\Gamma^i_{j[r,s]} - \Gamma^i_{j[r;s]}.$$

11. We will find the explicit form of the identities

$$X^r = Y^{(rs)} = 0,$$

and their analogues derived from (10.1), in the case where $\mathfrak{W}$ involves no derivatives of g_{ik}, and only first dervatives of ϕ_i. Let

$$\delta\mathfrak{W} = \mathfrak{W}^{ik}\,\delta g_{ik} + \mathfrak{w}^i\,\delta\phi_i + \frac{\partial}{\partial x^s}(\mathfrak{v}^{rs}\,\delta\phi_r), \tag{11.1}$$

$\mathfrak{W}^{ik}$ is evidently a tensor-density of weight $m - 2$. $\mathfrak{v}^{rs}$ *is also a density, of weight* m. For if δg_{ik} is everywhere zero and $\delta\phi_s = 0$ at P_0, $\delta\phi_{r,s}$ has tensor character at P_0 and

$$\delta\mathfrak{W} = \mathfrak{v}^{rs}\,\delta\phi_{r,s}.$$

Since the values of $\delta\phi_{r,s}$ are arbitrary, it follows that $\mathfrak{v}^{rs}$ is a tensor-density. Also $\delta\phi_{r,s}$ has the same weight as $\delta\phi_r$, namely 0.

If $\delta\phi_i$ has a general value, while δg_{ik} still remains zero,

$$\delta\mathfrak{W} - (\mathfrak{v}^{rs}\delta\phi_r)_{\|s} = \mathfrak{w}^i\delta\phi_i - m\phi_s\mathfrak{v}^{rs}\delta\phi_r.$$

The left-hand side of this identity being a scalar density of weight m, the right-hand side must be too; *i.e.*,

$$\mathfrak{u}^i = \mathfrak{w}^i - m\phi_s\mathfrak{v}^{is} \tag{11.2}$$

is a vector-density of weight m.

To find the required identities we observe that if instead of a function of g_{ik}, ϕ_i, and their derivatives only, a function involving also a scalar function K of weight 0 is considered, the identity I remains valid, but II requires a little modification. The increment of K is

$$\delta^* K = -\xi^r K_{,r},$$

and if $\mathfrak{k} = \dfrac{\partial\mathfrak{W}}{\partial K}$, the term

$$\tfrac{1}{2}\mathfrak{k}K_{,r}$$

must be added to the right-hand side of II.

Let us apply this to the scalar density $K\mathfrak{W}$ where $\mathfrak{W}$ is now the original function (not involving K), whose increment is given by (11.1). Then

$$\delta(K\mathfrak{W}) = K\mathfrak{W}^{ik}\delta g_{ik} + (K\mathfrak{w}^r - K_{,s}\mathfrak{v}^{rs})\,\delta\phi_r + \mathfrak{W}\delta K + \frac{\partial}{\partial x^s}(K\mathfrak{v}^{rs}\delta\phi_r).$$

Hence I and the modified II give

$$2K\mathfrak{W}^i_i + \frac{\partial}{\partial x^i}(K\mathfrak{w}^i - K_{,s}\mathfrak{v}^{is}) = mK\mathfrak{W}, \tag{11.3}$$

$$(K\mathfrak{W}^i_r)_{;i} - (K\mathfrak{w}^i - K_{,s}\mathfrak{v}^{is})\,\phi_{(i,r)} = \tfrac{1}{2}\mathfrak{W}K_{,r} - \tfrac{1}{2}mK\mathfrak{W}\phi_r. \tag{11.4}$$

Since K is arbitrary the coefficients of $K_{,rs}$, of $K_{,r}$, and of K in these equations must vanish separately. We find

(A₁)
$$\mathfrak{v}^{(is)} = 0$$

$$\frac{\partial \mathfrak{v}^{is}}{\partial x^i} - \mathfrak{w}^s = 0. \tag{11.5}$$

In view of (11.2) and the fact that $\mathfrak{v}^{ir}$ is of weight m, (11.5) can also be given the form

(A₂)
$$\mathfrak{v}^{is}_{\|i} = \mathfrak{u}^s,$$

which shows it to be a gauge-true relation. (11.3) now reduces simply to I.

From (11.4) we find similarly

(B₁)
$$\mathfrak{W}^i_r + \mathfrak{v}^{is}\phi_{[r,s]} = \tfrac{1}{2}\delta^i_r\,\mathfrak{W}.$$

This enables us to give I a simple gauge-true form. For

$$\begin{aligned}\frac{\partial \mathfrak{w}^i}{\partial x_i} &= \frac{\partial \mathfrak{u}^i}{\partial x_i} - m\phi_{s,i}\,\mathfrak{v}^{is} - m\phi_s\,\mathfrak{v}^{is}_{,i}\\ &= \frac{\partial \mathfrak{u}^i}{\partial x_i} + m\phi_i\mathfrak{u}^i + m\phi_{[i,s]}\mathfrak{v}^{is} \quad \text{(by (11.5) and } A_1)\\ &= \mathfrak{u}^i_{\|i} + m\,(\tfrac{1}{2}n\mathfrak{W} - \mathfrak{W}^i_i) \quad \text{(by } B_1),\end{aligned}$$

and so I is equivalent to

(A₃)
$$\mathfrak{u}^i_{\|i} = (m-2)\mathfrak{W}^i_i - \tfrac{1}{2}m\,(n-2)\,\mathfrak{W}.$$

Finally, to get the gauge-true form of II, let the gauge-system be such that

$$\phi^r = \frac{K_{,r}}{mK}$$

at a certain point P_0. (11.4) becomes

$$K\mathfrak{W}^i_{r;i} + mK\phi_i\mathfrak{W}^i_r - K\mathfrak{u}^i\phi_{[i,r]} = 0,$$

i.e.,

(B₂)
$$\mathfrak{W}^i_{r\|i} = \mathfrak{u}^i\phi_{[i,r]}.$$

This being a gauge-true equation, must be true in all gauge systems. (A_3 and B_2 could, of course, be deduced directly from I and II, which are the forms to which they reduce in a normal gauge-system.)

It will be noticed that A_2 and B_1 give expressions for the "first variations," $\mathfrak{W}^i_r$ and $\mathfrak{u}^i$, in terms of $\mathfrak{v}^{rs}$, which is

$$\frac{\partial \mathfrak{W}}{\partial \phi_{r,s}},$$

and therefore easily found.

Example 1.

$$\mathfrak{W} = \mathfrak{L} = 2\phi_{[i,k]}\,\phi_{[r,s]}\,g^{ir}g^{ks}\sqrt{g}.$$

Here $m = n - 4$ and

$$\mathfrak{v}^{rs} = 2\mathfrak{F}^{rs},$$

where

$$\mathrm{F}_{rs} = 2\phi_{[r,s]}, \qquad \mathfrak{F}^{rs} = \mathrm{F}_{ik}\,g^{ir}g^{ks}\sqrt{g}.$$

Hence, by B_1,

$$\mathfrak{W}^i_r = -\mathfrak{F}^{is}\mathrm{F}_{rs} + \tfrac{1}{4}\delta^i_r\,\mathfrak{F}^{pq}\mathrm{F}_{pq} \qquad (11.61)$$

$$= \mathfrak{S}^i_r,$$

say; and by A_2

$$\tfrac{1}{2}\mathfrak{u}^i = -\mathfrak{F}^{ik}_{\| k} = -\frac{\partial\mathfrak{F}^{ik}}{\partial x^k} - (n-4)\,\phi_k\mathfrak{F}^{ik}.$$

Equation B_2 gives the well-known identity in electromagnetism:

$$\mathrm{S}^i_{r\| i} = \mathrm{F}^{ik}_{\| k}\,\mathrm{F}_{ri} \qquad (11.62)$$

where

$$\mathrm{S}^i_k = \frac{1}{\sqrt{g}}\,\mathfrak{S}^i_k.$$

The ordinary form of this identity,

$$\mathrm{S}^i_{r\,;\,i} = \mathrm{F}^{ik}_{;\,k}\,\mathrm{F}_{ri},$$

is only true when $g_{rs\,;\,t} = 0$.

$\mathfrak{S}^i_i$ is $\tfrac{1}{2}(n-4)\,\mathfrak{L}$, $(= \tfrac{1}{2}m\mathfrak{L})$, and A_3 gives

$$\mathfrak{F}^{ik}_{\| ik} = \tfrac{1}{2}\mathfrak{u}^i_{\| i} = \longleftrightarrow (n-4)\,\mathfrak{L}. \qquad (11.63)$$

Example 2.—The weight, $n - 4$, of $\mathfrak{L}$ in Example 1 suggests the consideration of

$$\mathfrak{H} = \mathrm{R}^2\sqrt{g} - a\mathfrak{L}$$

as a "world-function," a being a numerical constant. Weyl investigated the law

$$\delta\int\mathfrak{H}\,dx = 0, \qquad (11.71)$$

but did not give the general gauge-true form of the resulting system of equations. Let us then set

$$\mathfrak{W} = \mathrm{R}^2\sqrt{g}.$$

The results (A_2) and (B_1) are not applicable, since R involves $g_{ik,rs}$ and the value of $\mathfrak{W}^{ik}$ must be found from first principles.

If the values

$$\Gamma^i_{rs} = \left\{ {i \atop rs} \right\} + \delta^i_r\phi_s + \delta^i_s\phi_r - g_{rs}\phi^i$$

are substituted in the general expression for R_{rs} it will be found that

$$R_{rs} = G_{rs} + 2\phi_{[r,s]} + (n-2)\,\phi_{r|s} + g_{rs}\,\phi^{i}_{|i} - (n-2)\,(g_{rs}\phi_i\phi^i - \phi_r\phi_s),^{*} \qquad (11.72)$$

where G_{rs} is the contracted curvature tensor formed with the quantities $\left\{\begin{matrix} i \\ rs \end{matrix}\right\}$. Hence

$$R = G + 2\,(n-1)\,\phi^{i}_{|i} - (n-1)\,(n-2)\,\phi_r\phi^r.^{\dagger} \qquad (11.73)$$

Using this value of R we find

$$\begin{aligned}\delta\,(R^2\sqrt{g}) &= 2R\,\delta\,(R\sqrt{g}) - R^2\,\delta\sqrt{g} \\ &= 2R\,[\delta\,(G\sqrt{g}) - \tfrac{1}{2}R\,\delta\sqrt{g} + 2\,(n-1)\,\delta\,(\phi^i\sqrt{g})_{,i} \\ &\qquad + (n-1)\,(n-2)\,\delta\,(\phi_r\phi_s g^{rs}\sqrt{g})].\end{aligned}$$

In general a further partial integration is necessary, but if we use Weyl's device of employing (after variation, of course) a gauge system in which R is constant we find

$$\delta\,(R^2\sqrt{g}) = 2X_{ik}\sqrt{g}\,\delta g^{ik} + 4\,(n-1)\,(n-2)\,R\sqrt{g}\,\phi^i\,\delta\phi_i + \frac{\partial}{\partial x_i}(\delta_i^i),$$

where

$$\begin{aligned}X_{ik} &= R\,[G_{ik} - \tfrac{1}{2}g_{ik}G + \tfrac{1}{4}g_{ik}R + (n-1)\,(n-2)\,(\phi_i\phi_k - \tfrac{1}{2}g_{ik}\phi_r\phi^r)] \\ &= R\,[R_{(ik)} - \tfrac{1}{4}g_{ik}R - (n-2)\,(\phi_{(i|k)} - g_{ik}\phi^{r}_{|r}) \\ &\qquad - (n-2)^2\,(g_{ik}\phi_r\phi^r - \phi_i\phi_k)]. \qquad (11.74)\end{aligned}$$

Now R is of weight -2, and therefore

$$\begin{aligned}R_{|i} &= R_{,i} - 2\phi_i R \\ R_{|ik} &= (R_{,i})_{|k} - 2\phi_{i|k}R - 2\phi_i\,(R_{,k} - 2\phi_k R).\end{aligned}$$

In a gauge system in which R is constant

$$R_{|ik} = -2R\,(\phi_{i|k} - 2\phi_i\phi_k). \qquad (11.75)$$

Hence, *when* $n = 4$ the tensor

$$R\,(R_{(ik)} - \tfrac{1}{4}g_{ik}\,R) + R_{|(ik)} - g_{ik}\,g^{rs}\,R_{|rs} \qquad (11.76)$$

is identical with X_{ik} in the gauge-system $R = \text{const.}$ Provided, then, that $R \neq 0$, the field equations derived by variation of g_{ik} in (11.71) are

$$R_{(ik)} - \tfrac{1}{4}g_{ik}R = -\frac{a}{2R}\,S_{ik} + \frac{1}{R}\,(g_{ik}g^{rs}R_{|rs} - R_{|(ik)}).^{\ddagger} \qquad (11.77)$$

---

* *Cf.* Eisenhart, *loc. cit.*, p. 236.

† RZM, p. 131. In comparing this expression with Weyl's it is to be remembered that our ϕ_r is one-half of his, that our G and R are his $-R$ and $-F$, and tha

$$\frac{\partial}{\partial x_r}(\phi^r\sqrt{g}) = \sqrt{g}\,(\phi^{r}_{|r} - (n-2)\,\phi^r\phi_r),$$

‡ $-\frac{a}{2R}$, because $\mathfrak{S}^{ik}\delta g_{ik} = -\mathfrak{S}_{ik}\delta g^{ik}$.

and these are tensor and gauge-true equations. Raising one index and contracting give

$$g^{rs}\,\mathrm{R}_{\|rs} = 0\,. \tag{11.78}$$

If $\phi_i = 0$ in the gauge system $\mathrm{R} = 0$ the equations reduce to

$$\mathrm{G}_{ik} - \tfrac{1}{4} g_{ik}\,\mathrm{G} = 0.$$

The ϕ_i-equation (coefficient of $\delta\phi_i$) is

$$\frac{\partial \mathfrak{F}^{ik}}{\partial x^k} = -\,12\,\frac{\mathrm{R}}{a}\phi^i\sqrt{g}. \tag{11.79}$$

In applying the identities I and II it must be remembered that in para. 10 the quantity varied was g_{ik}, not g^{ik}, and, therefore, we must set $-2\mathrm{X}^{ik}\sqrt{g}$ for $\mathfrak{W}^{ik}$.

From I there follows the identity

(R$_1$) $$g^{rs}\mathrm{R}_{\|rs} = -\,2\,(\mathrm{R}\phi^i)_{\|i},$$

which reduces, when $\phi_i = 0$, to

$$g^{rs}\,\mathrm{G}_{;rs} = 0.$$

The equation (11.78) obtained from the law (11.71) is therefore equivalent to

$$(\mathrm{R}\phi^i)_{\|i} = 0. \tag{11.8}$$

This equation, the " equation of continuity," also follows from (11.79), *i.e., it is a consequence both of the g_{ik}- and of the ϕ_i-equations.* (*Cf.* RZM, foot of p. 305.)

II gives the " equations of energy and momentum " :

$$(\mathrm{X}^i_k\sqrt{g})_{;i} = -\,12\mathrm{R}\phi^i\phi_{(i,k)}\sqrt{g}.$$

These are gauge-true equations in the 4-dimensional case, since $\mathrm{X}^i_k\sqrt{g}$ is then of weight 0. They are, therefore, equivalent to

(R$_2$) $$\mathrm{X}^i_{k\|i} = -\,12\mathrm{R}\phi^i\phi_{(i,k)}.$$

Using the values (11.76) and (11.74) of X_{ik} it is easy to verify this identity in the two " unmixed " cases, (*a*) when $\phi_i = 0$ (it reduces to

$$\mathrm{G}\,(\mathrm{G}^i_k - \tfrac{1}{2}\delta^i_k\mathrm{G})_{;i} + g^{ij}(\mathrm{G}_{;jki} - \mathrm{G}_{;ijk}) + \mathrm{G}^i_k\mathrm{G}_{,i} = 0)\,;$$

and (*b*) when $\mathrm{G}_{ik} = 0$ in the gauge system $\mathrm{R} = $ const.

Summary.

(§ 1) A differential calculus is developed capable of dealing with tensors of various " weights," as well as tensors of various ranks. The equations preserve their form both under a change of co-ordinates and under a change of gauge-system.

(§ 2) The theory is applied to find a tensor and gauge-true form for the identities given by the variation of integrals. The general gauge-true equations resulting from the law

$$\delta \int R^2 \sqrt{g} = 0$$

are obtained. The part independent of the " electrical " vector ϕ_i is found to be

$$G_{ik} - \tfrac{1}{4} G g_{ik},$$

a tensor which has been considered by Einstein from time to time in connection with the theory of gravitation. The identities found by small variations of gauge and co-ordinates are in this case

$$g^{rs} R_{\| rs} = -2 (R\phi^i)_{\| i}$$

$$X^i_{k \| i} = -12 R \phi^i \phi_{[i,k]},$$

where the stroke denotes " weighted covariant differentiation," and

$$X_{ik} = R (R_{(ik)} - \tfrac{1}{4} g_{ik} R) + R_{\| (ik)} - g_{ik} g^{rs} R_{\| rs}.$$

The Determination of the Elastic Moduli of the Piezo-Electric Crystal Rochelle Salt by a Statical Method.

By W. Mandell, M.Sc. (Physics Research Department, King's College, London).

(Communicated by O. W. Richardson, F.R.S.—Received July 5, 1927.)

Introduction.

Rochelle salt owes its importance to the fact that it possesses piezo-electric properties which are much greater in magnitude than in the case of any other known substance.

Nicholson* points out that whereas the larger of the two piezo-electric moduli of quartz is 0·0677 E.S.U. per kilogram, a usual value for Rochelle salt is 10 E.S.U., and this can be increased to 200 E.S.U. per kilogram for crystals grown in a special manner so as to develop what is known as a composite structure.

This piezo-electric effect is associated only with crystals having an asymmetric structure, and occurs when the crystal is submitted to mechanical stresses.

---

* 'Proc. Amer. I.E.E.,' vol. 38, pp. 1467–85.

It would therefore appear that the phenomenon may be closely related to its elastic properties. Experiments were therefore devised to measure the elastic moduli, for it should be of interest to determine the behaviour of the crystal, the amount of deformation, for example when submitted to pressures or torsion in a manner and in a direction which gives the greatest piezo-electric response.

Valasek* carried out an experiment to find how the piezo-electric effect varies with temperature. Starting at the temperature of carbon-dioxide snow, he gradually raised the temperature and measured the response. He found the effect was very small until a temperature of – 20° C. was reached, when it increased very suddenly and attained a maximum value at about 0° C. On still raising the temperature it almost disappeared in a very abrupt manner at about 23° C.

Another experiment was devised to find the variation in elasticity with change in temperature, for if these electric properties are due to some molecular rearrangement, we would expect a considerable change in the elastic properties as the temperature was varied through the point where this abrupt change takes place.

Properties of Rochelle Salt.

Rochelle salt or Seignette salt is a double tartrate of sodium and potassium, having the formula $NaKC_4H_4O_6 . 4H_2O$. It belongs to the rhombic-bisphenoidal or rhombic-hemihedral class and possesses three digonal axes of symmetry which are identical with the three crystallographic axes, but there are no planes of symmetry. Fig. 1 shows a section through the crystal parallel to the basal plane. This shows the hemihedrism very clearly, and, as in the figure, one of the pinacoid faces is almost invariably missing.

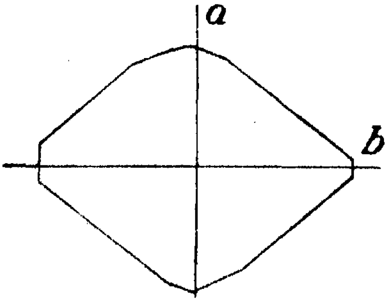

Fig. 1.

The substance, both as a solid and in solution, is optically active since it possesses an asymmetric arrangement of the atoms in the organic molecule.

It is exceedingly fragile, and care has to be used in handling it, as it is liable to fracture due to the heat of the hand.

Valasek† and others have shown that the crystal has a natural polarisation. It was used as a dielectric in a condenser and the potential varied between the plates in steps, deflections being obtained in a ballistic galvanometer in the same circuit for each change of potential. On carrying the process through a cycle, a hysteresis loop was obtained of the same form as with a magnetic substance in a magnetising field.

---

* 'Phys. Rev.,' p. 484 (1922).

† 'Phys. Rev.,' p. 475 (1921).

Hankel and Lindenberg* by heating the crystal and also by means of pressure have shown that the four electric axes are in the directions parallel to the normals to the two forms {111} and {1$\bar{1}$1}.

Perfectly clear crystals showing no composite structure can be grown in a thermostat in about a month, and of such a size that plates 6 cm. long can be obtained. Slabs were cut by means of a wet string, as the crystal is very soluble in water. It was found to be advisable not to attempt to cut the crystals until a period of about a month had elapsed after growth. A further period of three months was allowed before the beams were used.

Theory.

In the theory of elasticity, the number of quantities which must be specified in order that the stress at a point in a solid may be determined are six, viz., three normal tractions X_x, Y_y, Z_z and three tangential tractions Y_z, Z_x and X_y. These are called the six components of stress at the point. According to the generalised Hook's Law, each of the six components of stress at any point is a linear function of the six components of strain at the point, the equations being of the form :—

$$\left.\begin{array}{l} X_x = c_{11}x_x + c_{12}y_y + c_{13}z_z + c_{14}y_z + c_{15}z_x + c_{16}x_y \\ \quad\cdot\quad\cdot\quad\cdot\quad\cdot\quad\cdot\quad\cdot\quad\cdot \\ Y_z = c_{41}x_x + c_{42}y_y + c_{43}z_z + c_{44}y_z + c_{45}z_x + c_{46}x_y \\ \quad\cdot\quad\cdot\quad\cdot\quad\cdot\quad\cdot\quad\cdot\quad\cdot \end{array}\right\}, \tag{1}$$

where $c_{hk} = c_{kh}$ $(h, k = 1, 2, \ldots 6)$ are the elastic constants.

When a body is strained slowly by gradual increase of the load and is in continual equilibrium of temperature with surrounding bodies, the changes taking place are perfectly isothermal. Under these conditions it can be shown that a strain-energy-function exists, which is equal to the potential energy per unit of volume stored up in the body due to the strain. The amount of stored energy stored by work of amount δa would be given by

$$\delta a = X_x\,\delta x_x + Y_y\,\delta y_y + Z_z\,\delta z_z + Y_z\,\delta y_z + Z_x\,\delta z_x + X_y\,\delta x_y.$$

Hence, by equation (1) we obtain the strain-energy-function ξ in terms of the strain components, and owing to the relations between the elastic constants it can be written in the form

---

* 'Z. f. Kryst.,' vol. 27, p 515 (1897).

$$\left.\begin{array}{rl} 2\xi = c_{11}x_x^2 + 2c_{12}x_xy_y + 2c_{13}x_xz_z + 2c_{14}x_xy_z + 2c_{15}x_xz_x + 2c_{16}x_xx_y & \\ + c_{22}y_y^2 + 2c_{23}y_yz_z + 2c_{24}y_yy_z + 2c_{25}y_yz_x + 2c_{26}y_yx_y & \\ + c_{33}z_z^2 + 2c_{34}z_zy_z + 2c_{35}z_zz_x + 2c_{36}z_zx_y & \\ + c_{44}y_z^2 + 2c_{45}y_zz_x + 2c_{46}y_zx_y & \\ + c_{55}z_x^2 + 2c_{56}z_xx_y & \\ + c_{66}x_y^2 & \end{array}\right\} . \qquad (2)$$

If for $X_xY_y \ldots X_y$ and $x_xy_y \ldots x_y$, we write $X_1X_2 \ldots X_6$ and $x_1x_2 \ldots x_6$ respectively, then for short

$$2\xi = \sum_h \sum_k c_{hk}x_hx_k \qquad \text{(for } h \text{ and } k = 1, 2, \ldots 6).$$

In like manner each strain component is a function of the six stress components at the point according to the equations

$$x_x = s_{11}X_x + s_{12}Y_y + s_{13}Z_z + s_{14}Y_z + s_{15}Z_x + s_{16}X_y,$$
$$\cdot \quad \cdot \quad \cdot \quad \cdot \quad \cdot \quad \cdot$$
$$y_z = s_{41}X_x + s_{42}Y_y + s_{43}Z_z + s_{44}Y_z + s_{45}Z_x + s_{46}X_y,$$
$$\cdot \quad \cdot \quad \cdot \quad \cdot \quad \cdot \quad \cdot$$

where $s_{hk} = s_{kh}$ are the elastic moduli, and the strain-energy-function can be obtained in terms of the stress components, for it can be shown that

$$2\xi = \sum_h \sum_k s_{hk}X_hX_k \qquad \text{(for } h \text{ and } k = 1, 2 \ldots 6).$$

Thus, in the general case, a substance has 21 elastic constants and 21 elastic moduli, but in most crystals, they reduce in number according to the symmetry. Voigt* has shown that for crystals belonging to the rhombic system they reduce to nine, with the indices (11, 22, 33, 44, 55, 66, 23, 31, 12). These constants are obtained by bending and twisting suitably cut beams.

The bending of a plate of length L, breadth B, and thickness D, supported on knife-edges at both ends and carrying a central load, P, is given by the equation

$$\delta = \frac{EPL^3}{4BD^3} \quad \text{or} \quad \frac{PL^3}{4YBD^3}, \qquad (3)$$

where Y is Young's modulus and E is the extension modulus (Dehungs modul of German nomenclature).†

---

* 'Lehrbuch der Krystallphysik,' p. 585.

† Since this notation is used in practically all works on crystal physics, it will be retained here.

If $\alpha_1, \alpha_2, \alpha_3$, denote the direction cosines of the length L of equation (3) with the crystal axes, E is given by the formula

$$E = \frac{1}{Y} = s_{11}\alpha_1^4 + s_{22}\alpha_2^4 + s_{33}\alpha_3^4 + (s_{44} + 2s_{23})\alpha_2^2\alpha_3^2 + (s_{55} + 2s_{31})\alpha_3^2\alpha_1^2 + (s_{66} + 2s_{12})\alpha_1^2\alpha_2^2. \qquad (4)$$

For crystals in the rhombic system, six beams cut in suitable directions are required for the bending experiments alone. The orientations actually used in this paper are shown in fig. 2, and are denoted by the letters A, B. C, D, E, F.

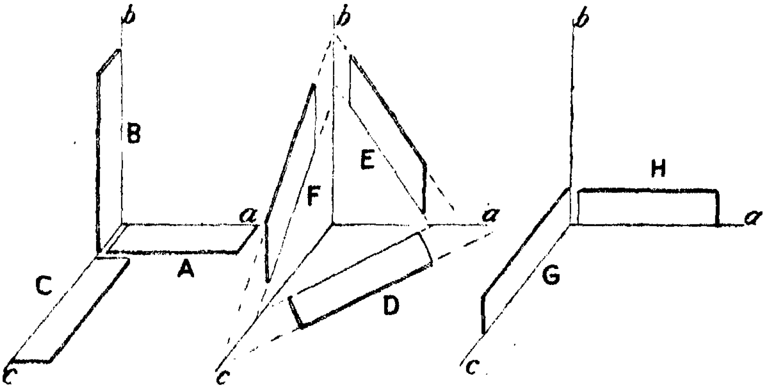

FIG. 2.

Beams A, B and C have their lengths parallel to the crystal axes; A and C have their breadths in the *ac* plane, while that of B is in the *bc* plane. The beams D, E and F have their breadths in the *ac*, *ab* and *bc* planes respectively, the directions of their lengths making angles of 45° with the *a* and *c* axes, 45° with the *a* and *b* axes, and 60° and 30° with the *b* and *c* axes. This last direction was used in order to obtain a slightly longer beam.

From equation (4) we obtain for the beams (whose direction-angles of the length with respect to the axes are given)

$$\left.\begin{array}{lll}
\text{A} & (0, 90, 90) & E_1 = s_{11} \\
\text{B} & (90, 0, 90) & E_2 = s_{22} \\
\text{C} & (90, 90, 0) & E_3 = s_{33} \\
\text{D} & (45, 90, 45) & E_4 = \frac{1}{4}\,[s_{11} + s_{33} + (s_{55} + 2s_{31})] \\
\text{E} & (45, 45, 90) & E_5 = \frac{1}{4}\,[s_{11} + s_{22} + (s_{66} + 2s_{12})] \\
\text{F} & (90, 60, 30) & E_6 = \frac{1}{16}\,[s_{22} + 9s_{33} + 3\,(s_{44} + 2s_{23})]
\end{array}\right\} . \qquad (5)$$

From these results the value of E for every direction in the crystal can be found.

The Bending Experiments.

A Fizeau interference method, fig. 3, was employed for determining the amounts of bending of the beams. By an adjustable arrangement the distance between the knife-edges could be easily varied. To obviate the necessity of preparing optically worked surfaces of the crystal for the production of interference fringes, a very small nickel saddle was cemented to the middle of the beam as shown. On this saddle was cemented a small optically worked piece of glass by which interference fringes were obtained on suitably adjusting the plate above it. Broad, straight fringes were obtained with a sodium flame; the knife-edges and upper plate were adjusted not only until the fringes were parallel to the knife-edges, but also until they remained parallel to them on adding the maximum load. This precaution ensured that the whole breadth of the beam was resting on the knife-edges and that the observed deflection was not partly due to any twisting of the beam on adding the load.

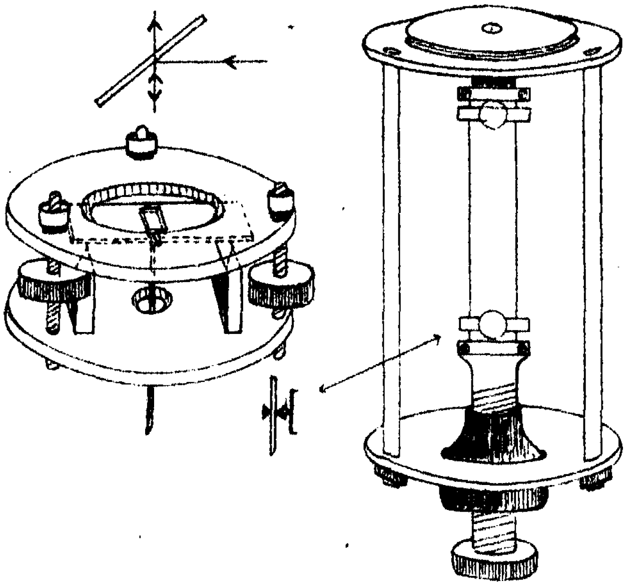

Fig. 3.

At first the knife-edges were of brass coated with nickel, as this metal is least attacked by the salt, but later agate knife-edges were used and were found to be more satisfactory.

Since any slight change in temperature during an experiment would vitiate the results, the apparatus had to be enclosed in a constant temperature enclosure.

The load had to be added from outside the enclosure. An attachment was therefore made to the nickel saddle, and passing through an opening in the bottom of the enclosure, carried a scale-pan. Below the scale-pan and attached rigidly to it was a vane which, when placed in water, damped out any vibratory motion.

In order to count the fringes accurately it was necessary to add the load gradually. A carefully graduated pipette with a very fine bore was used, and this held 58·245 gm. of mercury which constituted one load. Usually four or five loads were added, and then sufficient time was allowed for the beam to recover from fatigue before taking more readings.

To secure uniformity in the number of fringes for each beam and since the lengths were limited, a series of preliminary experiments was carried out to find the thickness of beams which would give roughly about 15 fringes per load. It will be noticed that the beams vary appreciably in thickness; beam A was left comparatively thick, as many cut in this direction were broken in grinding. They were measured by a screw-gauge, the average of twenty readings, which did not vary by more than 0·005 mm., was taken for each beam.

The fringes which were situated at the plane surfaces were seen in a long-focus microscope of low power, and measurements could easily be made to an accuracy of less than one-tenth of a fringe width.

A correction had to be applied which was mainly due to the "yield" of the apparatus on adding the load, and to the "bite" of the knife edges into the crystal. It was determined by using a very thick beam of crystal of which the elasticity was known, and consequently the deflection could be determined and compared with the observed deflection. Since, however, there was the possibility that different faces were of different hardness, the correction was checked by taking two, and in some cases three lengths of each beam. The "bite" effect was eliminated by a timing arrangement.

The following table gives the particulars of each beam, the dimensions being given in centimetres; the deflection is the corrected number of fringes per load for an average of ten loads, one length of beam only being given.

Beam.	Length.	Breadth.	Thickness.	Deflection.	E.
A	3·753	0·998	0·2332	9·5	46·0 $10^{-10} = E_1$
B	4·260	1·160	0·2037	12·24	31·4 $= E_2$
C	5·083	1·147	0·2198	14·7	27·6 $= E_3$
D	4·012	1·071	0·2590	14·2	82·8 $= E_4$
E	3·395	0·998	0·1694	14·0	35·1 $= E_5$
F	3·691	1·148	0·1867	11·6	34·8 $= E_6$

Hence from equation (5) we obtain

$$s_{11} = 46\cdot 0 \quad 10^{-10}, \qquad (s_{55} + 2s_{31}) = 257\cdot 6 \quad 10^{-10},$$
$$s_{22} = 31\cdot 4 \quad 10^{-10}, \qquad (s_{66} + 2s_{12}) = 63\cdot 1 \quad 10^{-10},$$
$$s_{33} = 27\cdot 6 \quad 10^{-10}, \qquad (s_{44} + 2s_{23}) = 92\cdot 7 \quad 10^{-10}.$$

the units being grams and centimetres.

On substituting these values, in equation (4), the value of E can be determined for any direction in the crystal; consequently a series of radii vectors expressed in terms of E will give the elasticity surface of the crystal.

Fig. 4 gives the sections obtained by planes containing two crystallographic axes; the circles are drawn merely for comparison, the lengths of the radii being given. Thus any vector drawn from the intersection of the axes to the surface of elasticity gives a numerical measure of the extension per centimetre length of a prism, the direction of whose length lies along the vector, when it is subjected to a tensile force of 1 gm. per square centimetre cross-section.

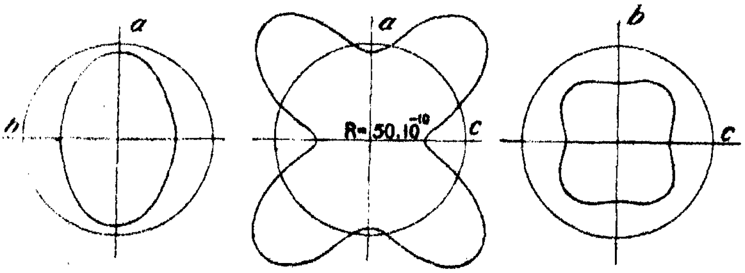

FIG. 4.

In connection with these elasticity surfaces, it is of interest to notice the elastic behaviour of the crystal when pressures are applied in directions which give the greatest piezo-electric effect.

Suppose plates are cut, their breadths lying in the principal sections of fig. 4 and the direction of their lengths making angles of 45° with the axes. If, then, pressures are applied in the planes of these principal sections in a direction bisecting the angles between the crystallographic axes, the electric polarisations produced are parallel to the axes, at right angles to the planes in which the pressure is exerted. Thus for plates in the *ab*, *ac* and *bc* planes, the piezo-electric moduli as found by Pockels[*] have the exceedingly large values $+ 35\cdot 4$ 10^{-8}, $- 165$ 10^{-8} and $+ 1180$ 10^{-8} E.S.U. for a force of 1 dyne per square centimetre along the *c*, *b* and *a* axes respectively.

---

[*] 'Abh. Gesch. d. Wiss. Gott.,' p. 39 (1894).

Theory of the Twisting Experiments.

So far by considering the results of the bending experiments alone, it has been possible to determine the surface of elasticity of the crystal. In order to find the absolute values of each of the elastic moduli, it is necessary to twist three suitably cut beams. Voigt* has shown that if T is the twisting modulus β_1, β_2, β_3, the direction-cosines of the length L and γ_1, γ_2, γ_3 of the breadth B of a beam cut in any direction, then

$$\begin{aligned} \mathrm{T} = \frac{1}{\eta} &= 4\,(s_{11}\beta_1^2\gamma_1^2 + s_{22}\beta_2^2\gamma_2^2 + s_{33}\beta_3^2\gamma_3^2) \\ &+ 2\,[(s_{44} + 4s_{23})\,\beta_2\gamma_2\beta_3\gamma_3 + (s_{55} + 4s_{31})\,\beta_3\gamma_3\beta_1\gamma_1 + (s_{66} + 4s_{12})\,\beta_1\gamma_1\beta_2\gamma_2] \\ &+ s_{44}\,(\beta_2^2\gamma_3^2 + \beta_3^2\gamma_2^2) + s_{55}\,(\beta_3^2\gamma_1^2 + \beta_1^2\gamma_3^2) + s_{66}\,(\beta_1^2\gamma_2^2 + \beta_2^2\gamma_1^2). \quad (6) \end{aligned}$$

It is most convenient to use three of the six orientations in which L, B and D are parallel to the crystal axes.

The actual beams used were G, C, and H of fig. 2, and on substituting the appropriate values for the direction cosines in equation (6), it is found that these give s_{44}, s_{55}, s_{66} respectively. There is a correction to apply, however, because, for any direction of the length, the angle of twist depends on two elastic moduli, beam G for instance depending on s_{44} and s_{55}.

The angle of twist θ for a rectangular beam of dimensions L, B and D when subjected to a couple of moment N about an axis parallel to its length and passing through its centre of cross-section is given for beams G and C respectively by

$$\theta_{\mathrm{G}} = 3s_{44}\mathrm{LN}\Big/\mathrm{BD}^3\left[1 - k\frac{\mathrm{D}}{\mathrm{B}}\sqrt{\frac{s_{55}}{s_{44}}}\right],$$

$$\theta_{\mathrm{C}} = 3s_{55}\mathrm{LN}\Big/\mathrm{BD}^3\left[1 - k\frac{\mathrm{D}}{\mathrm{B}}\sqrt{\frac{s_{44}}{s_{55}}}\right],$$

the constant k having to be determined by employing several thicknesses of the same beams.

The Twisting Experiments.

Fig. 3 shows the apparatus used in the twisting experiments, the beams usually being about 2 mm. thick and about 12 mm. broad. They were centred and fixed as shown in the diagram and the couple applied to the upper end. The angle of twist was determined for a length of beam between two bands which were so constructed as to grip the crystal plate along a line. Consequently the length could be accurately measured. These bands carried concave mirrors giving images on a scale at a distance of 261 cm. A couple of magnitude 229·1 gm. cm. was applied gradually by using mercury from a graduated pipette. Usually an average of six readings was taken for each beam, sufficient time being allowed to elapse for the recovery of the beam from fatigue. It was found that there was a very slow movement of the image on the scale after applying the full load. This was thought to be due to a tendency of the crystal to break down under continuous shearing forces and consequently a method of timing was employed.

---

* *Loc. cit.*, p. 759.

The most difficult part of the twisting experiments was the determination of the constant k. Beams about 6 cm. long were employed and readings were taken for 17 beams of different thicknesses.

The constant k was found to be approximately 1·198, most of the experiments being carried out on the long beams of types G and C. This constant is nearly twice as large with Rochelle salt as compared with other crystals of the rhombic system. A possible explanation may be that the electric charges produced by the shearing forces set up opposing stresses.

The beams of type H were found to be exceedingly fragile and were also considerably shorter than the others.

Details of six of the beams are given, the deflection being in millimetres on the scale:

Beam.	Length.	Breadth.	Depth.	Deflection per load.	T.	Average.
C	4·72	1·147	0·2198	46·67	301·4	
C	5·00	1·146	0·1797	88·06	299·3	300·4 = s_{55}
G	4·35	1·147	0·2193	15·85	59·7	
G	4·48	1·147	0·1990	19·90	59·7	59·7 = s_{44}
H	2·33	1·244	0·2253	8·06	78·9	
H	2·44	1·200	0·1930	12·80	78·6	78·7 = s_{66}

On substituting the values in equation (5), the values of the elastic moduli are as follows:—

$$\begin{array}{lccccccccc} & s_{11} & s_{22} & s_{33} & s_{44} & s_{55} & s_{66} & s_{23} & s_{31} & s_{12} \\ 10^{-10} \times & 46\cdot0, & 31\cdot4, & 27\cdot6, & 59\cdot7, & 300\cdot4, & 78\cdot7, & +16\cdot5, & -21\cdot4, & -7\cdot8 \end{array}$$

These values may be compared with two other crystals of the rhombic system:—

$$\begin{array}{llccccccccc} & & s_{11} & s_{22} & s_{33} & s_{44} & s_{55} & s_{66} & s_{23} & s_{31} & s_{12} \\ \text{Baryta} & 10^{-10} \times & 16\cdot3, & 18\cdot57, & 10\cdot42, & 82\cdot3, & 34\cdot2, & 35\cdot3, & -2\cdot46, & -1\cdot88, & -8\cdot80 \\ \text{Aragonite} & 10^{-10} \times & 6\cdot84, & 12\cdot9, & 12\cdot0, & 23\cdot8, & 38\cdot2, & 23\cdot0, & -2\cdot33, & +0\cdot42, & -2\cdot98 \end{array}$$

The most noteworthy fact about the results with Rochelle salt is the extremely large values of the elastic moduli as compared with other crystals, that is, the elasticity according to the English nomenclature is very small. Hence the crystals have low natural frequencies of vibration. The Young's modulus for the *a*, *b*, and *c* directions is 2·17 10^8, 3·18 10^8 and 3·62 10^8 as compared with 14·6 10^8, 7·78 10^8 and 8·35 10^8 for aragonite and 23·04 10^8, 28·9 10^8 and 26·53 10^8 for topaz.

The elastic constants c_{hk} for a crystal of the rhombic system are connected with the elastic moduli s_{hk} by the relations :—

$$\sigma c_{11} = \begin{vmatrix} s_{22} & s_{23} \\ s_{32} & s_{33} \end{vmatrix}, \quad \sigma c_{23} = \begin{vmatrix} s_{31} & s_{32} \\ s_{11} & s_{12} \end{vmatrix}, \quad c_{44} = \frac{1}{s_{44}}, \quad \text{where } \sigma = \begin{vmatrix} s_{11} & s_{12} & s_{13} \\ s_{21} & s_{22} & s_{23} \\ s_{31} & s_{32} & s_{33} \end{vmatrix}.$$

Hence values are obtained as follows :—

	c_{11}	c_{22}	c_{33}	c_{44}	c_{55}	c_{66}	c_{23}	c_{31}	c_{12}
$10^8 \times$	3·54	4·83	8·23	1·67	0·33	1·27	—3·51	3·23	—0·82

A theory of elasticity has been based on the hypothesis that the central forces between molecules are functions only of the distance between them. As a consequence of this hypothesis the coefficients in the strain-energy-function for a crystal of the rhombic system are connected by the so-called Cauchy-Poisson relations,

$$c_{44} = c_{23}, \quad c_{55} = c_{31}, \quad c_{66} = c_{12}$$

The fact that these relations do not hold for Rochelle salt indicates that there is a strong polar force between the molecules.

The general equation (6) for the twisting modulus T of a beam contains two directions, that of the length and of the breadth ; consequently it cannot be represented by one surface.

The torsion modulus T for a circular cylinder is given (Voigt, p. 760) in terms of the elastic moduli and the direction cosines of the axis of the cylinder as follows :—

$$\begin{aligned} T_0 = {} & \tfrac{1}{2}\gamma_1^4 (s_{55} + s_{66}) + \tfrac{1}{2}\gamma_2^4 (s_{66} + s_{44}) + \tfrac{1}{2}\gamma_3^4 (s_{44} + s_{55}) \\ & + \gamma_2^2\gamma_3^2 \{2 (s_{22} + s_{33} - 2s_{23}) + \tfrac{1}{2} (s_{55} + s_{66} - 2s_{44})\} \\ & + \gamma_3^2\gamma_1^2 \{2 (s_{33} + s_{11} - 2s_{31}) + \tfrac{1}{2} (s_{66} + s_{44} - 2s_{55})\} \\ & + \gamma_1^2\gamma_2^2 \{2 (s_{11} + s_{22} - 2s_{12}) + \tfrac{1}{2} (s_{44} + s_{55} - 2s_{66})\}. \end{aligned}$$

Substituting the values found experimentally

$$T_0 = 189{\cdot}5\,\gamma_1^4 + 69{\cdot}2\,\gamma_2^4 + 180{\cdot}0\,\gamma_3^4 + 181{\cdot}8\,\gamma_2^2\gamma_3^2 + 1{\cdot}6\,\gamma_3^2\gamma_1^2 + 287{\cdot}3\,\gamma_1^2\gamma_2^2.$$

Fig. 5 gives the torsion modulus T_0, for any circular cylinder the direction of whose axis is obtained by joining any point on the surface to the intersection of the co-ordinate axes.

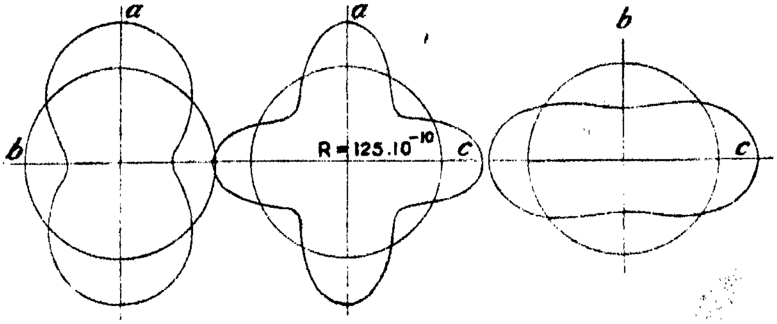

Fig. 5.

When comparing the values of the piezo-electric moduli with the extension moduli, simple pressures or tensions in directions bisecting the crystallographic axes were considered. It is evident, however, that the three piezo-electric moduli are merely determined by the electric polarisation along the directions of the crystal axes per unit shear in the respective planes normal to them, the maximum value according to Pockels being given along the *a* axis for shearing forces in the *bc* plane. Fig. 5 shows that the torsion moduli for cylinders whose axes coincide with the *a* and *c* axes are greatest.

Nicholson,[*] working mainly with crystals of Rochelle salt with a composite structure, states that a given force produces the greatest piezo-electric effect when it is applied in such a way as to twist the crystal about its principal *c* axis, and advises this method of use for producing electrical or mechanical results.

Elasticity and Temperature.

As was pointed out in the Introduction, Rochelle salt almost loses its piezo-electric properties very abruptly when heated above a temperature of about 23° C. Valasek has carried out a large number of experiments to see if various physical properties of the crystal change in the neighbourhood of this temperature. His experiments include the measurement of the refractive indices, the idea being that change in the restoring force on the ions producing the effect might alter the position of absorption bands, which, if not too far from the visible spectrum, should give a considerable change in refractive index. There was no unusual change, however, between temperatures of —70° and +40° C.

---

[*] *Loc. cit.*

Experiments on the coefficients of expansion through the same range indicated no sudden change in dimensions, nor was there any sharp heat transformation. Optical activity, like the piezo-electric effect, is associated with asymmetric structure. Difficulties occurred in the measurement of the rotatory power with the solid, but no marked change could be obtained with a solution. The same remark applied to the electrical conductivity, although it was found that it depended on the direction of the current over the piezo-electric temperature range, but the linear relation of current to field still applied.

The author carried out a bending experiment to determine if there was any sudden change in the elasticity, using a beam the direction of the length being parallel to the crystallographic c axis. The beam was enclosed in a constant temperature enclosure for at least 6 hours for each temperature and readings were taken for 12 different temperatures between —14° and +35° C. No discontinuity was evident near the critical temperature of 23° C. and the elasticity did not vary by more than 2 per cent. in the whole range. However, in a paper shortly to be published it will be shown, by a very sensitive method, that there is a slight abrupt change in elasticity at this critical temperature, although the change is exceedingly small.

Electro-Optical Effect.

Pockels* discusses a reversible electro-optical effect peculiar to crystals of asymmetric structure and carried out experiments on sodium chlorate, quartz and Rochelle salt. The effect consists of a change in double refraction somewhat similar to the Kerr effect exhibited by dielectrics which become double refracting when submitted to an electrostatic field. Pockels conducted experiments to decide the important question whether this electro-optical phenomenon in piezo-electric crystals was due solely to the mechanical deformation caused by the electric field, or whether there was also a direct influence of the electrostatic force on light motion in these crystals. He first shows that six constants are necessary in order to determine the orientation of the optical symmetry axes and the principal velocities. These constants are functions of an externally applied force, mechanical or electrostatic. Consequently in the former case they are functions of the elastic deformation, and in the last case of the dielectric polarisation. In the general case, there are 36 piezo-optic constants and 18 electro-optic constants, which reduce in number according to the symmetry of the crystal considered. It is also necessary to determine experimentally the piezo-electric moduli; from the energy principle it follows that a piezo-electric crystal, if brought in a suitable electric field, suffers a known deformation, and indeed gives a reciprocal relation between this deformation and the electrical effect through pressure. Knowing then these moduli by experiment, the resulting deformation can be calculated if the elastic moduli are known.

---

* *Loc. cit.*

The experiments of Pockels consisted therefore of a determination of the piezo-optical effect due to pressure alone and of the electro-optical effect in an electrostatic field, which would cause the same amount of deformation. If the electric field exerts no direct optical effect, then these two results should be the same.

In the case of sodium chlorate, the electro-optical effect was about 12 times as great as that due to the deformation alone, and in quartz it was about twice as great; for Rochelle salt, although the experimental results were obtained, no definite decision could be made since the elastic moduli had not been determined. Pockels, however, points out that this would be a decisive case as the experimental values are very large. On inserting the value found for s_{55} in the present paper, the electro-optical effect is about five times greater than that obtained by the mechanical effect alone.

Thus the result for this crystal agrees with that for sodium chlorate and quartz, namely, that an electrostatic field *does* exert a direct influence on light motion in piezo-electric crystals.

The author wishes to express his thanks to Prof. G. Owen and to Prof. O. W. Richardson for their kind interest, to Mr. L. E. Sulston for making the apparatus, and to Mr. R. M. Davies for advice on growing the crystals.

Gaseous Combustion at High Pressures. *Part* VIII.—*The Explosion of Methane with up to its own Volume of Oxygen at Initial Pressures up to* 150 *Atmospheres.*

By Donald T. A. Townend, Ph.D., D.I.C.

(Communicated by W. A. Bone, F.R.S.—Received July 18, 1927.)

In Part I of this series* an account was given of the behaviour of methane on explosion with less than its own volume of oxygen at initial pressures between 8·5 and 31·26 atmospheres. It was shown to be in agreement with the "hydroxylation" theory of hydrocarbon combustion; moreover, the oxygen-affinity of methane was found to be far greater than that of either hydrogen or carbonic oxide in like circumstances.

Other outstanding features of the experiments were (1) the formation of large quantities of both steam and carbon in explosions of $2CH_4 + O_2$ mixtures, (2) the disappearance of free carbon from the products when the proportion of oxygen in the mixture exploded exceeded 40 per cent., (3) the occurrence of oxides of carbon and steam in the products of all the mixtures fired, and (4) that the proportion of the original oxygen appearing as steam in the cooled products was smaller with a $3CH_4 + 2O_2$ mixture than with any other exploded between the limits $2CH_4 + O_2$ and $CH_4 + O_2$. These observations excited considerable interest on account of their theoretical importance and have since been much discussed.

In order to gain further insight into such explosions, it seemed desirable to extend the work, and particularly to make a systematic study of the pressure-time curves over a much wider range of initial pressure. A number of these were obtained by the late W. A. Haward during 1920, but they were incomplete, and not until recently have circumstances allowed of the matter being further pursued. More than a year ago Prof. Bone requested me to carry out a series of new experiments, and the present paper embodies the results obtained up to the present.

The experiments included herein fall into two series, namely, a systematic study of the behaviours on explosion of (1) a number of methane-oxygen mixtures between the limits $5CH_4 + 2O_2$ and $CH_4 + O_2$, and (2) of mixtures corresponding to $CH_4 + O_2 + 3{\cdot}76R$ (where $R = N_2$, Ar or He). With the apparatus now at our disposal it has been possible to employ much higher initial pressures than were possible in the earlier work, the range covered being from 6 up to (in some cases) 150 atmospheres.

---

* Bone, 'Phil. Trans.,' A, vol. 215, p. 275 (1915).

Experimental.

The Gases.—The methane used was prepared by the action of dilute hydrochloric acid on aluminium carbide, the gas evolved being then scrubbed by contact with a stream of 50 per cent. sulphuric acid in towers packed with pumice. Its final purification was by liquefaction and subsequent fractional distillation of the liquid, the first and last fractions being rejected. After compression into cylinders at 120 atmospheres the gas was found on analysis to be quite free from either hydrogen or higher hydrocarbons, and to contain less than 2 per cent. of adventitious nitrogen.

The oxygen used had been purchased in cylinders from the British Oxygen Company, its nitrogen content always being ascertained by chemical analysis before use. Whenever either argon or helium was used as a diluent in the explosions, it was taken from stock of about 98 per cent. purity in each case.

Deviations from Boyle's Law of the Experimental Mixtures at the Various Initial Firing Pressures.

The deviations from Boyle's law of the various explosive mixtures at all the initial pressures to be employed in these experiments were determined in a specially designed apparatus which has recently been installed in Professor Bone's laboratories for such purpose. An isotherm was first determined for each mixture and from it a series of pressures calculated corresponding with "corrected" values of 6, 10, 25, 50, 100, 125 and 150 atmospheres, respectively.

The following are the pressures, so determined, at which the various mixtures were actually fired in the subsequent explosions :—

Mixtures.	"Corrected" Initial Pressures (Atmospheres).						
	6	10	25	50	100	125	150
	Initial Pressures Actually Employed.						
$5CH_4 + 2O_2$	—	9·77	—	46·9	88·5	108·6	128·7
$2CH_4 + O_2$	5·91	9·78	24·1	47·0	88·9	109·8	—
$3CH_4 + 2O_2$	5·92	9·79	24·2	47·1	89·5	—	—
$4CH_4 + 3O_2$	5·93	9·80	24·2	47·2	—	—	—
$CH_4 + O_2$	5·94	—	24·2	—	—	—	—
$CH_4 + O_2 + 3{\cdot}76N_2$	—	9·93	—	48·7	95·6	—	143·8
$CH_4 + O_2 + 3{\cdot}76Ar$	—	9·84	—	48·2	94·7	—	139·3
$CH_4 + O_2 + 3{\cdot}76He$	—	10·11	—	50·5	101·7	—	152·0

In the tabulated results of the experiments :—

P_i obs. = the initial pressure in atmospheres, at which the mixture was actually fired.

P_i corrd. = the said initial pressure "corrected" for deviation of the mixture from Boyle's law.

P_m obs. = the maximum pressure in atmospheres, actually attained in the explosion.

P_m corrd. = the said maximum pressure "corrected" for cooling loss during the actual explosion period.

P_m/P_i corrd. = the ratio of the said "corrected" maximum pressure to the said "corrected" initial pressure.

t_m = the time (in seconds) taken for the attainment of maximum pressure after commencement of the pressure rise.

P_f obs. = the observed final pressure of the cooled explosion products.

It should also be noted that the numbering of the experiments follows on that adopted in the previous papers of this series.

FIRST SERIES OF EXPERIMENTS.

Explosions of Methane-Oxygen Mixtures of Compositions between $5CH_4 + 2O_2$ *and* $CH_4 + O_2$.

Although it is not possible at atmospheric pressure to explode a methane-oxygen mixture containing more than about 60 per cent. of the combustible gas, yet on increasing the initial pressure the upper "explosion limit" is raised, so that at high pressures mixtures containing much larger proportions of methane can be fired. Thus, for example, at an initial pressure of 10 atmospheres it has been found possible to explode a mixture containing 70 per cent. of methane. It was also discovered that the effect of increasing the initial pressure in cases of mixtures containing upwards of 60 per cent. of methane is not only to increase the violence of the explosions, but also to diminish carbon deposition, and in certain cases even to suppress it altogether.

In the experiments now to be described, a series of explosions was made with mixtures corresponding to (*a*) $5CH_4 + 2O_2$, (*b*) $2CH_4 + O_2$, (*c*) $3CH_4 + 2O_2$, (*d*) $4CH_4 + 3O_2$, and (*e*) $CH_4 + O_2$, respectively, in each case up to as high an initial pressure as the violence of the explosion would allow. For this purpose one or other of our spherical bombs No. 2 or No. 3 (explosion cavity = 240 c.c.), fitted with a Petavel gauge and optical recording accessories, was employed.

In all essentials the experimental procedure followed that described in previous papers* (*q.v.*), each gaseous mixture being made up in the bomb itself, which had been previously thoroughly dried out by means of $CaCl_2$-dried air blast. After thorough mixing of the gases by rotating the bomb, which is mounted on ball-bearings, the explosive medium was ignited by electrically fusing a thin platinum wire.

(*a*) *With a* $5CH_4 + 2O_2$ *Mixture.*—The experimental results with this mixture at initial pressures between 10 and 150 atmospheres are summarised in Table I, and four of the pressure-time records, namely, those obtained in experiments carried out at initial pressures of 10, 50, 100 and 150 atmospheres,† respectively, reproduced in fig. 1.

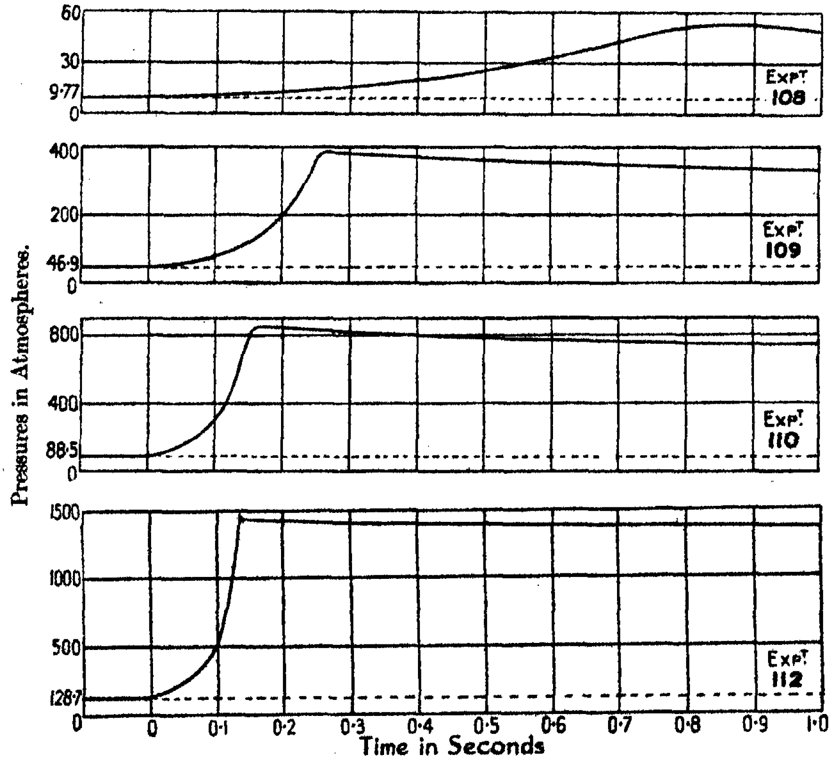

FIG. 1.—$5CH_4 + 2O_2$ Mixture.

It may here be observed that this mixture could not be fired at all at 6 atmospheres initial pressure, and that whilst it could be fired at 10 atmospheres, the resulting explosion was exceedingly slow. As the initial pressure was raised, however, the times taken for the attainment of maximum pressure were found to decrease rapidly. Also particular attention is directed to the fact that, whilst much carbon was deposited in the explosions at initial pressures up to 100 atmospheres, at higher pressures this feature became less, and at 150 atmospheres it almost disappeared.

---

* *Loc. cit.*; also 'Roy. Soc. Proc.,' A, vol. 103, p. 205 (1923); and vol. 108, p. 393 (1925).

† In discussing these results it will be more convenient to refer to the "corrected" initial pressure.

For each experiment gas balances have been drawn up (*vide* Table I), showing the units of carbon, hydrogen and oxygen, respectively, in the initial mixture as compared with those in the gaseous explosion products. From these values an approximate calculation has been made of the percentages of (*a*) the original methane-carbon deposited during the explosion, and (*b*) the oxygen and hydrogen accounted for by the formation of steam. Thus the percentage of free carbon progressively decreased from about 21 in the explosion at 10 atmospheres initial pressure to 0·4 in that at 150 atmospheres, while the percentage of the original oxygen appearing as steam decreased from about 51 at 10 atmospheres initial pressure to a minimum of about 36 at 100 atmospheres, increasing thereafter to 39 at 150 atmospheres. From the composition of the explosion products an estimate has also been made of the water-gas equilibrium constant.

One of the outstanding features of the pressure-time records was the abnormally slow rate of cooling which occurred in all these explosions. Thus, for example, in Experiment 110, where at an initial pressure of 100 atmospheres a maximum pressure of 850 atmospheres was developed, the rate of cooling two seconds after the attainment of maximum pressure was only 25 atmospheres per second, although a pressure of about 700 atmospheres still remained in the bomb. This circumstance seemed to be due mainly to the poor heat conductance of the carbon deposit on the walls of the bomb, and in part also to exothermic reactions occurring during the cooling period.

(*b*) *With a* $2CH_4 + O_2$ *Mixture.*—On increasing the percentage of oxygen the mixture was found to be far more easily ignitable, and the subsequent rate of pressure development more rapid, than in corresponding experiments of the previous series. No difficulty was experienced in exploding the mixture at 6 atmospheres initial pressure, and as the latter was raised the violence of the explosion increased until at 125 atmospheres the end of the pressure rise was accompanied by a slight "knock" (*vide* fig. 2). For this reason the initial pressure was not taken any higher.

Much the same general effects were observed in the case of this mixture (*vide* Table II) as with the previous one. Abundant carbon deposition occurred in the explosions at the lower initial pressures (*e.g.*, as much as 26 per cent. of the

Table I.—$5CH_4 + 2O_2$ Mixture.

	Bomb No. 2.		Bomb No. 3.		
Experiment No.	108	109	110	111	112
P_i (atms.) Obs. Corr.	9·77 10·00	46·9 50·0	88·5 100·0	108·6 125·0	128·7 150·0
P_m (atms.) Obs. Corr.	52·4 60·2	381 392	850 864	1175 1192	1440 1445
P_m/P_i Obs. Corr.	5·36 6·02	8·13 7·84	9·61 8·64	10·82 9·53	11·19 9·70
t_m (sec.)	0·84	0·26	0·19	0·16	0·14
Cooling Loss 1 sec. after t_m Atms. Per cent.	16·6 31·7	52 13·7	100 11·8	95 8·1	80 5·6
P_f obs.	10·3	61·5	117·8	142·6	166·0
†Original Mixture CH_4 O_2	70·4 29·6	71·0 29·0	71·1 28·9	71·9 28·1	71·3 28·7
†Gaseous Products CO_2 CO CH_4 H_2	4·0 20·2 29·6 46·2	3·7 21·6 22·6 52·1	4·6 22·3 30·2 42·9	4·5 22·2 33·9 39·4	4·9 22·1 37·2 35·8
Units in :— Original Mixture Gaseous Products	C H_2 O_2 70·4 140·8 29·6 55·4 108·6 14·5	C H_2 O_2 71·0 142·0 29·0 58·9 119·6 17·9	C H_2 O_2 71·1 142·2 28·9 67·1 121·5 18·5	C H_2 O_2 71·9 143·8 28·1 69·2 122·3 17·8	C H_2 O_2 71·3 142·6 28·7 71·0 121·8 17·5
Difference Per cent. ditto	15·0 32·2 15·1 21·3 22·9 51·0	12·1 22·4 11·1 17·1 15·8 38·5	4·0 20·7 10·4 5·6 14·5 36·2	2·7 21·5 10·3 3·8 14·9 36·5	0·3 20·8 11·2 0·4 14·6 39·0
Ratio $\frac{CO \times OH_2}{CO_2 \times H_2}$ in Products	3·4	2·1	2·0	[2·3]	[2·4]
Remarks	Abundant Carbon Deposit.			Small Carbon Deposit.	

† N_2-free.

Table II.—$2CH_4 + O_2$ Mixture.

		Bomb No. 2.			Bomb No. 3.	
Experiment No.	113	114	115	116	117	118
P_i (atms.) Obs.	5·91	9·78	24·1	47·0	88·9	109·8
P_i (atms.) Corr.	6·00	10·00	25·0	50·0	100·0	125·0
P_m (atms.) Obs.	36·0	74·8	200·0	462	1000	1445
P_m (atms.) Corr.	40·7	77·0	204·6	472	1007	1448
P_m/P_i Obs.	6·09	7·65	8·29	9·84	11·25	13·16
P_m/P_i Corr.	6·78	7·70	8·18	9·45	10·07	11·56
t_m (sec.)	0·42	0·17	0·16	0·11	0·05	0·045
Cooling Loss after 1 sec. Atms.	16·0	20·8	39	86	170	190
Cooling Loss after 1 sec. Per cent.	44·5	28·0	19·5	18·6	17·0	13·1
P_f obs.	6·70	12·0	32·8	66·7	122·1	144·4
†Original Mixture CH_4	65·9	65·8	66·4	66·3	67·1	66·5
†Original Mixture O_2	34·1	34·2	33·6	33·7	32·9	33·5
†Gaseous Products CO_2	3·7	3·6	3·4	3·3	5·6	6·1
†Gaseous Products CO	24·3	25·4	26·2	27·0	25·2	25·2
†Gaseous Products CH_4	15·5	14·8	11·9	12·1	23·5	26·1
†Gaseous Products H_2	56·5	56·2	58·5	57·6	45·7	42·6
Units in :—	C H_2 O_2	C H_2 O_2	C H_2 O_2	C H_2 O_2	C H_2 O_2	C H_2 O_2
Original Mixture	65·9 131·8 34·1	65·8 131·6 34·2	66·4 132·8 33·6	66·3 132·6 33·7	67·1 134·2 32·9	66·5 133·0 33·5
Gaseous Products	48·6 97·7 17·7	52·6 103·1 19·5	54·4 108·0 21·6	56·5 109·1 22·4	66·3 113·0 22·2	66·2 109·5 21·6
Difference	17·3 34·1 16·4	13·2 28·5 14·7	12·0 24·8 12·0	9·8 23·5 11·3	0·8 21·2 10·7	0·3 23·5 11·9
Per cent. ditto	26·3 25·9 48·0	20·1 21·6 42·9	18·1 18·7 35·7	14·7 17·7 33·6	1·2 15·8 32·4	0·4 17·5 35·7
Ratio $\frac{CO \times OH_2}{CO_2 \times H_2}$ in Products	3·5	3·0	2·5	2·5	1·7	[2·0]
Remarks	Abundant Carbon Deposit.				Slight Carbon Deposit.	Slight " knock."

† N_2-free.

original carbon in the explosion at 6 atmospheres initial pressure), but only a mere trace could be detected in the explosion at the highest initial pressure.

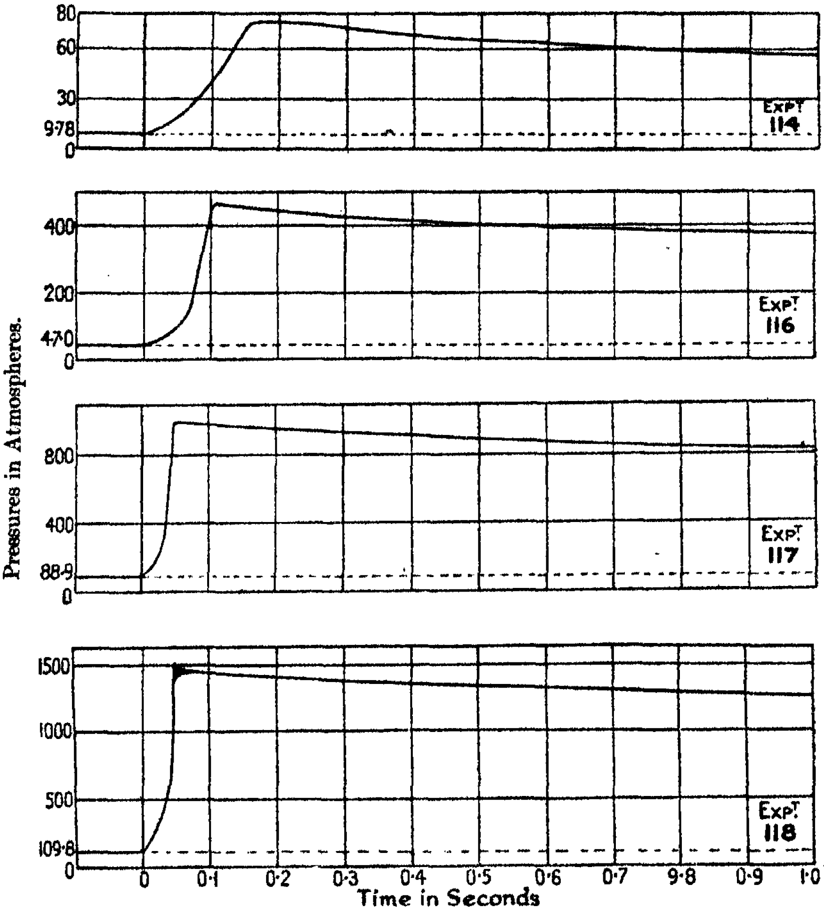

Fig. 2.—$2CH_4 + O_2$ Mixture.

At 10 atmospheres the percentage of oxygen appearing as steam in the products was much less than in the corresponding explosion with the previous mixture, but in this case also, as the initial pressure was raised, a minimum value was again found at 100 atmospheres.

The slowness of the rates of cooling in these explosions was not quite so marked as in those of the previous mixture.

(c) *With a* $3CH_4 + 2O_2$ *Mixture.*—A further addition of oxygen so as to produce a mixture of the composition $3CH_4 + 2O_2$ sufficed to ensure a fairly rapid pressure rise on explosion at comparatively low initial pressures. There was also a distinct change in the type of pressure-time curves obtained (*vide* fig. 3) as compared with those from the two previous mixtures; for not only was the time taken for the attainment of maximum pressure much less, but the rate of cooling much greater. The time taken for the attainment of maximum pressure decreased rapidly as the initial pressure was raised, until at 100 atmospheres the explosion was very violent, as is evident from the vibrations in the pressure-time record.

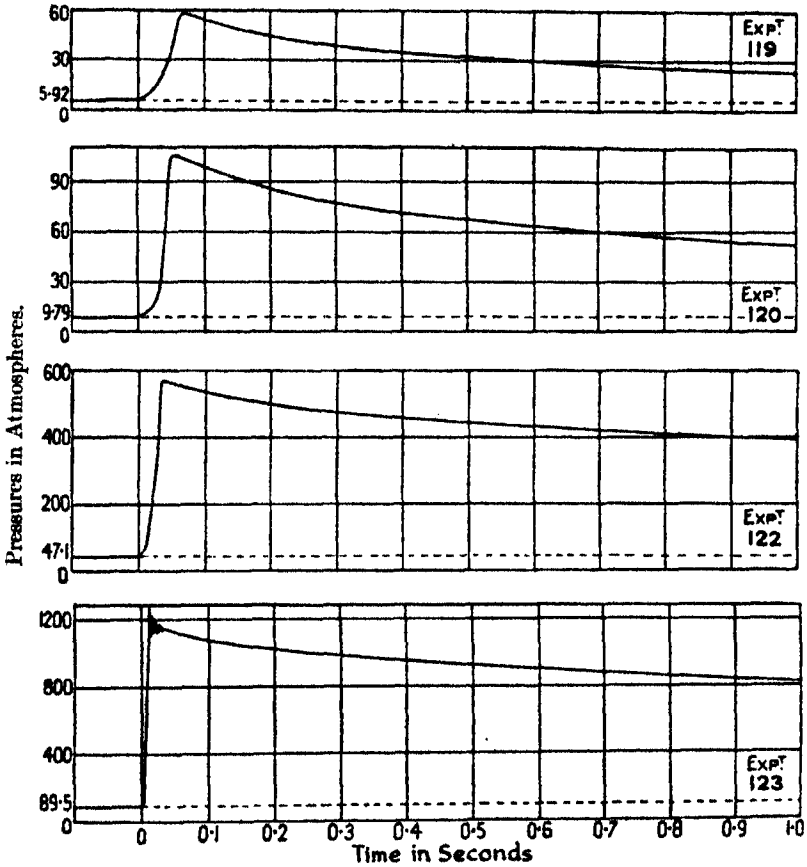

FIG. 3.—$3CH_4 + 2O_2$ Mixture.

Perhaps the most notable features of the explosions, however, were (1) that whereas in the explosion at an initial pressure of 6 atmospheres (*vide* Table III) a copious deposit of carbon was observed, only a very small amount was found at 25, and none whatever at 100 atmospheres initial pressure, and (2) that the proportions of oxygen appearing as steam were less than those in the corresponding experiments with any other mixture fired between the limits $5CH_4 + 2O_2$ and $CH_4 + O_2$. This last-named result confirmed over a wide range

Table III.—$3CH_4 + 2O_2$ Mixture.

	Bomb No. 2.				Bomb No. 3.
Experiment No.	119	120	121	122	123
P_i (atms.) Obs.	5·92	9·79	24·2	47·1	89·5
P_i (atms.) Corr.	6·00	10·00	25·0	50·0	100·0
P_m (atms.) Obs.	58·5	105	266	568	1200*
P_m (atms.) Corr.	63·0	108·5	274	577	1210*
P_m/P_i Obs.	9·88	10·72	10·74	12·06	13·41*
P_m/P_i Corr.	10·5	10·85	10·96	11·53	12·10*
t_m (sec.)	0·07	0·05	0·04	0·035	0·01
Cooling Loss 1 sec. after t_m Atms.	36·3	54·6	112	178	375*
Cooling Loss 1 sec. after t_m Per cent.	62·0	52·0	42·1	31·3	31·0*
P_f obs.	8·5	14·6	35·9	66·0	120·5
†Original Mixture CH_4	58·9	59·4	58·7	58·9	59·1
†Original Mixture O_2	41·1	40·6	41·3	41·1	40·9
†Gaseous Products CO_2	2·9	3·0	3·6	5·5	6·7
†Gaseous Products CO	34·0	33·9	33·8	33·0	31·5
†Gaseous Products CH_4	1·7	1·9	2·2	5·9	11·3
†Gaseous Products H_2	61·4	61·2	60·4	55·6	50·5
Units in :—	C H_2 O_2	C H_2 O_2	C H_2 O_2	C H_2 O_2	C H_2 O_2
Original Mixture	58·9 117·8 41·1	59·4 118·8 40·6	58·7 117·4 41·3	58·9 117·8 41·1	59·1 118·2 40·9
Gaseous Products	54·8 91·9 28·2	56·7 94·8 29·1	56·9 93·0 29·5	58·7 89·0 29·0	59·6 88·1 27·0
Difference	4·1 25·9 12·9	2·7 24·0 11·5	1·8 24·4 11·8	0·2 28·8 12·1	— 30·1 13·9
Per cent. ditto	6·9 22·0 31·4	4·5 20·2 28·2	3·1 20·7 28·6	0·3 24·4 29·5	— 25·4 34·0
Ratio $\frac{CO \times OH_2}{CO_2 \times H_2}$ in Products	3·5	3·0	2·6	2·4	2·3
Remarks	Copious Carbon Deposit.	Small Carbon Deposit.		Trace of Carbon.	Violent Explosion. No Carbon Deposited.

* Approximate Values. † N_2-free.

of initial pressure the observations made by Prof. Bone in his earlier investigation.* It may also be pointed out that as the initial pressure was raised the proportions of steam found in explosion products reached a minimum at 10 atmospheres.

(*d*) *With a* $4CH_4 + 3O_2$ *Mixture.*—Little comment is necessary on the explosion of this mixture, the results concerning which are tabulated in Table IV and the pressure-time records reproduced in fig. 4. The explosions were always rapid and at 50 atmospheres initial pressure were quite violent. It should be noted that no carbon was ever found in the bomb after any of these explosions.

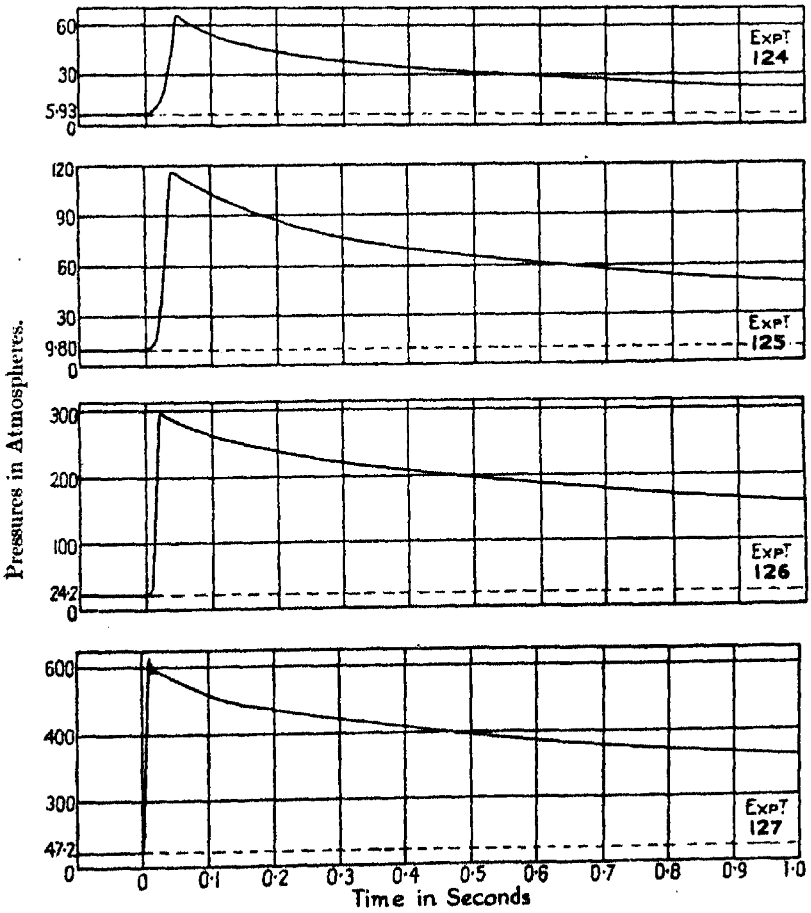

FIG. 4.—$4CH_4 + 3O_2$ Mixture.

(*e*) *With a* $CH_4 + O_2$ *Mixture.*—Owing to the violence of its explosion, an equimolecular mixture was not fired at more than 25 atmospheres initial

---

* *Loc. cit.*

Table IV.—$4CH_4 + 3O_2$ Mixture.

	Bomb No. 2.									Bomb No. 3.		
Experiment No.	124			125			126			127		
P_i (atms.) Obs.	5·93			9·80			24·2			47·2		
P_i (atms.) Corr.	6·00			10·00			25·0			50·0		
P_m (atms.) Obs.	65·0			116			298			625*		
P_m (atms.) Corr.	69·3			120·6			305			627*		
P_m/P_i Obs.	10·95			11·82			12·89			13·23*		
P_m/P_i Corr.	11·55			12·06			12·20			12·54*		
t_m (sec.)	0·045			0·04			0·025			0·01		
Cooling Loss 1 sec. after t_m Atms.	43			70			141			310*		
Cooling Loss 1 sec. after t_m Per cent.	66·2			60·3			47·3			49·6*		
P_f obs.	8·38			14·5			36·2			66·5		
†Original Mixture CH_4	56·4			56·8			57·0			56·6		
†Original Mixture O_2	43·6			43·2			43·0			43·4		
†Gaseous Products CO_2	3·5			3·6			4·2			6·1		
†Gaseous Products CO	35·5			35·1			33·4			33·0		
†Gaseous Products CH_4	0·8			0·4			1·6			3·5		
†Gaseous Products H_2	60·2			60·9			60·8			57·4		
Units in :—	C	H_2	O_2	C	H_2	O_2	C	H_2	O_2	C	H_2	O_2
Original Mixture	56·4	112·8	43·6	56·8	113·6	43·2	57·0	114·0	43·0	56·6	113·2	43·4
Gaseous Products	55·7	86·2	29·9	56·5	89·5	30·6	56·7	92·6	30·2	56·7	85·7	30·1
Difference	—	26·6	13·7	—	24·1	12·6	—	21·4	12·8	—	27·5	13·3
Per cent. ditto	—	23·5	31·4	—	21·2	29·2	—	18·8	29·8	—	24·2	30·7
Ratio $\frac{CO \times OH_2}{CO_2 \times H_2}$ in Products	3·2			2·7			2·0			1·9		
Remarks	—			—			—			Violent Explosion.		
	No Carbon ever Deposited.											

* Approximate Values. † N_2-free.

pressure. The two pressure-time curves obtained are illustrated in fig. 5 and the corresponding data tabulated in Table V. It is of interest to note the very high P_m/P_i ratios attained in the explosion of this mixture, namely, 14·8 and 17·2 at 6 and 25 atmospheres initial pressure respectively.

Table V.—$CH_4 + O_2$ Mixture.

		Bomb No. 2.					
Experiment No.		128			129		
P_i (atms.)	Obs.	5·94			24·2		
	Corr.	6·00			25·0		
P_m (atms.)	Obs.	88·0			418*		
	Corr.	90·3			427*		
P_m/P_i	Obs.	14·80			17·26*		
	Corr.	15·05			17·05*		
t_m (sec.)		0·01			$<$0·005		
Cooling loss 1 sec. after t_m	Atms.	62·6			223*		
	Per cent.	71·2			53·3*		
P_f obs.		6·48			26·4		
†Original Mixture	CH_4	50·7			49·9		
	O_2	49·3			50·1		
†Gaseous Products	CO_2	7·3			9·3		
	CO	38·4			36·4		
	CH_4	0·9			1·6		
	H_2	53·4			52·7		
Units in :—		C	H_2	O_2	C	H_2	O_2
	Original Mixture	50·7	101·4	49·3	49·9	99·8	50·1
	Gaseous Products	50·3	59·7	28·6	49·9	59·0	29·0
Difference		—	41·7	20·7	—	40·8	21·1
Per cent. ditto		—	41·0	42·1	—	40·9	42·1
Ratio $\frac{CO \times OH_2}{CO_2 \times H_2}$ in Products		3·8			2·8		
Remarks		—			Violent Explosion.		
		No Carbon ever Deposited.					

* Approximate Values. † N_2-free.

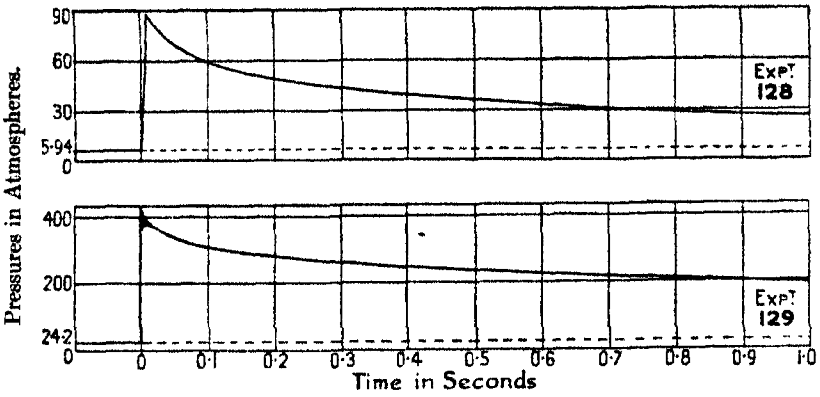

Fig. 5.—$CH_4 + O_2$ Mixture.

Rates of Cooling.

In order to compare the relative rates of cooling in the explosions of the five mixtures employed in the experiments, the differential cooling curves (in which rates of cooling dP/dt in atmospheres per second are plotted against the time in seconds after the attainment of maximum pressure) for each mixture when fired at 6 and 50 atmospheres initial pressure have been plotted in figs. 6 and 7. The influence of the deposition of free carbon on the walls of the bomb in retarding the rate of cooling is very marked.

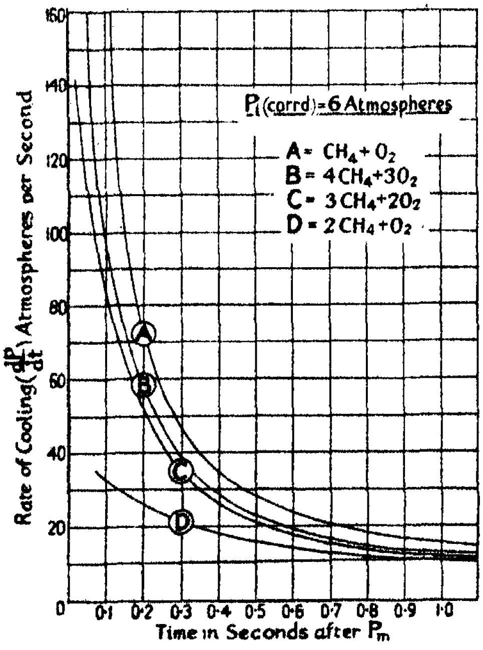

Fig. 6.

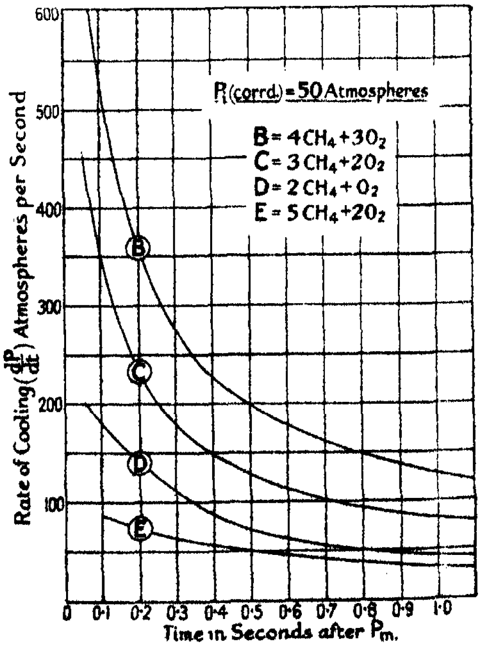

Fig. 7.

DISCUSSION OF RESULTS.

Reactions during the Explosion Period.

The results obtained are clearly inconsistent with any idea of preferential combustion of either carbon or hydrogen, for large quantities of both steam and oxides of carbon were found in the explosion products in all experiments.

It has been known since Dalton's time that the reactions involved in the explosion of an equimolecular methane-oxygen mixture are (*a*) a primary interaction producing a mixture of carbonic oxide, hydrogen and steam, probably as the result of the thermal decomposition of the incipiently formed dihydroxymethane—

$$CH_4 + O_2 = [CH_2(OH)_2] = CO + H_2 + H_2O,$$

followed during the cooling period by (*b*) a secondary interaction in the reversible system—

$$CO + OH_2 \rightleftharpoons CO_2 + H_2.$$

In considering the explosions of mixtures whose composition varied between $5CH_4 + 2O_2$ and $CH_4 + O_2$, the following facts must be borne in mind, namely, that (1) large quantities of carbon were deposited in the case of mixtures containing more than 60 per cent. of methane; (2) such carbon deposition was diminished, or even completely suppressed, when either (*a*) the oxygen content of the mixture was raised, or (*b*) higher initial pressures were employed; whilst (3) the proportion of oxygen appearing as steam in the cold explosion products (*a*) was greatest with the $5CH_4 + 2O_2$ mixture and least with the $3CH_4 + 2O_2$ mixture, and (*b*) in the case of any particular mixture was a maximum at the lowest initial pressure, decreasing as the latter was raised, and reaching a minimum in each case at some definite higher pressure.

The most probable explanation of these facts is essentially that advanced in Part I of this series (*loc. cit.*) by Prof. Bone, who considered the oxidation of methane and the decomposition of its primary oxidation products in explosions to proceed as follows:—

$$\begin{tikzcd}[column sep=huge, row sep=huge]
& \overbrace{\hspace{20em}}^{\text{Stage}} & \\
\underline{\text{A}} & \underline{\text{B}} & \underline{\text{C}} \\
CH_4 \arrow[r, "\text{oxidation}", "+\,30\ \text{K.C.Us.}"'] \arrow[d, "-\,21\cdot7\ \text{K.C.Us.}"] & H_3 : C\,.\,OH \arrow[r, "\substack{\text{oxidation via}\\ H_2 : C : (OH)_2}", "+\,49\ \text{K.C.Us.}"'] \arrow[d, "-\,22\cdot8\ \text{K.C.Us.}"] & H_2 : C : O + H_2O \arrow[d, "\substack{-\,13\cdot4\\ \text{K.C.Us.}}"] \\
C + 2H_2 & CO + 2H_2 & \overbrace{CO + H_2} \\
& \underline{B^1} & \underline{C^1}
\end{tikzcd}$$

It seems probable that where there is excess of methane present in explosions at low initial pressures, some of it is decomposed thermally into carbon and hydrogen ($CH_4 \rightleftharpoons C + 2H_2$). With increase of initial pressure, however, such methane would be more stable, and with a shorter time of attainment of maximum pressure there would become less tendency for its breaking down.

Accordingly, at the low initial pressures where some methane seems to be thermally decomposed, there would be a greater tendency for the oxidation to proceed as a "non-stop" run through the monohydroxy stage to dihydroxymethane, giving rise on thermal decomposition to steam, carbonic oxide and hydrogen (*i.e.*, $A \rightarrow B \rightarrow C \rightarrow C_1$), than for it to stop at the methyl alcohol stage (*i.e.*, $A \rightarrow B \rightarrow B_1$). For in the first case the heat liberated would be 79 units, of which only 13·4 would be absorbed in the passage from C to C_1, whereas in the second case for the use of the same amount of available oxygen 60, *i.e.*, (2×30) heat units would be evolved, of which 45·6, *i.e.*, ($2 \times 22\cdot8$) would be subsequently absorbed. Thus, at low pressures, where methane appears to be less stable, and consequently lower explosion temperatures are attained, the available oxygen is distributed over a smaller proportion of it than at higher pressures, a fact which is evident from the larger percentages of oxygen appearing as water in the products from the explosions at the low initial pressures. For a similar reason the percentages of oxygen appearing as steam on exploding the three mixtures, $5CH_4 + 2O_2$, $2CH_4 + O_2$, and $3CH_4 + 2O_2$ (*vide* Tables I, II and III) are greatest in the case of the mixture $5CH_4 + 2O_2$, where the explosion temperature is least.

Prof. Bone has also suggested to me recently that whereas at high explosion temperatures methyl-alcohol would break down into carbonic oxide and hydrogen, probably at lower temperatures a primary decomposition into $:CH_2$ and steam would also occur simultaneously.[*] Therefore in methane explosions where oxygen is greatly in defect some decomposition might occur at the mono-hydroxy stage according to the following simultaneous equations. In such case some methane would also subsequently be reformed by the hydrogenation of $:CH_2$ residues.

$$\begin{array}{l|c|l} \cline{2-2} (a)\ \mathrm{CH_3\,.\,OH} = & \mathrm{H_2} & + \mathrm{H_2} + \mathrm{CO.} \\ (b)\ \mathrm{CH_3\,.\,OH} = & \mathrm{:CH_2} & + \mathrm{OH_2.} \\ \cline{2-2} \end{array}$$

It may well be that the changes occurring during the explosion period are in accordance with both of the foregoing views, decomposition into $:CH_2$ and H_2O taking place to some extent at the mono-hydroxy stage, the remainder having a "non-stop" run to the dihydroxy stage, where decomposition into $CO + H_2 + H_2O$ would occur.

Reactions occurring during the Cooling Period.

Dealing with reactions which probably proceed during the cooling period, consideration must first be given to the reversible water-gas reaction—

$$CO + OH_2 \rightleftharpoons CO_2 + H_2 \quad .. \quad .. \quad .. \quad + 10{\cdot}1\ \text{K.C.Us.}$$

It may be noted that the composition at equilibrium is unaffected by pressure and dependent on temperature only. Values of 1·62 and 2·16 for the equilibrium constant $K = \frac{CO \times OH_2}{CO_2 \times H_2}$ were found experimentally by O. Hahn[†] at temperatures of 1000 and 1200° C., respectively, and extrapolation therefrom gives 3·43 at 1400° C. and 4·24 at 1600° C.

Reference to Tables I to V will show how the values for the water-gas equilibrium constant K, as determined from the cold gaseous products, varied between 3·8 and 1·7 according to the initial pressure of the explosion and the consequent rate of cooling. These values may be compared with the 4·0 found by Andrew,[‡] who exploded various hydrocarbon-oxygen mixtures in glass vessels at initial pressures of about half an atmosphere, where a greater rate of cooling would occur, and with the 4·8 to 5·8 found by Robertson and Garner* on detonating pellets of solid explosives in an evacuated calorimetric bomb. They should not be taken, however, as indicating in all cases the precise temperature at which the equilibrium mixture was "frozen out," because it is probable that at very high pressures the composition of the cold products might be affected by the subsequent operation of other reactions, as might be the case, for example, in the explosion of the $5CH_4 + 2O_2$ mixture at 125 and 150 atmospheres and the $2CH_4 + O_2$ mixture at 125 atmospheres initial pressure. Also, in cases where carbon deposition occurred during the explosion it would tend to diminish the ratio, both by its direct interaction with steam and by its retardation of the cooling.

---

[*] Bone and Davies, 'Trans. Chem. Soc.,' vol. 105, p. 1691 (1914).

[†] 'Z. Phys. Chem.,' vol. 48, p. 735 (1904).

[‡] 'Trans. Chem. Soc.,' vol. 105, p. 444 (1914).

Consideration should be given also to the possible occurrence of some reactions which might proceed even at comparatively low temperatures and in which methane-formation would be especially favoured by conditions of very high pressure combined with exceptionally slow cooling, such as were realised in the explosions carried out at initial pressures above 100 atmospheres. In these circumstances the following three reactions, each producing methane, might possibly come into play :—

(a) $CO + 3H_2 \rightleftharpoons CH_4 + H_2O$ .. .. .. + 50·8 K.C.Us.

(b) $2CO + 2H_2 \rightleftharpoons CH_4 + CO_2$ .. .. + 60·9 K.C.Us.

(c) $CO_2 + 4H_2 \rightleftharpoons CH_4 + 2H_2O$ .. .. + 40·7 K.C.Us.

The influence of high pressure on the equilibrium proportions of methane in such reactions is at once apparent.

In this connection some experiments made by Noble† on solid explosives may be recalled. On firing charges of explosive of increasing density, progressively higher percentages of methane were found in the gaseous products. As the charge density increased a proportionate increase in maximum gas pressure would occur, and a slower cooling rate ensue, conditions highly favourable to the formation of methane in the manner outlined above.

---

* 'Roy. Soc. Proc.,' A, vol. 103, p. 539 (1923).

† 'Phil. Trans.,' A, vol. 205, p. 201 (1905) (the effect of methane formation from solid explosives has been dealt with very thoroughly by Yamaga, 'J. Fac. Eng. Tokyo Imp. Univ.,' vol. 15, No. 7 (1924), and also by Muraour, 'C. R.,' vol. 168, p. 995 (1919)).

The following have been taken from Noble's figures :—

Cordite, Mark I.

Density	0·05	0·15	0·25	0·40	0·50
Percentage of methane in products	0·30	0·60	1·60	5·05	7·05

M.D. Cordite.

Ditto	0·35	1·90	4·65	9·30	10·70

As the conditions already referred to might possibly be favourable to the synthesis of liquid products during the cooling period, it was thought to be of interest to see if their presence could be detected in the bomb. Accordingly, tests were made in the cases of explosions of the mixtures $5CH_4 + 2O_2$ and $2CH_4 + O_2$ at an initial pressure of 125 atmospheres, by thoroughly washing out the bomb with chloroform and then alcohol both before and after each explosion. The bomb washings were subsequently examined by Dr. L. Horton (to whom the author expresses his indebtedness), who found, on evaporating the chloroform washings, yields in each case of about 0·2 to 0·3 gram (corresponding with about 1 per cent. of the weight of the original gaseous mixture) of high viscosity liquids. A representative sample was found on analysis to have the composition C = 77, H = 12, and O = 11 per cent. Furthermore, each chloroform washing gave a strong aldehydic reaction. The alcohol washings yielded on evaporation colloidal ferric hydroxide only.

SECOND SERIES OF EXPERIMENTS.

Explosions of $CH_4 + O_2 + 3{\cdot}76R$ *Mixtures, where* $R = N_2$, Ar *or* He.

In continuation of the investigation, it was thought desirable to compare the relative influences of nitrogen, argon and helium when present as diluents in explosions of methane-oxygen mixtures, with those previously observed in explosions of similarly diluted carbonic oxide-oxygen mixtures. Accordingly explosions of a mixture $CH_4 + O_2 + 3{\cdot}76R$ (where R = one or other of the diluents in question) were carried out at initial pressures of 10, 50, 100 and 150 atmospheres.

(*a*) *With a* $CH_4 + O_2 + 3{\cdot}76N_2$ *Mixture.*—The mixture $CH_4 + O_2 + 3{\cdot}76N_2$ could not be exploded at 6 atmospheres initial pressure, and at 10 atmospheres it was found to be almost an upper "limit" mixture. It will be seen from the pressure-time curve reproduced in fig. 8 that at this pressure a very slow explosion occurred, the time taken for the attainment of maximum pressure (t_m) being as long as 1·22 sec. This time was reduced considerably by raising

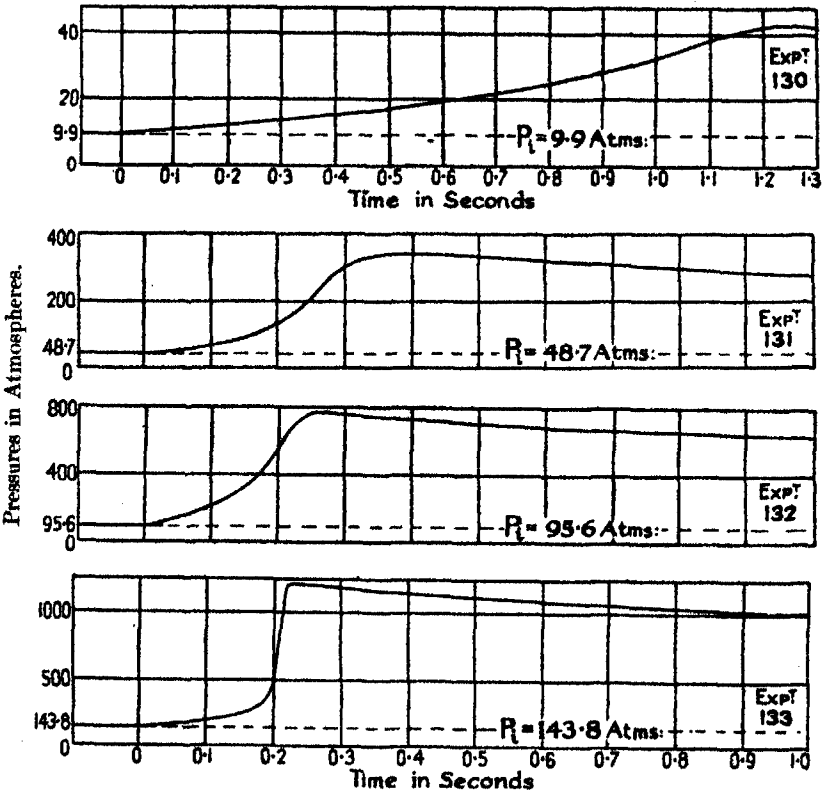

FIG. 8.—$CH_4 + O_2 + 3·76N_2$ Mixture.

the initial pressure to 100 atmospheres (*vide* Table VI). Increase of initial pressure above this, however, had little further effect on t_m. Slight carbon deposition accompanied the explosions at 10 and 50 atmospheres, but this was completely suppressed at initial pressures above 100 atmospheres.

From the balances of the units of carbon, hydrogen, and oxygen in the initial mixtures and in the gaseous explosion products, an approximate calculation of the water-gas equilibrium constant has been made in each case, as in the previous series of experiments. The latter values were again found to decrease as the initial pressure was raised.

(*b*) *With a* $CH_4 + O_2 + 3·76Ar$ *Mixture.*—The experimental data for explosions of this mixture are given in Table VII and the corresponding pressure-time curves illustrated in fig. 9. There was no difficulty in firing it at an initial pressure of 10 atmospheres, the time taken for the attainment of maximum

Table VI.—$CH_4 + O_2 + 3 \cdot 76N_2$ Mixture.

	Bomb No. 2.		Bomb No. 3.	
Experiment No.	130	131	132	133
P_i (atms.) Obs.	9·93	48·7	95·6	143·8
P_i (atms.) Corr.	10·00	50·0	100·0	150·0
P_m (atms.) Obs.	42·0	340	775	1200
P_m (atms.) Corr.	52·5	359	810	1234
P_m/P_i Obs.	4·23	6·98	8·11	8·35
P_m/P_i Corr.	5·25	7·18	8·10	8·23
t_m (sec.)	1·22	0·36	0·25	0·22
Cooling Loss 1 sec. after t_m Atms.	19·0	101	190	265
Cooling Loss 1 sec. after t_m Per cent.	45·2	29·8	24·5	22·1
P_f obs.	9·75	50·5	104·2	160·1
Ratio $\frac{CO \times OH_2}{CO_2 \times H_2}$ in Products	3·0	2·5	2·2	2·2
Remarks	This is almost an upper limit mixture. Slight Carbon Deposit.	Trace of Carbon Deposited.	No Carbon ever Deposited.	

Table VII.—$CH_4 + O_2 + 3 \cdot 76Ar$ Mixture.

	Bomb No. 2.		Bomb No. 3.	
Experiment No.	134	135	136	137
P_i (atms.) Obs.	9·84	48·2	94·7	139·3
P_i (atms.) Corr.	10·00	50·0	100·0	150·0
P_m (atms.) Obs.	72·0	430	960	1470
P_m (atms.) Corr.	77·5	450	990	1505
P_m/P_i Obs.	7·32	8·92	10·23	10·61
P_m/P_i Corr.	7·75	9·00	9·90	10·03
t_m (sec.)	0·24	0·17	0·14	0·12
Cooling Loss 1 sec. after t_m Atms.	43·0	171	420	595
Cooling Loss 1 sec. after t_m Per cent.	59·7	40·6	43·8	40·5
P_f obs.	9·96	53·0	99·4	152·0
Ratio $\frac{CO \times OH_2}{CO_2 \times H_2}$ in Products	3·0	2·7	2·5	2·4
Remarks	No Carbon ever Deposited.			

pressure being 0·24 sec. This time gradually decreased as the initial pressure was raised. In no case was any carbon deposited.

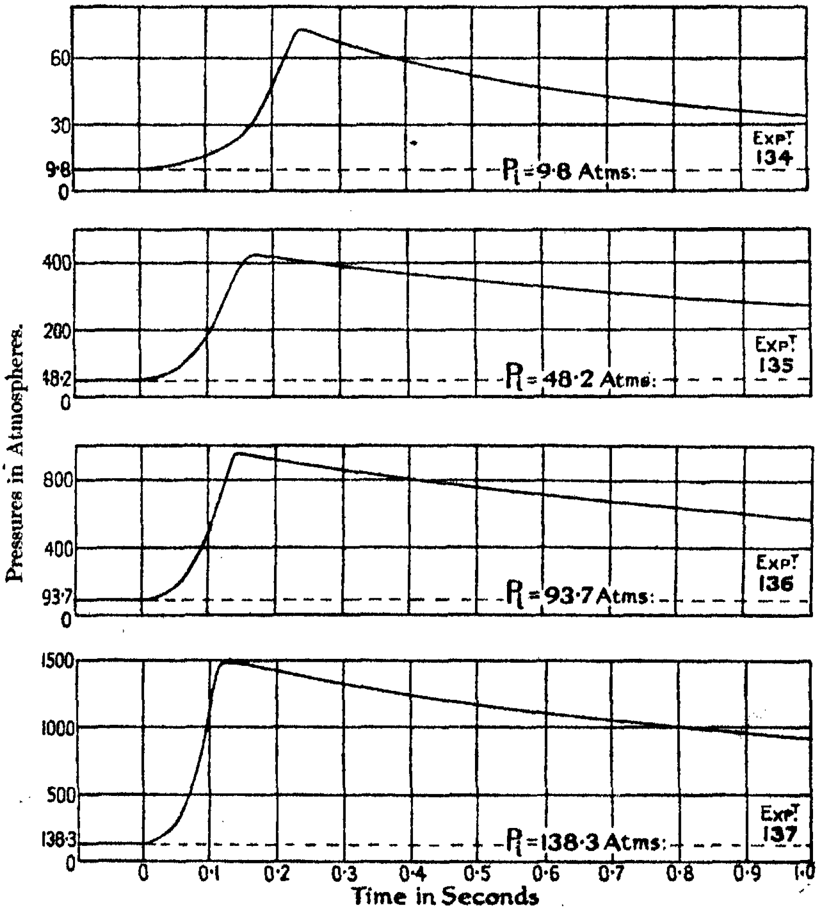

FIG. 9.—$CH_4 + O_2 + 3{\cdot}76Ar$ Mixture.

The values for the water-gas equilibrium constant as determined from the explosion products were higher than those obtained in the nitrogen series, and also decreased as the initial pressure was raised, thus showing their dependence on the relative rates of cooling.

The Non-Occurrence of Nitrogen Activation in Explosions of $CH_4 + O_2 + 3{\cdot}76N_2$ *Mixtures.*—In view of the "activation" of nitrogen by radiation previously observed in CO-air explosions at high initial pressures,* it was of interest to see whether or not any similar effect could be observed when methane was employed as the combustible gas. From a comparison of the curves obtained when argon and nitrogen, respectively, were present as diluents in a $CH_4 + O_2$ explosion (*vide* figs. 8 and 9), it will be seen that nitrogen does not behave abnormally in a $CH_4 + O_2 + 3{\cdot}76N_2$ mixture exploded at high initial pressures.

---

* Bone, Newitt and Townend, 'Roy. Soc. Proc.,' A, vol. 103, p. 205 (1923), and vol. 105, p. 406 (1924).

There are two reasons for this conclusion. In the first place, whereas in the case of a $2CO + O_2 + 3{\cdot}76N_2$ mixture the time required for the attainment of maximum pressure considerably increased as the initial pressure was raised, the reverse was found on exploding a $CH_4 + O_2 + 3{\cdot}76N_2$ mixture, as the following figures show :—

Mixtures.	t_m at initial pressures (atms.) of			
	10	50	100	150
	sec.	sec.	sec.	sec.
$2CO + O_2 + 3{\cdot}76N_2$	0·10	0·18	0·36	0·53
$CH_4 + O_2 + 3{\cdot}76N_2$	1·22	0·36	0·25	0·22

Secondly, whereas the ratio of the times taken for the attainment of maximum pressure in $2CO + O_2 + 4N_2$ and $2CO + O_2 + 4Ar$ explosions, respectively, at corresponding initial pressures rapidly increased with the initial pressure thus :—

Mixtures.	t_m at initial pressures (atms.) of		
	50	100	150
	sec.	sec.	sec.
$2CO + O_2 + 4Ar$	0·025	0·01	0·01
$2CO + O_2 + 4N_2$	0·18	0·36	0·53
Ratio of t_{ms}	7·2	36·0	53·0

The ratio observed in explosions of $CH_4 + O_2 + 3{\cdot}76N_2$ and $CH_4 + O_2 + 3{\cdot}76Ar$ mixtures, did not alter materially with pressure, as the following figures show :—

Mixtures.	t_m at initial pressures (atms.) of		
	50	100	150
	sec.	sec.	sec.
$CH_4 + O_2 + 3{\cdot}76Ar$	0·17	0·14	0·12
$CH_4 + O_2 + 3{\cdot}76N_2$	0·36	0·25	0·22
Ratio of t_{ms}	2·1	1·8	1·8

This last-named result shows no abnormality and is attributable merely to the greater molecular heat capacity of nitrogen as compared with monatomic argon.

(*c*) ***With a*** $CH_4 + O_2 + 3 \cdot 76He$ ***Mixture.***—The pressure-time curves of the explosion of helium diluted mixtures are shown in fig. 10 and the experimental data given in Table VIII. It will be seen that the general influence of helium, as compared with that of argon, as a diluent was to effect both a speeding up of the rate of pressure development and an increase in the subsequent rate of cooling, circumstances attributable to the greater mobility of helium as compared with that of argon.

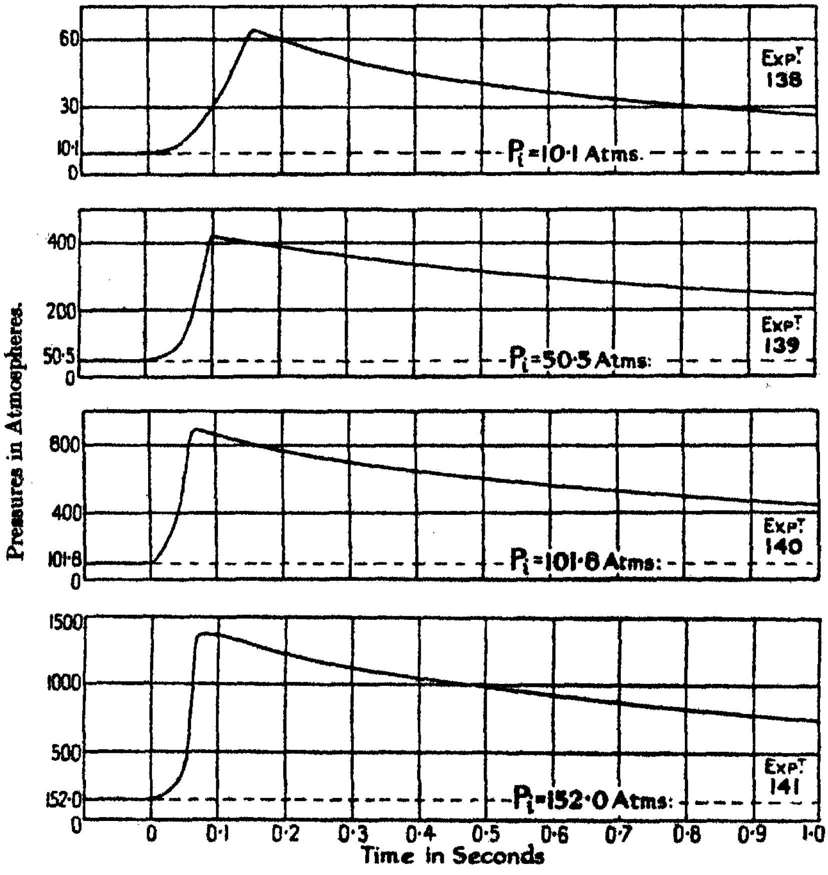

FIG. 10.—$CH_4 + O_2 + 3 \cdot 76He$ Mixture.

Table VIII.—$CH_4 + O_2 + 3 \cdot 76He$ Mixture.

		Bomb No. 2.		Bomb No. 3.	
Experiment No.		138	139	140	141
P_i (atms.)	Obs.	10·11	50·5	101·7	152·0
	Corr.	10·00	50·0	100·0	150·0
P_m (atms.)	Obs.	64·5	420	895	1370
	Corr.	71·0	434	920	1395
P_m/P_i	Obs.	6·37	8·31	8·80	9·01
	Corr.	7·10	8·68	9·20	9·30
t_m (secs.)		0·16	0·10	0·07	0·07
Cooling Loss 1 sec. after t_m	Atms.	40·3	198	460	650
	Per cent.	62·5	47·1	51·4	47·4
P_f obs.		9·56	49·5	99·4	155·6
Ratio $\frac{CO \times OH_2}{CO_2 \times H_2}$ in Products		3·4	2·9	2·7	2·6
Remarks		No Carbon ever Deposited.			

Perhaps the most striking difference between the two sets of experiments is the fact that the *corrected* P_m/P_i ratios were in most cases about 6 or 9 per cent. higher with the argon-diluted mixtures than with the corresponding helium-diluted mixtures, or, in other words, the available kinetic energy at the moment of maximum pressure was greater in the former case.

It may here be recalled that in the case of explosions of (*a*) $2CO + O_2 + 4R$, or (*b*) $2CO + O_2 + 6R$ mixtures, similar differences were observed between the influence of argon and helium as diluents, although in the case of (*a*) the rate of attainment of maximum pressure was greater in the explosion of the argon-diluted mixtures than in that of the corresponding helium-diluted ones, a result which was reversed in the case of (*b*). On the other hand, when helium or argon-diluted electrolytic gas mixtures were exploded little differences in corrected P_m/P_i ratios could be detected.* It seems probable that such results may be associated with radiation phenomena, and experiments are now in progress which it is hoped will further elucidate the matter.

Rates of Cooling.

The differential cooling curves obtained from a study of the pressure-time curves of the explosion at initial pressures of 50 and 150 atmospheres of the three mixtures of this series are given in figs. 11 and 12. It may be observed how the rate of cooling for a measurable time after the attainment of maximum pressure is always very much greater on exploding mixtures containing helium as a diluent as compared with those similarly diluted with argon. This has been found to be a characteristic feature of the cooling curves in such circumstances, whether the combustible gas be carbonic oxide, hydrogen or methane, and it may be that the heat lost by radiation as well as that by conduction is much greater when helium is the diluent employed.

---

* Bone, Newitt and Townend, 'Roy. Soc. Proc.,' A, vol. 110, p. 645 (1926).

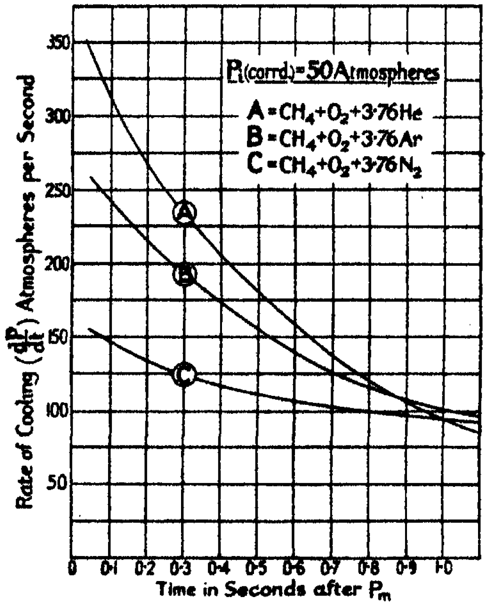

Fig. 11.

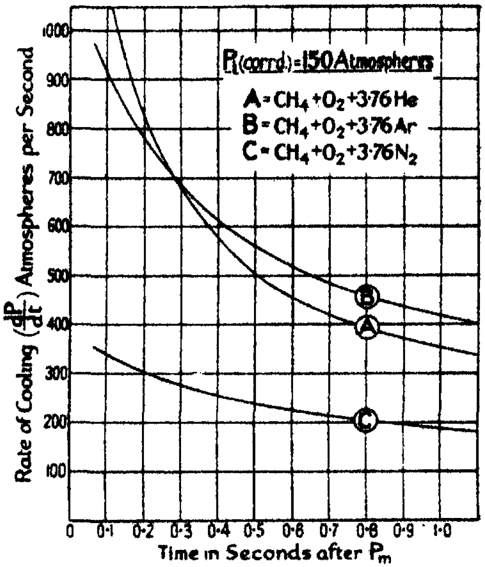

Fig. 12.

Summary.

It has been shown in the present investigation that :—

(i) Although at atmospheric pressure it is not possible to explode methane with less than two-thirds of its own volume of oxygen, at high pressures mixtures containing much smaller proportions of oxygen can be readily exploded.

(ii) The influence of increasing the initial pressure in exploding mixtures containing upwards of 60 per cent. of methane is not only to increase the violence of the explosion, but also to diminish, and in some cases to suppress altogether, carbon deposition. Such results are probably attributable to the influence of pressure in suppressing the thermal decomposition of methane.

(iii) Contrary to its behaviour in CO-air explosions, nitrogen is not "activated" in the explosion of a $CH_4 + O_2 + 3 \cdot 76N_2$ mixture, but appears to behave normally as a diluent only.

(iv) The influence of helium as compared with argon in the explosion of $CH_4 + O_2 + 3 \cdot 76R$ mixtures is to shorten the time taken for the attainment of maximum pressure, as well as to increase the subsequent rate of cooling, effects accounted for by the greater mobility of the helium molecule. The corrected P_m/P_i ratios, however, were always greater in the case of explosions of the argon-diluted mixtures.

The results have generally confirmed the observations made in earlier work and show that the mode of combustion of methane in explosions at high pressures accords well with the hydroxylation theory of hydrocarbon combustion.

In conclusion, my best thanks are due to Prof. Bone, in whose laboratories the research has been carried out, for his constant interest and advice ; to Mr. G. A. Scott, B.Sc., D.I.C., for valuable help, more particularly in connection with gas analysis and compressibility determinations, and, finally, to the Department of Scientific and Industrial Research for maintenance grants to Mr. Scott and myself. The cost of the bomb apparatus has also been defrayed by the Government Grant Committee of the Royal Society.

The Mobility of the Actinium A Recoil Atom measured by the Cloud Method.

By P. I. DEE, B.A., Sidney Sussex College, Cambridge.

(Communicated by C. T. R. Wilson, F.R.S.—Received July 22, 1927.)

[PLATES 15-19.]

1. *Introduction.*

This paper describes the measurement of the mobility of a single atom of actinium A immediately after it reaches the end of its recoil track.

Such a measurement is of importance for two main reasons. Firstly, it is of interest to obtain measurements of the mobility of individual atoms in order to ascertain whether the mobility has always a constant value, or whether a recoil atom possesses sometimes a mobility which is a multiple of the usually accepted value, namely, 1·56 cm./sec./volt/cm. Also, statistical experiments should give much better values of the relative numbers of recoil atoms of different mobilities than can be obtained from activity measurements as made by Erikson.*

Secondly, the present method enables one to obtain *definite* evidence when the mobility (and therefore presumably the charge) of the recoil atom is zero.

It has long been known that only a certain percentage of the recoil atoms bear a positive charge, the difference being attributed to neutral atoms. Briggs† has investigated this percentage for recoil atoms of different kinds in various gases by activity distribution methods, and it is felt that an extension of the present research should give more certain values of the percentages in question, by definite counting, than are obtainable by the activity methods; the latter involve considerable sources of possible error, since, in general, recoil atoms of more than one type are collected, while diffusion and loss of active emanations probably influence the results. Measurements of the mobility of recoil atoms have been made by Rutherford,‡ Franck,§ Erikson‖ and Briggs,¶ who all agree in attributing to the recoil atom the positive mobility, approximately 1·56 cm./sec./volt/cm., but Erikson finds the additional mobility 4·35 cm./sec./volt/cm., which value has not been assigned to any particular recoil atom.

---

* 'Phys. Rev.,' vol. 24, p. 622 (1924); vol. 26, p. 629 (1925).

† 'Phil. Mag.,' vol. 41, p. 357 (1921); and vol. 50, p. 600 (1925).

‡ 'Phil. Mag.,' vol. 5, p. 95 (1903).

§ 'Verh. Deutsch. Phys. Ges.,' vol. 7, p. 397 (1909).

‖ 'Phys. Rev.,' vol. 17, p. 400 (1921).

¶ 'Proc. Camb. Phil. Soc.,' vol. 23, p. 72 (1926).

2. *Theory of the Method.*

Suppose we have a "cloud track" chamber of the usual type which contains actininium, or thorium, emanation.

If a vertical electric field, directed upwards, exists in the chamber, then on making an expansion both sharp and diffuse tracks of α-particles will be obtained.*

For consider disintegration of a single emanation atom. If this occurs during the interval between the supersaturation and illumination, then the ions formed along the resulting α-track are immediately fixed by condensation of water vapour and photographed in their initial positions—the electric field having no effect.

If, however, the disintegration occurs before the supersaturation, the positive and negative ions in the α-track begin to move in opposite directions with constant velocities under the electric field. After a short time the result will be the presence of two parallel tracks, one containing all the positive, the other all the negative, ions. Separation will proceed either until the moment when critical supersaturation necessary for condensation on the ions is reached, with resultant destruction of mobility, or until the separated tracks are removed to the roof and floor of the chamber. We thus see that diffuse tracks may occur in parallel pairs, or in some cases singly, as when, for example, the α-track is initially formed near the roof, so that the positive ions reach the latter before the negative ions reach the floor. The diffuseness is due to self repulsion of the ions in the track, and to gaseous collisions of different kinds during the motion of the ions.

The number of diffuse tracks present is obviously inversely proportional to the strength of the electric field for a given strength of the active source.

When the emanation atom disintegrates, giving an α-track, the actinium A atom produced recoils only a short distance—and is therefore approximately at the origin of the α-track referred to at the instant of its formation. This enables one to determine the mobility of the A atom. If the photographs are taken through the side of the chamber, *i.e.*, in a direction perpendicular to the direction of the electric field, we shall obtain three main types of records of "double" disintegrations, that is, cases in which both the emanation α-track and the α-track formed by the disintegration of the resulting A atom are present.

---

* Wilson, 'Proc., Camb. Phil. Soc.,' vol. 21, p. 405 (1923).

Case (*a*).—The emanation atom and the resulting A atom both disintegrate during the time interval between the production of the supersaturation and the occurrence of the illuminating spark.

Case (*b*).—The emanation atom disintegrates before the supersaturation, and the resulting *A* atom after the supersaturation and before the illuminating spark.

Case (*c*).—Both the emanation atom and the resulting *A* atom disintegrate before the supersaturation.

We shall consider these cases separately.

Case (*a*).—In this case no information as to the mobility of the A atom can be obtained.

If we consider the case of actinium emanation, for which the mean life of the A recoil atom is 1/350 second, we see that in general, since the interval between the supersaturation and the illuminating spark is of the order 0·1 second, double disintegration will appear as two α-tracks starting from the same point. The A track is distinguished by a separation of its origin, giving the track the appearance of a "crutch." This is due to the absence of sufficient water vapour, the latter having been absorbed by the origin of the emanation track, so that the positive and negative ions in the origin of the A track moved under the electric field applied to the chamber into a region where there was sufficient water vapour to condense on the ions and reduce their mobility to zero. In the paper by Prof. C. T. R. Wilson referred to, a good photograph of this event is given.

Case (*b*).—Fig. I shows a vertical cross-section of an expansion chamber in which there is a vertical electric field as illustrated.

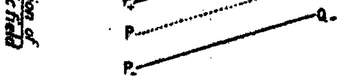

Fig. I.

P_+Q_+ and P_-Q_- are two parallel diffuse tracks formed as described previously—the emanation α-track being initially formed in the position PQ, at an instant previous to the production of the supersaturation. We here suppose that $P_+P = P_-P$, that is, that the positive and negative air ions have the same mobility under the experimental conditions—the correctness of this assumption is shown later.

Now during the time that the emanation α-track was being separated in this way, the recoil atom of actinium A has moved to some point R in the vertical line $P_- P_+$ (supposing it to be positively charged) and its mobility is given by $(PR/PP_+) \times$ the common mobility of the positive and negative air ions under the experimental conditions. At this instant the supersaturation is supposed to have occurred and fixed all the ions and the recoil atom in the positions shown. (In reality the expansion which produces the supersaturation increases all the vertical linear dimensions in a fixed ratio, but this effect can be neglected in the present discussion.)

If during the interval between this instant and the passage of the illuminating spark the *A* atom at R disintegrates, we shall obtain a sharp α-track whose origin is at *R*.

Thus a photograph of this type (obtained by a camera pointing horizontally through the side of the chamber) gives at once the mobility of the actinium A atom in terms of the common mobility of the positive and negative air ions under the experimental conditions. It does not, however, give the life of the A atom, namely, the time between the two disintegrations, since we cannot tell what interval elapsed between the occurrence of the supersaturation and the disintegration of the actinium *A* atom.

In order that photographs of this type shall be obtained frequently it is necessary that the electric field shall be of such a magnitude as to give an easily recognisable, but not too large, separation of the positive and negative ions of the emanation track in a time approximately equal to the mean life of the actinium A atom. It is obvious that the emanation atoms which disintegrate in a time before the supersaturation shorter than this value and whose A recoil atoms have lives greater than this value give doubles of this nature, since the time interval between the supersaturation and the illuminating spark is much greater than the mean life; or, in other words, the occurrence of the tracks P_+Q_+, P_-Q_- will almost invariably be accompanied by the tracks RS, provided PQ was due to an emanation atom.

Case (*c*).—It is also obvious that an emanation atom which disintegrates at a time before the supersaturation which is greater than the mean life of the recoil atom will, in general, give rise to a recoil atom which also disintegrates before the supersaturation—the result being that the track RS also undergoes separation.

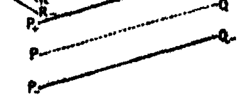

Fig. II.

Fig. II shows the general type of record to be expected in this case. Such a record will give both the mobility of the A recoil atom in terms of the common mobility of the positive and negative air ions under the experimental conditions, and the time interval between the two disintegrations, that is, the life of the A atom. An easy calculation shows that—

(1) The mobility of the recoil atom

$$= \frac{2\,.\,\mathrm{PR}}{(\mathrm{P}_-\mathrm{P}_+ - \mathrm{R}_-\mathrm{R}_+)} \times$$ the mobility of the positive air ion under the experimental conditions.

(2) The time interval between the two disintegrations is equal to the time taken for an air ion to travel a distance $= \frac{(\mathrm{P}_-\mathrm{P}_+ - \mathrm{R}_-\mathrm{R}_+)}{2}$ under the experimental conditions.

In this case it is to be noticed that the origins of the tracks again lie in a vertical line, the electric field being as before. The parallel pair of diffuse tracks due to the α-particle from the emanation atomic disintegration will naturally be more widely separated than the parallel pair due to the α-particle emitted in the disintegration of the resulting A atom. The former pair will also be more diffuse than the latter.

It has already been stated that the field applied to the chamber has to be adjusted to give a convenient separation of the emanation α-track in the mean life of the A atom.

The accuracy of determination of both the mobility of the A atom and its life is limited by the diffuseness of the tracks. This diffuseness is dependent upon the life of the A atom and is therefore not under control. The error introduced by the diffuseness could doubtless be diminished by the use of a deeper expansion chamber permitting the use of stronger electric fields, when the separations of the tracks would be greater.

On account of this diffuseness experiments with actinium A (mean life = 0·0029 second) are much more satisfactory than those with thorium A (mean life = 0·20 second), whilst the long life of radium A makes similar measurements with it impossible.

Plate 15, figs. 1 and 2, show the great advantage which lies in the use of actinium.

It is worthy of notice that in these experiments the mobility measured is that of the actinium A atom immediately after it has reached the end of its recoil track and during an interval equal to the life of the atom, *i.e.*, during a short time of mean value 1/350 second. The conditions are therefore more definite than in Erikson's experiments, where the recoil atoms, which were not all of one type, had first to pass through a region of dense ionisation before being affected by the electric field. In the experiments of this paper the recoil atom, if charged, was rapidly removed from ions of the opposite sign—if neutral, both positive and negative ions were rapidly removed from its neighbourhood.

3. *Apparatus and Experimental Method.*

The original expansion chamber used by Prof. C. T. R. Wilson in taking the photographs published in 1912 and 1923 was used in this work.* The illumination was by a Leyden-jar discharge through mercury vapour, and was oblique, photographs being taken through the side of the chamber with a stereoscopic camera.

The timing of the events—supersaturation and production of the illuminating spark—was effected by pendulums of adjustable period, as described in Prof. Wilson's 1923 paper on X-rays.

The interval between the two above events was made as short as possible (consistent with obtaining good tracks) to reduce the number of tracks formed after the expansion. Air was used in the chamber, at a pressure always less than atmospheric; the data for the photographs published are given in Section 7.

The field, applied by an annular ring of tinfoil fastened to the under side of the glass roof, was usually of the order of 30 volts/cm., but was adjusted so that the separation of the positive and negative ions of an emanation track in the mean life of the A atom (which depends also on the air pressure) was of a convenient magnitude.

The upper plate was always kept negative, this being convenient, since the emanation atoms are more numerous near the floor, and the positive tracks, which are the more important, are thus more probably caught.

The lenses were Beck Isostigmars—f. 8·0 being the aperture usually employed. Imperial Process Plates were used. Some difficulty was experienced in the introduction of the emanation. The method described by Prof. C. T. R. Wilson in a previous paper,† namely, laying a line of the radioactive source across a diameter of the floor of the chamber normal to the axis of the camera, and covering by a sheet of paper to cut off the direct α-tracks, proved unsatisfactory for actinium.

It was evident that a great number of the emanation atoms (mean life = 5·6 seconds) disintegrated while passing through the paper and shot α-tracks out into the chamber. These were separated by the field, and the ratio of the number of emanation tracks originating in the chamber to the total number of tracks present was very small. A number of methods were tried, the one finally adopted being the introduction of a small glass tube, about 1 mm. diameter and 1 cm. long, containing a thin layer of the radioactive source.* This tube was fastened horizontally to the gelatine floor of the chamber, on the diameter perpendicular to the axis of the camera, and close to the glass wall of the chamber. The open end of the tube pointed towards the centre of the chamber and faced a small vertical screen of copper about 1 cm. square.

---

* 'Roy. Soc. Proc.,' A, vol. 87, p. 277 (1912); vol. 104, pp. 1 and 192 (1923).

† 'Proc. Camb. Phil. Soc.,' vol. 21, p. 405 (1923).

By this means it was found possible to ensure that very few α-tracks starting near the mouth of the tube entered the central part of the chamber: this is, therefore, nearly free from all tracks except those due to emanation atoms which disintegrate in positions convenient for observation.

At fairly low pressures—about 0·25 atmosphere—the required event was then obtained with definition on nearly every plate exposed.

The depth of focus was about 2·0 cms., *i.e.*, tracks which were formed in that portion of the chamber bounded by two vertical planes at this distance apart were distinctly shown on the photographs. The diameter of the chamber perpendicular to the camera axis was, of course, equidistant from these planes. The magnification factor of the camera for vertical distances distributed over this depth of focus is, of course, not constant. The maximum error thus introduced is approximately 2 per cent. and was allowed for where appreciable. It was naturally impossible to prevent the formation of a number of tracks outside this depth of focus, but on examination of the plates with a stereoscope the different tracks were readily disentangled, and there was very little difficulty in interpreting the " rôle " of each track present.

The measurements of the plates were made by a travelling microscope. The magnification factor of the camera was determined by obtaining photographs of reticules placed in the chamber.

The main experiments were made with actinium, but a few preliminary trials were made using thorium.

4. *Results.*

Examination of the photographs obtained showed that five classes of associated tracks were obtained.

A large number of the pairs of type (*a*) were noticed.

The remaining four classes are discussed separately below; each can be accounted for theoretically by taking particular cases of the general theory (*b*) and (*c*) given above.

---

* The actinium source used was kindly lent by Dr. Chadwick.

Class (1). *Single separation. Mobility = that of the positive air ion under the existing conditions.*—Fig. III shows the nature of the group of tracks in this instance. This is obviously a particular form of *case* (*b*), given previously, corresponding to equality of the mobility of the actinium A atom with that of the positive air ion under the experimental conditions. The track RS was sharp—usually showing rays—the parallel tracks were diffuse.

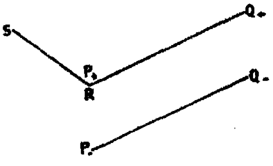

Fig. III.

Twenty photographs of cases of this nature were obtained—for typical plates see Plate 15, fig. 2, and Plate 18, fig. 8. In general the actinium A track was observed to start from the centre of the origin of the emanation α-track—or rather from the end of the positive ions of the recoil track. It is to be noticed that in the preceding discussion we neglected the length of the recoil track. This was about 0·5 mm. at the pressures used.

It is clear that the *ends* of the separated actinium A recoil tracks should be in the same vertical line as the *common origin* of the α-track from the actinium A atom and of the recoil actinium B track. This was in general found to be the case—but the great self-repulsion of the ions in the deeply ionised recoil tracks often masked this effect. In future, for convenience, we shall not refer to this effect, but it was taken into account in making the measurements of the plates. We may, therefore, conclude from these photographs that the mobility of the actinium A recoil atom in air saturated with water vapour is, in some cases, equal to the mobility of the positive air ion under similar conditions. It will be seen shortly, however, that the positive air ion in question is the *initial* short-lived positive air ion.

Class (2). *Double separation. Mobility = that of positive air ion under the existing conditions.*—Fig. IV shows the record obtained in this case. It is obviously a particular form of *case* (*c*), discussed previously, corresponding to the same mobility of the actinium A atom as in (1) above, and to a time interval between the two disintegrations equal to that required for the air ions to travel a distance $\frac{1}{2}(P_-R_-)$.

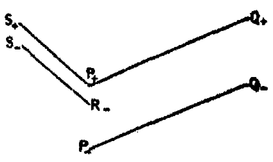

Fig. IV.

Fifty-six photographs of this type were obtained—for typical plates see Plate 17, fig. 6; Plate 18, fig. 7; Plate 19, fig. 9. The time intervals between the two disintegrations, *i.e.*, the lives of the A atoms, were calculated in a manner shown later.

It is of interest here to discuss the assumption we have made that the positive and negative air ions have equal mobilities under the conditions of these experiments. In a recent paper Tyndall and Grindley* have confirmed a result obtained by Erikson,† namely, that the positive air ion has a higher mobility at the instant of its formation than after an interval of about 0·02 second, and have shown in addition that the presence of moisture retards the transition from the initial to the final positive ion. They found that in the presence of moisture the positive ions are nearly all in their initial state after 0·014 second, whereas in dry air a considerable amount of transformation has occurred in 0·007 second. In these experiments the age of the positive ions *when the actinium A atom disintegrates* is never greater than 0·006 second, so that it must be the *initial* positive air ion which is effective in the cases described. Now Tyndall and Grindley found that in dry air the mobility of the initial positive ion equals that of the negative ion, namely, 2·15 cm./sec./volt/cm.—and both are affected by water vapour in the same way—tending to the value 1·60 for air with a saturation water-vapour pressure of 16·5 mm. This latter value is, therefore, the mobility of the positive air ion in the experiments of this paper.

Since the occurrence of groups of tracks belonging to classes (1) and (2) above fixes the mobility of the actinium A recoil atom as identical with that of the positive air ion under the experimental conditions, the mobility of the actinium A atom in air saturated with water vapour is in such cases equal to + 1·60 cm./sec./volt/cm.

In reality, as will be seen later, the mobility measured is that of the A atom in air for supersaturations less than the critical value for condensation upon the ions. The experiments of Tyndall and Grindley indicate, however, that this mobility will not differ much from the value for air saturated with water vapour. This is close to the value obtained by Erikson in ordinary air which had not been dried, and was probably also unsaturated, and suggests that the actinium A atom is not influenced by water vapour to the same extent as a negative or initial positive air ion.

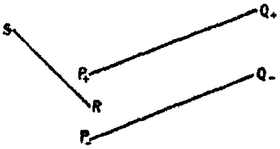

FIG. V.

Class (3). *Single separation. Mobility* = 0.—See fig. V. This, again, is a particular form of case (*b*) in the earlier part of the paper.

Four examples of this phenomenon were obtained. See Plate 15, fig. 3; Plate 16, fig. 4; and Plate 17, fig. 5.

---

* 'Roy. Soc. Proc.,' A, vol. 110, pp. 341 and 358 (1926).

† 'Phys. Rev.,' vol. 24, p. 502 (1924).

Although the positive and negative air ions have equal mobilities under the experimental conditions, we should not expect the distances RP_+ and RP_- to be exactly equal, for the critical supersaturations for the positive and negative ions are not attained simultaneously owing to the finite time of descent of the piston. The exact manner in which this time affects the calculations of the mean lives of the A atoms is shown later. The time of descent of the piston was approximately determined and found to be about 0·02 second. This corresponds to an interval of about 0·003 second between the instants at which critical supersaturations are reached for the negative and positive ions and to a further interval of the same amount between the latter instant and the attainment of the final supersaturation for which $v_2/v_1 = 1{\cdot}37$. The difference $(P_+R - P_-R)$ which would be obtained if the instants of occurrence of critical supersaturation and destruction of mobility for an ion were identical is about 3·0 mm. The experimental value obtained for this distance was never greater than 0·3 mm., and in two of the four cases it was approximately zero. It is to be expected that the time during which an ion is in the free state decreases very rapidly as the supersaturation increases beyond the critical value, and since the greater final supersaturation is reached in a very short time after the attainment of critical supersaturation, it is seen that the value for $(P_+R - P_-R)$ of 3·0 mm. is an upper limit, and that any value less than this magnitude is possible experimentally. For this and other reasons it has been assumed that destruction of mobility occurs at the same instant for positive as for negative ions.

Class (4). *Double separation. Mobility* = 0.—Fig. VI shows the modification of fig. II necessary to explain the photographs of this class. All four tracks are diffuse in this case. Eleven photographs of this type were obtained (see Plate 19, fig. 9). In general the distances between the two positive tracks and between the two negative tracks were not quite equal, but taking all the photographs the mean of the former was equal to the mean of the latter. This equality would be expected even for a comparatively large time between two critical supersaturations, since in this case the distances P_+R_+ and P_- R_- are determined completely by the velocity of the positive and negative ions and the interval between the two disintegrations.

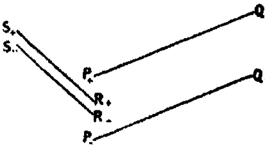

FIG. VI.

Photographs of the α-tracks produced by the use of actinium emanation in an expansion chamber have also been taken by Kinoshita and Ikeuti.* In their experiments the axis of the camera coincided with the direction of the electric field, making it extremely difficult to examine the relative positions of the origins of the tracks since separation occurred in the line of sight. No mention of neutral recoil atoms is made—the object of the study apparently being the determination of the relative numbers of the pairs "sharp-sharp," "sharp-diffuse," "diffuse-diffuse" with a view to the determination of the decay constant of actinium A.

---

* 'Nagaoka Anniv.,' 1925.

5. *Rare Occurrences.*

The above four classes, together with the double disintegrations which occurred between the supersaturation and illumination, embrace nearly all the cases experimentally observed.

In two cases photographs were obtained which apparently corresponded to a mobility of the actinium A atom higher than the value given in Classes (1) and (2) above. Unfortunately, in both of these cases the separation of the emanation track was very small, making the error due to diffuseness considerable. The distance of the origin of the actinium A track in these cases from the centre of the ions at the end of the positive separated track is, moreover, of the same order as the deviations occurring in the inequalities of positive and negative separations in Class (4) above, and it therefore seems unjustifiable to attribute these cases to a higher mobility than the value 1·60 but rather to assume that in these cases the A atom suffered greater gaseous diffusion than the average ion. One photograph was obtained which corresponded to the recoil atom being negatively charged of mobility 1·60. Little certainty is felt about this photograph—the origin was in a part of the chamber which was denser than the average with other tracks. Among the photographs taken by Prof. C. T. R. Wilson, using thorium emanation in the expansion chamber, there is a record of a double disintegration which apparently corresponds to a negative mobility 3·6 cm./sec./volt/cm. No such record was obtained in these experiments; conditions were such as to render its detection rather improbable.

6. *Experiments with Thorium.*

Only a few photographs were taken using thorium emanation. Plate 15, fig. 1, shows a typical case and emphasises the great advantage lying in the short life of actinium A.

The diffuseness of the separated tracks makes it impossible to give any value for the mobility of the thorium A atom.

Three cases in which the mobility was equal to that of the positive air ion, and one case of zero mobility, were obtained, in each of which only the emanation track was separated.

7. *Description of Plates.*

Plate 15.

Fig. 1.—Final pressure = 39 cms. of mercury.
Electric field = 1·5 volts/cm.

$$v_2/v_1 = 1\cdot 36.$$

This figure shows an example of Class (1) for thorium. The sharp track is, by chance, almost parallel to the initial emanation track.

Fig. 2.—Final pressure = 28 cms.
Electric field = 35 volts/cm.

$$v_2/v_1 = 1\cdot 37.$$

This photograph belongs to Class (1) for actinium, showing the smaller diffuseness of the parallel pair of separated tracks.

In all the following cases actinium emanation was in the chamber.

The magnification given below each figure indicates the ratio of the linear dimensions of the picture to those of the original object.

Fig. 3.—Final pressure = 26 cms.
Electric field = 34 volts/cm.

$$v_2/v_1 = 1\cdot 37.$$

This stereoscopic pair shows an example of Class (3). The enlarged " heads " of the tracks, due to the great ionisation produced by the recoil atoms, are clearly visible.

Plate 16.

Fig. 4.—An enlargement of the left-hand photograph of Plate 15, fig. 3.

Plate 17.

Fig. 5.—Final pressure = 28 cms.
Electric field = 35 volts/cm.

$$v_2/v_1 = 1\cdot 37.$$

This stereoscopic pair shows another example of Class (3).

Fig. 6.—Final pressure = 27 cms.
Electric field = 35 volts/cm.

$$v_2/v_1 = 1\cdot 37.$$

An example of Class (2) is shown ; the life of the A atom was 0·0016 second, Also near the roof there is a pair of sharp tracks with the same origin due to a double disintegration which occurred after supersaturation.

Plate 18.

Fig. 7.—Final pressure = 17 cms.

Electric field = 23 velts/cm.

$v_2/v_1 = 1 \cdot 39.$

Three records of double disintegrations are present on this stereoscopic pair. The three enlarged " heads " in a vertical line near the centre correspond to an example of Class (2). The more widely separated pair of parallel tracks are due to the α-particle from the emanation atom. This example also shows the effect previously discussed in Section 4, namely, that the *ends* of the separated actinium A recoil track are in the same vertical line as the common origins of the separated α-track from the A atom, and of the recoil actinium B track. The life of the A atom in this example was 0·0007 second. Above this, on the left, is seen a record of a double disintegration corresponding to a very short life of the A atom, certainly less than 0·0002 second. Near the bottom of the photograph there is an example of a double disintegration which occurred after the critical supersaturation had been reached.

Fig. 8.—Final pressure = 28 cms.

Electric field = 36 volts/cm.

$v_2/v_1 = 1 \cdot 36.$

The horizontal pair of parallel diffuse tracks correspond to an example of Class (1). The sharp track originating at the beginning of the positive separated track shows a crutch at its origin, due to want of water vapour at this point. The inclined pair of parallel diffuse tracks belong to an example of Class (2). The α-track from the A atom is, by chance, vertical ; so that the motion in opposite directions of the positive and negative ions in this track gives rise to separation only at the origin. This is visible, and combined with the diffuse character of the track justify the inclusion of this example in Class (2) rather than Class (1). On the left of each stereoscopic photograph there is a record of a double disintegration which occurred after the supersaturation. On the right of the right-hand photograph there is another example of the same type, but somewhat out of focus. The diffuse spot in each photograph is not a small cloud but an optical image of the source due to successive reflection by the glass cylinder.

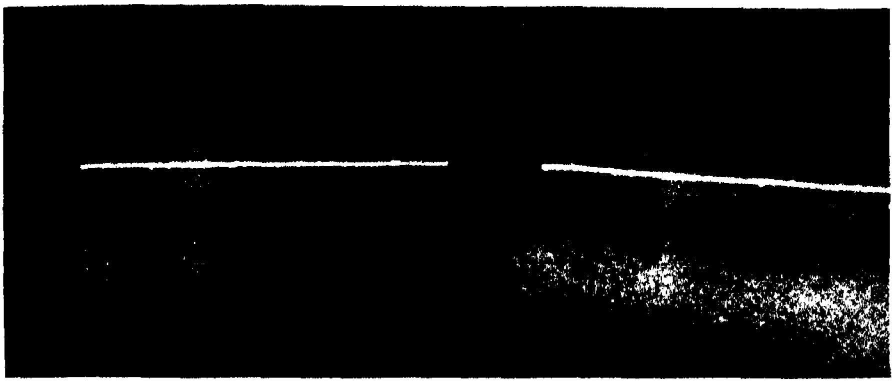

Fig. 1. (× 2.)

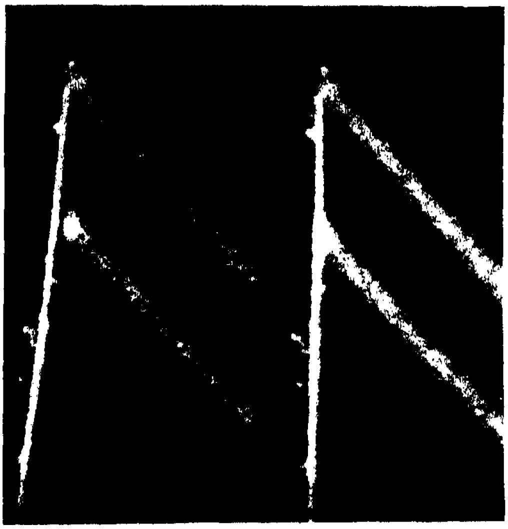

Fig. 2. (× 3.)

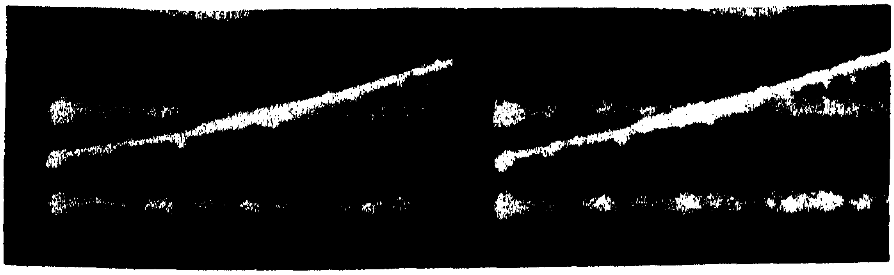

Fig. 3. (× 3·5.)

(*Facing p.* 676.)

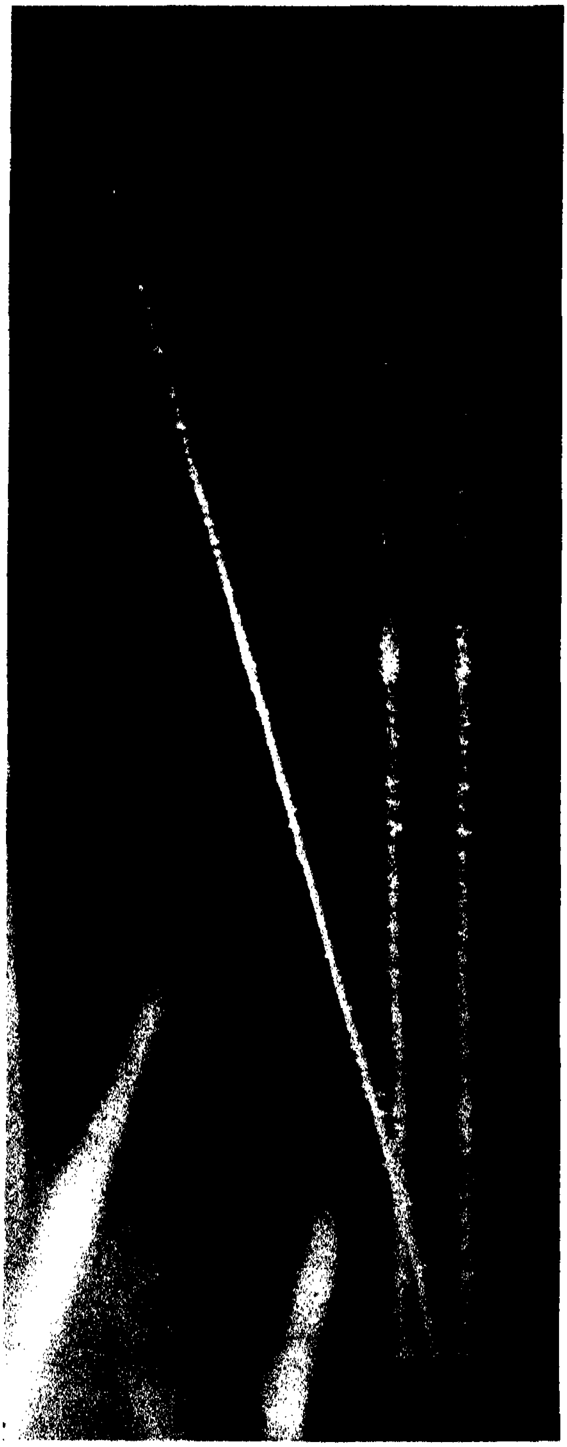

Fig. 4. (× 2·5.)

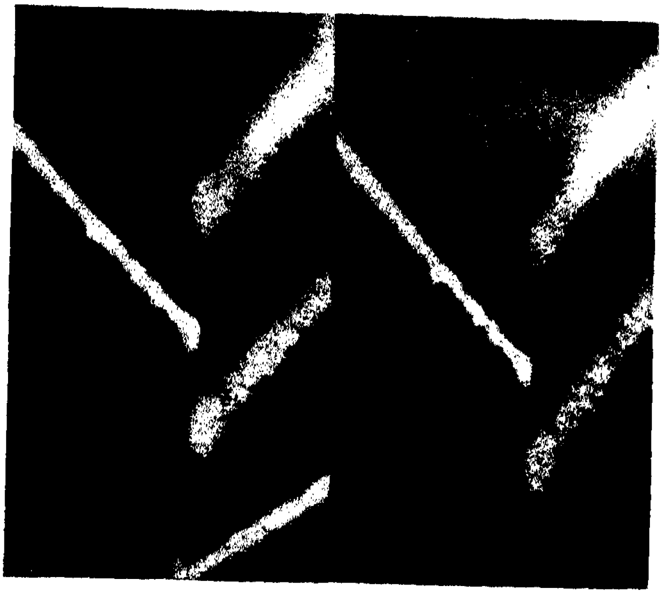

Fig. 5. (× 7.)

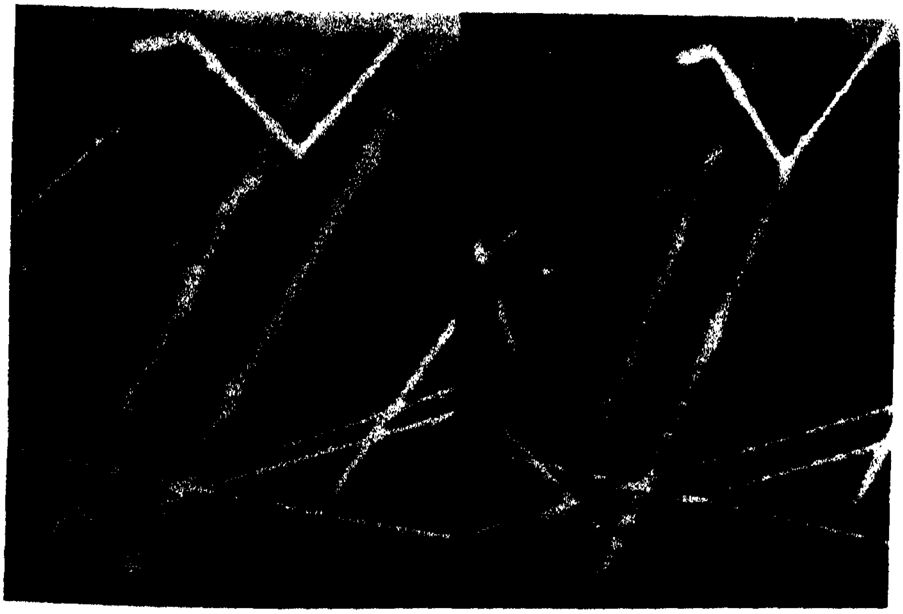

Fig. 6. (× 2·8.)

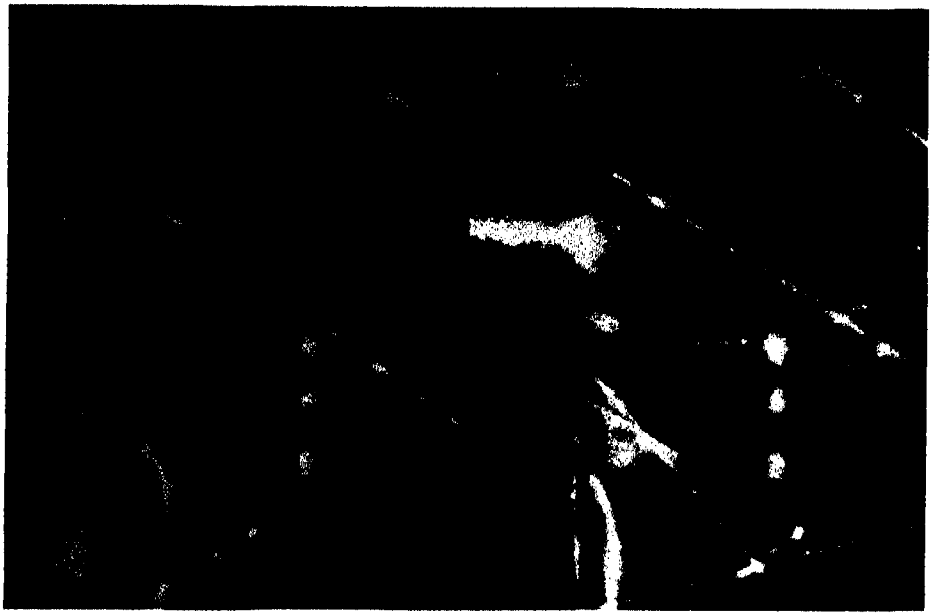

Fig. 7. (× 4.)

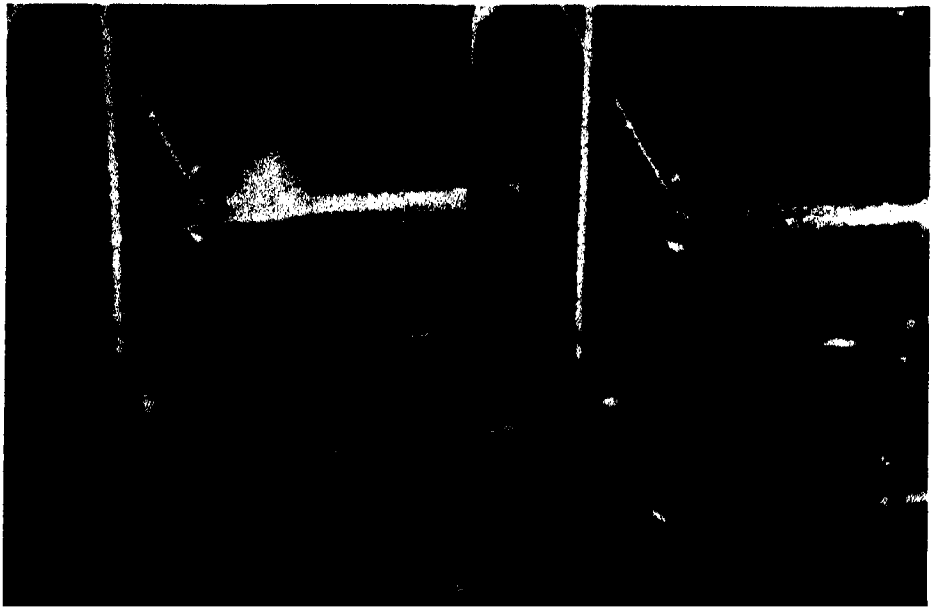

Fig. 8. (× 2·5.)

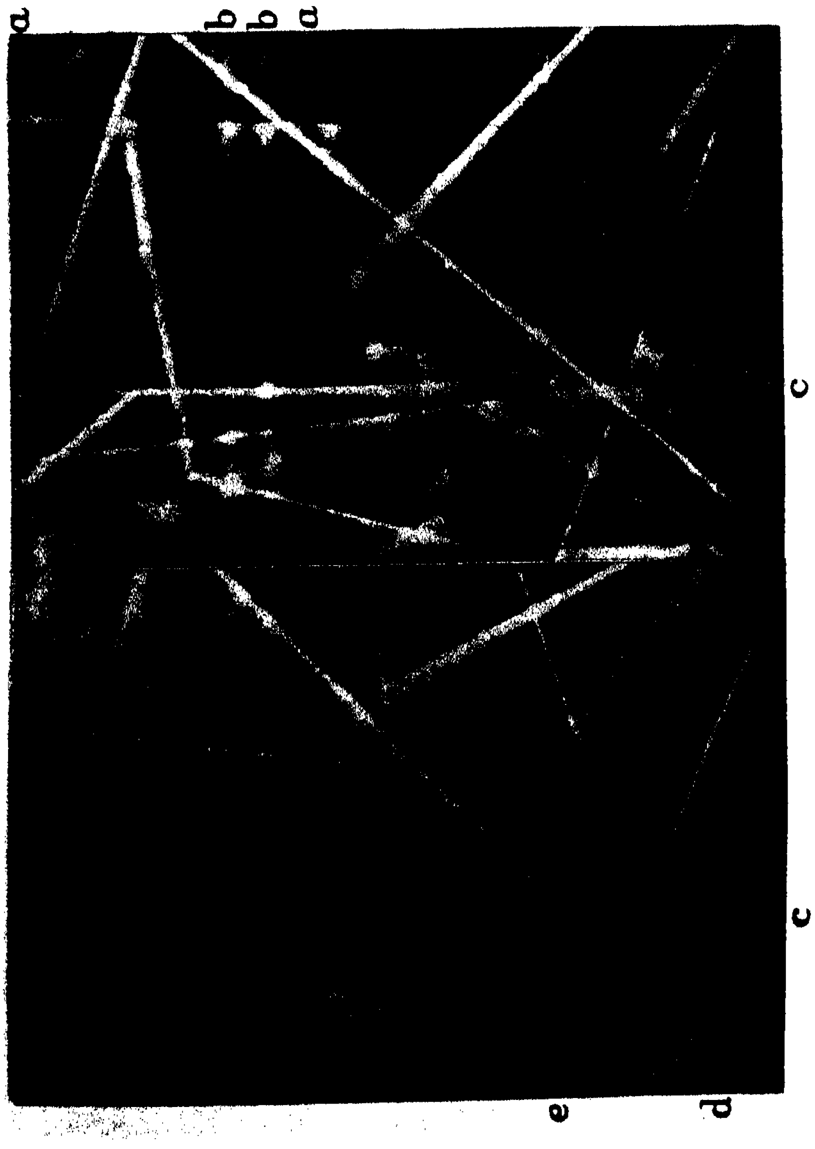

Fig. 9. (× 3·5.)

Plate 19.

Fig. 9.—Final pressure = 28 cms.

Electric field = 34 volts/cm.

$v_2/v_1 = 1{\cdot}37.$

This photograph contains a much greater number of tracks than was customary.

The four diffuse tracks, *aa*, *bb*, correspond to a double disintegration of Class (4), the life of the A atom being 0·0032 second. The tracks, *c*, *d*, belong to a record of Class (2); the α-track from the A atom is only slightly separated; the life of the A atom was 0·0032 second. Two double disintegrations which occurred after the expansion are also visible, one showing the crutch at the common origin of the two α-tracks. A similar effect is seen in the loop on the sharp track *e*.

8. *Calculations and Rough Statistics.*

The factor 0·40 was obtained for the magnification effect of the camera—vertical distances measured on the plates have to be multiplied by 2·50 to give the actual magnitude of vertical distances in the chamber.

The average number of tracks originating in the gas was, neglecting doubles of case (*a*), which are readily recognisable, about 3 per plate, so that the chance of records of the above classes being produced by the disintegrations of unrelated atoms is very small. It is realised that in the above method the actinium atom of mobility 4·35 as found by Erikson, even if due to actinium A, would in many cases escape capture owing to its greater separation from the emanation tracks, but in *32* cases of the total number (91) of double disintegrations (other than those of case (*a*)) which were recorded the position of the emanation track was such that had the A atom possessed the high mobility value it would have been detected.

The total number of positively charged recoil atoms of actinium A observed was *76*, the total number of neutral atoms was *15*, giving the value 84 per cent. of actinium A recoil atoms positively charged in air at the end of their recoil tracks.

This agrees well with Briggs's value 82 per cent. obtained for thorium A and radium A in air, since it is to be expected that these elements give the same percentage as actinium A, the three elements being isotopic, and this percentage depending only upon the nature of the atom and of the gas in which the recoil occurs, and not upon the velocity of recoil. Briggs has shown that isotopic elements do give identical percentages in the same gas, and using the value

82 per cent. for actinium A in air has explained Lucian's* results for the distribution of active deposit of actinium emanation.

By assuming that the whole separation occurs before the expansion commences, and that the latter occurs in an infinitely short time, it is possible to prove that the life of the actinium A atom is given by

$$\frac{2\cdot 5\,\mathrm{D}\,.\,v_0 v_1}{\mathrm{KV}v_2}\left\{(\mathrm{B}-p)+\frac{pv_1}{v_0}\right\} 1/76 \text{ sec.},$$

where

D cms. = the measured distance on the plates $\frac{1}{2}$(P₋R₋) for Class (2), (P₋R₋) for Class (4).

K cm./sec./volt/cm. = the mobility of the negative air ion for the water vapour pressure in question, and for total pressure = 76 cms.

B cms. of mercury = Barometric height.

V = Voltage applied to chamber.

v_0 cms. = depth of the cloud chamber at barometric pressure.

v_1 cms. = depth of the cloud chamber just before the expansion.

v_2 cms. = depth of the cloud chamber after the expansion.

p cms. of mercury = the water-vapour pressure.

The expansion, however, does not occur in an infinitely short time. Calculation shows that the whole separation which occurred took place after the piston had started to move. The equations giving the separation of the tracks for a life *L* seconds of the A atom were obtained and it was found that, if the electric field in the chamber remains constant during the expansion, the equation for the separation of the negative tracks where the piston is moving whilst the whole double event occurs was exactly the same as the equation obtained on the assumption of an infinitely fast expansion after the whole event has occurred at the pressure just before the expansion. The field remains constant during the expansion because the time of the latter is very much shorter than the time taken for the electric charge on the glass roof to diminish by leakage across the roof to the smaller value which corresponds to the smaller field, *i.e.*, to the field which corresponds to the greater depth of the chamber and the same applied voltage. By experiments with a gold leaf electroscope it was shown that the time taken for the leakage of the excess charge off the roof was certainly greater than 0·3 second, whilst the time of descent of the piston is of the order 0·02 second.

---

* 'Phil. Mag.,' vol. 28, p. 761 (1914).

The equality of the two cases can be seen in a simple manner as follows :—

Consider the motion of an ion under the electric field during the descent of the piston.

Let s = the *displacement* of the ion at the time t; that is, its distance from the gas molecules which were in its immediate neighbourhood at $t = 0$.

Then the increase of this, due to the mobility of the ion, in time dt is equal to

$$\mathrm{KF}\,\frac{v}{v_0}\,dt \text{ (assuming } v_0 \text{ corresponds to 76 cms. pressure),}$$

where

v = depth of the chamber at time t,

F = the constant field during the expansion $\left(= \frac{\mathrm{V}}{v_1}\right)$,

K and v_0 being as given above.

The final contribution of *this* separation to the final displacement of the ion

$$= \mathrm{KF} \cdot \frac{v}{v_0} \cdot dt \cdot \frac{v_2}{v}$$

$$= \mathrm{KF}\,\frac{v_2}{v_0}\,dt.$$

Thus the final displacement

$$= \mathrm{KF} \cdot \frac{v_2}{v_0} \cdot t,$$

where t = the time interval between the production of the ion and the instant when *its* mobility is destroyed by condensation.

Now on the elementary theory that the expansion occurs in an infinitely short time we have for this displacement $\left(\mathrm{KF}\,\frac{v_1}{v_0}\,t'\right)$ before the expansion—giving a final displacement

$$= \mathrm{KF}\,\frac{v_1}{v_0}\,t' \cdot \frac{v_2}{v_1},$$

$$= \mathrm{KF}\,\frac{v_2}{v_0}\,t',$$

t' in this case being the interval between the production of the ion and the instant of expansion. It may also be seen that the final result for the displacement is as if the motion occurred at the *final* pressure for a time t given above.

For the determination of the life of the A atom we need only consider the distance between the negative tracks, so that the correct result is obtained by considering the motion of the ions from the instant of their production to the instant of attainment of critical supersaturation for the negative ion.

Using the equation on p. 678 and substituting the values of all the different quantities for each case, the lives of the actinium A atoms were obtained in 47 cases of the total number of cases (67) in which the double separation occurred. The lives in the other 20 cases were not calculated as all the origins did not appear on the plate—this, however, did not prevent the recognition of these cases, as in general only a small length of the separated negative emanation track was missing.

The mean life of these 47 actinium A atoms was 0·0018(5) second. The highest life recorded was 0·0053 second, and in two of the cases the separation of the origins of the negative separated tracks was too small to be measured, the life being shorter than 0·0001 second. If we calculate the mean life to be expected for an infinitely large number of actinium A atoms, whose lives are all shorter than 0·0053 second, we obtain the value 0·0019 second. The agreement is better than would be expected, since the mean life thus calculated varies rapidly with change in the maximum value adopted.

The distribution of the lives was compared with that to be expected theoretically for A atoms whose lives are all shorter than 0·0053 second.

Life in seconds.	0–0·001.	0·001–0·002.	0·002–0·003.	0·003–0·004.	0·004–0·0053.
Calculated No.	17	11	8	5	5
Observed No.	18	13	8	3	5

The relative numbers of the three types of records, "sharp-sharp," "sharp-diffuse," "diffuse-diffuse," agreed approximately with the calculated numbers.

9. *The High Mobility Recoil Atom.*

It is very probable that the mobility 4·35 cm/sec./volt/cm. is due to one particular type of recoil atom. In Erikson's experiments about equal activities were found for the groups of atoms possessing mobilities 1·56 and 4·35 respectively, and the two groups were *B* products a short time after collection when their activities were measured. It is well known that emanation recoil atoms are all neutral. The agreement of my value 84 per cent. of actinium A atoms positively charged in air, combined with the fact that in a large number of cases the high mobility would have been observed had it been present, makes it improbable that more than a small percentage of the A atoms have the high mobility. This suggests that the high mobility recoil atoms obtained by Erikson were B atoms.

Summary.

A method is described by which the mobility of *individual* actinium A recoil atoms is measured at the instant of their reaching the ends of their recoil tracks. Photographs of four main types of grouped tracks were obtained, corresponding to the double disintegration—actinium emanation $\xrightarrow{\alpha}$ actinium A $\xrightarrow{\alpha}$ actinium B. The relative positions of the origins of these tracks gave the mobility and, in some cases, the life of the A atom. Results obtained for actinium A agree with the usually accepted value for the mobility, namely, 1·56 cm./sec./volt/cm. The method also gives *direct* evidence that some of the recoil atoms at the end of their recoil track are uncharged, and the percentage of such neutral recoil atoms agrees with Briggs's value, found by activity distribution methods. The lives of the actinium A atoms were deduced for 47 cases, and the rough statistics were satisfactory.

No cases of the mobility 4·35 found by Erikson for recoil from an active source were obtained. The method is well suited to a study of the percentages of actinium A and thorium A recoil atoms positively charged in different gases.

The above method was suggested by Prof. C. T. R. Wilson, to whom I am also indebted for valuable advice during the course of the work.

The research was carried out with the original apparatus installed by Prof. C. T. R. Wilson at the Solar Physics Observatory, Cambridge. I wish to thank the Director, Prof. Newall, for the use of all the facilities of the laboratory. I wish also to thank Mr. Manning for making the photographic enlargements.

APPENDIX.

Before the work described above was undertaken, Mr. Hamshue and I had repeated Briggs's* experiment on the mobility of recoil atoms from a mesothorium source. The method was that of deflection of the recoil atoms in an electric field and air blast acting at right angles. The method adopted is that fully described in the paper referred to with a few slight modifications.

The air velocity was measured by Pitot tubes connected to the apparatus—one facing the blast and one fitting in flush with the side wall of the box so that the air stream blew tangentially across its mouth. The pressure difference recorded was measured by a Chattock gauge.

The mobility calculated from the "peak" values of the photometer curves was (1·50 ± 0·04), which agrees with Erikson's and Briggs's values.

It is of interest to note that Briggs failed to obtain evidence of the 4·35 mobility recoil atom and suggested as the main point of difference between his experiment and Erikson's the fact that Erikson used fields of the order of 1,000 volts/cm. compared with his own field of about 140 volts/cm.

---

* 'Proc. Camb. Phil. Soc.,' vol. 23, p. 73 (1926).

We used fields of the order 750 volts/cm., and in one case 1,000 volts/cm., but obtained no evidence of the high mobility recoil atom.

Further Measurements on Wireless Waves received from the Upper Atmosphere.

By R. L. Smith-Rose, D.Sc., Ph.D., and R. H. Barfield, M.Sc.,

(Communicated by Admiral of the Fleet Sir Henry Jackson, F.R.S.—Received October 1, 1927.)

1. *Introductory.*

In previous papers* the authors have described the development of experimental methods of measuring the directions and relative intensities of both the electric and magnetic forces in wireless waves received at the earth's surface from a distant transmitting station. In this work it was seen that the detection of the arrival of waves deflected from the upper atmosphere, and polarised with their electric force in a horizontal plane, was rendered difficult owing to the relatively great reflecting power of the earth resulting from its high conductivity. By a suitable choice of wave-length and careful attention to detail in the design and construction of the apparatus, however, the methods employed enabled measurements to be made on both vertically and horizontally polarised waves. The results of such measurements enabled a direct proof to be given of the fact that the fading of wireless signals on a vertical aerial and the variations of bearings experienced on the closed-loop type of wireless direction-finder are due to the reception respectively of vertically and horizontally polarised waves deflected from the upper atmosphere in their passage from the transmitter to the receiver. On arrival at the receiver, these indirect or atmospheric waves interfere with the direct or ground waves, in a manner determined by their relative magnitude and phase, and produce the intensity and apparent directional variations mentioned above. The results of such interference phenomena have been investigated experimentally by Appleton and Barnett[*] and by Hollingworth.[†] In a more recent publication the present authors[‡] have provided experimental evidence showing that the path of the indirect waves is confined to the great circle plane between the transmitter and receiver.

---

* 'Roy. Soc. Proc.,' A, vol. 107, p. 587 (1925), and vol. 110, p. 580 (1926).

The measurements of the quantities in the received waves as previously described by the authors were confined to observations on the transmissions from the Bournemouth broadcasting station over a short period. The object of the present paper is to describe the continuation of these measurements and their extension to the transmissions from other stations.

2. *Procedure of Experiments.*

These measurements were carried out during the six months from July to December, 1925, the transmissions from the broadcasting stations at Bournemouth, Birmingham, London and Newcastle being utilised for the purpose. As previously described, the experiments comprised the carrying out of simultaneous observations on the following four sets of apparatus :—

(*a*) *Signal strength apparatus*, measuring the relative strength of the vertical electric force (Z).[§]

(*b*) *Hertzian rod apparatus*, measuring the angles of inclination of the electric force (A and B).

(*c*) *Tilting coil apparatus*, measuring the angles of inclination of the magnetic force (C, D and F).

(*d*) *Loop-aerial apparatus*, measuring the ratio of the horizontal magnetic to the vertical electric force α/Z and β/Z.

The observations on each of these instruments were taken simultaneously over a five-minute period which was repeated half-hourly for four hours. This programme was repeated on several occasions for each of the transmitting stations observed. Owing to the rapid variation in all the quantities measured, it was found necessary to make an observation every five seconds during the five-minute periods, and this naturally required accurate synchronisation of the watches of the four independent observers.

It will be seen that the four sets of apparatus provided measurements of eight quantities relating to the forces in the arriving wave-fronts, and the whole series of measurements provided a considerable mass of data, which has been systematically reduced in the following manner.

---

[*] 'Roy. Soc. Proc.,' A, vol. 109, p. 621 (1925), and vol. 113, p. 450 (1926).

[†] 'J. Inst. Elec. Eng.,' vol. 64, p. 579 (1926).

[‡] 'J. Inst. Elec. Eng.,' vol. 64, p. 831 (1926).

[§] The notation here used is the same as that employed in the previous paper ('Roy. Soc. Proc.,' A, vol. 110, pp. 581 and 592 (1926)).

3. *Treatment of Data obtained.*

The eight quantities measured during this investigation can best be defined with the system of rectangular co-ordinates formerly employed*; and they are as follows:—

(*a*) The strength of the vertical electric field = Z
(*b*) Angle A = $\tan^{-1}(Y/Z)$
(*c*) Angle B = $\tan^{-1}(X/Z)$
(*d*) Angle C = $\tan^{-1}(\alpha/\beta)$
(*e*) Angle D = $\tan^{-1}(\gamma/\beta)$
(*f*) Angle F = $\tan^{-1}(\gamma/\alpha)$
(*g*) Ratio α/Z
(*h*) Ratio β/Z

In addition to these directly observed quantities it was found desirable to derive two others, viz.:—

(*j*) The component of the horizontal magnetic force, α, derived from (*a*) and (*g*).
(*k*) The component of the horizontal magnetic force, β, derived from (*a*) and (*h*).

An inspection of the graphs of the above quantities showed immediately the general nature of their variations, the times at which each variation began and passed through its maximum value, and the presence or absence of downcoming waves polarised with the electric force either vertical or horizontal.

At selected instants at which the electric field (Z) passed through a maximum, the angle of incidence of the downcoming waves was calculated from the formula

$$\sin\theta = \left|\frac{Z - Z_0}{\beta - \beta_0}\right|,$$

using the curves of Z and β, whose day values are Z_0 and β_0 respectively. A similar procedure was adopted for peak values of β also. Owing to the limitations imposed by the instrumental accuracy in observing Z and β, the above calculations of the angle of incidence were only carried out for cases in which the values of Z or β differed by more than 30 per cent. from the day values as an arbitrarily chosen limit. Of the values of θ thus obtained for each five-minute run, the extremes and means were tabulated with those obtained from the other five-minute runs.

---

* See 'Roy. Soc. Proc.,' A, vol. 110, p. 592 (1926).

To obtain the angle of incidence of horizontally polarised waves the relation

$$\sin\theta = \sqrt{K'}\tan F$$

is employed, where $\sqrt{K'} = \sqrt{2\sigma/n}$ = refractive index of ground. Here again, owing to the falling off in instrumental accuracy for weak downcoming waves, it was necessary to impose a limiting condition which, in this case, was arbitrarily decided as

$$\alpha > \tfrac{1}{2}Z_1 \quad \text{or} \quad > \tfrac{1}{2}\beta_1.$$

The values of θ calculated for values of F, at times when α satisfied this condition, were treated in a similar manner to that mentioned above, the extremes and means being tabulated.

The relative intensity of the vertically polarised component of the downcoming waves is calculable from the relationship

$$\frac{E_1}{E_0} = \frac{1}{(1+v_v)}\cdot\frac{\beta_1}{Z_0}.$$

In a similar manner, for the horizontally polarised component of the downcoming waves, the following expression is used for obtaining its intensity (E_1) relative to that of the direct wave (E_0):—

$$\frac{E_1}{E_0} = \frac{\alpha}{(1+\rho_h)\cos\theta\,.\,Z_0}.$$

In this latter case, therefore, a value of E_1/E_0 can be obtained for each of the derived values of θ.

The extreme and mean values of the intensities and angles of incidence of both components of the downcoming waves during certain five-minute periods of observation are entered in the Tables II and III below for certain measurements made on the transmissions from Bournemouth and Newcastle. In the following section is given a detailed discussion of the results obtained from the measurements on the different transmitting stations.

4. *Discussion of Results.*

(*a*) *General.*—In Table I is given a summary of the D.F. bearing and signal strength observations made during these experiments on the transmissions from four broadcasting stations. Several general deductions may be made from these results on the direct and downcoming waves received from the various stations. For example, in the case of London's transmissions at a distance of 20 miles,

Table I.—Summary of Bearing and Signal Strength Observations.

Transmitting station.	Distance.	True bearing.	Date.	Period of test.	Time of sunset.	Mean day bearing.	Mean day value of s.s. Z.	Maximum deviations of bearing from mean.	Maximum variations of Z from day mean.	Remarks.
	Miles	Degrees		G.M.T.	G.M.T.	Degrees	Arbitrary units	Degrees		
Newcastle	245	350	12.11.25	1630–2030	1616	351·2	1·6	−21·2 +23·8	+17·2	
,, ...			19.11.25	1600–1930	1606	351·4	1·6	−26·4 +48·6	+18·4	
London	18	84	8.10.25	1640–2040	1724	84·0	—	− 4·0 + 3·5	—	Extreme variation of signal strength during these tests was less than 10 per cent. of the day value.
,, ...			15.10.25	1650–2030	1708	85·2	—	− 1·0 + 1·3	—	
,, ...			17.12.25	1730–2030	1552	85·4	—	− 1·4 + 1·1	—	
Birmingham	88	319	2.7.25	1450–1600 1930–2130	2020	321·0	7·0	−11·0 +19·0	+ 8·1 − 0·2	*I.e.*, lowest reading 6·8 at night.
,, ...			9.7.25	1450–1600 1845–2125	2016	320·9	8·0	−10·9 + 9·1	+ 7·2	*I.e.*, always above 8 at night.
,, ...			16.7.25	1440–1600 1845–2145	2010	321·4	13·0	− 4·4 + 6·6	+ 3·4 − 3·0	
,, ...			17.9.25	1725–2125	1812	321·4	7·0	−21·4 +22·6	+ 2·6 − 1·8	
,, ...			1.10.25	1445–1545 1725–2125	1739	320·9	6·6	−55·9 +39·1	+ 3·4 − 2·9	
,, ...			5.11.25	1630–2030	1627	321·0	6·0	−21·0 +39·0	+ 5·2 − 1·2	Morse interference.

Bournemouth	79	228	28.5.25	1450–1540 1845–2125	2002	226·8	12·0	+103·2 −116·8	+10·0 − 8·3	
"			4.6.25	1445–1600 1845–2125	2010	231·6	12·0	+ 38·4 − 36·6	+ 5·0 − 4·5	Fairly quiet night for 6 BM.
"			11.6.25	1445–1600 1845–2125	2016	232·0	12·0	—	+ 8·4 − 2·8	Observing F most of period.
"			18.6.25	1450–1605 1845–2125	2020	232·2	12·0	—	>+10·0 − 3·0	Observing D and F most of period.
"			25.6.25	1445–1605 1845–2125	2021	232·1	12·0	—	>+10·0 − 2·5	Do.
"			24.9.25	1510–1545 1715–2125	1755	231·1	8·0	+124 −161	+ 8·0 − 4·4	
"			29.10.25	1630–2030	1639	232·0	8·0	±180	+18·0 − 2·5	Complete rotation 2–3 occasions.
"			10.12.25	1540–1940	1551	232·0	—	±180	—	Do. on three occasions.

the variations of signal strength during any sunset or night period were less than 10 per cent. of the day value, while the corresponding variations in the apparent bearings had a maximum amplitude of 4°. It is, therefore, to be concluded that the intensity of the downcoming waves from this station is very small compared with that of the direct wave along the ground. On the other hand, the normal day signal intensity from Newcastle is 1·6 units, and this rises at night to as much as 18·4, or nearly twelve times as great. This indicates that the direct wave from this station is comparatively weak and that at night the reception is chiefly due to the downcoming wave. It is seen that the variations of apparent bearings due to the changing polarisation of these latter waves give a maximum error of 49°.

The results obtained on the transmissions from Birmingham occupy an intermediate position between those just discussed. The variations in signal intensity at night indicate that the downcoming waves at night contribute a vertical electric field component, which is from about 25 to 100 per cent. of the normal day value. This variation is accompanied by errors in the apparent bearing of the station ranging up to 56°. A somewhat different case, again, is presented by the results on transmissions from Bournemouth. While the normal day signal intensity is quite appreciable, the variations at night indicate that the downcoming waves can supply a vertical intensity component, which is equal to, and at times greater than, the day value. It is evident that in this case the conditions of wave-length, distance of transmission, etc., are such that the downcoming waves have an intensity which is of the same order as that of the direct waves. As a result, critical interference conditions may occur, giving the excessively large rotations of apparent bearings which have only been observed on this station.

With this introductory discussion the results may now be considered in more detail under the heading of each transmitting station.

(*b*) *Birmingham.*—The Birmingham transmitting station was observed on six occasions each consisting of four-hour continuous watches in the evening. It was at once found that the fading and other night effects were not so marked with this station as with Bournemouth. The total downcoming wave was, in fact, found to be only of the order of one-tenth the amplitude of the direct wave, whereas in the case of Bournemouth it averaged one-third. This fact, which is satisfactorily accounted for by the smaller surface attenuation of the direct Birmingham wave compared to the Bournemouth wave, rendered it impossible to make an accurate calculation of the angle of incidence of the downcoming wave by the method outlined above. A rough estimate, however, was made on the same lines, and this showed that the results were consistent with a downcoming wave having an angle of incidence lying between 30° and 40°. The distance from Birmingham to Slough being 88 miles, the mean of the above angles of incidence (35°) gives an effective height of the deflecting ionised layer of 63 miles or 101 km. for transmissions from this station.

(*c*) *Bournemouth.*—Since the results recorded in the last paper* this station has been observed on three occasions, each consisting of four-hour watches in the evening preceded by a day-time run of half an hour to establish normal conditions. The fading and other night effects observed on this station were, as before, very marked. Variations in Z of ± 50 per cent. to 100 per cent. were quite common, and variations in bearing (angle C) were particularly large—on several occasions a complete rotation of 360 degrees took place. Large forward and sideway tilts of the electric field were also observed.

The angles of incidence and relative intensities of the downcoming waves were measured when possible and are shown in Table II.

The apparent angle of incidence is seen to vary rapidly from minute to minute. The mean angle of incidence, — 42° for the vertically polarised waves, and 32° for the horizontally polarised waves—will give an approximation to the *mean* angle at which the total downcoming radiation is arriving. The vertically polarised mean is probably too high owing to the tendency of weak downcoming waves to instrumental error in this direction. For the same reason the horizontally polarised mean should be too low. Hence, we can take the average of the two (37°) for the true angle with considerable confidence. This angle gives 84 km. as the mean height to which the atmospheric waves penetrate, which is in good agreement with result (88 km.) given in the previous paper.†

The ratio of the field strength of the downcoming wave to the direct wave, as measured at the instants at which the angles of incidence were calculated, and, therefore, probably representing the maximum value, is found from Table II to average 0·34 for the vertically polarised and 0·67 for the horizontally polarised wave. Thus the total horizontally polarised wave appears to be about twice the intensity of the total vertically polarised wave. Of the two figures, however, it should be pointed out that the former is the more reliable, since the value for the horizontally polarised wave is the result of a less direct calculation.

---

* 'Roy. Soc. Proc.,' A, vol. 110, p. 580 (1926).

† *Ibid.*, p. 613.

Table II.—Transmissions from Bournemouth. (λ = 386 m.)

Date.	G.M.T.	Vertically polarised wave.				Horizontally polarised wave.			
		Angle of incidence.		Intensity.		Angle of incidence.		Intensity.	
		Extremes.	Mean.	Extremes.	Mean.	Extremes.	Mean.	Extremes.	Mean.
		Degrees	Degrees			Degrees	Degrees		
24.9.25	1845					(0)–58	30	0·23–1·10	0·59
	1900	59–(90)	75	0·20–0·29	0·26				
	1945					26–47	39	0·42–1·44	0·37
	2000	17–49	27	0·29–0·80	0·52				
	2015					26–76	39	0·32–1·26	0·58
	2030	20–38	25	0·35–0·62	0·46				
	2045					(0)–58	29	0·25–0·73	0·42
	2100	20–50	34	0·15–0·26	0·21				
	2115					(0)–47	15	0·25–0·69	0·46
29.10.25	1700	19–37	29	0·30–0·87	0·45				
	1745					16–76	35	0·43–4·90	1·67
	1800	24–48	38	0·21–0·26	0·23				
	1815					16–58	33	0·33–0·77	0·45
	1930	32–47	40	0·20–0·27	0·23				
	1945					47–58	52	0·48–0·61	0·54
	2000	29–(90)	58	0·20–0·44	0·34				
	2015					(3)–47	29	0·28–0·73	0·44

Reflection Coefficient of Heaviside Layer.—If we define the reflection (ρ) of the Heaviside layer as the ratio of the intensity of the electric field of the wave on leaving the layer to its value on entering, it can be shown that the expression for determining it is

$$\rho = \frac{a \, . \, E_1/E_0}{\sin \theta \, . \, f(\theta)},$$

where

E_1/E_0 is the ratio of downcoming to direct wave observed at the receiver, as recorded in Table II.

a is the surface attenuation factor of the direct wave due to earth resistivity.

θ is the angle of incidence of the downcoming wave.

$f(\theta)$ is the ratio of the field intensity radiated upwards by transmitter at angle θ to the value radiated along the ground.

In the case of Bournemouth we have

$$E_1/E_0 = 0 \cdot 34 \quad \text{(vertically polarised wave)}.$$

The value of a is obtained from Sommerfeld's attenuation theory utilising a value for the effective surface resistance obtained by actual attenuation measurements on a wave-length close to that of Bournemouth and over a considerable part of the same ground. Its value for the particular wave-length distance and soil condition relating to Bournemouth is approximately 0·04. The angle of incidence (θ) is obtained as in Table II and assumed to be 37°. The value of $f(\theta)$ is based on the assumption that the polar curve of radiation in a vertical plane is the same as that of a vertical aerial, and for $\theta = 37°$ is 0·2. Putting these values in the above equation we obtain $\rho = 0 \cdot 11$ as the value for the reflection coefficient of the Heaviside layer for waves from Bournemouth to Slough.

(*d*) *Newcastle.*—The transmissions from Newcastle were observed on two night periods of four hours each, with suitable day periods for obtaining the necessary day values. The results are shown in Table III.

The angle of incidence of the downcoming wave was found to remain more constant than for Bournemouth. The mean angle for the whole of the observations was 62°. The ratio of indirect to direct wave intensities averaged 2·0.

The intensity of the horizontally polarised component was not great enough to enable calculation of the angle of incidence of the horizontally polarised wave to be made. As already mentioned, however, the variations in apparent bearings recorded in Table I indicate that the intensity of the horizontally polarised downcoming waves was at times very appreciable.

Table III.—Transmissions from Newcastle. ($\lambda = 410$m.)

Date.	G.M.T.	Vertically polarised wave.			
		Angle of incidence.		Intensity.	
		Extremes.	Mean.	Extremes.	Mean.
		Degrees	Degrees		
12.11.25	1730	64–69	66	2·53–4·18	3·3
	1800	56–65	62	1·58–1·91	1·8
	1830	20–77	52	1·22–2·37	1·9
	1900	13–46	28	0·83–1·84	1·2
	1930	52–90	64	1·64–2·73	2·2
	2000	62–68	65	0·92–1·38	1·2
19.11.25	1630	58–73	63	0·92–1·48	1·2
	1700	58–70	63	1·05–1·15	1·1
	1730	51–90	68	1·25–2·04	1·6
	1800	60–90	68	0·92–1·64	1·2
	1830	66–72	70	2·76–3·95	3·4
	1930	62–90	73	3·26–5·69	4·3

Height of Layer. Reflection Coefficient.—The height of the Heaviside layer calculated from the average angle of incidence given above is 105 km. The reflection coefficient calculated in the same way as for Bournemouth and Birmingham is 0·14.

5. *Conclusions.*

The method of analysis of the electro-magnetic field in the presence of downcoming waves at receiving stations, which was applied to the waves received at Slough from the Bournemouth station, has been extended to deal with two other stations at different distances and on different wave-lengths, and further confirmatory observations have been made on Bournemouth.

From measurements of the mean angle of incidence of the downcoming waves by the loop-aerial method, the height of the layer from the various stations has been worked out. Also by making use of the results of some experiments on the attenuation of the surface wave over land, it has been possible to arrive at more exact values for the coefficient of reflection of the Heaviside layer from the three cases dealt with. These results are summarised in Table IV below.

The previously published paper* contained the results of measurements on downcoming waves received at Slough from Bournemouth during May and June, 1926. In the following Table V these results are compared with

---

* *Ibid.*, pp. 608 and 610.

Table IV.

Transmitter.	λ.	Height of layer.	Coefficient of reflection of ionised layer.
	m.	km.	
Bournemouth	386	84	0·11
Birmingham	470	101	0·17
Newcastle	410	105	0·14

the corresponding results in Table II of the present paper, referring to similar measurements made in September and October, 1926.

Table V.—Results of Measurements on Transmissions from Bournemouth made in the Summer and Autumn, 1926.

Date of measurement.	Vertically polarised waves.		Horizontally polarised waves.	
	Mean angle of incidence.	Mean intensity.	Mean angle of incidence.	Mean intensity.
18th and 25th June, 1926	21°	0·7	29°	0·8
24th Sept. and 29th Oct. 1926	40	0·35	33	0·7

It is interesting to note from this table that while the results of the measurements on the horizontally polarised waves are of the same order in the two cases, the vertically polarised waves in the autumn arrive at a smaller angle of incidence and with half the intensity of the waves received at midsummer. As already explained in the paper, these results probably give the mean value of two or more downcoming waves, and the above change may simply indicate a reduction of the intensity of those waves which have suffered two deflections at the ionised layer. Alternatively, the results may indicate a real change in the effective height of the ionised layer.

Acknowledgments.

This work was carried out as part of the programme of the Radio Research Board and is communicated by permission of the Department of Scientific and Industrial Research. The authors wish to acknowledge the general assistance rendered by Mr. S. R. Chapman, M.Sc., throughout the investigation, and the help given by Messrs. E. L. Hatcher, G. W. Warren, A. C. Haxton, and A. H. Free in connection with the large amount of simultaneous observation work carried out.

Tensile Tests on Alloy Crystals. Part IV.—A Copper Alloy containing Five Per Cent. Aluminium.

By C. F. Elam, D.Sc. (Armourer's and Brasier's Research Fellow).

(Communicated by H. C. H. Carpenter, F.R.S.—Received August 11, 1927.)

[Plate 20.]

A previous paper* described the preparation and tensile properties of brass crystals containing 25 to 30 per cent. zinc. Similar experiments have now been carried out with a copper-aluminium alloy containing 5 per cent. aluminium, which was kindly prepared by the Broughton Copper Company. Crystals of this alloy were easier to prepare than the brass crystals and the composition was more uniform, as unlike zinc, aluminium is not volatile. On the other hand, a very resistant oxide film forms on the surface, and the prepared surfaces of the crystals tarnish very readily. The bars were sound, except near the top, where very well-developed dendrites were formed. It was found on etching that the crystals were not always of uniform orientation throughout and were very much cored. Bands of very slightly differing orientation occurred, of which fig. 1 (Plate 20) is an example. This has almost the appearance of lamellar twinning. Actually, X-ray measurements showed that both parts had the same relationship to the vertical axis, but that one part was rotated 7° with regard to the other, about their plane of union, which in this case was nearly perpendicular to the axis.

Figs. 2 and 3 (Plate 20) are photographs of the cross-section and vertical section of the same crystal. The scratch in fig. 2 corresponds with the plane of the section shown in fig. 3. The cores are not developed uniformly, nor are they evenly spaced. In this particular crystal those perpendicular to the axis were most complete. X-ray measurements showed that both sections were $\{100\}$ planes, indicating that the cores followed the cubic axes of the crystal,† but as the photographs show, they were not equally developed along the three possible directions. This is in accordance with previous observations on the crystallization of metals.

Other crystals examined generally show two directions of cores irrespective of the orientation of the crystal to the axis of the rod (see figs. 6 and 8) and in every case the directions agreed with planes parallel to the cube faces. The positions of the principal cores are mentioned later in discussing the distortion of these crystals. Prolonged annealing failed to remove the coring completely, but distortion measurements were made on both annealed and unannealed crystals.

---

* Elam, 'Roy. Soc. Proc.,' A, vol. 115 (1927).

† 'The Crystallization of Metals,' Col. N. Belaiew.

Small square bars were machined from the crystals, polished, marked and measured as before. Complete distortion and X-ray measurements were made on one crystal (Cu-Al_1), and the results are given in Table I and figs. 4 and 5.

Table I.

Copper-Aluminium I. Reference Face II.

$\epsilon = 1\cdot393$. $f = 0\cdot9475$. $g = 0\cdot7725$. $\lambda_0 = 89\cdot9°$. $\lambda_1 = 76\cdot5°$.
$\beta_0 = 89° 20'$. $\beta_1 = 79° 30'$. $\gamma_0 = 90° 20'$. $\gamma_1 = 102° 30'$.

Unstretched cone.
Strained position.

$$(0\cdot1275 \cos^2 \phi + 0\cdot8689 \sin^2 \phi - 0\cdot5724 \cos \phi \sin \phi) \tan^2 \theta - (0\cdot1730 \cos \phi + 0\cdot2260 \sin \phi) \tan \theta - 0\cdot485 = 0.$$

$\epsilon = 1\cdot802$. $f = 0\cdot9360$. $g = 0\cdot6095$. $\lambda_0 = 89\cdot9°$. $\lambda_1 = 75°$.
$\beta_0 = 89° 20'$. $\beta_1 = 69° 30'$. $\gamma_0 = 90° 20'$. $\gamma_1 = 105° 10'$.

Unstretched cone.
Strained position.

$$(0\cdot1800 \cos^2 \phi + 2\cdot1294 \sin^2 \phi - 1\cdot0432 \cos \phi \sin \phi) \tan^2 \theta - (0\cdot2178 \cos \phi + 0\cdot2201 \sin \phi) \tan \theta - 0\cdot2925 = 0.$$

Extension. $\dfrac{\epsilon = 1\cdot802}{\epsilon = 1\cdot393}$.

$\epsilon = 1\cdot292$. $f = 0\cdot9890$. $g = 0\cdot8030$. $\lambda_0 = 76\cdot5°$. $\lambda_1 = 75°$.
$\beta_0 = 79° 30'$. $\beta_1 = 69° 30'$. $\gamma_0 = 102° 30'$. $\gamma_1 = 105° 10'$.

Unstretched cone.
Strained position.

$$(0\cdot0312 \cos^2 \phi + 0\cdot5406 \sin^2 \phi + 0\cdot0995 \cos \phi \sin \phi) \tan^2 \theta - (0\cdot1569 \cos \phi + 0\cdot0812 \sin \phi) \tan \theta - 0\cdot401 = 0.$$

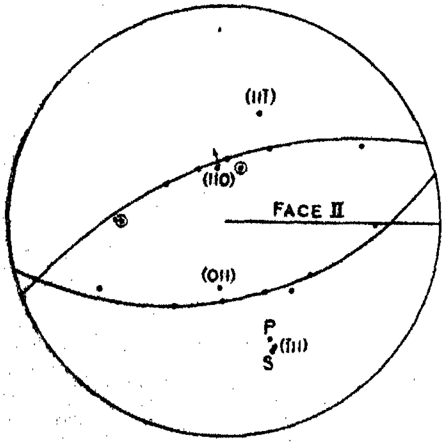

Fig. 4.

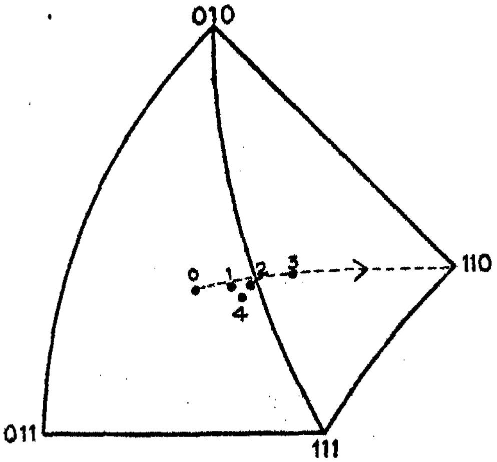

Fig. 5.

Copper-Aluminium I.

P = pole of slip-plane calculated from distortion. S = pole of slip-plane from measurements of slip-bands. The arrow indicates direction of slip.

It was calculated that, provided this crystal deformed in the same way as others of the same structure, it should slip on one octahedral plane until it had extended 27 per cent., when two octahedral planes would be equally inclined to the axis and slip might occur on both. X-ray and distortion measurements, however, showed that at an extension of 39 per cent. slip was still on the $(\bar{1}11)$ plane towards the (110) plane (using the notation previously employed). Slip-bands also agreed with these measurements. Fig. 4 illustrates all these points. This alloy therefore appeared to resemble the brass crystals, and this was confirmed on further extension. A second set of slip-bands suddenly appeared which agreed with the position of the $(11\bar{1})$ plane, and after an extension represented by $\varepsilon = 1 \cdot 802$, the axis of the test-piece was found to have moved back towards the (011) plane. This is shown in fig. 5. Distortion calculations indicated slip on both planes during this period, but the evidence is in favour of the assumption that the copper-aluminium crystal behaves like the copper-zinc and slips back on the $(11\bar{1})$ plane in the (011) direction. The final extension of this crystal was represented by the value $\varepsilon = 2 \cdot 38$, and from $\varepsilon = 1 \cdot 802$ onwards slip probably occurred on both octahedral planes, as the test-piece axis remained almost in the same position with regard to the crystal axes. The extension before fracture was not so great as the copper-zinc crystals, but was still much greater than pure copper. Test-pieces of normal, multi-crystalline alloy are also more ductile than pure copper.* It is considered to be due to the removal of oxygen by the zinc and aluminium respectively.

The crystal referred to above had been annealed for four days at 750° C. and coring was less marked, although not completely removed. In order to determine the influence of coring, some crystals were tested which had not been specially annealed and in which it was very prominent. Figs. 6 and 8 (Plate 20) are photographs of two faces of such a crystal, and figs. 7 and 9 (Plate 20) of the same crystal after an extension of 10 per cent. The appearance of the slip-bands nearly obliterated the cores, although they were just visible on the specimen; but if the photographs are compared, it will be seen at once that the slip-bands pass right across the faces quite regardless of the coring. It has already been pointed out that the coring follows the cubic-planes, while the slip-planes are octahedral planes, so that the two sets of planes make angles of 54° 40′ with each other. They intersect at points corresponding to the {110} planes, which represent the directions of slip. Usually two sets of cores are prominent, so that those {110} planes which are parallel to them—the cores

---

* Carpenter and Edwards, Eighth Alloys Research Report, 'Proc. Inst. Mec. Eng.' (1907).

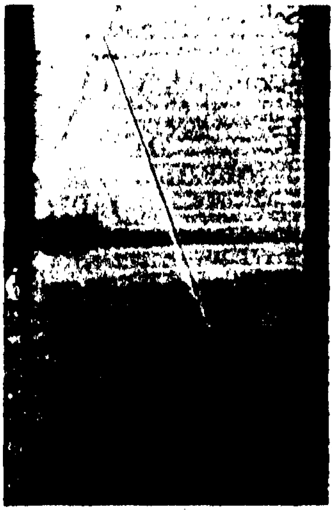
1

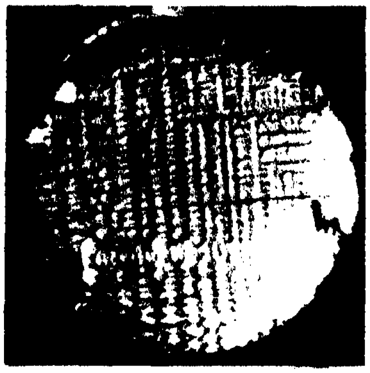
2

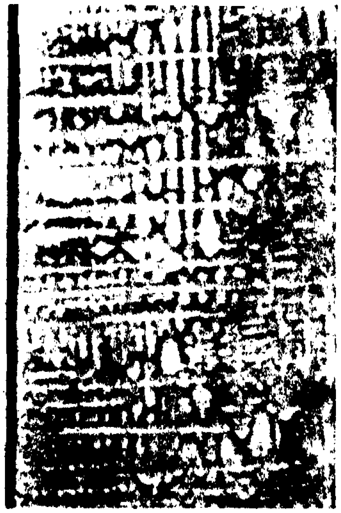
3

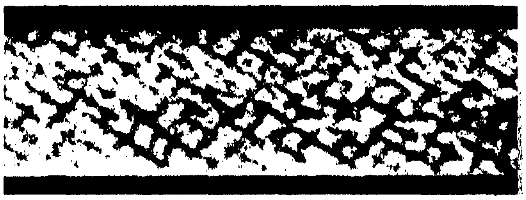
6

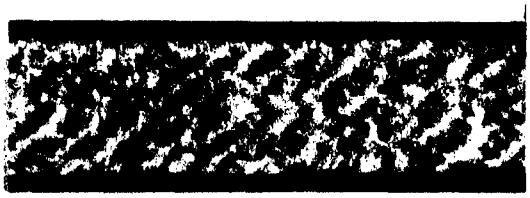
8

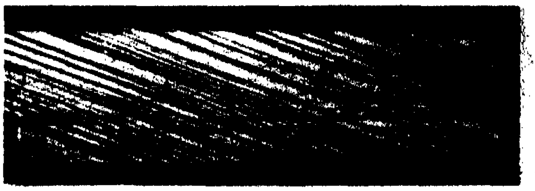
7

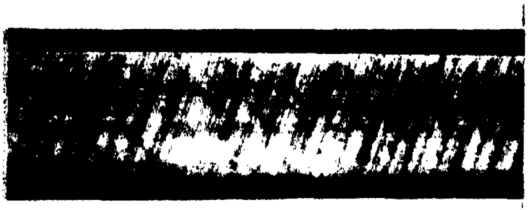
9

11

being parallel to {100} planes—may have a different composition from those that are parallel to the {100} plane, in which the cores are not well developed. Taking all these points into consideration, it seems unlikely that the octahedral planes would be influenced by coring, but that the directions of slip might be so.

It is difficult to see what factors determine the particular directions taken by coring. It so happened that two crystals were obtained of very nearly the same orientation with regard to the bar axis and prepared under similar conditions in which the coring was very differently developed.

The inclinations of the normals of the three cubic planes to the bar axis (the angle θ) in the two crystals were as follows :—

	1.	2.	3.
Cu-Al III	87° 30′	− 69° 30′	− 19°
Cu-Al IV	88° 30′	− 73° 30′	− 17°

In the former, two sets of cores were present agreeing with the first and second, and in the second only one, agreeing with the third. The coring has never been found to change in the same crystal, so that it must be determined at at the very beginning of growth.

Both these crystals were interesting because there were two octahedral planes almost equally inclined to the axis. In one case slip occurred on one plane only, in the other the middle portion slipped on one plane, and the two ends on the other. As it had already been determined that slip in this alloy occurred on an octahedral plane, only X-ray and slip-band measurements were made.

Crystal Cu-Al IV behaved normally and slipped uniformly on the $(\bar{1}11)$ plane towards the pole of the (101) plane (according to the diagram given, fig. 10), so further X-ray measurements were not made, but the extension and load were observed in order to calculate shear-stress, etc., and as a second set of slip-bands did not appear till after an extension of 52 per cent., this crystal also slipped farther on the first plane than the calculated distance, which was 32 per cent.

Fig. 10 illustrates the movement of the crystal in both specimens. Cu-Al IV is put into one of the outer triangles of the projection, but in order to show the movement of both parts of crystal III this is put into another pair of triangles which are crystallographically similar, and being adjacent, the movement of the axis from one to the other is clearly shown.

Table II gives details of measurements and calculations for both parts of crystal III. If the slip-plane in the top portion is called the $(11\bar{1})$ plane and the direction of slip the (011) plane, the corresponding planes in the middle portion are (111) and $(01\bar{1})$.* This is confirmed by the movement of the test-piece axis and the formation of slip-bands corresponding with these planes. From shear-stress considerations slip should have occurred only on the former, and the top and bottom parts therefore behaved normally. By slipping on the (111) plane in the $(01\bar{1})$ direction, the point representing the axis in the middle portion moved into the adjacent triangle, where this plane is the slip-plane required by theory, and distortion then proceeded in a perfectly normal manner, as shown in the diagram. Actually, therefore, the only abnormality shown by this crystal is that part of it started slipping on the wrong plane, and, as Table II shows, the differences in shear-stress on the two planes were small. At the foot of the table are given figures for the two planes in crystal IV, which are of the same order of difference, except for the value of η. As has been said already, this behaved normally and there is no explanation of the results obtained in crystal III.

Table II.

Load. lbs.	Top and Bottom.					Middle.				
	ϵ.	Area, sq. ins.	θ.	η.	S. lbs. per sq. ins.	ϵ.	Area, sq. ins.	θ.	η.	S. lbs. sq. ins.
			° ′	° ′				° ′	° ′	
Copper-Aluminium III.										
25	Yield	0·01101	45 0	8 30	1,123	Yield	0·01101	40 30	12 0	1,097
83	1·188	0·00914	53 30	8 0	4,325	1·177	0·0092	45 30	8 0	4,500
130	1·268	0·00858	56 30	4 30	5,355	1·257	0·00854	52 30	8 0	7,280
190	1·450	0·00754	60 0	6 0	10,880	1·411	0·00721	57 30	5 30	11,880
Copper-Aluminium IV.										
20	Yield	0·00952	47 0	5 30	1,039					
			41 30	16 30	975					

According to the position of the crystal axes, the top part should have started slipping on a second plane at an extension of 30 per cent. Actually, a second set of slip-bands appeared at an extension of 50 per cent. The middle portion should have commenced double slipping at an extension of 42 per cent. (it is evident from fig. 10 that it had farther to go than the top), but at an extension of 60 per cent. a second set of slip-planes had not appeared. At this point the top fractured, so that it was not possible to see if both parts of the same crystal behaved similarly with regard to the excess amount of slip on the first plane. On the other hand, the total amount of shear on the slip-plane in the middle part was already greater than that on the corresponding plane in the top, so that the amount of deformation alone does not appear to be the determining factor. The shear-stress on both planes shows that it was rather greater on the slip-plane in the middle portion than the ends. This may indicate a difference in hardness, but the evidence is insufficient to justify an assumption of this kind.

---

* Reference to the diagrams in previous papers will make this clear. G. I. Taylor and C. F. Elam, 'Roy. Soc. Proc.,' A, vol. 108 (1925).

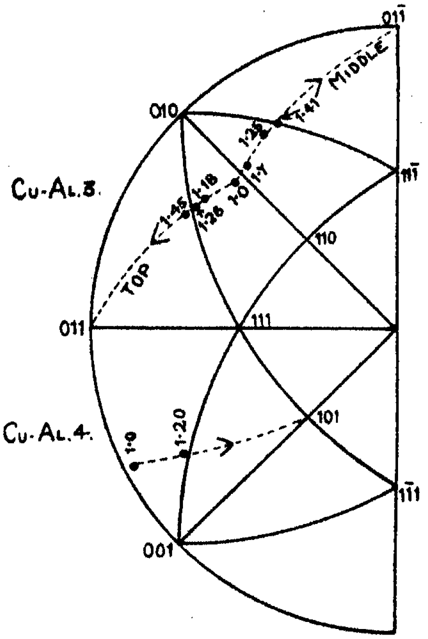

Fig. 10.

The external form of this specimen, of which fig. 11 (Plate 20) is a photograph, very much resembles a "twinned" crystal, and its method of formation is similar to other forms of so-called mechanical twinning. The formation of such a structure in this case is very simply explained, and the crystal is not "twinned" in the crystallographic sense at all. When once the deformation had begun in the two parts, each functioned as independent crystals, and behaved accordingly. But the two crystals, at different stages, are almost identical, relative to the axis of the specimen, if in one case the specimen is viewed from above, and in the other from below. Fig. 10 shows that the axis in the middle, after an extension equal to $\varepsilon = 1 \cdot 177$, occupied the same position in its triangle as the original position in the first triangle. Similarly, the position at $\varepsilon = 1 \cdot 257$ in the middle is equivalent to the position at $\varepsilon = 1 \cdot 188$ in the top. This only serves to emphasize the similarity existing between the two parts and also the fact that as soon as deformation began, they ceased to have any crystallographic relationship.

The shear-stress on the slip-plane was calculated for three crystals and is plotted against the amount of shear in fig. 12. Table III gives all the figures, together with similar figures obtained for a copper and two brass crystals. These figures only refer to that part of the test where slipping was confined to one plane. The shape of the curves indicates that copper hardens up much more rapidly than any of the alloys. This is further confirmed by the fact that Brass I which contained 70·9 per cent. copper is harder than Brass II which contained 74·47 to 77·75 per cent. copper. Of the copper-aluminium alloys, the annealed crystal is altogether harder than the unannealed crystal, which give very similar figures in spite of the different type of coring.

Table III.

ϵ.	θ.	η.	S. lbs. per sq. in.	s.	ϵ.	θ.	η.	S. lbs. per sq. ins.	s.
		Copper.					*Copper-Aluminium I.*		
	° ′	° ′				° ′	° ′		
1·0	42 03	18 0	—	—	1·0	52 30	7 0	—	—
1·10	—	—	3,320	0·2000	1·11	—	—	5,850	0·2365
1·25	—	—	8,430	0·4695	1·23	—	—	7,640	0·4750
1·30	—	—	10,250	0·5390	1·39	—	—	13,110	0·7795
		Brass I.					*Copper-Aluminium III.*		
1·0	55 40	8 30	—	—	1·0	45 0	8 30	—	—
1·17	—	—	4,001	0·3495	1·18	—	—	4,250	0·3515
1·27	—	—	6,710	0·5595	1·26	—	—	6,355	0·4235
1·38	—	—	9,025	0·7735	1·45	—	—	10,890	0·7955
		Brass II.					*Copper-Aluminium IV.*		
1·0	55 30	26 0	—	—	1·0	47 0	5 30	—	—
1·13	—	—	2,750	0·2115	1·08	—	—	4,155	0·1619
1·23	—	—	4,700	0·5220	1·20	—	—	4,880	0·3745
1·46	—	—	9,450	0·9925	1·35	—	—	6,190	0·6350
					1·42	—	—	9,695	0·7535
					1·52	—	—	12,750	0·9145

The experiments just described confirm the results obtained from the copper-zinc alloys, and have brought forward more evidence on the effect of non-homogeneity of structure on the distortion. Owen and Preston* have given the value of 3·62 Å for the dimensions of the lattice of copper containing 5 per cent. aluminium and 3·65 Å containing 8 per cent., as compared with 3·60 Å for pure copper. A crystal showing a cored structure must have variable lattice dimensions within these limits, according to the composition. Prolonged heating induces diffusion and an equalizing of the structure, but in single crystals this process is very slow. There is some evidence that it is even impossible in the case of pure metal crystals, and, in fact, it is difficult to see how one metal can diffuse into another if it is necessary to expand the lattice to any great extent, unless the lattice is first distorted by mechanical means. Deformation also acts as a mechanical distributor of the segregated areas. The slip-planes which cut across the cores break them up, and the material is actually transferred along the direction of slip according to the amount of shear.

---

* Owen and Preston, 'Journ. of the Physical Society' (1923).

The curves shown in fig. 12 indicate that the copper-aluminium alloy is harder than copper, and the copper-zinc alloy softer, at the beginning of the test, but that copper hardens more rapidly than either of the alloys. The alloying elements therefore appear to facilitate slip rather than impede it. This is also confirmed by the fact that very large extensions are obtained with the alloys. If the breaking load is calculated on the original cross-section, the alloys appear harder than copper, because the extension is much greater and consequently the hardening of the metal due to deformation is greater. This is brought out in the following table :—

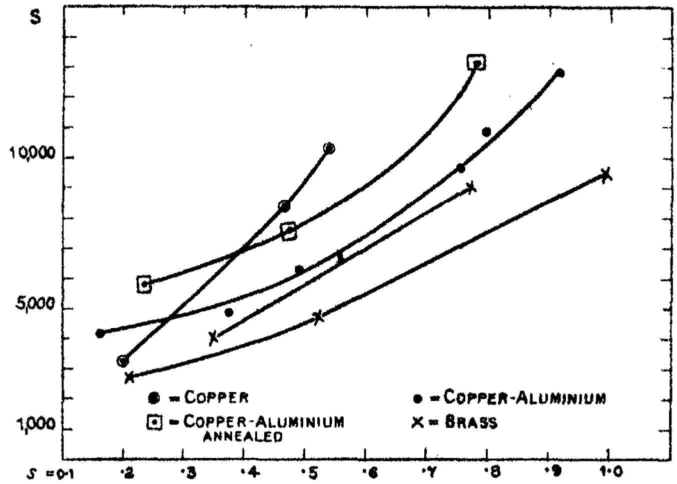

FIG. 12.

Table IV.

—	Breaking load. Tons per sq. ins.	Elongation. Per cent.
Copper XI	7·77	52
Brass I	7·925	72
„ II	10·51	159
„ III	10·26	168
Copper-Aluminium I	12·42	138
„ „ III	10·52	110
„ „ IV	10·79	120

The difference of behaviour between these alloys and those of aluminium and zinc previously described is still only to be explained on the assumption that their method of manufacture was different. It is shown above that both slip-plane and direction of slip appear to be uninfluenced by coring, but uniformity of structure tends towards greater strength, as is illustrated by the effect of annealing. This question, however, must remain unsettled until crystals of the same alloy can be prepared by both methods.

I wish to express my thanks to Prof. H. C. H. Carpenter, F.R.S., for his interest and kindness throughout the course of this work.

Series of Emission and Absorption Bands in the Mercury Spectrum.

By Lord RAYLEIGH, F.R.S.

(Received September 15, 1927.)

[PLATES 21 and 22.]

Introduction.

In a recent paper* some remarkable phenomena exhibited by the mercury band spectrum in emission were described. In particular it was shown that the band spectrum was intimately related to the resonance line $1\ {}^1S_0 - 1\ {}^3P_1$ (2537) and the "forbidden" lines $1\ {}^1S_0 - 1\ {}^3P_0$ (2656) and $1\ {}^1S_0 - 1\ {}^3P_2$ (2270) which appear strongly with it, in spite of the apparent violation of the inner quantum number rule which this implies.

A system of emission bands was described, extending from λ 3055 to λ 2697, with the spacing diminishing from 21 A to about 6 A. The starting point of the present investigation was to look for these bands in absorption, so as to determine whether they had for their lower energy level one associated with the normal state of the molecule.

Since previous workers had not given any account of such bands, it became necessary to consider in what respect their methods could be improved upon. One point which suggested itself was that the source used should have a continuous spectrum, free from lines. For some purposes the lines present in such a source as the cadmium spark are not important, but in the search for a faint band structure they may seriously distract the eye.

---

* 'Roy. Soc. Proc.,' A, vol. 114, p. 620 (1927).

Another point was to experiment with long as well as short mercury columns, so as to be sure of finding the most suitable conditions.

As regards the source, I have used a silica discharge tube, containing hydrogen at 2·5 mm. pressure, and giving the continuous spectrum of hydrogen in the ultra-violet to the limit of range of quartz spectrography. The tube was of the "end on" type, about 30 cm. long and 1·2 cm. bore. I am not sure that these dimensions are the most suitable. The tube was used because it happened to be at hand, having been constructed for other work.* The tube was excited by a transformer fed by a small rotatory converter. The power taken by the latter was a little under 1 kilowatt. No convenient means was at hand for measuring the alternating discharge current. Probably it might have been increased with advantage.

The absorption tubes were of silica, 2·5 cm. diameter with plane ends fused on. The length was varied in different experiments from 45 to 178 cm. In the final work, a layer of mercury lay on the bottom of the tube and extended along the whole length. The tube was heated electrically, and mercury kept boiling with reflux condensation from a small vertical branch tube. This latter communicated above with a bulb of 500 c.c. capacity and a manometer. The air pressure could be increased up to about 3 atmospheres, or diminished to any fraction of 1 atmosphere. The boiling mercury vapour had, of course, the same pressure as the air in the bulb above, and in this way its pressure could readily be controlled and measured without the use of any elaborate appliances. The density was sufficiently indicated by the pressure. It is convenient to use moderately high pressures, so as to avoid the trouble and expense of very long silica tubes.

§ 1. *Bands of the Less Refrangible Region.*

In the first experiments absorption bands similar to the emission bands above mentioned were found, but on close scrutiny they were seen not to be identical with them. The general aspect will best be studied from Plate 21. A represents the emission bands produced according to the methods described before (*loc. cit.*).

A mercury line spectrum has been put on the absorption spectra BCD for comparison with the mercury lines already present on A. These absorption spectra show the effect of successive increases in the quantity of vapour. The tube used was 87 cm. in length and the pressures 46 cm., 76 cm. and 193 cm.

---

* Lambrey and Chalonge in a recent paper recommend a tube 3 mm. in diameter ('C. R.,' vol. 184, p. 1057 (1927)).

The most important region of general absorption in mercury vapour is bounded on the short wave side by the resonance line 2537. On the side of long waves its boundary is much less definite, and is pushed farther towards the red as the quantity of vapour increases. These facts were noted by R. W. Wood in 1909. What is now to be added is that the intermediate region between free transmission and complete absorption is not uniformly graduated, as I believe has generally been supposed, but that, superposed upon the general increase of absorption towards λ 2537, there is an alternation between absorption and transmission. This constitutes the bands which have been mentioned.

They can be traced from about λ 2943 (spacing 146 cm.$^{-1}$) to λ 2614 (spacing 50 cm.$^{-1}$).

It is not possible to see the whole of this range on a single photograph. The less refrangible end is best seen with a dense column of vapour, which obliterates the more refrangible part entirely (Plate 21, D). To examine the latter part, it is necessary to reduce the length or the density of the vapour column. More bands then come into view. The most distinct part of the system is at about λ 2800. As we reduce the quantity of vapour still more light penetrates still farther into the region of intense general absorption, and yet more bands come into view, but they become increasingly difficult to make out. This behaviour is very similar to what was noted by Prof. Fowler and myself* in ozone absorption, observed in the laboratory and also in the solar spectrum with varying solar altitude.

The following table gives the wave-lengths and frequencies of these bands, with the same quantities for the emission bands. In the case of absorption, the absorption maximum is measured. In the case of emission, the emission maximum. This method was adopted in the absence of recognisable band heads. In order to facilitate comparison, those bands have been placed on the same line which do not differ in measured wave-length by more than one Ångström, which may be taken as approximately representing the experimental error. This method of arrangement shows that over a part of the range λ 2734 to 2696, for seven or eight periods, the two series were identical, within the limit of experimental error.

Beyond this range, on the side of long waves the absorption bands are more closely spaced than the emission bands; on the side of short waves the emission bands are closer than the absorption bands. It is clear, therefore, that no uniform shift on the scale of frequencies could bring the two series into coincidence.

---

* Fowler and Strutt, 'Roy. Soc. Proc.,' A, vol. 93, p. 577 (1917).

Table I.

Emission.			Absorption.		
Δν.	ν.	λ.	λ.	ν.	Δν.
	32278	3097·5			
250					
	32528	3073·7			
232					
	32760	3051·6			
225					
	32985	3030·8			
181					
	33166	3014·3			
220					
	33386	2994·4			
205					
	33591	2976·1			
181					
	33772	2960·2			
169					
	33941	2945·4			
182			2943·4	33964	
					148
	34123	2929·7	2930·7	34112	
					146
194			2918·2	34258	
	34317	2913·2			132
193			2907·0	34390	
	34510	2896·9			145
153			2894·8	34535	
					131
	34663	2884·1	2883·8	34666	
					123
150			2873·6	34789	
	34813	2871·6			122
132			2863·6	34911	
	34945	2860·8			128
162			2853·1	35039	
	35127	2846·0			121
132			2843·3	35160	
	35259	2835·3			125
			2833·2	35285	
141					99
			2825·3	35384	
	35400	2824·0			126
118					
	35518	2814·6	2815·3	35510	
					112
145			2807·4	35622	
	35663	2803·2			92
133			2799·2	35714	
	35796	2792·8			107
118			2790·8	35821	
	35914	2783·6	2784·3	35905	
					104
117			2776·3	36009	
	36031	2774·6			105
109			2768·2	36114	
	36140	2766·2			86
95			2761·6	36200	
	36235	2758·9			97

Table I—(continued).

Emission.			Absorption.		
Δν.	ν.	λ.	λ.	ν.	Δν.
112			2754·6	36297	
	36347	2750·4			93
110			2747·2	36390	
	36457	2742·1			84
101			2740·9	36474	
					93
	36558	2734·6	2733·9	36567	
89					90
	36647	2727·9	2727·2	36657	
88					85
	36735	2721·4	2720·9	36742	
82					75
	36817	2715·3	2715·3	36817	
86					82
	36903	2709·0	2709·3	36899	
87					90
	36990	2702·6	2702·7	36989	
85					100
	37075	2696·4	2695·4	37089	
75					
	37150	2691·0			76
74			2689·9	37165	
	37224	2685·6			78
67			2684·3	37243	
	37291	2680·8			68
62			2679·4	37311	
	37353	2676·4			78
72			2673·8	37389	
	37425	2671·2			70
55			2668·8	37459	
	37480	2667·3			69
49					
	37529	2663·8	2663·9	37528	
61					66
	37590	2659·5	2659·2	37594	
					71
			2654·2	37665	
					65
			2649·6	37730	
					66
			2645·0	37796	
					60
			2640·8	37856	
					62
			2636·5	37918	
					66
			2632·6	37974	
					58
			2628·6	38032	
					55
			2624·8	38087	
					62
			2620·5	38149	
					50
			2617·1	38199	
					47
			2613·9	38246	

An examination of the table, or of the spectra themselves, as shown on Plate 21, will show that both series, emission and absorption, have a considerable measure of regularity, which at first glance appears to extend over the whole range. The first differences diminish towards the shorter waves. The individual second differences are not uniform, but in any case the measurements are not accurate enough to make this irregularity of any significance. Diffuse bands like these are difficult objects on which to make a precise setting with the measuring machine. For, as already emphasised, they show no sharp heads; and in bisecting them the eye is likely to be distracted by the neighbourhood of atomic lines, or accidental markings on the plate. In general, if a band interval appears considerably too small from causes of this kind, one of its immediate neighbours will appear too large. By taking the average of four or five intervals a comparatively regular curve is obtained, and I have found by trial that it is possible to assign a series of positions with uniform second difference which smooth the apparently more irregular parts of the system, and which are within the limits of error of the actual measured band frequencies, relative to the comparison spectrum. But in the case of the absorption spectrum we can only get rid of the exceptionally large interval which appears between ν 36989 and ν 37089 by an extreme application of the powers of adjustment which this criterion would give; and I am inclined to believe that this interval is in fact really larger than regularity of the whole series would allow. The point should be examined by measurement of further negatives, which is unfortunately not possible at the time of writing.

There is undoubtedly at least one anomaly in the emission series of bands. The maximum at λ 2913·2 (ν 34317 cm.$^{-1}$) is exceptionally broad, as is clear on several negatives, and should be evident on the reproduction A, Plate 21. This anomaly, evident on inspection, is reflected in the table of first differences by an exceptional distance between this maximum and *both* of its neighbours.*

Since the bands which have been described tend to converge in a noticeable manner, it is natural to enquire, apart from all questions of theoretical interpretation, what is the position of the point of convergence? Evidently we cannot hope to determine it with much precision, since a considerable extrapolation is involved, without very precise data on which to base it. Nevertheless, it is desirable to make the attempt.

---

* In the provisional measurements published in 'Roy. Soc. Proc.,' *loc. cit.*, I regarded this maximum as double, the central minimum being abnormally faint. Reconsidering the matter with better negatives and with the help of a microphotometergraph, I now find no adequate evidence for this. The microphotometergraphs also made it possible to extend the series of emission bands farther towards the convergence point than was possible by eye measurement.

Two methods have been used by previous writers in cases of this kind.

In the *first*, the intervals of the observed bands are simply plotted as a function of the main position of each interval in the spectrum, using the frequency scale. A linear extrapolation to zero interval gives a value for the point of convergence.

This method has been used by Kuhn* to make a short extrapolation on the absorption spectra of bromime and chlorine. In the present case it has the justification that both the emission and absorption spectra yield graphs which, if somewhat irregular, are, on the whole, straight over the entire experimental range, and thus lend themselves to linear extrapolation.

A *second* method of extrapolation has been used by Birge and Sponer.† It amounts in effect to continuing the series of bands, with diminution of the band interval by a constant quantity at each step, until the interval is exhausted. This gives the convergence point. This method is more in harmony with the conceptions of the quantum theory of band spectra than the former one. On the other hand, if applied in the present case, it is equivalent to the linear extrapolation of a curve which, within the observable range, is not a straight line; for if we plot the band intervals as a function of their ordinal numbers, a curve decidedly convex to the origin is obtained. For this reason I prefer the former method; though the argument would lose some of its force if the bands are not regarded as forming an unbroken series; and as we have seen, this is somewhat uncertain. For comparison the results of both methods are given.

In fig. 1 (emission) and fig. 2 (absorption) the frequency interval is plotted

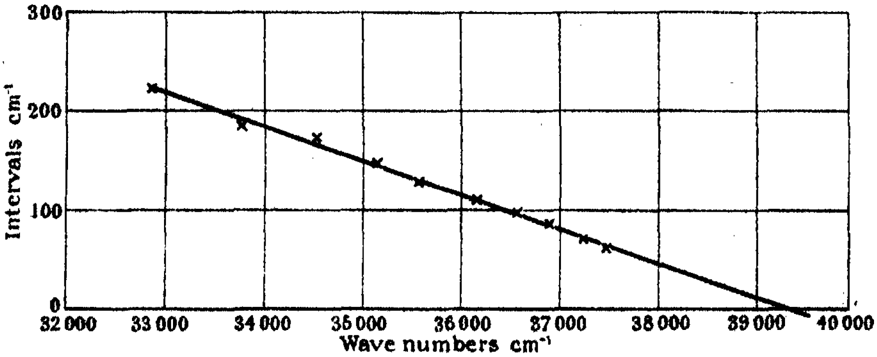

FIG. 1.—Emission.

---

* 'Z. f. Physik,' vol. 39, p. 77 (1926).

† 'Phys. Rev.,' vol. 28, p. 259 (Aug., 1926).

against the wave number (first method). The individual intervals are not regular enough for satisfactory discussion. To diminish the effect of experimental errors, the mean of 4 or in one instance 5 intervals has been taken and plotted against the mean position of the set. A similar plan was followed in extrapolating by the second method, but the graphs are not reproduced.

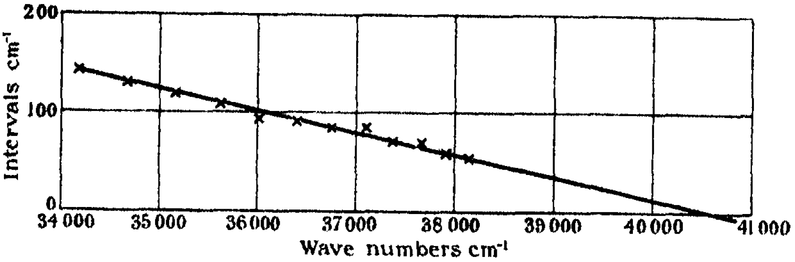

FIG. 2.—Absorption.

The results are—

—	Emission.		Absorption.	
	ν.	λ.	ν.	λ.
1st method (preferred)	39300	2544	40550	2465
2nd method	37945	2635	39030	2561

The discrepancy by the two methods of about 1400 cm.$^{-1}$ is large from some points of view. Measured electrically, however, it is equivalent to 0·17 volt, and Birge and Sponer (*loc. cit.*, p. 270) consider that 0·4 volt is a reasonable estimate of the error of their extrapolation for the stable series of levels of oxygen, which seems to be a not unfavourable example of the cases treated by them.

As already indicated, most reliance is here placed on the results of the first method of extrapolation.

In considering the interpretation of the bands shown in Plate 21, the idea that at first suggests itself is that these represent a long series of vibrational levels. The spacing is of the order of magnitude of, *e.g.*, the vibrational levels of the copper iodide bands investigated by Mulliken, and is of course much too large for rotational levels. The law of spacing is not at all that which we should expect in a series of electronic levels, such as occur in the band spectrum of helium.

The bands do not show definite edges or heads, but if this were the only difficulty, it would be possible to invent hypotheses which might explain it away. Thus the vibrational levels might, in some way, be selected from a complex spectrum of overlapping bands, as in Wood's resonance spectrum of iodine. Or again, each member might, in reality, be a sequence, as in the case of the visual bands (α bands) of active nitrogen, as seen in a small instrument. In some such way the edges might perhaps be obscured, without obscuring the series of vibrational levels themselves.

If any such view were taken, it would be necessary to assume that the series of vibrational levels revealed is attached to the upper and not the lower electronic level. For, if it were otherwise, the system of bands would converge to the red, and not to the violet as observed (*cf.* Wood's iodine resonance).

But the real difficulty arises when we try to explain the relation between emission and absorption spectra in this way. The general aspect and mode of convergence of the two spectra are very similar, and over part of the range they are apparently coincident. Nevertheless, it is impossible to bring them into coincidence by any simple shift on the scale of frequencies. This is obvious from the graphs, figs. 1 and 2. These graphs are not parallel, that for the emission spectrum being the steeper; and therefore they cannot be brought into coincidence by moving one of them parallel to itself. The graphs, in fact, cross at about $\nu = 3700$ cm.$^{-1}$, and it is near this part of the spectrum that several bands in the two spectra are coincident within the limits of error (see table of wave-lengths, p. 706). Any relative displacement would sacrifice the measure of agreement that already exists in this neighbourhood.

It seems therefore that on the view under discussion we should be driven to regard the emission and absorption spectra as revealing two independent sets of excited levels (n' levels) each presumably attached to a different electronic level. I cannot, without further evidence, feel satisfied with such a view, and judgment as to the true nature and relation of the bands must be suspended.

§ 2. *Bands of the More Refrangible System.*

In addition to the region of absorption already discussed, it is known that mercury vapour shows a peculiar series of absorption bands, beginning at λ 2345 downwards.[*] Similar bands have been observed by Grotian[†] in emission in a Geissler discharge tube, and by myself in the excited mercury vapour from a hot cathode discharge, with low current, the vapour being removed by rapid distillation out of the region of discharge. I shall return presently to these emission bands.

---

[*] R. W. Wood, 'Phil. Mag.,' vol. 18, p. 240 (1909); McLennan and Edwards, 'Phil. Mag.,' vol. 30, p. 695 (1915).

[†] 'Z. f. Physik,' vol. 5, p. 148 (1921).

These bands were very conspicuous in some of the absorption experiments described above, for which a medium-sized Hilger spectrograph was used. The wave-lengths measured were :—

1st band..	2341 to 2346
2nd band	2337
3rd band	2333
4th band	2330

These are a little lower (1 to 2A) than the values given by Wood, owing apparently to his having measured the less refrangible edges of the bands, whereas I measured the middle : allowing for this the agreement is satisfactory. The bands thus examined in absorption are seen in Plate 22, upper portion of photograph M. Their aspect is symmetrical, without a head.

However, a closer examination of the negatives under a magnifier gave signs of a much more complex structure which does not seem to have been suspected by previous observers. The dispersive power of the medium-size spectrograph used was not enough to allow of a satisfactory examination of this structure, which was too much interfered with by the grain of the plate.

A grant from the funds at the disposal of the Council of the Royal Society allowed me to procure a Hilger quartz spectrograph of the Littrow pattern, having about three times the dispersion of the instrument before available. With this it became possible to measure the spectrum, and to produce satisfactory photographs for reproduction (Plate 22, E–K). It must be explained, however, that these photographs have in all cases been intensified by the superposition of two original negatives, and sometimes by a second application of the same process, superposing two enlarged positives to make a new negative. It is only by procedure of this kind that pictures bold enough for satisfactory reproduction have been obtained. The reader may be reminded that if the phenomenon were very conspicuous, it would not have remained undescribed until now.

E shows absorption by a column of mercury vapour 45 cm. long, at 26 cm. pressure. The comparison spectrum was an iron arc, and the iron wave-lengths are marked. The bands, as shown by the medium-sized instrument, are seen, but their aspect has become more diffuse, and their finer underlying structure is apparent. F is from the same pair of negatives, further intensified by copying.

The appearance may be roughly described as a structure of about 1 Ångström spacing superposed upon the coarser structure of about 4 Ångströms spacing previously discussed. The finer structure continues, however, when the coarser one has died out and can be traced over an *additional* range of spectrum fully twice as long as that covered by the former. In all, the finer structure has been measured as far as λ 2297.

The bright, as well as the opaque, regions of the absorption spectrum as seen in M can in several cases each be resolved into two or three complete members of the finer structure. To obtain this resolution, it is necessary carefully to examine photographs taken at different densities of vapour. And even so, the resolution has not been observed in all cases. The first absorption region, 2346 to 2341, has not been resolved, nor has the transmission region between the absorption regions 2333 and 2330. On a general view of the evidence, and judging by the faintness of the finer structure, even where it is discernible, I am inclined to regard it as in reality present throughout. It is doubtless a vibrational structure, but the significance of the fluctuations of intensity in the region of longer wave-lengths (which represent all that can be seen in a small-scale photograph) remains obscure.

Returning to Plate 22, G is the absorption by a 45-cm. column at 36 cm. pressure, H at 51 cm. pressure, and K at 76 cm. pressure. It will be observed that with increasing density of vapour, the general absorption becomes more intense, and tends to blot out more and more of the spectrum at the more refrangible end. At the same time, the structure becomes more evident at the shorter wave-lengths. The ultimate limit is reached when increasing density causes absorption to advance (λ increasing) from the region of the resonance line 1849 $1\ {}^1S_0 - 1\ {}^1P_1$ of the principal singlet series so far as to meet the absorption which we have been discussing, which advances in the opposite direction (λ diminishing). Ultimately they meet, and blot out everything below wave-length 2345. The conditions under which this may be said to happen depend of course on the intensity of the source. In my experiments, with a column 45 cm. long, it was at about 120 cm. pressure.

Unlike the bands of the less refrangible system, these absorption bands are unsymmetrical, being definitely degraded to the red. This is best seen in Plate 22, G, which shows the clearest and most intense part of the system. The bands nearer either end are more difficult to make out, and at the short-wave end it is impossible to attempt more than to make a setting on the intensity minimum. The measurements have therefore been made throughout on this method. The important point is to determine the law of spacing rather than the absolute wave-lengths, and for this it is desirable to follow the system as far as possible. Undoubted signs of bands have been seen beyond the range measured, but I have resisted the temptation to measure anything dubious. With a more intense source of continuous background a few more bands might perhaps be obtained. Table II gives the measures.

Table II.

Band No.	Wave-length A.	Wave number cm.^{-1}.	Wave number differences cm.^{-1}.
8	2341·37	42696	
			17
9	2340·50	42713	
			20
10	2339·43	42733	
			18
11	2338·44	42751	
			18
12	2337·39	42769	
			17
13	2336·49	42786	
			16
14	2335·57	42802	
			21
15	2334·50	42823	
			18
16	2333·47	42841	
			19
17	Fails.	Fails.	
			18
18	2331·48	42878	
			19
19	Fails.	Fails.	
			19
20	2329·40	42916	
			19
21	2328·40	42935	
			18
22	2327·39	42953	
			21
23	2326·32	42974	
			16
24	2325·41	42990	
			18
25	2324·45	43008	
			19
26	2323·42	43027	
			16
27	2322·55	43043	
			18
28	2321·55	43061	
			20
29	2320·49	43081	
			18
30	2319·52	43099	
			17
31	2318·59	43116	
			17
32	2317·67	43133	

Table II—(continued).

Band No.	Wave-length A.	Wave number cm^{-1}.	Wave number differences cm^{-1}.
			17
33	2316·83	43150	
			16
34	2315·89	43166	
			19
35	2314·91	43185	
			17
36	2314·02	43202	
			19
37	2313·01	43221	
			17
38	2312·05	43238	
			14
39	2311·27	43252	
			18
40	2310-36	43270	
			17
41	2309·45	43287	
			16
42	2308·63	43303	
			17
43	2307·71	43320	
			15
44	2306·92	43335	
			16
45	2306·04	43351	
			16
46	2305·19	43367	
			17
47	2304·34	43384	
			14
48	2303-55	43398	
			14
49	2302·82	43412	
			15
50	2301·99	43427	
			17
51	2301·09	43444	
			15
52	2300·33	43459	
			15
53	2299·52	43474	
			12
54	2298·85	43486	
			17
55	2298·02	43503	
			14
56	2297·25	43517	

In this list, it will be noticed that the first observed band is numbered 8. This is largely hypothetical, but the reasons for it are as follows: We have seen that the region from λ 2346 to 2341, showing strong absorption (E, Plate 22), has not been resolved into fine bands; further, it is found that with dense vapour (K, Plate 22) absorption begins about λ 2349. I have therefore assumed that the whole of this region is really filled with fine bands, which are too faint for observation. They have been assigned the same spacing as the initial spacing (18·25 cm.$^{-1}$) of those which *are* detected, and the absent bands are numbered accordingly. On this hypothesis, the first band of the series (numbered 0) would have $\nu = 42550$ cm.$^{-1}$.

As in the previous case, the individual measured band-intervals are somewhat irregular. These irregularities are not larger than the probable errors of measurement, if we consider the extreme faintness of many of the bands. It is apparent that the intervals between the successive bands tend on the whole to grow less as we go down the list. To investigate the law of spacing, a number of intervals must be grouped together, and the mean taken, as in the case of the less refrangible bands. Thus if we group 9 or 10 intervals together, most of the irregularity is got rid of.

Band No.	ν cm^{-1}.	Mean position.	Mean interval cm^{-1}.
8	42696		
		42787	18·2
18	42878		
		42970	18·3
28	43061		
		43150	17·7
38	43238		
		43311	16·2
47	43384		
		43451	14·8
56	43517		

The band-interval remains appreciably constant for the first 20 observed intervals, and then begins sensibly to diminish. The data are hardly adequate for a satisfactory extrapolation to the point of convergence. However, the relation between band-interval and wave number is sensibly linear from $\nu =$ 43150 to 43451. The relation between band-interval and ordinal number of the band is also sensibly linear over this part of the range. We may apply either method of extrapolation as before (see above, p. 708), but in this instance the second method is preferred. The reasons are (*a*) that the first method has not in this case the advantage of giving a linear graph for all known bands; and (*b*) that the bands themselves are of the shaded type to which the quantum theory is known to be directly applicable; they are therefore more rationally discussed by the second method.

The results for the limit are—

	ν.	λ.
1st method	44980	2222
2nd method	44154	2264

The discrepancy 836 cm.$^{-1}$ is equivalent to about $\frac{1}{10}$th volt excitation potential.

We now return to the subject of the relatively coarse bands 2345, etc., in *emission*. Plate 22, M, lower part, shows these bands, in a Geissler tube discharge in rather dense mercury vapour.* They were photographed with the same medium-sized instrument as the absorption bands placed above them (Plate 22, M, upper part). The photographs are placed in register by means of the mercury emission lines which were present in the emission spectrum, and which were intentionally photographed over the absorption spectrum for this purpose. The emission bands are marked by dots below, the wave-length being 2345, 2338, 2334, 2330. The last three are coincident with the coarser absorption structure (which is all that can be seen on this small scale). But in the case of 2345 it will be seen that the two are by no means coincident. The mercury *line* 2345 happens to bisect the emission band precisely, but it lies quite unsymmetrically near the long wave limit of the absorption band. This should be very evident from the reproduction.

How much importance should be attached to the difference which has just been pointed out it is difficult to say. But a further point is to be noticed. Grotian found three additional emission bands 2325, 2321, 2317. It is clear that these have no counterpart in the absorption spectrum. The photograph G, Plate 22, of the finer structure, as obtained with the larger instrument, establishes this point. The coarse absorption structure ends with the member at 2330, though the underlying finer absorption structure is continued, with a spacing about one-quarter that of the emission bands in the same region.

I wish now to recall the results of my recent paper† in which the continued emission (afterglow) of mercury excited by a low current filament discharge is examined. It was found that the series of emission bands 2345, etc., extended towards short wave-lengths, being prolonged into an apparently continuous spectrum which becomes fainter as we approach the "forbidden" line $1\ {}^1S_0 - 1\ {}^3P_2$ λ 2270 and abruptly stops at this line, which itself appears in considerable strength. The photograph showing this is reproduced for convenience of reference in Plate 22, L. It was necessary to use a wide slit, but the limit of the band spectrum was determined within ± 1·5 A as coincident with λ 2270. The individual emission bands are not distinguishable in L, but they can be seen at N, which is printed from the same negative with longer exposure. This brings out individual bands but blots out the fainter part of the spectrum towards λ 2270. Five other bands can be made out on the negative, thus one more than has been seen in absorption under any circumstances. Possibly the slit was too wide to allow more to be distinguished.

---

* They were first obtained in this way by Grotian, *loc. cit.*

† *Loc. cit.*

§ 3. *General Discussion.*

According to the views first put forward by Franck* and afterwards applied by Birge and Sponer† the highest convergence frequency of a band system gives the work of dissociation starting from the unexcited state; for at this point the vibrational energy has reached its maximum possible value. It is not, however, necessarily the work of dissociation of the molecule into two neutral atoms which is concerned, for the products of dissociation may be a neutral and an excited atom. In that case the work of atomic excitation must be subtracted.

In the case of mercury the work of dissociation into two neutral atoms has been measured by Koernicke‡ using an independent method due originally to Franck and Grotian. The value found was 1·4 kilogram-calories per mole, equivalent spectroscopically to 494 cm.$^{-1}$, which is very small compared with the energy of excitation of the mercury atom to any of the P^1 states. These states are the lowest excited states known or likely to exist.

Thus, if the product of dissociation were a neutral atom and an atom in the 1 $^3P_2$ state, the frequency of the convergence point would be 44039 + 494 cm.$^{-1}$ or 44533 cm.$^{-1}$. This is in agreement with the value actually found for the high frequency absorption bands, which according to alternative methods of extrapolation was 44980 or 44154. The calculated value is about midway between these. It seems, therefore, very probable that these bands, which are of the ordinary type with heads, indicate a type of vibration which leads to the dissociation of the molecule with one normal atom and one excited to the 1 $^3P_2$ metastable state. This conclusion does not of course involve more than the order of magnitude of the work of dissociation of a molecule into two neutral atoms.

As already mentioned, it is very difficult at present to apply the quantum theory to the bands of the less refrangible system, described in Part I. These bands are without heads, and in this respect they are similar to the emission bands of the more refrangible system. There is another remarkable point to be noticed. The emission bands of the less refrangible system converge to a position which, as nearly as can be determined, coincides with the resonance line $1\ {}^1S_0 - {}^3P_1$ 2537. The emission bands of the more refrangible system seem to be similarly related to the forbidden line $1\ {}^1S_0 - {}^3P_2$ 2270. This is tentatively inferred from the photograph L, Plate 22, the limitations of which have already been mentioned.

---

* 'Trans. Faraday Soc.,' vol. 21, pt. 3 (1925).

† 'Phys. Rev.,' vol. 28, p. 250 (1926).

‡ 'Z. f. Physik,' vol. 33, p. 219 (1925).

It is hoped to make a better examination of the more refrangible emission bands. In the meantime these remarkable relations to the atomic lines are noted as decidedly suggested by the observations. If correct, they will add to the difficulty of regarding the symmetrical bands as vibrational progressions, for there should be an interval between the atomic line and the head of the band series, this interval representing the work of dissociation of the molecule into two neutral atoms. Other difficulties about so regarding the headless bands have already been emphasised.

§ 4. *Summary.*

In this paper are described extensive band series in the spectrum of metallic mercury. These are separately described as (I) the less refrangible, and (II) the more refrangible, group.

I. These are situated between λ 3000 and λ 2600 and consist of—

I (*a*).—Emission bands, of which 42 are observed. The initial spacing of those observed is 250 cm.^{-1} and the point of convergence is found by extrapolation to be near the resonance line 2537. The bands are diffuse and symmetrical, without heads.

I (*b*).—Absorption bands, 48 bands observed. Initial spacing 148 cm.^{-1}, convergence point found by extrapolation about λ 2645. Bands of the same character as I (*a*). The convergence points are subject to considerable uncertainty, but the absorption bands undoubtedly converge to a higher frequency than the others.

The puzzling feature about these band systems I (*a*) and I (*b*) is that they cannot be brought into coincidence over the whole range by any shift on the frequency scale. In fact, the two systems are already in apparent coincidence for about seven bands around λ 2715, and any shift designed to produce coincidence at other regions would upset the coincidence at this one. It has not therefore been possible to apply the quantum theory to their classification.

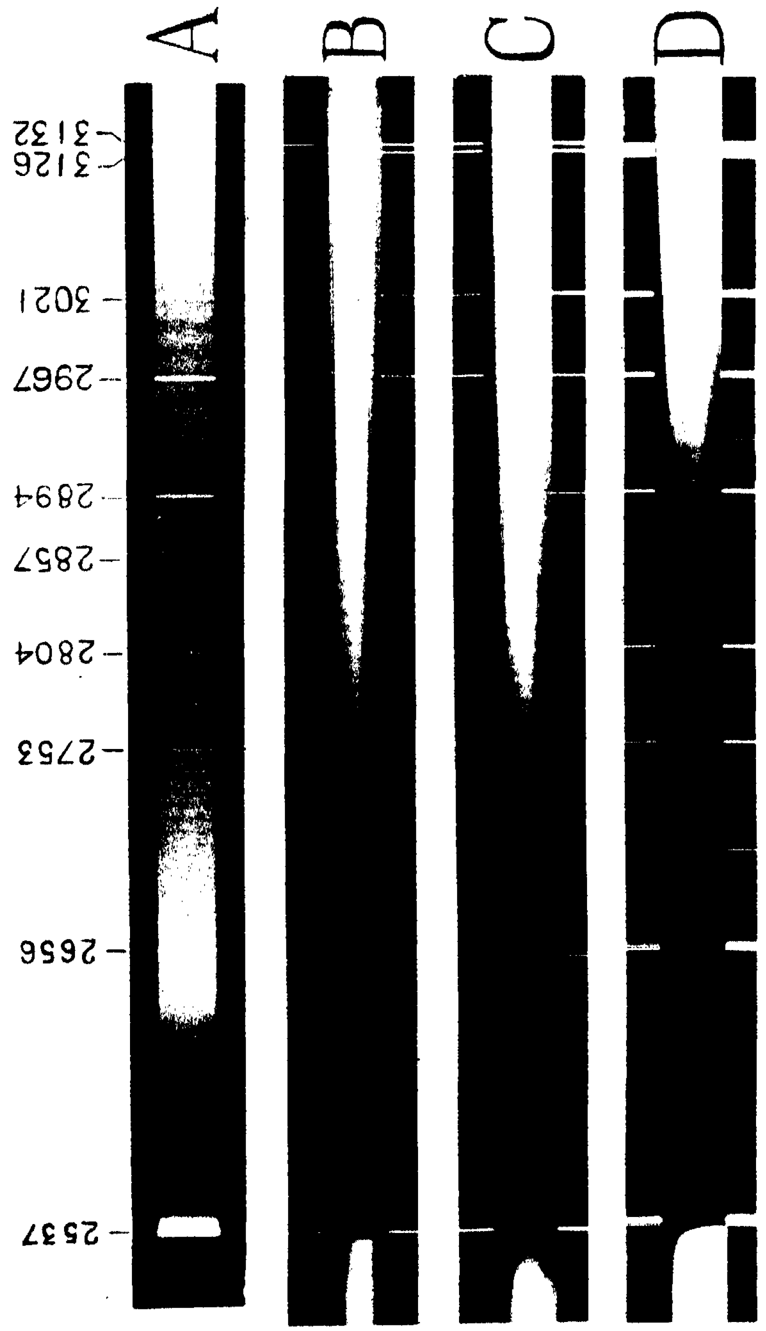
A
B
C
D
3132
3126
3021
2967
2894
2857
2804
2753
2656
2537

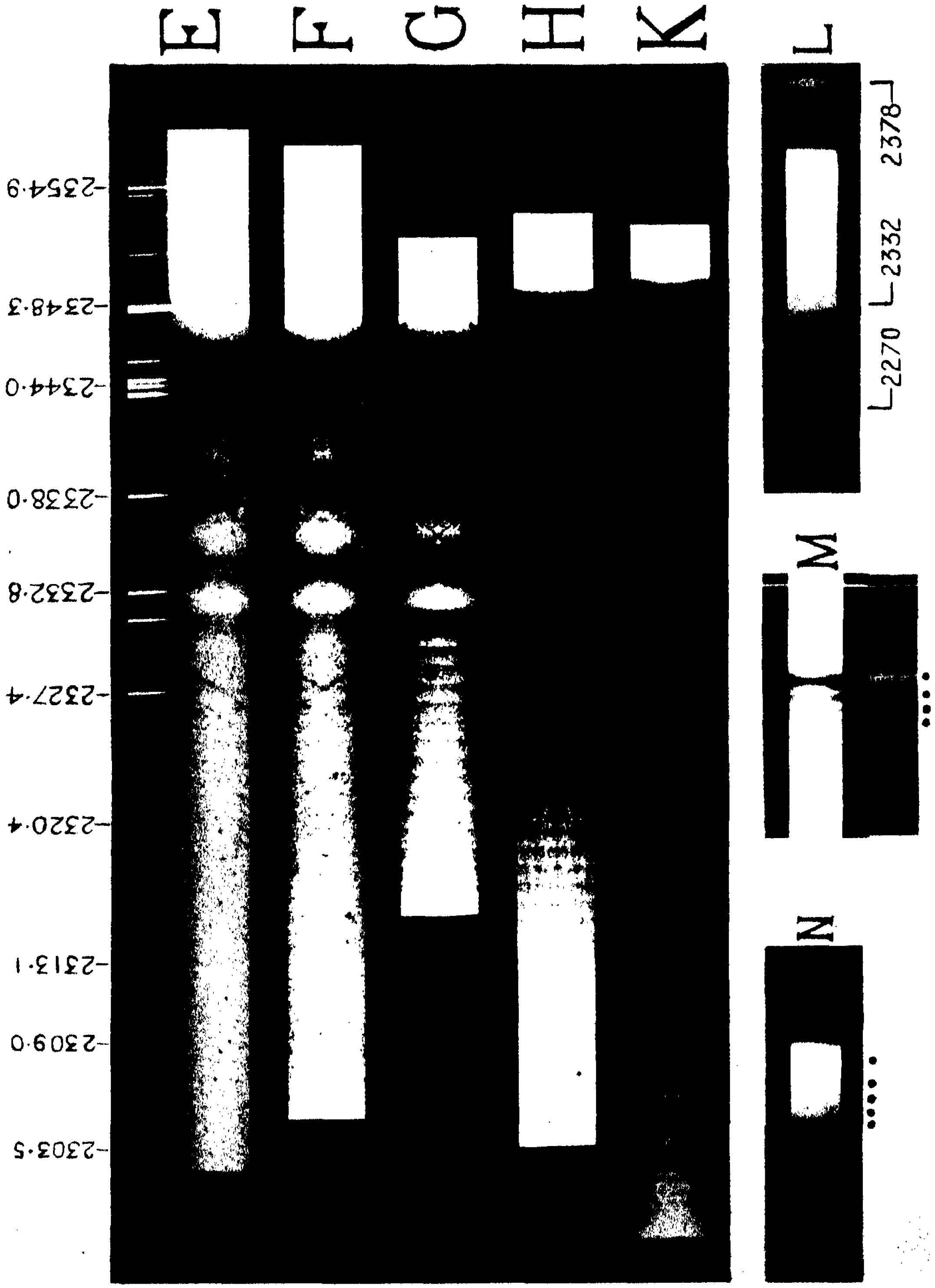
E
F
G
H
K
L
M
N
2354·9
2348·3
2344·0
2338·0
2332·8
2327·4
2320·4
2313·1
2309·0
2303·5
2378
2332
2270

II. The more refrangible group between λ 2350 and λ 2290. Under this we have—

II (*a*).—A series of emission bands, symmetrical, without heads, which have been only resolved for a short distance from 2345, but which merge into an apparently continuous spectrum ending exactly at the forbidden line λ 2270. From the work of Grotian seven of these bands are known. Spacing about 70 cm.$^{-1}$.

II (*b*).—A series of four bands, in absorption, which are nearly the counterpart of the first four bands in emission II (*a*). Like the latter, they are symmetrical, without heads. It is noteworthy that only four of these appear to exist, as against at least seven of the emission bands.

II (*c*).—A series of absorption bands, of finer spacing than II (*b*) and in part superposed on the latter. Forty-eight have been observed. The convergence point is found by extrapolation as λ 2264, though an alternative method of extrapolation would put it at a somewhat shorter wave-length.

The spacing of these bands is initially only 18 cm.$^{-1}$, much closer than any other vibrational series known to the writer. Unlike any of the other series here described, they are of the normal type with heads, and are shaded to the red. The convergence point probably represents dissociation into a neutral atom and one excited to the 1 $^3P_2$ state. The relation of these to the bands described under II (*b*) can be seen on the reproductions which accompany the paper, but so far it is unexplained.

DESCRIPTION OF PLATES.

PLATE 21.—LESS REFRANGIBLE REGION.

A.—Emission bands from stream of excited vapour. Mercury lines in addition.
B.—Absorption bands : 87 cm. column of mercury vapour at 46 cm. pressure.
C.—The same, 76 cm. pressure.
D.—The same, 193 cm. pressure.
Mercury comparison spectrum on BCD.

PLATE 22.—MORE REFRANGIBLE REGION.

E.—Absorption by 45 cm. of mercury at 26 c.m. pressure.
F.—The same. Photograph further intensified.
G.—45 cm. mercury column at 36 cm. pressure.
H.—45 cm. mercury column at 51 c.m. pressure.
K.—45 cm. mercury column at 76 cm. pressure.
L.—Emission in this region from stream of excited mercury vapour. Note that the emission ends at λ 2270.
N.—The same. More strongly printed to bring out the bands, which are marked by dots
M.—Top. The broad absorption structure as in E, but on a contracted scale.
Bottom : The same bands in emission, Geissler tube discharge. Bands marked by dots.

On Electric Phenomena in Gravitational Fields.

By E. T. Whittaker, F.R.S.

(Received September 23, 1927.)

§ 1. *Introduction.*

It is a consequence of general relativity that all electromagnetic and optical phenomena are influenced by a gravitational field. Indeed, the first prediction of relativity-theory, namely, the bending of light-rays when they pass near a massive body such as the sun, was a particular application of this principle. Evidently, therefore, the classical electromagnetic theory must be rewritten in order to take account of the interaction between electromagnetism and gravitation; but beyond laying down general principles, comparatively little progress has been made hitherto in this task, the mathematical difficulties of solving definite electrical problems in a gravitational field being somewhat formidable. The subject is, however, of some interest to atomic physics; for if we assume that the atom has a massive nucleus with electrons in its immediate neighbourhood, the behaviour of such electrons (especially with regard to radiation) will be affected by the gravitational field of the nucleus.

In the present paper two kinds of gravitational field are considered, namely, the field due to a single attracting centre (*i.e.*, the field whose metric was discovered by Schwarzschild) and a limiting form of it. Within these gravitational fields we suppose electromagnetic fields to exist. Strictly speaking, the electromagnetic field has itself a gravitational effect, *i.e.*, it changes the metric everywhere; but this effect is in general small, and we shall treat the ideal case in which it is ignored, so we shall suppose the metric to be simply that of the gravitational field originally postulated. The general equations of the electromagnetic field are obtained, and particular solutions are found, which are the analogues of well-known particular solutions in the classical electromagnetic theory; notably the fields due to electrons at rest, electrostatic fields in general, and spherical electromagnetic waves. The results of the investigation are for the most part expressible only in terms of Bessel functions and certain new functions which are introduced; but in some interesting cases the electromagnetic phenomena can be represented in terms of elementary functions, as, for instance, the electric field due to an electron in a quasi-uniform gravitational field (equations (15) and (19) below) and the spherical electromagnetic waves of short wave-length about a gravitating centre (equation (43) below).

§ 2. *The Electromagnetic Equations in a Gravitational Field.*

Let (x_0, x_1, x_2, x_3) be any generalised co-ordinates in space-time, and let the metric be specified by the equation $ds^2 = \sum\limits_{p,q} g_{pq}\, dx_p\, dx_q$.

Let X_{pq} denote the electromagnetic six-vector, so that with a Galilean metric the three components of the electric force would be (X_{10}, X_{20}, X_{30}), and the three components of the magnetic force would be (X_{23}, X_{31}, X_{12}). Then X_{pq} can be expressed in terms of the electromagnetic potential-vector $(\phi_0, \phi_1, \phi_2, \phi_3)$ (corresponding to Maxwell's scalar and vector potentials) by the equations

$$X_{pq} = \frac{\partial\phi_p}{\partial x_q} - \frac{\partial\phi_q}{\partial x_p} \qquad (p, q = 0, 1, 2, 3). \tag{1}$$

The potential-vector itself is to be determined from the partial differential equations which connect it with the electric current-vector (j_0, j_1, j_2, j_3); with a Galilean metric (*i.e.*, in the classical electrodynamics) these equations would be the ordinary equations of wave-motion

$$\frac{\partial^2\phi_p}{\partial t^2} - c^2\left(\frac{\partial^2\phi_p}{\partial x^2} + \frac{\partial^2\phi_p}{\partial y^2} + \frac{\partial^2\phi_p}{\partial z^2}\right) = j_p \qquad (p = 0, 1, 2, 3);$$

in place of these we have in general relativity

$$\sum_{q,r} g^{qr}(\phi_{pqr} - \phi_{rpq} + \phi_{rqp}) = j_p \qquad (p = 0, 1, 2, 3), \tag{2}$$

where ϕ_{prq} denotes the second covariant derivative of ϕ_p; with these equations must be associated the equation

$$\operatorname{div}(\phi^p) = 0$$

or

$$\sum_{p,q} g^{pq}\phi_{pq} = 0. \tag{3}$$

Now we have

$$-\phi_{rpq} + \phi_{rqp} = \sum_s K^s_{rqp}\phi_s,$$

where K^s_{rqp} denotes the Riemann-Christoffel mixed tensor, and thus equation (2) becomes

$$\sum_{q,r} g^{qr}\phi_{prq} + \sum_s K^s_p\phi_s = j_p \qquad (p = 0, 1, 2, 3), \tag{4}$$

where K_{pq} denotes the contracted Riemann tensor.

But in the kind of gravitational fields which we consider in this paper, there is no matter at the places where the electric fields are studied, and the effect of the electric field in altering the metric is (as explained in § 1) ignored; thus K_{pq} is zero, and equations (4) become

$$\sum_{q,r} g^{qr} \phi_{prq} = j_p \qquad (p = 0, 1, 2, 3). \tag{5}$$

These are the partial differential equations from which the electromagnetic potential (ϕ_p) *is to be determined in a gravitational field.*

§ 3. *The Quasi-Uniform Gravitational Field.*

The metric of space-time about a gravitating centre is specified by Schwarzschild's formula

$$ds^2 = \left(1 - \frac{\alpha}{r}\right) dt^2 - \frac{1}{c^2}\left(\frac{dr^2}{1 - \frac{\alpha}{r}} + r^2 d\theta^2 + r^2 \sin^2\theta \, d\phi^2\right). \tag{6}$$

There is a still simpler kind of space-time, which is a limiting form of Schwarzschild's metric, and which may be derived in the following way: Fixing our attention on the neighbourhood of a point O, we suppose the gravitating centre to be removed to a very great distance from O, while its mass is increased so that the attractive force at O (to use the language of the older physics) remains finite and equal to g; then (by passing to the limit from the above formula) we obtain a metric

$$ds^2 = \left(1 + \frac{2gx}{c^2}\right) dt^2 - \frac{1}{c^2}\left(\frac{dx^2}{1 + \frac{2gx}{c^2}} + dy^2 + dz^2\right) \tag{7}$$

which represents space-time in the simplest of all types of gravitational field.

We shall now proceed to study electromagnetic phenomena taking place in these fields (6) and (7); and first of all in the field (7), which we shall call the *quasi-uniform* field, since near the origin it corresponds to a uniform field of gravitational attraction parallel to the axis of x.

We have first to write down the equations (5) explicitly for the field specified by the metric (7). For this field, we have

$$g_{00} = 1 + \frac{2gx}{c^2}, \qquad g_{11} = -\frac{1}{2gx + c^2}, \qquad g_{22} = g_{33} = -\frac{1}{c^2},$$

$$g^{00} = \frac{c^2}{2gx + c^2}, \qquad g^{11} = -(2gx + c^2), \qquad g^{22} = g^{33} = -c^2.$$

The Christoffel symbols $\left\{\begin{matrix} pq \\ r \end{matrix}\right\}$ all vanish except the three following :—

$$\left\{\begin{matrix} 00 \\ 1 \end{matrix}\right\} = g\left(1 + \frac{2gx}{c^2}\right), \qquad \left\{\begin{matrix} 01 \\ 0 \end{matrix}\right\} = \frac{g}{c^2 + 2gx}, \qquad \left\{\begin{matrix} 11 \\ 1 \end{matrix}\right\} = -\frac{g}{c^2 + 2gx}.$$

Remembering the formulæ for covariant differentiation, namely,

$$\phi_{rq} = \frac{\partial \phi_r}{\partial x_q} - \sum_r \left\{\begin{matrix} pq \\ r \end{matrix}\right\} \phi_r,$$

$$\phi_{pqs} = \frac{\partial \phi_{pq}}{\partial x_s} - \sum_r \left\{\begin{matrix} ps \\ r \end{matrix}\right\} \phi_{rq} - \Sigma \left\{\begin{matrix} qs \\ r \end{matrix}\right\} \phi_{pr},$$

we can now calculate all the quantities ϕ_{pqs}; on substituting their values in the equations (5) we obtain

$$\frac{c^2}{c^2 + 2gx} \frac{\partial^2 \phi_0}{\partial t^2} - 2g \frac{\partial \phi_1}{\partial t} - (c^2 + 2gx) \frac{\partial^2 \phi_0}{\partial x^2} - c^2 \frac{\partial^2 \phi_0}{\partial y^2} - c^2 \frac{\partial^2 \phi_0}{\partial z^2} = j_0, \quad (8)$$

$$\frac{c^2}{c^2 + 2gx} \frac{\partial^2 \phi_1}{\partial t^2} - \frac{2gc^2}{(c^2 + 2gx)^2} \frac{\partial \phi_0}{\partial t} - 4g \frac{\partial \phi_1}{\partial x}$$
$$- (c^2 + 2gx) \frac{\partial^2 \phi_1}{\partial x^2} - c^2 \frac{\partial^2 \phi_1}{\partial y^2} - c^2 \frac{\partial^2 \phi_1}{\partial z^2} = j_1, \quad (9)$$

$$\frac{c^2}{c^2 + 2gx} \frac{\partial^2 \phi_2}{\partial t^2} - 2g \frac{\partial \phi_2}{\partial x} - (c^2 + 2gx) \frac{\partial^2 \phi_2}{\partial x^2} - c^2 \frac{\partial^2 \phi_2}{\partial y^2} - c^2 \frac{\partial^2 \phi_2}{\partial z^2} = j_2, \quad (10)$$

$$\frac{c^2}{c^2 + 2gx} \frac{\partial^2 \phi_3}{\partial t^2} - 2g \frac{\partial \phi_3}{\partial x} - (c^2 + 2gx) \frac{\partial^2 \phi_3}{\partial x^2} - c^2 \frac{\partial^2 \phi_3}{\partial y^2} - c^2 \frac{\partial^2 \phi_3}{\partial z^2} = j_3. \quad (11)$$

These are the four partial differential equations for determining the electric potential-vector (ϕ_0, ϕ_1, ϕ_2, ϕ_3) *in a quasi-uniform gravitational field.* With them must be associated the equation (3), which for the metric (7) becomes

$$\frac{c^2}{c^2 + 2gx} \frac{\partial \phi_0}{\partial t} - (c^2 + 2gx) \frac{\partial \phi_1}{\partial x} - 2g\phi_1 - c^2 \frac{\partial \phi_2}{\partial y} - c^2 \frac{\partial \phi_3}{\partial z} = 0. \quad (12)$$

§ 4. *Electrostatics in the Quasi-Uniform Field.*

We shall first consider electrostatical phenomena. For these, the function ϕ_0 is independent of the temporal co-ordinate t, j_0 is zero except at electrons, and j_1, j_2, j_3, ϕ_1, ϕ_2, ϕ_3 are all zero. The equations (8) to (12) now reduce to a single equation for the determination of ϕ_0 at places not occupied by electrons, namely, the equation

$$\left(1 + \frac{2gx}{c^2}\right) \frac{\partial^2 \phi_0}{\partial x^2} + \frac{\partial^2 \phi_0}{\partial y^2} + \frac{\partial^2 \phi_0}{\partial z^2} = 0. \quad (13)$$

This is the equation for the electric potential, corresponding to the equation

$$\frac{\partial^2\phi}{\partial x^2}+\frac{\partial^2\phi}{\partial y^2}+\frac{\partial^2\phi}{\partial z^2}=0$$

of Newtonian physics.

To solve this equation (13), we first try to find particular solutions of the form

$$\phi_0 = \mathrm{P}(x)\,\mathrm{Q}(\rho)\,\Phi(\phi),$$

where ρ denotes $(y^2+z^2)^{\frac{1}{2}}$, ϕ denotes arctan (y/z), and where P, Q, Φ, denote functions of x alone, ρ alone, and ϕ alone, respectively. The differential equation (13) becomes

$$\frac{1}{\mathrm{P}}\left(1+\frac{2gx}{c^2}\right)\frac{d^2\mathrm{P}}{dx^2}+\frac{1}{\mathrm{Q}}\left(\frac{d^2\mathrm{Q}}{d\rho^2}+\frac{1}{\rho}\frac{d\mathrm{Q}}{d\rho}\right)+\frac{1}{\rho^2\Phi}\frac{d^2\Phi}{d\phi^2}=0.$$

This evidently requires

$$\frac{1}{\mathrm{P}}\left(1+\frac{2gx}{c^2}\right)\frac{d^2\mathrm{P}}{dx^2}=k^2,\quad \text{a constant,}$$

of which the solution is

$$\mathrm{P}=\left(1+\frac{2gx}{c^2}\right)^{\frac{1}{2}}\mathrm{J}_1\left\{\frac{ic^2k}{g}\left(1+\frac{2gx}{c^2}\right)^{\frac{1}{2}}\right\},$$

where J_1 denotes Bessel's function of order one or, more generally, any solution of Bessel's equation of order one.

We must also evidently have

$$\frac{1}{\Phi}\frac{d^2\Phi}{d\phi^2}=-m^2,\quad \text{a constant,}$$

of which the solution is

$$\Phi=\frac{\sin}{\cos}\,m\phi,$$

and then the equation for the determination of Q is

$$\frac{d^2\mathrm{Q}}{d\rho^2}+\frac{1}{\rho}\frac{d\mathrm{Q}}{d\rho}+\left(k^2-\frac{m^2}{\rho^2}\right)\mathrm{Q}=0,$$

of which the solution is

$$\mathrm{Q}=\mathrm{J}_m(k\rho).$$

Thus we obtain particular solutions of the equation (13), *of the form*

$$\phi_0=\left(1+\frac{2gx}{c^2}\right)^{\frac{1}{2}}\mathrm{J}_1\left\{\frac{ikc^2}{g}\left(1+\frac{2gx}{c^2}\right)^{\frac{1}{2}}\right\}\mathrm{J}_m(k\rho)\frac{\sin}{\cos}\,m\phi. \tag{14}$$

From these we can build up solutions of the special problems of electrostatics, in the same say as we use the solutions $e^{-kx}J_m(k\rho) \begin{matrix}\cos\\ \sin\end{matrix}\, m\phi$ in the Newtonian potential-theory.

We may note in passing that it is easy to obtain any number of algebraic solutions. Thus summing with respect to m, and remembering that $\sum\limits_{m=-\infty}^{\infty} J_m(k\rho)\, e^{mi\phi} = e^{ik\rho\sin\phi}$, we obtain solutions of the type

$$\left(1+\frac{2gx}{c^2}\right)^{\frac{1}{2}} J_1\left\{\frac{rc^2}{g}\left(1+\frac{2gx}{c^2}\right)^{\frac{1}{2}}\right\} e^{-r(y\cos\theta+z\sin\theta)},$$

where r and θ are arbitrary constants. Multiplying this by dr/r and integrating with respect to r, remembering the formula

$$\int_0^\infty e^{-ar} J_1(br)\frac{dr}{r} = \frac{(a^2+b^2)^{\frac{1}{2}}-a}{b},$$

we obtain the algebraic solution

$$\left\{\frac{c^4}{g^2}+\frac{2c^2x}{g}+(y\cos\theta+z\sin\theta)^2\right\}^{\frac{1}{2}},$$

where θ is an arbitrary constant.

Again, taking $m = 0$ in (14), writing it

$$\phi_0 = \left(1+\frac{2gx}{c^2}\right)^{\frac{1}{2}} J_1\left\{\frac{rc^2}{g}\left(1+\frac{2gx}{c^2}\right)^{\frac{1}{2}}\right\} J_0\{ir(y^2+z^2)^{\frac{1}{2}}\},$$

multiplying by r^2dr and integrating, remembering that

$$\int_0^\infty J_0(t)\, J_1(tx)\, t^2\, dt = \text{constant} \times \frac{x}{(1-x^2)^{\frac{3}{2}}},$$

we obtain the rational solution

$$\frac{c^2+2gx}{\{c^4+2c^2gx+g^2(y^2+z^2)\}^{\frac{3}{2}}}.$$

§ 5. *The Potential of a Single Electron in the Quasi-Uniform Gravitational Field.*

Our main object at present, however, is to find the electric potential due to a single point-charge placed in a quasi-uniform gravitational field, say, at the origin. When we have found this, we can, of course, build up the solution of all other electrostatic problems from it.

The desired solution must reduce to $(x^2+y^2+z^2)^{-\frac{1}{2}}$ when g is replaced by zero. Now in the Newtonian theory, $(x^2+y^2+z^2)^{-\frac{1}{2}}$ can be expanded in terms of the solutions $e^{-kx}J_0(k\rho)$ of Laplace's equation by the integral

$$(x^2+\rho^2)^{-\frac{1}{2}} = \int_0^\infty e^{-kx} J_0(k\rho)\, dk\,;$$

so we naturally try to form a corresponding integral with solutions of the type (14). Using an integral due to G. N. Watson, namely,

$$2al\int_0^\infty k\mathrm{I}_1(lk)\,\mathrm{K}_1(ak)\,\mathrm{J}_0(bk)\,dk = \frac{a^2+b^2+l^2}{\{(a^2+b^2+l^2)^2-4a^2l^2\}^{\frac{1}{2}}}-1,$$

and putting in it

$$l=\frac{c^2}{g},\qquad a=\frac{c^2}{g}\left(1+\frac{2gx}{c^2}\right)^{\frac{1}{2}},\qquad b=(y^2+z^2)^{\frac{1}{2}},$$

we see that the algebraic solution which we should obtain in this manner would be

$$\phi_0=\frac{1+\frac{gx}{c^2}+\frac{g^2}{2c^4}(y^2+z^2)}{\left\{(x^2+y^2+z^2)+\frac{g}{c^2}x(y^2+z^2)+\frac{g^2}{4c^4}(y^2+z^2)^2\right\}^{\frac{1}{2}}}. \qquad (15)$$

Now it may be verified by direct differentiation that this value of ϕ_0 satisfies the differential equation (13); and it evidently reduces to $(x^2+y^2+z^2)^{-\frac{1}{2}}$ when $g\rightarrow 0$: therefore *it represents the electric potential due to a unit point-charge at rest at the origin in a quasi-uniform gravitational field.*

We have next to find the electric potential due to a unit point-charge at rest at some point (x_0, y_0, z_0) other than the origin. To find this, we perform the transformation

$$\left.\begin{aligned} t&=\left(1+\frac{2gx_0}{c^2}\right)^{-\frac{1}{2}}\mathrm{T}, & y&=y_0+\mathrm{Y}\\ x&=x_0+\left(1+\frac{2gx_0}{c^2}\right)^{\frac{1}{2}}\mathrm{X}, & z&=z_0+\mathrm{Z}\end{aligned}\right\}, \qquad (16)$$

when the metric (7) becomes

$$ds^2=\left(1+\frac{2\mathrm{GX}}{c^2}\,d\mathrm{T}^2\right)-\frac{1}{c^2}\left\{\frac{d\mathrm{X}^2}{1+\frac{2\mathrm{GX}}{c^2}}+d\mathrm{Y}^2+d\mathrm{Z}^2\right\}$$

where G stands for $g\left(1+\frac{2gx_0}{c^2}\right)^{-\frac{1}{2}}$. Since this line-element is of the same form as (7), an electric potential exists of the same form as (15), that is,

$$\Phi_0=\frac{1+\frac{\mathrm{GX}}{c^2}+\frac{\mathrm{G}^2}{2c^4}(\mathrm{Y}^2+\mathrm{Z}^2)}{\left\{(\mathrm{X}^2+\mathrm{Y}^2+\mathrm{Z}^2)+\frac{\mathrm{G}}{c^2}\mathrm{X}(\mathrm{Y}^2+\mathrm{Z}^2)+\frac{\mathrm{G}^2}{4c^4}(\mathrm{Y}^2+\mathrm{Z}^2)^2\right\}^{\frac{1}{2}}}. \qquad (17)$$

The covariant vector $(\Phi_0, 0, 0, 0)$ is transformed into the original system of co-ordinates (t, x, y, z) by the formula

$$\phi_0 = \frac{\partial \mathrm{T}}{\partial t}\Phi_0,$$

or

$$\phi_0 = \left(1 + \frac{2gx_0}{c^2}\right)^{\frac{1}{2}}\Phi_0. \tag{18}$$

Substituting for (T, X, Y, Z) in (17) their values in terms of (t, x, y, z) we have from (17) and (18)

$$\phi_0 = \frac{1 + \frac{g}{c^2}(x + x_0) + \frac{g^2}{2c^4}\{(y-y_0)^2 + (z-z_0)^2\}}{\left[(x-x_0)^2 + (y-y_0)^2 + (z-z_0)^2 + \frac{g(x+x_0)}{c^2}\{(y-y_0)^2 + (z-z_0)^2\} + \frac{g^2}{4c^4}\{(y-y_0)^2 + (z-z_0)^2\}^2\right]^{\frac{1}{2}}}. \tag{19}$$

This expression represents the electric potential due to a unit point-charge at rest at the point (x_0, y_0, z_0) *in a quasi-uniform gravitational field.* As in the Newtonian theory, by postulating an electric charge-density $\rho\,(x_0, y_0, z_0)$, and integrating, we obtain *the most general electrostatic potential in a quasi-uniform gravitational field*, namely,

$$\mathrm{V}\,(x, y\, z)$$
$$= \iiint \frac{\rho\,(x_0, y_0, z_0)\left[1 + \frac{g}{c^2}(x + x_0) + \frac{g^2}{2c^4}\{(y - y_0)^2 + (z - z_0)^2\}\right] dx_0\, dy_0\, dz_0}{\left[(x-x_0)^2 + (y-y_0)^2 + (z-z_0)^2 + \frac{g(x+x_0)}{c^2}\{(y-y_0)^2 + (z-z_0)^2\} + \frac{g^2}{4c^4}\{(y-y_0)^2 + (z-z_0)^2\}^2\right]^{\frac{1}{2}}}. \tag{20}$$

§ 6. *The Electromagnetic Equations in the Field due to a Single Gravitating Centre.*

We now pass from the consideration of the quasi-uniform gravitational field to the consideration of the field due to a single gravitating centre, for which the metric is specified by Schwarzschild's formula (6). We have first to write down the electromagnetic equations (5) explicitly for this field. Now with this metric we have

$$g^{00} = \frac{r}{r - \alpha}, \qquad g^{11} = -c^2\frac{r - \alpha}{r}, \qquad g^{22} = -\frac{c^2}{r^2}, \qquad g^{33} = -\frac{c^2}{r^2 \sin^2\theta},$$

and the Christoffel symbols $\begin{Bmatrix} pq \\ r \end{Bmatrix}$ all vanish except the following :—

$$\begin{Bmatrix} 10 \\ 0 \end{Bmatrix} = \begin{Bmatrix} 01 \\ 0 \end{Bmatrix} = \frac{\alpha}{2r(r-\alpha)}, \qquad \begin{Bmatrix} 00 \\ 1 \end{Bmatrix} = \frac{c^2\alpha(r-\alpha)}{2r^3},$$

$$\begin{Bmatrix} 11 \\ 1 \end{Bmatrix} = -\frac{\alpha}{2r(r-\alpha)}, \qquad \begin{Bmatrix} 21 \\ 2 \end{Bmatrix} = \begin{Bmatrix} 12 \\ 2 \end{Bmatrix} = \begin{Bmatrix} 31 \\ 3 \end{Bmatrix} = \begin{Bmatrix} 13 \\ 3 \end{Bmatrix} = \frac{1}{r},$$

$$\begin{Bmatrix} 22 \\ 1 \end{Bmatrix} = -(r-\alpha), \qquad \begin{Bmatrix} 32 \\ 3 \end{Bmatrix} = \begin{Bmatrix} 23 \\ 3 \end{Bmatrix} = \cot\theta,$$

$$\begin{Bmatrix} 33 \\ 1 \end{Bmatrix} = -(r-\alpha)\sin^2\theta, \qquad \begin{Bmatrix} 33 \\ 2 \end{Bmatrix} = -\sin\theta\cos\theta.$$

We are thus enabled to calculate all the covariant derivatives ϕ_{pq} and ϕ_{pqs}; on substituting their values in the equations (5), we obtain

$$\frac{r}{r-\alpha}\frac{\partial^2\phi_0}{\partial t^2} - c^2\frac{r-\alpha}{r}\frac{\partial^2\phi_0}{\partial r^2} - \frac{c^2}{r^2}\frac{\partial^2\phi_0}{\partial\theta^2} - \frac{c^2}{r^2\sin^2\theta}\frac{\partial^2\phi_0}{\partial\phi^2}$$

$$- \frac{c^2\alpha}{r^2}\frac{\partial\phi_1}{\partial t} - \frac{2c^2(r-\alpha)}{r^2}\frac{\partial\phi_0}{\partial r} - \frac{c^2\cot\theta}{r^2}\frac{\partial\phi_0}{\partial\theta} = j_0. \tag{21}$$

$$\frac{r}{r-\alpha}\frac{\partial^2\phi_1}{\partial t^2} - c^2\frac{r-\alpha}{r}\frac{\partial^2\phi_1}{\partial r^2} - \frac{c^2}{r^2}\frac{\partial^2\phi_1}{\partial\theta^2} - \frac{c^2}{r^2\sin^2\theta}\frac{\partial^2\phi_1}{\partial\phi^2} - \frac{2c^2}{r}\frac{\partial\phi_1}{\partial r}$$

$$- \frac{\alpha}{(r-\alpha)^2}\frac{\partial\phi_0}{\partial t} + \frac{2c^2(r-\alpha)}{r^3}\phi_1 + \frac{2c^2}{r^3}\frac{\partial\phi_2}{\partial\theta} + \frac{2c^2}{r^3\sin^2\theta}\frac{\partial\phi_3}{\partial\phi}$$

$$+ \frac{2c^2\cos\theta}{r^3\sin\theta}\phi_2 - \frac{c^2\cos\theta}{r^2\sin\theta}\frac{\partial\phi_1}{\partial\theta} = j_1, \tag{22}$$

$$\frac{r}{r-\alpha}\frac{\partial^2\phi_2}{\partial t^2} - c^2\frac{r-\alpha}{r}\frac{\partial^2\phi_2}{\partial r^2} - \frac{c^2}{r^2}\frac{\partial^2\phi_2}{\partial\theta^2} - \frac{c^2}{r^2\sin^2\theta}\frac{\partial^2\phi_2}{\partial\phi^2} - \frac{c^2\alpha}{r^2}\frac{\partial\phi_2}{\partial r}$$

$$+ \frac{c^2}{r^2\sin^2\theta}\phi_2 - \frac{2c^2(r-\alpha)}{r^2}\frac{\partial\phi_1}{\partial\theta} + \frac{2c^2\cos\theta}{r^2\sin^3\theta}\frac{\partial\phi_3}{\partial\phi} - \frac{c^2\cot\theta}{r^2}\frac{\partial\phi_2}{\partial\theta} = j_2, \tag{23}$$

$$\frac{r}{r-\alpha}\frac{\partial^2\phi_3}{\partial t^2} - c^2\frac{r-\alpha}{r}\frac{\partial^2\phi_3}{\partial r^2} - \frac{c^2}{r^2}\frac{\partial^2\phi_3}{\partial\theta^2} - \frac{c^2}{r^2\sin^2\theta}\frac{\partial^2\phi_3}{\partial\phi^2} - \frac{c^2\alpha}{r^2}\frac{\partial\phi_3}{\partial r}$$

$$+ \frac{c^2}{r^2}\cot\theta\frac{\partial\phi_3}{\partial\theta} - \frac{2c^2(r-\alpha)}{r^2}\frac{\partial\phi_1}{\partial\phi} - \frac{2c^2\cos\theta}{r^2\sin\theta}\frac{\partial\phi_2}{\partial\phi} = j_3. \tag{24}$$

These are the four partial differential equations for determining the electric potential-vector (ϕ_0, ϕ_1, ϕ_2, ϕ_3) in the gravitational field due to a single attracting centre.

§ 7. *Electrostatics in the Field due to a Single Gravitating Centre.*

Let us now consider electrostatical phenomena in this gravitational field. For these, j_1, j_2, j_3, ϕ_1, ϕ_2, ϕ_3, are all zero, j_0 is zero except at electrons, and

ϕ_0 is independent of t. The partial differential equations (21) to (24) thus reduce to the single equation

$$\left(1-\frac{\alpha}{r}\right)\frac{\partial^2\phi_0}{\partial r^2}+\frac{1}{r^2}\frac{\partial^2\phi_0}{\partial\theta^2}+\frac{1}{r^2\sin^2\theta}\frac{\partial^2\phi_0}{\partial\phi^2}+\frac{2}{r}\left(1-\frac{\alpha}{r}\right)\frac{\partial\phi_0}{\partial r}+\frac{\cot\theta}{r^2}\frac{\partial\phi_0}{\partial\theta}=0,$$

or

$$\left(1-\frac{\alpha}{r}\right)\frac{\partial}{\partial r}\left(r^2\frac{\partial\phi_0}{\partial r}\right)+\frac{1}{\sin\theta}\frac{\partial}{\partial\theta}\left(\sin\theta\frac{\partial\phi_0}{\partial\theta}\right)+\frac{1}{\sin^2\theta}\frac{\partial^2\phi_0}{\partial\phi^2}=0. \tag{25}$$

This replaces the equation $\nabla^2\phi=0$ which is satisfied by the electrostatic potential in the classical theory.

To solve this equation, let us first try to find particular solutions of the form

$$\phi_0=\mathrm{F}(r)\,\mathrm{G}(\theta)\,\mathrm{K}(\phi) \tag{26}$$

where F, G, H are respectively functions of r only, θ only, and ϕ only. Substituting in (25), we have

$$\frac{1}{\mathrm{F}}\left(1-\frac{\alpha}{r}\right)\frac{d}{dr}\left(r^2\frac{d\mathrm{F}}{dr}\right)+\frac{1}{\mathrm{G}\sin\theta}\frac{d}{d\theta}\left(\sin\theta\frac{d\mathrm{G}}{d\theta}\right)+\frac{1}{\mathrm{K}\sin^2\theta}\frac{d^2\mathrm{K}}{d\phi^2}=0,$$

and in the usual way we break this up into the equations

$$\left(1-\frac{\alpha}{r}\right)\frac{d}{dr}\left(r^2\frac{d\mathrm{F}}{dr}\right)-n(n+1)\,\mathrm{F}=0, \tag{27}$$

$$\frac{d^2\mathrm{K}}{d\phi^2}+m^2\mathrm{K}=0, \tag{28}$$

$$\frac{1}{\sin\theta}\frac{d}{d\theta}\left(\sin\theta\frac{d\mathrm{G}}{d\theta}\right)+\left\{n(n+1)-\frac{m^2}{\sin^2\theta}\right\}\mathrm{G}=0. \tag{29}$$

The solutions of (28) and (29) are

$$\mathrm{G}=\mathrm{P}_n^m(\cos\theta),\qquad \mathrm{K}=\frac{\sin}{\cos}\,m\phi. \tag{30}$$

As to equation (27), if we put $\mathrm{F}=\left(1-\frac{\alpha}{r}\right)^{\frac{1}{2}}\mathrm{H}$, and $r=\frac{1}{2}\alpha(z+1)$, it becomes

$$(1-z^2)\frac{d^2\mathrm{H}}{dz^2}-2z\frac{d\mathrm{H}}{dz}+\left\{n(n+1)-\frac{1}{1-z^2}\right\}\mathrm{H}=0,$$

which is the differential equation of the associated Legendre function $\mathrm{P}_n^1(z)$, so

$$\mathrm{F}=\text{constant}\times\left(1-\frac{\alpha}{r}\right)^{\frac{1}{2}}\mathrm{P}_n^1(z).$$

Now

$$P_n^1(z) = (1 - z^2)^{\frac{1}{2}} \frac{dP_n(z)}{dz},$$

and thus

$$F = \text{constant} \times (r - \alpha) \frac{dP_n(z)}{dz}, \qquad \text{where } z = \frac{2r}{\alpha} - 1.$$

We shall choose the arbitrary constant factor so that the coefficient of the leading term in F (namely, the term in r^n) is unity ; with this understanding, we have

$$F = \frac{2 \, . \, (n-1)! \; n!}{(2n)!} \alpha^{2-1} (r - \alpha) \frac{dP_n(z)}{dz},$$

and therefore, by (26) and (30), *a particular solution of equation* (25) *is*

$$\phi_0 = \frac{2 \, . \, (n-1)! \; n!}{(2n)!} \alpha^{n-1} (r - \alpha) \frac{dP_n(z)}{dz} P_n^m (\cos \theta) \, {\cos \atop \sin} (m\phi). \qquad (31)$$

This solution reduces ro $r^n P_n^m (\cos \theta) \, {\cos \atop \sin} \, m\phi$, *when* α *tends to zero, i.e., when the gravitational field disappears : and it can be used to construct solutions of electrostatical problems in the field of a single gravitating centre, just as the solutions* $r^n P_n^m (\cos \theta) \, {\cos \atop \sin} \, m\phi$ *are used in the Newtonian potential-theory.*

§ 8. *The Potential of an Electron in the Gravitational Field of a Single Centre.*

We now have to find the electric potential due to a unit point-charge of electricity, placed (say) at the point $r = l$, $\theta = 0$, in this gravitational field.

In classical electrostatics the electric potential would be $(r^2 + l^2 - 2rl \cos \theta)^{-\frac{1}{2}}$, which can be expanded in the form

$$\frac{1}{l} + \frac{r}{l^2} P_1 (\cos \theta) + \frac{r^2}{l^3} P_2 (\cos \theta) + \frac{r^3}{l^4} P_3 (\cos \theta) + \ldots \qquad (32)$$

The corresponding solution when the gravitational field exists will therefore be

$$\phi_0 = \frac{1}{l} + \frac{2(r - \alpha)}{l^2} \left\{ \frac{1}{2!} \frac{dP_1(z)}{dz} P_1 (\cos \theta) + \frac{1!\,2!}{4!} \frac{\alpha}{l} \frac{dP_2(z)}{dz} P_2 (\cos \theta) \right.$$
$$\left. + \frac{2!\,3!}{6!} \frac{\alpha^2}{l^2} \frac{dP_3(z)}{dz} P_3 (\cos \theta) + \ldots \right\}, \qquad (33)$$

since this is compounded of the solutions (31), and reduces to (32) when the gravitational field vanishes.

Let us first try to sum this series when θ is zero. In this case (33) becomes

$$(\phi_0)_{\theta=0} = \frac{1}{l} + \frac{2(r-\alpha)}{l}\frac{d}{dz}\left\{\frac{1}{2!}\frac{P_1(z)}{l} + \frac{1!\,2!}{4!}\frac{\alpha P_2(z)}{l^2} + \frac{2!\,3!}{6!}\frac{\alpha^2 P_3(z)}{l^3} + \ldots\right\}. \qquad (34)$$

Now, since $\dfrac{(n-1)!\,n!}{(2n)!} = \int_0^1 \nu^n (1-\nu)^{n-1}\,d\nu$, equation (34) may be written

$$(\phi_0)_{\theta=0} = \frac{1}{l} + \frac{2(r-\alpha)}{l^2}\int_0^1 \frac{d}{dz}\left\{P_1(z) + \frac{\nu(1-\nu)\alpha}{l}P_2(z) + \frac{\nu^2(1-\nu)^2\alpha^2}{l^2}P_3(z) + \ldots\right\}\nu\,d\nu$$

$$= \frac{1}{l} + \frac{2(r-\alpha)}{l^2}\int_0^1 \frac{l}{\nu(1-\nu)\alpha}\frac{d}{dz}\left\{1 - \frac{2\nu(1-\nu)\alpha z}{l} + \frac{\nu^2(1-\nu)^2\alpha^2}{l^2}\right\}^{-1/2}\nu\,d\nu$$

$$= \frac{1}{l} + \frac{2(r-\alpha)}{l^2}\int_0^1 \left\{1 - \frac{2\nu(1-\nu)\alpha z}{l} + \frac{\nu^2(1-\nu)^2\alpha^2}{l^2}\right\}^{-3/2}\nu\,d\nu,$$

or

$$(\phi_0)_{\theta=0} = \frac{1}{l} + \frac{2(r-\alpha)}{l^2}\int_0^1\left[\left\{1 + \frac{\alpha\nu(1-\nu)}{l}\right\}^2 - \frac{4r\nu(1-\nu)}{l}\right]^{-3/2}\nu\,d\nu.$$

Changing ν to $(1-\nu)$, and adding half the equation so obtained to half the original equation, we have

$$(\phi_0)_{\theta=0} = \frac{1}{l} + \frac{r-\alpha}{l^2}\int_0^1\left[\left\{1 + \frac{\alpha\nu(1-\nu)}{l}\right\}^2 - \frac{4r\nu(1-\nu)}{l}\right]^{-3/2}d\nu. \qquad (35)$$

This is the sum of the series (33) when θ is zero. We have now to extend it so as to represent the sum of the series (33) when θ is no longer zero. For this we remark that

$$P_n(\cos\theta) = \frac{1}{\pi}\int_0^\pi (\cos\theta + i\sin\theta\cos s)^n\,ds,$$

and therefore the effect of the Legendre functions $P_n(\cos\theta)$ in the series (33) is the same as if, in each term of the large bracket in equation (34), we replaced $\dfrac{1}{l}$ by $\dfrac{\cos\theta + i\cos s\sin\theta}{l}$ and then integrated with respect to s between the limits 0 and π, and divided by π. Performing these operations on the series in its integrated form (35), we have

$$\phi_0 = \frac{1}{l} + \frac{l(r-\alpha)}{\pi}\int_0^\pi\int_0^1 \frac{(\cos\theta + i\cos s\sin\theta)\,d\nu\,ds}{[\{l + \alpha\nu(1-\nu)(\cos\theta + i\cos s\sin\theta)\}^2 - 4r\nu(1-\nu)\,l\,(\cos\theta + i\cos s\sin\theta)]^{3/2}}. \quad (36)$$

This expression represents the electric potential at the point (r, θ) *due to a unit point-charge at rest at the point* $(r = l, \theta = 0)$, *in the gravitational field due to a mass at the origin.* It does not seem possible to perform the integrations so as to obtain an algebraic expression similar to that obtained in equation (19) for the quasi-uniform field. One consequence, however, follows immediately from (36), namely that ϕ_0 is constant over the sphere $r = \alpha$: so there are electric equipotential surfaces which enclose the gravitating centre and one wholly external to the electric charge—a result so surprising that it would seem worth while to pursue the matter farther by numerical calculation.

§ 9. *Spherical Electromagnetic Waves.*

Still considering the gravitational field of a single attracting centre, we shall now find the systems of spherical electromagnetic waves which have their centre at the gravitating mass.

For this we require solutions of the partial differential equations (21) to (24), for which j_0, j_1, j_2, j_3 are zero (except at the singularity at the origin) and ϕ_0, ϕ_1, ϕ_2, are also zero, while ϕ_3 is of the form

$$e^{ipt} \times (\text{a function of } r \text{ only}) \times (\text{a function of } \theta \text{ only}),$$

say,

$$\phi_3 = e^{ipt} f(r)\, g(\theta). \tag{37}$$

Equations (21), (22), (23) are satisfied automatically; and equation (24) becomes

$$\frac{r}{c^2(r-\alpha)}\frac{\partial^2\phi_3}{\partial t^2} - \frac{r-\alpha}{r}\frac{\partial^2\phi_3}{\partial r^2} - \frac{\alpha}{r^2}\frac{\partial\phi_3}{\partial r} - \frac{1}{r^2}\frac{\partial^2\phi_3}{\partial\theta^2} + \frac{1}{r^2}\cot\theta\,\frac{\partial\phi_3}{\partial\theta} = 0, \tag{38}$$

or by (37)

$$\frac{-p^2 r}{c^2(r-\alpha)} - \frac{r-\alpha}{r}\,\frac{1}{f(r)}\,\frac{d^2 f(r)}{dr^2} - \frac{\alpha}{r^2}\frac{1}{f(r)}\,\frac{\partial f(r)}{dr} - \frac{1}{r^2}\,\frac{1}{g(\theta)}\,\frac{d^2 g(\theta)}{d\theta^2}$$
$$+ \frac{1}{r^2}\,\frac{\cot\theta}{g(\theta)}\,\frac{dg(\theta)}{d\theta} = 0.$$

We break this up in the usual way into two equations, namely,

$$\frac{d^2 g}{d\theta^2} - \cot\theta\,\frac{dg}{d\theta} + n(n+1)g = 0,$$

of which the solution is

$$g = \sin^2\theta \,.\, \frac{d\,\mathrm{P}_n(\cos\theta)}{d(\cos\theta)} \tag{39}$$

and

$$\frac{r-\alpha}{r}\frac{d^2 f}{dr^2} + \frac{\alpha}{r^2}\frac{df}{dr} + \left\{\frac{p^2 r}{c^2(r-\alpha)} - \frac{n(n+1)}{r^2}\right\} f = 0. \tag{40}$$

This is a linear differential equation of the second order with three singular points, namely, 0, α, and ∞. The exponents at $r = 0$ are 0 and 2, and the exponents at $r = \alpha$ are $\frac{ip\alpha}{c}$ and $-\frac{ip\alpha}{c}$, while $r = \infty$ is an irregular singular point at which f behaves like $e^{\pm\frac{ipr}{c}} . r^{\pm\frac{i\alpha p}{c}}$. The equation (40) is therefore akin to Mathieu's equation, which also has two regular finite singular points and an irregular singularity at infinity, but it is not identical with Mathieu's equation. Denoting its solution by $f(r)$ (we shall show in the next two sections how to calculate it), we see by (37) and (39) that *the vector-potential of the spherical electromagnetic waves in the gravitational field is* $(0, 0, 0, \phi_3)$, *where*

$$\phi_3 = e^{ipt} f(r) \sin^2 \theta \frac{dP_n(\cos\theta)}{d(\cos\theta)}.$$

§ 10. *Case when the Waves are of High Frequency.*

When the waves are of high frequency, so that p is very large, the equation (40) can be integrated in terms of elementary functions: for we can then neglect the term $-\frac{n(n+1)}{r^2}$ in comparison with the term $\frac{p^2 r}{c^2(r-\alpha)}$, and thus equation (40) becomes

$$\frac{r-\alpha}{r}\frac{d^2 f}{dr^2} + \frac{\alpha}{r^2}\frac{df}{dr} + \frac{p^2 r}{c^2(r-\alpha)} f = 0 \tag{41}$$

of which the solution is

$$f = \mathrm{A}\, e^{\frac{ipr}{c}} (r-\alpha)^{\frac{ip\alpha}{c}} + \mathrm{B}\, e^{-\frac{ipr}{c}} (r-\alpha)^{-\frac{ip\alpha}{c}}, \tag{42}$$

where A and B are arbitrary constants. Thus *the vector-potential of spherical electromagnetic waves of high frequency in the gravitational field is* $(0, 0, 0, \phi_3)$, *where*

$$\phi_3 = e^{ipt} . e^{\pm\frac{ipr}{c}} . (r-\alpha)^{\pm\frac{ip\alpha}{c}} . \sin^2\theta . \frac{dP_n(\cos\theta)}{d(\cos\theta)}. \tag{43}$$

The ambiguous sign ± must, of course, be taken as plus for convergent waves and minus for divergent waves. From (43) we can at once find the velocity* with which the waves approach or recede from the origin at any point; for if the vector-potential is given by an expression of the form

$$\phi_3 = [\text{a function of } \{t - h(r)\}] \times [\text{a function of } \theta],$$

then the velocity of the waves at the point (r, θ) is $\frac{1}{h'(r)}$. Now from (43) we see that in our case, $h(r)$ has the value $\frac{r}{c} + \frac{\alpha}{c}\log(r - \alpha)$, and therefore $h'(r)$ has the value $\frac{r}{c(r - a)}$. Thus *the velocity of the waves at the point* (r, θ) is

---

* *I.e.*, the co-ordinate velocity.

$$c\left(1 - \frac{a}{r}\right). \tag{44}$$

This shows that convergent waves cannot approach nearer to the gravitating mass than the point $r = \alpha$. Now r is not the *distance* from the origin, but the area of the sphere $r = \alpha$ is $4\pi\alpha^2$, so we may say that *the area of the wave-front of a spherical wave can never become smaller than* $4\pi\alpha^2$.

The result (44) might, as a matter of fact, have been inferred by considering that these high-frequency waves are the "rays of light" which are the null geodesics of the metric, and therefore satisfy the equation $ds^2 = 0$, or by (6)

$$\frac{r - \alpha}{r}\,dt^2 - \frac{r}{c^2(r - \alpha)}\,dr^2 = 0,$$

or

$$\frac{dr}{dt} = \pm c\left(1 - \frac{\alpha}{r}\right),$$

in agreement with (44).

§ 11. *The General Case when the Frequency is Arbitrary.*

Let us now consider the general case, when the frequency p is no longer supposed to be necessarily very great. The results of the last section suggest that for convergent waves the solution of equation (40) may be represented by a series of the form

$$f(r) = e^{\frac{ipr}{c}}(r - \alpha)^{\frac{ip\alpha}{c}}\left\{1 + \frac{h_1(r)}{p} + \frac{h_2(r)}{p^2} + \frac{h_3(r)}{p^3} + \dots\right\}, \tag{45}$$

where $h_1(r), h_2(r), h_3(r), \dots$ are functions of r. To obtain these functions, we first transform equation (40) by writing

$$f = e^{\frac{ipr}{c}}(r - \alpha)^{\frac{ip\alpha}{c}}y, \tag{46}$$

when we find for y the differential equation

$$\frac{d}{dr}\left\{\left(1 - \frac{\alpha}{r}\right)\frac{dy}{dr}\right\} + \frac{2ip}{c}\frac{dy}{dr} - \frac{n(n+1)}{r^2}y = 0. \tag{47}$$

Substituting in this differential equation the series

$$y = 1 + \frac{h_1(r)}{p} + \frac{h_2(r)}{p^2} + \frac{h_3(r)}{p^3} + \dots,$$

and equating to zero the coefficient of p^{-s}, we have

$$\frac{d}{dr}\left\{\left(1-\frac{\alpha}{r}\right)h_s'(r)\right\}+\frac{2i}{c}h_{s+1}'(r)-\frac{n(n+1)}{r^2}h_s(r)=0,$$

where we see that $h_{s+1}(r)$ is determined in terms of $h_s(r)$ by the simple equation

$$h_{s+1}(r)=\tfrac{1}{2}ic\left\{\left(1+\frac{\alpha}{r}\right)h_s'(r)+n(n+1)\int_r^\infty\frac{h_s(r)\,dr}{r^2}\right\}. \tag{48}$$

This gives in succession

$$h_1(r)=\frac{n(n+1)ic}{2r},\quad h_2(r)=-\frac{n(n+1)c^2}{4}\left\{\frac{(n+2)(n-1)}{2r^2}+\frac{\alpha}{r^3}\right\},\text{ etc.,}$$

and so the series in (45) is completely determined. Evidently it will be closely related to the asymptotic expansion of the solution of equation (40) at its irregular singularity $r=\infty$. *The electromagnetic waves, in the general case when the frequency is arbitrary, are then determined by substituting the expression* (45), *thus obtained, in the equation*

$$\phi_3=e^{ipt}f(r)\sin^2\theta\,.\,\frac{dP_n(\cos\theta)}{d(\cos\theta)},$$

which was found in § 9 *for the vector-potential.*

INDEX TO VOL. CXVI. (A)

Acetylene, hydrogen and pentane mixtures, explosions in (Egerton and Gates), 516.
Actinium A recoil atom, mobility (Dee), 664.
Adsorption, electric condition of hot surfaces (Finch and Stimson), 379.
Alkali metals, magnetic susceptibility (McLennan and others), 468.
Allen (H. S.) and Sandeman (I.) Bands in the Secondary Spectrum of Hydrogen, II, 312.
Alloys, binary, magnetic susceptibility (Spencer and John), 61.
Alloy crystals, tensile tests, IV (Elam), 694.
Askey (P. J.) *See* Hinshelwood and Askey.
Atkinson (R. d'E.) On the Emission of Light from Hydrogen Atoms, 81.

Baly (E. C. C.), Davies (J. B.), Johnson (M. R.), and Shanassy (H.) The Photosynthesis of Naturally Occurring Compounds, I, 197.
Baly (E. C. C.), Stephen (W. E.), and Hood (N. R.) The Photosynthesis of Naturally Occurring Compounds, II, 212.
Baly (E. C. C.), Davies (J. B.) The Photosynthesis of Naturally Occurring Compounds, III, 219.
Barfield (R. H.) *See* Smith-Rose and Barfield.
Barrell (H.) *See* Rolt and Barrell.
Beckett (H. E.) *See* George and Beckett.
Bengough (G. D.), Stuart (J. M.), and Lee (A. R.) The Theory of Metallic Corrosion in the Light of Quantitative Measurements, 425.
Brazier (L. G.) On the Flexure of Thin Cylindrical Shells and other Thin Sections, 104.
Burgers (W. G.) Investigations of the Molecular Arrangement of Uniaxial Optically Active Crystals, 553.
Burt (F. P.) *See* Francis and Burt.

Coagulation of Smokes and the Theory of Smoluchowski (Nonhebel and others), 540.
Cohen (E.) *See* McLennan and others.
Combustion, gaseous at high pressures, VIII (Townend), 637.
Contact of flat surfaces (Rolt and Barrell), 401.
Collins (W. T.) *See* McLennan, Grayson-Smith and Collins.
Colvin (J.) *See* Nonhebel and others.
Corrosion, metallic (Bengough and others), 425.
Cowen (L. G.) *See* Finch and Cowen.
Crystals of alloys, tensile tests (Elam), 694.
Crystals of aluminium, distorsion under compression (Taylor), 16, 39.
Crystals, uniaxial, molecular arrangement (Burgers), 553.

Darwin (C. G.) The Electron as a Vector Wave, 227.
Davies (J. B.) *See* Baly and others.
Dee (P. I.) The Mobility of the Actinium A Recoil Atom, 664.
Diffraction of light by metallic screens (Raman and Krishnan), 254.

Egerton (A.) and Gates (S. F.) Further Experiments on Explosions in Gaseous Mixtures of Acetylene, of Hydrogen and of Pentane, 516.
Eisenbrand (J.) *See* Halban and Eisenbrand.
Elam (C. F.) Tensile Tests on Alloy Crystals, IV, 694.
Electric phenomena in gravitational fields (Whittaker), 720.
Electron as a vector wave (Darwin), 227.
Emission of light from hydrogen atoms (Atkinson), 81.
Energy of the struck string, II (George and Beckett), 115.
Explosions in gaseous mixtures of acetylene, hydrogen and pentane (Egerton and Gates), 516.

Fage (A.) and Johansen (F. C.) On the Flow of Air Behind an Inclined Flat Plate of Infinite Span, 170.
Finch (G. I.) and Cowen (L. G.) Gaseous Combustion in Electric Discharges, II, 529.
Finch (G. I.) and Stimson (J. C.) The Electrical Condition of Hot Surfaces during the Adsorption of Gases, 379.
Flexure of thin cylindrical shells (Brazier), 104.
Flow of air behind infinite inclined flat plate (Fage and Johansen), 170.
Forsdyke (A. G.) *See* Levy and Forsdyke.
Francis (M.) and Burt (F. P.) Sorption of Ammonia by Glass, 586.
Fresnel's convection coefficient in general relativity (Sen), 73.

Gamma rays, internal conversion (Swirles), 491.
Gaseous combustion in electric discharges, II (Finch and Cowen), 529.
Gates (S. F.) *See* Egerton and Gates.
Gauge-invariant tensor calculus (Newman), 603.
George (W. H.) and Beckett (H. E.) The Energy of the Struck String, II, 115.
Glass, sorption of ammonia (Francis and Burt), 586.
Gravitational fields, electric phenomena (Whittaker), 720.
Grayson-Smith (H.) *See* McLennan, Grayson-Smith and Collins.

Halban (H. von) and Eisenbrand (J.) On the Measurement of Light Absorption, 153.
Hill (L.) Measurement of the Biologically Active Ultra-Violet Rays of Sunlight, 268.
Hinshelwood (C. N.) and Askey (P. J.) The Influence of Hydrogen on Two Homogeneous Reactions, 163.
Homogeneous reactions, influence of hydrogen (Hinshelwood and Askey), 163.
Hood (N. R.) *See* Baly and others.
Hydrogen atoms, emission of light (Atkinson), 81.
Hydrogen, bands in secondary spectrum, II (Allen and Sandeman), 312.
Hydrogen, influence on homogeneous reactions (Hinshelwood and Askey), 163.
Hydrogen, intensities in secondary spectrum (McLennan and others), 277.
Hydrogen molecule, intensity distribution in spectrum (Richardson), 484.

Ireton (H. J. C.) *See* McLennan and others.

Jenkins (H. G.) *See* Johnson and Jenkins.
Johansen (F. C.) *See* Fage and Johansen.
John (M. E.) *See* Spencer and John.
Johnson (M. R.) *See* Baly and others.
Johnson (R. C.) and Jenkins (H. G.) The Band Spectra of Silicon Fluoride, 327.

Krishnan (K. S.) *See* Raman and Krishnan.

Lee (A. R.) *See* Bengough and others.

Levy (H.) and Forsdyke (A. G.) The Vibrations of an Infinite System of Vortex Rings, 352.

Light absorption, measurement (Halban and Eisenbrand), 153.

McLennan (J. C.), Grayson-Smith (H.) and Collins (W. T.) Intensities in the Secondary Spectrum of Hydrogen, 277.

McLennan (J. C.), Ireton (H. J. C.) and Thomson (K.) The Luminescence of Solid Nitrogen under Cathode Ray Bombardment, 1.

McLennan (J. C.), Ruedy (R.) and Cohen (E.) The Magnetic Susceptibility of the Alkali Metals, 468.

Magnetic susceptibility of alkali metals (McLennan and others), 468.

Magnetic susceptibility of some binary alloys (Spencer and John), 61.

Mandell (W.) The Determination of the Elastic Moduli of the Piezo-Electric Crystal Rochelle Salt, 623.

Mercury spectrum, series of emission and absorption bands (Rayleigh), 702.

Metallic corrosion (Bengough and others), 425.

Newman (M. H. A.) A Gauge-Invariant Tensor Calculus, 603.

Nitrogen, solid, luminescence under cathode ray bombardment (McLennan and others), 1.

Nonhebel (G.), Colvin (J.), Patterson (H. S.) and Whytlaw-Gray (R.) The Coagulation of Smokes and the Theory of Smoluchowski, 540.

Paraffins, chemical equilibrium in mixture (Wilson), 501.

Patterson (H. S.) *See* Nonhebel and others.

Photosynthesis of naturally occurring compounds (Baly and others), 197, 212, 219.

Raman (C. V.) and Krishnan (K. S.) The Diffraction of Light by Metallic Screens, 254.

Rawlins (F. I. G.) and Rideal (E. K.) The Absorption Spectra of Aragonite and Strontianite in the near Infra-Red, 140.

Rayleigh (Lord). Series of Emission and Absorption Bands in the Mercury Spectrum, 702.

Richardson (O. W.) On the Intensity Distribution among the Lines of certain Bands in the Spectrum of the Hydrogen Molecule, 484.

Rideal (E. K.) *See* Rawlins and Rideal.

Rochelle salt, determination of elastic moduli (Mandell), 623.

Rolt (F. H.) and Barrell (H.) Contact of Flat Surfaces, 401.

Ruedy (R.) *See* McLennan and others.

Sandeman (I.) *See* Allen and Sandeman.

Sen (N. R.) On Fresnel's Correction Coefficient in General Relativity, 73.

Shanassy (H.) *See* Baly and others.

Silicon fluoride, band spectra (Johnson and Jenkins), 327.

Smith-Rose (R. L.) and Barfield (R. H.) Further Measurements on Wireless Waves received from the Upper Atmosphere, 682.

Smoluchowski's theory and coagulation of smokes (Nonhebel and others), 540.

Sorption of ammonia by glass (Francis and Burt), 586.

Spectra, absorption, of aragonite and strontianite in infra-red (Rawlins and Rideal), 140.

Spectra, band, of silicon fluoride (Johnson and Jenkins), 327.

Spectrum, luminescence of solid nitrogen (McLennan and others), 1.

Spectrum, mercury, series of emission and absorption bands (Rayleigh), 702.

Spectrum of hydrogen molecule, intensity distribution (Richardson), 484.

Spectrum, secondary hydrogen, bands (Allen and Sandeman), 312.

Spectrum, secondary hydrogen, intensities (McLennan and others), 277.
Spencer (J. F.) and John (M. E.) The Magnetic Susceptibility of some Binary Alloys, 61.
Stephen (W. F.) *See* Baly and others.
Stimson (J. C.) *See* Finch and Stimson.
Stuart (J. M.) *See* Bengough and others.
Swirles (B.) The Internal Conversion of Gamma Rays, 491.

Taylor (G. I.) The Distorsion of Crystals of Aluminium under Compression, II, 16; III, 39.
Thomson (K.) *See* McLennan and others.
Townend (D. T. A.) Gaseous Combustion at High Pressures, VIII, 637.

Ultra-violet rays of sunlight, measurement (Hill), 268.
Uniaxial crystals, molecular arrangement (Burgers), 553.

Vortex rings, vibration of an infinite system (Levy and Forsdyke), 352.

Whittaker (E. T.) On Electric Phenomena in Gravitational Fields, 720.
Whytlaw-Gray (R.) *See* Nonhebel and others.
Wilson (H. A.) Chemical Equilibrium in a Mixture of Paraffin, 501.
Wireless waves from the upper atmosphere (Smith-Rose and Barfield), 682.

END OF THE ONE HUNDRED AND SIXTEENTH VOLUME (SERIES A).

[redacted] AGRICUL[redacted]R[redacted]
INSTITUTE LIBRARY
NEW DELHI.

Date of issue.	Date of issue.	Date of issue.
28-7-41		
1[illegible].12.45		